VOLUME 29 / NUMBER 8
APRIL 23, 1991
ACC. NOS. N91-15976 TO N91-16987

STAR

AN ABSTRACT JOURNAL

Scientific and Technical Aerospace Reports

PRODUCED BY THE
SCIENTIFIC AND TECHNICAL
INFORMATION
DIVISION

NASA

NATIONAL AERONAUTICS AND SPACE ADMINISTRATION

***Scientific and Technical Aerospace Reports* (*STAR*)** is an abstract journal that provides comprehensive coverage of worldwide aerospace-related reports. It is a major product of the International Aerospace Database managed by the NASA Scientific and Technical Information (STI) Program. The coverage includes reports on aeronautics, space, and supporting disciplines. *STAR* lists current, publicly available reports entered into the NASA STI Database during the 2-week period preceding publication. An explanation of items that appear in each citation is given on the last page of each volume.

NASA sponsors a companion journal, *International Aerospace Abstracts* (*IAA*), that lists abstracts of the open literature on aerospace subjects available worldwide. *IAA* is available through the American Institute of Aeronautics and Astronautics.

Entries found in *STAR* and *IAA* are available through NASA's online service, RECON, as the International Aerospace Database and through DIALOG as the Aerospace Database.

Information on aerospace and related subjects is gathered by the NASA STI Program through national and international agreements and exchanges and is made available to the NASA community as well as to the public in many forms through various outlets. The section on NASA STI Program Products and Services contains additional information.

US ISSN 0036-8741

Volume 29 Number 8 / April 23, 1991

TABLE OF CONTENTS

AERONAUTICS For related information see also *Astronautics.*

01 AERONAUTICS (GENERAL) **1089**

02 AERODYNAMICS **1089**
Includes aerodynamics of bodies, combinations, wings, rotors, and control surfaces; and internal flow in ducts and turbomachinery. For related information see also *34 Fluid Mechanics and Heat Transfer.*

03 AIR TRANSPORTATION AND SAFETY **1093**
Includes passenger and cargo air transport operations; and aircraft accidents. For related information see also *16 Space Transportation* and *85 Urban Technology and Transportation.*

04 AIRCRAFT COMMUNICATIONS AND NAVIGATION **1094**
Includes digital and voice communication with aircraft; air navigation systems (satellite and ground based); and air traffic control. For related information see also *17 Space Communications, Spacecraft Communications, Command and Tracking* and *32 Communications and Radar.*

05 AIRCRAFT DESIGN, TESTING AND PERFORMANCE **1094**
Includes aircraft simulation technology. For related information see also *18 Spacecraft Design, Testing and Performance* and *39 Structural Mechanics.* For land transportation vehicles see *85 Urban Technology and Transportation.*

06 AIRCRAFT INSTRUMENTATION ..... **N.A.**
Includes cockpit and cabin display devices; and flight instruments. For related information see also *19 Spacecraft Instrumentation* and *35 Instrumentation and Photography.*

07 AIRCRAFT PROPULSION AND POWER **1097**
Includes prime propulsion systems and systems components, e.g., gas turbine engines and compressors; and onboard auxiliary power plants for aircraft. For related information see also *20 Spacecraft Propulsion and Power, 28 Propellants and Fuels,* and *44 Energy Production and Conversion.*

08 AIRCRAFT STABILITY AND CONTROL **1098**
Includes aircraft handling qualities; piloting; flight controls; and autopilots. For related information see also *05 Aircraft Design, Testing and Performance.*

09 RESEARCH AND SUPPORT FACILITIES (AIR) **1098**
Includes airports, hangars and runways; aircraft repair and overhaul facilities; wind tunnels; shock tubes; and aircraft engine test stands. For related information see also *14 Ground Support Systems and Facilities (Space).*

ASTRONAUTICS For related information see also *Aeronautics.*

12 ASTRONAUTICS (GENERAL) **1099**
For extraterrestrial exploration see *91 Lunar and Planetary Exploration.*

13 ASTRODYNAMICS **1099**
Includes powered and free-flight trajectories; and orbital and launching dynamics.

14 GROUND SUPPORT SYSTEMS AND FACILITIES (SPACE) ..... **N.A.**
Includes launch complexes, research and production facilities; ground support equipment, e.g., mobile transporters; and simulators. For related information see also *09 Research and Support Facilities (Air).*

15 LAUNCH VEHICLES AND SPACE VEHICLES ..... **N.A.**
Includes boosters; operating problems of launch/space vehicle systems; and reusable vehicles. For related information see also *20 Spacecraft Propulsion and Power.*

16 SPACE TRANSPORTATION **1100**
Includes passenger and cargo space transportation, e.g., shuttle operations; and space rescue techniques. For related information see also *03 Air Transportation and Safety* and *18 Spacecraft Design, Testing and Performance.* For space suits see *54 Man/System Technology and Life Support.*

17 SPACE COMMUNICATIONS, SPACECRAFT COMMUNICATIONS, COMMAND AND TRACKING . **1101**
Includes telemetry; space communications networks; astronavigation and guidance; and radio blackout. For related information see also *04 Aircraft Communications and Navigation* and *32 Communications and Radar.*

N.A.—no abstracts were assigned to this category for this issue.

18 SPACECRAFT DESIGN, TESTING AND PERFORMANCE **1101**
Includes satellites; space platforms; space stations; spacecraft systems and components such as thermal and environmental controls; and attitude controls. For life support systems see *54 Man/System Technology and Life Support.* For related information see also *05 Aircraft Design, Testing and Performance, 39 Structural Mechanics,* and *16 Space Transportation.*

19 SPACECRAFT INSTRUMENTATION **1104**
For related information see also *06 Aircraft Instrumentation* and *35 Instrumentation and Photography.*

20 SPACECRAFT PROPULSION AND POWER **1104**
Includes main propulsion systems and components, e.g., rocket engines; and spacecraft auxiliary power sources. For related information see also *07 Aircraft Propulsion and Power, 28 Propellants and Fuels, 44 Energy Production and Conversion,* and *15 Launch Vehicles and Space Vehicles.*

CHEMISTRY AND MATERIALS

23 CHEMISTRY AND MATERIALS (GENERAL) **1105**

24 COMPOSITE MATERIALS **1105**
Includes physical, chemical, and mechanical properties of laminates and other composite materials. For ceramic materials see *27 Nonmetallic Materials.*

25 INORGANIC AND PHYSICAL CHEMISTRY **1107**
Includes chemical analysis, e.g., chromatography; combustion theory; electrochemistry; and photochemistry. For related information see also *77 Thermodynamics and Statistical Physics.*

26 METALLIC MATERIALS **1113**
Includes physical, chemical, and mechanical properties of metals, e.g., corrosion; and metallurgy.

27 NONMETALLIC MATERIALS **1117**
Includes physical, chemical, and mechanical properties of plastics, elastomers, lubricants, polymers, textiles, adhesives, and ceramic materials. For composite materials see *24 Composite Materials.*

28 PROPELLANTS AND FUELS **1121**
Includes rocket propellants, igniters and oxidizers; their storage and handling procedures; and aircraft fuels. For related information see also *07 Aircraft Propulsion and Power, 20 Spacecraft Propulsion and Power,* and *44 Energy Production and Conversion.*

29 MATERIALS PROCESSING ..... **N.A.**
Includes space-based development of products and processes for commercial application. For biological materials see *55 Space Biology.*

ENGINEERING For related information see also *Physics.*

31 ENGINEERING (GENERAL) **1123**
Includes vacuum technology; control engineering; display engineering; cryogenics; and fire prevention.

32 COMMUNICATIONS AND RADAR **1124**
Includes radar; land and global communications; communications theory; and optical communications. For related information see also *04 Aircraft Communications and Navigation* and *17 Space Communications, Spacecraft Communications, Command and Tracking.* For search and rescue see *03 Air Transportation and Safety,* and *16 Space Transportation.*

33 ELECTRONICS AND ELECTRICAL ENGINEERING **1130**
Includes test equipment and maintainability; components, e.g., tunnel diodes and transistors; microminiaturization; and integrated circuitry. For related information see also *60 Computer Operations and Hardware* and *76 Solid-State Physics.*

34 FLUID MECHANICS AND HEAT TRANSFER **1136**
Includes boundary layers; hydrodynamics; fluidics; mass transfer and ablation cooling. For related information see also *02 Aerodynamics* and *77 Thermodynamics and Statistical Physics.*

35 INSTRUMENTATION AND PHOTOGRAPHY **1147**
Includes remote sensors; measuring instruments and gauges; detectors; cameras and photographic supplies; and holography. For aerial photography see *43 Earth Resources and Remote Sensing.* For related information see also *06 Aircraft Instrumentation* and *19 Spacecraft Instrumentation.*

36 LASERS AND MASERS **1151**
Includes parametric amplifiers. For related information see also *76 Solid-State Physics.*

37 MECHANICAL ENGINEERING **1156**
Includes auxiliary systems (nonpower); machine elements and processes; and mechanical equipment.

38 QUALITY ASSURANCE AND RELIABILITY **1161**
Includes product sampling procedures and techniques; and quality control.

39 STRUCTURAL MECHANICS **1161**
Includes structural element design and weight analysis; fatigue; and thermal stress. For applications see *05 Aircraft Design, Testing and Performance* and *18 Spacecraft Design, Testing and Performance.*

GEOSCIENCES For related information see also *Space Sciences.*

42 GEOSCIENCES (GENERAL) ..... **N.A.**

43 EARTH RESOURCES AND REMOTE SENSING **1165**
Includes remote sensing of earth resources by aircraft and spacecraft; photogrammetry; and aerial photography. For instrumentation see *35 Instrumentation and Photography.*

44 ENERGY PRODUCTION AND CONVERSION **1169**
Includes specific energy conversion systems, e.g., fuel cells; global sources of energy; geophysical conversion; and windpower. For related information see also *07 Aircraft Propulsion and Power, 20 Spacecraft Propulsion and Power,* and *28 Propellants and Fuels.*

45 ENVIRONMENT POLLUTION **1171**
Includes atmospheric, noise, thermal, and water pollution.

46 GEOPHYSICS **1175**
Includes aeronomy; upper and lower atmosphere studies; ionospheric and magnetospheric physics; and geomagnetism. For space radiation see *93 Space Radiation.*

47 METEOROLOGY AND CLIMATOLOGY **1180**
Includes weather forecasting and modification.

48 OCEANOGRAPHY **1188**
Includes biological, dynamic, and physical oceanography; and marine resources. For related information see also *43 Earth Resources and Remote Sensing.*

LIFE SCIENCES

51 LIFE SCIENCES (GENERAL) **1189**

52 AEROSPACE MEDICINE **1190**
Includes physiological factors; biological effects of radiation; and effects of weightlessness on man and animals.

53 BEHAVIORAL SCIENCES **1191**
Includes psychological factors; individual and group behavior; crew training and evaluation; and psychiatric research.

54 MAN/SYSTEM TECHNOLOGY AND LIFE SUPPORT **1192**
Includes human engineering; biotechnology; and space suits and protective clothing. For related information see also *16 Space Transportation.*

55 SPACE BIOLOGY ..... **N.A.**
Includes exobiology; planetary biology; and extraterrestrial life.

MATHEMATICAL AND COMPUTER SCIENCES

59 MATHEMATICAL AND COMPUTER SCIENCES (GENERAL) ..... **N.A.**

60 COMPUTER OPERATIONS AND HARDWARE **1196**
Includes hardware for computer graphics, firmware, and data processing. For components see *33 Electronics and Electrical Engineering.*

61 COMPUTER PROGRAMMING AND SOFTWARE **1196**
Includes computer programs, routines, algorithms, and specific applications, e.g., CAD/CAM.

62 COMPUTER SYSTEMS **1206**
Includes computer networks and special application computer systems.

63 CYBERNETICS **1208**
Includes feedback and control theory, artificial intelligence, robotics and expert systems. For related information see also *54 Man/System Technology and Life Support.*

64 NUMERICAL ANALYSIS **1208**
Includes iteration, difference equations, and numerical approximation.

65 STATISTICS AND PROBABILITY **1211**
Includes data sampling and smoothing; Monte Carlo method; and stochastic processes.

66 SYSTEMS ANALYSIS ..... **N.A.**
Includes mathematical modeling; network analysis; and operations research.

67 THEORETICAL MATHEMATICS **1212**
Includes topology and number theory.

PHYSICS For related information see also *Engineering.*

70 PHYSICS (GENERAL) **1212**
For precision time and time interval (PTTI) see *35 Instrumentation and Photography;* for geophysics, astrophysics or solar physics see *46 Geophysics, 90 Astrophysics,* or *92 Solar Physics.*

71 ACOUSTICS **1213**
Includes sound generation, transmission, and attenuation. For noise pollution see *45 Environment Pollution.*

72 ATOMIC AND MOLECULAR PHYSICS **1219**
Includes atomic structure, electron properties, and molecular spectra.

73 NUCLEAR AND HIGH-ENERGY PHYSICS **1222**
Includes elementary and nuclear particles; and reactor theory. For space radiation see *93 Space Radiation.*

74 OPTICS **1223**
Includes light phenomena and optical devices. For lasers see *36 Lasers and Masers.*

75 PLASMA PHYSICS **1225**
Includes magnetohydrodynamics and plasma fusion. For ionospheric plasmas see *46 Geophysics.* For space plasmas see *90 Astrophysics.*

76 SOLID-STATE PHYSICS **1230**
Includes superconductivity. For related information see also *33 Electronics and Electrical Engineering* and *36 Lasers and Masers.*

77 THERMODYNAMICS AND STATISTICAL PHYSICS **1239**
Includes quantum mechanics; theoretical physics; and Bose and Fermi statistics. For related information see also *25 Inorganic and Physical Chemistry* and *34 Fluid Mechanics and Heat Transfer.*

SOCIAL SCIENCES

80 SOCIAL SCIENCES (GENERAL) ..... **N.A.**
Includes educational matters.

81 ADMINISTRATION AND MANAGEMENT **1239**
Includes management planning and research.

82 DOCUMENTATION AND INFORMATION SCIENCE **1240**
Includes information management; information storage and retrieval technology; technical writing; graphic arts; and micrography. For computer documentation see *61 Computer Programming and Software.*

83 ECONOMICS AND COST ANALYSIS ..... **N.A.**
Includes cost effectiveness studies.

84 LAW, POLITICAL SCIENCE AND SPACE POLICY ..... **N.A.**
Includes NASA appropriation hearings; aviation law; space law and policy; international law; international cooperation; and patent policy.

85 URBAN TECHNOLOGY AND TRANSPORTATION ..... **N.A.**
Includes applications of space technology to urban problems; technology transfer; technology assessment; and surface and mass transportation. For related information see *03 Air Transportation and Safety, 16 Space Transportation,* and *44 Energy Production and Conversion.*

SPACE SCIENCES For related information see also *Geosciences.*

88 SPACE SCIENCES (GENERAL) **1243**

89 ASTRONOMY **1243**
Includes radio, gamma-ray, and infrared astronomy; and astrometry.

90 ASTROPHYSICS **1244**
Includes cosmology; celestial mechanics; space plasmas; and interstellar and interplanetary gases and dust. For related information see also *75 Plasma Physics.*

91 LUNAR AND PLANETARY EXPLORATION **1268**
Includes planetology; and manned and unmanned flights. For spacecraft design or space stations see *18 Spacecraft Design, Testing and Performance.*

92 SOLAR PHYSICS **1268**
Includes solar activity, solar flares, solar radiation and sunspots. For related information see *93 Space Radiation.*

93 SPACE RADIATION **1268**
Includes cosmic radiation; and inner and outer earth's radiation belts. For biological effects of radiation see *52 Aerospace Medicine.* For theory see *73 Nuclear and High-Energy Physics.*

GENERAL

Includes aeronautical, astronautical, and space science related histories, biographies, and pertinent reports too broad for categorization; histories or broad overviews of NASA programs.

99 GENERAL **1269**

SUBJECT INDEX **I-1**

PERSONAL AUTHOR INDEX **I-71**

CORPORATE SOURCE INDEX **I-81**

CONTRACT NUMBER INDEX **I-93**

REPORT/ACCESSION NUMBER INDEX **I-97**

APPENDIX **A-1**

TYPICAL CITATION AND ABSTRACT

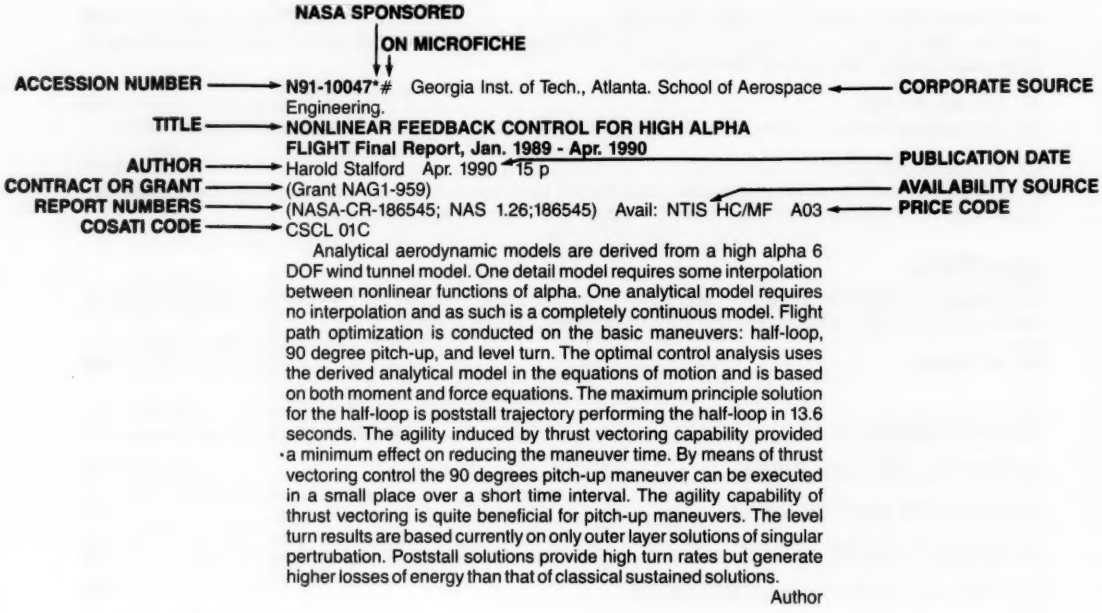
NASA SPONSORED
ON MICROFICHE
ACCESSION NUMBER
N91-10047*# Georgia Inst. of Tech., Atlanta. School of Aerospace Engineering.
CORPORATE SOURCE
TITLE
NONLINEAR FEEDBACK CONTROL FOR HIGH ALPHA FLIGHT Final Report, Jan. 1989 - Apr. 1990
PUBLICATION DATE
AUTHOR
Harold Stalford Apr. 1990 15 p
CONTRACT OR GRANT
(Grant NAG1-959)
AVAILABILITY SOURCE
REPORT NUMBERS
(NASA-CR-186545; NAS 1.26;186545) Avail: NTIS HC/MF A03
PRICE CODE
COSATI CODE
CSCL 01C
Analytical aerodynamic models are derived from a high alpha 6 DOF wind tunnel model. One detail model requires some interpolation between nonlinear functions of alpha. One analytical model requires no interpolation and as such is a completely continuous model. Flight path optimization is conducted on the basic maneuvers: half-loop, 90 degree pitch-up, and level turn. The optimal control analysis uses the derived analytical model in the equations of motion and is based on both moment and force equations. The maximum principle solution for the half-loop is poststall trajectory performing the half-loop in 13.6 seconds. The agility induced by thrust vectoring capability provided a minimum effect on reducing the maneuver time. By means of thrust vectoring control the 90 degrees pitch-up maneuver can be executed in a small place over a short time interval. The agility capability of thrust vectoring is quite beneficial for pitch-up maneuvers. The level turn results are based currently on only outer layer solutions of singular pertrubation. Poststall solutions provide high turn rates but generate higher losses of energy than that of classical sustained solutions.
Author

VOLUME 29 NUMBER 8 / APRIL 23, 1991

Scientific and Technical Aerospace Reports

A Semimonthly Publication of the National Aeronautics and Space Administration

01 AERONAUTICS (GENERAL)

N91-15976# General Accounting Office, Washington, DC. National Security and International Affairs Div.
TACTICAL FIGHTER AIRCRAFT: DIFFERENCES BETWEEN THE AIR FORCE'S ROADMAP AND THE FIVE YEAR DEFENSE PLAN Report to the Chairman, Committee on Armed Services, House of Representatives
Aug. 1990 23 p
(AD-A228882; GAO/NSIAD-90-262) Avail: NTIS HC/MF A03 CSCL 05/1

The tactical fighter roadmap presents a strategy for acquiring and maintaining the force structure desired by the tactical commanders. The roadmap, however, is not an official strategy approved by DOD or Air Force Headquarters. The Tactical Air Command (TAC), which represents the commanders of U.S. Tactical Air Forces (TAF), develops and revises a briefing on the roadmap based on threat considerations, force structure positions, and fiscal constraints. During the budget process, the roadmap is used by TAC and Air Force Headquarters in developing budget requests. Portions of the briefing have also been presented to the Congress during appropriations hearings. The October 1989 roadmap includes TAF's modernization plans for the 36 wings of tactical fighters assigned to its active, Air National Guard, and reserve forces. It reflects the fiscal year 1990/1991 budget request but presents a tactical force structure in the years beyond 1991 that is different from the force structure presented in the April 1989 defense plan. The defense plan and the roadmap do not agree on the number and type of aircraft scheduled to be purchased or retired after fiscal year 1991. GRA

N91-15977# Deutsche Forschungsanstalt fuer Luft- und Raumfahrt, Goettingen (Germany, F.R.). Forschungsbereich Stroemungsmechanik.
DOCUMENTS ON THE HISTORY OF THE AERODYNAMIC RESEARCH ESTABLISHMENT AT GOETTINGEN, 1907 - 1925
Julius C. Rotta Apr. 1990 174 p In GERMAN; ENGLISH summary
(DLR-MITT-90-05; ISSN-0176-7739; ETN-91-98261) Avail: NTIS HC/MF A08; DLR, VB-PL-DO, Postfach 90 60 58, Cologne, Fed. Republic of Germany, HC 27 DM

A supplement to a history of the Aerodynamic Research Establishment is presented. Subjects covered are the model research facilities; first interests in aeronautical engineering; the project of an institute for aerodynamics and hydrodynamics; permission given by military authorities during the First World War for the creation of an aerodynamic research institute; construction of the model research center for aerodynamics; and the research equipment used in the institute after the First World War. ESA

N91-15978* National Aeronautics and Space Administration, Washington, DC.
AERONAUTICAL ENGINEERING: A CONTINUING BIBLIOGRAPHY WITH INDEXES (SUPPLEMENT 260)
Jan. 1991 132 p
(NASA-SP-7037(260); NAS 1.21:7037(260)) Avail: NTIS HC A07; NTIS standing order as PB91-914100, $17.00 domestic, $34.00 foreign CSCL 01B

This bibliography lists 405 reports, articles, and other documents introduced into the NASA scientific and technical information system in December, 1990. Subject coverage includes: design, construction and testing of aircraft and aircraft engines; aircraft components, equipment and systems; ground support systems; and theoretical and applied aspects of aerodynamics and general fluid dynamics. Author

N91-15979* National Aeronautics and Space Administration, Washington, DC.
AERONAUTICAL ENGINEERING: A CONTINUING BIBLIOGRAPHY WITH INDEXES (SUPPLEMENT 259)
Dec. 1990 202 p
(NASA-SP-7037(259); NAS 1.21:7037(259)) Avail: NTIS HC A10; NTIS standing order as PB90-914100, $11.50 domestic, $23.00 foreign CSCL 01B

This bibliography lists 774 reports, articles, and other documents introduced into the NASA scientific and technical information system in November, 1990. Subject coverage includes: design, construction and testing of aircraft and aircraft engines; aircraft components, equipment and systems; ground support systems; and theoretical and applied aspects of aerodynamics and general fluid dynamics. Author

02 AERODYNAMICS

Includes aerodynamics of bodies, combinations, wings, rotors, and control surfaces; and internal flow in ducts and turbomachinery.

For related information see also *34 Fluid Mechanics and Heat Transfer.*

N91-15980 University Coll., Cardiff (Wales).
AERODYNAMIC SURFACE PRESSURE MEASUREMENT IN ATMOSPHERE AND WIND TUNNEL ON A VERTICAL AXIS WIND TURBINE BLADE USING PRESSURE TRANSDUCERS Ph.D. Thesis
C. E. Oram 1989 292 p
Avail: Univ. Microfilms Order No. BRDX89820

Blade aerodynamic loads during operation of a wind turbine are poorly understood. Better measurements of these forces are needed for the design of more cost effective turbines. Existing estimates were inferred from strain gauges in the blade structure, but such measurements are confused by the complexity of the blade's structural response. The blade surface was pressure tapped and recorded at high speed, giving a highly detailed picture of dynamic events and blade loads. A modular blade was concentrated for the 6 m diameter Rutherford Appleton Vertical Axis Wind Turbine and instrumented with 32 semiconductor pressure transducers. A flow probe using a further three transducers projected ahead of the blade during some of the tests. The instrumented module was also operated in the oscillating mounting of the University of Glasglow's 1.6 by 2.4 m wind tunnel. Data (1760 revolutions) were collected in atmosphere with blade speed ratios down to about 2.0 and with a variety of blade leanout angles. Some 118 runs of a variety of waveform types and Reynolds numbers from 0.3 to 1.1 million, were collected from the blade in tunnel. Analysis of transducer calibration concluded that the temperature correction technique used allowed pressure readings

to 40 Pa or better with 95 percent confidence. Confidence in measured pressures has allowed use of leading edge stagnation point pressure and position as a measure of wind in the rotor flowfield and as a surrogate measure of blade angle of attack. Blade surface pressures and integrated forces show the progression of dynamic stall with increase in wind speed, the dominance of the upstream blade pass in usefulness at low and moderate windspeeds and the rough equality at high windspeeds. Comparisons of wind tunnel and on-rotor data show much lower force and moment coefficients in atmosphere. Dissert. Abstr.

N91-15981*# Tennessee Univ. Space Inst., Tullahoma.
INVESTIGATION OF TRANSONIC FLOW OVER SEGMENTED SLOTTED WIND TUNNEL WALL WITH MASS TRANSFER Final Report
M. K. Bhat, A. D. Vakili, and J. M. Wu Dec. 1990 90 p
(Grant NAG2-193)
(NASA-CR-187760; NAS 1.26:187760; UTSI-90) Avail: NTIS HC/MF A05 CSCL 01A

The flowfield on a segmented multi-slotted wind tunnel wall was studied at transonic speeds by measurements in and near the wall layer using five port cone probes. The slotted wall flowfield was observed to be three-dimensional in nature for a relatively significant distance above the slot. The boundary layer characteristics measured on the single slotted wall were found to be very sensitive to the applied suction through the slot. The perturbation in the velocity components generated due to the flow through the slot decay rapidly in the transverse direction. A vortex-like flow existed on the single slotted wall for natural ventilation but diminished with increased suction flow rate. For flow on a segmented multi-slotted wall, the normal velocity component changes were found to be maximum for measurement points located between the segmented slots atop the active chamber. The lateral influence due to applied suction and blowing, through a compartment, exceeded only slightly that in the downstream direction. Limited upstream influence was observed. Influence coefficients were determined from the data in the least-square sense for blowing and suction applied through one and two compartments. This was found to be an adequate determination of the influence coefficients for the range of mass flows considered. Author

N91-15982# National Aerospace Lab., Tokyo (Japan). ACT Study Group.
WIND TUNNEL TESTS ON FLUTTER CONTROL OF A HIGH-ASPECT-RATIO CANTILEVERED WING: CONTROL WITH LEADING-EDGE AND TRAILING-EDGE CONTROL SURFACES Report No. 2
Jun. 1990 26 p In JAPANESE; ENGLISH summary
(NAL-TR-1070; ISSN-0389-4010) Avail: NTIS HC/MF A03

Control laws were synthesized for active flutter suppression of a transport-type high aspect-ratio wing using both the leading-edge and the trailing-edge control surfaces. Wind tunnel tests were conducted in the NAL 5.5m x 6.5m low-speed wind tunnel in order to verify these control laws. The wing model has two accelerometers as sensors co-located at the control surfaces. The Linear Quadratic Gaussian (LQG) optimal control law synthesis method was applied to this multi-input, multi-output system to yield full order control laws. The order reduction procedure based on chained aggregation, together with some engineering manipulation, reduced the original 17th order controller to the decoupled second order practical controller. This synthesis method was verified to be effective by wind tunnel tests. In spite of the violent nature of clean wing flutter, the control law attained 13 percent increase in flutter speed in the test. Author

N91-15983# National Aerospace Lab., Tokyo (Japan).
AN EXPERIMENT ON SUPERSONIC TURBULENT MIXING LAYERS: SUPERSONIC-SUBSONIC TWO-STREAM LAYERS
Atsuo Murakami, Tomoyuki Komuro, Kenji Kudou, Goro Masuya, and Nobuo Chinzei May 1990 17 p In JAPANESE; ENGLISH summary
(NAL-TR-1066; ISSN-0389-4010) Avail: NTIS HC/MF A03

An experimental study was made on supersonic-subsonic two-stream mixing layers with a high-velocity side free-stream Mach number of 2.3. The free-stream Mach number on the low-velocity side was 0.19, 0.49, 0.65, or 0.80. Self-similar velocity distributions approximately agreed with those of the single-stream incompressible mixing layers. Centers of the mixing layers moved to the low-velocity side with decreasing velocity ratio. Values of the maximum shear stress decreased with increasing compressibility effect, and simply correlated with the spreading rates irrespective of compressibility. Compressibility effect on the spreading rate appeared stronger to the visual thickness and the density thickness than to the velocity thickness. Author

N91-15984# National Aerospace Lab., Tokyo (Japan). Aircraft Aerodynamics Div.
LARGE-SCALE NUMERICAL AERODYNAMIC SIMULATIONS FOR COMPLETE AIRCRAFT CONFIGURATIONS
Susumu Takanashi Jul. 1990 14 p
(NAL-TR-1073-T; ISSN-0389-4010) Avail: NTIS HC/MF A03

Navier-Stokes simulations of transonic flows were carried out for complete configurations of two kinds of test models which were designed to investigate the aerodynamic characteristics of the airplanes under development using the transonic wind tunnel. An O-O grid system for the computation is constructed by the automatic procedure based on the electro-static theory. The Reynolds-averaged Navier-Stokes equations are solved on a supercomputer, FACOM VP-400, using an implicit finite volume, upwind Total Variation Diminishing (TVD) scheme. Computed pressure distributions as well as force coefficients are also compared with the experimental data. Author

N91-15985# National Aerospace Lab., Tokyo (Japan).
CALCULATIONS FOR UNSTEADY AERODYNAMIC CHARACTERISTICS ON A 3-D LIFTING BODY IN SUBSONIC FLOW USING BOUNDARY ELEMENT METHOD
Mitsunori Yanagizawa, Toshiyuki Morita, and Shigefumi Tatsumi May 1990 72 p In JAPANESE; ENGLISH summary
(NAL-TR-1065; ISSN-0389-4010) Avail: NTIS HC/MF A04

A boundary element method of unsteady compressible potential flow around lifting bodies having arbitrary configurations and harmonic oscillation motions was developed using Green's function. Morino described the form of the integral equation relating the perturbation potential and its normal derivative. The purpose is to present a new paneling and derivative technique which can be applied to any complex configuration for evaluating the derivative of unsteady velocity potential on the surface. Numerical results for a wing-store model are presented and compared to experimental results in a subsonic flow. Good agreement was obtained between the two. Author

N91-15986*# Pennsylvania State Univ., University Park. Dept. of Mechanical Engineering.
HYPERSONIC SHOCK/BOUNDARY-LAYER INTERACTION DATABASE
Gary S. Settles and Lori J. Dodson Dec. 1990 156 p
(Grant NAG2-565)
(NASA-CR-187769; NAS 1.26:187769; PSU-ME-90/91-003)
Avail: NTIS HC/MF A08 CSCL 01A

Turbulence modeling is generally recognized as the major problem obstructing further advances in computational fluid dynamics (CFD). A closed solution of the governing Navier-Stokes equations for turbulent flows of practical consequence is still far beyond grasp. At the same time, the simplified models of turbulence which are used to achieve closure of the Navier-Stokes equations are known to be rigorously incorrect. While these models serve a definite purpose, they are inadequate for the general prediction of hypersonic viscous/inviscid interactions, mixing problems, chemical nonequilibria, and a range of other phenomena which must be predicted in order to design a hypersonic vehicle computationally. Due to the complexity of turbulence, useful new turbulence models are synthesized only when great expertise is brought to bear and considerable intellectual energy is expended. Although this process is fundamentally theoretical, crucial guidance may be gained from

carefully-executed basic experiments. Following the birth of a new model, its testing and validation once again demand comparisons with data of unimpeachable quality. This report concerns these issues which arise from the experimental aspects of hypersonic modeling and represents the results of the first phase of an effort to develop compressible turbulence models. Author

N91-15987*# MCAT Inst., San Jose, CA.
ROTORCRAFT APPLICATION OF ADVANCED COMPUTATIONAL AERODYNAMICS Final Report
Sharon Stanaway Jan. 1991 8 p
(Contract NCC2-579)
(NASA-CR-187767; NAS 1.26:187767; MCAT-91-001) Avail: NTIS HC/MF A02 CSCL 01A

The objective was to develop the capability to compute the unsteady viscous flow around rotor-body combinations. In the interest of tractability, the problem was divided into subprograms for: (1) computing the flow around a rotor blade in isolation; (2) computing the flow around a fuselage in isolation, and (3) integrating the pieces. Considerable progress has already been made by others toward computing the rotor in isolation (Srinivasen) and this work focused on the remaining tasks. These tasks required formulating a multi-block strategy for combining rotating blades and nonrotating components (i.e., a fuselage). Then an appropriate configuration was chosen for which suitable rotor body interference test data exists. Next, surface and volume grids were generated and state-of-the-art CFD codes were modified and applied to the problem. Author

N91-15988# Stuttgart Univ. (Germany, F.R.).
FINITE ELEMENT APPROXIMATIONS FOR TRANSONIC FLOWS Ph.D. Thesis [FINITE-ELEMENT-APPROXIMATIONEN FUER TRANSONISCHE STROEMUNGEN]
Harald Berger 1989 96 p In GERMAN
(ETN-91-98491) Avail: NTIS HC/MF A05

The conservative nonlinear potential equation is examined using finite element methods. This equation describes a stationary, even, friction free, adiabatic, isoenergetical and homentropic flow for an ideal gas. In the case of a subsonic flow, the nonlinear potential equation is of elliptical type. The nonlinear potential equation is derived from the continuum mechanics general equations. It is shown that the solution of an hyperbolic conservation equation should fulfill a mathematical entropoy condition. It is established that some finite element functions satisfy the discrete entropy condition. It is underlined that the convergence behavior of finite element solutions of the nonlinear potential equation in subdomains of the flow field stays strictly subsonic, e.g., the potential equation stays uniformly elliptical. The global convergence properties of finite element solutions are examined. An error analysis can be derived for these finite element solutions. ESA

N91-15989# EMA, Mansfield, TX.
EVALUATION OF ROTORWASH CHARACTERISTICS FOR TILTROTOR AND TILTWING AIRCRAFT IN HOVERING FLIGHT Final Report
Samuel W. Ferguson Dec. 1990 263 p Prepared for Systems Control Technology, Inc., Arlington, VA
(Contract DTFA01-87-C-00014)
(SCT-90RR-18; DOT/FAA/RD-90/16) Avail: NTIS HC/MF A12

The rotorwash characteristics of eleven different types of tiltrotor and tiltwing aircraft in hovering flight are presented for comparison purposes. Rotorwash characteristics that were quantified include the mean and peak outwash velocity profiles off the left wing position (azimuth = 270 degrees) and nose position (azimuth = 0 degrees). Maximum values from each of the peak velocity and peak dynamic pressure profiles are also presented as a function of distance from the rotorcraft along both the 0 and 270 degree azimuths. Calculated personnel overturning forces are presented along both azimuths for a six foot tall person. All documented results were calculated with the ROTWASH analysis program. Flight test data, as correlated with the analysis program, are presented for the XV-15 tiltrotor and the CL-84 tiltwing. These hover characteristics do not represent the worst cast scenario characteristics which would be expected at a vertiport. Scenarios involving ambient winds and maneuvering flight near hover generate higher rotorwash velocities. Unfortunately, the identification and prediction of worst case scenario results for comparison purposes is not presently possible. Author

N91-15990# Ballistic Research Labs., Aberdeen Proving Ground, MD.
USE OF THE MAGNUS FORCE IN THE MODIFIED POINT MASS TRAJECTORY MODEL Final Report
Robert F. Lieske Oct. 1990 28 p
(DA Proj. 1L1-62618-AH-80)
(AD-A228194; BRL-MR-3870) Avail: NTIS HC/MF A03 CSCL 20/4

A method is presented for determining the Magnus force coefficient for use with the Modified Point Mass Trajectory model, to improve the simulated time of flight, based on the firing table experimental range firing impact and time-of-flight data. A comparison is made with the Magnus force coefficients determined from aerodynamic testing for the 155mm, HE, M107 and 8-Inch, HE, RA, M650 projectiles. The Magnus force coefficients contained in the firing table data base for artillery projectiles are presented. GRA

N91-15991*# Institute for Computer Applications in Science and Engineering, Hampton, VA.
ON A CLASS OF UNSTEADY THREE-DIMENSIONAL NAVIER STOKES SOLUTIONS RELEVANT TO ROTATING DISC FLOWS: THRESHOLD AMPLITUDES AND FINITE TIME SINGULARITIES Final Report
Philip Hall and P. Balakumar (High Technology Corp., Hampton, VA.) Dec. 1990 46 p Submitted for publication
(Contract NAS1-18605)
(NASA-CR-187482; NAS 1.26:187482; ICASE-90-86) Avail: NTIS HC/MF A03 CSCL 01A

A class of exact steady and unsteady solutions of the Navier Stokes equations in cylindrical polar coordinates is given. The flows correspond to the motion induced by an infinite disc rotating with constant angular velocity about the z-axis in a fluid occupying a semi-infinite region which, at large distances from the disc, has velocity field proportional to (x,-y,O) with respect to a Cartesian coordinate system. It is shown that when the rate of rotation is large, Karman's exact solution for a disc rotating in an otherwise motionless fluid is recovered. In the limit of zero rotation rate a particular form of Howarth's exact solution for three-dimensional stagnation point flow is obtained. The unsteady form of the partial differential system describing this class of flow may be generalized to time-periodic equilibrium flows. In addition the unsteady equations are shown to describe a strongly nonlinear instability of Karman's rotating disc flow. It is shown that sufficiently large perturbations lead to a finite time breakdown of that flow whilst smaller disturbances decay to zero. If the stagnation point flow at infinity is sufficiently strong, the steady basic states become linearly unstable. In fact there is then a continuous spectrum of unstable eigenvalues of the stability equations but, if the initial value problem is considered, it is found that, at large values of time, the continuous spectrum leads to a velocity field growing exponentially in time with an amplitude decaying algebraically in time. Author

N91-15992 Iowa State Univ. of Science and Technology, Ames.
COMPUTATION OF TURBULENT FLOW ABOUT UNCONVENTIONAL AIRFOIL SHAPES Ph.D. Thesis
Salahuddin Ahmed 1990 84 p
Avail: Univ. Microfilms Order No. DA9100414

A new nonequilibrium turbulence closure model was developed for computing wall bounded two-dimensional turbulent flows. This two-layer eddy viscosity model was motivated by the success of the Johnson-King model in separated flow regions. The influence of history effects are described by an ordinary differential equation developed from the turbulent kinetic energy equation. The performance of the present model was evaluated by solving the flow around three airfoils using the Reynolds time-averaged Navier-Stokes equations. Excellent results were obtained for both

attached and separated flows about the NACA 0012 airfoil, the RAE 2822 airfoil, and the Integrated Technology A 153W airfoil. Based on the comparison of the numerical solutions with the available experimental data, it is concluded that the new nonequilibrium turbulence model accurately captures the history effects of convection and diffusion on turbulence. Dissert. Abstr.

N91-15993 Purdue Univ., West Lafayette, IN.
PROPFAN SUPERSONIC PANEL METHOD ANALYSIS AND FLUTTER PREDICTIONS Ph.D. Thesis
Ching-Chywan Hwang 1990 141 p
Avail: Univ. Microfilms Order No. DA9031342

A supersonic panel method analysis for propfan performance and flutter predictions was developed by extending Williams' three dimensional unsteady lifting surface theory to the supersonic speed range. The method upgrades the capability of the original (subsonic) panel code, UPROP3S, to include the propfan operating conditions at subsonic axial speeds with subsonic/supersonic tip speeds and supersonic axial speeds. The original panel code, UPROP3S, is coded for the predictions of steady performance characteristics, forced vibration, static aeroelastic deformation, and flutter. This panel code is effective and inexpensive compared to full potential, Euler, or Navier-Stokes codes. In this method the unsteady aerodynamic model is based on the three dimensional linearized compressible aerodynamic theory. A piece-wise constant load paneling technique is applied to find the blade pressure difference distributions from the lifting surface integral equation. The aeroelastic model is formulated in terms of the in-vacuum normal modes of the blades. The flutter event is determined by solving the eigenvalue problem associated with the equations of motion. The surveyed propfan wind tunnel models include the SR2, SR3, SR5, and SR7 blades. The computed results correlate very well with the measured data in both performance and flutter predictions. It is thought that this study could also lead to the emergence of a supersonic cruise propeller. Dissert. Abstr.

N91-15994*# Institute for Computer Applications in Science and Engineering, Hampton, VA.
ON THE GOERTLER INSTABILITY IN HYPERSONIC FLOWS: SUTHERLAND LAW FLUIDS AND REAL GAS EFFECTS Final Report
Yibin B. Fu, Philip Hall, and Nicholas D. Blackaby (Manchester Univ., England) Dec. 1990 71 p Submitted for publication
(Contract NAS1-18605; AF-AFOSR-0042-89)
(NASA-CR-187481; ICASE-90-85; NAS 1.26:187481) Avail: NTIS HC/MF A04 CSCL 01A

The Goertler vortex instability mechanism in a hypersonic boundary layer on a curved wall is investigated. The precise roles of the effects of boundary layer growth, wall cooling, and gas dissociation is clarified in the determination of stability properties. It is first assumed that the fluid is an ideal gas with viscosity given by Sutherland's law. It is shown that when the free stream Mach number M is large, the boundary layer divides into two sublayers: a wall layer of O(M sup 3/2) thickness over which the basic state temperature is O(M squared) and a temperature adjustment layer of O(1) thickness over which the basic state temperature decreases monotonically to its free stream value. Goertler vortices which have wavelengths comparable with the boundary layer thickness are referred to as wall modes. It is shown that their downstream evolution is governed by a set of parabolic partial differential equations and that they have the usual features of Goertler vortices in incompressible boundary layers. As the local wavenumber increases, the neutral Goertler number decreases and the center of vortex activity moves towards the temperature adjustment layer. Goertler vortices with wavenumbers of order one or larger must necessarily be trapped in the temperature adjustment layer and it is this mode which is most dangerous. For this mode, it was found that the leading order term in the Goertler number expansion is independent of the wavenumber and is due to the curvature of the basic state. This term is also the asymptotic limit of the neutral Goertler numbers of the wall mode. To determine the higher order corrections terms in the Goertler number expansion, two wall curvature cases are distinguished. Real gas effects were investigated by assuming that the fluid is an ideal dissociating gas. It was found that both gas dissociation and wall cooling are destabilizing for the mode trapped in the temperature adjustment layer, but for the wall mode trapped near the wall the effect of gas dissociation can be either destabilizing or stabilizing. Author

N91-15995*# Institute for Computer Applications in Science and Engineering, Hampton, VA.
MODELLING THE TRANSITIONAL BOUNDARY LAYER Final Report
R. Narasimha (National Aeronautical Lab., Bangalore, India) Dec. 1990 25 p Submitted for publication
(Contract NAS1-18605)
(NASA-CR-187487; ICASE-90-90; NAS 1.26:187487) Avail: NTIS HC/MF A03 CSCL 01A

Recent developments in the modelling of the transition zone in the boundary layer are reviewed (the zone being defined as extending from the station where intermittency begins to depart from zero to that where it is nearly unity). The value of using a new non-dimensional spot formation rate parameter, and the importance of allowing for so-called subtransitions within the transition zone, are both stressed. Models do reasonably well in constant pressure 2-dimensional flows, but in the presence of strong pressure gradients further improvements are needed. The linear combination approach works surprisingly well in most cases, but would not be so successful in situations where a purely laminar boundary layer would separate but a transitional one would not. Intermittency-weighted eddy viscosity methods do not predict peak surface parameters well without the introduction of an overshooting transition function whose connection with the spot theory of transition is obscure. Suggestions are made for further work that now appears necessary for developing improved models of the transition zone. Author

N91-15996*# Institute for Computer Applications in Science and Engineering, Hampton, VA.
ON THE RECEPTIVITY AND NON-PARALLEL STABILITY OF TRAVELLING DISTURBANCES IN ROTATING DISK FLOW Final Report
P. Balakumar, P. Hall, and M. R. Malik (High Technology Corp., Hampton, VA.) Dec. 1990 32 p Submitted for publication
(Contract NAS1-18605)
(NASA-CR-187486; ICASE-90-89; NAS 1.26:187486) Avail: NTIS HC/MF A03 CSCL 01A

The generation and evolution of small amplitude wavelength traveling disturbances in rotating disk flow is discussed. The steady rotational speed of the disk is perturbed so as to introduce high frequency oscillations in the flow field. Secondly, surface imperfections are introduced on the disk such as roughness elements. The interaction of these two disturbances will generate the instability waves whose evolution is governed by parabolic partial differential equations that are solved numerically. For the class of disturbances considered (wavelength on the order of Reynolds number), it is found that eigensolutions exist which decay or grow algebraically in the radial direction. However, these solutions grow only for frequencies larger than 4.58 times the steady rotational speed of the disk. The computed receptivity coefficient shows that there is an optimum size of roughness for which these modes are excited the most. The width of these roughness elements in the radial direction is about .1 r(sub 0) where r(sub 0) is the radial location of the roughness. It is also found that the receptivity coefficient is larger for a negative spanwise wavenumber than for a positive one. Typical wave angles found for these disturbances are about -26 degrees. Author

N91-15997# Messerschmitt-Boelkow-Blohm G.m.b.H., Munich (Germany, F.R.). Hubschrauber und Flugzeuge.
NUMERICAL ANALYSIS OF VISCOUS HYPERSONIC FLOW PAST A GENERIC FOREBODY
K. M. Wanie and M. A. Schmatz 6 Jul. 1990 13 p Presented at the 17th Congress of the International Council of the Aeronautical

Sciences, Stockholm, Sweden, 9-14 Sep. 1990
(MBB/FE122/S/PUB/0407; ICAS-90-6.7.2; ETN-91-98544)
Copyright Avail: NTIS HC/MF A03

The viscous hypersonic flow past an analytically defined generic-transport aircraft forebody is numerically simulated using a Navier-Stokes code. The governing equations were written in general three dimensional curvilinear form. The sensitivity of the solutions to variations of physical parameters was investigated. Turbulence is shown to have a significant influence on boundary layer velocity profiles and boundary layer thickness but at Mach number, real gas effects and radiation play a minor role for these features while they considerably reduce the thermal loads. ESA

N91-15998# Deutsche Forschungsanstalt fuer Luft- und Raumfahrt, Goettingen (Germany, F.R.). Abt. Aerodynamik.
CALCULATION OF SUPPORT INTERFERENCES ON THE AERODYNAMIC COEFFICIENTS FOR A WIND TUNNEL CALIBRATION MODEL
Dieter Steinbach May 1990 63 p In GERMAN; ENGLISH summary Report will also be announced as translation (ESA-TT-1247) Original contains color illustrations
(DLR-FB-90-26; ISSN-0171-1342; ETN-91-98593) Avail: NTIS HC/MF A04; DLR, VB-PL-DO, Postfach 90 60 58, 5000 Cologne, Fed. Republic of Germany, HC 25 Deutsche marks

Model support interferences are calculated in form of corrections for the aerodynamic coefficients. Two different model support systems are investigated: the horizontal sting mounted model, and the vertical sting mounted model. The sting influences on the static longitudinal stability of the model are investigated. A three dimensional panel method is used, which allows simultaneous calculation of several displacing and lifting bodies of nearly arbitrary shapes in the flow. The aerodynamic coefficients are obtained by numerical integration of the surface pressure distribution of the model. ESA

N91-16268# Kyushu Univ., Fukuoka (Japan). Dept. of Aeronautical Engineering.
NUMERICAL SIMULATION OF SEPARATED FLOWS AROUND A WING SECTION AT STEADY AND UNSTEADY MOTION BY A DISCRETE VORTEX METHOD
Shigeru Aso, Atsushi Fujimoto, Naoki Futatsudera, and Masanori Hayashi (Nishinippon Inst. of Tech., Fukuoka, Japan) *In* Tokyo Univ., The Proceedings of the Symposium on Mechanics for Space Flight 1989 Mar. 1990 p 15-24 Original language document was announced in IAA as A90-33753 (For primary document see N91-16266 08-34)
Avail: NTIS HC/MF A09

N91-16272# Kyushu Univ., Fukuoka (Japan). Dept. of Aeronautical Engineering.
UNSTEADY VORTEX LATTICE CALCULATION OF THE FLOW AROUND A SLENDER DELTA WING
Akira Sakurai and Hiroshi Uchihori *In* Tokyo Univ., The Proceedings of the Symposium on Mechanics for Space Flight 1989 Mar. 1990 p 53-59 (For primary document see N91-16266 08-34)
Avail: NTIS HC/MF A09

03 AIR TRANSPORTATION AND SAFETY

Includes passenger and cargo air transport operations; and aircraft accidents.

For related information see also *16 Space Transportation* and *85 Urban Technology and Transportation.*

N91-15999# Civil Aeromedical Inst., Oklahoma City, OK.
DEVELOPMENT OF A CRASHWORTHY SEAT FOR COMMUTER AIRCRAFT Final Report
Van Gowdy Sep. 1990 13 p Sponsored by FAA, Washington, DC
(AD-A227486; DOT/FAA/AM-90/11) Avail: NTIS HC/MF A03 CSCL 01/3

A series of dynamic impact tests were conducted using a prototype seat with an energy absorbing mechanism as part of the seat pan. The seat frame was designed to represent a typical commuter aircraft passenger seat. Tests were conducted in an orientation simulating a vertical impact with a 30 deg nose-down aircraft attitude. The impact severity for these tests ranged from 15 to 33 Gs. Seat pan stroke and occupant lumbar reaction forces were measured. Results indicate the axial force measured in the lumbar spine of a fiftieth percentile Hybrid II dummy can be limited to a peak value less than 1500 pounds during vertical impact tests of 33 G with a seat pan stroke distance of 6.3 inches. GRA

N91-16000# Planungsbuero Luftraumnutzer, Frankfurt (Germany, F.R.).
THE EUROPEAN FLIGHT SAFETY CRISIS: COSTS AND SOLUTION [DIE KRISE DER EUROPAEISCHEN FLUGSICHERUNG: DIE KOSTEN UND IHRE LOESUNG]
Sep. 1989 69 p In GERMAN
(ETN-91-98490) Avail: NTIS HC/MF A04

The European airspace structure is based on political and not commercial considerations. The costs of the European flight safety crisis, in particular the costs of the delays, were rated at ten billion German marks. A drastic cost increase is still expected up to year 2000, as the air traffic is expected to double. It is necessary to harmonize the 22 different national safety systems. The long term solution is a unique, fully integrated flight safety system. A two phase planning is proposed, including the creation of a European flight safety organization. ESA

N91-16001*# National Aeronautics and Space Administration. Ames Research Center, Moffett Field, CA.
POTENTIAL USE OF TILTROTOR AIRCRAFT IN CANADIAN AVIATION
Denyse Gazdag (Versatec, Inc., Santa Clara, CA.) and Larry Alton Dec. 1990 37 p
(NASA-TM-102245; A-89269; NAS 1.15:102245) Avail: NTIS HC/MF A03 CSCL 01C

The aviation system in Canada is described as it relates to the potential applicability of tiltrotor technology. Commuter service in two corridors, the Vancouver-Victoria route on the west coast and the heavily traveled Montreal-Toronto corridor in eastern Canada, are examined. The operation of air service from the near-downtown Toronto STOLport and from the Vancouver-Victoria downtown heliport facilities is described. The emergency medical services, search and rescue, and natural resources development sectors are described with regard to the needs that tiltrotor technology could uniquely meet in these areas. The airport construction program in isolated communities of northern Quebec and possible tiltrotor service in northern regions are reviewed. The Federal and provincial governments' financial support policy regarding the aeronautical industry is to encourage the establishment and expansion of businesses in the field of aeronautics and to make possible the acquisition of new technology. This policy has implications for the tiltrotor program. Author

N91-16002 Bundesanstalt fuer Flugsicherung, Frankfurt am Main (Germany, F.R.).
[ACTIVITIES REPORT OF THE GERMAN FEDERAL INSTITUTE FOR FLIGHT SAFETY] Annual Report, 1989 [BUNDESANSTALT FUER FLUGSICHERUNG, JAHRESBERICHT 1989]
Jul. 1990 51 p In GERMAN
(ETN-91-98644) Copyright Avail: Fachinformationszentrum Karlsruhe, 7514 Eggenstein-Leopoldshafen 2, Fed. Republic of Germany

The air traffic flow, as well as the air traffic flow control and measures envisaged to increase the air traffic safety are presented. The problems raised by airplane noises, flight incidents and accidents are mentioned. The progress achieved in fields, such

as Doppler omnidirectional radio range, instrument and microwave landing systems, radar renewable and modernization airspace utilization, training simulation, weather data information system, and electronic data processing, are outlined. Subjects covered in testing were: computer oriented metering planning and advisory system, experimental working position simulation, radar data quality control and radar analysis support systems. The cooperation with international airflight organizations and the participation in international conferences are mentioned. ESA

04 AIRCRAFT COMMUNICATIONS AND NAVIGATION

Includes digital and voice communication with aircraft; air navigation systems (satellite and ground based); and air traffic control.

For related information see also *17 Space Communications, Spacecraft Communications, Command and Tracking* and *Communications and Radar.*

N91-16003# Air Force Inst. of Tech., Wright-Patterson AFB, OH. School of Engineering.

OPTIMAL KALMAN FILTER INTEGRATION OF A GLOBAL POSITIONING SYSTEM RECEIVER AND AN LN-94 INERTIAL NAVIGATION SYSTEM M.S. Thesis

James Lawrence Hirning Sep. 1990 121 p

(AD-A227222; AFIT/GE/ENG/90S-02) Avail: NTIS HC/MF A06 CSCL 17/7

This research develops and attempts to implement a Kalman filter integration of a Phase 3 Global Positioning System (GPS) five channel receiver and an LN-94 Inertial Navigation System (INS). The GPS provides highly accurate position and velocity information in low dynamic environments. An INS provides position and velocity information with lower accuracy over long periods of time, but it is highly responsive in dynamic maneuvers or at high frequencies. The INS has the added advantage of requiring no signals external to the vehicle to function. The integration of these two systems provide more precise information under a wider variety of situations. A truth model for the INS is verified. A GPS error model is developed and combined with the INS model to provide GPS-aided INS navigation. This model is used to predict baseline performance of all full ordered filter. Attempts are made to utilize the filter with empirical data. The data is analyzed, and suggestions are made about ways to account for the errors in evidence. Results to date are presented and analyzed. GRA

N91-16004# Mitre Corp., Bedford, MA.

A SUCCESSIVE PARTIAL-RELAXATION GAUSSIAN ALGORITHM FOR AREA NAVIGATION OPERATIONS WITH THE MICROWAVE LANDING SYSTEM (MLS) Final Report

Patricia M. Hatzis and Frederic D. Powell Oct. 1990 45 p

(Contract F19628-89-C-0001; AF Proj. 5420)

(AD-A228871; MTR-10910; ESD-TR-90-326) Avail: NTIS HC/MF A03 CSCL 17/7

Position reconstruction algorithms (PRAs) based on Gaussian techniques converge very slowly, or diverge, for some geometries of ground unit and aircraft location which are within MLS system coverage. On the other hand, algorithms based on Newton-Raphson techniques usually converge very rapidly but impose a significantly greater storage requirement and computational burden on the avionics. This report presents a modified Gaussian algorithm which uses a relaxation factor to achieve rapid convergence for all geometries, and with a computational burden much less than the equivalent Newton-Raphson algorithm. It presents the theoretical foundations of this algorithm and various results showing its effects. It also compares the algorithm's storage and computational burdens against Gaussian, rotated-coordinate Gaussian, and Newton-Raphson equivalent PRAs in the MLS context. GRA

N91-16005# Rijksluchtvaartdienst, Schiphol (Netherlands). Meetkundige Dienst.

[ACTIVITIES REPORT OF THE DUTCH CIVIL AERONAUTICS BOARD] Annual Report, 1989 [RIJKSLUCHTVAARTDIENST: JAARVERSLAG 1991]

Anne Marie Steendijk 1990 69 p In DUTCH and ENGLISH (ETN-91-98472) Avail: NTIS HC/MF A04

The activities in the fields of air traffic control air transportation and infrastructure, civil areronautics school, civil aeronautics museum aviodome, national aeronautics and astronautics laboratory, responsibility in the air, aerospace safety above the North Sea, and air traffic and environment are presented. ESA

05 AIRCRAFT DESIGN, TESTING AND PERFORMANCE

Includes aircraft simulation technology.

For related information see also *18 Spacecraft Design, Testing and Performance* and *39 Structural Mechanics.* For land transportation vehicles see *85 Urban Technology and Transportation.*

N91-16006 Maryland Univ., College Park.

A COUPLED ROTOR AEROELASTIC ANALYSIS UTILIZING ADVANCED AERODYNAMIC MODELING Ph.D. Thesis

Michael Scott Torok 1989 339 p

Avail: Univ. Microfilms Order No. DA9021593

The effects of improved aerodynamic modeling on rotor blade section and root loads, blade response, and blade stability are investigated. A nonlinear unsteady aerodynamic model for attached and separated flow and dynamic stall, as well as prescribed and free wake models, are incorporated into a coupled rotor aeroelastic analysis. Blade responses and loadings are calculated using a finite element formulation in space and time. A modified Newton iterative method is used to calculate blade response and trim controls as one coupled solution. Aeroelastic stability is determined utilizing Floquet theory for a linearized system, and a transient perturbation technique which can model nonlinear unsteady aerodynamic effects. Damping estimations are made using a Moving-Block analysis. Results of a parametric study of a soft in-plane hingeless rotor show that at high speed flight conditions, nonlinear effects dominate blade section forces, and significantly affect peak-to-peak values and the harmonic content of blade root loads. A correlation with SA349/2 Aerospatiale Gazelle flight test data is used to evaluate the analysis. Trim controls, blade section aerodynamic loads, and blade flap bending moments are satisfactorily predicted. The rotor stability analysis is correlated with model hingeless rotor data. A parametric study of a hingeless rotor in forward flight is examined. Dissert. Abstr.

N91-16007# Army Lab. Command, Watertown, MA. Material Technology Lab.

FAILURE ANALYSIS OF A MAIN ROTOR PITCH HORN BOLT LOCATED ON THE AH-1 COBRA HELICOPTER Final Report

Victor K. Champagne, Jr. Sep. 1990 36 p

(AD-A227679; MTL-TR-90-44) Avail: NTIS HC/MF A03 CSCL 01/3

A comprehensive metallurgical examination of the pitch horn bolt was conducted to determine the probable cause of failure. The component is part of the main rotor hub assembly and had failed while in service. Light optical microscopy revealed evidence of corrosion pitting in regions adjacent to the fracture. Chemical analysis verified that the part was fabricated from 4340 steel. It was determined by metallographic examination that the microstructure was tempered martensite. Hardness measurements taken on transverse cross sections of the bolt near the fracture indicated that the material had been hardened to the upper limit of the specified range. The surface finish was measured along the upper shank and conformed to the requirements of the engineering drawing. Fractographic examination utilizing the scanning electron microscope (SEM) revealed multiple crack origins which assumed a decohesion. Many of these crack sites were

initiated from corrosion pits. Energy dispersing spectroscopy (EDS) performed on areas within the crack initiation site showed the presence of chlorides. Beyond the thumbnail zone fast fracture occurred in a ductile manner, which was confirmed by a dimpled topography. The failure was attributed to stress corrosion cracking (SCC). GRA

N91-16008*# North Carolina State Univ., Raleigh. Dept. of Mechanical and Aerospace Engineering
DESIGN AND FABRICATION OF THE NASA HL-20 FULL SCALE RESEARCH MODEL Final Report
K. Dean Driver and Robert J. Vess 25 Jan. 1991 101 p Sponsored in part by NASA, Langley Research Center
(Grant NAGw-1331)
(NASA-CR-187801; NAS 1.26:187801) Avail: NTIS HC/MF A06 CSCL 01C

A full-scale engineering model of the HL-20 Personnel Launch System (PLS) was constructed for systems and human factors evaluation. Construction techniques were developed to enable the vehicle to be constructed with a minimum of time and cost. The design and construction of the vehicle are described. Author

N91-16009# Army Command and General Staff Coll., Fort Leavenworth, Kansas.
ARMY UNMANNED AERIAL VEHICLE (UAV) REQUIREMENTS AND THE JOINT UAV PROGRAM M.S. Thesis
William R. Harshman 1990 137 p
(AD-A228149) Avail: NTIS HC/MF A07 CSCL 01/3

The Department of Defense joint unmanned aerial vehicle program was studied to determine if it will satisfy the UAV needs of the Army to conduct tactical intelligence collection. First, UAV requirements, as defined by both the Army and DoD are identified. Next, the Army requirements are tested for validity within the framework of the Army's capstone war fighting doctrine, AirLand Battle, and supporting doctrine for the conduct of intelligence operations. Third, the operational characteristics specified by the Army are compared with the same criterias as defined by the Army for the equivalent joint UAV system. The final step is identification of differences in the two programs and determining the impact on future Army UAV operations. The study concludes that the Army has clearly defined its requirements for UAV operations. These requirements are valid and fully support the Army's war fighting doctrine. While the research finds significant differences exist between the Army and joint programs, these differences do not impact on the essential needs of the Army. The joint UAV program supports the UAV needs of the Army. After a slow start, the joint UAV program is proceeding rapidly. Barring funding constraints, the Army, and the other services, will soon possess an operational short range (out to 150 km) UAV system capable of performing tactical intelligence collection. GRA

N91-16010*# Rice Univ., Houston, TX. Dept. of Mechanical Engineering and Materials Science.
OPTIMIZATION AND GUIDANCE OF FLIGHT TRAJECTORIES FOR THE NATIONAL AEROSPACE PLANE Final Report, 22 Jun. 1989 - 31 Dec. 1990
Angelo Miele 1990 22 p
(Grant NAG1-1029)
(NASA-CR-187837; NAS 1.26:187837; AAR-252) Avail: NTIS HC/MF A03 CSCL 01C

The research on optimal trajectories for the National Aerospace Plane (NASP) performed by the Aero-Astronautics Group of Rice University from June 22, 1989 to December 31, 1990 is summarized. The aerospace plane is assumed to be controlled via the angle of attack and the power setting. The time history of the controls is optimized simultaneously with the switch times from one powerplant to another and the final time. The intent is to arrive at NASP guidance trajectories exhibiting many of the desirable characteristics of NASP optimal trajectories. Author

N91-16011*# Rice Univ., Houston, TX. Dept. of Mechanical Engineering and Materials Science.
OPTIMAL TRAJECTORIES FOR AN AEROSPACE PLANE. PART 2: DATA, TABLES, AND GRAPHS
Angelo Miele, W. Y. Lee, and G. D. Wu 1990 94 p Presented at the 1990 American Control Conference, San Diego, CA, 23-25 May 1990
(Grant NAG1-1029)
(NASA-CR-187848; NAS 1.26:187848; AAR-248-PT-2) Avail: NTIS HC/MF A05 CSCL 01C

Data, tables, and graphs relative to the optimal trajectories for an aerospace plane are presented. A single-stage-to-orbit (SSTO) configuration is considered, and the transition from low supersonic speeds to orbital speeds is studied for a single aerodynamic model (GHAME) and three engine models. Four optimization problems are solved using the sequential gradient-restoration algorithm for optimal control problems: (1) minimization of the weight of fuel consumed; (2) minimization of the peak dynamic pressure; (3) minimization of the peak heating rate; and (4) minimization of the peak tangential acceleration. The above optimization studies are carried out for different combinations of constraints, specifically: initial path inclination that is either free or given; dynamic pressure that is either free or bounded; and tangential acceleration that is either free or bounded. Author

N91-16012*# Purdue Univ., West Lafayette, IN. School of Mechanical Engineering.
APPLICATIONS OF FUZZY THEORIES TO MULTI-OBJECTIVE SYSTEM OPTIMIZATION
S. S. Rao and A. K. Dhingra Jan. 1991 74 p
(Contract NCA2-223)
(NASA-CR-177573; A-91029; NAS 1.26:177573) Avail: NTIS HC/MF A04 CSCL 01C

Most of the computer aided design techniques developed so far deal with the optimization of a single objective function over the feasible design space. However, there often exist several engineering design problems which require a simultaneous consideration of several objective functions. This work presents several techniques of multiobjective optimization. In addition, a new formulation, based on fuzzy theories, is also introduced for the solution of multiobjective system optimization problems. The fuzzy formulation is useful in dealing with systems which are described imprecisely using fuzzy terms such as, 'sufficiently large', 'very strong', or 'satisfactory'. The proposed theory translates the imprecise linguistic statements and multiple objectives into equivalent crisp mathematical statements using fuzzy logic. The effectiveness of all the methodologies and theories presented is illustrated by formulating and solving two different engineering design problems. The first one involves the flight trajectory optimization and the main rotor design of helicopters. The second one is concerned with the integrated kinematic-dynamic synthesis of planar mechanisms. The use and effectiveness of nonlinear membership functions in fuzzy formulation is also demonstrated. The numerical results indicate that the fuzzy formulation could yield results which are qualitatively different from those provided by the crisp formulation. It is felt that the fuzzy formulation will handle real life design problems on a more rational basis. Author

N91-16013*# Rice Univ., Houston, TX. Aero-Astronautics Group.
OPTIMAL TRAJECTORIES FOR AN AEROSPACE PLANE. PART 1: FORMULATION, RESULTS, AND ANALYSIS
Angelo Miele, W. Y. Lee, and G. D. Wu 1990 61 p Presented at the American Control Conference, San Diego, CA, 23-25 May 1990
(Grants NAG1-1029; TATP-003604020)
(NASA-CR-187868; NAS 1.26:187868; AAR-247) Avail: NTIS HC/MF A04 CSCL 01C

The optimization of the trajectories of an aerospace plane is discussed. This is a hypervelocity vehicle capable of achieving orbital speed, while taking off horizontally. The vehicle is propelled by four types of engines: turbojet engines for flight at subsonic

speeds/low supersonic speeds; ramjet engines for flight at moderate supersonic speeds/low hypersonic speeds; scramjet engines for flight at hypersonic speeds; and rocket engines for flight at near-orbital speeds. A single-stage-to-orbit (SSTO) configuration is considered, and the transition from low supersonic speeds to orbital speeds is studied under the following assumptions: the turbojet portion of the trajectory has been completed; the aerospace plane is controlled via the angle of attack and the power setting; the aerodynamic model is the generic hypersonic aerodynamics model example (GHAME). Concerning the engine model, three options are considered: (EM1), a ramjet/scramjet combination in which the scramjet specific impulse tends to a nearly-constant value at large Mach numbers; (EM2), a ramjet/scramjet combination in which the scramjet specific impulse decreases monotonically at large Mach numbers; and (EM3), a ramjet/scramjet/rocket combination in which, owing to stagnation temperature limitations, the scramjet operates only at M approx. less than 15; at higher Mach numbers, the scramjet is shut off and the aerospace plane is driven only by the rocket engines. Under the above assumptions, four optimization problems are solved using the sequential gradient-restoration algorithm for optimal control problems: (P1) minimization of the weight of fuel consumed; (P2) minimization of the peak dynamic pressure; (P3) minimization of the peak heating rate; and (P4) minimization of the peak tangential acceleration. Author

N91-16014# Technische Univ., Brunswick (Germany, F.R.). Fakultaet fuer Maschinenbau und Elektrotechnik.
TESTS FOR INTEGRATING MEASUREMENTS OF GAS PRESSURES IN AIRCRAFT MECHANISMS Ph.D. Thesis [VERSUCHE ZUR INTEGRIERENDEN MESSUNG VON GASDRUECKEN IN FLUGTRIEBWERKEN]
Gerardo Walle 1989 217 p In GERMAN
(ETN-91-98558) Avail: NTIS HC/MF A10

The possibility that the integral signal driven by a fiber is a measure for the mean value of the examined data, is studied. Examinations were carried out at a firmly inserted fiber, which was bent between two support teeth by a weight tooth (fiber deformation unity). The radial curvature distributions along the fiber was approximately simulated by the bend beam model. The relation between damping and bending was described by a nonlinear exponential function. For the practical realization of a sensor with optical fibers several prototypes were made and the conditions for a successful conception were defined. ESA

N91-16015# Messerschmitt-Boelkow-Blohm G.m.b.H., Munich (Germany, F.R.). Military Aircraft Div.
AEROTHERMODYNAMIC PHENOMENA AND THE DESIGN OF ATMOSPHERIC HYPERSONIC AIRPLANES
E. H. Hirschel 18 Jul. 1990 42 p Presented at the 3rd Joint Europe/US Short Course in Hypersonics, Aachen, Fed. Republic of Germany, 1-5 Oct. 1990
(MBB/FE122/S/PUB/0408; ETN-91-98545) Avail: NTIS HC/MF A03

The design problems of aerodynamic hypersonic airplanes and the aerodynamic tools such as wind tunnels and computation methods are reviewed simultaneously with their validation problems. Aerodynamic phenomena such as viscosity, heat loads, heat transfer and real gas effects are studied with consideration of the design and simulation problems. It is remarked that research and development must be increased in the area of turbulence and laminar turbulent transition. ESA

N91-16016# Messerschmitt-Boelkow-Blohm G.m.b.H., Munich (Germany, F.R.). Hubschrauber und Flugzeuge.
HYPERSONIC MODEL CONFIGURATIONS
K. M. Wanie, ed. and E. H. Hirschel 7 Aug. 1990 78 p In GERMAN; ENGLISH summary
(MBB/FE122/S/PUB/411; ETN-91-98546) Avail: NTIS HC/MF A05

Model configurations for the development of hypersonic aerothermodynamics are presented in order to create a common data base for hypersonic cruise flights. Each configuration is dedicated to a specific problem arising from the flight conditions. ESA

N91-16017# Messerschmitt-Boelkow-Blohm G.m.b.H., Munich (Germany, F.R.). Aircraft Div.
THE INTEGRATION OF STRUCTURAL OPTIMIZATION IN THE GENERAL DESIGN PROCESS FOR AIRCRAFT
O. Sensburg, J. Schweiger, H. Goedel, and A. Lotze 21 Jun. 1990 12 p Presented at the 17th Congress of the International Council of the Aeronautical Sciences, Stockholm, Sweden, 9-14 Sep. 1990
(MBB/FE122/S/PUB/0405; ETN-91-98547) Copyright Avail: NTIS HC/MF A03

A method for solving large linear equation systems by an iterative method is described and successfully applied with the MBB-LAGRANGE code which uses mathematical programming and gradients to fulfill different constraints simultaneously. As examples, heat flux and frequency optimization of a satellite structure, and design of a carbon fiber wing are presented and studied with the finite element method. In the first case, vector optimization method is added to obtain a compromise solution between dynamic and thermal constraints. ESA

N91-16018# Cranfield Inst. of Tech., Bedford (England). Dept. of Aerospace Vehicle Design.
TF89 AIRCRAFT CENTRE FUSELAGE M.S. Thesis
D. C. Ellis Apr. 1990 248 p
(ETN-91-98579) Copyright Avail: NTIS HC/MF A11

The design work undertaken on the TF89 tactical fighter aircraft center fuselage is detailed. The requirement is for a high performance, long range interceptor, comparable to the American Tactical Fighter (ATF) project, to replace the now ageing F15. Maneuver shear force and bending moment loading analyses of the fuselage are presented with explanations of longeron design using the computer program STRUCT and skin design. A fatigue analysis of a longeron is undertaken. The design solution uses aluminum lithium alloy throughout. ESA

N91-16019# Cranfield Inst. of Tech., Bedford (England). Dept. of Aircraft Design.
TF89 TACTICAL FIGHTER OUTER WING DESIGN M.S. Thesis
A. M. Leahy May 1990 230 p
(ETN-91-98580) Copyright Avail: NTIS HC/MF A11

The swept wing is largely designed using thermoplastic PEEK (PolyEtherEtherKetone) composite material which offers excellent specific strength, good fracture toughness and can be tailored to match the wing loading. A highly redundant multiple spar structure is used to meet the chosen failsafe design philosophy. The wing skins carry both shear and some bending and hence are reinforced by closely spaced spanwise stiffeners which prevent buckling. The wing was modeled on the finite element system to obtain the distribution of the loads though the structure. All detailed discussion and calculations are shown, as well as stress calculations and drawings. ESA

06 AIRCRAFT INSTRUMENTATION

Includes cockpit and cabin display devices; and flight instruments.

For related information see also *19 Spacecraft Instrumentation* and *35 Instrumentation and Photography.*

No abstracts in this category.

07 AIRCRAFT PROPULSION AND POWER

Includes prime propulsion systems and systems components, e.g., gas turbine engines and compressors; and onboard auxilliary power plants for aircraft.

For related information see also *20 Spacecraft Propulsion and Power, 28 Propellants and Fuels,* and *44 Energy Production and Conversion.*

N91-16020# Aeronautical Research Labs., Melbourne (Australia).

IFDIS: AN EXPERT SYSTEM FOR DIAGNOSIS OF FAILURES IN JET AIRCRAFT ENGINES

M. D. Larkin (Deakin Univ., Australia), D. A. Frith, and A. S. Findlay Jan. 1987 45 p

(AD-A227757; ARL-PROP-TM-439; DODA-AR-004-515) Avail: NTIS HC/MF A03

IFDIS (Interactive Fault Diagnosis and Isolation System) is being developed to aid in the F404 jet engines that are installed in the F/A-18 fighters. Existing documentation supporting troubleshooting for these engines is inflexible in the level of sophistication expected of the user and it does not explicitly use the reasoning with uncertain information which is inherent in human troubleshooting. Data, which is required for troubleshooting the F404, is currently or potentially available for computer processing from a number of sources. IFDIS will assist maintenance personnel by providing on-line access to relevant information and will perform much of the tedious interpretation of the available data. The expert knowledge embodied on some of the existing maintenance manuals has been re-expressed in a format that serves as the basis for the knowledge-base for an expert system. Expert systems techniques have been employed because they offer benefits of perspicuity, they can be developed incrementally and can cope with imprecise data. IFDIS is currently based on EMYCIN but will be reimplemented using a commercial expert system shell in the near future. Author

N91-16021*# General Motors Corp., Indianapolis, IN. Gas Turbine Div.

ADVANCED TURBINE TECHNOLOGY APPLICATIONS PROJECT (ATTAP) Final Annual Report, Jan. - Dec. 1989

2 Jul. 1990 137 p

(Contracts DEN3-336; DE-AI01-85CE-50111)

(NASA-CR-187039; NAS 1.26:187039; EDR-14585; DOE/NASA/0336-2) Avail: NTIS HC/MF A07 CSCL 21E

Advanced Turbine Technology Application Project (ATTAP) activities during the past year were highlighted by test-bed engine design and development activities; ceramic component design; materials and component characterization; ceramic component process development and fabrication; component rig testing; and test-bed engine fabrication and testing. Although substantial technical challenges remain, all areas exhibited progress. Test-bed engine design and development activity included engine mechanical design, power turbine flow-path design and mechanical layout, and engine system integration aimed at upgrading the AGT-5 from a 1038 C metal engine to a durable 1371 C structural ceramic component test-bed engine. ATTAP-defined ceramic and associated ceramic/metal component design activities include: the ceramic combustor body, the ceramic gasifier turbine static structure, the ceramic gasifier turbine rotor, the ceramic/metal power turbine static structure, and the ceramic power turbine rotors. The materials and component characterization efforts included the testing and evaluation of several candidate ceramic materials and components being developed for use in the ATTAP. Ceramic component process development and fabrication activities are being conducted for the gasifier turbine rotor, gasifier turbine vanes, gasifier turbine scroll, extruded regenerator disks, and thermal insulation. Component rig testing activities include the development of the necessary test procedures and conduction of rig testing of the ceramic components and assemblies. Four-hundred hours of hot gasifier rig test time were accumulated with turbine inlet temperatures exceeding 1204 C at 100 percent design gasifier speed. A total of 348.6 test hours were achieved on a single ceramic rotor without failure and a second ceramic rotor was retired in engine-ready condition at 364.9 test hours. Test-bed engine fabrication, testing, and development supported improvements in ceramic component technology that will permit the achievement of program performance and durability goals. The designated durability engine accumulated 359.3 hour of test time, 226.9 of which were on the General Motors gas turbine durability schedule. Author

N91-16022# Karlsruhe Univ. (Germany, F.R.). Fakultaet fuer Maschinenbau.

EXPERIMENTAL AND THEORETICAL EXAMINATIONS OF FILM COOLING OF GAS TURBINE BLADES Ph.D. Thesis [EXPERIMENTELLE UND THEORETISCHE UNTERSUCHUNGEN ZUR FILMKUEHLUNG VON GASTURBINENSCHAUFELN]

Wolfgang Haas 1989 245 p In GERMAN

(ETN-91-98554) Avail: NTIS HC/MF A11

Film cooling measurements are carried out in a grid channel with relatively low velocities to obtain data for the development and the safeguarding of calculation models. The influence of the density ratio, the Reynolds number and the turbulence degree on the cooling efficiency, and the heat transfer number was investigated. The formation and the development of velocity and temperature profiles were also investigated in the case of a plane blade grid. A calculation process based on a numerical solution of the stationary two dimensional conservation equations for mass, impulse, and energy in the boundary shape was developed which characterizes the velocity and temperature fields at turbine blades. ESA

N91-16023# Loughborough Univ. of Technology (England). Dept. of Transport Technology.

JET ENGINE PERFORMANCE ESTIMATION FROM MINIMAL INPUT DATA M.S. Thesis

Mark Pitt 27 Nov. 1990 234 p

(ETN-91-98582) Copyright Avail: NTIS HC/MF A11

From a photograph of a subject aircraft for which drag characteristics can be estimated, determination of an engine cycle which matches the engine thrust to the aircraft drag characteristics is attempted. A database collating the facets of engine design important to the analysis task is established. Computer routines are used to assist in the analysis. The expected output of the assessment methodology is defined. The performance of the method is critically examined to determine its strengths and weaknesses. The assessment was found to be highly sensitive to the values of total pressure at the engine inlet and as calulated at the nozzle exit. ESA

N91-16024# Loughborough Univ. of Technology (England). Dept. of Electrical and Electronic Engineering.

AN INTRODUCTION TO MODERN AERO-ENGINE CONTROL DESIGN M.S. Thesis

B. A. Moore 27 Nov. 1990 104 p

(ETN-91-98583) Copyright Avail: NTIS HC/MF A06

The fundamental requirements of aeroengine controllers are discussed. Using the example of a remotely piloted vehicle engine controller, a simple in service system is analyzed from the control engineer view. The relationship between theory and practice is discussed. The fundamental concepts underlying a unique research control system for a military gas turbine power plant are examined. The complexity of the technique needed for safe and efficient control of a modern jet engine is briefly discussed. The idea of employing multivariate techniques in a modern aeroengine controller is considered. A simple engine controller design exercise based on a military aeroengine is undertaken, using a modern control compensator design technique. ESA

08 AIRCRAFT STABILITY AND CONTROL

Includes aircraft handling qualities; piloting; flight controls; and autopilots.

For related information see also *05 Aircraft Design, Testing and Performance.*

N91-16025 Purdue Univ., West Lafayette, IN.
AEROSERVOELASTIC TAILORING FOR LATERAL CONTROL ENHANCEMENT Ph.D. Thesis
Changho Nam 1990 166 p
Avail: Univ. Microfilms Order No. DA9031368

A fundamental study of aeroservoelastic tailoring for roll control is presented. The effects of combining the structural tailoring of the lifting surface (ply orientation and thickness), together with the wing geometry (sweep angle and taper ratio), and the control surface geometry (spanwise position and chordwise size of the control surface) upon the lateral control effectiveness are discussed. Several optimization examples for the minimization of control surface hinge moment, subject to constant roll effectiveness, are performed. To understand the effects of aeroservoelastic tailoring, two different levels of approach are used. First, a simple beam model is used to represent a high aspect ratio flexible wing. Second, a plate model is used for the more accurate structural analysis. The ELAPS code, the general equivalent plate analysis program, is used for the structural analysis. The best spanwise location of the control surface for flutter suppression is found, by using Nissim's aerodynamic energy concept. The results are compared with those of the best spanwise position of the control surface for roll control. The formulation for optimization studies when the wing weight is included as a part of the objective function is presented. Optimization examples for the simultaneous minimization of wing and control surface hinge moment are considered. Results show that the control surface hinge moment can be minimized by reorienting the ply angle and redesigning the wing, control surface geometry. Even the hinge moment and wing weight can be minimized simultaneously.
Dissert. Abstr.

N91-16026# Loughborough Univ. of Technology (England). Dept. of Electrical and Electronic Engineering.
LONGITUDINAL STABILITY AUGMENTATION OF A LIGHTWEIGHT FIGHTER AIRCRAFT MODEL M.S. Thesis
W. A. Fernie 1989 161 p
(ETN-91-98585) Copyright Avail: NTIS HC/MF A08

Two control systems are assessed and tested over a range of incidence values, in order to evaluate the effectiveness of the designs. A suitable aircraft model is developed and aerodynamic data for the F16 fighter aircraft are used to ensure that the resulting longitudinal behavior of the model is unsatisfactory. The stability criteria are established and the existing defense standard criteria for the short period oscillation are selected. Both control systems produce better results when the designs are based on the fourth order model. The performance of a digital compensator is studied. The quantization and discretization errors are evaluated. An optimum sampling rate is selected. The effects of system delays on aircraft handling qualities are considered. ESA

09 RESEARCH AND SUPPORT FACILITIES (AIR)

Includes airports, hangars and runways; aircraft repair and overhaul facilities; wind tunnels; shock tubes; and aircraft engine test stands.

For related information see also *14 Ground Support Systems and Facilities (Space).*

N91-16027# Sandia National Labs., Albuquerque, NM. Fluid and Thermal Sciences Dept.
AEROSOL DYNAMICS LABORATORY
D. J. Rader and L. A. Mondy Apr. 1990 23 p
(Contract DE-AC04-76DP-00789)
(DE90-010275; SAND-89-2658) Avail: NTIS HC/MF A03

In the past five years, Department 1510 has developed a state-of-the-art Aerosol Dynamics Laboratory (ADL). This report documents the current instrumentation and capabilities that exist in this laboratory. The ADL was developed from a variety of sources, with a primary contribution from Department 1510's Independent Research and Development program in aerosol dynamics. Current capabilities of the ADL include: (1) generation of calibration-quality monodisperse particles with diameters between 0.005 to 100 microns; (2) real-time measurement of particle size distributions for particle diameters between 0.01 and 100 microns; (3) in situ, real-time measurement of particle size distributions for particle diameters between 0.3 and 100 microns; and (4) real-time measurement of particle charge distributions for particle diameters between 0.01 and 1.0 microns. DOE

N91-16028# Sandia National Labs., Albuquerque, NM. Explosive Subsystem.
GRAPHICAL ANALYSIS OF BARREL-TAMPED EXPLOSIVELY ACCELERATED FLYER PLATES
Manuel G. Vigil Apr. 1990 41 p
(Contract DE-AC04-76DP-00789)
(DE90-010299; SAND-90-0388) Avail: NTIS HC/MF A03

Analytical equations for barrel-tamped explosively accelerated flyer plates are used to generate graphical solutions to flyer problems. Given the problem geometrical dimensions, explosive weight, detonation velocity, explosive exponent, barrel-tamping weight, and flyer weight, the graphical representation of the calculated data allows for a fast approximation of the final or maximum flyer plate velocity. Graphically obtained flyer velocities are compared to experimentally published data. The graphical solution for flyer velocity is particularly useful when a computer is not available. The graphical representation of the various barrel-tamped flyer parameters results in a parametric study which illustrates the effect on final flyer velocity in varying parameters. The graphical analysis scheme can be used with any explosive, tamper and flyer materials. DOE

N91-16029# Ballistic Research Labs., Aberdeen Proving Ground, MD.
SMALL SCALE SHOCK TUBE EXPERIMENTS USING A COMPUTER CONTROLLED ACTIVE RAREFACTION WAVE ELIMINATOR Final Report, Aug. 1989 - Aug. 1990
Stephen J. Schraml and Richard J. Pearson Sep. 1990 82 p
(DA Proj. 1L1-62120-AH-25)
(AD-A227507; BRL-TR-3149) Avail: NTIS HC/MF A05 CSCL 14/2

The technology needed to construct a facility for testing full scale military equipment, termed the Large Blast/Thermal Simulator (LB/TS), is under development. One of the major components of the proposed facility will be a large valve controlling the flow exiting the downstream end, called a rarefaction wave eliminator (RWE). An active RWE, one which adapts its open area to changing flow conditions, will be used in the LB/TS. Using an active RWE allows a relatively short facility to produce the same range of blast simulations that would otherwise require a very long expansion section. A small scale active rarefaction wave eliminator was constructed and tested through a series of blast conditions. Shock overpressures ranged from 40 to 100 kPa, while positive phase durations were in range of 14 to 54 ms. Pressure histories and impulse values obtained from tests using the RWE compared well with long expansion section baseline data. The results of this program show that an active rarefaction wave eliminator can be used in place of a long expansion section to achieve successful nuclear blast simulation. Knowledge gained from the use of this RWE will be employed during construction and testing of the 1:6 scale and full scale active RWE's. GRA

N91-16030# Rutherford Appleton Lab., Chilton (England).
THE RADIATION HARDNESS TEST FACILITY

M. Edwards and D. R. Perry 14 Aug. 1990 23 p
(RAL-90-065; ETN-91-98408) Avail: NTIS HC/MF A03

The neutron radiation hardness test facility using the spallation neutron source ISIS is described. The ability to irradiate test structures with neutrons of about 1 MeV energy will be necessary in designing detectors for future high luminosity hadron colliders. The measurements of the neutron energy spectrum and flux available and the requirements placed on devices to be irradiated are detailed. Possible ways the facility could be improved in the future, should this become necesary, are indicated. ESA

N91-16031# Army Engineer Waterways Experiment Station, Vicksburg, MS. Geotechnical Lab.
EVALUATION PROCEDURE FOR REINFORCED CONCRETE BOX CULVERTS UNDER AIRFIELD PAVEMENTS Final Report, Jan. 1983 - Mar. 1990
David M. Coleman, James A. Harrison, and Stanley C. Woodson Sep. 1990 81 p Sponsored by Corps of Engineers, Washington, DC and AFESC, Tyndall AFB, FL
(AD-A227920; WES/TR/GL-90-25) Avail: NTIS HC/MF A05 CSCL 12/5

While most airfield pavements are periodically evaluated to determine their structural capacity, often little thought is given to the structural capacity of the culverts and other drainage structures beneath the pavement. The Department of Defense has never had a standard means of evaluating box culverts under airfields or landing strips. This capacity has been needed on several occasions, particularly overseas where landing strips are sometimes built into the local highway system. The research reported herein evaluated several different methods for performing the structural evaluation of reinforced concrete box culverts under aircraft loads, selected two computer programs (CANDE-1980 and CORTCUL) for detailed testing, and then developed a culvert evaluation methodology based on the CORTCUL program. To assist in determining the aircraft loads, an additional computer program was developed. This program, CULVERT, uses elastic layer theory and predefined aircraft data to calculate the vertical stress acting on the top of the culvert due to the aircraft and also provides output and plotting capabilities. Stress is then applied to the culvert model along with the member loads, soil loads, and other loads such as internal water. The CORTCUL program evaluates the culvert based on the requirements of ACI 318, Building Code Requirements for Reinforced Concrete. GRA

N91-16032*# Alabama Univ., Huntsville. Dept. of Chemical Engineering.
HIGH TEMPERATURE FURNACE MODELING AND PERFORMANCE VERIFICATIONS Semiannual Progress Report, 1 Apr. - 31 Aug. 1990
James E. Smith, Jr. Jan. 1991 30 p
(Grant NAG8-708)
(NASA-CR-187831; NAS 1.26:187831) Avail: NTIS HC/MF A03 CSCL 14B

A two dimensional conduction/radiation problem for an alumina crucible in a zirconia heater/muffle tube enclosing a liquid iron sample was solved numerically. Variations in the crucible wall thickness were numerically examined. The results showed that the temperature profiles within the liquid iron sample were significantly affected by the crucible wall thicknesses. New zirconia heating elements are under development that will permit continued experimental investigations of the zirconia furnace. These elements have been designed to work with the existing furnace and have been shown to have longer lifetimes than commercially available zirconia heating elements. The first element has been constructed and tested successfully. Author

N91-16033*# Vigyan Research Associates, Inc., Hampton, VA.
USER'S GUIDE TO PANCOR: A PANEL METHOD PROGRAM FOR INTERFERENCE ASSESSMENT IN SLOTTED-WALL WIND TUNNELS
William B. Kemp, Jr. Dec. 1990 50 p
(Contract NAS1-18585)
(NASA-CR-187479; NAS 1.26:187479) Avail: NTIS HC/MF A03 CSCL 14B

Guidelines are presented for use of the computer program PANCOR to assess the interference due to tunnel walls and model support in a slotted wind tunnel test section at subsonic speeds. Input data requirements are described in detail and program output and general program usage are described. The program is written for effective automatic vectorization on a CDC CYBER 200 class vector processing system. Author

12 ASTRONAUTICS (GENERAL)

For extraterrestrial exploration see *91 Lunar and Planetary Exploration.*

N91-16034# Bundesministerium fuer Forschung und Technologie, Bonn (Germany, F.R.).
THE SPACE FLIGHTS: SECOND GERMAN SPACELAB MISSION D-2 AND MIR 1992 [DIE RAUMFLUEGE ZWEITE DEUTSCHE SPACELAB-MISSION D-2 UND MIR '92]
8 Oct. 1990 39 p In GERMAN
(REPT-25/90; ETN-91-98551) Avail: NTIS HC/MF A03

The German research programs of the Spacelab missions are presented. The following topics were studied: fluid physics (capillarity, Marangoni convection), crystallography, biology, human physiology (heart function, respiration), robotics, microgravity, Earth observation (cartography), astronomy. The institutes which cooperated in these programs are reviewed. Some experiments are more precisely described, such as diffusion in metallic fusion, crystalization of biologic macromolecules or doximetry of spatial radiation. The experiments of Mir mission are also depicted, which are based on physiology and radiation protection. ESA

13 ASTRODYNAMICS

Includes powered and free-flight trajectories; and orbital and launching dynamics.

N91-16035# Royal Aerospace Establishment, Farnborough (England).
GEOPOTENTIAL HARMONICS OF ORDER 15 AND 30 FROM ANALYSIS OF 50 ORBIT DETERMINATIONS OF 1967-102B
Doreen M. C. Walker 11 Jun. 1990 32 p
(RAE-TR-90029; RAE-SS-12; BR115205; ETN-91-98409)
Copyright Avail: NTIS HC/MF A03

The orbital parameters of the satellite 1967-102B, Cosmos 184 rocket, were determined at 50 epochs from some 3900 observations. For 21 of these determinations, Hewitt camera observations were available. During the time of the orbit determinations the satellite passed through 15th order resonance. The variations in inclination and eccentricity were analyzed to obtain six lumped 15th order geopotential harmonics, with accuracies equivalent to between 0.2 and 3.3 cm in geoid height and four lumped 30th order geopotential harmonics, with accuracies better than 1 cm in geoid height. The lumped harmonics obtained were compared with those from GEM 10B and 10C models and with those from GRIM3-L1 and the RAPP 1981 models. A comparison was also mode with the lumped harmonics obtained from a new PGS-3337 model published by NASA, and the agreement with this model is very good. ESA

14 GROUND SUPPORT SYSTEMS AND FACILITIES (SPACE)

Includes launch complexes, research and production facilities; ground support equipment, e.g., mobile transporters; and simulators.

For related information see also *09 Research and Support Facilities (Air).*

No abstracts in this category.

15 LAUNCH VEHICLES AND SPACE VEHICLES

Includes boosters; operating problems of launch/space vehicle systems; and reusable vehicles.

For related information see also *20 Spacecraft Propulsion and Power.*

No abstracts in this category.

16 SPACE TRANSPORTATION

Includes passenger and cargo space transportation, e.g., shuttle operations; and space rescue techniques.

For related information see also *03 Air Transportation and Safety* and *18 Spacecraft Design, Testing and Performance.* For space suits see *54 Man/System Technology and Life Support.*

N91-16036 Joint Publications Research Service, Arlington, VA.
JPRS REPORT: SCIENCE AND TECHNOLOGY. USSR: SPACE
2 May 1989 77 p Transl. into ENGLISH from various Russian articles
(JPRS-USP-89-006) Copyright Avail: Issuing Activity

Science and technology topics addressed include: manned mission highlights; space science; space engineering; space applications; and space policy and administration. For individual titles, see N91-16037 through N91-16040.

N91-16037 Joint Publications Research Service, Arlington, VA.
BURAN AND THE FUTURE OF THE SOVIET SPACE PROGRAM
Yu. P. Semenov, V. A. Timchenko, and S. K. Gromov *In its* JPRS Report: Science and Technology. USSR: Space 2 May 1989 p 37-43 Transl. into ENGLISH from Zemlya i Vselennaya (Moscow, USSR), no. 2, Mar. - Apr. 1989 p 3-10 (For primary document see N91-16036 08-16)
Copyright Avail: Issuing Activity

On 15 November 1988, the versatile Energiya rocket and space transportation system was successfully launched, and it placed the Buran reusable orbital spacecraft into orbit. A new and important stage in the development of the Soviet Space Program began with that flight. Features that are specific to the development of the Buran spacecraft are discussed. Transport of cargo; ballistics of the Buran flight; reusable vs. disposable rockets; comparison of the U.S. Space Shuttle and Buran; and prospects for future use of Buran are briefly described. B.G.

N91-16038 Joint Publications Research Service, Arlington, VA.
DEVELOPMENTAL TESTS FOR SHUTTLE ORBITER
K. Vasilchenko, G. Lozino-Lozinskiy, and G. Svishchev *In its* JPRS Report: Science and Technology. USSR: Space 2 May 1989 p 43-46 Transl. into ENGLISH from Pravda (Moscow, USSR), 24 Nov. 1988 p 3 (For primary document see N91-16036 08-16)
Copyright Avail: Issuing Activity

Since it is simultaneously an orbital spacecraft and aircraft, the Buran combines the qualities of a satellite and an aircraft. One of the basic problems was that of attaining aerodynamic characteristics that would ensure performance of the missions in all sections of the flight during the descent from space. Wind tunnel tests, tests in airborne prototypes, and precise calculation techniques have made possible determination of the airframe aerodynamic characteristics. Development of the Heat-Resistant Vacuum Chamber for testing the thermal protection system is discussed. The impact of nondestructive tests, computer aided design, computer aided operation monitoring systems, automated tooling, and the automated quality assurance systems are briefly examined. Tests of the Buran have become a test of the scientific and technical arsenal. B.G.

N91-16039 Joint Publications Research Service, Arlington, VA.
GENERAL DESIGNER DESCRIBES BURAN FLIGHT CONTROL, AUTOPILOT SYSTEMS
V. Lapygin *In its* JPRS Report: Science and Technology. USSR: Space 2 May 1989 p 46-48 Transl. into ENGLISH from Sotsialisticheskaya Industriya (Moscow, USSR), 7 Dec. 1988 p 4 (For primary document see N91-16036 08-16)
Copyright Avail: Issuing Activity

Installed aboard Buran are around a thousand instruments, in which the most precise electromechanical equipment was combined with the latest equipment in electronics. The system determines where the Buran is at any given moment, selects the necessary trajectory, keeps it on course, and ensures a stable orientation in space. The components of the flight control and autopilot systems are briefly described. B.G.

N91-16040 Joint Publications Research Service, Arlington, VA.
SPECIALISTS AT FLIGHT CONTROL CENTER DISCUSS SHUTTLE COMPUTER SYSTEMS
Aleksandr Nemov *In its* JPRS Report: Science and Technology. USSR: Space 2 May 1989 p 48-52 Transl. into ENGLISH from Sovetskaya Rossiya (Moscow, USSR), 2 Dec. 1988 p 3 (For primary document see N91-16036 08-16)
Copyright Avail: Issuing Activity

The performance of the computers on-board Buran were described from launch, through malfunctions, to return landing. The process of decision making was briefly discussed. Outlined is the possible transfer of technology to other sectors. Author

N91-16041*# National Aeronautics and Space Administration. John F. Kennedy Space Center, Cocoa Beach, FL.
DEBRIS/ICE/TPS ASSESSMENT AND PHOTOGRAPHIC ANALYSIS FOR SHUTTLE MISSION STS-41
Scott A. Higginbotham and J. Bradley Davis Nov. 1990 151 p Original contains color illustrations
(NASA-TM-103814; NAS 1.15:103814) Avail: NTIS HC/MF A08; 60 functional color pages CSCL 22B

A Debris/Ice/Thermal Protection System (TPS) assessment and photographic analysis was conducted for Space Shuttle Mission STS-41. Debris inspections of the flight elements and launch pad were performed before and after launch. Ice/frost conditions on the External Tank were assessed by the use of computer programs, nomographs, and infrared scanner data during cryogenic loading of the vehicle followed by on-pad visual inspection. High speed photography was analyzed after launch to identify ice/debris sources and evaluate potential vehicle damage and/or in-flight anomalies. Documented here are the debris/ice/TPS conditions and photographic analysis of Mission STS-41, and their overall effect on the Space Shuttle Program. Author

17 SPACE COMM., SPACECRAFT COMM., COMMAND & TRACKING

Includes telemetry; space communications networks; astronavigation and guidance; and radio blackout.

For related information see also *04 Aircraft Communications and Navigation* and *32 Communications and Radar.*

N91-16042# Los Alamos National Lab., NM.
A LOW-COST INFRARED TELEMETRY SYSTEM FOR KILOHERTZ-BANDWIDTH DATA ACQUISITION
Michael D. Holder 1990 9 p Presented at the 3rd Test Technology Symposium, Laurel, MD, 19-21 Mar. 1990 Submitted for publication
(Contract W-7405-eng-36)
(DE90-010616; LA-UR-90-1434; CONF-9003149-2) Avail: NTIS HC/MF A02

A telemetry system is described that transmits data from three 8-kHz analog inputs by means of an infrared-optical-digital communications channel. This system is used to acquire accelerometer data on a rocket sled during its 300-m flight. An optical communications channel at 950 nm is used to send digitally encoded analog signals from the sled to a fixed receiver. The signal is recorded and decoded by a computer. The transmitter includes a differential amplifier and low-pass filter for each input channel. Excitation for piezoresistive accelerometers is also provided. Each input channel is sampled and digitized at a 16-kHz rate. The transmitter is built on a single printed-circuit card measuring 7.5 cm by 23 cm, weighing less than 450 g including batteries. This system can be used on tests involving destruction of the transmitter because of its low cost. DOE

18 SPACECRAFT DESIGN, TESTING AND PERFORMANCE

Includes satellites; space platforms; space stations; spacecraft systems and components such as thermal and environmental controls; and attitude controls.

For life support systems see *54 Man/System Technology and Life Support.* For related information see also *05 Aircraft Design, Testing and Performance, 39 Structural Mechanics,* and *16 Space Transportation.*

N91-16043# Sandia National Labs., Albuquerque, NM. Electromagnetic Applications Div.
MAGNETIC-FIELD SHIELDING OF SATELLITES FROM HIGH-ENERGY-ELECTRON ENVIRONMENTS
Charles N. Vittitoe May 1990 16 p
(Contract DE-AC04-76DP-00789)
(DE90-010296; SAND-89-2956) Avail: NTIS HC/MF A03

Magnet configurations are found that limit the 6-MeV electrons threatening satellite electronics to less than 1 percent of the incident flux. Successful configurations of permanent magnets and electromagnets require magnetic energies of approximately 8 to 12 kJ to protect each liter of electronics volume. The fundamental strength of materials leads to a required minimum mass of approximately 48 to 64 kg/liter to support the magnetic pressure. With the electronics requiring approximately 5 liters, several hundred kilograms are needed for this support. Except for protecting small apertures, magnetic shielding provides little, if any, advantage over that obtained by coating with an equivalent mass using traditional methods. DOE

N91-16044# Sandia National Labs., Albuquerque, NM.
SENSOR-BASED AUTOMATED DOCKING OF LARGE PAYLOADS
W. D. Drotning 1990 11 p Presented at the American Nuclear Society Annual Meeting, Nashville, TN, 10-14 Jun. 1990
(Contract DE-AC04-76DP-00789)
(DE90-011020; SAND-90-0348C; CONF-900608-17) Avail: NTIS HC/MF A03

A multiple degree of freedom robotic system is described for the sensor-based, automated remote manipulation and precision docking of large payloads. Computer vision and ultrasonic proximity sensing are used to control the automated precision docking of a large object with a passive target cavity. Real-time sensor processing and model-based analysis are used to control payload position to a precision of +/-0.5 mm. DOE

N91-16045*# Illinois Univ., Urbana-Champaign. Dept. of Aeronautical and Astronautical Engineering.
AEROSPACE VEHICLE DESIGN, SPACECRAFT SECTION. VOLUME 1: PROJECT GROUPS 1-4 Final Project Reports
May 1990 366 p
(Grant NGT-21-002-800)
(NASA-CR-186841; NAS 1.26:186841; AAE-241-VOL-1) Avail: NTIS HC/MF A16 CSCL 22B

Four spacecraft design proposals are presented for an unmanned probe to Pluto and its satellite, Charon: (1) the Pluto flyby exploration/research design; (2) the Intrepid spacecraft; (3) the Cerberus spacecraft; and (4) the Orbiting Plutonian Topographic Image Craft (OPTIC). The topics covered include: (1) scientific instrumentation; (2) mission management, planning, and costing; (3) power and propulsion system; (4) structural subsystem; (5) command, control, and communications; and (6) attitude and articulation control. For individual titles, see N91-16046 through N91-16049.

N91-16046*# Illinois Univ., Urbana-Champaign.
PFERD MISSION: PLUTO FLYBY EXPLORATION/RESEARCH DESIGN Final Design Report
Gary Lemke, Husni Zayed, Jason Herring, Doug Fuehne, Kevin Sutton, and Mike Sharkey *In its* Aerospace Vehicle Design, Spacecraft Section. Volume 1: Project Groups 1-4 May 1990 71 p (For primary document see N91-16045 08-18)
Avail: NTIS HC/MF A16 CSCL 22B

The Pluto Flyby Exploration/Research Design (PFERD) mission will consist of a flyby spacecraft to Pluto and its satellite, Charon. The mission lifetime is expected to be 18 years. The Titan 4 with a Centaur upper stage will be utilized to launch the craft into the transfer orbit. The proposal was divided into six main subsystems: (1) scientific instrumentation; (2) command, communications, and control: (3) altitude and articulation control; (4) power and propulsion; (5) structures and thermal control; and (6) mission management and costing. Tradeoff studies were performed to optimize all factors of design, including survivability, performance, cost, and weight. Problems encountered in the design are also presented. K.S.

N91-16047*# Illinois Univ., Urbana-Champaign.
INTREPID: A MISSION TO PLUTO
Michael Behling, Donald Buchman, Andres Marcus, Stephanie Procopis, Carl Wassgren, and Sarah Ziemer *In its* Aerospace Vehicle Design, Spacecraft Section. Volume 1: Project Groups 1-4 May 1990 97 p (For primary document see N91-16045 08-18)
Avail: NTIS HC/MF A16 CSCL 22B

A proposal for an exploratory spacecraft mission to Pluto/Charon system was written in response to the request for proposal for an unmannned probe to pluto (RFP). The design requirements of the RFP are presented and under the guidance of these requirements, the spacecraft Intrepid was designed. The RPF requirement that was of primary importance is the minimization of cost. Also, the reduction of flight time was of extreme importance because the atmosphere of Pluto is expected to collapse close to the Year 2020. If intrepid should arrive after the collapse, the mission would be a failure; for Pluto would be only a solid rock of ice. The topics presented include: (1) scientific instrumentation; (2) mission management, planning, and costing; (3) power and propulsion subsystem; (4) structural subsystem; (5) command, control, and communications; and (6) attitude and articulation control. K.S.

N91-16048*# Illinois Univ., Urbana-Champaign.
PROJECT CERBERUS: FLYBY MISSION TO PLUTO

K. Sivier, A. Koepke, Theodore W. Humphrey, Jeffrey P. Elbel, Bruce E. Hackett, Ralph G. Kennedy, Donald J. Leo, and Shery A. Zimmerman *In its* Aerospace Vehicle Design, Spacecraft Section. Volume 1: Project Groups 1-4 May 1990 99 p (For primary document see N91-16045 08-18)
Avail: NTIS HC/MF A16 CSCL 22B

The goal of the Cerberus Project was to design a feasible and cost-effective unmanned flyby mission to Pluto. The requirements in the request for proposal for an unmanned probe to Pluto are presented and were met. The design stresses proven technology that will avoid show stoppers which could halt mission progress. Cerberus also utilizes the latest advances in the spacecraft industry to meet the stringent demands of the mission. The topics covered include: (1) mission management, planning, and costing; (2) structures; (3) power and propulsion; (4) attitude, articulation, and control; (5) command, control, and communication; and (6) scientific instrumentation. K.S.

N91-16049*# Illinois Univ., Urbana-Champaign.
OPTIC: ORBITING PLUTONIAN TOPOGRAPHIC IMAGE CRAFT PROPOSAL FOR AN UNMANNED MISSION TO PLUTO Final Report
Jonathan E. Kelly, Randall John Hein, David Lee Meyer, David Mark Robinson, Mark James Endre, and Eric W. Summers *In its* Aerospace Vehicle Design, Spacecraft Section. Volume 1: Project Groups 1-4 May 1990 94 p (For primary document see N91-16045 08-18)
Avail: NTIS HC/MF A16 CSCL 22B

The proposal for an unmanned probe to Pluto is presented and described. The Orbiting Plutonian Topographic Image Craft's (OPTIC's) trip will take twenty years and after its arrival, will begin its data collection which includes image and radar mapping, surface spectral analysis, and magnetospheric studies. This probe's design was developed based on the request for proposal of an unmanned probe to Pluto requirements. The distinct problems which an orbiter causes for each subsystem of the craft are discussed. The final design revolved around two important factors: (1) the ability to collect and return the maximum quantity of information on the Plutonian system; and (2) the weight limitations which the choice of an orbiting craft implied. The velocity requirements of this type of mission severely limited the weight available for mission execution-owing to the large portion of overall weight required as fuel to fly the craft with present technology. The topics covered include: (1) scientific instrumentation; (2) mission management; (3) power and propulsion; (4) attitude and articulation control; (5) structural subsystems; and (6) command, control, and communication. K.S.

N91-16050*# Illinois Univ., Urbana-Champaign. Dept. of Aeronautical and Astronautical Engineering.
AEROSPACE VEHICLE DESIGN, SPACECRAFT SECTION. VOLUME 2: PROJECT GROUPS 5-7 Final Project Reports
May 1990 287 p
(Grant NGT-21-002-800)
(NASA-CR-186842; NAS 1.26:186842; AAE-241-VOL-2) Avail: NTIS HC/MF A13 CSCL 22B

Three spacecraft design proposals are presented for an unmanned probe to Pluto and its satellite, Charon: (1) the Pluto unmanned long-range scientific explorer (PULSE); (2) the Copernicus spacecraft; and (3) the Phoenix Pluto probe. The topics covered include: (1) scientific instrumentation; (2) mission management, planning, and costing; (3) power and propulsion system; (4) structural subsystem; (5) command, control, and communication; and (6) attitude and articulation control. For individual titles, see N91-16051 through N91-16053.

N91-16051*# Illinois Univ., Urbana-Champaign.
MISSION MANAGEMENT, PLANNING, AND COST: PULSE ATTITUDE AND CONTROL SYSTEMS (AACS)
In its Aerospace Vehicle Design, Spacecraft Section. Volume 2: Project Groups 5-7 May 1990 98 p (For primary document see N91-16050 08-18)
Avail: NTIS HC/MF A13 CSCL 22B

The Pluto unmanned long-range scientific explorer (PULSE) is a probe that will do a flyby of Pluto. It is a low weight, relatively low costing vehicle which utilizes mostly off-the-shelf hardware, but not materials or techniques that will be available after 1999. A design, fabrication, and cost analysis is presented. PULSE will be launched within the first decade of the twenty-first century. The topics include: (1) scientific instrumentation; (2) mission management, planning, and costing; (3) power and propulsion systems; (4) structural subsystem; (5) command, control, and communication; and (6) attitude and articulation control. K.S.

N91-16052*# Illinois Univ., Urbana-Champaign.
THE COPERNICUS PROJECT
Bob Barnstable, Hans Polte, Paul Kepes, Kevin Walker, Jeff Jacobs, and Stephen Williams *In its* Aerospace Vehicle Design, Spacecraft Section. Volume 2: Project Groups 5-7 May 1990 97 p (For primary document see N91-16050 08-18)
Avail: NTIS HC/MF A13 CSCL 22B

The Copernicus spacecraft, to be launched on May 4, 2009, is designed for scientific exploration of the planet Pluto. The main objectives of this exploration is to accurately determine the mass, density, and composition of the two bodies in the Pluto-Charon system. A further goal of the exploration is to obtain precise images of the system. The spacecraft will be designed for three axis stability control. It will use the latest technological advances to optimize the performance, reliability, and cost of the spacecraft. Due to the long duration of the mission, nominally 12.6 years, the spacecraft will be powered by a long lasting radioactive power source. Although this type of power may have some environmental drawbacks, currently it is the only available source that is suitable for this mission. The planned trajectory provides flybys of Jupiter and Saturn. These flybys provide an opportunity for scientific study of these planets in addition to Pluto. The information obtained on these flybys will supplement the data obtained by the Voyager and Galileo missions. The topics covered include: (1) scientific instrumentation; (2) mission management, planning, and costing; (3) power and propulsion system; (4) structural subsystem; (5) command, control, and communication; and (6) attitude and articulation control. K.S.

N91-16053*# Illinois Univ., Urbana-Champaign.
THE PHOENIX PLUTO PROBE
George R. Gunning, Jeff Spapperi, Jeffrey P. Wilkinson, Jim Eldred, Dennis Labij, and Meredith Strinni *In its* Aerospace Vehicle Design, Spacecraft Section. Volume 2: Project Groups 5-7 May 1990 90 p (For primary document see N91-16050 08-18)
Avail: NTIS HC/MF A13 CSCL 22B

A design proposal for an unmanned probe to Pluto is presented. The topics covered include: (1) scientific instrumentation; (2) mission management, planning, and costing; (3) power and propulsion system; (4) structural subsystem; (5) command, control, and communication; and (6) attitude and articulation control. K.S.

N91-16054# Sandia National Labs., Albuquerque, NM. Computational Aerodynamics Div.
JOINT COMPUTATIONAL/EXPERIMENTAL AERODYNAMICS RESEARCH ON A REENTRY VEHICLE. PART 2: COMPUTATIONAL RESULTS
Mary McWherter Walker and William L. Oberkampf 1990 15 p Presented at the 29th AIAA Aerospace Sciences Conference, Reno, NV, 7-10 Jan. 1991
(Contract DE-AC04-76DP-00789)
(DE90-012765; SAND-90-1384C-PT-2; CONF-910117-3-PT-2)
Avail: NTIS HC/MF A03

Computational aerodynamics simulation applied to supersonic and hypersonic flight vehicles has significantly increased during the last several years. Flow field simulations have been computed for a wide variety of vehicles from ballistic reentry vehicles to the Space Shuttle. Although computational aerodynamics simulation has been taking more responsibility during this time, wind tunnel experimentation has continued to play the major role in flight vehicle analysis and design. This role, however, is changing because of

the great strides in the capability and confidence in numerical simulations. Computational results are obtained for a spherically blunted cone with a slice parallel to the cone axis. Aerodynamic force and moment predictions from Sandia's CFD codes are compared with wind tunnel data from the Sandia Mach 8 hypersonic wind tunnel. These comparisons are made on a sliced reentry vehicle both with and without a windward flap. The windward flap will be deflected 10, 20 and 30 degrees. Inviscid/boundary layer codes and the Parabolized Navier-Stokes code are used to generate solutions for the slice vehicle. In the region of the flap, some reversed flow is apparent and a full Navier-Stokes code will be used to provide comparisons with the data. Force and moment and surface flow visualization comparisons are made for laminar, ideal gas flow. Author

N91-16055# National Environmental Satellite Service, Washington, DC. Office of Research and Applications.
EVALUATION OF THE GOES 1-M NORMALIZATION TECHNIQUE WITH THE VISIBLE IMAGES OF GOES-7
J. H. Lienesch, R. Xie (Satellite Meteorological Center, Beijing, China), and W. Y. Ramsey Apr. 1990 26 p
(AD-A227462; NESIDS-31) Avail: NTIS HC/MF A03 CSCL 14/4

The visible images of the earth from the current and future NOAA geostationary satellites are produced from observations by eight separate detectors. Because the detectors have different responses to the reflected solar energy and are not calibrated in flight, the signals from seven of the detectors are normalized to that of the eighth detector to avoid banding or striping the images. A technique employing matching of the channels' empirical distribution functions was proposed for minimizing the striping in the images from the future GOES I-M spacecraft. This method was evaluated in an operational setting with the data of GOES 7. The results from a series of comparisons between the images derived from the operational normalization technique and the new technique are discussed quantitatively. The new technique significantly reduces the level of striping in the visible images compared to that produced by the operational procedures. The new method improved the image quality to an extent that warranted its implementation for the GOES 7 operational images in June 1989. GRA

N91-16056*# Science Applications International Corp., Prospect, TN.
SCOPING ESTIMATES OF THE LDEF SATELLITE INDUCED RADIOACTIVITY Final Technical Report
Tony W. Armstrong and B. L. Colborn Sep. 1990 60 p
(Contract NAS8-38427)
(NASA-CR-184074; NAS 1.26:184074; SAIC-90/1462) Avail: NTIS HC/MF A04 CSCL 22B

The Long Duration Exposure Facility (LDEF) satellite was recovered after almost six years in space. It was well-instrumented with ionizing radiation dosimeters, including thermoluminescent dosimeters, plastic nuclear track detectors, and a variety of metal foil samples for measuring nuclear activation products. The extensive LDEF radiation measurements provide the type of radiation environments and effects data needed to evaluate and help resolve uncertainties in present radiation models and calculational methods. A calculational program was established to aid in LDEF data interpretation and to utilize LDEF data for assessing the accuracy of current models. A summary of the calculational approach is presented. The purpose of the reported calculations is to obtain a general indication of: (1) the importance of different space radiation sources (trapped, galactic, and albedo protons, and albedo neutrons); (2) the importance of secondary particles; and (3) the spatial dependence of the radiation environments and effects expected within the spacecraft. The calculational method uses the High Energy Transport Code (HETC) to estimate the importance of different sources and secondary particles in terms of fluence, absorbed dose in tissue and silicon, and induced radioactivity as a function of depth in aluminum. Y.S.

N91-16057*# National Aeronautics and Space Administration. Langley Research Center, Hampton, VA.
THE NASA CONTROLS-STRUCTURES INTERACTION TECHNOLOGY PROGRAM
Jerry R. Newsom, W. E. Layman, H. B. Waites, and R. J. Hayduk (National Aeronautics and Space Administration, Washington, DC.) Oct. 1990 19 p Presented at the 41st Congress of the International Astronautical Federation, Dresden, German Democratic Republic, 6-12 Oct. 1990 Previously announced in IAA as A91-13934 Submitted for publication
(NASA-TM-102752; NAS 1.15:102752; IAF-90-290) Avail: NTIS HC/MF A03 CSCL 22B

The interaction between a flexible spacecraft structure and its control system is commonly referred to as controls-structures interaction (CSI). The CSI technology program is developing the capability and confidence to integrate the structure and control system, so as to avoid interactions that cause problems and to exploit interactions to increase spacecraft capability. A NASA program has been initiated to advance CSI technology to a point where it can be used in spacecraft design for future missions. The CSI technology program is a multicenter program utilizing the resources of the NASA Langley Research Center (LaRC), the NASA Marshall Space Flight Center (MSFC), and the NASA Jet Propulsion Laboratory (JPL). The purpose is to describe the current activities, results to date, and future activities of the NASA CSI technology program. Author

N91-16058*# National Aeronautics and Space Administration. Langley Research Center, Hampton, VA.
DETERMINATION OF SHUTTLE ORBITER CENTER OF GRAVITY FROM FLIGHT MEASUREMENTS
E. W. Hinson, J. Y. Nicholson (Vigyan Research Associates, Inc., Hampton, VA.), and R. C. Blanchard Jan. 1991 55 p
(NASA-TM-102627; NAS 1.15:102627) Avail: NTIS HC/MF A04 CSCL 22B

Flight measurements of pitch, yaw, and roll rates and the resultant rotationally induced linear accelerations during three orbital maneuvers on Shuttle mission space transportation system (STS) 61-C were used to calculate the actual orbiter center-of-gravity location. The calculation technique reduces error due to lack of absolute calibration of the accelerometer measurements and compensates for accelerometer temperature bias and for the effects of gravity gradient. Accuracy of the technique was found to be limited by the nonrandom and asymmetrical distribution of orbiter structural vibration at the accelerometer mounting location. Fourier analysis of the vibration was performed to obtain the power spectral density profiles which show magnitudes in excess of 10(exp 4) ug (sup 2)/Hz for the actual vibration and over 500 ug (sup 2)/Hz for the filtered accelerometer measurements. The data from this analysis provide a characterization of the Shuttle acceleration environment which may be useful in future studies related to accelerometer system application and zero-g investigations or processes. Author

N91-16059*# Texas Univ., Austin. Center for Aeronautical Research.
A DECENTRALIZED LINEAR QUADRATIC CONTROL DESIGN METHOD FOR FLEXIBLE STRUCTURES Interim Report
Tzu-Jeng Su and Roy R. Craig, Jr. May 1990 118 p
(Grant NAG9-357)
(NASA-CR-187860; NAS 1.26:187860; CAR-90-1) Avail: NTIS HC/MF A06 CSCL 22B

A decentralized suboptimal linear quadratic control design procedure which combines substructural synthesis, model reduction, decentralized control design, subcontroller synthesis, and controller reduction is proposed for the design of reduced-order controllers for flexible structures. The procedure starts with a definition of the continuum structure to be controlled. An evaluation model of finite dimension is obtained by the finite element method. Then, the finite element model is decomposed into several substructures by using a natural decomposition called substructuring decomposition. Each substructure, at this point, still has too large a dimension and must be reduced to a size that is

Riccati-solvable. Model reduction of each substructure can be performed by using any existing model reduction method, e.g., modal truncation, balanced reduction, Krylov model reduction, or mixed-mode method. Then, based on the reduced substructure model, a subcontroller is designed by an LQ optimal control method for each substructure independently. After all subcontrollers are designed, a controller synthesis method called substructural controller synthesis is employed to synthesize all subcontrollers into a global controller. The assembling scheme used is the same as that employed for the structure matrices. Finally, a controller reduction scheme, called the equivalent impulse response energy controller (EIREC) reduction algorithm, is used to reduce the global controller to a reasonable size for implementation. The EIREC reduced controller preserves the impulse response energy of the full-order controller and has the property of matching low-frequency moments and low-frequency power moments. An advantage of the substructural controller synthesis method is that it relieves the computational burden associated with dimensionality. Besides that, the SCS design scheme is also a highly adaptable controller synthesis method for structures with varying configuration, or varying mass and stiffness properties. Author

N91-16060# Messerschmitt-Boelkow-Blohm G.m.b.H., Bremen (Germany, F.R.).
EVAPORATION PROCESS AND 3 PHASE FLOW IN A WATER EVAPORATOR ASSEMBLY
Bernhard J. G. Leidinger Jul. 1990 11 p Presented at the 1st International Fluid Congress INTERFLUID, Essen, Fed. Republic of Germany, 13 Sep. 1990
(MBB-UO-0108-90-PUB; ETN-91-98509) Avail: NTIS HC/MF A03

Evaporation coolers are used for rejecting waste heat from spaceplanes. In the case of a water evaporator, the vacuum conditions of space allow the cooling process to operate below the triple point. The cooling process of a water evaporator is studied. Some important activities of the development like the spray nozzle selection, the capillary structure development and the tooth fin heat exchanger investigations are summarized and main results are discussed. ESA

19 SPACECRAFT INSTRUMENTATION

For related information see also *06 Aircraft Instrumentation* and *35 Instrumentation and Photography.*

N91-16061# Danish Space Research Inst., Lyngby.
MAGNETIC MEASUREMENTS WITH FLUXGATE MAGNETOMETER IN ROCKET FLIGHT
Fritz Primdahl, Poul Anker Jensen, and Christian Boe (Technical Univ. of Denmark, Lyngby.) Apr. 1990 26 p
(DRI-4-90; ISSN-0109-6605) Avail: NTIS HC/MF A03

Since 1979 the Institute for Engineering Design and the Danish Space Research Institute have flow magnetic field measuring instruments on board 7 NASA and European ionosphere scientific sounding rockets reaching altitudes up to 1000 km. Several future rocket flights are planned, and an ultralight magnetometer sensor for satellite missions is under construction jointly with the Department of Electrophysics at the Technical University of Denmark. Ten compact spherical coil sensors were calibrated determining the magnetic axes' deviations from being exactly orthogonal. The deviations ranged from 0.4 x 10(exp -4) to 66.3 x 10(exp -4) rad averaging to 17.0 x 10(exp -4) rad. The six best sensors had an average deviation of 7.85 x 10(exp -4) rad from orthogonality of the angles between the individual magnetic axes. All the sensors' alignments compare favorably with the Magsat sensor alignment, and the best sensors had almost an order of magnitude smaller alignment errors. Author

20 SPACECRAFT PROPULSION AND POWER

Includes main propulsion systems and components, e.g., rocket engines; and spacecraft auxilliary power sources.

For related information see also *07 Aircraft Propulsion and Power, 28 Propellants and Fuels, 44 Energy Production and Conversion,* and *15 Launch Vehicles and Space Vehicles.*

N91-16062 Utah State Univ., Logan.
OPTIMAL ROCKET MOTOR DESIGN AND CONTROL FOR TACTICAL MISSILES Ph.D. Thesis
Steven R. Wassom 1990 105 p
Avail: Univ. Microfilms Order No. DA9034098

The necessary conditions for the optimal thrust of a solid-propellant rocket motor are derived, and the results are applied to the design of conventional motors and pulse motors. The necessary conditions are derived and first applied to missiles flying at constant altitude. The resulting optimum thrust profile boosts the missile to an optimum cruising velocity and sustains the velocity with thrust equal to drag. Near-optimum thrust and flight path for variable-altitude trajectories are found using a heuristic procedure. The numerical examples show that pulse motors achieve the largest flight envelope because of higher delivered impulse and the ability to vary the coast times to achieve near-optimum cruising velocity for a variety of target conditions. Dissert. Abstr.

N91-16063*# Aerojet TechSystems Co., Sacramento, CA. Propulsion Div.
HIGH TEMPERATURE OXIDATION-RESISTANT THRUSTER RESEARCH Final Report
John R. Wooten and P. Tina Lansaw Feb. 1990 282 p
(Contract NAS3-24643)
(NASA-CR-185233; NAS 1.26:185233) Avail: NTIS HC/MF A13 CSCL 21H

A program was conducted for NASA-LeRC by Aerojet Propulsion Division to establish the technology base for a new class of long-life, high-performance, radiation-cooled bipropellant thrusters capable of operation at temperatures over 2200 C (4000 F). The results of a systematic, multi-year program are described starting with the preliminary screening tests which lead to the final material selection. Life greater than 15 hours was demonstrated on a workhorse iridium-lined rhenium chamber at chamber temperatures between 2000 and 2300 C (3700 and 4200 F). The chamber was fabricated by the Chemical Vapor Deposition at Ultramet. The program culminated in the design, fabrication, and hot-fire test of an NTO/MMH 22-N (5-lbF) class thruster containing a thin wall iridium-lined rhenium thrust chamber with a 150:1 area ratio nozzle. A specific impulse of 310 seconds was measured and front-end thermal management was achieved for steady state and several pulsing duty cycles. The resulting design represents a 20 second specific impulse improvement over conventional designs in which the use of disilicide coated columbium chambers limit operation to 1300 C (2400 F). Author

N91-16064*# Thiokol Corp., Brigham City, UT. Space Operations.
SPACE SHUTTLE FLIGHT SUPPORT MOTOR NO. 1 (FSM-1) Final Test Report
Phil D. Hughes 13 Nov. 1990 124 p
(Contract NAS8-30490)
(NASA-CR-184078; NAS 1.26:184078; TWR-50068; PUBL-910801) Avail: NTIS HC/MF A06 CSCL 21H

Space Shuttle Flight Support Motor No. 1 (FSM-1) was static test fired on 15 Aug. 1990 at the Thiokol Corporation Static Test Bay T-24. FSM-1 was a full-scale, full-duration static test fire of a redesigned solid rocket motor. FSM-1 was the first of seven flight support motors which will be static test fired. The Flight Support Motor program validates components, materials, and manufacturing processes. In addition, FSM-1 was the full-scale motor for qualification of Western Electrochemical Corporation ammonium

perchlorate. This motor was subjected to all controls and documentation requirements CTP-0171, Revision A. Inspection and instrumentation data indicate that the FSM-1 static test firing was successful. The ambient temperature during the test was 87 F and the propellant mean bulk temperature was 82 F. Ballistics performance values were within the specified requirements. The overall performance of the FSM-1 components and test equipment was nominal. Author

23 CHEMISTRY AND MATERIALS (GENERAL)

N91-16065*# Eloret Corp., Sunnyvale, CA.
THEORETICAL STUDY OF THE C-H BOND DISSOCIATION ENERGY OF ACETYLENE
Peter R. Taylor, Charles W. Bauschlicher, Jr., and Stephen R. Langhoff (National Aeronautics and Space Administration. Ames Research Center, Moffett Field, CA.) 1990 15 p
(Contract NCC2-371)
(NASA-CR-187858; NAS 1.26:187858) Avail: NTIS HC/MF A03 CSCL 07A

The authors present a theoretical study of the convergence of the C-H bond dissociation energy (D sub o) of acetylene with respect to both the one- and n-particle spaces. Their best estimate for D sub o of 130.1 plus or minus 1.0 kcal/mole is slightly below previous theoretical estimates, but substantially above the value determined using Stark anticrossing spectroscopy that is asserted to be an upper bound. Author

24 COMPOSITE MATERIALS

Includes physical, chemical, and mechanical properties of laminates and other composite materials.

For ceramic materials see *27 Nonmetallic Materials*.

N91-16066# Edgerton, Germeshausen and Grier, Inc., Idaho Falls, ID.
ACOUSTICAL AND DYNAMIC MECHANICAL CHARACTERIZATION OF FIBER-MATRIX INTERFACE BONDS IN CERAMIC COMPOSITES
L. A. Lott and D. C. Kunerth 1989 7 p Presented at the 16th Annual Review of Progress in Quantitative Nondestructive Evaluation, Brunswick, ME, 23-28 Jul. 1989 Submitted for publication
(Contract DE-AC07-76ID-01570)
(DE90-010949; EGG-M-89151; CONF-890770-10) Avail: NTIS HC/MF A02

Ceramic matrix composites presently being developed are potentially well suited for high temperature structural applications. The character of the fiber-matrix bond plays a significant role in determining the fracture toughness of the material and thus its performance. Increased toughness is achieved by phenomena such as interface debonding and fiber slip or pull-out, which improve material toughness by increasing the energy required to propagate a crack. In a bond that is too weak, the toughening mechanisms are not significant. However, a bond that is too strong permits a crack to propagate directly through a fiber-matrix interface without being significantly affected, resulting in brittle fracture. As a result, care is required in the manufacture of these materials to achieve optimum fiber-matrix bonding. The objective of this work is to develop and evaluate techniques to nondestructively characterize the fiber-matrix interface bonds. The techniques being investigated include ultrasonic velocity and attenuation, acousto-ultrasonic response, and internal dynamic mechanical damping. DOE

N91-16067# California Univ., San Diego, La Jolla. Dept. of Applied Mechanics and Engineering Sciences.
MECHANICS OF INTERFACE CRACKS
27 Sep. 1990 84 p
(Contract N00014-90-J-1398)
(AD-A227579) Avail: NTIS HC/MF A05 CSCL 11/4

Fracture of advanced materials, such as intermetallic alloys, ceramics, and composite materials nearly always begins at interfaces of one sort or another. Fibrous fractures, for example, initiate at the interfaces between second phase particles and the ductile matrix; the conditions for this to occur are sensitive to both matrix constitutive properties as well as to the chemistry and structure of the interfaces between the two phases. Interfacial cleavage involves the initiation of micrto-cracks and their propagation along interfaces and transgranular cleavage often initiates at interfacial sites, e.g., twin boundaries in intermetallic compounds, especially those with non-cubic crystal structures. Here again, the conditions required for this to occur are sensitive to the constitutive properties of the matrix materials as well as to the interfacial properties themselves. Intermetallic alloys, in particular, are known to possess complicated thermal and strain rate dependencies that can lead to either brittle or ductile behavior which in any event are very much dependent upon the loading conditions. GRA

N91-16068# Army Materials Technology Lab., Watertown, MA. Polymer Research Branch.
FLAMMABILITY CHARACTERISTICS OF FIBER-REINFORCED COMPOSITE MATERIALS FOR THE COMPOSITE INFANTRY FIGHTING VEHICLE Final Report
Domenic P. Macaione Sep. 1990 34 p Presented at the 197th Meeting of the American Chemical Society, Dallas, TX, Apr. 1989
(DA Proj. 162-63102-D-071)
(AD-A227783; MTL-TR-90-45) Avail: NTIS HC/MF A03 CSCL 11/4

The use of composites in Army systems as a means of decreasing weight and enhancing survivability, without reducing personnel safety, has been considered for sometime. The U.S. Army Materials Technology Laboratory (MTL) has successfully demonstrated, in an earlier program, that a ground vehicle turret could be fabricated from fiber reinforced composite material. That technology has now been applied to the fabrication of a composite vehicle hull. Organic polymers are one of the major constituents of fiber reinforced composites. As components of military systems, these materials are expected to survive combustion and pyrolysis processes associated with fires. It is thus necessary to develop an understanding of the flammability behavior of composite materials in the early design stages of a military vehicle such as the Composite Infantry Fighting Vehicle (CIFV). An attempt was made to characterize the flammability behavior of composite materials associated with the CIFV Hull Program in terms of accepted fire resistance parameters. GRA

N91-16069# National Aerospace Lab., Tokyo (Japan).
FUNDAMENTAL VERIFICATION OF TAILORING TECHNOLOGY FOR CONTROL OF A COEFFICIENT OF THERMAL EXPANSION BY COMPOSITE TESTING FACILITIES
Takashi Ishikawa, Hisao Fukunaga, Yoichi Hayashi, Masamichi Matsushima, and Tatsuru Noguchi Mar. 1990 19 p
(NAL-TR-1058; ISSN-0389-4010) Avail: NTIS HC/MF A03

Fundamentals of lamination tailoring technology are proposed here in order to control one coefficient of thermal expansion of carbon/epoxy composites in one principal direction. The theory of this technology consists of the two concepts of thermoelastic invariants and lamination parameters. The expansion free condition yields to a parabola in the feasible region of the lamination parameters. The calculated curves for a wide range of temperatures intersect at almost the same point. A laminate with the lay-up construction corresponding to this point exhibits an approximately null coefficient of thermal expansion in one direction in that temperature range. Experimental results with plate and tubular specimens indicate that the present technology is fundamentally verified. Author

N91-16070# Aeronautical Research Inst. of Sweden, Stockholm. Dept. of Structures.
PILOT STUDY OF THE DYNAMIC IMPACT RESPONSE OF A COMPOSITE PLATE
Robin Olsson and Per Gren (Lulea Univ., Sweden) Oct. 1990 24 p Sponsored by Swedish Defence Material Administration
(FFA-TN-1990-27; ETN-91-98402) Avail: NTIS HC/MF A03

An experimental pilot study of the dynamic response of composite plates in low mass impacts is described. The purpose was to make an initial investigation of the validity of an analytical impact solution recently presented. In the experiments a small spherical pendulum was used to strike a carbon fiber/epoxy laminate at various impact velocities. The time histories of the impactor acceleration (contact force), plate displacement and flexural strains were recorded. The plate displacement history was studied using holographic laser interferometry. Only a limited number of displacement results were obtained, since the holographic method leads to a very large number of densely spaced interference fringes even at moderate impact velocities. The theoretical predictions of contact force and plate displacement were found to be very good, although the flexural strains were only predicted qualitatively. An almost linear relation was found between impact velocity and the maximum values of contact force, plate displacement and flexural strains, which is in excellent agreement with the analytical predictions. ESA

N91-16071# Naval Postgraduate School, Monterey, CA. Dept. of Mechanical Engineering.
CHARACTERIZATION OF THE CORROSION OF A P-130x GRAPHITE FIBER REINFORCED 6063 ALUMINUM METAL MATRIX COMPOSITE M.S. Thesis
Joel David King Dec. 1989 90 p
(AD-A228134) Avail: NTIS HC/MF A05 CSCL 11/4

The corrosion behavior of a P-130x graphite fiber reinforced 6063 aluminum 0-90 cross plied metal matrix composite was studied. Electrochemical tests were performed on the composite and the monolithic matrix metal in aqueous 3.5 percent NaCl solutions. Immersion tests were performed on the composite in aqueous 3.5 percent NaCl solutions. The effects of pH, the presence of sulfite ions, and various heat treatments were investigated. The electrochemical tests included studies of galvanic corrosion, corrosion potential, galvanostaircase cyclic polarization and polarization resistance. Immersion tests showed accelerated corrosion at the exposed interfaces, with preferential attack at transverse fiber layers. Galvanic corrosion was large at low pH values, large graphite area fractions and when the matrix was in the over-aged state. The corrosion potential of the composite was found to be electronegative to the monolith when the Gr-Al interfaces were exposed to the electrolyte. Low pH values and over-aging increased pitting susceptibility. Solutionizing and quenching lowered pitting susceptibility at pH 8 but increased it at pH 4. Low pH values, the presence of sulfite ions and over-aging increased general corrosion rates. GRA

N91-16072# Factory Mutual Research Corp., Norwood, MA.
FLAMMABILITY CHARACTERISTICS OF FIBER REINFORCED COMPOSITE MATERIALS Final Report, Jun. 1987 - Jun. 1989
A. Tewarson Aug. 1990 85 p
(Contract DAAL04-87-C-0078; DA Proj. 162-63102-DO-71)
(AD-A228215; MTL-TR-90-41) Avail: NTIS HC/MF A05 CSCL 11/4

Fiber reinforced composite (FRC) materials are used extensively because of their physicochemical properties and high strength-to-weight ratio. The use of composites in U.S. Army vehicles, to decrease weight and enhance survivability, has been considered for some time. This report describes the results of a study undertaken by the Factory Mutual Research Corporation (FMRC) on FRC materials for possible composite combat vehicle applications on behalf on the U.S. Army Materials Technology Laboratory. The objective of the study was to assess the flammability characteristics of FRC materials using small-scale experiments. In the study, five FRC samples (about 3 to 45 mm in thickness) were examined. Results from the study showed that FRC materials have high resistance to ignition, a high heat of gasification and a low Fire Propagation Index (FPI), indicating that self-sustained fire propagation is expected to be difficult for these materials (fire are not expected to propagate beyond the ignition zone). Thus, these results suggest that FRC materials would not present as severe a fire hazard as ordinary combustibles; i.e., cellulosics and most plastics. GRA

N91-16073# Army Lab. Command, Watertown, MA. Material Technology Lab.
MECHANICAL BEHAVIOR OF A SiC-FIBER/Si3N4 COMPOSITE
Jeffrey J. Swab, George D. Quinn, and Daniel J. Snoha Sep. 1990 20 p
(Contract DE-AI05-84OR-21411)
(AD-A228371; MTL-TN-90-2) Avail: NTIS HC/MF A03 CSCL 11/4

The room and elevated temperature mechanical properties of a silicon carbide fiber/silicon nitride matrix composite were examined. The findings showed that the addition of fiber layers to a ceramic matrix eliminates the catastrophic brittle failure at room temperature. As the test temperature increases, the tendency for failure to proceed in a brittle manner increases. This is most likely due to an increase in the fiber/matrix bond strength which does not allow for fiber pullout and crack bridging to occur. GRA

N91-16074 Pittsburgh Univ., PA.
THE OXIDATION BEHAVIOR OF CARBON-CARBON COMPOSITES AND THEIR COATINGS Ph.D. Thesis
Jon Conrad Schaeffer 1989 285 p
Avail: Univ. Microfilms Order No. DA9021452

The oxidation of carbon-carbon composites and coatings in oxygen at temperatures between 300 and 1400 C was investigated. State-of-the-art systems were characterized prior to the oxidation studies using optical and scanning electron microscopy. It was determined that uncoated carbon-carbon composites cannot be used at temperatures above about 400 C for extended periods of time because of oxidation. Oxidation does occur at temperatures below 400 C but at very low rates. Boron was found to be an ineffective inhibitor for carbon-carbon oxidation. Coatings were useful in protecting carbon-carbon composites from oxidation under isothermal test conditions but these coatings failed under cyclic conditions. The factors leading to the failure of coatings on carbon-carbon composites are described. Dissert. Abstr.

N91-16075*# National Aeronautics and Space Administration. Lewis Research Center, Cleveland, OH.
EFFECTS OF HIGH PRESSURE NITROGEN ON THE THERMAL STABILITY OF SiC FIBERS
Martha H. Jaskowiak Jan. 1991 18 p Submitted for publication
(NASA-TM-103245; E-5671; NAS 1.15:103245) Avail: NTIS HC/MF A03 CSCL 11D

Polymer-derived SiC fibers were exposed to nitrogen gas pressures of 7 and 50 atm at temperatures up to 1800 C. The fiber weight loss, chemical composition, and tensile strength were then measured at room temperature in order to understand the effects of nitrogen exposure on fiber stability. High pressure nitrogen treatments limited weight loss to 3 percent or less for temperatures up to 1800 C. The bulk Si-C-O chemical composition of the fiber remained relatively constant up to 1800 C with only a slight increase in nitrogen content after treatment at 50 atm; however, fiber strength retention was significantly improved. To further understand the effects of the nitrogen atmosphere on the fiber stability, the results of previous high pressure argon treatments were compared to those of the high pressure nitrogen treatments. High pressure inert gas can temporarily maintain fiber strength by physically inhibiting the evolution of gaseous species which result from internal reactions. In addition to this physical effect, it would appear that high pressure nitrogen further improved fiber temperature capability by chemically reacting with the fiber surface, thereby reducing the rate of gas evolution. Subsequent low pressure argon treatments following the initial nitrogen treatments resulted

in stronger fibers than after argon treatment alone, further supporting the chemical reaction mechanism and its beneficial effects on fiber strength. Author

N91-16076# Messerschmitt-Boelkow-Blohm G.m.b.H., Munich (Germany, F.R.). Hubschrauber und Flugzeuge.
BUMP EXAMINATIONS OF INTEGRALLY STRENGTHENED CARBON FIBER REINFORCED PLASTIC PANELS [BEULUNTERSUCHUNGEN AN INTEGRALVERSTEIFTEN CFK-PANELS]
K. Brunner and K. Pfister 20 Jul. 1990 15 p In GERMAN Presented at DGLR-Jahrestagung 1989, Hamburg, Fed. Republic of Germany, 2-4 Oct. 1989
(MBB/FE281/CFK/PUB/0013; ETN-91-98548) Copyright Avail: NTIS HC/MF A03

The appearance of bumps on carbon fiber reinforced plastic aircraft structures is investigated. Static and dynamic experiments were carried out with determination of the residual strength by means of tests which were carried out in accordance to the constructive requirements of modern high power aircraft. The bump initiation was detected with experimental measurement processes based on the failure charge. The functioning charge was shown to have no influence on the residual strength despite the high bump excess. The measurement Moire process was successfully implemented so that a routine utilization is possible. ESA

N91-16077# British Petroleum Co. Ltd., Sunbury-on-Thames (England).
METALLURGICAL DESIGN OF NOVEL METAL MATRIX COMPOSITES FOR AEROSPACE APPLICATIONS
W. S. Miller and A. D. Tarrant 22 Nov. 1990 39 p Presented at TMS Meeting on Lightweight Alloys for Aerospace Applications, 4, Las Vegas, NV, 27 Feb. 1989
(ETN-91-98573) Avail: NTIS HC/MF A03

The interactions between matrix alloys, ceramic reinforcement, and material processing parameters on the microstructure property relationship are discussed in relation to the potential future material requirements of the aerospace industry. Metal matrix composites were shown to be useful in aerospace design in terms of performance improvement and weight savings. The ceramic reinforcement directly influences the composite fracture but also modifies the matrix alloy structure. Aluminum-lithium alloys, magnesium alloys, or boron carbide are particularly recommended. ESA

25 INORGANIC AND PHYSICAL CHEMISTRY

Includes chemical analysis, e.g., chromatography; combustion theory; electrochemistry; and photochemistry.

For related information see also *77 Thermodynamics and Statistical Physics.*.

N91-16078*# Jet Propulsion Lab., California Inst. of Tech., Pasadena.
SPRAY COMBUSTION MODELING AND EVALUATION
Lloyd H. Back, Josette Bellan, P. Shakkottai, Eug Kwack, and K. Harstad Dec. 1989 137 p
(Contract DE-AI01-86CE-90237)
(NASA-CR-187887; NAS 1.26:187887; DE90-010058; JPL-D-6847) Avail: NTIS HC/MF A07 CSCL 21B

The overall objective of this task is to produce and evaluate an analytical model of multicomponent-fuel spray combustion. It is intended that such a model could ultimately be incorporated into a composite computer program for predicting the performance of furnace and boiler designs fired with arbitrary liquid fuels. The primary intermediate objectives for CY 1989 are to: model the evaporation of individual multicomponent fuel drops, and initiate experiments designed to validate evaporation models developed under this program. DOE

N91-16079# Sandia National Labs., Albuquerque, NM. Fluid Mechanics and Heat Transfer Div. 1.
THE EFFECT OF STRATIFICATION ON GRAVITATIONAL COAGULATION AND SETTLING OF AEROSOLS
L. A. Mondy and S. K. Griffiths Mar. 1990 16 p
(Contract DE-AC04-76DP-00789)
(DE90-010153; SAND-87-0645) Avail: NTIS HC/MF A03

The differential equations describing the gravitational collision and coalescence of aerosol particles were solved numerically, using an explicit two step marching procedure, for the simple case of a single component aerosol settling in a quiescent environment. The initial particle size distribution is arbitrary and is allowed to change in time due to coagulation and loss due to precipitation. These equations are solved at discrete heights, with the aerosol assumed to be homogeneous (well mixed) in each height interval. The term describing precipitation allows for the transfer of mass from one height to the next lower and, so on, to the ground. This allows 1-D spatial stratification to develop when larger particles, that continue to grow due to coagulation, settle faster than the smaller particles. Numerical studies show that stratification in particle size and concentration can be significant in some cases. Stratification rates increase as the initial concentration of particles increases and as the range of initial particle sizes increases. Comparison of results from a well mixed model and a height dependent model shows that significant differences in the predicted fallout rates can occur. DOE

N91-16080# Lawrence Livermore National Lab., CA.
A NUMERICAL STUDY OF SILANE COMBUSTION
J. A. Britten, J. Tong, and C. K. Westbrook Dec. 1989 17 p Presented at the 23rd Combustion Inst. Symposium on Combustion, Orleans, France, 22-27 Jul. 1990 Submitted for publication
(Contract W-7405-eng-48)
(DE90-006002; UCRL-102584; CONF-900704-4) Avail: NTIS HC/MF A03

A kinetic model of the mechanism of silane combustion was developed, using a system of 70 elementary reaction steps and 25 chemical species. The model was used to examine silane ignition at ordinary pressures under both shock tube conditions and low temperature constant-volume conditions. The agreement between model predictions and experimental data is very good, both with respect to shock tube ignition delay times and to the pronounced, nonlinear variation of autoignition time with initial pressure at near ambient temperatures. The model also reproduces observed trends in H2/H2O product yield as a function of the initial SiH4/O2 ratio. One key to this mechanism is competition between thermal stabilization and chain branching decomposition reactions of an excited state silylperoxy radical, and a second key is the reaction of water vapor with intermediate species containing a SiO double bond. DOE

N91-16081# Massachusetts Inst. of Tech., Cambridge.
MODELLING OF FLAMELET SURFACE-TO-VOLUME RATIO IN TURBULENT PREMIXED COMBUSTION
R. S. Cant, S. B. Pope, and K. N. C. Bray 1990 14 p Presented at the 23rd Combustion Inst. Symposium on Combustion, Orleans, France, 22-27 Jul. 1990
(Contract DE-FG02-86ER-13553)
(DE90-006312; CONF-900704-7) Avail: NTIS HC/MF A03

A model is proposed, valid in the laminar flamelet regime, for the surface-to-volume ratio of a turbulent premixed flame. The new model is in a form suitable for incorporation into an existing model of turbulent premixed combustion. Exact equations are derived which describe the dynamics of the constant-property surface representing the flame interface. Unknown terms in the exact equations are modelled for the simplified case of constant-density combustion in a specified turbulence field. Numerical solutions of the modelled equations are carried out for a 1-D test case. Preliminary results indicate that the model is capable of predicting effects present in turbulent flame propagation, and a parametric study shows that correct trends are observed. DOE

N91-16082# Lawrence Livermore National Lab., CA.
AUTO-IGNITION TEMPERATURES OF BINARY MIXTURES OF ALKANES IN A CLOSED VESSEL: COMPARISONS BETWEEN EXPERIMENTAL MEASUREMENTS AND NUMERICAL PREDICTIONS
J. F. Griffiths, D. Coppersthwaite, C. H. Phillips (Leeds Univ., England), C. K. Westbrook, and W. J. Pitz 1990 22 p Presented at the 23rd Combustion Inst. Symposium on Combustion, Orleans, France, 22-27 Jul. 1990 Sponsored in part by Health and Safety Executive, England
(Contract W-7405-eng-48)
(DE90-007856; UCRL-102778; CONF-900704-8) Avail: NTIS HC/MF A03

Autoignition temperatures of the binary mixtures methane + ethane and methane + butane in air were measured at atmospheric pressure in a 0.56 d cu m spherical reaction vessel. The method used followed that for standard ASTM and BS tests for gaseous fuels. Fixed proportions by volume of the total fuel in air were studied, which correspond at the extreme of each composition range to the equivalence ratios for methane, ethane and butane of phi = 0.93, 1.63 and 3.04, respectively. Supplementary experiments were carried out on butane alone under the same conditions, in which its proportion was varied in the equivalence range where phi is between 0 and 3.04. The autoignition of methane was sensitized by ethane most strongly when the ethane was present at up to 10 percent of the total fuel. The autoignition temperature (T sub a,cr) was reduced by 40 K with respect to that for pure methane (T sub a,cr = 900 K). There was an even stronger sensitization by similar proportions of butane added to methane, such that T sub a,cr decreased to 810 K. In neither case were the effects linearly dependent on the proportion of additive. There was an addition sensitive region when butane was present in the proportion 0.5 to 0.7 of the methane/butane mixture, at which T sub a,cr fell sharply by 50 K over this limited composition range. Remarkably, except at the leanest mixtures, the autoignition temperatures of compositions containing butane alone matched very closely the autoignition temperatures of the equivalent methane/butane mixtures. It is believed that this is a new and very important observation in relation to the understanding and interpretation of combustion hazards involving mixtures of fuels. DOE

N91-16083# Georgia Inst. of Tech., Atlanta. School of Chemistry.
FUNDAMENTAL STUDIES WITH A MONODISPERSE AEROSOL-BASED LIQUID CHROMATOGRAPHY/MASS SPECTROMETRY INTERFACE (MAGIC-LC/MS) Progress Report, 1 Sep. 1985 - 30 Nov. 1989
Richard F. Browner May 1989 12 p
(Contract DE-FG05-85ER-13435)
(DE90-010667; DOE/ER-13435/4) Avail: NTIS HC/MF A03

A number of accomplishments have been made during the term of this grant. These include both technical aspects of the project, and developments associated with commercial development of the MAGIC-LC/MS interface. Technical advances have been made through a number of detailed studies of fundamental processes occurring with the interface. These have led to substantial improvements in the performance of the interface many of which are detailed below. Of particular importance has been a major improvement in detection capabilities. At the beginning of this grant period, sensitivity for many compounds was in the high microgram to low mg range. Presently, full-scan (40 to 400 daltons) electron impacts mass spectra may be obtained for many compounds with typically 10 to 50 ng of material injected on column. Selected ion monitoring gives detection limits in the range of 100 to 1000 pg. These figures are particularly noteworthy because they represent values which fall between 3 to 10 times the lowest detection limits possible with the same instrument when used in a GC/MS mode. DOE

N91-16084# Lawrence Livermore National Lab., CA.
THE NEW LLNL AMS SPECTROMETER
J. R. Southon, M. W. Caffee, J. C. Davis, T. L. Moore, I. D. Proctor, B. Schumacher, and J. S. Vogel 18 Apr. 1990 12 p Presented at the 5th International Conference on Accelerator Mass Spectrometry, Paris, France, 23-27 Apr. 1990
(Contract W-7405-eng-48)
(DE90-010868; UCRL-102983; CONF-900491-4) Avail: NTIS HC/MF A03

The multi-user tandem laboratory at Lawrence Livermore is a new facility dedicated to AMS and a variety of other ion beam analysis techniques. The AMS spectrometer design aims and implementation are presented here, and present performance and planned improvements are discussed. DOE

N91-16085# Los Alamos National Lab., NM.
DESTRUCTION OF PROPELLANT COMPONENTS IN SUPERCRITICAL WATER
Steven J. Buelow, R. Brian Dyer, Cheryl K. Rofer, Jerry H. Atencio, and Joseph D. Wander (Air Force Engineering and Services Center, Tyndall AFB, FL.) 1990 14 p Presented at the Workshop on the Alternative To Open Burning/Open Detonation of Propellants and Explosives, Panama City, Panama, 27-28 Mar. 1990 Sponsored in part by AFESC, Tyndall AFB, FL
(Contract W-7405-eng-36)
(DE90-010600; LA-UR-90-1338; CONF-9003153-1) Avail: NTIS HC/MF A03

Supercritical water oxidation is an innovative, relatively low-temperature process that can give high destruction efficiencies for a wide variety of hazardous chemical wastes. It takes place in a water medium with added oxidant above the critical point of water. In this paper we present preliminary results for the destruction of propellant components in supercritical water without added oxidant. Reactions of ammonium perchlorate and nitromethane are examined using a flow reactor made of Hastelloy C276 operated at temperatures as high as 580 C at pressures near 38.7 MPa. (5500 psig). Over 99.8 percent of the ammonium perchlorate is destroyed in less than 15 seconds at 500 C. The reaction produces primarily chloride ion, nitrous oxide, and oxygen. A small amount of the nitrogen is converted into nitrate ion and nitrite ion. No reaction is detected in 180 seconds at temperatures below 400 C. For nitromethane, over 99 percent is destroyed at 500 C within 30 seconds. The reaction produces negligible amounts of nitrate and nitrite. Effluents from both ammonium perchlorate and nitromethane experiments were analyzed for metal ions that could result from corrosion of the reactor. DOE

N91-16086# Cornell Univ., Ithaca, NY. Dept. of Microbiology.
CONVERSION OF ACETIC ACID TO METHANE BY THERMOPHILES Progress Report, 15 May 1985 - 15 May 1990
S. H. Zinder 1990 9 p
(Contract DE-FG02-85ER-13370)
(DE90-010993; DOE/ER-13370/1) Avail: NTIS HC/MF A02

The goal of this project is to gain a more complete understanding of the microorganisms converting a lignocellulose waste to methane in a thermophilic (58 C) anaerobic bioreactor. To accomplish this, we have directly examined microbial populations in the bioreactor and have examined the properties of microorganisms isolated from the bioreactor. The primary focus has been on anaerobic thermophiles involved in the formation and degradation of acetic acid, the precursor of two thirds of the methane produced in the bioreactor. Also, novel organisms of fundamental and practical significance have been isolated and characterized. As the project has progressed there has been greater emphasis on the physiology of pure cultures. DOE

N91-16087# Lawrence Livermore National Lab., CA.
MICROWAVE MEASUREMENTS OF WATER VAPOR PARTIAL PRESSURE AT TEMPERATURES UP TO 350 C
Victor R. Latorre Sep. 1989 10 p Presented at the Nuclear Waste Isolation in the Unsaturated Zone: FOCUS 1989, Las Vegas, NV, 18-21 Sep. 1989
(Contract W-7405-eng-48)
(DE90-011484; UCRL-101866; CONF-890928-24) Avail: NTIS HC/MF A02

This paper describes the theory of operation, design, construction, calibration and installation of a microwave coaxial resonator system for measuring the partial pressure of water vapor in air at temperatures up to 350 C. This is a relevant measurement for characterizing the unsaturated zone because the partial pressure of water vapor in the air in equilibrium with a rock mass is related to the capillary pressure of the rock. Microwave resonators can operate at high temperatures and, therefore, are the subject of this discussion. DOE

N91-16088# Lawrence Livermore National Lab., CA.
THE DESIGN AND CONSTRUCTION OF AN AUTOMATED MULTI-OBJECT SPECTROSCOPY SYSTEM (AMOS)
Jean P. Brodie, R. Hank Donnelly, Jay V. Bixler, Charles J. Hailey, Lynn G. Seppala, and William W. Craig (California Univ., Berkeley.) 15 Mar. 1990 7 p Presented at the SPIE Astronomical Telescopes and Instrumentation for the 21st Century Symposium, Tucson, AZ, 11-17 Feb. 1990 Sponsored by Institute for Geophysics and Planetary Physics and CALCOR
(Contract W-7405-eng-48)
(DE90-011497; UCRL-JC-10397; CONF-900285-4) Avail: NTIS HC/MF A02

An automated multi-object spectroscopy system (AMOS) is being developed for use on the 3-meter telescope at Lick Observatory. The overall design is compatible with the eventual goal of acquiring up to one hundred spectra simultaneously in a one degree field of view. The speed and accuracy of AMOS preserve the real time decision making and field changing flexibility associated with traditional single-source observing techniques. AMOS will operate at the 3-meter prime focus and will feed a floor-mounted spectrography. We describe some engineering design details and the results of laboratory and 1-meter telescope testing of AMOS. DOE

N91-16089# Ames Lab., IA. Dept. of Chemical Engineering.
FUNDAMENTAL STUDIES OF HYDROCARBON CONVERSIONS OVER SUPPORTED BIMETALLIC CATALYSTS Ph.D. Thesis
Mark Wilton Smale Jan. 1990 169 p
(Contract W-7405-eng-82)
(DE90-011744; IS-T-1405) Avail: NTIS HC/MF A08

The reactions of ethane and ethylene over selected silica-supported group 8 metal catalysts have been investigated using reaction studies and nuclear magnetic resonance (NMR) spectroscopy. The activity of the ruthenium-group IB bimetallic system for the ethane hydrogenolysis reaction was investigated as a function of group IB metal content and ethane and hydrogen partial pressures, while the reactions of ethylene over silica-supported platinum catalysts were studied using NMR. The turnover frequency of the silica-supported ruthenium catalysts for ethane hydrogenolysis as either copper or silver was added. This tended to change as the group IB metal was first added until a critical point was reached. The apparent orders of reaction for ethane hydrogenolysis over the ruthenium-group IB catalysts was measured as a function of temperature. The reactions of ethylene over silica-supported platinum catalysts has been investigated using NMR. The ethylene to surface platinum atom ratio used in this work was in the 10 to 20 range, far higher than that used for typical single crystal studies. DOE

N91-16090# Los Alamos National Lab., NM.
IMPURITY TOLERANT ELECTROCATALYSTS
Mark T. Paffett 1990 10 p Presented at the Fuel Cells Contractors Review, Morgantown, WV, 2-3 May 1990
(Contract W-7405-eng-36)
(DE90-011960; LA-UR-90-1603; CONF-900591-2) Avail: NTIS HC/MF A02

Two central goals were persued. The primary research effort addresses fundamental aspects of Pt electrocatalyst poisoning by CO and an understanding of practical schemes for improving the CO tolerance of electrocatalytic materials. The second mission is an attempt to address, on a fundamental level, the surface chemical properties that enhance the direct electrooxidation of methanol at binary Pt alloy electrode surfaces. DOE

N91-16091# Los Alamos National Lab., NM.
TIME-RESOLVED COHERENT ANTI-STOKES RAMAN SPECTROSCOPY (CARS) AND THE MEASUREMENT OF VIBRATIONAL SPECTRA IN SHOCK-COMPRESSED MOLECULAR MATERIALS
David S. Moore and Stephen C. Schmidt 1990 8 p Presented at the Meeting on Optical Spectroscopic Instrumentation and Techniques for the 1990s: Applications in Astronomy, Chemistry and Physics, Las Cruces, NM, 4-6 Jun. 1990
(Contract W-7405-eng-36)
(DE90-012053; LA-UR-90-1809; CONF-900656-1) Avail: NTIS HC/MF A02

The use of coherent anti-Stokes Raman scattering (CARS) in conjunction with a two-stage light gas gun to obtain vibrational spectra of shock compressed liquid N2, O2, CO, and their mixtures is presented. The experimental spectra are compared to spectra calculated using a semiclassical model for CARS intensities to obtain vibrational frequencies, peak Raman susceptibilities, and linewidths. The derived spectroscopic parameters suggest thermal equilibrium of the vibrational populations is established in less than a few nanoseconds after shock passage. Vibrational temperatures obtained are compared to those derived from equation-of-state calculations. Shifts in the vibrational frequencies reflect the influence of increased density and temperature on the intramolecular motion. DOE

N91-16092 New South Wales Univ., Canberra (Australia). Dept. of Inorganic and Nuclear Chemistry.
SYNTHESIS, CHARACTERIZATION AND CATALYTIC ACTIVITY OF MICROPOROUS ALUMINOPHOSPHATE CATALYSTS Ph.D. Thesis, 1989 Abstract Only
Eric Miles Kennedy 13 Feb. 1990 3 p
Avail: Issuing Activity

The oxidative dehydrogenation of methane, to form C2 and higher hydrocarbons, over microporous aluminophosphate molecular sieves was studied. The aluminophosphate AlPO5 was synthesized with one or more of 60 additional elements incorporated into the catalyst framework. The microporous substituted aluminophosphates (XAlPOs) were synthesized hydrothermally, from a gel consisting of aluminum, phosphorus, water, an organic templating agent, and the element (X) to be incorporated into the crystal framework. Some synthesis parameters were studied and generalizations were made. The solids were dried after synthesis (110 C) and slowly calcined in air (heating of the catalyst from room temperature to 750 C at 35 degrees/hour) to remove water and the organic template. X ray powder diffraction patterns and Al-25 MAS NMR spectra of all samples both synthesized and after calcination, were obtained. Al-27 MAS NMR was used to monitor the presence of octahedral and tetrahedral aluminum phases present in the (X)AlPO sample. Nitrogen adsorption measurements were used to determine the surface area of the calcined (X)AlPO. Surface areas ranged from 25 to 620 sq m/gram. A total of 44 different XAlPO catalysts synthesized were tested for activity in the oxidative dehydrogenation of methane. Methane:oxygen mixtures were passed over a bed of (X)AlPO catalyst at elevated temperatures, and the conversion products analyzed by an on-line gas chromatograph. Author

N91-16093# Los Alamos National Lab., NM.
MAGNETIC STRUCTURES OF ACTINIDE MATERIALS BY PULSED NEUTRON DIFFRACTION
A. C. Lawson, J. A. Goldstone, J. G. Huber, A. L. Giorgi, J. W. Conant, A. Severing, B. Cort, and R. A. Robinson 1990 18 p Presented at the Conference on Magnetism and Magnetic Materials, San Diego, CA, 30 Oct. - 2 Nov. 1990
(Contract W-7405-eng-36)
(DE91-000373; LA-UR-90-3166; CONF-901004-5) Avail: NTIS HC/MF A03

Some attempts to observe magnetic structure in various actinide (5f-electron) materials are described. The experimental technique is neutron powder diffraction as practiced at a spallation (pulsed) neutron source. The investigations of (alpha)-Pu, (delta)-Pu, (alpha)-UD3 and (beta)-UD3 are discussed. The (beta)-UD3 is a

simple ferromagnet: surprisingly, the moments on the two non-equivalent uranium atoms are the same within experimental error. The (alpha)-UD3, (alpha)-Pu and (delta)-Pu are non-magnetic, within the limits of the observations. The work with pulsed neutron diffraction shows that it is a useful technique for research on magnetic materials. DOE

N91-16094# Oak Ridge National Lab., TN. Analytical Chemistry Div.
APPLICATION OF DIODE LASERS TO RESONANCE IONIZATION MASS SPECTROMETRY
J. P. Young, R. W. Shaw, and D. H. Smith 1990 5 p Presented at the DOE Workshop on Advanced Laser Technology for Chemical Measurements, Oak Ridge, TN, 12-14 Nov. 1990
(Contract DE-AC05-84OR-21400)
(DE91-000614; CONF-9011110-1) Avail: NTIS HC/MF A01

Detailed studies of the application of diode lasers to resonance ionization mass spectrometry (RIMS) have been made. These devices were used to excite the first transition of several 1+1+1 multiple photon processes for both lanthanum 138 and 139. Enhanced isotopic selectivity resulted; very-high resolution spectra were also obtained with the diode laser step to yield new atomic hyperfine structure constants. DOE

N91-16095# Oak Ridge National Lab., TN. Analytical Chemistry Div.
ULTRASENSITIVE MOLECULAR FLUORESCENCE SPECTROSCOPY IN LEVITATED MICRODROPLETS
J. M. Ramsey, W. B. Whitten, S. Arnold, and B. V. Bronk (Army Chemical Research and Development Center, Aberdeen Proving Ground, MD.) 1990 3 p Presented at the DOE Workshop on Advanced Laser Technology for Chemical Measurements, Oak Ridge, TN, 12-14 Nov. 1990
(Contract DE-AC05-84OR-21400)
(DE91-000621; CONF-9011110-3) Avail: NTIS HC/MF A01

The extreme sensitivity of fluorescence spectrophotometry results from the fact that a molecule can undergo many excitation-emission cycles before destruction by photochemical degradation. For example, Rhodamine 6G (R6G) can emit in excess of 10(exp 5) photons before photolysis takes place. The fraction of emitted photons collected and converted to countable pulses can be as high as 10(exp -3), although 10(exp -4) is more readily attainable. Therefore, sufficient signal exists for single molecules to be detectable. Detection limits for molecules in solution were limited by background signal from solvent Raman scattering and fluorescence. This background signal adds noise to the measurement and has effectively restricted the detectable concentration to about 10(exp -13) M. Over the past decade, advances in detection of fewer molecules have all been made by reducing the measurement volume and/or increasing the measuring time. Given the above concentration detection limit a reduction of the measurement volume to 1 pL leads to a minimum observable quantity of approximately 1 molecule. The ability to detect a single molecule in condensed phase could have many important applications in addition to being an interesting problem. The obvious application of this approach is situations where small quantities of material are available for analysis. The capability to reliably detect a single fluorophore might also allow the screening and/or sorting of a collection of molecules. Such abilities would have application to many biological problems such as DNA sequencing and detection of DNA adducts. DOE

N91-16096# Oak Ridge National Lab., TN.
PICOSECOND MULTIPHOTON IONIZATION OF ATOMIC AND MOLECULAR CLUSTERS
John C. Miller and D. Barton Smith 1990 10 p Presented at the 5th International Conference on Multiphoton Processes, Paris, France, 24-28 Sep. 1990
(Contract DE-AC05-84OR-21400)
(DE91-000641; CONF-900926-3) Avail: NTIS HC/MF A02

High peak-power picosecond laser pulses have been used for the first time to effect nonresonant or resonant multiphoton ionization (MPI) of clusters generated in a supersonic nozzle expansion. The resulting ions are subsequently detected and characterized by time-of-flight mass spectroscopy. Specifically, results are presented involving MPI of clusters of xenon and nitric oxide. Previous MPI studies of many molecular clusters using nanosecond lasers have not been successful in observing the parent ion, presumably due to fast dissociation channels. It is proposed that the present technique is a new and rather general ionization source for cluster studies which is complementary to electron impact but may, in addition, provide unique spectroscopic or dynamical information. DOE

N91-16097# Army Chemical Research and Development Center, Aberdeen Proving Ground, MD.
COMPUTER-ASSISTED DETERMINATION OF MINIMUM ENERGY CONFORMATIONS. PART 4: ALPHA1 AND ALPHA2 ADRENERGIIC COMPOUNDS Final Report, Jan. 1988 - Feb. 1990
William P. Ashman and Alexander P. Mickiewicz Jun. 1990 74 p
(AD-A226811; CRDEC-TR-168) Avail: NTIS HC/MF A04 CSCL 07/4

Conformational minimum energy calculations were performed on 3-D representations of 56 selected adrenergic compounds to achieve molecular mechanics structure optimization (optimized geometries) using the empirical Molecular Mechanics II (MM2) computer program developed by Allinger and Yuh. The 3-D Cartesian atom coordinates for the minimum energy conformation of the 56 adrenergic compound are reported. The calculated optimized geometries results can be used as initial structural configurations in future structure-activity relationships and molecular-modeling studies of adrenergic compounds. GRA

N91-16098# Cornell Univ., Ithaca, NY. Dept. of Chemistry.
IN SITU STUDIES OF POTENTIAL DEPENDENT STRUCTURAL AND DISTRIBUTIONAL CHANGES AT ELECTROCHEMICAL INTERFACES WITH X RAYS
Hector D. Abruna, Mark Bommarito, and David Acevedo 29 Aug. 1990 12 p Sponsored by NSF; ARO; Eastman Kodak Co., Rochester, NY; and Xerox Corp.
(Contract N00014-84-K-0656)
(AD-A226844; TR-20) Avail: NTIS HC/MF A03 CSCL 20/2

The x ray standing-wave technique is applied in the in situ study of potential dependent structural and distributional changes of the I/Pt system and to the structural characterization of redox active self-assembling monolayers. GRA

N91-16099# San Diego State Univ., CA. Dept. of Chemistry.
INVERSE GAS CHROMATOGRAPHY Final Report, Feb. 1987 - Jan. 1990
R. J. Laub Sep. 1990 153 p
(Contract F04611-87-K-0006)
(AD-A227677; AL-TR-90-047) Avail: NTIS HC/MF A08 CSCL 07/6

Some fundamental aspects of the physicochemical characterization of propellant prepolymers were explored for the purpose of developing and optimizing analytical procedures for molecular weight, degree of branching, and functionality distributions. Inverse gas and gel permeation chromatography, and Fourier-transform infrared spectroscopy, were employed with bulk and fractionated R-45M. The methodologies and techniques of analysis ultimately developed make use only of readily available equipment, and are applicable to characterization and routine quality control of virtually and prepolymer system. GRA

N91-16100# Ames Lab., IA.
ELECTROCATALYSIS OF ANODIC AND CATHODIC OXYGEN-TRANSFER REACTIONS Ph.D. Thesis - Iowa State Univ.
Brian Reid Wels 21 Sep. 1990 119 p
(Contract W-7405-eng-82)
(DE91-000611; IS-T-1450) Avail: NTIS HC/MF A06

The electrocatalysis of oxygen-transfer reactions is discussed in two parts. In Part 1, the reduction of iodate (IO3(-)) is examined

as an example of cathodic oxygen transfer. On oxide-covered Pt electrodes (PtO), a large cathodic current is observed in the presence of IO3(-) to coincide with the reduction of PtO. The total cathodic charge exceeds the amount required for reduction of PtO and IO3(-) to produce an adsorbed product. An electrocatalytic link between reduction of IO3(-) and reduction of PtO is indicated. In addition, on oxide-free Pt electrodes, the reduction of IO3(-) is determined to be sensitive to surface treatment. The electrocatalytic oxidation of CN(-) is presented as an example of anodic oxygen transfer in Part 2. The voltametric response of CN(-) is virtually nonexistent at PbO2 electrodes. The response is significantly improved by doping PbO2 with Cu. Cyanide is also oxidized effectively at CuO-film electrodes. Copper is concluded to serve as an adsorption site for CN(-). It is proposed that an oxygen tunneling mechanism comparable to electron tunneling does not occur at the electrode-solution interface. The adsorption of CN(-) is therefore considered to be a necessary prerequisite for oxygen transfer. DOE

N91-16101# Argonne National Lab., IL. Materials Science Div.
HIGH RESOLUTION ELECTRON MICROSCOPY OF INTERFACES IN FCC MATERIALS
Karl L. Merkle Aug. 1990 64 p Presented at the International Conference on Frontiers of Electron Microscopy, Oak Brook, IL, 21-24 May 1990 Submitted for publication
(Contract W-31-109-eng-38)
(DE91-004420; CONF-9005145-3) Avail: NTIS HC/MF A04

Modern high-resolution electron microscopy (HREM) instruments, which are capable of a point-to-point resolution of better than 0.2 nm, have allowed atomic-scale observations of a variety of internal interfaces. The application of the HREM technique to fcc model systems for the purpose of addressing a number of interface issues will be examined in this paper. Atomic structure observations for heterophase interfaces of metal/metal and metal/metal-oxide systems as well as HREM studies of grain boundaries in NiO and Au will be discussed with emphasis on generic structural features and the role of the interface plane. Comparisons between observed interface structures and atomistic computer modeling results have shown agreements for some interfaces, as well as certain differences in others. A number of structural features are common to both metal and oxide grain boundaries, as well as certain heterophase boundaries. Of particular importance in close-packed solids appears to be the tendency to preserve, as much as possible, local atomic coordination, giving rise to atomically well-matched regions that alternate along the interface with regions of misfit. It is commonly observed that heterophase interfaces are being preferentially formed on dense-packed planes. Low-index planes are also frequently observed in asymmetric grain boundaries. In addition to the observation of misfit dislocations in heterophase boundaries, misfit-dislocation-like defects were also found in asymmetric, incommensurate grain boundaries. The tendency for maintaining coherence between dense-packed planes across the interface has resulted in the formation of three-dimensional GB structures. HREM observations have brought new insights into the correlations between macroscopic geometry, interfacial energy, and microscopic atomic relaxations. DOE

N91-16102# National Aerospace Lab., Tokyo (Japan).
AUTOIGNITION AND FLAMEHOLDING IN A CYLINDRICAL SCRAMJET COMBUSTOR
Kenji Kudou, Goro Masuya, Tomoyuki Komuro, Atsuo Murakami, and Nobuo Chinzei May 1990 11 p In JAPANESE; ENGLISH summary
(NAL-TR-1067; ISSN-0389-4010) Avail: NTIS HC/MF A03

Autoignition and flameholding characteristics of hydrogen fuel injected transversely to a supersonic air flow were experimentally examined in a cylindrical scramjet combustor with a rearward-facing step. Autoignition occurred when the air total temperature was above 1500 K. There were three categories of autoignition: (1) ignition occurred in the separation region at the combustor exit produced by a shock wave due to over-expansion of the flow; (2) ignition occurred in the regions of shock wave impinging on the combustor wall; and (3) ignition occurred in the vicinity of the injection holes or the step. The flameholding position moved complicatedly with the change of air total temperature. The position was at the step for air total temperatures below 1600 K, while it moved downstream of the step for temperatures between 1600 K and 2500 K. For temperatures above 2500 K, the flame was anchored by the step again. Author

N91-16103# Ultramet, Pacoima, CA.
HYDROGEN STORAGE IN METAL HYDRIDES Final Report, Sep. 1989 - Mar. 1990
Mark J. DelaRosa Aug. 1990 32 p
(Contract F04611-89-C-0047; AF Proj. 5730)
(AD-A228150; ULT/TR-90-7197; AL-TR-90-031) Avail: NTIS HC/MF A03 CSCL 11/6

The primary objective of this program was to develop an economical process for producing a lightweight hydrogen storage medium by the chemical vapor infiltration (CVI) of a metal hydride former into a reticulated foam substrate. An investigation was conducted to determine the most favorable precursors for forming the candidate hydride-forming materials, along with optimization of their transport and deposition parameters. A substrate optimization study was also performed in order to derive the greatest surface area-to-volume ratio from the resulting metal hydride-forming foam. Thermogravimetric analysis (TGA) was performed on a metal foam sample to determine its hydriding capability. Results were inconclusive, showing only slight if any hydriding. GRA

N91-16104# Ballistic Research Labs., Aberdeen Proving Ground, MD.
AN APPROXIMATION TO TRUE PEAK ABSORBANCE FROM OBSERVED PEAK ABSORBANCE FOR GAS PHASE FOURIER TRANSFORM SPECTROSCOPY Final Report, May 1988 - Jun. 1990
Kevin L. McNesby and Robert A. Fifer Sep. 1990 18 p
(DA Proj. 1L1-61102-AH-43)
(AD-A228357; BRL-TR-3159) Avail: NTIS HC/MF A03 CSCL 20/5

An approximation is developed to yield true peak absorbance, A sub p, from observed peak absorbance, A sub obs, from gas phase infrared spectra obtained using low resolution Fourier transform spectroscopy employing triangular apodization of the interferogram. The approximation is of the form A sub p = k((A sub obs) exp 1)(rho exp n), where k, 1, and n constants and rho is equal to the ratio of the resolution of the instrument to twice the half width at half height of the absorbing line. Values of k, 1, and n are given as a function of A sub p and instrument resolution. Comparison is made with a previous approximation. GRA

N91-16105# Ballistic Research Labs., Aberdeen Proving Ground, MD.
ROTATIONAL TEMPERATURE ESTIMATION OF CO AT HIGH TEMPERATURES BY GRAPHICAL METHODS USING FTIR SPECTROMETRY Final Report, Jun. 1988 - Dec. 1989
Kevin L. McNesby and Robert A. Fifer Oct. 1990 29 p
(DA Proj. 1L1-61102-AH-43)
(AD-A228370; BRL-TR-3165) Avail: NTIS HC/MF A03 CSCL 07/2

Rotational temperatures are obtained from gas phase Fourier transform infrared spectra of CO using graphical methods over the temperature range 302 to 773 K. Peak absorbances of individual ro-vibrational transitions are corrected for instrumental distortion and are then fit to a Boltzman distribution to obtain the rotational temperature of the gas. A solution to the convolution integral for FTIR spectrometry is obtained by numerical integration. In all cases, temperatures obtained by graphical analysis yielded gas temperatures within 10 percent of actual. GRA

N91-16106# Ballistic Research Labs., Aberdeen Proving Ground, MD.
LASER MICROPLASMA-GAS CHROMATOGRAPHY DETECTOR. 2: DETECTION OF SPECIES-SPECIFIC FRAGMENT EMISSION Final Report, Nov. 1989 - Aug. 1990
Randy J. Locke, Jeffrey B. Morris, Brad E. Forch, and Andrzej W. Miziolek Oct. 1990 25 p
(Grant AF-AFOSR-0025-90; DA Proj. 1L1-61102-AH-43)
(AD-A228373; BRL-TR-3163) Avail: NTIS HC/MF A03 CSCL 09/3

Characteristic laser produced microplasma emissions from various simple carbon containing vapors entrained in a He carrier gas were observed and compared. A focused ArF (193 nm) excimer laser is used to induce microplasmas with modest pulse energies (15 mJ or less) in the effluent region of a gas chromatography (GC) capillary column. Strong atomic (C, H, O, C1, and F), as well as modular (C2, CH, and CC1) emissions are observed with very high signal to noise ratios. A plasma emission survey indicates that different classes of molecules show unique spectra which make it relatively easy to distinguish one chemical class from another. These results suggest that a laser microplasma gas chromatography detector (LM-GCD) should offer additional discrimination/resolution for unknown sample gas mixture analysis. In addition, the LM-GCD exhibits a significant advantage over certain other GC detectors, like the widely used flame ionization detector (FID), by readily detecting non-responsive gases such as CO, CO2, CC14, and freons. GRA

N91-16107# Pacific Northwest Lab., Richland, WA.
THE DEVELOPMENT OF IMPROVED CAPILLARY SUPERCRITICAL FLUID CHROMATOGRAPHY AND MASS SPECTROMETRY Final Report, 1 Aug. 1987 - 31 Jul. 1990
Clement R. Yonker and Richard D. Smith 1990 4 p
(Contract DAAL03-87-K-0042)
(AD-A228535; ARO-23921.5-CH) Avail: NTIS HC/MF A01 CSCL 14/2

The main thrust of the research initiative conducted under this contract was the study of supercritical fluid solvation and separation processes under extreme solvent conditions. The specific areas of research included studies of the cybotactic region of select probe molecules, determination of stationary phase solvation in supercritical fluid chromatography, and extension of supercritical fluids to the separation of highly polar (charged) solute molecules. GRA

N91-16108# Cornell Univ., Ithaca, NY. Dept. of Chemistry.
CHEMISORPTION OF CARBON MONOXIDE ON THREE METAL SURFACES: Ni(111), Pd(111) AND Pt(111): A COMPARATIVE STUDY
Yat-Ting Wong and Roald Hoffmann 12 Oct. 1990 37 p
(Contract N00014-89-J-1052)
(AD-A228579; TR-52) Avail: NTIS HC/MF A03 CSCL 07/4

At one-third coverage of carbon monoxide, a (sq root of 3 x sq root of 3)R30 degree low energy electron diffraction (LEED) pattern has been observed on Ni(111), Pd(111) and Pt(111). Interestingly, the C-O stretching frequency indicates three completely different adsorption sites; a 2-fold bridge site for Ni(111), a 3-fold site for Pd(111), and an on-top site for Pt(111). As the coverage increases to one-half, a c(4x2) Leed pattern appears. For Ni(111) and Pd (111), the adsorbate seems to prefer the 2-fold site. On Pt(111), half of the chemisorbed CO sits on the on-top site while the other half is located at the 2-fold site. Further increase in coverage results in titled CO molecules on Pt(111) and adsorption of CO at the on-top site of Ni(111) and Pd(111). To rationalize these observations, we carried out extended Huckel calculations within the tight-binding formalism. Our discussion is augmented by conceptual tools such as density of states and crystal orbital overlap population. We also examine the question of the adequacy of the Blyholder model in describing the adsorbate-surface interaction. GRA

N91-16109# Naval Research Lab., Washington, DC. Theoretical Chemistry Section.
INTRODUCTION (TO A BOOK ON APPLICATIONS OF LOCAL-DENSITY-FUNCTIONAL METHODS IN CHEMISTRY) Technical Report No. 3, 1 Apr. - 1 Sep. 1990
Brett I. Dunlap Oct. 1990 10 p Submitted for publication
(Contract N00014-90-WX-24264)
(AD-A228769) Avail: NTIS HC/MF A02 CSCL 07/4

This book contains the work of people who spoke and presented posters at the Ohio Supercomputer Center Workshop on Theory and Applications of Density Functional Theory in Chemistry, in Columbus Ohio that was organized by the editors, Jan Labanowski and Jan Andzelm. A large fraction of those attending the conference were people from different corners of chemistry who were simply curious about density functional theory in chemistry. As this book demonstrates, there was and is the expectation that density functional methods will enable first principles treatment of chemical systems that are significantly large and more complex than those accessible by ab initio methods. If the field of computational density functional chemistry is new to you, I thank you for letting your curiosity lead you to read at least a portion of this book. The field is rather new compared to most semiempirical and ab initio methods of quantum chemistry. Density functional theory has its origins in solid state physics, and that origin can be traced by simply considering the titles of two related earlier conference proceedings, which include work by many of the contributors to this volume. The field has evolved sufficiently to focus exclusively on the chemical aspects of density functional theory now. GRA

N91-16110# California Inst. of Tech., Pasadena.
EXPERIMENTAL STUDIES OF THE PROPERTIES OF TRIHYDROGEN AND TETRAHYDROGEN Final Report, 1 Jul. 1986 - 31 Dec. 1989
Aron Kuppermann Oct. 1990 72 p
(Contract F04611-86-K-0076; AF Proj. 5730)
(AD-A228869; AL-TR-90-038) Avail: NTIS HC/MF A04 CSCL 07/1

Results of theoretical calculations by Nicolaides et al. have suggested the existence of metastable tetrahydrogen (H4) molecules. The specific impulse of this species is estimated to be 1820 s, making it a very interesting candidate for a rocket propulsion system. The scattered products of the H3 + HI collisions are measured with the help of an electron bombardment quadrupole mass spectrometer, having two angular motion degrees of freedom. This complex apparatus was put together and made operational. Preliminary experiments were then performed and the results indicated that it would indeed permit the proposed reaction to be investigated in detail. At this point, further, more accurate calculations by Montgomery et al. found that H4 in the 1A' state is not bound. This result led us to concentrate on studying the properties of the metastable H3 beam. A sophisticated apparatus to produce and characterize a metastable beam of H3 molecules were designed, constructed and assembled. It consists of an arc heated metastable H3 beam source, a Stern-Gerlach magnetic velocity selector and an electron bombardment mass spectrometer detector. The resolution of the latter still needs improvement. Once this is achieved, experiments will be performed to determine the rovibrational composition, translation energy distribution, and radiative lifetime of the metastable H3 beam and to determine its chemical properties. GRA

N91-16111# Technische Univ., Delft (Netherlands).
FROM VISCO-ELASTICITY TOWARDS THERMAL RELAXATION: A NEUTRON SCATTERING STUDY OF DENSITY FLUCTUATIONS IN FLUID HELIUM Ph.D. Thesis
Wouter Theodorus Montfrooij 1990 103 p
(ETN-91-98486) Avail: NTIS HC/MF A06

The results of neutron scattering experiments on helium at temperatures between 4 and 40 K and at number densities between 15 mm and 32 mm (exp -3) are presented. The Young algorithm proved to be useful in explaining static properties and worked for the microscopic dynamical behavior of helium. The halfwidths of

the helium spectra are largely determined by the heat mode alone. The minimum value of the halfwidth compares very well with other simple model. The Enskog theory is successful in qualitatively predicting the heat mode and extended sound modes of the helium fluid. The relevance of the mode coupling theory for helium is shown. ESA

N91-16112# Karlsruhe Univ. (Germany, F.R.). Sonderforschungsbereich 167.
HIGH-LOADED COMBUSTION CHAMBERS STATIONARY CONSTANT PRESSURE COMBUSTION. PART 2: RESEARCH REPORTS Semiannual Report, 1987 - 1989 [HOCHBELASTETE BRENNRAEUME STATIONAERE GLEICHDRUCKVERBRENNUNG. FORSCHUNGSBERICHT 2 HALBJ. 1987 - 1988 - 1989]
1989 583 p In GERMAN
(ETN-91-98511) Avail: NTIS HC/MF A25

Subjects covered are: fuel preparation; combustion and noxious matter formation, flow and heat transfer, high temperature material behavior and insulating layers. The narrow link in the thermodynamical/fluid mechanical process with material behavior problems is outlined. The necessity to know the loads to which material in service conditions is submitted is pointed out, in the framework of the new and further development of combustion chambers. High thermal and mechanical stresses induced by start up, change of load and stopping processes, as well as temperature and pressure gradients are to be considered. ESA

N91-16113# Technische Univ., Eindhoven (Netherlands).
HIGH SPEED NARROW BORE CAPILLARY GAS CHROMATOGRAPHY Ph.D. Thesis
Andries Johannes Joz vanEs 1990 203 p
(ETN-91-98481) Avail: NTIS HC/MF A10

Technological solutions to exploit the potentially attainable speed of analysis in capillary gas chromatography are investigated. The advantages and limitations of the application of narrow bore columns are theoretically and experimentally evaluated. Among the factors modifying the analysis speed such as plate number, phase ratio or outlet pressure, the column diameter is emphasized. Specially developed systems capable of generating input bandwidths as low as 1 ms, allowing column diameters at least down to 10 microns, are described. The influence of column diameter and film thickness on the sample capacity of the column is theoretically and experimentally shown: the ratio between sample capacity and minimum detectable amount strongly decreases with column diameter. With a microchip thermal conductivity detector, the minimum diameter is limited to 15 microns. ESA

N91-16114# Technische Univ., Delft (Netherlands).
ELECTRICAL PROPERTIES OF GAS SENSOR MATERIALS Ph.D. Thesis
Menno Dekker 29 Nov. 1990 227 p
(ETN-91-98572) Avail: NTIS HC/MF A11

Chemical all solid state gas sensors are examined. Target gases were SOx, NOx and H2 for Nernst sensors and CO, alcohols, and alkanes for semiconductor sensors. For the first ones, the study was focused on the selection and the characterization of suitable electrolyte and electrode materials in order to optimize sensor properties such as stability or reliability, particularly by means of impedance spectroscopy. NiO/NiSO4 is found to be an adequate solid reference electrode and Na2SO4 is proved to be a solid electrolyte with good electrical properties and mechanical integrity. The stability and temperature dependence and the cross sensitivity of commercially available semiconductor sensors was studied but they showed too weak a selectivity to be reasonably used for quantitative measurements. ESA

26 METALLIC MATERIALS

Includes physical, chemical, and mechanical properties of metals, e.g., corrosion; and metallurgy.

N91-16115# Argonne National Lab., IL. Materials and Components Technology Div.
THERMAL AGING OF CAST STAINLESS STEELS: MECHANISMS AND PREDICTIONS
O. K. Chopra Jan. 1990 40 p Presented at the Pressure Vessels and Piping Conference: Be in Tune for the 90's, Nashville, TN, 17-21 Jun. 1990 Sponsored in part by US Nuclear Regulatory Commission
(Contract W-31-109-eng-38)
(DE90-010093; CONF-900617-11) Avail: NTIS HC/MF A03

Charpy impact, tensile, and J-R curve data are presented for several experimental and commercial heats, as well as for reactor aged material of CF-3, CF-8, and CF-8M grades of cast stainless steel. The effects of material variables on the embrittlement of cast stainless steels are evaluated. In general, the low carbon CF-3 grades of cast stainless steels are the most resistant, and the molybdenum containing high carbon CF-8M grades are the most susceptible, to low temperature embrittlement. While ferrite morphology has a strong effect on the extent or degree of embrittlement, material composition influences the kinetics of embrittlement, which can vary significantly with small changes in the constituent elements of the cast material. The mechanisms of embrittlement were also established. Mechanical property data were analyzed to develop the procedure and correlations for predicting the kinetics and extent of embrittlement of reactor components from known material parameters. The method and examples of estimating the impact strength and fracture toughness of cast stainless steel components during reactor service are described. The lower bound values of impact strength and fracture toughness for cast stainless steels at LWR operating temperatures are defined. DOE

N91-16116# Oak Ridge National Lab., TN.
WELDABILITY OF NICKEL ALUMINIDES
G. M. Goodwin and S. A. David 1990 6 p Presented at the International Inst. of Welding Conference, Montreal, Quebec, 23-24 Jul. 1990
(Contract DE-AC05-84OR-21400)
(DE90-008557; CONF-900774-1) Avail: NTIS HC/MF A02

The weldability of nickel aluminides, in terms of resistance to hot cracking, is evaluated based on testing of thin sheet using the Sigmajig hot cracking test and simulated repair welding of 2.5 x 2.5 x 7.5 cm ingots. The thin sheet tests showed that certain alloy compositions have cracking resistance within the range of commercial type 316 stainless steel. The ingot tests showed that only a few compositions could be welded without cracking. It is hypothesized that oxygen plays a role in the operative hot cracking mechanism. Rolled and welded tubing was produced successfully from some of these materials. DOE

N91-16117# Oak Ridge National Lab., TN. Metals and Ceramics Div.
HAZ LIQUATION CRACKING BEHAVIOR IN NEWLY DEVELOPED LEAN 316 STAINLESS STEELS
C. D. Lundin, C. Y. P. Qiao (Tennessee Univ., Knoxville.), G. M. Goodwin, and R. W. Swindeman 1990 40 p Presented at the ASME PVP Conference, Nashville, TN, 17-21 Jul. 1990
(Contract DE-AC05-84OR-21400)
(DE90-009409; CONF-900789-1) Avail: NTIS HC/MF A03

The development of an advanced austenitic alloy to meet the needs of new power generation units (650 C, 35 MPa) is being aggressively pursued in Japan and Europe and the U.S., the DOE through the AR and TD Fossil Energy Program managed by ORNL, has extensive studies underway. The Basic tenets of alloy design involve long time strength and creep rupture properties, metallurgical stability, corrosion resistance, and fabricability (including weldability). A modified 316 stainless steel (lean 316 stainless steel) has been recently developed at ORNL based upon standard composition of materials used in elevated temperature

service. The basic modification is effected by using carbide forming and solid solution elements plus a thermo-mechanical treatment consistent with superheater tube production procedures to improve the elevated temperature properties. Researchers at ORNL have shown that the added strength is achieved through the precipitation of fine carbides, nitrides, or phosphides that stabilize dislocation networks. DOE

N91-16118# Argonne National Lab., IL. Chemical Technology Div.
DESORPTION OF H2O AND H2 FROM STEEL AND LiAo2 BY TEMPERATURE PROGRAMMED DESORPTION
Albert K. Fischer and Carl E. Johnson 1989 12 p Presented at the 4th International Conference on Fusion Reactor Materials, Kyoto, Japan, 4-8 Dec. 1989
(Contract W-31-109-eng-38)
(DE90-011170; CONF-891204-33) Avail: NTIS HC/MF A03

Temperature programmed desorption (TPD) measurements with a steel sample tube and helium sweep gas in progress to provide data describing the kinetics of desorption of H2O(g) and H2(g) from ceramic tritium breeders. Preliminary blank experiments indicated that the steel can be a reactive participant with H2O being consumed and H2 being evolved. There is also evidence of some dissolution of H2 in the steel. However, it is possible to stabilize the steel in the absence of added H2 so that useful desorption measurements with H2O(g) can be made. Initial work was on the LiAlO2-H2O(g) system. Fresh samples of LiAlO2 bear large amounts of absorbed H2O. TPD spectra were measured for LiAlO2 that had been equilibrated in a helium stream with 200 ppm H2O(g) at temperatures from 473 to 773 K. Several techniques of data analysis were applied. Questions of possible peak overlap still remain to be resolved. An activation energy for desorption of H2O(g) of approx. 120 kJ/mol appears to be associated with the sample equilibrated at 673 K. This result agrees with the values reported in the literature for decomposition of LiOH, and suggests that some sites on LiAlO2 might resemble sites on Li2O on their adsorptive properties. For a 773 K equilibration, the activation energy of desorption appears considerably higher. DOE

N91-16119# California Univ., Berkeley. Lawrence Berkeley Lab. Materials and Chemical Sciences Div.
HIGH RESOLUTION PHOTOELECTRON SPECTROSCOPY OF METAL CLUSTERS AND HIGH TEMPERATURE SPECIES Ph.D. Thesis
Lai-Sheng Wang Feb. 1990 203 p Prepared in cooperation with California Univ., Berkeley
(Contract DE-AC03-76SF-00098)
(DE90-011598; LBL-28606) Avail: NTIS HC/MF A10

The high resolution photoelectron spectroscopy of metal clusters and high temperature species was investigated. To that end, a high temperature molecular beam source has been built, which is capable of generating continuous and internally cooled beams of cluster species and high temperature species. A number of high temperature species (SnSe, SnTe, PbSe, and PbTe; Se2 and Te2; ZnCl2, MnCl2, and NiCl2) and group V element clusters (As2, Sb2, and Bi2; P4, As4, and Sb4) were measured with 12 to 15 MeV resolution. Vibrational structure is resolved for the first time for most of these species, and fundamental spectroscopic constants are obtained. Information about the electronic structure and chemical bonding is derived from the high resolution spectra and from comparisons with theoretical calculations. DOE

N91-16120*# Columbia Univ., New York, NY.
UNDERSTANDING THE INTERDIFFUSION BEHAVIOR AND DETERMINING THE LONG TERM STABILITY OF TUNGSTEN FIBER REINFORCED NIOBIUM-BASE MATRIX COMPOSITE SYSTEMS Final Report
John K. Tien 14 Nov. 1990 22 p
(Grant NAG3-720)
(NASA-CR-187396; NAS 1.26:187396) Avail: NTIS HC/MF A03 CSCL 11F

The long term interdiffusional stability of tungsten fiber reinforced niobium alloy composites is addressed. The matrix alloy that is most promising for use as a high temperature structural material for reliable long-term space power generation is Nb1Zr. As an ancillary project to this program, efforts were made to assess the nature and kinetics of interphase reaction between selected beryllide intermetallics and nickel and iron aluminides. Author

N91-16121 New South Wales Univ., Canberra (Australia). Dept. of Chemical Engineering.
HIGH TEMPERATURE CORROSION OF ALLOYS IN MIXED GASES Ph.D. Thesis, Jun. 1989 Abstract Only
Grant McAdam 10 May 1990 3 p
Avail: Issuing Activity

The corrosion behavior of iron, manganese, and a range of iron based alloys containing 2, 15, 25, and 50 w/o manganese were evaluated. Controlled gas atmospheres of SO2-CO2-CO-N2 at 1073 K were used. A catalyst was used to help establish gas phase equilibrium. The conditions covered a wide range of sulfur and oxygen partial pressures, and could be considered as sulfidizing, sulfidizing-oxidizing, and oxidizing with respect to iron. At high sulfur partial pressure, when a catalyst was used, the scales generally consisted of sulfides. Under non-catalyzed conditions the scales were dual-phased, consisting of mixed oxide and sulfide. In most cases the kinetics were parabolic and the controlling mechanism was diffusion through the product layer. At sulfur dioxide partial pressures greater than 1 x 10(exp -2) atm the scale morphologies consisted of an inner region of mixed oxide and sulfide and an outer region of oxide. The kinetics were parabolic. A marked reduction in the corrosion rate was not achieved until 50 w/o manganese. At sulfur dioxide partial pressures less than 3 x 10(exp -4) atm the scale morphologies were composed almost entirely of oxide-sulfide lamellae. Reaction with sulfur dioxide was responsible for the mixed oxide-sulfide. Due to the low sulfur dioxide concentration, the rate of conversion of sulfide to oxide by reaction with sulfur dioxide was slow, preserving the mixed oxide-sulfide. A surface reaction was believed to be in control during the early stages of reaction, changing to diffusion through the product layer, leading to parabolic kinetics. The alloys exhibited an inner porous oxide layer under high and low sulfur dioxide partial pressures. It increased in thickness with increasing manganese concentration and was a result of scale-metal separation. The rate of reaction was higher at low sulfur dioxide partial pressures than high ones. The grain boundaries between the oxide-sulfide lamellae provided a more rapid pathway for diffusion than did an external oxide layer.
Author

N91-16122# Los Alamos National Lab., NM. Materials Science and Technology Div.
INFLUENCE OF STRAIN RATE ON THE STRUCTURE/PROPERTY OF Ti-48Al-1V
George T. Gray, III 1990 13 p Presented at the Fall Meeting of the Minerals, Metals and Materials Society on Physical Metallurgy and Materials in Conjunction With Materials Week and the Material Applications and Services Exposition, Detroit, MI, 7-11 Oct. 1990
(Contract W-7405-eng-36)
(DE91-000172; LA-UR-90-3347; CONF-901008-4) Avail: NTIS HC/MF A03

While the influence of strain rate on the structure/property response of pure titanium and a variety of titanium alloys has been extensively studied, the effect of strain rate on the stress-strain and deformation response of titanium aluminides remains largely unknown. In this paper, a preliminary study of the effect of strain rate and temperature on the substructure evolution and mechanical response of a (48Al-1V)TiAl alloy is presented. The compressive true stress-true strain response of Ti-48Al-1V was found to depend on both the applied strain rate, varied between 0.001 and 7500/s, and the test temperature, varied between 25 and 700 C. The rate of strain hardening in Ti-48Al-1V is seen to increase with increasing strain rate. The substructure evolution of Ti-48Al-1V was observed to depend on the applied strain rate and temperature of deformation. The substructure of Ti-48Al-1V deformed to epsilon = 0.20 at 0.001/s at 25 C was seen to consist of predominately random dislocation debris and isolated

grains containing a high density of stacking faults. The majority of the dislocations appear to be a set of (111) planes 1/2 group of zone (110) zone axes unit type ordinary dislocations which is consistent with previous observations on Ti-48Al. Increasing the rate of deformation at room temperature to 75000/s is seen to increase the density of deformation twins and the overall random dislocation debris density. The substructure of Ti-48Al-1V deformed at a high-strain-rate at elevated temperatures was seen to be quite similar to that observed following high-rate deformation at room temperature except for an even higher incidence of twinning. The defect generation and the rate sensitivity of TiAl are discussed as a function of strain rate and contrasted to that observed in conventional titanium alloys. DOE

N91-16123# State Univ. of New York, Stony Brook.
ATOMIC AND ELECTRONIC STRUCTURE OF METALS AND ALLOYS: CLEAN SURFACES AND CHEMISORBED MOLECULES
Sep. 1990 4 p
(Contract DE-FG02-86ER-45239)
(DE91-000267; DOE/ER-45239/T2) Avail: NTIS HC/MF A01

In this second period of support three subjects were exclusively examined, namely, rare earths, bulk and surfaces; ultrathin films of strained metallic phases; and improvement of experimental facilities. In the area of rare earths the photoemission data collected at beamline U7B of the National Synchrotron Light Source from a single-crystal platelet of Tb(0001) were analyzed. DOE

N91-16124# Dayton Univ., OH. Research Inst.
MECHANICAL PROPERTY DATA ON ALUMINUM ALLOY 7150-T7751 PLATE Interim Report, Jun. 1988 - Jun. 1989
Patrick W. Ertel Aug. 1990 29 p
(Contract F33615-88-C-5437; AF Proj. 2418)
(AD-A227506; UDR-TR-90-02; WRDC-TR-90-4068) Avail: NTIS HC/MF A03 CSCL 11/6

A mechanical properties investigation was performed on aluminum 7150-T7751, a product using a recently developed thermal processing technique. Properties examined were tensile, fracture toughness, fatigue crack growth, spectrum fatigue crack growth, constant amplitude fatigue, stress corrosion cracking, and stress corrosion cracking threshold. Test results indicate this material possesses high strength with somewhat greater resistance to corrosion and decreased fracture toughness over conventional 7000 series aluminums of similar strength. Fatigue properties were found to be similar to those of other 7000 series aluminums, while fatigue crack growth rates were greater in the lower stress intensity ranges and similar in the higher ranges. GRA

N91-16125# Structural Integrity Associates, Inc., San Jose, CA.
ELEVATED TEMPERATURE CRACK GROWTH IN TITANIUM ALUMINIDES Final Report, Oct. 1989 - Apr. 1990
An-Yu Kuo, Kuan-Luen Chen, Ashok Saxena, M. Khobaib, and Joseph P. Gallagher May 1990 111 p
(Contract F33615-89-C-3213)
(AD-A227700; SIR-90-017; WRDC-TR-90-3050) Avail: NTIS HC/MF A06 CSCL 11/6

Crack growth of Titanium intermetallics at elevated temperatures was studied. Based on limited amount of test data available in the literature, it is concluded that, for Titanium aluminides at temperatures over 700 C, creep temperature (Ct) correlates better with fatigue crack growth rate (da/dt) than the Linear Elastic Fracture Mechanics (LEFM) parameter Stress Intensity Factor (K). An alternative definition of Ct has also been derived in this study. The new Ct definition is based on a line integral along the outer boundary of the whole structure. Such an alternative definition has made it easier to calculate Ct for structural components. GRA

N91-16126# Oak Ridge National Lab., TN.
BIBLIOGRAPHY OF THE TECHNICAL LITERATURE OF THE MATERIALS JOINING GROUP, METALS AND CERAMICS DIVISION, 1951--JUNE 1989
S. A. David, comp., G. M. Goodwin, comp., and K. Gardner, comp. Oct. 1989 52 p
(Contract DE-AC05-84OR-21400)
(DE91-000530; ORNL/M-983) Avail: NTIS HC/MF A04

This document contains a listing of the written scientific information originating in the Materials Joining (formerly the Welding and Brazing Group), Metals and Ceramics Division, Oak Ridge National Laboratory during 1951 through June 1989. This registry of documents is as much as possible in the order of issue date. A complete cross-referenced listing of the technical literature of the Metals and Ceramics Division is also available. DOE

N91-16127# Sandia National Labs., Albuquerque, NM.
ATOMIC-SCALE SIMULATION OF ADHESION BETWEEN METALLIC SURFACES
Paul A. Taylor 1990 11 p Presented at the Fall Meeting of the Materials Research Society, Boston, MA, 24 Nov. - 1 Dec. 1990
(Contract DE-AC04-76DP-00789)
(DE91-004722; SAND-90-3057C; CONF-901105-29) Avail: NTIS HC/MF A03

We have performed molecular dynamics (MD) simulations of adhesive phenomena, on an atomic scale, between metals possessing both smooth and stepped-surfaces. Studies of adhesion between identical metals, consisting of either Au, Cu, or Ni, with (001) or (111) orientations, reveal the existence of adhesive avalanches as the bodies are brought to within a critical separation approximately 2 A. That is, as the surfaces approach one another, one or both surface layers becomes unstable, and abruptly moves toward the other. This signals a transition from an initial system with two distinct surfaces to one possessing no identifiable surfaces. The presence of adhesive avalanches will pose difficulties in determining adhesive forces and energies by means of atomic force microscopy at sub-nanometer separations of probe tip and sample surface. DOE

N91-16128*# National Aeronautics and Space Administration. Lewis Research Center, Cleveland, OH.
TENSILE BEHAVIOR OF TUNGSTEN/NIOBIUM COMPOSITES AT 1300 TO 1600 K Final Report
Hee Mann Yun (Cleveland State Univ., OH.) and Robert H. Titran 1989 25 p Presented at the Fall Meeting of the Metallurgical Society, Indianapolis, IN, 30 Sep. - 6 Oct. 1989
(Contract DE-AI03-86SF-16310)
(NASA-TM-103727; E-5961; NAS 1.15:103727; DOE/NASA/16310-15) Avail: NTIS HC/MF A03 CSCL 11F

The tensile behavior of continuous tungsten fiber reinforced niobium composites (W/Nb), fabricated by an arc-spray process, was studied in the 1300 to 1600 K temperature range. The tensile properties of the fiber and matrix components as well as of the composites were measured and were compared to rule of mixtures (ROM) predictions. The deviation from the ROM was found to depend upon the chemistry of the tungsten alloy fibers, with positive deviations for ST300/Nb (i.e., stronger composite strength than the ROM) and negative or zero deviations for 218/Nb. Author

N91-16129# Wisconsin Univ., Madison. Dept. of Materials Science and Engineering.
PHASE SELECTION AND PROCESSING OF HIGH TEMPERATURE INTERMETALLIC ALLOYS Final Report, 1 Oct. 1986 - 28 Feb. 1990
J. H. Perepezko 18 Sep. 1990 108 p
(Contract DAAL03-86-K-0164)
(AD-A227910; ARO-24548.3-MS-A) Avail: NTIS HC/MF A06 CSCL 11/6

A crucial issue in the development of high temperature intermetallic systems for structural applications is the formulation of materials processing strategies in order to achieve controlled microstructures that are designed to provide for the required mechanical performance in elevated temperature aggressive environments. In the research effort at University of Wisconsin-Madison an integrated approach coupling processing with microstructure control as guided by the operative phase equilibria has been used to identify several intermetallic alloys

that show promise for further development. The processing efforts have been directed to examining the phase selection, solidification pathways and product phase thermal stability to provide a basis for microstructural development and alloy design. In Ti and Nb base alloy systems such as Ti-Al, Tl-Al-Nb, Nb-Cr and Nb-Al the formation of alternate phases has been identified and examined in terms of the operative kinetics and metasable phase equilibria. Powder samples have been examined following atomization and containerless drop tube processing to analyze soldification structure development. Long term microstructural stability is a key issue in particulate consolidation and high temperature application. A detailed study in Ti-Al alloy has demonstrated that the thermal stability of (alpha 2 + gamma) phase structures can be changed by more than 150 C by controlled manipulations of the microstructural morphology. GRA

N91-16130# Army Lab. Command, Watertown, MA. Materials Technology Lab.
ASSESSMENT OF CORROSION RESISTANT COATINGS FOR A DEPLETED U-0.75 Ti ALLOY
F. Chang, M. Levy, B. Jackman, and W. B. Nowak (Northeastern Univ., Boston, MA.) Sep. 1990 20 p
(AD-A228237; MTL-TR-90-43) Avail: NTIS HC/MF A03 CSCL 11/6

Aluminum, zinc, magnesium, Al-Zn, Al-Mg, nickel, titanium, TiN and Al/TiN coatings were applied by the arc plasma physical vapor deposition (PVD) technique to a depleted uranium (DU) alloy for corrosion protection assessment. The as-deposited specimens were examined by scanning electron microscopy (SEM) for surface morphology and tested for adhesion. Electrochemical polarization tests and immersion tests were conducted in aerated 3.5 wt. percent NaCl solution. Results of electrochemical polarization scans and observations after long-term exposure tests indicated that both Al-Zn and Al-Mg alloys appear to be the best sacrificial coating materials for improving the corrosion resistance of DU-0.75 Ti. GRA

N91-16131 Case Western Reserve Univ., Cleveland, OH.
MODELING AND IDENTIFICATION OF CUMULATIVE CREEP FATIGUE DAMAGE IN AN AUSTENITIC STAINLESS STEEL Ph.D. Thesis
Michael Aaron McGaw 1990 138 p
Avail: Univ. Microfilms Order No. DA9035291

A model of cumulative creep-fatigue damage was developed which is based on the use of damage curve equations to describe the evolution of creep-fatigue damage for four basic creep-fatigue cycle types. These cycle types correspond to the four fundamental cycles of the strainrange partitioning life prediction approach of Manson, Halford, and Hirschberg. A concept referred to as damage coupling is introduced to analytically account for the differences in the nature of the damage introduced by each cycle type, and to provide a means of tracking the cumulative damage which accrues in complex loading histories composed of the fundamental cycle types. These concepts are synthesized into a general framework for the treatment of cumulative creep-fatigue damage problems. To make application of this model, the cumulative creep-fatigue damage behavior of 316 S.S. at 1500 F was experimentally established for the two-level loading cases involving fatigue and creep-fatigue in various permutations. These tests were conducted such that the lower life (high strain) cycling was applied first, for a controlled number of cycles, and the higher life (lower strain) cycling was applied at the second level, to failure. With the exception of the tensile-hold cycle followed by fully reversed cycling results, the proposed model correlates the observed cumulative creep-fatigue behavior considerably well. For the loading sequence which was not well correlated, the model provides a lower bound for the observed behavior. Dissert. Abstr.

N91-16132*# Maryland Univ., College Park. Center for Electronics Packaging.
INELASTIC STRAIN ANALYSIS OF SOLDER JOINT IN NASA FATIGUE SPECIMEN Final Report
Abhijit Dasgupta and Chen Oyan 28 Jan. 1991 60 p
(Grant NAG5-1331)
(NASA-CR-187864; NAS 1.26:187864) Avail: NTIS HC/MF A04 CSCL 11F

The solder fatigue specimen designed by NASA-GSFC/UNISYS is analyzed in order to obtain the inelastic strain history during two different representative temperature cycles specified by UNISYS. In previous reports (dated July 25, 1990, and November 15, 1990), results were presented of the elastic-plastic and creep analysis for delta T = 31 C cycle, respectively. Subsequent results obtained during the current phase, from viscoplastic finite element analysis of the solder fatigue specimen for delta T = 113 C cycle are summarized. Some common information is repeated for self-completeness. Large-deformation continuum formulations in conjunction with a standard linear solid model is utilized for modeling the solder constitutive creep-plasticity behavior. Relevant material properties are obtained from the literature. Strain amplitudes, mean strains, and residual strains (as well as stresses) accumulated due to a representative complete temperature cycle are obtained as a result of this analysis. The partitioning between elastic strains, time-independent inelastic (plastic) strains, and time-dependent inelastic (creep) strains is also explicitly obtained for two representative cycles. Detailed plots are presented for two representative temperature cycles. This information forms an important input for fatigue damage models, when predicting the fatigue life of solder joints under thermal cycling Author

N91-16133# Technische Univ., Eindhoven (Netherlands).
SURFACE ANALYSIS BY LOW-ENERGY ION SCATTERING: TWO-DIMENSIONAL DETECTION AND QUANTIFICATION Ph.D. Thesis
Paul Anton Josef Ackermans 1990 111 p
(ETN-91-98474) Avail: NTIS HC/MF A06

An ion scattering set up is developed, which allows one to simultaneously determine the composition and structure of a surface, with reduced surface damage and time savings. A cylindrically symmetric double toroidal electrostatic analyzer was used to represent the compositional information in the radial direction and the structural information in the azimuthal direction. The ions leaving the analyzer were detected by means of a two dimensional position sensitive detector, whose imaging properties were investigated by means of a computer simulation. Two Ni isotopes were separated with a good resolution. A quantification method was described, which uses both 3-Het+ and 4-Het+ as primary ions to measure two spectra. From the differences in scattered ion fields from the same element, the relative sensitivity and the composition are determined. ESA

N91-16134# Forschungszentrum Juelich G.m.b.H. (Germany, F.R.). Inst. fuer Reaktorwerkstoffe.
THE INFLUENCE OF SMALL SO2 CONTENTS ON THE CORROSION BEHAVIOR FOR NiCrAl ALLOYS IN TEMPERATURE ZONE FROM 1000 TO 1100 C Thesis
C. H. Wasserfuhr, W. J. Quadakkers, H. Schuster, and H. Nickel 1969 145 p In GERMAN; ENGLISH summary
(JUEL-2362; ISSN-0366-0885; ETN-91-98513) Avail: NTIS HC/MF A07

The corrosion behavior of NiCrAl alloys in air containing small amounts of SO2 was investigated. The alloys containing 9 to 20 percent weight chromium, and 6 to 10 percent weight aluminum were oxidized in air and in air containing one volume percent SO2. In addition to long term tests, the initial stages of oxidation were examined, using various surface analysis techniques. The results show that small SO2 additions to the test atmosphere cause a much higher oxidation rate, especially for cast alloys of low chromium and high aluminum contents. The mechanism of the deleterious effect of SO2 on the oxidation rate was studied by measurement of the gas metal reaction kinetics using gas chromotographical analysis of the test gas, and through investigating trace amounts of sulfur in the alloy. It is shown that the high oxidation rates caused by the presence of SO2 in the test atmosphere can be significantly reduced by increasing the chromium content of the alloy, by adding yttrium to the alloy. ESA

N91-16135# Technische Univ., Delft (Netherlands).
THE USE OF IMPEDANCE MEASUREMENTS IN CORROSION RESEARCH: THE CORROSION BEHAVIOUR OF CHROMIUM AND IRON-CHROMIUM ALLOYS Ph.D. Thesis
Johannes Augustinus Dobbelaar 29 Nov. 1990 145 p
(ISBN-90-9003693-8; ETN-91-98570) Avail: NTIS HC/MF A07

Experimental conditions and the methods of interpretation of the data are investigated. A new cell is developed in which the corrosion of metals and alloys can be studied. The two methods of data interpretation are evaluated. The first method is based on the use of equivalent circuits in which corrosion processes are compared to electrical components. The second method is based on the calculation of the impedence from a physical model representing the corrosion reactions. The influence of the chromium content in the alloy, the alloy, the heat pretreatment, and the potential on the corrosion behavior of the alloys is studied. The oxide layer porosity decreases with increasing chromium content in the alloy on increasing potential. ESA

N91-16136# Technische Univ., Delft (Netherlands). Lab. of Metallurgy.
GRAIN-BOUNDARY STRUCTURE IN ORDERED ALLOYS Ph.D. Thesis
Frans David Tichelaar (Aristotle Univ. of Thessaloniki, Greece) 29 Nov. 1990 165 p
(ETN-91-98571) Avail: NTIS HC/MF A08

Some properties of grain boundaries in B2 ordered Fe3Al and LI2 ordered Cu3Au are studied by transmission electron microscopy to explain the behavior of superdislocations at the boundary and slip transfer across grain boundaries. In Fe3Al a low angle tilt is shown to consist of a regular array of superdislocations in the boundary plane or a set of irregular ordinary dislocations associated with an antiphase boundary. The superdislocations in the regular array are made of two ordinary dislocations separated by a ribbon of antiphase boundary. The dislocation separation in each superdislocation is larger than the calculated value of the equilibrium separation using anisotropic elasticity theory. ESA

27 NONMETALLIC MATERIALS

Includes physical, chemical, and mechanical properties of plastics, elastomers, lubricants, polymers, textiles, adhesives, and ceramic materials.

For composite materials see *24 Composite Materials.*

N91-16137# Argonne National Lab., IL. Materials and Components Technology Div.
A STUDY OF THE FORMATION AND SELF-LUBRICATION MECHANISMS OF BORIC ACID FILMS ON BORIC OXIDE COATINGS
A. Erdemir, G. R. Fenske, and R. A. Erck 1990 19 p Presented at the 8th International Triennial Conference on Thin Films and the 17th International Conference on Metallurgical Coatings, San Diego, CA, 1-6 Apr. 1990
(Contract W-31-109-eng-38)
(DE90-010115; CONF-900419-4) Avail: NTIS HC/MF A03

An investigation on the formation and self-lubrication mechanisms of boric acid films on boric oxide coatings prepared by vacuum evaporation was performed. Measured friction coefficients of a steel ball sliding on a boric-oxide-coated-steel disk and a sapphire ball sliding on a boric-oxide-coated-alumina disk were 0.025 to 0.05 at steady state, depending on load and substrate material. This low friction was correlated with the formation of a lubricious boric acid film on boric oxide coatings exposed to open air. For the mechanism of self-lubrication, the layered-triclinic-crystal structure of boric acid was proposed. The atoms constituting each boric acid molecule are arrayed in closely packed and strongly bonded layers that are 0.318 nm apart and held together by weak forces, such as van der Waals. It is hypothesized that during sliding, these layers can align themselves parallel to the direction of relative motion, and once so aligned, can slide over one another with relative ease to provide low friction. Structural and chemical findings were included to substantiate the proposed solid lubrication mechanism. DOE

N91-16138# Johns Hopkins Univ., Baltimore, MD. Dept. of Chemical Engineering.
INITIAL STUDIES OF ELECTRIC FIELD EFFECTS ON CERAMIC POWDER FORMATION IN FLAMES
Joseph L. Katz and Cheng-Hung Hung Dec. 1989 23 p Presented at the 23rd Combustion Inst. Symposium on Combustion, Orleans, France, 22-27 Jul. 1990
(Contract DE-FG02-88ER-45356)
(DE90-007571; CONF-900704-6) Avail: NTIS HC/MF A03

The effect of an electric field on ceramic powder formation was studied in a counterflow diffusion flame burner. TiCl4, SiH4, SiCl4, and GeCl4 were used as source materials for the formation of TiO2, SiO2, and GeO2 in H2/Ar-O2/Ar flames. Particle size and number density were determined using dynamic light scattering measurements and 90 degs light scattering measurements. The effects of the electric field on flame temperature, current, OH emission intensity, and particle characteristics were measured. The results show that in the presence of an electric field, the peak temperature shifts toward the oxidizer side, and the peak OH emission intensity decreases at low field strengths. Particle diameter and number density measurements show that a factor of 3 change in size can be achieved. These results suggest that an electric field can be successfully used as a control variable in the formation of ceramic oxide powders. DOE

N91-16139# Midwest Research Inst., Golden, CO.
ELECTROCHROMIC SUN CONTROL COVERINGS FOR WINDOWS
D. K. Benson and C. E. Tracy Apr. 1990 6 p Presented at the 33rd Annual Technical Conference, New Orleans, LA, 29 Apr. - 4 May 1990; sponsored by Society of Coaters
(Contract DE-AC02-83CH-10093)
(DE90-000335; SERI/TP-212-3786; CONF-900486-1) Avail: NTIS HC/MF A02

The 2 billion square meters (sq m) of building windows in the United States cause a national energy drain almost as large as the energy supply of the Alaskan oil pipeline. Unlike the pipeline, the drain of energy through windows will continue well into the 21st century. A part of this energy drain is due to unwanted sun gain through windows. This is a problem throughout the country in commercial buildings because they generally require air conditioning even in cold climates. New commercial windows create an additional 1600 MW demand for peak electric power in the United States each year. Sun control films, widely used in new windows and as retrofits to old windows, help to mitigate this problem. However, conventional, static solar control films also block sunlight when it is wanted for warmth and daylighting. New electrochromic, switchable, sun gain control films now under development will provide more nearly optimal and automatic sun control for added comfort, decreased building operating expense, and greater energy saving. Switchable, electrochromic films can be deposited on polymers at high speeds by plasma enhanced chemical vapor deposition (PECVD) in a process that may be suitable for roll coating. The electrochromic coatings and the PECVD processes are described, and their adaptability to high speed roll coating is examined. DOE

N91-16140# Bowling Green State Univ., OH. Center for Photochemical Sciences.
PHOTOINDUCED CHARGE SEPARATION BY POLYMER-BOUND CHROMOPHORES
Michael A. J. Rodgers Dec. 1989 32 p
(Contract DE-FG02-88ER-13942)
(DE90-010997; DOE/ER-13942/2) Avail: NTIS HC/MF A03

The major thrust of the project has been to examine the photodynamic behavior of water-soluble polymers that have covalently linked hydrophobic chromophores spaced along the chains. These polymeric systems have been examined for photoinduced charge separation with electron-accepting ions

having different total charge. To date focus has been centered on the excited singlet (S(sub 1)) state formed by laser flash absorption. The effects of pH and ionic strength - factors that govern the conformational nature of the polymer in solution - have been studied. Most efforts have concerned the effect of such conditions, and of the nature of the chromophore, on the yield of separated charges. DOE

N91-16141# Argonne National Lab., IL. Materials and Components Technology Div.
DEVELOPMENT OF NONDESTRUCTIVE EVALUATION METHODS AND PREDICTION OF EFFECTS OF FLAWS ON THE FRACTURE BEHAVIOR OF STRUCTURAL CERAMICS
W. A. Ellingson, J. P. Singh, N. Gopalsami, S. L. Dieckman, C.-Y. Chu, T. Hentea, and P. Rizo (Commissariat a l'Energie Atomique, Grenoble, France) Apr. 1990 14 p Presented at the 4th Conference on Fossil Energy Materials, Oak Ridge, TN, 15-17 May 1990 Submitted for publication
(Contract W-31-109-eng-38)
(DE90-011092; CONF-900546-2) Avail: NTIS HC/MF A03

To establish predictive performance (i.e., fracture behavior) of structural ceramic composites, we undertook in combination (1) a study of flaws and material variations as they relate to mechanical properties, and (2) development of non-destructive devaluation (NDE) methods suitable for obtaining data on flaws and material variations. Effects of whisker addition on development of flaw population and the resulting mechanical properties were evaluated for both green (cold-pressed) and dense (hot-pressed) Si3N4-whisker-reinforced Si3N4 matrix composites. To detect critical flaws in these composites, microfocus x ray computed tomography and ultrasonic NDE methods were used. In addition, a nuclear magnetic resonance (NMR) facility was designed for use on composites. DOE

N91-16142# California Univ., Berkeley. Lawrence Berkeley Lab. Windows and Daylighting Group.
ELECTRON MICROSCOPY AND ELECTROCHEMISTRY OF NICKEL OXIDE FILMS FOR ELECTROCHROMIC DEVICES PRODUCED BY DIFFERENT TECHNIQUES
Carl M. Lampert and RSue Caron-Popowich Sep. 1989 15 p Presented at the 33rd SPIE Annual International Technical Symposium on Optical and Optoelectronic Applied Science and Engineering, San Diego, CA, 10-11 Aug. 1989 Submitted for publication
(Contract DE-AC03-76SF-00098)
(DE90-011596; LBL-27596; CONF-890836-25) Avail: NTIS HC/MF A03

In this study we report on our investigation of the microstructure of nickel oxide films produced by e-beam evaporation, sol-gel deposition and sputtering techniques. We give characteristic cyclic voltammetry, current-voltage relationships, and optical transmission data for films made by each technique. Data is shown for electrodes, both uncycled and cycled, for 17 to 20 hrs. We found all samples have at least one phase corresponding to cubic nickel oxide (NaCl structure). Other phases, such as nickel hydroxide, may exist but are not immediately identifiable. The structure of the films ranges from fine polycrystalline to amorphous and varies over the surface of the sample. Films that were cycled for 17 to 20 hours all tended to have improved transmittance, as high as a 20 percent change. Overall, after cycling the films appeared to be slightly more crystalline. In all films, after cycling there were increases in the coloration and bleaching current. Also, peak shifts were noted after cycling; the coloration peak tended to shift to higher and the bleaching peak shifted to lower potentials. The overall coloration efficiency (550 nm) for these films ranged from 26 to 36 sq cm/C. DOE

N91-16143# Oak Ridge National Lab., TN. Metals and Ceramics Div.
MICROWAVE SINTERING OF FUEL CELL MATERIALS
M. A. Janney and H. D. Kimrey 1990 7 p Presented at the 4th Conference on Fossil Energy Materials, Oak Ridge, TN, 15-17 May 1990
(Contract DE-AC05-84OR-21400)
(DE90-011643; CONF-900546-5) Avail: NTIS HC/MF A02

Microwave processing of LaCrO3-based ceramics for the interconnect layer in the solid oxide fuel cell is reviewed. The characteristics of an inexpensive microwave furnace are detailed. (La.79Ca.2) (Cr.9Co.1)O3 was shown to sinter at approximately 50 C lower in the microwave furnace than in a conventional furnace. DOE

N91-16144# Sandia National Labs., Albuquerque, NM.
COMPARISON OF THE THERMAL STABILITY OF THE CODEPOSITED CARBON/HYDROGEN LAYER TO THAT OF THE SATURATED IMPLANT LAYER IN GRAPHITE
R. A. Causey (Sandia Labs., Livermore, CA.), W. R. Wampler, and D. Walsh 1990 10 p Presented at the 9th Plasma Surface Interactions in Controlled Fusion Devices Conference, Bournemouth, England, 20-25 May 1990
(Contract DE-AC04-76DP-00789)
(DE90-012148; SAND-90-1394C; CONF-900505-4) Avail: NTIS HC A02

This paper presents the results of an experimental study of the thermal stability in air and vacuum of the codeposited carbon/hydrogen layer formed in a carbon-lined fusion reactor. Results are also presented for the stability of the saturated layer formed by the implantation of energetic hydrogen ions into a graphite surface. For both films, the hydrogen isotope release occurs at a much lower temperature in air than it does in a vacuum. At temperatures above 600 K, the hydrogen isotope release in air is very rapid and is emitted in a condensible form. It is speculated that isotopic exchange with the water present in air is responsible for this release. In vacuum, temperatures in excess of 1000 K are required to produce a rapid release from either film. The implications of these results to the safety of tritium in carbon-lined fusion reactors are discussed. DOE

N91-16145# Oak Ridge National Lab., TN.
GELCASTING OF SUB-MICRON ALUMINA, SIALON, AND SILICON NITRIDE POWDERS
O. O. Omatete, R. A. Strehlow, and C. A. Walls 1990 11 p Presented at the 37th Sagamore Army Materials Research Conference, Plymouth, MA, 1-4 Oct. 1990
(Contract DE-AC05-84OR-21400)
(DE91-000618; CONF-9010201-1) Avail: NTIS HC/MF A03

Gelcasting is a near-net-shape forming technique that is applicable to various types of powders. It is accomplished by casting a concentrated suspension of a commercial ceramic powder in a solution of a polymerizable monomer and then polymerizing. A filled gel is formed, which is dried and processed further. Alumina, sialon, and silicon nitride parts of various geometries have been made and are described. Emphasis is placed on the unit-operations of the process. Because a requirement of the process is a castable suspension of more than 50 vol percent solids loading, good dispersion is crucial. Drying, another key process, has been studied extensively. Shrinkage from the cast size occurs during drying and further shrinkage occurs during sintering. Data on the relationship of physical properties of products to some of the more significant processing variables is discussed. Emphasis is also placed on the machinability of the dried gelled body. Because the body at this stage is quite durable, green part machining is feasible. The monomer used in the process is acrylamide, which undergoes a vinyl polymerization. Environmental, safety and hygiene issues are summarized. DOE

N91-16146# University of Southern California, Los Angeles. Dept. of Chemistry.
MODEL FILLED POLYMERS VERSUS SYNTHESIS OF CROSSLINKED MONODISPERSE POLYMETHACRYLATE BEADS Technical Report No. 5, 1 Sep. 1989 - 1 Sep. 1990
D. Zou, S. Ma, R. Guan, M. Park, L. Sun, J. J. Aklonis, and R. Salovey 25 Sep. 1990 23 p Submitted for publication
Sponsored by DARPA

(Contract N00014-88-K-0302)
(AD-A227236; TR-5) Avail: NTIS HC/MF A03 CSCL 11/10

Monodisperse polymethacrylate beads of varied size and crosslink density are prepared by emulsion copolymerization of methacrylate and divinyl monomers in the absence of emulsifiers. The sizes of polybutyl and polyethyl methacrylate beads decreased with increasing polymerization temperature, while polymethyl methacrylate beads were largely unchanged in size. The molar mass of polymer in polymethyl methacrylate beads markedly exceeded that in polystyrene beads. The rate of polymerization increased, and bead size decreased, with increasing initiator concentration or decreasing monomer concentration. The polymethacrylate beads are used as filler particles in polymer composites. GRA

N91-16147# Stanford Univ., CA. High Temperature Gasdynamics Lab.
ON THE DEVELOPMENT OF IN-SITU RAMAN ANALYSIS OF PLASMA DEPOSITED DIAMOND
Mark A. Cappelli and H. Herchen 1990 9 p
(Contract N00014-89-J-1197)
(AD-A227453; REPT-5) Avail: NTIS HC/MF A02 CSCL 20/5

Progress towards the development of in-situ Raman capabilities for plasma deposited diamond films is described. The shift and broadening of the first order Raman-active phonon mode in natural and synthetic diamond is analyzed at temperatures within the range commonly employed in vapor phase diamond deposition (greater than 1000 K). At these temperatures, it was found that the Anti-Stokes component to the Raman signature can be detected and employed as an alternative diagnostic. Preliminary results are described in which in-situ Raman is employed to monitor the temperature of a heated natural diamond substrate exposed to both molecular and atomic hydrogen. It was found that variations in molecular hydrogen fraction in the reactant gas mixture can lead to substantial variation in substrate temperature. Following exposure to atomic hydrogen, the Raman line center is found to be shifted to lower energy (at ambient temperatures). The shift is in part attributed to the presence of interstitial hydrogen. GRA

N91-16148# Oak Ridge National Lab., TN.
UPDATED EVALUATION OF POLYMER FILMS FOR ELECTRICAL INSULATION
H. E. McCoy, Jr. Aug. 1990 66 p
(Contract DE-AC05-84OR-21400)
(DE91-000544; ORNL-6603) Avail: NTIS HC/MF A04

Several types of tests have been run on polymer film materials that could be useful for electrical insulation. The polymers studied were polyethylene terephtalate, polycarbonate, polysulfone, polyetherimide, ultrahigh-molecular-weight polyethylene, polyimide, polybutylene terephthalate, and a laminate of Kraft paper and polypropylene. Thermal aging tests were run to 60,000 h on several of the polymers, and the samples were evaluated by tensile tests, electrical breakdown tests, and immersion density measurements. Because of the wide range of potential service conditions, tensile tests were run on as-received materials over the temperature range of -196 to 200 C. Polyimide is probably the only material suitable for the extremes of this temperature range, but many of the other polymers would be suitable for intermediate temperatures. Creep tests were run in nitrogen and transformer oil at 90 C. It was found that some polymers are weaker and less ductile in oil than in nitrogen and that other polymers have equivalent properties in the two environments. A means of applying mechanical, thermal, and electrical stresses simultaneously to polymer samples was developed. Tests were run at 90 C in transformer oil on polyethylene terephthalate, polyimide, and polyethersulfone. Tests thus far do not indicate that the creep rate is affected by the application of a 5 kV dc potential. DOE

N91-16149# California Univ., Berkeley. Lawrence Berkeley Lab. Center for Advanced Materials.
SINTERING STRESS AND MICROSTRUCTURE IN CERAMIC POWDER COMPACTS Ph.D. Thesis
May-Ying Chu (California Univ., Berkeley.) Aug. 1990 135 p
(Contract DE-AC03-76SF-00098)
(DE91-004415; LBL-29643) Avail: NTIS HC/MF A07

The behavior of the sintering stress and microstructure during sintering is studied under various thermal and physical conditions. Specifically, the study includes sintering under isothermal or constant heating rate conditions; and altering the starting compact structure by pre-coarsening to increase the particle size, or by compaction to increase the starting density. Loading dilatometry is used to measure the ratio of the densification strain rate to the creep strain rate and the continuous shrinkage history of the systems. The data show that the ratio of the densification to the creep strain rate is remarkably constant within a wide temperature range for densification, from the earliest stages of densification to at least the onset of the final stage. As a consequence, the sintering stress, which is proportional to the strain rate ratio, is nearly independent of sintered density or of temperature. Analysis leads to a simple method for determining the simultaneous densification strain rate over the creep strain rate ratio. A rigorous densification strain rate equation is derived for a model system. The constant sintering stress allows progress on formulating a sintering equation to predict the densification behavior of powder compacts. Analysis of dilatometry data from compacts sintered at various heating rates, and of numerical computations, indicate the need to include separate coarsening processes with different activation energies. The same model is used to describe the differences in pore spacing evolution between pre-coarsened and as-received systems. DOE

N91-16150*# Rockwell International Corp., Canoga Park, CA. Rocketdyne Div.
FIBER-REINFORCED CERAMIC COMPOSITES FOR EARTH-TO-ORBIT ROCKET ENGINE TURBINES Final Report
Jerry W. Brockmeyer and Gary D. Schnittgrund Jul. 1990 142 p
(Contract NAS3-25468)
(NASA-CR-185264; NAS 1.26:185264; RI/RD-90-163) Avail: NTIS HC/MF A07 CSCL 11C

Fiber reinforced ceramic matrix composites (FRCMC) are emerging materials systems that offer potential for use in liquid rocket engines. Advantages of these materials in rocket engine turbomachinery include performance gain due to higher turbine inlet temperature, reduced launch costs, reduced maintenance with associated cost benefits, and reduced weight. This program was initiated to assess the state of FRCMC development and to propose a plan for their implementation into liquid rocket engine turbomachinery. A complete range of FRCMC materials was investigated relative to their development status and feasibility for use in the hot gas path of earth-to-orbit rocket engine turbomachinery. Of the candidate systems, carbon fiber-reinforced silicon carbide (C/SiC) offers the greatest near-term potential. Critical hot gas path components were identified, and the first stage inlet nozzle and turbine rotor of the fuel turbopump for the liquid oxygen/hydrogen Space Transportation Main Engine (STME) were selected for conceptual design and analysis. The critical issues associated with the use of FRCMC were identified. Turbine blades were designed, analyzed and fabricated. The Technology Development Plan, completed as Task 5 of this program, provides a course of action for resolution of these issues. Author

N91-16151# Texas Univ., Austin. Dept. of Chemistry and Biochemistry.
POLYMERS AT LIQUID-LIQUID INTERFACES: PHOTOPHYSICS AND PHOTOREDOX CHEMISTRY Progress Report, 1 Apr. 1990 - 31 Mar. 1991
S. E. Webber Nov. 1990 5 p
(Contract DE-FG05-86ER-13629)
(DE91-005032; DOE/ER-13629/4) Avail: NTIS HC/MF A01

Research continued on polymers at liquid-liquid interfaces. This quarter, work concentrated on: preparation of poly-(styrene-alt-maleic acid-co-chromophore) polymers; studies of vinylnapthalene-maleic acid polymers as emulsifying agents for water-octane; and assembly of optical fiber reticon-based transient absorption system. DOE

N91-16152*# National Aeronautics and Space Administration. Lewis Research Center, Cleveland, OH.
METHOD OF MAKING CONTAMINATION-FREE CERAMIC BODIES Patent Application
Warren H. Philipp, inventor (to NASA) 9 Nov. 1990 8 p
(NASA-CASE-LEW-14984-1; NAS 1.71:LEW-14984-1; US-PATENT-APPL-SN-610883) Avail: NTIS HC/MF A02 CSCL 11C

Ceramic structures having high strength at temperatures above 1000 C after sintering are made by mixing ceramic powders with binder deflocculants such as guanidine salts of polymeric acids, guanidine salts of aliphatic organic carboxylic acids or guanidine alkylsulfates with the foregoing guanidine salts. The novelty of the invention appears to lie in the substitution of guanidine salts for the alkalai metal salts components or organic fatty acids of the prior art binder-deflocculant, ceramic processing aids whereby no undesirable metal contaminants are present in the final ceramic structure. Guanidine alkyl sulfates also replace the Na or K alkyl sulfates commonly used with binder-deflocculants in making high temperature ceramic structures. NASA

N91-16153# Wichita State Univ., KS. National Inst. for Aviation Research.
COMPARATIVE STUDY OF PHOSPHOSILICATE GLASS ON (100) SILICON BY FURNACE AND RAPID ISOTHERMAL ANNEALING
R. P. S. Thakur, R. Singh, A. J. Nelson, H. S. Ullal (Midwest Research Inst., Golden, CO.), J. Chaudhuri, and V. Gondhalekar Aug. 1990 25 p
(NIAR-90-26) Avail: NTIS HC/MF A03

Phosphosilicate glass (PSG) is extensively used throughout the semiconductor industry in the fabrication of integrated circuits. Rapid isothermal annealing based on incoherent sources of light is a very promising technique for fabricating micron and submicron integrated circuits. For submicron devices, a reduced thermal budget (e.g., product of processing temperature and time) is essential for minimizing lateral and vertical diffusion of dopants as well as suppressing various unwanted physical and chemical phenomena. In the case of rapid isothermal processing (RIP), the sample is thermally isolated and the heating and cooling are dominated by thermal radiations. The results of RIP and furnace annealed PSG samples are reported and the electrical and structural characteristics based of these two thermal treatments are compared. Author

N91-16154# Texas Univ., Arlington. Dept. of Chemistry.
ELECTRONIC AND IONIC TRANSPORT IN PROCESSABLE CONDUCTING POLYMERS Quarterly Technical Report, 1 Jul. - 30 Sep. 1990
Martin Pomerantz, John R. Reynolds, Krishnan Rajeshwar, and Dennis S. Marynick 5 Oct. 1990 7 p
(Contract N00014-90-J-1320)
(AD-A227857; TR-23) Avail: NTIS HC/MF A02 CSCL 07/6

A number of polymers derived from 2,5-dialkoxy-1,4-bis-(2-thienyl)benzene have been prepared and studied. Symmetric polymer repeat units are obtained when the alkoxy substituents are equivalent and asymmetric repeat units when they are different. The symmetric polymers are partially crystalline whereas the asymmetric ones are completely amorphous. Interestingly, the former show a higher conductivity than the latter upon doping. A new type of chemical sensor has been developed based on the redox release of fluorophores from a conducting polymer. Sub ppm levels of several analytes have been measured. 5-Decylbenzo(c)-2',5'-dihydrothiophene has been prepared and polymerized to processable poly(5-decyl-benzo-(c)thiophene). This is a low band-gap polymer whose color gets much lighter upon doping. Another low band-gap polymer, poly(2,3-dihexylthieno(3,4-b)pyrazine) has been prepared and is also being investigated. GRA

N91-16155# Massachusetts Inst. of Tech., Cambridge. Dept. of Chemical Engineering.
GAS SOLUBILITY IN GLASSY POLYMERS: A CORRELATION WITH EXCESS ENTHALPY
D. H. Rein, R. F. Baddour, and R. E. Cohen 23 Oct. 1990 28 p
(Contract N00014-87-K-0517)
(AD-A228202; TR-11) Avail: NTIS HC/MF A03 CSCL 07/6

Solubility coefficients for CO2, Ar and CH4 in polystyrene (PS) films with glass transition temperatures (Tg) of 52 to 107 C were measured in a pressure decay sorption apparatus at 1 atm over a temperature range of 20 to 90 C. The gas solubility at 30 C increased as the Tg of the PS increased; the heat of solution was largest for the PS with the highest Tg. This observed dependence of gas solubility on Tg was analyzed in terms of enthalpy - temperature relationships for glassy polymers. The solubilities for PS samples with different glass transition temperatures converged when comparisons were made based on states of equal enthalpy instead of the temperature of measurement. GRA

N91-16156# State Univ. of New York, Buffalo. Dept. of Chemistry.
DESIGN, ULTRASTRUCTURE, AND DYNAMICS OF NONLINEAR OPTICAL INTERACTIONS IN POLYMERIC THIN FILMS Final Technical Report, 1 Mar. 1987 - 30 Mar. 1990
Paras N. Prasad 4 Oct. 1990 26 p
(Contract F49620-87-C-0042; AF Proj. 2303)
(AD-A228876; AFOSR-90-1066TR) Avail: NTIS HC/MF A03 CSCL 07/2

This program covered microscopic theory of optical nonlinearity, design and synthesis of novel structures, materials processing for guided waves, measurements of optical nonlinearities, and study of device processes. Both classical anharmonic oscillator approach as well as ab-initio calculations were used to understand the microscopic nature of optical nonlinearities in organic structures. The ultimate goal was to understand the structure-property relationship so that one may be able to predict structures with enhanced optical nonlinearities. The focus of our work was on third-order optical nonlinearity. We developed a simple model of coupled locally anharmonic oscillators which can be used to describe the optical nonlinearities in conjugated organic monomeric, oligomeric, and polymeric structures. We showed that the method can very readily be used to explain the dependence of the band gap, the polarizability (alpha), and the second hyperpolarizability (gamma) as a function of the number of repeat units for the oligomers of thiophene and benzene. The results predicted by the coupled anharmonic oscillator model are in good agreement with those of the experimental studies of thiophene and benzene oligomers recently reported by our group. In addition, the predicted power dependences of orientationally averaged (alpha) and (gamma) on the number of repeat units were compared with those predicted by a free electron model, PPP methods, sum-over-states method and ab initio calculations. GRA

N91-16157# Technische Univ., Delft (Netherlands).
FATIGUE OF AMORPHOUS POLYMERS Ph.D. Thesis
Johannes Antonius Ma Remmerswaal 1990 155 p
(ISBN-90-9003520-6; ETN-91-98483) Avail: NTIS HC/MF A08

The influence of temperature, frequency, and loading rate on fatigue of glassy amorphous polymers is studied and methods for the prediction of the lifetime under various loading conditions are developed. A specific hydraulic torsion fatigue device was developed. Stress-strain tests were carried out to determine the effects of temperature and the rate of straining of the yield stress. Tensile and torsion creep experiments were carried out to investigate the influence of the stressing rate on the time to creep failure. From the results, it is concluded that fatigue can be considered as an Eyring process with a correction for the frequency and the stress wave shape. ESA

28 PROPELLANTS AND FUELS

Includes rocket propellants, igniters, and oxidizers; their storage and handling procedures; and aircraft fuels.

For related information see also *07 Aircraft Propulsion and Power, 20 Spacecraft Propulsion and Power,* and *44 Energy Production and Conversion.*

N91-16158# Lawrence Livermore National Lab., CA.
THE SEARCH FOR HIGH ENERGY LOW VULNERABILITY EXPLOSIVES
Eric vonHoltz, Ken Scribner, Gordon Moody, and Ray McGuire 13 Mar. 1990 9 p Presented at the 21st International Conference of the Fraunhofer-Inst. fuer Chemische Technologie: Technology of Polymer Compounds and Energetic Materials, Karlsruhe, Fed. Republic of Germany, 3-6 Jul. 1990 Submitted for publication
(Contract W-7405-eng-48)
(DE90-009436; UCRL-102393; CONF-900712-2) Avail: NTIS HC/MF A02

Lawrence Livermore National Laboratory (LLNL) is currently attempting to formulate explosives which have approximately 30 percent greater energy than our current TATB/Kel-F explosive, while still passing the Department of Energy's (DOE) insensitive high explosive (IHE) criteria. The new formulations are comprised of HMX, TATB, and high density fluoropolymers and fluoroplasticizers. Variables in the study include the particle size of HMX, type of TATB (wet or dry aminated), the ratios of polymers to plasticizers, and formulation techniques. Initial small scale sensitivity tests and thermal testing have shown promising results. This paper will relate the up-to-date status of the project. DOE

N91-16159# Lawrence Livermore National Lab., CA.
PASTE EXTRUDABLE EXPLOSIVES: THEIR HISTORY AND THEIR CURRENT STATUS
Eric vonHoltz, Ken Scribner, Rich Whipple, and James Carley 13 Mar. 1990 16 p Presented at the 21st International Conference of the Fraunhofer-Inst. fuer Chemische Technologie: Technology of Polymer Compounds and Energetic Materials, Karlsruhe, Fed. Republic of Germany, 3-6 Jul. 1990
(Contract W-7405-eng-48)
(DE90-009438; UCRL-JC-103244; CONF-900712-1) Avail: NTIS HC/MF A03

Lawrence Livermore National Laboratory (LLNL) has a continuing effort in the development of paste extrudable explosives (PEX) for use in high performance munitions. Upon request, the paste could be injected into place just prior to warhead launch, giving enhanced safety during transport, storage, and deployment. The desire for high energy (greater than Comp B) required the development of an energetic plasticizer which would not freeze in the range of -54 to 74 C, and yet be compatible with the desired crystalline explosive. These materials are highly viscous and extremely pseudoplastic in nature. Extensive rheological testing has been done, using a capillary rheometer, and the behavior has been fit to power law (Ostwald-deWaele) and Buckingham-Reiner models. This report will also cover the safety testing conducted on these materials, as well as the processing techniques required for their manufacture. DOE

N91-16160# Sandia National Labs., Albuquerque, NM. Explosive Subsystems Div.
THE EFFECT OF CHARGE MIXTURE RATIO AND PARTICLE SIZE ON IGNITER PLUME HEAT TRANSFER CHARACTERISTICS
N. A. Evans and C. F. Brezowski 1990 16 p Presented at the 15th International Pyrotechnics Seminar, Boulder, CO, 9-13 Jul. 1990
(Contract DE-AC04-76DP-00789)
(DE90-010833; SAND-90-0230C; UC-742; CONF-900792-3)
Avail: NTIS HC/MF A03

Investigation of the heat transfer characteristics of igniter output plumes, first reported at the Fourteenth International Pyrotechnics Seminar in 1989, has continued, using two types of igniter to determine the effect of charge mixture ratio and fuel particle size on performance. While both of these igniters had the same metallic closure disc (scored Hastelloy with a capture cone), the bridgewire sensitizer (or ignition mixture) was barium styphnate for one type, and a particular blend of fine particle titanium/potassium perchlorate (PB) for the other type. The output mixture for both types was titanium/potassium perchlorate; two mixture ratios (33/67 and 41/59), and two titanium particle sizes (2 and 8 microns) were used. The results show that, for both types of igniter, the coarse particle size titanium produced the best performance. The overall best performance was obtained from the igniter using the PB ignition mixture and an output charge of 41/59 titanium/potassium perchlorate. DOE

N91-16161# Sandia National Labs., Albuquerque, NM.
MODELING LASER IGNITION OF EXPLOSIVES AND PYROTECHNICS: EFFECTS AND CHARACTERIZATION OF RADIATIVE TRANSFER
R. D. Skocypec, A. R. Mahoney, M. W. Glass, R. G. Jungst, N. A. Evans, and K. L. Erickson 1990 18 p Presented at the 15th International Pyrotechnics Seminar, Boulder, CO, 9-13 Jul. 1990
(Contract DE-AC04-76DP-00789)
(DE90-011052; SAND-90-0577C; CONF-900792-5) Avail: NTIS HC/MF A03

The ignition of explosives and pyrotechnics using commercial diode lasers has been demonstrated and is of interest as a potential replacement for hot-wire ignition. Initial laser diode ignitor (LDI) test results using the detonation-to-deflagration transition (DDT) explosive CP (2-(5-cyanotetrazolato) pentaamminecobalt(III) perchlorate, C2H15N10Co-Cl2O8) doped with carbon black and graphite have reinforced the need for a better understanding of the interaction of the radiant energy transfer within the pressed material. The present work is directed toward developing a model to predict the transfer of laser energy in the pressed particulate charges. It is shown here that scattering can have a major effect on the volumetric absorption of laser energy, significantly affecting the thermal response of the granular energetic material. This paper describes an effort to characterize the radiative properties of compacted granular beds of CP and CP doped with carbon black or graphite that were prepared using normal pressing techniques. Current estimates of the radiative properties are presented and indicate dramatic absorption for CP when even a minute amount of carbon black or graphite is added. Initial data indicate pressed, undoped CP scatters radiative energy significantly. The radiative properties are dependent upon both wavelength and packing density; the less-densely packed samples exhibit more scattering. Doped samples exhibit essentially wavelength-independent characteristics. DOE

N91-16162# Lawrence Livermore National Lab., CA. Energetic Materials Section.
DEVELOPMENT OF A HIGH-TENSILE-STRAIN PLASTIC-BONDED TATB EXPLOSIVE
Cesar O. Pruneda, Raymond R. McGuire, and Rochelle E. Clements Apr. 1990 10 p Presented at the 21st International Conference of the Fraunhofer-Inst. fuer Chemische Technologie: Technology of Polymer Compounds and Energetic Materials, Karlsruhe, Fed. Republic of Germany, 3-6 Jul. 1990
(Contract W-7405-eng-48)
(DE90-011463; UCRL-102395; CONF-900712-3) Avail: NTIS HC/MF A02

Typical plastic-bonded explosives (PBX) with greater than 90 weight-percent explosive filler in a fluorocarbon binder have tensile strains which range from 0.2 to 0.6 percent. We have recently developed a triaminotrinitrobenzine (TATB)-based PBX with a tensile strain approaching 1 percent while maintaining a high-volume loading of the crystalline explosive component. We discuss our formulation efforts and the critical processing parameters which affect the ultimate mechanical properties of this PBX. DOE

N91-16163*# Arizona Univ., Tucson.
COMPOSITE SOLID PROPELLANT PREDICTABILITY AND QUALITY ASSURANCE
Kumar Ramohalli 1989 126 p Meeting held in Tucson, AZ,

21 Apr. 1989
(Grant NAG8-757)
(NASA-CR-186404; NAS 1.26:186404) Avail: NTIS HC/MF A07 CSCL 21I

Reports are presented at the meeting at the University of Arizona on the study of predictable and reliable solid rocket motors. The following subject areas were covered: present state and trends in the research of solid propellants; the University of Arizona program in solid propellants, particularly in mixing (experimental and analytical results are presented). For individual titles, see N91-16164 through N91-16165.

N91-16164*# Arizona Univ., Tucson.
INTRODUCTION TO THE PROBLEM
Kumar Ramohalli *In its* Composite Solid Propellant Predictability and Quality Assurance 1989 p 2-28 (For primary document see N91-16163 08-28)
Avail: NTIS HC/MF A07 CSCL 21I

Solid propellant rockets were used extensively in space missions ranging from large boosters to orbit-raising upper stages. The smaller motors find exclusive use in various earth-based applications. The advantage of the solids include simplicity, readiness, volumetric efficiency, and storability. Important recent progress in related fields (combustion, rheology, micro-instrumentation/diagnostics, and chaos theory) can be applied to solid rockets to derive maximum advantage and avoid waste. Main objectives of research in solid propellants include: to identify critical parameters, to establish specification rules, and to develop quantitative criteria. Y.S.

N91-16165*# Arizona Univ., Tucson.
THE UNIVERSITY OF ARIZONA PROGRAM IN SOLID PROPELLANTS
Kumar Ramohalli *In its* Composite Solid Propellant Predictability and Quality Assurance 1989 p 29-58 (For primary document see N91-16163 08-28)
Avail: NTIS HC/MF A07 CSCL 21I

The University of Arizona program is aimed at introducing scientific rigor to the predictability and quality assurance of composite solid propellants. Two separate approaches are followed: to use the modern analytical techniques to experimentally study carefully controlled propellant batches to discern trends in mixing, casting, and cure; and to examine a vast bank of data, that has fairly detailed information on the ingredients, processing, and rocket firing results. The experimental and analytical work is described briefly. The principle findings were that: (1) pre- (dry) blending of the coarse and fine ammonium perchlorate can significantly improve the uniformity of mixing; (2) the Fourier transformed IR spectra of the uncured and cured polymer have valuable data on the state of the fuel; (3) there are considerable non-uniformities in the propellant slurry composition near the solid surfaces (blades, walls) compared to the bulk slurry; and (4) in situ measurements of slurry viscosity continuously during mixing can give a good indication of the state of the slurry. Several important observations in the study of the data bank are discussed. Y.S.

N91-16166*# National Aeronautics and Space Administration. John F. Kennedy Space Center, Cocoa Beach, FL.
AN ASSESSMENT OF THE GOVERNMENT LIQUID HYDROGEN REQUIREMENTS FOR THE 1995-2005 TIME FRAME INCLUDING ADDENDUM, LIQUID HYDROGEN PRODUCTION AND COMMERCIAL DEMAND IN THE UNITED STATES
Addison Bain Jul. 1990 85 p
(NASA-TM-103812; NAS 1.15:103812) Avail: NTIS HC/MF A05 CSCL 21I

Liquid hydrogen will continue to be an integral element in virtually every major space program, and it has also become a significant merchant product for certain commercial markets. Liquid hydrogen is not a universally available commodity, and the number of supply sources historically have been limited to regions having concentrated consumption patterns. With the increased space program activity it becomes necessary to assess all future programs on a collective and unified basis. An initial attempt to identify projected requirements on a long range basis is presented. For individual titles, see N91-16167 through N91-16168.

N91-16167*# National Aeronautics and Space Administration. John F. Kennedy Space Center, Cocoa Beach, FL.
AN ASSESSMENT OF THE GOVERNMENT LIQUID HYDROGEN REQUIREMENTS FOR THE 1995-2005 TIME FRAME
Addison Bain *In its* An Assessment of the Government Liquid Hydrogen Requirements for the 1995-2005 Time Frame Including Addendum, Liquid Hydrogen Production and Commercial Demand in the United States Jul. 1990 23 p (For primary document see N91-16166 08-28)
Avail: NTIS HC/MF A05 CSCL 21I

The results of government study of long range liquid hydrogen (LH2) requirements for the time period of 1995 through the year 2005 are presented. To assure an adequate supply of LH2 is available in support of various programs, it is imperative a long range projection of LH2 requirements be developed and maintained. This information is vital in planning for necessary procurement actions and assuring adequate industry lead time to acquiring the necessary production and distribution capabilities. The Advanced Launch System and High-Altitude Long-Endurance programs may represent the predominant government needs for LH2 in the long range. The assembled data clearly indicates a need for KSC (Kennedy Space Center) constant program/project surveillance. Also clear is the need for KSC to monitor industry's plans for LH2 plant production and distribution expansion. Y.S.

N91-16168*# SRI International Corp., Menlo Park, CA.
LIQUID HYDROGEN PRODUCTION AND COMMERCIAL DEMAND IN THE UNITED STATES Final Report
Barbara Heydorn *In* NASA. Kennedy Space Center, An Assessment of the Government Liquid Hydrogen Requirements for the 1995-2005 Time Frame Including Addendum, Liquid Hydrogen Production and Commercial Demand in the United States Jul. 1990 39 p (For primary document see N91-16166 08-28)
(SRI Proj. 8562)
Avail: NTIS HC/MF A05 CSCL 21I

Kennedy Space Center, the single largest purchaser of liquid hydrogen (LH2) in the United States, evaluated current and anticipated hydrogen production and consumption in the government and commercial sectors. Specific objectives of the study are as follows: (1) identify LH2 producers in the United States and Canada during 1980-1989 period; (2) compile information in expected changes in LH2 production capabilities over the 1990-2000 period; (3) describe how hydrogen is used in each consuming industry and estimate U.S. LH2 consumption for the chemicals, metals, electronics, fats and oil, and glass industries, and report data on a regional basis; (4) estimate historical and future consumption; and (5) assess the influence of international demands on U.S. plants. Y.S.

N91-16169# Army Chemical Research and Development Center, Aberdeen Proving Ground, MD.
SYMMETRY AND DESIGN IN MIXTURE EXPERIMENTS Final Report, Mar. 1989 - Jun. 1990
Ronald B. Crosier Aug. 1990 33 p
(AD-A226760; CRDEC-TR-218) Avail: NTIS HC/MF A03 CSCL 07/4

The central composite design and designs based on the icosahedron and the dodecahedron are given for four component mixture systems. A uniform shell design is applied to the development of an obscurant smoke. Oils, cements, gasolines, and perfumes, are mixtures of components. The development of better products of these types involves experimentation with different formulations, or blends, of the components. GRA

N91-16170# Human Systems Div., Brooks AFB, TX.
A COMPARISON OF THREE PROSPECTIVE ANALYTICAL METHODS FOR BENZENE ANALYSIS IN JET FUEL ENVIRONMENTS Final Report

Mohammad A. Hossain Aug. 1990 23 p
(AD-A227489; USAFOEHL-90-126SA00687HAE) Avail: NTIS HC/MF A03 CSCL 07/3

Accurate analysis of benzene in jet fuel has been a concern over the past several years. The method has been used to analyze benzene in jet fuel is the NIOSH 1501 method, a method specifically designed for aromatic hydrocarbons including benzene. However, the method is not designed for analysis of benzene in jet fuel environments. At the present time there is no approved (either by NIOSH or OSHA) method for analysis of benzene in fuel environments. At the request of HQ AAC/SGPB, a study was conducted to compare three prospective analytical methods (NIOSH method 1501 (Gas Chromatography/Flame Ionization Detection (GC/FID) with packed column), modified NIOSH 1501 method (GC/FID with capillary column), and High Pressure Liquid Chromatography with Ultraviolet Detection (HPLC/UV)). Spiked charcoal tube samples as well as air samples of known concentrations of benzene in JP-4 and Stoddard Solvents were analyzed by all three methods. The test results showed that modified NIOSH 1501 and HPLC methods had good correlation between spiked and measured amount of benzene in JP-4 and Stoddard Solvent mixtures. The NIOSH 1501 method utilizing packed column over estimated the test benzene concentration indicating positive interference from other hydrocarbons present in JP 4 and Stoddard Solvents. GRA

N91-16171# Coordinating Research Council, Inc., Atlanta, GA.
CRC VOLATILITY PROGRAM ON THE EFFECT OF OXYGENATED FUELS AND ALTITUDE ON COLD-START DRIVABILITY AT LOW AMBIENT TEMPERATURES
Jan. 1990 162 p
(AD-A227571; CRC-569) Avail: NTIS HC/MF A08 CSCL 21/4

The 1988 CRC driveability program investigated the effects of altitude and fuel oxygenates at low ambient temperature upon cold-start driveability with vehicles equipped with various fuel systems. This program was conducted because of the use of gasoline-oxygenate blends to reduce ambient air carbon monoxide levels. The test program was divided into two phases. A high-altitude phase was conducted new Denver, Colorado, from January 11 through February 10, 1988, at an altitude of 5,486 feet; and a low-altitude phase was conducted in Brainerd, Minnesota, from March 4 through March 31, 1988, at an altitude of 1,226 feet. Test temperatures were 10 F to 40 F. Twenty-four vehicles chosen to represent a variety of engines and fuel systems tested twelve test fuels, including hydrocarbon-only fuels, gasoline-ethanol blends, and gasoline-MTBE blends. The altitude change between the two sites was found to have no statistically significant effect on driveability for the overall fleet. Driveability performance decreased statistically significantly with declining ambient temperatures. For the overall fleet, the oxygenate-containing fuels evaluated performed poorer than hydrocarbon-only fuels at a statistically significant level. GRA

N91-16172# SRI International Corp., Menlo Park, CA.
IONIC SOLID HYDROGEN FUEL: PRODUCTION AND PROPERTIES OF HYDROGEN ION AND ENERGETIC NEUTRAL CLUSTERS Final Report, Apr. 1987 - Jun. 1990
Young K. Bae and Philip C. Cosby Sep. 1990 81 p
(Contract F04611-87-C-0025)
(AD-A227683; MP-90-080; AL-TR-90-049) Avail: NTIS HC/MF A05 CSCL 07/4

It was demonstrated that the production of intense beams of positive hydrogen cluster ions is quite feasible, and should allow their rapid embedment in a H2 matrix. However, stabilization of these species by codeposition of hydrogen cluster anions does not appear to be a useful approach, because of the extreme difficulty encountered in generating the negative hydrogen cluster beams. Whereas the hydrogen anion clusters may be unstable in the gas phase, with the matrix H may form a cavity by repelling the surrounding H2 molecules to produce a locally stable structure. A much more promising way of achieving an extremely high energy density for rocket propulsion is the use of hydrogen containing cluster ions for igniting nuclear fusion (cluster-impact fusion, CIF). GRA

N91-16173# Messerschmitt-Boelkow-Blohm G.m.b.H., Schrobenhausen (Germany, F.R.).
DIAGNOSTIC OF THE REACTION BEHAVIOUR OF INTENSIVE HIGH EXPLOSIVES UNDER JET ATTACK
Manfred Held 1990 9 p Presented at the International CHSPP, Cambridge, England, 16-22 Sep. 1990
(MBB-UA-1188-90-PUB; ETN-91-98508) Avail: NTIS HC/MF A02

Definitive conclusions about high and low order reactions can be drawn from individual framing mode pictures of a rotating mirror camera record, when both the velocity of the axial propagation of the reaction along the outer contour and the velocity of radial products are analyzed at various distances from the plane of initiation. In this, the intensity of the reaction can be assessed quantitatively from the radial expansion velocities, even when, for example, a penetrating shaped charged jet induces a bow wave in the test charge. A detailed description of the test set up and of the test results obtained with charges exposed to the impact of a shaped charge jet is given. ESA

29 MATERIALS PROCESSING

Includes space-based development of products and processes for commercial applications.

For biological materials see *55 Space Biology*.

No abstracts in this category.

31 ENGINEERING (GENERAL)

Includes vacuum technology; control engineering; display engineering; cryogenics; and fire prevention.

N91-16174# Los Alamos National Lab., NM.
SAFE VENTING OF HYDROGEN
W. F. Stewart, J. M. Dewart, and F. J. Edeskuty 1990 14 p Presented at the 8th World Hydrogen Energy Conference, Honolulu, HI, 23-27 Jul. 1990
(Contract W-7405-eng-36)
(DE90-008964; LA-UR-90-753; CONF-900705-2) Avail: NTIS HC/MF A03

The disposal of hydrogen is often required in the operation of an experimental facility that contains hydrogen. Whether the vented hydrogen can be discharged to the atmosphere safely depends upon a number of factors such as the flow rate and atmospheric conditions. Calculations have been made that predict the distance a combustible mixture can extend from the point of release under some specified atmospheric conditions. Also the quantity of hydrogen in the combustible cloud is estimated. These results can be helpful in deciding if the hydrogen can be released directly to the atmosphere, or if it must be intentionally ignited. DOE

N91-16175# Oak Ridge National Lab., TN.
INITIAL PARAMETRIC RESULTS USING CYCLEZ: A LMTD-SPECIFIED, LORENZ-MEUTZNER CYCLE REFRIGERATOR-FREEZER MODEL
C. Keith Rice and James R. Sand 1990 24 p Presented at the International Compressor Engineering Conference; USNC/IIR-Purdue Refrigeration Conference; and ASHRAE-Purdue CFC Conference, West Lafayette, IN, 17-20 Jul. 1990 Sponsored by EPA
(Contract DE-AC05-84OR-21400)
(DE90-010146; CONF-900742-1) Avail: NTIS HC/MF A03

A computer model representing a two-evaporator, two-intercooler refrigerator-freezer operating at steady-state with nonazeotropic refrigerant mixtures (CYCLEZ) has been developed

at Oak Ridge National Laboratory (ORNL). This model is being used to assess the effects of system design and operating parameters on the cycle performance of a refrigerator-freezer designed around the Lorenz-Meutzner (L-M) circuit. Separate evaporators for the freezer and fresh-food compartments are modeled, as well as two intercoolers that subcool liquid refrigerant from the condenser by heat transfer with low-pressure refrigerant. The CYCLEZ refrigerator/freezer model is derived from the CYCLEZ heat-pump model developed originally by the National Institute of Standards and Technology (NIST). CYCLEZ currently uses the Carnahan-Starling-DeSantis (CSD) equation-of-state to compute refrigerant thermodynamic properties, so that new refrigerants can easily be added. Condenser and evaporator heat-exchanger performance are defined by user-specified overall LMTDs which allow equivalent heat-exchanger sizing per unit refrigeration load to be maintained for different refrigerant mixtures. A more consistent formulation of overall heat-exchanger LMTD is applied across the condenser superheated and two-phase regions as well as over the two evaporators. Source and sink conditions are specified in terms of inlet and outlet temperatures of the external fluid streams. Intercooler high-side (subcooling) delta Ts and relative fresh-food-to-freezer load ratio are also user-specified. These features make this model well suited for evaluating the optimal thermodynamic cycle requirements of the five heat exchangers used in the L-M refrigerator/freezer circuit. DOE

N91-16176# Allied-Signal Corp., Kansas City, MO. Bendix Kansas City Div.
DEBURRING AND SURFACE FINISHING: THE PAST TEN YEARS AND PROJECTIONS FOR THE NEXT TEN YEARS
LaRoux K. Gillespie Sep. 1990 21 p Presented at the Deburring Salon Conference, Nagoya, Japan, 23-25 Oct. 1990
(Contract DE-AC04-76DP-00613)
(DE91-000579; KCP-613-4437; CONF-9010203-1) Avail: NTIS HC/MF A03

The 1970s were a decade of significant growth in deburring and surface finishing. In the 1980s progress was made in robotic finishing, burr formation models, surface finish measurement, new processes, equipment and tooling. The centers of burr and surface related research changed. The decade of the 1990s will bring greater competition, environmental restrictions, more processes, more automation, and better characterization and simulation of processes. DOE

N91-16177# RAND Corp., Santa Monica, CA.
IMPACTS OF ADVANCED MANUFACTURING TECHNOLOGY ON PARAMETRIC ESTIMATING
Paul G. Hough Dec. 1989 30 p
(AD-A228232; RAND/P-7543) Avail: NTIS HC/MF A03 CSCL 13/8

The introduction of advanced manufacturing technology in the aerospace industry poses serious challenges for government cost analysts. Traditionally, the analysts have relied on parametric estimating techniques for both planning and budgeting. Despite its problems, this approach has proven to be a remarkably useful and robust tool for estimating new weapon system costs. However, rapid improvements in both product and process technology could exacerbate current difficulties, and diminish the utility of the parametric approach. This paper reviews some weakness associated with parametrics, then proceeds to examine how specific aspects of the factory of the future may further impact parametric estimating, and suggests avenues of research for their resolution. This paper is an extended version of Cost Estimating for the Factory of the Future. Parametric estimating is a method by which aggregated costs are derived as a function of high-level product characteristics or parameters. The resulting equations are known as cost estimating relationships (CERs). Such equations are particularly useful when detailed technical specifications are not available. GRA

N91-16178# Technische Univ., Eindhoven (Netherlands). Dept. of Mathematics and Computing Science.
GEOMETRICAL ASPECTS OF THE PRODUCTION OF TOOTHED DISKS [MEETKUNDIGE ASPECTEN VAN DE PRODUCTIE VAN KROONWIELEN]
D. A. Overdijk Jan. 1990 29 p In DUTCH
(MEMO-COSOR-90-02; ETN-91-98433) Avail: NTIS HC/MF A03

The formulas that are important for the geometrical description of toothed disk transmission are reviewed. A cartesian coordinate system is introduced for the geometrical considerations. The parameter representations of the tooth slopes on the toothed disk slope is analyzed. New handy formulas are given. Three control surfaces which approximate the toothed disk slope are discussed; the accuracy of the approximations is tabulated. ESA

N91-16179# Technische Univ., Delft (Netherlands).
CONTROL OF INDUSTRIAL CRYSTALLIZERS: THE PHYSICAL ASPECTS Ph.D. Thesis
Johan Jager 1990 154 p Sponsored by Akzo Zout Chemie, Hengelo, Netherlands; Dow Chemical Co., Terneuzen, Netherlands; DSM/nv Nederlandse Staatsmijnen, Geleen; Du Pont de Nemours (E. I.) and Co.; Rhone-Poulenc Industries; Suiker Unie; Unilever Research, Vlaardingen, Netherl
(ETN-91-98488) Avail: NTIS HC/MF A08

Three major requirements are to be met in order to establish Crystal Size Distribution (CSD) control: an on line CSD measurement, an accurate dynamic model, and effective process inputs. The continuous crystallization of ammonium sulfate in a draft tube baffled crystallizer serves as an example of the process. The design and the results of a dilution technique used to measure CSD transients are discussed. The results obtained are roughly in accordance with sieve analysis. Various aspects of the modeling of a continuous evaporative crystallizer are shown. A general technique for the estimation of parameters at unsteady state conditions is applied to the phenomenon of crystal birth. Crystal attrition causes a reduction in the number of larger crystals. The experimental data obtained so far, indicate that CSD is relatively invariant towards changes in the residence time, the heat input, and the rate of fines removal. ESA

32 COMMUNICATIONS AND RADAR

Includes radar; land and global communications; communications theory; and optical communications.

For related information see also *04 Aircraft Communications and Navigation* and *17 Space Communications, Spacecraft Communications, Command and Tracking.* For search and rescue see *03 Air Transportation and Safety,* and *16 Space Transportation.*

N91-16180# Sandia National Labs., Albuquerque, NM.
NUMERICAL MODELING TOOLS FOR TRANSIENT ELECTROMAGNETIC PROBLEMS
Douglas J. Riley, C. David Turner, Larry D. Bacon, and Joseph D. Kotulski Apr. 1990 163 p
(Contract DE-AC04-76DP-00789)
(DE90-010328; SAND-90-0519) Avail: NTIS HC/MF A08

Finite difference time domain (FDTD) codes can, in principle, be used to determine the electromagnetic response of complex scatterers. However, the extent to which structural details can be accommodated is limited by computer resources and one's ability to specify necessary parameters. By embedding into the FDTD code alternative numerical methods that solve the aspects of the problem which are not practical, or possible, for the FDTD code to handle, power and flexibility can be added. Three such hybrid schemes are investigated. Topics include: (1) embedding a transient multiconductor circuit analysis code so that coupling down to the component level can be directly computed; (2) the effectiveness of using a multiconductor transmission line code to analyze shielded multiwire cables in FDTD calculations; and (3) the effectiveness of using 2-D and 3-D aperture transfer functions to model narrow

apertures in FDTD formulations. These topics were selected because of their immediate need in system assessments. Experimental measurements and/or alternative solution methods are used to verify the hybrid approaches. DOE

N91-16181# Lawrence Livermore National Lab., CA.
COMPARISON OF PROPAGATION AND ABSORPTION OF FEL-GENERATED MICROWAVES WITH THEORY
M. E. Fenstermacher May 1990 21 p
(Contract W-7405-eng-48)
(DE90-010369; UCRL-ID-103808) Avail: NTIS HC/MF A03

The ECH propagation and absorption experiments performed in MTX during November, 1989 were analyzed in detail. These experiments used a microwave horn mounted behind the microwave calorimeter on the tokamak inside wall to measure the ECH power transmitted through the plasma from the injection port. The transmitted power fraction was obtained by normalizing this measurement with the incident power measured by a horn in the last mirror (M4) of the microwave transmission line. Analysis of shots without plasma showed that the powers measured by the two horns were linearly dependent. The remainder of this report is organized as follows. The next section presents the analysis of the data from the FEL experiments. A broad comparison of the data with ray tracing results using fixed density and temperature profiles is described. Following this, detailed analysis of individual shots are given in which density profiles inferred from FIR interferometer measurements and electron temperature profiles from ECE measurements are used in the ray tracing and absorption calculations. The next section discusses possible causes for the scatter in the experimental data and the differences between the measurements and calculational predictions. DOE

N91-16182# Lawrence Livermore National Lab., CA.
MODELING PULSE DRIVEN ANTENNA SYSTEMS WITH FINITE DIFFERENCES
Marvin Barth, Steve Pennock, Richard Ziolkowski, and Robert McLeod Mar. 1990 7 p Presented at the 6th Annual Review of Progress in Applied Computational Electromagnetics, Monterey, CA, 20-22 Mar. 1990
(Contract W-7405-eng-48)
(DE90-010682; UCRL-JC-103302; CONF-9003128-3) Avail: NTIS HC/MF A02

The capability was developed of modeling the performance of general, pulse driven, antenna systems. The approach is to use TSAR, a three dimensional finite difference time domain (FDTD) code, to model the antenna structure and the surrounding near field environment. A far field project algorithm was used to obtain its far field response. Specifically, this algorithm utilizes the tangential electric and magnetic fields at a specified surface of the TSAR FDTD computational volume and calculates the resulting fields far from the equivalent magnetic and electric sources. This approach is illustrated by considering the TEB antenna system. The system is modeled with the code and the results are compared with anechoic chamber data. DOE

N91-16183# Stanford Linear Accelerator Center, CA.
SLED II: A NEW METHOD OF RF PULSE COMPRESSION
P. B. Wilson, Z. D. Farkas, and R. D. Ruth Sep. 1990 3 p Presented at the 1990 LINAC Conference, Albuquerque, NM, 10-14 Sep. 1990
(Contract DE-AC03-76SF-00515)
(DE91-000058; SU-SLAC-PUB-5330; CONF-9009200-12) Avail: NTIS HC/MF A01

In the SLED method of RF pulse compression, two high Q resonators store energy from an RF source for a relatively long time interval (typically 3 to 5 microsec). Triggered by a reversal in RF phase, this stored energy is then released during a much shorter interval equal to the filling time of the accelerating structure. A peak power gain on the order of three and a compression efficiency on the order of 60 percent are typically attained. The shape of the output pulse is, however, a sharply decaying exponential. In SLED-2 the two cavities are replaced by two lengths of resonant line, forming a Resonant Line SLED (RELS) and resulting in a flat output pulse. Therefore, RELS stages can be cascaded to give a greater peak power gain. Using two stages, a peak power gain greater than ten can be achieved with a reasonable compression efficiency. Unlike the BEC, the RELS compression factor per stage is not limited to two, albeit at the expense of intrinsic efficiency. Like the BEC, it uses long lines rather than short cavities. DOE

N91-16184# Texas Univ., Austin. Dept. of Electrical and Computer Engineering.
SOME APPLICATIONS OF PROBABILITY AND STATISTICS IN COMMUNICATION THEORY AND SIGNAL PROCESSING Final Technical Report, 1 Nov. 1986 - 30 Apr. 1990
Gary L. Wise 16 Aug. 1990 22 p
(Grant AF-AFOSR-0026-86; AF Proj. 2304)
(AD-A226869; AFOSR-90-1034TR) Avail: NTIS HC/MF A03 CSCL 12/1

This Final Technical Report constitutes a summary of the research performed under Grant AFSOR-86-0026 during the period November 1, 1986 through April 30, 1990. First a list is presented of the personnel involved in the research effort. Then in the following section a brief summary is presented of the research results that were achieved. Each of these results is well documented in technical articles, and references to these articles are made in the summary of the research results. GRA

N91-16185# Woods Hole Oceanographic Inst., MA.
THE HIGH SPEED BUFFER BOARD: A SAIL EIA-485 COMMUNICATIONS ACCELERATOR CARD FOR THE VECTOR MEASURING CURRENT METER
Robin Singer and Douglas M. Butler Jul. 1990 52 p
(Contracts N00014-84-C-0134; N00014-90-J-1495)
(AD-A227181; WHOI-90-33) Avail: NTIS HC/MF A04 CSCL 17/2

A High Speed Buffer Board (HSBB) was developed for the Vector Measuring Current Meter (VMCM) to implement the transmission of data at 9600 baud over an EIA-485 link. The HSBB significantly extends the VMCM communication functionality, which was previously limited to 300 baud transmission via 20mA current loop or FSK telemetry. The increased speed allows rapid sampling of a large number of current meters on a common cable and the EIA-485 circuitry, which was designed for low power operation, provides a useful multipoint communication method for data transmission over long cable lengths. SAIL protocol (IEEE 997) was utilized to coordinate data transfer by the instruments on a common link. An MC68HC11 microcontroller resides in the VMCM, buffering data it receives at 300 baud from the VMCM UART. In response to a jumper selectable SAIL address, the MC68HC11 offloads the data 9600 baud via EIA-485 to the SAIL controller. Synchronous data collection from many instruments is ensured by the SAIL synoptic set command and an embedded resynchronization/reset command. The low power consumption allows deployments of six months or more with a standard VMCM battery stack. GRA

N91-16186# Naval Research Lab., Washington, DC. Communication Systems Branch.
MOVABLE-BOUNDARY CHANNEL-ACCESS SCHEMES FOR INTEGRATED VOICE/DATA NETWORKS Memorandum Report, Jan. - Jun. 1989
Jeffrey E. Wieselthier and Anthony Ephremides (Maryland Univ., College Park.) 20 Aug. 1990 47 p Sponsored by ONR, Arlington, VA
(AD-A227331; NRL-MR-6706) Avail: NTIS HC/MF A03 CSCL 17/2

Channel-access protocols for integrated radio networks must reflect the different communication requirements associated with voice and data, as well as the impact each type of traffic has on the other. A new class of protocols are introduced which were developed for this application, they are known as the Voice/Data Interleaved-Frame Fixed-Length (VD-IFFL) protocols. As a first step in the discussion of the VD-IFFL protocols, the IFFL protocols are introduced, which are similar to the Interleaved-Frame-Flush-Out

(IFFO) protocols (a class of schemes developed for data only applications) except that they have a fixed frame length, a desirable feature in voice communication. The VD-IFFL protocols use a movable boundary mechanism to share the channel between voice and data traffic. Voice traffic is handled on a reservation basis, while data traffic is handled using a hybrid IFFL scheme that combines reservation and contention. These protocols are characterized by infinite Markov chains, whose transition probabilities were evaluated exactly. GRA

N91-16187# Air Force Inst. of Tech., Wright-Patterson AFB, OH.
ELECTRON DENSITY COMPARISONS BETWEEN RADAR OBSERVATIONS AND 3-D IONOSPHERIC MODEL CALCULATIONS M.S. Thesis
Michael W. Johnson 1990 111 p
(AD-A227703; AFIT/CI/CIA-90-109) Avail: NTIS HC/MF A06 CSCL 20/14

A comparison of electron densities calculated from the Utah State University First-Principals Ionospheric Model with simultaneous observations taken at Sondrestrom, Millstone, and Arecibo incoherent scatter radars was undertaken to better understand the response of the ionosphere at these longitudinally similar yet latitudinally separated locations. The comparison included over 50 days distributed over 3 1/2 years roughly symmetrical about the last solar minimum in 1986. The overall trend of the comparison was that to first-order the model reproduces electron densities responding to diurnal, seasonal, geomagnetic, and solar cycle variations for all three radars. However, some model observation discrepancies were found. These include, failure of the model to correctly produce an evening peak at Millstone, fall-spring equinox differences at Sondrestrom, tidal structure at Arecibo, and daytime NmF2 values at Arecibo. GRA

N91-16188# Air Force Inst. of Tech., Wright-Patterson AFB, OH.
SHIFT-INVARIANT IMAGE RECONSTRUCTION OF SPECKLE-DEGRADED IMAGES USING BISPECTRUM ESTIMATION M.S. Thesis - Rochester Inst. of Technology
Steven M. Wear May 1990 156 p
(AD-A227728; AFIT/CI/CIA-90-094) Avail: NTIS HC/MF A08 CSCL 20/14

Coherent speckle noise is modeled as a multiplicative noise process that has a negative exponential probability density function. Using a homomorphic transformation, this speckle noise is converted to a signal-independent, additive process. The speckled images are randomly jittered from frame-to-frame against a uniform background to simulate image motion and/or platform jitter. Multiple images are logarithmically transformed and ensemble averaged in the bispectral domain. The bispectrum ignores this image motion so no blurring results from the ensemble averaging. Object Fourier magnitude and phase information are also retained in the bispectrum so that the resultant image can be uniquely reconstructed. This value is then exponentiated to complete the image reconstruction process. Since speckle masks the resolution of details in the noisy image and effectively destroys the object structure within the image, it is seen that image reconstruction using bispectrum estimation results in images that regain their object structure. Both one-dimensional and two-dimensional images were tested using separate bispectral signal reconstruction algorithms for each. GRA

N91-16189 British Broadcasting Corp., Kingswood (England). Engineering Div.
SATELLITE BROADCASTING: A COMMON-FREQUENCY APPROACH TO WIDEBAND HDTV WITH A HAND-MADE EXAMPLE PLAN
J. H. Stott 1990 17 p
(BBC-RD-1990/7) Avail: Issuing Activity

The generation and analysis of a hand-made plan for satellite broadcasting are described. The plan is intended as an example of what could be achieved within any band which may be allocated for wide-band high definition TV (HDTV) at a forthcoming World Administrative Radio Conference. It is shown that the whole of such a band could be used by every country simultaneously, each country being assigned an orbit location and the use of one or the other hand of polarization, provided digital modulation is used with receiving antennas of sufficient directivity. As a guide, 0.9 m at 17 GHz or 0.7 m at 22 GHz appear to be adequate receiving-antenna diameters as far as controlling interference is concerned. Use of digital modulation in this way makes more efficient usage of spectrum than analogue modulation, offering more programs per country per MHz of allocated band. It also permits greater flexibility of exploitation of the band. Author

N91-16190 British Broadcasting Corp., Kingswood (England). Engineering Div.
NICAM 728: FACTORS AFFECTING THE ASSESSMENT OF UHF TRANSMITTER LINEARITY
K. L. Beeke and A. G. Lyner 1990 18 p Original contains color illustrations
(BBC-RD-1990/9; RA-253) Avail: BBC, Kingswood Warren, Tadswoth, Surrey, England

Work was carried out to investigate the need for change in the specification of transmitter distortion levels once the digital stereo sound carrier has been introduced. New test signals were proposed and subjective tests were conducted to determine the visibility of the original distortion products and, hence, to determine appropriate limits. Author

N91-16191*# Ohio State Univ., Columbus. Dept. of Electrical Engineering.
THE REFLECTION AND TRANSMISSION PROPERTIES OF A TRIPLE BAND DICHROIC SURFACE Final Report
S. W. Schneider and B. A. Munk Dec. 1990 89 p
(Contract NCC3-158)
(NASA-CR-187776; NAS 1.26:187776; ESL-FTR-723108-1)
Avail: NTIS HC/MF A05 CSCL 20N

The development of a triple-band dichroic surface design is detailed that is reflective in the Ka-band from 22.5 to 27.3 GHz and the Ku-band from 13.7 to 15.1 GHz, yet transparent in the S-band from 2.0 to 2.3 GHz, for all planes of incidence, and for all angles of incidence out to eta = 45 deg. The design is comprised of two gangbuster whole-surfaces separated by a distance, d, that is comparable to a fraction of a wavelength in S-band, and enhanced by the addition of a dielectric matching plate. The gangbuster array is comprised of tightly packed straight skewed dipole elements referred to as half-surfaces. Two of these half-surfaces are oriented orthogonal to each other and placed an array separation distance, s, apart to form the gangbuster whole-surface which allows any arbitrary plane of incidence. Results are given for the triple-band design with and without dielectric and conduction losses. The cross polarization properties of the dichroic surface was further investigated. It is shown that the reflection cross polarized component is dominated by the geometry of the front whole surface of the design (particularly the array separation s) and is never more than -22.5 dB in the frequency band 0 to 30 GHz. The transmission cross polarization component is dependent on both whole-surfaces and is never more than -30 dB in the same frequency band. Author

N91-16192# Royal Signals and Radar Establishment, Malvern (England).
MODELS FOR SURFACE SCATTERING FROM SOLIDS AND LIQUIDS
D. L. Jordan Mar. 1990 13 p
(RSRE-MEMO-3699; BR114980; ETN-91-98412) Copyright
Avail: NTIS HC/MF A03

Some work on surface scattering of electromagnetic radiation is outlined. In particular, it is intended to present some of the data that suggests that fractals seem to provide realistic models for rigid surface scattering. For agitated fluid surfaces the experimental data is more tenuous. Some new but limited experimental findings that are reported, together with other briefly

mentioned work, suggests that something approximating to a marginal fractal may be more appropriate for liquids. ESA

N91-16193# Royal Signals and Radar Establishment, Malvern (England).
ANALYSIS OF THE PERFORMANCE OF A SINGLE-AUXILIARY SIDELOBE CANCELLER
I. Day and A. C. Fairhead Aug. 1990 37 p
(RSRE-MEMO-4375; BR115187; ETN-91-98413) Copyright
Avail: NTIS HC/MF A03

The geometrical approach to analyzing the performance of simple sidelobe canceller systems is illustrated. Systems with a single degree of freedom and with a two tap transversal filter are analyzed. Throughout, examples are given based on the BYSON antenna. These show that a single auxiliary channel containing a two tap transversal filter allows jamming arriving from any azimuth to be nulled over the radar signal bandwith. More general results may be deduced from the analysis. ESA

N91-16194*# Ohio State Univ., Columbus. Dept. of Electrical Engineering.
A PLANAR NEAR-FIELD SCANNING TECHNIQUE FOR BISTATIC RADAR CROSS SECTION MEASUREMENTS
S. Tuhela-Reuning and E. K. Walton Dec. 1990 47 p
(Grant NAG3-1125)
(NASA-CR-187794; NAS 1.26:187794; ESL-TR-723105-1) Avail: NTIS HC/MF A03 CSCL 20N

A progress report on the development of a bistatic radar cross section (RCS) measurement range is presented. A technique using one parabolic reflector and a planar scanning probe antenna is analyzed. The field pattern in the test zone is computed using a spatial array of signal sources. It achieved an illumination pattern with 1 dB amplitude and 15 degree phase ripple over the target zone. The required scan plane size is found to be proportional to the size of the desired test target. Scan plane probe sample spacing can be increased beyond the Nyquist lambda/2 limit permitting constant probe sample spacing over a range of frequencies.
Author

N91-16195# Massachusetts Inst. of Tech., Lexington. Lincoln Lab.
THE 1/f FREQUENCY NOISE EFFECTS ON SELF-HETERODYNE LINEWIDTH MEASUREMENTS FOR COHERENT COMMUNICATIONS
Linden B. Mercer 31 Jul. 1990 32 p
(Contract F19628-90-C-0002)
(AD-A227942; TR-881; ESD-TR-90-011) Avail: NTIS HC/MF A03 CSCL 12/9

The effects of 1/f frequency noise on self-heterodyne detection are described and the results are applied to the problem of laser-diode-linewidth measurement. Laser diode linewidths determined by self-heterodyne methods are not adequate predictors of coherent communications system performance because the measurements often include significant broadening due to 1/f frequency noise. In this report, the autocorrelation function and power spectrum of the detected self-heterodyne photocurrent are developed in terms of an arbitrary frequency noise. From numerical analysis, the power spectrum resulting from the 1/f frequency noise is shown to be approximately Gaussian and an empirical expression is given for its linewidth. These results are applied to the problem of self-heterodyne linewidth measurements for coherent optical communications, and the amount of broadening due to 1/f frequency noise is predicted. Two methods are then provided for estimating the portion of the measured self-heterodyne linewidth due to the white component of the frequency noise and the portion due to 1/f frequency noise. GRA

N91-16196# Rome Air Development Center, Griffiss AFB, NY.
STATISTICALLY THINNED ARRAYS WITH QUANTIZED ELEMENT WEIGHTS Report, 30 Nov. 1987 - 30 Nov. 1989
Robert J. Malloux and Edward Cohen Jan. 1990 44 p
(AF Proj. 4600)
(AD-A227965; RADC-TR-89-391) Avail: NTIS HC/MF A03 CSCL 09/1

This report investigates the use of statistical thinning and quantized element weights to produce low sidelobe patterns using large circular array apertures. The major result of the analysis is a comparison of several thinning algorithms and the evaluation of sidelobe levels, gain and effective radiated power data for large, but otherwise arbitrary size arrays. GRA

N91-16197# Naval Research Lab., Washington, DC. Beam Physics Branch.
DIFFUSION FIELDS IN A TOROIDAL CONDUCTING SHELL OF CIRCULAR CROSS SECTION
D. Dialetis, L. K. Len, J. Golden, and C. A. Kapetanakos (Berkeley Research Association, Springfield, VA.) 1 Oct. 1990 32 p
(AD-A228021; NRL-MR-6719) Avail: NTIS HC/MF A03 CSCL 20/7

The diffusion of an external magnetic field through a toroidal conducting shell is studied under the assumption of a small aspect ratio. The external magnetic field can have an arbitrary field index and magnetic flux on the minor axis of the torus. The diffused field, field index, magnetic flux and wall current are computed analytically and compared with the numerical results from the TRIDIF code. The analytical and numerical results are in good agreement. Measurements in the toroidal chamber of the modified betatron gave a delay time of 34 microseconds, which is less than 10 percent from the theoretical prediction fo 37 microseconds. GRA

N91-16198# Naval Postgraduate School, Monterey, CA.
TACTICAL HF FIELD EXPEDIENT ANTENNA PERFORMANCE, VOLUME 1 M.S. Thesis
Gurkan Turkes Mar. 1990 78 p
(AD-A228057) Avail: NTIS HC/MF A05 CSCL 09/1

This thesis investigates the performance of various configurations of tactical High Frequency (HF) field deployable antennas in the presence of lossy earth. Antennas investigated include horizontal dipoles, short sloping wires, inverted vees, and monopoles with buried and elevated radials. Numerical models of the antennas are exercised via the Numerical Electromagnetics Code (NEC) for radiation pattern performance. Antennas are analyzed for applicability to (1) short-range Near Vertical Incident Skywave (NVIS), where high elevation radiation angles are required; (2) medium-and long-range low radiation angle use; and (3) vertically polarized low-angle radiation for ground wave communication. Good NVIS and ground wave performance occurs for horizontal dipoles. Sloping wires and sloping dipoles are similar to horizontal dipoles but exhibit a moderate amount of azimuth plane directivity. Vertical monopoles with at least 15 buried radials produce medium-and long-range skywave coverage and good ground wave performance. Four elevated radials for quarter-wavelength monopoles are shown to out-perform 15 buried radials and are much easier to erect. The larger and more difficult-to-erect inverted vee dipole slightly outperforms a monopole by virtue of modest azimuth plane directivity. The results of this study can be included in an antenna engineering handbook and can be used to interface with existing ionospheric propagation codes in order to obtain optimum communication effectiveness. GRA

N91-16199# Naval Postgraduate School, Monterey, CA.
MEASUREMENT OF THE CAPTURE EFFECT OF FREQUENCY MODULATION M.S. Thesis
Dennis G. Bevington Dec. 1989 76 p
(AD-A228058) Avail: NTIS HC/MF A05 CSCL 25/2

Capture Effect is a phenomenon associated with frequency modulation (FM). The capture effect relates the ability of the receiver demodulator to recover the message of the dominant carrier when two or more FM carriers of unequal power level are present. In this research, an experimental system is constructed that generates the sum of two FM signals and demodulates that sum using a phase-locked loop (PLL). The effect on capture by

several parameters is measured. These parameters are the frequency deviation of the FM signal, the frequency of the message, and the lowpass filter design of the PLL demodulator. Capture ratios as small as 0.387 dB are observed. Results show that the frequency deviation of the stronger signal affects capture. The frequency deviation of the weaker signal has no effect on capture. Frequencies of the message have small effects on capture. GRA

N91-16200# Princeton Univ., NJ. Dept. of Electrical Engineering.
NEAR/FAR RESISTANT RECEIVERS FOR DS/SSMA COMMUNICATIONS Final Report, 1 Apr. 1987 - 31 Jul. 1990
Sergio Verdu 27 Sep. 1990 200 p
(Contract DAAL03-87-K-0062)
(AD-A228147; ARO-24543.13-EL) Avail: NTIS HC/MF A09
CSCL 25/5

In Code-Division Multiple-Access (CDMA), each transmitter is assigned a fixed, distinct signature waveform which he uses to modulate his message in the same fashion as in single-user communication. Then the information sent by each user can be demodulated by correlating the received signal with each of the signature waveforms. This demodulator, whose use is widespread in practice, is referred to as the conventional single-user detector. As is well-known, when the channel output is corrupted by additive white Gaussian noise, the conventional single-user detector minimizes the probability of error in a single-user channel, i.e., in the absence of interfering users. The fact that this is no longer true in the multiple-access channel is the raison d'etre of the area of multiuser detection. The performance of the conventional single-user detector is acceptable provided that the energies of the received signals are not too dissimilar and that the signature waveforms are designed so that their crosscorrelations are low enough (this depends on the desired maximum number of simultaneous users). In practice, low crosscorrelations are usually achieved employing Spread-Spectrum Pseudonoise sequences of long periodicity. If the received signal energies are indeed dissimilar, i.e., some users are very weak in comparison to others, then the conventional single-user detector is unable to recover the messages of the weak users reliably, even if the signature waveforms have very low crosscorrelation. GRA

N91-16201# Nebraska Univ., Lincoln. Dept. of Electrical Engineering.
SCATTERING AND DEPOLARIZATION BY ROUGH TERRAIN AND SEA: A UNIFIED FULL WAVE APPROACH Final Report, 1 Jul. 1987 - 30 Jun. 1990
Ezekiel Bahar 31 Jul. 1990 73 p
(Contract DAAL03-87-K-0085)
(AD-A228295; ARO-25130.21-GS) Avail: NTIS HC/MF A04
CSCL 20/6

The principal results are summarized from the project. (1) Two separate approaches are developed to account for multiple scatter from rough surfaces. (2) In the high frequency limit shadowing is accounted for by limiting the angles of incidence and scatter to less than 90 deg. (3) The random rough surfaces are often characterized by Gaussian surface height and slope probability density functions. (4) To determine the rough surface cross sections, the random rough surfaces need to be characterized by their joint characteristic functions. (5) The medium below the rough interface is characterized by its complex permittivity and permeability. (6) To make the problem of evaluating the scattering cross sections of random rough surfaces more tractable, it is assumed that the rough surface heights and slopes are statistically uncorrelated. (7) The observed phenomena of enhanced backscatter from very rough surfaces (including particles with rough surfaces) was examined in some detail. (8) Investigations were conducted to determine the scattering cross sections of rough surfaces modified by the presence of oil slicks, ship wakes, swells and other anisotropic surface features. (9) For the vector problem of electromagnetic scattering by two dimensional rough surfaces, the excitations considered are in general elliptically polarized waves. (10) In the past several attempts have been made to obtain experimental validation of the numerical/analytical results based on the full wave approach. The full wave solutions, with the singly and multiple (two bounce) contributions accounted for in the analyses of scattering from very rough surfaces provide an analytical and physical interpretation of the observed enhanced backscatter at both normal and oblique incidence. GRA

N91-16202# Scientific Research Associates, Inc., Glastonbury, CT.
NUMERICAL SIMULATION OF THE COMPARATIVE ELECTRICAL PERFORMANCE OF THE PERMEABLE BASE TRANSISTOR, OPPOSED GATE-SOURCE TRANSISTOR AND HETEROSTRUCTURE LAUNCHED BALLISTIC FIELD EFFECT TRANSISTOR Final Report, 1 Sep. 1986 - 31 Aug. 1989
H. L. Grubin, J. P. Kreskovsky, M. Meyyappan, and B. J. Morrison Oct. 1990 111 p
(Contract N00014-86-C-0567)
(AD-A228545; SRA-R90-910032-F) Avail: NTIS HC/MF A06
CSCL 09/1

Devices operate under large signal conditions. Thus large signal simulations are required. This is illustrated for the permeable base transistor, the heterostructure bipolar transistor, and the opposed source-gate transistor. There were a number of ground-breaking results during the course of this study. The most significant is that a simulation was developed that coupled the large signal two dimensional device behavior to the large signal properties of an external circuit. The study was applied most extensively to the permeable base transistor, where it was determined that if fabrication properties could be addressed successfully, the permeable base transistor could be a significant device in terms of output power and frequency. These results are summarized in the discussion of the permeable base transistor. Studies on the heterostructure bipolar transistor confirm that the long recombination times serve to yield superior performance for the indium based HBTs. Finally, the discussion of the OGST points to its promise as a high frequency switching devices. GRA

N91-16203# Naval Ocean Systems Center, San Diego, CA.
INTEGRATED REFRACTIVE EFFECTS PREDICTION SYSTEM (IREPS) USER'S MANUAL, REVISION PC-2.0
W. L. Patterson Aug. 1990 46 p
(AD-A228549; NOSC/TD-1874) Avail: NTIS HC/MF A03
CSCL 20/14

The purpose of this manual is to introduce the contents and operation of the integrated refractive effects prediction system, personal computer version 2.0 (IREPS PC-2.0). IREPS is a system designed to assess the electromagnetic propagation effects of the lower atmosphere on radar, electronic warfare, communication, and weapon guidance systems. The IREPS models account for effects from optical interference, diffraction, tropospheric scatter, refraction, and evaporation and surface-based ducting under horizontally homogeneous atmospheric conditions. GRA

N91-16204# Electronics Research Lab., Adelaide (Australia). Communications Div.
METEOR BURST COMMUNICATIONS STUDY
John A. Hackworth Jul. 1990 31 p
(AD-A228641; ERL-0519-RE; DODA-AR-006-418) Avail: NTIS HC/MF A03 CSCL 25/2

The results are documented of a study into the use of a meteor burst communication system over the southern part of the Australian continent. Also included is a description of the equipment used and some suggestions for further work. GRA

N91-16205# Hughes Research Labs., Malibu, CA.
APPLICATIONS RESEARCH STUDIES ON MICROTUBULES Final Report, 12 Aug. 1987 - 11 Jul. 1990
J. David Margerum, K. C. Lim, Anna M. Lackner, Leroy J. Miller, Elena Sherman, Willis H. Smith, Jr., and Camille I. vanAst 28 Sep. 1990 82 p
(Contract N00014-87-C-2354)
(AD-A228756; HAC-REF-G3338-1) Avail: NTIS HC/MF A05
CSCL 09/1

This final report describes progress completed on two of three phases of work aimed at defining new applications areas for microtubules formed as self-organizing microstructures from lipids with diacetylenic lecithin structures. The emphasis in the first phase was on the suspension, orientation, and electro-optical properties of metalized microtubule dispersions in fluids, liquid crystals, and polymers, and on techniques for controlling the orientation and attachment of microtubules to surfaces. The emphasis in the second phase was on phase shift effects in the millimeter wave region with field effects on metalized microtubule dispersions, in regard to potential applications such as scanning radar antennas and radar lenses. In these studies it was discovered that composite fluids consisting of metalized microtubules dispersed in liquid crystals have the highest birefringence values which have been reported in the millimeter wave region and that these composite fluids are readily aligned by applied electrical and magnetic fields. GRA

N91-16206# Massachusetts Inst. of Tech., Lexington. Lincoln Lab.
RESULTS OF THE KANSAS CITY 1989 TERMINAL DOPPLER WEATHER RADAR (TDWR) OPERATIONAL EVALUATION TESTING
J. E. Evans, ed. 17 Aug. 1990 87 p
(Contract DTFA01-83-4-10579)
(AD-A228784; ATC-171; DOT/FAA/NR-90/1) Avail: NTIS HC/MF A05 CSCL 17/9

The Terminal Doppler Weather Radar (TDWR) testbed was used at the Kansas City International (KCI) airport during the summer of 1989. The objective was to test and refine previous tested techniques for the automatic detection of low-altitude wind shear phenomena (specifically microbursts and gun fronts) and heavy precipitation in a midwest weather environment, as well as to assess possible new products such as storm movement predictions. A successful operation evaluation of the TDWR products took place at the KCI tower and terminal radar control room (TRACON). Several supervisor and controller display refinements were assessed as effective. The system was successful in terms of aircraft at KCI avoiding wind shear encounters during the operational period, and it was assessed as very good in usefulness for continuing operation by the KCI air traffic control (ATC) personnel. The probability of detection for microbursts was substantially better than that in Denver. However, the false-alarm probability was found to be substantially higher in Kansas City due to a combination of weather and clutter phenomena. By optimizing the site-adaptation capabilities of the TDWR meteorological and data quality algorithms, the required false-alarm probability was achieved. The gust front performance was generally poorer than in Denver due to a combination of unfavorable radar-airport-gust front geometry of false alarms induced by low-level jets. Gust front algorithm refinements which should provide improved performance are discussed. GRA

N91-16207# Syracuse Univ., NY.
NUMERIC AND SYMBOLIC SIGNAL PROCESSING FOR VERY HIGH SUBCLUTTER VISIBILITY Final Report, Jun. - Dec. 1988
Donald Weiner and Braham Himed Oct. 1990 28 p
(Contract F30602-88-D-0027)
(AD-A228812; RADC-TR-90-251) Avail: NTIS HC/MF A03 CSCL 17/9

This effort deals with the compensation of mutual coupling effects in a sensor array when using the subspace approach known as the matrix pencil. This method is easy to implement and is applicable even in the presence of coherent sources. Computer simulation shows that use of the mutual impedance matrix effectively compensates for the presence of mutuals. GRA

N91-16208# Syracuse Univ., NY.
AN EXPERIMENTAL DEMONSTRATION OF HIGH-RESOLUTION DOPPLER PROCESSING Final Report, Jan. 1989 - Jan. 1990
Russell D. Brown and Hong Wang Sep. 1990 18 p
(Contract F30602-88-D-0027)
(AD-A228813; RADC-TR-90-245) Avail: NTIS HC/MF A03 CSCL 17/9

This correspondence reports the experimental results of applying the coherent wideband modified forward-backward linear prediction (CWB-MFBLP) to processing of the radar data obtained in a real target-clutter environment for the resolution improvement in the Doppler frequency domain. Significant resolution improvement is obtained and further research topics are suggested. GRA

N91-16209# Syracuse Univ., NY.
INTRA-PULSE FREQUENCY DIVERSITY (IPFD) LAB DEMONSTRATION Final Report, Jan. - Sep. 1989
Hong Wang Sep. 1990 21 p
(Contract F30602-88-D-0027)
(AD-A228814; RADC-TR-90-246) Avail: NTIS HC/MF A03 CSCL 17/9

A new approach is described to wideband adaptive beamforming for correlated signal and interference. Unlike other approaches, such as spatial smoothing, the new approach solves the signal cancellation problem by employing the idea of frequency domain smoothing. Advantages of frequency domain smoothing method show that proper spatial filtering can be achieved by frequency domain smoothing, whether the desired signal and the interference are correlated or not. GRA

N91-16210# Rochester Univ., NY. Dept. of Computer Science.
LINGUISTIC AND PRAGMATIC CONSTRAINTS ON UTTERANCE INTERPRETATION Ph.D. Thesis
Elizabeth A. Hinkelman May 1990 166 p
(Contracts N00014-82-K-0193; DACA76-85-C-0001)
(AD-A228815; TR-288) Avail: NTIS HC/MF A08 CSCL 05/7

In order to model how people understand language, it is necessary to understand not only grammar and logic but also how people use language to affect their environment. This area of study is known as natural language pragmatics. Speech acts, for instance, are the offers, promises, announcements, etc., that people make by talking. The same expression may be different acts in different contexts, and yet not every expression performs every act. We want to understand how people are able to recognize other's intentions and implications in saying something. Previous plan-based theories of speech act interpretation do not account for the conventional aspect of speech acts. They can, however, be made sensitive to both linguistic and propositional information. This dissertation presents a method of speech act interpretation which uses patterns of linguistic features (e.g., mood, verb form, sentence adverbials, thematic roles) to identify a range of speech act interpretations for the utterance. These are then filtered and elaborated by inferences about agents' goals and plans. In many cases the plan reasoning consists of short, local inference chains (that are in fact conversational implicatures) and, extended reasoning is necessary only for the most difficult cases. The method is able to accommodate a wide range of cases, from those which seem very idiomatic to those which must be analyzed using knowledge about the world and human behavior. It explains how, Can you pass the salt, can be a request while, Are you able to pass the salt, is not. GRA

N91-16211*# Michigan Univ., Ann Arbor. Radiation Lab.
HIGH FREQUENCY SCATTERING BY A SMOOTH COATED CYLINDER SIMULATED WITH GENERALIZED IMPEDANCE BOUNDARY CONDITIONS Technical Report, Sep. 1990 - Feb. 1991
Hasnain H. Syed and John L. Volakis Jan. 1991 31 p Sponsored by Pacific Missile Test Center, Point Mugu, CA
(Grant NAG2-541)
(NASA-CR-187829; NAS 1.26:187829; REPT-025921-17-T)
Avail: NTIS HC/MF A03 CSCL 20N

Rigorous uniform geometrical theory of diffraction (UGTD) diffraction coefficients are presented for a coated convex cylinder simulated with generalized impedance boundary conditions. In particular, ray solutions are obtained which remain valid in the

transition region and reduce uniformly to those in the deep lit and shadow regions. These involve new transition functions in place of the usual Fock-type integrals, characteristic to the impedance cylinder. A uniform asymptotic solution is also presented for observations in the close vicinity of the cylinder. As usual, the diffraction coefficients for the convex cylinder are obtained via a generalization of the corresponding ones for the circular cylinder. Author

N91-16212*# Arizona State Univ., Tempe. Dept. of Electrical Engineering.
HIGH-FREQUENCY TECHNIQUES FOR RCS PREDICTION OF PLATE GEOMETRIES Semiannual Progress Report, 1 Aug. 1990 - 31 Jan. 1991
Constantine A. Balanis and Lesley A. Polka 1991 30 p
(Grant NAG1-562)
(NASA-CR-187865; NAS 1.26:187865) Avail: NTIS HC/MF A03 CSCL 20N

Several different high-frequency methods for modeling the radar cross sections (RCSs) of plate geometries are examined. The Method of Equivalent Currents and a numerically derived corner diffraction coefficient are used to model the RCS of a rectangular, perfectly conducting plate in nonprincipal planes. The Uniform Theory of Diffraction is used to model the RCS of a rectangular, perfectly conducting plate in principal planes. For the soft polarization case, first-order and slope-diffraction terms are included. For the hard polarization case, up to four orders of diffraction are included. Finally, the Uniform Theory of Diffraction for impedance wedges and the Impedance Boundary Condition are used to model the RCS of a coated, rectangular plate in principal planes. In most of the cases considered, comparisons are made between theoretical and experimental results. Author

N91-16213 Institute for Perception RVO-TNO, Soesterberg (Netherlands).
ERICC: CONSTRUCTION AND APPLICATION OF THE COMMAND AND CONTROL RESEARCH FACILITY Final Report
P. J. M. D. Essens, H. vanDoorne, and C. Vijlbrief 13 Dec. 1989 24 p In DUTCH; ENGLISH summary
(Contract A87/KLu/131)
(IZF-1989-55; TD-89-4553; ETN-91-98305) Copyright Avail: Institute for Perception RVO-TNO, P.O. Box 23, 3769 ZG Soesterberg, Netherlands

A computer network facility was set up to simulate command and control task situations. Tools were developed for the presentation and manipulation of dynamic and more static information and for the registration of responses. The experimental approach chosen is the partial task simulation. The application of the research facility in the analysis of an air defense task is discussed. ESA

N91-16214# Laboratoire d'Automatique et d'Analyse des Systemes, Toulouse (France).
MODELING AND VERIFICATION OF DISTRIBUTED SYSTEMS WITH LABELED PREDICATE TRANSITION NETS Ph.D. Thesis - Toulouse Univ.
Jean-Christophe Lloret 1990 154 p In FRENCH; ENGLISH summary
(LAAS-90215; ETN-91-98541) Avail: NTIS HC/MF A08

Two main steps in the design of distributed systems are modeling and verification. Petri nets and CCS are two basic formal models. CCS is a modular language supporting compositional verification. Conversely, the petri net theory requires an accurate description of parallelism and focuses on property global verification. A structuring technique based on CCS concepts is introduced for predicate/transition nets. It consists of a high level petri net that permits expression of communication with value passing. In particular, a petri net composition operator, that can be interpreted as a multi-rendezvous between communicating systems, is defined. The multi rendezvous allows abstract modeling, with small state graphs. The developed formalism is highly convenient for refining abstract models relative to less abstract levels. Based on this work, a software tool, supporting distributed system design and verification, is developed. The advantage of this approach is shown in many research and industrial applications. ESA

N91-16215# Loughborough Univ. of Technology (England). Dept. of Electrical and Electronic Engineering.
A PAPER-ASSESSMENT OF THE PERFORMANCE OF A MODERN AIRBORNE MULTI-MODE PULSE DOPPLER RADAR DEPLOYED AS A GROUND-BASED FIRE-CONTROL RADAR M.S. Thesis
Charles Edwards 1989 123 p
(ETN-91-98584) Copyright Avail: NTIS HC/MF A06

It is attempted to determine whether any of the well established airborne radar techniques are appropriate to the task of detecting targets in clutter with a ground installation. Airborne radar modes are discussed and the selected design configuration and operation are described. The radar performance in its new environment is analyzed. The results are summarized and the applicability of such a radar design to the ground environment is assessed. It is clear that some of the techniques which have become established in airborne pulse Doppler radar designs could have a valuable role to play in the future of ground based fire control radars. ESA

N91-16216# Deutsche Forschungsanstalt fuer Luft- und Raumfahrt, Oberpfaffenhofen (Germany, F.R.). Abt. HF-Physik.
SCATTERING CENTER ANALYSIS OF SIMPLE METALLIC OBJECTS Ph.D. Thesis - Ulm Univ.
Ulrich Fuchs May 1990 186 p In GERMAN; ENGLISH summary Report will also be announced as translation (ESA-TT-1250)
(DLR-FB-90-32; ISSN-0171-1342; ETN-91-98596) Avail: NTIS HC/MF A09; DLR, VB-PL-DO, Postfach 90 60 58, 5000 Cologne, Fed. Republic of Germany, HC 59.50 Deutsche marks

Measurements of the complex signal backscattered by metallic cubes, plates, cylinders, and combinations of these objects are given. The measurements are used to generate microwave images wich typically exhibit only a few intensity maxima, so called scattering centers. Methods are developed for analyzing the dependence of the corresponding scattering mechanisms on frequency, aspect angle and polarization. Interpretations of the experimental results are compared with model calculations on the basis of the geometrical theory of diffraction. ESA

33 ELECTRONICS AND ELECTRICAL ENGINEERING

Includes test equipment and maintainability; components, e.g., tunnel diodes and transistors; microminiaturization; and integrated circuitry.

For related information see also *60 Computer Operations and Hardware* and *76 Solid-State Physics.*

N91-16217# Sandia National Labs., Albuquerque, NM. Product Engineering Div.
CHARACTERIZATION AND DEVELOPMENT REPORT FOR THE SA2859: A SILICON CONTROLLED RECTIFIER
C. E. McCarty 12 Feb. 1990 118 p
(Contract DE-AC04-76DP-00789)
(DE90-010196; SAND-88-2174) Avail: NTIS HC A06

The design, development, and testing of the SA2859, a diffused planar epitaxial silicon controlled rectifier manufactured by Texas Instruments (TI) is thoroughly studied. DOE

N91-16218# Sandia National Labs., Albuquerque, NM.
TOTAL-DOSE DEGRADATION OF THIN FILM FERROELECTRIC CAPACITORS
J. R. Schwank, S. L. Miller, R. D. Nasby, M. S. Rodgers, and P. V. Dressendorfer 1990 5 p Presented at the 27th IEEE Annual International Nuclear and Space Radiation Effects Conference, Reno, NV, 16-20 Jul. 1990

(Contract DE-AC04-76DP-00789)
(DE90-007152; SAND-90-0367C; CONF-900723-3) Avail: NTIS HC/MF A01

The effects of total dose irradiation on PbO-ZrO2-TiO2 ferroelectric capacitors were studied in detail. It is shown that significant total dose degradation of ferroelectrics can occur at dose levels greater than 1 Mrad(Si). DOE

N91-16219# Sandia National Labs., Albuquerque, NM.
THE 1/f NOISE IN IRRADIATED MOS DEVICES
T. L. Meisenheimer, R. V. Jones, and D. M. Fleetwood 1990 5 p Presented at the 27th IEEE Annual International Nuclear and Space Radiation Effects Conference, Reno, NV, 16-20 Jul. 1990
(Contract DE-AC04-76DP-00789)
(DE90-007288; SAND-90-0410C; CONF-900723-6) Avail: NTIS HC/MF A01

The 1/f noise of MOS transistors was measured as a function of total ionizing dose and postirradiation biased annealing time. Comparison to oxide and interface trapped-charge buildup and annealing is discussed. DOE

N91-16220# Sandia National Labs., Albuquerque, NM.
RADIATION HARDENING OF A HIGH VOLTAGE IC TECHNOLOGY (BCDMOS)
John C. Desko, Jr., Mohamed N. Darwish, Martin C. Dolly, Charles A. Goodwin, William R. Dawes, Jr., and Jeffrey L. Titus (Naval Weapons Support Center, Crane, IN.) 1990 4 p Presented at the 27th IEEE Annual International Nuclear and Space Radiation Effects Conference, Reno, NV, 16-20 Jul. 1990
(Contract DE-AC04-76DP-00789)
(DE90-008345; SAND-90-0501C; CONF-900723-11) Avail: NTIS HC/MF A01

PIC's (Power Integrated Circuits) are becoming increasingly important because they allow integration of high voltage and high current power transistors, precision linear control circuitry, and low voltage logic gates on the same monolithic chip. Integration of power and control functions provide benefits in reduced weight and size, enhanced reliability, and lower costs over conventional designs using these same components packaged separately. However, commercial PIC technologies, including AT and T's commercial BCDMOS technology, are susceptible to failure in radiation environments. The relative lack of radiation hardness of the AT and T BCDMOS technology was previously reported at this conference. Radiation hardening of PIC technologies is significantly more difficult than for other IC technologies, primarily because of the integration of many different types of devices into the technology. To facilitate integration, different devices share processing sequences. Thus, no one device can be optimized independently of the remaining devices. Since each device has its own distinct radiation response, this adds another set of constraints on the optimization of the overall technology from the point of view of device performance and radiation response. The high voltage requirements further complicates efforts to harden a PIC technology. Modifying one device to optimize one aspect of its performance can severely impact all the other devices in the technology. DOE

N91-16221# Sandia National Labs., Albuquerque, NM.
A TRANSFORMER COUPLED SEMICONDUCTOR BRIDGE IGNITER FOR LOW VOLTAGE IGNITION FROM A HIGH VOLTAGE SOURCE
R. W. Bickes, Jr. and S. L. Schlobohm 1990 9 p Presented at the 15th International Pyrotechnics Seminar, Boulder, CO, 9-13 Jul. 1990 Sponsored in part by AFSC, Eglin AFB, FL
(Contract DE-AC04-76DP-00789)
(DE90-009974; SAND-90-0001C; CONF-900792-1) Avail: NTIS HC/MF A02

Some missile systems have high voltage, short (less than 1 microsec) current pulses available for ignition of the missile's rocket motor. Such high voltage systems are desirable for enhanced safety considerations. However, application of high voltage firing pulses to conventional 1-omega bridgewire igniters can result in a detonation in the igniter rather than a well controlled burn. We present in this paper a concept proposed by Eglin Air Force Base for converting the high voltage (2 kV) firing signal pulse to the appropriate low voltage (less than 50 V) and low energy (approximately 1.5 mJ) input required for semiconductor bridge, SCB, igniters. The Eglin concept makes use of a pot core transformer to step down the input voltage. Our transformer is a Ferroxcube pot core (10 mil air gap) with a 50-turn primary and 1-turn secondary. In our prototype design, the 1-turn secondary is a Kapton-laminated copper loop with the SCB directly bonded to the ends of the copper loop. The igniter assembly consist of the primary spool and secondary loop mounted in the pot core transformer with a hole, which serves as the charge holder for the igniter material, drilled in one of the pot core halves and positioned directly over the SCB. The igniter material is pressed into the charge holder against the SCB. Application of a 2 kV (less than 1 microsec) pulse to the primary, produces a 40-V signal in the secondary that functions the SCB and ignites the explosive material. In addition to the 2-kV all-fire ignition requirement, the ignition system must be able to withstand 500-V no-fire signals and electrostatic discharge, ESD inputs. We will discuss in this paper various design configurations of this component and their output and also the ability of this concept to successfully withstand the no-fire and ESD inputs. DOE

N91-16222# Argonne National Lab., IL. Fusion Power Program.
NEOCLASSICAL EFFECTS ON RF CURRENT DRIVE
David A. Ehst and Charles F. F. Karney (Princeton Univ., NJ.) Apr. 1990 21 p
(Contract W-31-109-eng-38)
(DE90-010302; ANL/FPP/TM-247) Avail: NTIS HC/MF A03

A functional form is derived for the efficiency of current drive in toroidal geometry with low frequency waves (frequencies below the electron cyclotron frequency). By fitting constants in order to duplicate numerical results for the efficiency we obtain an accurate function which will be useful for computer calculations of current drive. DOE

N91-16223# Idaho National Engineering Lab., Idaho Falls.
PCB/TRANSFORMER TECHNO-ECONOMIC ANALYSIS MODEL: USER MANUAL, VOLUME 2
Martin M. Plum and Ray M. Geimer Feb. 1989 39 p
(Contract DE-AC07-76ID-01570)
(DE90-010654; EGG-EA-8245-VOL-2) Avail: NTIS HC/MF A03

This model is designed to evaluate the economic viability of replacing or retrofilling a PCB transformer with numerous non-PCB transformer options. Replacement options include conventional, amorphous, amorphous-liquid filled, or amorphous-liquid filled-high performance transformers. The retrofill option is the process that removes and disposes this with non-PCB dielectric. Depending on data available, the skills of the user, and the intent of the analysis, there are three model options available to the user. For practical purposes, Level 1 requires the least amount of input data from the user while Level 3 requires the greatest quantity of data. This manual is designed for people who have a minimum experience with Lotus 123 and are familiar with electric transformers. This manual covers system requirements, how to install the model on your system, how to get started, how to move around in the model, how to make changes in the model data, how to print information, how to save your work, and how to exit from the model. DOE

N91-16224# Lawrence Livermore National Lab., CA.
MULTIFRAME X RAY IMAGES FROM A SINGLE MEANDER STRIPLINE COATED ON A MICROCHANNEL PLATE
P. M. Bell, J. D. Kilkenny, G. Power, R. Bonner, and D. K. Bradley (Rochester Univ., NY.) Aug. 1989 11 p Presented at the 33rd SPIE Annual International Technical Symposium on Optical and Optoelectronic Applied Science and Engineering, San Diego, CA, 14-18 Aug. 1989 Submitted for publication
(Contract W-7405-eng-48)
(DE90-010741; UCRL-101659; CONF-890836-24) Avail: NTIS HC/MF A03

The electrical gating of microchannel plates can produce shutter times shorter than 100 ps. Previously, several different microstrip lines with independent electrical gating have been coated on a microchannel plate in order to obtain several image areas on one microchannel plate. We describe here design considerations and results from a microstrip line coated as a meander on a microchannel plate, from which 14, 100 ps images, gated at different times are obtained from a single gate. DOE

N91-16225# Edgerton, Germeshausen and Grier, Inc., Idaho Falls, ID.
LABORATORY TESTING OF CHLORIDE 3ET205 6 VOLT TRACTION BATTERY
Jasper E. Hardin Oct. 1989 24 p
(Contract DE-AC07-76ID-01570)
(DE90-010926; EGG-EP-8919) Avail: NTIS HC/MF A03

The purpose of this report is to describe the testing performed on the Chloride 3ET205 6 volt traction battery by the INEL Battery Laboratory, to present the results and conclusions of this testing, and to make appropriate recommendations. The Chloride 3ET205 is a tubular plate lead-acid battery made in England by the Chloride Battery Company and imported into the U.S. The traction battery division of Chloride has been sold, although Chloride assured its customers that the 3ET205 would continue to be available for their consumption. The new owners of the factory are Tudor and Fulman of France. The joint venture company name is C. E. Ac. It is our understanding that all orders are to be sent to the factory at Salford Rd., Bolton, Lancashire, England BL5 1DD. DOE

N91-16226# Sandia National Labs., Albuquerque, NM.
AN ALGORITHM FOR USING A SLIDE-SCREW TUNER AS A COMPUTER-CONTROLLED IMPEDANCE
George Sloan 1990 10 p Presented at the Automatic RF Technology Group Conference, Dallas, TX, 10-11 May 1990
(Contract DE-AC04-76DP-00789)
(DE90-010657; SAND-90-1209C; CONF-9005175-1) Avail: NTIS HC/MF A02

In the testing of active microwave components, a common test procedure is to evaluate a device's performance when subjected to an all-phase, constant-standing-wave-ratio (APCS) load pull. Such a test specification is useful in verifying a device's stability and mismatch performance. Typically, APCS pulls are tediously performed by hand, with manually operated tuners. However, with the advent of mechanical, computer-controlled tuners, it is now possible to automate this procedure. At Sandia, the goal was to integrate an APCS pull capability into a multi-test, single-connection tester. (The single-connection concept implies that many test, such as network analysis, spectral analysis, and noise figure measurements can be made from a one-time, device-to-tester connection). Consequently, the slide-screw tuner was the obvious choice due to its removable probe capability. Hence, it became necessary to develop a custom algorithm capable of utilizing the tuner in an impedance-finding mode. The general concept used in implementing this capability was to empirically characterize the tuner over and acceptable range of tuner positions, and then use this characterization to intelligently predict the tuner positions needed to present the desired impedance. DOE

N91-16227# Edgerton, Germeshausen and Grier, Inc., Idaho Falls, ID.
ASSESSMENT OF BATTERY TECHNOLOGIES FOR ELECTRIC VEHICLES. VOLUME 2, PART 1: APPENDICES
G. L. Henriksen, ed. and E. Z. Ratner (Sheladia Associates, Inc., Rockville, MD.) Feb. 1990 475 p
(Contract DE-AC07-76ID-01570)
(DE90-010907; DOE/ID-10243/2-VOL-2-APP-PT-1; MISC-90024-VOL-2-APP-PT-1) Avail: NTIS HC/MF A20

To help guide future EV battery R and D programs, the U.S. Department of Energy (DOE) commissioned a comprehensive assessment of viable secondary battery technologies. A total of 55 battery developers, from the United States, Canada, Europe, Asia, and Africa, were solicited to submit battery design concepts for an Improved Dual-Shaft Electric Propulsion (IDSEP) van. A team of 7 representatives from DOE laboratories and 10 independent EV and Battery consultants evaluated 42 design concepts. Using six criteria, five technical/economic criteria and a maturity/technical barriers criterion, the Assessment Team identified 12 most-promising batteries. This document Volume 2, Part 1 provides the following appendices to the report: information solicitation package; listing of battery technology developers; improved dual-shaft electric propulsion van; and battery design concepts. DOE

N91-16228# California Univ., Berkeley. Lawrence Berkeley Lab. Physics Div.
MEASUREMENTS OF 1/f NOISE IN a-Si:H PIN DIODES AND THIN-FILM-TRANSISTORS
Gyuseong Cho, J. S. Drewery, I. Fujieda, T. Jing, S. N. Kaplan, V. Perez-Mendez, S. Qureshi, D. Wildermuth, and R. A. Street (Xerox Palo Alto Research Center, CA.) May 1990 6 p Presented at the Spring Meeting of the Materials Research Society, San Francisco, CA, 16-21 Apr. 1990
(Contract DE-AC03-76SF-00098)
(DE90-011218; LBL-28836; CONF-900466-41) Avail: NTIS HC/MF A02

The equivalent noise charge was measured of a-Si:H p-i-n diodes (5 approx. 45 micron i-layer) with a pulse shaping time of 2.5 microsec under reverse biases up to 30 V/micron and analyzed it as a four component noise source. The frequency spectra of 1/f noise on the soft-breakdown region and of the Nyquist noise from contact resistance of diodes were measured. Using the conversion equations for a CR-RC shaper, the contact resistance noise was identified and the 1/f noise as the main noise sources in the low bias and high bias regions respectively. The 1/f noise of a-Si:H Thin Film Transistors (TFTs) with channel length of 15 micron was measured to be the dominant component up to approx. 100 kHz for both saturation and linear regions. DOE

N91-16229# Argonne National Lab., IL. Chemical Technology Div.
STATUS OF ARGONNE LIFE EVALUATION OF VALVE REGULATED LEAD-ACID BATTERIES
W. H. DeLuca, R. L. Hogrefe, C. E. Webster, and A. F. Tummillo 1990 12 p Presented at the International Lead Zinc Research Organization Meeting, San Francisco, CA, 27-28 Apr. 1990
(Contract W-31-109-eng-38)
(DE90-011098; CONF-9004196-2) Avail: NTIS HC/MF A03

Argonne is conducting a life evaluation of valve-regulated lead-acid (VRLA) batteries for cycling applications. Two technologies are being evaluated: (1) gelled-electrolyte modules from Johnson Controls, Inc. (JCI), and (2) absorbed electrolyte modules from GNB, Inc. A matrix of operating temperature and depth-of-discharge (DOD) conditions is being used to accelerate the end-of-life for given modules. In May 1989, two modules from each manufacturer were placed on life test at 30 C (80 and 100 percent DOD), and a third module was placed on accelerated life testing at 50 C (100 percent DOD). The GNB module operating to 100 percent DOD at 30 C still retains approximately 87 percent of its initial capacity after more than 400 cycles. The GNB module operating to 80 percent DOD at 30 C has accrued more than 500 cycles and retains approximately 93 percent of its initial 80 percent DOD capacity. After a high-temperature charge procedure was established, a fourth GNB module was placed on test at 50 C (80 percent DOD) in September 1989. Both GNB modules tested at 50 C have accrued approximately 150 cycles: the 100 percent DOD module retains approximately 84 percent of its initial capacity, and the 80 percent DOD module retains approximately 89 percent of its initial 80 percent DOD capacity. The three gelled-electrolyte JCI modules were removed from test because they reached end-of-life. Preliminary teardown analysis indicate that a manufacturing defect caused premature failure of the modules. DOE

N91-16230# Argonne National Lab., IL. Electrochemical Technology Program.
REQUIREMENTS FOR A FUEL CELL FOR TRANSPORTATION APPLICATION
Romesh Kumar 1990 8 p Presented at the Direct Methanol/Air Fuel Cell Workshop, Washington, DC, 14-16 May 1990
(Contract W-31-109-eng-38)
(DE90-011146; CONF-9005196-1) Avail: NTIS HC/MF A02

Fuel cells are being considered as replacements for internal combustion engines in buses, vans, and ultimately passenger cars. Low emissions of pollutants, high fuel energy conversion efficiencies, and the possibility of using coal- or biomass-derived alcohols rather than petroleum-based fuels are the major motivations. The challenges are to reduce the capital costs of the fuel cell power systems, to make the systems capable of meeting the dynamic power requirements of the different driving profiles, and to increase the systems' volumetric and mass power densities to enable their use within the space and weight limitations imposed by the vehicle design. Other considerations in adapting fuel cells to automotive applications include start up, idling (or standby) operation, drivability, ruggedness, useful life (in terms of both the delivered kWh and lifetime), safety, and operation at ambient temperatures from less than 0 C to 50 C. DOE

N91-16231# Argonne National Lab., IL.
EVALUATION OF NOVEL SOLID ELECTROLYTE MATERIALS Report, 1 Apr. 1989 - 1 Apr. 1990
I. Bloom, M. Krumpelt, D. W. Dees, and M. C. Hash 1990 4 p Presented at the METC Contractors Review Meeting, Morgantown, WV, 2-3 May 1990 Sponsored in cooperation with the Gas Research Inst. and EPRI
(Contract W-31-109-eng-38)
(DE90-011164; CONF-9005195-1) Avail: NTIS HC/MF A01

Solid-state fuel cells have the potential for becoming one of the most trouble-free fuel cell systems. The use of solid electrolyte virtually eliminates corrosion reactions and redistribution due to a liquid electrolyte. The project is structured to first focus on developing new candidate electrolyte materials. Once suitable electrolyte materials have been identified, compatible electrode and interconnect materials will be developed. Central to the theme of the project is to find an electrolyte that could function as the basis of all four cell components, depending on dopant. In this way, the stresses due to thermal mismatch could be much smaller than those in a cell made from different materials. Following this approach, two classes of compounds were chosen initially for evaluation: perovskites scheelites. DOE

N91-16232# Sandia National Labs., Albuquerque, NM.
MICROWAVE COUPLING ON PRINTED CIRCUIT BOARDS
Larry D. Bacon and Richard P. Toth 1989 5 p Presented at the 5th National Conference on High-Power Microwave Technology, West Point, NY, 10-15 Jun. 1990
(Contract DE-AC04-76DP-00789)
(DE90-011237; SAND-89-2769C; CONF-9006179-2) Avail: NTIS HC/MF A01

The bottom line for any susceptibility assessment of a system to an electromagnetic threat is whether or not components are upset or damaged. To predict this, we have to understand the distribution of energy on pc boards, and its interaction with the functioning circuits on the boards. LineCAP is a code that computes this energy distribution and the circuit's response. It includes the effects of trace-to-trace coupling, discontinuities (bends, vias), passive circuit components, and nonlinear devices. The theory, comparisons with measurements, applications, and limitations of this code will be presented. DOE

N91-16233# Sandia National Labs., Albuquerque, NM. Exploratory Batteries Div.
DEVELOPMENT OF A MODERATE RATE LITHIUM/THIONYL-CHLORIDE D CELL
Wendy R. Cieslak and Henry K. Street 1990 4 p Presented at the 34th International Power Sources Symposium, Cherry Hill, NJ, 25-28 Jun. 1990
(Contract DE-AC04-76DP-00789)
(DE90-011909; SAND-89-2245C; CONF-9006146-8) Avail: NTIS HC/MF A01

We have designed a lithium/thionyl chloride D cell for efficient performance at the moderate rate of approximately 500 mA (6.25 omega load). The SNL-MR-D cell has 345 sq cm of active electrode area, 1.0 M LiAlCl4 electrolyte that may have SO2 additive, and a cathode blended of Shawinigan Acetylene Black, Cabot Black Pearls 2000, and Teflon binder. The average performance of cells built in-house and discharged at 25 C and 6.25 omega has been 14.9 Ah (50 Wh). We have aged the cells at 30 C and 50 C, and measured complex impedance and microcalorimetry during the aging period. The cells have been discharged after the aging period at 25 C and 0 C. This preliminary study has allowed us to establish an initial cell design and estimate the rate of capacity loss on storage or long-term usage. DOE

N91-16234 New South Wales Univ., Canberra (Australia). School of Chemical Engineering and Industrial Chemistry.
ELECTROLYTE OPTIMIZATION AND ELECTRODE MATERIAL EVALUATION FOR THE VANADIUM REDOX BATTERY M.S. Thesis, Feb. 1989 Abstract Only
Michael Kazacos 17 May 1990 3 p
Avail: Issuing Activity

The preparation of the electrolyte for the all vanadium redox flow battery was investigated using both chemical and electrolytic reduction of V2O5 powder. Oxalic acid and SO2 reduction were found to be unsuitable as only the V(IV) state could be produced directly. With suspended powder hydrolysis, however, vanadium sulphate of any oxidation state, in this case 50 percent V(IV) plus 50 percent V(III) in sulphuric acid can readily be prepared from V2O5 powder, thus allowing a significant reduction in the cost of the vanadium battery electrolyte. Results from conductivity and electrolyte stability tests at elevated temperature have led to modification of the electrolyte composition for the vanadium redox cell, from the 2 M V plus 2 M H2SO4, originally employed, to the use of 3 M H2SO4, much higher energy efficiencies and greater electrolyte stability was demonstrated with the 3 M H2SO4 supporting electrolyte. Spectroscopy and electrolyte conductivity were demonstrated as suitable techniques for state-of-charge monitoring. A number of electrode materials were also evaluated and a Toray graphite bonded to a carbon plastic electrode was selected for further prototype development. Energy efficiencies of between 83 and 86 percent obtained for a current density of 30 mA/sq cm for a temperature range of 5 to 45 C, and between 0 and 100 percent state-of-charge. A wide range of construction materials was tested for long term stability in the vanadium redox electrolyte. Author

N91-16235# Purdue Univ., West Lafayette, IN. School of Electrical Engineering.
INVESTIGATION OF A NEW CONCEPT IN SEMICONDUCTOR MICROWAVE OSCILLATORS Final Report, 1 May 1985 - 30 Apr. 1990
James A. Cooper, Jr. 30 Jun. 1990 19 p
(Grant AF-AFOSR-0193-85; AF Proj. 2305)
(AD-A226785; AFOSR-90-0971TR) Avail: NTIS HC/MF A03
CSCL 09/1

A new type of millimeter wave oscillator device based on a resistive gate MESFET structure was studied. The resistive gate establishes a uniform electric field in the regime of negative differential mobility for electrons in GaAs. At these fields, dipolar charge domains form in the channel and drift into the drain, producing microwave oscillations in the drain current. In the contiguous domain mode, a continuous sequence of charge domains forms throughout the channel. This mode is possible because the resistive gate screens the self-induced fields of each dipolar domain, keeping the field outside the domain unperturbed. Frequencies up to 100+ GHz are produced, independent of channel length, and the frequency should be tunable over at least one octave by varying the gate-to-source voltage. This mode has not yet been observed experimentally, since the gate resistivity on the prototype devices has been too large. These devices are

presently operating a single domain transit time mode, producing oscillations in the 6 to 28 GHz range for channel lengths from 5 to 20 micron. Work is continuing to reduce the gate resistivity so that the contiguous domain mode can be observed. GRA

N91-16236# Naval Postgraduate School, Monterey, CA. Dept. of Electrical and Computer Engineering.
THE USE OF WINDOW FUNCTIONS AND KALMAN FILTERING IN SPECTRAL ESTIMATION M.S. Thesis
William W. Go Mar. 1990 137 p
(AD-A227482) Avail: NTIS HC/MF A07 CSCL 09/1

The periodogram, the square of the magnitude of the Fourier Transform, is widely used to estimate the spectral content of sampled processes. The performance of the periodogram is degraded by spectral leakage. This is the consequence of processing finite length data records. Classical means of enhancing periodogram performance are the use of tapered window functions and averaging of several periodograms. These methods smooth the spectral estimate, but at a loss of resolution. A nonstationary Kalman filter was applied to the periodogram of untapered (i.e., rectangular windowed) time data in an effort to smooth the noise portions of the periodogram while leaving the main spectral response unaltered. The Kalman filter was able to enhance the periodogram. Best results were obtained in the single spectral peak case. Even in the case of multiple spectral peaks, the resolution of the unfiltered periodogram was largely preserved since the filtering algorithm was designed to selectively smooth the noise-only segments of the spectral estimate. GRA

N91-16237# Stanford Univ., CA. Lab. of Physics.
JOINT SERVICES ELECTRONICS PROGRAM Annual Progress Report, 10 Oct. 1989 - 9 Oct. 1990
S. E. Harris, David M. Bloom, R. L. Byer, C. F. Quante, and A. Kapitulnik 9 Oct. 1990 47 p
(Contract N00014-87-K-0327)
(AD-A227576; SU-GL-4738) Avail: NTIS HC/MF A03 CSCL 09/1

During this period the research activities were organized into four work units: Development of an All-Silicon Integrated Optical Modulator for High Speed Data Communications; Synthetic Nonlinear Media; Scanning Tunneling Microscopy; and Device Related Properties of High-Temperature Superconductors. GRA

N91-16238# Electronics Research Lab., Adelaide (Australia).
NONRADIATIVE DIELECTRIC WAVEGUIDE MILLIMETRE-WAVE INTEGRATED CIRCUITS: A REVIEW
Bevan D. Bates and Kym Jordon Jun. 1990 27 p
(AD-A227760; ERL-0521-RN; DODA-AR-006-421) Avail: NTIS HC/MF A03 CSCL 09/1

Nonradiative dielectric waveguide has been shown to be a practical method for the realization of a wide range of millimetre-wave circuit components. However there is still much work to be done before use of the transmission-line media becomes more widespread especially in the areas of active components, design and analysis methods, and fabrication techniques. This report reviews research achievements to date and identifies the important areas requiring further development. GRA

N91-16239# Mitre Corp., McLean, VA. JASON Program Office.
SOME COMMENTS ON THE ACOUSTIC COUPLING OF ELEMENTS IN AN ARRAY
K. Watson May 1990 39 p Sponsored by DARPA, Arlington, VA
(AD-A227762; JSR-89-290) Avail: NTIS HC/MF A03 CSCL 09/1

The effects of acoustic coupling between radiators is investigated for linear and planar acoustic arrays. To provide a simple model for calculation and inversion of the acoustic impedance matrices, spherical radiators are chosen. Considerations of total radiated beam power are addressed. The principal effect of element interaction on array performance found is in the effective impedance of individual radiators in the array. GRA

N91-16240# Sandia National Labs., Albuquerque, NM.
NOVEL APPLICATIONS OF Tl-Ca-Ba-Cu-O THIN FILMS TO ACTIVE AND PASSIVE HIGH FREQUENCY DEVICES
J. S. Martens, D. S. Ginley, T. E. Zipperian, V. M. Hietala, and C. P. Tigges 1990 6 p Presented at the 3rd International Symposium on Superconductivity, Sendai, Japan, 6-9 Nov. 1990 Sponsored in part by NSF
(Contracts DE-AC04-76DP-00789; N00173-90-WR-00172)
(DE91-004507; SAND-90-2192C; CONF-901169-2) Avail: NTIS HC/MF A02

Applications of high temperature superconducting thin films to the development of new passive and active circuitry operating up to 40 GHz are presented. Thin film deposition (including new results on the effect of low temperature anneals), patterning Tl-based films to linewidths of 3 microns, and contacting are discussed. A number of high-temperature superconducting devices are discussed including passive resonators, passive filters, and an active device. The active device is the superconducting flux flow transistor (SFFT), that can be used in applications such as amplifiers and phase shifters. DOE

N91-16241# Royal Aerospace Establishment, Farnborough (England).
MOLTEN SALT ELECTROLYTES IN HIGH TEMPERATURE BATTERIES
A. G. Ritchie 1 Aug. 1990 20 p Presented at Royal Society of Chemistry Molten Salts Discussion Group Summer Meeting, Swansea, England, 4-6 Jul. 1990 Original contains color illustrations
(RAE-TM-MAT/STR-1155; BR115041; ETN-91-98411) Copyright Avail: NTIS HC/MF A03

The use of molten salt electrolytes in high temperature batteries, both single use thermal batteries and high temperature rechargeable batteries is described. The properties of the existing electrolytes are discussed and current research on new electrolytes is described. ESA

N91-16242# Sandia National Labs., Albuquerque, NM.
PROPERTIES AND CHARACTERIZATION OF THIN FILM FERROELECTRIC CAPACITORS FOR NONVOLATILE MEMORIES
R. D. Nasby, J. R. Schwank, M. S. Rodgers, S. L. Miller, Bruce A. Tuttle, A. Y. Liang, and P. V. Dressendorfer 1990 3 p Presented at the IEEE Nonvolatile Semiconductor Memory Workshop, Monterey, CA, 19-22 Feb. 1991
(Contract DE-AC04-76DP-00789)
(DE91-004037; SAND-90-2933C; CONF-910251-1) Avail: NTIS HC/MF A01

Thin film ferroelectric materials are the basis for a new, promising IC nonvolatile memory technology. The primary material being studied for ferroelectric memories is PZT. One of the key factors in determining the feasibility of PZT ferroelectric memories for weapon or space applications is whether PZT ferroelectric technology can be integrated into a radiation-hardened CMOS or bipolar process. Sandia National Laboratories has a program to study ferroelectric/CMOS process integration issues. The primary goal of this program is to determine if radiation-hardened reliable ferroelectric/CMOS IC memories can be fabricated. This program includes both the fabrication and characterization of ferroelectric test capacitors. In this one page summary accompanied by graphs, we will give a brief overview of the program, discuss techniques developed to characterize ferroelectric devices for retention and endurance, and give results on studies of fatigue and retention of capacitors. DOE

N91-16243# Michigan Univ., Ann Arbor. Dept. of Nuclear Engineering.
ION BEAM MODIFICATION OF SURFACE FOR IMPROVED HIGH TEMPERATURE PERFORMANCE Final Report, 1 Sep. 1986 - 31 Apr. 1990
Gary S. Was and Daniel Cavasin 27 Jul. 1990 110 p
(Contract DAAL03-86-G-0052)

(AD-A228067; ARO-23802.1-MS-F) Avail: NTIS HC/MF A06 CSCL 09/1

A novel experimental technique, Thin Film Calorimetry (TFC), has been developed to determine the enthalpy of transformation from metastable to stable equilibrium structures in thin films. This technique has been applied to investigate metastable stable transformations occurring in thin films of nominal composition NiAl3. Elemental Ni and Al are codeposited directly onto the surface of a pure Al calorimeter sample pan to form a 0.75 solid solution of NiAl3. The as-deposited microstructure in this case is a metastable configuration, and the reaction heat accompanying its transformation to the stable, equilibrium NiAl3 phase is measured directly in the calorimeter. The mean change in enthalpy, DeltaH, for a series of such measurements, is -4.16 kcal/mole. A second approach involves annealing the as-deposited film to form the epsilon phase, then irradiating the as-annealed film, using 1.5 MeV Ni++ ions, to form an amorphous structure. The enthalpy associated with the transformation of this structure to the equilibrium is then measured in the DSC. The mean DeltaH found for this reaction is -5.02 kcal/mole. GRA

N91-16244# Massachusetts Inst. of Tech., Cambridge. Artificial Intelligence Lab.

NOISE REDUCTION USING LOW WEIGHT AND CONSTANT WEIGHT CODING TECHNIQUES M.S. Thesis

Jeffrey F. Tabor Jun. 1990 78 p

(Contracts N00014-88-K-0825; N00014-85-K-0124)

(AD-A228346; AI-TR-1232) Avail: NTIS HC/MF A05 CSCL 12/6

Signalling off-chip requires significant current. As a result, a chip's power supply current changes drastically during certain output-bus transitions. These current fluctuations cause a voltage drop between the chip and circuit board due to the parasitic inductance of the power supply package leads. Digital designers often go to great lengths to reduce this transmitted noise. Cray, for instance, carefully balances output signals using a technique called differential signalling to guarantee a chip has constant output current. Transmitted noise reduction costs Cray a factor of two in output pins and wires. Coding achieves similar results at smaller costs. In a circuit using parallel terminated transmission lines such as the Cray-1, a chip exhibits nearly constant output current throughout a single clock cycle. However, since current for an output 1 differs greatly from that for an output 0, current can change drastically at the end of a cycle generating an intolerable amount of transmitted noise as successfully as differential signalling. Experimental results substantiate this. Information capacity of a word is greatest when the word has half 1's. Coding requires fewer output signals than differential signalling. For example, an 8-bit byte can be encoded as eleven bits with but requires a more costly coding scheme. GRA

N91-16245# Illinois Univ., Urbana-Champaign. Coordinated Science Lab.

ICHARM: HIERARCHICAL CMOS CIRCUIT EXTRACTION WITH POWER BUS EXTRACTION M.S. Thesis

Russell Makoto Iimura 5 Sep. 1990 111 p

(Contracts F30602-88-D-0028; N00014-90-J-1270)

(AD-A228613; UILU-ENG-90-2242; DAC-25) Avail: NTIS HC/MF A06 CSCL 20/3

Circuit extraction is critical in the validation of VLSI circuits since it provides the link between the design and the simulation phases. The use of hierarchical design techniques and hierarchical analysis methods increases design productivity. The development of iCHARM, a hierarchical circuit extractor, is described. The extractor takes its input layout in either the CIF format or the Oct. VLSI database format. The extractor produces circuit parasitics including capacitances and resistances. A power bus extraction mode was developed to calculate power bus currents for reliability estimation. The primary contribution is a method to extract a circuit hierarchically without flattening and with minimal overhead. A full-chip layout was used to test the extractor's functionality and to allow a comparison of the hierarchical and flat extraction modes. GRA

N91-16246# North Carolina State Univ., Raleigh. Dept. of Materials Science and Engineering.

RESEARCH AND DEVELOPMENT ON ADVANCED SILICON CARBIDE THIN FILM GROWTH TECHNIQUES AND FABRICATION OF HIGH POWER AND MICROWAVE FREQUENCY SILICON CARBIDE-BASED DEVICE Annual Report, FY 90

Robert F. Davis Oct. 1990 11 p

(Contract N00014-88-K-0341)

(AD-A228758) Avail: NTIS HC/MF A03 CSCL 09/1

The RF operation of bipolar transistors fabricated from alpha-(6H)SiC by Cree Research investigated and improved from the standpoints of parasitic resistances and capacitances as well as device design and fabrication procedures. In addition IMPATT diode structures have been further developed, ohmic and Schottky contact materials selected and deposited and the design and construction of a new MBE/ALE system virtually completed. GRA

N91-16247# EIC, Inc., Norwood, MA.

STUDIES OF THE FUNDAMENTALS OF SOLIDS STATE BATTERIES Final Report, Sep. 1987 - Jun. 1990

K. M. Abraham and M. Alamgir 6 Nov. 1990 52 p Submitted for publication

(Contract N00014-87-C-0857)

(AD-A228772; C-937) Avail: NTIS HC/MF A04 CSCL 10/2

Several methods have been developed to dimensionally stabilize polymer electrolytes based on poly-(bis (methoxy ethoxy ethoxide) phosphazene), known as MEEP. In contrast to the poor dimensional stability exhibited by complexes of MEEP with most Li salts, those prepared with LiAlCl4 have been isolated as the first example of free-standing MEEP-(LiX)n films. The mechanical properties of dimensionally unstable MEEP-(LIX)n complexes can be significantly improved by forming composites with polymers such as poly(ethylene oxide), poly(propylene oxide), poly(ethylene glycol diacrylate) and poly(vinyl pyrrolidinone). The conductivity of 6.7 x 10(exp -5) ohm(exp -1) cm(exp -1) at 25 C exhibited by 55 w/o MEEP/45 w/o PEO-(LiN(CF3SO2)2)0.13 is among the highest values reported to date for a dimensionally stable electrolyte. The preparation, and conductivity, calorimetric and electrochemical studies of these electrolytes are described. Cyclic voltammetric data indicated that these electrolytes have anodic stability at least up to 4.5V versus Li(+)/Li. They have shown excellent compatibility with Li metal making them suitable for use as Li(+) conductive solid electrolytes in solid-state Li batteries. Li/TiS2 solid-state cells utilizing some of these electrolytes have exceeded 200 cycles. GRA

N91-16248# Aerospace Corp., El Segundo, CA. Electronics Research Lab.

THRESHOLD VOLTAGE AND I-V CHARACTERISTICS OF AlGaAs/GaAs MODFETs

Richard J. Krantz, Walter L. Bloss, and Michael J. OLoughlin 30 Sep. 1990 23 p

(Contract F04701-88-C-0089)

(AD-A228844; TR-0090(5925-01)-3; SSD-TR-90-44) Avail: NTIS HC/MF A03 CSCL 09/1

A strong inversion model, in the depletion layer approximation, of the I-V characteristics for MODFETs has been developed. The model describes MODFET I-V characteristics from subthreshold through saturation, over nine orders of magnitude in current. The saturation current is calculated and used to derive the experimental threshold voltage, which is determined by extrapolation of the saturation current (or square root of the current) vs gate voltage to zero current. It is shown that, for certain regions of acceptor doping, the experimentally determined threshold voltage can differ appreciably from the strong inversion definition. We show that this discrepancy is due to the effect of the depletion layer charge in the saturation region. Inclusion of the depletion layer charge in the analysis accounts for this difference and the difference between the saturation device capacitance per unit area and the AlGaAs layer capacitance per unit area. GRA

N91-16249# Nationaal Inst. voor Kernfysica en Hoge Energiefysica, Amsterdam (Netherlands). Afd. DIGEL.
DIGITAL TIME INTERPOLATOR Thesis - Algemene Hogeschool [DIGITALE TIDJ-INTERPOLATOR]
S. Schuller 22 Jun. 1990 48 p In DUTCH
(DIGEL-1990-4; ETN-91-98323) Avail: NTIS HC/MF A03

A digital time measuring instrument was designed. The best principle for interpolation was selected by computer simulation using a PASCAL program. Part of the circuit was built to test the interpolation, the rest of the circuit was computer simulated. The interpolation part is the most critical one, the rest of the circuit is more or less simple logic. The time measuring instrument interpolates every 100 ns and has an accuracy of 50 ps. ESA

N91-16250# Technische Univ., Delft (Netherlands).
SYSTEMATIC DESIGN OF REGULAR VLSI PROCESSOR ARRAYS Ph.D. Thesis
Jichun Bu May 1990 142 p
(ETN-91-98482) Avail: NTIS HC/MF A07

A systematic way to design regular Very Large Scale Integrated (VLSI) processor arrays in particular systolic arrays, is presented. The problem of the systematic design of fixed size arrays for Regular Algorithms (RAs) is dealt with. The problem of systematic conversion of imperative nested loop programs into RAs is studied. A parallel VLSI architecture for the fast synthesis of high quality realistic method in computer graphics is presented, as well as a ray tracing algorithm, for the computation of the form factors. ESA

N91-16251# Max-Planck-Inst. fuer Radioastronomie, Bonn (Germany, F.R.).
NATURAL WAVES OF MICROSTRIP TRANSMISSION LINES IN WAVE GUIDES Thesis - Siegen Univ. [EIGENWELLEN VON MIKROSTREIFENLEITUNGEN IN HOHLLEITERN]
Reiner Schueller Jun. 1990 107 p In GERMAN
(BER-68; ETN-91-98512) Avail: NTIS HC/MF A06

A microstrip transmission line immerged in a special wave guide was analyzed. Filters for radio astronomical receivers are to be built using this special microstrip transmission line. The waveguide shape is such that its mechanical stability be guaranteed at low temperatures. For the field development, the non dissipation of dielectrics, and of the conductor, were taken as unique approximation. A method was found to describe analytically the electromagnetic field in the wave guide, which can be demounted in homogeneous rectangular subdomains, where the wave equation is to be solved in closed form. It gives an homogeneous equation system of the form MP equals zero, where P is an unknown split vector. A program was developed in this way. The solutions found were graphically represented as dispersion diagrams. The cut off frequencies of the higher mode are exactly determined. This is important for the filter development, in order to determine the effective bandwidth. ESA

N91-16252# Laboratoire d'Automatique et d'Analyse des Systemes, Toulouse (France).
DESIGN AND FABRICATION OF HIGH VOLTAGE PLANAR DEVICES Ph.D. Thesis - Toulouse Univ.
Georges Charitat 1990 253 p In FRENCH; ENGLISH summary
(LAAS-90306; ETN-91-98543) Avail: NTIS HC/MF A12

In order to design modern power and high voltage devices, specific tools, either analytical for a first order evaluation, and numerical, solving the basic electrical equations of those devices in two dimensions are developed. Two kinds of electrical behavior: off and on state, both static are dealt with. The peculiar data extracted with those tools are the voltage handling capability and the on resistance of the device. For off state behavior, analytical models are able to rate the avalanche breakdown criterion. To complete the first order evaluation, a special purpose software dedicated to power and high voltage devices, is elaborated to solve in two dimensions the basic semiconductor equations, namely Poisson and current equations, and to give the value of the breakdown voltage, using either holes or electrons integral ionization, and its location. ESA

N91-16253# Karlsruhe Univ. (Germany, F.R.). Inst. fuer Rechnerentwurf und Fehlertoleranz.
SAFETY AS A DESIGN GOAL FOR APPLICATIONS OF MICROELECTRONIC CONTROL SYSTEMS
Winfried Goerke Jul. 1990 25 p Presented at the 2nd Workshop on Test Methods and Reliability of Circuits and Systems, Gut Ising, Chiemsee, Fed. Republic of Germany, 18-20 Mar. 1990
(REPT-23/90; ETN-91-98552) Avail: NTIS HC/MF A03

The possibility of using microelectronics such as ASIC (Application Specific Integrated Circuits) to eliminate the risks of computers such as programmed logic and the related fault mechanisms, is discussed in the case of safety problems. The substitution of classical systems by digital programmable electronics for economical and functional reasons was first observed but neglected because of the abundant failure possibilities. A classification scheme was achieved, for which three risk parameters were chosen such as consequences of an accident, frequency of damage and possibilities for reduction of danger. Microprocessors are preferred to very large scale integration components because their larger number of standard components lead to more realistic and reliable failure rate data. ESA

N91-16254# Loughborough Univ. of Technology (England). Dept. of Electrical and Electronic Engineering.
ELECTRONICALLY STEERABLE ARRAYS: CURRENT AND FUTURE TECHNOLOGY AND APPLICATIONS M.S. Thesis
Adrian James Parrish 1989 149 p
(ETN-91-98581) Copyright Avail: NTIS HC/MF A07

The key differences between mechanically and electronically steered arrays are established and are subsequently used to highlight the importance of balancing economic considerations against performance needs in procurement decision making. The previous generation of technology for microwave generation, transmission and radiation is discussed. Using only unclassified information, the applications of the technology in present aircraft systems are described. Electronically steerable arrays will be used only where the high costs and technological risks are not unacceptable, and for certain operational needs. The integration of optical processors into active electronically steerable array modules and advances in digital computing will enable the full benefits of electronically steerable arrays to be realized through the use of techniques such as beam forming. ESA

34 FLUID MECHANICS AND HEAT TRANSFER

Includes boundary layers; hydrodynamics; fluidics; mass transfer; and ablation cooling.

For related information see also *02 Aerodynamics* and *77 Thermodynamics and Statistical Physics.*

N91-16255# Los Alamos National Lab., NM.
TRANSIENT NATURAL CONVECTION IN HEATED INCLINED TUBES
Donald M. McEligot (Westinghouse Electric Corp., Middletown, RI.), David A. Denbow, and Hugh D. Murphy May 1990 60 p
(Contract W-7405-eng-36)
(DE90-008217; LA-11813-MS) Avail: NTIS HC/MF A04

To simulate natural convection flow patterns in directionally drilled wellbores, experiments and analyses were conducted for a circular tube with length-to-diameter (L/D) ratio of 36 at angles of 0, 20, and 35 degrees from the vertical. The tube was heated at the bottom and cooled at the top, and the insulation was adjusted so that approximately one- to two-thirds of the power dissipated was transferred through the tube wall to the surroundings. An aqueous solution of polyvinyl alcohol was employed as the working fluid in order to obtain low Rayleigh numbers corresponding to conditions in geothermal wellbores. Results were primarily

qualitative but were useful in providing insight into the phenomena occurring. Steady-state temperature distributions were measured for the three orientations and for several heating rates to demonstrate the effects of tube angle and Rayleigh number. Transient measurements of the temperature distribution were obtained during cooling from a higher temperature without a heat source to calibrate the heat losses. With the electrical heat source, temporal data were taken during heating to examine the approach to steady state. Quasi-steady flow conditions were approached rapidly, but the overall time constant of the apparatus was of the order of one-third of a day. Predictions with the three-dimensional TEMPEST code were first tested by comparison with simple conduction analyses. Comparison with actual data showed good agreement of the predicted temperature levels for the maximum inclination, 35 degrees, and slightly poorer agreement for the other limit, a vertical tube. Trends of temperature level and Nusselt number with heating rate or Rayleigh number were reasonable, but the predicted variation of the end Nusselt number versus inclination was in the opposite direction from the experiment. DOE

N91-16256# Conserve Resources, Inc., Prescott, WA.
ROTARY ABSORPTION HEAT PUMP SENSITIVITY ANALYSIS
J. A. Bamberger and F. R. Zalondek Mar. 1990 84 p Prepared in cooperation with Pacific Northwest Lab., Richland, WA
(Contract DE-FG01-86CE-15256)
(DE90-010006; DOE/CE-15256/1) Avail: NTIS HC/MF A05

Conserve Resources, Incorporated is currently developing an innovative, patented absorption heat pump. The heat pump uses rotation and thin film technology to enhance the absorption process and to provide a more efficient, compact system. The results are presented of a sensitivity analysis of the rotary absorption heat pump (RAHP) performance conducted to further the development of a 1-ton RAHP. The objective of the uncertainty analysis was to determine the sensitivity of RAHP steady state performance to uncertainties in design parameters. Prior to conducting the uncertainty analysis, a computer model was developed to describe the performance of the RAHP thermodynamic cycle. The RAHP performance is based on many interrelating factors, not all of which could be investigated during the sensitivity analysis. Confirmatory measurements of LiBr/H2O properties during absorber/generator operation will provide experimental verification that the system is operating as it was designed to operate. Quantities to be measured include: flow rate in the absorber and generator, film thickness, recirculation rate, and the effects of rotational speed on these parameters. DOE

N91-16257# Oak Ridge National Lab., TN.
MEETINGS TO SHARE ADVANCEMENTS IN HEAT PUMP TECHNOLOGIES
F. A. Creswick, R. C. DeVault, and P. D. Fairchild Apr. 1990 25 p
(Contract DE-AC05-84OR-21400)
(DE90-010008; ORNL/FTR-3561) Avail: NTIS HC/MF A03

The Conference brought together researchers, engineers, managers, and government policy makers from the various participating countries and provided a forum to share information on heat pump technological advancements and related environmental issues. From interactions with the Japanese participants in various working meetings and site visits, it is clear that heat pumps represent a major technology emphasis in Japan for industry and utility supported R and D, as well as government sponsored programs. The Super Heat Pump (SHP) project sponsored by the Agency of Industrial Science and Technology (AIST), Ministry of International Trade and Industry (MITI) and aimed at leveling electric power demand in addition to higher heat pump performance, is a notable example of this emphasis and of the way in which industry, research institutes, and government are working together in Japan. A joint industry R and D association established for the SHP effort, for example, includes sixteen (16) major corporate members (Mitsubishi, Toshiba, etc.). Also, gas fired heat pumps have moved beyond laboratory prototypes and field tests and have emerged in Japan in production quantities. These first market entry products use near conventional small I.C. engines and are sized for residential and small commercial building applications. Sales are already in the ten thousands annually, and are increasing. Four major companies are already manufacturing and marketing such units (Yamaha, Yanmar, Aisin Seiki, and Sanyo). The Japanese companies and research organizations were much more open and frank about their research activities and progress than anticipated. The new Heat Pump Technology Center of Japan (HPTCJ) was an excellent host and established a positive atmosphere for international dialogue and cooperation. DOE

N91-16258# Washington Univ., Seattle. Dept. of Applied Mathematics.
ANALYTICAL AND NUMERICAL STUDIES IN FLOW DEVELOPMENT Progress Report, 1 Jul. 1989
W. O. Criminale and L. M. Adams Mar. 1990 8 p
(Contract DE-FG06-88ER-25061)
(DE90-010424; DOE/ER-25061/6) Avail: NTIS HC/MF A02

Analytical bases were established for a wide variety of shear flows under general initial conditions. In addition, provisions were made for study of both spatial and temporal development of disturbances. This combination is the essential framework for eventual direct numerical simulation of the three major prototypes of flow, namely bounded (channel) flow; semi-infinite (boundary layer) flow; and unbounded (mixing layer) flows. Besides the asset of having closed form solutions in all spatial coordinates and time, the important transient (initial) state of the motion can be determined explicitly. Of particular note is the fact that nonlinearity can be triggered by algebraic growth of disturbances, and therefore an alternate route for the breakdown to turbulence is possible. Such events were termed bypass because they can occur in a shorter time (or spatial) scale than that of the more common asymptotic exponential growth due to the instability of the flow. It is for these reasons that the eventual linking of the solutions to the numerical simulation is awaited with optimism. DOE

N91-16259# West Virginia Univ., Morgantown. Dept. of Mechanical and Aerospace Engineering.
AERODYNAMIC DRAG CHARACTERIZATION AND DEPOSITION STUDIES OF IRREGULAR PARTICLES. PART 3: ANALYSIS OF FLOW AND TEMPERATURE FIELD INSIDE THE COMBUSTION DEPOSITION ENTRAINED REACTOR (CDER) Final Report
I. Celik, S. Katragadda, and R. Nagarajan Jan. 1990 95 p
(Contract DE-FG21-86MC-23161)
(DE90-000466; DOE/MC-23161/2806) Avail: NTIS HC/MF A05

An experimental and numerical analysis was performed of the temperature and flow field involved in co-axial, confined, non-reacting heated jets in a drop tube reactor. An electrically heated 2-inch (50.8 mm) diameter drop tube reactor was utilized to study the jet characteristics. Profiles of gas temperature, typically in the range of 800 to 1600 K were measured in the mixing zone of the jet with a K-Type thermocouple. Measured temperatures were corrected for conduction, convection, and radiation heat losses. Because of limited access to the mixing zone, characterization of the flow field at high temperatures with laser Doppler or hot wire anemometry were impractical. A computer program which solves the full equations of motion and energy was employed to simulate the temperature and flow fields. The location of the recirculation region, the flow regimes, and the mixing phenomena were studied. The wall heating, laminar and turbulent flow regimes were considered in the simulations. The predictions are in fairly good agreement with the corrected temperature measurements provided that the flow is turbulent. The results of this study demonstrate how a numerical method and measurement can be used together to analyze the flow conditions inside a reactor which has limited access because of very high temperatures. DOE

N91-16260# Argonne National Lab., IL.
A METHOD FOR PRESSURE-PULSE SUPPRESSION IN FLUID-FILLED PIPING
Y. W. Shin, E. F. Bielick, A. H. Wiedermann, and C. E. Ockert

(Department of Energy, Washington, DC.) 1989 30 p Presented at the Winter Annual Meeting of the American Society of Mechanical Engineers, San Francisco, CA, 10-15 Dec. 1989
(Contract W-31-109-eng-38)
(DE90-010408; CONF-891208-31) Avail: NTIS HC/MF A03

A simple, nondestructive method to suppress pressure pulses in fluid-filled piping was proposed and theoretically analyzed earlier. In this paper, the proposed method is verified experimentally. The results of experiments performed for the range of parameters of practical importance indicated that the attenuation of pressure pulses was in accordance with the theoretical predictions. This paper describes the experimental setup and the test models of the proposed pulse suppression devices and discusses the experimental results. In particular, the measured attenuation factors are presented and compared with the theoretical predictions. DOE

N91-16261# Syracuse Univ., NY. Dept. of Chemical Engineering and Materials Science.
PARTICLE DEPOSITION IN GRANULAR MEDIA Progress Report
Tien Chi 1990 51 p
(Contract DE-FG02-88ER-13930)
(DE90-010810; DOE/ER-13930/T1) Avail: NTIS HC/MF A04

The purpose of the studies is aimed at obtaining a quantitative understanding of the process of deposition of aerosol particles from gas streams flowing through granular media and the formulation of a basic framework for describing the process. During the period June 1, 1988 to date, a number of investigations have been carried out including: transient behavior of granular filtration, modification of porous media model for aerosol deposition studies, stochastic simulation of particle deposition, and analysis of filter candle performance. Results of the studies are discussed separately. DOE

N91-16262# Argonne National Lab., IL. Dept. of Engineering Physics.
PARAMETRIC STUDY OF ELECTROSTATICALLY CHARGED SPRAYS
John S. Barnhart, Thomas E. Durbin, James E. Peters (Illinois Univ., Urbana.), and Keng H. Leong Dec. 1989 6 p Presented at the 4th Annual Conference on Liquid Atomization and Spray Systems, Hartford, CT, 20-23 May 1990
(Contract W-31-109-eng-38)
(DE90-010580; CONF-9005168-1) Avail: NTIS HC/MF A02

Electrostatically charged sprays are used in a wide range of applications. They include the coating of surfaces as with paint spraying, the production of fine powders, and the control of pollutants. The phenomenon of electrostatic spraying has been much researched particularly for the cases of dielectric fluids in paint spraying and conductive fluids in fine metallic powder production. Although the literature on electrostatic spraying is voluminous, the parametric dependence of the size distribution of the spray under various conditions still lacks precise definition. The focus of this study is the generation of charged water droplets for the production of ions and radicals in flue gases by pulsed corona discharges to control SO2 and NOx. As a first step in evaluating charged sprays for such use, a laboratory-scale injection system was evaluated by measuring atomization performance of needle injectors over a wide range of parameters. Sauter mean diameter (SMD) determined with a phase/Doppler particle analyzer (PDPA) was used as the measure of atomization performance. The independent parameters investigated include applied voltage, needle size, flow rate, and NaNO3 concentration (used to vary the solution conductivity). Because the spray was only about 2 mm wide at the sampling point, SMD measured at a single location was taken to be representative of the spray. This assumption was tested by taking radial traverses through the spray. Current flow from the needle to a collector plate 6 cm below was measured with and without solution flow to quantify the relative current-carrying capacities of the spray and the surrounding air. DOE

N91-16263# Los Alamos National Lab., NM.
STATE OF AN ADIABATIC EXPANDING AND CONDENSING VAPOR OR SLOW, MEDIUM, AND FAST EXPLOSIONS INTO A VACUUM
George L. Strobel (Georgia Univ., Athens.) Apr. 1990 63 p
(Contract W-7405-eng-36)
(DE90-010815; LA-11641-MS) Avail: NTIS HC/MF A04

A hot dense vapor expanding adiabatically into a vacuum is studied. A condensed phase develops after saturation and supercooling conditions have been achieved. The final state of the system consists of liquid drops in a expanding, cooling vapor. The final condensed mole fraction depends on the drop growth rate compared to the fractional volume rate of expansion at the time saturation is achieved. Drops are produced by a nonequilibrium collision process during supercooling of the vapor. The dependence of the number of drops on various factors is established. The First Law of Thermodynamics is used to solve for the evolution of the system, assuming the volume expansion rate is known. The initial vapor can include an inert gas that does not condense in the temperature range of interest. The vapors are treated as ideal gases until saturation occurs. Slow expansions result in the highest condensed mole fractions. Slow expansions are the result of one-dimensional versus three-dimensional expansions and from saturation occurring at high temperatures and densities. The size per drop depends mostly on how many drops are formed in the nonequilibrium supercooling process. DOE

N91-16264# Sandia National Labs., Albuquerque, NM.
AEROSOL CLOUD GENERATION EXPERIMENTS
A. C. Ratzel and E. J. Constantineau 1990 20 p Presented at the 15th International Pyrotechnics Seminar, Boulder, CO, 9-13 Jul. 1990
(Contract DE-AC04-76DP-00789)
(DE90-011051; SAND-90-0125C; CONF-900792-4) Avail: NTIS HC/MF A03

This paper provides results from an experimental study performed to evaluate the use of homogeneous and granulated explosive mixture concepts for creating spherical aerosol clouds. In the explosive mixture concept, a small mass of explosive is added to a larger mass of fine inert particulate, and the blend is hand-tamped into a confining cylindrical or spherical structure thereby creating a bed of explosive mixture. The mixture proportions are selected such that the mixture is able to sustain a reaction, be it a detonation or deflagration, throughout the bed. This approach generates gas for aerosol dispersal throughout the bed rather than from the center of the bed (as from a center-driven concept device). As such, a uniformly dispersed aerosol, rather than a thin shell of aerosol, would be expected to be dispersed. The two mixture concepts considered in this work differed only in the assembly and blending of the inert and explosive. Of interest in this work was the evaluation of the explosive mixture concepts relative to providing uniform spherical clouds of fine oxide aerosols of characteristic dimension less than 10 microns. Programmatic constraints dictated that the mass and quantity of extraneous materials such as the external structure and other peripherals associated with initiation also be minimized. Experiments were conducted in air with spherical devices ranging in size from 3 to 15 in. in diameter and with cylindrical and conical shotgun devices of length 4 to 7 inches. The latter test were performed to assess reaction sustainability for different explosive mixture ratios. Trends obtained from the studies as well as an assessment of the explosive mixture dispersal concept are included. DOE

N91-16265# Argonne National Lab., IL.
CIRCUMFLUOUS MOTION OF A CONDUCTIVE LIQUID AROUND SOLID OBJECTS IN A MAGNETIC FIELD
A. B. Tsinober, A. G. Shtern, and E. V. Shcherbinin (Academy of Sciences of the Latvian SSR, Riga.) 1 Dec. 1989 14 p Transl. into ENGLISH from Izvestiya Akademii Nauk Latviiskoi SSR, Seriya Fizicheskikh i Technicheskikh Naul (USSR), no. 4, p 31-40
(Contract W-31-109-eng-38)
(DE90-011335; ANL-TRANS-89-52) Avail: NTIS HC/MF A03

Experiments aimed at an investigation of the influence exerted

by a magnetic field on the resistance associated with the circumfluous motion of mercury around conductive solids are described in the first part of this work. It is learned that when good electrical contract is present between the mercury and the solid that it flows around, the resistance of the solid increases with an increase in its electric conduction. The second part of this text is devoted to a study of the influence exerted by a magnetic field on the distribution of pressure along a circular cylinder. It is shown that when a magnetic field is applied, pressure along the front portion of the cylinder increases, so that the pressure coefficient in place at the leading stagnation point becomes greater than unity. Pressure along the afterbody of the cylinder decreases. The resistance increase resulting from pressure variation accounts for 40 to 50 percent of the increase in total resistance. DOE

N91-16266# Tokyo Univ. (Japan). Inst. of Space and Astronautical Science.

THE PROCEEDINGS OF THE SYMPOSIUM ON MECHANICS FOR SPACE FLIGHT 1989

K. Oshima, ed. Mar. 1990 188 p Symposium held in Tokyo, Japan, 30 Nov. - 2 Dec. 1989

(ISAS-SP-12; ISSN-0288-433X) Avail: NTIS HC/MF A09

The symposium on Mechanics for Space Flight, 1989 was held at the Institute of Space and Astronautical Science on November 30, and December 1 and 2, 1989. Topics discussed included numerical simulation of unsteady flow around a wing, Navier-Stokes solvers, flow around a slender Delta wing, vortical flows inside a circular pipe, atmospheric diffusion of pollutants, heat transfer characteristics of a radial heat pipe and heat transfer characteristics of a closed two-phase thermosyphon. For individual titles, see N91-16267 through N91-16280.

N91-16267# Kyushu Univ., Fukuoka (Japan). Dept. of Aeronautical Engineering.

NUMERICAL SIMULATIONS OF UNSTEADY SHOCK REFLECTION PROCESSES BY A RAMP

Shigeru Aso, Masanori Hayashi (Nishinippon Inst. of Tech., Fukuoka, Japan), and Masanori Takano *In* Tokyo Univ., The Proceedings of the Symposium on Mechanics for Space Flight 1989 Mar. 1990 p 3-14 (For primary document see N91-16266 08-34)

Avail: NTIS HC/MF A09

Numerical simulations of unsteady shock reflections by a ramp were conducted. The two-dimensional Euler equations are solved numerically by a Total Variation Diminishing (TVD) scheme proposed by Harten with modified flux approach and resolution enhancement by artificial compression. The calculations were carried out for regular reflections, single Mach reflections, complex Mach reflections and double Mach reflections under the conditions of shock Mach number from 1.34 to 3.10 and ramp angles from 35 to 48 degrees. The results show good agreements with experiments. In particular the slip layers and Mach stems in Mach reflections under the conditions of shock Mach number of 2.35 and 2.75 respectively with ramp angle of 42.5 degrees. The unsteady aerodynamic heating induced by shock impingement is simulated numerically. The results show good agreements with experiments. In particular, the second peak heating caused by the impingement of the slip layer generated from the triple point is properly predicted. Also weak Mach reflection processes are simulated properly. Viscous effects to the shock reflection processes are proved to be significant for weak Mach reflection. Author

N91-16268# Kyushu Univ., Fukuoka (Japan). Dept. of Aeronautical Engineering.

NUMERICAL SIMULATION OF SEPARATED FLOWS AROUND A WING SECTION AT STEADY AND UNSTEADY MOTION BY A DISCRETE VORTEX METHOD **c02**

Shigeru Aso, Atsushi Fujimoto, Naoki Futatsudera, and Masanori Hayashi (Nishinippon Inst. of Tech., Fukuoka, Japan) *In* Tokyo Univ., The Proceedings of the Symposium on Mechanics for Space Flight 1989 Mar. 1990 p 15-24 Original language document was announced in IAA as A90-33753 (For primary document see N91-16266 08-34)

Avail: NTIS HC/MF A09

Separated flows around a wing section at pitching motion are simulated numerically by a discrete vortex method combined with a panel method. The potential flows around wing sections are expressed by vortex sheets and separated shear layers are expressed by discrete vortices. In the calculation, a separation point is determined by solving boundary layer equations. The strength of shed vortex is estimated using local velocity near separation point. Separated flows around pitching airfoils are simulated. A hysteresis of lift of airfoil at dynamic stall is obtained in the calculation. These results suggest that this method is useful to simulate separated flows around a wing section at pitching motions. Author

N91-16269# Chiba Univ. (Japan). Faculty of Engineering.

SOME TOPICS OF NAVIER-STOKES SOLVERS

H. Honma and N. Nishikawa *In* Tokyo Univ., The Proceedings of the Symposium on Mechanics for Space Flight 1989 Mar. 1990 p 25-39 (For primary document see N91-16266 08-34)

Avail: NTIS HC/MF A09

The process of numerical simulation consists of selection of some items: a mathematical model, a numerical scheme, the level of the computer, and post processing. From this point of view, recent numerical studies of viscous flows are described especially for the fluid engineering laboratories in the Chiba University. The examples of simulations are Mach reflection on a wedge using a kinetic model equation and a cylinder-plate juncture flow using incompressible Navier Stokes equation. Some attempts at graphic monitoring of fluid mechanical calculations are also shown for some combinations of computers with Computational Fluid Dynamics (CFD) solvers. Author

N91-16270# Tohoku Univ., Sendai (Japan). Inst. of Fluid Science.

SIMULATION OF EXCITED SHEAR FLOWS

Osamu Inoue *In* Tokyo Univ., The Proceedings of the Symposium on Mechanics for Space Flight 1989 Mar. 1990 p 41-44 (For primary document see N91-16266 08-34)

Avail: NTIS HC/MF A09

The purpose is to increase our understanding of the effects of artificial excitation on the development of turbulent shear flows. As an example, two-dimensional, spatially growing, turbulent mixing layers are studied numerically by a vortex method. Special attention is paid to the effect of multiple-frequency forcing. Forcing frequencies selected are various combinations of the predominant frequency of an unforced flow with its subharmonics or high-harmonics. Results are in good agreement with experiments. Author

N91-16271# Tokyo Univ. (Japan). Dept. of Aeronautical Engineering.

NUMERICAL SIMULATION OF PULSATILE FLOWS PASSING THROUGH A PIPE WITH SUDDEN EXPANSION

Y. Ishii *In its* The Proceedings of the Symposium on Mechanics for Space Flight 1989 Mar. 1990 p 45-52 (For primary document see N91-16266 08-34)

Avail: NTIS HC/MF A09

Pulsating flows in a circular pipe were numerically investigated in order to obtain a basic understanding of the generating mechanism of Post-Stenotic Dilatation (PSD) from the fluid dynamic point of view. The vorticity and steamfunction formulation of the Navier-Stokes equation was solved for a pipe flow with a sudden expansion using the finite difference method. The velocity distribution and the reattachment point were determined. These results showed fairly good agreement with the analytical results, and the reattachment point obtained is coincided with the experimental result. Author

N91-16272# Kyushu Univ., Fukuoka (Japan). Dept. of Aeronautical Engineering.
UNSTEADY VORTEX LATTICE CALCULATION OF THE FLOW AROUND A SLENDER DELTA WING **c02**
Akira Sakurai and Hiroshi Uchihori *In* Tokyo Univ., The Proceedings of the Symposium on Mechanics for Space Flight 1989 Mar. 1990 p 53-59 (For primary document see N91-16266 08-34)
Avail: NTIS HC/MF A09

The unsteady vortex lattice method was applied to the calculation of the unsteady flow field around a slender delta wing at a high angle of attack. The result shows that the essential feature of the flow such as the formation of the leading edge vortex can be described by this model, while the detail of the calculated flow field still depends on the practical aspects of the scheme such as the selection of the viscous core radius. Author

N91-16273# Tokyo Univ. (Japan). Dept.of Aeronautical Engineering.
NUMERICAL SIMULATION OF A COMPLICATED TRANSITION-BREAKDOWN OF VORTICAL FLOWS INSIDE A CIRCULAR PIPE
H. L. Chen and K. Oshima (Tokyo Univ., Sagamihara, Japan) *In its* The Proceedings of the Symposium on Mechanics for Space Flight 1989 Mar. 1990 p 73-104 (For primary document see N91-16266 08-34)
Avail: NTIS HC/MF A09

Entrance flows to a circular pipe which has an axisymmetric sudden expansion were numerically simulated for a wide range of Reynolds numbers. Particularly, shear layer instabilities observed behind the sudden expansion were studied. Experimental observation of the flow fields at the corresponding flow conditions were also carried out. Taylor-Helmholtz type instability was observed along the shear layer behind the sudden expansion, and its breakdown into turbulent blobs were observed. Numerical results successfully simulated this vortex breakdown process. The process whereby flows grow into chaos was also successfully simulated. Author

N91-16274# Academia Sinica, Beijing (China). Inst. of Mathematics.
ANALYSIS OF ATMOSPHERIC DIFFUSION OF POLLUTANTS BASED ON THE LIMITED OBSERVATION OF HORIZONTAL WIND **c45**
Lier Wang and Huamo Wu *In* Tokyo Univ., The Proceedings of the Symposium on Mechanics for Space Flight 1989 Mar. 1990 p 105-113 (For primary document see N91-16266 08-34)
Avail: NTIS HC/MF A09

A numerical method of predicting the pollutant concentration in the atmosphere is suggested. A variational method approach to determinate the three dimensional wind field from the measured data at irregularly located observation stations is improved. A numerical algorithm for obtaining the physically relevant distribution of the pollutant concentrations by solving a convection-diffusion equation is presented and an example of analyzed data is demonstrated. Numerical results of the wind fields and the pollutant concentrations are given. Author

N91-16275# Academia Sinica, Beijing (China). Computing Center.
MmB: A NEW CLASS OF ACCURATE HIGH RESOLUTION SCHEMES FOR CONSERVATION LAWS IN TWO DIMENSIONS
Huamo Wu and Shuli Yang *In* Tokyo Univ., The Proceedings of the Symposium on Mechanics for Space Flight 1989 Mar. 1990 p 115-146 (For primary document see N91-16266 08-34)
Avail: NTIS HC/MF A09

The MmB schemes, which preserve the local maximum and minimum bounds of the initial data in the smallest union of mesh elements of the previous time step containing the domain of dependence of the solution on the mesh element with center at point P under consideration are presented. In 1-D, the MmB schemes are almost identical with Total Variation Diminishing (TVD) schemes. There is no second-order TVD scheme in 2-D. Nevertheless, researchers present here two classes of 2-D second-order accurate MmB schemes. It is proved that 1-D discrete MmB (or TVD) and 1-D semi-discrete TVD schemes may have second-order accuracy at (nonsonic) critical points, but cannot be uniformly second-order accurate in the whole neighborhood of the critical point. New accurate high resolution flux limiters are suggested. Numerical results for 1-D and 2-D test problems are given. Author

N91-16276# Ibaraki Univ., Hitachi (Japan). Faculty of Engineering.
HEAT TRANSFER CHARACTERISTICS OF A RADICAL HEAT PIPE
Fumito Kaminaga, Yoshizo Okamoto, Terumitsu Yotsukura, Haruhiko Ito, Takasi Saito, and Hiroo Amezawa (Japan Atomic Energy Research Inst., Oarai.) *In* Tokyo Univ., The Proceedings of the Symposium on Mechanics for Space Flight 1989 Mar. 1990 p 147-153 (For primary document see N91-16266 08-34)
Avail: NTIS HC/MF A09

Heat transfer characteristics of a newly designed heat pipe which transports thermal energy in a radial direction of the heat pipe are examined experimentally, using Freon R-113 working fluid. The heat pipe produces a much higher overall heat transmission than the current heat pipe due to a direct contact condensation instead of a filmwise condensation. An unheated vapor space above a heated section and a higher charge rate over 70 percent are required to use it in a wide range of heat flux. A normal screen wick presents an insufficient capillary force to pump up the working fluid to the heated section against the gravity force. Author

N91-16277# National Space Development Agency, Ibaraki (Japan).
DEVELOPMENT OF A TWO-PHASE COLD PLATE
Y. Miyazaki, M. Furukawa, Y. Ishii, M. Shigehara, M. Komori, K. Mimura, and S. Oshima (Toshiba Corp., Tokyo, Japan) *In* Tokyo Univ., The Proceedings of the Symposium on Mechanics for Space Flight 1989 Mar. 1990 p 155-165 (For primary document see N91-16266 08-34)
Avail: NTIS HC/MF A09

A two-phase cold plate using evaporators of grooved double-pipe type was tested in order to examine its heat transfer and hydrodynamic characteristics under practical operating conditions. Under a uniform heat load, excellent temperature uniformity of the cold plate was obtained. Under an uneven heat load, however, the temperature distributions were not uniform; they were high in active areas and low in inactive areas. It seems to be due to ineffective liquid flow through inactive pipes, which causes liquid shortage in active tubes and over-cooling by sub-cooled liquid in inactive tubes. Parallel operations with two cold plates were performed successfully, demonstrating that both temperatures were kept at the same level even under different heat loads. In a certain operating condition, the individual flow rate of the two cold plates was observed to oscillate symmetrically to each other, while total flow rate was kept constant and no anomalous behavior on heat transfer was induced. Through the tests, a design approach for the cold plate from the viewpoint of a loop control technology was obtained. Author

N91-16278# Tsukuba Univ., Ibaraki (Japan). Inst. of Engineering Mechanics.
EFFECT OF INCLINATION ANGLE ON HEAT TRANSFER CHARACTERISTICS OF CLOSED TWO-PHASE THERMOSYPHON
P. Terdtoon, M. Shiraishi (Mechanical Engineering Lab., Tsukuba, Japan), and M. Murakami *In* Tokyo Univ., The Proceedings of the Symposium on Mechanics for Space Flight 1989 Mar. 1990 p 167-173 (For primary document see N91-16266 08-34)
Avail: NTIS HC/MF A09

The results of the effect of inclination angle on heat transfer characteristics of a thermosyphon are given. The steel-R113 thermosyphon system is used in the investigation, with the filling

ratios of 80, 50 and 30 percent. The heat transfer characteristics of the thermosyphon are obtained in the range from 90 deg. to the horizontal position. It is found from the experiments that there is a tendency for the transported heat at any inclination angle to be higher than that of the vertical state. The ratio of critical heat transfer rate at any inclination angle and that of the vertical state reach the maximum value of 1.6 in the case of a filling ratio of 50 percent. The range of the isothermal operating state depends deeply on the filling ratio. From the preliminary consideration, the effect of inclination angle can be divided into 4 major regions, which are described. Author

N91-16279# Ishikawajima-Harima Heavy Industries Co. Ltd., Yokohama (Japan).
NUMERICAL SIMULATION OF BUFFER FLOW IN A FREE FLOW ELECTROPHORESIS CHAMBER
Hiromi Yamaguchi, Masahiro Ishii, Kazuo Uematsu, Hiroyuki Uchida, Sintaro Enya, and Hisao Azuma (National Aerospace Lab., Tokyo, Japan) *In* Tokyo Univ., The Proceedings of the Symposium on Mechanics for Space Flight 1989 Mar. 1990 p 176-182 (For primary document see N91-16266 08-34)
Avail: NTIS HC/MF A09

Free flow electrophoresis facilities used for the refining of biological materials such as blood and protein are limited in their performance by the disturbance of buffer flow. Two types of convection which cause the flow disturbance in an electrophoresis chamber were studied. Numerical investigation on natural convection by Joule heat proved that the flow field in the electrophoretic chamber is characterized by the Reynolds, the Grashof and the Prandtl numbers. It was also found that the critical condition where the convective flow arises is evidenced by a relationship between the Reynolds and the Grashof numbers. Electroosmotic convection combined with the natural one in a three-dimensional model was calculated. Horizontal and vertical flow are not individually conserved in their flux because a complex three-dimensional flow pattern is formed. Author

N91-16280# National Research Inst. for Pollution and Resources, Tokyo (Japan).
EXPERIMENTAL STUDY ON MERCURY HEAT PIPES (ON EFFECT OF SCREEN MESH WICK UNDER BOTTOM HEAT MODE)
M. Tashiro, Y. Tanaka, T. Yamamoto, and Y. Ikeda (Nippon Inst. of Tech., Japan) *In* Tokyo Univ., The Proceedings of the Symposium on Mechanics for Space Flight 1989 Mar. 1990 p 183-189 (For primary document see N91-16266 08-34)
Avail: NTIS HC/MF A09

The purpose is to obtain the fundamental information required for the development of the mercury heat pipe. As a part of the study, the influence of the presence of the screen mesh wick on the performance of the mercury heat pipe was examined experimentally in the bottom heat mode. Author

N91-16281 Council for National Academic Awards (England).
FAR-FIELD BOUNDARIES AND THEIR NUMERICAL TREATMENT Ph.D. Thesis
S. Karni 1989 227 p
Avail: Univ. Microfilms Order No. BRDX89813

Many computational problems of theoretical and practical interest are not naturally bounded by physical boundaries. Aerodynamic examples include flow calculations past airfoils or past wing-body configurations, semi-bounded channel flows. Other examples include simulations of turbomachinery flows, problems in underwater acoustics. To obtain a numerical solution, the problem has first to be converted to a finite region by introducing an artificial boundary at some finite distance. Boundary conditions must be specified at the artificial boundary for well-posedness of the truncated problem. An open boundary across which the fluid flows are simulated should ideally allow outgoing waves to pass through without generating reflections. A thorough numerical study is presented for the efficiency of several widely used boundary conditions in absorbing outgoing waves. The key parameters upon which the level of absorption at the boundaries depends, are examined and the limitations of some of the existing recipes expressed. Substantial reflections may occur even under conditions which are considerably milder than those encountered in practical calculations. Two closely related far field modifications are derived and analyzed: slowing down the outgoing waves; and attenuating the outgoing waves. Analytic conditions are derived to ensure that no reflections are generated due to the change of coefficients in the governing equations. Reflection analysis is also performed on the discrete level. The modifications are extended to two space dimensions and are applied to a variety of one and multidimensional test problems. Dissert. Abstr.

N91-16282 Lehigh Univ., Bethlehem, PA.
PRESSURE GRADIENT EFFECTS ON THE DEVELOPMENT OF HAIRPIN VORTICES IN AN INITIALLY LAMINAR BOUNDARY LAYER Ph.D. Thesis
Blaine Keith Taylor 1990 313 p
Avail: Univ. Microfilms Order No. DA9030349

An experimental study was conducted in Lehigh University's low-speed water channel to examine the effects of a zero, adverse, and favorable pressure gradients on the development of single hairpin vortices. Single hairpin vortices were generated in an initially laminar environment using controlled fluid injection through a streamwise slot at a Re(delta)* = 380, 440, and 570. Behavior of hairpin structures was determined by the use of dye and hydrogen bubble flow visualization techniques. Visualization results indicate that as a single hairpin vortex convects downstream a complicated growth process due to viscous-inviscid interactions and Biot-Savart deformation results in the generation of secondary and subsidiary vortices, eventually yielding a turbulent spot-like structure. The hairpin vortex structures are observed to be strongly affected by the presence of a pressure gradient, undergoing significant spatial growth changes, as well as experiencing significant flow structure modifications. As the hairpin initiation location is moved further into an adverse pressure gradient, the hairpin vortex lifts and rotates farther away from the surface relative to the behavior in a zero pressure gradient. Regions of low and high-velocity fluid near the surface are accentuated within an adverse pressure gradient, which amplifies the low-speed streak formation and breakdown process, accelerating the formation of vortical substructures and ejection of fluid from the surface. Dissert. Abstr.

N91-16283# Los Alamos National Lab., NM.
AFDM: AN ADVANCED FLUID-DYNAMICS MODEL. VOLUME 2: TOPOLOGIES, FLOW REGIMES AND INTERFACIAL AREAS
D. Wilhelm Sep. 1990 123 p
(Contract W-7405-eng-36)
(DE91-000581; LA-11692-MS-VOL-2) Avail: NTIS HC/MF A06

This volume describes the Advanced Fluid-Dynamics Model (AFDM) for topologies, flow regimes, and interfacial areas. The objective of these models is to provide values for the interfacial areas between all components existing in a computational cell. The interfacial areas are then used to evaluate the mass, energy, and momentum transfer between the components. A new approach has been undertaken in the development of a model to convect the interfacial areas of the discontinuous velocity fields in the three-velocity-field environment of AFDM. These interfacial areas are called convectible surface areas. The continuous and discontinuous components are chosen using volume fraction and levitation criteria. This establishes so-called topologies for which the convectible surface areas can be determined. These areas are functions of space and time. Solid particulates that are limited to being discontinuous within the bulk fluid are assumed to have a constant size. The convectible surface areas are subdivided to model contacts between two discontinuous components or discontinuous components and the structure. The models have been written for the flow inside of large pools. Therefore, the structure is tracked only as a boundary to the fluid volume without having a direct influence on velocity or volume fraction distribution by means of flow regimes or boundary layer models. DOE

N91-16284# Minnesota Univ., Minneapolis. Dept. of Mechanical Engineering.
THE IMPACT OF SEPARATED FLOW ON HEAT AND MASS TRANSFER
R. J. Goldstein and M. Y. Jabbari 1990 11 p
(Contract DE-FG02-87ER-13800)
(DE91-000592; DOE/ER-13800/T2) Avail: NTIS HC/MF A03

An investigation of the effect of flow separation on heat (or mass) transfer is underway. This research is planned to enhance the understanding of the fundamental mechanisms governing the process. This report summarizes previous accomplishments and briefly describes works done during period May 1, 1989 through April 30, 1990. Future plans and studies under preparation are also mentioned. DOE

N91-16285# Cornell Univ., Ithaca, NY.
UNSTEADY SEPARATION OVER MANEUVERING BODIES Final Progress Report, 1 Oct. 1989 - 31 Jan. 1990
Shan-Fu Shen, Txuyin Wu, Z. Xiao, and J. S. Kim 15 Aug. 1990 21 p
(Grant AF-AFOSR-0229-88; AF Proj. 2307)
(AD-A226829; AFOSR-90-0948TR) Avail: NTIS HC/MF A03 CSCL 20/4

Development of a new boundary layer code has reached the status to permit meaningful applications. Computations were carried out for the initiation of separation in the symmetry plane of a prolate spheroid of slenderness ratio 1/4, impulsively started into forward motion at zero incidence and also at 50 degrees angle. This case serves as validation by comparing with previously published results of Xu and Wang, and also demonstrates that the method gives information of flow near the rear stagnation point not available in the literature. More studies were performed on the optimization of surface suction to delay or prevent the unsteady separation for an impulsively started circular cylinder. Here the methodology should be of interest. Work on an unsteady three-dimensional thin-layer Navier-Stokes code, however, is progressing slowly. GRA

N91-16286# Army Cold Regions Research and Engineering Lab., Hanover, NH. Applied Research Branch.
HEAT TRANSFER FROM WATER FLOWING THROUGH A CHILLED-BED OPEN CHANNEL
Paul W. Richmond and Virgil J. Lunardini May 1990 56 p
(DA Proj. 4A7-62730-A4-AL)
(AD-A226855; CRREL-90-3) Avail: NTIS HC/MF A04 CSCL 20/13

Observations and experiments have shown that the transfer is greater for water flowing over ice than for water flowing over flat plates without melting. The mechanisms that contribute to this increased heat transfer are not completely understood. One possible cause is the density inversion of water at 4 C. In order to investigate this effect on heat transfer, a small open-channel flume was designed and constructed. Experiments were conducted with the flume bed at temperatures slightly above 0 C and at temperatures above 4 C. Bulk water temperatures ranged from 5 to 33 C. Flow data were obtained for 2500 is less than Re(sub H) is less than 100000. At high flow rates (fully developed turbulent flow) heat transfer correlations obtained from these experiments initially showed higher heat transfer rates than those obtained from experiments in larger flumes with ice present. This thought to be due to a difference in velocity profiles caused by the flume width. Once velocity corrections were made to the data, they agreed more closely with experiments from wider flumes. The results indicate that the density inversion of water could account for most of the increased turbulent heat transfer observed between melting and nonmelting systems. The heat transfer data at low flow rates are more qualitative than quantitative due to difficulty in obtaining accurate data. GRA

N91-16287# Ballistic Research Labs., Aberdeen Proving Ground, MD.
EVALUATION OF THE HULL AND SHARC HYDROCODES IN SIMULATING THE REFLECTION OF MACH 2.12 NON-DECAYING SHOCK ON WEDGES OF VARIOUS ANGLES
Richard E. Lottero and John D. Wortman Sep. 1990 122 p
(AD-A227581; BRL-TR-3153) Avail: NTIS HC/MF A06 CSCL 20/4

Hydrodynamic computer code simulations of the interaction of a non-decaying Mach 2.12 shock wave with wedges of various angles are presented. Techniques for simulating this interaction with the HULL and SHARC hydrocodes are evaluated by running the codes in various geometric configurations commonly used to simulate Mach reflection. Fluid dynamics aspects of each geometry are evaluated and discussed. The codes are also run with systematic variations in differencing method and artificial viscosity options. Most of these variations done in the SHARC also includes the option of using half hydrodynamic and half rigid flow field cells to simulate a smooth wedge surface in a rectangular finite difference grid. These computations are based on experimental and computational work performed at the Ernst Mach Institute, Freiburg, Federal Republic of Germany. Author (GRA)

N91-16288# Los Alamos National Lab., NM. Physics Div.
ROTATING RAYLEIGH-BENARD CONVECTION: THE KUEPPERS-LORTZ TRANSITION
Fang Zhong, Robert Ecke, and Victor Steinberg 1990 17 p Presented at the 10th Annual Conference on Nonlinear Science: The Next Decade, Los Alamos, NM, 21-25 May 1990 Submitted for publication
(Contract W-7405-eng-36)
(DE91-004835; LA-UR-90-3819; CONF-9005237-8) Avail: NTIS HC/MF A03

Rayleigh-Benard convection with rotation about a vertical axis is investigated for small dimensionless rotation rates Omega between 0 and 50. The convection cell is cylindrical with aspect ratio Gamma equal to 10 and the convecting fluid is water with a Prandtl number of 6.8 at temperature 23.8 C. Comparisons are made between experimental data and linear stability theory for the onset Rayleigh number and for the wave number dependence of the convective pattern. The nonlinear Kueppers-Lortz transition is found to occur significantly below the theoretically expected rotation rate Omega(sub c) and to be nucleated by defects created at the lateral cell walls. DOE

N91-16289*# Florida State Univ., Tallahassee. Fluid Mechanics Research Lab.
THE DEVELOPMENT OF LASER SPECKLE VELOCIMETRY FOR THE STUDY OF VORTICAL FLOWS Final Technical Report, 1 Oct. 1984 - 31 Mar. 1990
A. Krothapalli Jan. 1991 116 p
(Grant NAG2-314)
(NASA-CR-187756; NAS 1.26:187756) Avail: NTIS HC/MF A06 CSCL 20D

A new experimental technique commonly known as PIDV (particle image displacement velocity) was developed to measure an instantaneous two dimensional velocity fluid in a selected plane of the flow field. This technique was successfully applied to the study of several problems: (1) unsteady flows with large scale vortical structures; (2) the instantaneous two dimensional flow in the transition region of a rectangular air jet; and (3) the instantaneous flow over a circular bump in a transonic flow. In several other experiments PIDV is routinely used as a non-intrusive measurement technique to obtain instantaneous two dimensional velocity fields. Y.S.

N91-16290 Princeton Univ., NJ.
ANALYSIS AND APPLICATION OF THE DISCRETE VORTEX METHOD Ph.D. Thesis
Marie Dillon Dahleh 1990 108 p
Avail: Univ. Microfilms Order No. DA9027574

Two dimensional, inviscid, incompressible vortex methods were studied and the implementation of these methods for problems in

atmospheric and oceanic fluid dynamics is presented. The accuracy of the vortex method is examined computationally. Specifically the point vortex and higher order methods based on kernels built from a rational function approximation to the delta function are discussed. In order to learn more about the accuracy of these methods for flows which are not radially symmetric, the Kirchhoff ellipse and the Kida ellipse are studied. The Kida ellipse serves both as a good test for the vortex method and it is a physically interesting flow which is studied in its own right. For the Kirchhoff ellipse the error at the initial time is studied as a function of the aspect ratio of the ellipse, the kernel function, the blob radius, and the distance between the centers of the blobs. The long term error for the point vortex and the fourth order blob vortex for both the Kirchhoff and Kida ellipses is examined by comparing the computed rotation rate with the exact rotation rate. The applicability of the vortex method for the study of the Kida vortex is examined. The Liapunov exponents for a chaotic region of the flow are computed and the effect of the addition of vorticity to these particles is studied. The applicability of these methods to the equivalent barotropic equations of potential vorticity is determined by comparing the continuous linear dispersion relation with the continuous limit of the discrete linear dispersion relation for the two vortex methods. A convergence extension of the modulated point vortex proposed by Zabusky and McWilliams (1982) is developed. The order of this method is determined. A formally O(N) fast multipole vortex method was implemented and its utility was studied. Given the size of the problems considered and the machines used, the fast multipole method did not yield improved speed. Dissert. Abstr.

N91-16291# Stanford Univ., CA. Dept. of Mechanical Engineering.
NUMERICAL STUDY OF A THREE-DIMENSIONAL TURBULENT BOUNDARY LAYER Final Report, 1 Jul. 1987 - 30 Jun. 1990
Parviz Moin 31 Aug. 1990 12 p
(Grant AF-AFOSR-0285-87; AF Proj. 2307)
(AD-A227835; AFOSR-90-1027TR) Avail: NTIS HC/MF A03 CSCL 20/4

The effects of transverse strain on an initially 2-D turbulent boundary layer are studied in a direct numerical simulation of a planar channel flow with impulsively started transverse pressure gradient. Consistent with experiments in 3-D boundary layers, the simulation shows a decrease in the Reynolds shear stress with increasing transverse strain. Also, the directions of the Reynolds shear stress vector and the mean velocity gradient vector were found to differ. In addition, the simulation shows a drop in the turbulent kinetic energy. Terms in the Reynolds stress transport equations were computed. The balances indicate that the decrease in turbulent kinetic energy is a result of a decrease in turbulence production, along with an increase in turbulent dissipation. The effects of the transverse pressure gradient on the instantaneous flow structures were investigated. GRA

N91-16292# California Inst. of Tech., Pasadena. Dept. of Applied Mathematics.
RESEARCH IN NONLINEAR WATER WAVES Quarterly Letter Progress Report, 1 Jul. - 30 Sep. 1990
P. G. Saffman 30 Sep. 1990 2 p
(Contract N00014-89-J-1164)
(AD-A227948) Avail: NTIS HC/MF A01 CSCL 20/4

Satisfactory progress has been made with the continuing studies of the effect of a thin drift layer on the stability and shape of capillary gravity waves. The problem about the counting for the integro-differential equation formulation of the shape of finite amplitude waves of permanent form has been resolved. The equations now seem to describe a well-posed problem, and the task now is to calculate solutions for problems of physical relevance. The calculation of stability for smooth profiles has been carried out. This proved to be more difficult than anticipated but rather interesting. It uncovered new features of the way in which the Rayleigh equation (inviscid Orr-Sommerfeld equation) describes the onset of instability. The work was extended to three-dimensional disturbances, and it was shown that the Squire theorem still applies, so that the most unstable disturbances, are two dimensional. Further studies of the results indicate that the new instabilities may not be closely relevant to the generation of waves by wind, as the surface drift velocities are not likely to be large enough. However, there is a possibility that there may be some relevance to situations where the shear layers are generated mechanically. GRA

N91-16293# Calspan Corp., Arnold AFS, TN.
INVESTIGATION OF THE INFLUENCE OF CONSTANT ADVERSE PRESSURE GRADIENTS ON LAMINAR BOUNDARY-LAYER STABILITY AT MACH NUMBER 8 Final Report, 7-11 May 1990
J. C. Donaldson, J. P. Grubb, and D. W. Sinclair AEDC Oct. 1990 59 p Sponsored by AF
(AD-A228231; AEDC-TSR-90-V13) Avail: NTIS HC/MF A04 CSCL 20/4

Measurements of fluctuating flow and mean flow parameters were made in the boundary layer on each of two axisymmetric, constant pressure gradient bodies in an investigation of the influence of adverse pressure gradients on the stability of a laminar boundary layer in hypersonic flow. Each test article was slender, constant pressure gradient flare combined with a sharp cone forebody with a 7-deg half angle. The test articles differed in the magnitude of the pressure gradient. The flow fluctuation measurements were made using constant current hot-wire anemometry techniques. Boundary layer profiles and model surface conditions were measured to supplement the hot-wire data. Testing was done at Mach number 8 with a free-stream unit Reynolds number of 1.0-million per foot. The test equipment, test techniques, and the data acquisition and reduction procedures are described. The test was the ninth in a series of efforts which have investigated various aspects of hypersonic boundary layer stability. GRA

N91-16294# Colorado Univ., Boulder.
NONLINEAR WAVES AND INVERSE SCATTERING Annual Technical Report
Mark J. Ablowitz 18 Sep. 1990 4 p
(Contract N00014-90-J-1218)
(AD-A228757) Avail: NTIS HC/MF A01 CSCL 20/4

We are continuing our research in the development of the Inverse Scattering Transform (IST). IST is a method which allow's one to solve nonlinear wave equations by solving certain related direct and inverse scattering problems. Research is really two pronged. It is necessary for us to understand and effectively solve both classical and new direct and inverse scattering problems. We use these results to find solutions to nonlinear wave equations much like one uses Fourier analysis for linear problems. Moreover the nonlinear wave equations arise naturally in physical problems. We are particularly interested in fluid dynamical applications. Although original discoveries employed IST in one spatial dimension, we have developed effective procedures to carry forth the method for multidimensional problems. In one spatial dimension solving the inverse scattering problem requires one to solve a vector Riemann-Hilbert boundary value problem. In multidimensions we have shown that the DBAR method is essential to solve the increase problem. In a special case it reduces to a Riemann-Hilbert problem (sometimes a nonlocal Riemann-Hilbert problem). The method applies to the multidimensional Schrodinger scattering problem (i.e., the Helmboltz equation) higher order scalar differential operators, multidimensional first order systems and even discrete equations, i.e., difference equations. The multidimensional DBAR method is an extremely powerful method to analyze and solve inverse scattering problems. The DBAR method was extended to solve a variety of novel and important inverse scattering problems in multidimensions. GRA

N91-16295# Berkeley Research Associates, Inc., CA.
DEVELOPMENT AND APPLICATION OF NUMERICAL MODELS FOR REACTIVE FLOWS Final Report, 28 Oct. 1985 - 30 Sep. 1989
15 Aug. 1990 536 p

(Contract N00014-86-C-2021)
(AD-A228884; BRA-91-W001R) Avail: NTIS HC/MF A23
CSCL 20/4

This report focused on developing mathematical and computational models which accurately and efficiently describe the behavior of complex physical systems such as: chemically reacting flows; transition from laminar to turbulent flow in reacting gas mixtures; laser-induced shock waves in an explosive medium; initiation, propagation, extinguishment, and structure of laminar flames. Work carried out in extending the flux-corrected transport (FCT) flow models to three dimensions and to generalize meshes is described. The extension to three dimensions required the development of surface definition software and sophisticated data structures to avoid excessive CPU-time overheads for the search operations involved. The hybrid method developed in combining the finite element method with the flux-corrected transport method (FEM-FCT) is useful for solving problems involving steady and unsteady transonic and supersonic flow in irregular geometries. The VOYEUR graphics system is described. It is used in conjunction with two instruments, namely a color hardcopy device (a Tektronix 4115 compatible printer/plotter, VOYEUR being implemented on a Tektronix 4115) or a DICOMED graphic output device. It is a menu driven system which builds up from a simple set-up to more complicated plots compiled from this initial information. Work carried out on transverse and axisymmetric jets, mixing enhancement in supersonic shear layers, unforced spatially-developing mixing layer and subgrid closures is described. GRA

N91-16296*# Old Dominion Univ., Norfolk, VA. Dept. of Mechanical Engineering and Mechanics.
EXPERIMENTAL PARAMETRIC STUDY OF JET VORTEX GENERATORS FOR FLOW SEPARATION CONTROL Final Report, period ending 31 Dec. 1990
Gregory Selby Jan. 1991 45 p
(Grant NAG1-1071)
(NASA-CR-187836; NAS 1.26:187836) Avail: NTIS HC/MF A03
CSCL 20D

A parametric wind-tunnel study was performed with jet vortex generators to determine their effectiveness in controlling flow separation associated with low-speed turbulence flow over a two-dimensional rearward-facing ramp. Results indicate that flow-separation control can be accomplished, with the level of control achieved being a function of jet speed, jet orientation (with respect to the free-stream direction), and orifice pattern (double row of jets vs. single row). Compared to slot blowing, jet vortex generators can provide an equivalent level of flow control over a larger spanwise region (for constant jet flow area and speed). Dye flow visualization tests in a water tunnel indicated that the most effective jet vortex generator configurations produced streamwise co-rotating vortices. Author

N91-16297 Harvard Univ., Cambridge, MA.
STREAMWISE VORTICES IN LAMINAR-TURBULENT TRANSITION Ph.D. Thesis
Joseph Dwan Myers 1990 203 p
Avail: Univ. Microfilms Order No. DA9035524

The characteristics of a single streamwise vortex embedded in plane Poiseuille flow were analyzed. On short time scales, computations show that velocity profiles evolve similarly to those previously derived in unbounded Couette flow. As boundary effects begin to be felt at later times, a perturbation solution is derived whose profiles and decay rates are found to agree with calculations. Both solutions are used to answer questions about the strength and motion of the vortex, the presence and strength of any counterrotating vortices induced at the viscous boundary, and the possible, or impossible, role of such induced vortices in transition. Time scale arguments are used to derive a neutral curve with a minimum critical Reynolds number close to 1000. The dynamics of a simple model of an isolated polymer molecule embedded in a single vortex flow were also investigated. First, a streamwise vortex embedded in plane Poiseuille flow was numerically simulated, including the effects of streamwise gradients. Then the dynamics of an embedded polymer molecule were introduced using a hybrid ellipsoid-dumbbell model. Regions of positive streamwise strain rate develop within the flow which are of sufficient strength to stretch the polymer to experimentally observed elongations, and then to allow the polymer to relax or entangle. The resulting local increase in viscosity is interpreted within the context of the single streamwise vortex model to infer the local decrease in strength of the associated vortex, the reduced inflectional velocity profiles within the vortex core, and the increased stability of the flow in that region. Dissert. Abstr.

N91-16298 California Univ., Los Angeles.
LOCAL AND GLOBAL INSTABILITY OF HEATED 2-D JETS AND WAKES Ph.D. Thesis
Ming-Huei Yu 1990 143 p
Avail: Univ. Microfilms Order No. DA9034009

The stability of heated two-dimensional jets and wakes is analyzed, and an experiment on a two-dimensional hot jet in the transitional regime is described. By applying linear theory to the problem of a hot jet, it is shown that it exhibits absolute instability when the density ratio of the jet to the ambient is less than 0.95, the Reynolds number is infinite, buoyancy effects are negligible and the Mach number is zero. Linear theory applied to low Reynolds number wake flows shows that absolute instability is suppressed by heating the wake. These results suggest that self-excited oscillations develop in the hot jet, while the self-excited Karman vortex shedding in the wake can be suppressed by heating. Experiments using flow visualizations, mean flow measurements and spectral analyses in the near-field of an initially laminar jet illustrated that the broad band amplitude spectra which characterize cold jets indeed become line-dominated for hot jets. The jet becomes globally unstable via a Hopf bifurcation when the density ratio decreases below approximately 0.9. Furthermore, bicoherence measurements show that the dominant frequency and its harmonic become then phase-locked. Flow visualizations reveal that in the self-excited hot jet organized structures develop and contribute to the jet spreading. However, the spreading of the two-dimensional hot jet is not as spectacular as in the axisymmetric case. Author

N91-16299 Minnesota Univ., Minneapolis.
INCOMPRESSIBLE FLOW SIMULATIONS USING THE VELOCITY-PRESSURE FORMULATION Ph.D. Thesis
Deepak Kumar Ganjoo 1990 145 p
Avail: Univ. Microfilms Order No. DA9029684

Various formulations used in the simulation of the incompressible Navier-Stokes equation are introduced. A comparative study indicates that the velocity-pressure formulation is the most general. The numerical difficulties associated with this formulation are addressed, especially those related to: (1) different orders of interpolation for velocity and pressures; (2) time integration schemes and solution strategies for the discretized equations; and (3) the dissipative nature of the time integration schemes. Two new multi-step time integration schemes are introduced and compared with the one-step scheme. Various velocity-pressure elements are studied in order to identify robust elements in two-dimension. Implicit and explicit strategies are developed for various elements in conjunction with different temporal integration schemes. The numerical examples chosen are the standing vortex, lid-driven cavity, and flow past a circular cylinder. Numerical tests indicate that one of the multi-step algorithms is less dissipative and that two elements show potential for extension to three-dimensions. One of the multi-step algorithms is extended to three-dimensions and compared with the one-step algorithm. The lid-driven cavity problem is tested and satisfactory results are obtained. Dissert. Abstr.

N91-16300 Colorado Univ., Boulder.
STUDY OF TIME ACCURACY OF FLOW VARIABLES ACROSS DISCONTINUOUS BOUNDARIES Ph.D. Thesis
Jyh-Horng Kuan 1990 133 p
Avail: Univ. Microfilms Order No. DA9032848

The Chimera grid scheme, a multiple overset mesh technique, was coupled with an implicit Euler flow solver (ARC3D) and was

successfully applied to a number of steady and unsteady aerodynamics problems. Errors were identified when an overset mesh is moved with respect to a stationary global mesh. Several methods were developed to try to reduce the errors across the moving boundary: (1) solving the Euler equations with a relaxation scheme; (2) solving the Euler equations with a predictor-corrector scheme; (3) improving the interpolation sequence to reflect the motion of the moving grid; and (4) reducing the errors using grid-based studies. The time lag error is found to be quite small; the resulting error is found to be largely due to spatial interpolation. Accuracy across an interface is improved for a given time step using a relaxation scheme, and this scheme was successfully applied to a more realistic three-dimensional problem designed to take full advantage of the scheme. A predictor-corrector method developed for the one-dimensional and three-dimensional Euler equations proved promising but has a stability limitation. A change in the interpolation procedure to include the time metrics gives a small improvement for the accuracy in the test cases. Removing the one-sided differencing for the metric terms on the updated outer boundary, and selecting a suitable grid size also give minor improvements for accuracy. Dissert. Abstr.

N91-16301 Pennsylvania State Univ., University Park.
ACCELERATION OF ITERATIVE ALGORITHMS FOR EULER AND NAVIER-STOKES EQUATIONS Ph.D. Thesis
Seungsoo Lee 1990 207 p
Avail: Univ. Microfilms Order No. DA9032326

A method for enhancing convergence rates of iterative schemes for the numerical integration of systems of partial differential equations was developed. It is termed the distributed minimal residual (DMR) method, and is based on general Krylov subspace methods. The DMR method differs from the Krylov subspace methods by the fact that the iterative acceleration factors are different from equation to equation in the system. Using different acceleration factors effectively, provides preconditioning effects to the system. At the same time, the DMR method can be viewed as an incomplete Newton iteration method. The DMR method was applied to a number of systems of highly non-linear partial differential equations: Euler equations of gasdynamics, incompressible Navier-Stokes equations, and Boussinesq equations. The DMR method was tested extensively with respect to the common difficulties encountered by the stiffness of the system associated with low Mach number flows and the stiffness associated with source terms. All numerical test cases were obtained using explicit four stage Runge-Kutta or Euler implicit time integration. The DMR method was found capable of reducing the computation time by 10 to 80 percent depending on the test case and grid used. When directly compared with an implicit residual smoothing, the DMR method performed consistently better and more reliably. The formulation for the DMR method is general in nature and can be applied to explicit and implicit iterative algorithms for arbitrary systems of partial differential equations.
Dissert. Abstr.

N91-16302 Minnesota Univ., Minneapolis.
FINITE ELEMENT SOLUTION TECHNIQUES FOR THE VORTICITY-STREAM FUNCTION FORMULATION OF TWO-DIMENSIONAL INCOMPRESSIBLE FLOWS Ph.D. Thesis
Jianntyng James Liou 1990 134 p
Avail: Univ. Microfilms Order No. DA9033201

Finite element solution techniques for the vorticity-stream function formulation of two-dimensional incompressible flows are presented. While both the viscous and inviscid cases are considered, the derivation of the proper finite element formulations for multiply-connected domains is emphasized. Implementation of various types of boundary conditions are discussed, including those related to internal obstacle, downstream, periodic, and outer boundaries. In all formulations associated with the vorticity transport equation, the streamline-upwind/Petrov-Galerkin method is used. Both direct and iterative solution schemes are introduced. The adaptive implicit-explicit, grouped element-by-element, generalized minimum residual solution strategies and their combined versions are employed to maximize the computational efficiency. The solutions obtained in all test cases compare well with those from previously published investigations. The convergence and benchmark studies demonstrate that the solution techniques presented are accurate and efficient. Dissert. Abstr.

N91-16303 California Inst. of Tech., Pasadena.
SIMULATION OF THE FLOW PAST AN IMPULSIVELY STARTED CYLINDER USING A DISCRETE VORTEX METHOD Ph.D. Thesis
Francois Michel Pepin 1990 150 p
Avail: Univ. Microfilms Order No. DA9031480

Vortex methods are a powerful tool for the simulation of incompressible flows at high Reynolds number and can be modified to simulate bluff body flows at moderate Reynolds numbers. The so-called deterministic treatment of viscous diffusion is extended to problems where a flux of vorticity is used to enforce the no-slip boundary condition. In addition, multi-range approximations are used to reduce the time complexity of the convective step from O(N exp 2) to O(N log N). The implementation of this particular fast algorithm on concurrent processors allows simulations with as many as 80,000 discrete vortex particles. The resulting combination of a fully viscous vortex method with a fast parallel algorithm is used to compute the flow past an impulsively started cylinder. The numerical scheme is able to capture the asymptotic behavior of the drag that immediately follows the impulsive start. In addition, the simulations successfully reproduce the behavior of the secondary eddies over a wide range of Reynolds numbers (Re = 550 to 9500). Tertiary separation is even observed at Re = 3000 and Re = 9500. It is also shown that by redirecting the flux of vorticity, the secondary phenomena can significantly affect the drag experienced by the cylinder. Dissert. Abstr.

N91-16304*# National Aeronautics and Space Administration. Lewis Research Center, Cleveland, OH.
EXTENSION OF TRANSONIC FLOW COMPUTATIONAL CONCEPTS IN THE ANALYSIS OF CAVITATED BEARINGS
D. Vijayaraghavan, T. G. Keith, Jr., and D. E. Brewe (Army Aviation Systems Command, Cleveland, OH.) Oct. 1990 14 p Presented at the Joint Tribology Conference, Toronto, Ontario, 7-10 Oct. 1990; cosponsored by the STLE and ASME
(DA Proj. 1L1-61102-AH-45)
(NASA-TM-103214; E-5625; NAS 1.15:103214;
AVSCOM-TR-91-C-002) Avail: NTIS HC/MF A03 CSCL 20D

An analogy between the mathematical modeling of transonic potential flow and the flow in a cavitating bearing is described. Based on the similarities, characteristics of the cavitated region and jump conditions across the film reformation and rupture fronts are developed using the method of weak solutions. The mathematical analogy is extended by utilizing a few computational concepts of transonic flow to numerically model the cavitating bearing. Methods of shock fitting and shock capturing are discussed. Various procedures used in transonic flow computations are adapted to bearing cavitation applications, for example, type differencing, grid transformation, an approximate factorization technique, and Newton's iteration method. These concepts have proved to be successful and have vastly improved the efficiency of numerical modeling of cavitated bearings. Author

N91-16305*# Institute for Computer Applications in Science and Engineering, Hampton, VA.
ASYMPTOTIC-INDUCED NUMERICAL METHODS FOR CONSERVATION LAWS Final Report
Marc Garbey (Lyon-1 Univ., France) and Jeffrey S. Scroggs Dec. 1990 25 p
(Contracts NAS1-18605; W-31-109-eng-38)
(NASA-CR-187483; ICASE-90-87; NAS 1.26:187483) Avail: NTIS HC/MF A03 CSCL 20D

Asymptotic-induced methods are presented for the numerical solution of hyperbolic conservation laws with or without viscosity. The methods consist of multiple stages. The first stage is to obtain a first approximation by using a first-order method, such as the Godunov scheme. Subsequent stages of the method involve solving internal-layer problems identified by using techniques derived via

asymptotics. Finally, a residual correction increases the accuracy of the scheme. The method is derived and justified with singular perturbation techniques. Author

N91-16306*# Institute for Computer Applications in Science and Engineering, Hampton, VA.
MODELING THE DISSIPATION RATE IN ROTATING TURBULENT FLOWS Final Report
Charles G. Speziale, Rishi Raj, and Thomas B. Gatski (National Aeronautics and Space Administration. Langley Research Center, Hampton, VA.) Dec. 1990 29 p Submitted for publication
(Contract NAS1-18605)
(NASA-CR-187485; ICASE-90-88; NAS 1.26:187485) Avail: NTIS HC/MF A03 CSCL 20D

A variety of modifications to the modeled dissipation rate transport equation that have been proposed during the past two decades to account for rotational strains are examined. The models are subjected to two crucial test cases: the decay of isotropic turbulence in a rotating frame and homogeneous shear flow in a rotating frame. It is demonstrated that these modifications do not yield substantially improved predictions for these two test cases and in many instances give rise to unphysical behavior. An alternative proposal, based on the use of the tensor dissipation rate, is made for the development of improved models. Author

N91-16307# Technische Univ., Eindhoven (Netherlands).
INTERNAL SOLITARY WAVES IN COMPRESSIBLE FLUIDS Ph.D. Thesis
Robertus Henricus Ma Miesen 1990 136 p Sponsored by Netherlands Organization for Applied Scientific Research TNO, Delft
(ETN-91-98475) Avail: NTIS HC/MF A07

Several basic properties of acoustic gravity waves are discussed, using the linearized equations of motion for an inviscid nonrotating compressible fluid that is stratified under gravity. A critical analysis of the frequently used hydrostatic approximation and of the Boussinesq approximation is given. Both approximations are applied to finite amplitude waves in stratified fluids. The influence of the compressibility on the properties of internal solitary waves in compressible stratified fluids is studied. Internal solitary waves are described by the Koterweg de Vries equation if the fluid is shallow, e.g., if the total depth of the fluid is much smaller than the characteristic horizontal length scale of the wave. They are described by the Benjamin-Davis-Ono equation if the fluid is deep, e.g., the total depth of the fluid is much larger than the characteristic horizontal length scale of the wave. ESA

N91-16308# Technische Univ., Eindhoven (Netherlands).
SHEAR THICKENING OF CONCENTRATED DISPERSIONS Ph.D. Thesis
Willem Hein Boersma 1990 192 p
(ETN-91-98477) Avail: NTIS HC/MF A09

Rheological experiments were performed on a number of different concentrated dispersions in a concentric cylinder system. Steady shear and oscillatory shear experiments were carried out. The volume fractions of the dispersions varied between 0.45 and 0.6. A theory was developed to predict the shear rate at which shear thickening starts to occur in a concentrated dispersion of electrostatically stabilized particles. Computer simulations were performed. It was shown that the agreement between theory and experiments is good. The attention was drawn to the rheological phenomena occurring in the different regimes. The measurements of the viscoelastic properties in the dispersions were given. It was shown that the dispersions mostly show only viscous behavior. ESA

N91-16309# Technische Univ., Eindhoven (Netherlands).
FINE PARTICLE FLOTATION IN A CENTRIFUGAL FORCE FIELD Ph.D. Thesis
Henricus Martinus Ge Tils 1990 152 p
(ETN-91-98480) Avail: NTIS HC/MF A08

The effect of a centrifugal force field on hydrodynamic characteristics, flotation kinetics and separation behavior was examined. Flotation devices were designed that combine a centrifugal force field and flotation action in one apparatus. The relation between rotational velocity and centrifugal force field, the loss of rotation due to wall friction and the effect of the centrifugal force field on bubble characteristics were studied. The formation and stability of froth in a centrifugal force field were examined. The fact that the bubbles are smaller in a centrifugal force field causes a reduction of solid solid interaction. This effect was found to also result in an improved flotation efficiency. ESA

N91-16310# Stuttgart Univ. (Germany, F.R.). Inst. fuer Thermische Stroemungsmaschinen und Maschinenlab.
A PROCESS FOR UNSTATIONARY VELOCITY AND TURBULENCE MEASUREMENTS WITH A PNEUMATIC MEASURING WEDGE PROBE [EIN VERFAHREN ZUR INSTATIONAEREN GESCHWINDIGKEITS- UND TURBULENZMESSUNG MIT EINER PNEUMATISCH MESSENDEN KEILSONDE]
Gerhard Ruck Dec. 1989 147 p In GERMAN
(MITT-33; ETN-91-98553) Avail: NTIS HC/MF A07

A process for the evaluation of the unstationary three dimensional profile of the flow vector with a probe equipped with four pressure captors and a thermoelement is presented. A system that estimates the transmission behavior of the pressure captors is proposed. This is accomplished with an acoustic device which produces an unstationary pressure field and measures the reference magnitudes. The probe allowed the Reynolds stress tensor to be obtained. The probe proved to be easily implemented and reproducible. ESA

N91-16311# Technische Hochschule, Aachen (Germany, F.R.). Fakultaet fuer Maschinenwesen.
UNSTATIONARY SHOCK AND BOUNDARY LAYER PHENOMENA AT PROFILES AND IN A PLANE GRID BY TRANSONIC FLOW Ph.D. Thesis [INSTATIONAERE STOSS- UND GRENZSCHICHTPHAENOMENE AN EINZELPROFILEN UND IN EINEM EBENEN GITTER BEI TRANSSONISCHER STROEMUNG]
Joerg Michael Henne 1989 186 p In GERMAN
(ETN-91-98557) Avail: NTIS HC/MF A09

A double circle arc profile is analyzed by high velocity Schlieren films in the case of autoexcited periodic flow oscillations for Mach numbers varying from 0.82 to 0.87. The boundary layer was laminar before the shock. If the Reynolds number increases until the boundary layer is turbulent, the flow is stabilized. Pressure oscillations were produced in a wind tunnel by a rotating body in the flow. The amplitude of the forced shock oscillations increases exponentially with increasing frequency, which agrees with theoretical and experimental results. The shock boundary layer configurations correspond to those of a quasistationnary variation of the state magnitudes. ESA

N91-16312# Universitaet der Bundeswehr Muenchen, Neubiberg (Germany, F.R.). Fakultaet fuer Luft- und Raumfahrttechnik.
THEORETICAL AND EXPERIMENTAL EXAMINATIONS OF TRANSITION BEHAVIOR OF THE PROFILE BOUNDARY LAYER AT COMPRESSOR AND TURBINE GRIDS Ph.D. Thesis [THEORETISCHE UND EXPERIMENTELLE UNTERSUCHUNGEN ZUM UMSCHLAGVERHALTEN DER PROFILGRENZSCHICHT AN VERDICHTER- UND TURBINENGITTERN]
Nicolaus Roemer 1990 193 p In GERMAN
(ETN-91-98559) Avail: NTIS HC/MF A09

Empirically correlated criteria for the laminar turbulent transition were developed and improved. The thin film measuring technique was implemented at a high velocity grid wind channel and compared with usual methods. The results, combined with pressure distribution data allowed the examination of the influence of the Reynolds number and the turbulence degree on the transition way and the transition area profile. Calculations were achieved with an integral boundary layer computation process and correlated with the empirical data from the measurements. Only the

Aby-Ghannam criterium gives the laminar-turbulent transition point with the desired precision. ESA

N91-16313# Technische Univ., Delft (Netherlands).
NATURAL-CONVECTION BOUNDARY LAYERS Ph.D. Thesis
Rudolphus Aloysius W Henkes 1990 212 p
(ISBN-90-9003467-6; ETN-91-98489) Copyright Avail: NTIS HC/MF A10

The natural convection flow for two geometries positioned in the gravitational field is considered: a square cavity differentially heated over the vertical walls and a semi infinite hot vertical plate in an isothermal environment. The flow of both air and water is calculated by numerically solving the 2-D, incompressible Navier-Stokes equations, including the energy equation. The Boussinesq approximation is applied. The spatial derivatives in the equation are discretized with the finite volume method whereas the time derivatives are discretized with an implicit scheme using three time levels. The accuracy of the numerical results is checked by grid and time step refinement. ESA

N91-16314# Bonn Univ. (Germany, F.R.). Sonderforschungsbereich 256.
THE STATIONARY EXTERIOR THREE DIMENSIONAL NAVIER-STOKES PROBLEM OF VISCOUS FLOW PAST A BODY IN ANISOTROPICALLY WEIGHTED SOBOLEV SPACES
Reinhard Farwig May 1990 105 p In GERMAN; ENGLISH summary Sponsored by DFG
(REPT-110; ETN-91-98560) Avail: NTIS HC/MF A06

The stationary Navier-Stokes equations of a viscous incompressible fluid are considered. The velocity is assumed to be approximated by a constant non-vanishing vector. The equations were linearized to obtain Oseen equations which were studied in weighted Sobolev spaces. The weights were anisotropic and linked to the decay properties of the fundamental solution. The method of the boundary integral equation and a variational approach to a related elliptic equation in exterior domains were used. A solution of the Navier-Stokes equations for sufficiently small data by Banach fixed point theorem was achieved. ESA

N91-16315# Warwick Univ., Coventry (England). Dept. of Engineering.
A SEGREGATED FINITE ELEMENT SOLUTION TO THE INCOMPRESSIBLE NAVIER-STOKES EQUATIONS
C. T. Shaw 22 Nov. 1990 30 p
(ME-69; ETN-91-98575) Avail: NTIS HC/MF A03

The development of a segregated solution scheme for the incompressible steady state Navier Stokes equations is presented. A pressure correction equation is derived from the momentum and continuity equations, and equal order interpolation for both the velocities and pressure is utilized. Several benchmark problems are solved to illustrate the application of the method. They are described together with details of how the solutions are obtained. ESA

35 INSTRUMENTATION AND PHOTOGRAPHY

Includes remote sensors; measuring instruments and gages; detectors; cameras and photographic supplies; and holography.

For aerial photography see *43 Earth Resources and Remote Sensing*. For related information see also *06 Aircraft Instrumentation*, and *19 Spacecraft Instrumentation*.

N91-16316# Fermi National Accelerator Lab., Batavia, IL.
SELF-PROPELLED IN-TUBE SHUTTLE AND CONTROL SYSTEM FOR AUTOMATED MEASUREMENTS OF MAGNETIC FIELD ALIGNMENT
W. N. Boroski, T. H. Nicol, S. V. Pidcoe, and R. A. Zink (Superconducting Super Collider Lab., Dallas, TX.) Mar. 1990 7 p Presented at the 2nd International Industrial Symposium on the Super Collider, Miami, FL, 14-16 Mar. 1990
(Contract DE-AC02-76CH-03000)
(DE90-008210; FNAL-TM-1654; CONF-900348-2) Avail: NTIS HC/MF A02

A magnetic field alignment gauge is used to measure the field angle as a function of axial position in each of the magnets for the Superconducting Super Collider (SSC). Present measurements are made by manually pushing the gauge through the magnet bore tube and stopping at intervals to record field measurements. Gauge location is controlled through graduation marks and alignment pins on the push rods. Field measurements are recorded on a logging multimeter with tape output. Described is a computerized control system being developed to replace the manual procedure for field alignment measurements. The automated system employs a pneumatic walking device to move the measurement gauge through the bore tube. Movement of the device, called the Self-Propelled In-Tube Shuttle (SPITS), is accomplished through an integral, gas driven, double-acting cylinder. The motion of the SPITS is transferred to the bore tube by means of a pair of controlled, retractable support feet. Control of the SPITS is accomplished through an RS-422 interface from an IBM-compatible computer to a series of solenoid-actuated air valves. Direction of SPITS travel is determined by the air-valve sequence, and is managed through the control software. Precise axial position of the gauge within the magnet is returned to the control system through an optically-encoded digital position transducer attached to the shuttle. Discussed is the performance of the transport device and control system during preliminary testing of the first prototype shuttle. DOE

N91-16317# Sandia National Labs., Albuquerque, NM. Target Experiments Div.
X-RAY DETECTOR: AN X-RAY RADIATION DETECTOR DESIGN CODE
Rick B. Spielman Apr. 1990 38 p
(Contract DE-AC04-76DP-00789)
(DE90-008235; SAND-85-0699) Avail: NTIS HC/MF A03

X-Ray Detector (XRD) is an x-ray detector design code. It is intended to aid in the rapid design of x-ray detector packages. The design capabilities of XRD include filters, x-ray mirrors, x-ray diodes, silicon PIN diodes, GaAs PIN diodes, photoconducting detectors, bolometers, and x-ray film. XRD uses x-ray cross-section information stored in easily-modified external libraries. Interactive calculations are completed in seconds using a DEC VAX 8650. Some of the more notable features of XRD are edge handling in the x-ray photoelectric cross-section data, I/O error handling, internal error messages, nearly bomb-proof design, and extensive documentation. DOE

N91-16318# Ceramphysics, Inc., Westerville, OH.
A MINIATURE INEXPENSIVE, OXYGEN SENSING ELEMENT Quarterly Report, 31 Jan. - 30 Apr. 1990
R. W. Arenz 30 Apr. 1990 5 p
(Contract DE-FG01-88CE-15401)
(DE90-009938; DOE/CE-15401/T7) Avail: NTIS HC/MF A01

This paper is a progress report by Ceramphysics, Inc. on their efforts to design and fabricate an instrument to measure oxygen. This report discusses the project's two tasks. The first task consisted of choosing the sensor ceramics, developing the sealing techniques, and designing the heating element. The second task's objective was the preliminary fabrication of the measuring instrument. DOE

N91-16319# Idaho National Engineering Lab., Idaho Falls.
A CONVENIENT SYSTEM FOR THE MANUFACTURE OF HOLOGRAPHIC DIFFRACTION GRATINGS
V. A. Deason and M. B. Ward 1989 5 p Presented at the 3rd International Conference on Laser Interferometry, San Diego, CA, 6-11 Aug. 1989
(Contract DE-AC07-76ID-01570)
(DE90-009481; EGG-M-89048; CONF-8908222-2) Avail: NTIS HC/MF A01

A device that provides a very convenient facility for the manufacture of holographic diffraction gratings is described. The

system employs single mode polarization maintaining optical fibers and a simple opto-mechanical design to permit great flexibility in grating manufacture. The intended application of these gratings is diffraction moire interferometry. A variety of gratings ranging from less than 100 to more than 2000 1/mm can be made with minimal time required for changing between grating frequencies. Furthermore, the rational design of the device permits one to easily generate more complex gratings, including crossed gratings, gratings having two or more superimposed groove spatial frequencies, or gratings having other unusual features such as induced aberrations. DOE

N91-16320# Oak Ridge National Lab., TN.
CONCEPTS FOR FUTURE DEVELOPMENTS IN ELECTRON MICROSCOPY Foreign Trip Report
L. F. Allard and T. A. Nolan 30 Apr. 1990 8 p
(Contract DE-AC05-84OR-21400)
(DE90-010630; ORNL/FTR-3589) Avail: NTIS HC/MF A02

At the request of Hitachi, Ltd. and JEOL, Ltd., the travelers visited the JEOL factory and the Hitachi Central Research Laboratory in Tokyo, and the Hitachi Naka Works Factory in Katsuta. At these three facilities the travelers presented seminars explaining both ORNL's significance in materials research and electron microscopy and concepts relating to transmission electron microscopy resolution improvements, instruments, and concepts that the manufacturers are developing. Additionally, they had the opportunity to assess the performance of the recently introduced Hitachi 200-kV Field Emission Gun TEM. The visit provided the travelers a unique opportunity to influence the directions for future instrumental developments by two major electron microscope manufacturers. DOE

N91-16321# EG and G Energy Measurements, Inc., Goleta, CA.
GABOR ZONE PLATE APERTURES FOR IMAGING WITH THE MERCURIC IODIDE GAMMA RAY CAMERA
B. E. Patt, A. Meyyappan, A. Cai, and G. Wade (California Univ., Santa Barbara.) 1990 11 p Presented at the 7th Symposium on Radiation Measurements and Applications, Ann Arbor, MA, 21-24 May 1990
(Contract DE-AC08-88NV-10617)
(DE90-011193; EGG-10617-2066; CONF-900563-6) Avail: NTIS HC/MF A03

Gabor zone plate (GZP) apertures were developed for use in EG and G EM's mercuric iodide (HgI2) gamma ray camera. The purpose of such an aperture is to increase efficiency, while maintaining good resolution. The GZP is similar to the Fresnel zone plate (FZP) but it has continuous transitions between opaque and transparent regions. Because there are no sharp transitions in the transmission the inherent interference noise in GZP imaging is lower than that in FZP imaging. GZP parameters were chosen by considering the effects of constraints such as detector pixel size, number of pixels, minimum field of view required, maximum angle of incidence tolerated, and the Nyquist criterion for the minimum sampling rate. As a result an aperture was designed and fabricated with eight zones and a diameter of 3 cm. Lead was chosen as the aperture medium due to its high attenuation coefficient. Experimental data were obtained from the camera with the above GZP aperture. The point spread function was determined and compared to the calculated response. Excellent agreement was obtained. The reconstruction process involves simulating, by computer, planar wave illumination of a scaled transparency of the image and recording the intensity pattern at the focal plane. DOE

N91-16322# California Univ., Berkeley. Lawrence Berkeley Lab.
A TUNABLE X RAY MICROPROBE USING SYNCHROTRON RADIATION
Y. Wu, A. C. Thompson, J. H. Underwood, R. D. Giauque, K. Chapman, M. L. Rivers, and K. W. Jones (Brookhaven National Lab., Upton, NY.) Aug. 1989 16 p Presented at the 1989 Synchrotron Radiation Instrumentation National Conference, Berkeley, CA, 6-10 Aug. 1989
(Contract DE-AC03-76SF-00098)
(DE90-011219; LBL-28904; CONF-890802-28) Avail: NTIS HC/MF A03

We describe an x ray microprobe using multilayer mirrors. Previously, we had demonstrated a Kirkpatrick-Baez type focusing system working at both 8 and 10 keV and successfully applied it to a variety of applications, including the determination of elemental contents in fluid inclusions. In this paper, we show that the usable excitation energy for this microprobe is not restricted to between 8 and 10 keV, and furthermore, it can be simply tuned in operation. A 10-keV x ray fluorescence microprobe can be used to measure the concentration of the elements from potassium ($Z = 19$) to zinc ($Z = 30$) using K x ray lines, and from cadmium ($Z = 48$) to erbium ($Z = 68$) using L x-ray lines. There are a number of geologically important elements in the gap between gallium ($Z = 31$) and silver ($Z = 47$) and also with Z greater than 68. In order to cover this range, a higher excitation energy is required. On the other hand, for samples that contain major elements with absorption edges lower than the excitation energy, it would be hard to detect other mirror elements because of the strong signal from the major elements and the background they produce. In this case, a tunable x ray source can be used to avoid the excitation of the major elements. We demonstrate that, with the existing setup, it is possible to tune the excitation energy from 6 keV to 14 keV, in this range, the intensity does not decrease by more than one order of magnitude. As an illustration, a geological sample was examined by using two different excitation energies to show the advantage of a tunable source. Finally, we discuss the possibility of further extension of the excitation energy range as well as the possibility of improving the intensity. DOE

N91-16323# Los Alamos National Lab., NM.
COMPARISON OF SOME X RAY SENSORS FOR VERIFICATION
C. E. Moss, G. J. Berzins, H. E. Felthauser, M. R. Sweet, and J. E. Valencia 1990 5 p Presented at the AFTAC Sensors Conference, Patrick AFB, FL, 2-3 May 1990
(Contract W-7405-eng-36)
(DE90-011990; LA-UR-90-1921; CONF-9005212-1) Avail: NTIS HC/MF A01

More efficient alternatives to silicon sensors in an instrument to measure x rays over several channels, or energy windows, offer some advantages. First if the source is cool, the responses in the high energy channels measured with silicon sensors will be low. If these responses do not exceed the electronic thresholds of their uncertainties are large, then they can not be used to determine the spectral shape. Using more efficient sensors will mitigate this problem. Second, if the efficiency of the high energy channels is high enough so that their thresholds are exceeded, then coincidence between low energy channels and high energy channels can be used to greatly reduce false event rates. Two potential disadvantages are higher sensitivity to radiation damage and slower rise time. The results are described for the high-Z semiconductor CdTe, the high-Z scintillator CsI(Tl) mounted on a silicon photodiode, and scintillation fiber. DOE

N91-16324# Lawrence Livermore National Lab., CA.
STABILITY AND ACCURACY OF THE SWEEP RATE MEASUREMENTS FOR LLNL OPTICAL STREAK CAMERAS
D. S. Montgomery Aug. 1989 10 p Presented at the International Conference on Optical and Opto-Electronics and Applied Science, San Diego, CA, 14-18 Aug. 1989
(Contract W-7405-eng-48)
(DE90-012080; UCRL-101660; CONF-8908185-2) Avail: NTIS HC/MF A02

Precise pulse shaping is vital for present and future high-power lasers that will attempt to achieve low-entropy laser-fusion implosions. Multichannel, streak-camera-based systems are used to make such measurements. Such systems must be accurately calibrated in order to correct for time-base and flat-field variations. We use an on-line calibration system in order to measure the sweep rate, and in our recent work we have evaluated the accuracy of this measurement technique. By analyzing a large number of

calibrations, and the effect of noise on our measurement technique, we have concluded that the sweep rate for our streak camera systems is reproducible to a least +/-1.2 percent and that our measurement technique contributes an additional +/-0.5 percent uncertainty in the measurement. DOE

N91-16325# Sandia National Labs., Albuquerque, NM.
ION CONTAMINATION OF X RAY PINHOLE CAMERA IMAGES ON PBFA 2
A. R. Moats and T. A. Mehlhorn 1990 14 p Presented at the 8th Topical Conference on High-Temperature Plasma Diagnostics, Hyannis, MA, 6-10 May 1990
(Contract DE-AC04-76DP-00789)
(DE90-012180; SAND-90-0300C; CONF-900557-9) Avail: NTIS HC/MF A03

Inner-shell x ray pinhole cameras are an important diagnostic for time-averaged beam profile measurements on PBFA-2 experiments which require no shielding from the diode magnetic field. However, the same ions that create the inner-shell x rays can also Rutherford scatter and directly expose the x ray film. A double image, due to this effect, has been observed in PBFA-2 data. In this paper, we derive the expected film density die to these scattered ions relative to the film density from the ion-induced x ray line radiation from Titanium, Aluminum, and Gold targets. We then show that our calculated degree of ion contamination for a Gold target M(sub (alpha)) camera recently fielded on PBFA-2 is consistent with the actual images observed --- a phantom image tentatively identified as proton contamination with a film density of the same order of magnitude as the x ray image. The amount of ion contamination is strongly dependent on the optical filtering used. For less heavily-filtered cameras, we will show that this contamination will be less of a concern. We propose a different camera geometry for which this ion contamination will be a 5 percent effect in the Titanium and Aluminum K(sub alpha) cameras, but may be a 16 percent effect in the Gold M(sub alpha) cameras. DOE

N91-16326# Allied-Signal Corp., Kansas City, MO.
CHARACTERIZATION OF ULTRASONIC TRANSDUCERS USING PATTERN RECOGNITION TECHNIQUES
J. W. Ekis, M. S. Obaidar, and S. A. Bleha (Missouri Univ., Columbia.) Sep. 1990 5 p Presented at the Fall Conference of the American Society for Nondestructive Testing, Seattle, WA, 9-12 Oct. 1990
(Contract DE-AC04-76DP-00613)
(DE91-000580; KCP-613-4426; CONF-901053-1) Avail: NTIS HC/MF A01

This paper describes an automated method for characterizing ultrasonic transducers. A computer based test system will collect test data for a given transducer. This data set is then subjected to a pattern recognition algorithm. The results from this classification will place the transducer in a group of similar units. All the transducers in a group will have similar performance characteristics. DOE

N91-16327# Allied-Signal Aerospace Co., Phoenix, AZ. Engine Div.
MAGNETIC DOMAIN STRAIN SENSOR PROGRAM Final Report, Sep. 1986 - Mar. 1990
Bernard OHalloran, Harvey Niska, Steve Mina, and Gordon Fish 1 Aug. 1990 136 p
(Contract F33615-86-C-2646; AF Proj. 3036)
(AD-A227225; REPT-21-7574; WRDC-TR-90-2050) Avail: NTIS HC/MF A07 CSCL 11/6

The Magnetic Domain Strain Sensor Program was to demonstrate the feasibility of using the magnetostrictive properties of magnetic alloys in the design of a new type of strain gage. The Magnetic Domain Strain Sensor offered advantages over the resistive strain gage in the areas of digital data acquisition, increased temperature capability, and potentially determining residual strain and fatigue. Theory development bore out a modified Sixtus-Tonks model, measuring domain inversion time instead of magnetic pulse propagation. The modified theory that developed led to improved gage measurement accuracy. Phase 1 testing of wire and ribbon magnetic alloy sensors supported the theory development. Phase 2 developed the thin film technology for both the amorphous metallic glass sensor and the coils for eventual full gage fabrication in the program's Phase 3 portion. Many obstacles had to be overcome, especially in developing the thin film sputtering technology. The feasibility of the magnetic domain strain gage was demonstrated, but significant development still remains to be performed before the sensor can be considered a production test device. GRA

N91-16328# United Technologies Research Center, East Hartford, CT.
ADVANCED STRUCTURAL INSTRUMENTATION, VOLUME 1 Final Report, Feb. 1983 - Nov. 1989
A. J. Dennis and Graham B. Fulton 11 Jun. 1990 24 p
(Contract F33615-83-C-2330; AF Proj. 3066)
(AD-A227226; R-89-2330-VOL-1; WRDC-TR-90-2020-VOL-1)
Avail: NTIS HC/MF A03 CSCL 21/5

The results are presented of the development and test of a variety of steady state strain and temperature sensors specifically aimed at application in hot sections of advanced gas turbines. In each case, the sensors have shown success in the laboratory, and tests and results described herein were designed to simulate the actual turbine environment. Most of the testing was carried out in the UTRC vacuum spin rig which was able to achieve speeds and temperatures characteristic of advanced gas turbines. Volume 1 is an overview of the sensors, physical description, summary comparison of results and conclusions and recommendations. The report is divided into the sections each of which gives the details of a specific sensor tested in this program. Temperature sensors tested in the present program include conventional wire thermocouples and an advanced type of thin film thermocouple deposited directly on the test piece. The temperature measuring capability of twin core optical fiber sensor technology was also demonstrated. Remote sensing of temperature was achieved with a thermographic phosphor technique, and optical pyrometry was used as a control throughout the program. Additionally, the feasibility of advanced concept heat flux sensors on a turbine blade was demonstrated. GRA

N91-16329# Naval Academy, Annapolis, MD. Dept. of Physics.
DEVELOPMENT OF AN EXTERNAL BEAM ION MILLIPROBE Final Report, 1989 - 1990
Stephan A. MacLaren 22 May 1990 54 p
(AD-A227247; USNA-TSPR-170) Avail: NTIS HC/MF A04 CSCL 20/7

The goals of this Trident Project were the design, construction, testing, and initial application of an external beam ion milliprobe. The ion milliprobe is a tool for elemental analysis that employs the 1.7 million volt tandem electrostatic accelerator in Michelson C-7 to provide a beam of charged particles. The mechanism used for the analysis of elemental concentration is particle induced x ray emission (PIXE). This technique involves detecting and counting the x rays produced when the focused beam of charged particles strikes the sample to be analyzed. The design and construction of several essential specialized devices is described including an electrostatic quadrupole triplet lens, a current measuring collimator, an exit tip, and a sample enclosure. The procedures necessary to align, focus, and determine the size of the beam are discussed. Finally, the results of the initial analysis are evaluated and presented. GRA

N91-16330# United Technologies Research Center, East Hartford, CT.
ADVANCED STRUCTURAL INSTRUMENTATION, VOLUME 2 Final Report, Feb. 1983 - Nov. 1989
A. J. Dennis and Graham B. Fulton 11 Jun. 1990 171 p
(Contract F33615-83-C-2330; AF Proj. 3066)
(AD-A227473; UTRC-R-89-2330-VOL-2;
WRDC-TR-90-2020-V2-VOL-2) Avail: NTIS HC/MF A08 CSCL 21/5

The results are presented of the development and tests of a

variety of steady state strain and temperature sensors specifically aimed at application in hot sections of advanced gas turbines. In each case, the sensors have shown success in the laboratory, and tests and results described herein were designed to simulate the actual turbine environment. Most of the testing was carried out in the UTRC vacuum spin rig which was able to achieve speeds and temperatures characteristic of advanced gas turbines. Volume 1 is an overview of the sensors, physical description, summary comparison of results and conclusions and recommendations. Volume 2 gives the details of the sensor fabrication and installation as well as evaluation of the data acquired. The details are given of a specific sensor tested in this program. Temperature sensors tested in the present program include conventional wire thermocouples and an advanced type of thin film thermocouple deposited directly on the test piece. The temperature measuring capability of twin core optical fiber sensor technology was also demonstrated. Remote sensing of temperature was achieved with a thermographic phosphor technique, and optical pyrometry was used as a control throughout the program. Additionally, the feasibility of advanced concept heat flux sensors on a turbine blade was demonstrated. GRA

N91-16331# Electronics Research Lab., Adelaide (Australia).
ANALYSIS OF EMISSION DATA FROM A PERKIN-ELMER 1710 FTIR SPECTROMETER
Adrian Tudini and Soi-Sang Ti Apr. 1990 23 p
(AD-A227759; ERL-0517-RR; DODA-AR-006-413) Avail: NTIS HC/MF A03 CSCL 14/2

The principles of analysis of radiant output of an emitter in the atmospheric windows using a Perkin-Elmer 1710 FTIR Spectrometer equipped with an emission accessory are presented. From the raw emission data, experimentally measured for standard blackbody sources, the radiant intensities were analyzed using the principles discussed. The analyzed results are in good agreement with those theoretically calculated. GRA

N91-16332*# General Electric Co., Philadelphia, PA. Astro Space Div.
DEFINITION AND PRELIMINARY DESIGN OF THE LASER ATMOSPHERIC WIND SOUNDER (LAWS) PHASE 1. VOLUME 1: EXECUTIVE SUMMARY Final Report
15 May 1990 33 p Original contains color illustrations
(Contract NAS8-37589)
(NASA-CR-184071; NAS 1.26:184071) Avail: NTIS HC/MF A03; 2 functional color pages CSCL 14B

The laser atmospheric wind sounder (LAWS) is a facility instrument of the Earth Observing System (EOS) and is the culmination of over 20 years of effort in the field of laser Doppler wind sensing. LAWS will by the first instrument to fly in space with the capability of providing global-scale tropospheric wind profiles at high spatial resolutions. Global-scale wind profiles are necessary for: (1) more accurate diagnostics of large-scale circulation and climate dynamics; (2) improved numerical weather prediction; (3) improved understanding of mesoscale systems; (4) improved understanding of global biogeochemical and hydrologic cycles. The objective of phase 1 of the LAWS study was to evaluate competing concepts and develop a baseline configuration for the LAWS instrument. The first phase of the study consisted of identifying realistic concepts for LAWS and analyzing them in sufficient detail to be able to choose the most promising one for the LAWS application. System configurations were then developed for the chosen concept. The concept and subsequent configuration were to be compatible with two prospective platforms: the Japanese polar orbiting platform (JPOP) and the Space Station Freedom (as an attached payload). After an objective and comprehensive concept selection process, a heterodyne detection Doppler lidar using a CO2 laser transmitter operating at 9.1 microns over a 2.1 micron system with a solid state laser was chosen. The CO2 lidar concept was then analyzed in detail to arrive at a configuration for the instrument and its major subsystems. A configuration for LAWS was arrived at which meets the performance requirements, and this design is presented. Author

N91-16333*# General Electric Co., Philadelphia, PA. Astro Space Div.
DEFiNITION AND PRELIMINARY DESIGN OF THE LASER ATMOSPHERIC WIND SOUNDER (LAWS) PHASE 1. VOLUME 2 Final Report
15 May 1990 206 p
(Contract NAS8-37589)
(NASA-CR-184072; NAS 1.26:184072) Avail: NTIS HC/MF A10 CSCL 14B

The steps and engineering trades and analyses used in establishing the initial requirements and in developing a concept and configuration for the laser atmospheric wind sounder (LAWS) instrument. A summary of the performance anticipated from the baseline configuration, and a bibliography are presented. LAWS, which is a facility instrument of the Earth observing system (EOS), is the culmination of over 20 years of effort in the field of laser Doppler wind sensing and will be the first instrument to fly in space capable of providing global-scale tropospheric wind profiles at high spatial resolutions. Global-scale wind profiles are necessary for: (1) more accurate diagnosis of large-scale circulation and climate dynamics; (2) improved numerical weather prediction; (3) improved understanding of mesoscale systems; and (4) improved understanding of global biogeochemical and hydrologic cycles. The objective of phase 1 was to define and perform a preliminary design for the LAWS instrument. The definition phase consisted of identifying realistic concepts for LAWS and analyzing them in sufficient detail to be able to choose the most promising one for the LAWS instrument. Systems and subsystems configurations were then developed for the chosen concept. The concept and subsequent configuration were to be compatible with two prospective platforms: the Japanese polar orbiting platform (JPOP) and as an attached payload on the Space Station Freedom. After a thorough and objective concept selection process, a heterodyne detection Doppler lidar using a CO2 laser transmitter operating a 9.1 micron over a 2.1 micron solid state system was chosen. A configuration for LAWS that meets the performance requirements was designed at the conclusion of phase 1. Author

N91-16334*# General Electric Co., Philadelphia, PA. Astro Space Div.
DEFINITION AND PRELIMINARY DESIGN OF THE LASER ATMOSPHERIC WIND SOUNDER (LAWS) PHASE 1. VOLUME 3: PROGRAM COST ESTIMATES Final Report
15 May 1990 50 p
(Contract NAS8-37589)
(NASA-CR-184073; NAS 1.26:184073) Avail: NTIS HC/MF A03 CSCL 14B

Cost estimates for phase C/D of the laser atmospheric wind sounder (LAWS) program are presented. This information provides a framework for cost, budget, and program planning estimates for LAWS. Volume 3 is divided into three sections. Section 1 details the approach taken to produce the cost figures, including the assumptions regarding the schedule for phase C/D and the methodology and rationale for costing the various work breakdown structure (WBS) elements. Section 2 shows a breakdown of the cost by WBS element, with the cost divided in non-recurring and recurring expenditures. Note that throughout this volume the cost is given in 1990 dollars, with bottom line totals also expressed in 1988 dollars (1 dollar(88) = 0.93 1 dollar(90)). Section 3 shows a breakdown of the cost by year. The WBS and WBS dictionary are included as an attachment to this report. Author

N91-16335 Colorado Univ., Boulder.
A RING LASER GYROSCOPE WITH OPTICAL SUBTRACTION Ph.D. Thesis
Nicholas Michael Sampas 1990 335 p
Avail: Univ. Microfilms Order No. DA9032872

A prototype passive ring laser gyroscope uses heterodyne detection of optically derived common mode and differential mode error signals. A 7 x 7 sq cm ring cavity demonstrates a rotation rate sensitivity of 1.3 degrees/hr for integration periods from 1 t0 30 sec. Long-term sensitivity is limited by AM contamination of the phase modulated input beams and phase drifts in the injection

loop interferometer. The alignment of the injected beams is stabilized to the reference cavity by heterodyne detection of misalignment-induced coupling to the off-axis modes. Phase sensitive detection of partially transmitted sidebands produces error signals that are nulled by a control system that steers the input beams. The alignment technique demonstrates sensitivities to tilts of 0.1 nrad/sq root of Hz and to lateral beam displacements of 0.08 nm/sq root of Hz in the 1 to 1000 Hz frequency range for a two degree-of-freedom system. Maximum alignment error suppression is 80 dB. A proposed Earth-based experiment capable of measuring the gravitomagnetic frame-dragging effect to 1 percent requires a large passive ring laser gyroscope (300 m optical path length) integrated with a long-baseline (100 m) stellar interferometer located at the South Pole. Author

N91-16336# Texas Univ., Arlington.
VISUALIZATION OF UNSTEADY TRANSONIC FLOW BY HOLOGRAPHIC INTERFEROMETRY USING PHOTOREFRACTIVE MEDIA Final Report, 1 Jul. 1986 - 30 Jun. 1990
Robert Magnusson and Donald R. Wilson 31 Aug. 1990 33 p
(Contract DAAL03-86-K-0149)
(AD-A228802; ARO-23915.6-EG) Avail: NTIS HC/MF A03
CSCL 14/1

The primary objective of the proposed research was to quantify the applicability of photorefractive media in holographic interferometry as applied to the visualization of unsteady transonic flow. Photorefractive crystals possess properties that make them well suited for holographic interferometry applications. These properties include instantaneous hologram formation (self-development), huge data storage capacity via volume superposition (three dimensional storage), high sensitivity and resolution, erasability and reusability, real-time recording and readout, hologram fixing (archival storage), and sensitivity to the recording light only. Photorefractive crystals will be important recording media in future holographic interferometry. For aerodynamics, heat transfer, acoustics, and other areas where a large number of interferograms must be rapidly recorded and processed, photorefractive materials have significant advantages over photographic film. This works focus was to carry out a program of research and development to define in detail the applicability of photorefractive crystals to interferometry for the visualization of dynamic flow fields and to establish the techniques necessary for efficient utilization of such media. Concepts developed included volume hologram superposition, real-time interferometry, hologram fixing, coherent image subtraction, and asymmetric recording/readout hologram characteristics (two photon recording). The application of these concepts to the visualization of unsteady transonic flow-fields was emphasized. GRA

N91-16337# Nationaal Inst. voor Kernfysica en Hoge Energiefysica, Amsterdam (Netherlands). Afd. DIGEL.
TIME INTERPOLATOR Thesis - Algemene Hogeschool [TIJD-INTERPOLATOR]
M. deBlok 8 Jun. 1990 45 p In DUTCH
(DIGEL-1990-3; ETN-91-98322) Avail: NTIS HC/MF A03

A time interpolator for the measurement of time difference using digital and analog techniques is described. Emitter Coupled Logic (ECL) and high frequency techniques were used. The difficulty with ECL is to keep the connections as short as possible and to properly terminate the output to avoid reflections. The digital part of the interpolator consists of a continuous clock and logic which converts the input signal into a start and stop signal. The analog part consists of a time to amplitude converter and an analog to digital convertor. The maximum measuring time is 6.4 microns with a 100 ps resolution. ESA

N91-16338# Technische Univ., Delft (Netherlands).
HIGH-PURITY SILICON SOFT X RAY SENSOR ARRAYS Ph.D. Thesis
Sarah Anne Steigerwa Audet 1990 199 p
(ETN-91-98484) Avail: NTIS HC/MF A09

The fundamental properties of 2-D position sensitive soft x ray sensors made of high purity silicon are investigated. The interactions that take place when electromagnetic radiation is incident upon silicon are discussed. High purity silicon soft x ray sensor arrays are theoretically characterized. Their fabrication is detailed. The measurement system used for the detection of soft x radiation is defined. Experimental results are presented. The low leakage currents, good energy resolutions and minimal degrees of cross talk associated with the high purity silicon soft x ray sensor arrays establish their useful application in the imaging of soft x rays. ESA

N91-16339# Warwick Univ., Coventry (England). Centre for Microengineering and Metrology.
DYNAMIC ASPECTS OF SCANNING SURFACE INSTRUMENTS AND MICROSCOPES
D. J. Whitehouse 22 Nov. 1990 25 p Sponsored by United Kingdom Science and Engineering Research Council
(ME-84; ETN-91-98577) Avail: NTIS HC/MF A03

Particular emphasis is placed on the role of damping in the mechanical system. Two concepts are introduced, integrated damping and differential spatial damping. The use of scanning velocity to couple the instrument and surface coordinate systems is demonstrated. ESA

36 LASERS AND MASERS

Includes parametric amplifiers.
For related information see also *76 Solid-State Physics.*

N91-16340# Lawrence Livermore National Lab., CA.
SHORT PULSE DRIVEN RECOMBINATION X RAY LASERS
C. J. Keane, J. N. Bardsley, L. daSilva, N. Landen, and D. Matthews 16 Mar. 1990 7 p Presented at the SPIE Optics, Electro-Optics and Laser Applications in Science and Engineering Conference and Exhibition, Los Angeles, CA, 15-19 Jan. 1990
(Contract W-7405-eng-48)
(DE90-009945; UCRL-JC-103338; CONF-900140-21) Avail: NTIS HC/MF A02

The advent of compact high peak power short pulse lasers has made tabletop recombination x ray lasers pumped by these systems a real responsibility. In this paper we discuss some of the relevant issues for these lasers and highlight a number of issues that require consideration. Results of simulations designed to estimate potential gains in the quasi-steady-state region are also described. DOE

N91-16341# Washington Univ., Seattle. Dept. of Applied Mathematics.
NONLINEAR RESONANCE Progress Report, 1 Aug. 1989 - 31 Mar. 1990
J. Kevorkian, Mark Pernarowski, and David L. Bosley 12 Apr. 1990 4 p
(Contract DE-FG06-86ER-25019)
(DE90-010428; DOE/ER-25019/17) Avail: NTIS HC/MF A01

The subjects discussed are: transient and sustained resonance for systems with very slowly varying parameters; free electron lasers with very slow wiggler taper; and bursting oscillations in biological systems. Plans are discussed for: FEL applications; transient and sustained resonance; and bursting oscillations. DOE

N91-16342# Los Alamos National Lab., NM. Chemical and Laser Science Div.
DEVELOPMENT OF FREE-ELECTRON LASERS FOR XUV PROJECTION LITHOGRAPHY
Brian E. Newnam 1990 19 p Presented at the SPIE Optics, Electro-Optics and Laser Applications in Science and Engineering Conference and Exhibition, Los Angeles, CA, 15-19 Jan. 1990 Submitted for publication
(Contract W-7405-eng-36)
(DE90-010566; LA-UR-90-1125; CONF-900140-23) Avail: NTIS HC/MF A03

Future RF-linac-driven FELs, operating in the range from 4 nm to 100 nm, could be excellent exposure tools for extending the resolution limit of projection optical lithography to less than or equal to 0.1 microns and with adequate total depth of focus (1 to 2 microns). When operated at a moderate duty rate of greater than or equal 1 percent, XUV FELs should be able to supply sufficient average power to support high-volume chip production. Recent developments of the electron beam, magnetic undulator, and resonator mirrors are described which raise our expectation that FEL operation below 100 nm is almost ready for demonstration. Included as a supplement is a review of initial design studies of the reflecting XUV projection optics, fabrication of reflection masks, characterization of photoresists, and the first experimental demonstrations of the capability of projection lithography with 14-nm radiation to produce lines and spaces as small as 0.05 microns. DOE

N91-16343# Los Alamos National Lab., NM.
DROPLET SHATTERING, VAPORIZATION, AND RECONDENSATION IN CLOUD CLEARING WITH LONG PULSE INFRARED CHEMICAL LASERS
E. J. Caramana, J. L. Kindel, R. L. Morse, G. P. Quigley, R. B. Webster, and G. W. York 1990 8 p Presented at the 1989/90 Conference on Cloud Impacts on DOD Operations and Systems, Monterey, CA, Jan. 1990
(Contract W-7405-eng-36)
(DE90-010584; LA-UR-90-1275; CONF-900189-1) Avail: NTIS HC/MF A02

Results of experimental attempts to produce an optically clear channel in a water cloud by evaporating the cloud droplets with a CO2 laser are presented. The use of scattered light makes it possible to visualize the clear channel produced. Measurements of the fraction of power transmitted through the channel at visible wavelengths give insight into the clearing mechanisms. The present data suggest that the water droplets explode in the process of clearing. A theoretical explanation of why this should occur is presented and predictions of the onset of droplet explosions are made. DOE

N91-16344# Lawrence Livermore National Lab., CA.
CLUSTER FORMATION IN LASER-INDUCED ABLATION AND EVAPORATION OF SOLIDS OBSERVED BY LASER IONIZATION TIME-OF-FLIGHT MASS SPECTROMETRY AND SCANNING TUNNELING MICROSCOPY
R. J. Tench, M. Balooch, L. Bernardez, Mike J. Allen, W. J. Siekhaus, D. R. Olander, and W. Wang (California Univ., Berkeley. Lawrence Berkeley Lab.) 1990 6 p Presented at the Spring Meeting of the Materials Research Society, San Francisco, CA, 16-21 Apr. 1990 Submitted for publication
(Contracts W-7405-eng-48; DE-AC03-76SF-00098)
(DE90-010876; UCRL-JC-103629; CONF-900466-31) Avail: NTIS HC/MF A02

Laser ionization time-of-flight mass analysis (LIMA) used pulses (5ns) of a frequency-quadrupled Nd-YAG laser (266 nm) focused onto spots of 4 to 100 microns diameter to ablate material, and a reflectron time of flight tube to mass-analyze the plume. The observed mass spectra for Si, Pt, SiC, and UO 2 varied in the distribution of ablation products among atoms, molecules and clusters, depending on laser power density and target material. Cleaved surfaces of highly oriented pyrolytic graphite (HOPG) positioned at room temperature either 10 cm away from materials ablated at 10(exp -5) Torr by 1 to 3 excimer laser (308 nm) pulses of 20 ns duration or 1 m away from materials vaporized at 10(exp -8) Torr by 10 Nd-Glass laser pulses of 1 ms duration were analyzed by Scanning Tunneling Microscopy (STM) in air with angstrom resolution. Clusters up to 30 A in diameter were observed. DOE

N91-16345# Sandia National Labs., Albuquerque, NM. Combustion Research Facility.
INTERFEROMETRIC SECOND-HARMONIC-GENERATION AUTOCORRELATOR FOR CHARACTERIZING FEMTOSECOND PULSES
Michelle Kuska Nov. 1989 15 p
(Contract DE-AC04-76DP-00789)
(DE90-010331; SAND-89-8253; UC-700) Avail: NTIS HC/MF A03

An interferometric second harmonic generation (SHG) autocorrelator for characterizing femtosecond pulses generated by a colliding pulse, mode locked ring dye laser is discussed. The autocorrelator consists of a modified Michelson interferometer. One arm provides a variable time delay through the use of a corner cube oscillating at 60 Hz. Electronic filters are used to display the pulse envelope and the second harmonic interference fringes. Since this autocorrelator produces an interferometric autocorrelation signal, it is possible to monitor the effects of pulse chirping, as well as the pulse width. DOE

N91-16346# Maryland Univ., College Park. Lab. for Plasma Research.
MODE COMPETITION EFFECTS IN FREE ELECTRON LASERS AND GYROTRONS
B. Levush and T. M. Antonsen, Jr. 1990 5 p Presented at the Topical Conference on Research Trends in Nonlinear and Relativistic Effects in Plasmas, San Diego, CA, 5-8 Feb. 1990 Submitted for publication
(Contract DE-FG05-87ER-52147)
(DE90-011084; CONF-900264-6) Avail: NTIS HC/MF A01

In many cases in high frequency, high power coherent radiation generators (such as free electron laser and gyrotrons) the linear gain is positive for many modes and therefore these modes will grow and compete for the beam energy. The questions related to mode competition, coherency of the radiation and maximization of the interaction efficiency are of great importance. To address these issues simple multi-mode models have been formulated. This paper is a short review of the recent results from both simulation and analyses of these models. DOE

N91-16347# Ames Lab., IA. Dept. of Chemistry.
NEW DEVELOPMENT OF LASER-BASED TECHNIQUES IN APPLICATIONS OF THIN-LAYER CHROMATOGRAPHY, MICROPROBE ELEMENTAL ANALYSIS, AND GAS PHASE PYROLYSIS Ph.D. Thesis
Jianzhong Zhu Jan. 1990 186 p
(Contract W-7405-eng-82)
(DE90-011740; IS-T-1429) Avail: NTIS HC/MF A09

The laser has made dramatic impact on today's technologies since its invention in 1960s. The development of the laser in analytical atomic and molecular spectroscopy as a primary light source has remarkably improved both sensitivity and spectral resolution. In addition, the laser has also offered a unique approach to challenging problems of both fundamental and applicable natures, such as isotope separation, remote sensing, selective photochemistry, solid sample vaporization, multiphoton spectroscopy and studies of transient events. However, many new applications of laser-based techniques are still rapidly developing. It is the main goal of the this research to explore new laser applications in the areas of thin layer chromatography, microprobe elemental analysis, and gas phase pyrolysis. The three sections are titled: (1) quantitative thin-layer chromatography by laser pyrolysis and flame ionization or electron capture detection; (2) direct coupling of thin-layer chromatography to gas chromatography by laser desorption; and (3) elemental analysis based on chemiluminescence in the laser microprobe. DOE

N91-16348# Los Alamos National Lab., NM.
INTEGRATED NUMERICAL EXPERIMENTS (INEX) AND THE FREE-ELECTRON LASER PHYSICAL PROCESS CODE (FELPPC)
L. E. Thode, K. C. D. Chan, M. J. Schmitt, J. McKee, J. Ostic, C. J. Elliott, and B. D. McVey 1990 34 p Presented at the Accelerator Computer Code Meeting, Los Alamos, NM, 22-25 Jan. 1990
(Contract W-7405-eng-36)
(DE90-011957; LA-UR-90-1483; CONF-900163-9) Avail: NTIS HC/MF A03

The strong coupling of subsystem elements, such as the accelerator, wiggler, and optics, greatly complicates the understanding and design of a free electron laser (FEL), even at the conceptual level. Given the requirements for high-performance FELs, the strong coupling between the laser subsystems must be included to obtain a realistic picture of the potential operational capability. To address the strong coupling character of the FEL the concept of an Integrated Numerical Experiment (INEX) was proposed. Unique features of the INEX approach are consistency and numerical equivalence of experimental diagnostics. The equivalent numerical diagnostics mitigates the major problem of misinterpretation that often occurs when theoretical and experimental data are compared. The INEX approach has been applied to a large number of accelerator and FEL experiments. Overall, the agreement between INEX and the experiments is very good. Despite the success of INEX, the approach is difficult to apply to trade-off and initial design studies because of the significant manpower and computational requirements. On the other hand, INEX provides a base from which realistic accelerator, wiggler, and optics models can be developed. The Free Electron Laser Physical Process Code (FELPPC) includes models developed from INEX, provides coupling between the subsystems models and incorporates application models relevant to a specific trade-off or design study. DOE

N91-16349# Lawrence Livermore National Lab., CA. Beam Research Program.

GENERATION OF XUV LIGHT BY RESONANT FREQUENCY TRIPLING IN A TWO-WIGGLER FEL AMPLIFIER

R. Bonifacio, L. deSalvoSouza, P. Pierini (Milan Univ., Italy), and E. T. Scharlemann 1989 13 p Presented at the 11th International Free Electron Laser Conference, Naples, Italy, 28 Aug. - 1 Sep. 1989

(Contract W-7405-eng-48)

(DE90-012120; UCRL-102746; CONF-8908134-32) Avail: NTIS HC A03

FEL operation at short wavelength is limited by electron beam quality, by the availability of mirrors for oscillators, and by the availability of input sources for FEL amplifiers. It is possible to use and FEL amplifier as a resonant frequency tripling device, generating light and strong bunching at the 3rd harmonic of a conventional input source in an initial section of wiggler, then using a second section of wiggler resonant at the tripled frequency to amplify the short wavelength light. Neither mirrors nor a short-wavelength input source are required, and some relaxation of electron beam quality appears to be possible. We illustrate the scheme with a one-dimensional model and then with NUTMEG simulations of an 80 nm FEL amplifier initiated by a 240 nm input signal, in which an efficiency of conversion of electron beam power to 80 nm light of nearly 10(exp -4) was obtained. DOE

N91-16350*# Case Western Reserve Univ., Cleveland, OH.

DEVELOPMENT OF A VERSATILE LASER LIGHT SCATTERING INSTRUMENT Final Report

William V. Meyer and Rafat R. Ansari Oct. 1990 25 p

(Contract NCC3-74)

(NASA-CR-182474; NAS 1.26:182474) Avail: NTIS HC/MF A03 CSCL 20E

A versatile laser light scattering (LLS) instrument is developed for use in microgravity to measure microscopic particles of 30 A to above 3 microns. Since it is an optical technique, LLS does not affect the sample being studied. A LLS instrument built from modules allows several configurations, each optimized for a particular experiment. The multiangle LLS instrument can be mounted in the rack in the Space Shuttle and on Space Station Freedom. It is possible that a Space Shuttle glove-box and a lap-top computer containing a correlator card can be used to perform a number of experiments and to demonstrate the technology needed for more elaborate investigations. This offers simple means of flying a great number of experiments without the additional requirements of full-scale flight hardware experiments. Y.S.

N91-16351# Los Alamos National Lab., NM. Chemical and Laser Science Div.

ANGULAR DEPENDENCE OF THIN-FILM DIELECTRIC COATING DAMAGE THRESHOLDS

J. D. Boyer, S. R. Foltyn, B. R. Mauro, and V. E. Sanders 1989 8 p Presented at the 21st Annual Symposium on Optical Materials for High Power Lasers, Boulder, CO, 1-3 Nov. 1989

(Contract W-7405-eng-36)

(DE91-000237; LA-UR-90-3129; CONF-891163-4) Avail: NTIS HC/MF A02

Newman et al. reported experiments showing that the angular dependence of 351-nm laser damage thresholds in HfO2/SiO2 multilayer dielectric reflectors was much weaker than even the 1/cos theta expected from simple geometric fluence dilution. Several plausible explanations were suggested, but none were convincing. We propose a simple geometric model based on a cylindrical form for the coating defect responsible for damage initiation. We have measured 248-nm damage thresholds for bare fused silica, evaporated aluminum films, and HfO2/SiO2 and Al2O3/SiO2 dielectric reflectors at angles out to 85 degrees. The measured data agree well with our simple model. DOE

N91-16352# Aerospace Corp., El Segundo, CA. Chemistry and Physics Lab.

EFFECTS OF NEUTRON FLUENCE ON THE OPERATING CHARACTERISTICS OF DIODE LASERS USED IN ATOMIC FREQUENCY STANDARDS

R. P. Frueholz, J. C. Camparo, S. B. Delcamp, and C. E. Barnes (California Inst. of Tech., Pasadena.) 15 Aug. 1990 14 p

(Contract F04701-88-C-0089)

(AD-A226763; TR-0090(5945-05)-3; SSD-TR-90-21) Avail: NTIS HC/MF A03 CSCL 09/3

One of the next major advances in rubidium and cesium atomic clock technology will center on the use of diode lasers for optical pumping. The atomic clocks used on board satellites have the potential to interact with various forms of radiation that are not present in the laboratory environment, and the effects of this radiation on the laser's operating characteristics relevant to clock applications are not well known. The effects were studied of neutron fluence on the operating characteristics of Mitsubishi Transverse Junction Stripe (TJS) AlGaAs diode lasers. Different models of the TJS diode laser produce optical radiation in both the 780 and 850 nm range, appropriate for optical pumping in rubidium and cesium atomic clocks, respectively. In this phase, a set of TJS diode lasers was exposed to a neutron fluence of 2 x 1012 n/sq cm, and four laser characteristics were examined after each exposure. The laser's light output versus injection current and single mode linewidth versus output power both influence the efficiency of optical pumping and hence the atomic clock's signal to noise ratio. The laser's single mode wavelength versus injection current (laser tuning) was also measured. Since the diode laser must remain tuned to the appropriate atomic transition, any degradation in the ability to tune the laser will impact atomic clock reliability. Finally, the diode laser's gain curve was studied at several injection currents below threshold. GRA

N91-16353# University of Central Florida, Orlando.

TIMING MARGIN MEASUREMENT USING A LASER TECHNIQUE Final Technical Report, Oct. 1987 - Dec. 1989

Harold K. Brown, Glenn C. Fuller, and Shane S. Clammae Jul. 1990 227 p

(Contract F30602-87-C-0100; AF Proj. 2338)

(AD-A226821; RADC-TR-90-147) Avail: NTIS HC/MF A11 CSCL 09/3

A noncontact technique is described for obtaining information about the timing margins of internal signal paths in CMOS circuits. A controlled photocurrent is injected by spot illumination of an OFF transistor drain loading a node. The collected photocurrent aids or opposes transistors driving the node. This increases (or decreases) node switching times, and many manifest as a change in the maximum operating frequency of the overall circuit. An approach for extracting timing margin values from plots of maximum operating frequency vs illumination intensity was developed, which

does not require estimation of the drive strength or capacitive load of the node tested. Theory, implementation details, difficulties, and test results on a CMOS microprocessor are discussed.
GRA

N91-16354# Arizona State Univ., Tempe. Dept. of Mechanical and Aerospace Engineering.
RESEARCH ON CERTAIN ASPECTS OF LASER DIFFRACTION PARTICLE SIZE ANALYSIS RELEVANT TO AUTONOMOUS SELF-DIAGNOSING INSTRUMENTATION Final Report, 1 Oct. 1984 - 31 May 1990
E. Dan Hirleman 27 Jul. 1990 24 p
(Grant AF-AFOSR-0187-84; AF Proj. 2308)
(AD-A226822; AFOSR-90-0972TR) Avail: NTIS HC/MF A03 CSCL 17/5

The results of a multi-year research effort addressing fundamental scientific issues relevant to the application of laser diagnostic methods as on-line sensors in next-generation propulsion systems are summarized. The overall objective effort was to contribute to the scientific knowledge base necessary to characterize and then extend the capabilities of near-forward scattering (laser diffraction) particle sizing techniques in terms of application as intelligent sensors capable of on-line, autonomous, and self-diagnosing operation in hostile propulsion system environments. The project scope encompassed three research areas: (1) steering or deflection of the probe laser beam due to refractive index (temperature or concentration) gradients; (2) inverse scattering algorithms; and (3) multiple scattering and measurements in optically thick media. The important technical contributions of this project included: development and demonstration of a concept which allows on-line configuration of optimal detector arrays using transmission-mode spatial light modulators and which can obviate the beam steering problem; derivation of the optimal scaling law for Fraunhofer diffraction particle sizing systems which integrated the optical detector array geometry and the inversion software; systematic formulation and synthesis of the family of integral transform solutions to the inverse Fraunhofer diffraction particle sizing problem and development of a new integral transform; development of a radiation transfer model for near forward scattering by optically thick particle media; and development of a general solution and technique for solving the inverse scattering problem for optically thick dispersions of particles large compared to the wavelength. GRA

N91-16355# Aerospace Corp., El Segundo, CA. Chemistry and Physics Lab.
OPTIMIZATION OF HYDROGEN CONSUMPTION IN HYDROGEN MASERS
B. Jaduszliwer and Yat C. Chan 6 Aug. 1990 19 p
(Contract F04701-88-C-0089)
(AD-A227267; TR-0090(5945-05)-02; SSD-TR-90-22) Avail: NTIS HC/MF A03 CSCL 07/2

Hydrogen consumption is an important reliability issue for space-qualified hydrogen masers. An excess of atoms in the upper state of the maser transition must be continuously fed into the maser bulb. Atomic hydrogen is produced in an RF discharge dissociator, and state selection is accomplished by a multipole magnet which focuses atoms in the desired state at the masers' bulb entrance orifice. The focusing properties of these magnets depend strongly on atomic speed. The quality of the match between the speed distribution of the atoms leaving the dissociator and the velocity-dependent transmission of the state selector plays an important role in determining the masers' hydrogen consumption budget. Speed distributions of hydrogen atoms effusing from an RF dissociator were determined and were found to be significantly narrower than Maxwellians. Realistic calculations were performed of the focusing properties of hexapole magnet atomic state selectors, and explored the conditions under which good matches between atomic speed distribution and state selector transmission can be achieved. GRA

N91-16356# Illinois Univ., Urbana. Coordinated Science Lab.
TWO-DIMENSIONAL SIMULATION OF QUANTUM-WELL LASERS INCLUDING ENERGY TRANSPORT Ph.D. Thesis
Ghie Hugh Song Aug. 1990 82 p Sponsored by NSF
(Contract N00014-86-K-0512)
(AD-A227487; UILU-ENG-90-2241) Avail: NTIS HC/MF A05 CSCL 09/3

A versatile, 2-D simulator for various types of semiconductor lasers for both steady state and transients has been developed. The simulator is capable of spectral analysis of quantum well semiconductor lasers, such as gain-spectrum analysis, as well as analysis of the 2-D current flow and optical intensity patterns. The simulator is based on the drift-diffusion model with full Fermi Dirac statistics for the transport equations as well as for the Pisson equation. Simulation of the thermionic emission current is required at the abrupt hetero-interfaces of the quantum well. Energy transfer among the change carriers, crystal lattice, and optical radiation in an optoelectronic semiconductor device is analyzed in order to obtain details of the internal temperature distribution. Fermi Dirac statistics and the spatial band gap variation in a degenerate semiconductor device with nonuniform band structure are included in the analysis. The boundary conditions for the energy flow equation are discussed. The photon rate equation is used for the spectral analysis of quantum well lasers for each Fabry-Perot mode. The transient simulation is done by the backward Euler method in conjunction with the full Newton approach for the entire semiconductor equations. To demonstrate the simulator, a model GaAs-AlGaAs graded index separate confinement heterostructure buried quantum well laser is analyzed. GRA

N91-16357# Los Alamos National Lab., NM.
DESIGN REQUIREMENTS AND CALCULATED PERFORMANCE OF AN XUV FEL OSCILLATOR OPERATING ON A HIGHER HARMONIC
John C. Goldstein, Roger W. Warren, and Brian E. Newnam 1990 11 p Presented at the 12th International Free Electron Laser Conference, Paris, France, 17-21 Sep. 1990
(Contract W-7405-eng-36)
(DE91-004833; LA-UR-90-3788; CONF-9009166-12) Avail: NTIS HC/MF A03

We study, using numerical simulation methods, the design requirements for the electron beam, wiggler, and optical resonator of an extreme-ultraviolet (XUV, lambda is equal or between 10 and 100 nm) free-electron laser oscillator operating on a higher harmonic. Our previous theoretical studies of an XUV FEL oscillator have assumed operation at the fundamental wavelength. Higher harmonic operation is attractive because the energy of the electrons can be reduced, thus reducing the cost of the linac. A further reduction in beam energy is possible with the use of short-period wigglers: in the present work, we use the expected properties of pulsed-wire wigglers. Operation of an FEL oscillator on the third harmonic has been experimentally demonstrated at Stanford University and Los Alamos, and this mode of operation may also be both possible and desirable for an XUV device. DOE

N91-16358# California Univ., Berkeley. Lawrence Berkeley Lab.
SOME NONLINEAR PROBLEMS IN THE MANIPULATION OF BEAMS
Andrew M. Sessler 1 Oct. 1990 22 p Presented at the US-Japan Workshop on Nonlinear Dynamics and Acceleration Mechanisms, Tsukuba, Japan, 22-25 Oct. 1990
(Contract DE-AC03-76SF-00098)
(DE91-005211; LBL-29716; CONF-9010270-1) Avail: NTIS HC/MF A03

An overview is given of nonlinear problems that arise in the manipulation of beams. Beams can be made of material particles or photons, can be intense or dilute, can be energetic or not, and they can be propagating in vacuum or in a medium. The nonlinear aspects of the motion are different in each case, and this diversity of behavior is categorized. Many examples are given, which serves to illustrate the categorization and, furthermore, display the richness of behavior encountered in the physics of beams. DOE

N91-16359 Rochester Univ., NY.
STOCHASTIC AND CHAOTIC EFFECTS IN THE RING LASER Ph.D. Thesis
Thomas Herman Chyba 1990 334 p
Avail: Univ. Microfilms Order No. DA9032736

Experimental and theoretical distinctions are drawn between chaotic and stochastic laser processes. Elementary notions of stochastic and chaotic processes are introduced and the relevant laser theory is outlined. The spontaneous switching between the two counterpropagating cavity modes in the bidirectional dye ring laser is experimentally shown to be a stochastic rather than a chaotic process - a macroscopic manifestation of quantum fluctuations. However, the rapid intensity fluctuations in the laser are experimentally demonstrated to be chaotic. The underlying source of this behavior is the turbulent flow of the dye through the dye cell. For the standing wave single-mode dye laser, a first order phase transition analogy is observed which is induced by stochastic noise with a finite bandwidth. The phase jump instability of the bidirectional He:Ne ring laser with backscattering is investigated. The deterministic equations for this laser are shown to be exactly soluble and not chaotic. Conditions are derived under which the field phases are unstable and may exhibit discontinuities. An experiment is also described which compares the calculated absorbed photon flux, the measured absorbed photon flux, and the measured photocurrent when a quasimonochromatic collimated laser beam falls upon a vacuum photodiode. Dissert. Abstr.

N91-16360 Bryn Mawr Coll., PA.
HOMOGENEOUSLY BROADENED BIDIRECTIONAL RING LASER: THEORETICAL ANALYSIS, NUMERICAL SIMULATION, AND EXPERIMENT IN HELIUM-XENON Ph.D. Thesis
Lois Marion Hoffer 1990 314 p
Avail: Univ. Microfilms Order No. DA9032027

Theoretical and experimental studies of a homogeneously broadened bidirectional ring laser are reported. A model for a homogeneously broadened bidirectional ring laser is derived. The material variables, the population inversion and the atomic polarization, are written as infinite spatial harmonic series. Each of those series is truncated at fourth order in the spatial frequency, yielding a system of fifteen real equations. A numerical investigation of the validity of this truncation is performed. The rate of convergence of the spatial harmonic series of the population inversion and thereby the validity of the truncation of the series, is found to depend on the ratio of the relaxation rates of the population difference and the field and on the regularity of the dynamics. The four steady-state solutions to this problem are found and a linearized stability analysis is performed on the zero-intensity steady state and the unidirectional steady states. The stability of the bidirectional solution is explored numerically. Plots of intensity versus time from a numerical integration of the fifteen equations, is presented for parameter values appropriate to a Helium-Xenon laser and for a range of pump and detuning values, for later comparison with experimental values. The experimental set-up is described and the determination of the values for the various parameters appearing in the model is presented. A summary and comparison of experimental findings and theoretical predictions is given. Dissert. Abstr.

N91-16361# Massachusetts Inst. of Tech., Lexington. Lincoln Lab.
MATERIALS SYSTEMS FOR 2- TO 5-MICROMETERS WAVELENGTH DIODE LASERS Technical Report, 1 Nov. 1988 - 30 Sep. 1989
J. N. Walpole, T. C. Harman, S. H. Groves, R. C. Williamson, and A. J. Strauss 22 Aug. 1990 67 p
(Contract F19628-90-C-0002)
(AD-A228218; TR-898; ESD-TR-90-066) Avail: NTIS HC/MF A04 CSCL 09/3

Several materials systems are reviewed in attempt to determine the most favorable for use in the fabrication of diode lasers emitting in the 2- to 5-micron wavelength range. Eight possible systems, along with several of their variations, are identified among the III-V, IV-VI, and II-VI semiconductors. All meet the following criteria: optical and carrier confinement can be obtained, a significant portion of the desired wavelength range can be achieved, and the layers that are required to fabricate a double-heterostructure (DH) laser can be lattice matched to a suitable substrate. The performance of III-V laser devices is limited by Auger recombination and free-carrier absorption. The role of the valence band structure in these effects is of particular importance. The III-V system identified as the most promising is GaInAsSb/AlGaAsSb/GaSb, with the quaternary alloy GaInAsSb for the active layer, the quaternary alloy AlGaAsSb for the cladding layers, and GaSb for the substrate. This system offers substrate availability, a wide range of wavelengths, good metallurgical properties and favorable device physics. In this system, DH lasers emitting at approximately 2.3 micron have been operated CW at room temperature with threshold current densities as low as 1.5 A/sq cm, and differential quantum efficiencies as high as 18 percent per facet have been obtained in pulsed room-temperature operation. According to theoretical projections, the threshold current density of such GaInAsSb/AlGaAsSb/GaSb lasers will increase with increasing wavelength because of increased Auger recombination and free-carrier absorption. GRA

N91-16362# Aerospace Corp., El Segundo, CA. Aerophysics Lab.
DIRECT OBSERVATION OF NF(X) USING LASER-INDUCED FLUORESCENCE: KINETICS OF THE NF 3 SIGMA - GROUND STATE
Raymond F. Heidner, III, John S. Holloway, Henry Helvajian, and John B. Koffend 6 Aug. 1990 35 p
(Contract F04701-88-C-0089)
(AD-A228294; TR-0090(5930-04)-3; SSD-TR-90-31) Avail: NTIS HC/MF A03 CSCL 07/5

Vibrational relaxation of NF(X) produced from the 249 nm photolysis of NF2 was investigated with CO2 and SF6 as the quenching partners. State-to-state vibrational quenching rate constants were obtained for NF(X, v' = 1-3). SF6 is seen to be an efficient vibrational quencher of NF(X), while CO2 is relatively inefficient, contrary to what is observed for HF vibrational relaxation. The bimolecular disproportionation of NF(X) is seen to be much smaller than previously reported, while the reaction of NF(X) with NF2 is surprisingly fast and may be the dominant removal mechanism for NF(X 3 Sigma). GRA

N91-16363# Colorado Univ., Boulder.
SPONTANEOUS FORCE OPTICAL TRAPS Final Report, 1 Jun. 1987 - 30 Sep. 1990
Carl E. Wieman 1 Oct. 1990 14 p
(Contract N00014-87-K-0396)
(AD-A228539; CU-153-1200) Avail: NTIS HC/MF A03 CSCL 20/5

Extensive studies were carried out on the use of laser light to cool and trap neutral cesium atoms. High density samples were obtained of trapped cesium with temperatures as low as 0.3 mK, and the interactions between these atoms studied. Because of the very low temperatures and high densities, these atoms show unique short range interactions as well as unexpected long range interactions. At short range, the laser excitation of the atoms induces inelastic collisions which lead to loss from the trap. Multiple scattering of photons leads to long range interactions between the atoms which cause the trapped cloud to behave in a collective manner, and undergo abrupt changes in shape. The ability to optically trap atoms directly from a low pressure vapor demonstrated along with potential of this technology for making an improved atomic clock. GRA

N91-16364# Erlangen-Nuremberg Univ. (Germany, F.R.). Lehrstuhl fuer Stroemungsmechanik.
OPTIMIZATION OF A LASER DIODE ANEMOMETRY SYSTEM
R. Mueller and A. Naqwi Dec. 1988 89 p
(Contract DFG-Na-189/1-1)
(LSTM-239/T/88; ETN-91-97874) Avail: NTIS HC/MF A05

A laser Doppler anemometry system using a laser diode as the light source is investigated. A computational procedure for

optimizing a Doppler anemometry unit is developed. The aim is the minimization of the following measurement uncertainties: broadening of the signal frequency due to distortion of wavefronts in the measuring volume; frequency broadening caused by misalignment of the lens that collimates the diverging beam of the laser diode; changes in the wavelength of laser and hence the calibration constant of the system resulting from fluctuations in the operating temperature and current. The calculations are based on a generalized relation for the frequency broadening combined with a simulation model for the anemometry system. The optical field of a laser diode is described as a product of a Gaussian and a truncated Lorentzian distribution. The influence of design parameters is examined by means of a computational study and an experimental evaluation of the measuring volume. Flow measurements are taken. The performance is found to improve with the use of a small focal length collimator and a large focal length front lens. ESA

N91-16365 Physics and Electronics Lab. TNO, The Hague (Netherlands).
EXPERIMENTAL SET-UP FOR A PULSED CO2 LASER RANGEFINDER WITH HETERODYNE DETECTION Final Report
J. Bloem Aug. 1990 58 p In DUTCH; ENGLISH summary
(Contract A84/KL/121)
(FEL-90-A125; TD-89-4464; ETN-91-98392) Copyright Avail: Physics and Electronics Lab. TNO, P.O. Box 96864, 2509 JG The Hague, Netherlands

The creation of a pulsed CO2 laser range finder with heterodyne detection is described. The range finder uses a hybrid CW-TEA (Continuous Wave-Transversely Excited Atmospheric pressure) laser as emitter and an RF laser as local oscillator. The laser stabilization is described. The frequency offset between the transmitted laser pulse and the local oscillator laser is locked at 20 MHz. The long term (20 to 30 min) variation of this offset frequency is limited to 50 kHz. The effects of pulsing on this stabilization were eliminated. The signal processing was started. A rough model of the laser pulse and its frequency characteristics was developed. An AM demodulator was developed to determine the envelope of the reflected pulses. The system created can be used to measure the range to (and in the future also the speed of) diffuse reflecting targets. ESA

N91-16366 Physics and Electronics Lab. TNO, The Hague (Netherlands).
GENERATION OF HIGH POWER 1.54 MICROMETER RADIATION BY STIMULATED RAMAN SCATTERING IN METHANE Final Report
F. J. M. vanPutten Aug. 1990 62 p In DUTCH; ENGLISH summary
(FEL-90-B098; TD-90-2788; ETN-91-98395) Copyright Avail: Physics and Electronics Lab. TNO, P.O. Box96864, 2509 JG The Hague, Netherlands

Experiments with a Nd:YAG laser operating at 1.064 microns were carried out to obtain an efficient source of eye safe 1.54 microns radiation. This conversion was obtained using stimulated Raman scattering in methane by applying a focusing and a dichroic mirror for feedback. The varied parameters were laser power, pulse repetition rate, gas pressure, gas constitution, beam width, and the optical strength of the lenses. With a spherical lens a 61 percent conversion efficiency was obtained with a 22 mJ input. For a combination of two cylindrical lenses of 100 mm focal length and 200 mJ input a value of 74 percent was found. The output degrades at pulse repetition frequencies higher than 5 Hz, probably due to thermal effects. Adding helium to the methane up to 39 percent partial pressure to increase the thermal conductivity does not degrade the conversion, however, no improvements at higher repetition rates were found. ESA

N91-16367# Deutsche Forschungsanstalt fuer Luft- und Raumfahrt, Stuttgart (Germany, F.R.). Inst. fuer Technische Physik.
ANALYTICAL AND EXPERIMENTAL INVESTIGATION OF TRANSVERSE FLOW AERODYNAMIC WINDOWS FOR HIGH POWER LASERS Ph.D. Thesis - Stuttgart Univ.
Eberhard Wildermuth Aug. 1990 194 p In GERMAN; ENGLISH summary Report will also be announced as translation (ESA-TT-1251)
(DLR-FB-90-33; ISSN-0171-1342; ETN-91-98597) Avail: NTIS HC/MF A01; DLR, VB-PL-DO, Postfach 90 60 58, 5000 Cologne, Fed. Republic of Germany, HC 58 Deutche marks

Different concepts of transverse flow aerodynamic windows to be used as outcoupling element in CO2 high power lasers are presented. A gas jet transverse to the optical axis seals the laser cavity against the ambient atmosphere. The respective layout and the experiments to investigate the optical and fluid mechanical properties show the application range of each concept. Design and experimental operations of a prototype combined with a 5 kW CO2 laser are discussed. Calculations of the beam quality are compared with experimental results. ESA

37 MECHANICAL ENGINEERING

Includes auxiliary systems (nonpower); machine elements and processes; and mechanical equipment.

N91-16368# Oak Ridge National Lab., TN. Center for Engineering Systems Advanced Research.
EXPERIMENTATION AND CONCEPT FORMATION BY AN AUTONOMOUS MOBILE ROBOT
P. F. Spelt, G. deSaussure, G. Oliver, and M. Silliman 1990 18 p Presented at the Japan-USA Symposium on Flexible Automation, Kyoto, Japan, 9-11 Jul. 1990
(Contract DE-AC05-84OR-21400)
(DE90-003063; CONF-900729-1) Avail: NTIS HC/MF A03

The Center for Engineering Systems Advanced Research (CESAR) conducts basic research in the area of intelligent machines. In this paper, we describe our approach to a class of machine learning which involves autonomous concept formation using feedback from trial-and-error experimentation with the environment. Our formulation was experimentally validated on an autonomous mobile robot, which learned the task of control panel monitoring and manipulation for effective process control. Conclusions are drawn concerning the applicability of the system to a more general class of learning problems, and implications for the use of autonomous mobile robots in hostile and unknown environments are discussed. DOE

N91-16369# Oak Ridge National Lab., TN. Center for Engineering Systems Advanced Research.
ULTRASOUND AND VISUAL SENSOR FEEDBACK AND FUSION
M. Beckerman, D. L. Barnett, and S. M. Killough 1990 12 p Presented at the Japan-USA Symposium on Flexible Automation, Kyoto, Japan, 9-11 Jul. 1990
(Contract DE-AC05-84OR-21400)
(DE90-005280; CONF-900729-2) Avail: NTIS HC/MF A03

The HERMIES-IIB mobile robot developed at Oak Ridge National Laboratory's (ORNL's) Center for Engineering Systems Advanced Research was designed to carry out autonomous sensing, navigation and manipulation tasks in an unstructured laboratory environment. In this paper we report on the use of sensor feedback and sensor fusion as means of compensating for HERMIES-IIB sensor and mechanical errors, uncertainties and limitations. DOE

N91-16370# Argonne National Lab., IL. Center for Transportation Research.
A SUMMARY OF PROSPECTS FOR METHANOL VEHICLES IN THE UNITED STATES
Robert P. Larsen 1990 10 p Presented at the National

Symposium on Methanol Vehicles, Tokyo, Japan, 6-8 Feb. 1990
(Contract W-31-109-eng-38)
(DE90-009719; CONF-9002120-1) Avail: NTIS HC/MF A02

Interest in alternatives to petroleum as fuel for the U.S. transportation system has been increasing steadily over the last 10 years. Initiatives from the Federal and state governments have advanced the likelihood of the use of alternative fuels in the U.S. in significant volumes in the 1990's. In a rare convergence of governmental and industrial perspectives, methanol has emerged as the most likely alternative fuel to displace large quantities of petroleum as a transportation fuel. Methanol has attained this position because of its favorable economics from infrastructure, vehicle conversion, and production standpoints. In addition, the necessarily lengthy transition period for any alternative fuel is facilitated using methanol, a liquid fuel with a great many similarities to gasoline and diesel fuel. The environmental benefits from a transition to alternative fuels, and from methanol in particular, have emerged as the largest motivation to begin a transition to a non-petroleum fuel. This paper will summarize recent developments in alternative fuel policy, research and development, and legislative initiatives in the U.S., highlighting the leading position of methanol fuel. DOE

N91-16371# Sandia National Labs., Albuquerque, NM.
HAPTIC PERCEPTION WITH AN ARTICULATED, SENSATE ROBOT HAND
S. A. Stansfield Mar. 1990 36 p
(Contract DE-AC04-76DP-00789)
(DE90-010195; SAND-90-0085) Avail: NTIS HC/MF A03

In this paper we present a series of haptic exploratory procedures, or EPs, implemented for a multi-fingered, articulated, sensate robot hand. These EPs are designed to extract specific tactile and kinesthetic information form an object via their purposive invocation by an intelligent robotic system. Taken together, they form and active robotic touch perception system to be used both in extracting information about the environment for internal representation and in acquiring grasps for manipulation. The haptic system presented utilizes an integrated robotic system consisting of PUMA 560 robot arm, a JPL/Stanford robot hand, with joint torque sensing in the fingers, a wrist force/torque sensor, and 256 element, spatially-resolved fingertip tactile array. We describe the EPs implemented for this system and provide experimental results which illustrate how they function and how the information which they extract may be used. In addition to the sensate hand and arm, the robot also contains structured-lighting vision and a Prolog-based reasoning system capable of grasp generation and object categorization. We present a set of simple tasks which show how both grasping and recognition may be enhanced by the addition of active touch perception. DOE

N91-16372# Oak Ridge National Lab., TN. Center for Engineering Systems Advanced Research.
MULTI-CRITERIA POSITION AND CONFIGURATION OPTIMIZATION FOR REDUNDANT PLATFORM/MANIPULATOR SYSTEMS
F. G. Pin and Jean-Christophe Culioli 1990 6 p Presented at the IROS 1990: IEEE International Workshop on Intelligent Robots and Systems, Tsuchiura, Japan, 3-6 Jul. 1990 Submitted for publication Sponsored in part by Army Lab. Command
(Contract DE-AC05-84OR-21400)
(DE90-010705; CONF-900795-1) Avail: NTIS HC/MF A02

An important characteristic of practical mobile manipulators, i.e., manipulators mounted on mobile platforms, is their particular kinematic redundancy created by the addition of the degrees of freedom of the platform to those of the manipulator. This paper is concerned with the resolution of this kinematic redundancy, and in particular with the local optimization of the position and configuration on the system during task commutations when changes occur in both task requirements and task constraints. Optimization criteria for obstacle avoidance, manipulability, least torque norm and maximum actuator torque are first discussed. Emphasis is them placed on optimization methods for problems involving multi-requirements and multi-criteria optimization. Sample results of the methods for a system including a three-link manipulator mounted on a mobile platform are presented and discussed. DOE

N91-16373# Argonne National Lab., IL.
TECHNICAL AND ECONOMIC EVALUATION OF DIESEL ENGINE WITH OXYGEN ENRICHMENT AND WATER INJECTION
R. L. Cole, R. R. Sekar, T. J. Marciniak, and F. Stodolsky (Argonne National Lab., Washington, DC.) 1990 8 p Presented at the 13th Energy-Sources Technology Conference and Exhibition, New Orleans, LA, 14-18 Jan. 1990
(Contract W-31-109-eng-38)
(DE90-009723; CONF-900102-5) Avail: NTIS HC/MF A02

Technical and economic feasibility of diesel engines for stationary cogeneration applications using oxygen-enriched combustion air, water injection, and low-grade fuels was examined. The effects of these modifications on the diesel engine were studied with a computer simulation: results are presented in a companion paper. Four methods of oxygen enrichment, purchases LOX, cryogenic separation, pressure-swing adsorption (PSA), and membrane enrichment (ME) were investigated. Two of these methods, PSA and ME, are particularly amenable to integration with a stationary engine. After the technical evaluation was completed, the economic performance of the options was analyzed. Results show that the economic viability of the system depends primarily on switching to a cheaper, low-grade fuel; the optimum oxygen enrichment is the minimum that will enable the engine to burn the low-grade fuel. Economic benefit is also derived from increased power production. Both of the methods that can be integrated with the engine show economic benefits, but one is more attractive that the other. Cryogenic separation systems are generally too large to be technically feasible for this application. The use of low-grade fuels, oxygen enrichment, and water injection affect ignition delay and combustion times, cylinder temperatures and pressures, and emissions (especially smoke, particulates, and NOx). There appears to be an optimum combination of these parameters that will allow short ignition delay, reasonable cylinder temperatures and pressures, and low emissions. DOE

N91-16374# Department of Energy, Washington, DC. Office of the Deputy Assistant Secretary for Coal Technology.
HEAT ENGINES PROGRAM
Sep. 1989 38 p
(DE90-010276; DOE/FE-0183P) Avail: NTIS HC/MF A03

The Office of Coal Technology (OCT) in FE is concentrating its efforts on two internal combustion engines - the open cycle gas turbine and the diesel engine - that utilize gas- and oil-based fuels today but have the potential for burning coal in the future. Research in these areas is briefly described, along with a discussion on program strategy. DOE

N91-16375# Argonne National Lab., IL. Technical Evaluation Group.
MAGNETIC HEAT PUMPS
R. F. Giese Feb. 1990 85 p
(Contract W-31-109-eng-38)
(DE90-010305; ANL/ESD-3) Avail: NTIS HC/MF A05

The effect of the development of high temperature superconductors on the use of magnetic heat pumps was evaluated for two applications: refrigeration for commercial food processing and industrial production of hot water or low quality steam. Background discussion are included on magnetic heat pumps and their operation and on the selection of the two applications that were evaluated. The design of magnetic heat pumps and how designs will be affected by the use of high temperature superconductors are analyzed. The heat pump designs used in the evaluations were a Brayton cycle with an active magnetic regenerator and a Brayton cycle with external recuperation. The economics of the active magnetic regenerator design are compared with conventional vapor compression devices for the two applications. DOE

N91-16376# Oak Ridge National Lab., TN. Engineering Physics and Mathematics Div.
TIME OPTIMAL TRAJECTORIES FOR A TWO WHEELED ROBOT
D. B. Reister May 1990 29 p
(Contract DE-AC05-84OR-21400)
(DE90-010335; ORNL/TM-11510; CESAR-90/12) Avail: NTIS HC/MF A03

The objective is to move a two wheeled robot from one posture to the next in the minimum time in a planar environment without obstacles. It was assumed that the maximum acceleration on each wheel is bounded. Pontryagin's Maximum Principle was used to find the optimum paths. The optimal trajectories are bang-bang; at every point on the optimum path the acceleration on each wheel is either at the upper limit or at the lower limit. A coordinate transformation was used to move the initial posture to the origin. Any point was reached by a rotation followed by a translation. Adding a final rotation moves the robot to an arbitrary posture. A switch point is a point at which the acceleration on one of the wheels changes sign. A trajectory was characterized by the number of switch points. A path with a smaller number of switch points will have a higher average velocity and a longer distance traveled by the wheels. The path with the smallest number of switch points has two (one of each wheel). For translation, both wheels accelerate from zero to the maximum velocity. After the switch point, both wheels decelerate to zero. However, there are only two paths with two switch points: translation and rotation. Rotation followed by translation requires five switch points, while rotation, translation, rotation has eight switch points. Paths were explored with three and four switch points. The paths with three switch points and initial rotation can reach any point faster than a rotation followed by a translation. Paths with three switch points and initial translation or paths with four switch points are useful if the final orientation is considerably different than the direction of travel.
DOE

N91-16377# Edgerton, Germeshausen and Grier, Inc., Idaho Falls, ID.
SENSING OF METAL-TRANSFER MODE FOR PROCESS CONTROL OF GMAW (GAS METAL ARC WELDING)
Nancy M. Carlson, John A. Johnson, and Herschel B. Smartt 1989 9 p Presented at the 16th Annual Review of Progress in Quantitative Nondestructive Evaluation, Brunswick, ME, 23-28 Jul. 1989
(Contract DE-AC07-76ID-01570)
(DE90-010946; EGG-M-89148; CONF-890770-9) Avail: NTIS HC/MF A02

One of the requirements of a sensing system for feedback control of gas metal arc welding (GMAW) is the capability to determine the metal-transfer mode. Because the operating boundary for the desired transfer mode, expressed as a function of mass input and heat input, may vary due to conditions beyond the control of the system, a means of detecting the transfer mode during welding is necessary. A series of sensing experiments was performed during which the ultrasonic emissions, audio emissions, welding current fluctuations and welding voltage fluctuations were recorded as a function of the transfer mode. In addition, high speed movies (5000 frames/s) of the droplet formation and detachment were taken synchronously with the sensing data. An LED mounted in the camera was used to mark the film at the beginning and end of the data acquisition period. A second LED was pulsed at a 1 kHz rate and the pulses recorded on film and with the sensor data. Thus events recorded on the film can be correlated with the sensor data. Data acquired during globular transfer, spray transfer, and stiff spray or streaming transfer were observed to correlate with droplet detachment and arc shorting. The audio, current, and voltage data can be used to discriminate among these different transfer modes. However, the current and voltage data are also dependent on the characteristic of the welding power supply.
DOE

N91-16378# Oak Ridge National Lab., TN.
OPTIMAL POSITIONING OF REDUNDANT MANIPULATOR-PLATFORM SYSTEMS FOR MAXIMUM TASK EFFICIENCY
Francois G. Pin and Jean-Christophe Culioli 1990 8 p Presented at the ISRAM '90: International Symposium on Robotics and Automation, Vancouver, British Columbia, 18-20 Jul. 1990
(Contract DE-AC05-84OR-21400)
(DE90-011061; CONF-900780-3) Avail: NTIS HC/MF A02

Mobile manipulators are attracting significant interest in the industrial, military and public service communities because of the potential they provide for increased efficiency in material handling and manipulation tasks. Corresponding interest has arisen in the robotic research community since the combination and coordination of the mobility of an autonomous platform with the robotic motion of a manipulator introduce complex problems. This paper focuses on a subset of these problems, namely the utilization of the redundancy occurring in most mobile manipulators to optimize their initial positioning and configuration in the accomplishment of given tasks. Optimization schemes are developed for cases when force and position constraints are applied at the end-effector. Various optimization criteria are investigated for optimizing the position of the platform and the configuration of the manipulator with respect to obstacle avoidance, maneuverability and several torque functions. Sample results are presented for a system involving a three-link manipulator on a mobile platform. The various optimization schemes are discussed and compared, and several directions including multi-criteria optimization, tunneling algorithms, and minimax optimization are outlined for further extensions of the methods to the general problem of optimal positioning and configuring of redundant robotic systems with combined mobility and manipulation capabilities.
DOE

N91-16379*# Oak Ridge National Lab., TN.
DESIGN OF A TELEROBOTIC CONTROLLER WITH JOINT TORQUE SENSORS USING 2-PORT NETWORK THEORY
J. F. Jansen and J. N. Herndon 1990 9 p Presented at the 3rd International Symposium on Robotics and Automation, Vancouver, British Columbia, 18-20 Jul. 1990 Sponsored by NASA. Langley Research Center
(Contract DE-AC05-84OR-21400)
(NASA-CR-186543; NAS 1.26:186543; DE90-011389; CONF-900780-5) Avail: NTIS HC/MF A02 CSCL 13I

The purpose of this paper is to show how to design a joint controller for a telerobotic system when joint torque sensors are available based on 2-port network theory. Mechanical manipulators with high levels of friction are assumed in this study. Very high levels of friction for the master have been reduced using high-gain feedback while avoiding limit cycles. Finally, the results are applied to a telerobotic system built for NASA and called the laboratory telerobotic manipulator (LTM).
DOE

N91-16380# Sandia National Labs., Albuquerque, NM.
EXPERIMENTAL VERIFICATION OF PHYSICAL MODEL OF PULSED LASER WELDING
J. L. Jellison and D. M. Keicher 1990 9 p Presented at the Modeling of Casting, Welding and Advanced Solidification Processes Engineering Foundation Conference, Davos, Switzerland, 16-21 Sep. 1990
(Contract DE-AC04-76DP-00789)
(DE91-000025; SAND-90-0449C; CONF-9009258-1) Avail: NTIS HC/MF A02

Whereas most experimental and theoretical studies of the role of convection in fusion welding have been concerned with continuous heat sources, a pulsed heat source is the focus of this study. This is primarily an experimental study of the pulsed Nd:YAG laser welding of austenitic stainless steels.
DOE

N91-16381# Martin Marietta Space Systems, Inc., Denver, CO. Dept. of Research and Technology.
LARGE SPACE MANIPULATORS STUDY Final Report, May 1988 - May 1990
Eric Schmitz and Madison Ramey Jun. 1990 59 p

(Contract F49620-88-C-0037)
(AD-A227276; MCR-90-513; AFOSR-90-1031TR) Avail: NTIS HC/MF A04 CSCL 22/1

The derivation of nonlinear dynamic models for a simple 3-D articulated, elastic structure is discussed. Kane's dynamics equations are used to obtain equations of motion is closed form; the bending deformations of the elastic links, modelled as slender elastic beams, are described with the assumed-modes method. A 2-D planar version of the dynamic model is used to predict the dynamic behavior of an experimental, articulated two-link elastic structure. Both links consist of thin elastic beams with rectangular cross section. The outer link has a tip payload of variable mass and moment of inertia. The structure is instrumented with position/rate acceleration sensors mounted at the articulations and at the end-point; strain gauges are mounted along the links at several locations. Close agreement between the analytical predictions and the experimental measurements is documented for modal tests and for slew maneuvers of the structure. The design and implementation of several digital compensators to actively control the single elastic beam as well as the 2-DOF elastic structure are presented. The compensators are obtained using classical design techniques and the Linear Quadratic Gaussian/Loop Transfer Recovery (LQG/LTR) method. GRA

N91-16382# Implant Sciences Corp., Danvers, MA.
WEAR MEASUREMENT OF CERAMIC BEARINGS IN GAS TURBINES Final Report, Aug. 1989 - Mar. 1990
A. J. Armini and S. N. Bunker Mar. 1990 58 p
(Contract F33615-89-C-2942; AF Proj. 3005)
(AD-A227505; WRDC-TR-90-2078) Avail: NTIS HC/MF A04 CSCL 13/9

The objective was to determine the feasibility of measuring ceramic bearing wear in real time. The method chosen is to selectively introduce a radioactive tag into the surface of a ceramic part and to measure the wear amount by monitoring the strength of the tagging activity as the test progresses. Although this method has been used for many years in the automobile and heavy machinery industries, it has not yet been used to measure the extremely minute amounts of wear which are experienced by ball bearings. This program was analytical in nature, and its principal task was to show the feasibility and accuracy of such a technique applied to Si3N4 and SiC ceramic bearing components. In addition the goal was to develop the analytical theory and operational techniques needed for wear tests. GRA

N91-16383# Rock Island Arsenal, IL. Science and Engineering Directorate.
MANUFACTURING GUIDE FOR ELASTOMERIC SEALS Final Report
Frank B. Testroet 27 Dec. 1989 40 p
(AD-A227511; SE-90-04) Avail: NTIS HC/MF A03 CSCL 11/10

Elastomeric seals used in gun mounts have a hard to achieve combination of properties, so acceptable seals are difficult to procure and few sources are available. Therefore, two rubber formulations were developed, each for a different hydraulic oil, with the intention of providing the manufacturing data to U.S. Government activities and potential vendors. As in-house Army fabrication capability is needed for the seal kit for the M140 gun mount, polytetrafluoroethylene (PTFE) tubes and cloth filled phenolic sheet were procured for back up rings in the kit. Subsequent gymnastication demonstrated Rock Island Arsenal has the capability of fabricating all the seals in the kit according to the technical data. For improved producibility and storage and lower cost, nylon filled phenolic and polyester thermoplastic back up rings were fabricated to replace the phenolic and PTFE, respectively. GRA

N91-16384# National Aerospace Lab., Tokyo (Japan).
DETECTION OF SOLID LUBRICANT FILM FAILURE DURING SLIDING BY VIBRATION MONITORING
Mineo Suzuki, Makoto Nishimura, and Hiroshi Sagawa Mar. 1990 29 p
(NAL-TR-1060; ISSN-0389-4010) Avail: NTIS HC/MF A03

Pin-on-disk friction tests were carried out to examined the feasibility of acceleration vibration monitoring for detection of solid lubricant film failure during sliding. MoS2 sputtered film on a steel disk and on a Si3N4 disk, and MoS2 bonded film on a steel disk were rubbed against a 440C steel ball. From the measured acceleration vibration signal, kurtosis of amplitude distribution and rms were calculated, and frequency analysis was made. A partial failure of sputtered MoS2 film can be clearly detected by the increase in kurtosis. A high value of kurtosis is due to an impulse-like shock imposed by a pin/substrate contact. At the same time, the rms, the component of natural frequency of pin bending mode and the component of disk rotating frequency of envelope detected signal also increased. The changes were small, indicating that these parameters were not relevant to detection of partial film failure. However, a marked increase of these parameters was observed as film failure progressed. These parameters are effective for detection of complete film failure. For MoS2 bonded film, many small metal contacts were observed from the initial stage of the test. The wear process seems to be different with bonded MoS2 film. The appearance of a vibration wave was also different from that of a sputtered film; more continuous shocks seem to excite the arm. This leads to a lower value of kurtosis, thus resulting in effectiveness of kurtosis. However, the film failure can be detected by monitoring the rms value. Author

N91-16385*# Oak Ridge National Lab., TN. Robotics and Process Systems Div.
NASA LABORATORY TELEROBOTIC MANIPULATOR CONTROL SYSTEM ARCHITECTURE
J. C. Rowe, P. L. Butler, R. L. Glassell, and J. N. Herndon 1991 9 p Presented at the 4th Topical Meeting on Robotics and Remote Systems, Albuquerque, NM, 24-28 Feb. 1991 Sponsored in part by NASA
(Contract DE-AC05-84OR-21400)
(NASA-CR-187751; NAS 1.26:187751; DE91-002880; CONF-910223-2) Avail: NTIS HC/MF A02 CSCL 13I

In support of the National Aeronautics and Space Administration (NASA) goals to increase the utilization of dexterous robotic systems in space, the Oak Ridge National Laboratory (ORNL) has developed the Laboratory Telerobotic Manipulator (LTM) system. It is a dexterous, dual-arm, force reflecting teleoperator system with robotic features for NASA ground-based research. This paper describes the overall control system architecture, including both the hardware and software. The control system is a distributed, modular, and hierarchical design with flexible expansion capabilities for future enhancements of both the hardware and software. DOE

N91-16386*# Massachusetts Inst. of Tech., Cambridge. Artificial Intelligence Lab.
THE PHD: A PLANAR, HARMONIC DRIVE ROBOT FOR JOINT TORQUE CONTROL M.S. Thesis
Bruce Robert Thompson Jul. 1990 115 p Sponsored by NASA, Goddard Space Flight Center
(Contract N00014-86-K-0685)
(NASA-CR-187924; NAS 1.26:187924; AD-A228691; AI-TR-1247) Avail: NTIS HC/MF A06 CSCL 13/9

Many efforts are underway to extend the abilities of robots into the domain of space, where they can be used to perform simple tasks in environments where it is difficult or dangerous for humans to work. One such effort, the flight telerobotic servicer (FTS) is being undertaken for NASA by Martin Marietta. The FTS is a two arm manipulator system mounted on a mobile platform. A third arm is used to anchor the platform while working. The two manipulators on the FTS are seven degree of freedom arms which will be used to perform a variety of tasks. MIT was contracted, in conjunction with the University of Iowa, to build an accurate simulation of a seven degree of freedom manipulator similar to that proposed for the FTS. This thesis documents the development of that model. In order to perform some tasks, the FTS will need some sort of force control ability. To assist in the development of

that ability a robot, the PHD, was designed and built with the capability to be used for two purposes. First, it can be used to perform research on joint torque control schemes, and second it can be used to determine the important dynamic characteristics of the harmonic drive gear reducer. The PHD, is a planar, three degree of freedom arm with torque sensors integral to each joint allowing joint torque feedback to be implemented. Preliminary testing using the PHD has shown that a simple linear spring model of the harmonic drive's flexibility is suitable in many situations.
GRA

N91-16387# Rochester Univ., NY. Dept. of Computer Science.
REAL-TIME VERGENCE CONTROL FOR BINOCULAR ROBOTS
Thomas J. Olson and David J. Coombs Jun. 1990 37 p
(Contracts N00014-82-K-0193; DACA76-85-C-0001)
(AD-A228817; TR-348) Avail: NTIS HC/MF A03 CSCL 17/5

In binocular systems, vergence is the process of adjusting the angle between the eyes (or cameras) so that both eyes are directed at the same world point. Its utility is most obvious for foveate systems such as the human visual system, but it is a useful strategy for non-foveate binocular robots as well. This paper discusses the vergence problem and outlines a general approach to vergence control, consisting of a control loop driven by an algorithm that estimates the vergence error. As a case study this approach is used to verge the eyes of the Rochester Robot in real time. Vergence error is estimated with the cepstral disparity filter. The cepstral filter is analyzed, and it is shown in this application to be equivalent to correlation with an adaptive prefilter; carrying this idea to its logical conclusion converts the cepstral filter into phase correlation. The demonstration system uses a PD controller in cascade with the error estimator. An efficient real-time implementation of the error estimator is discussed, and empirical measurements of the performance of both the disparity estimator and the overall system are presented. GRA

N91-16388# Federal Railroad Administration, Washington, DC.
MOVING AMERICA; NEW DIRECTIONS, NEW OPPORTUNITIES: ASSESSMENT OF THE POTENTIAL FOR MAGNETIC LEVITATION TRANSPORTATION SYSTEMS IN THE UNITED STATES
Jun. 1990 143 p
(PB91-104596) Avail: NTIS HC/MF A07 CSCL 13F

This supplement to the report to Congress includes a more detailed discussion of technological, economic, and legal issues involved in advancing a U.S. maglev system. A glossary of terms and a bibliography are included. Author

N91-16389 Iowa State Univ. of Science and Technology, Ames.
MODELING AND CONTROL OF A TWO-ARM ELASTIC ROBOT IN GRAVITY Ph.D. Thesis
Chaeyoun Oh 1990 164 p
Avail: Univ. Microfilms Order No. DA9100490

A model of a two arm robot with highly elastic arms is developed and experimentally verified. The model is later used in this research to evaluate control algorithms. The model includes the effects of gravity. The dimensions of the arms are chosen to maximize the coupling between the flexible and large scale motion of the robot. The model is then linearized and a new analytical solution is presented for the natural frequencies and mode shapes of the robot at given equilibrium positions. This analytical solution is then compared to the assumed mode shape solutions to determine the accuracy relative to the number of assumed modes included in the model. An experimental test rig is built and tests are conducted to verify the model. A number of different amounts of end mass and torsional stiffness at the joints are used during the validation. For 12 cases tested, the measured first four natural frequencies are within +/- 7 percent of the frequencies predicted by the model with an average error of only 2.89 percent. Finally, the model is used to design a control algorithm for end effector control of the robot using a torque input at each of the two joints. An optimal control algorithm developed using a linear quadratic regulator (LQR) with the prescribed degree of stability method results in effective end effector control with short response time and little overshoot. Dissert. Abstr.

N91-16390 Iowa State Univ. of Science and Technology, Ames.
CAMERA SPACE MANIPULATION OF A MOBILE ROBOT Ph.D. Thesis
Issac Yalda-Mooshabad 1990 146 p
Avail: Univ. Microfilms Order No. DA9035128

The method of camera space manipulation is applied to accomplish positioning of the mobile robot's end effector. First, the method is developed and illustrated experimentally with a point placement task. This is done using a sequential estimation scheme which permits placement of a point on the end effector relative to a target point in each of the two-dimensional image planes of a minimum of two monitoring cameras, resulting in a precise manipulation strategy that is compatible with real time. Then, the method is generalized to rigid-body placement. This requires the placement of points on the end effector (or the object in its grasp) of an n-degree-of-freedom manipulator relative to another body where the wheels on the mobile manipulator are included among these degrees of freedom. Although the experimental point placement illustrations make use of a very simple trajectory planning scheme for the wheels of the base, a smoother, optimal trajectory planning scheme which makes use of the Pontryagin maximum principle is also developed and illustrated. Dissert. Abstr.

N91-16391 Oregon State Univ., Corvallis.
KINEMATICS OF ARTHROPOD LEGS: MODELING AND MEASUREMENT Ph.D. Thesis
Stephen Lawrence Albright 1990 187 p
Avail: Univ. Microfilms Order No. DA9032644

A method for determining the kinematic geometry of arthropod legs is presented. A kinematic description makes the analysis of arthropod leg motion possible as a prelude to investigating how various arthropod species are able to negotiate diverse terrains. Such knowledge will aid in design of legged vehicles. The focus is on three areas: leg modeling; leg measurement for model-parameter determination; and effects of model-parameter accuracy. Three characteristics are considered important to arthropod leg modeling. The model must show proportionality to differences in leg geometry, physically resemble the leg being modeled, and be adaptable to various joint types found in arthropods. In successfully addressing all these concerns, the model presented in this work is an improvement over other available models. Measuring the small arthropod leg requires specialized equipment design and measurement technique. A microscope mounted over a positioner which measures three translations and two rotations makes it possible to determine position, orientation, and range-of-motion of each successive joint. Model parameters are calculated from these measurements. Measurement errors in positioning equipment are quantified. A technique for representing these measurement errors as errors in the position and orientation of each joint axis is presented. Joint axis errors are superposed to form an error volume surrounding the foot position. Foot-position error can be used to evaluate accuracy of leg-model parameters computed from the measurement method. This technique was used to measure the right middle leg of a darkling beetle and proved to be an effective tool for quantifying kinematic parameters of a small articulated biological mechanism. Such methods may also prove useful for measuring small engineering mechanisms.
Dissert. Abstr.

N91-16392# Warwick Univ., Coventry (England). Dept. of Engineering.
A HYDRAULICALLY DRIVEN MICRODISPLACEMENT UNIT
Hu Jianhua and D. G. Chetwynd Jun. 1987 9 p
(ME-56; ETN-91-98574) Avail: NTIS HC/MF A02

A high stiffness, small range displacement device can be constructed, in which the active element of the mechanical drive loop is reduced to a single metal member which changes dimension elastically under the action of hydrostatic pressure. A very simple design of such a device was constructed to demonstrate that the principle of operation is sound. Its initial evaluation is described.

Simple tests indicate behavior close to theoretical expectations. It is concluded that the idea is worthy of further study involving more nearly optimal designs and fuller evaluation. ESA

38 QUALITY ASSURANCE AND RELIABILITY

Includes product sampling procedures and techniques; and quality control.

N91-16393# Pacific Northwest Lab., Richland, WA.
PROCEDURES FOR QUALITY ASSURANCE PROGRAM
R. L. Schaub and D. E. Ryder Dec. 1989 384 p
(Contract DE-AC06-76RL-01830)
(DE90-010001; PNL-MA-70-VOL-1) Avail: NTIS HC/MF A17

These administrative procedures were developed to implement the quality assurance program described in PNL-MA-70, Quality Assurance Manual. The manual and procedures establish requirements, responsibilities, and methods for execution of the program consistent with U.S. Department of Energy (DOE) policies and requirements. When specified by a QA Plan, a Statement of Work or other governing document, PNL activities affecting quality shall be performed in accordance with the administrative procedures. The procedures are controlled documents assigned to the person named on the cover sheet. The assignee is responsible for maintaining the procedures in an up-to-date condition, consistent with Controlled Document Lists, by incorporating subsequent changes or new procedures promptly as they are issued. These procedures shall be available and used at the location where the prescribed activity is performed. A Controlled Document List (CDL) for each type of administrative procedure is included for use as a table of contents. The CDL lists procedure numbers, titles, revisions and/or amendments and the effective date. Work shall be performed in accordance with the latest effective procedure revision and/or amendment identified in the CDL unless a Controlled Document Transmittal Record (CDT/R), a QA Plan, or a Statement of Work allows or requires otherwise. This document is Volume 1 of a two volume set. DOE

N91-16394# Sandia National Labs., Albuquerque, NM.
STATISTICAL PROCESS CONTROL FOR QML (QUALIFIED MANUFACTURER'S LIST) RADIATION HARDNESS ASSURANCE
P. S. Winokur, F. W. Sexton, D. M. Fleetwood, J. R. Schwank, M. R. Shaneyfelt, and M. D. Terry 1990 4 p Presented at the 27th IEEE Annual International Nuclear and Space Radiation Effects Conference, Reno, NV, 16-20 Jul. 1990
(Contract DE-AC04-76DP-00789)
(DE90-007413; SAND-90-0368C; CONF-900723-5) Avail: NTIS HC/MF A01

Effective testing of highly-complex VLSI circuits employing ever decreasing feature sizes is becoming extremely difficult. This difficulty arises from the inability to routinely provide 100 percent fault coverage during testing of these complex functions, as well as by a scarcity of functional parts inherent in low volume high product mix military component manufacturing lines. Under the sponsorship of RADC and DESC, the government has proposed a Qualified Manufacturer's List (QML) methodology to qualify ICs for high reliability and radiation hardness. In this approach, a production line is certified on a one time basis, and all product from that line is subsequently qualified per the requirements of MIL-STD-38535. The approach places a large burden on the manufacturer or production source, who is tasked with demonstrating that the quality of the part is built in, as opposed to being tested in. This built-in quality is assured by the proper control of the IC manufacturing sequence from design through assembly. DOE

N91-16395# Edgerton, Germeshausen and Grier, Inc., Idaho Falls, ID.
LIVING PRAS (PROBABILISTIC RISK ANALYSIS) MADE EASIER WITH IRRAS (INTEGRATED RELIABILITY AND RISK ANALYSIS SYSTEM)
K. D. Russell, M. B. Sattison, and D. M. Rasmuson (Nuclear Regulatory Commission, Washington, DC.) 1989 33 p Presented at the 10th International Conference on Structural Mechanics in Reactor Technology (SMIRT), Anaheim, CA, 14-18 Aug. 1989
(Contract DE-AC07-76ID-01570)
(DE90-010938; EGG-M-89329; CONF-890855-60) Avail: NTIS HC/MF A03

The Integrated Reliability and Risk Analysis System (IRRAS) is an integrated PRA software tool that gives the user the ability to create and analyze fault trees and accident sequences using an IBM-compatible microcomputer. This program provides functions that range from graphical fault tree and event tree construction to cut set generation and quantification. IRRAS contains all the capabilities and functions required to create, modify, reduce, and analyze event tree and fault tree models used in the analysis of complex systems and processes. IRRAS uses advanced graphic and analytical techniques to achieve the greatest possible realization of the potential of the microcomputer. When the needs of the user exceed this potential, IRRAS can call upon the power of the mainframe computer. The role of the Idaho National Engineering Laboratory of the IRRAS program is that of software developer and interface to the user community. Version 1.0 of the IRRAS program was released in February 1987 to prove the concept of performing this kind of analysis on microcomputers. This version contained many of the basic features needed for fault tree analysis and was received very well by the PRA community. Since the release of Version 1.0, many user comments and enhancements have been incorporated into the program providing a much more powerful and user-friendly system. This version is designated IRRAS 2.0. Version 3.0 will contain all of the features required for efficient event tree and fault tree construction and analysis. DOE

N91-16396# National Aerospace Lab., Tokyo (Japan).
APPLICATION OF FUZZY-BAYESIAN ANALYSIS TO STRUCTURAL RELIABILITY
Seiichi Ito and Hiroshi Itagaki May 1990 21 p In JAPANESE; ENGLISH summary
(NAL-TR-1063; ISSN-0389-4010) Avail: NTIS HC/MF A03

The purpose is to develop a fuzzy-Bayesian approach for decisions on the proper inspection schedule needed to maintain structural reliability. It is pointed out that subjective information is often given in inspection results because of the fuzzy environment which arises from the inspectors' judgement. Therefore, it is difficult to make use of the fuzzy information under conventional statistical theories. Here, an attempt is made to investigate the fuzzy information expressed in terms of linguistic variables and to consider the fuzzified Bayes' theorem in order to obtain posterior probability from the information. According to this approach, a priori uncertain parameters are estimated from the data collected during in-service inspections. Numerical examples are presented to demonstrate the effectiveness of fuzzy information which is useful for maintaining structural integrity. Author

39 STRUCTURAL MECHANICS

Includes structural element design and weight analysis; fatigue; and thermal stress.

For applications see *05 Aircraft Design, Testing and Performance* and *18 Spacecraft Design, Testing and Performance.*

N91-16397# Oak Ridge National Lab., TN.
TEST METHODS FOR EVALUATING HOT CRACKING: REVIEW AND PERSPECTIVE
G. M. Goodwin 1990 26 p Presented at the 1st US-Japan Symposium on Advances in Welding Metallurgy, San Francisco,

CA, 12-13 Jun. 1990; 7-8 Jun. 1990
(Contract DE-AC05-84OR-21400)
(DE90-009820; CONF-9006162-2; CONF-9006149-2) Avail: NTIS HC/MF A03

The phenomenon of hot cracking is described and discussed, and criteria for tests to assess hot cracking are elucidated. The historical development of hot cracking tests is traced from the 1930s to present with categorization of tests into several types. It is noted that the number of tests developed continues to increase dramatically. The number of literature citations also increases with time, with few popular tests receiving a major share of interest. Predominant countries of origin of both tests and citations shift with time, and a few journals account for most of the published information. Reviews of hot cracking are reviewed, and it is predicted that modeling and other developing analytical techniques will contribute greatly to an increased understanding of hot cracking. DOE

N91-16398# Argonne National Lab., IL. Reactor Safety and Analysis Div.
STUDY OF THE INFLUENCE OF IMPERFECTIONS ON THE DYNAMIC STABILITY OF TANKS
Rasim Aziz Uras, Wing Kam Liu, and Yi-Jung Chen (Northwestern Univ., Evanston, IL.) 1990 9 p Presented at the Pressure Vessels and Piping Conference, Nashville, TN, 17-21 Jun. 1990
(Contract W-31-109-eng-38; NSF CES-86-14957)
(DE90-011094; CONF-900617-15) Avail: NTIS HC/MF A02

The influence of geometrical imperfections on the dynamic stability of liquid-filled shells under horizontal ground excitation is studied. Some basic concepts in the large deformation and large deformation thin shell theory are recalled. The work done by inertial and internal forces are given in the Gaussian surface coordinate system. A general imperfection pattern in the circumferential direction is introduced. The emphasis is particularly dedicated to the analysis of the geometrical stiffness term. Different patterns are studied to explain the occurrence of additional instability regions. DOE

N91-16399# Oak Ridge National Lab., TN. Metals and Ceramics Div.
SPECIMEN SIZE EFFECTS IN CHARPY IMPACT TESTING
David J. Alexander and Ronald L. Klueh 1989 13 p Presented at the Symposium on Charpy Impact Test: Factors and Variables, Orlando, FL, 8-9 Nov. 1989
(Contract DE-AC05-84OR-21400)
(DE90-011369; CONF-8911193-1) Avail: NTIS HC/MF A03

Full-size, half-size, and third-size specimens from several different steels have been tested as part of an ongoing alloy development program. The smaller specimens permit more specimens to be made from small trail heats and are much more efficient for irradiation experiments. The results of several comparisons between the different specimen sizes have shown that the smaller specimens show qualitatively similar behavior to large specimens, although the upper-shelf energy level and ductile-to-ductile transition temperature are reduced. The upper-shelf energy levels from different specimen sizes can be compared by using a simple volume normalization method. The effect of specimen size and geometry on the ductile-to-ductile transition temperature is more difficult to predict, although the available data suggest a simple shift in the transition temperature due to specimen size changes. The relatively shallower notch used in smaller specimens alters the deformation pattern, and permits yielding to spread back to the notched surface as well as through to the back. This reduces the constraint and the peak stresses, and thus, the initiation of cleavage is more difficult. A better understanding of the stress and strain distributions is needed. DOE

N91-16400 Cleveland State Univ., OH.
A MODULAR STIFFNESS-BASED APPROACH TO ROTATING SYSTEMS ANALYSIS Ph.D. Thesis
John Walter Spring 1990 84 p
Avail: Univ. Microfilms Order No. DA9026936

The primary product is the creation of an improved methodology to analyze rotating systems. The framework of this technique is implemented by the ROTATE computer program. It was designed to provide maximum flexibility in program development and in its application to engineering problems. All six degrees-of-freedom are retained at each node in order to include related translational and bending effects. The program's modular structure facilitates the addition or replacement of component models and solution techniques to suit the particular needs of each individual researcher or analyst. Each program module provides a distinct function, so that any may be readily replaced with an improved algorithm, or alternative techniques may be included in the program with modifications needed only in the calling routines. Another major feature of the approach is its emphasis on making the component descriptions logical and easy to input. Unlike existing structural analysis finite element programs, which require the input of computed element properties such as inertia and stiffness, this system uses the physical dimensions of the actual parts to compute the element properties directly. Modules were developed for the more common components present in rotating systems to demonstrate program capabilities. Solution routines taken from STAP and SAP4 finite element programs were implemented. Program accuracy was verified by comparison to results obtained from other finite element programs, and from other calculations. The ROTATE program provides an integrated problem solving environment which can be used to quickly determine the behavior of a system of rotating parts without prior hand calculation of element properties. This system permits the creation of better designs because incremental and minor design modifications can be quickly evaluated. Dissert. Abstr.

N91-16401 California Inst. of Tech., Pasadena.
TIME-TEMPERATURE RESPONSE OF MULTIPHASE VISCOELASTIC SOLIDS THROUGH NUMERICAL ANALYSIS Ph.D. Thesis
Lynda Catherine Brinson 1990 147 p
Avail: Univ. Microfilms Order No. DA9031436

A numerical model was constructed for the study of the properties of multiphase viscoelastic composites. The model utilizes the dynamic correspondence principle of viscoplasticity in a finite element program to solve boundary value problems simulating uniaxial tension or simple shear and obtains the global complex Young's or shear moduli of the composite. Each phase of the composite is considered to be thermorheologically simple. The resulting modulus properties of the composite however, are thermorheologically complex and the nature of time-temperature behavior of multiphase composite materials is examined. The specific composite considered contains viscoelastic inclusions embedded in a different viscoelastic matrix material. The deviation of the composite moduli from thermorheologically simple behavior of the matrix material is shown to occur at frequencies and temperatures where the glass-to-rubber transition of the included phases are reached. Properties of polystyrene and polybutadiene are used to investigate the thermorheological complexity (non-shiftability) of a Styrene Butadiene Styrene (SBS) block copolymer. To achieve congruence of the results with experimental data, it is necessary to consider a transition phase of properties intermediate to those of styrene and butadiene. Using accurate physical information on the individual phase properties and on the interphase region, it is possible to utilize the numerical model to predict long term properties of multi-phase composites from short term laboratory data. Lacking detailed information on the properties of a particular phase, but knowing the time dependent properties for the composite material at a broad range of temperatures, it is also possible to use the numerical tool to solve an inverse problem and determine the unknown properties of the phase in question. Dissert. Abstr.

N91-16402 California Inst. of Tech., Pasadena.
DYNAMIC CRACK PROPAGATION IN ELASTIC-PLASTIC SOLIDS Ph.D. Thesis
Xiaomin Deng 1990 308 p
Avail: Univ. Microfilms Order No. DA9031446

The present finite element study addresses several issues of interest pertaining to the phenomenon of dynamic crack propagation in elastic-plastic solids. Three classes of materials, namely elastic-perfectly plastic materials, linear hardening materials, and power-law hardening materials, are considered. The materials are assumed to obey the von Mises yield criterion and the associated flow rule. Under conditions of mode 1, plane stress, steady state, and small scale yielding, the structures of the near-tip stress and deformation fields were investigated. A preliminary asymptotic analysis for crack-tip stress and velocity fields in elastic-perfectly plastic solids was provided to reveal and explain some special features of the crack-tip fields observable only in the case of rapid crack propagation. The theoretical basis of a fracture criterion was studied based on the dynamic stress intensity factor for crack growth in materials which fail in a locally ductile manner. The behavior of crack-tip fields was explored under non-K-dominance conditions and its effects on dynamic fracture toughness vs. crack propagation speed relationship. An Eulerian finite element scheme is employed. Finite element meshes with extremely small elements near the crack tip are carefully designed. The ratio of the crack-tip plastic zone size to that of the element nearest to the crack tip is of the order of 1.6 x 10(exp 4). In order to overcome numerical difficulties associated with crack-tip strain singularities and the use of small near-tip elements, an efficient stress integration algorithm is devised. The existing stress state determination procedure is modified to prevent the occurrence of negative plastic flow and to avoid mistakenly treating elastic unloading as plastic flow. The above measures are proven to be essential for the convergence of the numerical solution.

Dissert. Abstr.

N91-16403 Missouri Univ., Rolla.
FINITE ELEMENT SOLUTION OF STEADY STATE AXISYMMETRIC PENETRATION PROBLEMS Ph.D. Thesis
Thulasiram Gobinath 1990 98 p
Avail: Univ. Microfilms Order No. DA9032103

Steady state axisymmetric deformations of a homogeneous, isotropic, compressible and rigid perfectly plastic target being penetrated by a rigid cylindrical penetrator with a hemispherical nose are studied by the finite element method. Contact between the penetrator and the target is assumed to be smooth. The effect of compressibility of the material delineated by comparing results for compressible and incompressible materials. Also studied is the effect of the penetrator speed on the target deformations. Steady state axisymmetric deformations of a deformable penetrator striking a deformable thick target are analyzed by the finite element method. Both the target and penetrator are assumed to be made of rigid/perfectly plastic materials and the contact between them is assumed to be smooth. The shape of the deformed penetrator, which involves determining two a-priori unknown surfaces, one the target/penetrator interface and the other free surface of the penetrator flowing rearward, was computed. Results computed and presented graphically include the distribution of the velocity field, the hydrostatic pressure and the second invariant of the strain rate tensor. The work is extended to the case when the rod and target materials are viscoplastic and exhibit strain rate hardening and thermal softening. The dependence of the location and shapes of the free and intermediate surfaces and the distribution of normal tractions on the intermediate surface on parameters such as strain-rate hardening exponent, the speed of the stagnation point, and the thermal softening coefficient was also determined. Also the histories of the stress, temperature, second invariant of strain-rate tensor and the plastic spin for four penetrator and two target particles are computed. Dissert. Abstr.

N91-16404 Oklahoma Univ., Norman.
DIRECT DISC IMPACT INVESTIGATION OF DYNAMIC LARGE FINITE PLASTIC BEHAVIOR OF 1100 ALUMINUM Ph.D. Thesis
Sujian Huang 1990 171 p
Avail: Univ. Microfilms Order No. DA9033282

A numerical analysis using finite difference method is performed to solve a problem with historical controversy on the sensitivity of measured strain histories to the constitutive models and the material constants in the model. Special attention is paid to the large finite deformation. Two viscoplastic models, proposed by Malvern and Chalupnik, are studied and it was shown that the strain histories are very sensitive to different models and the material constants in the model, especially in the case of large finite strains. A Direct Disc Impact technique is introduced. This technique uses only one hard transmitted bar to infer the stress in the specimen, while the strains in the specimen are directly measured using strain gages bonded to it. The use of strain gages for measuring finite dynamic plastic strains is investigated in detail and the problem of variation of the strain gage factor with strain was solved by both dynamic and quasi-static experiments. A linear relation between the gage factor and strain was established. The Direct Disc Impact technique is used to study the mechanical behavior of fully annealed 1100 aluminum and 1100-0 aluminum at high strain rates, while a MTS system is used to obtain the stress-strain curves of 1100-0 aluminum at low strain rates. The experimental results show that fully annealed 1100 aluminum is negligibly strain rate sensitive and its behavior at high strain rates can be described by Bell's parabolic law, while 1100-0 aluminum is quite strain rate sensitive and a rate-dependent theory has to be used to describe its behavior. Bodner-Partom model is then used to predict the experimental results. It was found that this model can not accurately describe the work-hardening behavior and can only predict the strain rate sensitivity in a limited range for 1100-0 aluminum. A new viscoplasticity model is then proposed which can predict the experimental results in a very large strain rate range, including the high work-hardening region which the Bodner-Partom model is unable to predict. Dissert. Abstr.

N91-16405 Alabama Univ., Huntsville.
NEW METHODS FOR PRODUCING, RECORDING, AND PROCESSING INTERFEROMETRIC MOIRE PATTERNS Ph.D. Thesis
Helen Sue Johnson 1990 170 p
Avail: Univ. Microfilms Order No. DA9032138

Moire interferometry is a highly sensitive full-field optical method useful for measurement of surface displacement. In prior research, a reflective phase-type sinusoidal grating was generated interferometrically and transferred to a specimen. This grating, which exhibits only first order diffraction, was produced and interrogated using conventional optical components. Displacement patterns were usually recorded using a double exposure technique and fringes were interpreted by eye. Prior research is discussed and new techniques are explored for enhancing the potential of moire interferometry. Fiber optics are introduced to produce a grating mold and to measure deformations with moire interferometry. The deformations are monitored in real-time using a technique which employs a thermoplastic device to holographically record phase information. The technique is applied to study deformations in a notched beam subjected to three point bending. The capabilities of moire interferometry are further expanded when gratings which produce multiple diffraction orders are generated using micro-optical lithography. Generalized expressions are derived which show that customized gratings produced by micro-optical lithography can be used to vary sensitivity for displacement measurement. Experimental tests are conducted to verify these arguments and an analysis of grating profiles is performed to establish diffraction efficiency in each diffraction order. Finally, an automated approach for measuring surface deformation using moire interferometry is described. The method relies on the introduction of a carrier fringe pattern to achieve fringe linearization, and the application of image digitization and computer analysis to determine the magnitude and direction of a specific displacement component. Dissert. Abstr.

N91-16406 Illinois Inst. of Tech., Chicago.
ADAPTIVE MESH REFINEMENT FOR MESHES WITH SINGULAR ELEMENTS Ph.D. Thesis
Maria Kaltsouni 1990 204 p
Avail: Univ. Microfilms Order No. DA9032906

A self-adaptive optimization technique was developed for the finite element solution of elliptic boundary-value problems with

singularities. The method was applied on meshes with a layer of singular elements surrounding the singular point as well as meshes with regular elements only. The procedure is based upon a-posteriori bounds of the error in the energy norm generated during an initial finite element solution. These error estimates depend on the elements' residual and on the jump of the normal derivatives of the approximate solution over the elements' boundaries. The error bounds were developed for singular and regular elements. Numerical experiments were performed for one and two dimensional problems, in order to investigate the efficiency of the method. The rate of convergence of the approximate solution in the energy norm was monitored for optimal meshes with or without singular elements as well as for uniform meshes with or without singular elements. From the experimental results it was concluded that the coupling of the optimization procedure with singular elements can produce optimal rates of convergence for the finite element approximation for coarse as well as for fine meshes. The absolute error in the approximation of the stress intensity factor was monitored. From the experimental results, as well as analytical ones, it was concluded that, when the optimization procedure is applied on meshes with singular elements, convergence of the approximate value to the analytical one with a high rate is possible. All other approaches produced approximations to the stress intensity factor, which could not converge to the exact value. Dissert. Abstr.

N91-16407*# National Aeronautics and Space Administration. Langley Research Center, Hampton, VA.

FINITE ELEMENT THERMO-VISCOPLASTIC ANALYSIS OF AEROSPACE STRUCTURES

Ajay K. Pandey, Pramote Dechaumphai, and Earl A. Thornton (Virginia Univ., Charlottesville.) Nov. 1990 23 p Presented at the 1st Thermal Structures Conference, Charlottesville, VA, 13-15 Nov. 1990 Previously announced in IAA as A91-16034

(NASA-TM-102761; NAS 1.15:102761) Avail: NTIS HC/MF A03 CSCL 20K

The time-dependent thermo-viscoplastic response of aerospace structures subjected to intense aerothermal loads is predicted using the finite-element method. The finite-element analysis uses the Bodner-Partom unified viscoplastic constitutive relations to determine rate-dependent nonlinear material behavior. The methodology is verified by comparison with experimental data and other numerical results for a uniaxially-loaded bar. The method is then used (1) to predict the structural response of a rectangular plate subjected to line heating along a centerline, and (2) to predict the thermal-structural response of a convectively-cooled engine cowl leading edge subjected to aerodynamic shock-shock interference heating. Compared to linear elastic analysis, the viscoplastic analysis results in lower peak stresses and regions of plastic deformations. Author

N91-16408# Illinois Univ., Urbana-Champaign. Dept. of Theoretical and Applied Mechanics.

DYNAMIC RESPONSE OF COMPOSITE BEAMS USING SHEAR-DEFORMABLE FINITE ELEMENTS Ph.D. Thesis

Stephen Robert Whitehouse 1990 244 p Sponsored by AFIT, Wright-Patterson AFB, OH

(AD-A227975; AFIT/CI/CIA-90-028D) Avail: NTIS HC/MF A11 CSCL 11/4

The goal of this effort is to develop shear-deformable finite elements which can be used to find the natural frequencies of composite beams. The first objective of the study is to derive the mass and stiffness matrices for the elements of interest and incorporate them into computer programs which can be used to estimate the natural frequencies of composite beams. Composite beams of interest include sandwich beams and those of fiber-reinforced laminated construction. Elements based on the beam theories of Bernoulli-Euler, Timoshenko, Levinson-Bickford, as well as general third-order beam theory are considered. The elements ignore transverse normal strain, coupling between longitudinal and lateral motion caused by Poisson effects, and damping, and are limited to linear, elastic materials. However, both isotropic and orthotropic layers in symmetric and nonsymmetric and configurations can be accommodated. In addition, the elements can impose a kinematic constraint on the entire beam or individual layers within the beam. This study refers to elements which employ the latter approach as stacked elements. GRA

N91-16409# Cornell Univ., Ithaca, NY. Dept. of Structural Engineering.

PROBABILISTIC FRACTURE MECHANICS: A VALIDATION OF PREDICTIVE CAPABILITY Final Report, 4 Jan. 1987 - 30 Dec. 1989

Anthony R. Ingraffea and Mircea Grigoriu Aug. 1990 155 p

(Contract F49620-87-C-0054; AF Proj. 2302)

(AD-A228877; REPT-90-8; AFOSR-90-1074TR) Avail: NTIS HC/MF A08 CSCL 12/5

A two-phase task was undertaken to the probabilistic fracture analysis code (PROFRANC) developed under this project. Phase one consisted in predicting deterministically the outcome of a subset of a larger number of experiments in which variability in geometry and material parameters was purposely minimized. The purpose of this phase was to verify that PROFRANC could predict nearly deterministic events accurately. This phase was shown to be highly successful. This verification was based on experimental results which had to be obtained within this project due to a paucity of comprehensive mixed-mode fracture propagation data in the open literature. In Phase two all currently available data involving inherent uncertainties in some material and geometrical parameters was assembled in a probabilistic framework and subsequently compared to the probabilistic predictions of PROFRANC qualitatively and quantitatively. These comparisons were shown to be very successful. The quantitative comparison was performed by hypothesis testing, which is a mathematical rule deciding whether to except or reject PROFRANC predictions using experimental data. GRA

N91-16410# Massachusetts Inst. of Tech., Cambridge. Dept. of Mechanical Engineering.

VOID NUCLEATION IN NONLINEAR SOLID MECHANICS Final Report, 20 Jan. 1987 - 19 Jul. 1990

Rohan Abeyaratne 1990 28 p

(Contract DAAL03-87-K-0016)

(AD-A228890; ARO-24377.9-EG) Avail: NTIS HC/MF A03 CSCL 20/11

Consider a solid sphere of unit radius subjected to a uniformly-distributed radial tensile traction p on its surface. In response to this loading, the body can expand into a larger solid sphere. However, for certain materials, when p is sufficiently large, it is energetically more favorable for the body to develop an internal spherical cavity. A bifurcation analysis yields the value P(sub cr) of the applied stress at which this instability occurs, without the need for an ad hoc failure criterion. This phenomenon of internal rupture is closely related to the well-known phenomenon of cavitation in fluids; therefore, it has been dubbed 'cavitation' even in solids. Since the nucleation of a void in a stressed solid is often a precursor to failure, it would be useful to be able to predict the conditions under which cavitation occurs. The present project has been aimed at trying to determine whether cavitation, viewed as an intrinsic material instability, provides insight into the phenomenon of void nucleation. The project had two principal goals: (1) to better understand the phenomena of spherically (of cylindrically) symmetric cavitation; and (2) to study the phenomenon of cavitation in circumstances that do not possess such symmetry. GRA

N91-16411*# Old Dominion Univ., Norfolk, VA. Dept. of Civil Engineering.

PASSIVE DAMPING CONCEPTS FOR TUBULAR BEAMS WITH PARTIAL ROTATIONAL AND TRANSLATIONAL END RESTRAINTS Final Report, period ending 20 Sep. 1989

Zia Razzaq and David K. Muyundo Feb. 1991 79 p

(Grant NAG1-336)

(NASA-CR-187833; NAS 1.26:187833) Avail: NTIS HC/MF A05 CSCL 20K

The main objectives of the study are: (1) identification of

potential passive damping concepts for slender tubular structural members with rotational and translational end springs under natural and forced-free vibrations; (2) evaluation of damping efficiencies of the various damping concepts; and (3) evaluation of the suitability of a theoretical finite difference analysis by comparison to the experimental results for the case of natural vibrations. Only member flexural an translation motion is considered. The natural vibration study is conducted on the seven damping concepts and for only one specific initial deflection. The most suitable of the seven dampers is further investigated under forced-free vibrations. In addition only one set of end springs is used for all of the experiments. The results show that passive damping provides a possible approach to structural vibration reduction. Y.S.

N91-16412 Colorado Univ., Boulder.
SCATTERING OF LAMB WAVES IN AN ELASTIC PLATE FOR ULTRASONIC NONDESTRUCTIVE EVALUATION OF WELDMENTS AND CRACKS Ph.D. Thesis
Yaagoub Nassar Al-Nassar 1990 122 p
Avail: Univ. Microfilms Order No. DA9032806

The problem of scattering of guided waves by a defect in an isotropic or anisotropic structure is a basic problem in nondestructive evaluation. The analytical approaches to the problem fail if the plate contains anisotropic welds or flaws of complex geometry. A hybrid numerical technique for analyzing scattering of time harmonic Lamb waves by normal rectangular weldments and surface-breaking cracks is presented. This method combines the finite element discretization and modal representation. In this method, media inhomogeneities are enclosed in a finite region containing the defects. The incident wave is taken to be a single propagating mode. Imposing continuity of displacements and traction forces at the nodal points along the fictitious boundaries separating the inner finite-element region containing the defects from the exterior region, a set of equations is obtained to solve for the unknown coefficients of the modal expansion. Three cases considered here are those of scattering by a normal rectangular weldment, normal surface-breaking cracks, and normal surface-breaking cracks situated in a butt welded plate. The reflection and transmission coefficients are computed for the first two incident wave modes A (sub 0) and S (sub 0). The validity and accuracy of the results are checked by satisfaction of the energy conservation principle. Dissert. Abstr.

N91-16413*# National Aeronautics and Space Administration. Marshall Space Flight Center, Huntsville, AL.
PLATE AND BUTT-WELD STRESSES BEYOND ELASTIC LIMIT, MATERIAL AND STRUCTURAL MODELING
V. Verderaime Washington Jan. 1991 63 p
(NASA-TP-3075; M-654; NAS 1.60:3075) Avail: NTIS HC/MF A04 CSCL 20K

Ultimate safety factors of high performance structures depend on stress behavior beyond the elastic limit, a region not too well understood. An analytical modeling approach was developed to gain fundamental insights into inelastic responses of simple structural elements. Nonlinear material properties were expressed in engineering stresses and strains variables and combined with strength of material stress and strain equations similar to numerical piece-wise linear method. Integrations are continuous which allows for more detailed solutions. Included with interesting results are the classical combined axial tension and bending load model and the strain gauge conversion to stress beyond the elastic limit. Material discontinuity stress factors in butt-welds were derived. This is a working-type document with analytical methods and results applicable to all industries of high reliability structures. Author

N91-16414*# National Aeronautics and Space Administration. Ames Research Center, Moffett Field, CA.
A FINITE ELEMENT PROCEDURE FOR CALCULATING FLUID-STRUCTURE INTERACTION USING MSC/NASTRAN
Mladen Chargin and Otto Gartmeier (Daimler-Benz A.G., Stuttgart, Germany, F.R.) Dec. 1990 168 p Original contains color illustrations
(NASA-TM-102857; A-90262; NAS 1.15:102857) Avail: NTIS HC/MF A08; 6 functional color pages CSCL 20K

This report is intended to serve two purposes. The first is to present a survey of the theoretical background of the dynamic interaction between a non-viscid, compressible fluid and an elastic structure is presented. Section one presents a short survey of the application of the finite element method (FEM) to the area of fluid-structure-interaction (FSI). Section two describes the mathematical foundation of the structure and fluid with special emphasis on the fluid. The main steps in establishing the finite element (FE) equations for the fluid structure coupling are discussed in section three. The second purpose is to demonstrate the application of MSC/NASTRAN to the solution of FSI problems. Some specific topics, such as fluid structure analogy, acoustic absorption, and acoustic contribution analysis are described in section four. Section five deals with the organization of the acoustic procedure flowchart. Section six includes the most important information that a user needs for applying the acoustic procedure to practical FSI problems. Beginning with some rules concerning the FE modeling of the coupled system, the NASTRAN USER DECKs for the different steps are described. The goal of section seven is to demonstrate the use of the acoustic procedure with some examples. This demonstration includes an analytic verification of selected FE results. The analytical description considers only some aspects of FSI and is not intended to be mathematically complete. Finally, section 8 presents an application of the acoustic procedure to vehicle interior acoustic analysis with selected results. Author

42 GEOSCIENCES (GENERAL)

No abstracts in this category.

43 EARTH RESOURCES AND REMOTE SENSING

Includes remote sensing of earth resources by aircraft and spacecraft; photogrammetry; and aerial photography.

For instrumentation see *35 Instrumentation and Photography.*

N91-16415 Purdue Univ., West Lafayette, IN.
MAGSAT INVESTIGATIONS OVER THE GREATER AFRICAN REGION Ph.D. Thesis
Dhananjay Narendra Ravat 1989 256 p
Avail: Univ. Microfilms Order No. DA9018887

A high-resolution, wide-band Magsat total intensity magnetic anomaly map of the greater African region was prepared that is useful for constraining regional geologic and tectonic interpretations. Magnetic anomaly discrepancies in the Magsat dawn and dusk orbital cross-overs (mis-ties) are used to establish improved data selection criteria and problem-oriented data processing techniques. Empirical and random data handling techniques were developed to minimize both the spatially coherent and random errors in the data. The processing has yielded wide-band dawn and dusk orbital Magsat data sets of the greater African region which have substantially reduced dawn-dusk discrepancies compared to other published wide-band maps. High correlation between the two data sets suggests that they are internally consistent, relatively free from external field effects, and hence, useful for broad-scale lithospheric magnetic anomaly interpretation. The ridge-regression method was used in a large-scale equivalent source inversion of Magsat data. The optimum damping parameter is selected based on the rate of increase of the variance in the residual between the observed and the calculated anomaly and the variance of the solution for a

series of damping parameters. Solutions obtained by the damping parameter selected in this manner are numerically stable and geologically meaningful. There is a high degree of correspondence between Magsat anomalies and regional Euro-African geotectonic provinces. Three-dimensional quantitative magnetic models constrained by available geologic and geophysical data were generated for West Africa, Central African, Southern Africa, Europe, and Northeastern Walvis Ridge that demonstrate the utility of the Magsat maps in regional geotectonic studies. Dissert. Abstr.

N91-16416# Army Construction Engineering Research Lab., Champaign, IL.
CARTOGRAPHIC ISSUES IN THE DEVELOPMENT OF A DIGITAL GRASS DATABASE Final Report
Marilyn S. Ruiz and Jean M. Messersmith Sep. 1990 47 p
(AD-A227582; CERL-SR-N-90/16) Avail: NTIS HC/MF A03
CSCL 12/7

The process of building a complete and useful database for the Geographic Resource Analysis Support System (GRASS), a geographic information system (GIS), is complex and costly. If data are entered or manipulated incorrectly, the result can be large, costly body of useless geographic information. The likelihood of such mistakes arises in part from a user's misunderstanding of basic differences between digital map data and conventional analog paper maps. Additionally, a number of environmental planners have been faced with the necessity of creating or editing GRASS databases without substantial training in cartographic concepts or the use of GIS. This report provides information that will help minimize mistakes commonly made in the creation and modification of GRASS databases. GRASS is now used widely at military installations, and by numerous other public and private agencies. This report answers some of the questions most frequently asked by GRASS users throughout the public and private sectors. The contents of this report are drawn largely from the collective experience of researchers at the U.S. Army Construction Engineering Research Laboratory (USACERL), where GRASS was developed. Issues addressed include software-specific matters, the characteristics of digital cartographic databases, the relationship between digital and analog maps in general, and the preparation of analog map information for conversion into digital data. GRA

N91-16417 Colorado Univ., Boulder.
THE EFFECTS OF THE SOLID INNER CORE AND NONHYDROSTATIC STRUCTURE ON THE EARTH'S FORCED NUTATIONS AND EARTH TIDES Ph.D. Thesis
Daniel Neville deVries 1990 113 p
Avail: Univ. Microfilms Order No. DA9032820

Recent highly-accurate nutation results from Very Long Baseline Interferometry (VLBI) disagree with the 1980 IAU nutation model by about 2 milli-arcseconds (mas). Most of the discrepancy is at the retrograde annual frequency. The discrepancy was interpreted as being due to a non-hydrostatic core-mantle boundary (CMB) ellipticity, an interpretation which is consistent with inferences from tidal gravity measurements. The ellipticity affects the eigenfrequency of the Free Core Nutation (FCN) normal mode, predominantly a relative rotation between the solid mantle and the fluid outer core (OC), assuming that the inner core (IC) is fluid. Furthermore, the earth is presumed to be hydrostatically prestressed, and so it is inconsistent to use results from this theory to infer information about non-hydrostatic structure. The theoretical results are extended to include the effects of a solid IC, and of non-hydrostatic structure. The presence of the IC is responsible for a new, nearly diurnal, prograde normal mode, the Free Inner Core Nutation (FICN) that involves a relative rotation between the IC and OC. The FICN causes a perturbation in the prograde semi-annual nutation amplitude of 0.2 mas, but the contribution to the retrograde annual nutation is not enough to explain the VLBI discrepancy. Effects on the earth tide are negligible. Non-hydrostatic structure affects the eigenfrequency of this mode. It causes the nutation and tide amplitudes to depend on the IC-OC boundary, CMB, and outer surface topography at all spatial scales, but falls off as the (l-1)-th power of the ratio of the IC radius to the OC radius, for the simplified case of a homogeneous, rigid IC and mantle, and homogeneous, incompressible OC. Dissert. Abstr.

N91-16418 Utah Univ., Salt Lake City.
IMAGE-BASED TERRAIN MODELING WITH THEMATIC MAPPER Ph.D. Thesis
John A. Merola 1989 114 p
Avail: Univ. Microfilms Order No. DA9033440

The LANDSAT Thematic Mapper (TM) scanner records reflected solar energy from the Earth's surface in six wavelength regions, or bands, and one band that records emitted energy in the thermal region, giving a total of seven bands. The goal to extract useful information about terrain morphometry from remote sensing measurements and to use this information in an image-based terrain model for selected coastal geomorphic features in the Great Salt Lake Desert (GSLD). Technical developments include the incorporation of Aerial Profiling of Terrain System (APTS) data in satellite image analysis, and the production and use of three-dimensional surface plots of TM reflectance data. Also included in the technical development is the analysis of the ground control point spatial distribution and its affects on geometric correction, and the terrain mapping procedure; using satellite data in a way that eliminates the need to degrade the data by resampling. The most common approach for terrain mapping with multispectral scanner data includes the techniques of pattern recognition and image classification, as opposed to direct measurement of radiance for identification of terrain features. The research approach was based on an understanding of the characteristics of reflected light resulting from the variations in moisture and geometry related to terrain as described by the physical laws of radiative transfer. The image-based terrain model provides quantitative information about the terrain morphometry based on the physical relationship between TM data, the physical character of the GSLD, and the APTS measurements. Dissert. Abstr.

N91-16419 Nebraska Univ., Lincoln.
CARBON DIOXIDE AND ENERGY EXCHANGES IN A TEMPERATE GRASSLAND ECOSYSTEM Ph.D. Thesis
Joon Kim 1990 97 p
Avail: Univ. Microfilms Order No. DA9030132

A micrometeorological study was conducted to evaluate the surface exchanges of carbon dioxide and energy at a temperate grassland site in northeastern Kansas. The fluxes of CO2 (FC), latent heat (LE), sensible heat (H), and momentum were measured using the eddy correlation technique. Pertinent microclimatic, plant and soil variables were also monitored through the season. The prairie was dominated by three C4 grass species: Andropogon gerardii, Sorghastrum nutans, and Panicum virgatum. The energy partitioning was controlled mainly by net radiation and by soil water availability. Considerable daily and seasonal variability of CO2 flux was observed. The dependence of the daytime FC on pertinent controlling variables (e.g., light, temperature, vapor pressure deficit, soil water availability, and canopy surface conductance) was investigated. A leaf stomatal conductance model was developed for the major grass species in this ecosystem, and was scaled up to a canopy level using a canopy radiative transfer model. Comparisons with field measurements indicated that the model provided reasonable estimates of canopy stomatal conductance for well-watered conditions. The modelled half-hourly values of LE agreed well with those measured, under these conditions. A biochemical leaf photosynthesis model was adapted to the major grass species studied here, and was scaled up to a canopy level. Comparisons with field measurements showed that the model realistically simulated the magnitudes and the diurnal variations of canopy photosynthesis under well-watered conditions. Although the modelled canopy photosynthesis overestimated the measured values under moisture stress conditions, the model did simulate the diurnal patterns adequately. Dissert. Abstr.

N91-16420 Colorado State Univ., Fort Collins.
INVESTIGATION OF A REMOTE SENSING TECHNIQUE FOR

DROPLET EFFECTIVE RADIUS Ph.D. Thesis
Melanie Ann Wetzel 1990 147 p
Avail: Univ. Microfilms Order No. DA9029453

Theoretical and observational studies are carried out to evaluate the use of cloud near-infrared spectral reflectance to determine cloud droplet size. A multiple scattering radiative transfer model for plane-parallel clouds is developed in order to determine monochromatic cloud reflectance in the 0.85 and 1.6 micrometer atmospheric windows. The results are applied to an objective retrieval technique for droplet effective radius. It is shown that the retrieval technique provides accurate droplet size estimates from known values of bispectral reflectance. Potential uncertainties due to measurement or viewing geometry errors are identified. The influence of cloud structure variability on the retrieval accuracy is determined through numerical simulations representing vertical inhomogeneity of cloud microphysical characteristics, limited horizontal extent of the cloud, and the presence of aerosol vertically adjacent to and within the cloud. The results of the simulations indicate little sensitivity of the retrieved droplet size due to typical cloud inhomogeneity, except in the case of a shallow cloud atop a hazy marine boundary layer. The ability to correctly identify droplet effective radius variations is shown to require a cloud of sufficient optical depth. Analysis of field measurement data demonstrate a retrieval accuracy within an uncertainty of 3 micrometers for cloud areas of sufficient optical depth, and a bias towards larger retrieved sizes for an optically thin cloud. The results suggest the utility and some possible limitations of satellite remote sensing of cloud droplet size. Dissert. Abstr.

N91-16421# Rochester Inst. of Tech., NY. Center for Imaging Science.
MERGING PANCHROMATIC AND MULTISPECTRAL IMAGES FOR ENHANCED IMAGE ANALYSIS M.S. Thesis
Curtis K. Munechika Aug. 1990 215 p Sponsored by AFIT, Wright-Patterson AFB, OH
(AD-A227902; AFIT/CI/CIA-90-114) Avail: NTIS HC/MF A10 CSCL 14/4

This study evaluates several methods that enhance the spatial resolution of multispectral images using a finer resolution panchromatic image. The resultant hybrid, high resolution, multispectral data set has increased visible interpretation and improved classification accuracy, while preserving the radiometry of the original multispectral images. These methods can therefore be applied to create simulated high resolution multispectral data, as well as to enhance image analysis. GRA

N91-16422# Colorado Univ., Boulder. Center for Astrodynamics Research.
[ANALYSIS OF SATELLITE AND EXPENDABLE BATHYTHERMOGRAPH (XBT) DATA FOR THE ABRUPT TOPOGRAPHY PROGRAM] Annual Progress Report
Bill Emery 1990 1 p
(Contract N00014-89-J-1189)
(AD-A228870) Avail: NTIS HC/MF A01 CSCL 08/3

Our project involves the analysis of satellite and expendable bathythermograph data for the abrupt topography program. The satellite data analysis concentrated on the analysis of GEOSAT altimeter data since it was established that the surface temperature gradients (in the region around the Fieberling seamount) were too weak to be viewed and monitored by the AVHRR on NOAA satellites. Using GEOSAT data we have been able to isolate the modes of sea surface height variability in the Fieberling region. A total of 7 XBT surveys have now been collected over the Fieberling site. GRA

N91-16423 Leicester Univ. (England).
IONOSPHERIC CORRECTIONS FOR SHF SATELLITE RADAR ALTIMETRY Ph.D. Thesis
Richard Peter Leigh 1989 282 p
Avail: Univ. Microfilms Order No. BRD-90625

To measure the satellite-ocean altitude, a radar altimeter transmits a nadir-directed microwave pulse and times the return of the surface reflection. The intervening free electrons of the ionosphere cause group delay of the pulse resulting in an overestimate of the platform altitude by an amount directly proportional to the sub-satellite electron content. In effect the figure of the ocean surface detected by the altimeter is modulated by the spatial and temporal variation of the ionospheric electron content. A two stage technique was developed to remove the bias imposed by the ionosphere on altimetric measurements. The first stage generates a prediction of electron content based on ionospheric climatology. The second stage is an adaptive modeling procedure which makes use of data from satellite-ranging radar systems. An in introduction to the Earth's ionosphere is given. Its effect is described on radar altimetry and a technique is suggested to correct for this influence. Previous work in related areas is reviewed. The spatial and temporal behavior of electron content are described. The mathematical sub-models are described which form the basis of the empirical model. The calibration and validation of this model are presented. The calculation of the coherence functions of electron content which are crucial for the operation of the adaptive procedure is covered. The new model is compared with one employed for a previous altimeter mission. What has gone before is summarized and topics suggested for future research. Dissert. Abstr.

N91-16424 Texas Univ., Austin.
TERRAIN MATCHING USING IMAGE SEQUENCE ANALYSIS Ph.D. Thesis
Jeffrey Joel Rodriguez 1990 120 p
Avail: Univ. Microfilms Order No. DA9031700

A terrain matching algorithm is presented for use in a passive aircraft navigation system. A monocular sequence of aerial, optical images is matched to a reference digital map of the three-dimensional terrain. Stereoscopic analysis of each successive pair of images in the sequence yields a recovered elevation map of the observed terrain in the field of view. A two-dimensional cliff map is then used as a compact representation of both the recovered elevation map and the reference map. This representation makes it possible to match the sparse, stereoscopic data to the dense reference map. A terrain matching algorithm is presented which achieves its efficiency by matching high-curvature points along the two-dimensional cliff contours. The observed cliff map is found within the reference cliff map, and the associated translation and rotation parameters provide the desired position and heading of the aircraft. The robustness of the terrain matching algorithm is demonstrated by experimental results using real terrain data. A detailed analysis of the performance is presented, including results using both simulated and real stereo implementations. Dissert. Abstr.

N91-16425# Beleidscommissie Remote Sensing, Delft (Netherlands).
EXTRACTION OF MARKETABLE INFORMATION FROM ERS-1 DATA
C. F. deValk, G. J. Wensink, R. W. vanSwol, and J. C. Venema (National Aerospace Lab., Amsterdam, Netherlands) Jun. 1990 83 p
(BCRS Proj. CO-2.20)
(BCRS-90-03; ETN-91-98463) Avail: NTIS HC/MF A05

Ways in which marketable information can be extracted from ERS-1 data are discussed. Recommendations for ways of processing and disseminating the data are presented. Use of ERS-1 data to support marine and coastal activities, for instance, requires integration of ERS-1 observations with conventional observations to generate a set of wind, wave and flow data covering the requirements for a wide range of applications. A functional design of an information system providing easy access to ERS-1 data in generic form is presented. A system definition study to specify the functional and technical requirements of the system and arrive at a well founded cost estimate, is described. ESA

N91-16426# Beleidscommissie Remote Sensing, Delft (Netherlands).
SAHELIAN VEGETATION MONITORING PROJECT Final Report

A. Rosema (Environmental Analysis and Remote Sensing, Delft, Netherlands) Jun. 1990 46 p
(BCRS-90-04; ETN-91-98464) Avail: NTIS HC/MF A03

Midnight and noon infrared and visible channel Meteosat images are used to map evapotranspiration and biomass development in the Sahelian zone in and around Burkina Faso. They are compared with NOAA derived NDVI imagery from the same area and period. Both types of data are tested on the rain gauge data from stations in Burkina and Mali as well as biomass observations performed in the Gourma area of Mali. It is concluded that both the Meteosat derived evapotranspiration and biomass values can be useful tools in regional water budget studies and early crop warning. ESA

N91-16427# Beleidscommissie Remote Sensing, Delft (Netherlands).
DETECTION OF SOIL MOISTURE USING X-BAND SLAR RECORDS IN A SANDY AREA [DETEKTIE VAN BODEMVOCHT MET X-BAND SLAR OPNAMEN IN EEN ZANDGEBIED]
F. P. Hagedoorn (Winand Staring Centre, Wageningen, Netherlands) Jun. 1990 47 p In DUTCH
(BCRS-90-08; ICW-1942; ETN-91-98465) Avail: NTIS HC/MF A03

The correlation between X band radar images and soil moisture was studied in order to find locations which are sensitive to water nuisance. The radar observation and the SLAR (Side Looking Airborne Radar) measuring system are described. A digitized topographical map of the area was projected over six radar images. The pixel values of each of the nine parcels were determined, allowing the calculation of the average radar backscatter of each parcel. The visual interpretation shows that moisture patterns of the false color picture can be retrieved on the radar image for many parcels to a certain degree. It is concluded that there exists a correlation between the average moisture content and the backscatter of the X band SLAR. However, the quality ot the correlation is moderate. ESA

N91-16428# Beleidscommissie Remote Sensing, Delft (Netherlands).
THE USEFULNESS OF MSS PICTURES FOR MAPPING AND BIOMASS ESTIMATION OF MACRO-ALGAE AND SEAWEED IN THE EASTERN SCHELDT [DE BRUIKBAARHEID VAN VLIEGTUIG-MSS OPNAMEN BIJ DE KARTERING EN BIOMASSASCHATTING VAN MACRO-ALGEN EN ZEEGRASSEN IN DE OOSTERSCHELDE]
C. Meulstee and H. C. Bakker (Rijksluchtvaartdienst, Schiphol, Netherlands) Jul. 1990 49 p In DUTCH; ENGLISH summary
(BCRS-90-09; ETN-91-98466) Avail: NTIS HC/MF A03

The use of airborne MSS (Multi Spectral Scanning) imagery and digital image processing for mapping and biomass estimation of macrophytes following a method based on aerial photography was investigated. Radiometric and geometric corrections to the MSS images were carried out and principal components were calculated to reduce the amount of data. The results of supervised classification using the maximum likelihood algorithm are not satisfactory. By means of unsupervised classification of transparent overlay of the vegetation borders it was shown that the conformity to the vegetation map requires a certain amount of field investigation. The results of biomass estimation are promising. The total biomass estimated amounts to 93 percent compared to the total biomass estimate of the same area based on aerial photography. ESA

N91-16429# Beleidscommissie Remote Sensing, Delft (Netherlands).
THE DIELECTRIC PROPERTIES OF WET SOILS
G. P. deLoor (Physics and Electronics Lab. TNO, The Hague, Netherlands) Jul. 1990 41 p
(BCRS-90-13; ETN-91-98468) Avail: NTIS HC/MF A03

In microwave remote sensing, knowledge of the dielectric properties of the materials observed (soils, vegetation) is important for the interpretation of the recorded reflection or emission and for the design of models for this reflection and emission. Many data sets giving the dielectric properties of soils are now available in the literature, some of them even in numerical form. These last data sets are compiled. They cover the whole soil textural triangle reasonably well. All sets are summarized, discussed, and compared with the available theories. These theories offer no simple law to describe the electrical properties of a wet soil, but boundaries can be given between which the permittivity must lie. Empirical relations can be applied. The available data give a linear relation with volumetric soil moisture. ESA

N91-16430# Beleidscommissie Remote Sensing, Delft (Netherlands).
PROCEDURE FOR THE CORRECTION OF ERRORS IN THE DUTSCAT DATA 1987/1988 [WERKWIJE VOOR HET CORRIGEREN VAN FOUTEN IN DE DUTSCAT DATA 1987/1988]
P. C. Luik (Physics and Electronics Lab. TNO, The Hague, Netherlands) Jul. 1990 25 p In DUTCH; ENGLISH summary
(BCRS-90-14; FEL-90-C082; ETN-91-98469) Avail: NTIS HC/MF A03

Error correction procedures for data obtained with the DUTSCAT (Delft University of Technology SCATterometer) for the benefit of agricultural fields in the Fleropolder (The Netherlands) are presented. Due to instrument problems the database contains false and dubious measurements which must to be removed by a number of selection procedures. The stringency level of the tests was varied in order to create a sequence of data bases containing varying numbers of false or dubious measurements. The corrected data set is shown to be reliable. ESA

N91-16431# Winand Staring Centre, Wageningen (Netherlands).
EVALUATION OF CROP TRANSPIRATION WITH REMOTE SENSING AND COMPUTER SIMULATION MODELS
J. W. Miltenburg and W. Beekman 1989 40 p
(REPT-1; ETN-91-98470) Copyright Avail: NTIS HC/MF A03

A Geo Information System (GIS) in which remotely sensed imagery is used to extrapolate and verify agrohydrological model simulations is developed. A one dimensional model is applied to simulated crop transpiration for different soil types. Simulation maps are obtained by combining model results with a digital soil map and a land use map. A land use map is obtained through classification of reflection images. Digital reflection and thermal airborne scanner images are used, after radiometric and geometric corrections, to map actual crop transpiration. It was found that in general an important improvement of the hydrological description of an area can be achieved by a combination of remote sensing data and hydrological model simulations. Future research should be directed towards the minimization and assessment of errors due to the combined use of maps and remote sensing data in the developed GIS. ESA

N91-16432# Institut fuer Angewandte Geodaesie, Frankfurt am Main (Germany, F.R.).
REPORTS ON CARTOGRAPHY AND TOPOGRAPHY. SERIES 1, REPORT 104 [NACHRICHTEN AUS DEM KARTEN- UND VERMESSUNGSWESEN. REIHE 1, HEFT NR. 104]
1990 45 p In GERMAN; ENGLISH summary Cartographic imagery as supplement
(ISSN-0469-4236; ETN-91-98643) Avail: NTIS HC/MF A03

Possibilities of supporting and extending photogrammetric techniques by using inexpensive serially produced instruments of video electronics with stereo plotters are described. A method to produce multisensor image maps from SPOT 1 HRV (High Resolution Visible) and Landsat 5 TM (Thematic Mapper) satellite data is presented. For individual titles, see N91-16433 through N91-16434.

N91-16433# Institut fuer Angewandte Geodaesie, Frankfurt am Main (Germany, F.R.).
THE PHOTOGRAMMETRIC EVALUATION BY VIDEO TECHNIQUE: A SUPPORTING STUDY [UNTERSTUETZUNG DER PHOTOGRAMMETRISCHEN AUSWERTUNG DURCH VIDEO-TECHNIK]

Werner Kolb *In its* Reports on Cartography and Topography. Series 1, Report 104 1990 p 5-26 In GERMAN; ENGLISH summary (For primary document see N91-16432 08-43)
Avail: NTIS HC/MF A03

Possibilities of supporting and extending photogrammetric techniques by using inexpensive serially produced instruments of video electronics with stereo plotters are described. A new method to produce point sketches automatically, as well as the three dimensional projection of stereo model on a color screen by using the anaglyph method, are presented. The technical bases of the applied methods are described. The results are explained and discussed. ESA

N91-16434# Institut fuer Angewandte Geodaesie, Frankfurt am Main (Germany, F.R.).
THE MULTISENSOR IMAGE MAP 1:50,000 RHEINHESSEN [DIE MULTISENSORBILDKARTE 1:50000 RHEINHESSEN]
Berthold Pfeiffer *In its* Reports on Cartography and Topography. Series 1, Report 104 1990 p 27-39 In GERMAN; ENGLISH summary (For primary document see N91-16432 08-43)
Avail: NTIS HC/MF A03

A method to produce multisensor image maps from SPOT 1 HRV (High Resolution Visible) and LANDSAT 5 TM (Thematic Mapper) satellite data is presented. Digital image processing methods are applied for geometric registration, rectification, contrast enhancement and color transformations. A practical realization example is given and described by the enclosed thematic satellite image map 1:50,000 Rheinhessen. It is demonstrated that an operational production of such maps in a purely digital way is possible. Time consumption amounts to about two months, starting from the satellite image data reading until the presentation of the printed map. ESA

44 ENERGY PRODUCTION AND CONVERSION

Includes specific energy conversion systems, e.g., fuel cells; global sources of energy; geophysical conversion; and windpower.

For related information see also *07 Aircraft Propulsion and Power, 20 Spacecraft Propulsion and Power,* and *28 Propellants and Fuels.*

N91-16435# Colorado State Univ., Fort Collins. Solar Energy Applications Lab.
COLORADO STATE UNIVERSITY PROGRAM FOR DEVELOPING, TESTING, EVALUATING AND OPTIMIZING SOLAR HEATING AND COOLING SYSTEMS
May 1990 17 p
(Contract DE-FG03-86SF-16306)
(DE90-010107; DOE/SF-16306/21) Avail: NTIS HC/MF A03

The results are presented of efforts to develop and test various integrated solar heating, cooling and domestic hot water systems, and to evaluate their performance. DOE

N91-16436# Argonne National Lab., IL. Materials and Components Technology Div.
CONTEMPORARY ISSUES IN SOLAR POND RESEARCH
John H. Huff 1990 4 p Presented at the 19th American Solar Energy Society Annual Conference, Austin, TX, 18-20 Mar. 1990
(Contract W-31-109-eng-38)
(DE90-010094; CONF-900315-3) Avail: NTIS HC/MF A01

Technical issues that are vital to the economic viability of salinity gradient solar ponds include gradient zone erosion, brine transparency, ground heat loss, and salt recycling. Present knowledge of these issues is summarized, and a number of promising research problems are suggested for each issue. DOE

N91-16437# Lawrence Livermore National Lab., CA.
ELECTRICAL POWER FROM INERTIAL CONFINEMENT FUSION: ISSUES AND PROSPECTS
Michael T. Robin, John H. Pitts, Charles D. Orth, Ralph W. Moir, William J. Hogan, and Roger O. Bangerter Oct. 1989 15 p
(Contract W-7405-eng-48)
(DE90-010200; UCID-21849) Avail: NTIS HC/MF A03

This report discusses the following topics on using inertial confinement for electrical power generation: General Economic Issues; Design of Reactors; Safety and Environmental Issues; and Development Issues. DOE

N91-16438# Sandia National Labs., Albuquerque, NM. Battery Development Div.
SELF-DISCHARGE STUDY OF LI-ALLOY/FeS2 THERMAL CELLS
Ronald A. Guidotti, Frederick W. Reinhardt, and John A. Smaga (Argonne National Lab., IL.) 1990 4 p Presented at the 34th International Power Sources Symposium, Cherry Hill, NJ, 25-28 Jun. 1990
(Contract DE-AC04-76DP-00789)
(DE90-010659; SAND-89-2229C; CONF-9006146-4) Avail: NTIS HC/MF A01

The capacities of Li-alloy/FeS2 thermal batteries are influenced by the extent of self-discharge reactions that occur during operation. For some thermal-battery applications involving open-circuit (i.e., wet-stand) conditions, this self-discharge can result in a significant loss incapacity. A study was undertaken to obtain a better understanding of the factors influencing the self-discharge of thermal cells, such as temperature, electrolyte composition, and processing of the catholyte (i.e., lithiation and fusion). The cells were discharged after prescribed times at open circuit under isothermal conditions and the capacity to a cutoff voltage was measured. Postmortem characterization of the cells was used to correlate the results of the electrochemical experiments. DOE

N91-16439# Los Alamos National Lab., NM.
DIRECT METHANOL/AIR FUEL CELLS: SYSTEMS CONSIDERATIONS
James R. Huff 1990 6 p Presented at the Direct Methanol/Air Fuel Cell Workshop, Washington, DC, 14-16 May 1990
(Contract W-7405-eng-36)
(DE90-011971; LA-UR-90-1688; CONF-9005196-2) Avail: NTIS HC/MF A02

Successful operation of a direct methanol/air fuel cell system depends upon appropriate integration of the fuel cell components and accommodation of the need for heat and mass transfer within the system. The features of the system that must be considered separately and in an interactive fashion are: (1) the physical state of the fuel feed stream; (2) electrode characteristics; (3) characteristics of the electrolyte; (4) product water removal; (5) heat transfer into and out of the stack; and (6) methanol loss modes. The operating temperature and pressure will be determined, to a large extent, by these features. An understanding of the component features and their interactions is necessary for initial system considerations for direct methanol/air fuel cells. DOE

N91-16440 Council for National Academic Awards (England).
SOLAR REFRIGERATION: EVALUATION OF TECHNICAL OPTIONS AND DESIGN OF A SOLAR-GENERATOR-ADSORBER FOR A NOVEL ADSORPTION REFRIGERATOR, VOLUMES 1 AND 2 Ph.D. Thesis
Salim Abid Tabassum 1989 498 p
Avail: Univ. Microfilms Order No. BRDX89771

Various technical options for developing a solar operated refrigerator were discussed. Their suitability for being used as a vaccine store for the conditions specified by the World Health Organization Expanded Program on Immunization (EPI) were evaluated. A model to predict the performance of a photovoltaic refrigerator was developed and used to identify factors which influence its performance. It was concluded that it can be more competitive in areas where insolation is high and sunshine hours

are long. It was proposed that ice-lined refrigerators, which would run during the day, may be more economical and eliminate the need for battery storage. The option of operating an Electrolux absorption refrigerator with evacuated tube heat pipe collectors was assessed. It was concluded that the operation was not possible without a major re-design of the commercially available models. However, it was proposed that coordination of the EPI with other development programs may be useful. The building of biogas plants was proposed. Biogas can then fuel the modified burner of the kerosene fueled absorption refrigerators. This may prove to be a cheaper option. Characterization of various adsorption pairs was done using the experimental rig. The influence of various properties of adsorption pairs on the performance of an adsorption refrigeration cycle was studied. A relationship between the refrigerant properties and the generating temperature for specified operating conditions was developed. A idea of direct absorption of solar radiation into the activated carbon bed is put forward to combat the temperature differential of 24 C, in a conventional design of SGA, between the carbon and the metal contained. A new tubular design of the SGA is proposed finally which is hoped will bring improvement to the performance of the activated carbon adsorption refrigerators. Dissert. Abstr.

N91-16441 New South Wales Univ., Canberra (Australia).
HIGH EFFICIENCY SILICON CONCENTRATOR SOLAR CELLS Ph.D. Thesis, Mar. 1989 Abstract Only
Jianhua Zhao 1 Jun. 1990 3 p
Avail: Issuing Activity

Techniques were investigated for improving the energy conversion efficiency of silicon concentrator solar cells. This aim was achieved with the demonstration of bifacially contacted silicon concentrator solar cells of markedly superior performance. An additional achievement was the demonstration of substantial improvements in the performance of non-concentrating, one-sun cells. The improvements in the one-sun cell area were achieved by optimization of the Passivated Emitter Solar Cell (PESC) technology. Aluminum gettering and emitter surface oxide-passivation played key roles for the PESC cells. The optimized PESC one-sun cell demonstrated an independently confirmed efficiency of 21.4 percent. The optimized PESC technology was also successfully applied to the fabrication of silicon concentrator cells on low resistivity substrates. The effects of metal contact resistance and heavy phosphorus diffusion were areas requiring additional careful investigation in this case. A concentrator cell after optimization demonstrated 23.4 percent efficiency at 100 suns, again independently confirmed. Although very high by normal standards, the efficiency was limited by the trade-off of the resistance and the shading of the front metal fingers. The need for the trade-off was eliminated by the application of prismatic covers, which steer the incident light onto the cell active areas avoiding metal fingers. The Passivated Emitter and Rear Cells (PERC) incorporating TCA (trichloro-ethane) processing improved the one-sun cell efficiency further to 21.8 percent. The improvement came from low recombination at surfaces and in the bulk resulting from the TCA processing and from reduced rear contact area. Antireflection coatings and prismatic cover design were also theoretically optimized. When combined with light trapping techniques, 27 percent efficiency silicon concentrator cell will be obtained with this approach in the near future. Author

N91-16442# Giner, Inc., Waltham, MA.
IMPROVED ANODE CATALYSTS FOR COAL GAS-FUELED PHOSPHORIC ACID FUEL CELLS
N. D. Kackley, S. A. McCatty, and J. A. Kosek Jul. 1990 52 p
(Contract DE-AC21-88MC-25170)
(DE90-009683; DOE/MC-25170/2861) Avail: NTIS HC/MF A04

The feasibility of adapting phosphoric acid fuel cells to operate on coal gas fuels containing significant levels of contaminants such as CO, H2S and COS was investigated. The overall goal was the development of low-cost, carbon-supported anode fuel cell catalysts that can efficiently operate with a fossil fuel-derived hydrogen gas feed contaminated with carbon monoxide and other impurities. This development would reduce the cost of gas cleanup necessary in a coal gas-fueled PAFC power plant, thereby reducing the final power cost of the electricity produced. The problem to date was that the contaminant gases typically adsorb on catalytic sites and reduce the activity for hydrogen oxidation. An advanced approach investigated was to modify these alloy catalyst systems to operate efficiently on coal gas containing higher levels of contaminants by increasing the alloy catalyst impurity tolerance and ability to extract energy from the CO present through (1) generation of additional hydrogen by promoting the CO/H2 water shift reaction or (2) direct oxidation of CO to CO2 with the same result. For operation on anode gases containing high levels of CO, a Pt-Ti-Zn and Pt-Ti-Ni anode catalyst showed better performance over a Pt baseline or G87A-17-2 catalyst. The ultimate aim was to allow PAFC-based power plants to operate on coal gas fuels containing increased contaminant concentrations, thereby decreasing the need for and cost of rigorous coal gas cleanup procedures. DOE

N91-16443# Midwest Research Inst., Golden, CO.
HIGH-EFFICIENCY LARGE-AREA CdTe PANELS
Scot P. Albright, Rhodes R. Chamberlin, and John F. Jordan Nov. 1990 39 p Prepared in cooperation with Photon Energy, Inc., El Paso, TX
(Contract DE-AC02-83CH-10093)
(DE91-002117; SERI/TP-211-4034) Avail: NTIS HC/MF A03

The objective of this three year effort has been to develop an improved materials technology and fabrication process for limited volume production of 1 and 4 sq ft CdS/CdTe photovoltaic modules. The module stability objective by the end of this three year subcontract was to develop techniques to provide ten year life exploration with no greater than 10 percent degradation. In order to achieve these efficiency and stability objectives, the research program has been separated into tasks including: (1) analysis and characterization of CdS/CdTe devices; (2) performance optimization on small cells; (3) encapsulation and stability testing; and (4) module efficiency optimization. DOE

N91-16444# Midwest Research Inst., Golden, CO.
LOW-COST CdZnTe DEVICES FOR CASCADE CELL APPLICATION Final Report, 15 May 1989 - 15 May 1990
Bulent M. Basol and Vijay K. Kapur (International Solar Electric Technology, Inglewood, CA.) Nov. 1990 22 p
(Contract DE-AC02-83CH-10093)
(DE91-002116; SERI/TP-211-4033) Avail: NTIS HC/MF A03

This report describes a research program to develop a low-cost technique for producing Cd(1-x)Zn(x)Te devices for cascade solar cell applications. The technique involves a two-stage process for fabricating such devices with a band gap of about 1.7 eV and a transparent contact layer of low-resistivity ZnTe. In the first stage, thin films of Cd, Zn, and Te are deposited in stacked layers as Cd(1-x)An(x)Te. The second stage involves hearing and reacting the layers to form the compound. At first, electrodeposition was used for depositing the layers to successfully fabricate Cd(1-x)Zn(x)Te thin-film devices. These films were also intrinsically doped with copper. For the first time, transparent ZnTe films of low resistivity were obtained in a two-stage process; preliminary solar cells using films with low Zn content were demonstrated. A second phase of the project involved growing films with higher Zn content (greater than 15 percent). Such films were grown on CdS-coated substrates for fabricating devices. The effects of the solar-cell processing steps on the Cd(1-x)Zn(x)Te and CdS/Cd(1-x)Zn(x)Te interfaces were studied; results showed that the nature of the interface depended on the stoichiometry of the Cd(x-1)Zn(x)Te thin film. A sharp interface was observed for the CdS/CdTe structures, but the interface became highly diffused as the Zn content in the absorber layer increased above 15 percent. The interaction between the CdS window layer and the Cd(1-x)Zn(x)Te absorber layer was found to result from an exchange reaction between Zn in the absorber layer and the thin CdS film. DOE

45 ENVIRONMENT POLLUTION

Includes atmospheric, noise, thermal, and water pollution.

N91-16445# Pacific Northwest Lab., Richland, WA.
MULTIMEDIA ENVIRONMENTAL POLLUTANT ASSESSMENT SYSTEM (MEPAS) SENSITIVITY ANALYSIS OF COMPUTER CODES
P. G. Doctor, T. B. Miley, and C. E. Cowan Apr. 1990 134 p
(Contract DE-AC06-76RL-01830)
(DE90-010005; PNL-7296) Avail: NTIS HC/MF A07

The Multimedia Environmental Pollutant Assessment System (MEPAS) is a computer-based methodology developed to estimate health impacts from the release of hazardous chemicals and radioactive materials. The health impacts are estimated from the environmental inventory and release or emission rate, constituent transport, constituent uptake and toxicity, and exposure route parameters. As part of MEPAS development and evaluation, PNL performed a formal parametric sensitivity analysis to determine the sensitivity of the model output to the input parameters, and to provide a systematic and objective method for determining the relative importance of the input parameters. The sensitivity analysis determined the sensitivity of the Hazard Potential Index (HPI) values to combinations of transport pathway and exposure routes important to evaluating environmental problems at DOE sites. Two combinations of transport pathways and exposure routes were evaluated. The sensitivity analysis focused on evaluating the effect of variation in user specified parameters, such as constituent inventory, release and emission rates, and parameters describing the transport and exposure routes. The constituents used were strontium-90, yttrium-90, tritium, arsenic, mercury, polychlorinated biphenyls, toluene, and perchloroethylene. DOE

N91-16446# Brookhaven National Lab., Upton, NY. Dept. of Applied Science.
SOLVING GLOBAL ENVIRONMENTAL PROBLEMS THROUGH TECHNOLOGICAL INNOVATION
Meyer Steinberg Mar. 1990 15 p Presented at the GISPRI Symposium '90 Meeting, Tokyo, Japan, 28 Feb. 1990
(Contract DE-AC02-76CH-00016)
(DE90-010018; BNL-44417; CONF-9002113-1) Avail: NTIS HC/MF A03

Much of the environment problems arise from the supply and utilization of energy for industrial, transportation and domestic markets. The use of fossil fuels can result in environmental, atmospheric, and terrestrial problems, including organic, acid rain, and global warming hazards. The CO2 global greenhouse problem is addressed along with the nuclear industry and its dilemma as well. The possibility is recognized of global natural feedback phenomena which may limit and mitigate anthropomorphic global greenhouse climate change, however, the discussion is limited to anthropomorphic (man made) technological mitigation process as opposed to adaptation which means adapting to change. DOE

N91-16447# Argonne National Lab., IL. Center for Transportation Research.
TECHNOLOGICAL AND POLICY OPTIONS FOR MITIGATING GREENHOUSE GAS EMISSIONS FROM MOBILE SOURCES
Christopher Saricks 1990 33 p Presented at the Transportation Research Board Meeting, Washington, DC, 7-11 Jan. 1990
(Contract W-31-109-eng-38)
(DE90-010151; CONF-900121-6) Avail: NTIS HC/MF A03

This paper presents issues and explores options for reducing emissions of carbonaceous pollutants from mobile sources. It discusses first what can be expected from current and proposed emission control system designed chiefly to reduce the output of regulated pollutants, then explores opportunities for incremental control of emissions of carbon (bound in gaseous form) that appear at this time to have good potential for success. The presentation of current and anticipated control technologies is organized by vehicle type, considering, in turn, passenger vehicles and light-duty trucks, medium- and heavy-duty vehicles, and non-highway vehicular modes. The discussion of incremental control opportunities focuses first on hardware and (existing) fuels modification for reduced emissions and improved fuel efficiency, then turns to advanced vehicular technologies and fuels, new refrigerants (to replace CFCs, which, in addition to being implicated in the destruction of stratospheric ozone, are molecule for molecule more potent than carbon dioxide as greenhouse gases), and in-use emissions testing and travel reduction strategies. Finally, opportunities for continuation of the current (net) downward trend in fuel consumption by most non-highway transportation activities are described. The paper concludes that evolutionary developments in most transportation activities, developments driven in large measure by simple economics, could be at least as effective in mitigating the contribution of (domestic) mobile sources to greenhouse warming as any specific revolutionary change. DOE

N91-16448# Argonne National Lab., IL.
GREENHOUSE GAS EMISSIONS FROM SELECTED ALTERNATIVE TRANSPORTATION FUELS MARKET NICHES
D. J. Santini, M. A. DeLuchi, A. Vyas, and M. Walsh 1989 37 p Presented at the American Institute of Chemical Engineer's Summer National Meeting, Philadelphia, PA, 20-23 Aug. 1989
(Contract W-31-109-eng-38)
(DE90-010491; CONF-890814-10) Avail: NTIS HC/MF A03

The incremental worldwide effects on greenhouse gases are estimated for the substitution of natural gas- or methanol-based light-duty vehicles for current gasoline-based vehicles in the United States. The effects are estimated on a per-vehicle mile basis, holding acceleration, passenger capacity, engine technology, and range of the vehicle constant. The relative merits of natural gas- or methanol-based vehicles for commuting and other household vehicle market niches are considered. In terms of net global greenhouse gas emissions, the replacement of crude-oil-derived gasoline by non-gasoline fuels derived from natural gas is superior to the use of gasoline derived from natural gas. The transition paths from oil to natural-gas-based light-duty vehicle fuels is examined, considering the effects of the substitution of currently flared natural gas for crude oil as the raw material for transition transportation fuels. Greenhouse gas emissions arising from raw material pathways are compared. These pathways include oil to gasoline and natural gas to the following: (1) atmosphere; (2) flared combustion products to the atmosphere; (3) compressed natural gas in vehicles; (4) methanol in vehicles; (5) methyl tert-butyl ether in vehicles; (6) gasoline in vehicles; and (7) coal to methanol. The comparisons show that continued dependence on a gasoline-based transportation infrastructure ultimately implies the production of gasoline from natural gas. This pathway would result in substantially greater greenhouse gas emissions than if the infrastructure were altered to use natural gas or methanol directly in vehicles. DOE

N91-16449# Oak Ridge National Lab., TN. Energy Div.
PREPARATIONS FOR A MAJOR INTERNATIONAL SYMPOSIUM ON ELECTRICITY AND THE ENVIRONMENT
T. J. Wilbanks 27 Apr. 1990 16 p
(Contract DE-AC05-84OR-21400)
(DE90-010539; ORNL/FTR-3602) Avail: NTIS HC A03

At the request of eleven international agencies and with the approval of the Department of Energy, this trip was conducted in order for the traveler to serve as U.S. representative to an international advisory group on energy and electricity supply and demand. This group was established to assist with preparations for a major international symposium on electricity and the environment, scheduled for Helsinki, Finland, in May 1991. At the meeting, the topics of energy and electricity supply and demand patterns, projections, issue and background papers to be prepared for the symposium, symposium program, and participation were discussed. DOE

N91-16450# Council on Environmental Quality, Washington, DC.
ENVIRONMENTAL TRENDS
1989 152 p Sponsored in part by Interagency Advisory

Committee on Environmental Trends
(DE90-010530; CEQ-90010530) Avail: NTIS HC/MF A08

The Council on Environmental Quality is required, by the National Environmental Policy Act of 1969, to report on the status and condition of the environment; current and foreseeable trends in the quality, management, and utilization of the environment; and the effects of environmental trends. The Council reports to Congress in an annual report and maintains an archive of national environmental statistics, which it updates and publishes periodically in the annual report as statistical tables and in environmental trends report as charts, graphs, and maps. Environmental Trends updates the Council's 1981 report by that name. This sourcebook contains 367 graphics, most of which are computer generated and indicate current conditions and trends in the environment of the United States. The statistical series for Environmental Trends was compiled from data available through government agencies, private studies, or the literature of each discipline. The data were reviewed and verified by experts at various Federal agencies. National data are used wherever possible, with breakdowns shown when especially meaningful. The text is drawn from the published sources cited. DOE

N91-16451# Oak Ridge National Lab., TN. Environmental Sciences Div.
POTENTIAL RESPONSES OF LANDSCAPE BOUNDARIES TO GLOBAL ENVIRONMENTAL CHANGE
Monica G. Turner, Robert H. Gardner, and Robert V. ONeill 1990 35 p Presented at the Annual Conference of Ecological Society of America, Snowbird, NC, 29 Jul. - 2 Aug. 1990
(Contract DE-AC05-84OR-21400)
(DE90-008568; CONF-900775-1) Avail: NTIS HC/MF A03

Global change is likely to affect the location, size, shape, or composition of landscape boundaries. Neutral models were used to study two general mechanisms by which landscape boundaries may respond to global change: (1) disturbance regimes may change in response to climate, leading to rapid alterations in landscape structure; and (2) in the absence of disturbance, suitable habitat for different species may move gradually and directionally. The spread of disturbance was simulated as a function of the proportion of the landscape occupied by a disturbance-prone habitat and the frequency and intensity of a habitat-specific disturbance. The effects of changing disturbance regimes on landscape boundaries were different in connected and fragmented landscapes. In connected landscapes, an increase in disturbance intensity caused landscape boundaries to decrease. In landscapes that were fragmented, an increase in disturbance frequency resulted in a decrease in landscape boundaries. Habitat displacement and species migration were simulated as a function of the proportion of half of a landscape occupied by a community, migration, extinction, and the rate at which potential habitat is displaced.
Author

N91-16452# Oak Ridge National Lab., TN. American Chemistry Div.
DETERMINATION OF AIRBORNE ORGANICS BY DIRECT SAMPLING MASS SPECTROMETRY
Marcus B. Wise, Michelle V. Buchanan, and Michael Guerin 1990 7 p Presented at the 5th International Conference on Indoor Air Quality and Climate, Toronto, Ontario, 29 Jul. - 3 Aug. 1990 Sponsored by Army Toxic and Hazardous Materials Agency, Aberdeen Proving Ground, MD and National Cancer Inst., Bethesda, MD
(Contract DE-AC05-84OR-21400)
(DE90-009422; CONF-900724-6) Avail: NTIS HC/MF A02

Two new state-of-the-art mass spectrometer systems are currently being evaluated for the determination of part-per-billion levels of organics in ambient air. These instruments include an ion trap mass spectrometer (ITMS) and a glow discharge quadrupole mass spectrometer (GDMS). Both of these instruments can be configured for direct air sampling or may be operated in conjunction with thermal desorbers for the analysis of samples preconcentrated on resin traps. Glow discharge ionization is particularly amenable to direct air monitoring; however, the use of a single quadrupole mass analyzer limits the ultimate specificity of this particular system. Important features of the ITMS include the ability to perform selective chemical ionization as well as collision induced dissociation (CID) tandem mass spectrometry (MS/MS) for compound identification. Applications of this technology have included the determination of ambient nicotine in environmental tobacco smoke (ETS), the determination of trace levels of organo-phosphonates in air, and the detection of target volatile organics in indoor atmospheres. DOE

N91-16453# Brookhaven National Lab., Upton, NY. Dept. of Applied Science.
BIOMASS AND HYDROCARB TECHNOLOGY FOR REMOVAL OF ATMOSPHERIC CO2
Meyer Steinberg Mar. 1990 10 p Presented at the 8th World Hydrogen Energy Conference, Honolulu, HI, 22-27 Jul. 1990
(Contract DE-AC02-76CH-00016)
(DE90-010016; BNL-44410; CONF-900705-3) Avail: NTIS HC/MF A02

All mitigation scenarios proposed to date either tend to slow down the rate of atmospheric CO2 emissions or level out the CO2 concentration in the atmosphere. A unique system has been devised which offers a method of actually reducing the CO2 concentration in the atmosphere while still generating energy from fossil fuel. The only economically and technically reasonable method for removal of CO2 from the atmosphere is by the process of solar photosynthesis which extracts carbon from atmospheric CO2 by formation of biomass, e.g., hemi-cellulose. The biomass is then thermochemically converted by the HYDROCARB technology with fossil fuel, gas, oil or coal to produce carbon black and methanol. The carbon is returned to the earth, for long-term storage, while the methanol is used as fuel. There is also an energy enhancement in utilizing gas and oil for producing methanol compared to conventional methanol processes using these fuels. Co-processing with coal results in no net CO2 generated or removed per unit of methanol energy generated; however, a 2 percent increase in coal utilization is realized compared to conventional steam refining and methanol production. The process chemistry system is described and quantified in this paper. DOE

N91-16454# Oak Ridge National Lab., TN. Energy Div.
INTERNATIONAL DECISION MAKING AND GLOBAL CLIMATE CHANGE: LESSONS OF PRIOR RESOURCE MANAGEMENT EFFORTS FOR CONSENSUS BUILDING
David L. Feldman 1990 56 p Presented at the 3rd Symposium on Social Science in Resource Management, College Station, TX, 16-19 May 1990
(Contract DE-AC05-84OR-21400)
(DE90-010714; CONF-9005171-1) Avail: NTIS HC/MF A04

International cooperation aimed at furthering awareness of anthropogenic climate change has been relatively rapid, but developing strategies for prevention or mitigation has taken more time. This is because anthropogenic climate change poses several particularly difficult obstacles to an integrated global strategy. These include conceiving of the atmosphere as a shared, sustainable resource, agreeing upon the causes, rates, and responsibilities of induced change among national actors, minimizing collateral effects of economic development while optimizing growth, particularly in LDCs, and encompassing the complexity of the problem's various ramifications in a multilateral policy. This paper addresses the availability of an incremental and iterative learning process for enhancing international cooperation in the management of global climate change. Through an examination of three case studies: regional seas, ozone, and nuclear materials regulation, models for global cooperation are identified which effectively encompass concerns over the size and distribution of correction costs among countries, the uncertainties involved in identifying cause-effect relationships, the vulnerability of shared resources, and the divergent needs of developed and developing countries. DOE

N91-16455# Lawrence Livermore National Lab., CA.
STUDY OF THE GLOBAL DISTRIBUTIONS OF ATMOSPHERIC RADIONUCLIDES Final Progress Report
1990 10 p Submitted for publication
(Contract W-7405-eng-48)
(DE90-010749; UCRL-CR-103753) Avail: NTIS HC/MF A02

Radon-222, which emanates from the decay chain of Radium-226 found in soils, has a half-life of 3.8 days after which it decays to lead-210. We simulate transport of these species using GRANTOUR, a three dimensional Lagrangian chemical transport model. The model uses wind, precipitation and temperature fields from the NCAR Community Climate Model (CCM1). Radon and lead are used as tracers in the model to examine meso-scale transport and convection in the GCM and to verify the meteorological representation of the GCM. This study was performed running GRANTOUR in continuous January and July mode with 25000 parcels and a 12 hr time step. The standard or control model for this analysis is run using a vertical diffusion coefficient of 0.5 sq m/s. Sensitivity studies have been performed to determine the model's response to convection, vertical diffusion coefficient and wind speed. DOE

N91-16456# Department of Energy, Washington, DC. Office of Health and Environmental Research.
SUBSURFACE SCIENCE PROGRAM: PROGRAM OVERVIEW AND RESEARCH ABSTRACTS Report, FY 1989 - FY 1990
May 1990 150 p
(DE90-010321; DOE/ER-0432) Avail: NTIS HC/MF A07

The Subsurface Science Program, described in this document, supports an interdisciplinary university and national laboratory research program in geochemistry, microbiology, and hydrology. Long-term, fundamental research in subsurface science is critical to ensuring that new concepts for predicting environmental risk and facilitating cleanup are available in the future. The Subsurface Science Program is DOE's (Department of Energy) primary basic research program concerned with subsoils and groundwater. This document describes the core areas for fundamental research that have been identified thus far for priority research attention within the Subsurface Science Program. The fundamental research supported in each of these high-priority scientific areas is such that substantial resources have been concentrated on them for 3 to 5 years to ensure that scientific progress can be made. Although predicting the outcome of basic research is very difficult, selected goals for each subprogram that have been identified in consultation with investigators and the scientific community are included in this document. DOE

N91-16457# Lawrence Livermore National Lab., CA.
NUMERICAL SIMULATION OF AEROSOL SCAVENGING BY ICE-BEARING CONVECTIVE CLOUDS
Michael M. Bradley and Charles R. Molenkamp Apr. 1990 3 p Presented at the American Meteorological Society Conference on Cloud Physics, San Francisco, CA, 23-27 Jul. 1990
(Contract W-7405-eng-48)
(DE90-010676; UCRL-101997; CONF-900796-1) Avail: NTIS HC/MF A01

Precipitation is the most effective mechanism for cleansing the atmosphere of small aerosol particles. Although there are many process paths by which precipitation can ultimately deposit aerosol on the ground, each path begins with the initial capture, or scavenging, of an aerosol particle. One of the most effective of these processes, at least in the absence of strong electric fields, is condensation nucleation scavenging, in which an aerosol particle serves as a cloud condensation nucleus. Although scavenging is a necessary precursor to aerosol removal by precipitation, scavenging does not guarantee that an aerosol particle will be removed from the atmosphere. For example, the particle will be resuspended if its host cloud droplet evaporates or if the droplet is collected by a raindrop which subsequently evaporates. The removal process becomes further complicated if ice is present in the cloud. The purpose of this research is to study the effects of various ice processes on the net aerosol removal efficiency of convective clouds. DOE

N91-16458# Lawrence Livermore National Lab., CA.
PARAMETERIZATION OF AEROSOL SCAVENGING IN A CONVECTIVE CLOUD MODEL
Charles R. Molenkamp and Michael M. Bradley Apr. 1990 5 p Presented at the American Meteorological Society Conference on Cloud Physics, San Francisco, CA, 23-27 Jul. 1990
(Contract W-7405-eng-48)
(DE90-010865; UCRL-101998; CONF-900796-2) Avail: NTIS HC/MF A01

A three-dimensional numerical cloud model (OCTET) is developed to simulate the transport, diffusion and scavenging of aerosol particles. The initial purpose of the model is to estimate the fraction of smoke particles emitted by large fires that are scavenged by precipitation immediately above the fire and the fraction that is injected into the upper troposphere and stratosphere. Because large fires generate strong updrafts, the clouds penetrate above the freezing level and contain frozen hydrometeors; therefore, interactions of the aerosol with the ice phase must be included in the model. This paper is a description of the current microphysics and scavenging parameterization. DOE

N91-16459# Lawrence Livermore National Lab., CA.
CLIMATE CAUCUS REPORT: OPPORTUNITIES FOR BRIDGING THE GAPS FROM EFFECTS TO IMPACTS
Michael C. MacCracken Apr. 1990 10 p Presented at the Workshop on Global Climate Change and Its Effects on California, Davis, CA, 10-12 Jul. 1989
(Contract W-7405-eng-48)
(DE90-010877; UCRL-101735; CONF-8907191-1) Avail: NTIS HC/MF A02

The workshop provided an important opportunity for those studying climate research to meet with those evaluating potential impacts as a bridge to formulating and developing effective policy responses. Participants identified an extensive range of capabilities at the University of California campuses and laboratories, spanning experience in biogeochemical cycling, atmospheric and oceanic modeling, data and model analysis and intercomparison, monitoring and observation capabilities, and hydrology and surface processes. These diverse capabilities together create a significant strength in study of the physical and chemical environment. Climate Caucus members identified a number of important initiatives that could extend understanding of potential changes in California. More detailed analysis of existing model simulations, model improvements including nesting of mesoscale models, and more extensive analyses of available data sets could provide important insights into potential changes in hydrology and in the intensity of the California current. Increased computer resources could provide both an incentive and the glue to enhance collaboration between physical and biological studies. A strong commitment to pursue these opportunities could assure significantly more definitive assessments of the potential impacts of climate change on California and provide a firmer basis for policy consideration. DOE

N91-16460# Lamont-Doherty Geological Observatory, Palisades, NY.
MULTI-DIMENSIONAL ASPECTS OF RECENT CLIMATE CHANGE IN NORTH AMERICA Progress Report, 15 Aug. 1989 - 1 Apr. 1990
George J. Kukla, Joyce E. Gavin, and Thomas R. Karl (National Climatic Data Center, Asheville, NC.) Apr. 1990 17 p
(Contract DE-FG02-85ER-60372)
(DE90-010958; DOE/ER-60372/5) Avail: NTIS HC/MF A03

Work on the project began in August 1989. The objectives are: to identify and analyze time related changes in the properties and frequency of individual air masses over North America, and to determine the degree to which the observed changes agree with the predictions of climate models testing the CO2 impact. Climate models predict a substantial warming of the surface air temperature due to increased levels of atmospheric CO2 and other trace gases. These greenhouse gases are expected to affect various air masses differently. Changes in the properties of

individual air masses and their frequency will be used to assess climate change. Particular attention will be given to moisture dependent variables which can mask the CO2 signal. DOE

N91-16461# Edgerton, Germeshausen and Grier, Inc., Idaho Falls, ID.
THE ROLE OF QUALITY ASSURANCE IN THE MONITORING OF TERRESTRIAL ECOSYSTEMS
R. P. Breckenridge, G. L. Olson, G. B. Wiersma, and K. B. Jones (Environmental Monitoring and Support Lab., Las Vegas, NV.) 1990 7 p Presented at the 3rd Ecological Quality Assurance Workshop, Ontario, 24-26 Apr. 1990
(Contract DE-AC07-76ID-01570)
(DE90-010986; EGG-M-90102; CONF-9004200-1) Avail: NTIS HC/MF A02

Quality assurance in ecosystem monitoring helps reduce the variability associated with human factors, and increase the probability that if the work is duplicated by other scientists, the results will be comparable. This paper addresses quality assurance issues related to program design, field work, and subjective measurements in terrestrial monitoring. The purpose of this paper is to provide topics for discussion for participants at the Ecological Quality Assurance Workshop, and is not intended to be an exhaustive study of these topics. DOE

N91-16462# Lawrence Livermore National Lab., CA. Environmental Sciences Div.
OZONE AND ACID-PRECIPITATION ON WESTERN CONIFEROUS FORESTS
S. Cowles, J. L. J. Houpis, and J. R. Kercher May 1990 26 p
(Contract W-7405-eng-48)
(DE90-011014; UCRL-21221) Avail: NTIS HC/MF A03

Reviews of airborne pollution problems and their effects on plants are numerous. The authors of these reviews integrate and synthesize the plethora of observations reported in the literature. In contrast, the focus here is a review of research into mechanistic processes. This brief literature review addresses the mechanistic effects of air pollutants on western coniferous forests in the United States and on the primary inhabitants of these forests. To accomplish this goal, literature from other regions was examined. This inclusion was necessary because most biological work examines the effects of air pollutants in the regions of heaviest impact, the eastern United States and Europe. The purpose of this review is to provide an introduction to various processes that have been identified as potentially important in relating air pollution to observed growth and metabolic changes. In particular, the mechanisms that are emphasized are those appropriate for inclusion in simulation models. DOE

N91-16463# Oak Ridge National Lab., TN.
FINALIZATION OF THE INTERNATIONAL BIOSPHERIC MODEL VALIDATION STUDY Foreign Trip Report
F. O. Hoffman May 1990 30 p
(Contract DE-AC05-84OR-21400)
(DE90-011087; ORNL/FTR-3603) Avail: NTIS HC/MF A03

The primary objectives of this meeting were to finalize the drafting of the International Biospheric Model Validation Study (BIOMOVS) final report and to discuss a draft proposal announcing continuation of BIOMOVS into Phase 2. The meeting was held in Paris, France, from April 23 through April 28, 1990, at the offices of INTAKTA, a French subsidiary of the Swedish firm KEMAKTA. The Swedish firm functions as the present secretariat for BIOMOVS. BIOMOVS has provided an international forum for testing and critically evaluating models commonly used to predict the transfer of radionuclides through the biosphere. Although other international efforts have addressed the evaluation and testing of radionuclides and other pollutants in primary environmental media such as the atmosphere and the oceans, BIOMOVS has been the first organization devoted to model testing in the field of radioecology. The task undertaken by BIOMOVS has been especially important because model testing and evaluation involve the transboundary transport between the primary environmental media and the biological elements within these media. DOE

N91-16464 New South Wales Univ., Canberra (Australia). School of Accountancy.
ENVIRONMENTAL UNCERTAINTY, PLANNING AND ORGANIZATIONAL PERFORMANCE Ph.D. Thesis, 1989 Abstract Only
Graham William Bradley 27 Jun. 1990 3 p
Avail: Issuing Activity

The relationship between planning and organizational performance was examined. Organizations which develop appropriate planning and control systems, and internal planning environments relative to the level of uncertainty in their external environments achieving higher relative performance than other organizations which do not, were studied. The findings showed that organizations do appear to obtain benefits through the adoption of appropriate planning and control systems and internal planning environments relative to the level of uncertainty in their external environments. The level of development of organizations' planning and control systems and the congeniality of their internal planning environments related to the level of uncertainty in their external environments was examined. The findings showed that there was a positive relationship between the level of perceived uncertainty in organizations' external environments; the level of development of their planning and control systems; and the congeniality of their internal planning environments. It appears that organizations which develop appropriate planning and control systems and internal planning environments enhance their ability to survive. Whether those organizations which correctly perceived their external environments achieved a higher relative performance than those organizations which did not, was examined. In order to test these relationships it was necessary to develop a number of measurement systems specifically for this research, namely: perceived external environmental uncertainty; potential organizational performance; and past organizational performance. These measurement systems were tested successfully for reliability and validity. Author

N91-16465# Oak Ridge National Lab., TN. Environment Sciences Div.
MONITORING CHALLENGES AND INNOVATIVE IDEAS
Robert V. ONeill, C. T. Hunsaker, and D. A. Levine 1990 33 p Presented at the Ecological Indicators Conference, Ft. Lauderdale, FL, 16-19 Oct. 1990
(Contract DE-AC05-84OR-21400)
(DE91-000586; CONF-9010198-1) Avail: NTIS HC/MF A03

Monitoring programs are difficult to design even when they focus on specific problems. Ecosystems are complex, and it is often impossible to predetermine what aspects of system structure or dynamics will respond to a specific insult. It is equally difficult to interpret whether a response is a stabilizing compensatory mechanism or a real loss of capacity to maintain the ecosystem. The problems are compounded in a broad monitoring program designed to assess ecosystem health at regional and continental scales. It is challenging in the extreme to monitor ecosystem response, at any scale, to past insults as well as an unknown future array of impacts. Some of the fundamental issues and challenges raised by large-scale monitoring efforts are examined. The challenges will serve as a framework and as an excuse to discuss several important topics in more detail. Following the discussion of challenges, some basic innovations are suggested that could be important across a range of monitoring programs. The innovations include integrative measures, innovative methodology, and creative interpretation. DOE

N91-16466*# National Aeronautics and Space Administration, Washington, DC.
THE ATMOSPHERIC EFFECTS OF STRATOSPHERIC AIRCRAFT: A TOPICAL REVIEW
Harold S. Johnston (California Univ., Berkeley.), M. J. Prather, and R. T. Watson Jan. 1991 32 p
(NASA-RP-1250; NAS 1.61:1250) Avail: NTIS HC/MF A03
CSCL 13B

In the late 1960s the aircraft industry became interested in developing a fleet of supersonic transports (SSTs). Between 1972

and 1975, the Climatic Impact Assessment Program (CIAP) studied the possible environmental impact of SSTs. For environmental and economic reasons, the fleet of SSTs was not developed. The Upper Atmosphere Research Program (UARP) has recently undertaken the responsibility of directing scientific research needed to assess the atmospheric impact of supersonic transports. The UARP and the High-Speed Research Program asked Harold Johnston to review the current understanding of aircraft emissions and their effect on the stratosphere. Johnston and his colleagues have recently re-examined the SST problem using current models for stratospheric ozone chemistry. A unique view is given here of the current scientific issues and the lessons learned since the beginning of CIAP, and it links the current research program with the assessment process that began two years ago. Author

N91-16467*# National Aeronautics and Space Administration. Goddard Space Flight Center, Greenbelt, MD.
THE ATMOSPHERIC EFFECTS OF STRATOSPHERIC AIRCRAFT: A CURRENT CONSENSUS
A. R. Douglass, M. A. Carroll, W. B. DeMore, J. R. Holton, I. S. A. Isaksen, H. S. Johnston, and M. K. W. Ko (Atmospheric and Environmental Research, Inc., Cambridge, MA.) Jan. 1991 46 p
(NASA-RP-1251; NAS 1.61:1251) Avail: NTIS HC/MF A03 CSCL 13B

In the early 1970's, a fleet of supersonic aircraft flying in the lower stratosphere was proposed. A large fleet was never built for economic, political, and environmental reasons. Technological improvements may make it economically feasible to develop supersonic aircraft for current markets. Some key results of earlier scientific programs designed to assess the impact of aircraft emissions on stratospheric ozone are reviewed, and factors that must be considered to assess the environmental impact of aircraft exhaust are discussed. These include the amount of nitrogen oxides injected in the stratosphere, horizontal transport, and stratosphere/troposphere assessment models are presented. Areas in which improvements in scientific understanding and model representation must be made to reduce the uncertainty in model calculations are identified. Author

N91-16274# Academia Sinica, Beijing (China). Inst. of Mathematics.
ANALYSIS OF ATMOSPHERIC DIFFUSION OF POLLUTANTS BASED ON THE LIMITED OBSERVATION OF HORIZONTAL WIND
Lier Wang and Huamo Wu *In* Tokyo Univ., The Proceedings of the Symposium on Mechanics for Space Flight 1989 Mar. 1990 p 105-113 (For primary document see N91-16266 08-34)
Avail: NTIS HC/MF A09

46 GEOPHYSICS

Includes aeronomy; upper and lower atmosphere studies; ionospheric and magnetospheric physics; and geomagnetism.

For space radiation see *93 Space Radiation.*

N91-16468# Sandia National Labs., Albuquerque, NM. Ground Motion and Seismic Div.
SEISMIC SIGNAL PROCESSING OPTIMIZED FOR A SPECIFIC SOURCE AND RECEIVER
Samuel D. Stearns Apr. 1990 26 p
(Contract DE-AC04-76DP-00789)
(DE90-010189; SAND-90-0462) Avail: NTIS HC/MF A03

A seismic signal processing procedure is designed so that its performance is optimized for a specific seismic array looking for explosions at a specific teleseismic location. In this report we first describe the processing procedure, which essentially estimates beamformer signal power as a function of time in a specified frequency band. Then we calibrate the procedure for the Norwegian Regional Seismic array (NRSA) in terms of equivalent body magnitude (emb) level versus signal power using U.S. Department of Interior/Geological Survey (USGS) epicenter data from documented explosions at the USSR Semipalatinsk test area in Eastern Kazakh. Finally, we test the performance of the procedure on actual NRSA data and estimate that explosions above approximately mb 4.0 at Semipalatinsk correspond with an event rate in the emb signal on the order of one to ten events per hour. We conclude that, to detect and analyze events around the clock at levels below mb 4.0, an automatic event locator must be used to process the output of the procedure described here. DOE

N91-16469# Lawrence Livermore National Lab., CA.
SEISMIC IMAGING FOR VELOCITY AND ATTENUATION STRUCTURE IN GEOTHERMAL FIELDS
J. J. Zucca and J. R. Evans (Geological Survey, Menlo Park, CA.) Jun. 1989 5 p Presented at the Annual Meeting of the Geothermal Resources Council: The Geysers - Three Decades of Achievement: A Window on the Future, Santa Rosa, CA, 1-4 Oct. 1989
(Contract W-7405-eng-48)
(DE90-010742; UCRL-100841; CONF-891031-11) Avail: NTIS HC/MF A01

We have applied the attenuation inversion technique developed by Evans and Zucca (1988) to a seismic tomographic data set taken at Newberry Volcano by Achauer et al. (1988). Our preliminary results suggest that the interpretation of the velocity data by Achauer et al. that a magma chamber is present 3 km beneath the caldera is not confirmed by the attenuation data. DOE

N91-16470# Geological Survey, Menlo Park, CA.
PRINCIPAL FACTS FOR ABOUT 16,000 GRAVITY STATIONS IN THE NEVADA TEST SITE AND VICINITY
R. N. Harris, D. A. Ponce, H. W. Oliver, and D. L. Healey (Geological Survey, Denver, CO.) 1989 78 p
(Contract DE-AI08-78ET-44802)
(DE90-011521; USGS-OFR-89-682-A) Avail: NTIS HC/MF A05

The Nevada Test Site (NTS) and vicinity includes portions of the Goldfield, Caliente, Death Valley, and Las Vegas. This report documents and consolidates previously published and recently compiled gravity data to establish a gravity data base of about 16,000 stations for the NTS and vicinity. While compiling data sets, redundant stations and stations having doubtful locations or gravity values were excluded. Details of compiling the gravity data sets are discussed in later sections. Where feasible, an accuracy code has been assigned to each station so that the accuracy or reliability of each station can be evaluated. This data base was used in preparing complete Bouguer and isostatic gravity maps of the NTS and vicinity. Since publication of the complete Bouguer gravity map, additional data were incorporated into the isostatic gravity map. Gravity data were compiled from five sources: 14,183 stations from the U.S. Geological Survey (USGS), 326 stations from Exploration Data Consultants (EDCON) of Denver, Colorado, 906 stations from the Los Alamos National Laboratory (LANL), 212 stations from the University of Texas at Dallas (UTD), and 48 stations from the Defense Mapping Agency (DMA). This investigation is an effort to study several areas for potential storage of high-level radioactive waste. Gravity stations established under YMP are shown. The objective of this gravity survey was to explore for the presence of plutons. DOE

N91-16471# EG and G Energy Measurements, Inc., Pleasanton, CA.
TURBULENCE AND DIFFUSION IN THE ATMOSPHERIC BOUNDARY LAYER Foreign Trip Report
Ronald L. Baskett 10 May 1990 33 p
(Contract DE-AC08-88NV-10617)
(DE90-011582; EGG-10617-7008) Avail: NTIS HC/MF A03

This conference addressed recent theoretical advancements of turbulence and diffusion in the atmospheric boundary layer (ABL). Activities were centered on the technical sessions of the conference. Sessions addressed clouds and the marine atmospheric boundary layer, field experimental techniques, physical and numerical simulations, transport and diffusion, surface

properties, general boundary layer, stratified turbulence and turbulence in complex terrain. A jointly authored poster on an evaluation of the ARAC emergency response models with and without on-site sound detection and ranging systems (sodars) which measure vertical wind profiles was presented. Several scientists commented on our work and some requested further information. In addition, there was a workshop on dispersion around groups of buildings and a tour of Riso National Laboratory. Developments relevant to our work included work on dispersion model evaluation, especially using Monte Carlo random walk techniques, parameterizations of mixing height and turbulence from remote sensing systems such as sodars and radars, and measurements and parameterizations of enhanced turbulence around groups of buildings. DOE

N91-16472*# Kansas State Univ., Manhattan. Evapotranspiration Lab.

AN INTER-COMPARISON OF SURFACE ENERGY FLUX MEASUREMENT SYSTEMS USED DURING FIFE, 1987

D. Nie, E. T. Kanemasu, L. J. Fritschen, H. Weaver, E. A. Smith, S. B. Verma, R. T. Field, W. Kustas, and J. B. Stewart (Institute of Hydrology, Wallingford, England) 1990 36 p
(Grant NAG5-389)
(NASA-CR-187699; NAS 1.26:187699) Avail: NTIS HC/MF A03 CSCL 04A

During the first International Satellite Land Surface Climatology Program Field Experiment (FIFE-87), surface energy fluxes were measured at 22 flux sites by nine groups of scientists using different measuring systems. A rover Bowen ratio station was taken to nearly all the flux stations to serve as a reference for estimating the instrument related differences. The rover system was installed within a few meters from the host instrument of a site. Net radiation, Bowen ratio, and latent heat fluxes were compared between the rover and the host for the stations visited. Linear regression analysis was used to examine the relationship between rover measurements and host measurements. These inter-comparisons are needed to examine the influence of instrumentation on measurement uncertainty. Highly significant effects of instrument type were detected from these comparisons. Instruments of the same type showed average differences of less than 5 percent for net radiation, 10 percent for Bowen ratio, and 6 percent for latent heat flux. The corresponding average differences for different types of instruments can be up to 10, 30, and 20 percent respectively. The Didcot net radiometer gave higher net radiation while the Swissteco type showed lower values, as compared to the corrected REBS model. The 4-way components methed and the Thornswaite type give similar values to the REBS. The SERBS type Bowen ratio systems exhibit slightly lower Bowen ratios and thus higher latent heat fluxes, compared to the AZET systems. Eddy correlation systems showed slightly lower latent heat flux in comparison to the Bowen ratio systems. Author

N91-16473*# Kansas State Univ., Manhattan. Evapotranspiration Lab.

A STUDY OF THE SURFACE ENERGY BALANCE ON SLOPES IN A TALLGRASS PRAIRIE

D. Nie, T. Demetriades-Shah, and E. T. Kanemasu (Georgia Univ., Griffin.) 1990 40 p
(Grant NAG5-389)
(NASA-CR-187698; NAS 1.26:187698) Avail: NTIS HC/MF A03 CSCL 04A

Four slopes (north, south, east, and west) were selected on the Konza Prairie Research Natural Area to study the effect of topography on surface energy balance and other micrometeorological variables. Energy fluxes, air temperature, and vapor pressure were measured on the sloped throughout the 1988 growing season. Net radiation was the highest on the south-facing slope and lowest on the north-facing slope, and the difference was more than 150 W/sq m (20 to 30 percent) at solar noon. For daily averages, the difference was 25 W/sq m (15 percent) early in the season and increased to 60 W/sq m (30 to 50 percent) in September. The east-facing and west-facing slopes had the same daily average net radiation, but the time of day when maximum net radiation occurred was one hour earlier for the east-facing slope and one hour later for the west-facing slope relative to solar noon. Soil heat fluxes were similar for all the slopes. The absolute values of sensible heat flux (h) was consistently lower on the north-facing slope compared with other slopes. Typical difference in the values of H between the north-facing and the south-facing slopes was 15 to 30 W/sq m. The south-facing slope had the greatest day to day fluctuation in latent heat flux as a result of interaction of net radiation, soil moisture, and green leaf area. The north-facing slope had higher air temperatures during the day and higher vapor pressures both during the day and at night when the wind was from the south. Author

N91-16474# Air Force Inst. of Tech., Wright-Patterson AFB, OH. School of Engineering.

MONTE CARLO SIMULATION OF ATMOSPHERIC NEUTRON TRANSPORT AT HIGH ALTITUDES USING MCNP

Donald R. Culp, David L. Monti, James R. Shoemaker, David Wesley, and Kirk A. Mathews Aug. 1990 72 p
(AD-A226773; AFIT/EN-TR-90-5) Avail: NTIS HC/MF A04 CSCL 04/1

Neutron transport calculations were performed using the Monte Carol code, MCNP. The transport problem considered has a point source at high altitude (40 km). Since atmospheric density decreases with altitude, 2-D effects (cylindrical coordinates) can be important. Results were compared to those obtained with the SMAUG-II computer code, which performs mass-integral scaling of approximate fits to 1-D spherical discrete ordinates solutions. These comparisons show the importance of 2-D computations. Practical issues are discussed of applying MCNP to this problem, without code modifications and includes example input files for MCNP and for SMAUG-II. Computational modelling of neutron transport in the atmosphere is complicated by the variation of air density with altitude. GRA

N91-16475# California Univ., Los Angeles.

ATTENUATION OF SEISMIC WAVES IN THE NEAR-SOURCE REGION Final Report, 17 Feb. 1987 - 16 Feb. 1989

Leon Knopoff 14 Dec. 1989 64 p
(Contract F19628-87-K-0020; AF Proj. 7A10)
(AD-A226814; GL-TR-89-0338) Avail: NTIS HC/MF A04 CSCL 08/10

Consider a model of elastic wave propagation through a material permeated by a dilute ensemble of cracks. The excitation strains are large enough to cause the cracks to grow either by fatigue or by stress corrosion. As the cracks grow, energy is removed from the excitation. The dominant mechanism of growth, and hence for absorption, is creep in the slip-weakening zone at the edges of the cracks. Because of non-linearity, the attenuation in the time domain in this case is significantly waveform dependent. For harmonic excitation and narrow bandwidth detection, 1/Q varies as the cube of the excitation amplitude and is independent of the frequency. For broad band impulsive excitation and detection, an equivalent transfer function for the attenuation has a Q which varies as the first power of the frequency for low frequencies, both for simulated explosion and extended noisy waveshapes. GRA

N91-16476# National Climatic Data Center, Asheville, NC.

JOINT US NAVY/US AIR FORCE CLIMATIC STUDY OF THE UPPER ATMOSPHERE. VOLUME 1: JANUARY Final Report

Michael J. Changery, Claude N. Williams, Michael L. Dickenson, and Brian L. Wallace Jul. 1989 236 p Sponsored by Naval Oceanography Command
(AD-A227122; NAVAIR-50-1C-VOL-1; AWS-TR-89/001-VOL-1)
Avail: NTIS HC/MF A11 CSCL 04/1

The upper atmosphere was studied based on 1980 to 1985 twice daily gridded analyses produced by the European Centre for Medium Range Weather Forecasts. This volume is for the month of January. Included are global analyses of: (1) Mean temperature standard deviation; (2) Mean geopotential height standard deviation; (3) Mean density standard deviation; (4) Mean density standard deviation (all for 13 levels - 1000, 850, 700, 500,

400, 300, 250, 200, 150, 100, 70, 50, 30 mb); (5) Mean dew point standard deviation for the 13 levels; and (6) Jet stream at levels 500 through 30 mb. Also included are global 5 degree grid point wind roses for the 13 pressure levels. Author

N91-16477# National Climatic Data Center, Asheville, NC.
JOINT US NAVY/US AIR FORCE CLIMATIC STUDY OF THE UPPER ATMOSPHERE. VOLUME 2: FEBRUARY Final Report
Michael J. Changery, Claude N. Williams, Michael L. Dickenson, and Brian L. Wallace Sep. 1989 236 p Sponsored by Naval Oceanography Command
(AD-A227123; NAVAIR-50-1C-VOL-2; AWS-TR-89/002-VOL-2)
Avail: NTIS HC/MF A11 CSCL 04/1

The upper atmosphere was studied based on 1980 to 1985 twice daily gridded analyses produced by the European Centre for Medium Range Weather Forecasts. This volume is for the month of February. Included are global analyses of: (1) Mean temperature standard deviation; (2) Mean geopotential height standard deviation; (3) Mean density standard deviation; (4) Height and vector standard deviation (all for 13 pressure levels - 1000, 850, 700, 500, 400, 300, 250, 200, 150, 100, 70, 50, 30 mb); (5) Mean dew point standard deviation for the 13 levels; and (6) Jet stream for levels 500 through 30 mb. Also included are global 5 degree grid point wind roses for the 13 pressure levels. Author

N91-16478# National Climatic Data Center, Asheville, NC.
JOINT US NAVY/US AIR FORCE CLIMATIC STUDY OF THE UPPER ATMOSPHERE. VOLUME 3: MARCH Final Report
Michael J. Changery, Claude N. Williams, Michael L. Dickenson, and Brian L. Wallace Nov. 1989 236 p Sponsored by Naval Oceanography Command
(AD-A227124; NAVAIR-50-1C-VOL-3; AWS-TR-89/003-VOL-3)
Avail: NTIS HC/MF A11 CSCL 04/2

The upper atmosphere was studied based on 1980 to 1985 twice daily gridded analysis produced by the European Centre for Medium Range Weather Forecasts. This volume is for the month of March. Included are global analyses of: (1) Mean Temperature Standard Deviation; (2) Mean Geopotential Height Standard Deviation; (3) Mean Density Standard Deviation; (4) Height and Vector Standard Deviation (all for 13 pressure levels - 1000, 850, 700, 500, 400, 300, 250, 200, 150, 100, 70, 50, 30 mb); (5) Mean Dew Point Standard Deviation for levels 1000 through 30 mb; and (6) Jet stream for levels 500 through 30 mb. Also included are global 5 degree grid point wind roses for the 13 pressure levels. GRA

N91-16479# National Climatic Data Center, Asheville, NC.
JOINT US NAVY/US AIR FORCE CLIMATIC STUDY OF THE UPPER ATMOSPHERE. VOLUME 4: APRIL Final Report
Michael J. Changery, Claude N. Williams, Michael L. Dickenson, and Brian L. Wallace Jul. 1989 236 p Sponsored by Naval Oceanography Command
(AD-A227125; NAVAIR-50-1C-VOL-4; AWS-TR-89/004-VOL-4)
Avail: NTIS HC/MF A11 CSCL 04/1

The upper atmosphere was studied based on 1980 to 1985 twice daily gridded analyses produced by the European Centre for Medium Range Weather Forecasts. This volume is for the month of April. Included are global analyses of: (1) Mean temperature standard deviation; (2) Mean geopotential height standard deviation; (3) Mean density standard deviation; (4) Height and vector standard deviation (all for 13 pressure levels - 1000, 850, 700, 500, 400, 300, 250, 200, 150, 100, 70, 50, 30 mb); (5) Mean dew point standard deviation for the 13 levels; and (6) Jet stream for levels 500 through 30 mb. Also included are global 5 degree grid point wind roses for the 13 pressure levels. Author

N91-16480# National Climatic Data Center, Asheville, NC.
JOINT US NAVY/US AIR FORCE CLIMATIC STUDY OF THE UPPER ATMOSPHERE. VOLUME 7: JULY Final Report
Michael J. Changery, Claude N. Williams, Michael L. Dickenson, and Brian L. Wallace Jul. 1989 236 p Sponsored by Naval Oceanography Command
(AD-A227126; NAVAIR-50-1C-VOL-7; AWS-TR-89/007-VOL-7)
Avail: NTIS HC/MF A11 CSCL 04/1

The upper atmosphere was studied based on 1980 to 1985 twice daily gridded analysis produced by the European Centre for Medium Range Weather Forecasts. This volume is for the month of July. Included are global analyses of: (1) Mean temperature/standard deviation; (2) Mean geopotential height/standard deviation; (3) Mean density/standard deviation; (4) Height and vector standard deviation (all at 13 pressure levels - 1000, 850, 700, 500, 400, 300, 250, 200, 150, 100, 70, 50, 30 mb); (5) Mean dew point standard deviation at levels 1000 through 30 mb; and (6) Jet stream at levels 500 through 30 mb. Also included are global 5 degree grid point wind roses for the 13 pressure levels. Author

N91-16481# National Climatic Data Center, Asheville, NC.
JOINT US NAVY/US AIR FORCE CLIMATIC STUDY OF THE UPPER ATMOSPHERE. VOLUME 10: OCTOBER Final Report
Michael J. Changery, Claude N. Williams, Michael L. Dickenson, and Brian L. Wallace Jul. 1989 236 p Sponsored by Naval Oceanographic Command
(AD-A227127; NAVAIR-50-1C-VOL-10; AWS-TR-89/010-VOL-10)
Avail: NTIS HC/MF A11 CSCL 04/1

The upper atmosphere was studied based on 1980 to 1985 twice daily gridded analysis produced by the European Centre for Medium Range Weather Forecasts. This volume is for the month of October. Included are global analyses of: (1) Mean temperature/standard deviation; (2) Mean geopotential height/standard deviation; (3) Mean density/standard deviation; (4) Height and vector standard deviation (all at 13 pressure levels - 1000, 850, 700, 500, 400, 300, 250, 200, 150, 100, 70, 50, 30 mb); (5) Mean dew point/standard deviation at levels 1000 through 30 mb; and (6) Jet stream at levels 500 through 30 mb. Also included are global 5 degree grid point wind roses for the 13 pressure levels. Author

N91-16482# Yap Analytics, Inc., Lexington, MA.
UPPER ATMOSPHERE IR RADIATION MODELING AND ANALYSIS Annual Report No. 1, 20 Apr. 1989 - 30 Apr. 1990
J. M. Sindoni, R. J. Healey, and B. K. Yap 14 May 1990 62 p
(Contract F19628-89-C-0033)
(AD-A227214; YAI-TR-101; GL-TR-90-0129; SR-1) Avail: NTIS HC/MF A04 CSCL 04/1

The mechanisms involved in the emissions of the infrared (IR) radiation of the upper atmosphere and the related impacts of this background clutter on surveillance sensors were studied. The models for non-equilibrium phenomena leading to emission from very high rotational levels were investigated. One critical parameter in the model is the scattering cross section in a complex multi-body collision and interaction. The impulse approach (IA) is being applied to atom-molecule collisions which accounts for the total scattering amplitude of an atom incident upon a complex system by summation of independent two particle interactions. A resultant momentum distribution of each constituent particle is then evaluated. Studies to date by various investigators uses simplifications, the peaking approximation (PA), to evaluate the complex integral for the momentum of non-interaction (spectator) particles. The validity and accuracy of the PA was investigated. GRA

N91-16483# Air Force Inst. of Tech., Wright-Patterson AFB, OH.
A COMPARISON OF OPTICALLY MEASURED AND RADAR-DERIVED HORIZONTAL NEUTRAL WINDS M.S. Thesis
Michael S. Christie 1990 106 p
(AD-A227690; AFIT/CI/CIA-90-108) Avail: NTIS HC/MF A06 CSCL 04/1

Nighttime thermospheric winds for Sondrestrom, Greenland from 11 nights between 1983 and 1988, were compared to learn about the O(+)-O collision cross section and the high latitude atomic oxygen density. The horizontal winds in the magnetic meridian were derived indirectly from incoherent scatter radar (ISR) measurements on ion velocities antiparallel to the magnetic field

and directly from Fabry-Perot interferometer (FPI) measurements of Doppler shifts of the (6300A) emission of atomic oxygen. In deriving the radar winds, the O(+)-O collision frequency, which involves the product of the atomic oxygen density and the O(+)-O collision cross section, was scaled by a factor of f that was varied from 0.5 to 5.1. On the basis of several arguments the altitude of the 6300A emission was assumed to be 230 km. The best agreement between the ISR and FPI winds was obtained when f was increased substantially, to between 1.7 and 3.4. If the average peak emission altitude were higher, these factors would be larger; if it were lower, they would be somewhat smaller. However, if the average altitude were substantially lower it would have been more difficult to have obtained agreement between the two techniques. GRA

N91-16484# Air Force Inst. of Tech., Wright-Patterson AFB, OH.
DERIVATION OF EXOSPHERIC TEMPERATURE AT HIGH LATITUDES FROM INCOHERENT-SCATTER RADAR DATA M.S. Thesis - Utah State Univ.
Willow Cliffswallow 1990 114 p
(AD-A227721; AFIT/CI/CIA-90-110) Avail: NTIS HC/MF A06 CSCL 04/1

This thesis investigates the feasibility of using statistical methods to derive representative exospheric temperatures in the high-latitude ionosphere despite Joule heating effects. The study was based on two main premises: that Joule heating is spatially and temporally localized in the radar's field of view and that a contaminated neutral temperature population representing Joule heating can be separated from the non-enhanced temperature population by statistical means. Exospheric temperatures were derived from Sondrestrom incoherent-scatter radar data using the ion energy balance equation. The effect of the 0(+) -0 section was tested by increasing it in the ion energy equation by factor of 1.7. Since exospheric temperatures increased only an average of 10 K, the original cross section was used in the calculations. Tests also showed the calculations to be fairly insensitive to variations in the s parameter and the neutral temperature at 120 km, used in the Bates neutral temperature profile, as long as the s value was .02 or greater. Input parameters were drawn from the MSIS86 model atmosphere, and the s values used were always greater than .02. Three tests were used to delimit the lower (non-Joule-heated) population in each cycle of radar observations: the Student t test, the normal distribution test, and the chi-squared test. A mean exospheric temperature was computed for each temperature population determined by the tests. GRA

N91-16485# Air Force Inst. of Tech., Wright-Patterson AFB, OH.
ON THE DEVELOPMENTAL DYNAMICS OF SUDDEN STRATOSPHERIC WARMINGS M.S. Thesis - Creighton Univ.
Ann R. Ostdiek 31 Jul. 1990 91 p
(AD-A227731; AFIT/CI/CIA-90-079) Avail: NTIS HC/MF A05 CSCL 04/1

A Sudden Stratispheric Warming (SSW) is an event which causes a drastic temporary disruption of the zonal winter configuration of the stratosphere. High latitudes in the stratosphere experience temperature increases of over 25 C in less than a week. At the peak of the warming, the temperature can increase by much as 80 C. Typically, within six weeks the atmosphere returns to a more normal configuration, ending the SSW. The onset of a warming is defined by the first appearance of a closed -35 C isotherm at 10 mb (McQuirck and Douglas, 1988). The warming levels ends when temperatures warmer than -35 C are no longer observed. SSWs were first observed in 1952 by Scherhag over Berlin. Until recently, data on SSW were sporadic due to a total dependence on the sparse radiosonde/rocketsonde network. Since the advent to satellite mounted sensors which routinely probe the stratosphere, observational data has become much more abundant. While tremendous advances in the research on SSW have been made in the past decade, few operational meteorologists know much about them. This paper will provide an overview of research done in the following areas: what SSWs are; what synoptic events occur during SSWs; and the dynamics involved with SSWs. GRA

N91-16486# California Univ., Los Angeles.
A STATISTICAL SURVEY OF ELECTRON PITCH ANGLE DISTRIBUTIONS IN THE NIGHTSIDE CENTRAL PLASMA SHEET M.S. Thesis
Timothy F. Alsruhe 1990 88 p Sponsored by AFIT, Wright-Patterson AFB, OH
(AD-A227763; AFIT/CI/CIA-90-077) Avail: NTIS HC/MF A05 CSCL 04/1

The diffuse aurora is produced by precipitating electrons whose origin is believed to be the central plasma sheet. The process by which these electrons are continually scattered into the atmospheric loss cone is unresolved. Arguments included processes which cause pitch angle scattering at the strong diffussion limit. A survey of equatorial pitch angle distributions of about 0.2 to 20 keV electrons was conducted to determine the extent of pitch angle diffusion. Pitch angle distributions were binned by location and geomagnetic activity for the nightside near earth plasma sheet. The average pitch angle anisotropy was determined for each bin. Representative samples were selected from geomagnetically quiet distributions. Of the three energies examined (1.09, 4.52, 19.4 keV), only distributions consistent with moderate to weak diffusion were observed. Even test cases were consistent with only moderate diffusion. These results conclude that strong diffusion is usually not in effect in the quiet near earth plasma sheet. Electron Cyclotron Harmonic (ECH) waves at the 3/2 harmonic are suggested as the scattering mechanism responsible for maintaining the diffuse aurora. The necessary ECH wave amplitudes required to recreate average distributions were calculated. Derived amplitudes were one to three orders of magnitude greater than those amplitudes observed. Thus, it is concluded ECH do not occur with the frequency and amplitude necessary to sustain the continuous diffuse aurora. GRA

N91-16487# Maryland Univ., College Park. Inst. for Physical Science and Technology.
A CASE STUDY OF THE 19 OCTOBER 1989 POLAR CAP ABSORPTION EVENT USING THE IMAGING RIOMETER FOR IONOSPHERIC STUDIES M.S. Thesis
Timothy C. Davis 1990 118 p Sponsored by AFIT, Wright-Patterson AFB, OH
(Grants NSF UPP-84-19272; NSF DPP-88-18229)
(AD-A227764; AFIT/CI/CIA-90-076) Avail: NTIS HC/MF A06 CSCL 04/1

A polar cap absorption (PCA) event, beginning on 19 October 1989, is examined using the Imaging Riometer for Ionospheric Studies (IRIS) developed at the Univ. of Maryland. IRIS is a 49-beam (7 x 7) phased array 38.2 MHz radiowave imaging system and operating at Amundsen-Scott South Pole Station, Antarctica. After applying a low pass filter, a cross correlation was performed between the central beam and the other beams in the array. From the cross correlation analysis, whether there is any delay of effects during event onset and early main phase (plateau) within the array was determined. For most of the period studied, no delay was detected; i.e., features of each beam's absorption time series were essentially simultaneous. However, significant delays (approx. 2 minutes) occurred at the equatorward edge during a local absorption peak occurring just prior to magnetic local noon. The peak is coincident with short term energetic particle flux enhancements detected by GOES-7. Two possible mechanisms are proposed: a local time variation of cutoff rigidities possibly associated with the relative position of the dayside cusp, and a short term change in energetic particle rigidity spectrum. GRA

N91-16488# ST Systems Corp., Lexington, MA.
A STUDY OF THE INTERACTION OF PHYSICAL AND NUMERICAL PARAMETERIZATIONS WITH REGARD TO MOISTURE FORECASTING IN A REGIONAL MODEL OF THE ATMOSPHERE Final Report, May 1988 - May 1990
Isadore M. Halberstam, S.-L. Tung, L. Knowlton, and G. Zolotusky

25 Jul. 1990 66 p
(Contract F19628-88-C-0072; AF Proj. 2310)
(AD-A227966; GL-TR-90-0173) Avail: NTIS HC/MF A04
CSCL 04/1

This is the final report produced under contract F19628-88-C-0072. It summarizes the research performed with STX's Relocatable Limited-Area Model (RLAM) in assessing the necessary ingredients for forecasting moisture. The report describes the experiments involving lateral boundary treatment and physical parameterizations of the planetary boundary layer (PBL) and convective systems. It also explains how these interact with the numerical schemes that are available in RLAM and what effects these have on moisture forecasts. GRA

N91-16489# Aerospace Corp., El Segundo, CA. Lab. Operations.
THE MAGNETOSPHERIC RESPONSE TO 8-MINUTE PERIOD STRONG-AMPLITUDE UPSTREAM PRESSURE VARIATIONS
D. G. Sibeck, A. T. Lui, R. W. McEntire, T. A. Potemra, and K. Takahashi 6 Aug. 1990 65 p
(Contract F04701-88-C-0089)
(AD-A228038; TR-0089(4940-05)-1; SSD-TR-89-30) Avail: NTIS HC/MF A04 CSCL 04/1

This report documents a series of brief, strong (Delta p/p = 1), dynamic pressure oscillations that occurred in the region upstream of the Earth's bow shock during a period of radial interplanetary magnetic field (IMF). The analyzed set of oscillations, which may be either intrinsic solar wind or bow shock-related phenomena, recur approximately every 8 to 10 minutes, and their magnetic field signatures occur nearly simultaneously over great distances transverse to the Earth-sun line. The pressure oscillations appear to drive tailward-moving magnetopause surface wavelets. In turn, the surface wavelets can be identified as hydromagnetic waves with strong compressional components in the outer magnetosphere and as quasi-periodic variations in electron precipitation and high-latitude ground pulsations. We use observations by spacecraft in the outer dayside magnetosphere to predict geosynchronous and subsolar magnetic field strengths, the location of the subsolar magnetopause, the solar wind dynamic pressure, and variations in the energetic magnetospheric ion flux. GRA

N91-16490 Harvard Univ., Cambridge, MA.
CONTINUUM MODELS OF CONTINENTAL DEFORMATION Ph.D. Thesis
Shimon Wdowinski 1990 150 p
Avail: Univ. Microfilms Order No. DA9035585

Viscous flow models are used to investigate continental deformation above subduction zones and isostatic rebound due to tectonic denudation. These models are applied to the extensional and compressional tectonic environments of the Andes, the Aegean, and the Basin and Range province. Large scale continental tectonics of back-arc (extensional) and Andean-type (compressional) environments are investigated by using a thin viscous sheet model to calculate the deformation of the overlying continental lithosphere and a corner flow model to calculate the asthenospheric flow underneath. For a compressional environment, the model predicts that a broad region of uplifted topography will tend to develop above a more steeply dipping slab, as is observed in the various segments of the central Andes. For an extensional environment, the model predicts that a zone of compression can develop near the trench, and that extensional strain rates increase with distance from the trench, as is observed in the Aegean. A different approach is taken to calculate the deformation of the central Andes, where the overriding continental lithosphere and the asthenosphere are investigated as a single system by using a plane strain viscous flow model of the upper 700 km of the Earth. The same formulation and numerical methods of solution are used to investigate the extension in the Basin and Range province. A four-layer model of the upper 150 km of the earth is used to calculate the viscous response of continental crust and the underlying mantle to tectonic denudation. The model predicts footwall uplift, Moho deflection, and surface topography which are similar to that which was observed in the Basin and Range province. Overall, continuum models of continental deformation enable a quantitative investigation of continental tectonics and provides a physical explanation of the causes of the deformation. Dissert. Abstr.

N91-16491 Michigan Univ., Ann Arbor.
EXCURSIONS TO THE BASE OF THE MANTLE Ph.D. Thesis
Christopher John Young 1990 219 p
Avail: Univ. Microfilms Order No. DA9034551

The core mantle boundary (CMB) region, consisting of the core mantle interface itself and the few hundred kms above and below it, is investigated in two different types of large-scale seismological studies. In the first, a large set of long-period S phases is analyzed to determine large scale shear velocity structures in the CMB region beneath Alaska. Subdivision of the data by depth, source region, and source to receiver azimuth established that the observations exhibit stable behavior, which is consistent with extensive local stratification of D double prime. The preferred model SYLO, has a 2.75 percent velocity increase 243 km above the CMB and a negative velocity gradient within the D double prime layer. Analysis of the core-penetrating phases indicates that the outermost 100 km of the core below the fast D double prime region underlying Alaska must be slower than the PREM structure. In the second, a set of short-period P-wave amplitude profiles near the core shadow zone is utilized to explore lateral variation in P velocity structure at the base of the mantle. Various radially symmetric models are tested by comparison of the data with amplitudes measured from synthetics. The observed amplitude versus distance profiles exhibit significant regional variations of the apparent shadow zone boundary, with as much as a 5 deg shift in onset distance, but it is possible to model the overall behavior using simple, regionally varying positive P velocity gradients in the lowermost mantle. The strong lateral variations required by the data support the presence of compositional heterogeneity in D double prime. The results from these two studies, as well as those from previous studies of the CMB region, are used to evaluate several simple schemes for the role of D double prime in mantle conversion. Dissert. Abstr.

N91-16492 California Univ., Los Angeles.
SEISMIC STRUCTURE OF THE UPPER MANTLE UNDER THE PACIFIC OCEAN Ph.D. Thesis
Ke-Shan Zou 1990 147 p
Avail: Univ. Microfilms Order No. DA9035235

The seismic structure of the upper mantle under the Pacific Ocean was studied by inverting fundamental-mode Rayleigh wave phase velocities in the ultra-long period range of 100 to 300 s. The results from various regionalization models have indicated that lateral heterogeneities in the Pacific are strongly associated with sea floor age to a depth of 200 km. Some important results include: the geometry of the bottom of the low velocity channel under the ocean was resolved for the first time using seismic data. Although the thickness of the low velocity zone (LVZ) decreases with age, the bottom of the LVZ deepens monotonically with increasing age. Thus age-related variations of properties under the Pacific extend as deeply as the bottom of the low velocity channels which is at a depth around 200 km, and extends as far as the oldest oceans with age greater than 117 m.y. A significant low velocity anomaly in the mantle associated with major hot-spots in the Pacific plate was found. The anomalous structure around the Hawaii and the Austral-Tuamotu hot spots, is characterized by a thin lithosphere with a prominent, thick asthenosphere. This hot spot structure is embedded in the main frame of age-related heterogeneity. The lateral variations of the lower boundary to the sub-channel cannot be well defined. Either the limited path coverage or the poor resolution and accuracy of the measurements of fundamental mode long-period data lead to a poor resolution of the phase transition zone at depths of the order of 420 km. Hence, very little is known about regional variations in this depth. The temperature and the degree of partial melting in the low velocity channel under different ages of the ocean floor are

estimated according to published laboratory data. A discussion is made whether the low velocity channel is in a partial melting or a subsolidus state. Dissert. Abstr.

N91-16493# Bonn Univ. (Germany, F.R.). Inst. fuer Physik.
THE CABANNES-LIDAR FOR THE EXAMINATION OF THE STRATOSPHERE: SELECTED DESIGN ELEMENTS FOR THE EXPERIMENTAL CONSTRUCTION Thesis [DAS CABANNES-LIDAR ZUR UNTERSUCUNG DER STRATOSPHAERE: AUSGEWAEHLTE BAUELEMENTE DES EXPERIMENTELLEN AUFBAUS]
Heinz-Juergen Schaefer Sep. 1990 115 p In GERMAN; ENGLISH summary
(BONN-IR-90-39; ISSN-0172-8741; ETN-91-98563) Avail: NTIS HC/MF A06

A new lidar experiment for the measurement of temperature profiles and the aerosol content of the Arctic stratosphere is described. Several backscattering mechanisms are presented and the spectral distribution of expected signals is derived. Light pulses emitted by a laser and backscattered in the atmosphere are spectrally analyzed in the receiving branch with an excellent resolution. Four possible interferometer systems were compared. The reasons for choosing the Nd:YAG laser system were discussed. The transfer optics from the laser to the atmosphere were described. Technical characteristics for different photomultiplier tubes were discussed and compared. Simulations of the expected signals for several spectral resolutions were presented. ESA

N91-16494 Max-Planck-Inst. fuer Physik und Astrophysik, Garching (Germany, F.R.). Inst. fuer Extraterrestrische Physik.
THE ROLE OF THE EQUATORIAL ELECTROJET IN THE EVENING IONOSPHERE
G. Haerendel and J. V. Eccles Jun. 1990 42 p Submitted for publication
(MPE-PREPRINT-184; ETN-91-98608) Copyright Avail: Fachinformationszentrum Karlsruhe, 7514
Leopoldshafen-Eggenstein 2, Fed. Republic of Germany

The role of the equatorial E region in the electrodynamics of the evening ionosphere is examined. It is proposed that the equatorial electrojet current near sunset has a significant role in the determination of the post sunset enhancement of the horizontal electric field. The electrojet region provides the best avenue for current to be channeled from the dayside to meet the vertical current demands of the F region neutral wind dynamo after sunset. The conductivity reduction in the E region due to the recombination of ionization and the plasma uplift enhances the horizontal (eastward) electric field and thereby increases the speed of the uplift. Thus, the dynamic adjustment of ionization has an unstable, feedback relationship with the electrical fields which may explain the night to night variability of the horizontal electric field enhancement. ESA

N91-16495 Max-Planck-Inst. fuer Physik und Astrophysik, Garching (Germany, F.R.). Inst. fuer Extraterrestrische Physik.
THEORY FOR MODELING THE EQUATORIAL EVENING IONOSPHERE AND THE ORIGIN OF THE SHEAR IN THE HORIZONTAL PLASMA FLOW
G. Haerendel, J. V. Eccles, and S. Cakir (Middle East Technical Univ., Ankara, Turkey) Jun. 1990 49 p Submitted for publication
(MPE-PREPRINT-185; ETN-91-98609) Copyright Avail: Fachinformationszentrum Karlsruhe, 7514
Leopoldshafen-Eggenstein 2, Fed. Republic of Germany

Equations describing the time evolution of the equatorial ionosphere are developed using flux tube integrated and flux tube weighted quantities which model the chemistry, dynamics and electrodynamics of the equatorial ionosphere. The resulting two dimensional set of equations can be used to investigate equatorial electric fields neglecting small scale phenomena. An immediate result derived from the integrated current equations is an equation describing the physics of the shear in the horizontal flow of the equatorial plasma during the evening hours. The profile of the horizontal flow has three imortant contributing terms relating to the neutral wind dynamo, Hall conduction, and the equatorial electrojet current divergence. Using a one dimensional model of the velocity shear equation and the integrated ionospheric transport equations, a time history of the development of the shear feature during post sunset hours is presented. The one dimensional model results are compared to the velocity shear measurements from the colored bubbles experiments. ESA

N91-16496 Max-Planck-Inst. fuer Physik und Astrophysik, Garching (Germany, F.R.). Inst. fuer Extraterrestrische Physik.
COMPUTER SIMULATIONS OF MEDIUM WAVELENGTH IRREGULARITIES IN THE EQUATORIAL IONOSPHERE RESULTING FROM ARTIFICIALLY PRODUCED DENSITY ENHANCEMENTS
S. Cakir (Middle East Technical Univ., Ankara, Turkey), G. Haerendel, and J. V. Eccles Jun. 1990 46 p Submitted for publication
(MPE-PREPRINT-186; ETN-91-98610) Copyright Avail: Fachinformationszentrum Karlsruhe, 7514
Leopoldshafen-Eggenstein 2, Fed. Republic of Germany

The motion of plasma density enhancements (barium clouds) artificially introduced into the post sunset equatorial F region is investigated with a two dimensional model incorporating flux tube integrated quantities. The temporal development of the ionosphere, in which the density perturbations are embedded, is derived from a one dimensional set of relations modeling plasma transport and the vertical electric field from initial conditions and a prescribed variation of the horizontal electric field as a function of time. The calculations show that the strong horizontal shear flows existing at the night time F region ledge (where the perturbations were placed) reduce the growth of polarization fields associated with the enhancements and adjacent relative depletions of plasma for weak perturbations. These simulations show why experimental efforts of initiating rising bubbles and equatorial spread F were not successful. The experiments require larger scale and stronger density perturbations than can be achieved with conventional sounding rocket releases of barium vapors. ESA

47 METEOROLOGY AND CLIMATOLOGY

Includes weather forecasting and modification.

N91-16497# Lawrence Livermore National Lab., CA.
GCM (GENERAL CIRCULATION MODEL) PREDICTIONS FOR SURFACE AIR TEMPERATURE AND PRECIPITATION OVER THE SOUTHEASTERN UNITED STATES
Stanley L. Grotch Mar. 1990 17 p Presented at the Southeast Regional Climate Symposium: Global Change - A Southern Perspective, Charleston, SC, 19-22 Feb. 1990
(Contract W-7405-eng-48)
(DE90-009434; UCRL-JC-103166; CONF-900255-2) Avail: NTIS HC/MF A03

For regional assessments of the effects of possible global climate change due to increasing greenhouse gases, two of the most significant variables predicted by general circulation models (GCM's) are surface air temperature and precipitation. In an earlier Department of Energy report, the results from four GCMs and several historical climate data sets for each of these variables (both seasonally and annually averaged) were intercompared over different regional scales using a variety of techniques. In the work reported here, several more recent, higher resolution simulations are included and attention is focused primarily on the southeastern United States. Two graphical/statistical techniques are applied: (1) cuts intercomparing model/historical data predictions at both fixed latitudes and longitudes, and (2) side-by-side boxplots showing the quartiles of the distributions for a particular variable for a selected subset of gridpoints in a specified region. DOE

N91-16498# Lawrence Livermore National Lab., CA.
THE VALUE OF ON-SITE SODAR DATA IN REGIONAL MODELING
John S. Nasstrom, Ronald L. Baskett, and Rolf Lang Feb. 1990

4 p Presented at the 9th Symposium on Turbulence and Diffusion, Roskilde, Denmark, 30 Apr. - 3 May 1990
(Contracts W-7405-eng-48; DE-AC08-88NV-10617)
(DE90-009921; UCRL-JC-103279; CONF-9004180-1) Avail: NTIS HC/MF A01

Three-dimensional dispersion modeling has many applications. At Lawrence Livermore National Laboratory, it is used both as a research tool and, by the Atmospheric Release Advisory Capability (ARAC), as an emergency response tool. ARAC uses a diagnostic three-dimensional regional modeling system built around the MATHEW (Mass-Adjusted Three-dimensional Wind field) and ADPIC (Atmospheric Dispersion Particle-In-Cell) models. Initializing these models requires meteorological observations to estimate the horizontal and vertical variation of the wind in the atmospheric boundary layer. These observations may be obtained from meteorological towers, tethersondes, rawinsondes, or remote sensing instruments. Standard twice-daily rawinsonde observations are readily available but may be outside the modeling domain and up to 12 hours old. Sodars such as the Doppler acousting sounder show promise in providing the necessary vertical wind inputs. If properly sited, one would expect that real-time soundings within the modeling domain would provide the best initialization of the upper level wind field. This paper attempts to assess the value of on-site vertical wind measurements to dispersion modeling in two different settings. One is the Savannah River, Georgia. The second is the Diablo Canyon Power Plant, California. Author

N91-16499# Los Alamos National Lab., NM.
NUMERICAL SIMULATIONS OF THE MOUNTAIN IRON TRACER DATA
Tetsuji Yamada and Susan S. Bunker 1990 7 p Presented at the International Symposium on Measurement of Toxic and Related Air Pollutants, Raleigh, NC, 30 Apr. - 4 May 1990 Sponsored by AFESC, Tyndall AFB, FL
(Contract W-7405-eng-36)
(DE90-009749; LA-UR-90-1332; CONF-900435-1) Avail: NTIS HC/MF A02

Extensive field experiments were conducted during 1965 and 1966 near Vandenberg Air Force Base. The experiments included wind speed and wind direction measurements at several towers, upper air soundings by radiosondes, and fluorescent particle releases to characterize the diffusion processes. The data provide a unique opportunity to test numerical models under realistic boundary conditions: land-sea contrast and complex topography. We used high order turbulence model for air circulations (HOTMAC), a three-dimensional mesoscale model based on simplified turbulence-closure equations, to simulate temporal and spatial variations of wind, temperature, mixing ratio of water vapor, and turbulence distributions. Surface concentrations were computed by using a three-dimensional transport and diffusion model random puff transport and diffusion (RAPTAD). RAPTAD is a Lagrangian puff code based on the Monte Carlo statistical diffusion process. The center location and standard deviation of concentration distribution for each puff are computed by using wind and turbulence modeled by HOTMAC. Then, the concentration at any location is computed by summing concentrations contributed by all the puffs. The purpose of this study is to simulate the transport and dispersion of atmospheric pollutants in the complex terrain surroundings at Vandenberg Air Force Base by using the Los Alamos National Laboratory (LANL) atmospheric models HOTMAC and RAPTAD. DOE

N91-16500*# National Aeronautics and Space Administration. Marshall Space Flight Center, Huntsville, AL.
NASA/MSFC FY90 GLOBAL SCALE ATMOSPHERIC PROCESSES RESEARCH PROGRAM REVIEW
Fred W. Leslie, ed. Washington Oct. 1990 58 p Conference held in Huntsville, AL, 20-21 Aug. 1990
(NASA-CP-3093; M-651; NAS 1.55:3093) Avail: NTIS HC/MF A04 CSCL 04B

Research supported by the Global Atmospheric Research Program at the Marshall Space Flight Center on atmospheric remote sensing, meteorology, numerical weather forecasting, satellite data analysis, cloud precipitation, atmospheric circulation, atmospheric models and related topics is discussed. For individual titles, see N91-16501 through N91-16517.

N91-16501*# National Aeronautics and Space Administration. Marshall Space Flight Center, Huntsville, AL.
COMPARISON OF SSM/I MEASUREMENTS TO NUMERICALLY-SIMULATED CLOUD AND PRECIPITATION DURING ERICA
Franklin R. Robertson, Charles Cohen, Donald J. Perkey (Drexel Univ., Philadelphia, PA.), and William Lapenta *In its* NASA/MSFC FY90 Global Scale Atmospheric Processes Research Program Review Oct. 1990 p 1-3 (For primary document see N91-16500 08-47)
Avail: NTIS HC/MF A04 CSCL 04B

These investigations focused essentially on the macroscale organization of cloud and precipitation which occurred during the 4th Intensive Observing Period (IOP-4) of the Experiment for Rapidly Intensifying Cyclones over the Atlantic (ERICA). This experiment, held off the East Coast of the United States and Canada during the winter of 1989, documented several episodes of rapid cyclonic storm development. Also playing a major role as validation and ground truth in these studies are Special Sensor Microwave Imager (SSM/I) retrievals of precipitable water, total liquid water and ice, generated by other Marshall Space Flight Center (MSFC) supported investigations. Model simulations produced to date suggest that, while the large-scale atmospheric dynamics was an essential driving mechanism, the role of condensation was crucial in facilitating the exceptionally rapid spinup of the cyclone and the low surface pressure. A model simulation of the precipitation rate at the time of most rapid storm intensification is shown in the accompanying figure. Heavier precipitation rates in the crescent shaped region are associated with deep convection along the leading edge of a dry intrusion behind the surface low. The majority of precipitation in the stratiform region to the northeast involved the production of ice with deposition from vapor to ice being the dominant process of growth. Some small amount of mixed phase cloudiness was present. Model condensate distributions matched well with SSM/I observations. The accompanying SSM/I imagery which delineates areas of large (greater than several hundred micron effective radius) precipitating ice over the ocean suggests that the model has done well in capturing the essential mechanisms responsible for the horizontal distribution of precipitation. Author

N91-16502*# National Aeronautics and Space Administration. Marshall Space Flight Center, Huntsville, AL.
OBSERVATION SIMULATION EXPERIMENTS WITH REGIONAL PREDICTION MODELS
George Diak, Donald J. Perkey, Michael Kalb (Universities Space Research Association, Huntsville, AL.), Franklin R. Robertson, and Gary Jedlovec *In its* NASA/MSFC FY90 Global Scale Atmospheric Processes Research Program Review Oct. 1990 p 5-8 (For primary document see N91-16500 08-47)
Avail: NTIS HC/MF A04 CSCL 04B

Research efforts in FY 1990 included studies employing regional scale numerical models as aids in evaluating potential contributions of specific satellite observing systems (current and future) to numerical prediction. One study involves Observing System Simulation Experiments (OSSEs) which mimic operational initialization/forecast cycles but incorporate simulated Advanced Microwave Sounding Unit (AMSU) radiances as input data. The objective of this and related studies is to anticipate the potential value of data from these satellite systems, and develop applications of remotely sensed data for the benefit of short range forecasts. Techniques are also being used that rely on numerical model-based synthetic satellite radiances to interpret the information content of various types of remotely sensed image and sounding products. With this approach, evolution of simulated channel radiance image features can be directly interpreted in terms of the atmospheric dynamical processes depicted by a model. Progress is being made in a study using the internal consistency of a regional prediction model to simplify the assessment of forced diabatic heating and

moisture initialization in reducing model spinup times. Techniques for model initialization are being examined, with focus on implications for potential applications of remote microwave observations, including AMSU and Special Sensor Microwave Imager (SSM/I), in shortening model spinup time for regional prediction. Author

N91-16503*# National Aeronautics and Space Administration. Marshall Space Flight Center, Huntsville, AL.
SOUTH PACIFIC CONVERGENCE ZONE AND GLOBAL-SCALE CIRCULATIONS
Dayton G. Vincent (Purdue Univ., West Lafayette, IN.) and Franklin R. Robertson *In its* NASA/MSFC FY90 Global Scale Atmospheric Processes Research Program Review Oct. 1990 p 9-11 (For primary document see N91-16500 08-47)
(Contract NAS8-37127)
Avail: NTIS HC/MF A04 CSCL 04B

Current research is focused on four topics. First, the GLA Global Circulation Model (GCM) is used for a series of experiments to examine the relationship between tropical heating and subtropical westerly wind maxima. Second, barotropic and baroclinic energy mechanisms associated with summertime subtropical wind maxima in the Southern Hemisphere is studied. Third, tropical/extratropical interactions in the Southern Hemisphere summer circulation is studied; the focus is on the importance of the 30 to 60 day tropical oscillation as a cause of enhancing the subtropical westerly winds. Finally, a study of precipitation efficiency in the tropics, comparing mean monthly distributions of precipitation over a three-year period to precipitable water and moisture convergency is being conducted. Author

N91-16504*# National Center for Atmospheric Research, Boulder, CO.
RESEARCH ON DIABATIC INITIALIZATION
Akira Kasahara *In* NASA, Marshall Space Flight Center, NASA/MSFC FY90 Global Scale Atmospheric Processes Research Program Review Oct. 1990 p 13-17 (For primary document see N91-16500 08-47)
Avail: NTIS HC/MF A04 CSCL 04B

The objective of this research project is to contribute to improvement in the synoptic analyses in the tropics for numerical weather prediction and climate research. In addition to a prediction model, four dimensional data assimilation systems have two principal components. One is objective analysis and the other is initialization. Various methods of objective analysis are designed primarily to analyze the mass and rotational wind fields. Methods of initialization are developed to obtain the irrotational wind and its associated vertical velocity field which are balanced with the mass field and free from meteorological noise. There are essentially three approaches to the problem of initialization: quasi-geostrophic theory, bounded derivative method and nonlinear normal mode method. In the midlatitudes, these approaches generally produce satisfactory results even without diabatic effects for large-scale motions. In the tropics, the situation is quite different from that in the midlatitudes. Because of a small magnitude of the Coriolis parameter and a weak horizontal temperature gradient in the tropics, any method of initialization must incorporate diabatic effects. In fact, it can be said that understanding the problem of diabatic initialization is the key to improving the analysis and weather forecasting in the tropics. Author

N91-16505*# Colorado Univ., Boulder. Center for Atmospheric Theory and Analysis.
PLANETARY CIRCULATIONS IN THE PRESENCE OF TRANSIENT AND SELF-INDUCED HEATING Abstract Only
Murry L. Salby *In* NASA, Marshall Space Flight Center, NASA/MSFC FY90 Global Scale Atmospheric Processes Research Program Review Oct. 1990 p 19 (For primary document see N91-16500 08-47)
Avail: NTIS HC/MF A04 CSCL 04B

The linearized global primitive equation model of Salby and Garcia (1987) was modified to study tropospheric circulations and their interaction with tropical convection. The vertical resolution was increased to approximately 1.5 km, with the effective vertical domain extending the approximately 40 km (higher altitudes in the calculation are used to ensure the radiation upper boundary condition is satisfied). A formal wave conditional instability of the second kind (CISK) parameterization was introduced. That parameterization allows low-frequency disturbances to interact with convection by organizing surface moisture. Boundary layer friction has two important effects in these calculations: it exaggerates surface convergence near the equator by driving the flow out of geostrophic balance; and it introduces a phase shift between the convergence pattern and the circulation, which drives the heating out of quadrature with the temperature field and allows a positive feedback to take place. The observational complement of this theoretical work involves Global Cloud Imagery (GCI) composited from six satellites in the International Satellite Cloud Climatology Project (ISCCP) which were simultaneously observing the Earth's cloud field. Having global coverage, horizontal resolution of half a degree, and produced synoptically every 3 hours, the GCI affords an unprecendented view of global convection. A full year (1983 to 1984) of GCI has now been successfully created. Among other phenomena, that imagery reveals a regular progression of easterly waves in the convective pattern of the Western Pacific. Those disturbances have odd symmetry about the equator and organize convection into a pattern with similar symmetry. In time-mean maps of cloud cover, these propagating disturbances produce a split Inter-Tropical Convergence Zone (ITCZ) in the western Pacific. Author

N91-16506*# Pennsylvania State Univ., University Park. Dept. of Meteorology.
STRATIFORM CLOUDS AND THEIR INTERACTION WITH ATMOSPHERIC MOTION
John H. E. Clark and Hampton N. Shirer *In* NASA, Marshall Space Flight Center, NASA/MSFC FY90 Global Scale Atmospheric Processes Research Program Review Oct. 1990 p 21-25 (For primary document see N91-16500 08-47)
Avail: NTIS HC/MF A04 CSCL 04B

During 1989 and 1990, the researchers saw the publication of two papers and the submission of a third for review on work supported primarily by the previous contract, NAS8-36150; the delivery of an invited talk at the SIAM Conference on Dynamical Systems in Orlando, Florida; and the start of two new projects on the radiative effects of stratocumulus on the large-scale flow. The published papers discuss aspects of stratocumulus circulations (Laufersweiler and Shirer, 1989) and the Hadley to Rossby regime transition in rotating spherical systems (Higgins and Shirer, 1990). The submitted paper (Haack and Shirer, 1990) discusses a new nonlinear model of roll circulations that are forced both dynamically and thermally. The invited paper by H. N. Shirer and R. Wells presented an objective means for determining appropriate truncation levels for low-order models of flows involving two incommensurate periods; this work has application to the Hadley to Rossby transition problem in quasi-geostrophic flows (Moroz and Holmes, 1984). The new projects involve the development of a multi-layered quasi-geostrophic channel model for study of the modulation of the large-scale flow by stratocumulus clouds that typically develop off the coasts of continents. In this model the diabatic forcing in the lowest layer will change in response to the (parameterized) development of extensive fields of stratocumulus clouds. To guide creation of this parameterization scheme, researchers are producing climatologies of stratocumulus frequency and the authors correlate these frequencies with the phasing and amplitude of the large-scale flow pattern. Researchers discuss the above topics in greater detail. Author

N91-16507*# National Aeronautics and Space Administration. Marshall Space Flight Center, Huntsville, AL.
GLOBAL VARIABILITY OF WATER VAPOR AND CONDENSATE FROM SSM/I
Franklin R. Robertson *In its* NASA/MSFC FY90 Global Scale Atmospheric Processes Research Program Review Oct. 1990 p 27-28 (For primary document see N91-16500 08-47)
Avail: NTIS HC/MF A04 CSCL 04B

In the three years since its launch, the Special Sensor Microwave Imager (SSM/I) provided the beginnings of a data set crucial to the study of the Earth's global hydrologic cycle. Investigations with SSM/I centered largely on two themes: (1) an analysis of the variability in atmospheric moisture as a signature of dynamic and kinematic processes, and (2) development of high quality data sets for determining moisture balance and, eventually, diabatic heating on regional and planetary scales. To date, most of the emphasis has been on the precipitable water field since algorithms for this quantity appear to be the most mature. In addition, researchers began work with liquid water, precipitating ice and ocean surface wind stress fields. The retrievals used in these studies are from algorithms developed by Wentz (RSS Tech Rpt. 1989) and Spencer (1988 JTECH). Author

N91-16508*# Alabama Univ., Huntsville.
GLOBAL-SCALE, INTRASEASONAL FLUCTUATIONS OF DIABATIC FORCING OF THE ATMOSPHERE
John R. Christy *In* NASA, Marshall Space Flight Center, NASA/MSFC FY90 Global Scale Atmospheric Processes Research Program Review Oct. 1990 p 29-30 (For primary document see N91-16500 08-47)
Avail: NTIS HC/MF A04 CSCL 04B

Fields of diabatic heating rate estimates (H) for 5-day periods were calculated from the European Center for Medium Weather Forecasts (ECMWF) analyses since 1985 as the residual of the dry thermodynamic equation. Included in these fields are the horizontal and vertical divergences of heat for both mean and eddy statistics. Previous work dealt with 4-day periods, however, with the emphasis in the Global Precipitation Climatology Project (GPCP) for 5-day period totals the change was made to accommodate the GPCP product. H has long been associated with cold tropical cloud-top temperatures as measured by polar orbiting outgoing longwave radiation (OLR) sensors. Correlations between H and OLR fields on three time scales indicate a moderate amount of agreement. For periods less than 90 days, significant negative correlations are found between H and OLR for (1) tropical and NH midlatitude oceanic areas, and (2) for zonal and hemispheric mean values. Positive correlations are seen in NH mean and continental areas of N. Africa, N. America, N. Asia and Antarctica. These latter results reflect seasonal heating and cooling. Comparisons have been made between H as H as calculated from the ECMWF analyses and output from the CCM1 T42 simulations. The CCM1 tends to have a more cellular structure with more heating (precipitation) over land versus that observed (ECMWF) over oceans. Author

N91-16509*# Texas A&M Univ., College Station. Dept. of Meteorology.
TROPICAL PACIFIC MOISTURE VARIABILITY
James P. McGuirk *In* NASA, Marshall Space Flight Center, NASA/MSFC FY90 Global Scale Atmospheric Processes Research Program Review Oct. 1990 p 31-33 (For primary document see N91-16500 08-47)
Avail: NTIS HC/MF A04 CSCL 04B

The objectives are to describe synoptic scale variability of moisture over the tropical Pacific Ocean and the systems leading to this variability; implement satellite analysis procedures in support of this effort, and to incorporate additional satellite information into operational analysis forecast systems at the National Meteorological Center (NMC). Composite satellite radiance patterns describe features detectable well before the development of synoptic scale tropical plumes. These typical features were extracted from historical files of Tiros Operational Vertical Sounder (TOVS) radiance observations for a pair of tropical plumes which developed during January 1989. Signals were inserted into the NMC operational medium range forecast model and a suite of model integrations were conducted. Many of the 48 h model errors of the historical forecasts were eliminated by the inclusion of more complete satellite observations. Three studies in satellite radiance analysis progressed. An analysis which blended TOVS moisture channels, OLR observations and European Center for Medium Weather Forecasts (ECMWF) model analysis to generate fields of total precipitable water comparable to those estimated from Scanning Multichannel Microwave Radiometer (SMMR) mu-wave observations. This study demonstrated that a 10 y climatology of precipitable water over the oceans is feasible, using available infrared observations (OLR and TOVS) and model analysis (ECMWF, NMC or similar quality). The estimates are sensitive to model quality and the estimating model must be updated with operational model changes. Coe developed a set of tropical plume and ITCZ composites from TOVS observations, and from NMC and ECMWF analyses which had been passed through a radiative transfer model to simulate TOVS radiances. The composites have been completed as well as many statistical diagnostics of individual TOVS channels. Analysis of the computations is commencing. Chung has initiated a study of the differences between TOVS observed vapor structure during El Nino Southern Oscillation (ENSO) (1983) and non-ENSO (1984) years. Preliminary diagnosis demonstrates gross moisture changes between warm and cold sea surface temperature episodes. Author

N91-16510*# Yale Univ., New Haven, CT. Dept. of Geology and Geophysics.
NONLINEAR DYNAMICS OF GLOBAL ATMOSPHERIC AND EARTH-SYSTEM PROCESSES
Barry Saltzman, Wesley Ebisuzaki, Kirk A. Maasch, Robert Oglesby, and Lionel Pandolfo *In* NASA, Marshall Space Flight Center, NASA/MSFC FY90 Global Scale Atmospheric Processes Research Program Review Oct. 1990 p 35-37 (For primary document see N91-16500 08-47)
Avail: NTIS HC/MF A04 CSCL 04B

Researchers are continuing their studies of the nonlinear dynamics of global weather systems. Sensitivity analyses of large-scale dynamical models of the atmosphere (i.e., general circulation models i.e., GCM's) were performed to establish the role of satellite-signatures of soil moisture, sea surface temperature, snow cover, and sea ice as crucial boundary conditions determining global weather variability. To complete their study of the bimodality of the planetary wave states, they are using the dynamical systems approach to construct a low-order theoretical explanation of this phenomenon. This work should have important implications for extended range forecasting of low-frequency oscillations, elucidating the mechanisms for the transitions between the two wave modes. Researchers are using the methods of jump analysis and attractor dimension analysis to examine the long-term satellite records of significant variables (e.g., long wave radiation, and cloud amount), to explore the nature of mode transitions in the atmosphere, and to determine the minimum number of equations needed to describe the main weather variations with a low-order dynamical system. Where feasible they will continue to explore the applicability of the methods of complex dynamical systems analysis to the study of the global earth-system from an integrative viewpoint involving the roles of geochemical cycling and the interactive behavior of the atmosphere, hydrosphere, and biosphere. Author

N91-16511*# Colorado Univ., Boulder. Dept. of Astrophysical, Planetary, and Atmospheric Sciences.
LABORATORY AND THEORETICAL MODELS OF PLANETARY-SCALE INSTABILITIES AND WAVES
John E. Hart and Juri Toomre *In* NASA, Marshall Space Flight Center, NASA/MSFC FY90 Global Scale Atmospheric Processes Research Program Review Oct. 1990 p 39-42 (For primary document see N91-16500 08-47)
Avail: NTIS HC/MF A04 CSCL 04B

Meteorologists and planetary astronomers interested in large-scale planetary and solar circulations recognize the importance of rotation and stratification in determining the character of these flows. In the past it has been impossible to accurately model the effects of sphericity on these motions in the laboratory because of the invariant relationship between the uni-directional terrestrial gravity and the rotation axis of an experiment. Researchers studied motions of rotating convecting liquids in spherical shells using electrohydrodynamic polarization forces to generate radial gravity, and hence centrally directed buoyancy

forces, in the laboratory. The Geophysical Fluid Flow Cell (GFFC) experiments performed on Spacelab 3 in 1985 were analyzed. Recent efforts at interpretation led to numerical models of rotating convection with an aim to understand the possible generation of zonal banding on Jupiter and the fate of banana cells in rapidly rotating convection as the heating is made strongly supercritical. In addition, efforts to pose baroclinic wave experiments for future space missions using a modified version of the 1985 instrument led to theoretical and numerical models of baroclinic instability. Rather surprising properties were discovered, which may be useful in generating rational (rather than artificially truncated) models for nonlinear baroclinic instability and baroclinic chaos. Author

N91-16512*# National Aeronautics and Space Administration. Marshall Space Flight Center, Huntsville, AL.

THEORETICAL AND EXPERIMENTAL STUDIES OF BAROCLINIC PROCESSES

Tim Miller, Fred W. Leslie, Shih-Hung Chou, Nathaniel Reynolds, H.-I. Lu, and Karen Butler (NTI, Inc., San Antonio, TX.) *In its* NASA/MSFC FY90 Global Scale Atmospheric Processes Research Program Review Oct. 1990 p 43-44 (For primary document see N91-16500 08-47)

Avail: NTIS HC/MF A04 CSCL 04B

The geophysical fluid flow simulation code, GEOSIM, is being used to study the phenomenon of vacillation in the baroclinic annulus. Having verified that the code predicts vacillation for the same points as the experiments, the work is aiming toward explaining the mechanics of vacillation and pointing out some of the sensitivities of the results to the numerical method. Researchers are finding that there is a structural change associated with amplitude vacillation, where the structural changes are in the vertical. The results disagree with the premise of Lindzen et al, that the vacillation is due to constructive and destructive interference of neutral modes with different phase speeds. The researchers are continuing to study the Spacelab 3 Geophysical Fluid Flow Cell (GFFC) results with horizontal temperature gradients and heating from below. GEOSIM has been used to compute a wide range of cases, and these are being compared with the observations. The computations and observations compare well, and the model is being used to extend the results beyond cases studied in the experiments and to study the mechanics and predictability of the flows. The study of fully nonlinear baroclinic instability using the GFFC apparatus is proceeding with the numerical code. While the first instability that occurs is of planetary scale, secondary instabilities consisting of small-scale, penetrative convection occurs where cold fluid flows over a warm surface. The simultaneous modeling of the planetary scale and the convective scale is possible because of the nonhydrostatic formulation of the model. Some of these results have been animated on the Stardent computer, which shows the explosive nature of the small-scale convection. Author

N91-16513*# Purdue Univ., West Lafayette, IN. Dept. of Earth and Atmospheric Sciences.

SYNOPTIC/PLANETARY-SCALE INTERACTIONS AND BLOCKING OVER THE NORTH ATLANTIC OCEAN

Phillip J. Smith, Mary A. Uhl, Anthony R. Lupo, Gregory L. Lamberty, and Richard D. Knabb *In* NASA, Marshall Space Flight Center, NASA/MSFC FY90 Global Scale Atmospheric Processes Research Program Review Oct. 1990 p 45-46 (For primary document see N91-16500 08-47)

Avail: NTIS HC/MF A04 CSCL 04B

Work was completed on the height tendency diagnoses of two extratropical cyclones that occurred upstream from the blocking event studied previously. One developed explosively over water 60 to 36 hours before the block first appeared, while the second developed explosively over the southeastern United States during the time of block formation. In both cases, both vorticity and temperature advection were consistently important forcing mechanisms. This is in contrast to the block itself, in which vorticity advection was easily the dominant forcing mechanism. Latent heat release was also significant, accounting for about 50 percent of the total height falls in the cyclone below 850 mb. Estimates of latent heat release were greatly enhanced by coupling parameterized estimates with values derived from GOES IR data using an algorithm developed by Marshall's F. R. Robertson. Among the difficulties encountered in this work was the identification of an appropriate lower boundary condition for the solution of the height tendency equation. The zero value currently used tends to yield underestimates of the lower troposphere height tendencies. To address this problem a new diagnostic technique was developed in cooperation with Dr. Peter Zwack of the University of Quebec at Montreal. Based on an equation Dr. Zwack had previously developed (the Zwack-Okossi development equation), researchers now have a relationship that is completely consistent with the height tendency equation and provides estimates of lower boundary geostrophic vorticity or height tendencies. Finally, comparison of the SAT (satellite data) and NOSAT (no satellite data) analyses is progressing well. The present focus is on both the new diagnostic technique and the SAT/NOSAT comparisons. The former is being tested on the southeastern United States cyclone case previously mentioned and compared with the height tendency diagnoses already completed. The latter are being examined for the blocking case described in the publications cited in this summary. In addition to obtaining statistics that will allow general comparison of the two analyses, it will be possible to determine whether conclusions about the dynamics of the block development are influenced by the analysis set used. Author

N91-16514*# Environmental Dynamics Research, Miami, FL.

THE EFFECT OF LATENT HEAT RELEASE ON SYNOPTIC-TO-PLANETARY WAVE INTERACTIONS AND ITS IMPLICATION FOR SATELLITE OBSERVATIONS: THEORETICAL MODELING

Lee E. Branscome, Rainer Bleck, and Enda OBrien (Miami Univ., FL.) *In* NASA, Marshall Space Flight Center, NASA/MSFC FY90 Global Scale Atmospheric Processes Research Program Review Oct. 1990 p 47-49 (For primary document see N91-16500 08-47)

Avail: NTIS HC/MF A04 CSCL 04B

The project objectives are to develop process models to investigate the interaction of planetary and synoptic-scale waves including the effects of latent heat release (precipitation), nonlinear dynamics, physical and boundary-layer processes, and large-scale topography; to determine the importance of latent heat release for temporal variability and time-mean behavior of planetary and synoptic-scale waves; to compare the model results with available observations of planetary and synoptic wave variability; and to assess the implications of the results for monitoring precipitation in oceanic-storm tracks by satellite observing systems. Researchers have utilized two different models for this project: a two-level quasi-geostrophic model to study intraseasonal variability, anomalous circulations and the seasonal cycle, and a 10-level, multi-wave primitive equation model to validate the two-level Q-G model and examine effects of convection, surface processes, and spherical geometry. It explicitly resolves several planetary and synoptic waves and includes specific humidity (as a predicted variable), moist convection, and large-scale precipitation. In the past year researchers have concentrated on experiments with the multi-level primitive equation model. The dynamical part of that model is similar to the spectral model used by the National Meteorological Center for medium-range forecasts. The model includes parameterizations of large-scale condensation and moist convection. To test the validity of results regarding the influence of convective precipitation, researchers can use either one of two different convective schemes in the model, a Kuo convective scheme or a modified Arakawa-Schubert scheme which includes downdrafts. By choosing one or the other scheme, they can evaluate the impact of the convective parameterization on the circulation. In the past year researchers performed a variety of initial-value experiments with the primitive-equation model. Using initial conditions typical of climatological winter conditions, they examined the behavior of synoptic and planetary waves growing in moist and dry environments. Surface conditions were representative of a zonally averaged ocean. They found that moist

convection associated with baroclinic wave development was confined to the subtropics. Author

N91-16515*# Cornell Univ., Ithaca, NY. Dept. of Soil, Crop, and Atmospheric Sciences.
THE EFFECT OF LATENT HEAT RELEASE ON SYNOPTIC-TO-PLANETARY SCALE WAVE INTERACTIONS AND IMPLICATIONS FOR SATELLITE OBSERVATIONS: OBSERVATIONAL STUDY
Stephen J. Colucci and Timothy L. Alberta *In* NASA, Marshall Space Flight Center, NASA/MSFC FY90 Global Scale Atmospheric Processes Research Program Review Oct. 1990 p 51-54 (For primary document see N91-16500 08-47)
Avail: NTIS HC/MF A04 CSCL 04B

Researchers have been exploring methods to facilitate the prediction of rapidly intensifying surface cyclones. Recognizing that synoptic-scale systems, such as these cyclones, are less predictable at medium range and beyond than are planetary-scale circulations, researchers propose that the planetary-scale environment for explosive cyclogenesis could be better predicted than the cyclones themselves. Researchers have therefore constructed a planetary-scale climatology of explosive cyclogenesis by compositing together filtered 500 mb height fields (retaining planetary waves only) corresponding to a large sample of rapidly intensifying surface cyclones, stratified geographically and according to the direction of 500 mb geostrophic flow (southwesterly, northwesterly or westerly) over the cyclone center. The composites are calculated from five days preceding to five days following each rapid cyclogenesis event, and have climatology subtracted so that the evolution of planetary-scale anomalies before and after cyclogenesis can be followed. Whether the anomalies are distinct from background variability and thus provide predictive value is now being evaluated. Following explosive cyclogenesis over which the filtered 500 mb flow is southwesterly, there appear in the composites large positive 500 mb height anomalies downstream. In some cases, these anomalies are associated with blocking patterns. Whether the objectively-defined blocking patterns in the data set are preceded by upstream intense surface cyclone activity is being investigated. Finally, the contribution of synoptic-scale processes, notably warm air advection, to planetary-scale height rises during a block formation following an explosive cyclogenesis event is being diagnosed. Researchers hope to eventually evaluate the impact of satellite derived latent heat release upon the warm air advection in this case. Author

N91-16516*# Florida State Univ., Tallahassee. Geophysical Fluid Dynamics Inst.
POTENTIAL VORTICITY INDEX
Albert Barcilon and Hengyi Weng *In* NASA, Marshall Space Flight Center, NASA/MSFC FY90 Global Scale Atmospheric Processes Research Program Review Oct. 1990 p 54-56 (For primary document see N91-16500 08-47)
Avail: NTIS HC/MF A04 CSCL 04B

Using standard data analysis techniques, researchers explore the links between disturbance growth and quasi-geostrophic potential vorticity (PV) gradients; appearance and disappearance of cutoff lows and blocking highs and their relation to a zonal index (properly defined in terms of PV); and teleconnections between different flow patterns and their relation to the zonal index. It was found that the PV index and the eddy index correlate better than a zonal index (defined by zonal wind) and the eddy index. In the frequency domain there are three frequencies (.03, .07 and .17 cpd (cycle per day) corresponding to periods of 33, 14 and 6 days) at which PV index and the eddy index exhibit local maxima. The high correlation found at periods of 33 days is mainly due to eddy activity at high latitudes while the local correlation maxima found at the shorter periods are mainly due mid-latitude eddy activity. The correlation between the PV index and the geopotential height anomaly at 500 mb, at each grid point in the Northern Hemisphere, shows the existence of most of the teleconnection patterns summarized by Wallace and Gutzler (1981): the North Atlantic Oscillation, the North Pacific Oscillation, and the Pacific/North American patterns. Results show that the Isentropic Potential Vorticity (IPV) analysis can be a very useful and powerful tool when used to understand the dynamics of several large scale atmospheric systems. Although the data are limited to only one winter, and it is difficult to assess the statistical significance of the correlation coefficients presented here, the results are encouraging from physical viewpoint. Author

N91-16517*# California Univ., Davis. Dept. of Land, Air, and Water Resources.
USE OF SATELLITE DATA AND MODELING TO ASSESS THE INFLUENCE OF STRATOSPHERIC PROCESSES ON THE TROPOSPHERE
Terrence Nathan *In* NASA, Marshall Space Flight Center, NASA/MSFC FY90 Global Scale Atmospheric Processes Research Program Review Oct. 1990 p 57-59 (For primary document see N91-16500 08-47)
Avail: NTIS HC/MF A04 CSCL 04B

Current research focused on the examination of the effects of ozone heating and Newtonian cooling on the linear stability of transient planetary waves. A finite difference numerical model was developed in which the basic state wind, temperature, and ozone distributions were constructed using ground-based and satellite data. Preliminary results indicate that ozone dynamics interaction may play a more important role in the stability and maintenance of planetary waves than previously thought, particularly in summer when the mean solar zenith angle is smallest and thus ozone heating largest. Examination of the finite amplitude interactions among radiation, ozone, and dynamics was carried out. Self-consistent, coupled equations governing the weakly nonlinear interactions are currently being analyzed to provide a better understanding of wave-mean flow interactions and ozone transport in a continuously stratified model of the troposphere-stratosphere coupled system. Author

N91-16518# Air Force Inst. of Tech., Wright-Patterson AFB, OH.
A TWO-DIMENSIONAL BALANCED MODEL OF INTERNAL FRONTOGENESIS IN GEOSTROPHIC AND ISENTROPIC COORDINATES M.S. Thesis
Norman H. Mandy 1990 70 p
(AD-A227644; AFIT/CI/CIA-90-081) Avail: NTIS HC/MF A04 CSCL 04/2

Using a 2-D form of the geostrophic momentum approximation in geostrophic/isentropic coordinates, our dynamic model reduces to a predictive equation for the potential pseudo-density (inverse Rossby-Ertel potential vorticity), with associated diagnostic equation for the Bernoulli function from which the wind and mass fields can be calculated. Ageostrophic motions are implicit, and vertical motions retained for the adiabatic case employed, by this choice of coordinates. Initialization of the domain incorporates a realistic vertical distribution of the mass field along with upper/lower boundaries which are either isobaric/isentropic or constant potential vorticity surfaces. Vertical wind shears such as are commonly associated with baroclinic waves are idealized and act as the forcing mechanism for frontogenesis. Major model results include the formation of upper fronts with associated wind and thermal fields which, when viewed together, are well correlated with observations of these parameters in terms of magnitude and gradient as well as their proximity to one another. Well defined folding of the dynamic tropopause occurs in geostrophic space; thus, unlike previous balanced models, the transformation back to physical space is not required in order to produce the desired results. However, performing the coordinate transformation enhances the realism of the results. GRA

N91-16519# Air Force Inst. of Tech., Wright-Patterson AFB, OH.
AN INVESTIGATION OF A GRAVITY WAVE DURING GALE: FEBRUARY 6, 1986 M.S. Thesis
Kenneth S. Smith 1990 79 p
(AD-A227655; AFIT/CI/CIA-90-078) Avail: NTIS HC/MF A05 CSCL 04/2

A mesoscale inertia-gravity wave that propagated

northeastward across the southeastern United States on 6 February 1986 is investigated. Barograph traces and surface pressure perturbations based on hourly observations were used to trace the wave to its origin in the northwest Gulf of Mexico. The analysis shows that the wave propagated in the direction of the mid- and upper tropospheric flow for over 19 hours at a mean speed of 25 m/s. The wave initially expanded as an arc, but the northern edge became bounded by a frontal system. Over the entire event, the half-period ranged from 25 minutes near its origin to 2 hours at the U.S. east coast. The half-wavelength is about 130 km with a crest to trough pressure range of less than 1.0 up to 5.7 mb along the axis of propagation. Potential source mechanisms for the gravity wave were examined. These included orographic forcing; shear instability; geostrophic adjustment; density impulses and convection. Available evidence leads to the conclusion that intense and explosively growing convection provided the initial energy. After its initiation the gravity wave marked the sharp western edge of a convective line moving eastward along the Gulf Coast. The long lived horizontal propagation of the gravity wave is shown to be the result of a ducting structure within the mean flow. This structure was revealed by Richardson number and critical level profiles at several sounding stations along the wave path. The duct is eventually disrupted by the frontal structure which marks the northern edge of the gravity wave. GRA

N91-16520# Air Force Inst. of Tech., Wright-Patterson AFB, OH.
PREDICTION OF TROPICAL CYCLONE RAPID INTENSIFICATION EVENTS M.S. Thesis
Dan B. Mundell 1990 207 p
(AD-A227668; AFIT/CI/CIA-90-104) Avail: NTIS HC/MF A10 CSCL 04/2

The largest errors in tropical cyclone intensity forecasting are usually the result of rapid intensification events, where rapid intensification is defined as a change in minimum central pressure of at least 42 hP sub a in a 24 hour period, or a satellite-inferred increase in maximum sustained winds of a least 23 m/s per day when no measurement of central pressure is possible. An observational and theoretical study is made of the unique characteristics of rapidly intensifying typhoons in the western North Pacific. Climatological data, digital infrared satellite imagery and composited rawinsonde sounding data within 5 deg of the center of tropical cyclones were used to identify the distinctive features associated with rapid intensifiers when compared to other stratifications of non-rapid intensifiers and non-intensifiers. Rapid intensity change is indicated on satellite imagery as an extreme concentration of convection near the cyclone center. Relative concentrations of inner and outer deep cumulus convection reveal a predictive relationship between the ratio of inner core to outer core convection and the onset of rapid intensity change 12 hours later. This prediction technique was found to successfully forecast rapid or non-rapid intensification in over 90 percent of the cases in a three-year study of 70 northwest Pacific tropical cyclones. A physical explanation of the likely processes associated with rapid intensification is also presented. Rapid intensification is believed to be the result of weak asymmetrical wind flow across the cyclone center at upper levels of the troposphere. GRA

N91-16521# Air Force Inst. of Tech., Wright-Patterson AFB, OH.
EXAMPLES OF ISALLOBARIC FORCING IN SURFACE FRONTAL MOTION AND SURFACE FRONTOGENESIS OVER THE CENTRAL UNITED STATES M.S. Thesis
Steven R. Christy 23 Feb. 1990 109 p
(AD-A227687; AFIT/CI/CIA-90-098) Avail: NTIS HC/MF A06 CSCL 04/2

The extent to which the isallobaric component of the ageostrophic wind influences surface frontal motion and frontogenesis is not well understood. The isallobaric contribution to surface frontal propagation is subjectively ascertained by diagnosis of isallobaric influence on the actual wind crossfrontal components and frontogenetical forcing. Hourly average surface frontal motions are calculated over a several hour period for three case studies and compared to surface actual, geostrophic, and frictionless isallobaric wind crossfrontal components. In addition, isallobaric crossfrontal contribution to surface frontal motion appears somewhat random and has a very limited geographical extent. In contrast, the isallobaric influence on actual wind frontogenetical forcing can be substantial. In many areas where frontogenetically induced frontal motion by the actual wind is indicated, the issallobaric contribution appears to be significant. GRA

N91-16522# Air Force Inst. of Tech., Wright-Patterson AFB, OH.
A COMPARISON OF DIAGNOSTIC AND KINEMATIC VERTICAL MOTION FIELDS ASSOCIATED WITH CURVED AND STRAIGHT JET STREAK ADJUSTMENT PROCESSES M.S. Thesis - St. Louis Univ.
Glenn Ernest VanKnowe 1990 156 p
(AD-A227724; AFIT/CI/CIA-90-099) Avail: NTIS HC/MF A08 CSCL 04/2

Investigative research was performed on real and simulated jet streaks to determine the relationship of the diagnostic Rossby number with kinematic, balanced and non-balanced omega fields as a function of magnitude, wind shear, and curvature. Hydrodynamic instability was also examined as influencing omega values. A two-layer primitive equation model was used to produce forty five jet streak cases. Seven cases were quasi-barotropic with upper winds equal to the lower level winds. Twenty four were equivalent barotropic with the upper level winds set to equal three times the magnitude of the lower level winds. Four cases were run with a beta plane versus a constant f plane. The remaining ten cases were simulated baroclinic conditions. One cyclonic jet streak using operational data also examined. Model results indicated a consistent weakening for both the 800 mb and 400 mb wind maximums for all jet streak cases when the upper and lower-level waves were in phase and of the same speed. When the upper level was set to equal 3 times the magnitude of the lower jet while maintaining the upper and lower level waves in phase resulted in a larger wind decrease while the 800 mb level showed an increase over the 24 hours of the run in each jet streak case. For the beta and easterly jet streak cases the upper level decrease was somewhat less. The baroclinic cases showed a very slight decrease of increase over the 24 hours of the run. GRA

N91-16523*# FWG Associates, Inc., Tullahoma, TN.
ANALYSIS OF WIND PROFILE MEASUREMENTS FROM AN INSTRUMENTED AIRCRAFT Interim Final Report
Terry S. Paige and Patrick J. Murphy 30 Nov. 1990 159 p
(Contract NAS8-37377)
(NASA-CR-184084; NAS 1.26:184084) Avail: NTIS HC/MF A08 CSCL 04B

The results of an experimental program to determine the capability of measuring wind profiles on support of STS operations with an instrumented aircraft are discussed. These results are a compilation of the flight experiments and the statistical data comparing the quality of the aircraft measurements with quasi-simultaneous and quasi-spatial overlapping Jimsphere measurements. An instrumented aircraft was chosen as a potential alternative to the Jimsphere/radar system for expediting the wind profile calculation by virtue of the ability of an aircraft to traverse the altitudes of interest in roughly 10 minutes. The two aircraft which participated in the study were F-104 and ER-2. Y.S.

N91-16524 Colorado Univ., Boulder.
A GLOBAL CLIMATOLOGY OF MIDDLE ATMOSPHERE INERTIO-GRAVITY WAVES Ph.D. Thesis
Eric Joseph Fetzer 1990 284 p
Avail: Univ. Microfilms Order No. DA9032826

Inertio-gravity wave signals in the limb infrared monitor of the stratosphere (LIMS) satellite instrument temperature data are examined. The height, geographic, and time coverage includes most of the middle atmosphere, almost the entire glove and late October 1978 to late May 1979. The inertio-gravity wave signal is

defined by differencing profiles of total state temperatures and globally mapped planetary waves. These residual temperature profiles are characterized by growth with height and strong correlation between adjacent profiles. The inertio-gravity wave signals are quantified further by examining residual temperature variance, vertical spectra, and horizontal spectra. A strong correlation in time and space is seen between the LIMS inertio-gravity wave variance and the total gravity wave forcing. This correlation implies that inertio-gravity waves may be dominating the total gravity wave momentum transport in the lower to middle mesosphere. An alternative interpretation is that the inertio-gravity wave distribution is the same as that of the high frequency gravity waves. The vertical inertio-gravity wave spectra are variable in shape, being red in winter but showing pronounced long wavelength rollover in the tropics and during summer. The inertio-gravity wave horizontal spectra are truly universal in shape, with slight rollover at long wavelengths, very nearly like k(exp -3/5)(sub H) at intermediate wavelengths, and slight flattening due to aliasing at short wavelengths. Horizontal spectra of the inverted temperature profiles are also examined. Such profiles contain signals of both inertio-gravity waves and planetary waves, but allow direct comparison with other high horizontal resolution measurements of the middle atmosphere. In contrast with the inertio-gravity wave spectra, these spectra are seen to have shapes which vary with height. Dissert. Abstr.

N91-16525# Florida State Univ., Tallahassee. Dept. of Meteorology.

THE VERTICAL STRUCTURE OF THE MARINE ATMOSPHERIC BOUNDARY LAYER ACROSS A SEA SURFACE TEMPERATURE FRONT M.S. Thesis

Christopher G. Herbster Jul. 1990 179 p

(Contract N00014-89-J-1660)

(AD-A227931) Avail: NTIS HC/MF A09 CSCL 04/2

The response of the lower marine atmospheric boundary layer to a sharp change in sea-surface temperature was studied in the (FASINEX) Experiment with ships and aircraft instrumented for turbulence measurements. Synoptic conditions on 14th and 16th Feb. 1986 presented the opportunity to study the vertical structure of the turbulence for the case of a North wind blowing from the cold to warm side of the front. A moving boxcar averaging technique was used to determine the turbulent statistics and fluxes for the meteorological variables, and their associated changes, as the air made the transition from the cold to warm side of the front. Aircraft flight tracks for the two days were designed to investigate somewhat different aspects of the marine atmospheric boundary layer, concentrating on either the vertical structure alone (14 Feb.) or on both the vertical and horizontal structure (16 Feb.) in the vicinity of an oceanic temperature front. The depth of the atmospheric boundary layer was found to be approx. 200 m deeper over the warm water than was found over the cold water. The potential temperature was found to respond very rapidly to the underlying warm water throughout the entire depth of the boundary layer. The vertical heat flux for each day showed a pronounced increase over the warm water. Heat flux for the 14th showed two organized convective cells in the immediate vicinity of the front; this type of organized convection was not found on the 16th.

GRA

N91-16526# Colorado Univ., Boulder. Cooperative Inst. for Research in Environmental Sciences.

STABILITY CRITERIA FOR STRATOCUMULUS-TOPPED BOUNDARY LAYERS EVALUATED THROUGH CONDITIONAL SAMPLING OF TURBULENCE ELEMENTS Annual Report, 1 Nov. 1989 - 31 Oct. 1990

Siri Jodha Singh Khalsa 31 Oct. 1990 6 p Presented at the 9th Symposium on Turbulence and Diffusion, Roskilde, Denmark, 30 Apr. - 3 May 1990 Submitted for publication

(Contract N00014-84-K-0405)

(AD-A228433; CU-1531940) Avail: NTIS HC/MF A02 CSCL 04/2

The stability of stratocumulus layers to breakup is in large part determined by the nature of turbulent exchanges across cloud base and across the capping inversion. Conditional sampling techniques were applied to aircraft measurements of boundary layer turbulence in the stratocumulus regime off the southern California coast in order to evaluate processes believed important to the breakup of stratocumulus. Results show that cloud layers can persist despite the production of evaporatively cooled, negatively buoyant parcels near cloud top, a condition known as cloud top entrainment instability. The drying effect produced by the sinking of such parcels through the cloud layer is compensated for by the supply of moisture from surface-based plumes, contrary to implications that the cloud layer was decoupled from the subcloud layer as indicated by weak mean buoyancy flux at cloud base. Measurement and analysis of individual turbulence elements will continue to assist in the testing of proposed theories of stratocumulus breakup as well as help guide the formulation of new theories. GRA

N91-16527# Texas A&M Univ., College Station.

SPATIAL AND TEMPORAL CLIMATE VARIATIONS INFLUENCING MEDIUM-RANGE TEMPERATURE PREDICTIONS OVER SOUTH-CENTRAL EUROPEAN RUSSIA M.S. Thesis

Jeffrey Edward Johnson May 1990 151 p Sponsored by AFIT, Wright-Patterson AFB, OH

(AD-A228623; AFIT/CI/CIA-90-103) Avail: NTIS HC/MF A08 CSCL 04/2

To issue medium range forecasts, forecasters should integrate climatology, synoptic meteorology, statistics, local topography, computer science, human experience and judgment. Often, if forecasts extend beyond 72 hours, a systematic approach is abandoned for a more haphazard one. A forecaster's guesswork is reduced and the forecast method are made more objective. A general climatology was developed for south central European Russia. Monthly and diurnal trends are easily noted. One station, Astrakhan, was selected for a more detailed climatology. A monthly overview for 9 stations in the region is given for the weather elements as stated above. Pentad and 3-hourly averages are also included. Detailed climatology is helpful in orienting a new weather forecaster to the peculiarities of a novel region. Regression equations were developed using lag functions of 1 to 5 days. Low and high temperatures for the forecast period were regressed back to day zero. Low and high temperatures were predicted for 1 to 5 days past the initial forecast day. The regression equations developed from 24 years of data have a higher percentage of correctly predicting temperatures at the times mentioned than do climatology, persistence, or combinations thereof. GRA

N91-16528# Cranfield Inst. of Tech., Bedford (England). Dept. of Electronic System Design.

THE DESIGN OF A METEOROLOGICAL FACSIMILE CONVERTER M.S. Thesis

Anthony W. Andrews 27 Nov. 1990 126 p

(ETN-91-98578) Copyright Avail: NTIS HC/MF A07

The facsimile transmission of weather maps and charts which are of use, for example, to sea farers, is presented. The design of a Meteorological Facsimile Converter (MFC) is detailed. The input of the MFC would be the facsimile signal received by an external radio. The radio signal is converted to a form suitable for printing by a dot matrix printer. An Intel 80188 microprocessor chip is used as the basis of the MFC. ESA

48 OCEANOGRAPHY

Includes biological, dynamic, and physical oceanography; and marine resources.

For related information see also *43 Earth Resources and Remote Sensing.*

N91-16529# Pennsylvania State Univ., University Park. Applied Research Lab.

FOURTH MOMENTS OF ACOUSTIC WAVES FORWARD SCATTERED BY A ROUGH OCEAN SURFACE Final Technical Report, 15 Feb. 1989 - 14 Feb. 1990

C. C. Yang and S. T. McDaniel 9 Aug. 1990 41 p

(Contract N00014-89-J-1690)

(AD-A227469; ARL/PSU/TM-90-227) Avail: NTIS HC/MF A03 CSCL 20/1

Three types of statistical fourth moments of acoustic waves forward scattered by a randomly rough ocean surface are derived and numerically evaluated. The first one is related to the scintillation index which characterizes intensity fluctuations. The second one is the two-position intensity correlation function which describes the spatial correlation of wave intensity. The third is the two-position coherence function which carries information on the phase fluctuations of the scattered wave. In the range of weak scattering, the ratio of the absolute value of the two-position coherence function over the two-position intensity correlation exactly describes the mean square fluctuation of the relative phase between the two positions. The acoustic frequency is high so that the Kirchhoff approximation can be used. Two types of spectral functions for surface-height fluctuations are considered: a Gaussian spectrum and the Donelan/Pierson spectrum. The latter is obtained from a model for the fluctuations of the ocean surface height which are controlled by the wind at the ocean surface. GRA

N91-16530 Rhode Island Univ., Kingston.

FORMIC AND ACETIC ACIDS IN THE BOUNDARY LAYER OVER THE NORTH ATLANTIC OCEAN Ph.D. Thesis

Joseph John SchmultzTokos 1989 242 p

Avail: Univ. Microfilms Order No. DA9023244

Gaseous formic acid (HCOOH) and acetic acid (CH3COOH) abbreviated as HFo(sub g) and HAc(sub g), respectively, are significant contributors to the acidity of precipitation on a global scales. Both are reactive in the atmosphere in both liquid and gas phases, and are important in the trace-gas chemistry of the remote marine atmosphere. The first reliable measurements of HFo(sub g) and HAc(sub g) in the lower atmospheric boundary layer over the North Atlantic Ocean are described. Gas-phase organic acid concentrations were measured using an aqueous mist-chamber sampler on a cruise from Iceland to Barbados in the summer of 1988. Particulate and aqueous phase acids were also collected. HFo(sub g) and HAc(sub g) concentrations exhibited diurnal cycles, ranging from minima near the detection limit during the night to maxima of 2.0 to 9.0 nmol/cu m of either acid at midday. Maximum concentrations of both acids increased with decreasing latitude. Continental influences were not apparent, except when samples were collected in the lee of islands in the Azores. A marine photochemical source of these species is implied by effective residence times less than or equal to 12 hours. The source of HFo(sub g) appears to be the heterogeneous conversion of gaseous formaldehyde (CH2O) to aqueous HFo within clouds. The uptake of acetaldehyde (CH3CHO) by cloud water is too slow to account for the observed rate of change of concentrations of HAc(sub g) by the same mechanism. The source of HAC(sub g) remains unknown. Dry gaseous deposition onto the sea surface was the largest measureable atmospheric removal process for either acid. The net daytime depositional fluxes of HFo(sub g) nad HAc(sub g) ranged from 600 to 3000 nmol/sq m/day, and 100 to 500 nmol/sq m/day respectively, and were independent of latitude. The carboxylic acid gases may contribute a significant fraction of the organic carbon cycling within the marine atmosphere when compared to the air-sea fluxes of CH4 or CO.

Dissert. Abstr.

N91-16531 California Univ., San Diego.

VARIABILITY OF LATENT AND SENSIBLE HEAT FLUXES OVER THE OCEANS Ph.D. Thesis

Daniel Richard Cayan 1990 220 p

Avail: Univ. Microfilms Order No. DA9023996

The spatial and temporal variability of latent and sensible heat flux is explored. Monthly flux anomalies are estimated using bulk formulae applied to COADS marine data over 1946 to 1986. Emphasis is on behavior during fall and winter over the well-sampled North Atlantic and North Pacific Oceans, but available data from the Indian Ocean, from the tropics, and from the Southern Hemisphere is also included. From the bulk formulae, it appears that the latent and sensible flux anomalies outweigh those of the radiative fluxes, except in the tropics or in the summer extratropics, where net solar flux variations become important. Coexisting spatial patterns of anomalous wind speed (w), sea-air humidity difference (delta q), and sea-air temperature difference (delta t) show how the anomalous circulation organizes the flux difference. Relative to major sea level pressure (SLP) anomaly centers, w anomalies occur to the north and south in the strongest westerly wind zones, while delta q (and delta t) anomalies lie to the west and east in response to meridional air advection. The flux anomalies are a hydrid of these, shifted meridionally and zonally, with enhanced sea-to-air fluxes to the southwest and diminished fluxes to the east of an anomalous low. In the extratropics, the monthly atmospheric circulation also systematically arranges the Bowen Ratio (sensible flux/latent flux), as well as the shorter period intramonthly variability of the fluxes. The flux anomalies show a definite link to the upper ocean temperature field, which was represented by sea surface temperature (SST). In the tropics there is a tendency for flux anomalies and SST anomalies to be positively correlated. Dissert. Abstr.

N91-16532*# Jet Propulsion Lab., California Inst. of Tech., Pasadena.

BIO-OPTICAL PROFILE DATA REPORT COASTAL TRANSITION ZONE PROGRAM, R/V THOMAS WASHINGTON, JUNE 24 - JULY 21, 1988

Curtiss O. Davis and W. Joseph Rhea 1 Dec. 1990 58 p Prepared in cooperation with Naval Research Lab., Washington, DC

(Contract NAS7-918)

(NASA-CR-187808; JPL-PUBL-90-40; NAS 1.26:187808) Avail: NTIS HC/MF A04 CSCL 08C

Twenty-three vertical profiles of the bio-optical properties of the ocean were made during a research cruise on the R/V Thomas Washington, June 24 to July 21, 1988, as part of the Coastal Transition Zone Program off Point Arena, California. A summary is given, to provide investigators with an overview of the data collected. The entire data set is available in digital form for interested researchers. Author

N91-16533*# Jet Propulsion Lab., California Inst. of Tech., Pasadena.

BIO-OPTICAL PROFILE DATA REPORT COASTAL TRANSITION ZONE PROGRAM, R/V POINT SUR, JUNE 15-28, 1987

Curtiss O. Davis and W. Joseph Rhea 1 Dec. 1990 54 p Prepared in cooperation with Naval Research Lab., Washington, DC

(Contract NAS7-918)

(NASA-CR-187807; JPL-PUBL-90-39; NAS 1.26:187807) Avail: NTIS HC/MF A04 CSCL 08C

Twenty vertical profiles of the bio-optical properties of the ocean were made during a research cruise on the R/V Point Sur, June 15 to 28, 1987, as part of the Coastal Transition Zone Program off Point Arena, California. Extracted chlorophyll values were also measured at some stations to provide calibration data for the in situ fluorometer. This summary provides investigators with an overview of the data collected. The entire data set is available in digital form. Author

N91-16534*# Jet Propulsion Lab., California Inst. of Tech., Pasadena.
BIO-OPTICAL PROFILE DATA REPORT: JOINT GLOBAL OCEAN FLUX STUDY, HAWAII OCEAN TIME-SERIES, HOT-3, R/V MOANA WAVE, 6-10 JANUARY 1989
Donald J. Collins, W. Joseph Rhea, and An Van Tran 1 Sep. 1990 37 p
(Contract NAS7-918)
(NASA-CR-187805; JPL-PUBL-90-36; NAS 1.26:187805) Avail: NTIS HC/MF A03 CSCL 08C

Time-series measurements of the incident surface downwelling irradiance and vertical profiles of the Bio-optical properties of the ocean have been measured during the third cruise of the Hawaii Ocean Time-Series to the ALOHA site, 22 degrees 56.4 minutes N, 157 degrees 54.6 minutes W, north of the island of Oahu, Hawaii, during the period January 6 to 10, 1989. A summary of these data is presented to permit investigators an overview of the data collected. The data are available in digital form for scientific investigators. Author

N91-16535*# Jet Propulsion Lab., California Inst. of Tech., Pasadena.
CONTENTS OF THE NASA OCEAN DATA SYSTEM ARCHIVE, VERSION 11-90
Elizabeth A. Smith, ed. and Ruby A. Lassanyi, ed. 15 Nov. 1990 28 p
(Contract NAS7-918)
(NASA-CR-187812; JPL-PUBL-90-49; NAS 1.26:187812) Avail: NTIS HC/MF A03 CSCL 08C

The National Aeronautics and Space Administration (NASA) Ocean Data System (NODS) archive at the Jet Propulsion Laboratory (JPL) includes satellite data sets for the ocean sciences and global-change research to facilitate multidisciplinary use of satellite ocean data. Parameters include sea-surface height, surface-wind vector, sea-surface temperature, atmospheric liquid water, and surface pigment concentration. NODS will become the Data Archive and Distribution Service of the JPL Distributed Active Archive Center for the Earth Observing System Data and Information System (EOSDIS) and will be the United States distribution site for Ocean Topography Experiment (TOPEX)/ POSEIDON data and metadata. Author

N91-16536*# National Aeronautics and Space Administration. Goddard Space Flight Center, Greenbelt, MD.
EFFECTS OF SWITCH LEAKAGES UPON NIMBUS-7 SMMR CALIBRATION
Daesoo Han and Seung T. Kim (ST Systems Corp., Lanham, MD.) Washington Jun. 1988 21 p
(Contract NAS5-29386)
(NASA-TM-100705; REPT-88B0238; NAS 1.15:100705) Avail: NTIS HC/MF A03 CSCL 08C

A calibration model for the Nimbus 7 Scanning Multichannel Microwave Radiometer (SMMR) is studied. This model not only removes major drawbacks of the current calibration model but also helps in the understanding of the performance degradation of the aging instrument. The current Nimbus 7 SMMR calibration algorithm was derived without considering the interference effect between the two orthogonally polarized signals merging at a ferrite polarization selector switch. The resulting calibrated brightness temperatures, considered as a function of scan angle, are not symmetric around scan angle = 0. However, neither the origin of the asymmetry nor the manner in which the two orthogonal components are mixed has been fully understood. The new calibration model proposed incorporates all the leakage factors associated with the ferrite switches along the signal paths. The resulting calibration equations clarify how the orthogonal components of surface brightness are coupled at radiometers. As a consequence, the origin of the asymmetry is clearly identified and explained. In addition, the feasibility of absolute calibration using in-orbit data is discussed. Author

51 LIFE SCIENCES (GENERAL)

N91-16537# Southwest Research Inst., San Antonio, TX.
INVESTIGATION OF EFFECTS OF 60-Hz ELECTRIC AND MAGNETIC FIELDS ON OPERANT AND SOCIAL BEHAVIOR AND ON THE NEUROENDOCRINE SYSTEM OF NONHUMAN PRIMATES Annual Report
John L. Orr Oct. 1989 88 p
(Contract DE-AC02-80RA-50219)
(DE90-010809; DOE/RA-50219/T10) Avail: NTIS HC/MF A05

The objective is to investigate, using the baboon as a nonhuman primate surrogate for the human, behavioral and neuroendocrine effects associated with exposure to 60-Hz electric and magnetic fields. Results from this program could be used to estimate and evaluate the likelihood of deleterious consequences resulting from exposure of humans to the electric and magnetic fields associated with electric power transmission. This project year has focused on two technical areas: the modification of the facility to include 60-Hz magnetic fields, and development of the capability for studies of neuroendocrine parameters by obtaining blood samples from baboons during electric and magnetic field exposure. Activities in the social behavior, operant behavior, and laboratory animal sciences during this project year have been in preparation for the start of experiment 3. DOE

N91-16538# Lawrence Livermore National Lab., CA.
APPLICATION OF AMS TO THE BIOMEDICAL SCIENCES
J. S. Vogel, B. L. Gledhill, I. D. Proctor, K. W. Turteltaub, D. E. Nelson, J. C. Davis, J. S. Felton, and J. R. Southon 18 Apr. 1990 16 p Presented at the 5th International Conference on Accelerator Mass Spectrometry, Paris, France, 23-27 Apr. 1990
(Contract W-7405-eng-48)
(DE90-010869; UCRL-102985; CONF-900491-5) Avail: NTIS HC/MF A03

Radioisotopic tracers are a useful tool in numerous areas of biomedical research, including metabolism, pharmacokinetics, and the detailed study of biomolecular interactions. Accelerator mass spectrometry (AMS) was suggested as a tool for the biomedical sciences shortly after its invention, but few attempts to use its sensitivity in such research have been reported. We have examined some of the strengths and limitations of the technique and find that AMS has a sensitivity advantage over decay-counting for the long-lived radioisotopes and for shorter-lived, common radiotracers. The advantage can be translated into the use of much smaller sample sizes and much lower radioisotope concentrations, both of which present new opportunities for biochemical tracing and human research. New approaches to separation and preparation of the material to be assayed for radiotracers will be developed to take advantage of the sensitivity and specificity. Most biochemical laboratories have used radioactive isotopes as tracers and their facilities have been contaminated with unacceptably high levels of these tracers. Careful protocols and/or new facilities are required to prevent contamination of the AMS samples. DOE

N91-16539# Southwest Research Inst., San Antonio, TX.
INVESTIGATION OF EFFECTS OF 60-Hz ELECTRIC AND MAGNETIC FIELDS ON OPERANT AND SOCIAL BEHAVIOR AND ON THE NEUROENDOCRINE SYSTEM OF NONHUMAN PRIMATES Quarterly Technical Progress Report No. 28, 1 Nov. 1988
John L. Orr 24 Mar. 1989 84 p
(Contract DE-AC02-80RA-50219; SwRI Proj. 14-6253)
(DE90-011557; DOE/RA-50219/T13) Avail: NTIS HC/MF A05

The objective of this program is to investigate, using the baboon as a nonhuman primate surrogate for the human, behavioral and nonendocrine effects associated with exposure to 60-Hz electric and magnetic fields. Results from this program, along with information from experiments conducted elsewhere, could be used to estimate and evaluate the likelihood of deleterious consequences resulting from exposure of humans to the electric and magnetic fields associated with electric power transmission. The test facility is being modified to include combined electric and magnetic field

capability. This will be accomplished by the installation of a magnetic field exposure system and modification of the electric field exposure equipment. The purpose of this document is to provide information on the design. DOE

N91-16540# Tennessee Univ., Memphis. Dept. of Anatomy and Neurobiology.
CHANGES IN SOMATOSENSORY RESPONSIVENESS IN BEHAVING MONKEYS Annual Technical Report No. 2, 1 Jul. 1989 - 30 Jun. 1990
Randall J. Nelson 31 Jul. 1990 24 p
(Grant AF-AFOSR-0179-88; AF Proj. 2312)
(AD-A226832; AFOSR-90-0956TR) Avail: NTIS HC/MF A03
CSCL 06/4

Four research goals were accomplished: (1) It was determined that sensory responsiveness of primary somatosensory (SI) cortical neurons to vibratory stimuli is quantitatively different depending upon whether monkeys make wrist movements in response to the stimuli or withhold movement. (2) For a special class of SI neurons, it was determined that activity occurring before movement is comprised of a reactivation of the neuron's sensor response and a presumably centrally generated component. (3) It was determined that sensory responsiveness and premovement activity are elevated when behavioral conditions are unpredictable as compared to when they are predictable. (4) It was determined that human subjects can acquire a positional target by wrist movements more quickly if vibratory go-cues are presented in addition to the illumination of a visual signal lamp. The neurophysiological experiments suggest that the responsiveness of SI neurons is profoundly affected by behavioral conditions and an animal's expectation of correct performance. The human psychophysical experiments suggest that the addition of vibratory go-cues to control systems may have benefits without seeming to degrade performance. GRA

N91-16541# Warwick Univ., Coventry (England). Dept. of Engineering.
ELECTRONIC ANALOGUE FOR A BIOLOGICAL NOSE
H. V. Shurmer Sep. 1989 37 p Sponsored by United Kingdom Science and Engineering Research Council
(ME-78; ETN-91-98576) Avail: NTIS HC/MF A03

The various facets of progress towards instrumentation capable of replacing or surpassing in performance the biological nose are described. Key areas providing continuing advances relate to sensor materials, integration of sensing elements, and information processing. The process of devising instrumentation has begun for some of the numerous applications awaiting exploitation. The topics discussed include: (1) an electronic model; (2) linearization and gas analysis; (3) test systems; (4) arrays of non-identical sensing elements; (5) information processing (pattern recognition); and (6) instrumentation. Also, different types of sensors are covered: inorganic semiconductors, conducting polymers, Langmuir-Blodgett films, and others. ESA

52 AEROSPACE MEDICINE

Includes physiological factors; biological effects of radiation; and effects of weightlessness on man and animals.

N91-16542# Brookhaven National Lab., Upton, NY. Atomic and Applied Physics Group.
GALLIUM AS A UNIQUE ANTI-RESORPTIVE AGENT IN BONE: PRECLINICAL STUDIES ON ITS MECHANISMS OF ACTION
Richard Bockman, Robert Adelman, Robert Donnelly, Lynn Brody, Raymond Warrell (Hospital for Special Surgery, New York, NY.), and Keith W. Jones 1990 8 p Presented at the 1st International Symposium on Metal Ions in Biology and Medicine, Champagne, France, 16-19 May 1990 Sponsored in part by Department of Health and Human Services, Washington, DC
(Contract DE-AC02-76CH-00016; NIH-RR-01838)
(DE90-010650; BNL-44536; CONF-9005170-1) Avail: NTIS HC/MF A02

The discovery of gallium as a new and unique agent for the treatment of metabolic bone disorders was in part fortuitous. Gallium is an exciting new therapeutic agent for the treatment of pathologic states characterized by accelerated bone resorption. Compared to other therapeutic metal compounds containing platinum or germanium, gallium affects its antiresorptive action without any evidence of a cytotoxic effect on bone cells. Gallium is unique amongst all therapeutically available antiresorptive agents in that it favors bone formation. DOE

N91-16543 New South Wales Univ., Canberra (Australia).
ELECTRICAL RESISTANCE VOLUMETRY IN THE CIRCULATION Ph.D. Thesis - 1988 Abstract Only
John Campbell Woodard 1 Jun. 1990 3 p
Avail: Issuing Activity

The measurement of changes in blood volume is examined using electrical resistance techniques. The utility of such cardiovascular measurements was assessed for use with implantable devices. Intracardiac measurements were made in both greyhound dogs and human volunteers with an 8-electrode catheter which was also used for intravascular resistance measurements. Transcardiac resistance of greyhound hearts was obtained from epicardial electrodes used with implantable defibrillators. These in-vivo experiments were supplemented with in-vitro investigations using canine tissues and computer simulation, to determine the geometric factors influencing the performance of the conductance catheter and the magnitude of changes in tissue resistivity under various conditions. Good transduction of ventricular volume change was obtained from the multi-electrode catheter in the right ventricle under a variety of interventions. However anatomical factors, principally the location of the tricuspid valve, limited the proportion of the ventricle that could be effectively transduced and necessitated careful positioning of the catheter to obtain acceptable volume transduction. Computer simulation and in-vitro measurements showed that the radial position of the catheter in a vessel of constant cross-section could result in errors in volume measurement, and that this error could be minimized by a large separation of the current-injecting electrodes. Transcardiac resistance was found to be unrelated to ventricular volume changes, but was strongly associated with the level of coordinated mechanical activity of the heart. Both transcardiac resistance and volume measurements from a right ventricular catheter appear suitable for detection of ventricular fibrillation. Although volume transduction using a right ventricular catheter is subject to error during arrhythmias, this technique could be used for rate-regulation of an artificial pacemaker. Author

N91-16544# Federal Aviation Administration, Washington, DC. Office of Aviation Medicine.
THE USE OF CONTACT LENSES IN THE CIVIL AIRMAN POPULATION Final Report
Van B. Nakagawara Sep. 1990 15 p
(AD-A227450; DOT/FAA/AM-90/10) Avail: NTIS HC/MF A03
CSCL 06/4

Federal Aviation Regulations permit the routine use of contact lenses by civilian pilots to satisfy the distant visual acuity requirements for obtaining medical certificates. Specific information identifying the prevalence of both defective distant vision and contact lenses in the civil airman population is required to guide future medical certification decisions, policy changes, and education safety programs for aviation personnel. A descriptive, retrospective epidemiologic study was performed of active airmen by 5-year intervals for a 20-year period (1967 to 1987) using FAA databases and publications. The percentage of airmen who use contact lenses quadrupled during the study period. When stratified by class of medical certificate and age, the prevalence rates for airmen with first-class medical certificates and older airmen showed the largest increases. The increasing use of contact lenses and the variety of design, materials, and applications which may be employed by the pilot population mandate ongoing review for adverse changes and safety consequences. GRA

N91-16545# Army Research Inst. of Environmental Medicine, Natick, MA.
QUANTIFICATION OF LOWER BOUNDS FOR ENDURANCE TIMES IN THERMALLY INSULATED FINGERS AND TOES EXPOSED TO COLD STRESS
Avraham Shitzer, Leander A. Stroschein, William R. Santee, Richard R. Gonzales, and Kent B. Pandolf Jul. 1990 56 p
(DA Proj. 3E1-62787-A-878)
(AD-A227782; USARIEM-T18-90) Avail: NTIS HC/MF A04 CSCL 06/5

The model developed is useful in calculating temperature variations along insulated digits and in predicting their endurance times to cold exposures. Calculated results compared very favorably with data obtained on human subjects. The present version of the model does not include the effect of cold induced vasodilation. Expansion of the model to include this important natural mechanism will tend, as a general rule, to predict longer, less conservative endurance times. Thus, predictions based on the present model should be useful whenever conservative, lower bounds of endurance times to cold exposures are required. GRA

N91-16546# California Univ., Berkeley. Lawrence Berkeley Lab. Theoretical Physics Group.
A QUANTUM THEORY OF THE MIND-BRAIN INTERFACE
Henry P. Stapp 30 Jul. 1990 35 p Presented at the Conference on Consciousness Within Science, San Francisco, CA, 17-18 Feb. 1990
(Contract DE-AC03-76SF-00098)
(DE91-004431; LBL-28574; CONF-9002159-1) Avail: NTIS HC/MF A03

The Heisenberg quantum mechanical conception of nature is extended and applied to the brain. Strict adherence to the principle of parsimony, and to quantum thinking, produces naturally, on the basis of an overview of brain operation compatible with the information provided by the brain sciences, a unified description of the physical and mental aspects of nature that can account in principle for the full content of felt human experience. DOE

N91-16547* National Aeronautics and Space Administration, Washington, DC.
AEROSPACE MEDICINE AND BIOLOGY: A CUMULATIVE INDEX TO A CONTINUING BIBLIOGRAPHY (SUPPLEMENT 345)
Jan. 1991 233 p
(NASA-SP-7011(345); NAS 1.21:7011(345)) Avail: NTIS HC A11; NTIS standing order as PB91-912300, $15.00 domestic, $30.00 foreign CSCL 06E

This publication is a cumulative index to the abstracts contained in Supplements 333 through 344 of Aerospace Medicine and Biology: A Continuing Bibliography. Seven indexes are included -- subject, personal author, corporate source, foreign technology, contract number, report number, and accession number. Author

N91-16554# Institute of Aviation Medicine, Farnborough (England).
CEREBRAL OXYGEN STATUS AND G-INDUCED LOSS OF CONSCIOUSNESS
David H. Glaister *In* AGARD, Safety Network to Detect Performance Degradation and Pilot Incapacitation Sep. 1990 4 p (For primary document see N91-16553 08-54)
Copyright Avail: NTIS HC/MF A06; Non-NATO Nationals requests available only from AGARD/Scientific Publications Executive

N91-16555# Laboratoire de Medecine Aerospatiale, Bretigny-sur-Orge (France).
DETECTION OF LOSS OF CONSCIOUSNESS IN FLIGHT BY DOPPLER METHOD [DETECTION DES PERTES DE CONNAISSANCE EN VOL PAR METHODE DOPPLER]
J. M. Clere, G. Ossard, D. Lejeune, A. Leger, and A. Roncin (Tours Univ., France) *In* AGARD, Safety Network to Detect Performance Degradation and Pilot Incapacitation Sep. 1990 6 p In FRENCH (For primary document see N91-16553 08-54)
Copyright Avail: NTIS HC/MF A06; Non-NATO Nationals requests available only from AGARD/Scientific Publications Executive

53 BEHAVIORAL SCIENCES

Includes psychological factors; individual and group behavior; crew training and evaluation; and psychiatric research.

N91-16548# Yale Univ., New Haven, CT. Dept. of Ophthalmology and Visual Science.
LIMITS OF HUMAN VISUAL DISCRIMINATION: TOWARD A GENERAL MODEL OF VISUAL GEOMETRY Final Technical Report, 1 Jan. 1986 - 31 Dec. 1989
Joy Hirsch 1 Mar. 1990 10 p
(Grant AF-AFOSR-0077-86; AF Proj. 2313)
(AD-A226826; AFOSR-90-0965TR) Avail: NTIS HC/MF A02 CSCL 06/4

The goal was to understand the neural computations that mediate the precision of human spatial vision. This goal was approached along three interrelated lines of research: (1) direct investigation of human and monkey retinal sampling mosaics; (2) psychophysical measurements of the precision of human spatial vision; and (3) computer simulations of human visual processes based on 'biologically correct' sampling lattices and 'behaviorally constrained' neural models of human spatial information processing. GRA

N91-16549# South Carolina Univ., Columbia. Dept. of Psychology.
SKILL AND SKILLED MEMORY Final Report, 1985 - 1988
James J. Staszewski 18 Feb. 1990 46 p
(Contract N00014-85-K-0524; NR Proj. 667549)
(AD-A227697) Avail: NTIS HC/MF A03 CSCL 05/8

The findings are summarized of two longitudinal studies of expert-level cognitive skills and their acquisition. Their empirical, theoretical, and methodological contributions are described and some practical implications are discussed. Comprehensive analyses of subjects' learning and performance demonstrate that acquired knowledge, rather than exceptional native talents or general aptitudes, constitutes the foundation of expertise in the skills studied. They show that the knowledge structures and processing supporting expertise can be analyzed at a fine grain. Theoretically motivated analyses reveal that rapid and reliable storage and retrieval of information in Long Term Memory (LTM) appears to be a key general characteristic experts' information processing, and that acquired memory skills enable experts to use LTM efficiently to reduce the constraints that limited working memory capacity imposes upon performance in complex tasks. The studies also document the efficient information processing strategies on cognitive skill acquisition and expert performance. GRA

N91-16550# Johns Hopkins Univ., Baltimore, MD. Dept. of Psychology.
PRE-ATTENTIVE AND ATTENTIVE VISUAL INFORMATION PROCESSING Final Report, 1 Apr. 1987 - 30 Jun. 1990
Howard E. Egeth 5 Sep. 1990 12 p
(Grant AF-AFOSR-0180-87; AF Proj. 2313)
(AD-A228541; AFOSR-90-1118TR) Avail: NTIS HC/MF A03 CSCL 05/8

Research project abstracts on several interrelated topics are presented. These projects are all in the area of visual cognition, and focus on feature and object perception, models of selective attention, and the nature of visual routines such as curve tracing and subitizing. The major thrust of this endeavor has been to explore the nature of visual processes to determine the extent to which they are carried out in parallel or in series. GRA

N91-16551# University of Southern California, Los Angeles. Signal and Image Processing Inst.
RESEARCH IN OPTICAL SYMBOLIC TASKS Final Technical Report, 1 Jun. 1986 - 29 Nov. 1989
Keith Jenkins 29 Nov. 1989 151 p
(Grant AF-AFOSR-0196-86; AF Proj. 2305)
(AD-A228797; AFOSR-90-1130TR) Avail: NTIS HC/MF A08 CSCL 09/5

The research findings of the AFOSR Grant AFOSR-86-0196, Optical Symbolic Computing Tasks are summarized. The grant period was 1 June 1986 to 29 November 1989. Specifically, we have concentrated on the following topics: complexity studies for optical neural and digital systems, architecture and models for optical computing, learning algorithms for neural networks and applications of neural networks for early vision problems such as image restoration, texture segmentation, computation of optical flow and stereo. A number of conference and journal papers reporting the research findings have been published. A list of publications and presentation is given at the end of the report along with a set or reprints. GRA

N91-16558# Army Aeromedical Research Lab., Fort Rucker, AL.
A COMPARISON OF COMPUTERIZED MEASUREMENT OF HELICOPTER PILOT PERFORMANCE WITH ATROPINE SULFATE DURING ACTUAL AND SIMULATED FLIGHT
J. A. Caldwell, Jr. and H. D. Jones *In* AGARD, Safety Network to Detect Performance Degradation and Pilot Incapacitation Sep. 1990 10 p (For primary document see N91-16553 08-54)
Copyright Avail: NTIS HC/MF A06; Non-NATO Nationals requests available only from AGARD/Scientific Publications Executive

N91-16561# Paris V Univ. (France). Lab. d'Anthropologie Appliquee.
STUDY OF PILOT VIGILANCE DURING LONG RANGE FLIGHT [ETUDE DE LA VIGILANCE DES PILOTES AU COURS DE VOLS LONG-COURRIERS]
A. Coblentz, R. Mollard, Ph. Cabon, J. P. Fouillot, and Vincent Carmigniani (Direction Generale de l'Aviation Civile, Paris, France) *In* AGARD, Safety Network to Detect Performance Degradation and Pilot Incapacitation Sep. 1990 17 p In FRENCH (For primary document see N91-16553 08-54)
Copyright Avail: NTIS HC/MF A06; Non-NATO Nationals requests available only from AGARD/Scientific Publications Executive

N91-16562# Johann-Wolfgang-Goethe-Univ., Frankfurt am Main (Germany, F.R.). Zentrum der Physiologie.
COMPUTER AIDED PHYSIOLOGICAL ASSESSMENT OF THE FUNCTIONAL STATE OF PILOTS DURING SIMULATED FLIGHT
Kurt Offenloch and Gisela Zahner *In* AGARD, Safety Network to Detect Performance Degradation and Pilot Incapacitation Sep. 1990 9 p Sponsored by Dornier G.m.b.H. and Inspektion des Sanitaetswesens der Bundeswehr (For primary document see N91-16553 08-54)
Copyright Avail: NTIS HC/MF A06; Non-NATO Nationals requests available only from AGARD/Scientific Publications Executive

N91-16564# Dialogics S.A., Labege Innopole (France).
INTELLIGENT ASSISTANT SYSTEMS: AN ARTIFICIAL INTELLIGENCE APPROACH TO DETECTING PERFORMANCE DEGRADATION AND PILOT INCAPACITATION
Guy A. Boy *In* AGARD, Safety Network to Detect Performance Degradation and Pilot Incapacitation Sep. 1990 6 p (For primary document see N91-16553 08-54)
Copyright Avail: NTIS HC/MF A06; Non-NATO Nationals requests available only from AGARD/Scientific Publications Executive

54 MAN/SYSTEM TECHNOLOGY AND LIFE SUPPORT

Includes human engineering; biotechnology; and space suits and protective clothing.

For related information see also *16 Space Transportation.*

N91-16552# Air Force Human Resources Lab., Brooks AFB, TX.
HUMAN FACTORS DESIGN GUIDANCE DURING THE CONCEPTUAL DESIGN PHASE OF SYSTEM DEVELOPMENT: A METHODOLOGICAL APPROACH Final Technical Report, Aug. 1985 - Sep. 1989
Lawrence S. Finegold and Michael T. Lawless Jun. 1990 14 p
(AF Proj. 3017)
(AD-A224667; AFHRL-TR-89-66) Avail: NTIS HC/MF A03 CSCL 23/2

Current design process limitations inhibit the most effective use of human factors data in the design of complex man-machine systems. These limitations are described and a possible methodological solution is offered that incorporates human factors issues into the conceptual phase of system design. A current Air Force weapon system is reviewed historically and an application of the methodology to this system is reported. The methodological approach uses subject matter experts to assess various human performance issues on hypothetical systems through mental imagery. In-depth research was required to fully describe the hypothetical systems so that conceptualized operations could be conducted. Lessons learned are presented. GRA

N91-16553# Advisory Group for Aerospace Research and Development, Neuilly-Sur-Seine (France). Aerospace Medical Panel.
SAFETY NETWORK TO DETECT PERFORMANCE DEGRADATION AND PILOT INCAPACITATION
Sep. 1990 120 p In ENGLISH and FRENCH Symposium held in Tours, France, 2 Apr. 1990
(AGARD-CP-490; ISBN-92-835-0580-8) Copyright Avail: NTIS HC/MF A06; Non-NATO Nationals requests available only from AGARD/Scientific Publications Executive

The proceedings from this conference are presented. Recent advances in technology are making feasible the concept of a Safety Net system temporarily overriding the authority of the partially or fully incapacitated pilot until he/she is able to resume full control of the aircraft. The current status of technological developments as well as philosophical issue which must be addressed are reviewed. For individual titles, see N91-16554 through N91-16564.

N91-16554# Institute of Aviation Medicine, Farnborough (England).
CEREBRAL OXYGEN STATUS AND G-INDUCED LOSS OF CONSCIOUSNESS **c52**
David H. Glaister *In* AGARD, Safety Network to Detect Performance Degradation and Pilot Incapacitation Sep. 1990 4 p (For primary document see N91-16553 08-54)
Copyright Avail: NTIS HC/MF A06; Non-NATO Nationals requests available only from AGARD/Scientific Publications Executive

G-induced loss of consciousness (G-LOC) is a common event and has led to the loss of many aircraft and aircrew. While most body systems are ultimately affected, the final common path for its initiation is an inadequate supply of oxygen to the brain. Thus, a measure of cerebral oxygen sufficiency could provide a specific monitor for incipient G-LOC and serve either as a warning to the pilot or as a trigger for an autorecovery system. Multiwavelength near IR spectrophotometry permits the noninvasive in vivo measurement of the oxygen content of blood within the cerebral microcirculation, and also of the oxygen status of cytochrome-c oxidase within the brain cells. This technique was validated in human subjects during exposure to hypoxia; in presyncope induced by lower body negative pressure; and during +G sub z induced

loss of consciousness. As well as providing an important new tool for acceleration research, the technique has the potential to be developed into an inflight monitor for aircrew. Author

N91-16555# Laboratoire de Medecine Aerospatiale, Bretigny-sur-Orge (France).
DETECTION OF LOSS OF CONSCIOUSNESS IN FLIGHT BY DOPPLER METHOD [DETECTION DES PERTES DE CONNAISSANCE EN VOL PAR METHODE DOPPLER] c52
J. M. Clere, G. Ossard, D. Lejeune, A. Leger, and A. Roncin (Tours Univ., France) *In* AGARD, Safety Network to Detect Performance Degradation and Pilot Incapacitation Sep. 1990 6 p In FRENCH (For primary document see N91-16553 08-54)
Copyright Avail: NTIS HC/MF A06; Non-NATO Nationals requests available only from AGARD/Scientific Publications Executive

The use of transcranial Doppler monitoring is recommended for detecting acceleration induced loss of consciousness (LOC). One transcranial Doppler pulse device was developed specifically to function in a centrifuge and another for use in a Mirage 2000, causing limitations to respect the secure environment required by use in flight. During a study conducted for the evaluation of acceleration tolerance of 9 subjects at +8 Gz, the transcranial Doppler device showed the existence in 23 instances of a relationship between velocimetric signal reduction of an average cerebral arterial circulation and the decrease of the field of view; in 9 instances, this relationship was not observed, and in 1 case a weak decrease of the Doppler signal was followed by LOC. The detection and analysis of LOC in flight of many physiological and flight factors will cause the release of automatic safety procedures by the onboard computer. This necessitates the development of new and complex procedures. In this case, the best treatment for LOC consist of being put in a preventive position thanks to new anti-G protection (inclined seat, positive pressure respiration, anti-G pants for the lower body). Transl. by E.R.

N91-16556# Aerospace Medical Research Labs., Wright-Patterson AFB, OH. Acceleration Effects Branch.
CURRENT STATUS OF AN ARTIFICIAL INTELLIGENCE-BASED LOSS OF CONSCIOUSNESS MONITORING SYSTEM FOR ADVANCED FIGHTER AIRCRAFT
William B. Albery and Robert E. VanPatten (Van Patten, Robert E., Bellbrook, OH) *In* AGARD, Safety Network to Detect Performance Degradation and Pilot Incapacitation Sep. 1990 8 p (For primary document see N91-16553 08-54)
Copyright Avail: NTIS HC/MF A06; Non-NATO Nationals requests available only from AGARD/Scientific Publications Executive

During the past decade, fourteen U.S. Air Force pilots lost their lives and aircraft to gravity induced loss of consciousness (GLOC). GLOC is not a new problem, it has been around for over 70 years. Because of the emergence of high performance aircraft such as the F-16 and F-15 and the fact that these aircraft can perform beyond the acceleration tolerance limits of the human, GLOC has become the U.S. Tactical Air Force's second most serious human factors problem, second only to spatial disorientation. To date, there exists no monitoring system in USAF aircraft to detect when a pilot has become incapacitated due to GLOC. The incorporation of high G onset training and a special centrifuge training facility will help reduce, but not eliminate, the GLOC problem. The current status is presented of a LOC detection and recovery system being developed. Author

N91-16557# Defense Advanced Research Projects Agency, Arlington, VA. Tactical Technology Office.
FRAMEWORK FOR AN EFFICIENT TWO FILTER GLOC MONITOR
Dennis K. McBride and Elizabeth A. Davies (Naval Air Test Center, Patuxent River, MD.) *In* AGARD, Safety Network to Detect Performance Degradation and Pilot Incapacitation Sep. 1990 7 p (For primary document see N91-16553 08-54)
Copyright Avail: NTIS HC/MF A06; Non-NATO Nationals requests available only from AGARD/Scientific Publications Executive

A multiple filter Gravitational Loss of Consciousness (GLOC) design framework was derived. The framework recognizes the computational limitations of current and modified airborne avionics suites. The sequential gating approach minimizes load on supporting computer resources. As context and symptoms dictate, however, appropriate processing is applied. The framework is introduced as a provocative statement of design constraints inherent in 1970's jet architectures. The simplicity of design and implementation minimizes software engineering requirements, and holds hardware/interface development to but one requisite innovation; a helmet integrated, ICS capable earplug that would serve as a blood velocity, Doppler sensing and transdusing agent. Author

N91-16558# Army Aeromedical Research Lab., Fort Rucker, AL.
A COMPARISON OF COMPUTERIZED MEASUREMENT OF HELICOPTER PILOT PERFORMANCE WITH ATROPINE SULFATE DURING ACTUAL AND SIMULATED FLIGHT c53
J. A. Caldwell, Jr. and H. D. Jones *In* AGARD, Safety Network to Detect Performance Degradation and Pilot Incapacitation Sep. 1990 10 p (For primary document see N91-16553 08-54)
Copyright Avail: NTIS HC/MF A06; Non-NATO Nationals requests available only from AGARD/Scientific Publications Executive

The requirement for aviators to operate under stressful circumstances raises concerns over both safety and effectiveness. Although appropriate countermeasures for stress induced performance deteriorations are available, the implementation of these countermeasures require that commanders know the time course and extent of the problem. For this reason, the U.S. Army has focused research on the practical assessment of helicopter pilot degradation using flight performance assessments which combine enhanced automation and objectivity with optimized data analysis procedures. Recently, the sensitivity, accuracy, and consistency of these assessment systems were demonstrated while studying the effects of atropine sulfate on aviator performance. Both simulator and helicopter systems detected atropine related performance problems across a variety of aircraft control parameters. Also, analysis of combined simulator and helicopter data showed remarkable consistency of effects across the two flight platforms. This verification of performance measurement using computerized schemes in both simulator and aircraft has substantiated a feasible methodology, and has helped the concept development of better assessment devices. Author

N91-16559# British Aerospace Public Ltd. Co., Bristol (England).
EEG INDICATORS OF MENTAL WORKLOAD: CONCEPTUAL AND PRACTICAL ISSUES IN THE DEVELOPMENT OF A MEASUREMENT TOOL
M. R. Hicks *In* AGARD, Safety Network to Detect Performance Degradation and Pilot Incapacitation Sep. 1990 7 p (For primary document see N91-16553 08-54)
Copyright Avail: NTIS HC/MF A06; Non-NATO Nationals requests available only from AGARD/Scientific Publications Executive

A first objective in the development of a pilot state monitor is the development of a lab tool capable of measuring mental workload. Several general performance benchmarks are identified that facilitate the evaluation of such techniques and a recent program of research is described and assessed in the light of these criteria. Author

N91-16560# Royal Aerospace Establishment, Farnborough (England).
OPTIMISATION OF OPERATIONAL WORKLOAD LEVELS USING NEUROPHYSIOLOGICAL AND COGNITIVE TECHNIQUES
D. W. Burgess, J. A. Chillery, S. Jensen, and A. Hall *In* AGARD, Safety Network to Detect Performance Degradation and Pilot Incapacitation Sep. 1990 7 p (For primary document see N91-16553 08-54)
Copyright Avail: NTIS HC/MF A06; Non-NATO Nationals requests available only from AGARD/Scientific Publications Executive

Extremes of operational workloads were identified and assessed

using either existing measures, e.g., NASA TLX, SWAT, etc., together with neurological measurements. Data already exists from specialist labs which show a reliable increase in the DC levels of brain activity with increasing workloads. In order to optimize workloads, the objective of future missions are predicted and analyzed. Following this detailed task analysis, timeline analysis and attentional demand analysis are used to identify the extent to which particular cognitive channels, e.g., visual, auditory, and psychomotor are being used at any one time. In parallel with this analysis, evoked response techniques are developed from the lab studies towards man mountable apparatus for in-flight use. This requires the development of low noise electrically isolated DC amplifiers of high dynamic range design to obtain physiological data from the man with the minimum of operator support. An aim is to provide a high degree of perceived realism in lab tasks including the accomplishment of secondary tasks. Author

N91-16561# Paris V Univ. (France). Lab. d'Anthropologie Appliquee.

STUDY OF PILOT VIGILANCE DURING LONG RANGE FLIGHT [ETUDE DE LA VIGILANCE DES PILOTES AU COURS DE VOLS LONG-COURRIERS] **c53**

A. Coblentz, R. Mollard, Ph. Cabon, J. P. Fouillot, and Vincent Carmigniani (Direction Generale de l'Aviation Civile, Paris, France) *In* AGARD, Safety Network to Detect Performance Degradation and Pilot Incapacitation Sep. 1990 17 p In FRENCH (For primary document see N91-16553 08-54)

Copyright Avail: NTIS HC/MF A06; Non-NATO Nationals requests available only from AGARD/Scientific Publications Executive

The various states of alertness and performance during the course of monotonous activity has been demonstrated by many authors. In transport aviation, the monotony often found associated with the cycle of irregular work and timeshift is important. The interaction of these factors contribute to the amplification of a drop in performance and vigilance. After a study of pilot behavior during long range flight, a project was started. The objective was to identify phases of hypovigilance and to evaluate the repercussions on pilot performance. The method used rest deprivation as an objective evaluation of physiological levels of pilot alertness together with an analysis of different activities of electroencephalogram (EEG), electro-oculagram (EOC), and electrocardiogram (ECG) during flight. The cardiac frequency and driving wrist activity were both recorded during flight and periods of rest. The driving wrist activity allows the acquisition of data on the activity-rest cycles of pilots. The observation of activity and of crew task is made simultaneously in this recording using a coded grid. Eight long range transmeridian flights, north-south was used during the first stage of protocol completion. The first results show large variations in the EEG spectra and in the frequency of eye movements. The alternation of phases during which the pilots show elevated vigilance with drowsiness were seen in each crew member. The deprivation of sleep during stopover show repercussions on pilot behavior. In particular, the lowest vigilance appear most pronounced during flight following a night with sleep deprivation, especially if the flight is during the next day.

Transl. by E.R.

N91-16562# Johann-Wolfgang-Goethe-Univ., Frankfurt am Main (Germany, F.R.). Zentrum der Physiologie.

COMPUTER AIDED PHYSIOLOGICAL ASSESSMENT OF THE FUNCTIONAL STATE OF PILOTS DURING SIMULATED FLIGHT **c53**

Kurt Offenloch and Gisela Zahner *In* AGARD, Safety Network to Detect Performance Degradation and Pilot Incapacitation Sep. 1990 9 p Sponsored by Dornier G.m.b.H. and Inspektion des Sanitaetswesens der Bundeswehr (For primary document see N91-16553 08-54)

Copyright Avail: NTIS HC/MF A06; Non-NATO Nationals requests available only from AGARD/Scientific Publications Executive

Multichannel (polygraphic) analysis of cardiovascular and neurophysiological parameters provides very sensitive indicators of the functional state of subjects such as pilots during real or simulated flight missions which thus can be objectively assessed. In 6 pilots flying a fighter jet simulator with ALPHA JET dynamic characteristics without self motion, systolic and diastolic blood pressure, four channel electroencephalogram (EEG), electro-oculogram (EOG), and electrocardiogram (ECG) were continuously recorded during a rest-activity-rest sequence for 60 min. The activities consisted of tracking another plane flying ahead of the piloted plane with four different degrees of difficulty. The analysis of the data, especially those of the EEG by Fast Fourier Transformation (FFT), revealed task dependent, and in the case of EEG, topographically different cortical activities depending upon whether sensory and/or motor systems were involved. The physiological measures thus obtained can serve as an objective criterion to assess the functional state of pilots and may serve as part of an automatic safety network not only in the event of sudden loss of consciousness but also in cases of lowered cases of pilot vigilance due to fatigue. Author

N91-16563# Man-Made Systems Corp., Ellicott City, MD.

DEVELOPMENT OF A TEST-BED FOR REAL-TIME MONITORING OF PILOT MENTAL STATUS

Richard L. Horst, Dan T. Smith, and John K. Nebel (Advanced Resource Development Corp., Columbia, MD.) *In* AGARD, Safety Network to Detect Performance Degradation and Pilot Incapacitation Sep. 1990 9 p (For primary document see N91-16553 08-54)

Copyright Avail: NTIS HC/MF A06; Non-NATO Nationals requests available only from AGARD/Scientific Publications Executive

The real time determination of pilot mental and physical status is a critical feature of the workload monitoring and Mindware subsystems that have been envisioned for future jet aircraft. Recent lab and simulator studies, using retrospective data analyses, have suggested the value of various behavioral and physiological indices for reflecting task performance. Software algorithms were developed to derive some of these measures in real time and to develop a test bed in which to explore the efficacy of these measures for inferring operationally relevant changes in pilot status. The project showed the feasibility and usefulness of the approach. Data processing algorithms were developed for characterizing and integrating physiological indices based on heart rate and heart rate variability, eye blinks, and single trial, scalp recorded event related potentials. These physiological measures were obtained concurrently with behavioral measures as subjects performed a PC based, aviation simulation task. The data processing algorithms were implemented in a distributed processing configuration, using multiple personal computers, with the derived measures being integrated by a decision maker multiprocessor. Author

N91-16564# Dialogics S.A., Labege Innopole (France).

INTELLIGENT ASSISTANT SYSTEMS: AN ARTIFICIAL INTELLIGENCE APPROACH TO DETECTING PERFORMANCE DEGRADATION AND PILOT INCAPACITATION **c53**

Guy A. Boy *In* AGARD, Safety Network to Detect Performance Degradation and Pilot Incapacitation Sep. 1990 6 p (For primary document see N91-16553 08-54)

Copyright Avail: NTIS HC/MF A06; Non-NATO Nationals requests available only from AGARD/Scientific Publications Executive

An artificial intelligence approach is presented to detecting performance degradation and pilot incapacitation. The motivations are discussed for Intelligent Assistant Systems in such situations. The problem of constructing procedures is shown to be a very critical issue. In particular, keeping procedural experience in both design and operation is critical. It is suggested what artificial intelligence can offer in this direction, and the concept of Integrated Human-Machine Intelligence is presented. Some crucial problems induced by this approach are discussed in detail. Finally, the various roles are analyzed that would be shared by both the pilot and the intelligent assistant system. Author

N91-16565# Ballistic Research Labs., Aberdeen Proving Ground, MD.

REMOVAL OF NO AND NO2 FROM CONTAMINATED ATMOSPHERES Final Report, 22 Jun. - 18 Aug. 1989

Anthony E. Finnerty, Gould Gibbons, Jr., Matthew Schroeder, Lisa

Copland, and Tanya Swiderski Sep. 1990 37 p
(AD-A227260; BRL-MR-3860) Avail: NTIS HC/MF A03 CSCL 07/2

Laboratory studies were carried out to determine the feasibility of removing certain toxic gases from a vehicle atmosphere. Both nitrogen dioxide (NO2) and nitric oxide (NO) were studied in the concentration range 200 to 2000 parts per million (ppm). Only non-toxic agents were considered for removal of these gases. The most efficient scrubbing agents found were: water, diammonium phosphate and Monnex with NO2, MAP (monoammonium phosphate) and alum with NO. Unfortunately, no single powder showed promise of removing both the toxic gases. The presence of a base (sodium bicarbonate) in the water mist did not enhance the removal of NO2 from the atmosphere. GRA

N91-16566*# National Aeronautics and Space Administration. Lyndon B. Johnson Space Center, Houston, TX.
WHOLE BODY CLEANSING AGENT Patent Application
Steven E. Lentsch, inventor (to NASA) (ECO-Labs., Cleveland, OH.) 29 May 1990 15 p
(NASA-CASE-MSC-21589-1; NAS 1.71:MSC-21589-1; US-PATENT-APPL-SN-529427) Avail: NTIS HC/MF A03 CSCL 06K

The subject invention relates to a human cleansing agent particularly suitable for use in long duration spaceflight and a method of bathing with the agent. The agent of the subject invention is in the form of a paste having a pH of 5.0 to 7.9 which comprises an acyltaurate, a skin conditioner, a hair conditioner, and a preservative. More specifically, it includes sodium N-coconut acid-N-methyl taurate, in combination with soybean lecithin, polyquaternium 16, and formalin. This particular combination satisfies the following objectives: (1) that it be usable with a minimum amount of water per shower (approximately 1 gallon); (2) that it be easily separated from the water for purposes of water reclamation; (3) that it be pH compatible with skin and hair; (4) that it rinse well in deionized water; (5) that it be mild to skin and eyes; (6) that it effectively clean both skin and hair; (7) that it be suitable for use in zero gravity; and (8) that it provide ease of combing of wet and dry hair. The method of the invention includes the steps of wetting the skin and hair with a small quantity of water, lathering the skin with the paste, rinsing the lather from the skin and hair with a small quantity of water to produce a rinse water containing the cleansing agent, defoaming the rinse water, and supplying the defoamed rinse water to a water reclamation unit for recycling the water. The novelty of the invention appears to lie in the particular formulation of the cleansing agent and its method of use which provide optimal results under the given constraints and objectives. NASA

N91-16567# National Academy of Sciences - National Research Council, Washington, DC. Committee on Human Factors.
APPLICATION PRINCIPLES FOR MULTICOLORED DISPLAYS: A WORKSHOP REPORT
JoAnn S. Kinney, ed. and Beverly Messick Huey, ed. National Academy Press 1990 73 p Workshop held in Washington, DC, 22 Oct. 1990
(Grants N00014-85-G-0093; MDA903-88-C-0031; MDA903-89-K-0074)
(AD-A227961) Avail: NTIS HC/MF A04 CSCL 12/6

The Committee on Human Factors organized the Workshop on Application Principles for Multicolored Displays to examine a subset of problems associated with the current use of color in displays. Multicolored displays are used in a variety of civilian and military systems, and the rapid expansion of the field has technical developments from diverse fields. A great number of complex, interacting factors determine the effectiveness of a color display system. Although many of these factors characterize visual displays in general, many others are specifically related to the production and use of color. The latter include both human visual perceptual factors and color display hardware characteristics that cannot reasonably be treated in isolation. There is substantial evidence that people prefer color. The significantly higher sales of color television sets and color photographic film and the almost exclusive production of motion pictures in color are examples of the preference. Since color will probably be used, even demanded, in displays, whether essential or not, a high priority should be given to employing it effectively, even though multicolored displays are not necessary or advantageous for all applications. GRA

N91-16568 Institute for Perception RVO-TNO, Soesterberg (Netherlands).
ORGANIZATION OF THE MISSION PATTERN IN THE AIR PICTURE Final Report
P. J. M. D. Essens 28 Feb. 1990 22 p In DUTCH; ENGLISH summary
(Contract A87/KLu/131)
(IZF-1990-A-12; TD-90-0026; ETN-91-98311) Copyright Avail: Institute for Perception RVO-TNO, P.O. Box 23, 3769 ZG Soesterberg, Netherlands

In an experiment with fighter allocators the organization of the mission pattern in a dynamic air picture was investigated with two types of presentation. A comparison, in terms of search times and mental image of the mission pattern, was made between an air picture in which the own and enemy aircraft coupled in the mission have the same color, and one in which those elements of a mission pattern shows that the mental image with color coding is richer than with line coding. The number of recalled missions is about 10 percent higher. There is no difference in the spatial accuracy for the two types of presentation. The search time (about 3 sec) is the same in the two conditions. The subjects strongly preferred color coding. The comments of the subjects indicate that the air picture is more organized. ESA

N91-16569 Institute for Perception RVO-TNO, Soesterberg (Netherlands).
HEAT TRANSFER IN CLOTHING DURING HEAT RADIATION Final Report
A. M. J. Pieters and W. A. Lotens 22 Jan. 1990 61 p In DUTCH; ENGLISH summary
(IZF-1990-B-2; TD-89-4561; ETN-91-98390) Copyright Avail: Institute for Perception RVO-TNO, P.O. 23, 3768 ZG Soesterberg, Netherlands

A model to calculate temperatures and heat flows with one-sided heat radiation is suggested. Two clothing layers were taken into account in the model. The model is based on a network and calculates the temperatures in both layers, the microclimate, and the heat flow from skin and clothing. For the experimental verification only the dry heat flow was measured by wrapping the subjects in plastic foil. Wind and movement decrease clothing temperature and insulation. Measured and calculated temperatures agree very well. In an experiment where the subjects wore absorbing, reflecting, and transmitting garments while walking, the radiation properties were determined; the mean difference between measured and calculated temperatures and heat flows was 1.2 C and 2.2 W, respectively. ESA

N91-16570# Messerschmitt-Boelkow-Blohm G.m.b.H., Bremen (Germany, F.R.).
COMMON APPROACH FOR PLANETARY HABITATION SYSTEMS IMPLEMENTATION
Frank Steinsiek and Uwe Apel 1990 11 p Presented at the 20th International Conference on Environmental Systems, Williamsburg, VA, 9-12 Jul. 1990 Previously announced in IAA as A90-49425 Prepared in cooperation with Erno Raumfahrttechnik G.m.b.H.
(MBB-UO-0115-90-PUB; ETN-91-98549) Avail: NTIS HC/MF A03

Possible concepts for orbital, lunar and Martian habitations are based on ESA-European Manned Space Infrastucture (EMSI) program philosophy are presented. The key requirements for the design of an orbital habitat were reviewed, such as atmospheric pressure, temperature, radiation and gravity levels. The human factors such as life cycle, ergonomy and psychological needs were examined. A common approach for these three cases may be to use as much available hardware in each step of the scenario as

possible. The implementation of the habitation systems offers the possibility to work in an evolutionary way, starting with the EMSI Columbus based hardware. ESA

55 SPACE BIOLOGY

Includes exobiology; planetary biology; and extraterrestrial life.

No abstracts in this category.

59 MATHEMATICAL AND COMPUTER SCIENCES (GENERAL)

No abstracts in this category.

60 COMPUTER OPERATIONS AND HARDWARE

Includes hardware for computer graphics, firmware, and data processing.

For components see *33 Electronics and Electrical Engineering.*

N91-16571# Stanford Univ., CA. Computer Systems Lab.
MICROSUPERCOMPUTERS: DESIGN AND IMPLEMENTATION
Semiannual Progress Report, Nov. 1989 - Mar. 1990
John L. Hennessy and Mark A. Horowitz Mar. 1990 67 p
(Contract N00014-87-K-0828; DARPA Order 1133)
(AD-A228741) Avail: NTIS HC/MF A04 CSCL 12/6

The following topics are presented: (1) Parallel Processor Architecture -- The primary focus of the architecture effort has been on completing the design of DASH and starting the construction of the prototype; (2) Parallel Software -- A compiler system is being built that supports the research in a broad spectrum of topics, ranging from advanced scalar optimizations to parallel loop transformations and code scheduling for multiprocessors and superscalar processors; (3) Uniprocessor Architecture -- Work on investigating efficient methods of extracting the parallelism available at the lowest-level, by issuing multiple instruction per cycle has been continued; (4) Computer-Aided Design -- Recent research has been focusing on partitioning techniques at the behavioral-level of abstraction; and (5) VLSI Design -- During this period, work in high-speed BiCMOS circuits has been continued. GRA

N91-16572# Stanford Univ., CA. Computer Systems Lab.
MICROSUPERCOMPUTERS: DESIGN AND IMPLEMENTATION
Semiannual Progress Report, Apr. - Oct. 1990
John L. Hennessy and Mark A. Horowitz Oct. 1990 52 p
(Contract N00014-87-K-0828; DARPA Order 1133)
(AD-A228744) Avail: NTIS HC/MF A04 CSCL 12/5

The project goals are as follows: (1) to investigate fundamental properties of parallel programs and the implications for multiprocessor architectures, parallel programming, and compilers; (2) to explore architectural approaches that can be used to build scalable multiprocessors capable of supporting a shared memory programming paradigm; (3) to develop compiler and programming language technology that supports the construction of efficient, machine-independent parallel programs; (4) to investigate architectural approaches that will lead to substantial improvements in uniprocessor performance and that can be incorporated in scalable multiprocessors; and (5) to develop computer aided design tools and very large scale integration technology needed to construct high performance machines. GRA

61 COMPUTER PROGRAMMING AND SOFTWARE

Includes computer programs, routines, alogorithms, and specific applications, e.g., CAD/CAM.

N91-16573# Argonne National Lab., IL. Mathematics and Computer Science Div.
A BLOCK QR FACTORIZATION ALGORITHM FOR RANK-DEFICIENT MATRICES
Christian H. Bischof 1989 6 p Presented at the 4th SIAM Conference on Parallel Processing for Scientific Computing, Chicago, IL, 11-13 Dec. 1989
(Contract W-31-109-eng-38; NSF ASC-87-15728)
(DE90-010066; CONF-891273-4) Avail: NTIS HC/MF A02

A new algorithm is presented for computing the QR factorization of a rank deficient matrix that is well suited for high performance machines. These machines typically employ a memory hierarchy and matrix-matrix operations perform better on those machines than matrix-vector or vector-vector operations since they require significantly less data movement per floating point operation. The traditional QR factorization algorithm with column pivoting is not well suited for such environments since it precludes the use of matrix-matrix operations. Instead, a restricted pivoting strategy is suggested based on incremental condition estimation which allows the formulation of a block QR factorization algorithm where the bulk of the work is in matrix-matrix operations. Performance results on the Cray 2, Cray X-MP and Cray Y-MP show that the new algorithm performs significantly better than the traditional scheme and can more than halve the cost of computing the QR factorization. DOE

N91-16574# Edgerton, Germeshausen and Grier, Inc., Idaho Falls, ID.
AUTOMATIC, HIGH-RESOLUTION ANALYSIS OF LOW-NOISE FRINGES
Gordon D. Lassahn 1990 6 p Presented at the SPIE's International Symposium on Optical and Optoelectronic Applied Science and Engineering and Exhibit, San Diego, CA, 8-13 Jul. 1990
(Contract DE-AC07-76ID-01570)
(DE90-009779; EGG-M-90027; CONF-900756-1) Avail: NTIS HC/MF A02

We outline a fringe analysis algorithm that is completely automatic and has been demonstrated to give individual pixel resolution with good accuracy for very general types of fringe patterns, but is slow and quite sensitive to noise in the raw fringe image. The purpose of this work was to develop a fringe analysis system that can handle any type of fringe pattern arising from diffraction Moire interferometry and can calculate the phase accurately at each pixel. DOE

N91-16575# Sandia National Labs., Albuquerque, NM. Computational Physics and Mechanics Div.
ANEOS: ANALYTIC EQUATIONS OF STATE FOR SHOCK PHYSICS CODES INPUT MANUAL
Samuel L. Thompson Mar. 1990 69 p
(Contract DE-AC04-76DP-00789)
(DE90-010198; SAND-89-2951) Avail: NTIS HC/MF A04

ANEOS is an in-line software package which provides thermodynamic information for shock physics codes. Solids, liquids, vapors, plasmas and phase mixtures are considered in a thermodynamically consistent and complete manner. The package is flexible and easy to use. This users manual contains input instructions, examples, and descriptions of user output. DOE

N91-16576# Argonne National Lab., IL. Mathematics and Computer Science Div.
USING MAPLE FOR SYMBOLIC COMPUTATIONS IN ROBOTICS
Man Kam Kwong, Rongdong Wang, and Peng-Yung Woo (University of Northern Illinois, De Kalb.) 1990 30 p Presented at the IEEE Robotics and Automation Conference, Cincinnati, OH, 13-18 May 1990
(Contract W-31-109-eng-38)
(DE90-010405; CONF-900559-14) Avail: NTIS HC/MF A03

Programs are presented for deriving forward kinematics, Jacobians and dynamic equations of robotic manipulators in symbolic closed forms by using the algebraic manipulation software MAPLE. Examples are given. Efficiency of these computations are discussed. DOE

N91-16577# Lawrence Livermore National Lab., CA. Computing Research Group.
POSC: A PARTITIONING AND OPTIMIZING SISAL COMPILER
Vivek Sarkar (International Business Machines Corp., Yorktown Heights, NY.) and David C. Cann Apr. 1990 14 p Presented at the 4th ACM International Conference on Supercomputing, Amsterdam, Netherlands, 11-15 Jun. 1990 Revised
(Contract W-7405-eng-48)
(DE90-010679; UCRL-102737-REV-1; CONF-9006114-1-REV-1)
Avail: NTIS HC/MF A03

Single assignment languages like SISAL offer parallelism at all levels (arbitrary operations, conditionals, loop iterations, and function calls). All control data dependences are local, and can be easily determined from the program. Various studies of SISAL programs have shown that they contain massive amounts of potential parallelism. There are two major challenges in converting this potential parallelism into real speedup on multiprocessor systems. First, it is important to carefully select the useful parallelism in a SISAL program, so as to obtain good speedup by trading off parallelism with overhead. Second, it is important to do sequential optimizations, so that the sequential components (tasks) of the SISAL program have comparable execution times with sequential languages such as FORTRAN, Pascal and C. The POSC compiler system described addresses both issues by integrating previous work on efficient sequential implementation of SISAL programs with previous work on selecting the useful parallelism in a SISAL program. The combined approach is validated by real speedup measurements on a Sequent Balance multiprocessor. DOE

N91-16578# Los Alamos National Lab., NM.
A GRAPHICAL USER-INTERFACE-DRIVEN WAVEFORM DATA ACQUISITION AND ANALYSIS SYSTEM
Alan Chamberlin, Michael D. Holder, and John M. McAfee 1990 11 p Presented at the 3rd Test Technology Symposium, Laurel, MD, 19-21 Mar. 1990
(Contract W-7405-eng-36)
(DE90-011948; LA-UR-90-1546; CONF-9003149-3) Avail: NTIS HC/MF A03

We have developed a computerized waveform data acquisition and analysis system that uses the graphic user interface of the Macintosh computer. The system provides the means for acquiring single-shot waveforms from a variety of recorders and digital oscilloscopes on an IEEE-488 instrument bus. The computer interrogates each address on the bus to determine the identity and configuration of any combination of CAMAC crates and oscilloscopes connected to the IEEE-488 bus. Graphic representations of each instrument and/or CAMAC module are displayed on the computer screen. A unique method is used to configure the software to represent graphically the signal path and content. The operator may draw connections through intermediate modules and enter calibrations for signal sources to give a complete data base of transfer functions and signal paths. The data base is used to generate graphs of the waveforms reduced to the desired engineering units. This system is designed to reduce the operator workload and specialized knowledge by providing guidance for the use of a particular instrument. Once acquired, the data may be manipulated by means of several signal-processing functions, such as smoothing, filtering, fitting, and Fourier analysis. Waveforms may be combined into complex data sets for complete Fourier analysis. The data are normally stored in a compact binary format to minimize the impact on archival storage. However, they may be translated to more general ASC2 formates, if desired. Any waveform graphic may be transferred to word-processing and page layout software for publication. DOE

N91-16579# Sandia National Labs., Albuquerque, NM.
IMPLEMENTATION OF THE PHASE GRADIENT ALGORITHM
Daniel E. Wahl, Paul H. Eichel, and Charles V. Jakowatz, Jr. 1990 6 p Presented at the SPIE's International Symposium on Optical and Optoelectronic Applied Science and Engineering and Exhibit, San Diego, CA, 8-13 Jul. 1990
(Contract DE-AC04-76DP-00789)
(DE90-012160; SAND-89-2985C; CONF-900756-4) Avail: NTIS HC/MF A02

The recently introduced Phase Gradient Autofocus (PGA) algorithm is a non-parametric autofocus technique which has been shown to be quite effective for phase correction of Synthetic Aperture Radar (SAR) imagery. This paper will show that this powerful algorithm can be executed at near real-time speeds and also be implemented in a relatively small piece of hardware. A brief review of the PGA will be presented along with an overview of some critical implementation considerations. In addition, a demonstration of the PGA algorithm running on a 7 x 10 in. printed circuit board containing a TMS320C30 digital signal processing (DSP) chip will be given. With this system, using only the 20 range bins which contain the brightest points in the image, the algorithm can correct a badly degraded 256 x 256 image in as little as 3 seconds. Using all range bins, the algorithm can correct the image in 9 seconds. DOE

N91-16580 Florida Univ., Gainesville.
A QUERY MODEL AND QUERY AND KNOWLEDGE DEFINITION LANGUAGES FOR OBJECT-ORIENTED DATABASES Ph.D. Thesis
Abdallah Mohammed Alashqur 1989 175 p
Avail: Univ. Microfilms Order No. DA9028489

A query model for object-oriented databases is introduced in which the closure property is preserved. Furthermore, the query model is made concrete by introducing an object-oriented query language named OQL as an example of this query model. A query in this language returns a subdatabase whose structure consists of some selected object classes and their associations. The objects that fall in the patterns of object associations specified in the query constitute the extension of the resulting subdatabase. A knowledge definition language for defining deductive rules and integrity constraints pertaining to an object-oriented database is introduced. Deductive rules in this language derive new patterns of associations among objects based on existing and/or other derived patterns. Deductive reasoning about a large number of objects stored in a database is a needed functionality in several new database application domains (e.g., CAD/CAM databases). The OQL and the knowledge definition language are tightly coupled. This facilitates the integration of concepts and techniques, which are typically found in different categories of systems such as database management systems and expert systems, into one integrated, object-oriented knowledge base management system (OKBMS) that meets the specifications and requirements of the new database application domains. Dissert. Abstr.

N91-16581# Sandia National Labs., Albuquerque, NM.
A TRELLIS-SEARCHED APC (ADAPTIVE PREDICTIVE CODING) SPEECH CODER
Kevin T. Malone and Thomas R. Fischer (Washington State Univ., Pullman.) 1990 11 p Presented at the 1990 International Symposium on Information Theory and Its Applications, Honolulu, HI, 27-30 Nov. 1990
(Contract DE-AC04-76DP-00789; NSF NCR-88-21764)
(DE91-000866; SAND-90-2589C; CONF-9011114-1) Avail: NTIS HC/MF A03

A speech coding system was formulated that incorporates trellis coded vector quantization (TCVQ) and adaptive predictive coding (APC). A method for optimizing the TCVQ codebooks is presented and experimental results concerning survivor path mergings are reported. Simulation results are given for encoding rates of 16 and 9.6 kbps for a variety of coder parameters. The quality of the encoded speech is deemed excellent at an encoding rate of 16 kbps and very good at 9.6 kbps. DOE

N91-16582# Midwest Research Inst., Golden, CO. Solar Energy Research Inst.
SMOOTHING AND SCALING AIRFOIL COORDINATES ON A PERSONAL COMPUTER
Peter K. C. Tu and George N. Scott Dec. 1989 79 p
(Contract DE-AC02-83CH-10093)
(DE89-000878; SERI/TR-257-3372) Avail: NTIS HC/MF A05

A mainframe computer program written for smoothing and scaling coordinates was successfully adapted for use on personal computers (IBM PC or compatible microcomputers). The program was modified with a new format for input/output files, keyboard selection of plotting and printing options, and the ability to preview plots on a PC monitor before pen plotting. The new source code was then recompiled on a PC and used mainly for the purpose of supporting in-house aerodynamic research work. It was made compatible with other in-house codes. The system specifications for PCs are listed and the NASA Langley program and its theories used for smoothing and scaling airfoil coordinates are briefly described. A flow chart of the program and the input/output files are explained in detail. A step-by-step manual of executing the code on a PC and the results of sample runs are included. Also included is an evaluation section of airfoil performance characteristics by using a low Reynolds number airfoil design and analysis computer code created to demonstrate the significance or any discrepancies as a result of the smoothing and scaling. DOE

N91-16583# Pattern Analysis and Recognition Corp., New Hartford, NY. Government Systems.
DISTRIBUTED SYSTEM MODELING ENVIRONMENT (DSME) Final Report, Aug. 1986 - Mar. 1990
C. L. Brown and F. K. Frantz Jul. 1990 157 p
(Contract F30602-86-C-0195)
(AD-A226698; RADC-TR-90-140) Avail: NTIS HC/MF A08
CSCL 12/7

The DSME is a computer-based environment that will assist the development and analysis of distributed computer systems by providing support for the simulation modeling of these systems and their components. During the development of the overall DSME concept, PGSC/Harris and RADC defined an overall context for the proposed DSME and defined the framework of that system. In addition, the particular goals of the current effort were established in relation to the overall target system, which is expected to evolve through long term development. The current effort focuses on the initial design and implementation of a limited prototype demonstration of the DSME concept. GRA

N91-16584# Carnegie-Mellon Univ., Pittsburgh, PA. Software Engineering Inst.
IMPLEMENTING SPORADIC SERVERS IN Ada Final Report
Brinkley Sprunt and Lui Sha May 1990 53 p
(Contract F19628-85-C-0003)
(AD-A226723; CMU/SEI-90-TR-6; ESD-90-TR-207) Avail: NTIS HC/MF A04 CSCL 12/5

The data structures and algorithms are presented for implementing sporadic servers in real time systems programmed in Ada. The sporadic server algorithm is an extension of the rate monotonic scheduling algorithm (6). Sporadic servers are tasks created to provide limited and usually high priority service for other tasks, especially aperiodic tasks. Sporadic servers can be used to guarantee deadlines for hard-deadline aperiodic tasks and provide substantial improvements in average response times for soft-deadline aperiodic tasks over polling techniques. Sporadic servers also provide a mechanism for implementing the Period Transformation technique that can guarantee that a critical set of periodic tasks will always meet their deadlines during a transient overload. Sporadic servers can also aid fault detection and containment in a real time system by limiting the maximum execution time consumed by a task and detecting attempts to exceed a specified limit. Two types of implementations for the sporadic server algorithm are discussed: a partial implementation using an Ada task that requires no modifications to the Ada runtime system and a full implementation and options for reducing this overhead. GRA

N91-16585# Carnegie-Mellon Univ., Pittsburgh, PA. Software Engineering Inst.
UNDERSTANDING THE ADOPTION OF Ada: RESULTS OF AN INDUSTRY SURVEY
Marthena Carlson and Gordon N. Smith May 1990 62 p
(Contract F19628-85-C-0003)
(AD-A226725; CMU/SEI-90-SR-10) Avail: NTIS HC/MF A04
CSCL 12/5

In 1983, the U.S. Department of Defense (DoD) established a policy requiring the use of a new programming language, Ada, for the development of all new Mission-Critical Computer Resource (MCCR) software that it purchases. Firms that supply the DoD with these systems have show considerable variation in their decisions to incorporate this new technology into their products and production processes. This survey is part of a multi-stage research project that sought to understand the variability in firms' adoption and use of new information technologies. Herein is a follow-up and elaboration on a case study of the adoption of Ada which is described in CMU/SEI-89-TR-28, Understanding the Adoption of Ada: A Field Study Report. Participants in the survey were 123 business and technical people form 69 business units that supply the DoD with the MCCR software systems and services. The survey explored factors pertaining to respondents' technical and market environments in an attempt to describe depth of adoption and to describe the differences between the firms with active Ada contracts and those without the active contracts. For firms that have adopted Ada, aspects are described of the language and tools that are considered most useful in different application areas. GRA

N91-16586# Kestrel Inst., Palo Alto, CA.
AUTOMATED DESIGN OF DISPLAYS FOR TECHNICAL DATA Interim Technical Paper, Jun. 1989 - May 1990
Stephen Westfold, Cordell Green, and David Zimmerman Sep. 1990 45 p Submitted for publication
(Contract F33615-88-C-0004; AF Proj. 2950)
(AD-A226729; AFHRL-TP-90-66) Avail: NTIS HC/MF A03
CSCL 12/5

A theory is examined of a graphical display that automatically designs tables and diagrams that represent relations occurring in technical data. The theory is based upon a small number of principles such as using visual adjacency and visual connectedness to reflect semantic relations among the data. The theory uses techniques adapted from automated programming for display reformulation and display optimization. A prototype display synthesis system that implements the theory as a set of transformation rules was written. The system takes a relational specification as input and produces a display as output. The theory is illustrated by showing an annotated trace of the prototype generating a large number of tables and diagrams from relational technical data. The examples show the generation of displays from aircraft maintenance technical data that is free of all formatting and display instructions. GRA

N91-16587# Carnegie-Mellon Univ., Pittsburgh, PA. Software Engineering Inst.
HARTSTONE BENCHMARK RESULTS AND ANALYSIS Final Report
Patrick Donohue, Ruth Shapiro, and Nelson Weiderman Jun. 1990 197 p
(Contract F19628-85-C-0003)

(AD-A226817; CMU/SEI-90-TR-7; ESD-90-TR-208) Avail: NTIS HC/MF A09 CSCL 12/5

Hartstone is a series of timing requirements for testing a system's ability to handle hard real time applications. It is specified as a set of processes with well defined workloads and timing constraints. The name Hartstone derives from Hard Real Time and the fact the workloads are based on the well known Whetstone benchmark. This report describes the results obtained by running Version 1.0 of the Hartstone benchmark, an Ada implementation of one of the requirements, on a number of complier/target processor combinations. The characteristics and expected behavior of the benchmark are described, actual results are presented and analyzed, and the lessons learned about the compliers and processors, and the benchmark itself, are discussed. Nothing should be taken as an endorsement of, or an indictment of, a particular product. Users of Ada technology are encouraged to experiment with the Hartstone benchmark relative to their own application requirements. GRA

N91-16588# Rockwell International Corp., Anaheim, CA.
RELIABILITY/MAINTAINABILITY/LOGISTICS SUPPORT ANALYSIS COMPUTER AIDED TAILORING SOFTWARE PROGRAM (R/M/L CATSOP) Final Report, Jul. 1987 - Dec. 1989
Robin L. Webster and Keith J. Gibson Jun. 1990 149 p
(Contract F30602-87-C-0133)
(AD-A226820; RADC-TR-90-120) Avail: NTIS HC/MF A07 CSCL 12/5

The objective was to develop a prototype expert system to improve tailoring of MIL-STD-785, MIL-STD-470 and MIL-STD-1388-1A to system acquisition needs. Specifically, CATSOP takes into account the information pertinent to system requirements, maintenance concepts, mission needs, acquisition phases, funding levels and use environment. This information provides a definition of scope, character and makeup of each task in each standard. The expert system is capable of providing guidance with respect to the above that experienced engineering specialists in reliability, maintainability and logistics are capable of providing a consistent and repeatable fashion given the same set of program characteristics and needs. R/M/L CATSOP, which runs on the M.1 Expert System Shell prompts the user with a series of system acquisition related questions. Each user response provides a pathway for applicable follow-on questions. Once the user has responded to all applicable questions, CATSOP determines and prioritizes all R/M/L tasks that are necessary for the acquisition program. The user then has the option to: add or delete tasks with CATSOP giving consequences of either, editing any previous inputs, or looking at the audit trail to determine why a given task was called out. CATSOP is written for the novice as well as the expert. GRA

N91-16589# Ballistic Research Labs., Aberdeen Proving Ground, MD.
BLAST2D COMPUTATIONS OF THE REFLECTION OF PLANAR SHOCKS FROM WEDGE SURFACES WITH COMPARISON TO SHARC AND STEALTH RESULTS Final Report, Jan. - Jul. 1990
Dixie M. Hisley Sep. 1990 57 p
(DA Proj. 1L1-62120-AH-25)
(AD-A227261; BRL-TR-3147) Avail: NTIS HC/MF A04 CSCL 19/9

Computations of the reflection of planar shocks from wedge surfaces are performed with BLAST2D in order to compare to computational results from the SHARC, and the STEALTH codes and for comparison to experimental data obtained from the Ernst Mach Institute. Results are presented for an incident shock with Mach number equal to 2.12 impinging on 30, 45, 60 degree wedges. Also, BLAST2D results are presented for an incident shock with Mach number equal to 1.295 impinging on 25 and 60 degree double wedge for comparison to SHARC results and to an experimental shadowgraph published by Takayama and Ben-Dor. A new type of contour plot (the computational shadowgraph) is shown to produce excellent agreement with the experimental shadowgraph for the double wedge case. GRA

N91-16590# Carnegie-Mellon Univ., Pittsburgh, PA. Software Engineering Inst.
NATIONAL SOFTWARE CAPACITY: NEAR-TERM STUDY EXECUTIVE SUMMARY
Jane A. Siegel, Shelby Stewman, Suresh Konda, Patrick D. Larkey, and W. G. Wagner May 1990 19 p
(Contract F19628-85-C-0003)
(AD-A227564; SEI-90-SR-12) Avail: NTIS HC/MF A03 CSCL 12/5

The assessment is that the United States has a serious software capacity problem that may worsen substantially unless action is taken on several fronts. An initial overall assessment of the nation's capacity to produce military software, is provided with a focus on mission-critical software. National capacity is dependent upon and impacted by other software development and PDSS that is occurring in the non-DoD commercial and government sectors. In a survey of senior executives from corporations and government, 88 percent indicate that the nation will have a serious capacity problem in being able to produce mission-critical software over the next five years. Moreover, of those who expect a problem, the severity of the problem was ranked at 4 on a scale of 1 to 5, where 3 = serious and 5 = very serious. Both the degree of consensus and the level of criticality indicate that the United States is facing a serious software capacity problem. GRA

N91-16591# Pratt and Whitney Aircraft, West Palm Beach, FL. Government Products Div.
GEOMETRIC MODELING APPLICATIONS INTERFACE PROGRAM Final Report, 1 Aug. 1985 - 31 Mar. 1989
R. Helldoerfer, C. VanWie, and D. Emmerson Nov. 1990 80 p
Prepared in cooperation with McDonnell Aircraft Co., Saint Louis, MO
(Contracts F33615-85-C-5122; F33615-82-C-5036; AF Proj. MTFI)
(AD-A227651; FR-20674; WRDC-TR-90-8022) Avail: NTIS HC/MF A05 CSCL 12/5

This User Manual provides a description of the data exchange software developed under the Air Force sponsored Product Definition Data Interface contract and is applicable to Geometric modeling applications interface program. GRA

N91-16592# LabTek Corp., Woodbridge, CT.
SCHEDULER ISSUES FOR REAL-TIME Ada Final Report
Thomas E. Griest 11 Jun. 1990 44 p
(Contract MDA903-87-C-0056)
(AD-A227766) Avail: NTIS HC/MF A03 CSCL 12/5

Problems associated with providing a user-defined scheduler for use with an Ada program application are discussed from both a single processor and distributed processor viewpoint. The limitations on scheduling, imposed by Ada language semantics, are addressed. Some recent rulings on language interpretations are especially relevant since they seem to provide greater flexibility in the scheduling of prioritized tasks than what was previously considered legal. Runtime architectures which provide an interface for user-defined schedulers are examined to determine their strengths and weaknesses. An Ada runtime scheduler interface was designed to allow a high degree of flexibility users to configure the scheduling of Ada tasks. A conscious decision was made to provide an extremely low level and efficient interface from which higher level abstractions could be built. GRA

N91-16593# LabTek Corp., Woodbridge, CT.
TAILORING AN Ada RUNTIME ENVIRONMENT PROOF-OF-CONCEPT Final Report
Laura Griest 8 Jun. 1990 58 p
(Contract MDA903-87-C-0056)
(AD-A227767) Avail: NTIS HC/MF A04 CSCL 12/5

The need to modify Ada runtime environments in order to achieve the necessary performance and/or functionality of applications has been reported frequently by Ada application developers. The effort involved with making and maintaining custom

runtimes is also known to be quite substantial. For developers that are inexperienced in tailoring Ada runtime systems, the customization work can grow into a major undertaking and place the entire project at risk. To help organizations in managing a first-time runtime customization project, a guideline was developed. This paper describes a proof-of-concept effort designed to verify the accuracy and completeness of this guideline for tailoring Ada runtimes. To evaluate the guideline, an Ada runtime was purchased and several changes were made to implement features of an extended runtime interface. During each step of the project the guideline was examined and followed. In several cases, new information that was believed to be important was identified during the tailoring effort. This information has been provided as comments to the guideline in a detailed review. GRA

N91-16594# Pratt and Whitney Aircraft, West Palm Beach, FL. Government Products Div.
GEOMETRIC MODELING APPLICATION INTERFACE PROGRAM. SYSTEM COMPONENTS OPERATOR'S MANUAL Final Report, 1 Aug. 1985 - 31 Mar. 1989
C. Magnuson, C. VanWie, and D. Emmerson Nov. 1990 55 p
(Contract F33615-85-C-5122)
(AD-A227827; PWA-FR-20435; WRDC-TR-90-8025) Avail: NTIS HC/MF A04 CSCL 12/5

This Operator's Manual describes the system operating commands and software installation procedures for the 3 major system components of the Computer Integrated Manufacturing program known as GMAP (Geometric Modeling Applications Interface Program). These components are the System Translator, Schema Manager, and Model Access Software with Name Value Interface. GRA

N91-16595 British Broadcasting Corp., Kingswood (England). Engineering Div.
THE COMPUTER SIMULATION OF DIGITAL RECORDING SYSTEMS
C. H. Williams 1990 20 p
(BBC-RD-1990/14) Avail: Issuing Activity

Digital recording systems for television are becoming more widely used in the broadcasting industry. Traditionally, the design, evaluation and performance monitoring of such recorders has relied on conventional laboratory methods and equipment. An improved approach to these tasks based on the use of a computer to process electrical signals which have been captured from the circuits of the recording system under test is discussed. This computer simulation technique provides a clearer insight into the factors affecting the performance and reliability of digital recording systems, so that quantitative measures of confidence in them can be derived before valuable program material is finally stored. The simulation also provides a convenient framework for optimizing recording system design. Author

N91-16596*# Notre Dame Univ., IN. Dept. of Electrical Engineering.
REAL-TIME FILTERING AND DETECTION OF DYNAMICS FOR COMPRESSION OF HDTV Status Report, 11 Jun. 1990 - 10 Jan. 1991
Ken D. Sauer and Peter Bauer 1991 39 p
(Grant NAG3-1186)
(NASA-CR-187777; NAS 1.26:187777) Avail: NTIS HC/MF A03 CSCL 09B

The preprocessing of video sequences for data compressing is discussed. The end goal associated with this is a compression system for HDTV capable of transmitting perceptually lossless sequences at under one bit per pixel. Two subtopics were emphasized to prepare the video signal for more efficient coding: (1) nonlinear filtering to remove noise and shape the signal spectrum to take advantage of insensitivities of human viewers; and (2) segmentation of each frame into temporally dynamic/static regions for conditional frame replenishment. The latter technique operates best under the assumption that the sequence can be modelled as a superposition of active foreground and static background. The considerations were restricted to monochrome data, since it was expected to use the standard luminance/chrominance decomposition, which concentrates most of the bandwidth requirements in the luminance. Similar methods may be applied to the two chrominance signals. Author

N91-16597# Center for Mathematics and Computer Science, Amsterdam (Netherlands). Dept. of Computer Science.
INTRODUCTION TO ASPECTS OF OBJECT ORIENTED GRAPHICS
E. H. Blake Mar. 1990 21 p Sponsored by Netherlands Organization for the Advancement of Research
(CWI-CS-R9009; ETN-91-98422) Copyright Avail: NTIS HC/MF A03

Any attempt to deal with the complexity of interactive computer graphics should have a well founded and appropriate underlying abstraction. The object oriented paradigm is introduced and its suitability as a foundation for computer graphics is critically examined. It is found to be a good basis for graphics standards and particularly useful in dynamic graphics, that is, animation and interaction. The need for extensions to overcome some shortcomings, such as the lack of part-whole hierarchy, are discussed. Comparison is made with the other major abstraction for computer graphics: the functional approach. ESA

N91-16598# Technische Univ., Eindhoven (Netherlands). Dept. of Mathematics and Computing Science.
COLUMN REDUCTION OF POLYNOMIAL MATRICES: AN ITERATIVE ALGORITHM
W. H. L. Neven and C. Praagman Nov. 1989 22 p
(MEMO-COSOR-89-30; ETN-91-98428) Avail: NTIS HC/MF A03

The structure indices of polynomial matrices are studied. Results proved on the indices of the associated polynomials are presented. A minimal basis is calculated. An algorithm using the iterative step is described. ESA

N91-16599# Technische Univ., Delft (Netherlands). Faculty of Technical Mathematics and Informatics.
SOME GENERALIZATIONS OF THE CRISS-CROSS METHOD FOR QUADRATIC PROGRAMMING
E. Klafszky and T. Terlaky (Eoetvoes Lorand Univ., Budapest, Hungary) 1990 19 p Revised
(REPT-90-52; ISSN-0922-5641; ETN-91-98455) Copyright Avail: NTIS HC/MF A03

Three generalizations of the criss-cross method for quadratic programming are presented. Tucker's, Cottle's and Dantzig's principal pivoting is specialized as diagonal and exchange pivots for the linear complementarity problem obtained from a convex quadratic program. A finite criss-cross method, based on least index resolution, is constructed for solving LCP (Linear Complementarity Problems). In proving finiteness orthogonality properties of pivot tableaux and positive semidefiniteness of quadratic matrices are used. Some special cases and two further variants of the quadratic criss-cross method are discussed. If the matrix of the LCP has full rank, then a surprising simple algorithm follows, which coincides with Murty's Bard type schema in the P matrix case. ESA

N91-16600# Technische Univ., Delft (Netherlands). Faculty of Technical Mathematics and Informatics.
A LONG STEP BARRIER METHOD FOR CONVEX QUADRATIC PROGRAMMING
K. M. Anstreicher, D. denHertog, C. Roos, and T. Terlaky (Eoetvoes Lorand Univ., Budapest, Hungary) 1990 24 p
(REPT-90-53; ISSN-0922-5641; ETN-91-98456) Copyright Avail: NTIS HC/MF A03

A long step, logarithmic barrier function method for convex quadratic programming with linear equality constraints is proposed. After a reduction of the barrier parameter, a series of long steps along projected Newton directions are taken until the iterate is in the vicinity of the center associated with the current value of the barrier parameter. The total number of iterations is proved to be

O((square root of n)(L)) or O(nL) dependent on how the barrier parameter is updated. ESA

N91-16601*# National Aeronautics and Space Administration, Washington, DC.
SOFTWARE FOR AEROSPACE EDUCATION: A BIBLIOGRAPHY, 2ND EDITION
Gregory L. Vogt, Susan Kies Roth, and Malcom V. Phelps (Oklahoma State Univ., Stillwater.) 1990 89 p
(NASA-PED-106-ED-2; NAS 1.84:106-ED-2) Avail: NTIS HC/MF A05 CSCL 09B

This is the second aerospace education software bibliography to be published by the NASA Educational Technology Branch in Washington, DC. Unlike many software bibliographies, this bibliography does not evaluate and grade software according to its quality and value to the classroom, nor does it make any endorsements or warrant scientific accuracy. Rather, it describes software, its subject, approach, and technical details. This bibliography is intended as a convenience to educators. The specific software included represents replies to more than 300 queries to software producers for aerospace education programs. Author

N91-16602*# National Aeronautics and Space Administration. Goddard Space Flight Center, Greenbelt, MD.
ANNOTATED BIBLIOGRAPHY OF SOFTWARE ENGINEERING LABORATORY LITERATURE
Paula Groves and Jon Valett Nov. 1990 253 p
(NASA-TM-103415; NAS 1.15:103415; SEL-82-906) Avail: NTIS HC/MF A12 CSCL 09B

An annotated bibliography of technical papers, documents, and memorandums produced by or related to the Software Engineering Laboratory is given. More than 100 publications are summarized. These publications cover many areas of software engineering and range from research reports to software documentation. This document has been updated and reorganized substantially since the original version (SEL-82-006, November 1982). All materials have been grouped into eight general subject areas for easy reference: the Software Engineering Laboratory; the Software Engineering Laboratory-software development documents; software tools; software models; software measurement; technology evaluations; Ada technology; and data collection. Subject and author indexes further classify these documents by specific topic and individual author. Author

N91-16603# LabTek Corp., Woodbridge, CT.
DISTRIBUTED ISSUES FOR Ada REAL-TIME SYSTEMS Final Report
Thomas E. Griest 23 Jul. 1990 315 p
(Contract MDA903-87-C-0056)
(AD-A227852) Avail: NTIS HC/MF A14 CSCL 12/7

This work addresses an approach to reduce the complexity of distributed systems by extending the standard Ada tasking model to handle the distributed processing and by introducing a failure model for reliability issues. It uses software developed in a previous CECOM research project, the Border Defense System (BDS) distributed demonstration application, that addressed the performance benefits that could be gained by the distribution of real-time Ada systems. To achieve increased performance, a new approach to improving parallel execution was studied. The approach was to create a data structure consisting of an array of tasks and distribute the elements of the array across a set of processors. Performance benefits are then achieved as a function of the available processors. A simple failure model appropriate for a class of applications which can tolerate interruptions in service for up to one second was introduced. GRA

N91-16604# Carnegie-Mellon Univ., Pittsburgh, PA. Dept. of Electrical and Computer Engineering.
DECENTRALIZED REAL-TIME SCHEDULING Final Technical Report, Feb. 1989 - Feb. 1990
J. Duane Northcutt, Raymond K. Clark, David P. Maynard, and Jeffrey E. Trull Aug. 1990 246 p
(Contract F30602-88-D-0026; AF Proj. 5581)
(AD-A227856; RADC-TR-90-182) Avail: NTIS HC/MF A11 CSCL 12/5

This document describes experiments designed to evaluate the behavior and performance of various scheduling policies for the Alpha real-time distributed operating system. Alpha is an adaptable decentralized operating system being developed as a part of the Archons project's on-going research into real-time distribution systems. Timely completion of an application's computational activities is one of the most important functions of a real-time system. Therefore, the proper scheduling of those activities is of critical importance. The Alpha programming model provides simple mechanisms for an application to specify its timeliness requirements. The scheduler may consider this time constraint information when scheduling activities for execution. To gauge the effectiveness of Alpha as an operating system for real-time applications, an understanding of its scheduling facility is necessary. To this end, a study of the effects of various different scheduling policies was made. To evaluate these policies, a real-time application was created to serve as an experimental workload. The application was designed to simplify the modeling of tasks with a wide range of timeliness requirements and to provide a visual indication of scheduler performance. Alpha provides a clean well-defined interface between the scheduling subsystem and the kernal proper. GRA

N91-16605# Purdue Univ., West Lafayette, IN. Dept. of Computer Sciences.
VISUALIZATION OF SURFACES IN FOUR-DIMENSIONAL SPACE
Christoph M. Hoffmann and Jianhua Zhou Mar. 1990 39 p
(Contract N00014-90-J-1599; NSF CCR-86-19817; NSF DMC-88-07550)
(AD-A227858; CSD-TR-960; CER-90-12) Avail: NTIS HC/MF A03 CSCL 12/3

The authors discuss some issues of displaying two-dimensional surfaces in four-dimensional (4D) space, including the behavior of surface normals under projection, the silhouette points due to the projection, and methods for object orientation and projection center specification. We have implemented an interactive 4D display system on z-buffer based graphics workstations. Preliminary experiments show that such a 4D display system can give valuable insights into high-dimensional geometry. We present some pictures from the examples using high-dimensional geometry, offset curve tracing and collision detection problems, and explain some of the insights they convey. GRA

N91-16606# Rensselaer Polytechnic Inst., Troy, NY. Dept. of Computer Science.
EXPRESSING USER-DEFINED PARALLELISM IN EPL (EQUATIONAL PROGRAMMING LANGUAGE)
Can Ozturan Oct. 1990 69 p
(Contracts N00014-86-K-0442; DAAL03-90-G-0096; NSF CCR-86-13353; NSF CCR-89-20694)
(AD-A227875; RPI-TR-90-29) Avail: NTIS HC/MF A04 CSCL 12/5

EPL is a high level language which aims at producing efficient parallel code for a variety of architectures. EPL is an equational language and requires the computations to be expressed as systems of recurrent equations. This project describes two additions to EPL language which greatly simplifies the way user expresses parallelism. The first addition is that of a general purpose reduction operator called all. The second addition is the extension of the language to include annotations which the user can use to indicate parallelism at medium-grain level. The annotations are processed by the annotation preprocessor which has two functions. The first is determining a mapping of annotated processes onto a logical hierarchical tree structure which minimizes the total communication cost. We give an O(n2) heuristic algorithm to do this. The second function is to generate EPL code for each process. This part involves parallel scheduling of systems of recurrence equations and is beyond the scope of this project. We, however, discuss

the issues that should be addressed in the code generator part which is left for future implementation. GRA

N91-16607# San Diego State Univ., CA. Dept. of Electrical Engineering.
OPTIMIZATION OF A POWER TRANSIENT STABILITY PROGRAM ON A VECTOR SUPERCOMPUTER: THEORY AND APPLICATIONS M.S. Thesis
Gregg Francis Degen 18 Apr. 1990 133 p Sponsored by Army Military Personnel Center, Alexandria, VA
(AD-A227884) Avail: NTIS HC/MF A07 CSCL 12/6

Detailed simulations of large interconnected power distribution systems currently cannot be performed. Vector supercomputers have the capability to solve the great number of differential and non-linear simultaneous equations associated with the models, but programs have not been developed for them. This thesis investigates the optimization of a current power stability program installed on a Cray Y-MP vector supercomputer. Theory and models for power system stability are reviewed and an outline of the program is given. A discussion of vector supercomputer pipelining and the Cray Y-MP architecture are included. Programming constructs in FORTRAN which inhibit compiler optimization and vectorization are discussed, and program modification techniques to overcome these are presented. The modifications made to the power stability program are discussed and their effects on program execution time and output are presented. It is shown that significant speed up in program execution time can be achieved with no change in program output. GRA

N91-16608# Dynamics Research Corp., Andover, MA.
THE ASSISTANT FOR SPECIFYING THE QUALITY SOFTWARE (ASQS). VOLUME 1: OPERATIONAL CONCEPT DOCUMENT Final Technical Report, Mar. 1988 - Jan. 1990
Larry Kahn and Steve Keller Sep. 1990 96 p
(Contract F30602-87-D-0086; AF Proj. 2527)
(AD-A227893; RADC-TR-90-195-VOL-1) Avail: NTIS HC/MF A05 CSCL 12/5

The ASQS, a knowledge base software tool, assists software acquisition managers which specify software quality requirements. In the consultation mode, questions are presented to the acquisition manager in terms related to the mission area of interest. Answers are transformed by ASQS into tailored quantitative quality goals based on the thirteen software quality factors of the RADC software quality framework. The current version supports the Intelligence and Satellite mission areas. ASQS serves the purpose of transitioning the Software quality specification methodology found in the RADC final report RADC-TR-85-37, Vol. 2 (of three), Specification of Software Quality Attributes - Software Quality Specification Guidebook, into use in the DOD acquisition process. In so doing, it reduces the amount of time and the expertise required to specify meaningful software quality goals. It bridges the gap between software quality concepts and terminology and the system needs and terminology understood by the acquisition manager. GRA

N91-16609# Dynamics Research Corp., Andover, MA.
THE ASSISTANT FOR SPECIFYING THE QUALITY SOFTWARE (ASQS). VOLUME 2: USER'S MANUAL. VOLUME 2 Final Technical Report, Mar. 1988 - Jan. 1990
Larry Kahn and Steve Keller Sep. 1990 201 p
(Contract F30602-87-D-0086; AF Proj. 2527)
(AD-A227894; RADC-TR-90-195-VOL-2) Avail: NTIS HC/MF A10 CSCL 12/5

The ASOS, (The Assistant for Specifying the Quality of Software) a knowledge base software tool, assists software acquisition managers which specify software quality requirements. In the consultation mode, questions are presented to the acquisition manager in terms related to the mission area of interest. Answers are transformed by ASQS into tailored quantitative quality goals based on the thirteen software quality factors of RADC software quality framework. The current version supports the Intelligence and Satellite mission areas. ASQS serves the purpose of transitioning the software quality specification methodology found in the RADC final report RADC-TR-85-37, Vol. 2 (of three), Specification of Software Quality Attributes - Software Quality Specification Guidebook, into use in the DOD acquisition process. In so doing, it reduces the amount of time and the expertise required to specify meaningful software quality goals. It bridges the gap between software quality concepts and terminology and the system needs and terminology understood by the acquisition manager. GRA

N91-16610# Carnegie-Mellon Univ., Pittsburgh, PA. Software Engineering Inst.
KERNAL FACILITIES DEFINITION, KERNEL VERSION 3.0 Final Report
Judy Bamberger, Currie Colket, Robert Firth, Daniel Klein, and Roger VanScoy Dec. 1989 124 p
(Contract F19628-85-C-0003)
(AD-A228027; CMU/SEI-88-TR-16; ESD-88-TR-17) Avail: NTIS HC/MF A06 CSCL 12/5

This document defines the functionality of the Distributed Ada Real-Time Kernel (hereafter called the Kernel). The Kernel is being developed as one artifact of the Distributed Ada Real-Time Kernel Project (hereafter called the project). The goal of the Kernel is to support effectively the execution of the distributed Ada applications in an embedded computer environment. The Kernel provides user's with support for language functionality (i.e., the ability to execute Ada programs in a distributed, real-time environment); it does not provide support for language features (i.e., Ada tasking primitives). As a result, the Kernel specification places certain requirements (restrictions and conventions) on the Ada application programs that use the Kernel. These will become apparent to the reader as the definition of the Kernel is expounded. This document is divided into three parts: (1) Kernel Background describes the models on which the Kernel is based and outlines the scope of its capabilities; (2) Requirements describes the functionality and performance required of the Kernel; and (3) Kernel Primitives describes the mechanisms and primitive capabilities the Kernel provides to implement the requirements. GRA

N91-16611# Massachusetts Inst. of Tech., Cambridge. Lab. for Computer Science.
DISTRIBUTED ALGORITHM SIMULATION USING INPUT/OUTPUT AUTOMATA Ph.D. Thesis
Kenneth J. Goldman Sep. 1990 245 p
(Contracts N00014-83-K-0125; N00014-85-K-0168; N00014-89-J-1988; NSF CCR-86-11442)
(AD-A228113; MIT/LCS/TR-490) Avail: NTIS HC/MF A11 CSCL 12/5

This document presents the Spectrum Simulation System, a new research tool for the design and study of distributed algorithms. Based on the formal Input/Output automation model of Lynch and Tuttle, Spectrum allows one to express distributed algorithms as collections of I/O automata and simulate them directly in terms of the semantics of that model. This permits integration of algorithm specification, design, debugging, analysis, and proof of correctness within a single formal framework that is natural for describing distributed algorithms. Spectrum provides a language for expressing algorithms as I/O automata, a simulator for generating algorithm executions, and a graphics interface for constructing systems of automata and observing their executions. It is shown that the properties of the I/O automation model provide a solid foundation for algorithm development tools. For example, using I/O automation composition, Spectrum users may define composed types hierarchically, study simulations at varying levels of detail, and create specialized debugging and analysis devices. These devices, called spectators, are written in the Spectrum language just as any other system component, and can monitor algorithm executions for correctness and performance without interfering with the algorithm. GRA

N91-16612# New York Univ., New York. Inst. of Mathematical Sciences.
IMPLEMENTATION AND EXPERIMENTATION WITH MOTION PLANNING ALGORITHMS Annual Report, 1 Oct. 1989 - 30 Sep. 1990
Micha Sharir Sep. 1990 13 p
(Contract N00014-90-J-1284)
(AD-A228278) Avail: NTIS HC/MF A03 CSCL 12/9

The main charter of this contract is the implementation and experimentation with motion planning algorithms that emphasize the exact combinatorial and purely geometric approach. Motion planning is considered to be one of the major research areas in robotics, and is one of the main stages in the design and implementation of autonomous intelligent systems, which is an important long-range goal in robotics research. Motion planning is one of the basic capabilities that such a system must possess. In purely geometric terms, the simplest version of the problem can be stated as follows. The system is given complete information about the geometry of the environment in which it is to operate (and of its own structure), and has to process it so that, when commanded to move from its current position to some target position, it can determine whether it can do so without colliding with any of the obstacles around it, and if so plan (and execute) such a motion. There are many variants of the problem. A few of those are: motion planning in environments that are only partially known to the system, compliant motion planning that allows contact with obstacles, which might be unavoidable due to measurement errors, optimal motion planning, motion planning with kino-dynamics constraints, and motion planning amidst moving obstacles. GRA

N91-16613# Stanford Univ., CA. Dept. of Operations Research.
ANALYSIS OF PARALLEL, REPLICATED SIMULATIONS UNDER A COMPLETION TIME CONSTRAINT
Peter W. Glynn and Philip Heidelberger (International Business Machines Corp., Yorktown Heights, NY.) Feb. 1990 28 p Sponsored in part by IBM
(Contract DAAL03-88-K-0063)
(AD-A228292; SU-TR-56; ARO-25839.32-MA) Avail: NTIS HC/MF A03 CSCL 12/6

This paper analyzes properties associated with a simple yet effective way to exploit parallel processors in discrete event simulations: averaging the results of multiple, independent replications that are run, in parallel, on multiple processors. We focus on estimating expectations from terminating simulations, or steady state parameters from regenerative simulations. We assume that there is a Central Processing Unit time constraint, t, on each of P processors. Unless the replication lengths are bounded, one must be willing to simulate beyond any fixed, finite time t on at least some processors in order to always obtain a strongly consistent estimator (as the number of processors increases). We therefore consider simulation experiments in which t is viewed as either being a strict constraint, or a guideline, in which case simulation beyond time t is permitted. The statistical properties, including strong laws, central limit theorems, bias expansions and completion time distributions, of a variety of estimators obtainable from such an experiment are derived. We propose an unbiased estimator for a simple mean value. This estimator requires pre-selecting a fraction of the processors. Simulation beyond time t may be required on pre-selected processor, but only if no replications have yet been completed on that processor. GRA

N91-16614# California Univ., Berkeley. Dept. of Civil Engineering.
A SOFTWARE DEVELOPMENT SPECIFICATION FOR NONLINEAR STRUCTURAL ANALYSIS Final Report, Sep. 1987 - Oct. 1988
Joseph A. Landers Jul. 1990 27 p Sponsored by Office of Naval Technology, Arlington, VA and ACEL, Port Hueneme, CA
(AD-A228427; NCEL-CR-90-016) Avail: NTIS HC/MF A03 CSCL 12/5

A programming environment for structural engineering computations is described. Offering many advantages over the current state of technology in this area, the software system discussed here is highly flexible and portable. In addition to carrying out sophisticated calculations efficiently on today's engineering workstations, the environment can also exploit the power of larger computers by linking tasks over a local area network. Furthermore, the system is programmable and extensible. Finally, the software system may be integrated with existing programs such as finite element codes and mathematical libraries. GRA

N91-16615# Syracuse Univ., NY.
ALOPEX OPTIMIZATION ALGORITHM Final Technical Report, Jan. 1989 - Dec. 1989
E. Harth, T. Kalogeropoulos, W. Liu, and A. U. Joshi Sep. 1990 54 p
(Contract F30602-88-D-0027)
(AD-A228442; RADC-TR-90-205) Avail: NTIS HC/MF A04 CSCL 12/4

Results are provided of the investigation and application of the Alopex Algorithm to optimization problems. The Alopex Algorithm is a stochastic multiparameter optimization procedure. This algorithm addresses the two optimization problems of resource allocation and pattern recognition. The assigned tasks consist of two parts: recognition of 3-D objects given a 2-D projection, and optimal resource allocation. Both assignments involved application of the optimization algorithm Alopex which was developed by the principal investigators. Some 3-D objects were studied with a view toward identification of airplanes. A rapid aircraft identification system can be built based on the findings. For the second assignment, the problem of assigning in an optimal way a number of guns to targets was investigated. Alopex has been found to converge rapidly to optimal assignments. The performance was also compared of the Alopex algorithm with the widely used method of simulated annealing. Alopex was found to converge considerably faster in all examples tried. GRA

N91-16616# Electronics Research Lab., Adelaide (Australia). Communications Div.
XSHELL: A GENERAL PURPOSE EXPERT SYSTEM SHELL
Allan J. Mack May 1990 31 p
(AD-A228454; ERL-0509-RE; DODA-AR-005-997) Avail: NTIS HC/MF A03 CSCL 12/5

An expert system shell is a computer program which is ideally independent of the domain (subject) of application. A problem is represented by facts and rules which the shell processes as data. Although it may be large, the shell is a conventional procedural program. The shell described is the result of a study of existing shells and of the needs of the Intelligent Frequency Management System. The outcome is a comprehensive tool for the development, execution and maintenance of rule-based expert systems. Several unique features can ensure a high level of completeness, reliability and maintainability in the application. The degree of detail which follows is provided not only as a guide to users but also as a reference for the assessment of specification of other shells. This issue refers to XSHELL version 2.11. Expert systems usually divide the rules and facts into the domain, which describes the general case, and the context, which is the part that can vary from one problem to another. In XSHELL, facts and rules describe the problem domain. The assignment of certainties and values to the facts describes the context. The solution of problems is goal driven using a combination of backward and forward chaining. Each fact is described by a text. Associated with each fact is either a set of descriptive states each having a probability (certainty), or a numeric value (or array of values). The descriptive facts are referred to as being qualified and the numeric facts as quantified. GRA

N91-16617# IBM Federal Systems Div., Gaithersburg, MD.
PRACTICAL ASPECTS OF REPOSITORY OPERATIONS FOR THE SOFTWARE TECHNOLOGY FOR ADAPTABLE, RELIABLE SYSTEMS (STARS) PROGRAM Final Report
S. Kutoroff 10 Jan. 1990 32 p
(Contract F19628-88-D-0032)
(AD-A228455) Avail: NTIS HC/MF A03 CSCL 12/5

The operation is described of the STARS Repository computer

and the basis for the policies under which it operates. The STARS Repository acts as a focal point of the STARS (Software Technology for Adaptable Reliable Systems) program and supports many STARS activities. It stores all deliverable software and technical reports. It is also a means of communication amongst the prime contractors, the subcontractors, the consultants, and the contracting agency. Electronic mail is interchanged, other electronic documents are shared, software is developed, and software is shared and reused by the STARS contract participants using the STARS repository computer. GRA

N91-16618# Science Applications International Corp., Clearwater, FL. Software and Systems Integration Group.
BRIEFING DTD USER'S GUIDE FOR THE SOFTWARE TECHNOLOGY FOR ADAPTABLE, RELIABLE SYSTEMS (STARS) PROGRAM Final Report
S. Kutoroff 1 Jul. 1990 126 p
(Contract F19628-88-D-0032)
(AD-A228473; CDRL-1820) Avail: NTIS HC/MF A07 CSCL 12/5

SGML (Standard Generalized Markup Language) is an international standard for representing the elements and structure of electronically stored exit. SGML uses Document Type Definitions (DTD's) to unify the structure of various kinds of documents. Recommendations on style are made. GRA

N91-16619# IBM Federal Systems Div., Gaithersburg, MD.
DTD CREATION FOR THE SOFTWARE TECHNOLOGY FOR ADAPTABLE, RELIABLE SYSTEMS (STARS) PROGRAM Final Technical Report
S. Kutoroff 23 Jun. 1990 18 p
(Contract F19628-88-D-0032)
(AD-A228475; CDRL-1810) Avail: NTIS HC/MF A03 CSCL 12/5

Within the Software Technology for Adaptable Reliable Systems (STARS) there exists a need to exchange source code and documents between the prime contractors. Even within this program there are multiple hardware vendors, operating systems, and applications software. The problems experienced by the DoD in exchanging revisable documents are apparent within STARS. Part of the problem was addressed by the selection of the Standard Generalized Markup Language as the standard for document exchange. SGML defines a standard means to specify the organization and relationships between the elements of structured documents. SGML is intended to be used in the preparation of documents using descriptive markup to denote document elements. The Document Type Definition (DTD) defines the elements of a document and specifies the relationship of each element to other elements. The section on the history of electronic document production explains some of the reasons why descriptive markup is important and why SGML is the appropriate tool for use in the STARS program for document interchange. The DTDs as used in the STARS program as well as those used in other DoD programs are introduced. The features and rationale for the DTDs are discussed and the foundation for a STARS DTD is presented. GRA

N91-16620# Rochester Univ., NY. Dept. of Computer Science.
PENGUIN: A LANGUAGE FOR REACTIVE GRAPHICAL USER INTERFACES Ph.D. Thesis
Sue-Ken Yap Apr. 1990 123 p
(Contract N00014-82-K-0193; NSF CCR-83-20136)
(AD-A228580) Avail: NTIS HC/MF A06 CSCL 12/5

Programming environment for graphical user interfaces (PENGUIN) is a computer language that supports grammar-based specification of control flow in event-driven graphical programs. The PENGUIN model of intercomponent connection extends and subsumes the older Seeheim model of UIMS design, allowing large programs to be constructed as co-operating components. Traditional approaches to graphical program design have treated the user interface code as something that can be written independently of the application. This dissertation argues that the reactive nature of graphical programs should be taken into account from the beginning of design, that a graphical program be composed as a collection of modules whose input behavior is specified, and that modules be grouped into separately-compiled components along lines of clear division of labor and responsibility for resources. Such partitions result in components that are more likely to be reusable. Our experiences indicate that the use of PENQUIN can reduce the volume of user interface code by a factor of two to three and result in code which is clearer than functionally equivalent code using traditional control structures. Uniform handling of I/O and signals as PENQUIN events leads to programs that are more portable across systems. PENQUIN encourages the construction of reactive modules which are clearer than modules that use polling or a mixed approach. GRA

N91-16621# Ada Joint Program Office, Arlington, VA.
Ada COMPILER VALIDATION PROCEDURES, VERSION 2.1 Executive Summary
Aug. 1990 29 p
(AD-A228614) Avail: NTIS HC/MF A03 CSCL 12/5

The Ada certification body consists of the Ada Joint Program Office, (AJPO), the Ada Validation Organization (AVO), the ACVC Maintenance Organization (AMO), and the Ada Validation Facilities (AVFs). The AJPO, a component of the Department of Defense, establishes the policies of the Ada certification system issues validation certificates for AVF tested Ada implementations and registers Ada implementations that are untested by an AVF. The AVO, the Institute for Defense Analyses, provides the technical and administrative support required to operate the Ada certification system. The AMO, Wright-Patterson Air Force Base, provides the technical and administrative support required to supply the Ada Compiler Validation Capability (ACVC) for use in the operation of the Ada certification system. There are five AVFs charted by the AJPO to conduct validation (see Section 3 and Appendix E). The Ada certification body operates in conjunction with the U.S. Department of Commerce which has the responsibility for establishing and maintaining a certification system for the Federal Information Processing Standards (FIPS). GRA

N91-16622# North Carolina Univ., Chapel Hill. Dept. of Computer Science.
DISPLAYING ALPHANUMERIC CHARACTERS ON PIXEL-PLANES 5
Andrei State Dec. 1989 12 p
(Contracts N00014-86-K-0680; F33615-89-C-1848; NSF DCI-86-01152; DARPA Order 6090)
(AD-A228616; TR89-049) Avail: NTIS HC/MF A03 CSCL 12/1

The Pixel-Planes 5 system (Fuchs89) is an implementation of a high-performance graphics architecture design primarily for high-speed rendering of 3 dimensional data from surface or volumetric databases. However, particular applications may require the additional display of alphanumeric text, either as superimposed (overlayed) alphanumeric text, or as true 3 dimensional text capable of interacting with other 3 dimensional elements (shading, hiding/intersecting, etc.). Different approaches that have been proposed and partially implemented so far will be described and compared. GRA

N91-16623# Illinois Univ., Urbana-Champaign. Applied Computation Theory Group.
AN O(LOG n) TIME COMMON CRCW PRAM ALGORITHM FOR MINIMUM SPANNING TREE
Michael M. Wu Oct. 1990 12 p
(Contract N00014-85-K-0570)
(AD-A228740; UILU-ENG-90-2250; ACT-114) Avail: NTIS HC/MF A03 CSCL 12/5

The minimum spanning tree problem is an important problem of combinatorial optimization. Some practical applications of MST's include the design of computer, communication, and transportation networks. An algorithm is presented for finding the minimum spanning tree of a graph with n vertices and m edges on a common concurrent-read concurrent-write (CRCW) parallel random access machine (PRAM) using m+n(exp 1+2epsilon) processors and

O(m+n)(exp 1+epsilon) space in O(log n) time, where epsilon is a constant such that 0 is less than epsilon and epsilon is less than or equal to 1/2. GRA

N91-16624# Massachusetts Inst. of Tech., Cambridge. Artificial Intelligence Lab.
SUPPORTING REUSE AND EVOLUTION IN SOFTWARE DESIGN
Yang M. Tan Oct. 1990 106 p
(Contract N00014-85-K-0124)
(AD-A228782; MIT-AI-M-1256) Avail: NTIS HC/MF A06 CSCL 12/5

Program design is an area of programming that can benefit significantly from machine-mediated assistance. A proposed tool, called the Design Apprentice (DA), can assist a programmer in the detailed design of programs. The DA supports software reuse through a library of commonly-used algorithmic fragments, or cliches, that codifies standard programming. The cliche library enables the programmer to describe the design of a program concisely. The DA can detect some kinds of inconsistencies and incompleteness in program descriptions. It automates detailed design by automatically selecting appropriate algorithms and data structures. It supports the evolution of program designs by keeping explicit dependencies between the design decisions made. These capabilities of the DA are underlaid by a model of programming, called programming by successive elaboration, which mimics the way programmers interact. Programming by successive elaboration is characterized by the use of breadth-first exposition of layered program descriptions and the successive modifications of descriptions. A scenario is presented to illustrate the concept of the DA. Techniques for automating the detailed design process are described. A framework is given in which designs are incrementally augmented and modified by a succession of design steps. A library of cliches and a suite of design steps needed to support the scenario are presented. GRA

N91-16625# Stanford Univ., CA. Dept. of Computer Science.
MATRIX ALGORITHMS IN SIGNAL PROCESSING Final Report, 18 May 1987 - 17 May 1990
Gene H. Golub Aug. 1990 7 p
(Contract DAAL03-87-K-0095)
(AD-A228851; ARO-25323.6-MA-SDI) Avail: NTIS HC/MF A02 CSCL 09/1

A final report describes the results obtained under the contract title, Matrix Algorithms in Signal Processing. A number of algorithms are described which have the properties that they are numerically stable, robust, and useful. A basic tool for many of these algorithms is the Lanczos class of algorithms. These algorithms have the virtue that they can be used in a dynamic environment and require little storage. Abstracts of several of the reports are included. GRA

N91-16626# Carnegie-Mellon Univ., Pittsburgh, PA. Graduate School of Industrial Administration.
LINEAR-TIME SEPARATION ALGORITHMS FOR THE THREE-INDEX ASSIGNMENT POLYTOPE
Liqun Qi (New South Wales Univ., Sydney, Australia) and Egon Balas Sep. 1990 19 p Sponsored in part by Australian Research Council
(Contract N00014-85-K-0198; NSF DDM-89-01495)
(AD-A228854; MSRR-562) Avail: NTIS HC/MF A03 CSCL 12/4

Balas and Saltzman identified several classes of facet inducing inequalities for the three-index assignment polytope, and gave O(n(exp 4)) separations algorithms for two of them. We give O(n cubed) separation algorithms for these two classes of facets, and also for a third class. Since the three-index assignment problem has n cubed variables. These algorithms are linear-time and their complexity is best possible. GRA

N91-16627*# Clemson Univ., SC. Dept. of Computer Science.
TOWARDS CONSERVATIVE RELIABILITY PREDICTIONS FOR REAL-TIME SOFTWARE Final Report
Robert Geist, A. Jefferson Offutt, and Frederick C. Harris, Jr. 1991 20 p
(Grant NAG1-1024)
(NASA-CR-187863; NAS 1.26:187863) Avail: NTIS HC/MF A03 CSCL 09B

A method for obtaining numerical estimates of the reliability of N-version, real-time software is proposed. An extended stochastic Petri net is used to represent the synchronization structure of N versions of the software, where dependencies among versions are modeled through correlated sampling of module execution times. The distributions of execution times are derived through an automated generation of test cases that is based on mutation analysis. Since these test cases are designed to reveal software errors, the associated execution times are likely to provide a worst case scenario. Experimental results using specifications for NASA's planetary lander control software suggest that mutation-based testing could hold greater potential for reliability enhancement than the desirable but perhaps unachievable goal of independence among N versions. Author

N91-16628# Nationaal Inst. voor Kernfysica en Hoge Energiefysica, Amsterdam (Netherlands). Afd. DIGEL.
PROGRAMMABLE PSEUDORANDOM DETECTOR PULSE PATTERN GENERATOR Thesis - Hogeschool Alkmaar [PROGRAMMEERBARE PSEUDO RANDOM DETECTOR PLUS PATROON GENERATOR]
Ronald vanderPutten 1990 68 p In DUTCH
(ETN-91-98321) Avail: NTIS HC/MF A04

The design and realization of the digital part of a programmable pseudorandom detector pulse pattern generator for the electron accelerator Medium Energy Accelerator (MEA) are discussed. For the design and realization F-TTL and high speed special purpose integrated circuits, especially Programmable Logics (PAL's) were used. The design possibilities offered by the software for PAL programming were utilized as much as possible. Counters, registers and a state machine with extensive control possibilities were designed. An advanced eight channel pulse generator, controlled via a VME system bus, was realized. The generator has a 16 MHz internal clock generator. The pulse generation instant can be adjusted in 250 ps steps, and 2000 different time windows can be stored to generate a pattern. ESA

N91-16629# Laboratoire d'Automatique et d'Analyse des Systemes, Toulouse (France).
VECTORIAL AND PARALLEL ALGORITHMS IN DYNAMIC PROGRAMMING FOR OPTIMAL CONTROL PROBLEMS Ph.D. Thesis - Toulouse Univ.
Jorge DantasdeMelo 1990 125 p In FRENCH; ENGLISH summary Sponsored by Instituto de Pesquisas Espaciais, Brazil and Universidade Federal do Rio Grande do Norte, Natal, Brazil
(LAAS-90256; ETN-91-98542) Avail: NTIS HC/MF A06

The numerical resolution of optimal control problems relying on dynamic programming methods is discussed. The approach proposed makes use of a new type of computer architecture, namely parallel machines capable of handling in a concurrent way, the various independent parts of a same program. Some methodological aspects of the parallelism are analyzed: the expression of concurrence in the algorithms and the complexity in its implementation. Following the analysis of some approaches in dynamic programming found in the current literature, different possibilities in the exploration of parallelism are presented, relying on domain decomposition methods and on synchronism relaxation. Under some previously defined conditions, an original parallel algorithm is deduced. Such algorithms permit reduction in the space complexity of the method. The implementation of this kind of algorithm in MIMD machines (in particular on a CRAY-2 computer) is studied. A general tool for the resolution of discrete-time optimal control problems by means of dynamic programming is developed and tested for various applications problems, emphasizing the interest of using the parallelism for the resolution of some complex problems in the area of automatic control. ESA

N91-16630# Messerschmitt-Boelkow-Blohm G.m.b.H., Munich (Germany, F.R.). Hubschrauber und Flugzeuge.
THERMOPT: AN OPTIMIZER FOR ESATAN MODELS
Wolfgang Hartzheim and Martin Sander 14 Aug. 1990 59 p (MBB/FW522/S/PUB/427; ETN-91-98550) Copyright Avail: NTIS HC/MF A04

A computer program for optimization with an external analysis program is presented. THERMOPT is a FORTRAN-77 code and is divided into three main parts: the structural analysis, optimization model, and the optimization methods. The function to minimize is real valued, scalar, nonlinear and twice continuously differentiable. Two optimization algorithms were implemented, the sequential programming method and the method of multipliers, which need gradient information which is numerically obtained. ESA

N91-16631# Technische Univ., Delft (Netherlands).
LOW-LEVEL IMAGE PROCESSING ARCHITECTURES COMPARED FOR SOME NON-LINEAR RECURSIVE NEIGHBORHOOD OPERATIONS Ph.D. Thesis
Erwin Ronald Komen 29 Nov. 1990 192 p Sponsored by Netherlands Foundation for Computer Science, and Netherlands Organization for Scientific Research
(ISBN-90-9003713-6; ETN-91-98569) Avail: NTIS HC/MF A09

A method is developed for the comparison of computer architectures for image processing designed to work for low level operations, e.g., image to image transformations. A division is made between three different groups: square processor arrays, linear processor arrays, and pipelines. The development of a theoretical framework for recursive neighborhood operations is initiated. The use of these operations for image processing is demonstrated. It is shown how they can be implemented on the architecture groups. The performance of the architecture groups is investigated for six nonlinear recursive neighborhood operations. ESA

62 COMPUTER SYSTEMS

Includes computer networks and special application computer systems.

N91-16632# Argonne National Lab., IL. High Energy Physics Div.
WAKEFIELD CALCULATIONS ON PARALLEL COMPUTERS
Paul Schoessow 1990 10 p Presented at the Accelerator Computer Code Meeting, Los Alamos, NM, 22-25 Jan. 1990
(Contract W-31-109-eng-38)
(DE90-009712; ANL-HEP-CP-90-05; CONF-900163-8) Avail: NTIS HC/MF A02

The use of parallelism in the solution of wakefield problems is illustrated for two different computer architectures (SIMD and MIMD). Results are given for finite difference codes which have been implemented on a connection machine and an Alliant FX/8 and which are used to compute wakefields in dielectric loaded structures. Benchmarks on code performance are presented for both cases. DOE

N91-16633# Lawrence Livermore National Lab., CA. National Magnetic Fusion Energy Computer Center.
MASSIVELY PARALLEL FOKKER-PLANCK CALCULATIONS
Arthur A. Mirin 1990 8 p Presented at the 5th Distributed Memory Computing Conference, Charleston, SC, 9-12 Apr. 1990
(Contract W-7405-eng-48)
(DE90-010691; UCRL-102438; CONF-9004159-5) Avail: NTIS HC/MF A02

The Fokker-Planck package FPPAC, which solves the complete nonlinear multispecies Fokker-Planck collision operator for a plasma in two-dimensional velocity space, has been rewritten for the Connection Machine 2 (CM2). This has involved allocation of variables either to the front end or the CM2, minimization of data flow, and replacement of Cray-optimized algorithms with ones suitable for a massively parallel architecture. Coding has been done utilizing Connection Machine FORTRAN. Calculations have been carried out on various connection machines throughout the country. Results and timings on these machines have been compared to each other and to those on the static memory Cray-2 at the National Magnetic Fusion Energy Computer Center. For large problem size, the CM2 is found to be cost-efficient. DOE

N91-16634# Pennsylvania State Univ., University Park.
REAL-TIME SYSTEM SPECIFICATION AND VERIFICATION Annual Report, 1 Oct. 1989 - 30 Sep. 1990
K. T. Narayana 30 Sep. 1990 8 p Submitted for publication
(Contract N00014-89-J-1171)
(AD-A227682) Avail: NTIS HC/MF A02 CSCL 12/6

A major revision was made to the formal semantic model for real-time concurrency under limited parallelism. The revision was required to simplify the model. The basic elements of the revision dealt with observing processes against the local clocks of processors and relating those observations to the global clock. Several notational simplifications have been brought forth in the formal specifications of the dialog system. The specification notation is made to conform to the latest Z-Language Standard. A part of the work dealing with the Formal Specification of a Look Manager has been published in the special issue on formal methods of the IEEE Transactions on Software Engineering, Sep. 1990. Another part dealing with the Invariant Properties in the Dialog System has appeared in the Proceedings of the ACM Workshop on Formal Methods, May 1990. The specification of the design of the complete dialog system is currently going through a second iteration. Meanwhile, a lot of effort was spent in implementing a syntax directed incremental specification environment for the Z-notation. The environment interfaces nicely with the X-Window system. Currently type inference systems are being integrated to the incremental editing environment. GRA

N91-16635# Naval Research Lab., Washington, DC. Integrated Warfare Technology Branch.
PARALLEL ACCESS MAIN MEMORY (PAMM) USER'S MANUAL, VERSION 1.0 Final Report, Jun. 1987 - Mar. 1990
Todd J. Rosenau and Mona El-Kadi (Locus, Inc., Alexandria, VA.) 15 Sep. 1990 42 p
(AD-A227744; NRL-9267) Avail: NTIS HC/MF A03 CSCL 12/5

The structure and use of the parallel access main memory (PAMM) data base management system (DBMS) interface for C programmers is described. PAMM is a high-speed, high-throughout DBMS that allows concurrent access to data stored in a distributed data structure across all of the processors in a general-purpose, multiprocessor computer. Concurrency is achieved by allowing several tasks executing on different processors to access the database at the same time with a minimum of locking. This allows an application's task to proceed with a minimum of delay. Its high speed is achieved by keeping most of the data and index structures resident in main memory, thus reducing the number of disk accesses performed. The data structure and storage method for the DBMS are a multidirectory hashing, distributed lock system that Sakti Pramanik and Charles Severance at Michigan State University developed for the Naval Research Laboratory (NRL). PAMM has been implemented on a 32-processor BBN Butterfly GP1000 at NRL. GRA

N91-16636# Stanford Univ., CA. Dept. of Operations Research.
EXPERIMENTS WITH INITIAL TRANSIENT DELETION FOR PARALLEL, REPLICATED STEADY-STATE SIMULATIONS
Peter W. Glynn and Philip Heidelberger (International Business Machines Corp., Yorktown Heights, NY.) May 1990 26 p Sponsored by IBM
(Contract DAAL03-88-K-0063)
(AD-A227879; SU-TR-59; ARO-25839.34-MA) Avail: NTIS HC/MF A03 CSCL 12/4

A simple and effective way to exploit parallel processors in discrete event simulations is to run multiple independent replications, in parallel, on multiple processors and to average the results at the end of the runs. We call this the method of parallel replications. This paper is concerned with using the method of

parallel replications for estimating steady-state performance measures. We report on the results of queueing estimators that can be formed using this method. The theoretical asymptotic properties of these estimators were determined in Glynn and Heidelberger (1989a and 1989b). Both the theory and the experimental results reported here strongly indicate that a nonstandard (in the context of steady-state simulation), yet easy to apply, estimator procedure is required on highly parallel machines. This nonstandard estimator is a ratio estimator. The experiments also show that use of the ratio estimator is advantageous even on machines with only a moderate degree of parallelism. GRA

N91-16637# Navy Personnel Research and Development Center, San Diego, CA.
A COMPUTER-BASED INSTRUCTIONAL SUPPORT NETWORK: DESIGN, DEVELOPMENT, AND EVALUATION Interim Technical Report
Henry Simpson and H. Lauren Pugh Sep. 1990 47 p Sponsored by Office of Naval Technology, Arlington, VA
(AD-A227922; NPRDC-TR-90-6) Avail: NTIS HC/MF A03 CSCL 12/7

The objective of the work was to design, develop, and evaluate an experimental, computer-based Instructional Support Network (ISN) consisting of an electronic communication network linking students to instructional resources such as instructors and instructional materials. A key element of the ISN concept was to provide very simple, easy to use workstations for instructor and students, enabling effective system use with minimal training and technical support. Without outside support, users were successfully able to set up and operate prototype workstations in less than two hours. During a field test, the ISN was used to link continuing education calculus students with a tutor at the Naval Postgraduate School. The majority ISN messages during this test were administrative (72.9 percent), 17.3 percent were technical, and 9.8 percent were motivational. Students initiated 40.9 percent of messages, and the tutor initiated the remainder. Some evidence shows that use of the ISN reduced student attrition and helped students with weak mathematics background. GRA

N91-16638# Texas A&M Univ., College Station. Dept. of Computer Science.
HORIZONTAL FAULT TOLERANCE IN A FULLY DISTRIBUTED LOOSELY COUPLED ENVIRONMENT Ph.D. Thesis
Peter Schiavi Dec. 1990 351 p Sponsored by AFIT, Wright-Patterson AFB, OH
(AD-A227972; AFIT/CI/CIA-90-030D) Avail: NTIS HC/MF A16 CSCL 12/5

The increasing use of local area networks to divide up the processing power once allocated to a single central processor has a side benefit which allows for the implementation of levels of fault tolerance at minimal cost. With a central processor, hardware replication is mandatory to continue processing in the face of hardware failures. Otherwise, processing must generally halt for a period of hardware repair. A local area network already contains replicated hardware, along with software to support communications over links connecting the individual nodes. The existence of duplicated hardware, and independent processing ability within each node, allows for a concentration on software support for fault tolerance. Hardware replication can be limited to such areas as network topologies which employ multiple links among the nodes. This research concentrates on software approaches to fault tolerance in a (loosely coupled) network environment. Current approaches are studied. These turn out to emphasize special purpose languages and operating systems designed to allow for transparent distribution of tasks amongst the nodes. The failure scenarios under which faults will be masked varies widely. Specifically, this research develops a set of language and operating system protocols to implement a level of fault tolerance. This Fault Tolerant Monitor (FTM) system is layered above the operating system. GRA

N91-16639*# Pathology Associates, Inc., Frederick, MD.
RESEARCH PATHOLOGY AND SPECIAL TECHNIQUES Annual Report, 15 May 1989 - 14 May 1990
William E. Hall 14 Jun. 1990 13 p
(Contract NAG2-593; MDA972-88-C-0024; DA Proj. 3M2-63763-D-807)
(NASA-CR-187828; NAS 1.26:187828; AD-A228256) Avail: NTIS HC/MF A03 CSCL 06/16

Immunoperoxidase procedures using the ABC and/or PAP methods have been completely developed for CCHF (KFD, RSSE) and Oropouche viruses, and partially developed for tularemia. Extensive support was provided for continuation fo the work accomplished in previous years especially Ebolavirus in the only known outbreak in the United States, and in the dengue outbreak which occurred in Venezuela in late 1989 and early 1990. As a result of the latter, PAHO has requested that USAMRIID develop a workship on these techniques for South American pathologists. The workshop is scheduled for October 1990. A training program and additional laboratory space has been established for performing the routine work of the Institute. A military technician is working in the Immunopathology Laboratory full-time on the Ebola project; it is anticipated that technical personnel from PAI will need to continue at USAMRIID on a full-time basis. Collaboration with other Institute investigators from various Divisions has taken place on a routine basis. An adequate bank of resource materials has been archived to include animal tissues containing virus, adequate reagents, and aliquots of antibodies. Tissue preparation for immunoelectron microscopy has been completed. Work with the molecular probes has begun. GRA

N91-16640# Massachusetts Inst. of Tech., Cambridge. Artificial Intelligence Lab.
PI: A PARALLEL ARCHITECTURE INTERFACE FOR MULTI-MODEL EXECUTION Ph.D. Thesis
Donald Scott Wills Jul. 1990 199 p Revised
(Contracts N00014-88-K-0738; N00014-87-K-0825; N00014-85-K-0124)
(AD-A228345; AI-TR-1245) Avail: NTIS HC/MF A09 CSCL 12/5

Existing parallel architectures are constructed monolithically, with no well defined boundaries separating model and machine issues. This makes it difficult to evaluate the effect of a single component of an architecture, or compare it with the corresponding components of other architectures. Machine hardware is specialized to support a single programming model, even though similar but more general mechanisms could support a variety of models. Often details of an implementation become visible in the programming environment, restricting future implementation improvements because of compatibility. The lack of an interface between model and machine issues also complicates the translation of a machine improvement into a performance improvement for model applications. This thesis defines Pi, a parallel architecture interface that separates model and machine issues, allowing them to be addressed independently. This provides greater flexibility for both the model and machine builder. Pi addresses a set of common parallel model requirements including low latency communication, fast task switching, low cost synchronization, efficient storage management, the ability to exploit locality, and efficient support for sequential code. Since Pi provides generic parallel operations, it can efficiently support many parallel programming models including hybrids of existing models. GRA

63 CYBERNETICS

Includes feedback and control theory, artificial intelligence, robotics and expert systems.

For related information see also *54 Man/System Technology and Life Support.*

N91-16641# Argonne National Lab., IL. Mathematics and Computer Science Div.

SKOLEM FUNCTIONS AND EQUALITY IN AUTOMATED DEDUCTION

William McCune 6 Feb. 1990 14 p Presented at the AAAI 1990 8th National Conference on Artificial Intelligence, Boston, MA, 29 Jul. - 3 Aug. 1990

(Contract W-31-109-eng-38)

(DE90-009703; CONF-900793-1) Avail: NTIS HC/MF A03

We present a strategy for restricting the application of the inference rule paramodulation. The strategy applies to problems in first-order logic with equality and is designed to prevent paramodulation into subterms of Skolem expressions. A weak completeness result is presented (the functional reflexive axioms are assumed). Experimental results on problems in set theory, combinatory logic, Tarski geometry, and algebra show that the strategy can be useful when searching for refutations and when applying Knuth-Bendix completion. The emphasis of the paper is on the effectiveness of the strategy rather than on its completeness. DOE

N91-16642# Los Alamos National Lab., NM.

ARTIFICIAL INTELLIGENCE TECHNOLOGIES APPLIED TO TERRAIN ANALYSIS

J. C. Wright (Army Training and Doctrine Command, Fort Leavenworth, KS.) and D. R. Powell 1990 16 p Presented at the 2nd French/US Conference on Analysis Techniques, Paris, France, 4-5 Jun. 1990

(Contract W-7405-eng-36)

(DE90-011985; LA-UR-90-1747; CONF-9006189-1) Avail: NTIS HC/MF A03

The U.S. Army Training and Doctrine Command is currently developing, in cooperation with Los Alamos National Laboratory, a Corps level combat simulation to support military analytical studies. This model emphasizes high resolution modeling of the command and control processes, with particular attention to architectural considerations that enable extension of the model. A planned future extension is the inclusion of a computer based planning capability for command echelons that can be dynamically invoked during the execution of the model. Command and control is the process through which the activities of military forces are directed, coordinated, and controlled to achieve the stated mission. To perform command and control the commander must understand the mission, perform terrain analysis, understand his own situation and capabilities as well as the enemy situation and his probable actions. To support computer based planning, data structures must be available to support the computer's ability to understand the mission, terrain, own capabilities, and enemy situation. The availability of digitized terrain makes it feasible to apply artificial intelligence technologies to emulate the terrain analysis process, producing data structures for uses in planning. DOE

N91-16643# SRI International Corp., Menlo Park, CA. Artificial Intelligence Center.

AN EVOLUTIONARY APPROACH TO DESIGNING NEURAL NETWORKS Annual Report No. 1

Stephen Barnard and Aviv Bergman Sep. 1990 25 p

(Contract F49620-89-K-0005; SRI Proj. ECU-7929)

(AD-A228874) Avail: NTIS HC/MF A03 CSCL 12/9

One of the most interesting properties of neural networks is their ability to learn appropriate behavior by being trained on examples. Established learning algorithms, which typically work by minimizing error through backpropagation in weight space, tend to get stuck in local optima: a tendency typical of gradient-descent methods applied to nonconvex objective functions. Therefore, for problems of nontrivial complexity these systems must be handcrafted to a significant degree, but the distributed nature of neural network representations make this handcrafting difficult. We are investigating an evolutionary approach to learning what will avoid this problem. This approach simulates a variable population of networks which, through processes of mutation, combination, selection, and differential reproduction, converge to a group of networks well suited to solving the task at hand. The important components of the approach are a genetic language for coding a large variety of networks, a procedure for constructing networks from these genetic codes, a nondeterministic process for mutating and combining genetic codes, and a function that measures the overall fitness of networks in the context fo the task at hand. We use a connection machine to exploit the inherent parallelism in the simulations. GRA

N91-16644# Technische Univ., Eindhoven (Netherlands).

IDENTIFICATION OF NON-LINEAR MECHANICAL SYSTEMS FOR CONTROL APPLICATION Ph.D. Thesis

Marinus Jacobus Gera vandeMolengraft 1990 114 p

(ISBN-90-9003596-6; ETN-91-98479) Avail: NTIS HC/MF A06

Experimentally obtained data are used to determine unknown parameters in a mathematical model of the mechanical system so that the model provides a suitable basis for controller design. The method was based on the mathematical minimization of a quadratic function, in which the model residuals were weighted with consideration of their interrelationships. The method determined estimates parameters, positions, velocities, accelerations and inputs of the system. The optimal estimation problem is shown to be similar to the optimal control problem, that allows the development of new estimation methods, such as the sliding surface filter. The method was applied to an experimental system whose unknown parameters were related to inertia, friction and elastic deformation. A global identification of the system is shown to lead to a useful description of the system. ESA

N91-16645# Laboratoire d'Automatique et d'Analyse des Systemes, Toulouse (France).

IMPLEMENTATION AND SIMULATION OF THE MANUFACTURING SYSTEMS CONTROL COORDINATION LEVEL: A MIXED APPROACH OF PETRI NETS AND RULE-BASED SYSTEMS Ph.D. Thesis - Toulouse Univ.

Babou Bako 1990 146 p In FRENCH; ENGLISH summary

(LAAS-90355; ETN-91-98592) Avail: NTIS HC/MF A07

A simultaneous utilization of artificial intelligence and petri nets techniques is presented. The main classes of high level petri nets and the possibilities to include time in the models were examined and compared. For the implementation of rule based systems controlled by petri nets, the petri net tokens player techniques were simultaneously used with the production rules compilation techniques. A conservative distributed simulation approach was developed and the example of a manufacturing system was given. ESA

64 NUMERICAL ANALYSIS

Includes iteration, difference equations, and numerical approximation.

N91-16646# New York Univ., New York. Inst. of Mathematical Sciences.

LIMIT BEHAVIORS OF APPROXIMATE SOLUTIONS TO CONSERVATION LAWS

Gui-Quiang Chen (Chicago Univ., IL.) 1989 27 p Presented at the Workshop on Multi-Dimensional Hyperbolic Problems and Computations, Minneapolis, MN 3-14 Apr. 1989 Sponsored in part by CYNSF

(Contract W-31-109-eng-38; NSF DMS-85-0403)

(DE90-010069; CONF-8904308-2) Avail: NTIS HC/MF A03

Limit behaviors of approximate solutions to hyperbolic systems of conservation laws were studied. Several mathematical compactness theories and their roles in this direction are described. Some recent and ongoing developments in this direction are reviewed and analyzed. DOE

N91-16647# Sandia National Labs., Albuquerque, NM.
LINEAR ALGEBRA FOR DENSE MATRICES ON A HYPERCUBE
Mark P. Sears 1990 4 p Presented at the 5th Distributed Memory Computing Conference, Charleston, SC, 9-12 Apr. 1990
(Contract DE-AC04-76DP-00789)
(DE90-010533; SAND-89-2930C; CONF-9004159-6) Avail: NTIS HC/MF A01

A set of routines has been written for dense matrix operations optimized for the NCUBE/6400 parallel processor. This work was motivated by a Sandia effort to parallelize certain electronic structure calculations. Routines are included for matrix transpose, multiply, Cholesky decomposition, triangular inversion, and Householder tridiagonalization. The library is written in C and is callable from FORTRAN. Matrices up to order 1600 can be handled on 128 processors. For each operation, the algorithm used is presented along with typical timings and estimates of performance. Performance for order 1600 on 128 processors varies from 42 MFLOPs (Householder tridiagonalization, triangular inverse) up to 126 MFLOPs (matrix multiply). We also present performance results for communications and basic linear algebra operations (saxpy and dot products). DOE

N91-16648# Ohio State Univ., Columbus. Dept. of Physics.
SOLVABLE TWO-DIMENSIONAL SUPERSYMMETRIC MODELS AND THE SUPERSYMMETRIC VIRASORO ALGEBRA
K. Tanaka 1990 12 p
(Contracts DE-AC02-76ER-01545; EY-75-C-02-141500)
(DE90-012140; DOE/ER-01545/439) Avail: NTIS HC/MF A03

The simplest extension of a variety of solvable 2 dimensional models to supersymmetric models is obtained and classical solutions are discussed. It is found that these supersymmetric models are closely related. DOE

N91-16649# Naval Underwater Systems Center, New London, CT.
TWO-DIMENSIONAL CONVOLUTIONS, CORRELATIONS, AND FOURIER TRANSFORMS OF COMBINATIONS OF WIGNER DISTRIBUTION FUNCTIONS AND COMPLEX AMBIGUITY FUNCTIONS
Albert H. Nuttall 6 Aug. 1990 58 p Sponsored by ONR, Arlington, VA
(AD-A226852; NUSC-TR-8759) Avail: NTIS HC/MF A04 CSCL 12/3

A number of new two-dimensional Fourier transforms of combinations of cross Wigner distribution functions, W, of convolution form or correlation form are derived. In addition, similar relations are obtained for combinations of cross complex ambiguity functions, X. Their great generality subsumes most of the already known available properties, such as: the volume constraint of magnitude-squared ambiguity functions; the positivity of the convolution of two Wigner distribution functions; and Moyal's theorem. GRA

N91-16650# Tennessee State Univ., Nashville. Dept. of Psychology.
VALIDITY STUDY IN MULTIDIMENSIONAL LATENT SPACE AND EFFICIENT COMPUTERIZED ADAPTIVE TESTING Final Report, 1987 - 1990
Fumiko Samejima Sep. 1990 82 p
(Contract N00014-87-K-0320)
(AD-A227742) Avail: NTIS HC/MF A05 CSCL 05/8

The following subject areas are covered: backgrounds and basic concepts used throughout the research; proposal of two modification formulae of the test information function; reliability coefficient and standard error of measurement in classical mental test theory predicted in the context of latent trait models; validity measures in the context of latent trait models; further investigation of the nonparametric approach to the estimation of the operating characteristics of discrete item responses; content-based observation of informative distractors and efficiency of ability estimation; efficient computerized adaptive testing. GRA

N91-16651# Technische Univ., Eindhoven (Netherlands). Dept. of Mathematics and Computing Science.
THE DISCRETE TIME H INFINITY CONTROL PROBLEM WITH MEASUREMENT FEEDBACK
A. A. Stoorvogel 20 Nov. 1989 28 p
(MEMO-COSOR-89-31; ETN-91-98429) Avail: NTIS HC/MF A03

The discrete time H sub infinity control problem with measurement feedback is addressed. It turns out that, as in the continuous time case, the existence of an internally stabilizing controller which makes the H sub infinity norm strictly less than 1 is related to the existence of stabilizing solutions to two algebraic Riccati equations. However in the discrete time have to satisfy extra conditions. ESA

N91-16652# Technische Univ., Eindhoven (Netherlands). Dept. of Mathematics and Computing Science.
THE FINITE HORIZON SINGULAR TIME-VARYING H INFINITY CONTROL PROBLEM WITH DYNAMIC MEASUREMENT FEEDBACK
A. A. Stoorvogel and H. L. Trentelman 12 Dec. 1989 43 p
(MEMO-COSOR-89-33; ETN-91-98430) Avail: NTIS HC/MF A03

The finite horizon version of the H sub infinity problem with measurement feedback is addressed. Given a finite dimensional linear, time varying system, together with a positive real number, necessary and sufficient conditions for the existence of a possibly time varying dynamic compensator such that the L sub 2 ((0, t sub 1)) induced norm of the closed loop operator is smaller than the positive real number are obtained. These conditions are expressed in terms of a pair of quadratic differential inequalities, generalizing the well known Riccati differential equations introduced recently in the context of finite horizon H sub infinity control. ESA

N91-16653# Technische Univ., Delft (Netherlands). Faculty of Technical Mathematics and Informatics.
RELATIVE EXTREMA, ZEROS, AND INEQUALITIES FOR GEGENBAUER FUNCTIONS OF THE FIRST AND SECOND KIND
H. vanHaeringen 1990 38 p
(REPT-90-54; ISSN-0922-5641; ETN-91-98457) Copyright Avail: NTIS HC/MF A03

Let C sup lambda sub nu (x) denote ultraspherical or Gegenbauer function of the first kind, and D sup lambda sub nu (x) the Gegenbauer function of the second kind, as introduced by Durand. Inequalities are derived for these functions and for their relative extrema and on -1 less than x less than 1, generalizing thereby similar facts, known for the ultraspherical polynomial C sup lambda sub nu (x) and for D sup 1/2 sub n (x) where n= 0, 1. ESA

N91-16654# Technische Univ., Delft (Netherlands). Faculty of Technical Mathematics and Informatics.
RELATIVE EXTREMA, ZEROS, AND INEQUALITIES FOR JACOBI FUNCTIONS OF THE FIRST AND SECOND KIND
H. vanHaeringen 1990 69 p
(REPT-90-55; ISSN-0922-5641; ETN-91-98458) Copyright Avail: NTIS HC/MF A04

Let P sup alpha, beta sub nu (x) denote the Jacobi function of the first kind. A Jacobi function of the second kind, Q sub alpha, beta sub nu (x) is introduced, in analogy with the ultraspherical or Gegenbauer function of the second kind, D sup lambda sub nu (x), introduced by Durand. Inequalities for these functions and for their relative extrema on -1 less than x less than 1, generalizing thereby similar facts known for the Jacobi polynomials P sup alpha, beta sub n (x), n = 0,1, ..., with alpha less than beta = -1/2, and the P and Q functions above. ESA

N91-16655# Technische Univ., Delft (Netherlands). Faculty of Technical Mathematics and Informatics.
A SIGN-CHANGING GLOBAL MINIMIZER ON A CONVEX DOMAIN

Guido Sweers 1990 10 p Sponsored by Netherlands Organization for Applied Scientific Research TNO, Delft
(REPT-90-57; ISSN-0922-5641; ETN-91-98460) Copyright
Avail: NTIS HC/MF A02

The existence of stable sign changing solutions for the elliptic problem -delta u = f(u) in omega, u = 0 on delta omega was previously established. The existence of a sign changing stable solution on a convex domain with f(0) = 0 was shown. The next question will be: does a global minimizer have a fixed sign. The answer was guessed to be positive if the domain is convex. A study which recalls a proof for the ball is presented and a counterexample with f(0) = 0 for a triangle is given. The example uses a triangle for a domain and a piecewise linear right hand side. ESA

N91-16656# Technische Univ., Delft (Netherlands). Faculty of Technical Mathematics and Informatics.
STABILITY PROPERTIES OF A FLOW PROCESS IN GRAPHS
J. v.d.Berg and R. W. J. Meester 1990 12 p
(REPT-90-58; ISSN-0922-5641; ETN-91-98461) Copyright
Avail: NTIS HC/MF A03

A flow process in infinite graphs where vertices with large resources tend to attract resources from neighbors is studied. The initial resources are random. An interesting question is whether in each finite region all motion stops after a finite time. Under certain assumptions, this is proved to be true. For some other cases, a weaker stability result is proved. Attention is mainly paid of the set Z squared, but several results can be easily generalized to the set Z to the power d. ESA

N91-16657# Technische Univ., Delft (Netherlands). Faculty of Technical Mathematics and Informatics.
AN ELEMENTARY PROOF OF THE AMBARTZUMIAN-PLEIJEL IDENTITY
A. J. Cabo 1990 10 p
(REPT-90-59; ISSN-0922-5641; ETN-91-98462) Copyright
Avail: NTIS HC/MF A02

The aim is to show that Stokes' theorem may be used to prove Ambartzumian's Pleijel type identity for convex polygons directly. It turns out that the use of differential forms leads to considerable simplifications. ESA

N91-16658# Sheffield Univ. (England). Dept. of Control Engineering.
PERIODIC SOLUTIONS OF NEUTRAL DIFFERENTIAL EQUATIONS
Zhang Yi, S. P. Banks, and Y. Zhang (Xuzhou Teacher's Coll., China) Feb. 1990 14 p
(RR-390; ETN-91-98520) Avail: NTIS HC/MF A03

The existence of periodic solutions of neutral differential equations with infinite delay and delay equations of nth order are studied. Some necessary and sufficient conditions for existence of periodic solutions are obtained. A simple lemma on Fourier series is proved and applied to equations with infinite delay. ESA

N91-16659# Oak Ridge National Lab., TN. Mathematical Sciences Section.
AN AUTOMATIC ORDERING METHOD FOR INCOMPLETE FACTORIZATION ITERATIVE SOLVERS
P. A. Forsyth, W. P. Tang (Waterloo Univ., Ontario), and E. F. D. DAzevedo 1991 18 p Presented at the 1991 SPE Symposium on Reservoir Simulation, Anaheim, CA, 17-20 Feb. 1991 Sponsored in part by Natinal Sciences and Engineering Research Council of Canada
(Contract DE-AC05-84OR-21400)
(DE91-001974; CONF-910238-2; RR-CS-90-32) Avail: NTIS HC/MF A03

The minimum discarded fill (MDF) ordering strategy for incomplete factorization iterative solvers is developed. MDF ordering is demonstrated for several model non-symmetric problems, as well as a water-flooding simulation which uses an unstructured grid. The model problems show a three to five fold decrease in the number of iterations compared to natural orderings. Greater than twofold improvement was observed for the waterflooding simulation. DOE

N91-16660# Yale Univ., New Haven, CT. Dept. of Computer Science.
SPARSE REPRESENTATION OF SMOOTH LINEAR OPERATORS Ph.D. Thesis
Bradley Kevin Alpert Aug. 1990 87 p Sponsored in part by IBM
(Contract N00014-86-K-0310; NSF DMS-90-12751)
(AD-A228142; YALEU/DCS/RR-814) Avail: NTIS HC/MF A05 CSCL 12/1

A wide variety of problems in differential and integral equations require application and inversion of linear operators. For large-scale physical problems, the size of the problem n is such that the work expended by general algorithms, O(n squared) for application of a transformation and O(n cubed) for application of its inverse, is often prohibitive. Several methods have been devised in recent years to reduce these complexities by exploiting the structure of particular problems. This thesis puts earlier methods into a unified framework by developing new wavelet-like bases for spaces, which lead to efficient algorithms for operator application and inversion. It is based on the observation that in many cases of interest, while the matrices involved are dense, their elements vary smoothly as a function of their indices, except along a collection of bands of fixed width. Algorithms are presented for transforming such locally smooth matrices into matrices which are sparse (to a finite but arbitrarily high accuracy). The resulting sparse representations support fast algorithms for matrix application and inversion, requiring variously O(n), O(n log n), and O(n log squared n) operations. Programs have been developed applying these techniques to the solution of second-kind integral equations with non-oscillatory kernels. Numerical results are presented to demonstrate the effectiveness of the approach. GRA

N91-16661# Southern Methodist Univ., Dallas, TX. Dept. of Statistical Science.
ADAPTIVE BANDWIDTH CHOICE FOR KERNEL REGRESSION
R. L. Eubank (Texas A&M Univ., College Station.) and William R. Schucany 19 Oct. 1990 22 p Submitted for publication
(Contract F19628-88-K-0042; NSF DMS-89-02576)
(AD-A228437; SMU/DS/TR/241; GL-TR-90-0277) Avail: NTIS HC/MF A03 CSCL 12/3

A data based procedure is introduced for local bandwidth selection for kernel estimation of a regression function at a point. The estimated bandwidth is shown to be consistent and asymptotically normal as an estimator of the (asymptotic) optimal value for minimum mean square estimation. The rate of convergence is identical to that of plug-in bandwidth estimators. The proposed method has the practical advantage that it reduces the need for a priori values and does not require pilot estimates of the regression function, optimization of estimated objective functions or resampling. A small Monte Carlo study is used to examine the behavior of the new bandwidth estimator in a variety of situations. The resulting finite-sample mean square errors of the corresponding curve estimates are generally found to be less than or equal to those of an idealized plug-in estimator. GRA

N91-16662# Stanford Univ., CA. Dept. of Operations Research.
PATHWISE CONVEXITY AND ITS RELATION TO CONVERGENCE OF TIME-AVERAGE DERIVATIVES
Peter W. Glynn Jul. 1990 14 p
(Contract DAAL03-88-K-0063)
(AD-A228888; TR-61; ARO-25839.35-MA) Avail: NTIS HC/MF A03 CSCL 12/1

In this note, we further develop the pathwise convexity approach introduced by Hu (1990) to prove consistency of infinitesimal perturbation analysis for the derivative of the steady-state waiting time of the G/G/1 queue. In addition to generalizing the argument, we illustrate the technique with applications to stochastic storage theory and networks of queues. GRA

N91-16663# Texas A&M Univ., College Station. Dept. of Mathematics.
MATHEMATICAL METHODS AND ALGORITHMS FOR REAL-TIME APPLICATIONS Final Report, 1 Feb. 1987 - 30 Jul. 1990
Charles K. Chui 25 Sep. 1990 24 p
(Contract DAAL03-87-K-0025)
(AD-A228889; ARO-24862.11-MA-SDI) Avail: NTIS HC/MF A03 CSCL 12/1

The notion of super splines and vertex splines is introduced and studied. Quasi-interpolation formulas for real-time applications are constructed. The method of noncommutative blending of quasi-interpolation and vertex spline interpolation is introduced to yield interpolation schemes which are local, flexible, and of optimal approximation orders. These formulas can be applied to real-time interpolation by means of table-look-up or FIR implementation. Applications to engineering problems such as parallel implementation of the extended Kalman filter and Hankel-norm frequency domain methods are studied. Wavelets are constructed by applying cardinal splines, and hence, they are readily available for real-time interpolation and orthogonal wavelet decompositions and reconstructions. GRA

N91-16664*# Institute for Computer Applications in Science and Engineering, Hampton, VA.
RESOLUTION OF THE 1D REGULARIZED BURGERS EQUATION USING A SPATIAL WAVELET APPROXIMATION Final Report
J. Liandrat and Ph. Tchamitchian (Centre National de la Recherche Scientifique, Marseilles, France) Dec. 1990 37 p Submitted for publication
(Contract NAS1-18605; AF-AFOSR-0093-90)
(NASA-CR-187480; ICASE-90-83; NAS 1.26:187480) Avail: NTIS HC/MF A03 CSCL 12A

The Burgers equation with a small viscosity term, initial and periodic boundary conditions is resolved using a spatial approximation constructed from an orthonormal basis of wavelets. The algorithm is directly derived from the notions of multiresolution analysis and tree algorithms. Before the numerical algorithm is described these notions are first recalled. The method uses extensively the localization properties of the wavelets in the physical and Fourier spaces. Moreover, the authors take advantage of the fact that the involved linear operators have constant coefficients. Finally, the algorithm can be considered as a time marching version of the tree algorithm. The most important point is that an adaptive version of the algorithm exists: it allows one to reduce in a significant way the number of degrees of freedom required for a good computation of the solution. Numerical results and description of the different elements of the algorithm are provided in combination with different mathematical comments on the method and some comparison with more classical numerical algorithms.
Author

65 STATISTICS AND PROBABILITY

Includes data sampling and smoothing; Monte Carlo method; and stochastic processes.

N91-16665# Florida Univ., Gainesville. Dept. of Electrical Engineering.
ANALYSIS OF MULTIVARIABLE CONTROL SYSTEMS IN THE PRESENCE OF STRUCTURED UNCERTAINTIES Ph.D. Thesis
Robert Jeffrey Norris Aug. 1990 141 p Sponsored by AFIT, Wright-Patterson AFB, OH
(AD-A227976; AFIT/CI/CIA-90-026D) Avail: NTIS HC/MF A07 CSCL 12/4

An analysis of the stability properties of uncertain multivariable control systems in the frequency domain is presented. Necessary and sufficient stability criteria are reviewed along with singular value scaling techniques for characterizing permissible uncertainties. Such scaling methods have become widely accepted tools for the analysis of control systems in the presence of structured uncertainties. Included in this study are the general block similarity scaling techniques advanced by Doyle and the nonsimilarity scaling approach of Kouvaritakis and Latchman. For element-by-element structured uncertainties, both scaling methods reliably compute Doyle's structured singular value, mu, which provides an indication of system stability. However, the similarity scaling formulation has the disadvantage of expanding an n x n system matrix to an sq n x sq n matrix requiring sq n - 1 optimization variables to compute mu. Using nonsimilarity scaling, the system size remains n with the additional benefit of requiring only 2(n-1) optimization variables. The results of this work show that for scalar uncertainties, the structure may be exploited to yield a similarity scaling method which requires no more than the 2(n-1) optimization variables needed for nonsimilarity scaling. Substantial savings in floating point operations are observed for various system sizes enhancing the capability of this method for analysis and iterative design. A similar reduction in optimization variables is shown to hold for the important class of general block structured uncertainties. This reduction leads to a complete solution for the 2 x 2 block uncertainty problem. GRA

N91-16666# Stanford Univ., CA. Dept. of Statistics.
HIERARCHICAL BAYESIAN ANALYSIS OF CHANGE POINT PROBLEMS
Bradley P. Carlin, Alan E. Gelfand, and Adrian F. M. Smith 18 Oct. 1990 53 p
(Contract N00014-89-J-1627; NR Proj. 042-267)
(AD-A228179; SU-TR-437) Avail: NTIS HC/MF A04 CSCL 12/3

A general approach to hierarchical Bayes change point models is presented. In particular, desired marginal posterior densities are obtained utilizing the Gibbs sampler, an iterative Monte Carlo method. This approach avoids sophisticated analytic and numerical high dimensional integration procedures. We include application to changing regressions, changing Poisson processes, and changing Markov chains. Within these contexts we handle several previously inaccessible problems. GRA

N91-16667# Stanford Univ., CA. Dept. of Operations Research.
ESTIMATING THE ASYMPTOTIC VARIANCE WITH BATCH MEANS
Peter W. Glynn and Ward Whitt (Bell Telephone Labs., Inc., Murray Hill, NJ.) Mar. 1990 9 p
(Contract DAAL03-88-K-0063)
(AD-A228293; SU-TR-57; ARO-25839.33-MA) Avail: NTIS HC/MF A02 CSCL 12/4

In this paper it is shown that there does not exist a procedure to consistently estimate the asymptotic variance constant in a stochastic simulation using batch means when the number of batches is held fixed as the run length increases. Thus, if consistency is desired, then the number of batches must increase as the run length increases. To be precise, we must first specify what we mean by an estimation procedure. To be interesting, an estimation procedure should apply to a large family of stochastic processes. GRA

N91-16668# Stanford Univ., CA. Dept. of Operations Research.
THE ASYMPTOTIC VALIDITY OF SEQUENTIAL STOPPING RULES FOR STOCHASTIC SIMULATIONS
Peter W. Glynn and Ward Whitt Jan. 1990 32 p
(Contract DAAL03-88-K-0063)
(AD-A228896; TR-55; ARO-25839.31-MA) Avail: NTIS HC/MF A03 CSCL 12/4

We establish general conditions for the asymptotic validity of sequential stopping rules to achieve fixed-volume confidence sets for simulation estimators of vector-valued parameters. The asymptotic validity occurs as the prescribed volume of the confidences set approaches zero. There are two requirements: a functional central limit theorem for the estimation process and a strong consistency (with-probability-one convergence) for the variance or scaling matrix estimator. Applications are given for:

sample means of i.i.d. random variables and random vectors, nonlinear functions of such sample means, jackknifing, Kiefer-Wolfowitz and Robbins-Monro stochastic approximation, and both regenerative and non-regenerative steady-state simulation. GRA

N91-16669# Messerschmitt-Boelkow-Blohm G.m.b.H., Schrobenhausen (Germany, F.R.).
FRAGMENT MASS DISTRIBUTION OF DEBRIS
Manfred Held 1990 20 p Presented at the 24th DOD Explosive Safety Seminar, Saint Louis, MO, 27-30 Aug. 1990
(MBB-UA-1187-90-PUB; ETN-91-98507) Avail: NTIS HC/MF A03

An equation is established for the mass distribution of the natural fragments of an explosive filled projectile, or for that of secondary fragments behind one or several spaced target plates, which can also be applied with very good results to the mass distribution of the debris from an exploded aircraft shelter. The two constants required for this, namely, the scale parameter and the shape parameter, can be determined to a usually high confidence level, with a correlation coefficient close to 1, especially when the given total mass is changed to a best mass that best describes the actual fragment mass distribution. ESA

N91-16670# Laboratoire d'Automatique et d'Analyse des Systemes, Toulouse (France). Groupe Systeme de Production.
ABOUT PETRI NETS WITH FUZZY MARKINGS Ph.D. Thesis - Toulouse Univ.
Janette Cardoso 1990 133 p In FRENCH; ENGLISH summary Sponsored by Coordenacao de Aperfeicoamento de Pessoal de Nivel Superior; Santa Catarina Univ, Florianopolis, Brazil; and COFECUB
(LAAS-90354; ETN-91-98591) Avail: NTIS HC/MF A07

A model combining petri nets with objects, probability theory and notions of fuzzy time knowledge is elaborated with a view to an application to the monitoring of flexible manufacturing systems, at the global coordination level. Notions of imprecise and fuzzy markings were introduced in the petri nets. In case of a disruption, in addition to the current marking to which the object localizations are certain, some tokens whose localizations are uncertain were introduced. The monitoring and the recovery in an automated manufacturing system was given as an example. ESA

66 SYSTEMS ANALYSIS

Includes mathematical modeling; network analysis; and operations research.

No abstracts in this category.

67 THEORETICAL MATHEMATICS

Includes topology and number theory.

N91-16671# Hiroshima Univ., Takehara (Japan). Research Inst. for Theoretical Physics.
SOME ASPECTS OF QUANTUM GROUPS AND SUPERGROUPS
E. Corrigan, D. B. Fairlie, P. Fletcher, and R. Sasaki (Durham Univ., England) Jul. 1989 17 p
(DE90-777884; RRK-89-23; DTP-89/29) Avail: NTIS (US Sales Only) HC A03

The paper concentrates upon certain algebraic aspects of the quantum inverse scattering theory and develops ideas arising principally from the viewpoint of Manin, who considers a quantum group as effecting linear transformations upon a space whose elements are non-commutative. The conditions for such a mapping to be an endomorphism constitute the quantum group relations. In fact, since this idea underlies the classical transformation groups, it is a very natural, though at first sight unfamiliar, approach to the deformation of classical groups. The idea of Manin is recounted for the simplest example of GLq(2) and develop properties of this quantum group. A natural extension leads to the definition of the dual group GLq(2) whose elements are Grassmannian, and GLq(1/1) which is connected with the quantum extension of the superalgebra SU(1/1), just as GLq(2) is connected with the quantum extension of SU(2). These groups are then displayed in a more familiar way as bilinear relations specified by an R-matrix satisfying the Yang-Baxter equation. The minimal set of relations imposed by the R-matrix relations is shown to be equivalent to those imposed by Manin's construction, and in fact, Manin's construction can be used to infer the structure of the R-matrix for the classical groups. DOE

70 PHYSICS (GENERAL)

For precision time and time interval (PTTI) see *35 Instrumentation and Photography;* for geophysics, astrophysics or solar physics see *46 Geophysics, 90 Astrophysics,* or *92 Solar Physics.*

N91-16672# Lawrence Livermore National Lab., CA. Computational Physics Group.
COMPUTATIONAL PHYSICS AT THE NATIONAL ENERGY RESEARCH SUPERCOMPUTER CENTER
Arthur A. Mirin Apr. 1990 112 p
(Contract W-7405-eng-48)
(DE90-010283; UCRL-ID-103429) Avail: NTIS HC/MF A06

The principal roles of the Computational Physics Group are (1) to develop efficient numerical algorithms, programming techniques and applications software for current and future generations of supercomputers, (2) to develop advanced numerical models for the investigation of plasma phenomena and the simulation of contemporary magnetic fusion devices, and (3) to serve as a liaison between the Center and the user community, in particular, to provide NERSC with an application-oriented viewpoint and to provide the user community with expertise on the effective usage of the computers. In addition, many of our computer codes employ state-of-the-art algorithms that test the prototypical hardware and software features of the various computers. This document describes the activities of the Computational Physics Group and was prepared with the assistance of the various Group members. The fist part contains overviews on a number of our important projects. The second section lists our important computational models. The third part provides a comprehensive list of our publications. DOE

N91-16673# Naval Underwater Systems Center, New London, CT.
OPERATING CHARACTERISTICS FOR WEIGHTED ENERGY DETECTOR WITH GAUSSIAN SIGNALS
Albert H. Nuttall 16 Jul. 1990 98 p Sponsored by Naval Sea Systems Command, Washington, DC
(AD-A226851; NUSC-TR-8753) Avail: NTIS HC/MF A05
CSCL 12/9

The performance of several weighted energy detectors of Gaussian signals in noise are investigated, both by exact procedures and by five different approximation procedures. In particular, receiver operating characteristics, for false alarm probabilities ranging from 1E-10 to .1 and detection probabilities ranging from .01 to .999, are quantitatively compared. The standard Gaussian approximation is found to be severely deficient and generally optimistic for small false alarm probabilities, while two different fourth-order approximations have excellent capability over the entire range of probabilities considered. A method of avoiding the calculation of the eigenvalues of a covariance matrix, and yet accurately predicting performance of a fading medium, is presented. It requires only sums of products of the covariance elements directly, the precise number depending on the order of the approximation. GRA

N91-16674# National Lab. for High Energy Physics, Ibaraki (Japan).
INVESTIGATION OF WIRE MOTION IN SUPERCONDUCTING MAGNETS
T. Ogitsu, K. Tsuchiya, and A. Devred Sep. 1990 5 p Presented at the Applied Superconductivity Conference, Aspen, CO, 24-28 Sep. 1990 Prepared in cooperation with Superconducting Super Collider Lab., Dallas, TX
(Contract DE-AC02-89ER-40486)
(DE91-004952; SSCL-330; CONF-900944-26) Avail: NTIS HC/MF A01

The large Lorentz forces occurring during the excitation of superconducting magnets can provoke sudden motions of wire, which eventually release enough energy to trigger a quench. These wire motions are accompanied by two electromagnetic effects: an induced emf along the moved wire, and a local change in flux caused by the minute dislocation of current. Both effects cause spikes in the coil voltage. Voltage data recorded during the excitation of a superconducting quadrupole magnet which early exhibit such events are here reported. Interpretations of the voltage spikes in terms of energy release are also presented, leading to insights on the spectrum of the disturbances which occur in real magnets. DOE

71 ACOUSTICS

Includes sound generation, transmission and attenuation. For noise pollution see *45 Environmental Pollution.*

N91-16675# Sandia National Labs., Albuquerque, NM. Microsensor Div.
MULTIPLE-FREQUENCY SURFACE ACOUSTIC WAVE DEVICES AS SENSORS
Antonio J. Ricco and Stephen J. Martin 1990 5 p Presented at the Solid State and Sensor Actuator Workshop, Hilton Head Island, SC, 4-7 Jun. 1990
(Contract DE-AC04-76DP-00789)
(DE90-009972; SAND-90-0139C; CONF-9006172-1) Avail: NTIS HC/MF A01

We have designed, fabricated, and tested a multiple-frequency acoustic wave (MUFAW) device on ST-cut quartz with nominal surface acoustic wave (SAW) center frequencies of 16, 40, 100, and 250 MHz. The four frequencies are obtained by patterning four sets of input and output interdigital transducers of differing periodicities on a single substrate. Such a device allows the frequency dependence of AW sensor perturbations to be examined, aiding in the elucidation of the operative interaction mechanism(s). Initial measurements of the SAW response to the vacuum deposition of a thin nickel film show the expected frequency dependence of mass sensitivity in addition to the expected frequency independence of the magnitude of the acoustoelectric effect. By measuring changes in both wave velocity and attenuation at multiple frequencies, extrinsic perturbations such as temperature and pressure changes are readily differentiated from one another and from changes in surface mass. DOE

N91-16676# Sandia National Labs., Albuquerque, NM.
UTILIZATION OF POLYMER VISCOELASTIC PROPERTIES IN ACOUSTIC WAVE SENSOR APPLICATIONS
Stephen J. Martin, Antonio J. Ricco, and G. C. Frye 1990 4 p Presented at the Solid State Sensor and Actuator Workshop, Hilton Head Island, SC, 4-7 Jun. 1990
(Contract DE-AC04-76DP-00789)
(DE90-010534; SAND-89-0126C; CONF-9006171-1) Avail: NTIS HC/MF A01

The changes which occur in polymer viscoelastic properties in response to cross-linking reactions and due to absorption of gas phase species were used advantageously in several acoustic wave-based sensor applications. When a polymer film is present on the surface of an acoustic wave device, changes in the visoelastic properties of the film induce changes in wave porpagation velocity and attenuation, providing two sensor responses. Film changes which occur polymer cross-linking allow photopolymerization to be monitored in real time using acoustic devices. A photoaction spectrum of photoresist reveals the cross-linking wavelength with maximum quantum yield. Changes in the viscoelastic properties of a polysiloxane film induces by vapor absorption are found to be unique for each of several species, enabling differentiation of species with a single film. A Maxwell model for polymer viscoelasticity, in combination with mass loading effects, provides a sound theoretical basis for explaining observed results for both polysiloxane and polybytadiene/polystyrene copolymer films. DOE

N91-16677# Naval Ocean Systems Center, San Diego, CA.
CANONICAL EIGENVALUES. PART 2: APPLICATION TO ONE-LAYER, BOUNDED, UNDERWATER ACOUSTIC DUCTS Technical Report, Mar. 1986 - Sep. 1989
Melvin A. Pedersen, David F. Gordon, and Fell Hosmer Jun. 1990 42 p
(AD-A227451; NOSC/TR-1333-PT-2) Avail: NTIS HC/MF A03 CSCL 20/1

The general theory of canonical eigenvalues, as developed by the authors, is applied to underwater sound propagation in one-layer bounded duct. For this type of duct, the eigenvalues apply to an entire class of single layer profiles (slopes may be either negative or positive). Three classes are considered with different upper and lower boundary conditions. They are free-rigid, free-free, and rigid-rigid boundary pairs. Numerical results are given for phase velocity, group velocity, and eigenfunction normalization coefficient, all plotted as functions of frequency. GRA

N91-16678# Johns Hopkins Univ., Baltimore, MD. Dept. of Materials Science and Engineering.
FULL FIELD VISUALIZATION OF SURFACE AND BULK ACOUSTIC WAVES Final Report
James W. Wagner and Robert E. Green, Jr. Sep. 1990 18 p
(Contract N00014-82-K-0741)
(AD-A227676) Avail: NTIS HC/MF A03 CSCL 14/1

The objective was to apply optical holographic techniques coupled with electronic signal and image processing to provide quantitative, full field measurements of acoustic wave disturbances. High speed pulsed holographic methods were developed to permit visualization of transient acoustic wave fields on the surfaces of solids and plates. In addition, it was possible to produce tomographic displays of acoustic energy flow in optically transparent fluids and solids. Special adaptations for heterodyne analysis made it possible to extract data from the holographic interferograms with sensitivities 900 times greater than conventional visual analysis. GRA

N91-16679*# National Aeronautics and Space Administration. Langley Research Center, Hampton, VA.
WIND TURBINE ACOUSTICS
Harvey H. Hubbard and Kevin P. Shepherd Dec. 1990 49 p Submitted for publication Prepared in cooperation with NASA, Lewis Research Center and American Society of Mechanical Engineers
(Contract DE-AI01-76ET-20320)
(NASA-TP-3057; E-5663; DOE/NASA/20320-77; NAS 1.60:3057) Avail: NTIS HC/MF A03 CSCL 20A

Available information on the physical characteristics of the noise generated by wind turbines is summarized, with example sound pressure time histories, narrow- and broadband frequency spectra, and noise radiation patterns. Reviewed are noise measurement standards, analysis technology, and a method of characterizing wind turbine noise. Prediction methods are given for both low-frequency rotational harmonics and broadband noise components. Also included are atmospheric propagation data showing the effects of distance and refraction by wind shear. Human perception thresholds, based on laboratory and field tests, are given. Building vibration analysis methods are summarized. The bibliography of this report lists technical publications on all aspects of wind turbine acoustics. Author

N91-16680 British Broadcasting Corp., Kingswood (England). Engineering Div.
A REVIEW OF THE AIRBORNE SOUND INSULATION REQUIREMENTS FOR BROADCASTING STUDIOS AND ANCILLARY AREAS
R. Walker 1990 24 p
(BBC-RD-1990/10) Avail: Issuing Activity

Experience over the past nine years with the airborne sound insulation criteria has shown that they are stringent. In new developments their application is limited by financial constraints and additionally in refurbishments by structural constraints. Discussions during the past years have taken place on attempts and methods to reduce the requirements. This review began as a study of existing criteria in order to define more closely some of the categories and thus, perhaps, reduce some of the apparent requirements. It has been found that the original bases of the majority of the sound insulation criteria are still appropriate, but that a small number of categories can be adjusted. The opportunity has been taken to incorporate some new data and to allow for changes in background noise level criteria for some area categories. A study of a possible relaxation of the criteria for the special case of a studio to its own control area was abandoned, when it became clear that the same relaxations could be applied to all areas. Author

N91-16681 British Broadcasting Corp., Kingswood (England). Engineering Div.
PROVING EXPERIMENTS ON AN ACOUSTIC TRANSMISSION SUITE AND ITS REVERBERATION ROOM
G. D. Plumb 1990 20 p
(BBC-RD-1990/13) Avail: Issuing Activity

An Acoustic Transmission Suite is a facility used for the laboratory measurement of the airborne sound transmission properties of partitions. It consists of a pair of adjoining rooms, the source room and the receive room, with a hole for the construction of the test partition in their common walls. The building is designed to minimize the sound power flow by paths other than that through the test partition. Such a facility has recently been built at the British Broadcasting Corporation (BBC) Research Department. A double brick cavity wall was built to allow the limiting sound insulation performance between the source and receive rooms in the Transmission Suite to be measured. This performance is effectively equal to that which would be measured with a perfectly isolating partition in place, and limits the maximum insulation that could be measured using the Suite. The actual isolation was shown to be impaired by a rigid bond between the test wall and the receive room walls. A demountable lightweight partition was fitted firstly to the receive and then to the source room side of the test wall. This improved the isolation of the test wall and proved that the rigid bond at its edges had been the cause of the impaired isolation. It also revealed a void above the test wall, and a further weakness through the cavity between the source and receive rooms. The mean limiting sound reduction index between the source and receive rooms was shown to be 65 dB, provided that the cavity between source and receive rooms was sealed. In future, a mechanism must be employed which provides vibration isolation between the test wall and the Transmission Suite building structure. The receive room was designed to meet the specifications detailed in the ISO-Standard for reverberation rooms. Proving tests were carried out on the reverberation room and repeatability tests were carried out to evaluate the minimum number of decays needed in each frequency band for absorption coefficient measurements. The amount of additional diffusion needed in the reverberation room to ensure reliable results was determined. Author

N91-16682*# National Aeronautics and Space Administration. Langley Research Center, Hampton, VA.
FOURTH INTERNATIONAL SYMPOSIUM ON LONG-RANGE SOUND PROPAGATION
William L. Willshire, Jr., comp. Washington Dec. 1990 274 p Symposium held in Hampton, VA, 16-17 May 1990; sponsored by NASA, Langley Research Center, Mississippi Univ., and Open Univ. of England
(NASA-CP-3101; L-16875; NAS 1.55:3101) Avail: NTIS HC/MF A12 CSCL 20A

Long range sound propagation is an aspect of many acoustical problems ranging from en route aircraft noise to the acoustic detection of aircraft. Over the past decade, the University of Mississippi and the Open University of England, together with a third institution, have held a symposium approx. every 2 years so that experts in the field of long range propagation could exchange information on current research, identify areas needing additional work, and coordinate activities as much as possible. The Fourth International Symposium on Long Range Sound Propagation was jointly sponsored by the University of Mississippi, the Open University of England, and NASA. Papers were given in the following areas: ground effects on propagation; infrasound propagation; and meteorological effects on sound propagation. A compilation of the presentations made at the symposium is presented along with a list of attendees, and the agenda. For individual titles, see N91-16683 through N91-16704.

N91-16683*# Sutherland (Louis C.), Rancho Palos Verdes, CA.
LONG-RANGE SOUND PROPAGATION: A REVIEW OF SOME EXPERIMENTAL DATA
Louis C. Sutherland *In* NASA, Langley Research Center, 4th International Symposium on Long-Range Sound Propagation Dec. 1990 p 1-1 (For primary document see N91-16682 08-71)
Avail: NTIS HC/MF A12 CSCL 20A

Three experimental studies of long range sound propagation carried out or sponsored in the past by NASA are briefly reviewed to provide a partial prospective for some of the analytical studies presented in this symposium. The three studies reviewed cover (1) a unique test of two large rocket engines conducted in such a way as to provide an indication of possible atmospheric scattering loss from a large low-frequency directive sound source, (2) a year-long measurement of low frequency sound propagation which clearly demonstrated the dominant influence of the vertical gradient in the vector sound velocity towards the receiver in defining excess sound attenuation due to refraction, and (3), a series of excess ground attenuation measurements over grass and asphalt surfaces replicated several times under very similar inversion weather conditions. Author

N91-16684*# Utah Univ., Salt Lake City. Dept. of Mechanical Engineering.
ON THE PROPAGATION OF PLANE WAVES ABOVE AN IMPEDANCE SURFACE
F. H. Zhong and W. K. VanMoorhem *In* NASA, Langley Research Center, 4th International Symposium on Long-Range Sound Propagation Dec. 1990 p 13-25 (For primary document see N91-16682 08-71)
Avail: NTIS HC/MF A12 CSCL 20A

The propagation of grazing incidence plane waves along a finite impedance boundary is investigated. A solution of the semi-infinite problem, where a harmonic motion, parallel to the boundary, is imposed along a line perpendicular to the boundary, is obtained. This solution consists of quasiplane waves, waves moving parallel to the boundary with amplitude and phase variations perpendicular to the boundary. Several approximations to the full solution are considered. Author

N91-16685*# National Research Council of Canada, Ottawa (Ontario). Div. of Physics.
AIR-GROUND INTERFACE: SURFACE WAVES, SURFACE IMPEDANCE AND ACOUSTIC-TO-SEISMIC COUPLING COEFFICIENT
Gilles Daigle and Tony Embleton *In* NASA, Langley Research Center, 4th International Symposium on Long-Range Sound Propagation Dec. 1990 p 27-40 (For primary document see N91-16682 08-71)
Avail: NTIS HC/MF A12 CSCL 20A

In atmospheric acoustics, the subject of surface waves has been an area of discussion for many years. The existence of an acoustic surface wave is now well established theoretically. The

mathematical solution for spherical wave propagation above an impedance boundary includes the possibility of a contribution that possesses all the standard properties for a surface wave. Surface waves exist when the surface is sufficiently porous, relative to its acoustical resistance, that it can influence the airborne particle velocity near the surface and reduce the phase velocity of sound waves in air at the surface. This traps some of the sound energy in the air to remain near the surface as it propagates. Above porous grounds, the existence of surface waves has eluded direct experimental confirmation (pulse experiments have failed to show a separate arrival expected from the reduced phase speed) and indirect evidence for its existence has appeared contradictory. The experimental evidence for the existence of an acoustical surface wave above porous boundaries is reviewed. Recent measurements including pulse experiments are also described. A few years ago the acoustic impedance of a grass-covered surface was measured in the frequency range 30 to 300 Hz. Here, further measurements on the same site are discussed. These measurements include core samples, a shallow refractive survey to determine the seismic velocities, and measurements of the acoustic-to-seismic coupling coefficient. Author

N91-16686*# Mississippi Univ., University. Dept. of Physics and Astronomy.

EXPONENTIAL GROUND IMPEDANCE MODELS AND THEIR INTERPRETATION

Richard Raspet and Mark Sprague *In* NASA, Langley Research Center, 4th International Symposium on Long-Range Sound Propagation Dec. 1990 p 41-50 (For primary document see N91-16682 08-71)

Avail: NTIS HC/MF A12 CSCL 20A

The authors compare the results of Donato's exponentially varying ground model, Attenborough's exponentially varying ground model and the rigid backed thin layer model. They show that these models produce similar results for slow variations. For rapid variations the results are quite different, but the basic theory used is only correct for the thin layer model. These results suggest that the exponentially varying models are not necessary for fitting ground impedance data. Author

N91-16687*# Army Cold Regions Research and Engineering Lab., Hanover, NH.

PRELIMINARY ANALYSIS OF MEASURED SOUND PROPAGATION OVER VARIOUS SEASONAL SNOW COVERS

Donald G. Albert *In* NASA, Langley Research Center, 4th International Symposium on Long-Range Sound Propagation Dec. 1990 p 51-57 Sponsored in part by Army (For primary document see N91-16682 08-71)

Avail: NTIS HC/MF A12 CSCL 20A

Measurements of acoustic pulse propagation in the 5 to 500-Hz frequency band were conducted under various snow cover conditions during the 1989 to 1990 winter in New Hampshire. The objective was to determine the effect of snow cover thickness and other snow properties on the absorption of acoustic pulses. Blank pistol shots were used as the source of the acoustic waves, and geophones and microphones in an 80 m-long linear array served as receivers. Snow thicknesses ranged from 0.05 to 0.35 m, and densities varied from 100 to 350 kg m(sup -3) during the 10 separate measurement days. Preliminary analysis indicates that the peak pulse amplitude decayed in proportion to approx. gamma (sup -1.7) for most conditions and that the acoustic-to-seismic ratios varied from about 4 to 15 x 10(exp -6) m s(sup -1) Pa(sup -1). Theoretical waveforms were calculated for propagation in a homogeneous atmosphere using Attenborough's model of ground impedance. An automatic fitting procedure for the normalized experimental and theoretical waveforms was used to determine the effective flow resistivity of the snow covers, and gave values of 10 to 35 kN s m(sup -4), in agreement with earlier results. Author

N91-16688*# Bradford Univ. (England). Dept. of Civil Engineering.

LONG-DISTANCE SOUND PROPAGATION OVER DISCONTINUOUS IMPEDANCES

Simon N. Chandler-Wilde, Joseph N. B. Harriott, and David C. Hothersall *In* NASA, Langley Research Center, 4th International Symposium on Long-Range Sound Propagation Dec. 1990 p 59-73 (For primary document see N91-16682 08-71)

Avail: NTIS HC/MF A12 CSCL 20A

A calculation method is presented for sound propagation over an impedance discontinuity in flat ground with a homogeneous, still atmosphere. The method is based on an approximate solution to a two dimensional boundary integral equation formulation of the problem, which expresses the wave field as the solution for homogeneous ground plus an integral over half of the boundary. Through recognizing this integral as a generalized Fourier integral, asymptotic methods are applied to evaluate the part of the integral most expensive to compute by numerical quadrature. Single frequency excess attenuation results for propagation from a point source above rigid ground to a receiver above absorbing ground are discussed. The results are applied, with air attenuation and A-weighting, to a notional jet engine noise source. Simple trends are noted. Author

N91-16689*# Army Tank-Automotive Command, Warren, MI. Countermeasures Branch.

ADRPM-VII APPLIED TO THE LONG-RANGE ACOUSTIC DETECTION PROBLEM

Edward Shalis and Gerald Koenig *In* NASA, Langley Research Center, 4th International Symposium on Long-Range Sound Propagation Dec. 1990 p 75-83 (For primary document see N91-16682 08-71)

Avail: NTIS HC/MF A12 CSCL 20A

An acoustic detection range prediction model (ADRPM-VII) has been written for IBM PC/AT machines running on the MS-DOS operating system. The software allows the user to predict detection distances of ground combat vehicles and their associated targets when they are involved in quasi-military settings. The program can also calculate individual attenuation losses due to spherical spreading, atmospheric absorption, ground reflection and atmospheric refraction due to temperature and wind gradients while varying parameters effecting the source-receiver problem. The purpose here is to examine the strengths and limitations of ADRPM-VII by modeling the losses due to atmospheric refraction and ground absorption, commonly known as excess attenuation, when applied to the long range detection problem for distances greater than 3 kilometers. Author

N91-16690*# Textron Defense Systems, Wilmington, MA.

VEHICULAR SOURCES IN ACOUSTIC PROPAGATION EXPERIMENTS

Gervasio Prado, James Fitzgerald, Anthony Arruda, and George Parides *In* NASA, Langley Research Center, 4th International Symposium on Long-Range Sound Propagation Dec. 1990 p 85-99 (For primary document see N91-16682 08-71)

Avail: NTIS HC/MF A12 CSCL 20A

One of the most important uses of acoustic propagation models lies in the area of detection and tracking of vehicles. Propagation models are used to compute transmission losses in performance prediction models and to analyze the results of past experiments. Vehicles can also provide the means for cost effective experiments to measure acoustic propagation conditions over significant ranges. In order to properly correlate the information provided by the experimental data and the propagation models, the following issues must be taken into consideration: the phenomenology of the vehicle noise sources must be understood and characterized; the vehicle's location or 'ground truth' must be accurately reproduced and synchronized with the acoustic data; and sufficient meteorological data must be collected to support the requirements of the propagation models. The experimental procedures and instrumentation needed to carry out propagation experiments are discussed. Illustrative results are presented for two cases. First, a

helicopter was used to measure propagation losses at a range of 1 to 10 Km. Second, a heavy diesel-powered vehicle was used to measure propagation losses in the 300 to 2200 m range. Author

N91-16691*# Michigan Technological Univ., Houghton.
SCATTERING MEASUREMENTS ON NATURAL AND MODEL TREES
James C. Rogers and Sung M. Lee *In* NASA, Langley Research Center, 4th International Symposium on Long-Range Sound Propagation Dec. 1990 p 101-113 (For primary document see N91-16682 08-71)
Avail: NTIS HC/MF A12 CSCL 20A

The acoustical back scattering from a simple scale model of a tree has been experimentally measured. The model consisted of a trunk and six limbs, each with 4 branches; no foliage or twigs were included. The data from the anechoic chamber measurements were then mathematically combined to construct the effective back scattering from groups of trees. Also, initial measurements have been conducted out-of-doors on a single tree in an open field in order to characterize its acoustic scattering as a function of azimuth angle. These measurements were performed in the spring, prior to leaf development. The data support a statistical model of forest scattering; the scattered signal spectrum is highly irregular but with a remarkable general resemblance to the incident signal spectrum. Also, the scattered signal's spectra showed little dependence upon scattering angle. Author

N91-16692*# Open Univ., Milton (England).
USING A FAST FOURIER METHOD TO MODEL SOUND PROPAGATION IN A STRATIFIED ATMOSPHERE OVER A STRATIFIED POROUS-ELASTIC GROUND
S. Tooms and K. Attenborough *In* NASA, Langley Research Center, 4th International Symposium on Long-Range Sound Propagation Dec. 1990 p 115-126 (For primary document see N91-16682 08-71)
Avail: NTIS HC/MF A12 CSCL 20A

Using a Fast Fourier integration method and a global matrix method for solution of the boundary condition equations at all interfaces simultaneously, a useful tool for predicting acoustic propagation in a stratified fluid over a stratified porous-elastic solid was developed. The model for the solid is a modified Biot-Stoll model incorporating four parameters describing the pore structure corresponding to the Rayleigh-Attenborough rigid-porous structure model. The method is also compared to another Fast Fourier code (CERL-FFP) which models the ground as an impedance surface under a horizontally stratified air. Agreement with the CERL FFP is good. The effects on sound propagation of a combination of ground elasticity, complex ground structure, and atmospheric conditions are demonstrated by theoretical results over a snow layer, and experimental results over a model ground surface. Author

N91-16693*# National Aeronautics and Space Administration. Langley Research Center, Hampton, VA.
LONG-RANGE VERTICAL PROPAGATION
William L. Willshire, Jr. and Donald P. Garber (Lockheed Engineering and Sciences Co., Hampton, VA.) *In its* 4th International Symposium on Long-Range Sound Propagation Dec. 1990 p 127-132 (For primary document see N91-16682 08-71)
Avail: NTIS HC/MF A12 CSCL 20A

Development of the advanced turboprop has led to concerns about en route noise. Advanced turboprops generate low-frequency, periodic noise signatures at relatively high levels. As demonstrated in a flight test of NASA Lewis Research Center's Propfan Test Assessment (PTA) airplane in Alabama in October 1987, the noise of an advanced turboprop operating at cruise altitudes can be audible on the ground. The assessment of the en route noise issue is difficult due to the variability in received noise levels caused by atmospheric propagation and the uncertainty in predicting community response to the relatively low-level en route noise, as compared to noise associated with airport operations. The En Route Noise Test was designed to address the atmospheric propagation of advanced turboprop noise from cruise altitudes and consisted of measuring the noise of an advance turboprop at cruise in close proximity to the turboprop and on the ground. Measured and predicted ground noise levels are presented. Author

N91-16694*# Los Alamos National Lab., NM.
INFRASONIC OBSERVATIONS OF LARGE-SCALE HE EVENTS
Rodney W. Whitaker, J. Paul Mutschlecner, Masha B. Davidson, and Susan D. Noel *In* NASA, Langley Research Center, 4th International Symposium on Long-Range Sound Propagation Dec. 1990 p 133-141 Sponsored in part by DOE (For primary document see N91-16682 08-71)
Avail: NTIS HC/MF A12 CSCL 20A

The Los Alamos Infrasound Program has been operating since about mid-1982, making routine measurements of low frequency atmospheric acoustic propagation. Generally, the authors work between 0.1 Hz to 10 Hz; however, much of the work is concerned with the narrower range of 0.5 to 5.0 Hz. Two permanent stations, St. George, UT, and Los Alamos, NM, have been operational since 1983, collecting data 24 hours a day. For the purposes of this discussion, the authors concentrate on their measurements of large, high explosive (HE) events at ranges of 250 km to 5330 km. Because their equipment is well suited for mobile deployments, they can easily establish temporary observing sites for special events. The measurements are from the permanent sites, as well as from various temporary sites. A few observations that are typical of the full data set are given. Author

N91-16695*# Los Alamos National Lab., NM.
THE CORRECTION OF INFRASOUND SIGNALS FOR UPPER ATMOSPHERIC WINDS
J. Paul Mutschlecner and Rodney W. Whitaker *In* NASA, Langley Research Center, 4th International Symposium on Long-Range Sound Propagation Dec. 1990 p 143-153 Sponsored in part by DOE (For primary document see N91-16682 08-71)
Avail: NTIS HC/MF A12 CSCL 20A

Infrasound waves propagate in the atmosphere by a well known mechanism produced by refraction of the waves, return to earth, and reflection at the surface into the atmosphere for subsequent bounces. A figure illustrates this phenomenon with results from a ray trace model. In this instance three rays are returned to earth from a region centered at about 50 kilometers in altitude and two from a region near 110 kilometers in altitude. The control of the wave refraction is largely dominated by the temperature-height profile and inversions; however, a major influence is also produced by the atmospheric wind profile. Another figure illustrates the considerable ray differences for rays moving in the wind direction (to the right) and in the counter direction (to the left). It obviously can be expected that infrasonic signal amplitudes will be greatly influenced by the winds in the atmosphere. The seasonal variation of the high altitude atmospheric winds is well documented. A third figure illustrates this with average statistics on the observed zonal wind in the region of 50 plus or minus 5 kilometers in altitude. The results are based upon a survey by Webb; Webb terms this parameterization the Stratospheric Circulation Index (SCI). The very strong seasonal variation has the ability to exert a major seasonal influence on infrasonic signals. The purpose here is to obtain a method for the correction of this effect. Author

N91-16696*# Oldenburg Univ. (Germany, F.R.).
METEOROLOGICAL EFFECTS ON LONG-RANGE OUTDOOR SOUND PROPAGATION
Helmut Klug *In* NASA, Langley Research Center, 4th International Symposium on Long-Range Sound Propagation Dec. 1990 p 155-164 (For primary document see N91-16682 08-71)
Avail: NTIS HC/MF A12 CSCL 20A

Measurements of sound propagation over distances up to 1000 m were carried out with an impulse sound source offering reproducible, short time signals. Temperature and wind speed at several heights were monitored simultaneously; the meteorological data are used to determine the sound speed gradients according to the Monin-Obukhov similarity theory. The sound speed profile

is compared to a corresponding prediction, gained through the measured travel time difference between direct and ground reflected pulse (which depends on the sound speed gradient). Positive sound speed gradients cause bending of the sound rays towards the ground yielding enhanced sound pressure levels. The measured meteorological effects on sound propagation are discussed and illustrated by ray tracing methods. Author

N91-16697*# Massachusetts Inst. of Tech., Lexington. Lincoln Lab.

EFFECT OF WIND AND TEMPERATURE GRADIENTS ON RECEIVED ACOUSTIC ENERGY

Richard K. Brienzo *In* NASA, Langley Research Center, 4th International Symposium on Long-Range Sound Propagation Dec. 1990 p 165-185 Sponsored in part by AF (For primary document see N91-16682 08-71)

Avail: NTIS HC/MF A12 CSCL 20A

The effect of refraction due to wind and temperature gradients on energy received from low flying aircraft is examined. A series of helicopter and jet flyby's were recorded with a microphone array on two separate days, each with distinctly different meteorological conditions. Energy in the 100 to 200 Hertz band is shown as a function of aircraft range from the array, and compared with the output of the Fast Field Program. Author

N91-16698*# Pennsylvania State Univ., University Park. Dept. of Meteorology.

COMPARISON OF FFP PREDICTIONS WITH MEASUREMENTS OF A LOW-FREQUENCY SIGNAL PROPAGATED IN THE ATMOSPHERE

K. Keith Wilson and Dennis W. Thomson *In* NASA, Langley Research Center, 4th International Symposium on Long-Range Sound Propagation Dec. 1990 p 187-200 (For primary document see N91-16682 08-71)

Avail: NTIS HC/MF A12 CSCL 20A

An experimental study of low-frequency propagation over a distance of 770 m was previously reported (J. Acoust. Soc. Am. Suppl. 1 86, S120 (1989)). For that study, sound speed profiles were reconstructed entirely from surface-layer micrometeorological data. When the acoustic data were compared with theoretical predictions from a fast field program (FFP), it was found that the FFP underpredicted sound levels measured in a shadow zone. Here, the effect on the predictions of including meteorological data for heights greater than the surface layer, i.e., wind profiles measured by a Doppler sodar, is discussed. Vertical structure of turbulence is simulated by stochastically perturbing the mean profiles, and the agreement between the acoustic data and FFP predictions is improved. Author

N91-16699*# Salford Univ. (England). Dept. of Applied Acoustics.

NEW CORRECTION PROCEDURES FOR THE FAST FIELD PROGRAM WHICH EXTEND ITS RANGE

M. West and R. A. Sack *In* NASA, Langley Research Center, 4th International Symposium on Long-Range Sound Propagation Dec. 1990 p 201-209 (For primary document see N91-16682 08-71)

Avail: NTIS HC/MF A12 CSCL 20A

A fast field program (FFP) algorithm was developed based on the method of Lee et al., for the prediction of sound pressure level from low frequency, high intensity sources. In order to permit accurate predictions at distances greater than 2 km, new correction procedures have had to be included in the algorithm. Certain functions, whose Hankel transforms can be determined analytically, are subtracted from the depth dependent Green's function. The distance response is then obtained as the sum of these transforms and the Fast Fourier Transformation (FFT) of the residual k dependent function. One procedure, which permits the elimination of most complex exponentials, has allowed significant changes in the structure of the FFP algorithm, which has resulted in a substantial reduction in computation time. Author

N91-16700*# National Center for Physical Acoustics, University, MS.

DISTORTED-WAVE BORN APPROXIMATION CALCULATIONS FOR TURBULENCE SCATTERING IN AN UPWARD-REFRACTING ATMOSPHERE

Kenneth E. Gilbert, Xiao Di, and Lintao Wang *In* NASA, Langley Research Center, 4th International Symposium on Long-Range Sound Propagation Dec. 1990 p 211-225 Sponsored in part by Navy (For primary document see N91-16682 08-71)

Avail: NTIS HC/MF A12 CSCL 20A

Weiner and Keast observed that in an upward-refracting atmosphere, the relative sound pressure level versus range follows a characteristic 'step' function. The observed step function has recently been predicted qualitatively and quantitatively by including the effects of small-scale turbulence in a parabolic equation (PE) calculation. (Gilbert et al., J. Acoust. Soc. Am. 87, 2428-2437 (1990)). The PE results to single-scattering calculations based on the distorted-wave Born approximation (DWBA) are compared. The purpose is to obtain a better understanding of the physical mechanisms that produce the step-function. The PE calculations and DWBA calculations are compared to each other and to the data of Weiner and Keast for upwind propagation (strong upward refraction) and crosswind propagation (weak upward refraction) at frequencies of 424 Hz and 848 Hz. The DWBA calculations, which include only single scattering from turbulence, agree with the PE calculations and with the data in all cases except for upwind propagation at 848 Hz. Consequently, it appears that in all cases except one, the observed step function can be understood in terms of single scattering from an upward-refracted 'skywave' into the refractive shadow zone. For upwind propagation at 848 Hz, the DWBA calculation gives levels in the shadow zone that are much below both the PE and the data. Author

N91-16701*# Oldenburg Univ. (Germany, F.R.).

WAVE PROPAGATION THROUGH RANDOM MEDIA: A LOCAL METHOD OF SMALL PERTURBATIONS BASED ON THE HELMHOLTZ EQUATION

Ralf Grosse *In* NASA, Langley Research Center, 4th International Symposium on Long-Range Sound Propagation Dec. 1990 p 227-230 (For primary document see N91-16682 08-71)

Avail: NTIS HC/MF A12 CSCL 20A

Propagation of sound through the turbulent atmosphere is a statistical problem. The randomness of the refractive index field causes sound pressure fluctuations. Although no general theory to predict sound pressure statistics from given refractive index statistics exists, there are several approximate solutions to the problem. The most common approximation is the parabolic equation method. Results obtained by this method are restricted to small refractive index fluctuations and to small wave lengths. While the first condition is generally met in the atmosphere, it is desirable to overcome the second. A generalization of the parabolic equation method with respect to the small wave length restriction is presented. Author

N91-16702*# Atmospheric Sciences Office, White Sands Missile Range, NM.

A NOISE ASSESSMENT AND PREDICTION SYSTEM

Robert O. Olsen and John M. Noble *In* NASA, Langley Research Center, 4th International Symposium on Long-Range Sound Propagation Dec. 1990 p 231-244 (For primary document see N91-16682 08-71)

Avail: NTIS HC/MF A12 CSCL 20A

A system has been designed to provide an assessment of noise levels that result from testing activities at Aberdeen Proving Ground, Md. The system receives meteorological data from surface stations and an upper air sounding system. The data from these systems are sent to a meteorological model, which provides forecasting conditions for up to three hours from the test time. The meteorological data are then used as input into an acoustic ray trace model which projects sound level contours onto a two-dimensional display of the surrounding area. This information is sent to the meteorological office for verification, as well as the range control office, and the environmental office. To evaluate

the noise level predictions, a series of microphones are located off the reservation to receive the sound and transmit this information back to the central display unit. The computer models are modular allowing for a variety of models to be utilized and tested to achieve the best agreement with data. This technique of prediction and model validation will be used to improve the noise assessment system. Author

N91-16703*# Planning Systems, Inc., Slidell, LA.
SCATTERING OF SOUND BY ATMOSPHERIC TURBULENCE PREDICTIONS IN A REFRACTIVE SHADOW ZONE
Walton E. McBride, Henry E. Bass, Richard Raspet, and Kenneth E. Gilbert (Mississippi Univ., University.) *In* NASA, Langley Research Center, 4th International Symposium on Long-Range Sound Propagation Dec. 1990 p 245-254 (For primary document see N91-16682 08-71)
Avail: NTIS HC/MF A12 CSCL 20A

According to ray theory, regions exist in an upward refracting atmosphere where no sound should be present. Experiments show, however, that appreciable sound levels penetrate these so-called shadow zones. Two mechanisms contribute to sound in the shadow zone: diffraction and turbulent scattering of sound. Diffractive effects can be pronounced at lower frequencies but are small at high frequencies. In the short wavelength limit, then, scattering due to turbulence should be the predominant mechanism involved in producing the sound levels measured in shadow zones. No existing analytical method includes turbulence effects in the prediction of sound pressure levels in upward refractive shadow zones. In order to obtain quantitative average sound pressure level predictions, a numerical simulation of the effect of atmospheric turbulence on sound propagation is performed. The simulation is based on scattering from randomly distributed scattering centers ('turbules'). Sound pressure levels are computed for many realizations of a turbulent atmosphere. Predictions from the numerical simulation are compared with existing theories and experimental data. Author

N91-16704*# Atmospheric Sciences Office, White Sands Missile Range, NM.
EFFECTS OF LARGE-SCALE WIND DRIVEN TURBULENCE ON SOUND PROPAGATION
John M. Noble, Henry E. Bass, and Richard Raspet (Mississippi Univ., University.) *In* NASA, Langley Research Center, 4th International Symposium on Long-Range Sound Propagation Dec. 1990 p 255-270 (For primary document see N91-16682 08-71)
Avail: NTIS HC/MF A12 CSCL 20A

Acoustic measurements made in the atmosphere have shown significant fluctuations in amplitude and phase resulting from the interaction with time varying meteorological conditions. The observed variations appear to have short term and long term (1 to 5 minutes) variations at least in the phase of the acoustic signal. One possible way to account for this long term variation is the use of a large scale wind driven turbulence model. From a Fourier analysis of the phase variations, the outer scales for the large scale turbulence is 200 meters and greater, which corresponds to turbulence in the energy-containing subrange. The large scale turbulence is assumed to be elongated longitudinal vortex pairs roughly aligned with the mean wind. Due to the size of the vortex pair compared to the scale of the present experiment, the effect of the vortex pair on the acoustic field can be modeled as the sound speed of the atmosphere varying with time. The model provides results with the same trends and variations in phase observed experimentally. Author

N91-16705# Southampton Univ. (England). Inst. of Sound and Vibration Research.
A LOW COST END-FIRE ACOUSTIC RADIATOR
K. R. Holland and F. J. Fahy Sep. 1990 44 p
(ISVR-TR-188; ETN-91-98403) Avail: NTIS HC/MF A03

A low cost end fire directional acoustic radiator for sound reinforcement applications in highly reverberant spaces was developed which consists of an array of holes drilled in a pipe to which is attached a horn compression driver. A mathematical model allows the size, spacing and number of holes to be optimized. Prototype pipes were constructed and tested in an anechoic chamber, and the results show satisfactory agreement between theoretical and measured results. ESA

N91-16706# Aeronautical Research Inst. of Sweden, Stockholm. Dept. of Aerodynamics.
ENVIRONMENTAL NOISE FROM THE NAESUDDEN (SWEDEN) AND MAGLARP (SWEDEN) PROTOTYPE WIND TURBINES: A STUDY OF MACHINERY NOISE
Sten Ljunggren, Melker Johansson, and Per Sahlin (DNV Ingemansson A.B., Sweden) Aug. 1990 102 p
(Contract STEV-506-266-4)
(FFA-TN-1990-34; ETN-91-98530) Avail: NTIS HC/MF A06

The noise generated by the machinery of the two prototypes contains pure tones, which are very important with respect to the environmental impact. The gearbox is shown to be the most important source in both units. It is also shown that a predominant part of the noise is transmitted as structure borne sound from the source to the radiating parts of the structure in the Naesudden unit and as airborne sound in the Maglarp case. The transmission depends heavily on the load bearing properties of the power line. Thus, the noise level around the Naesudden turbine is significantly higher due to its monocoque design than the level of the Maglarp unit where a separate frame is used. Add on measures to reduce this transmission are not easily found as the gearbox acts as a velocity source. The measurements at the Naesudden turbine also show that the radiation from the load bearing hub and the steel blades may be important beside that from the nacelle. The results from Maglarp show in a similar way that the radiation from a steel tower must not be neglected. ESA

N91-16707*# National Aeronautics and Space Administration. Langley Research Center, Hampton, VA.
LAMINA TRANSDUCER COUPLER AND METHOD OF MAKING Patent Application
John A. Companion, inventor (to NASA) (PRC Kentron, Inc., Hampton, VA.) 25 Sep. 1990 15 p
(NASA-CASE-LAR-14361-1; NAS 1.71:LAR-14361-1; US-PATENT-APPL-SN-587920) Avail: NTIS HC/MF A03 CSCL 20A

The invention is a novel lamina transducer coupler and method of making same from a solidified layer of gel-like material. The properties and thickness of the layer determine the acoustical impedance which may also be detachably formed on a suitable substrate. This invention provides a disposable transducer coupler that detachably conforms to the surface of an object to be scanned such as a burn victim. It is essentially self-lubricating though a coating of lubricant may be applied to further reduce the friction between a scanning transducer and the coupler. Since the coupler can be preformed, sterilized and packaged for subsequent use, it is believed to have important ultrasonic medical diagnostic applications. NASA

N91-16708# Wisconsin Univ., Madison. Hearing Development Research Lab.
FIELD MEASUREMENT OF HEAD RELATED TRANSFER FUNCTIONS Final Report, May 1988 - Aug. 1989
Frederic Wightman and Doris J. Kistler Apr. 1990 187 p
(Contract F33615-87-C-0534; AF Proj. 7184)
(AD-A227850; AAMRL-TR-90-019) Avail: NTIS HC/MF A09 CSCL 23/3

This effort sought to refine and simplify techniques for generating acoustic signals that could be used in 3-D auditory displays. Such signals are presented to a listener over headphones and create the illusion of a virtual sound source at a predetermined position in 3-D space. The signals are generated digitally, using algorithms based on the acoustic effects of human outer ear structures on sound waves reaching the ears. To date, the main area of difficulty inhibiting development of practical (3-D) displays is in obtaining estimates of these outer ear effects. The work was divided into three areas: (1) acoustic measurements of free

field-to-eardrum transfer functions (also called head related transfer functions, of HRTFs); (2) analysis of HRTFs; and (3) psychophysical assessment of human performance in sound localization tasks involving stimuli presented both in real and in simulated (virtual) auditory space. The focus was on evaluating means for making HRTF measurements faster and easier, thus simplifying synthesis of auditory stimuli for 3-D displays. GRA

N91-16709# David Taylor Research Center, Bethesda, MD. Dept. of Ship Systems Integration.
SCATSPHERE2: A COMPUTATION FOR THE PLANE-WAVE SCATTERING FROM A SUBMERGED, ELASTIC, SPHERICAL, EVACUATED OR FLUID-FILLED, THIN SHELL Final Report, Oct. 1989 - May 1990
Raymond S. Cheng and Francis M. Henderson Oct. 1990 29 p
(AD-A228867; DTRC-90/029) Avail: NTIS HC/MF A03 CSCL 20/1

Program SCATSPHERE2, a modification of program SCATSPHERE, computes the series solution for the time-harmonic plane-wave scattering by a submerged, elastic, spherical, evacuated, or fluid-filled, thin shell. For program SCATSPHERE2, this report presents the basic scattering theory and the user's instructions. Three examples are also presented involving underwater plane-wave scattering by: (1) an evacuated steel spherical thin shell; (2) a fluid-filled aluminum spherical thin shell; and (3) a fluid-filled aluminum spherical thin shell. GRA

N91-16710# Technische Univ., Delft (Netherlands).
A TIME-DOMAIN FINITE-ELEMENT METHOD FOR THE COMPUTATION OF THREE-DIMENSIONAL ACOUSTIC WAVE FIELDS IN INHOMOGENEOUS FLUIDS AND SOLIDS Ph.D. Thesis
Hendrik Johannes Stam 1990 232 p Sponsored by Shell Exploration and Production Lab., Rijswijk, Netherlands
(ETN-91-98485) Avail: NTIS HC/MF A11

A hybrid method is presented that solves numerically space time acoustic wave problems in a configuration that may consist of fluid and solid parts. The fluids and solids are taken to be linear, locally and instantaneously reacting, and time invariant in their mechanical behavior. The computation of the wave fields in the bounded domain of numerical computation is carried out by a finite element method that is suited to handle the conditions at arbitrarily shaped boundaries and interfaces of the solid-solid, fluid-fluid, and the solid-fluid types. The geometry is discretized into elementary subdomains that are cylindrical in the time direction in four dimensional space time. ESA

72 ATOMIC AND MOLECULAR PHYSICS

Includes atomic structure, electron properties, and molecular spectra.

N91-16711# Ohio State Univ., Columbus. Dept. of Chemistry.
MOLECULAR ORBITAL STUDIES OF THE BONDING IN HEAVY ELEMENT ORGANOMETALLICS
Bruce E. Bursten 23 Mar. 1990 7 p
(Contract DE-FG02-86ER-13529)
(DE90-009732; DOE/ER-13529/2) Avail: NTIS HC/MF A02

This progress report contains highlights of research projects in actinide chemistry. Projects covered are bonding in Np, Pu, and transplutonium organometallic compounds, applications of the discrete variational X(sub alpha) method to actinide chemistry, ab initio calculations on actinide molecules, and experimental comparisons of organoactinide and organotransition metal chemistry. Also included is brief discussions on budgets, funding, invited papers and invited presentations. DOE

N91-16712# Washington Univ., Seattle. Dept. of Physics.
PARITY VIOLATION AND ELECTRON SCATTERING
Ernest M. Henley 1990 10 p Presented at the Workshop on Parity Violation in Electron Scattering, Pasadena, CA, 22-24 Feb. 1990
(Contract DE-FG06-88ER-40427)
(DE90-010429; DOE/ER-40427/04-N90; CONF-9002117-1)
Avail: NTIS HC/MF A02

The history is reviewed of parity nonconservation in electron scattering. In electron scattering, parity violation (PV) is the unique signal which allows the study of the weak interactions among the much stronger electromagnetic ones. It is observed through the detection of a pseudoscalar quantity in the cross section or rate of a reaction. These pseudoscalars usually involve a spin or polarization. Since it is known that spin effects are more sensitive to dynamics than differential or total cross sections, which are partially determined by geometry, PV measurements allows the study of the weak interactions and nucleon and nuclear structure. Because the weak interactions are of short range, the measurements are sensitive to different aspects of the target structure than the long range electromagnetic scattering. DOE

N91-16713# Lawrence Livermore National Lab., CA.
A NEW APPROACH FOR THE DETERMINATION OF ELECTRONIC STRUCTURE
A. Gonis, Eric C. Sowa, and X.-G. Zhang (California Univ., Berkeley. Lawrence Berkeley Lab.) Apr. 1990 34 p Presented at the 20th Annual International Symposium on Electronic Structures of Solids, Gaussig (German Democratic Republic), 16-20 Apr. 1990
(Contract W-7405-eng-48)
(DE90-010479; UCRL-JC-103520; CONF-900455-1) Avail: NTIS HC/MF A03

A new real space multiple scattering theory method for the solution of the Schroedinger equation and the calculation of the electronic structure of solid materials is presented. The fundamental basis of the method is discussed and illustrated with the results of numerical calculations. DOE

N91-16714# Argonne National Lab., IL.
STATE-TO-STATE INELASTIC AND REACTIVE MOLECULAR BEAM SCATTERING FROM SURFACES
Keith R. Lykke and Bruce D. Kay 1990 12 p Presented at the SPIE Optics, Electro-Optics and Laser Applications in Science and Engineering Conference and Exhibition, Los Angeles, CA, 14-19 Jan. 1990
(Contract W-31-109-eng-38)
(DE90-010492; CONF-900140-22) Avail: NTIS HC/MF A03

Resonantly enhanced multiphoton ionization (REMPI) laser spectroscopic and molecular beam surface scattering techniques are coupled to study inelastic and reactive gas surface scattering with state-to-state specificity. Rotational, vibrational, translational and angular distributions were measured for the inelastic scattering of HCl and N2 from Au(111). In both cases the scattering is direct-inelastic in nature and exhibits interesting dynamical features such as rotational rainbow scattering. In an effort to elucidate the dynamics of chemical reactions occurring on surfaces, the quantum resolved scattering studies were extended to include the reactive scattering of a beam of gas phase H-atoms from a chlorinated metal surface M-Cl. The nascent rotational and vibrational distributions of the HCl product are determined using REMPI. The thermochemistry for this reaction on Au indicates that the product formation proceeding through chemisorbed H-atoms is slightly endothermic while direct reaction of a gas phase H-atom with M-Cl is highly exothermic (ca. 50 kcal/mole). Details of the experimental techniques, results and implications regarding the scattering dynamics are discussed. DOE

N91-16715# Toledo Univ., OH. Dept. of Physics and Astronomy.
MEASUREMENTS OF SCATTERING PROCESSES IN NEGATIVE ION-ATOM COLLISIONS Progress Report, 1 Sep. 1989 - 31 Aug. 1990
Thomas J. Kvale 1990 8 p
(Contract DE-FG05-88ER-13971)
(DE90-010666; DOE/ER-13971/6) Avail: NTIS HC/MF A02

This research is designed to study scattering processes which occur in negative ion-atom collisions in the intermediate energy

region. These include: elastic scattering, electron detachment, and possible target inelastic processes. The experimental technique is Ion Energy-Loss Spectroscopy (IELS), which will positively identify the elastic scattering channel as well as any target inelastic processes. The measurements will provide total cross sections initially, and once the angular positioning apparatus is installed, will provide angular differential cross sections. In order to accomplish these goals, construction of an apparatus was necessary, and much of the progress this year involved this construction. DOE

N91-16716# Los Alamos National Lab., NM.
ELECTRON STOPPING POWERS OF SOME ELEMENTS AND COMPOUNDS FROM 0 TO 10,000 eV: A COMPILATION
Joseph J. Devaney Jul. 1989 18 p
(Contract W-7405-eng-36)
(DE90-010675; LA-11625-MS) Avail: NTIS HC/MF A03

Electron stopping powers of hydrogen, helium, nitrogen, oxygen, aluminum, silicon, silicon dioxide, nickel, copper, silver, tungsten, gold, air, collodion, liquid water, polystyrene, polyethylene, aluminum oxide, kaptan, mylar (polyethylene terephthalate), bakelite, lucite, plexiglas (polymethyl methacrylate), perspex, PMMA resist, melinex, and nylon 6,6 are given from 0 to 10,000 eV where available. Ashley's formulae for the stopping power of some organic solids are included. Iskef and Watt's simple formulae are given. The NBS Bethe stopping powers for 51 materials from 1 to 10 keV are reproduced. DOE

N91-16717# Florida State Univ., Tallahassee. Inst. of Molecular Biophysics.
SELECTIVE EXCITATION, RELAXATION, AND ENERGY CHANNELING IN MOLECULAR SYSTEMS Progress Report, May 1987 - Apr. 1990
William C. Rhodes Apr. 1990 18 p
(Contract DE-FG05-86ER-60473)
(DE90-010793; DOE/ER-60473/T1) Avail: NTIS HC/MF A03

These theoretical studies involve the response, relaxation, and correlated motion in the time-dependent behavior of rather large molecular systems. By large systems, it is meant that they have a large number or degrees of freedom. They range in size from a single large polyatomic molecule to a protein molecule in its natural environment. By response, it is meant that changes in the electronic and vibrational motion of a molecule (or a portion of a molecule called a chromophore) due to interactions with an externally applied field (such as light) or to intermolecular interactions in systems not at equilibrium. Such responses are the associated relaxation and the channeling of energy as the system moves toward a new equilibrium. The following topics are covered: davydov soliton theory, squeezed states, multimode molecular quantum mechanics, the phase operator of quantum mechanics, and quantum thermodynamics. DOE

N91-16718# Sandia National Labs., Albuquerque, NM.
THERMAL EMISSION MODEL FOR THE ANNEAL OF RADIATION-INDUCED TRAPPED HOLES
P. J. McWhorter, S. L. Miller, and W. M. Miller 1990 5 p Presented at the 27th IEEE Annual International Nuclear and Space Radiation Effects Conference, Reno, NV, 16-20 Jul. 1990
(Contract DE-AC04-76DP-00789)
(DE90-007285; SAND-90-0344C; CONF-900723-7) Avail: NTIS HC/MF A01

It was found that the anneal of trapped holes can be predicted through the use of a first order thermal emission model. This model allows accurate prediction of long term hole anneal from short term laboratory measurements. DOE

N91-16719# Oak Ridge National Lab., TN.
INTERATOMIC FORCES AND BONDING MECHANISMS IN MgO CLUSTERS
Nancy F. Wright and Gayle S. Painter 1990 6 p Presented at the Spring Meeting of the Materials Research Society, San Francisco, CA, 16-21 Apr. 1990
(Contract DE-AC05-84OR-21400)
(DE90-010148; CONF-900466-15) Avail: NTIS HC/MF A02

We report results from a first-principles local spin density quantum mechanical study of the energetics and elastic properties of a series of magnesium-oxygen clusters of various morphologies. The role of quantum effects, e.g., covalency, in the bonding character of diatomic MgO is determined by comparison of classical and quantum restoring force curves. The dependence of binding properties on geometry and metal to oxygen ratio is determined by comparison of binding energy curves for a series of clusters. Results show that while gross features of the binding curves may be represented by simple interatomic potentials, details require the many body corrections of a full quantum treatment. DOE

N91-16720# Argonne National Lab., IL. Chemistry Div.
PUZZLES OF ELECTRON TRANSFER
John R. Miller 1989 15 p Presented at the International Chemical Congress of Pacific Basin Societies, Honolulu, HI, 17-22 Dec. 1989
(Contract W-31-109-eng-38)
(DE90-010541; CONF-891206-12) Avail: NTIS HC/MF A03

Major progress has been made to dramatically change our concepts of electron transfer reactions over the last several years by defining the distances, energetics, and even orientation of electron donor and acceptors groups. Despite this progress, several open questions remain. These include the lack of clear understanding of the factors controlling the dependence of the rate on distance. Distance dependence of long distance electron transfer rates is often similar in a variety of experimental situations including rigid glasses, donor and acceptors bound to rigid spacer groups, monolayer assemblies and proteins. But two puzzling cases in which the distance dependence is dramatically weaker have not been understood and interpreted. An even more serious lack of understanding for control of rate by orientation. In some cases strong dependence of rates on solvent polarity have been obtained, but in at least one other case, the rates seem to be independent of polarity. Important energetic quantities such as the free energy change and the solvent reorganization energy are often difficult to obtain and are particularly difficult to predict due to inaccuracies of the dielectric continuum model. This chapter compiles a list of many of these problems, but makes no attempt to suggest the nature of their solutions. DOE

N91-16721# Oak Ridge National Lab., TN. Physics Div.
THE THEORY OF ELECTRON-ION COLLISIONS: THE ROLE OF DOUBLY EXCITED STATES
D. C. Griffin, M. S. Pindzola (Auburn Univ., AL.), and C. Bottcher 1989 28 p Presented at the Summer School of Computational Atomic and Nuclear Physics, Sewanee, TN, 26 Jun. - 7 Jul. 1989
(Contracts DE-AC05-84OR-21400; DE-FG05-86ER-53217)
(DE90-011078; CONF-8906270-5) Avail: NTIS HC/MF A03

The important contributions of doubly excited autoionizing states to electron-impact excitation, ionization, and recombination are reviewed. Various theoretical methods of treating these states are considered, and theoretical cross sections are presented and compared to experimental measurements where available. DOE

N91-16722# Columbia Univ., New York, NY. Center for Radiological Research.
RADIATION PHYSICS, BIOPHYSICS, AND RADIATION BIOLOGY Progress Report, 1 Dec. 1989 - 30 Nov. 1990
E. J. Hall and M. Zaider May 1990 109 p
(Contract DE-FG02-88ER-60631)
(DE90-011544; DOE/ER-60631/5) Avail: NTIS HC/MF A06

This annual report contains a summary of our current research. Some highlights include: experimental microdosimetry, track structure, extension of the Dual Radiation Action model to be time dependent, experiments showing that the reverse dose-rate effect for onogenic transformation, first rated for neutrons, has also been observed for charged particles of intermediate LET, an analysis of low dose-rate, research in hyperthermia, studies in molecular cloning, low dose rate studies, experimental studies on high LET, and molecular studies on DNA. DOE

N91-16723# Vanderbilt Univ., Nashville, TN.
THEORETICAL STUDIES OF ATOMIC TRANSITIONS Progress Report, 1 Apr. 1990 - 31 Mar. 1991
Charlotte Froese Fischer Oct. 1990 7 p
(Contract DE-FG05-88ER-13867)
(DE91-000931; DOE/ER-13867/8) Avail: NTIS HC/MF A02

Topics addressed include: lifetime of excited states; core-polarization studies; large relativistic calculations; Monte Carlo Hartree-Fock (MCHF) atomic structure package; and MCHF codes for the hypercube. DOE

N91-16724# Princeton Univ., NJ.
TECHNIQUE FOR DETERMINING THE STATIC POLARIZABILITIES OF REFRACTORY METAL ATOMS
Keith D. Bonin and W. Happer 15 May 1990 26 p
(Contract W-7405-eng-48)
(DE90-017088; UCRL-CR-104249) Avail: NTIS HC/MF A03

A technique is being developed for determining the static polarizabilities of refractory metal atoms. The technique involves producing a dense, cold atomic beam (n is approximate or = to 10(exp 11) to 10 (exp 12) atoms/cu cm, T(perpendicular) is approximate or = to 5 mK) that is illuminated for a short time by a standing wave formed by a Nd:YAG laser. This technique would have an impact on laser isotope separation, ion mobility physics, and theoretical atomic physics. The interaction between the atoms and the laser light results in velocity kicks to the atoms along the two directions defined by the photons in the laser standing wave. The velocity kicks force the atoms to form into planes of alternating high and low density downstream. By Bragg scattering near-resonant light off these planes the static polarizability can be determined. The velocity kicks will also cause the atomic density distribution further downstream to take on a bimodal appearance. A measurement of the separation of the peaks of this distribution can be used to determine the polarizability. Here progress is reported on this technique and the present status of the experiments. A new method for producing focused beams of neutrals, ions, and clusters using two-stage laser ablation was developed as a result of the experiments. DOE

N91-16725# Michigan Univ., Ann Arbor. Dept. of Physics.
THEORY OF NON-EQUILIBRIUM GROWTH Summary Report, 1987 - 1990
1990 43 p
(Contract DE-FG02-85ER-45189)
(DE91-004159; DOE/ER-45189/4) Avail: NTIS HC/MF A03

This report discusses the following topics in growth of solids: pattern formation; disorderly growth; general nonlinear phenomona; and electronic structure. DOE

N91-16726# Stanford Linear Accelerator Center, CA.
THEORETICAL TOPICS IN B-PHYSICS
James D. Bjorken Dec. 1990 29 p Presented at the 18th SLAC Summer Inst. on Particle Physics: Heavy Quarks and Gauge Bosons, Stanford, CA, 16-27 Jul. 1990
(Contract DE-AC03-76SF-00515)
(DE91-004911; SU-SLAC-PUB-5389; CONF-900799-1) Avail: NTIS HC/MF A03

The bottom quark should need no introduction. Other than the undiscovered top quark, it is by far the most fashionable of the six. There is good reason for this. It is bottom-quark behavior which holds out the most hope of measuring and understanding some of the most fundamental and delicate parameters of the standard model -- those having to do with the origin of electroweak mixing - and thereby in all probability also the origin of quark mass. Also interwoven into this is the subject of CP violation, and its proposed interpretation in terms of electroweak mixing. In this section we shall review the basics of electroweak mixing and how it is impacted by the study of b-quark properties. There are by now many lecture series and workshop proceedings devoted to this topic, so I will not try to be comprehensive, but only hit some highlights. DOE

N91-16727*# Eloret Corp., Sunnyvale, CA.
COMPARISON OF THE QUADRATIC CONFIGURATION INTERACTION AND COUPLED CLUSTER APPROACHES TO ELECTRON CORRELATION INCLUDING THE EFFECT OF TRIPLE EXCITATIONS
Peter R. Taylor, Timothy J. Lee, and Alistair P. Rendell (National Aeronautics and Space Administration. Ames Research Center, Moffett Field, CA.) 1990 23 p
(Contract NCC2-371)
(NASA-CR-187855; NAS 1.26:187855) Avail: NTIS HC/MF A03 CSCL 20H

The recently proposed quadratic configuration interaction (QCI) method is compared with the more rigorous coupled cluster (CC) approach for a variety of chemical systems. Some of these systems are well represented by a single-determinant reference function and others are not. The finite order singles and doubles correlation energy, the perturbational triples correlation energy, and a recently devised diagnostic for estimating the importance of multireference effects are considered. The spectroscopic constants of CuH, the equilibrium structure of cis-(NO)2 and the binding energies of Be3, Be4, Mg3, and Mg4 were calculated using both approaches. The diagnostic for estimating multireference character clearly demonstrates that the QCI method becomes less satisfactory than the CC approach as non-dynamical correlation becomes more important, in agreement with a perturbational analysis of the two methods and the numerical estimates of the triple excitation energies they yield. The results for CuH show that the differences between the two methods become more apparent as the chemical systems under investigation becomes more multireference in nature and the QCI results consequently become less reliable. Nonetheless, when the system of interest is dominated by a single reference determinant both QCI and CC give very similar results. Author

N91-16728*# National Aeronautics and Space Administration. Ames Research Center, Moffett Field, CA.
TRIPLE AND QUADRUPLE EXCITATION CONTRIBUTIONS TO THE BINDING IN Be CLUSTERS: CALIBRATION CALCULATIONS ON Be3
John D. Watts, Ivan Cernusak, Jozef Noga, Rodney J. Bartlett, Charles W. Bauschlicher, Jr., Timothy J. Lee, Alistair P. Rendell, and Peter R. Taylor (Eloret Corp., Palo Alto, CA.) 1991 16 p
(Contract NCC2-371)
(NASA-TM-103391; NAS 1.15:103391) Avail: NTIS HC/MF A03 CSCL 20H

The contribution of connected triple and quadruple excitations to the binding in Be3 is investigated by comparing various coupled-cluster (CC) and truncated configuration interaction (CI) treatments with multireference CI (MRCI) and full CI(FCI) calculations. The CC method with single and double excitations (CCSD) produces results that differ substantially from more elaborate treatments, but most extensions to CCSD that account approximately for connected triple excitations perform very well. In constrast, good agreement with FCI for Be2 can be achieved only with the highest level CC and MRCI methods. Author

N91-16729# Bonn Univ. (Germany, F.R.). Inst. fuer Physik.
DESIGN AND TESTING OF A PROTON DETECTOR Thesis [BAU UND TEST EINES PROTONENDETEKTORS]
Georg Kranefeld Aug. 1990 57 p In GERMAN; ENGLISH summary
(BONN-IR-90-34; ISSN-0172-8741; ETN-91-98561) Avail: NTIS HC/MF A04

A prototype of a proton telescope for nonmagnetic proton detectors is designed. The detector was made of three scintillation counters which are used as dE/dx counter, energy counter and veto counter. The telescope was calibrated by using elastic electron proton scattering and was tested with quasielastic electrodisintegration of the deuteron, in which a missing mass resolution of 5.1 MeV was achieved. It was shown that such detectors are well suited for proton detection and identification. ESA

N91-16730# Bonn Univ. (Germany, F.R.). Inst. fuer Physik.
TESTING OF LEAD GLASS DETECTORS FOR ELECTRON PROOF IN THE ELAN EXPERIMENT Thesis [TEST VON BLEIGLASDETEKTOREN ZUM ELEKTRONENNACHWEIS IM ELAN-EXPERIMENT]
Ruth Tauchen Sep. 1990 53 p In GERMAN; ENGLISH summary
(BONN-IR-90-38; ISSN-0172-8741; ETN-91-98562) Avail: NTIS HC/MF A04

The ELAN (Electron Diffusion At Nucleons) experiment investigates scattering of electrons at light nuclei at the ELSA (Electron Stretcher and Accelerator), which allows nonmagnetic spectrometers to detect electrons and hadrons. For measurements of small cross sections, large solid angle detectors must be used. Lead glass detectors were employed for elastic scattered electrons. It was shown that the relative energy resolutions and the energies in a counter depend on the input location of the primary particles. ESA

N91-16731# Bonn Univ. (Germany, F.R.). Inst. fuer Physik.
A MOLLER POLARIMETER FOR THE EXTRACTED ELSA-RAY Thesis [ARBEITEN AN EINEM MOELLERPOLARIMETER FUER DEN EXTRAHIERTEN ELSA-STRAHL]
Renate Reuter Sep. 1990 44 p In GERMAN; ENGLISH summary
(BONN-IR-90-42; ISSN-0172-8741; ETN-91-98564) Avail: NTIS HC/MF A03

Experiments with a polarized electron beam, planned at ELSA (Electron Stretcher and Accelerator), are described. The polarization degree of longitudinally polarized electrons can be measured by using the spin dependence of the elastic electron-electron cross section (Moller-scattering). Because of their lower energy, the Moller electrons can be separated from the primary beam by a dipole magnet at the beam line, whose field must be measured to compare measured and theoretical counting rates. The field chart was used in a Monte-Carlo simulation of the experiment. ESA

N91-16732# Max-Planck-Inst. fuer Physik und Astrophysik, Garching (Germany, F.R.).
MEASUREMENT OF THE e+e- ANNIHILATION IN mu+mu- PAIRS AT THE Z SUP o RESONANCE Thesis - Ludwig-Maximilians-Univ. [MESSUNG DER E+E- ANNIHILATION IN MU+MU- -PAARE AN DER Z SUP 0-RESONANZ]
Alexander Jahn Sep. 1990 105 p In GERMAN
(MPI-PAE/EXP.EL-231; ETN-91-98567) Copyright Avail: NTIS HC/MF A06

The total effective cross section and the charge asymmetry for the process e+e- in mu+mu- are investigated for gravity center energies in the area 88.3 to 95 GeV. The 1,001 muon pairs and 242,264 hadronic Z-decays, which could be filtered from 540,000 solved events, were analyzed. The background of particles from high cosmic radiation was experimentally evaluated at (0.43 + or - 0.22) percent. The charge asymmetry for muons was studied as a function of the Weinberg angle. The function profile corresponds to the ultrarelativistic Born approximation without consideration of radiation corrections. ESA

73 NUCLEAR AND HIGH-ENERGY PHYSICS

Includes elementary and nuclear particles; and reactor theory.

For space radiation see *93 Space Radiation.*

N91-16733# Brookhaven National Lab., Upton, NY.
AGS SILICON GOLD COLLISIONS MEASURED IN THE E-810 TPC (TIME PROJECTION CHAMBER)
B. E. Bonner, J. A. Buchanan, C. S. Chan, C. S. Chiou, J. M. Clement, M. D. Corcoran, A. Etkin, K. J. Foley, R. W. Hackenburg, and T. J. Hallman (Johns Hopkins Univ., Baltimore, MD.) et al 26 Mar. 1990 12 p Presented at the Heavy Ion Physics at the Alternating Gradient Synchrotron, Upton, NY, 5-7 Mar. 1990 Submitted for publication
(Contracts DE-AC02-76CH-00016; DE-AS05-81ER-40032; DE-AC02-83ER-40107; DE-AC02-76ER-03274)
(DE90-010015; BNL-44431; CONF-900331-2) Avail: NTIS HC/MF A03

The tracking detector of Alternating Gradient Synchrotron (AGS) Experiment 810 is a three-piece Time Projection Chamber (TPC) intended to measure all charged tracks in the forward hemisphere of the nucleon-nucleon center of mass system, i.e., forward of an angle of about 20 degrees in the lab. Each module of the TPC contains twelve rows of short anode wires which give 3-D space points on each track, but no dE/dx information useable for particle identification. The TPC was operated in a beam of silicon ions at the end of June 1989 and the results are reported of analysis of the data taken with a thin gold target in that run. A similar amount of data was gathered from thin copper and silicon targets, the analysis of which is in a less advanced state. The results of the investigation of the neutral strange particle decays appear in a separate contribution by Al Saulys. The current state of the analysis of the charged tracks from the silicon gold collisions is presented. DOE

N91-16734# Maryland Univ., College Park. Dept. of Physics and Astronomy.
ADVANCED METHODS FOR THE COMPUTATION OF PARTICLE BEAM TRANSPORT AND THE COMPUTATION OF ELECTROMAGNETIC FIELDS AND BEAM-CAVITY INTERACTIONS
Alex J. Dragt and Robert L. Gluckstern Apr. 1990 8 p
(Contract DE-AS05-80ER-10666)
(DE90-011071; DOE/ER-10666/8) Avail: NTIS HC/MF A02

The University of Maryland Dynamical Systems and Accelerator Theory Group carries out research in two broad areas: the computation of charged particle beam transport using Lie algebraic methods and advanced methods for the computation of electromagnetic fields and beam-cavity interactions. Important improvements in the state of the art are believed to be possible in both of these areas. In addition, applications of these methods are made to problems of current interest in accelerator physics including the theoretical performance of present and proposed high energy machines. The Lie algebraic method of computing and analyzing beam transport handles both linear and nonlinear beam elements. Tests show this method to be superior to the earlier matrix or numerical integration methods. It has wide application to many areas including accelerator physics, intense particle beams, ion microprobes, high resolution electron microscopy, and light optics. With regard to the area of electromagnetic fields and beam cavity interactions, work is carried out on the theory of beam breakup in single pulses. Work is also done on the analysis of the high frequency behavior of longitudinal and transverse coupling impedances, including the examination of methods which may be used to measure these impedances. Finally, work is performed on the electromagnetic analysis of coupled cavities and on the coupling of cavities to waveguides. DOE

N91-16735# California Univ., Berkeley. Lawrence Berkeley Lab. Nuclear Science Div.
PRODUCTION OF HIGH INTENSITY RADIOACTIVE BEAMS
J. M. Nitschke Apr. 1990 15 p Presented at the Workshop on the Science of Intense Radioactive Ion Beams, Los Alamos, NM, 10-12 Apr. 1990
(Contract DE-AC03-76SF-00098)
(DE90-011340; LBL-28924; CONF-9004209-1) Avail: NTIS HC/MF A03

The production of radioactive nuclear beams world-wide is reviewed. The projectile fragmentation and the ISOL approaches are discussed in detail, and the luminosity parameter is used throughout to compare different production methods. In the ISOL approach, a thin and a thick target option are distinguished. The role of storage rings in radioactive beam research is evaluated. It is concluded that radioactive beams produced by the projectile

fragmentation and the ISOL methods have complementary characteristics and can serve to answer different scientific questions. The decision of which kind of facility to build has to depend on the significance and breadth of these questions. Finally, a facility for producing a high intensity radioactive beams near the Coulomb barrier is proposed, with an expected luminosity of approximately 10(exp 39)/(sq cm x sec), which would yield radioactive beams in excess of 10(exp 11)/sec. DOE

N91-16736# Lawrence Livermore National Lab., CA.
IS THERE HOPE FOR FUSION
T. Kenneth Fowler (California Univ., Berkeley.) 12 Apr. 1990 11 p Presented at the 2nd University of California Global Climate Change Workshop, Davis, CA, 6-8 Sep. 1989
(Contract W-7405-eng-48)
(DE90-012095; UCRL-JC-103526; CONF-8909192-2) Avail: NTIS HC/MF A03

From the outset in the 1950's, fusion research has been motivated by environmental concerns as well as long-term fuel supply issues. Compared to fossil fuels both fusion and fission would produce essentially zero emissions to the atmosphere. Compared to fission, fusion reactors should offer high demonstrability of public protection from accidents and a substantial amelioration of the radioactive waste problem. Fusion still requires lengthy development, the earliest commercial deployment being likely to occur around 2025 to 2050. However, steady scientific progress is being made and there is a wide consensus that it is time to plan large-scale engineering development. A major international effort, called the International Thermonuclear Experimental Reactor (ITER), is being carried out under IAEA auspices to design the world's first fusion engineering test reactor, which could be constructed in the 1990's. DOE

N91-16737# Argonne National Lab., IL. High Energy Physics Div.
ANALYTIC MULTI-REGGE THEORY AND THE POMERON IN QCD
Alan R. White 10 May 1990 139 p
(Contract W-31-109-eng-38)
(DE90-012153; ANL-HEP-PR-90-28) Avail: NTIS HC/MF A07

The formalism of Analytic Multi-Regge Theory is developed as a basis for the study of abstract Critical and Super-Critical Pomeron high-energy behavior and for related studies of the Regge behavior of spontaneously broken gauge theories and the Pomeron in QCD. Asymptotic domains of analyticity for multiparticle amplitudes are shown to follow from properties of Field Theory and S-Matrix Theory. General asymptotic dispersion relations are then derived for such amplitudes in which the spectral components are described by the graphical formalism of hexographs. Further consequences are distinct Sommerfeld-Watson representations for each hexograph spectral component, together with a complete set of angular momentum plane unitarity equations which control the form of all multi-Regge amplitudes. Because of this constraint of Reggeon Unitarity the Critical Pomeron solution of the Reggeon Field Theory gives the only known non-trivial unitary high-energy S-Matrix. By exploiting the full structure of multi-Regge amplitudes as the Pomeron becomes Super-Critical, the simultaneous modification of hadrons and the Pomeron can be studied. The result is a completely consistent description of the Super-Critical Pomeron appearing in hadron scattering. Reggeon Unitarity is satisfied in the Super-Critical Phase by the appearance of a massive gluon (Reggeised vector particle) coupling pair-wise to the Pomeron. DOE

74 OPTICS

Includes light phenomena; and optical devices.
For lasers see *36 Lasers and Masers.*

N91-16738# Mound Lab., Miamisburg, OH.
PC-BASED DIGITAL IMAGING FOR STORING MICROSCOPY IMAGES FOR SURVEILLANCE PROGRAMS
Patrick M. Schleitweiler and Mark H. Ransick 1990 7 p Presented at the 16th DOE Compatibility, Aging and Service Life Conference, Livermore, CA, 24-26 Apr. 1990
(Contract DE-AC04-88DP-43495)
(DE90-010080; MLM-3633(OP); CONF-9004146-8) Avail: NTIS HC/MF A02

Advances in video technology and digital imaging have resulted in the ability to produce an image in high quality digital format. Images that are created and viewed in a digital format can be quantitatively measured and then stored on disk for later examination. Write-once read many (WORM) optical disks are excellent media for permanently archiving digital images. One of the best applications for this image storage technology is storage of microscopy images for surveillance programs. Currently, the most common type of recording medium used in service laboratories is Polaroid instant developing film. The short developing time and ease in processing make it well suited for most high volume laboratories. But the convenience of this film has a substantial price tag. Depending on the type of film, each picture can cost about $1.50. The two metallurgical support laboratories at Mound are frequently required to make multiple copies for design agencies or program managers. Permanent archiving of photos is required for both WR and surveillance samples. This has made Polaroid film a significant part of the expense budget. In addition, the thousands of photos taken annually present a considerable storage problem. DOE

N91-16739# Edgerton, Germeshausen and Grier, Inc., Idaho Falls, ID.
A CONVENIENT SYSTEM FOR DIFFRACTION MOIRE MEASUREMENTS
V. A. Deason and M. B. Ward 1989 10 p Presented at the Western Regional Strain Gage Committee Meeting, Idaho Falls, ID, 22 Aug. 1989
(Contract DE-AC07-76ID-01570)
(DE90-010980; EGG-M-89360; CONF-8908128-2) Avail: NTIS HC/MF A02

This device utilizes single mode polarization maintaining optical fibers to generate the pair of laser beams required by diffraction moire interferometry. Design of the device permits extremely rapid and convenient setup for measurement of in-plane displacement distributions on the surfaces of specimens. The device, applications, and typical data are described. DOE

N91-16740# Columbia Univ., New York, NY.
DEVELOPMENT OF LIQUID XENON IMAGING GAMMA-RAY SPECTROPHOTOMETERS Final Report, 1 Jun. 1983 - 30 Nov. 1989
Robert Novick and Elena Aprile Jul. 1990 48 p
(Contracts N00014-83-K-0494; N00014-86-C-0086)
(AD-A227575; CAL-1811R) Avail: NTIS HC/MF A03 CSCL 20/6

The application of liquid xenon in high resolution, low background and efficient gamma-ray detectors for the observation in space of weak sources emitting in the 0.1 to 10 MeV energy region is investigated. The basic requirement of ultra-high purity liquid xenon, necessary for the successful operation of these detectors was satisfied with the development of an efficient and reliable purification system, capable of reducing and maintaining the concentration of electronegative impurities below one part in 109. The charge and energy resolution response of a liquid xenon (and liquid argon) ionization chamber has been systematically measured as a function of electric field strength, using various radioactive sources. The results of 4.5 percent FWHM and 2.6 percent FWHM at 1 MeV in liquid xenon and liquid argon, respectively are the best reported in the literature. Their deviation from theoretical estimates based on Fano factor statistics was interpreted as due to recombination straggling on low energy delta-electrons produced along the primary ionizing particle. The effect of photosensitive dopants in the liquid was also measured. Improved charge collection and energy resolution is observed for the case of alpha particles. In view of its application for event

triggering in an imaging ionization chamber, the yield of the primary scintillation light abundantly emitted in liquid Xenon was measured using both electrons and alpha particles. GRA

N91-16741# OPTRA, Inc., Beverly, MA.
FIBER OPTIC SYNTHETIC APERTURE INTERFEROMETER Final Technical Report, Aug. 1987 - Mar. 1990
Michael Hercher Aug. 1990 50 p
(Contract F19628-87-C-0204)
(AD-A227891; RADC-TR-90-177) Avail: NTIS HC/MF A03 CSCL 20/6

This report describes a Fiber Optic Stellar Interferometer built by Optra, Inc. for the purposes of (1) measuring stellar diameters using a pair of small portable telescopes (rather than a large observatory telescope), and (2) measuring atmospheric turbulence. The key element of this concept is the use of singlemode optical fibers to link the separate small telescopes with the interferometer module. We have shown that the proposed turbulence measurements are entirely feasible using a distant light source (preferably a laser). The demonstration of the ability to obtain white light fringes through the fibers was not successful. We believe that this is due to a mismatch in the lengths of the fibers, and we have proposed a simple and flexible solution to this problem. GRA

N91-16742# Rochester Univ., NY. Inst. of Optics.
NONLINEAR OPTICAL SYSTEMS INTERACTING WITH AMPLITUDE-MODULATED OPTICAL FIELDS Ph.D. Thesis
Stephen H. Chakmakjian Jul. 1990 201 p
(Contract DAAL03-86-K-0173)
(AD-A228221; ARO-24626.155-PH-UIR) Avail: NTIS HC/MF A10 CSCL 09/3

The interaction is studied of amplitude-modulated (AM) optical fields with various nonlinear systems. An experimental and theoretical analysis of three distinct nonlinear systems is treated: two level atoms interacting with a 100 percent AM field; a four level laser amplifier with an AM pump intensity; and a multimode dye laser with an AM pump intensity. A 100 percent AM field is the limiting case of strong modulation in which the energy at the carrier frequency is completely suppressed, and only the modulation sidebands remain. The interaction of such an optical field with an ensemble of radiatively broadened two level atoms (an optically pumped sodium atomic beam is used) yields a complicated series of parametric resonances when both the Rabi frequency and the modulation frequency are large compared with the atomic transition linewidth. The time averaged fluorescence, and therefore, the absorption of energy exhibits parametric resonant enhancement whenever the modulation frequency is equal to a subharmonic of the Rabi frequency. Population oscillations in a multilevel laser amplifier are studied using weak AM spectroscopy. Two laser fields are applied to a four level laser amplifier (alexandrite is used as the amplifier). GRA

N91-16743# Colorado Univ., Boulder. Dept. of Physics.
APPLICATIONS OF NON-LINEAR OPTICS Final Report, 1 Mar. 1987 - 28 Feb. 1990
Dana Z. Anderson 28 Feb. 1990 20 p Submitted for publication
(Grant AF-AFOSR-0163-87; AF Proj. 2301)
(AD-A228872; AFOSR-90-1103TR) Avail: NTIS HC/MF A03 CSCL 20/6

Spatial mode-multiplexing is used to transmit several communication channels on a single multimode optical fiber. Each channel is encoded by an orthogonal pattern produced by a spatial light modulator. A photorefractive medium holographically decodes the output speckle pattern at a receiver station. A ring and star architectures for interconnection networks is demonstrated. Typical crosstalk to signal ratios, for fully interconnected 3 processor networks, are -24 and -26 dB for the ring and star respectively. GRA

N91-16744 Texas Univ., Austin.
THE DESIGN OF A TWO-DIMENSIONAL OPTICAL IMAGE CORRELATOR AND ITS APPLICATION IN IMAGE TRACKING Ph.D. Thesis
Shahriar Ghaffari 1990 142 p
Avail: Univ. Microfilms Order No. DA9031573

The design and characteristics of an optical image correlator was investigated. The optical image correlator uses an acousto-optic (A-O) cell to convert the real-time video information (1-dimensional) into a spatial light intensity controller system. A 2-dimensional template is utilized to store the reference image to be correlated to the real-time video frames. As a result of the multiplication effects of the 2-D template light distribution by the pixel values of the real-time video signals, through the A-O cell, new light distribution is generated. The new light distribution in conjunction with the spatial movement results in an equivalent of the image correlation if integrated on a CCD detector. The application of the optical image correlator is primarily concentrated in a general purpose tracking system. One frame of the video images is stored as the reference image and all of the proceeding images are correlated with a sub-section of the stored image. The result of the image correlation is a video image with a relative maximum gray level located at the center of the best match between the reference image and the real-time images. The tracking system is based on finding the maximum intensity location within the output of the optical image correlator. The movement of the target can be calculated by measuring the location of the maximum intensity from one frame to the next. The detected movement provides a signal for feedback control of the image position. Dissert. Abstr.

N91-16745# Messerschmitt-Boelkow-Blohm G.m.b.H., Munich (Germany, F.R.). Information und Dokumentation.
OPTICAL TRANSCEIVER FRONTEND FOR HIGH SPEED BUS STANAG 3910 WITH ONE FIBER ONLY
Bodo Tilly 1990 9 p Presented at the EMFFOC/LAN 1990, Munich, Fed. Republic of Germany 25-26 Jun. 1990
(MBB-UA-1182-90-PUB; ETN-91-98506) Avail: NTIS HC/MF A02

The 200/280 micron glass fiber bus system is planned to be installed into the European Fighter Aircraft (EFA). Hybrid integration includes an optical fiber bidirectional T-coupler for aeronautical use. This mode of acting saves 50 percent of the cost intensive glass fiber installation, one reflective star coupler included, and therefore doubles the reliability of the new system. Significant transceiver frontend requirements had to be considered due to the concept of high speed bus STANAG 3910. In particular it is the intertransmission dynamic range on the receiver side: control of 23 dB signal level swing within the short time of 2 microseconds. And the optical power output of 0.5 dBm at the wavelength of 830 nm with the rise and fall times of 10 ns, using a surface emitting light emitting diode on the transmitter side. The data rate is 20 Mbit/s encoded in Manchester 2 format. That requires a wide receiver bandwidth (greater than 30 MHz) and a wide dynamic range (greater than 25 dB) to guarantee a bit error rate less than or equal to 10 (exp -10). The minimum optical power obtained is -37 dBm. Further details with values near to theoretical limits are given. ESA

N91-16746# Technische Univ., Delft (Netherlands).
PROGRAMMABLE SURFACE ACOUSTIC WAVE DETECTION IN SILICON: DESIGN OF PROGRAMMABLE FILTERS Ph.D. Thesis
Jacobus Cornelis Haartsen 29 Nov. 1990 217 p
(ETN-91-98568) Avail: NTIS HC/MF A10

The design and implementation of programmable surface acoustic wave (SAW) detectors in ZnO-SiO2-Si layered structures is explained. An overview is given of the application of programmable filters in radar and communication systems. The fundamentals of SAW techniques are reviewed. The realization of SAW detectors, whose output can be controlled electronically, is investigated. A new active SAW detector composed merely of

junction electrodes is presented. The complete monolithic programmable filter is considered. An overview of the electronic circuitry is given. ESA

75 PLASMA PHYSICS

Includes magnetohydrodynamics and plasma fusion.
For ionospheric plasmas see *46 Geophysics*. For space plasmas see *90 Astrophysics*.

N91-16747# Brookhaven National Lab., Upton, NY.
V(SUP 0) PRODUCTION WITH 14.5 GeV/c SILICON BEAMS
B. E. Bonner, J. A. Buchanan, C. S. Chan, C. N. Chious, J. M. Clement, M. D. Corcoran, A. Etkin, K. J. Foley, R. W. Hackenburg, and T. J. Hallman (Johns Hopkins Univ., Baltimore, MD.) 26 Mar. 1990 18 p Presented at the Heavy Ion Physics at the Alternating Gradient Synchrotron, Upton, NY, 5-7 Mar. 1990 Submitted for publication
(Contracts DE-AC02-76CH-00016; DE-AC02-83ER-40107; DE-AS05-81ER-40032; DE-AC02-76ER-03274)
(DE90-010014; BNL-44429; CONF-900331-3) Avail: NTIS HC/MF A03

Lambda, K sub s sup 0 and bar Lambda production with 14.5 GeV/c Silicon beams is dealt with. Lambda sup 0 production is studied. Because the study of strangeness is an important part of the search for Quark Gluon Plasma (QGP). Many models predict an enhancement of strangeness in a QGP as compared to the amount of strangeness produced in a superposition of nucleon-nucleon interactions. The amount of enhancement varies from model to model. Even if no QGP is detected at Alternating Gradient Synchrotron (AGS) energies using Si beams, it is important to understand the production mechanisms in quantitative detail so that standard nucleon-nucleon production mechanism can be distinguished from QGP formation. The advantage of measuring strangeness production by measuring V sup 0 production is that V sup 0's can be identified by kinematics without the use of any special particle ID detectors. The disadvantage is that usually large aperture detectors are required. Experiment 810 has the needed large aperture. The technique and results of V sup 0 production from approx. 9000 interactions of Si in a 1 mil (25 micron) Au target are described. DOE

N91-16748# Texas Univ., Austin. Inst. for Fusion Studies.
WAVE-PARTICLE POWER TRANSFER IN A STEADY-STATE DRIVEN SYSTEM
H. L. Berk, B. N. Breizman (Academy of Sciences, USSR, Novosibirsk), and S. Hamaguchi Mar. 1990 11 p
(Contract DE-FG05-80ET-53088)
(DE90-010031; DOE/ET-53088/424; IFSR-424) Avail: NTIS HC/MF A03

The general expression of the power transfer from a high energy ion beam to a background electrostatic plasma wave is obtained as a function of an arbitrary wave amplitude. The injection ions are assumed to slow down through classical transport processes and form a weakly destabilizing distribution function. It is verified that phase space gradients produced by a finite amplitude wave enhances the power transfer significantly, as was also indicated in earlier work. DOE

N91-16749# General Atomic Co., San Diego, CA.
SCALING DIMENSIONALLY SIMILAR TOKAMAK DISCHARGES TO IGNITION
R. E. Waltz, J. C. DeBoo, and M. N. Rosenbluth Apr. 1990 5 p Presented at the 17th European Conference on Controlled Fusion and Plasma Heating, Amsterdam, Netherlands, 25-29 Jun. 1990 Prepared in cooperation with California Univ., San Diego Submitted for publication
(Contract DE-AC03-89ER-51114)
(DE90-010079; GA-A-20077; CONF-900602-7) Avail: NTIS HC/MF A01

The tokamak operates in a variety of confinement regimes suggesting there may be several transport mechanisms in combination. The detailed parametric dependence of each is likely to be very complicated. However, it can be argued that all plasma diffusion mechanisms can be divided into the extremes of gyro-Bohm (gB) or Bohm (B) types depending on their scaling with ion gyroradius rho sub s relative to the minor radius a: rho sub s a. These correspond to turbulent diffusion processes with short or long step sizes scaled to rho sub s or a, respectively. The local diffusivities and confinement times can be written as D sub gB = (c sub s/a) rho sub s sup 2 F sub gB or D sub B = c sub s rho sub s F sub B and tau sub gB = B sup -1 (rho sub s/a) sup -3 bar F sub gB or tau sub B = B sup -1 (rho sub s/a) sup -2 bar F sub B, respectively. The form factors are possibly complicated functions of the dimensionless parameters associated with geometry, atomic and profile parameters, and the plasma parameters collisionality (cflx nu) (proportional to) nu a/c sub s and beta. Discharges with all these dimensionless parameters including rho sub s/a the same would have tau (proportional to) B sup -1 and could be called dimensionally identical in their transport properties. It is well known that isolating the dependence on the dimensionless variables imposes a single constraint on the scaling of tau with respect to machine variables. It is observed that while dimensionally identical discharges cannot be scaled to ignition, existing and proposed ignition regime tokamak discharges can have all these dimensionless parameters the same except rho sub s/a. Such discharges are called dimensionally similar and focus on the scalings with respect to rho sub s/a. DOE

N91-16750# Los Alamos National Lab., NM.
A MIRNOV LOOP ARRAY FOR FIELD-REVERSED CONFIGURATIONS
Michel Tuszewski 1990 13 p Presented at the 8th Topical Conference on High-Temperature Plasma Diagnostics, Hyannis, MA, 6-10 May 1990
(Contract W-7405-eng-36)
(DE90-010607; LA-UR-90-1366; CONF-900557-2) Avail: NTIS HC/MF A03

An array of 64 magnetic pick-up loops has been used for stability studies of large field-reversed configurations in the FRX-C/LSM device. This array proved reliable, could resolve signals of a few Gauss, and allowed the detection of several plasma instabilities. DOE

N91-16751# InterScience, Inc., Troy, NY.
STATUS OF TARGET PHYSICS FOR INERTIAL CONFINEMENT FUSION
Mar. 1990 36 p Presented at a review at DOE Headquarters, Germantown, MD, 14-17 Nov. 1988
(DE90-008221; DOE/DP-0078T) Avail: NTIS HC/MF A03

A four day review to assess the status of target physics of inertial confinement fusion was held at U.S. Department of Energy (DOE) Headquarters on November 14 to 17, 1988. This review completes the current series of reviews of the inertial fusion program elements to assess the status of the data base for a decision to proceed with the proposed Laboratory Microfusion Facility (LMF) that is being planned. In addition to target physics, the program elements that have been reviewed previously include the driver technology development for KrF and solid-state lasers, and the light-on beam pulsed power system. This series of reviews was undertaken for internal DOE assessment in anticipation of the ICF program review mandated by the Congress in 1988 to be completed in 1990 to assess the significance and implications of the progress that has been realized in the laboratory and the underground Halite/Centurion experiments. For this target physics review, both the direct and the indirect drive approaches were considered. The principal issues addressed in this review were: (1) the adequacy of the present target physics data base in making a decision to proceed with design and construction of LMF now as opposed to continuing planning activities at this time; (2) the desirability of specific additional target physics data in reducing the risk involved in a DOE decision to construct an LMF; (3) the continuing role of Halite/Centurion experiments; (4) the priority given to the direct drive approach; and (5) the optimal

program-elements structure to resolve the critical issues of an LMF decision. Specific findings relating to these five issues are summarized. DOE

N91-16752# General Atomic Co., San Diego, CA.
D3-D RESEARCH OPERATIONS Annual Report, 1 Oct. 1988 - 30 Sep. 1989
P. Politzer, ed. Apr. 1990 139 p
(Contract DE-AC03-89ER-51114)
(DE90-008232; GA-A-19922) Avail: NTIS HC/MF A07

This paper discusses research at the D3-D tokamak reactor. The topics covered under the general heading of research program/scientific progress are: confinement, boundary physics, beta and stability, rf heating, and current drive. The operations section includes: tokamak operations, neutral beam operations, ECH/ICH operations, and shielding radiation studies. Program development focuses on: transport diagnostics, advanced divertor, 110 GHz ECH system, fast wave current drive, pellet injector. Collaborative work on D3-D and international cooperation are addressed and the following topics are covered under support services: quality assurance, planning and control, computer operations, and safety. ITER/CIT contributions are also covered and a list of FY89 publications is presented. DOE

N91-16753# Sandia National Labs., Albuquerque, NM. Nuclear Energy Science and Material Technology Div.
PLASMA-FACING MATERIALS
W. B. Gauster Apr. 1990 24 p
(Contract DE-AC04-76DP-00789)
(DE90-008243; SAND-90-0396) Avail: NTIS HC/MF A03

The interaction of plasmas with materials is reviewed and a status summary is given based on experience in large fusion experiments, laboratory investigations, and design studies. The phenomena that are discussed limit the power densities and confinement properties attainable in plasmas; their control is an essential element of the design of future fusion devices. DOE

N91-16754# Argonne National Lab., IL.
A FREE BOUNDARY PROBLEM ARISING IN PLASMA PHYSICS
Hans G. Kaper and Kam Kwong Man 1989 11 p Presented at the Gregynog International Conference on Nonlinear Diffusion Equations and Their Equilibrium States, Newton, England, 20-29 Aug. 1989
(Contract W-31-109-eng-38)
(DE90-010065; CONF-8908178-2) Avail: NTIS HC/MF A03

This article is concerned with free boundary problems for the differential equation u'' + (1/x)u' + f(u) = 0, x greater than 0. In particular, it addresses the questions of existence and uniqueness of a finite point P and a solution u satisfying the conditions u'(0) = 0; u(x) greater than 0, x between 0 and P; u(P) = u'(P) = 0. Among the admissible nonlinearities are functions of the type f(u) = u(exp p) - u(exp q) for certain combinations (p, q), where 0 less than or equal to q less than p less than or equal to 1, including the special case f(u) = square root of u - 1, which has been proposed in plasma physics as a simple model for Tokamak equilibria with magnetic islands. DOE

N91-16755# Los Alamos National Lab., NM.
US-JAPAN WORKSHOP ON FIELD-REVERSED CONFIGURATIONS WITH STEADY-STATE HIGH-TEMPERATURE FUSION PLASMAS AND THE 11TH US-JAPAN WORKSHOP ON COMPACT TOROIDS
D. C. Barnes, comp., J. C. Fernandez, comp., and D. J. Rej, comp. May 1990 220 p Workshop held in Los Alamos, NM, 7-9 Nov. 1989
(Contract W-7405-eng-36)
(DE90-010253; LA-11808-C; CONF-8911130) Avail: NTIS HC/MF A10

The U.S.-Japan Workshop on Field-Reversed Configurations with Steady-State High-Temperature Fusion Plasma and the 11th U.S.-Japan Workshop on Compact Toroids were held at Los Alamos National Laboratory, Los Alamos, New Mexico on November 7 to 9, 1989. These proceedings contain the papers presented at the workshops as submitted by the authors. These papers have been indexed separately. DOE

N91-16756# Oak Ridge National Lab., TN. Physics Div.
INITIAL CALORIMETRY EXPERIMENTS IN THE PHYSICS DIVSION, ORNL (OAK RIDGE NATIONAL LABORATORY)
D. P. Hutchinson, C. A. Bennett, R. K. Richards, J. S. Bullock, IV, and G. L. Powell (Oak Ridge Y-12 Plant, TN.) May 1990 14 p
(Contract DE-AC05-84OR-21400)
(DE90-010301; ORNL/TM-11356) Avail: NTIS HC/MF A03

Four calorimetry experiments were performed with palladium cathode electrolysis cells to investigate the possibility of cold fusion heat production based on the reported results of Fleischmann and Pons. Two of the cells contained 6.35-mm-diam x 10-cm-long palladium cathodes in a 0.2-M (6)LiOD electrolyte; one cell contained a similar cathode in a 0.1-M (6)LiOD electrolyte solution; and one cell used a cast 1.27-cm-diam x 10-cm-long palladium rod in a 0.2-M electrolyte. All four cells were constructed with platinum wire anodes. One of the cells exhibited an apparent 2-3 W power excess for a period of approximately 300 hours of a total operating time of 1800 hours; each of the remaining cells remained in power balance for the 1800 hour period. DOE

N91-16757# Wisconsin Univ., Madison. Dept. of Physics.
THE MADISON SYMMETRIC TORUS
R. N. Dexter, D. W. Kerst, T. W. Lovell, S. C. Prager, and J. C. Sprott Mar. 1990 21 p
(Contract DE-FG02-85ER-53198)
(DE90-010306; DOE/ER-53198/154) Avail: NTIS HC/MF A03

The Madison Symmetric Torus (MST) is the newest and largest reversed field pinch presently in operation. It incorporates a number of design features that set it apart from other pinches, including the use of the conducting shell as both a vacuum vessel and single-turn toroidal field coil. Specially insulated voltage gaps are exposed to the plasma. Magnetic field errors at these gaps as well as at the various diagnostic and pumping ports are minimized through a variety of techniques. The physics goals of MST include study of the effect of large plasma size on confinement and the investigation, in detail, of RFP turbulence, dynamo and transport. Details of the design and initial operation of the device are presented. DOE

N91-16758# Lawrence Livermore National Lab., CA.
MICROWAVE TOKAMAK EXPERIMENT (OMTX): OVERVIEW AND STATUS
May 1990 19 p
(Contract W-7405-eng-48)
(DE90-010287; UCRL-ID-103486) Avail: NTIS HC/MF A03

The Microwave Tokamak Experiment, now under construction at the Laboratory, will use microwave heating from a free electron laser. The intense microwave pulses will be injected into the tokamak to realize several goals, including a demonstration of the effects of localized heat deposition within magnetically confined plasma, a better understanding of energy confinement in tokamaks, and use of the new free electron laser technology for plasma heating. DOE

N91-16759# Lawrence Livermore National Lab., CA.
ELECTRICAL POWER FROM INERTIAL CONFINEMENT FUSION: ISSUES AND PROSPECTS
Michael T. Tobin, John H. Pitts, Charles D. Orth, Ralph W. Moir, William J. Hogan, Roger O. Bangerter, and Wayne R. Meier Mar. 1990 20 p Revised
(Contract W-7405-eng-48)
(DE90-010332; UCID-21849-REV-1) Avail: NTIS HC/MF A03

The following topics are discussed on using inertial confinement for electrical power generation: general economic issues; design of reactors; safety and environmental issues; and development issues. DOE

N91-16760# Columbia Univ., New York, NY. Dept. of Applied Physics.
TRANSPORT SIMULATION OF THE EFFECT OF IMPURITY RADIATION ON THE HIGH BETA, OHMIC START-UP OF THE HBT-EP TOKAMAK
M. K. VijayaSankar and M. E. Mauel 1990 17 p
(Contract DE-FG02-86ER-53222)
(DE90-010333; DOE/ER-53222/102) Avail: NTIS HC/MF A03

The effect is given of impurity radiation on the attainment of high beta and high temperature for an ohmic discharge in the case of a tokamak like (High Beta Tokamak) HBT-EP. Time dependent, one dimensional transport calculations were done using the HERMES code. The permissible impurity influx from the wall was found to decrease with increase in the magnetic field. For attaining a plasma temperature around 100 eV with the value of (beta) close to the Troyon (beta) limit, the maximum magnetic field was found to be around 0.6 Tesla with a maximum permissible impurity influx of about 0.2 percent of the hydrogen ion flux reaching the wall. DOE

N91-16761# Lawrence Livermore National Lab., CA.
CHARACTERIZATION OF DISRUPTIONS IN THE MICROWAVE TOKAMAK EXPERIMENT (MTX)
E. B. Hooper and M. A. Makowski (TRW, Inc., Redondo Beach, CA.) 30 Mar. 1990 35 p
(Contract W-7405-eng-48)
(DE90-010352; UCRL-ID-103473) Avail: NTIS HC/MF A03

The Microwave Tokamak Experiment (MTX) has a substantial number of fast diagnostics, especially for electrons, as part of its mission for pulsed, high-power electron cyclotron heating. As part of its contribution to ITER R and D, these diagnostics are being used to characterize disruptions in MTX. This report is the first of two, with the second planned for submittal in September 1990, at the end of the ITER conceptual design activity. Here, we analyze the characteristics of disruptions during normal operation of MTX, discuss some new data pertaining to the Granetz limit, and describe preliminary data on ramped density shorts which will be used for fast measurements on density limit disruptions. The final report will discuss measurements using the fast diagnostics to characterize the disruption. DOE

N91-16762# Texas Univ., Austin. Fusion Research Center.
TEXAS EXPERIMENTAL TOKAMAK Technical Progress Report, Apr. 1989 - Apr. 1990
Alan J. Wootton Apr. 1990 19 p
(Contract DE-FG05-88ER-53267)
(DE90-011070; DOE/ER-53267/3) Avail: NTIS HC/MF A03

The following work on the text tokamak is discussed: data systems; particle confinement; impurity transport; plasma rotation; runaway electrons; electron cyclotron heating; FIR system; transient transport; internal turbulence; edge turbulence; ion temperature; EML experiments; impurity pellet experiments; MHD experiments and analysis; TEXT Upgrade; and Upgrade diagnostics. DOE

N91-16763# Maryland Univ., College Park. Lab. for Plasma Research.
MICROWAVE GENERATION FOR MAGNETIC FUSION ENERGY APPLICATIONS, TASK B Progress Report, 15 Sep. 1989 - 14 Sep. 1990
T. M. Antonsen, Jr., W. W. Destler, V. L. Granatstein, B. Levush, I. D. Mayergoyz, and A. Singh May 1990 40 p
(Contract DE-FG05-87ER-52147)
(DE90-011079; DOE/ER-52147/T1) Avail: NTIS HC/MF A03

One of the main issues in the development of high power gyrotrons is the present discrepancy between the theoretically predicted efficiency and that observed in the experiments. Recent 140 GHz experiments by MIT employed three cavities; two of the cavities have different interaction lengths and the third cavity is a complex two-section cavity. In all cases, the maximum experimental efficiency is well below the theoretically predicted one. A better theoretical understanding of the causes of these discrepancies is essential to the scaling of gyrotrons to higher power and higher frequency. We continued our investigation with the objective of determining whether mode competition and velocity spread in the electron beam could in some way be influencing the current result from the MIT 140 GHz gyrotrons experiments and determining to what extent these effects would influence operation of a 1 MW, 280 GHz, TE(sub 42,7) gyrotron as conceived at MIT. In our investigations, we used two models, the fixed axial field profile model and the self-consistent determination of the axial field profile model. With the fixed axial field profile model we studied the effect of thermal spread on the efficiency of gyrotrons operation, mode competition between unequally spaced modes, and we simulated the start up of the MIT 140 GHz gyrotrons. Our main conclusions from all these studies are discussed in this paper. DOE

N91-16764# Maryland Univ., College Park. Lab. for Plasma Research.
MICROWAVE GENERATION FOR MAGNETIC FUSION ENERGY APPLICATIONS, TASK C Progress Report, 15 Sep. 1989 - 14 Sep. 1990
T. M. Antonsen, Jr., W. W. Destler, V. L. Granatstein, B. Levush, I. D. Mayergoyz, and A. Singh May 1990 29 p
(Contract DE-FG05-87ER-52147)
(DE90-011080; DOE/ER-52147/T2) Avail: NTIS HC/MF A03

This report discusses: depressed collectors for a radially extracted beam; depressed collectors for quasi optical gyrotrons; general approach to design of depressed collectors; and effect on alpha of non-adiabatic changes in B-field. DOE

N91-16765# Argonne National Lab., IL. Fusion Power Program.
ELECTROMAGNETIC COMPUTATIONS FOR FUSION DEVICES
Larry R. Turner Sep. 1989 7 p Presented at the COMPUMAG Tokyo Conference, Tokyo, Japan, 3-7 Sep. 1989
(Contract W-31-109-eng-38)
(DE90-011097; CONF-8909331-1) Avail: NTIS HC/MF A02

Among the difficulties in making nuclear fusion a useful energy source, two important ones are producing the magnetic fields needed to drive and confine the plasma, and controlling the eddy currents induced in electrically conducting components by changing fields. All over the world, researchers are developing electromagnetic codes and employing them to compute electromagnetic effects. Ferromagnetic components of a fusion reactor introduce field distortions. Eddy currents are induced in the vacuum vessel, blanket and other torus components of a tokamak when the plasma current disrupts. These eddy currents lead to large forces, and 3-D codes are being developed to study the currents and forces. DOE

N91-16766# Argonne National Lab., IL.
THE MEASUREMENT OF GAMMA HEATING IN A FUSION BLANKET TEST ASSEMBLY
H. K. Chiu (Illinois Univ., Urbana.), E. F. Bennett, and B. J. Micklich 1989 4 p Presented at the 13th IEEE Symposium on Fusion Engineering, Knoxville, TN, 2-6 Oct. 1989
(Contract W-31-109-eng-38)
(DE90-011154; CONF-891007-120) Avail: NTIS HC/MF A01

Determining the distribution of gamma heating in fusion test assemblies will help guide the construction and operation of future experiments. Currently the dominant technique for spatial characterization of heating is the wide dispersal of thin film TLD's, which are limited to measurement of the total neutron + gamma dose. Heating is measured using calibrated proportional counters, which allows for the rejection of fast pulse rise events characteristic of ionizations produced by neutron induced atomic recoils. A coupled calculational and experimental program designed to demonstrate this capability was initiated at ANL. An irradiation assembly composed of graphite filled 5 x 5 x 61 cm Mg sleeves in cubic geometry was constructed. This assembly was then irradiated in turn with Co-60 gammas and 14.8 MeV neutrons produced by a D-T neutron generator in two sets of measurements with the proportional counter occupying various positions in the central channel of the assembly. Calculation of the expected dose in the assembly due to the sources at the positions of interest were made. These calculations first generated the neutral flux

profile in the assembly with either ANISN or MCNP depending on the degree of detail used in the modelling of the counter. The profile is then fed into a charged particle generation model to obtain the charged particle profiles, hence energy deposition in the assembly. A comparison was made between these calculations of the energy deposition and measured energy deposition in the assembly. It is hoped that by understanding this comparison a clear picture of gamma heating in a mixed gamma and neutron environment will be obtained. DOE

N91-16767# Pennsylvania State Univ., University Park. Dept. of Nuclear Engineering.
KINETIC STABILITY OF FIELD-REVERSED CONFIGURATIONS Progress Report, 15 Dec. 1989 - 15 May 1990
Ming-Yuan Hsiao and Joseph L. Staudenmeier May 1990 4 p
(Contract DE-FG02-90ER-53302)
(DE90-011530; DOE/ER-53302/2) Avail: NTIS HC/MF A01

This project studies the linear stability of global MHD-like modes in the Field Reversed Configuration (FRC) within the context of the Vlasov-fluid model (Vlasov ions, cold massless fluid electrons). The approach taken is to use unstable MHD eigenfunctions as basis functions to solve a variational form of the linearized Vlasov-fluid equations. In this approach the Vlasov-fluid dispersion functional is separated into a fluid-like part and a part that depends on the ion orbits in the equilibrium electric and magnetic fields. The fluid-like part is equivalent in form to the MHD energy principle without the compressibility term. The part that depends on the equilibrium particle orbits contains finite larmor radius effects, the Hall effect and the parallel kinetic effects. The dispersion functional is solved by numerical computation. This project will try to determine the scaling of the Vlasov-fluid growth rates of unstable modes with variations in FRC equilibrium parameters such as s (the approximate number of ion gyroradii between the magnetic axis and the separatrix of the FRC), elongation, and other profile parameters. DOE

N91-16768# Lawrence Livermore National Lab., CA.
THEORETICAL STUDIES OF TOKAMAKS
T. Kenneth Fowler, L. M. Grossman, and J. P. Holdren Apr. 1990 34 p Prepared in cooperation with California Univ., Berkeley, CA
(Contract W-7405-eng-48)
(DE90-011332; UCRL-CR-103859) Avail: NTIS HC/MF A03

Work since the interim report, September 1988, has concentrated on development of a simplified fusion reactor design code and fusion reactor risk analysis. Also work has continued on the transport models discussed in the interim report but with little further progress. On further analysis, the result reported for a model yielding tau(sub E) proportional to kappa(sup 2P) was found to be an artifact of the normalization chosen. Other models have been explored but none so far looks promising to explain the empirically observed scaling of tau(sub E) with elongation kappa. DOE

N91-16769# Lawrence Livermore National Lab., CA.
SCALING LAWS FOR FEMTOSECOND LASER-PLASMA INTERACTIONS
M. D. Rosen Dec. 1989 11 p Presented at the SPIE Optics, Electro-Optics, and Laser Applications in Science and Engineering Conference and Exhibition, Los Angeles, CA, 15-19 Jan. 1990
(Contract W-7405-eng-48)
(DE90-011496; UCRL-102484; CONF-900140-27) Avail: NTIS HC/MF A03

We present scaling laws for the interaction of femtosecond high power lasers with solid targets. We solve for scale lengths and temperatures of the hot dense plasma in both the classical and flux limited electron thermal conduction regimes, and apply those results to the prediction of radiation output from these targets. The radiative yield and duration are given as functions of both laser and target conditions. Our results compare quite favorably with sophisticated numerical simulations. DOE

N91-16770# Ames Lab., IA. Dept. of Chemistry.
FUNDAMENTAL CHARACTERISTICS AND APPLICATIONS OF AN INDUCTIVELY COUPLED PLASMA AS AN ION SOURCE FOR MASS SPECTROMETRY Ph.D. Thesis
Jeffrey Scott Crain Jan. 1990 102 p
(Contract W-7405-eng-82)
(DE90-011746; IS-T-1413) Avail: NTIS HC/MF A06

Noise power spectra of the (85)Rb(+) signal and the (93)Nb(+) signal from an inductively coupled plasma-mass spectrometer were compared to the noise power spectrum of Sr 2 emission from the plasma. Discrete frequency noise in the emission at the mass spectrometer sampling orifice was found to be nearly identical to that in the mass spectrometer signal. However, discrete frequency noise in emission from the plasma alone differed substantially in frequency from that in the mass spectrometer signal. The dependence of noise frequencies on plasma operating conditions was generally the same for the mass spectrometric measurements and both emission measurements. These results indicate that the plasma was the source of discrete frequency noise in the mass spectrometric signal. The major source of signal instability in this particular ICP-mass spectrometer was found to be 1/f noise. A new, home-made ICP-mass spectrometer was used to study the influence of Na, K, and U on ion signals from Y, Co, and As. In general, analyte signals were suppressed in the presence of excess matrix element. The extent of suppression was greatest for the element with high ionization energy and least for the element with the smallest ionization energy. These trends in the interference effect could be altered by applying a positive voltage to the first element of the ion optics. When the skimmer orifice diameter was made smaller than the sampling orifice diameter, analyte signal suppression was uniform and more extensive. Under these conditions, the heavy matrix element induced more suppression than did the light matrix element. DOE

N91-16771# Lawrence Livermore National Lab., CA.
STARK-EFFECT MEASUREMENT OF HIGH FEL ELECTRIC FIELDS IN MTX BY LASER-AIDED PARTICLE-PROBE SPECTROSCOPY
T. Oda, K. Odajima, K. Mizuno, K. Ohasa, M. Shiho, K. Takiyama (Hiroshima Univ., Japan), J. Foote, and D. G. Nilson May 1990 12 p Presented at the 8th Topical Conference on High-Temperature Plasma Diagnostics, Hyannis, MA, 6-10 May 1990
(Contract W-7405-eng-48)
(DE90-011911; UCRL-102939; CONF-900557-5) Avail: NTIS HC/MF A03

A diagnostic system was constructed to measure the electric field (greater than 100 kV/cm) of a free electron laser (FEL) beam when injected into the plasma of the Microwave Tokamak Experiment (MTX). The apparatus allows a crossed beam measurement, with 2 cm spatial resolution in the plasma, involving the FEL beam (with 140 GHz, approx. 1-GW ECH pulses), a neutral helium beam, and a dye laser beam. After the laser beam pumps metastable helium atoms to higher excited states, their decay light is detected by a collimated optical system. Because of the Stark effect due to the FEL electric field (rvec E), a forbidden transition can be strongly induced. The intensity of emitted light resulting from the forbidden transition is proportional to E sq. Because photon counting rates are calculated to be low, extra effort is made to minimize background and noise levels. It is possible that the lower (rvec E) of an MTX gyrotron produced ECH beam with its longer duration pulses also can be measured using this method. Other applications may include measurements of ion temperature (using charge exchange recombination), edge density fluctuations, and core impurity concentrations. DOE

N91-16772# Los Alamos National Lab., NM.
SPATIAL DISTRIBUTIONS OF THE EMITTING SPECIES IN A PENNING SURFACE-PLASMA SOURCE
H. Vernon Smith, Jr., Paul Allison, J. David Schneider, and Kourosh Saadatmand (Grumman Aerospace Corp., Bethpage, NY.) 1990 4 p Presented at the 2nd European Particle Accelerator Conference, Nice, France, 11-16 Jun. 1990

(Contract W-7405-eng-36)
(DE90-011996; LA-UR-90-1878; CONF-900603-1) Avail: NTIS HC/MF A01

Using optical spectroscopy, the spatial and temporal distributions were studied of the H(sub alpha), CsI(4555A), CsII(4604A), and MoI(3903A) emissions lines in a Penning surface plasma source (SPS). A diagnostic slit exposes the entire SPS discharge gap either parallel or perpendicular to the magnetic field. The spatial and temporal distributions of the emitting species are recorded using a 1 m monochromator. The visible light and the H(sub alpha) and CsII(4604A) spatial distributions are also recorded with a video camera. The cesium atomic and ionic light, and molybdenum atomic light, is strongly concentrated near the cathodes; the visible light and the H(sub alpha) light is almost uniform in both directions. These measurements are presented and discussed. DOE

N91-16773# Lawrence Livermore National Lab., CA.
MOTIONAL STARK EFFECT POLARIMETRY FOR THE CURRENT PROFILE DIAGNOSTIC IN D3-D
D. Wroblewski, K. H. Burrell, L. Lao, P. Politzer, and W. P. West (General Atomic Co., San Diego, CA.) Apr. 1990 15 p Presented at the 8th Topical Conference on High-Temperature Plasma Diagnostics, Hyannis, MA, 6-10 May 1990
(Contracts W-7405-eng-48; DE-AC03-89ER-51114)
(DE90-012071; UCRL-JC-103464; CONF-900557-8) Avail: NTIS HC/MF A03

Motional Stark effect produces large net linear polarization of hydrogenic beam emissions. Measurement of the polarization direction permits the determination the local magnetic field pitch angle. Design of a single point, spatially scannable, high sensitivity polarimeter installed on DIII-D is described. Excellent signal-to-noise ratio with good temporal and spatial resolution was obtained in preliminary measurements of magnetic field pitch angle. DOE

N91-16774# Oak Ridge National Lab., TN.
THE CIT PHYSICS PROGRAM
R. Goldston, G. Bateman, M. Bell, P. Colestock, S. Jardin, S. Medley, R. Perkins, N. Pomphrey, J. Schmidt, and D. Stotler et al 1990 5 p Presented at the 17th European Conference on Controlled Fusion and Plasma Heating, Amsterdam, Netherlands, 25-29 Jun. 1990 Prepared in cooperation with Princeton Univ., NJ.;Texas Univ., Austin; Massachusetts Inst. of Technology; Lawrence Livermore National Lab.; California Univ., Los Angeles; and General Atomics, San Diego, CA
(Contract DE-AC05-84OR-21400)
(DE90-012134; CONF-900602-13) Avail: NTIS HC/MF A02

The mission of the CIT device is to determine the physics behavior of self-heated fusion plasmas, and to demonstrate the production of substantial amounts of fusion power. In order to achieve this mission at minimum risk and cost, CIT is designed to be a high field, compact, copper-coil device, of modest pulse length. The best measure of extrapolation in confinement properties is the dimensionless parameter omega(sub c)tau(sub E). CIT is projected to stand midway between JET and ITER in this parameter, and so represents a relatively modest step. Nonetheless, because nTtau(sub E) is proportional to B for dimensionlessly similar devices (aB(exp 4/5) = const.). CIT should have about the same nTtau(sub E) as ITER, -10x that of JET. Standard assumptions on confinement, impurity levels, and profile shapes project to Q = 25, with 20 MW of heating power, corresponding to beta = 3 percent (=21/aB) and a total fusion output power of 500 MW. Even given pessimistic projection assumptions, CIT can achieve its basic mission to determine the confinement physics, operational limits, and alpha-particle dynamics of self-heated fusion plasmas with alpha power greater than auxiliary heating power, while producing more than 100 MW of fusion power. In order to reach these conditions CIT will also demonstrate heating, fueling, and plasma handling techniques necessary to produce reactorlike power density, self-heated fusion plasmas. DOE

N91-16775# Lawrence Livermore National Lab., CA.
A MODEL FOR THE PREDICTION OF Nb3Sn CRITICAL CURRENT AS A FUNCTION OF FIELD, TEMPERATURE, STRAIN, AND RADIATION DAMAGE
L. T. Summers, M. W. Guinan, J. R. Miller, and P. A. Hahn 21 Sep. 1990 6 p Presented at the Applied Superconductivity Conference, Aspen, CO, 24-28 Sep. 1990
(Contract W-7405-eng-48)
(DE91-000656; UCRL-100531; CONF-900944-7) Avail: NTIS HC/MF A02

Conductors designed for fusion machines must operate at high fields, under large mechanical loads, and in a high neutron flux. Present designs favor the use of Nb3Sn with force-cooling by supercritical helium to extract large nuclear and ac loss heat loads. Consequently, the magnet designer must have a good knowledge of the critical current of the superconductor as a function of field, strain, temperature, and radiation damage. Expanding on work by Hampshire, et al. and Ekin, combined with radiation damage studies of Nb3Sn, the critical field (B sub c20) is expressed as function of temperature, strain and damage energy (E sub d). Similarly, the zero-field critical temperature (T sub c0) is expressed as a function of strain and damage energy. The expressions of B(sub c20) and T(sub c0) are combined into a functional form that allows an accurate and consistent estimate of the critical current density at the operating conditions of fusion magnet conductors. DOE

N91-16776# Mission Research Corp., Nashua, NH.
IR PLASMA EMISSIONS Final Report, Aug. 1986 - Mar. 1990
Precila C. F. Ip and Russell A. Armstrong Apr. 1990 118 p
(Contract F19628-86-C-0100; AF Proj. 2310)
(AD-A227713; MRC-MSH-R-90-003; GL-TR-90-0131) Avail: NTIS HC/MF A06 CSCL 20/9

This final report summarized the latest results in data acquisition and various modeling efforts of the GL-LINUS plasma. Plasma radiance equations relevant to the LINUS plasma are first reviewed. Experimental data on the early-time plasma continuum are next presented. This is followed by discussions of the calculations on Stark broadening, hydrodynamics, and kinetics. Finally, recommendations on future experiments and calculations are made based on the present results. GRA

N91-16777# Los Alamos National Lab., NM.
THE LOS ALAMOS MEGAMP FIBER Z-PINCH EXPERIMENT
D. W. Scudder, J. S. Shlachter, J. E. Hammel, F. Venneri, R. Chrien, R. Lovberg, and R. Riley (California Univ., San Diego.) 1990 13 p Presented at the Workshop on Physics of Alternative Magnetic Confinement Schemes, Varenna, Italy, 14-15 Oct. 1990
(Contract W-7405-eng-36)
(DE91-004842; LA-UR-90-3877; CONF-9010209-6) Avail: NTIS HC/MF A03

The HDZP-II experiment uses a 2 MV, 1.9 Ohm, 1.2 MA, 100 ns risetime pulsed-power driver. Preliminary experiments have been performed at 600 to 800 kA (half the bank energy). Preliminary results show the plasma heating to several kilovolts (although a non-Maxwellian distribution is likely) while maintaining an overall straight and reasonably uniform axial configuration. However, interferograms and x ray pinhole photographs show the column expanding rapidly with considerable small-scale structure, presumably due to m equal 0 activity. The neutron yield (typically 5 x 10(exp 9)) is consistent with thermonuclear reactions at the reduced density although detailed study of the neutron characteristics has not been performed. Preliminary isotropy measurements do not show significant neutron anisotropy. DOE

N91-16778# Los Alamos National Lab., NM.
NEUTRON MEASUREMENTS IN SEARCH OF COLD FUSION
R. E. Anderson, C. A. Goulding, M. W. Johnson, K. B. Butterfield, S. Gottesfeld, D. A. Baker, T. E. Springer, F. H. Garzon, R. D. Bolton, and E. M. Leonard et al 1990 19 p Presented at the Conference on Anomalous Nuclear Effects in Deuterium/Solid Systems, Provo, UT, 22-24 Oct. 1990
(Contract W-7405-eng-36)

(DE91-004855; LA-UR-90-3964; CONF-9010266-1) Avail: NTIS HC/MF A03

We have conducted a research for neutron emission from cold fusion systems of the electrochemical type and, to a lesser extent, the high-pressure gas cell type. Using a high-efficiency well counter and an NE 213 scintillator, the experiments were conducted on the earth's surface and in a shielded cave approximately 50 ft underground. After approximately 6500 h of counting time, we have obtained no evidence for cold fusion processes leading to neutron production. However, we have observed all three types of neutron data that have been presented as evidence for cold fusion: large positive fluctuations in the neutron counting rate, weak peaks near 2.5 MeV in the neutron energy spectrum, and bursts of up to 145 neutrons in 500-microsecond intervals. The data were obtained under circumstances that clearly show our results to be data encountered as a part of naturally occurring neutron background, which is due primarily to cosmic rays. Thus, observing these types of data does not, in itself, provide evidence for the existence of cold fusion processes. Artifacts in the data that were due to counter misbehavior were also to lead to long-term neutron bursts whose time duration varied from several hours to several days. We conclude that any experiments which attempt to observe neutron emission must include strong steps to ensure that the experiments deal adequately with both cosmic-ray processes and counter misbehavior. DOE

N91-16779# SFA, Inc., Landover, MD.
INVESTIGATION AND MODELING OF RADIATION ABSORPTION PROCESSES AND OPACITIES IN DENSE PLASMAS Final Report, 1 Apr. 1988 - 28 Feb. 1990
Uday Gupta Sep. 1990 101 p
(Contract F49620-88-C-0055)
(AD-A228749; SFA-0184Z; AFOSR-90-1073TR) Avail: NTIS HC/MF A06 CSCL 20/9

A variety of atomic processes contribute to absorption of radiation in dense plasmas. Most existing atomic data are for low density, high temperature plasmas. At high densities and low temperatures, realistic modeling to incorporate the important additional effects in order to generate atomic data in needed. This is addressed in the present work. The models and computer codes developed for the project includes effects of non-linear screening, electron degeneracy, exchange-correlation and ion interactions self-consistently. These were applied to ions of specific configurations in dense plasmas and represent improvements over average atom models often used in dense plasma physics. The focus of this work is mainly on the bound-bound, bound-free and free-free photoprocesses, the contribute to radiation absorption and opacity of dense, low temperature plasmas. We discuss a model to generate ionic distribution that is computationally faster than rate equation method. We also discuss a model to investigate the d.c. electron conduction in dense plasmas, which incorporates effects of multiple scattering and improves over the Ziman type model. These self-consistent models and computer codes are very useful tools to generate large data bases for atomic processes contributing to radiation absorption and opacities in dense plasmas. Those data would be a useful input to simulation of radiative properties of dense plasmas in various laboratory and astrophysical conditions. GRA

N91-16780# Technische Univ., Eindhoven (Netherlands).
MICROWAVE INTERFEROMETER AND REFLECTOMETER TECHNIQUES FOR THERMONUCLEAR PLASMAS Ph.D. Thesis
Coenraad Albertus Ja Hugenholtz 1990 136 p Sponsored by Netherlands Organization for Applied Scientific Research TNO, Delft and EURATOM
(ETN-91-98478) Avail: NTIS HC/MF A07

A description of the 2 mm microwave interferometer designed and built for the Joint European Torus (JET) experiment is given. Results of measurements of the plasma density show a high phase resolution. The three CO2 laser interferometers built for experiments are described. A detailed description of the 12 channel heterodyne reflectometer designed and built for JET is given. Measurements in a mock up, using a plane mirror, show that it is possible to obtain the required accuracy. First results of measurements are shown. A description is given of a heterodyne reflectometer to measure high velocities of plasmoids. ESA

N91-16781# Stuttgart Univ. (Germany, F.R.). Inst. fuer Plasmaforschung.
STUDY ON ECW TRANSMISSION LINES FOR NET/ITER Final Report
W. Henle, A. Jacobs, W. Kasparek, H. Kumric, G. A. Mueller, P. G. Schueller, and M. Thumm Brussels, Belgium Commission of the European Communities Oct. 1990 104 p In GEORGIAN
(Contracts EES-333/88-11/FU-D; NET-88-1-82)
(EUR-FU/80/90-99; ETN-91-98503) Avail: NTIS HC/MF A06

The use of ECW (Electron Cyclotron Waves) in NET/ITER is considered for plasma formation and local current density profile control by Doppler upshifted non inductive current drive near the q = 2 magnetic surface, in order to prevent major disruptions. The general philosophy adopted for the design of the ECW system, is to place the most critical components as far as possible from the plasma and the machine. The parametric study of a 20 MW, CW reference transmission line system, at 140 GHz and of a corresponding optional system at 200 GHz showed that the hybrid system employing quasi optical gyrotron output mode converters, polarizers and antenna reflectors together with low loss long distance transmission through tubular HE11 wave guide using elbow bends, is most attractive. ESA

N91-16782# Max-Planck-Inst. fuer Physik und Astrophysik, Garching (Germany, F.R.). Inst. fuer Extraterrestrische Physik.
NUMERICAL EXAMINATIONS OF KELVIN-HELMHOLTZ INSTABILITY IN RESISTIVE COMPRESSIBLE MAGNETOHYDRODYNAMICS Thesis - Tech. Univ. Munich [NUMERISCHE UNTERSUCHUNGEN ZUR KELVIN-HELMHOLTZ INSTABILITAET IN DER RESISTIVEN KOMPRESSIBLEN MAGNETOHYDRODYNAMIK]
Stefan Cronjaeger Sep. 1990 90 p In GERMAN
(MPE-221; ISSN-0178-0719; ETN-91-98566) Copyright Avail: NTIS HC/MF A05

Simulations of the compressible and resistive magneto-hydrodynamic equations are achieved in the linear or non-linear cases. A particular configuration of the magnetic field was chosen in which the field component parallel to the plasma flows was in different directions on both sides of the boundary surface. The growth rates and the formation of magnetic islands was investigated by varying magnetic field intensities, pressure and density. Magnetic islands are found to be limited by field lines, in an area whose size is independent of the sound velocity and magnetic field intensity and always have the same shape. The transport of kinetic and magnetic energy was studied and the mixture of the materials through the boundary surface was analyzed. ESA

76 SOLID-STATE PHYSICS

Includes superconductivity.

For related information, see also *33 Electronics and Electrical Engineering* and *36 Lasers and Masers.*

N91-16783# Argonne National Lab., IL.
HYPERFINE INTERACTIONS ASSOCIATED WITH IRON SUBSTITUTED SUPERCONDUCTING OXIDES
D. E. Ellis, B. D. Dunlap, E. Baggio Saitovich, J. Souza Azevedo, R. B. Scorzelli, and C. W. Kimball (University of Northern Illinois, De Kalb.) Jun. 1989 11 p Presented at the Latin American Conference on the Applications of the Moessbauer Effect, Rio de Janeiro, Brazil, 31 Oct. - 4 Nov. 1988
(Contract W-31-109-eng-38)
(DE90-010411; CONF-8810423-1) Avail: NTIS HC/MF A03

Theoretical and experimental Moessbauer spectroscopy studies have been made concerning charge and spin densities and magnetic hyperfine fields H(sub hf), in iron-substituted

superconducting oxides. Calculations were carried out in the self-consistent-field embedded cluster model using local density theory SCF-X(alpha), with a variational atomic orbital basis. Spectral densities and changes in charge and spin density were monitored around neighboring Cu sites, as well as Fe impurity site, and La2Cu(1-x)Fe(x)O4 and YBa2Cu(3-x)Fe(x)O(7-y) compounds. Moessbauer isomer shifts (IS), quadrupole splittings (QS), and H(sub hf) are obtained by fitting multiline models to the observed spectra and are compared with SCF-X(alpha) results for specific lattice sites. The influence of oxygen vacancies and partial oxygen disorder is modeled and compared with the experimental data on variable oxygen content and disorder. DOE

N91-16784# Argonne National Lab., IL. Advanced Photon Source Div.
MODELING THE PERFORMANCE OF WATER AND LIQUID GALLIUM COOLED X RAY OPTICAL COMPONENTS: A COMPARISON WITH EXPERIMENT
J. Chrzas, A. M. Khounsary, D. M. Mills, and P. J. Viccaro Dec. 1989 17 p Presented at the 7th Synchrotron Radiation Instrumentation National Conference, Berkeley, CA, 7-10 Aug. 1989
(Contract W-31-109-eng-38)
(DE90-010460; CONF-890802-27) Avail: NTIS HC/MF A03

Thermal and structural analyses of a water or liquid gallium cooled silicon crystal x ray monochromator subjected to high heat loads were carried out using a finite element method. From the computed strain distributions in the crystal rocking curves were produced and compared with experimentally measured rocking curves. Good agreement between the general width and shape of the calculated and measured rocking curve profiles was obtained. This initial agreement between calculation and measurement provides the foundation for the extension of the modeling to the prediction of x ray optical component performance with more complex cooling schemes. Such elaborate cooling techniques may be required for the increased power loadings that will be produced by insertion devices in the next generation of low emittance storage ring sources such as the Advanced Photon Source (APS) to be constructed at Argonne National Laboratory. DOE

N91-16785# Stanford Linear Accelerator Center, CA.
DEEP INELASTIC STRUCTURE FUNCTIONS FROM ELECTRON SCATTERING ON HYDROGEN, DEUTERIUM, AND IRON AT 0.6 GeV2 LESS THAN OR EQUAL TO Q2 LESS THAN OR EQUAL TO 30.0 GeV2 Ph.D. Thesis
L. W. Whitlow Mar. 1990 203 p
(Contract DE-AC03-76SF-00515)
(DE90-010169; SU-SLAC-357) Avail: NTIS HC/MF A10

The final results are reported from experiment E140, a recent deep inelastic electron-deuterium and electron-iron scattering experiment at SLAC. In addition, the results are presented of a combined global analysis of all SLAC deep inelastic electron-hydrogen and electron-deuterium cross section measurements between 1970 and 1983. Data from seven earlier experiments are re-radiatively corrected and normalized to experiment E140. Extractions are reported of R(x,Q sq) and F2 (x,Q sq) for hydrogen and deuterium over the entire SLAC kinematic range: .06 less than or = x less than or = .90 and 0.6 less than or = Q sq less than or = 30.0 (GeV sq). It was found that R(sup p) = R(sup d), as expected by QCD. Extracted values of R(x,Q sq) are significantly larger than predictions based on QCD and on QCD with the inclusion of kinematic target mass terms. This difference indicates that dynamical higher twist effects may be important in the SLAC kinematic range. A best fit empirical model of R(x,Q sq) is used to extract F2 from each cross section measurement. These F2 extractions are compared with F2 data from EMC and BCDMS. Agreement is observed with EMC when the EMC data are multiplied by 1.07. Agreement is observed with BCDMS over a limited range in x. The ratios of F2 exp D/F2 exp p are examined for Q sq dependence. A significant negative slope was observed for x less than or = .6, and a significant positive slope above x greater than .7, in excellent agreement with predictions based on QCD with the inclusion of kinematic target mass terms. DOE

N91-16786# Los Alamos National Lab., NM.
MOLECULAR CRYSTALS AND LOCALIZED VIBRATIONAL STATES
A. Migliori, A. M. Clogston, P. M. Maxton (California Univ., Los Angeles.), J. R. Hill, D. S. Moore, and H. K. McDowell 1989 12 p Presented at the NATO Conference on Dynamical Localization, Lyngby, Denmark, 26 Jul. 1989
(Contract W-7405-eng-36)
(DE90-010602; LA-UR-90-1354; CONF-8907189-1) Avail: NTIS HC/MF A03

The normal modes arising from a simple linear model of a crystalline solid predict many important properties such as the specific heat, the sound velocity, and the Raman and infrared response. Such a model fails, however, to produce thermal expansion and finite thermal conductivity. The introduction of weak non-linear couplings between the normal modes immediately corrects these simpler problems, while preserving the usual phonon representation of the purely linear system as a useful first approximation for small phonon amplitudes. What we wish to consider here is the next step in the process, taken by keeping the weak non-linearities but introducing large phonon amplitudes. Putting aside, for the moment, the question of how to achieve the necessary amplitudes, we can consider the consequences if certain normal conditions are obtained which put the phonon equation of motion in correspondence with the non-linear Schroedinger equation. We can then be guided by classical solutions of this equation which predict spontaneous symmetry breaking and vibrational localization. To focus our thoughts, we outline in physical terms the processes leading to the localization of vibrational energy. We use the insight gained to guide our choice of materials, and we describe the measurements we have made to begin the establishment of a rigorous connection between real solids and the theoretical constructs related to this problem. DOE

N91-16787# Fermi National Accelerator Lab., Batavia, IL.
CHERN-SIMONS AND ANYONIC SUPERCONDUCTIVITY
Joseph D. Lykken Apr. 1990 11 p Presented at the Strings 1990: Superstring Workshop, College Station, TX, 12-17 Mar. 1990
(Contract DE-AC02-76CH-03000)
(DE90-010663; FERMILAB-CONF-90/72-T; CONF-9003152-1)
Avail: NTIS HC/MF A03

Anyons are particles with fractional statistics. They can exist as point particles in a 2+1 dimension, or as quasiparticles in quasiplanar condensed matter systems in the real world. Anyonic particles can be modeled by ordinary bosons or fermions coupled to a statistical Chern-Simons abelian gauge field. For certain values of the statistics phase, a plasma of anyons in the Chern-Simons description is a superconductor. Anyonic superconductivity may represent an idealized limit of a new type of superconductor in real systems, perhaps encompassing the recently discovered high Tc copper oxides. DOE

N91-16788# Oak Ridge National Lab., TN. Solid State Div.
YBa2Cu3O(7-x) THIN FILM GROWTH ON SINGLE CRYSTAL AND POLYCRYSTALLINE YTTRIA-STABILIZED ZIRCONIA
David P. Norton, Douglas H. Lowndes, D. K. Christen, J. D. Budai, E. C. Jones, Thomas D. Ketcham, Dell St.Julien, K. W. Lay, and J. E. Tkaczyk (General Electric Co., Schenectady, NY.) Apr. 1990 9 p Presented at the Conference on the Science and Technology of Thin Film Superconductors, Denver, CO, 30 Apr. - 4 May 1990 Submitted for publication Sponsored in part by Corning Glass Works and General Electric Co.
(Contract DE-AC05-84OR-21400)
(DE90-010707; CONF-900424-1) Avail: NTIS HC/MF A02

In this paper, we report on the growth of Y-123 thin films on single crystal and randomly-oriented polycrystalline YSZ substrates. High quality epitaxial Y-123 thin films were grown on (100) YSZ in order to identify the factors that determine the optimum growth conditions for this substrate material. In addition, we have grown

Y-123 thin films that are highly c-axis oriented with a zero resistance T(sub co) between 85 and 89 K on both rigid and flexible randomly-oriented polycrystalline YSZ. Critical current densities in excess of 10(exp 4) A /sq cm at 77 K in zero magnetic field were obtained for the films on rigid polycrystalline substrates. According to recent work, this value for J(sub c) approaches what appears to be the upper limit for J(sub c) when large-angle grain boundaries are present in the film. DOE

N91-16789# Sandia National Labs., Albuquerque, NM.
CHARACTERIZATION OF CHEMICALLY PREPARED PZT THIN FILMS
Bruce A. Tuttle, R. W. Schwartz, D. H. Doughty, J. A. Voigt, and A. H. Carim (New Mexico Univ., Albuquerque.) 1990 11 p Presented at the Symposium on Ferroelectric Thin Films, San Francisco, CA, 18-20 Apr. 1990
(Contract DE-AC04-76DP-00789)
(DE90-010831; SAND-90-1077C; CONF-9004193-1) Avail: NTIS HC/MF A03

We have systematically varied processing parameters to fabricate PbZr(x)Ti(1-x)O3 (PZT) 53/47 thin films. Polycrystalline PZT thin films were fabricated by spin depositing Pt coated SiO2/Si substrates with alkoxide solutions. Our study focused on two process parameters: (1) heating rate, and (2) excess Pb additions. We used rapid thermal processing techniques to vary heating rates from 3 deg C/min to 8400 deg C/min. Films were characterized with the following excess Pb additions: 0, 3, 5, and 10 mol percent. For all process variations, films with greater perovskite content had better ferroelectric properties. Our best films were fabricated using the following process parameters: an excess Pb addition of 5 mol percent, a heating rate of 8400 deg C/min and annealing conditions of 700 C for 1 min. Films fabricated using these process conditions had a remnent polarization of 0.27 C/sq m and a coercive field of 3.4 MV/m. DOE

N91-16790# Stanford Linear Accelerator Center, CA.
PERFORMANCE MEASUREMENTS OF HYBRID PIN DIODE ARRAYS
J. Garrett Jernigan, John F. Arens, Gordon Kramer, Tim Collins, Jim Herring, Stephen L. Shapiro, and Colin D. Wilburn (Micron Semiconductor, Inc., Longwood, FL.) May 1990 12 p Presented at the 2nd International Industrial Symposium on the Super Collider, Miami Beach, FL, 14-19 Mar. 1990
(Contract DE-AC03-76SF-00515)
(DE90-010308; SU-SLAC-PUB-5211; CONF-900348-5) Avail: NTIS HC/MF A03

The successful effort to develop hybrid PIN diode arrays and to demonstrate their potential as components of vertex detectors is reported. Hybrid pixel arrays were fabricated by the Hughes Aircraft Co. by bump bonding readout chips developed by Hughes to an array of PIN diodes manufactured by Micron Semiconductor Inc. These hybrid pixel arrays were constructed in two configurations. One array format having 10 x 64 pixels, each 120 micron square, and the other format having 256 x 256 pixels, each 30 micron square. In both cases, the thickness of the PIN diode layer is 300 microns. Measurements of detector performance show that excellent position resolution can be achieved by interpolation. By determining the centroid of the charge cloud which spreads charge into a number of neighboring pixels, a spatial resolution of a few microns was attained. The noise was measured to be about 300 electrons (rms) at room temperature, as expected from KTC and dark current considerations, yielding a signal-to-noise ratio of about 100 for minimum ionizing particles. DOE

N91-16791# Argonne National Lab., IL. Materials Science Div.
CALCULATION OF FREE ENERGY FROM THE INTERNAL-ENERGY DISTRIBUTION FUNCTION
S. R. Phillpot and J. M. Rickman May 1990 8 p Presented at the Spring Meeting of the Materials Research Society, San Francisco, CA, 16-21 Apr. 1990 Submitted for publication
(Contracts W-31-109-eng-38; N00014-88-F-0019)
(DE90-011111; CONF-900466-38; REPT-58922-00-105) Avail: NTIS HC/MF A02

A new method is outlined for the calculation of free energies from a cumulant analysis of the internal energy distribution function obtained from a Monte Carlo simulation. The new methodology is validated by comparing the free energy calculated for a perfect crystal from this approach with the free energy calculated by a temperature integration scheme. By comparing the two methods for an inhomogeneous system containing grain boundaries, the effects were investigated of the local strain distribution on the free energy; for the superlattice of twist grain boundaries studied here, the effects are found to be small. DOE

N91-16792# Argonne National Lab., IL. Materials Components and Technology Div.
HIGH Tc OXIDE SOLID STATE REACTION KINETICS VIA COMPLEX IMPEDANCE SPECTROSCOPY
E. A. Cooper, T. O. Mason, U. Balachandran, and M. L. Kullberg (Amoco Oil Co., Naperville, IL.) 1989 4 p Presented at the Materials Research Society Fall Meeting, Boston, MA, 27 Nov. - 2 Dec. 1989
(Contract W-31-109-eng-38; NSF DMR-88-09854)
(DE90-011178; CONF-891119-132) Avail: NTIS HC/MF A01

Impedance spectra (5Hz to 13MHz) were collected during the solid state reaction of YBa2Cu3O(6+y) from large monosized CuO particles imbedded in a finely divided Y2O3/BaCO3 matrix. No particle size effect was observed, but a large temperature effect was observed corresponding to an activation energy of approx. 1.8 eV (175 kJ/mol) over the range 700 to 900 C. DOE

N91-16793# Lawrence Livermore National Lab., CA.
APPLICATIONS OF STRAINED LAYER SUPERLATTICES
D. L. Smith, B. K. Laurich (Los Alamos National Lab., NM.), and C. Mailhiot Apr. 1990 21 p Presented at the Spring Meeting of the Materials Research Society, San Francisco, CA, 16-21 Apr. 1990 Submitted for publication
(Contract W-7405-eng-48)
(DE90-011204; UCRL-102758; CONF-900466-42) Avail: NTIS HC/MF A03

Because of different band edge lineups, strain conditions, and growth orientations, various strained layer superlattice (SLS) materials can exhibit qualitatively new physical behavior in their optical properties. Two examples are given of new physical behavior in SLS: strain generated electric fields in polar growth axis superlattices and strained type 2 superlattices. In SLS, large electric fields can be generated by the piezoelectric effect. The fields are largest for SLS with a (111) growth axis; they vanish for SLS with a (100) growth axis. The strain generated electric fields strongly modify the optical properties of the superlattice. Photogenerated electron-hole pairs screen the fields leading to a large nonlinear optical response. Application of an external electric field leads to a large linear electrooptical response. The absorption edge can be either red or blue shifted. Optical studies of (100), (111), and (211) oriented GaInAs/GaAs superlattices confirm the existence of the strain generated electric fields. Small band gap semiconductors are useful for making intrinsic long wavelength infrared detectors. Arbitrarily small band gaps can be reached in the type 2 superlattice InAs/GaSb. However, for band gaps less than 0.1 eV, the layer thicknesses are large and the overlap of electron and hole wavefunctions are small. Thus, the absorption coefficient is too small for useful infrared (IR) detection. Including In in the GaSb introduces strain in he InAs/GaInSb superlattice which shifts the band edges so that small band gaps can be reached in thin layer superlattices. Good absorption at long IR wavelengths is thus achieved. DOE

N91-16794# Lawrence Livermore National Lab., CA.
NEW SURFACE ATOMIC STRUCTURES FOR III-V(110)-p(1 X 1)-Sb(1ML): CHEMICAL BONDING AND ELECTRONIC STRUCTURE
J. P. LaFemina, C. B. Duke (Xerox Corp., Webster, NY.), and C. Mailhiot Apr. 1990 6 p Presented at the Spring Meeting of the Materials Research Society, San Francisco, CA, 16-21 Apr. 1990

(Contract W-7405-eng-48)
(DE90-011230; UCRL-JC-103872; CONF-900466-40) Avail: NTIS HC/MF A02

Tight-binding total energy computations are used to examine the chemical bonding and electronic structure for two new minimum-energy surface atomic structures for p(1 x 1) overlayers of Sb on III-V(110) surfaces. The bonding in each of these structures is unique, having no analog in either the bulk or small molecule coordination chemistry of these materials, and is a phenomena uniquely associated with the constrained epitaxical growth of the Sb overlayer. DOE

N91-16795# Sandia National Labs., Albuquerque, NM.
MICROWAVE-DETECTED PHOTOCONDUCTANCE DECAY
Paul A. Basore and Barry R. Hansen 1990 10 p Presented at the 21st IEEE Photovoltaic Specialists Conference, Kissimmee, FL, 21-25 May 1990
(Contract DE-AC04-76DP-00789)
(DE90-011505; SAND-89-2464C; CONF-900542-4) Avail: NTIS HC/MF A02

Microwave detected photoconductance decay (micron W-PCD) provides a contactless measurement of the recombination lifetime of free carriers in semiconductors following a pulse of optical excitation. Several complications in interpreting the results obtained by this method have prevented its widespread acceptance. Detailed models are proposed and verified experimentally using a commercially available apparatus. The model adequately predicts the behavior of the microwave reflectance as a function of wafer conductivity and system configuration. A new light based variation of the technique is described which makes it possible to characterize lifetime as a function of excess carrier density. This capability makes it possible to measure the emitter saturation current density for diffusions in high resistivity wafers, a valuable process control tool. DOE

N91-16796# Georgia Univ., Athens. Center for Simulational Physics.
DYNAMICS OF STRONG-COUPLING MODELS FOR CUPRATE SUPERCONDUCTORS: EXACT RESULTS ON FINITE LATTICES
H. B. Schuettler, C.-X. Chen, and A. J. Fedro (Argonne National Lab., IL.) 1989 12 p Presented at the Los Alamos Workshop on Quantum Simulations of Condensed Matter Phenomena, Los Alamos, NM, 8-11 Aug. 1989
(Contract W-31-109-eng-38; NSF DMR-89-13878)
(DE90-011155; CONF-8908106-6) Avail: NTIS HC/MF A03

We discuss recent applications of exact numerical continued fraction expansion (CFE) techniques to calculate dynamical correlation functions of various strong-coupling models related to the high-temperature cuprate superconductors. For the two-dimensional square-lattice spin-1/2 Heisenberg antiferromagnet, we present exact results for the zero-temperature dynamical structure factor on finite-sized lattices and compare them to approximate results from a Schwinger boson mean-field theory, recently proposed by Arovas and Auerbach. We find that the mean-field theory represents a very good approximation to the exact spin excitation spectra and to the static spin correlations. We then investigate the dynamical spin-spin structure factor and the single-particle spectral function for finite model clusters with dopant induced hole-type charge carriers, in the strong-coupling limit of both the single-band Hubbard model (t-J-model) and the three-band Hubbard model (Kondo-Heisenberg model). Our results are consistent with the physical picture recently proposed by Zhang and Rice which implies an approximate mapping of the low-energy states in the three-band model onto an effective single-band theory. DOE

N91-16797# California Univ., Berkeley. Lawrence Berkeley Lab. Materials and Chemical Sciences Div.
QUASIPERIODIC TRANSITION TO CHAOS IN Ge; AND MAGNETIC SUSCEPTIBILITY OF HIGH-T(c) SUPERCONDUCTORS Ph.D. Thesis
Youngtae Kim Apr. 1990 252 p
(Contract DE-AC03-76SF-00098)
(DE90-011304; LBL-28950) Avail: NTIS HC/MF A12

This thesis consists of the study of two topics in condensed matter physics: nonlinear dynamics in a Ge crystal; and magnetic properties of the high temperature superconductor YBa2Cu3O7. These are given as two parts, each of which can be read independently. The first part is concerned with the measurement of the universal spectrum of scaling indices of the critical attractor of the quasiperiodic route to chaos with golden mean winding number for the helical instability of the electron-hole plasma in a germanium crystal in a magnetic field. The second part consists of measurements of the complex ac magnetic susceptibility of the ceramic superconductor YBa2Cu3O7, and together with theoretical models of the material, assumed to be composed of intergranular junctions and superconducting grains. DOE

N91-16798# Lawrence Livermore National Lab., CA.
PROPERTIES OF SUPERDEFORMED BANDS IN THE A = 194 REGION
E. A. Henry, A. Kuhnert, S. W. Yates, M. J. Brinkman, J. A. Cizewski, M. A. Deleplanque, R. M. Diamond, F. S. Stephens, C. W. Beausang (California Univ., Berkeley. Lawrence Berkeley Lab.), and J. A. Becker et al Apr. 1990 7 p Presented at the Nuclear Structure in the 1990's, Oak Ridge, TN, 23-27 Apr. 1990 Submitted for publication Sponsored in part by Strategic Defense Initiative Organization and NSF
(Contracts W-7405-eng-48; DE-AC03-76SF-00098)
(DE90-011482; UCRL-JC-103608; CONF-900450-3) Avail: NTIS HC/MF A02

At least eighteen superdeformed (SD) bands have been identified in mercury, thallium, and lead nuclei since the report of a SD band in (191)Hg. Systematic information is beginning to emerge on the properties of the SD bands in this mass region, and comparisons with SD bands in the A = 150 region are now possible. Recently, data were obtained with the HERA spectrometer at the Lawrence Berkeley Laboratory 88 Cyclotron on SD bands in (194)Pb and (196)Pb. In these experiments, we bombarded (176)Yb with (24)Mg and (26)Mg. The cross bombardment was necessary to make the assignment of the band to (196)Pb certain. These bands are typical of other SD bands in the region in many ways. The gamma rays have energies that range from about 200 to 800 keV. The gamma-ray spacing decreases from about 40 to 30 keV as the transition energy increases. Their intensities gradually increase as the gamma-ray energies decrease over the upper half of of the sequence, and then sustain a constant value until the one or two lowest energy transitions. DOE

N91-16799# Ames Lab., IA. Dept. of Physics.
A PHOTOEMISSION STUDY OF SAMARIUM ON SILICON Ph.D. Thesis
An-Ban Yang Jan. 1990 113 p
(Contract W-7405-eng-82)
(DE90-011509; IS-T-1399) Avail: NTIS HC/MF A06

A photoemission study was performed on the chemisorption of samarium on three different kinds of silicon substrates, i.e., crystal Si(11), amorphous Si (a-Si), and hydrogenated amorphous Si (a-Si:H) to understand completely the chemical and physical phenomena underlying the interface formation. The core-level spectra clearly indicate the existence of three interface-formation regimes. Two chemically reacted shifts are observed and identified as disilicide phase and solid solution, respectively, and a critical coverage corresponding to the onset of strong chemical reaction is also shown. Moreover, the Si atoms show no sign of surface-segregation behavior, and a heterogeneous interface is indicated by the coexistence of two reacted species. Analogous growth behavior is shown on three different substrates, suggesting that morphological and surface structure differences in the reacted film play a second role in the interfacial development. However, the Schottky-barrier-lowering phenomenon is only observed in the crystal substrate. Combining the results of three complementary experiments, we conclude that the three interface-formation stages are the weakly-absorbed, chemically- and metallic-reacted phases,

respectively, and the nucleation and growth processes occuring in Sm thin film formation are sublayer plus island growth mode. Furthermore, only trivalent Sm is involved in the chemical reactions. DOE

N91-16800# Brookhaven National Lab., Upton, NY. National Synchrotron Light Source.
INFRARED RESPONSE OF YBa2Cu3O(7-DELTA) FILMS TO PULSED, BROADBAND SYNCHROTRON RADIATION
G. L. Carr, M. Quijada, D. B. Tanner, C. J. Hirschmugl, G. P. Williams, S. Etemad, F. DeRosa, T. Venkatesan, B. Dutta, and X. Xi (Rutgers Univ., Piscataway, NJ.) 1990 6 p Presented at the Technical Symposia on Optical Engineering and Photonics in Aerospace Sensing, Orlando, FL, 16-20 Apr. 1990
(Contracts DE-AC02-76CH-00016; MDA972-88-J-1006)
(DE90-011519; BNL-44573; CONF-900451-3) Avail: NTIS HC/MF A02

We report studies of a thin high Tc film operating as a fast bolometric detector of infrared radiation. The film has a response of infrared radiation. The film has a response of several mV when exposed to a 1 W, 1 ns duration broadband infrared pulse. The decay after the pulse was about 4 ns. The temperature dependence of the response accurately tracked dR/dT. A thermal model, in which the film's temperature varies relative to the substrate, provides a good description of the response. We find no evidence for other (non-bolometric) response mechanisms for temperatures near or well below Tc. DOE

N91-16801# Missouri Univ., Columbia. Dept. of Physics and Astronomy.
PHOTOREFLECTANCE STUDIES OF ELECTRONIC TRANSITIONS IN QUANTUM WELL STRUCTURES UNDER HIGH PRESSURE
H. R. Chandrasekhar and Meera Chandrasekhar 1990 14 p Presented at the SPIE's Symposium on Advances in Semiconductors and Superconductors: Physics Toward Device Applications, San Diego, CA, 17-21 Mar. 1990 Submitted for publication
(Contracts DE-FG02-89ER-45402; DAAL03-86-K-0083)
(DE90-011583; CONF-900302-2; REPT-1286-17) Avail: NTIS HC/MF A03

The unique feature of quantum confinement of carriers has made possible unusual devices. By combining various semiconductors and alloys of III-V, II-IV and group IV materials, unusual band lineups between neighboring layers have been obtained. Both lattice matched and strained layer structures have been grown. In this article we will focus on the electronic structure of the quantum well heterostructures under the external perturbation of hydrostatic pressure. Pressure has been used extensively to investigate materials in regions of phase space not otherwise accessible. In the study of quantum well structures, it has also been used to move band edges in a controlled fashion, and alter band lineups, allowing the determination of band offsets with an accuracy that was not possible without the use of pressure. As in bulk semiconductors, optical techniques provide powerful tools in studying the electronic states in quantum well heterostructures. Photoluminescence spectroscopy is only sensitive to spectral features associated with energy states close to the bottom of the well due to rapid thermalization of carriers. Photoluminescence excitation is often limited by the availability of tunable lasers. Photoreflectance, on the other hand, can provide a rich structure due to both symmetry allowed and forbidden transitions encompassing the entire quantum well. This sensitivity is due to the derivative nature of the spectroscopy. DOE

N91-16802 Cornell Univ., Ithaca, NY.
FABRICATION AND ELECTRICAL CHARACTERIZATION OF DEEP-SUBMICRON TRENCH-ISOLATED CMOS DEVICE STRUCTURES Ph.D. Thesis
Asanga Hiran Perera 1990 261 p
Avail: Univ. Microfilms Order No. DA9027044

The magnitude of the extrinsic parasitic MOSFET series resistance was experimentally evaluated in the deep-submicron domain and its consequence on device performance was determined. The series resistance of depletion mode MOSFET test structures were measured for source-drain sizes as small as 0.2 microns by 0.3 microns at room temperature and 100 K. To build the test structures, a multilevel-full electron beam lithography fabrication process was developed. Positive tone novalac resist, SYSTEM-9, was developed for electron beam application. A shallow trench isolation technology capable of defining 0.2 microns wide active areas was developed. A rapid thermal annealing based silicidation scheme using TiSi2 was established. MOSFET sidewall spacer formation using PECVD SiO2 was calibrated. Antimony and gallium were investigated as possible alternatives to arsenic and boron, respectively, and well behaved substrate diodes were successfully fabricated. Two patterning techniques for the metal bi-layer metalization of TiW and Al were developed. The source drain resistance of the test structures was measured at room temperture and at 100 K. An LN2 flushed cold chuck for low temperature device probing was designed and constructed. The extrinsic source-drain resistance increased rapidly as the contact size decreased below 0.5 microns, and showed an almost two order of magnitude change when the source-drain area was reduced from 2 x 1.7 sq microns to 0.2 x 0.3 sq microns. The effect of this resistance increase on a CMOS inverter switching speed was estimated. A first order empirical model to predict the series resistance was also formulated. Good correspondence was observed between results from the device simulator PISCES-2B and measured data for larger source-drain sizes. Dissert. Abstr.

N91-16803# Brookhaven National Lab., Upton, NY. Materials Science Div.
MICROSTRUCTURES AND dc CRITICAL CURRENTS IN TEXTURED Y-Ba-Cu-OXIDES
J. Orehotsky, H. J. Wiesmann, A. R. Moodenbaugh, M. Suenaga, H.-G. Wang, and H. Herman (State Univ. of New York, Stony Brook.) 24 Sep. 1990 3 p Presented at the Applied Superconductivity Conference, Aspen, CO, 24-28 Sep. 1990
(Contract DE-AC02-76CH-00016)
(DE91-000895; BNL-45207; CONF-900944-10) Avail: NTIS HC/MF A01

Sintered bars of Y-Ba-Cu oxide were partially melted using a quartz halogen lamp zone heating apparatus. The resulting multiphase samples showed varying degrees of melt texturing. It was found that the addition of YBa2CuO5 powders to the sintered YBa2Cu3O7 prior to the zone melting process enhanced the growth of large textured grains. The best value of the critical current density was approximately 10(exp 3) A/sq cm at 1.0 T and 77 K for the starting composition of YBa2Cu3O7-(0.2)Y2BaCuO5. DOE

N91-16804# Brookhaven National Lab., Upton, NY. Materials Science Div.
OBSERVATIONS OF VORTEX STRUCTURE IN YBa2Cu3O7
H. Muller, H. J. Wiesmann, and M. Suenaga 24 Sep. 1990 4 p Presented at the Applied Superconductivity Conference, Aspen, CO, 24-28 Sep. 1990
(Contract DE-AC02-76CH-00016)
(DE91-000900; BNL-45227; CONF-900944-11) Avail: NTIS HC/MF A01

The remnant magnetic flux distribution in a single crystal and a sintered polycrystal was examined using the magnetic particle decoration technique. The single crystal, which was heavily twinned, showed only local order in the flux lattice. This was probably due to lattice distortions caused by interaction between twin boundaries and fluxons. In the polycrystal, flux pinning effectiveness was seen to vary significantly between grains, depending on size and orientation. Grains with the c axis nearly perpendicular to the applied magnetic field were most effective at pinning flux. Some features of the decoration patterns implied that the flux distribution was influenced by more than just the grains at the sample surface. DOE

N91-16805# Sandia National Labs., Albuquerque, NM.
FAR-INFARED LASER SPECTROSCOPY OF TWO DIMENSIONAL HOLES IN STRAINED-LAYER HETEROSTRUCTURE AND SUPERLATTICES
S. Y. Lin, D. C. Tsui, J. F. Klem, E. D. Jones, and L. R. Dawson 1990 4 p Presented at the Fall Meeting of the Materials Research Society, Boston, MA, 24 Nov. - 1 Dec. 1990 Prepared in cooperation with Princeton Univ., NJ
(Contract DE-AC04-76DP-00789; AF-AFOSR-0248-88)
(DE91-000027; SAND-90-1772C; CONF-901105-15) Avail: NTIS HC/MF A01

Far-infrared magneto-transmission data at 4.2 K on a series of p-type strained layer Al(x)Ga(1-x)As/In(y)Ga(1-y)As/GaAs quantum well (QW) structure and InAs(0.15)Sb(0.85)/InSb superlattices (SLS) are reported. The Al(x)Ga(1-x(As/In(y)-Ga(1-y)As/GaAs QW structure consists of strained In(y) Ga-(1-y)As layers of 100 A in thickness and space layer having thickness (W(sub sp)) ranging from 30 to 700 A. The InAs(0.85)/InSb SLS was grown on top of a 1.0(mu)m InAs(0.15)Sb(0.95) strain relief buffer layer consisting of alternating layers of 100 A InAs(0.15)Sb(0.85) and 200 A InSb. The detail of the sample structures has been described elsewhere. The two-dimensional (2D) hole density (p(sub 2D)) of the sample is obtained from the period of the Shubnikov-de Hass oscillations in quantum transport measurements made at 4.2 K. The magneto-transimission experiments are performed in magnetic field (B) up to 8.5 T using polarized radiation and the spectrum is displayed as 4 Log(sub 10)(T(B)/T(0)), where T(B) is the transmittance at B. DOE

N91-16806# Oak Ridge National Lab., TN. Solid State Div.
DOSE RATE EFFECTS ON DAMAGE FORMATION IN ION-IMPLANTED GALLIUM ARSENIDE
T. E. Haynes and O. W. Holland Sep. 1990 14 p Presented at the 7th International Conference on Ion Beam Modification of Materials, Knoxville, TN, 9-14 Sep. 1990 Submitted for publication
(Contract DE-AC05-84OR-21400)
(DE91-000394; CONF-900936-9) Avail: NTIS HC/MF A03

The residual damage in GaAs was measured by ion channeling following implantation of either 100 keV Si-120(+) at temperatures of 300 or 77 K, or 360 keV Sn-120(+) at 300 K. For room-temperature Si implants and fluences between 1 and 10 x 10(exp 14) Si/sq cm, the amount of damage created was strongly dependent upon the ion current density, which was varied between 0.05 and 12 micro A/sq cm. Two different stages of damage growth were identified by an abrupt increase in the damage growth rate as a function of fluence, and the threshold fluence for the onset of the second stage was found to be dependent on the dose rate. The dose rate effect on damage was substantially weaker for Sn-120(+) implants and was negligible for Si implants at 77 K. The damage was found to be most sensitive to the average current density, demonstrating that the defects which are the precursors to the residual dose-rate dependent damage have active lifetimes of at least 3 x 10(exp -4) s. The dose rate effect and its variation with ion mass and temperature are discussed in the context of homogeneous nucleation and growth of damage during ion irradiation. DOE

N91-16807# Lowell Univ., MA. Dept. of Chemistry.
THIN FILM SINGLE CRYSTAL GROWTH OF A NONLINEAR OPTICAL POLYMER
J. Lee, Sukant Tripathy, H. Matsuda, S. Okada, and H. Nakaishi (Research Inst. for Polymers and Textiles, Ibaraki, Japan) Apr. 1990 4 p Presented at the Polymer Preprint ACS Meeting, Boston, MA, Apr. 1990
(Contract N00014-90-J-1148)
(AD-A227692; TR-14) Avail: NTIS HC/MF A01 CSCL 20/2

Over the past decade macromolecules with an extended chain geometry and conjugated backbone electronic structure have been established as novel electronic and optical materials. This includes photo-, thermo-, solvato-, and electro-chromism, large electrical and photoconductivities and unique linear and nonlinear optical properties among others. Polydiacetylenes, a class of a conjugated polymers are considered possible candidate material for all optical switching and logic applications. In the transparent regime they possess some of the largest third order nonlinear optical susceptibilities. In general, it is extremely difficult to grow bulk polymeric single crystals. Polydiacetylenes, however, can be grown to large size in single crystal form. Single crystals of polydiacetylene can be directly grown from monomer single crystals through solid state polymerization by heat. GRA

N91-16808# EG and G Mound Applied Technologies, Miamisburg, OH.
COMPARISON OF HYDROGEN DIFFUSION IN Ti2PdH(x) TO THE BEHAVIOR FOR Ti2CuH(x) AND Zr2PdH(x)
R. C. Bowman, Jr., A. Attalla, G. C. Abell, J. S. Cantrell, and A. J. Maeland (Concrete Solutions, Meriden, CT.) 1990 11 p Presented at the International Symposium on Metal-Hydrogen Systems, Banff, British Columbia, 2-7 Sep. 1990
(Contract DE-AC04-88DP-43495)
(DE91-002711; MLM-3659(OP); CONF-9009141-6) Avail: NTIS HC/MF A03

Nuclear magnetic resonance measurements of the proton spin-lattice and rotating-frame relaxation times were made on Ti2PdH(x) over the temperature range 100 to 580 K. Analyses of the NMR data for Ti2PdH(x) gave hydrogen diffusion parameters that corresponded with the results previously obtained from Ti2CuH(x) and Zr2PdH(x) when the hydrogen atoms occupied a single type of tetrahedral interstitial site. However, the diffusion activation energy decreases in the sequence Ti2PdH1.9, Ti2CuH1.9, and Zr2PdH1.9. DOE

N91-16809# Argonne National Lab., IL. Mathematics and Computer Science Div.
A SEARCH FOR GOOD LATTICE RULES BASED ON THE RECIPROCAL LATTICE GENERATOR MATRIX
James N. Lyness and W. Newman 1989 8 p Presented at the 1st Great Lakes Computer Science Conference, Kalamazoo, MI, 18-20 Oct. 1989
(Contract W-31-109-eng-38)
(DE91-004425; CONF-8910401-2) Avail: NTIS HC/MF A02

The search for cost-effective lattice rules is a time-consuming and difficult process. After a brief overview of some of the lattice theory relevant to these rules, a new approach to this search is suggested. This approach is based on a classification of lattice rules using the upper triangular lattice form of the reciprocal lattice generator matrix. DOE

N91-16810# Argonne National Lab., IL. Materials Science Div.
CORRELATION BETWEEN THE ELASTIC-SHEAR-INSTABILITY-MECHANISM AND EMPIRICAL CRITERIA FOR IRRADIATION-INDUCED AMORPHIZATION
J. Koike, P. R. Okamoto, L. E. Rehn, and M. Meshii (Northwestern Univ., Evanston, IL.) Sep. 1990 13 p Presented at the 7th International Conference on Ion Beam Modification of Materials, Knoxville, TN, 9-14 Sep. 1990
(Contract W-31-109-eng-38; NSF DMR-88-02487)
(DE91-004481; CONF-900936-20) Avail: NTIS HC/MF A03

In an attempt to correlate the shear instability mechanism with empirical criteria for irradiation-induced amorphization, shear moduli of an A3B-type fcc crystal were calculated as a function of the chemical long range order parameter (S) using a Morse potential. The shear moduli were found to decrease with decreasing S. When the depth and the curvature of the A-B potential were changed while keeping the A-A and B-B potentials constant, the magnitude of the decrease in shear moduli is greater for deeper and narrower A-B potentials. The present results indicate that a shear instability should occur more readily in compounds with larger ordering energy and larger elastic moduli. These results agree with the reported empirical criteria for irradiation-induced amorphization, therefore providing further support for the shear instability mechanism for solid-state amorphization. DOE

N91-16811# Oak Ridge National Lab., TN. Metals and Ceramics Div.

CHARACTERIZATION OF GaAs/Si INTERFACE STRUCTURE BY X RAY DIFFRACTION

E. D. Specht, G. E. Ice, C. J. Peters, C. J. Sparks, N. Lucas, X.-M. Zhu, R. Moret, and H. Morkoc (Illinois Univ., Urbana.) 1990 6 p Presented at the Fall Meeting of the Materials Research Society, Boston, MA, 24 Nov. - 1 Dec. 1990

(Contracts DE-AC05-84OR-21400; DE-AC02-76ER-01198; DE-AC02-76CH-00016)

(DE91-004769; CONF-901105-30) Avail: NTIS HC/MF A02

By measuring the intensity profiles along the crystal truncation rods of a Si(001) substrate, we obtain the depth sensitivity necessary for x ray diffraction measurements of the structure of its interface with a thick GaAs overlayer which is epitaxial to, but not in registry with the substrate. By comparing the diffraction with a model based on a grid of misfit dislocations, we find that the atoms at the interface have a root mean square displacement of 1.09 +/- 0.1 A from this ideal structure, and that the interface has a roughness of 2.9 +/- 1 A. The diffraction indicates an anomalously small strain perpendicular to the interface in the GaAs near the interface. DOE

N91-16812# Sandia National Labs., Albuquerque, NM.

THERMAL DESORPTION STUDIES OF ISOTOPICALLY-LABELED OXYGEN-INDUCED SUPERCONDUCTIVITY IN La2CuO(4+DELTA)

N. D. Shinn, M. E. Bartram, J. E. Schirber, D. L. Overmyer, J. W. Rogers, Jr., Z. Fisk, and S. W. Cheong (Los Alamos National Lab., NM.) 1990 6 p Presented at the Fall Meeting of the Materials Research Society, Boston, MA, 24 Nov. - 1 Dec. 1990

(Contract DE-AC04-76DP-00789)

(DE91-004898; SAND-90-1875C; CONF-901105-36) Avail: NTIS HC/MF A02

Isotopically-labeled oxygen enrichment and thermal desorption mass spectroscopy (TDMS) have been combined to study interstitial oxygen desorption from superconducting La2CuO(4+delta) (delta less than or equal to 0.032). Single crystal samples of magnetic insulating La2CuO(4.00) were annealed at 860 K under 1-3 kbar oxygen pressure for 12-100 hours to yield hole-doped, superconducting La2CuO(4+delta) samples with Tc between 35 and 40 K. Whereas no TDMS signals were observed for the insulator, rapid bursts (full width at half maximum less than 0.5 sec) of molecular oxygen were observed above 350 K while heating the superconductor at less than 1 K per sec in high vacuum. A kinetic model is proposed in which the interstitial oxygen diffuses to internal grain boundaries and defects during heating, thereby inducing stress in the lattice as it attempts to revert to the LaCuO(4.00) crystal structure. This stress is relieved by lattice fracture at grain boundaries during the TDMS experiment, releasing the trapped oxygen from the sample as micro-cracks are formed. In addition, the facile oxygen exchange between interstitial and lattice oxygen sites has been discovered by TDMS and weight gain measurements from isotopically-enriched crystals, supporting the structural model of Chaillout, et al. in which the interstitial oxygen atom dimerizes with a lattice oxygen ion. DOE

N91-16813*# Wisconsin Univ., Madison. Applied Superconductivity Center.

ASTROMAG COIL COOLING STUDY

Ben-Zion Maytal (Technion - Israel Inst. of Tech., Haifa.) and Steven W. VanSciver Dec. 1990 127 p

(Grant NAG5-1417)

(NASA-CR-187768; NAS 1.26:187768) Avail: NTIS HC/MF A07 CSCL 20L

ASTROMAG is a planned particle astrophysics magnetic facility. Basically it is a large magnetic spectrometer outside the Earth's atmosphere for an extended period of time in orbit on a space station. A definition team summarized its scientific objectives assumably related to fundamental questions of astrophysics, cosmology, and elementary particle physics. Since magnetic induction of about 7 Tesla is desired, it is planned to be a superconducting magnet cooled to liquid helium 2 temperatures. The general structure of ASTROMAG is based on: (1) two superconducting magnetic coils, (2) dewar of liquid helium 2 to provide cooling capability for the magnets; (3) instrumentation, matter-anti matter spectrometer (MAS) and cosmic ray isotope spectrometer (CRIS); and (4) interfaces to the shuttle and space station. Many configurations of the superconducting magnets and the dewar were proposed and evaluated, since those are the heart of the ASTROMAG. Baseline of the magnet configuration and cryostat as presented in the phase A study and the one kept in mind while doing the present study are presented. ASTROMAG's development schedule reflects the plan of launching to the space station in 1995. Author

N91-16814# Oak Ridge National Lab., TN. Metals and Ceramics Div.

DOMAIN BOUNDARIES FORMED DURING EPITACTICAL GROWTH OF ALPHA-Al2O3

J. Bentley and P. S. Sklad 1990 7 p Presented at the Fall Meeting of the Materials Research Society, Boston, MA, 24 Nov. - 1 Dec. 1990

(Contract DE-AC05-84OR-21400)

(DE91-005018; CONF-901105-38) Avail: NTIS HC/MF A02

Domain boundaries have been characterized by transmission electron microscopy in single crystal (0001) alpha-Al2O3 epitactically regrown after being amorphized by stoichiometric ion implantation. The domains are faceted on (1120) and have dislocation-like features at facet intersections. End-of-range dislocation loops on (0001) appear to be the nucleation site for the domains. Diffraction contrast, high resolution imaging, and convergent beam electron diffraction techniques showed that two types of domains are present which involve cation stacking sequences which are out of phase with the matrix as a result of translation along and/or inversion of (0001). The non-inverted regions can be described as anti-phase domains, whereas those with (0001) inverted also have a basal twin character. DOE

N91-16815*# National Aeronautics and Space Administration. Marshall Space Flight Center, AL.

HANGING DROP CRYSTAL GROWTH APPARATUS Patent Application

Robert J. Naumann, inventor (to NASA), William K. Witherow, inventor (to NASA), Daniel C. Carter, inventor (to NASA), Charles E. Bugg, inventor (to NASA), and Fred L. Suddath, inventor (to NASA) (Alabama Univ., Birmingham.) 31 Aug. 1990 18 p

(NASA-CASE-MFS-26061-1; NAS 1.71:MFS-26061-1; US-PATENT-APPL-SN-575708) Avail: NTIS HC/MF A03 CSCL 20L

This invention relates generally to control systems for controlling crystal growth, and more particularly to such a system which uses a beam of light refracted by the fluid in which crystals are growing to detect concentration of solutes in the liquid. In a hanging drop apparatus, a laser beam is directed onto drop which refracts the laser light into primary and secondary bows, respectively, which in turn fall upon linear diode detector arrays. As concentration of solutes in drop increases due to solvent removal, these bows move farther apart on the arrays, with the relative separation being detected by arrays and used by a computer to adjust solvent vapor transport from the drop. A forward scattering detector is used to detect crystal nucleation in drop, and a humidity detector is used, in one embodiment, to detect relative humidity in the enclosure wherein drop is suspended. The novelty of this invention lies in utilizing angular variance of light refracted from drop to infer, by a computer algorithm, concentration of solutes therein. Additional novelty is believed to lie in using a forward scattering detector to detect nucleating crystallites in drop. NASA

N91-16816*# Massachusetts Inst. of Tech., Lexington. Lincoln Lab.

SOLID STATE RESEARCH Quarterly Technical Report, 1 Nov. 1989 - 31 Jan. 1990

Alan L. McWhorter 22 Aug. 1990 96 p Sponsored by NASA, Washington, DC; Army; DARPA; Navy; Strategic Defense Initiative

Organization; and DOE
(Contract F19628-90-C-0002)
(NASA-CR-187871; NAS 1.26:187871; AD-A227941; REPT-1990:1; ESD-TR-90-027) Avail: NTIS HC/MF A05 CSCL 20/12

This report covers in detail the research work of the Solid State Division at Lincoln Laboratory for the period 1 November 1989 through 31 January 1990. The topics covered are Electrooptical Devices, Quantum Electronics, Materials Research, Submicrometer Technology, Microelectronics, and Analog Device Technology. Funding is provided primarily by the Air Force, with additional support provided by the Army, DARPA, Navy, SDIO, NASA, and DOE. GRA

N91-16817# Massachusetts Inst. of Tech., Cambridge. Research Lab. of Electronics.
CHEMICAL BEAM EPITAXY OF ZnSe Final Report, 1 Aug. 1988 - 31 Jul. 1990
Leslie A. Kolodziejski 17 Oct. 1990 17 p
(Contract N00014-88-K-0564)
(AD-A228045) Avail: NTIS HC/MF A03 CSCL 20/2

ZnSe, ZnTe, and ZnSe/ZnTe layered quantum well structures have room temperature direct energy bandgaps which span the blue/blue-green optical spectrum. These II-VI semiconductors possess significant technological potential for visible optoelectronic device applications. Both military and commercial applications are envisioned. Blue/blue-green semiconductor injection lasers for underwater to satellite communications, visible flat panel electroluminescent displays, optical disc recording using blue wavelengths to increase the density of recorded information, color laser printers, and short range domestic or industrial communications via polymer fibers are examples of frequently quoted potential markets. The magnitude in U.S. dollars offered by these varied and large commercial markets warrants substantial investment in both research time and funds to push these materials to their ultimate potential for optoelectronic device fabrication testing, and marketing. Substantial effort is currently underway in Japan and Europe with major investment in funds and manpower. GRA

N91-16818# CPS Superconductors, Inc., Milford, MA.
COMPOSITE CERAMIC SUPERCONDUCTING WIRES FOR ELECTRIC MOTOR APPLICATIONS Quarterly Report No. 9, 1 Jul. - 30 Sep. 1990
James D. Hodge 30 Sep. 1990 57 p
(Contract N00014-88-C-0512; DARPA Order 9525)
(AD-A228359; CPSS-0990-1) Avail: NTIS HC/MF A04 CSCL 20/3

A scaled-up process for producing sintered, silver coated YBCO mono filament wire was developed and is currently able to produce 30 meters of wire/day. Efforts aimed at improving the electrical performance of this wire are well underway. Two approaches are being used: Continuously melt-texturing sintered YBCO wire/fiber to produce a macro-crystalline, strong-linked wire, and adaptation the TBCO process to the production of BiSCCO wire which can be subsequently mechanically textured by rolling the wire into ribbon. Work has also proceeded on the fabrication of a brushless DC trapped flux motor in which melt-textured YBCO rings are used as permanent magnet replicas. This motor design holds the potential for a high power HTSC motor which can be fabricated using current HTSC technology. GRA

N91-16819# State Univ. of New York, Buffalo. Dept. of Chemistry.
THEORETICAL STUDIES OF ELECTRON TRANSPORT IN QUANTUM-WELL STRUCTURES
Lakshmi N. Pandey, Mark I. Stockman, Thomas F. George, and Devaraj Sahu (Computer Sciences Corp., Lanham, MD.) Oct. 1990 11 p Submitted for publication
(Contract N00014-90-J-1193)
(AD-A228429; UBUFFALO/DC/90/TR-27) Avail: NTIS HC/MF A03 CSCL 20/10

The study of resonant tunneling structures (RTS) has become increasingly important because of possible device applications and also because of the basic physics they involve. Within the static picture, the dwell time, i.e., the average time an electron spends inside an RTS was calculated. The actual time involved in the tunneling process can be described by the solution of the time dependent effective mass Schrodinger equation (TDEMSE), and a code based on the fast Fourier transform method is developed to solve the TDEMSE for a potential profile such as RTS. The physical properties of an RTS investigated are the build-up time, which is the time taken by an electron to accumulate probability inside the well, and the escape time. GRA

N91-16820# Illinois Univ., Urbana.
INTEGRATED SEMICONDUCTOR MODULATORS Final Report, 1 Jun. 1986 - 31 Aug. 1990
Thomas A. DeTemple 31 Aug. 1990 14 p
(Contract DAAL03-86-K-0089)
(AD-A228615; XA-23383.3-PH) Avail: NTIS HC/MF A03 CSCL 09/1

Studies have shown that impurity induced layer disordering can be used to fabricate buried channel optical waveguides from the same heterostructure as is used for lasers and the routing properties of these waveguides are exceeded only by those fabricated by non-planar techniques. The importance of this is that of providing an existence-proof for this technology for other than straight waveguides. It has been demonstrated that, by using vacancy induced disordering, the band gap can be selectively increased thus rendering a heterostructure transparent to radiation at it's native band gap without any loss in waveguide routing ability. This provides a means for integrating lasers, amplifiers, modulators, detectors, and passive waveguides from the same wafer without severe band edge attenuation. It has also been demonstrated that a single quantum well graded barrier laser heterostructure has a significant electroabsorption tail which can be used for a modulator or detector. GRA

N91-16821# Carnegie-Mellon Univ., Pittsburgh, PA. Dept. of Metallurgical Engineering and Materials Science.
THE ROLE OF LEDGES IN PHASE TRANSFORMATIONS Final Report, 1 Jun. 1989 - 28 Feb. 1990
H. I. Aaronson 17 Sep. 1990 5 p Presented at a Fall 1989 Symposium, Indianapolis, IN
(Grant AF-AFOSR-0334-89; AF Proj. 2306)
(AD-A228750; AFOSR-90-1105TR) Avail: NTIS HC/MF A01 CSCL 20/2

Research workers in many countries and in many different research areas have gradually come to realize that ledges play a central role in the growth of crystals from the vapor, liquid and solid phases. However, the structure of ledges is not easy to study experimentally or to analyze theoretically. Similarly, the kinetics of ledgewise growth pose substantial problems to the experimentalist intent on their measurement and to the theoretician studies attempting to account for these data mathematically. Both experimental and theoretical studies during the three major types of phase transformation enumerated have tended to develop more or less independently of each other. The observation of ledges with TEM and field ion microscopy was discussed with emphasizing methods of distinguishing between ledges and dislocations. One speaker make clear the theoretical as well as the experimental problems involved in making this distinction by referring to certain linear defects displayed in his slides as thingies! This issue has greatly worried us in our recent AFOSR-sponsored research, and it was somewhat of a relief to find that this concern is shared by the best of the experts in the field. However, it is now clear that special efforts must be expended upon making this very important distinction--particularly when the ledges are only a few atomic layers high. GRA

N91-16822 Wisconsin Univ., Milwaukee.
FROM LOW TO HIGH Tc: AN ULTRASONIC INVESTIGATION OF NIOBIUM SINGLE CRYSTAL AND YBaCuO SUPERCONDUCTING THIN FILMS WITH SURFACE ACOUSTIC

WAVES Ph.D. Thesis
Hugues-Pierre Baum 1990 157 p
Avail: Univ. Microfilms Order No. DA9035144

New results of surface acoustic waves (SAW) measurements on superconducting thin films from low critical temperature Tc (niobium, 8.6 K) to high Tc (Y1Ba2Cu3O(7-delta), 87 K) are reported. All films were less than 1 micron thick. The 700 MHz Rayleigh type SAW were used for the Nb investigation, whereas all other measurements were performed at 170 MHz. Critical findings about environmental, and internal, electromagnetic (e-m) noise are detailed, and those led to the initiation of a last study, the SAW attenuation in the substrate itself, under similar conditions. Some experiments reported were performed in a Faraday cage, to screen out all external e-m influences. This allowed for exceptional resolution (better than 0.01 dB) and for the discovery of small attenuation changes (0.2 dB) at the superconducting transition. A single crystal Nb film was studied and the results appear to follow the electron-phonon nature of the interaction of SAW with this type of superconductor. In Y1Ba2Cu3O(7-delta)(high Tc superconductor) however, the small change in attenuation observed at the transition is explained by the acousto-electric effect and the percolation theory. The direct measurements of ultrasonic surface wave attenuation on bare LiNbO3 substrates at 170 MHz appear to confirm results obtained elsewhere with a laser probe, and extend their range of validity down to 4 K. An example of potential application of the use of SAW with the new high Tc superconducting thin films, the Frequency Adjustable Surface Acoustic Wave device (FASAW) to be used as a tunable filter, chirp, encoder-decoder, and other, device is presented. Some ideas for new types of measurements of thin films and bulk material, with SAW are developed. Dissert. Abstr.

N91-16823 Harvard Univ., Cambridge, MA.
DYNAMICAL PROPERTIES OF TWO-DIMENSIONAL JOSEPHSON JUNCTION ARRAYS Ph.D. Thesis
Samuel Paul Benz 1990 147 p
Avail: Univ. Microfilms Order No. DA9035438

The dynamical properties of two-dimensional (2D) Josephson junction arrays are investigated at temperatures below the Kosterlitz-Thouless phase transition. A comprehensive study, based on experiments and simulations, is completed, on the effects of large direct (dc) and radio-frequency (RF) bias currents on 2D arrays in the presence of perpendicular magnetic fields. Experiments were performed on large 1000 by 1000 arrays of Nb-Cu-Nb proximity-effect junctions that were fabricated using various photolithographic and thin-film deposition techniques. A complete explanation of the dynamic resistance in arrays is presented as a function of both dc bias current and magnetic field. For certain fields, when the number of flux quanta per array unit cell is the ratio of two integers, the field-induced vortices are commensurate with the array and are arranged in ordered superlattices with q x q unit cells. Prominent peaks in the dynamic resistance are observed for these commensurate magnetic fields, and the currents at these peaks are related with the depinning currents of the vortex superlattices. New exact calculations of the critical current are presented for the cases where f = 1/2 and 1/3. When RF currents are applied to the 2D arrays in commensurate magnetic fields, fractional giant steps appear in the current-voltage curves at voltages, V(sub n) = n(N/q)h(nu)/2e, (where N = 1000 is the number of junctions in the direction of applied current) directly related to the vortex superlattice unit cell size, q. These steps are confirmed through computer simulations on arrays of resistively shunted Josephson junctions. A phenomenological model is proposed to explain these steps, based on the locking of the motion of the vortex superlattices with the applied RF current. The results of simulations of positionally-diordered superconducting wire networks are also presented. The critical field is determined from the decay of oscillations in the calculated transition temperature as a function of magnetic field. Dissert. Abstr.

N91-16824 Leicester Univ. (England).
EPITAXIAL GROWTH AND SURFACE MORPHOLOGY OF SOME METAL AND SEMICONDUCTOR STRUCTURES Ph.D. Thesis
Andrew David Johnson 1989 204 p
Avail: Univ. Microfilms Order No. BRD-90624

Forward focusing of medium energy Auger and photoelectrons were used along with LEED and Auger electron spectroscopy to investigate the initial stages of growth of both Cr and Co on Ag(001). Chromium was found to grow epitaxially on Ag in the bcc phase up to approximately 2 ML, in agreement with previous results. Cobalt also grows epitaxially on Ag up to 3 ML although it is proposed that the Co lattice is in the FCC phase but no comment can be made as to whether the overlayer is laterally expanded. Polarized neutron reflection (PNR) measurements were made on Ag/Cr/Ag sandwich structures with varying thicknesses of Cr. It is shown that for the Cr thickness of 2 and 3 ML, the Cr is ordered nonferromagnetically and it is proposed that at these thicknesses the Cr has reverted to its bulk antiferromagnetic order. However measurements on samples with Cr thicknesses of 0.33 ML indicate ferromagnetic ordering with a greatly enhanced magnetic moment per atom over the bulk Cr value, in partial agreement with previous theoretical predictions. The PNR measurements on a Ag/Fe/Ag(001) structure with a thickness of Fe of 8 ML have yielded an accurate measurement of the magnetic moment per atom for the Fe film of 1.0 + or - 0.15 microB, indicating a reduced value from that of bulk Fe of 2.22 microB. X ray scattering from a Ge(001) surface was used to show that the surface undergoes a reversible phase transition at T = 954 + or - 7 K. It is proposed that the transition occurs due to the formation of vacancy-adatom pairs as some of the surface dimers break with increasing temperature. The data are explained in terms of a three level model used to describe the vacancy-adatom creation. The three level model results are compared with results from a simple Monte Carlo simulation. Dissert. Abstr.

N91-16825# Technische Univ., Eindhoven (Netherlands).
PHYSICO-CHEMICAL INVESTIGATIONS ON Co-Mn-OXIDE SPINELS Ph.D. Thesis
Anna Dorothea Dagmar Broemme 1990 144 p
(ETN-91-98476) Avail: NTIS HC/MF A07

The processes of electronic transitions and the charge transport mechanisms are investigated. Extrinsic charge carriers were introduced by incorporating dope ions in the crystal, such as titanium or lithium. The spinels were prepared with ceramic methods by sintering. Single phase samples were selected by means of optical microscopy and x ray diffraction. Thermogravimetric measurements were performed to determine the oxygen content. The Seebeck coefficient, the conductivity and the thermal expansion were determined as a function of temperature. X ray photoemission spectra were recorded. It was remarked that the thermal expansion coefficient of Co3O4 spinels increases significantly above 750K, which is not observed in other oxidic materials and can be explained by a low spin to high spin transition of the trivalent Co ion on octohedral sites without charge transfer. ESA

N91-16826# Technische Univ., Delft (Netherlands).
IMAGE INTERPRETATION FOR TRANSMISSION ELECTRON MICROSCOPY OF THIN SEMICONDUCTOR LAYERS AND INTERFACES Ph.D. Thesis
Alan Frank deJong 1990 188 p
(ETN-91-98487) Avail: NTIS HC/MF A09

It is shown how computer simulation and computer processing can contribute to the interpretation of transmission electron microscopy (TEM) images of thin semiconductor layers and interfaces. For image simulations, a model of the structure of the material or interface under investigation is postulated. From this model, images are calculated and compared with experimental images. Several examples show that it is possible to obtain quantitative results. The greatest strength of the TEM, and certainly of high resolution electron microscopy (HREM) is to enable the distinction between a limited number of structural models. ESA

77 THERMODYNAMICS AND STATISTICAL PHYSICS

Includes quantum mechanics; theoretical physics; and Bose and Fermi statistics.

For related information see also *25 Inorganic and Physical Chemistry* and *34 Fluid Mechanics and Heat Transfer.*

N91-16827# Ohio State Univ., Columbus. Dept. of Physics.
FERMIONS IN THE HYPERCHARGE SECTOR OF THE STANDARD LATTICE ELECTROWEAK THEORY: GLOBAL LIMIT
Sinya Aoki, I-Hsiu Lee, Junko Skigemitsu, and Robert E. Shrock (State Univ. of New York, Stony Brook.) 1990 13 p
(Contracts DE-AC02-76ER-01545; DE-AC02-87ER-40325; NSF PHY-80-08495)
(DE90-009731; DOE/ER-01545/440; ITP-SB-89-40; RU-89/B1/55) Avail: NTIS HC/MF A03

We study the global limit of the hypercharge U(1)(sub Y) sector of the standard lattice electroweak theory. We show that for fermions with both Y(sub R) = 0 and Y(sub R) not equal to 0 the doubler modes can be removed in the continuum limit while the physical fermion masses can be tuned to agree with physical values. DOE

N91-16828# Kentucky Univ., Lexington.
RESEARCH IN THEORETICAL NUCLEAR PHYSICS
Keh-Fei Liu 13 Sep. 1989 28 p
(Contract DE-FG05-84ER-40154)
(DE90-010792; DOE/ER-40154/T2) Avail: NTIS HC/MF A03

This paper discusses: the role of nuclear binding in EMC effect; skyrmion quantization and phenomenology; lattice gauge Monte Carlo calculations; identification of tensor glueball; evidence of mesoniums in pn annihilation and gamma gamma reactions; Skyrme-Landau parameterization of effective NN interactions; and quark-gluon plasma. DOE

N91-16829# Lawrence Livermore National Lab., CA.
A NEW PERTURBATION THEORY OF SOLIDS AND FLUIDS AND ITS APPLICATIONS TO HIGH-PRESSURE MELTING PROBLEMS
Francis H. Ree May 1990 29 p Presented at the 2nd Archimedes Workshop on Molecular Solids Under Pressure, Catania, Italy, 28-31 May 1990
(Contract W-7405-eng-48)
(DE90-011502; UCRL-JC-103943; CONF-9005203-1) Avail: NTIS HC/MF A03

A statistical mechanical theory that can describe both solids and fluids in a self-consistent way is described. This theory utilizes a optimized reference potential whose repulsive range shrinks with density. A unique feature of the new theory is that solid- and fluid-phase thermodynamic properties are both computed within a single theoretical framework. Hence, it allows us to study melting phenomena in a self-consistent manner. For solids, the new theory treats both harmonic and anharmonic effects in thermodynamic properties on equal footing. Applications to several model and rare gas systems show that the new theory can accurately predict fluid, solid, and fluid-solid transition properties. Effective pair potentials inferred from the analysis of krypton and xenon isotherms contain short- and long-range modifications to the Aziz-Slaman pair potential. The long-range correction is repulsive and originates from the Axilrod-Teller three-body force, while the short-range correction probably originates from many-body forces. Using the computed melting curves of krypton and neon, we discuss the range of validity of the corresponding states principle for rare gas systems. DOE

80 SOCIAL SCIENCES (GENERAL)

Includes educational matters.

No abstracts in this category.

81 ADMINISTRATION AND MANAGEMENT

Includes management planning and research.

N91-16830# Logistics Management Inst., Bethesda, MD.
MANAGEMENT INFORMATION: A KEY TO BETTER ACQUISITION AT NIH Final Report
Harry H. Moore, Cynthia W. Shockley, and Robert A. Spargo Apr. 1990 106 p
(Contract MDA903-85-C-0139)
(AD-A226867; LMI-NI801R1) Avail: NTIS HC/MF A06 CSCL 05/1

The acquisition process at the National Institutes of Health (NIH) provides a wide variety of supplies and services to the on-campus research and administrative staff. Management of the process must balance responsiveness with frugal procedures that meet all statutory and regulatory requirements. Achieving the appropriate balance is a challenge, particularly since NIH has no objective, quantifiable, acquisition performance standards. It is recommended that it develop such standards and use them to measure how well the acquisition process is meeting its goals. In addition, NIH is not managing its information resources to best support its organizational goals and objectives. We recommend that it do so in a systematic process that we term a a management information system (MIS). The MIS should be defined by a MIS team - a partnership of acquisition information specialists and functional managers who work together to define the data and system needed to make good decisions. We believe that NIH can improve its automated resources to better support the MIS. GRA

N91-16831# Department of Energy, Washington, DC. Office of Small and Disadvantaged Business Utilization.
REPORT TO CONGRESS ON THE SMALL BUSINESS PROGRAM
1989 53 p
(DE91-004622; DOE/MA-0422) Avail: NTIS HC/MF A04

The Department of Energy's (DOE) Small Business Program is characterized by its diligent involvement in the procurement process to enhance participation by small businesses, small disadvantaged businesses, labor surplus area firms, and women-owned businesses. The DOE's primary means of securing an equitable proportion of transactions for these businesses are total set-asides, partial set-asides, 8(a) sole source procurements, and 8(a) competitive procurements. Throughout the DOE's infrastructure, all DOE organizational elements are committed to successfully implement the Small Business Program. The Department's commitment includes developing substantial opportunities in both prime contracting and subcontracting and encompasses special preference programs to enhance awards to such businesses. DOE

N91-16832*# National Aeronautics and Space Administration. Langley Research Center, Hampton, VA.
SPACE STATION FREEDOM RESOURCE ALLOCATION ACCOMMODATION OF TECHNOLOGY PAYLOAD REQUIREMENTS
Don E. Avery, Lisa D. Collier, and Charles F. Gartrell (General Research Corp., Washington, DC.) Nov. 1990 32 p
(NASA-TM-102766; NAS 1.15:102766) Avail: NTIS HC/MF A03 CSCL 05A

An overview of the Office of Aeronautics, Exploration, and Technology (OAET) Space Station Freedom Technology Payload

Development Program is provided, and the OAET Station resource requirements are reviewed. The requirements are contrasted with current proposed resource allocations. A discussion of the issues and conclusions are provided. It is concluded that an overall 20 percent resource allocation is appropriate to support OAET's technology development program, that some resources are inadequate even at the 20 percent level, and that bartering resources among U.S. users and international partners and increasing the level of automation may be viable solutions to the resource constraint problem. Author

N91-16833# Advisory Group for Aerospace Research and Development, Neuilly-Sur-Seine (France).
CALENDAR OF SELECTED AERONAUTICAL AND SPACE MEETINGS: JANUARY 1991 ONWARDS
Dec. 1990 130 p
(AGARD-CAL-91/1; ISBN-92-835-0599-9) Copyright Avail: NTIS HC/MF A07; Non-NATO Nationals requests available only from AGARD/Scientific Publications Executive

Three kinds of events are covered by this calendar: technical meetings, conferences, and symposia; exhibitions and technical displays; and educational courses. For each meeting, exhibition, or course, the following information is given: reference number, data, location, title and sponsor, keywords indicating main topic covered, and contact code for inquiries. A subject index in the form of keywords is given, each keyword being followed by reference numbers of all the meetings relevant to that particular keyword. B.G.

N91-16834# Messerschmitt-Boelkow-Blohm G.m.b.H., Ottobrunn (Germany, F.R.). Zentralbereich Technik.
TECHNOLOGICAL MANAGEMENT AS AN ELEMENT OF STRATEGY FOR AN EFFICIENT COMPANY MANAGEMENT [TECHNOLOGIEMANAGEMENT ALS STRATEGIEELEMENT EINER EFFIZIENTEN UNTERNEHMENSFUEHRUNG]
H. Prem Apr. 1990 10 p In GERMAN Presented at the Fachtagung Integriertes Innovati onsmnagement, Forum Inst. fuer Management, Duesseldorf, Fed. Republic of Germany, 19-20 Jun. 1990
(MBB-Z-0307-90-PUB; ETN-91-98504) Avail: NTIS HC/MF A02

The acquisition of abilities, so that industrial companies can successfully realize technological projects, are examined. The air and space industries are considered as typical fields, in which one cannot speak of mass production, as is mostly the case in other industries. It requires a very effective analysis of the total surrounding field, as each deviation exerts a stronger effect on the product costs, than in mass production. Four situations are examined: protection, transport, space flight and energy. The planning of resources utilization is studied. The Parametric Review of Information for Costing and Evaluation (PRICE) system is used for the evaluation of development costs. Development curves are presented. ESA

82 DOCUMENTATION AND INFORMATION SCIENCE

Includes information management; information storage and retrieval technology; technical writing; graphic arts; and micrography.

For computer documentation see *61 Computer Programming and Software.*

N91-16835# Oak Ridge National Lab., TN.
SUBJECT BIBLIOGRAPHY OF THE PMA 205 (PROGRAM MANAGER AIR 205) NETWORK TECHNICAL LIBRARY AT OAK RIDGE NATIONAL LABORATORY
Marilyn V. Ayers 1 May 1990 109 p
(Contract DE-AC05-84OR-21400)
(DE90-009988; ORNL/TM-11534) Avail: NTIS HC/MF A06

The PMA 205 (Program Manager Air 205) Network Technical Library at the Oak Ridge National Laboratory (ORNL) contains documents relating to U.S. Department of Defense standards for computer-based training technology and training and American National Standards Institute international standards for user interfaces and computer-aided acquisition and logistic support. The collection emphasizes supporting research in instructional system design, software engineering, user system interfaces, human factors engineering, and cognitive psychology as it differentiates between higher and lower cognitive tasking. The collection currently consists of about 670 documents of various types. These include military standards and specifications, reports, conference proceedings, dissertations, technical manuals, books, journal articles, and military instructions and directives. The documents have been added to the library as the result of literature searches and personal submission from team members. It is a selective collection and not a comprehensive one. A database, written in Procite/PC, contains the cataloged holdings of the library. Each record contains the bibliographic information and an abstract. The database provides access to information in the records by either full text searches using Boolean logic or individual field searching. One-word quick searches can be performed on the date, title, or author fields. The browsing capability for retrieved items is by full record or brief format. Search results can be read from the screen, printed to hard copy, or transferred to a disk file for later use. Disks containing the database and printed bibliographies are available to PMA 205 network team members upon request. Bibliographies created from the database are listed alphabetically by subject. The subject headings used are based on Defense Technical Information Center subject terms and other selected terms suited to the scope of the collection. Author

N91-16836 New South Wales Univ., Canberra (Australia).
GEOGRAPHIC DATA TRANSFER M.S. Thesis, 1989 Abstract Only
Timothy James Ramsay Mollison 3 May 1990 2 p
Avail: Issuing Activity

The expanding role and increased diversity of application of computer based spatial information systems has meant an increasing demand for the facility to incorporate various data sets. Meanwhile, the computer industry has engineered products such that various makes and models are frequently of incompatible format, so that the ease of transmission of data between parties with a common interest or sphere of operation has often been a function of computer trademark. The determination of appropriate protocols and interchange standards has alleviated this problem for many areas, but these have not met the special needs of spatial data structures. Eminent American groups have recently proposed a new standard for the interchange of digital cartographic data. This proposed Standard is also under consideration as the basis for an Australian Standard for Digital Geographic Data Transfer. This project was concerned with the development of data transfer software implementing the provisions of the Proposed Standard. Emphasis was placed upon the content of the transfer files and an illustration of output data representation under the vector form is provided. The application of spatial data and spatial information systems to the modeling of global environmental problems indicates the importance of the Standard in an Australian and international context. Author

N91-16837# Virginia Univ., Charlottesville. Dept. of Computer Science.
THE STARLITE PROJECT Annual Report, 1 Oct. 1989 - 30 Sep. 1990
Robert P. Cook and Sang H. Son Sep. 1990 52 p
(Contract N000143-86-K-0245)
(AD-A226722; UVA/525410/CS91/104) Avail: NTIS HC/MF A04 CSCL 12/5

The StarLite Project has the goal of constructing a program library for real time applications. The initial focus of the project is on operating system and database support. The project also involves the construction of a prototyping environment that supports experimentation with concurrent and distributed algorithms in a host environment before down-loading to a target system for performance testing. The components of the project include a Modula-2 compiler, a symbolic Modula-2 debugger, an

interpreter/runtime package, the Pheonix operating system, the meta-file system, a visual simulation package, a database system, and documentation. GRA

N91-16838# Assistant Secretary of the Air Force, Washington, DC. Deputy Director for Scientific and Technical Information.
THE USAF STINFO PROGRAM OVERVIEW
Walter R. Blados and Charlie Maiorana Jun. 1989 199 p
Prepared in cooperation with INFO/tek, Washington, DC
(AD-A226969; USAF-STINFO-MANAGEMENT-90/1; SAF/AQT-SR-90-001) Avail: NTIS HC/MF A09 CSCL 05/2

The critical elements of the USAF STINFO (Scientific and Technical Information) Program are summarized, covering the topics and materials in the STINFO Program Manager training course. The purpose is to impart an in-depth understanding of what the STINFO Program Management duties are and to give instruction in carrying out the STINFO function. The overall objective is to support the DoD Scientific and Technical Information (STI) Program, in order to increase the effectiveness of the scientific and technical efforts in the DoD community. Author

N91-16839# Air Force Inst. of Tech., Wright-Patterson AFB, OH.
MANAGING EMERGING TECHNOLOGY: CASE STUDIES IN DOCUMENT IMAGING SYSTEMS M.S. Thesis
Richard K. Brown 1990 152 p
(AD-A227688; AFIT/CI/CIA-90-068) Avail: NTIS HC/MF A08 CSCL 14/5

A document imaging system (DIS) digitizes paper-based information, such as graphics and text, into images for storage, maintenance and retrieval. This technology promises and, in many cases of actual DIS implementation, has delivered many benefits to organizations. Document imaging technology is enabling organizations to handle their information more efficiently than in the past. However, organizations face many issues while implementing this technology. Six case studies of organizations which appraised Document Imaging Systems (DIS) are presented and detailed. The research had two thrusts. The first aimed to identify critical management issues relating to the successful assimilation of DIS. Actions identified included ensuring integration into the existing technical architecture, designing adequate image distribution channels, preparing for future technology changes, choosing the right applications to implement, selecting appropriate indexes, overhauling the work process, alleviating the concerns of the users, securing adequate management support, and justifying the technology. The second goal sought to examine how organizations implementing document imaging technology progress through six stages of technology assimilation: Awareness/Observation, Evaluation/Justification, Acquisition/Installation/Modification, Pilot Test/Experiment, Limited Production, and Full Production. GRA

N91-16840 Texas Univ., Austin.
INFORMATION TECHNOLOGY POLICIES: A FOUR COUNTRY COMPARATIVE STUDY Ph.D. Thesis
Woochun Song 1990 232 p
Avail: Univ. Microfilms Order No. DA9031720

In recent years, the development of information technologies has been so rapid that a new age is being entered. In this new era, knowledge and communication are perceived as the main forces of social change and the possession of these technologies has become a serious concern of many countries. Governments in both industrialized and developing countries adopted national policies and plans to respond to this new change. However, what motivates the effort to develop information technologies, and what affects the process of this technological development largely remain unanswered. The justifications of policies implemented to develop information technology industries is being explored; policy measured adopted are being examined; and the outcomes of those approached are being discovered. Dissert. Abstr.

N91-16841# Naval Ocean Research and Development Activity, Bay Saint Louis, MS. Mapping, Charting, and Geodesy Div.
DATA BASE STRUCTURE TO SUPPORT THE PRODUCTION OF THE DIGITAL BATHYMETRIC DATA BASE Final Report
James E. Braud, John L. Breckenridge, James E. Current, and Jerry L. Landrum Nov. 1989 56 p
(AD-A227915; NORDA-236) Avail: NTIS HC/MF A04 CSCL 08/3

NORDA was tasked to develop a computer model that would support the storage and retrieval of the 7 billion points of collected bathymetry that are used to support the Ocean Survey Program. These data points are stored at a resolution that is beyond the noise level induced by the collection sensors. Gridding these bathymetric data on an acceptable resolution of 0.1 minute for areas of actual coverage can greatly reduce storage requirements. Further reductions can be achieved through the use of the compression algorithms developed as a result of this project. An overall compression ratio of 500 to 1 was demonstrated using actual data supplied by the Naval Oceanographic Office. Once the data base is reduced in size to a manageable level, relational data base management systems become practical for organizing information related to the bathymetry in order to provide easy multikeyed access. The Structured Query Language, a de facto standard for data base retrieval, can be used to query the data base to obtain tables of path names for the files that contain the compressed bathymetry. A suggested format for these files and the relational data base structure is presented. GRA

N91-16842# Institute of Electrical and Electronics Engineers, New York, NY.
IEEE INTERNATIONAL SYMPOSIUM ON INFORMATION THEORY Final Report, 1 Oct. 1989 - 31 May 1990
L. B. Milstein and A. J. Viterbi 1990 217 p Symposium held in San Diego, CA, 14-19 Jan. 1990 Sponsored by NSF and ONR
(Contract DAAL03-89-G-0122)
(AD-A228239; ARO-27283.1-EL-CF) Avail: NTIS HC/MF A10 CSCL 12/9

This volume consists of abstracts of papers presented at sessions on the following topics: Spread spectrum communications; Detection theory; Neural networks; Data compression; Channel capacity; Coding theory; Trellis coding; Communications systems; Broadcast channels; Estimation; Quantization; Shannon theory; Error control and other coding; Communication theory; Modulation; Optical communications; Source coding; Stochastic processes; Multiple access; Signal processing; Cyclic codes; Error correcting codes; Cryptography; Speech processing; Block coding; Viterbi decoders; Communications networks; Magnetic recording; Information theory applications; Pattern recognition; Entropy; and Convolutional codes. GRA

N91-16843# Stanford Univ., CA. Dept. of Computer Science.
RESEARCH INTO THE DESIGN AND IMPLEMENTATION OF KNOWLEDGE BASE SYSTEMS Final Report, 1 Aug. 1988 - 31 Jul. 1990
Jeffrey D. Ullman 31 Jul. 1990 8 p
(Grant AF-AFOSR-0266-88; AF Proj. 2304)
(AD-A228873; AFOSR-90-1106TR) Avail: NTIS HC/MF A02 CSCL 12/7

The general goal of the work has been to develop the techniques needed to process queries, expressed as logic programs, efficiently. A system called NAIL was developed, by mid-1989, to test out our ideas. It was fully declarative, which we found an interesting challenge, and its implementation exposed a number of issues that lead to important new ideas and research. However, the full declarativeness proved too much of a burden in writing some applications that we hoped would be facilitated by a logic/database language, and NAIL was abandoned in favor of a new language, called GLUE, that is logical, but that allows for controlled-flow, sets as data values, and aggregation operators such as sums of average. NAIL now serves as the view facility for GLUE, and we are in the process of writing a NAIL-to-GLUE

translator that will offer both nondeclarative capabilities of GLUE and the declarative capabilities of NAIL, whichever is more appropriate in a given situation. GRA

N91-16844# North Carolina Univ., Chapel Hill. Dept. of Computer Science.
USING COMPUTER-GENERATED PROTOCOLS TO STUDY WRITERS' PLANNING STRATEGIES
Marcy Lansman, John B. Smith, and Irene Weber Sep. 1990 22 p
(Contracts N00014-86-K-0680; MDA903-86-C-0345; NSF IRI-85-19517)
(AD-A228875; TR90-033) Avail: NTIS HC/MF A03 CSCL 12/6

Research has shown that extensive planning is typical of skilled adult writers. Yet word processors tend to discourage high level planning. In this research, we used the Writing Environment, a computer-based authoring tool that encourages planning, to study the strategies of adult writers. Nine graduate students and eight technical writers used the Writing Environment to write technical reports, while the computer recorded their activities. Analysis of computer-generated protocols revealed that subjects spent a large proportion of their time on the organizational structures for their reports and that these structures were quite elaborate. Subjects varied widely in the extent to which they completed their plans before they wrote. Surprisingly, the overall quality of the reports, as rated by two judges, was negatively related to time spent planning. Some writers apparently spent too much time on complex organizational structures and too little time composing text. GRA

N91-16845 Rutgers - The State Univ., New Brunswick, NJ.
A SECTORIAL ANALYSIS OF THE INFORMATION SECTOR IN THE INFORMATION ECONOMY: ITS COMPARATIVE MEASUREMENT AND NEW CLASSIFICATION MODEL Ph.D. Thesis
Dong Youl Jeong 1990 225 p
Avail: Univ. Microfilms Order No. DA9034913

The production, processing, and distribution of information is fast becoming a major economic activity for many nations of the world. Information is becoming the strategic resources and transforming agents in the information society. Two major objectives are fulfilled with regard to the analysis of the information sector in the information economy. First, an empirical study of the information sector-the information work force, and information goods and services (information activities) - of the selected nations are investigated. Second, a theoretical explanation of the major factors of the growth of the information sector is advanced, and a new classification model of the information economy is developed. In order to answer the objectives, the emergence of the information work force is derived and compared using the industry occupation matrix table, and of the information goods and services using the value added proportion of the gross domestic products (GDP) by analyzing both the primary information sector (PIS) and secondary information sector (SIS) separately. Based on the empirical data analysis, results show that the information sector in all selected countries, is consistently increasing, regardless of the levels of industrialization. The growth rate of the information sector in a developed country tends to slow down as a nation becomes a mature information economy. In addition, each country varies the internal structure of the information work force and the divisional contribution of the information goods and services. From a statistical view point, the growth of the information sector has a very strong relationship with the information work force, primary information sector, and secondary information sector among other. Dissert. Abstr.

N91-16846 Institute for Perception RVO-TNO, Soesterberg (Netherlands).
A NORMATIVE DATABASE FOR, AND ANALYSIS OF, THE DUAL TASK OF THE TASKOMAT Final Report
S. A. Los and L. C. Boer 19 Feb. 1990 39 p In DUTCH; ENGLISH summary
(Contract A88/M/319)
(IZF-1990-A-11; TD-90-0025; ETN-91-98310) Copyright Avail: Institute for Perception RVO-TNO, P.O. Box 23, 3769 ZG Soesterberg, Netherlands

The dual task test of the TASKOMAT was investigated. The TASKOMAT is a test battery on a personal computer to test several aspects of the human information acquisition system. It consists of a tracking task and a Continuous Memory Task (CMT). The analysis of the tracking task shows a test retest correlation of about 0.75, and a small relation between tracking and intelligence. The reliability of the CMT was estimated to be at least 0.55; no relation with intelligence was found. An experimental visual version of the CMT yields tables was established, based on 344 flight training candidates in the Dutch Government Civil Aviation Flying School and 194 conscripts in the Royal Dutch Army. The differences are thought to reflect motivational factors. Some remarks concerning the use and optimization of the dual task are given. ESA

N91-16847*# National Aeronautics and Space Administration, Washington, DC.
NASA THESAURUS AERONAUTICS VOCABULARY
Jan. 1991 220 p
(NASA-TM-104230; NAS 1.15:104230) Avail: NTIS HC/MF A10 CSCL 05B

The controlled vocabulary used by the NASA Scientific and Technical Information effort to index documents in the area of aeronautics is presented. The terms comprise a subset of the 1988 edition of the NASA Thesaurus and its supplements issued through the end of 1990. The Aeronautics Vocabulary contains over 4700 terms presented in a hierarchical display format. In addition to aeronautics per se, the vocabulary covers supporting terminology from areas such as fluid dynamics, propulsion engineering, and test facilities and instrumentation. Author

83 ECONOMICS AND COST ANALYSIS

Includes cost effectiveness studies.

No abstracts in this category.

84 LAW, POLITICAL SCIENCE AND SPACE POLICY

Includes NASA appropriation hearings; aviation law; space law and policy; international law; international cooperation; and patent policy.

No abstracts in this category.

85 URBAN TECHNOLOGY AND TRANSPORTATION

Includes applications of space technology to urban problems; technology transfer; technology assessment; and surface and mass transportation.

For related information see also *03 Air Transportation and Safety, 16 Space Transportation,* and *44 Energy Production and Conversion.*

No abstracts in this category.

88 SPACE SCIENCES (GENERAL)

N91-16848# Space Research Organization Netherlands, Utrecht.
[ACTIVITIES REPORT OF THE SPACE RESEARCH ORGANIZATION NETHERLANDS] Annual Report, 1989
Mar. 1990 241 p
(ETN-91-98473) Avail: NTIS HC/MF A11

The leading fields of research were x ray astronomy, infrared astronomy, solar research, ultraviolet and visual astronomy, gamma ray astronomy. The SRON scientific program is not limited to astronomy. It contains a substantial component on solid Earth research, as well as on the physics and the biology under conditions of (near) weightlessness. In 1989 the core instrument selection for XMM, the x ray observatory, took place. SRON contributed to the manufacture of the detector electronics for Hipparcos launching. The x ray instrument on board the Russian Space Station MIR operated satisfactorily. The Italian-Dutch x ray mission continued according to plan. ESA

N91-16849# Deutsche Forschungsgemeinschaft, Bonn (Germany, F.R.). COSPAR-Landesausschuss.
SPACE RESEARCH IN THE FEDERAL REPUBLIC OF GERMANY, 1988 AND 1989
1990 48 p
(ETN-91-98514) Avail: NTIS HC/MF A03

The following subject areas are covered: space astronomy and solar physics; solar wind, magnetospheres and energetic particles; atmospheres and ionospheres; Earth observations; material sciences; life sciences. Missions contributing to research include: the two Soviet Phobos spacecraft; the ESA astrometry mission Hipparcos; the Jupiter probe Galileo; the solar maximum mission; the x ray observatory EXOSAT; the German Helios probes; the AMPTE mission; the Giotto flyby by comet Halley; the ROSAT x ray telescope. ESA

89 ASTRONOMY

Includes radio, gamma-ray, and infrared astronomy, and astrometry.

N91-16850# Lawrence Livermore National Lab., CA.
LOW-COST, HIGH-RESOLUTION TELESCOPES FOR IMAGING LOW-EARTH ORBIT SATELLITES
N. A. Massie, Yale Oster, Greg Poe, Lynn G. Seppala, and Mike Shao (Harvard-Smithsonian Center for Astrophysics, Cambridge, MA.) Jan. 1989 18 p Presented at the SPIE Astronomical Telescopes and Instrumentation for the 21st Century Symposium, Tucson, AZ, 11-17 Feb. 1990
(Contract W-7405-eng-48)
(DE90-012081; UCRL-101665; CONF-900285-5) Avail: NTIS HC/MF A03

Telescopes designed for non-conventional imaging of near-earth satellites must follow the unique set of design rules. Cost must be reduced substantially and the design must accommodate a technique to circumvent the atmospheric distortion of the image. Apertures to 12 m and beyond are required along with alt-alt mounts providing high tracking rates. A novel design for such a telescope gas been generated which is optimized for speckle imaging. Its mount closely resembles a radar mount and it does not employ the conventional dome. Costs for this design are projected to be considerably reduced compared to conventional designs. Results of a detailed design study will be presented. Applications to astronomy will be discussed. DOE

N91-16851 Louisiana State Univ., Baton Rouge.
USING TILTED-RING MODELS AND NUMERICAL HYDRODYNAMICS TO STUDY THE STRUCTURE, KINEMATICS AND DYNAMICS OF HI DISKS IN GALAXIES Ph.D. Thesis
Dimitris Michael Christodoulou 1989 292 p
Avail: Univ. Microfilms Order No. DA9017253

The structure, kinematics, and dynamics of neutral hydrogen gas in galaxies is modeled. Attention is focused on specific features that are commonly observed mainly in the 21-cm line, such as twists, warps, and polar rings. The intimate connection between these features and the presumed dark halos of galaxies is analyzed with the intention to discover ways to probe the dark matter of individual galaxies by simply observing the distribution and kinematics of the luminous matter. An important, intermediate step in this analysis is to demonstrate that the twists that appear in the isovelocity maps of many spiral galaxies (and that are reproduced by the corresponding kinematical models) have a dynamical origin, owing their existence to the differential precession of gas-particle orbits. The main conclusions from this work are: (1) the kinematics of normal spiral galaxies can be modeled satisfactorily by a tilted-ring model; (2) the galaxies NGC5033 and NGC5055 show the signature of a prolate halo in their kinematics; (3) strongly twisted warps form naturally when a gaseous disk attempts to settle toward a preferred orientation in the external potential well of a weakly distorted halo, but only if the disks start from low or moderate inclinations relative to the preferred orientation; (4) highly and moderately inclined disks, as well as disks at all inclinations under the influence of a strongly non-spherically-symmetric halo, show significant matter inflow: and (5) polar rings and highly inclined disks can only survive for a Hubble time if the superimposed halo is nearly spherical.
Dissert. Abstr.

N91-16852 Pennsylvania State Univ., University Park.
MULTIPLE-PHOTON COMPTON SCATTERING IN A STRONG MAGNETIC FIELD: CROSS-SECTIONS AND RADIATIVE TRANSPORT Ph.D. Thesis
Stephen George Alexander 1990 129 p
Avail: Univ. Microfilms Order No. DA9032237

Astrophysical plasmas in the vicinity of a neutron star are believed to be threaded by a strong magnetic field. The physics of electron-photon scattering in such a field is investigated quantum electrodynamically, and calculations of the cross sections reveal that one-photon Compton scattering is the dominant process for photon energies in the continuum and near the fundamental cyclotron harmonic. The presence of the strong field permits two multiple photon processes that are analytically of the same order in the fine structure constant as one-photon scattering, and these are shown to dominate near the higher cyclotron harmonics. These processes are two-photon scattering where the electron is scattered into an excited state from which it radiatively decays with the emission of a second photon; and two-photon emission where an electron cyclotron absorbs a photon and then decays to the ground state with the emission of two photons. Since several of the terms that describe the two-photon processes in the differential equation of radiative transport are nonlinear, the discrete ordinate finite difference Feautrier method is extended to include nonlinear effects. This technique is used with the one- and two-photon processes to calculate model spectra that extend to the higher cyclotron harmonics for x ray pulsars and gamma ray bursters. The x ray pulsar model is a self-radiating optically thick slab, and the results show general agreement with observations of Hercules X-1. The model for the hard x ray spectrum of gamma ray bursts consists of radiation that is transmitted through an optically thin sheet of plasma. The results give excellent agreement with observations of the gamma ray burster GB 880205.
Dissert. Abstr.

N91-16853 Leicester Univ. (England).
X RAY EMISSION FROM LOW-MASS BINARY SYSTEMS Ph.D. Thesis
Lorraine Maria Breedon 1989 226 p
Avail: Univ. Microfilms Order No. BRD-89525

The bright galactic x ray sources, which possess (1 to 10 keV) luminosities above approximately 10(exp 36) ergs/s can be roughly divided into two groups: the young, massive x ray binaries and the old, low mass x ray binaries (including burst sources and

globular cluster x ray sources). In these groups the x ray emitting compact object is almost always a neutron star (in a few cases perhaps, a black hole). Only with the radiation from material in the vicinity of a neutron star, specifically in the low mass x ray binaries is examined. The pre-1983 knowledge of the low-mass x ray binaries (hereafter LMXRBs) is summarized and how Exosat has made a contribution is indicated. Contributions from the Japanese x ray satellite TENMA, in operation at the same time as Exosat, are also considered. Since the understanding of the massive x ray binaries is often applied to the LMXRBs where there is considerable less information available, the properties of the massive x ray binaries are also briefly discussed.

Dissert. Abstr.

N91-16854 California Inst. of Tech., Pasadena.
A NON-LTE ANALYSIS OF A SAMPLE OF O STARS SELECTED FROM GALACTIC OB ASSOCIATIONS Ph.D. Thesis
Kent Grimmett Budge 1990 286 p
Avail: Univ. Microfilms Order No. DA9031437

The tables of non-LTE line profiles and equivalent widths published by Mihalas and collaborators were revised and extended to four different values of the abundance ratio He/H. Bolometric corrections to V magnitudes were calculated. The theoretical line profiles were fit to echelle spectrograms of 22 galactic O stars by chi squared minimization. It is found that the stars with the lowest surface gravities are fitted best by theoretical spectra with unexpectedly high helium abundances, while the stars with higher surface gravities are fitted best by theoretical spectra with He/H of approximately 0.10, the accepted cosmic ratio. This suggests a systematic failure of conventional non-LTE, plane-parallel models for the more luminous O stars, probably as a result of the neglect of geometrical dilution. The formula, log He/H = 1.1234-0.4791 log g, gives a good fit to the relation between the apparent helium abundance and log g. Using the relationship, the apparent abundances were reduced to what are probably true abundances relative to the normal cosmic abundance. It is found that there is no significant difference in the average helium abundances of the associations observed. However, the stars HD 12993, HD 242908, and HD 19595 may be blue stragglers with moderately enhanced helium abundance. Relative carbon abundances were determined empirically by comparison of the CIV 5812 and He II 4542 A equivalent widths. It is found that the association Cyg OB2 is overabundant in carbon by approximately 50 percent. Likewise, the blue straggler HD 236894 is underabundant in carbon by a factor of two. The estimated effective temperatures of the sample are compared to the previously accepted calibration of MK spectral types to the effective temperature. Estimates of the radii and masses of the stars in the sample were calculated from their physical parameters and their absolute visual magnitude.

Dissert. Abstr.

N91-16855# Optical Sciences Co., Placentia, CA.
PHASED ARRAY IMAGING Final Report, 1 Sep. 1988 - 30 Apr. 1990
Sep. 1990 251 p
(Contract N00014-88-C-0692)
(AD-A228774; TOSC-DR-514) Avail: NTIS HC/MF A12 CSCL 12/1

The problem of recoverable image resolution is investigated for the case where an imaging array is used which array has an optical transfer function that may be described as consisting of islands of nonzero value in a sea of zero values. Can the missing spatial frequency information can be provided--can, in effect, a form of (interpolative) super resolution. The CLEAN algorithm used by radio astronomers suggests that this should be possible. The results developed here indicate that this can be done, with no significant price in terms of signal-to-noise ratio to be paid, and further show that a nonlinear algorithm, like CLEAN, is not required. The results show that the feasibility of doing this depends on the angular size of the object being imaged. We find that its size must be less than the inverse of the largest gap between islands in the array's optical transfer function. GRA

N91-16856 Max-Planck-Inst. fuer Physik und Astrophysik, Garching (Germany, F.R.). Inst. fuer Extraterrestrische Physik.
THE X RAY EMISSION OF SS433
W. Brinkmann, N. Kawai, M. Matsuoka (Institute of Physical and Chemical Research, Saitama, Japan), and H. H. Fink Jul. 1990 48 p Submitted for publication Sponsored in part by STA
(MPE-PREPRINT-189; ETN-91-98613) Copyright Avail: Max-Planck-Institut fuer Physik und Astrophysik, 8046 Garching-bei-Muenchen, Fed. Republic of Germany

Recent x ray observations of SS433 with the Ginga satellite, centered at the phases of optical primary minimum revealed new information about the systems properties. The main observational result is that the spectrum of the source is extremely hard, best fitted with a thermal bremsstrahlung law with kT approximately less than or equal to 30 keV, which softens during eclipse to kT approximately 12 keV. The 6.7 keV iron line region appears to be very complex and varies with the precessional phase. It is argued that the x ray flux from the jets is strongly modulated by large structures on the disc. If these can be modeled properly they will provide important clues to the disc's physical properties which might lead to a better understanding of the precession mechanism. ESA

90 ASTROPHYSICS

Includes cosmology; celestial mechanics; space plasmas; and interstellar and interplanetary gases and dust.
For related information see also *75 Plasma Physics*.

N91-16857 Newcastle-upon-Tyne Univ. (England).
STELLAR CONVECTION AND DYNAMO THEORY Ph.D. Thesis
Richard Leonard Jennings 1989 138 p
Avail: Univ. Microfilms Order No. BRDX89704

Two aspects of astrophysics are considered, large scale stellar convection and the generation of magnetic fields by a dynamo. In the convection problem the outer layers of a star are modeled as two co-rotating plane layers, one on top of the other, coupled at a fluid/fluid interface. The system is such that heating from below causes only the upper fluid to convect, although this convection can penetrate into the lower fluid. Stability analysis is then used to find the most unstable mode of convection. When considering stars, certain parameters are found to be asymptotically large or small, and with parameters appropriate to the Sun the most unstable mode is steady convection in thin cells filling the convection zone. There is negligible vertical motion in the lower fluid, but considerable thermal penetration, and a large jump in helicity at the interface, which has implications for dynamo theory. Next, an alpha omega dynamo is investigated in isolation from the convection problem. Certain aspects of the model are made as simple as possible, yet complexity is included by allowing both latitudinal and time dependence in the magnetic fields. The nonlinear dynamics of the resulting partial differential equations is being analyzed in considerable detail. On varying the main control parameter D (the dynamo number), many transitions of behavior are found involving many forms of time dependence, but not chaos. Further, solutions which break equatorial symmetry are common and provide a theoretical explanation of solar observations which have this asymmetry. Overall the behavior was more complicated than expected, providing insight into the qualitative observations that can be expected from other stars. In particular, there were multiple stable solutions at fixed D, meaning that similar stars can have very different magnetic patterns, with that attained depending upon the star's history. Dissert. Abstr.

N91-16858*# National Aeronautics and Space Administration. Marshall Space Flight Center, Huntsville, AL.
PAIRED AND INTERACTING GALAXIES: INTERNATIONAL ASTRONOMICAL UNION COLLOQUIUM NO. 124
Jack W. Sulentic, ed., William C. Keel, ed. (Alabama Univ., Tuscaloosa.), and C. M. Telesco, ed. Nov. 1990 738 p Colloquium held in Tuscaloosa, AL, 4-7 Dec. 1989; sponsored by NASA, the International Astronomical Union, and Alabama Univ.,

Tuscaloosa
(NASA-CP-3098; M-652; NAS 1.55:3098) Avail: NTIS HC/MF A99 CSCL 03B

The proceedings of the International Astronomical Union Colloquium No. 124, held at the University of Alabama at Tuscaloosa, on December 4 to 7, are given. The purpose of the conference was to describe the current state of theoretical and observational knowledge of interacting galaxies, with particular emphasis on galaxies in pairs. For individual titles, see N91-16859 through N91-16964.

N91-16859*# Special Astrophysical Observatory, Zelenchukskaya (USSR).
A HOMOGENEOUS SAMPLE OF BINARY GALAXIES: BASIC OBSERVATIONAL PROPERTIES
I. D. Karachentsev *In* NASA, Marshall Space Flight Center, Paired and Interacting Galaxies: International Astronomical Union Colloquium No. 124 Nov. 1990 p 3-17 (For primary document see N91-16858 08-90)
Avail: NTIS HC/MF A99 CSCL 03B

A survey of optical characteristics for 585 binary systems, satisfying a condition of apparent isolation on the sky, is presented. Influences of various selection effects distorting the average parameters of the sample are noted. The pair components display mutual similarity over all the global properties: luminosity, diameter, morphological type, mass-to-luminosity ratio, angular momentum etc., which is not due only to selection effects. The observed correlations must be caused by common origin of pair members. Some features (nuclear activity, color index) could acquire similarity during synchronous evolution of double galaxies. Despite the observed isolation, the sample of double systems is seriously contaminated by accidental pairs, and also by members of groups and clusters. After removing false pairs estimates of orbital mass-to-luminosity ratio range from 0 to 30 f(solar), with the mean value (7.8 plus or minus 0.7) f(solar). Binary galaxies possess nearly circular orbits with a typical eccentrity e = 0.25, probably resulting from evolutionary selection driven by component mergers under dynamical friction. The double-galaxy population with space abundance 0.12 plus or minus 0.02 and characteristic merger timescale 0.2 H(exp -1) may significantly influence the rate of dynamical evolution of galaxies. Author

N91-16860*# Arizona Univ., Tucson.
PAIRS OF GALAXIES IN LOW DENSITY REGIONS OF A COMBINED REDSHIFT CATALOG
Jane C. Charlton and Edwin E. Salpeter (Cornell Univ., Ithaca, NY.) *In* NASA, Marshall Space Flight Center, Paired and Interacting Galaxies: International Astronomical Union Colloquium No. 124 Nov. 1990 p 19-23 (For primary document see N91-16858 08-90)
Avail: NTIS HC/MF A99 CSCL 03B

The distributions of projected separations and radial velocity differences of pairs of galaxies in the CfA and Southern Sky Redshift Survey (SSRS) redshift catalogs are examined. The authors focus on pairs that fall in low density environments rather than in clusters or large groups. The projected separation distribution is nearly flat, while uncorrelated galaxies would have given one linearly rising with r sub p. There is no break in this curve even below 50 kpc, the minimum halo size consistent with measured galaxy rotation curves. The significant number of pairs at small separations is inconsistent with the N-body result that galaxies with overlapping halos will rapidly merge, unless there are significant amounts of matter distributed out to a few hundred kpc of the galaxies. This dark matter may either be in distinct halos or more loosely distributed. Large halos would allow pairs at initially large separations to head toward merger, replenishing the distribution at small separations. In the context of this model, the authors estimate that roughly 10 to 25 percent of these low density galaxies are the product of a merger, compared with the elliptical/SO fraction of 18 percent, observed in low density regions of the sample. Author

N91-16861*# Tokyo Astronomical Observatory, Mitaka (Japan).
MORPHOLOGICAL TYPE CORRELATION BETWEEN NEAREST NEIGHBOR PAIRS OF GALAXIES
Tomohiko Yamagata *In* NASA, Marshall Space Flight Center, Paired and Interacting Galaxies: International Astronomical Union Colloquium No. 124 Nov. 1990 p 25-31 Sponsored in part by Ministry of Education, Science and Culture, Sagamihara, Japan (For primary document see N91-16858 08-90)
Avail: NTIS HC/MF A99 CSCL 03B

Although the morphological type of galaxies is one of the most fundamental properties of galaxies, its origin and evolutionary processes, if any, are not yet fully understood. It has been established that the galaxy morphology strongly depends on the environment in which the galaxy resides (e.g., Dressler 1980). Galaxy pairs correspond to the smallest scales of galaxy clustering and may provide important clues to how the environment influences the formation and evolution of galaxies. Several investigators pointed out that there is a tendency for pair galaxies to have similar morphological types (Karachentsev and Karachentseva 1974, Page 1975, Noerdlinger 1979). Here, researchers analyze morphological type correlation for 18,364 nearest neighbor pairs of galaxies identified in the magnetic tape version of the Center for Astrophysics Redshift Catalogue. Author

N91-16862*# Landesternwarte auf dem Koenigstuhl, Heidelberg (Germany, F.R.).
STELLAR KINEMATICS OF ELLIPTICAL GALAXIES IN PAIRS
Rainer Madejsky (German-Spanish Astronomical Center, Calar Alto, Spain) and Ralf Bender *In* NASA, Marshall Space Flight Center, Paired and Interacting Galaxies: International Astronomical Union Colloquium No. 124 Nov. 1990 p 33-36 (For primary document see N91-16858 08-90)
Avail: NTIS HC/MF A99 CSCL 03B

In both galaxy pairs Arp 166 and 3C 278 the authors find radially increasing velocity dispersions indicating a perturbed, non-equilibrium state of the galaxies after the tidal interaction. In all galaxies, the increase is most pronounced in the regions which correspond to the centers of the outer isophotes. The authors suggest a scenario in which the galaxies are strongly decelerated on their orbits during the encounter. The deceleration depends on the radial position in the perturbed galaxy and vanishes in the center of the perturbed galaxy (Spitzer, 1958). In addition, the crossing time of the stars near the center is very short, implying that the tidal perturbations can be averaged over several orbital periods (e.g., Binney and Tremaine, 1987). In consequence, the central parts are not affected by the tidal interaction while the outer parts are strongly decelerated. This leads to a displacement of the central parts of the galaxies with respect to their envelopes in an anti-symmetrical way for the two components of each galaxy pair. The motions of the central parts subsequently are opposed by dynamical friction with the surrounding envelopes. Due to dynamical friction, the density of the stars increases in the wakes of the moving central parts (Mulder, 1983). The overdensity of stars in the wakes of the moving central parts efficiently decelerates the motions of the central parts. The reaction of the stars in the overdensity regions leads to an increase of the velocity dispersion mainly along the orbits of the moving central parts. The presented observations, especially the asymmetrical luminosity profiles and the radially increasing velocity dispersions support consistently the above scenario of tidal interaction between galaxies. Further spectroscopic observations are necessary in order to investigate the degree of anisotropy in the kinematically perturbed regions.
Author

N91-16863*# Catholic Univ., Santiago (Chile). Astrophysics Group.
DYNAMICS OF GROUPS AROUND INTERACTING DOUBLE ELLIPTICALS: MEASURING DARK MATTER HALOES
H. Quintana *In* NASA, Marshall Space Flight Center, Paired and Interacting Galaxies: International Astronomical Union Colloquium No. 124 Nov. 1990 p 37-41 (For primary document see N91-16858 08-90)
Avail: NTIS HC/MF A99 CSCL 03B

Binary galaxies, as binary stars, are important to measure masses, as suggested by Page (1952). Because three orbit parameters are measurable for galaxies at one instant of time, severe uncertainties remain in the orbit and mass determinations. These uncertainties can partly be overcome by statistical studies of selected samples and/or n-body simulations. Close double galaxies (and isolated galaxies) could also be useful to estimate dynamical masses if we can find test particles around them. Interacting elliptical pairs or dumb-bell galaxies are found with a large range, between 0-1200 km s(exp -1), of relative radial velocities. Standard 2-body orbit calculations, highly uncertain due to projection factors, suggest for the largest velocity differences very large galaxy masses, if the systems are bound and stationary. However, recent n-body simulations model these binaries as galaxies captured from hyperbolic orbits, requiring masses of order a few times 10(exp 11) solar maximum (Borne et al. 1988), but producing systems that are short lived. A different picture appears when we study observationally the dynamical mass of interacting double ellipticals using faint satellite galaxies. These satellites contribute little luminosity and, presumably, little mass to the system. The authors present results of two such groups, basically forming systems of test particles, around the dumb-bells NGC 4782/3 and IC 5049. They also briefly discuss the satellite group around the central dumb-bell in the cluster Sersic 40/6. Apparently, they detect large quantities of dark matter in the vicinity of these dumb-bell galaxies, because the system masses of approx. 4.5 times 10(exp 13) solar mass and 8 times 10(exp 13) solar mass for NGC 4782/3 and IC 5049, respectively, are quite high. Likewise, the mass of the Sersic 40/6 inner core is 7 times 10(exp 13) solar mass. The possibility that a common massive dark matter halo increases the merging times of these types of galaxies is suggested. Here, the authors assume H sub o = 100 km s (exp -1) Mpc(exp -1). Author

N91-16864*# Goettingen Univ. (Germany, F.R.).
THE INTERACTING PAIR Mkn 305/306
Matthias Dietrich *In* NASA, Marshall Space Flight Center, Paired and Interacting Galaxies: International Astronomical Union Colloquium No. 124 Nov. 1990 p 43-46 (For primary document see N91-16858 08-90)
Avail: NTIS HC/MF A99 CSCL 03B

Direct images and spectra at different slit positions of the interacting system Mkn 305/306 are discussed. Both galaxies show starburst properties due to tidal interaction. The morphology and velocity structure of Mkn 306 reveals the strongest warp of a stellar disk so far known. The galaxies Mkn 305 and Mkn 306 form a double system with 30 arcsec separation and having a common envelope at m sub B greater than or equal to 24.5. Furthermore a small tidal tail west of Mkn 305A, an isophote twist of Mkn 305 and the near identical redshifts of the two galaxies prove that this is a physical pair. Mkn 306 itself was classified as a double nucleus galaxy (Petrosyan et al., 1978). The optical morphology of Mkn 306 has the form of an integral sign which is similar to the radio morphology of strongly warped galaxies (Bottema et al., 1987). But in the optical the warp of the stellar component is normally far weaker than in the radio for the HI-gas. Therefore the authors investigate whether the double nucleus structure of Mkn 306 is real or an artifact due to an extreme warp in the optical. The origin for the warp phenomenon is not clear yet. Direct images of the galaxy system were taken with the Calar Alto 2.2m telescope in the B-band and at La Silla in the r-band using the 2.2m telescope; low dispersion spectra (240 A/mm) as well as high dispersion spectra (56 A/mm) for studying the velocity field were taken with the Calar Alto 3.5m telescope at different position angles. Also a spectrum of Mkn 305 was taken at Calar Alto with the 3.5m telescope covering the whole spectral range (240 A/mm). Author

N91-16865*# Osservatorio Astronomico, Brera, Milan (Italy).
GEOMETRICAL PARAMETERS OF E+S PAIRS
Roberto Rampazzo and Jack W. Sulentic (Alabama Univ., Tuscaloosa.) *In* NASA, Marshall Space Flight Center, Paired and Interacting Galaxies: International Astronomical Union Colloquium No. 124 Nov. 1990 p 47-51 (For primary document see N91-16858 08-90)
Avail: NTIS HC/MF A99 CSCL 03B

Local environmental conditions (i.e., density and angular momentum properties of protogalactic clouds) are thought to be factors affecting the ultimate morphology of a galaxy. The existence of significant numbers of mixed morphology (E/SO+S) pairs of galaxies would represent a direct challenge to this idea unless all early-type components are formed by mergers. The authors wished to isolate candidate E+S pairs for detailed study. The authors have observed 22 pairs of mixed morphology galaxies (containing at least one early-type component) selected from a catalog of Sulentic (1988: unpublished) based upon the ESO sky survey. The observed sample and relevant morphological and interaction characteristics are summarized in tabular form. The authors report the relevant geometrical properties of the galaxies in another table. They list the maximum values measured for the ellipticity and the a(4)/a shape parameter together with the total measured twisting along the profile beyond the seeing disk (they set an inner limit of 3 arcsed). An asterisk indicates objects in which a(4)/a is neither predominantly boxy nor disky. They found a large number of true mixed pairs with 13/22 E+S pairs in the present sample. The remaining objects include 5 disk pairs (composed of SO and S members) and 3 early-type pairs comprising E and SO members. They estimate that between 25 and 50 percent of the pairs in any complete sample will be of the E+S type. This suggests that 100 to 200 such pairs exist on the sky brighter than m sub pg = 16.0. They found no global evidence for a difference between E members of this sample and those in more general samples (e.g., Bender et al. 1989). In particular, they found that about 30 percent of the early-type galaxies cannot be classified either predominantly boxy or disky because the a(4)/a profile shows both of these features at a comparable level or does not show any significant trend. Isophotal twisting is observed with a range and distribution consistent with general samples (delta PA between 0 to 70 degrees). Two spirals show significant twisting in their bulge components. They observed two early-type components with shell structure and at least 6 objects with twisting values greater than about 30 degrees. Author

N91-16866*# National Optical Astronomy Lab. Tucson, AZ.
AN ATLAS OF MIXED-MORPHOLOGY PAIRS
N. A. Sharp *In* NASA, Marshall Space Flight Center, Paired and Interacting Galaxies: International Astronomical Union Colloquium No. 124 Nov. 1990 p 53-54 (For primary document see N91-16858 08-90)
Avail: NTIS HC/MF A99 CSCL 03B

Current theories of galaxy formation imply that environment is the most important factor in deciding whether a collapsing region becomes a spiral galaxy or an elliptical galaxy. If this is the case, then isolated pairs comprising a galaxy of each morphology provide an especially interesting test, since, strictly speaking, they should not exist. The first phase of studying E-S pairs is to define a sample which is genuinely isolated and genuinely E-S. The catalog compiled by Karachentsev is the most useful Northern Hemisphere starting point, containing 603 pairs which obeyed certain well-defined angular isolation criteria. All of these pairs now have velocities, enabling further removal of at least some of the non-physical binaries. The conventional cutoff at 500 km s(exp -1) was used for this purpose. However, the morphological types were estimated from Palomar Sky Survey prints, and are consequently not very accurate. It was therefore decided to obtain good charge coupled device (CCD) images in the B-band of all pairs from the Karachentsev sample which were classified as either E-S (73 pairs) or E-SO (91 pairs), for a total of 164 pairs. This includes the 24 pairs with known redshift differences greater than 500 km s(exp -1) (9 E-S and 15 E-SO), which were also imaged in this survey, not only for completeness but also in case the criteria were later changed, or the redshifts were found to be in error. A total of 198 CCD frames were obtained between February 1986 and the present, with most of the observations being completed by the summer of 1987. A number of missing stragglers and replacements for poor quality images were taken more recently.

Most observations used the number 1-0.9m telescope at Kitt Peak, with a few frames from the 2.1m. Some pairs required more than one image due to their separation. The morphological study did not require photometric conditions, but calibrations were made for almost all images anyway, and the weather was probably photometric at least half of the time, at least to an accuracy of around 0.1 magnitudes. The results of this first phase will be published in the form of an Atlas, from which any interested readers will be able to select their own sub-sample using their preferred morphological criteria. Author

N91-16867*# National Aeronautics and Space Administration. Goddard Space Flight Center, Greenbelt, MD.

MULTI-COLOR IMAGING OF SELECTED SOUTHERN INTERACTING GALAXIES

Eric P. Smith and Paul Hintzen *In* NASA, Marshall Space Flight Center, Paired and Interacting Galaxies: International Astronomical Union Colloquium No. 124 Nov. 1990 p 55-58 (For primary document see N91-16858 08-90)

Avail: NTIS HC/MF A99 CSCL 03B

The authors present preliminary results from a study of selected Arp-Madore Southern Hemisphere peculiar galaxies. Broadband charge coupled device (CCD) images (BVRI) of a subset of these galaxies allow us to study each galaxy's optical morphology, color, and (in a crude manner) degree of nuclear activity, and to compare them with similar data we possess on other active galaxies. Many of these galaxies have optical morphologies closely resembling those of powerful radio galaxies (Smith and Heckman 1989), yet their radio emission is unremarkable. Accurate positions for subsequent spectroscopic studies have been determined along with broad band photometry and morphology studies. Detailed observations of these comparatively bright, low-redshift, well-resolved interacting systems should aid our understanding of the role interactions play in triggering galaxy activity. This work is the initial effort in a long term project to study the role played by the dynamics of the interaction in the production and manifestations of activity in galaxies, and the frequency of galaxy mergers. Author

N91-16868*# Iowa State Univ. of Science and Technology, Ames.

MULTI-WAVEBAND OBSERVATIONS OF COLLIDING GALAXIES

P. N. Appleton, E. I. Robson, and James M. Schombert (Michigan Univ., Ann Arbor.) *In* NASA, Marshall Space Flight Center, Paired and Interacting Galaxies: International Astronomical Union Colloquium No. 124 Nov. 1990 p 59-64 (For primary document see N91-16858 08-90)

Avail: NTIS HC/MF A99 CSCL 03B

Colliding galaxies represent a major challenge to both theorists and observers because of the large variety of phenomena which are expected to come into play during the interaction. Strong gravitational fluctuations may drive non-linear waves and instabilities throughout the stars and gas leading to enhanced star formation, nuclear activity and ultimately a mixing of the morphological components of the original galaxies. One relatively uncomplicated class of colliding galaxy where stellar waves play an important role in star formation are ring galaxies. Ring galaxies are probably formed when a companion galaxy passes through the center of a disk system driving circular waves through the disk (Lynds and Toomre 1976, Toomre 1978, Struck-Marcell 1990). Off-center collisions can generate non-circular waves and can be loosely described as banana-shaped although they may exhibit more complex forms as the waves expand into the disk. The propagation of such stellar and gaseous waves through the disk leads to enhanced star formation (e.g., Appleton and Struck-Marcell 1987a; Jeske 1986) and provides a unique probe of the response of the interstellar medium (ISM) to a propagating wave (see Appleton and Struck-Marcell 1987b). Here, the authors report results for 3 systems; the irregular ring Arp 143 (=VV 117); Wakamatsu's Seyfert ring (A0959-755; see Wakamatsu and Nishida 1987) and the brighter member of the pair of ring galaxies comprising of AM 1358-221. The most complete multi-wavelength data is for Arp 143. Optical charge coupled device (CCD) observations made with the 60 inch Palomar telescope at BV and r band, near-IR images at J (1.25 microns), H (1.65 microns) and k (2.2 microns) bands from the infrared camera (IRCAM) InSb array camera on the 3.8m United Kingdon Infrared Telescope (UKIRT) telescope and very large array (VLA) observations at 20cm in both the neutral hydrogen line and radio continuum are described. The observations of Wakamatsu's ring and AM 1358 were made only in the near-IR, and a comparison is made with available optical plate material. Author

N91-16869*# European Southern Observatory, Garching (Germany, F.R.).

TIDAL DISTORTIONS IN PAIRS OF EARLY-TYPE GALAXIES

Philippe Prugniel and E. Davoust (Observatoire de Midi-Pyresnees, Toulouse, France) *In* NASA, Marshall Space Flight Center, Paired and Interacting Galaxies: International Astronomical Union Colloquium No. 124 Nov. 1990 p 65-68 (For primary document see N91-16858 08-90)

Avail: NTIS HC/MF A99 CSCL 03B

The authors are conducting an imaging survey of pairs of elliptical galaxies which has already produced interesting results. Some pairs present a common pattern of distortion interpreted in terms of tidal effects (Davoust and Prugniel, 1988; Prugniel et al., 1989). Other examples drawn from the literature (Borne and Hoessel, 1988; Colina and Perez-Fournon, 1990) share the same morphology. New cases and lists of the characteristics of 24 such systems. The authors' pairs are drawn from a sample of binary and multiple galaxies which has in turn been extracted from the CGCG, UGC (Nilson, 1973) and VV (Vorontsov-Velyaminov, 1959) catalogues. This sample includes that of Karachentsev (1972). It contains 1800 pairs, among which 700 are S - S or mixed morphology pairs. The authors are working on the remainder to produce a sample of close physical pairs of elliptical galaxies (they also include bulge dominated SO's since the morphological discrimination from ellipticals is often ambiguous, in particular for interacting galaxies). One of the interests of this work is to provide a sample selected on purely optical criteria, at variance with other works (e.g., Valentijn and Casertano, 1988). This will allow statistical studies of non-optical properties of these pairs (in particular radio emission). The authors have so far obtained charge-coupled device (CCD) images of 125 pairs with a 2m telescope and velocities' differences of 78 pairs were obtained using the 1.93 meter telescope of Observatoire de Haute Provence and from the literature. One is an optical pair (VV 190). Eighteen of our pairs present the morphological effect described in Davoust and Prugniel (1988): the external parts of each member are stretched in opposite senses in a direction rougly perpendicular to the pair axis. The proportion of 15 plus or minus 4 percent distorted pairs confirms previous estimates. Except for a few cases involving flattened galaxies with nearly aligned major axes which deserve careful detailed analysis (Prugniel, 1989), the apparent distortions do correspond to physical distortions. We have searched the literature for isophote maps showing this effect. In the survey of radio galaxies by Colina and Perez-Fournon (1990), 7 out of 20 pairs show this characteristic distortion. Author

N91-16870*# Toronto Univ. (Ontario). Dept. of Astronomy.

A MULTI-FREQUENCY STUDY OF THE PECULIAR INTERACTING SYSTEM Arp 206

Louis Noreau (Laval Univ., Quebec) and Philipp P. Kronberg *In* NASA, Marshall Space Flight Center, Paired and Interacting Galaxies: International Astronomical Union Colloquium No. 124 Nov. 1990 p 69-73 Sponsored in part by Natural Sciences and Engineering Research Council, Canada (For primary document see N91-16858 08-90)

Avail: NTIS HC/MF A99 CSCL 03B

Arp 206 is a nearby, relatively large, and bright interacting system comprising unequal members: NGC 3432 and UGC 5983. A third anonymous galaxy, Arp 206c, is visible in the field. The CCD images show a well-developed bridge between NGC 3432 and UGC 5983. On the other hand, the complex H I tails are not visible in the optical. In the total H I map, the bridge is lost in a

general envelope encompassing both galaxies. The bridge also appears to have some radio emission. On the Total H I map the system is rather edge-on, far more than it would appear in optical wavelengths. UGC 5983 falls exactly in line with NGC 3432. The velocity of the centers of mass of NGC 3432 and UGC 5983 are 530 km s(exp -1) and 630 km s(exp -1), respectively. In view of the considerable damage sustained by NGC 3432 and the apparent low mass of UGC 5983, it appears that the passage must have been at near parabolic speed, with a small pericentric distance and a very low inclination with rspect to the disk of NGC 3432. The apparent distribution of H I along the z axis of the galaxy could be accounted for by projection effects. The tidal appendage found at higher velocities, which rises at a P.A. approx. equal to 25 degrees west of the main body of the galaxy is probably the tail, the part of the tidal damage away from the perturbing companion. The bridge may be rising north-east from the galaxy and then continue under to the south of the galaxy. The relative sizes of the appendages would indicate that the pericenter was crossed recently. Any further inferences about the collision parameters will need to await the results of detailed computational modelling of the interaction. The authors also summarize the observational characteristics of NGC 3432, UGC 5983, and Arp 206c. Author

N91-16871*# British Columbia Univ., Vancouver. Dept. of Geophysics and Astronomy.

OBSERVATIONAL PROPERTIES OF COMPACT GROUPS OF GALAXIES

Paul Hickson *In* NASA, Marshall Space Flight Center, Paired and Interacting Galaxies: International Astronomical Union Colloquium No. 124 Nov. 1990 p 77-91 Sponsored in part by Natural Sciences and Engineering Research Council, Canada (For primary document see N91-16858 08-90)

Avail: NTIS HC/MF A99 CSCL 03B

Compact groups are small, relatively isolated, systems of galaxies with projected separations comparable to the diameters of the galaxies themselves. Two well-known examples are Stephan's Quintet (Stephan, 1877) and Seyfert's Sextet (Seyfert 1948a,b). In groups such as these, the apparent space density of galaxies approaches 10(exp 6) Mpc(sub -3), denser even than the cores of rich clusters. The apparent unlikeliness of the chance occurrence of such tight groupings lead Ambartsumyan (1958, 1975) to conclude that compact groups must be physically dense systems. This view is supported by clear signs of galaxy interactions that are seen in many groups. Spectroscopic observations reveal that typical relative velocities of galaxies in the groups are comparable to their internal stellar velocities. This should be conducive to strong gravitational interactions - more so than in rich clusters, where galaxy velocities are typically much higher. This suggests that compact groups could be excellent laboratories in which to study galaxy interactions and their effects. Compact groups often contain one or more galaxies whose redshift differs greatly from those of the other group members. If these galaxies are at the same distance as the other members, either entire galaxies are being ejected at high velocities from these groups, or some new physical phenomena must be occurring. If their redshifts are cosmological, we must explain why so many discordant galaxies are found in compact groups. In recent years much progress has been made in addressing these questions. Here, the author discusses the current observational data on compact groups and their implications. Author

N91-16872*# Delaware Univ., Newark.

VLA NEUTRAL HYDROGEN IMAGING OF COMPACT GROUPS

B. A. Williams, P. M. McMahon, and J. H. vanGorkom (National Radio Astronomy Observatory, Socorro, NM.) *In* NASA, Marshall Space Flight Center, Paired and Interacting Galaxies: International Astronomical Union Colloquium No. 124 Nov. 1990 p 93-98 (For primary document see N91-16858 08-90)

Avail: NTIS HC/MF A99 CSCL 03B

Images of the neutral hydrogen (H I) in the direction of the compact groups of galaxies, HCG 31, HCG 44, and HCG 79 are presented. The authors find in HCG 31 and HCG 79, emission contained within a cloud much larger than the galaxies as well as the entire group. The H I emission associated with HCG 44 is located within the individual galaxies but shows definite signs of tidal interactions. The authors imaged the distribution and kinematics of neutral hydrogen at the two extremes of group sizes represented in Hickson's sample. HCG 44 is at the upper limit while HCG 18, HCG 31, and HCG 79 are at the lower end. Although the number of groups that have been imaged is still very small, there may be a pattern emerging which describes the H I morphology of compact groups. The true nature of compact groups has been the subject of considerable debate and controversy. The most recent observational and theoretical evidence strongly suggests that compact groups are physically dense, dynamical systems that are in the process of merging into a single object (Williams and Rood 1987, Hickson and Rood 1988, Barnes 1989). The neutral hydrogen deficiency observed by Williams and Rood (1987) is consistent with a model in which frequent galactic collisions and interactions have heated some of the gas during the short lifetime of the group. The H I disks which are normally more extended than the luminous ones are expected to be more sensitive to collisions and to trace the galaxy's response to recent interactions. Very Large Array observations can provide in most cases the spatial resolution needed to confirm the dynamical interactions in these systems. Author

N91-16873*# Space Telescope Science Inst., Baltimore, MD.

BLUE ELLIPTICALS IN COMPACT GROUPS

Stephen E. Zepf (Johns Hopkins Univ., Baltimore, MD.) and Bradley C. Whitmore *In* NASA, Marshall Space Flight Center, Paired and Interacting Galaxies: International Astronomical Union Colloquium No. 124 Nov. 1990 p 99-103 (For primary document see N91-16858 08-90)

Avail: NTIS HC/MF A99 CSCL 03B

By studying galaxies in compact groups, the authors examine the hypothesis that mergers of spiral galaxies make elliptical galaxies. The authors combine dynamical models of the merger-rich compact group environment with stellar evolution models and predict that roughly 15 percent of compact group ellipticals should be 0.15 mag bluer in B - R color than normal ellipticals. The published colors of these galaxies suggest the existence of this predicted blue population, but a normal distribution with large random errors can not be ruled out based on these data alone. However, the authors have new ultraviolet blue visual data which confirm the blue color of the two ellipticals with blue B - R colors for which they have their own colors. This confirmation of a population of blue ellipticals indicates that interactions are occurring in compact groups, but a blue color in one index alone does not require that these ellipticals are recent products of the merger of two spirals. The authors demonstrate how optical spectroscopy in the blue may distinguish between a true spiral + spiral merger and the swallowing of a gas-rich system by an already formed elliptical. The authors also show that the sum of the luminosity of the galaxies in each group is consistent with the hypothesis that the final stage in the evolution of compact group is an elliptical galaxy. Author

N91-16874*# Special Astrophysical Observatory, Zelenchukskaya (USSR).

WHAT IS THE NUMBER OF SPIRAL GALAXIES IN COMPACT GROUPS

N. A. Tikhonov *In* NASA, Marshall Space Flight Center, Paired and Interacting Galaxies: International Astronomical Union Colloquium No. 124 Nov. 1990 p 105-114 (For primary document see N91-16858 08-90)

Avail: NTIS HC/MF A99 CSCL 03B

The distribution of morphological types of galaxies in compact groups is studied on plates from the 6 m telescope. In compact groups there are 57 percent galaxies of late morphological types (S + Irr), 23 percent lenticulars (SO) and 20 percent elliptical galaxies. The morphological content of compact groups is very nearly the same as in loose groups. There is no dependence of galaxy morphology on density in all compact groups (and possibly

in loose groups). Genuine compact groups form only 60 percent of Hickson's list. Author

N91-16875*# Special Astrophysical Observatory, Zelenchukskaya (USSR).
TRIPLE GALAXIES AND A HIDDEN MASS PROBLEM
I. D. Karachentsev, V. E. Karachentseva, and V. S. Lebedev *In* NASA, Marshall Space Flight Center, Paired and Interacting Galaxies: International Astronomical Union Colloquium No. 124 Nov. 1990 p 115-127 (For primary document see N91-16858 08-90)
Avail: NTIS HC/MF A99 CSCL 03B

The authors consider a homogeneous sample of 84 triple systems of galaxies with components brighter than m = 15.7, located in the northern sky and satisfying an isolation criterion with respect to neighboring galaxies in projection. The distributions of basic dynamical parameters for triplets have median values as follows: radial velocity dispersion 133 km/s, mean harmonic radius 63 kpc, absolute magnitude of galaxies M sub B equals -20.38, crossing time tau = 0.04 H(sup minus 1). For different ways of estimation the median mass-to-luminosity ratio is (20 - 30). A comparison of the last value with the ones for single and binary galaxies shows the presence of a virial mass excess for triplets by a factor 4. The mass-to-luminosity ratio is practically uncorrelated with linear size of triplets or with morphological types of their components. We note that a significant part of the virial excess may be explained by the presence of nonisolated triple configurations in the sample, which are produced by debris of more populous groups of galaxies. Author

N91-16876*# Montreal Univ. (Quebec).
H I STUDIES OF THE SCULPTOR GROUP GALAXIES
Claude Carignan and Daniel Puche (National Radio Astronomy Observatory, Socorro, NM.) *In* NASA, Marshall Space Flight Center, Paired and Interacting Galaxies: International Astronomical Union Colloquium No. 124 Nov. 1990 p 129-131 (For primary document see N91-16858 08-90)
Avail: NTIS HC/MF A99 CSCL 03B

Results from large-scale mapping of the H I gas in the Sculptor group are presented. From this kinematic analysis, a mean global (M/L sub B) approx. equals 9 solar maximum/solar luminosity (at the last observed velocity point) is found for the individual galaxies. This is only a factor approx. 10 smaller than the (M/L sub B) dyn approx. equals 90 solar maximum/solar luminosity derived from a dynamical study of the whole group. The parameters derived from the mass models suggest that most of the unseen matter has to be concentrated around the luminous galaxies. Under the assumption that the Sculptor group is a virialized system and that all the mass is associated with the galaxies, an upper limit of approx. 40 kpc is derived for the size of the dark halos present in the five late-type spirals of the group. Author

N91-16877*# Kitt Peak National Observatory, Tucson, AZ.
A STUDY OF THE COMPACT GROUP OF GALAXIES SHAHBAZIAN 4
C. R. Lynds, E. Ye. Khachikian, and A. S. Amirkhanian (Byurakan Observatory, Mount Aragatz, USSR) *In* NASA, Marshall Space Flight Center, Paired and Interacting Galaxies: International Astronomical Union Colloquium No. 124 Nov. 1990 p 133-142 Original language document was announced in IAA as A90-32601 (For primary document see N91-16858 08-90)
Avail: NTIS HC/MF A99 CSCL 03B

The radial velocities of members of Shakhbazian 4 are determined. It is found that the dispersion of the radial velocities is 440 km/s. The apparent and absolute magnitudes of galaxies in V color are obtained. It is found that the M/L ratio of the group is about 220 solar mass/solar luminosity. The crossing time for the Shakhbazian 4 group is equal to 47 Myr. Author

N91-16878*# Bulgarian Academy of Sciences, Sofia. Dept. of Astronomy.
ISOLATED GALAXIES, PAIRS, AND GROUPS OF GALAXIES
I. Kuneva and M. Kalinkov *In* NASA, Marshall Space Flight Center, Paired and Interacting Galaxies: International Astronomical Union Colloquium No. 124 Nov. 1990 p 143-148 Sponsored in part by Bulgarian Committee for Science (For primary document see N91-16858 08-90)
Avail: NTIS HC/MF A99 CSCL 03B

The authors searched for isolated galaxies, pairs and groups of galaxies in the CfA survey (Huchra et al. 1983). It was assumed that the distances to galaxies are given by R = V/H sub o, where H sub o = 100 km s(exp -1) Mpc(exp -1) and R greater than 6 Mpc. The searching procedure is close to those, applied to find superclusters of galaxies (Kalinkov and Kuneva 1985, 1986). A sphere with fixed radius r (asterisk) is described around each galaxy. The mean spatial density in the sphere is m. Let G (sup 1) be any galaxy and G (sup 2) be its nearest neighbor at a distance R sub 2. If R sub 2 exceeds the 95 percent quintile in the distribution of the distances of the second neighbors, then G (sup 1) is an isolated galaxy. Let the midpoint of G (sup 1) and G (sup 2) be O sub 2 and r sub 2=R sub 2/2. For the volume V sub 2, defined with the radius r sub 2, the density D sub 2 less than k mu, the galaxy G (sup 2) is a single one and the procedure for searching for pairs and groups, beginning with this object is over and we have to pass to another object. Here the authors present the groups - isolated and nonisolated - with n greater than 3, found in the CfA survey in the Northern galactic hemisphere. The parameters used are k = 10 and r (asterisk) = 5 Mpc. Table 1 contains: (1) the group number, (2) the galaxy, nearest to the multiplet center, (3) multiplicity n, (4) the brightest galaxy if it is not listed in (2); (5) and (6) are R.A. and Dec. (1950), (7) - mean distance D in Mpc. Further there are the mean density rho (8) of the multiplet (galaxies Mpc (exp -3), (9) the density rho (asterisk) for r (asterisk) = 5 Mpc and (10) the density rho sub g for the group with its nearest neighbor. The parenthesized digits for densities in the last three columns are powers of ten. Author

N91-16879*# Bulgarian Academy of Sciences, Sofia. Dept. of Astronomy.
CORRELATION FUNCTIONS FOR PAIRS AND GROUPS OF GALAXIES
M. Kalinkov and I. Kuneva *In* NASA, Marshall Space Flight Center, Paired and Interacting Galaxies: International Astronomical Union Colloquium No. 124 Nov. 1990 p 149-155 Sponsored in part by Bulgarian Committee for Science (For primary document see N91-16858 08-90)
Avail: NTIS HC/MF A99 CSCL 03B

There are many studies on the correlation functions of galaxies, of clusters of galaxies, even of superclusters (e.g., Groth and Peebles 1977; Davies and Peebles 1983; Kalinkov and Kuneva 1985, 1986; Bahcall 1988 and references therein) but not so many on pairs and groups of galaxies. Results of the calculations of two-point correlation fuctions for some catalogs of pairs and groups of galaxies are given. It is assumed that the distances to pairs and groups of galaxies are given by their mean redshifts according to R = sigma (sup n, sub i-1) V sub i/nH (sub 0), where n is the number of galaxies in the system and H sub 0 = 100 km s(exp -1) Mpc(exp -1). Author

N91-16880*# Padua Univ. (Italy). Dipartimento di Astronomia.
HIDDEN INTERACTION IN SBO GALAXIES
G. Galletta, D. Bettoni, T. Oosterloo, and G. Fasano (Osservatorio Astronomico, Padova, Italy) *In* NASA, Marshall Space Flight Center, Paired and Interacting Galaxies: International Astronomical Union Colloquium No. 124 Nov. 1990 p 159-164 (For primary document see N91-16858 08-90)
Avail: NTIS HC/MF A99 CSCL 03B

Galaxies, like plants, show a large variety of grafts: an individual of some type connects physically with a neighborhood of same or different type. The effects of these interactions between galaxies have a broad range of morphologies depending, among other quantities, on the distance of the closest approach between systems and the relative size of the two galaxies. A sketch of the possible situations is shown in tabular form. This botanical classification is just indicative, because the effects of interactions can be notable also at relatively large separations, when additional

conditions are met, as for example low density of the interacting systems or the presence of intra-cluster gas. In spite of the large variety of encounters and effects, in the literature the same terms are often used to refer to different types of interactions. Analysis indicates that only few of the situations show evident signs of interaction. They appear to be most relevant when the size of the two galaxies is comparable. Bridges and tails, like the well known case of NGC 4038/39, the Antennae, are only observed for a very low percentage of all galaxies (approx. 0.38 percent, Arp and Madore 1977). In most cases of gravitational bond between two galaxies, the effects of interactions are not relevant or evident. For instance, the detection of stellar shells (Malin and Carter 1983), which have been attributed to the accretion of gas stripped from another galaxy or to the capture and disruption of a small stellar system (Quinn 1984), requires particular observing and reduction techniques. Besides these difficulties of detection, time plays an important role in erasing, within a massive galaxy, the effects of interactions with smaller objects. This can happen on a timescale shorter than the Hubble time, so the number of systems now showing signs of interaction suggests lower limits to the true frequency of interactions in the life-time of a stellar system.

Author

N91-16881*# Space Telescope Science Inst., Baltimore, MD.
THE ENVIRONMENTS OF MARKARIAN GALAXIES
John W. MacKenty, Caroline Simpson (Florida Univ., Gainesville.), and Brian McLean *In* NASA, Marshall Space Flight Center, Paired and Interacting Galaxies: International Astronomical Union Colloquium No. 124 Nov. 1990 p 165-167 (For primary document see N91-16858 08-90)
Avail: NTIS HC/MF A99 CSCL 03B

The extensively studied Markarian sample of 1500 ultraviolet excess galaxies contains many Seyfert, starburst, and peculiar galaxies. Using the 20 minute V plates obtained for the construction of the Hubble Space Telescope Guide Star Catalog, the authors investigated the morphologies of the Markarian galaxies and the environments in which they are located. The relationship between the types of nuclear activity and the morphologies and environments of the Markarian galaxies is discussed. The authors conclude that the type of nuclear activity present in the galaxies of the Markarian sample is not dependent on either the morphology or the local environment of the galaxy. This is not to imply that nuclear activity per se is not influenced by the environment in which the nucleus is located. Rather the type of nuclear activity (at least in the Markarian population) does not appear to be determined by the environment. Author

N91-16882*# Padua Univ. (Italy). Dept. of Astronomy.
THE COMPLEX NATURE OF THE SEYFERT GALAXY NGC 7592
Piero Rafanelli and Paolo Marziani (International School for Advanced Studies, Trieste, Italy) *In* NASA, Marshall Space Flight Center, Paired and Interacting Galaxies: International Astronomical Union Colloquium No. 124 Nov. 1990 p 169-173 (For primary document see N91-16858 08-90)
Avail: NTIS HC/MF A99 CSCL 03B

Long slit spectra of NGC 7592 were taken on Sep. 26 to 30, 1989 at the 1.52 cm European Southern Observatory (ESO) telescope, equipped with a Boller and Chivens spectrograph and an RCA High Resolution charge coupled device (CCD) camera. The problem of the nature of Region C is addressed at first. C shows an heliocentric radial velocity very similar to that of Regions A and B. Moreover, the arm departing from C is most probably a tidal tail, because its extension is large and its orientation is peculiar. The high H alpha luminosity of C is typical of a starburst nucleus. These facts argue in favor of C being the nucleus of a third galactic component (southern component S) physically interacting with the SE component of NGC 7592. The directions of the velocity vectors in various regions of NGC 7592 are marked. It is noteworthy that the SE component rotates clockwise, if the radial velocity difference delta v sub r from its nucleus B is due to rotation. Under the same assumption for the delta v sub r = v sub r-v sub r, A, the NW component seems to rotate counterclockwise. Thus, the gas in the regions where the two galactic bodies are in contact moves in the same way, suggesting that a prograde encounter is occurring. It is known (e.g., Toomre and Toomre, 1972) that prograde encounters have the most disruptive effects on the interacting galaxies, leading to the formation of tidal tails. The interpretation of the wing of the NW component in terms of a tidal tail thus appears very likely. A similar situation holds for the interaction between SE and S too, where S rotates counterclockwise. The interpretation of the arm departing from C as a tidal tail is supported also in this case. The difference in radial velocity between A and B (delta v sub r approx. equal - 40 km s(exp-1)) and the morphology of NGC 7592 suggests that the NW component is beyond the SE one and is approaching it. The most heavily reddened regions (E(B - V) approx. equals 0.7, derived from the H alpha/H beta ratio) are B2 and B4, namely the regions between A and B. Moreover, the small difference in radial velocity between A,B,C suggests that the three galaxies form a bound system, and their kinematics hints that they are most probably in the early stage of a merging phenomenon. Author

N91-16883*# Sternberg Astronomical Inst., Moscow (USSR).
THE H I CONTENT OF NON-ISOLATED GALAXIES
Anatoli V. Zasov *In* NASA, Marshall Space Flight Center, Paired and Interacting Galaxies: International Astronomical UUnion Colloquium No. 124 Nov. 1990 p 175-182 (For primary document see N91-16858 08-90)
Avail: NTIS HC/MF A99 CSCL 03B

It seems obvious that the evolution of star formation rate and hence of gas content in galaxies strongly depends on their environment. It reveals itself in particular in enhanced star formation or even in a strong burst of activity of massive stars often observed in interacting galaxies. Nevertheless it should be noted that the time scale for the gas to be exhausted in these galaxies is unknown even approximately. To clarify a role of surroundings in the evolution of disk galaxies we should compare the H I content of isolated and non-isolated galaxies otherwise similar by their properties. It is concluded that there are no systematic differences between H I content in isolated and non-isolated late-type galaxies; in spite of the differences of star formation rates their hydrogen mass is determined by slowly evolving kinematic parameters of the disk. Enhanced star formation in interacting galaxies, if it lasts long enough, must have an initial mass function enriched in massive stars in order not to significantly reduce the supply of gas. Certainly these conclusions are not valid for galaxies which are members of rich clusters such as Virgo or Coma, where H I-deficiency really exists, possibly due to the interaction of interstellar H I with hot intergalactic gas. Author

N91-16884*# Space Telescope Science Inst., Baltimore, MD.
H I AND MASS DISTRIBUTION OF GR8
Sylvie Beaulieu and Claude Carignan (Montreal Univ., Quebec) *In* NASA, Marshall Space Flight Center, Paired and Interacting Galaxies: International Astronomical Union Colloquium No. 124 Nov. 1990 p 183-187 (For primary document see N91-16858 08-90)
Avail: NTIS HC/MF A99 CSCL 03B

The dwarf irregular galaxy GR8, which is at the extreme faint end of the luminosity and mass functions, is studied using optical photometry and 21 cm H I line observations. It is shown that rotation is only important to the gravitational support of the system in the inner parts (r less than 250 pc). GR8 is one of the very few non-elliptical systems known (with M81dwA) where the random motions provide essentially all the support in the outer parts (4 greater than or equal to 500 pc). The Gaussian nature of the H I distribution and the isothermal distribution of the H I velocity dispersion implies M is directly proportional to R(exp 3) in the outer regions of GR8 (i.e., the stellar disk and the H I lie in the approximately uniform density core of the dark halo). Author

N91-16885*# Alabama Univ., Tuscaloosa. Dept. of Physics and Astronomy.
THE RINGED X-GALAXY NGC 7020
Ronald Buta *In* NASA, Marshall Space Flight Center, Paired

and Interacting Galaxies: International Astronomical Union Colloquium No. 124 Nov. 1990 p 189-193 (For primary document see N91-16858 08-90)
Avail: NTIS HC/MF A99 CSCL 03B

The southern SO (sup +) galaxy NGC 7020 presents an unusual morphology: it includes a very regular outer ring which is completely detached and which envelops an inner ring/lens zone with a hexagon surrounding an X shape. The outer ring has a high contrast compared to those usually observed in barred galaxies, yet NGC 7020 is not obviously barred. The morphology of this galaxy poses an interesting puzzle in that the hexagonal/X zone is not a typical type of feature to find in the interior of such a regular ring. Instead, the zone bears a striking resemblance to the edge-on galaxy IC 4767, recently studied by Whitmore and Bell (1988 = WB88) and dubbed by them as the X-galaxy because its inner regions appear to be crossed by two distinct enhancements lined at plus or minus 22 deg with respect to the major axis. The observation of a similar phenomenon in NGC 7020 is interesting because of the suggestion by WB88 that X structures could be related to accretion of matter associated with a merger or tidal encounter between an SO and a small satellite galaxy. If this interpretation is correct for NGC 7020, then it has important implications for the nature of the outer ring. An alternative interpretation is that the inner hexagonal/X zone is a region where resonant periodic orbits in a weak bi-symmetric potential perturbation are influencing the morphology more strongly than might be expected. A brief summary of a more extensive paper (Buta 1990c = B90c) and a few other details concerning this interesting galaxy are given. Author

N91-16886*# Space Telescope Science Inst., Baltimore, MD.
THE cD GALAXY IN ABELL CLUSTER 1775
J. J. E. Hayes and B. Bhattacharya *In* NASA, Marshall Space Flight Center, Paired and Interacting Galaxies: International Astronomical Union Colloquium No. 124 Nov. 1990 p 195-199 (For primary document see N91-16858 08-90)
Avail: NTIS HC/MF A99 CSCL 03B

Over the last 20 years, a number of workers have studied the multiple nuclei cD galaxy in the rich Abell cluster 1775, trying to discover its nature. In all the cases though, very little has been published concerning its morphology. The majority of arguments about the nature of this object have been based on the relative radial velocities of the 2 components with each other and with the other galaxies in the cluster, or its radio morphology. Very little work has been done on the optical morphology. To rectify that lack of data, the authors have obtained charge coupled device (CCD) images of the cD. The authors find from the CCD data that the cD is unlikely to be a bound object and that there is strong evidence for a collision. Author

N91-16887*# Byurakan Observatory, Mount Aragatz (USSR).
NEW DATA ON THE PECULIAR GALAXY MRK 273
A. S. Asatrian, A. R. Petrosian, and F. Boerngen (Karl Schwarzschild Observatory, Tautenburg, German, D.R.) *In* NASA, Marshall Space Flight Center, Paired and Interacting Galaxies: International Astronomical Union Colloquium No. 124 Nov. 1990 p 201-208 Original language document was announced in IAA as A90-44888 (For primary document see N91-16858 08-90)
Avail: NTIS HC/MF A99 CSCL 03B

Colorimetric and spectral investigations of Markarian 273 and its three neighbors were performed on the basis of direct ultraviolet blue visual (UBV) and spectral observations with the 2-m Tautenburg telescope and the 6-m telescope of the Special Astrophysical Observatory of the USSR Academy of Sciences. The results obtained suggest that this galaxy is a close system of two objects with active nuclei. The observed straight tail with a thermal emission character is probably the result of the interaction of these galaxies. Author

N91-16888*# Florida Univ., Gainesville. Dept. of Astronomy.
H I OBSERVATIONS OF THE PECULIAR GALAXY NGC 660
Stephen T. Gottesman and Mary Elaine Mahon *In* NASA, Marshall Space Flight Center, Paired and Interacting Galaxies: International Astronomical Union Colloquium No. 124 Nov. 1990 p 209-213 (For primary document see N91-16858 08-90)
Avail: NTIS HC/MF A99 CSCL 03B

The authors present observations of H I emission from the peculiar galaxy NGC 660. H I was detected in the companion galaxy UGC 01195 as well. Sixteen hours of observations were obtained with the VLA telescope of the National Radio Astronomy Observatory during December 1986 and March 1987. Author

N91-16889*# Amsterdam Univ. (Netherlands). Astronomical Inst.
A SPIRAL-LIKE DISK OF IONIZED GAS IN IC 1459: SIGNATURE OF A MERGING COLLISION
Paul Goudfrooij, H. U. Norgaard-Nielsen, H. E. Jorgensen, L. Hansen (Copenhagen Observatory, Denmark), and T. deJong *In* NASA, Marshall Space Flight Center, Paired and Interacting Galaxies: International Astronomical Union Colloquium No. 124 Nov. 1990 p 215-219 (For primary document see N91-16858 08-90)
Avail: NTIS HC/MF A99 CSCL 03B

The authors report the discovery of a large (15 kpc diameter) H alpha + (NII) emission-line disk in the elliptical galaxy IC 1459, showing weak spiral structure. The line flux peaks strongly at the nucleus and is more concentrated than the stellar continuum. The major axis of the disk of ionized gas coincides with that of the stellar body of the galaxy. The mass of the ionized gas is estimated to be approx. 1 times 10 (exp 5) solar mass, less than 1 percent of the total mass of gas present in IC 1459. The total gas mass of 4 times 10(exp 7) solar mass has been estimated from the dust mass derived from a broad-band color index image and the Infrared Astronomy Satellite (IRAS) data. The authors speculate that the presence of dust and gas in IC 1459 is a signature of a merger event. Author

N91-16890*# Technische Univ., Goettingen (Germany, F.R.).
OBSERVATIONS OF MULTIPLE NUCLEUS GALAXIES
W. Kollatschny *In* NASA, Marshall Space Flight Center, Paired and Interacting Galaxies: International Astronomical Union Colloquium No. 124 Nov. 1990 p 221-224 (For primary document see N91-16858 08-90)
Avail: NTIS HC/MF A99 CSCL 03B

Disturbed galaxies with two nuclei display the final state of the interaction process of two galaxies (Kollatschny et al., 1986; Fricke and Kollatschny, 1989). A few of these double nucleus galaxies contain Seyfert nuclei. Making the assumption that the Seyfert galaxies Mkn 231 and Mkn 273 are galaxies in the final state of merging, having strong tidal arms but unresolved nuclei, one can estimate that 4 percent of all Seyfert galaxies are in the merging process. The luminosities of multiple nucleus Seyfert galaxies are extremely high in comparison to morphologically undisturbed Seyfert galaxies. In a table, mean values of the visual and blue luminosities and of the far-infrared and radio (6 cm) luminosities as well as the H alpha fluxes are listed for both classes are shown. In addition, the authors have separated Seyfert 1 and Seyfert 2 galaxies. In all cases the luminosities of double nucleus Seyfert galaxies are higher by a factor of more than two with respect to undisturbed Seyfert galaxies. This result might be explained by higher luminosities in the early phases of a Seyfert's life-under the assumption that the nonthermal activity is triggered by tidal interaction-and/or additional strong starburst phenomena. Due to strong nuclear absorption, the UV spectra of these Seyfert nuclei are unusually weak. Corresponding to the Seyfert survey, the authors obtained the H alpha and far infrared radiation (FIR) luminosities as well as the (0III)5007/H beta line ratios of a small sample of non-Seyfert nuclei in double nucleus galaxies. The direct image and the velocity field of the double starburst galaxy Mkn 788 (Kollatschny et al., 1986) are shown. The authors compared their measurements with those of normal interacting galaxies of Keel et al. (1985) and Bushouse (1987). The mean FIR luminosity per nucleus in multiple systems is the same as that of interacting galaxies. But the mean H alpha luminosities as well as the (OIII)/H beta line ratios are higher by a factor of 1.5-2 than those of normal interacting galaxies. Author

N91-16891*# Padua Univ. (Italy). Dept. of Astronomy.
THE DOUBLE NUCLEUS GALAXIES Mkn 423 AND Mkn 739
Piero Rafanelli and Paolo Marziani (International School for Advanced Studies, Trieste, Italy) *In* NASA, Marshall Space Flight Center, Paired and Interacting Galaxies: International Astronomical Union Colloquium No. 124 Nov. 1990 p 225-229 (For primary document see N91-16858 08-90)
Avail: NTIS HC/MF A99 CSCL 03B

Long slit spectroscopy and imaging of Mkn 423 and Mkn 739 were performed on the 2.2 m and 3.5 m telescopes of the Calar Alto Observatory using both change coupled device (CCD) and photographic detectors. Low and medium resolution spectra (1.8A, 3.5A, 6.0A) together with V images have permitted the demonstration of the merging nature of Mkn 423 and the double structure of the narrow line region (NLR) of its Seyfert component. This last feature has been found also in the NLR of the Seyfert component of Mkn 739, a double system the two components of which are counterrotating. Author

N91-16892*# Leningrad State Univ. (USSR). Astronomical Observatory.
THE POLAR-RING GALAXIES NGC 2685 AND NGC 3808B (VV 300)
V. P. Reshetnikov and V. A. Yakovleva *In* NASA, Marshall Space Flight Center, Paired and Interacting Galaxies: International Astronomical Union Colloquium No. 124 Nov. 1990 p 231-244 (For primary document see N91-16858 08-90)
Avail: NTIS HC/MF A99 CSCL 03B

Polar-ring galaxies (PRG) are among the most interesting examples of interaction between galaxies. A PRG is a galaxy with an elongated main body surrounded by a ring (or a disk) of stars, gas, and dust rotating in a near-polar plane (Schweizer, Whitmore, and Rubin, 1983). Accretion of matter by a massive lenticular galaxy from either intergalactic medium or a companion galaxy is usually considered as an explanation of the observed structure of PRG. In the latter case there are two possibilities: capture and merging of a neighbor galaxy, and accretion of mass from a companion galaxy during a close encounter. Two PRG formation scenarios just mentioned are illustrated here by the results of our observations of the peculiar galaxies NGC 2685 and NGC 3808B. Author

N91-16893*# Nuffield Radio Astronomy Labs., Jodrell Bank (England).
THE MORPHOLOGY OF SERSIC-PASTORIZA GALAXIES
G. J. Yates, A. Pedlar, D. J. Saikia, S. W. Unger (Royal Greenwich Observatory, Hailsham, England), and D. J. Axon *In* NASA, Marshall Space Flight Center, Paired and Interacting Galaxies: International Astronomical Union Colloquium No. 124 Nov. 1990 p 245-249 (For primary document see N91-16858 08-90)
Avail: NTIS HC/MF A99 CSCL 03B

The authors present the preliminary results of their radio-continuum and neutral hydrogen observations of Sersic-Pastoriza (S-P) galaxies. They show that the central regions contain a population of compact features thought to be young supernova remnants (SNRs) and discuss the overall morphology of the nuclei. Author

N91-16894*# Alabama Univ., Tuscaloosa.
INTERACTING NUCLEI IN DISTANT GALAXIES
Wei Zheng and Steven A. Grandi (National Optical Astronomy Lab. Tucson, AZ.) *In* NASA, Marshall Space Flight Center, Paired and Interacting Galaxies: International Astronomical Union Colloquium No. 124 Nov. 1990 p 251-253 (For primary document see N91-16858 08-90)
Avail: NTIS HC/MF A99 CSCL 03B

The N-galaxy 3C 390.3 has been monitored spectroscopically since 1974 (Osterbrock, Koski and Phillips 1975; Oke 1988). From various archives and literature, it is found that the Balmer lines change their intensities and profiles in a dramatic manner. The H alpha profile is very broad and peculiar, and the relative intensities of its two humps changes consistently with time, possibly periodically. Before 1980, the blue hump was significantly stronger than the one in the red. From 1980 to 1983 the blue hump became stronger (see Oke 1988). After 1983 the H alpha profile has returned to its early shape and seems to have completed a full circle. Unlike the rapid (on the order of a month or even less) and aperiodic variation in the continuum and integrated line intensities, the change in broad profile seems slow and consistent. Taking the analogy of cataclysmic variables, the double-horn profiles have been observed in cases of interacting stars. For example, the emission lines, both in He II and hydrogen Balmer lines in GD 552 (Stover 1985) show double-horn profiles and periodical changes in their line profiles, including the change in ratios of two humps. It is understood that the D-wave components (Smak 1976) are the signature of an emitting disk and the S-wave component is from the emission at a hot spot which rotates and results in a moving component in the velocity space. The mass flow from the nearby interacting star provides the stream toward the core of a neutron star or white dwarf. Therefore, it is proposed that the variation of broad line profiles observed in 3C 390.3 may be the result of a pair of interacting massive cores. The rotational velocity dominates and produces a variable double-horn profile. However, the line widths observed in broad line radio galaxies are one order larger than that in interacting stars. The Balmer decrements imply a much smaller density (10(exp 10-12) cm(exp-3)) than that in the cataclysmic variables. The much larger velocity and much thinner density make it unlikely that the broad line emission is simply formed in an accretion disk. The authors postulate that a significant rotational motion is involved. If the observed squared profiles are indeed due to the rotational velocity field, one can naturally explain their rare occurrence. Author

N91-16895*# Leiden Univ. (Netherlands).
ALIGNMENT OF cD-GALAXIES WITH THEIR SURROUNDINGS
Eelco vanKampen and George Rhee *In* NASA, Marshall Space Flight Center, Paired and Interacting Galaxies: International Astronomical Union Colloquium No. 124 Nov. 1990 p 255-260 (For primary document see N91-16858 08-90)
Avail: NTIS HC/MF A99 CSCL 03B

For a sample of 122 rich Abell clusters the authors find a strong correlation of the position angle (orientation) of the first-ranked galaxy and its parent cluster. This alignment effect is strongest for cD-galaxies. Formation scenarios for cD galaxies, like the merging scenario, must produce such a strong alignment effect. The authors show some N-body simulations done for this purpose. Author

N91-16896*# Istituto di Radioastronomia, Bologna (Italy).
DUMB-BELL GALAXIES IN SOUTHERN CLUSTERS: CATALOG AND PRELIMINARY STATISTICAL RESULTS
G. Vettolani, L. Gregorini, P. Parma, and H. R. deRuiter (Bologna Observatory, Italy) *In* NASA, Marshall Space Flight Center, Paired and Interacting Galaxies: International Astronomical Union Colloquium No. 124 Nov. 1990 p 261-264 (For primary document see N91-16858 08-90)
Avail: NTIS HC/MF A99 CSCL 03B

The dominant galaxy of a rich cluster is often an object whose formation and evolution is closely connected to the dynamics of the cluster itself. Hoessel (1980) and Schneider et al. (1983) estimate that 50 percent of the dominant galaxies are either of the dumb-bell type or have companions at projected distances less than 20 kpc, which is far in excess of the number expected from chance projection (see also Rood and Leir 1979). Presently there is no complete sample of these objects, with the exception of the listing of dumb-bell galaxies in BM type I and I-II clusters in the Abell statistical sample of Rood and Leir (1979). Recent dynamical studies of dumb-bell galaxies in clusters (Valentijn and Casertano, 1988) still suffer from inhomogeneity of the sample. The fact that it is a mixture of optically and radio selected objects may have introduced an unknown biases, for instance if the probability of radio emission is enhanced by the presence of close companions (Stocke, 1978, Heckman et al. 1985, Vettolani and Gregorini 1988) a bias could be present in their velocity distribution. However, this situation is bound to improve: a new sample of Abell clusters in the Southern Hemisphere has been constructed

(Abell et al., 1988 hereafter ACO), which has several advantages over the original northern catalog. The plate material (IIIaJ plates) is of better quality and reaches fainter magnitudes. This makes it possible to classify the cluster types with a higher degree of accuracy, as well as to fainter magnitudes. The authors therefore decided to reconsider the whole problem constructing a new sample of dumb-bell galaxies homogeneously selected from the ACO survey. Details of the classification criteria are given.

Author

N91-16897*# Arizona Univ., Tucson.
GLOBAL EFFECTS OF INTERACTIONS ON GALAXY EVOLUTION
Robert C. Kennicutt, Jr. *In* NASA, Marshall Space Flight Center, Paired and Interacting Galaxies: International Astronomical Union Colloquium No. 124 Nov. 1990 p 269-284 (For primary document see N91-16858 08-90)
(Grant NSF AST-89-96123)
Avail: NTIS HC/MF A99 CSCL 03B

Recent observations of the evolutionary properties of paired and interacting galaxies are reviewed, with special emphasis on their global emission properties and star formation rates. Data at several wavelengths provide strong confirmation of the hypothesis, proposed originally by Larson and Tinsley, that interactions trigger global bursts of star formation in galaxies. The nature and properties of the starbursts, and their overall role in galactic evolution are also discussed. Author

N91-16898*# National Aeronautics and Space Administration. Ames Research Center, Moffett Field, CA.
A MULTIWAVELENGTH SURVEY OF INTERACTING GALAXIES
Howard A. Bushouse, Susan A. Lamb, K.-Y. Lo (Illinois Univ., Urbana.), S. Lord, and M. Werner *In* NASA, Marshall Space Flight Center, Paired and Interacting Galaxies: International Astronomical Union Colloquium No. 124 Nov. 1990 p 285-290 (For primary document see N91-16858 08-90)
Avail: NTIS HC/MF A99 CSCL 03B

Galaxy-galaxy collisions are known to produce drastic changes in morphology and, in many cases, enhance the level of star formation activity in galaxies. In order to better quantify the effects that interactions have on the star formation characteristics of galaxies the authors undertook a multiwavelength survey of a large sample of interacting disk-type galaxies. The sample is optically-selected, the inclusion of systems having been based upon the presence of unusual morphological features--such as tidal tails, plumes, rings, warped disks--suggestive of tidal interaction. The sample is composed of about 115 systems, most of which are spiral-spiral pairs, with a few spiral-elliptical pairs and a few merging systems (see Bushouse 1986 for more details of the sample selection). This sample has now been studied in the optical, infrared, and radio regimes, including optical spectra and H alpha images, near-infrared photometry and imaging, far-infrared photometry, H I 21 cm emission-line measurements, Very Large Array (VLA) 20 cm maps, and CO emission-line measurements. This paper presents an overview and comparison of the results of the optical, infrared and CO surveys. With these data the authors can compare the far-infrared and CO properties of the galaxies with the classic optical and radio indicators of star formation activity and thereby determine what, if any, relationships exist between star formation activity and the far-infrared and CO properties of the galaxies. Author

N91-16899*# Alabama Univ., Tuscaloosa.
FIR STATISTICS OF PAIRED GALAXIES
Jack W. Sulentic *In* NASA, Marshall Space Flight Center, Paired and Interacting Galaxies: International Astronomical Union Colloquium No. 124 Nov. 1990 p 291-296 (For primary document see N91-16858 08-90)
Avail: NTIS HC/MF A99 CSCL 03B

Much progress has been made in understanding the effects of interaction on galaxies (see reviews in this volume by Heckman and Kennicutt). Evidence for enhanced emission from galaxies in pairs first emerged in the radio (Sulentic 1976) and optical (Larson and Tinsley 1978) domains. Results in the far infrared (FIR) lagged behind until the advent of the Infrared Astronomy Satellite (IRAS). The last five years have seen numerous FIR studies of optical and IR selected samples of interacting galaxies (e.g., Cutri and McAlary 1985; Joseph and Wright 1985; Kennicutt et al. 1987; Haynes and Herter 1988). Despite all of this work, there are still contradictory ideas about the level and, even, the reality of an FIR enhancement in interacting galaxies. Much of the confusion originates in differences between the galaxy samples that were studied (i.e., optical morphology and redshift coverage). Here, the authors report on a study of the FIR detection properties for a large sample of interacting galaxies and a matching control sample. They focus on the distance independent detection fraction (DF) statistics of the sample. The results prove useful in interpreting the previously published work. A clarification of the phenomenology provides valuable clues about the physics of the FIR enhancement in galaxies. Author

N91-16900*# International Centre for Theoretical Physics, Trieste (Italy).
QUANTIFYING THE FIR INTERACTION ENHANCEMENT IN PAIRED GALAXIES
Cong Xu and Jack W. Sulentic (Alabama Univ., Tuscaloosa.) *In* NASA, Marshall Space Flight Center, Paired and Interacting Galaxies: International Astronomical Union Colloquium No. 124 Nov. 1990 p 297-301 Previously announced as N90-29281 (For primary document see N91-16858 08-90)
Avail: NTIS HC/MF A99 CSCL 03B

The Catalog of Isolated Pairs of Galaxies in the Northern Hemisphere, by Karachentsev (1972), was studied and a well-matched comparison sample taken from the Catalog of Isolated Galaxies, by Karachentseva (1973), in order to quantify the enhanced FIR emission properties of interacting galaxies.

Author

N91-16901*# Illinois Univ., Urbana. Dept. of Physics.
STAR FORMATION IN INFRARED BRIGHT AND INFRARED FAINT STARBURST INTERACTING GALAXIES
Susan A. Lamb, Howard A. Bushouse, and John W. Towns (Northwestern Univ., Evanston, IL.) *In* NASA, Marshall Space Flight Center, Paired and Interacting Galaxies: International Astronomical Union Colloquium No. 124 Nov. 1990 p 303-308 (For primary document see N91-16858 08-90)
Avail: NTIS HC/MF A99 CSCL 03B

Short wavelength IUE spectra of Arp 248b and UGC 8315N are combined with optical spectra and interpreted using a combination of spectrum synthesis and spectral diagnostics to place constraints on the massive star populations of the central regions of these galaxies and to deduce information about the star formation histories in the last 10(exp 8) years. The authors find that both galaxies have substantial fractions of their optical light coming from massive stars and that Arp 248b may be dominated in the UV by WR stars. The UV spectra are dominated by radiation from evolved massive stars and the authors place and age on the burst in Arp 248b of a few tens of millions of years. Author

N91-16902*# California Univ., Berkeley. Dept. of Astronomy.
RADIO LOUD FAR-INFRARED GALAXIES
Arjun Dey, Wil vanBreugel (Lawrence Livermore National Lab., CA.), and Joseph C. Shields *In* NASA, Marshall Space Flight Center, Paired and Interacting Galaxies: International Astronomical Union Colloquium No. 124 Nov. 1990 p 309-314 Previously announced as N90-26786 (For primary document see N91-16858 08-90)
Avail: NTIS HC/MF A99 CSCL 03B

The first results are presented of a multiwavelength study of Infrared Astronomy Satellite (IRAS) galaxies with excess radio emission. The sample was selected by cross correlating the IRAS Faint Source Survey, and the Point Source Catalogue with the Texas radio survey. Recent optical (imaging and spectroscopic)

and radio (VLA) observations are discussed. These observations will be used to investigate possible connections between radio galaxy activity, star formation and galaxy interactions. Author

N91-16903*# Indian Inst. of Astrophysics, Bangalore.
ON A CONNECTION BETWEEN SUPERNOVA OCCURRENCE AND TIDAL INTERACTION IN EARLY TYPE GALAXIES
R. K. Kochhar *In* NASA, Marshall Space Flight Center, Paired and Interacting Galaxies: International Astronomical Union Colloquium No. 124 Nov. 1990 p 315-320 (For primary document see N91-16858 08-90)
Avail: NTIS HC/MF A99 CSCL 03B

There are three types of supernovae: two subtypes SNIa and Ib; and SNII. Late type galaxies produce all types of SN, whereas early types (E, SO, and non-Magellanic irregulars IO) have hosted only SNIa. The recently identified SNIb, like SNII, have massive stars as their progenitors. Reviving Oemler and Tinsley's (1979) suggestion that SNIa also come from short-lived stars, the author asserts that they need not occur in all early-type galaxies. SNIa occur only in those galaxies that have access to gas and can form stars in their main body. (SN in nuclear regions are a different matter altogether). In this model, SNIa are not associated with typical stellar population of E/SOs but with regions of localized star formation. Note that data on SNIa from spirals is already consistent with this model. Author

N91-16904*# Joint Astronomy Centre, Hilo, HI.
INFRARED IMAGES OF MERGING GALAXIES
G. S. Wright, P. A. James, R. D. Joseph, I. S. McLean, and R. Doyon (Imperial Coll. of Science and Technology, London, England) *In* NASA, Marshall Space Flight Center, Paired and Interacting Galaxies: International Astronomical Union Colloquium No. 124 Nov. 1990 p 321-326 (For primary document see N91-16858 08-90)
Avail: NTIS HC/MF A99 CSCL 03B

Infrared imaging of interacting galaxies is especially interesting because their optical appearance is often so chaotic due to extinction by dust and emission from star formation regions, that it is impossible to locate the nuclei or determine the true stellar distribution. However, at near-infrared wavelengths extinction is considerably reduced, and most of the flux from galaxies originates from red giant stars that comprise the dominant stellar component by mass. Thus near infrared images offer the opportunity to study directly components of galactic structure which are otherwise inaccessible. Such images may ultimately provide the framework in which to understand the activity taking place in many of the mergers with high Infrared Astronomy Satellite (IRAS) luminosities. Infrared images have been useful in identifying double structures in the nuclei of interacting galaxies which have not even been hinted at by optical observations. A striking example of this is given by the K images of Arp 220. Graham et al. (1990) have used high resolution imaging to show that it has a double nucleus coincident with the radio sources in the middle of the dust lane. The results suggest that caution should be applied in the identification of optical bright spots as multiple nuclei in the absence of other evidence. They also illustrate the advantages of using infrared imaging to study the underlying structure in merging galaxies. The authors have begun a program to take near infrared images of galaxies which are believed to be mergers of disk galaxies because they have tidal tails and filaments. In many of these the merger is thought to have induced exceptionally luminous infrared emission (cf. Joseph and Wright 1985, Sanders et al. 1988). Although the optical images of the galaxies show spectacular dust lanes and filaments, the K images all have a very smooth distribution of light with an apparently single nucleus. Author

N91-16905*# Institute of Astronomy, Cambridge (England).
GALAXY INTERACTIONS AND STAR FORMATION: RESULTS OF A SURVEY OF GLOBAL H-ALPHA EMISSION IN SPIRAL GALAXIES IN 8 CLUSTERS
C. Moss *In* NASA, Marshall Space Flight Center, Paired and Interacting Galaxies: International Astronomical Union Colloquium No. 124 Nov. 1990 p 327-330 (For primary document see N91-16858 08-90)
Avail: NTIS HC/MF A99 CSCL 03B

Kennicutt and Kent (1983) have shown that the global H alpha emission from a spiral galaxy is an indicator of the formation rate of massive stars. Moss, Whittle and Irwin (1988) have surveyed two clusters (Abell 347 and 1367) for galaxies with H alpha emission using a high dispersion objective prism technique. The purpose of the survey is to investigate environmental effects on star formation in spiral galaxies, and in particular to ascertain whether star formation is enhanced in cluster spirals. Approximately 20 percent of CGCG galaxies were detected in emission. Two plates of excellent quality were obtained for each of the two clusters, and galaxies were only identified to have emission if this was detected on both plates of a plate pair. In this way, plate flaws and other spurious identifications of emission could be rejected, and weak emission confirmed. The results of this survey have been discussed by Moss (1987). The detected galaxies are of types SO-a and later. The frequency with which galaxies are detected in emission increases towards later morphological type as expected (cf. Kennicutt and Kent 1983). There is no evidence of any dependence of the frequency of detected emission on the absolute magnitude of the galaxy (cf. Moss and Whittle 1990), but there is a strong correlation between a disturbed morphological appearance of the galaxy and the detection of emission. Furthermore it is found that the emission is more centrally concentrated in those galaxies which show a disturbed morphology. It may be noted that the objective prism plate gives a spectrum of a 400 A region around rest wavelength H alpha, but superposed on this is the H alpha emission from the galaxy which, because the light is essentially monochromatic, results in a true two-dimensional image of the H alpha distribution. The visual appearance of the emission on the prism plates was classified according to its diffuseness on a 5 point scale (very diffuse, diffuse, intermediate, compact, and very compact). In tabular form, the relation is shown between this classification and a morphologically disturbed appearance for the galaxy. Author

N91-16906*# Crimean Astrophysical Observatory (USSR).
OBSERVATIONAL EFFECTS OF INTERACTION IN THE SEYFERT GALAXY NGC 7469
I. I. Pronik and L. Metik *In* NASA, Marshall Space Flight Center, Paired and Interacting Galaxies: International Astronomical Union Colloquium No. 124 Nov. 1990 p 331-342 (For primary document see N91-16858 08-90)
Avail: NTIS HC/MF A99 CSCL 03B

Some pecularities of the circummucleus of the Seyfert galaxy NGC 7469 were revealed, plausibly caused by interaction with the satellite IC 5283 and a starlike detail, situated on the edge of the west spiral branch 14 seconds from the nucleus. Shock excited H II regions were noted in the part of NGC 7469 turned toward the satellite IC 5283. The galaxy's central radio structure (lambda approx. 6 cm) stretches in the direction toward the satellite IC 5283 and the starlike detail. The spectum and color index of the starlike detail suggest that it is a cluster of early type stars (M sub V = -19 sup m) and dust clouds (A sub V = 3 sup m), in NGC 7469. Author

N91-16907*# Sao Paulo Univ. (Brazil). Inst. Astronomico e Geofisico.
RADIO EMISSION IN PECULIAR GALAXIES
Dulia F. deMelloRabaca and Zulema Abraham *In* NASA, Marshall Space Flight Center, Paired and Interacting Galaxies: International Astronomical Union Colloquium No. 124 Nov. 1990 p 343-346 Sponsored in part by CNPq, Brazil and FAPESP, Brazil (For primary document see N91-16858 08-90)
Avail: NTIS HC/MF A99 CSCL 03B

During the last decades a number of surveys of peculiar galaxies have been carried out and accurate positions become available. Since peculiarities are a possible evidence of radio emission (Wright, 1974; Sulentic, 1976; Stocke et al., 1978), the authors selected a sample of 24 peculiar galaxies with optical jet-like features or extensions in different optical catalogues, mainly

the Catalogue of Southern Peculiar Galaxies and Associations (Arp and Madore, 1987) and the ESO/Uppsala Survey of the ESO(B) Atlas (Lauberts, 1982) for observation at the radio continuum frequency of 22 GHz. The sample is listed in a table. Sol (1987) studied this sample and concluded that the majority of the jet-like features seem to admit an explanation in terms of interactive galaxies with bridges and/or tails due to tidal effects. Only in a few cases do the jets seem to be possibly linked to some nuclear activity of the host galaxy. The observations were made with the 13.7m-radome enclosed Itapetinga Radiotelescope (HPBW of 4.3 arcmin), in Brazil. The receiver was a 1 GHz d.s.b. super-heterodine mixer operated in total-power mode, with a system temperature of approximately 800 K. The observational technique consisted in scans in right ascention, centralized in the optical position of the galaxy. The amplitude of one scan was 43 arcmin, and its duration time was 20 seconds. The integration time was at least 2 hours (12 ten-minute observations) and the sensibility limit adopted was an antenna temperature greater than 3 times the r.m.s. error of the baseline determination. Virgo A was used as the calibrator source. Three galaxies were detected for the first time as radio sources and four other known galaxies at low frequencies had their flux densities measured at 22 GHz. The results for these sources are presented. Author

N91-16908*# Wisconsin Univ., Madison.
THE KINEMATICS AND MORPHOLOGY OF NGC 520: ONE, TWO, OR THREE GALAXIES
S. A. Stanford and M. Balcells *In* NASA, Marshall Space Flight Center, Paired and Interacting Galaxies: International Astronomical Union Colloquium No. 124 Nov. 1990 p 347-351 (For primary document see N91-16858 08-90)
(Contracts NAS5-25451; NAS7-918)
Avail: NTIS HC/MF A99 CSCL 03B

The peculiar galaxy NGC 520 (Arp 157) is often interpreted as an interacting pair of galaxies. The identification of the two bulges and overall morphology of the two galaxies has long been a puzzle which the authors attempt to solve here. New longslit optical spectroscopy and near-infrared images of NGC 520 are presented. These data suggest that the northwest peak is the bulge of one of two galaxies in the system. The other larger bulge is clearly evident in the K band image in the middle of the dust lane. The stellar radial velocity profile in the central 10 seconds of the larger bulge is consistent with counterrotation seen in the molecular gas component. This kinematic subsystem could be the remains of a merged gas-rich irregular. Author

N91-16909*# Alabama Univ., Tuscaloosa. Dept. of Physics and Astronomy.
STATISTICS OF ASSOCIATIONS AMONG IR GALAXIES
Jack F. Gallimore and William C. Keel *In* NASA, Marshall Space Flight Center, Paired and Interacting Galaxies: International Astronomical Union Colloquium No. 124 Nov. 1990 p 353-356 (For primary document see N91-16858 08-90)
Avail: NTIS HC/MF A99 CSCL 03B

In the course of expanding the search of Kleinmann et. al. (1988) for distant, infrared-luminous objects, the authors noticed (as is often remarked) that a large number of infrared-selected galaxies have close neighbors or show merger characteristics (e.g., tidal tails, distorted disks). Because the sample size is large (567 infrared galaxies and 2182 field galaxies), this sample is ideal for statistically examining the importance of interactions among infrared galaxies. In particular, the authors compare the nearest-neighbor distribution and the two-point correlation function of their sample with that of a control sample of field galaxies. Author

N91-16910*# Johns Hopkins Univ., Baltimore, MD. Dept. of Physics and Astronomy.
GALAXY INTERACTIONS AND THE STIMULATION OF NUCLEAR ACTIVITY
Timothy M. Heckman (Space Telescope Science Inst., Baltimore, MD.) *In* NASA, Marshall Space Flight Center, Paired and Interacting Galaxies: International Astronomical Union Colloquium No. 124 Nov. 1990 p 359-382 (For primary document see N91-16858 08-90)
Avail: NTIS HC/MF A99 CSCL 03B

The author discusses the idea that interactions between galaxies can lead to enhanced galactic activity. He discusses whether, apart from the observational evidence, there is a strong theoretical or heuristic motivation for investigating galaxy interactions as stimulators of nuclear activity in galaxies. Galactic interactions as mechanisms for triggering nuclear starbursts are covered. Author

N91-16911*# National Aeronautics and Space Administration. Goddard Space Flight Center, Greenbelt, MD.
TIDAL EVENTS AND GALACTIC ACTIVITY
J. B. Hutchings (Dominion Astrophysical Observatory, Victoria, British Columbia) and S. G. Neff *In* NASA, Marshall Space Flight Center, Paired and Interacting Galaxies: International Astronomical Union Colloquium No. 124 Nov. 1990 p 383-386 (For primary document see N91-16858 08-90)
Avail: NTIS HC/MF A99 CSCL 03B

Researchers report some results from recent and ongoing work which relate to the connection between nuclear activity and tidal interactions. They suggest that tidal events are in general a necessary but not sufficient condition for nuclear activation. They also suggest that nuclear activity generally develops at a 'late stage' of a tidal encounter, following star-formation and dust evaporation, and when the most obvious morphological disturbances may have disappeared. The quantitative results from quasi-stellar object imaging, radio source evolution, HI observations, and an Infrared Astronomy Satellite (IRAS) source survey are given in tabular form. Author

N91-16912*# Commonwealth Scientific and Industrial Research Organization, Epping (Australia).
ARE EXTREMELY LUMINOUS FAR-INFRARED GALAXIES THE RESULT OF MERGING QUASAR CORES
R. P. Norris *In* NASA, Marshall Space Flight Center, Paired and Interacting Galaxies: International Astronomical Union Colloquium No. 124 Nov. 1990 p 387-392 (For primary document see N91-16858 08-90)
Avail: NTIS HC/MF A99 CSCL 03B

Extremely Luminous far-infrared galaxies (ELFs) are a class of galaxy discovered independently by several groups. The class is characterized by a quasar-like total luminosity (10(exp 11) to 10(exp 13) solar luminosity) which is radiated almost entirely in the far-infrared. It has been suggested that obscured quasar cores may be responsible for generating this luminosity. Here the author demonstrates that ELFs appear in several guises which can be characterized by the number of quasar cores they contain (zero, one or two). The author develops a unified model to account for these differences. Author

N91-16913*# Yale Univ., New Haven, CT. Dept. of Astronomy.
CENTRAL ACTIVITY IN 60 MICRON PEAKERS
Charlene A. Heisler, J. P. Vader, and Jay A. Frogel (Ohio State Univ., Columbus.) *In* NASA, Marshall Space Flight Center, Paired and Interacting Galaxies: International Astronomical Union Colloquium No. 124 Nov. 1990 p 393-398 (For primary document see N91-16858 08-90)
Avail: NTIS HC/MF A99 CSCL 03B

The authors present charge coupled device (CCD) imaging results of their sample of Infrared Astronomy Satellite (IRAS) galaxies with spectral energy distributions peaking at 60 microns (Vader et al 1988). The results support the author's suggestion that the activity in 60 micron peaking galaxies is centrally concentrated, and represents an early stage of dust-embedded nuclear activity. This activity is probably triggered by a recent interaction/merger event as indicated by their peculiar optical morphologies. The authors propose that 60 micron peakers are the precursors of SO's in the case of amorphous systems, and ellipticals in the case of interacting galaxies. Author

N91-16914*# Michigan State Univ., East Lansing.
GALAXY INTERACTIONS AND STRENGTH OF NUCLEAR ACTIVITY
S. M. Simkin *In* NASA, Marshall Space Flight Center, Paired and Interacting Galaxies: International Astronomical Union Colloquium No. 124 Nov. 1990 p 399-402 (For primary document see N91-16858 08-90)
Avail: NTIS HC/MF A99 CSCL 03B

Analysis of data in the literature for differential velocities and projected separations of nearby Seyfert galaxies with possible companions shows a clear difference in projected separations between type 1's and type 2's. This kinematic difference between the two activity classes reinforces other independent evidence that their different nuclear characteristics are related to a non-nuclear physical distinction between the two classes. The differential velocities and projected separations of the galaxy pairs in this sample yield mean galaxy masses, sizes, and mass to light ratios which are consistent with those found by the statistical methods of Karachentsev. Although the galaxy sample discussed here is too small and too poorly defined to provide robust support for these conclusions, the results strongly suggest that nuclear activity in Seyfert galaxies is associated with gravitational perturbations from companion galaxies, and that there are physical distinctions between the host companions of Seyfert 1 and Seyfert 2 nuclei which may depend both on the environment and the structure of the host galaxy itself. Author

N91-16915*# Space Telescope Science Inst., Baltimore, MD.
COOL INFALLING GAS AND ITS INTERACTION WITH THE HOT ISM OF ELLIPTICAL GALAXIES
W. B. Sparks and F. D. Macchetto (European Space Agency. European Space Research and Technology Center, ESTEC, Noordwijk, Netherlands) *In* NASA, Marshall Space Flight Center, Paired and Interacting Galaxies: International Astronomical Union Colloquium No. 124 Nov. 1990 p 403-408 (For primary document see N91-16858 08-90)
Avail: NTIS HC/MF A99 CSCL 03B

The authors describe work leading to the suggestion that interaction between infalling cool gas and ambient hot, coronal plasma in elliptical galaxies is responsible for emission filaments, and might remove the need for large mass depositions in cooling flows. A test of the hypothesis is undertaken - the run of surface brightness with radius for the emission lines - and the prediction agrees well with the data. Author

N91-16916*# Johns Hopkins Univ., Baltimore, MD.
THE NATURE OF THE EMISSION-LINE NEBULAE IN POWERFUL FAR-INFRARED GALAXIES
Lee Armus, Timothy M. Heckman, and George K. Miley (Leiden Univ., Netherlands) *In* NASA, Marshall Space Flight Center, Paired and Interacting Galaxies: International Astronomical Union Colloquium No. 124 Nov. 1990 p 409-413 (For primary document see N91-16858 08-90)
Avail: NTIS HC/MF A99 CSCL 03B

The authors discuss their program of narrow-band (H alpha + (NII)) imaging of a sample of 30 powerful far-infrared galaxies (FIRG's) chosen to have far-infrared spectral energy distributions similar to the prototype FIRG's Arp 220, NGC 3690, NGC 6240, and M82. The emission-line nebulae of these IR color-selected sample (ICSS) galaxies as a class are both impressively large (mean half light radius, r approx. 1.3 Kpc, and mean diameter, D approx. 16 Kpc) and luminous (L sub TOT approx. 10(exp 8) solar lumninosity; uncorrected for internal extinction). The mean total H alpha + (NII) luminosity of the FIRG's is comparable to that found for pairs of optically selected interacting galaxies (Bushouse, Lamb, and Werner 1988), but is a factor of approx. 5 greater than that of isolated spirals (Kennicutt and Kent 1983). Only approx. 25 percent of the nearby (z approx. less than 0.10) FIRG's have morphologies suggesting that large HII-regions contribute significantly to their emission-line appearance. The broad-band morphologies of our IR color-selected galaxies fall into three major categories. Nearly 75 percent are single galaxy systems, with the remaining FIRG's being either multiple nuclei systems, or members of interacting pairs. Since the authors saw few (10 percent) currently interacting FIRG's, yet many (80 percent) with highly distorted continuum morphologies, their IR color criteria may be preferentially selecting galaxies that have undergone highly inelastic, rapidly merging interactions. Author

N91-16917*# Arizona Univ., Tucson.
NUCLEAR AND EXTENDED INFRARED EMISSION IN PAIRED AND ISOLATED GALAXIES
Roc M. Cutri *In* NASA, Marshall Space Flight Center, Paired and Interacting Galaxies: International Astronomical Union Colloquium No. 124 Nov. 1990 p 415-419 (For primary document see N91-16858 08-90)
Avail: NTIS HC/MF A99 CSCL 03B

The empirical connection between gravitational and collisional interactions among galaxies and enhanced activity has been well-documented. However, the physical mechanisms which are responsible for triggering the various forms of activity have not been determined. The author presents the preliminary results of a study of the nuclear and integrated infrared properties of galaxies chosen from the Catalog of Isolated Pairs of Galaxies in the Northern Hemisphere (Karachentsev 1972; hereafter CPG) and the Catalog of Isolated Galaxies (Karachentseva 1973; hereafter KI). Observations of these large, unbiased samples of paired and isolated galaxies are analyzed with the hope of identifying which aspects of galaxy encounters are most closely coupled to the presence of activity. Author

N91-16918*# Kharkov State Univ. (USSR). Astronomical Observatory.
SIGNS OF INTERACTION OF THE NGC 1275 NUCLEUS WITH THE HIGH-VELOCITY SYSTEM ACCORDING TO 0.7 SEC SEEING OBSERVATIONS
V. N. Dudinov, V. S. Tsvetkova, S. B. Novikov, and I. I. Pronik (Crimean Astrophysical Observatory, USSR) *In* NASA, Marshall Space Flight Center, Paired and Interacting Galaxies: International Astronomical Union Colloquium No. 124 Nov. 1990 p 421-429 (For primary document see N91-16858 08-90)
Avail: NTIS HC/MF A99 CSCL 03B

The nucleus of the Seyfert galaxy NGC 1275 was observed in the B system on 1 December 1989 with seeing 0, 7 seconds using the Zeiss-1000 telescope on Mount Majdanak in Central Asia. Special methods of processing reveal low-contrast details. The nucleus and circumnucleus are stretched in NW-SE direction. There are two narrow filaments near the nucleus in position angles roughly 340 degrees and 320 degrees. The first is directed near the radio jet of the nucleus, the second has broken details curved to the NW or toward the high-velocity system of NGC 1275.
Author

N91-16919*# Space Telescope Science Inst., Baltimore, MD.
DUST AND IONIZED GAS IN ACTIVE RADIO ELLIPTICAL GALAXIES
D. A. Forbes, W. B. Sparks, and F. D. Macchetto (European Space Agency. European Space Research and Technology Center, ESTEC, Noordwijk, Netherlands) *In* NASA, Marshall Space Flight Center, Paired and Interacting Galaxies: International Astronomical Union Colloquium No. 124 Nov. 1990 p 431-435 (For primary document see N91-16858 08-90)
Avail: NTIS HC/MF A99 CSCL 03B

The authors present broad and narrow bandwidth imaging of three southern elliptical galaxies which have flat-spectrum active radio cores (NGC 1052, IC 1459 and NGC 6958). All three contain dust and extended low excitation optical line emission, particularly extensive in the case of NGC 1052 which has a large H alpha + (NII) luminosity. Both NGC 1052 and IC 1459 have a spiral morphology in emission-line images. All three display independent strong evidence that a merger or infall event has recently occurred, i.e., extensive and infalling HI gas in NGC 1052, a counter-rotating core in IC 1459 and Malin-Carter shells in NGC 6958. This infall event is the most likely origin for the emission-line gas and dust, and the authors are currently investigating possible excitation mechanisms (Sparks et al. 1990). Author

N91-16920*# Technische Univ., Goettingen (Germany, F.R.).
CORRELATIONS BETWEEN ENVIRONMENTAL PARAMETERS AND NUCLEAR ACTIVITY
W. Kollatschny and K. J. Fricke *In* NASA, Marshall Space Flight Center, Paired and Interacting Galaxies: International Astronomical Union Colloquium No. 124 Nov. 1990 p 437-440 (For primary document see N91-16858 08-90)
Avail: NTIS HC/MF A99 CSCL 03B

The occurrence and quantitative properties of Seyfert 1 and Seyfert 2 galaxies as a function of the galaxy environment were studied in a systematic way. For this investigation the authors selected from the Catalogue of Quasars and Active Nuclei (Veron & Veron, 1989) all Seyfert galaxies with the following properties: (1) m sub V less than or equal to 15; (2) listed classification as Sey 1, Sey 2, or Sey 3; (3) v sub rad less than or equal to 20,000 km s(sup -1). This results in a sample size of 242 Seyfert galaxies. For all these objects their galaxy environment was inspected on plates. The vicinity of each sample Seyfert galaxy was searched for companion galaxies out to at least 0.5 Mpc. Lacking redshift information, the authors adopted as a companion galaxy any galaxy in this area having a size between 20 and 200 percent of the Seyfert galaxy size. As an important environmental parameter for Seyfert activity, the authors consider the galaxy density within an environment of 500 kpc radius. They distinguish four density classes: D1: no companion (isolated Seyfert); D2: 1 companion; D3: 2 to 5 companions (group); and D4: less than or equal to 6 companions (dense group). The distribution of the various Seyfert classes among these density classes is listed in tabular form, both in absolute numbers and in percentages (given in brackets). From these statistics the environments of Sey 1, Sey 2, and Sey 3 galaxies do not differ in general with the exception that among the isolated galaxies the Seyfert 1 galaxies dominate conspicuously. No significant dependence of morphological type (de Vaucouleurs T-type) on density class is observed both for Sey 1 and Sey 2 galaxies. On the basis of an extensive search of the Seyfert literature the authors also investigated the dependence of the intrinsic parameters of the sample Seyfert galaxies on density class. Author

N91-16921*# Alabama Univ., Tuscaloosa.
THE ROLE OF SHOCKS IN NGC 6240
William C. Keel *In* NASA, Marshall Space Flight Center, Paired and Interacting Galaxies: International Astronomical Union Colloquium No. 124 Nov. 1990 p 441-444 Sponsored in part by EPSCoR (For primary document see N91-16858 08-90)
Avail: NTIS HC/MF A99 CSCL 03B

The case of the infrared-bright system NGC 6240 encapsulates in many ways the major issues in understanding processes in infrared-bright systems in general. Its morphology strongly suggests that this is a merger in progress, with energetic phenomena being triggered as evidenced by strong radio emission and optical emission lines as well as the strong far-infrared output. Evidence has been produced supporting various schemes for producing the energy being radiated by this object. Early work on the optical spectrum suggested a Seyfert 2 classification, but the ionization level and spatial extent of the emission implied a more distributed source of energy. IR line studies found evidence for young supergiants, and for immense amounts of H2 excited by low-velocity shocks, which might contribute to a large enhancement in star-formation rate. Finally, the radio-continuum morphology shows compact sources possibly associated with active nuclei in both remnants of the merger. This is one of the nearest IR-bright galaxies objects at high luminosity (Cz = 7500 km s(exp -1), so that spatially resolved studies can yield further insight into which of these processes are most important - star formation, nuclear activity, or shock excitation. The velocity field, linewidth distribution, and ionization structure of the gas in NGC 6240 was mapped with the Dense-Pak fiber-optic array on the Kitt Peak 4-m telescope. In all, 135 spectra were obtained through an array of 2 inch apertures, with considerable overlap between many of the adjacent apertures produced by offsetting the telescope between the exposures. As the strongest features with lambda less than 1.1 ma, H alpha and the adjacent (NII) lines were observed, along with the neighboring (O I) and (S II) features. Maps of velocity and linewidth were constructed by interpolating measurements from these spectra onto a regular grid, and show irregular patterns with large velocity gradients and, particularly, an extended region of large local (shear?) velocity width. Author

N91-16922*# Rice Univ., Houston, TX. Dept. of Space Physics and Astronomy.
DEEP FABRY-PEROT IMAGING OF NGC 6240: KINEMATIC EVIDENCE FOR MERGING GALAXIES
J. Bland Hawthorn, A. S. Wilson, and R. B. Tully (Hawaii Univ., Honolulu.) *In* NASA, Marshall Space Flight Center, Paired and Interacting Galaxies: International Astronomical Union Colloquium No. 124 Nov. 1990 p 445-449 (For primary document see N91-16858 08-90)
(Grant NSF AST-88-18900)
Avail: NTIS HC/MF A99 CSCL 03B

The authors have observed the superluminous, infrared galaxy NGC 6240 (z = 0.025) at H alpha with the Hawaii Imaging Fabry-Perot Interferometer (HIFI - Bland and Tully 1989). During the past decade, observational evidence from all wavebands indicates that the unusual appearance of NGC 6240 has resulted from a collision between two gas-rich systems, a view which is supported by our spectrophotometric data. However, the origin of the enormous infrared luminosity (4 times 10(exp 11) solar luminosity) detected by the Infrared Astronomy Satellite (IRAS) remains highly controversial, where opinions differ on the relative roles of large-scale shocks, massive star formation or a buried 'active' nucleus. These mechanisms are discussed in the light of the author's Fabry-Perot observations. Author

N91-16923*# Space Telescope Science Inst., Baltimore, MD.
IC5063: A MERGER WITH A HIDDEN LUMINOUS ACTIVE NUCLEUS
L. Colina, W. B. Sparks, and F. D. Macchetto (European Space Agency. European Space Research and Technology Center, ESTEC, Noordwijk, Netherlands) *In* NASA, Marshall Space Flight Center, Paired and Interacting Galaxies: International Astronomical Union Colloquium No. 124 Nov. 1990 p 451-455 (For primary document see N91-16858 08-90)
Avail: NTIS HC/MF A99 CSCL 03B

IC5063 is a nearby galaxy classified as an SO and containing a system of dust lanes parallel to its major optical axis (Danziger, Goss and Wellington, 1981; Bergeron, Durret and Boksenberg, 1983). Extended emission line regions with high excitation properties have been detected over distances of up to 19 kpc from the nucleus. This galaxy has been classified as Seyfert 2 on the basis of its emission line spectrum. These characteristics make IC5063 one of the best candidates for a merger remnant and an excellent candidate for a hidden luminous active nucleus. Based on new broad and narrow band images and long-slit spectroscopy obtained at the ESO 3.6 m telescope, the authors present some preliminary results supporting this hypothesis. Author

N91-16924*# Nigeria Univ., Nsukka. Astrophysics Group.
RADIO STRUCTURES IN QSO-GALAXY PAIRS
Chidi E. Akujor *In* NASA, Marshall Space Flight Center, Paired and Interacting Galaxies: International Astronomical Union Colloquium No. 124 Nov. 1990 p 467-472 (For primary document see N91-16858 08-90)
Avail: NTIS HC/MF A99 CSCL 03B

It is now generally agreed that if quasars and nearby low redshift galaxies are associated, then there should be luminous connections between them. However, most of the observational evidence being presented is in the optical domain, whereas such evidence should also exist at radio frequencies. The author is, therefore, investigating some quasar-galaxy pairs at radio frequencies to search for luminous connections and other structural peculiarities. Radio maps of some of these sources are presented. Author

N91-16925*# Smithsonian Astrophysical Observatory, Cambridge, MA.
RADIO LINE AND CONTINUUM OBSERVATIONS OF QUASAR-GALAXY PAIRS AND THE ORIGIN OF LOW RESHIFT QUASAR ABSORPTION LINE SYSTEMS
C. L. Carilli, J. H. vanGorkom, E. M. Hauxthausen, J. T. Stocke, and J. Salzer (Michigan Univ., Ann Arbor.) *In* NASA, Marshall Space Flight Center, Paired and Interacting Galaxies: International Astronomical Union Colloquium No. 124 Nov. 1990 p 473-477 (For primary document see N91-16858 08-90)
Avail: NTIS HC/MF A99 CSCL 03B

There are a number of known quasars for which our line of sight to the high redshift quasar passes within a few Holmberg radii of a low redshift galaxy. In a few of these cases, spectra of the quasar reveal absorption by gas associated with the low redshift galaxy. A number of these pairs imply absorption by gas which lies well outside the optical disk of the associated galaxy, leading to models of galaxies with 'halos' or 'disks' of gas extending to large radii. The authors present observations of 4 such pairs. In three of the four cases, they find that the associated galaxy is highly disturbed, typically due to a gravitational interaction with a companion galaxy, while in the fourth case the absorption can be explained by clouds in the optical disk of the associated galaxy. They are led to an alternative hypothesis concerning the origin of the low redshift absorption line systems: the absorption is by gas clouds which have been gravitationally stripped from the associated galaxy. These galaxies are rapidly evolving, and should not be used as examples of absorption by clouds in halos of field spirals. The authors conclude by considering the role extended gas in interacting systems plays in the origin of higher redshift quasar absorption line systems. Author

N91-16926*# Arizona Univ., Tucson.
PROPERTIES OF THE REDSHIFT
William G. Tifft and W. J. Cocke *In* NASA, Marshall Space Flight Center, Paired and Interacting Galaxies: International Astronomical Union Colloquium No. 124 Nov. 1990 p 479-483 (For primary document see N91-16858 08-90)
Avail: NTIS HC/MF A99 CSCL 03B

Central to any analysis of dynamical systems, or large scale motion, is the interpretation of redshifts of galaxies as classical Doppler velocity shifts. This is a testable assumption and for many years evidence has accumulated that is inconsistent with the assumption. Here, the authors review recent evidence suggesting systematic radial dependence and temporal variation of redshifts. Author

N91-16927*# Massachusetts Univ., Amherst.
SELECTION EFFECTS AND BINARY GALAXY VELOCITY DIFFERENCES
Stephen E. Schneider and Edwin E. Salpeter (Cornell Univ., Ithaca, NY.) *In* NASA, Marshall Space Flight Center, Paired and Interacting Galaxies: International Astronomical Union Colloquium No. 124 Nov. 1990 p 485-490 (For primary document see N91-16858 08-90)
Avail: NTIS HC/MF A99 CSCL 03B

Measurements of the velocity differences (delta v's) in pairs of galaxies from large statistical samples have often been used to estimate the average masses of binary galaxies. A basic prediction of these models is that the delta v distribution ought to decline monotonically. However, some peculiar aspects of the kinematics have been uncovered, with an anomalous preference for delta v approx. equal to 72 km s(sup-1) appearing to be present in the data. The authors examine a large sample of binary galaxies with accurate redshift measurements and confirm that the distribution of delta v's appears to be non-monotonic with peaks at 0 and approx. 72 km s (exp -1). The authors suggest that the non-zero peak results from the isolation criteria employed in defining samples of binaries and that it indicates there are two populations of binary orbits contributing to the observed delta v distribution. Author

N91-16928*# Alabama Univ., Huntsville. Dept. of Physics.
A TENTATIVE EXPLANATION OF COSMOLOGICAL RED SHIFT
T. Chang and D. G. Torr *In* NASA, Marshall Space Flight Center, Paired and Interacting Galaxies: International Astronomical Union Colloquium No. 124 Nov. 1990 p 491-495 (For primary document see N91-16858 08-90)
Avail: NTIS HC/MF A99 CSCL 03B

The authors suggest a possible alternative explanation of cosmological red shift. They consider that there exists a background field in the universe, and that light (the photon) has an extremely weak interaction with this background, and as result, experiences an energy loss. By analogy with damped oscillations, the authors introduce a dumping term with the first derivative with respect to time in the wave equation. The solution yields a linearly reduced frequency of the light with travel distance. The purpose of this exercise is to demonstrate how a simple alternative interpretation of the Hubble relation can be generated. Author

N91-16929*# Turku Univ. (Finland).
MERGING GALAXIES AND BLACK HOLE EJECTIONS
M. J. Valtonen *In* NASA, Marshall Space Flight Center, Paired and Interacting Galaxies: International Astronomical Union Colloquium No. 124 Nov. 1990 p 497-502 (For primary document see N91-16858 08-90)
Avail: NTIS HC/MF A99 CSCL 03B

In mergers of galaxies their central black holes are accumulated together. Researchers show that few black hole systems arise which decay through black hole collisions and black hole ejections. The ejection statistics are calculated and compared with two observed systems where ejections have been previously suggested: double radio sources and high redshift quasars near low redshift galaxies. In both cases certain aspects of the associations are explained by the merger hypothesis. Author

N91-16930*# Observatoire de Marseille (France).
DYNAMICAL INTERACTIONS OF GALAXY PAIRS
E. Athanassoula *In* NASA, Marshall Space Flight Center, Paired and Interacting Galaxies: International Astronomical Union Colloquium No. 124 Nov. 1990 p 505-516 (For primary document see N91-16858 08-90)
Avail: NTIS HC/MF A99 CSCL 03B

Here the author briefly reviews the dynamics of sinking satellites and the effect of companions on elliptical galaxies. The author then discusses recent work on interacting disk systems, and finally focuses on a favorite interacting pair, NGC 5194/5195. Author

N91-16931*# Universidad Autonoma de Puebla (Mexico). Facultad de Ciencias.
A STATISTICAL STUDY OF MERGING GALAXIES: THEORY AND OBSERVATIONS
Tapan K. Chatterjee *In* NASA, Marshall Space Flight Center, Paired and Interacting Galaxies: International Astronomical Union Colloquium No. 124 Nov. 1990 p 519-535 (For primary document see N91-16858 08-90)
Avail: NTIS HC/MF A99 CSCL 03B

A study of the expected frequency of merging galaxies is conducted, using the impulsive approximation. Results indicate that if we consider mergers involving galaxy pairs without halos in a single crossing time or orbital period, the expected frequency of mergers is two orders of magnitude below the observed value for the present epoch. If we consider mergers involving several orbital periods or crossing times, the expected frequency goes up by an order of magnitude. Preliminary calculation indicate that if we consider galaxy mergers between pairs with massive halos, the merger is very much hastened. Author

N91-16932*# Space Telescope Science Inst., Baltimore, MD.
PROBING THE TIDES IN INTERACTING GALAXY PAIRS
Kirk D. Borne *In* NASA, Marshall Space Flight Center, Paired and Interacting Galaxies: International Astronomical Union Colloquium No. 124 Nov. 1990 p 537-542 (For primary

document see N91-16858 08-90)
Avail: NTIS HC/MF A99 CSCL 03B

Detailed spectroscopic and imaging observations of colliding elliptical galaxies revealed unmistakable diagnostic signatures of the tidal interactions. It is possible to compare both the distorted luminosity distributions and the disturbed internal rotation profiles with numerical simulations in order to model the strength of the tidal gravitational field acting within a given pair of galaxies. Using the best-fit numerical model, one can then measure directly the mass of a specific interacting binary system. This technique applies to individual pairs and therefore complements the classical methods of measuring the masses of galaxy pairs in well-defined statistical samples. The 'personalized' modeling of galaxy pairs also permits the derivation of each binary's orbit, spatial orientation, and interaction timescale. Similarly, one can probe the tides in less-detailed observations of disturbed galaxies in order to estimate some of the physical parameters for larger samples of interacting galaxy pairs. These parameters are useful inputs to the more universal problems of (1) the galaxy merger rate, (2) the strength and duration of the driving forces behind tidally stimulated phenomena (e.g., starbursts and maybe quasi steller objects), and (3) the identification of long-lived signatures of interaction/merger events. Author

N91-16933*# European Southern Observatory, Garching (Germany, F.R.).
DYNAMICAL FRICTION IN PAIRS OF ELLIPTICAL GALAXIES
Philippe Prugniel and Francoise Combes (Observatoire de Paris-Meudon, France) *In* NASA, Marshall Space Flight Center, Paired and Interacting Galaxies: International Astronomical Union Colloquium No. 124 Nov. 1990 p 543-548 (For primary document see N91-16858 08-90)
Avail: NTIS HC/MF A99 CSCL 03B

The authors present numerical experiments on dynamical friction in pairs of elliptical galaxies of unequal mass. They confirm that the self-gravity of the response is not important and show the drastic effect of the deformability of the companion which reduces the decay time by more than a factor of 2. Almost the same amount of orbital energy is dissipated within the satellite as within the large galaxy. Finally, the authors discuss the importance of distant encounters for the dynamical evolution of systems of galaxies. Author

N91-16934*# National Aeronautics and Space Administration. Ames Research Center, Moffett Field, CA.
AN EXPERIMENTAL STUDY OF COUNTER-ROTATING CORES IN ELLIPTICAL GALAXIES
R. H. Miller, G. R. Roelofs, and B. F. Smith (Chicago Univ., IL.) *In* NASA, Marshall Space Flight Center, Paired and Interacting Galaxies: International Astronomical Union Colloquium No. 124 Nov. 1990 p 549-554 (For primary document see N91-16858 08-90)
Avail: NTIS HC/MF A99 CSCL 03B

Recent observational studies (Franx and Illingworth 1987; Jedrzejewski and Schechter 1988; Bender 1988; Illingworth and Franx 1989) have shown that some elliptical galaxies have a small region near the center that rotates in the opposite direction from the outer parts of the galaxy. Often the rotation in the central part is much faster than that in the outer part. A few other galaxies show a small region near the center that rotates in the same direction as the rest of the galaxy, but much faster. Either way, the part near the center that shows a strange pattern of rotation (the 'core') has been interpreted as a distinct dynamical subsystem. Very briefly, the observational data seem to be that anomalies show up in rotation curves near the centers of some elliptical galaxies and that galaxies with these strange rotational properties do not show a photometric signature: there are no noticeable bumps in the brightness profile and no unusual shapes of isophotal contours that would suggest an excess of matter concentrated near the center. No strong color variations have been reported. The puzzle is to learn what we can about elliptical galaxies in general, and about galaxies with strange central regions in particular, from these observational facts. The authors' approach is experimental. They make a guess about the form of the dynamically distinct subsystem, and then build a galaxy model to test experimental consequences such as the amount of matter required to produce observable effects and the length of time over which these effects would remain observable. They sidestep questions about how the galaxy might have gotten to be that way in the first place. That gives them more freedom to explore a variety of suggestions about what kind of dynamical system might give rise to the observed rotational patterns. Author

N91-16935*# Academy of Sciences (USSR), Moscow. Astronomical Council.
ON LEADING SPIRAL ARMS IN CLOSE PAIRS OF GALAXIES
A. M. Fridman *In* NASA, Marshall Space Flight Center, Paired and Interacting Galaxies: International Astronomical Union Colloquium No. 124 Nov. 1990 p 555-563 (For primary document see N91-16858 08-90)
Avail: NTIS HC/MF A99 CSCL 03B

It is explained why one can observe a leading spiral pattern in close pairs of galaxies where the direction of the orbital momentum of the satellite is opposite to the direction of the spin of the spiral galaxy. Author

N91-16936*# Alabama Univ., Tuscaloosa.
A SIMULATION SURVEY OF GALAXY INTERACTIONS
Gene G. Byrd, William C. Keel, and S. Howard (Los Alamos National Lab., NM.) *In* NASA, Marshall Space Flight Center, Paired and Interacting Galaxies: International Astronomical Union Colloquium No. 124 Nov. 1990 p 565-568 Sponsored in part by Cray Research, Inc. (For primary document see N91-16858 08-90)
(Grant NSF RII-86-10669)
Avail: NTIS HC/MF A99 CSCL 03B

Many carefully selected samples of interacting galaxies have been observed extensively in attempts to clarify whether interaction produces activity in galaxies. Because the sample members represent a wide range of encounter parameters and times, one can then study whether there are correlations between observable encounter features and, for example, Seyfert activity. On the other hand, in theoretical studies, simulations typically deal with either time-consuming detailed modelling of single galaxy pairs or tracing a few model encounters over time. The authors extend the observational survey approach by combining it with a simulation survey. The authors are conducting a survey of model encounters, covering the most important encounter parameters over a wide range. Some parameters, such as companion structure and initial velocity, are demonstratably less important and can be ignored in a first pass. The parameter range must be richly enough sampled so that the authors can evaluate the uniqueness of the observable morphology and velocity structure of the resulting simulated pairs to diagnose unobservable companion orbit parameters. They are using a self-gravitating polar n-body code run on the Cray X-MP at the Alabama Supercomputer Network. For each simulation, the authors have stellar and gas distributions predicted over, typically, a billion years, along with information on gas motions within the disk and any material captured by the companion or lost to the system. Features of disturbed spiral galaxies are sensitive enough to time and encounter parameters so that a match of the simulation survey results to observations can be applied as starting points to infer unobservable orbital or system parameters in actual sample members. This should enable them to examine whether interesting observed properties (Seyfert activity, nuclear star-formation rate) are functions of unobservable dynamical properties which characterize each encounter. Any correlations (or lack of some expected ones) will provide strong clues as to how or whether these phenomena are related to interactions. Aside from its use with such observed samples, this survey should greatly speed determination of initial orbital parameters for more detailed subsequent simulations of individual systems. Author

N91-16937*# Universidad Autonoma de Puebla (Mexico). Facultad de Ciencias.
A DYNAMICAL PROXIMITY ANALYSIS OF INTERACTING GALAXY PAIRS

Tapan K. Chatterjee *In* NASA, Marshall Space Flight Center, Paired and Interacting Galaxies: International Astronomical Union Colloquium No. 124 Nov. 1990 p 569-575 (For primary document see N91-16858 08-90)
Avail: NTIS HC/MF A99 CSCL 03B

Using the impulsive approximation to study the velocity changes of stars during disk-sphere collisions and a method due to Bottlinger to study the post collision orbits of stars, the formation of various types of interacting galaxies is studied as a function of the distance of closest approach between the two galaxies. Author

N91-16938*# Los Alamos National Lab., NM.
M51'S SPIRAL STRUCTURE
S. Howard and Gene G. Byrd (Alabama Univ., Tuscaloosa.) *In* NASA, Marshall Space Flight Center, Paired and Interacting Galaxies: International Astronomical Union Colloquium No. 124 Nov. 1990 p 577-581 Previously announced as N90-20916 Sponsored in part by Cray Research, Inc. (For primary document see N91-16858 08-90)
(Grant NSF RII-86-10669)
Avail: NTIS HC/MF A99 CSCL 03B

The M51 system (NGC 5194/5195) provides an excellent problem both in spiral structure and in galaxy interactions. The authors present an analytic study of a computer experiment on the excitation mechanisms for M51's spiral arms and whether or not a halo is important for these mechanisms. This work extends previous numerical studies of the M51 system by including self-gravitation in a two component disk: gas and stars, and a dark halo. The analytic study provides two new observational constraints: the time (approx. 70 to 84 million years ago) and position angle of perigalacticon (300 degrees). By using these constraints and a simple conic approximation, the search for the companion's possible orbit is greatly simplified. This requires fewer N-body simulations than a fully self-gravitating orbit search. Author

N91-16939*# Alabama Univ., Tuscaloosa. Dept. of Physics and Astronomy.
THE SPIRAL-COMPACT GALAXY PAIR AM 2208-251: COMPUTER SIMULATIONS VERSUS OBSERVATIONS
Mario Klaric and Gene G. Byrd *In* NASA, Marshall Space Flight Center, Paired and Interacting Galaxies: International Astronomical Union Colloquium No. 124 Nov. 1990 p 583-587 (For primary document see N91-16858 08-90)
Avail: NTIS HC/MF A99 CSCL 03B

The system AM2208-251 is a roughly edge-on spiral extending east-west with a smaller round compact E system about 60 arcsec east of the spiral nucleus along the major axis of the spiral. Bertola, Huchtmeier, and Zeilinger (1990) have presented optical spectroscopic as well as single dish 21 cm observations of this system. Their spectroscopic data show, via emission lines lambda lambda 3727-29A, a rising rotation curve near the nucleus. These spectroscopic observations may indicate a tidal interaction in the system. In order to learn more about such pairs, the authors simulated the interaction using the computer model developed by Miller (1976 a,b, 1978) and modified by the authors (Byrd 1986, 1987, 1988). To do the simulation they need an idea of the mutual orbits of the two galaxies. Their computer model is a two-dimensional polar N-body program. It consists of a self-gravitating disk of particles, within an inert axially symmetric stabilizing halo potential. The particles are distributed in a 24(radial) by 36(azimuthal) polar grid. Self consistent calculations can be done only within the grid area. The disk is modeled with a finite Mestel disk, where all the particles initially move in circular orbits with constant tangential velocities (Mestel 1963), resulting in a flat rotation curve. The gas particles in the spiral's disk, which make up 30 percent of its mass, collide in the following manner. The number of particles in each bin of the polar grid is counted every time step. If it is greater than a given critical density, all the particles in the bin collide, obtaining in the result the same velocities, equal to the average for the bin. This process produces clumps of gas particles-the star formation sites. The authors suppress the collision in the inner part of the disk (within the circle r = 6) to represent the hole seen in the gas in the nuclear bulge of spirals. They thus avoid spurious effects due to collisions in that region. They also varied the size of the collisional bins, which did not affect their conclusions. Author

N91-16940*# Indian Inst. of Astrophysics, Bangalore.
ENERGY AND ANGULAR MOMENTUM TRANSFER IN BINARY GALAXIES
P. M. S. Namboodiri and R. K. Kochhar *In* NASA, Marshall Space Flight Center, Paired and Interacting Galaxies: International Astronomical Union Colloquium No. 124 Nov. 1990 p 589-593 (For primary document see N91-16858 08-90)
Avail: NTIS HC/MF A99 CSCL 03B

The authors numerically studied tidal effects of a massive perturber on a satellite galaxy. The model consists of a spherical satellite galaxy and a point mass perturber and the encounter is non-penetrating. A wide range of density ratios and eccentricities of the relative orbits have been considered. The disruption of the satellite galaxy has been observed when the numerical value of the fractional change in the energy is greater than two. The changes in the energy and angular momentum show smooth variation in the case of unbound orbits and irregular variation in the bound orbit cases. It is shown that for a constant pericentral distance, increasing the density ratio decreases the tidal effects; and for a given density ratio an increase in the eccentricity decreases the tidal effects. Author

N91-16941*# Helsinki Univ. (Finland).
SIMULATION OF DISK-DISK ENCOUNTERS WITH CO-MOVING POLAR GRIDS
Heikki Salo *In* NASA, Marshall Space Flight Center, Paired and Interacting Galaxies: International Astronomical Union Colloquium No. 124 Nov. 1990 p 595-599 (For primary document see N91-16858 08-90)
Avail: NTIS HC/MF A99 CSCL 03B

The two-grid simulation method combining advantages of both polar and Cartesian mesh-codes is described. In addition to the stellar component reacting solely to gravitational forces, the gas component is included with dissipatively colliding particles. This allows fairly realistic simulation of planar encounters where both systems contain star plus gas disks. Author

N91-16942*# Leiden Univ. (Netherlands).
WHAT DETERMINES THE BULGE TO DISK RATIO OF GALAXIES
Nico Roos *In* NASA, Marshall Space Flight Center, Paired and interacting Galaxies: International Astronomical Union Colloquium No. 124 Nov. 1990 p 601-606 (For primary document see N91-16858 08-90)
Avail: NTIS HC/MF A99 CSCL 03B

Galaxies having the same luminosity may have very different bulge to disk ratios, while the mean bulge to disk ratio slowly increases with total luminosity (Schecter and Dressler, 1987, Sandage et al., 1985). Such a behavior is expected if ellipticals and the spheroidal components of disk galaxies are produced by secondary accretion of galaxies by larger galaxies. This is illustrated using a simple toy model of the evolution of the mass function of galaxies due to galaxy mergers. Author

N91-16943*# Observatoire de Paris-Meudon (France).
DYNAMICAL THEORY OF DENSE GROUPS OF GALAXIES
Gary A. Mamon *In* NASA, Marshall Space Flight Center, Paired and Interacting Galaxies: International Astronomical Union Colloquium No. 124 Nov. 1990 p 609-618 (For primary document see N91-16858 08-90)
Avail: NTIS HC/MF A99 CSCL 03B

It is well known that galaxies associate in groups and clusters. Perhaps 40% of all galaxies are found in groups of 4 to 20 galaxies (e.g., Tully 1987). Although most groups appear to be so loose that the galaxy interactions within them ought to be insignificant, the apparently densest groups, known as compact groups appear so dense when seen in projection onto the plane of the sky that their members often overlap. These groups thus appear as dense

as the cores of rich clusters. The most popular catalog of compact groups, compiled by Hickson (1982), includes isolation among its selection critera. Therefore, in comparison with the cores of rich clusters, Hickson's compact groups (HCGs) appear to be the densest isolated regions in the Universe (in galaxies per unit volume), and thus provide in principle a clean laboratory for studying the competition of very strong gravitational interactions. The $64,000 question here is then: Are compact groups really bound systems as dense as they appear? If dense groups indeed exist, then one expects that each of the dynamical processes leading to the interaction of their member galaxies should be greatly enhanced. This leads us to the questions: How stable are dense groups? How do they form? And the related question, fascinating to any theorist: What dynamical processes predominate in dense groups of galaxies? If HCGs are not bound dense systems, but instead 1D change alignments (Mamon 1986, 1987; Walke & Mamon 1989) or 3D transient cores (Rose 1979) within larger looser systems of galaxies, then the relevant question is: How frequent are chance configurations within loose groups? Here, the author answers these last four questions after comparing in some detail the methods used and the results obtained in the different studies of dense groups. Author

N91-16944*# Observatoire de Paris-Meudon (France).
EXPLAINING COMPACT GROUPS AS CHANGE ALIGNMENTS
Gary A. Mamon *In* NASA, Marshall Space Flight Center, Paired and Interacting Galaxies: International Astronomical Union Colloquium No. 124 Nov. 1990 p 619-627 (For primary document see N91-16858 08-90)
Avail: NTIS HC/MF A99 CSCL 03B

The physical nature of the apparently densest groups of galaxies, known as compact groups is a topic of some recent controversy, despite the detailed observations of a well-defined catalog of 100 isolated compact groups compiled by Hickson (1982). Whereas many authors have espoused the view that compact groups are bound systems, typically as dense as they appear in projection on the sky (e.g., Williams & Rood 1987; Sulentic 1987; Hickson & Rood 1988), others see them as the result of chance configurations within larger systems, either in 1D (chance alignments: Mamon 1986; Walke & Mamon 1989), or in 3D (transient cores: Rose 1979). As outlined in the companion review to this contribution (Mamon, in these proceedings), the implication of Hickson's compact groups (HCGs) being dense bound systems is that they would then constitute the densest isolated systems of galaxies in the Universe and the privileged site for galaxy interactions. In a previous paper (Mamon 1986), the author reviewed the arguments given for the different theories of compact groups. Since then, a dozen papers have been published on the subject, including a thorough and perceptive review by White (1990), thus more than doubling the amount written on the subject. Here, the author first enumerates the arguments that he brought up in 1986 substantiating the chance alignment hypothesis, then he reviews the current status of the numerous recent arguments arguing against chance alignments and/or for the bound dense group hypothesis (both for the majority of HCGs but not all of them), and finally he reconsiders each one of these anti-chance alignment arguments and shows that, rather than being discredited, the chance alignment hypothesis remains a fully consistent explanation for the nature of compact groups. Author

N91-16945*# Leningrad Univ. Observatory (USSR).
TYPICAL MOTIONS IN MULTIPLE SYSTEMS
Joanna P. Anosova *In* NASA, Marshall Space Flight Center, Paired and Interacting Galaxies: International Astronomical Union Colloquium No. 124 Nov. 1990 p 629-631 (For primary document see N91-16858 08-90)
Avail: NTIS HC/MF A99 CSCL 03B

In very old times, people counted - one, two, many. The author wants to show that they were right. Consider the motions of isolated bodies: (1) N = 1 - simple motion; (2) N = 2 - Keplerian orbits; and (3) N = 3 - this is the difficult problem. In general, this problem can be studied only by computer simulations. The author studied this problem over many years (see, e.g., Agekian and Anosova, 1967; Anosova, 1986, 1989 a,b). The principal result is that two basic types of dynamics take place in triple systems. The first special type is the stable hierarchical systems with two almost Keplerian orbits. The second general type is the unstable triple systems with complicated motions of the bodies. By random choice of the initial conditions, by the Monte-Carlo method, the stable systems comprised about approx. 10% of the examined cases; the unstable systems comprised the other approx. 90% of cases under consideration. In N greater than 3, the studies of dynamics of such systems by computer simulations show that we have in general also the motions roughly as at the cases 1 - 3 with the relative negative or positive energies of the bodies. In the author's picture, the typical trajectories of the bodies in unstable triple systems of the general type of dynamics are seen. Such systems are disrupted always after close triple approaches of the bodies. These approaches play a role like the gravitational slingshot. Often, the velocities of escapers are very large. On the other hand, the movie also shows the dynamical processes of a formation, dynamical evolution and disruption of the temporary wide binaries in triples and a formation of final hard massive binaries in the final evolution of triples. Author

N91-16946*# Leningrad Univ. Observatory (USSR).
DYNAMICS AND CONFIGURATIONS OF GALAXY TRIPLETS
Joanna P. Anosova, Victor V. Orlov, Arthur D. Chernin, Alexei V. Ivanov, and Ljudmila G. Kiseleva (Leningrad Electrotechnical Inst., USSR) *In* NASA, Marshall Space Flight Center, Paired and Interacting Galaxies: International Astronomical Union Colloquium No. 124 Nov. 1990 p 633-643 (For primary document see N91-16858 08-90)
Avail: NTIS HC/MF A99 CSCL 03B

The purpose is to infer the probable dynamical states of galaxy triplets by the observed data on their configurations. Two methods are proposed for describing the distributions of the triplet configuration parameters characterizing a tendency to alignment and hierarchy: (1) obtaining a representative sample of configurations and determining its statistical parameters (moments and percentages); and (2) dividing the region of possible configurations of triple systems (Agekian and Anosova, 1967) into a set of segments and finding the probabilities for the configurations to find themselves in each of them. Both these methods allow representation of the data by numerical simulations as well as observations. The effect of projection was studied. It rather overestimates the alignment and hierarchy of the triple systems. Among the parameters of interest there are found some parameters that are least sensitive to projection effects. The samples consist of simulated galaxy triplets (with hidden mass) as well as of 46 probably physical triple galaxies (Karachentseva et al., 1979). The observed triples as well as numerical models show a tendency to alignment. The triple galaxies do not show any tendency to hierarchy (formation of the temporary binaries), but this tendency may be present for simulated triplets without significant dark matter. The significant hidden mass (of order ten times the total mass of a triplet) decreases the probability of forming a binary and so weakens the hierarchy. Small galaxy groups consisting of 3 to 7 members are probably the most prevalent types of galaxy aggregate (Gorbatsky, 1987). Galaxy triplets are the simplest groups, but dynamically nontrivial ones. Author

N91-16947*# Kyoto Sangyo Univ. (Japan). Dept. of Physics.
DRAGGING FORCE ON GALAXIES DUE TO STREAMING DARK MATTER
Tetsuya Hara and Shigeru Miyoshi (Cambridge Univ., England) *In* NASA, Marshall Space Flight Center, Paired and Interacting Galaxies: International Astronomical Union Colloquium No. 124 Nov. 1990 p 645-649 (For primary document see N91-16858 08-90)
Avail: NTIS HC/MF A99 CSCL 03B

It has been reported that galaxies in large regions (approx. 10(exp 2) Mpc), including some clusters of galaxies, may be streaming coherently with velocities up to 600 km/sec or more with respect to the rest frame determined by the microwave background radiation. On the other hand, it is suggested that the

dominant mass component of the universe is dark matter. Because we can only speculate the motion of dark matter from the galaxy motions, much attention should be paid to the correlation of velocities between the observed galaxies and cold dark matter. So the authors investigated whether such coherent large-scale streaming velocities are due to dark matter or only to baryonic objects which may be formed by piling up of gases due to some explosive events. It seems that, although each galaxy will not follow the motion of dark matter, clusters of galaxies may represent the velocity field of dark matter. The origin of the velocity field of dark matter would be due to the initial adiabatic perturbations and, in fact, the observed peculiar velocities of clusters are within the allowed region constrained from the isotropy of the microwave background radiation. Author

N91-16948*# Leningrad State Univ. (USSR).
TRIPLETS OF GALAXIES: THEIR DYNAMICS, EVOLUTION, AND THE ORIGIN OF CHAOS IN THEM
Arthur D. Chernin and Alexei V. Ivanov (Academy of Sciences of the Tajik SSR, Doushanbe.) *In* NASA, Marshall Space Flight Center, Paired and Interacting Galaxies: International Astronomical Union Colloquium No. 124 Nov. 1990 p 651-658 (For primary document see N91-16858 08-90)
Avail: NTIS HC/MF A99 CSCL 03B

Recently Karachentsev's group at The Smithsonian Astrophysical Observatory (SAO) (6-meter Telescope Observatory) published a list of 84 triple systems of galaxies with their distances, radial (line of sight) velocities, and angular sizes (Karachentseva et al., 1988). This gives a new ground for studies of the dark matter problem which fills the gap between the large cosmic scales (White, 1987; Dekel and Rees, 1987, and Einasto et al., 1977) and the scale of individual galaxies (Erickson et al., 1987). The data on the typical velocity dispersions and linear dimension of the triplets indicate that they contain considerable amounts of dark matter (see also earlier work of Karachentseva et al., 1979). Numerical simulations show that the statistical characteristics of the Karachentsev triplets can be imitated by model ensembles of triple systems with dark matter masses M sub d = (1-3 x 10(exp 12) M sub O, which is almost ten times greater than the typical mass of stellar galaxies estimated by the standard mass-to-luminosity ration (Kiseleva and Chernin, 1988). Here, the authors report that important information can be drawn from the data on the visible configurations of these systems. The statistics of configurations provide an independent evidence for dark matter in the triplets; moreover, it enables one to argue that dark matter seems to be distributed over the whole volume of the typical triplet forming its common corona rather than concentrated within individual coronae (or haloes) of the member galaxies. Author

N91-16949*# Leningrad Univ. Observatory (USSR).
A CLASSIFICATION OF THE GALAXY GROUPS
Joanna P. Anosova *In* NASA, Marshall Space Flight Center, Paired and Interacting Galaxies: International Astronomical Union Colloquium No. 124 Nov. 1990 p 659-665 (For primary document see N91-16858 08-90)
Avail: NTIS HC/MF A99 CSCL 03B

A statistical criterion has been proposed to reveal the random and physical clusterings among stars, galaxies and other objects. This criterion has been applied to the galaxy triples of the list by Karachentseva, Karaschentsev and Scherbanovsky, and the double galaxies of the list by Dahari where the primary components are the Seyfert galaxies. The confident physical, probable physical, probable optical and confident optical groups have been identified. The limit difference of radial velocities of components for the confident physical multiple galaxies has also been estimated.
Author

N91-16950*# Leningrad Univ. Observatory (USSR).
VIRAL COEFFICIENT AND HIDDEN MASS IN THE GALAXY GROUPS
Joanna P. Anosova, Victor V. Orlov, and Ljudmila G. Kiseleva (Leningrad Electrotechnical Inst., USSR) *In* NASA, Marshall Space Flight Center, Paired and Interacting Galaxies: international Astronomical Union Colloquium No. 124 Nov. 1990 p 667-676 (For primary document see N91-16858 08-90)
Avail: NTIS HC/MF A99 CSCL 03B

The purpose is the verification of the virial mass estimations for small galaxy groups. The dynamical evolution of triple and quintuple galaxies was studied by the numerical simulations. The dependence of the virial coefficient k(t) versus time was derived. Initial k(O) = O. The function k(t) has some strong oscillations from 0.02 to 0.99. Generally, these oscillations are quasiperiodical ones. Such a behavior of k(t) is caused by formation in a system of close isolated temporary double subsystems. A strong correlation between the virial coefficient and the least mutual distance in the system is observed. Such wide oscillations may add into the estimation of virial mass of the galaxy groups an uncertainty of more than one order. An additional uncertainty is introduced by the projection effect. This uncertainty for the individual estimations of the masses approach three orders. Thus any individual estimation of the virial mass is impossible for small galaxy groups. Some possibility of statistical estimation (median or average) of the total mass, including a hidden mass, is shown for the homogeneous samples. The authors propose a method for these estimations based on a comparison of the medians of dynamical parameters (a mean size in projection and a dispersion of relative radial velocities) for the simulated and observed ensembles of the galaxy groups. This method has been applied to a sample of 46 probably physical triplets of galaxies. The probable median of the hidden mass in a volume of the triplet is about 4 M, where M is the total mass of visible matter. Author

N91-16951*# Kyoto Sangyo Univ. (Japan). Dept. of Physics.
ON THE LARGE-SCALE STRUCTURES FORMED BY WAKES OF OPEN COSMIC STRINGS
Tetsuya Hara, Shoji Morioka, and Shigeru Miyoshi (Cambridge Univ., England) *In* NASA, Marshall Space Flight Center, Paired and Interacting Galaxies: International Astronomical Union Colloquium No. 124 Nov. 1990 p 677-681 (For primary document see N91-16858 08-90)
Avail: NTIS HC/MF A99 CSCL 03B

Large-scale structures of the universe have been variously described as sheetlike, filamentary, cellular, bubbles or spongelike. Recently cosmic strings became one of viable candidates for a galaxy formation scenario, and some of the large-scale structures seem to be simply explained by the open cosmic strings. According to this scenario, sheets are wakes which are traces of moving open cosmic strings where dark matter and baryonic matter have accumulated. Filaments are intersections of such wakes and high density regions are places where three wakes intersect almost orthogonally. The wakes formed at t sub eq become the largest surface density among all wakes, where t sub eq is the epoch when matter density equals to radiation density. If we assume that there is one open cosmic string per each horizon, then it can be explained that the typical distances among wakes, filaments and clusters are also approx. 10(exp 2) Mpc. This model does not exclude a much more large scale structure. Open cosmic string may move even now and accumulate cold dark matter after its traces. However, the surface density is much smaller than the ones formed at t sub eq. From this model, it is expected that the typical high density region will have extended features such as six filaments and three sheets and be surrounded by eight empty regions (voids). Here, the authors are mainly concerned with such structures and have made numerical simulations for the formation of such large scale structures. Author

N91-16952*# Indian Inst. of Astrophysics, Bangalore. Dept. of Physics.
COLLISIONAL REMOVAL OF HI FROM THE INNER DISKS OF VIRGO CLUSTER GALAXIES
Monica Valluri and Chanda J. Jog *In* NASA, Marshall Space Flight Center, Paired and Interacting Galaxies: International Astronomical Union Colloquium No. 124 Nov. 1990 p 683-686 Previously announced in IAA as A90-41784 (For primary document see N91-16858 08-90)
Avail: NTIS HC/MF A99 CSCL 03B

There is sufficient observational evidence to show that many Virgo Cluster spirals are HI deficient in their inner disks (in addition to being HI deficient globally, as previously established). It is shown here that collisions between galaxies in a cluster can lead to the removal of HI gas from these galaxies while leaving the H2 gas, undisturbed. This follows directly from the application of the Spitzer-Baade collisional gas removal mechanism to galaxies consisting of stars and a two-component interstellar medium (ISM) consisting of HI and H2, with HI having the largest filling factor. This can account for both the observed HI deficiency in the inner regions and the normal H2 content of these galaxies. The frequency of galaxy collisions in the Virgo Cluster is shown to be large enough to make collisional gas removal a viable mechanism.

Author

N91-16953*# California Inst. of Tech., Pasadena. Theoretical Astrophysics Div.

INDUCED STARBURST AND NUCLEAR ACTIVITY: FAITH, FACTS, AND THEORY

Isaac Shlosman *In* NASA, Marshall Space Flight Center, Paired and Interacting Galaxies: International Astronomical Union Colloquium No. 124 Nov. 1990 p 689-704 (For primary document see N91-16858 08-90)

(Grant NSF AST-84-51725)

Avail: NTIS HC/MF A99 CSCL 03B

The problem of the origin of starburst and nuclear (nonstellar) activity in galaxies is reviewed. A physical understanding of the mechanism(s) that induce both types of activity requires one to address the following issues: (1) what is the source of fuel that powers starbursts and active galactic nuclei; and (2) how is it channeled towards the central regions of host galaxies? As a possible clue, the author examines the role of non-axisymmetric perturbations of galactic disks and analyzes their potential triggers. Global gravitational instabilities in the gas on scales approx. 100 pc appear to be crucial for fueling the active galactic nuclei.

Author

N91-16954*# Academy of Sciences (USSR), Moscow. Astronomical Council.

STATIONARY ORBITS OF SATELLITES OF DISK GALAXIES

Valerij L. Polyachenko *In* NASA, Marshall Space Flight Center, Paired and Interacting Galaxies: International Astronomical Union Colloquium No. 124 Nov. 1990 p 705-710 (For primary document see N91-16858 08-90)

Avail: NTIS HC/MF A99 CSCL 03B

The satellite of an S-galaxy will experience opposing dynamical-friction forces from the stars of the disk and the halo. If these forces are in balance, the satellite may travel in a stable, near-circular orbit whose radius, for a wide range of physical parameters, should be limited to a zone 1.2 to 1.4 times the disk radius, much as is observed. The idea is very simple. The dynamical friction acting on a small satellite, moving through a stellar galactic halo, makes this satellite slow down. On the other hand, a stellar disk, rotating faster than a satellite, makes it speed up. But the density distributions in radius for disk's and halo's stars in real flat galaxies are quite different (respectively, exponential and power-law). Moreover, the observational data show that the exponential profile for disk's surface density drops abruptly at some radius (r sub d). So it is natural to expect that a stationary orbit could be near the edge of a disk (where two effects are mutually compensated).

Author

N91-16955*# University Coll., Cardiff (Wales).

NUMERICAL SIMULATIONS OF INTERACTING DISK GALAXIES

Masafumi Noguchi *In* NASA, Marshall Space Flight Center, Paired and Interacting Galaxies: International Astronomical Union Colloquium No. 124 Nov. 1990 p 711-716 (For primary document see N91-16858 08-90)

Avail: NTIS HC/MF A99 CSCL 03B

Galaxy-galaxy interactions have long attracted many extragalactic astronomers in various aspects. A number of computer simulations performed in the 1970s have successfully reproduced the peculiar morphologies observed in interacting disk galaxies and clarified that tidal deformation explains most of the observed global peculiarities. However, most of these simulations have used test particles in modelling the disk component. Tidal response of a self-gravitating disk remains to be further clarified. Another topic which is intensely discussed at present is the relation between galaxy-galaxy interactions and activity. Many observations suggest that interactions trigger strong starbursts and possibly active galactic nuclei (AGN). However, the detailed mechanism of triggering is not yet clear. It is vital here to understand the dynamics of interstellar gas. In order to understand various phenomena related to galaxy-galaxy interactions (mainly for disk galaxies), the author performed a series of numerical simulations on close galaxy encounters which includes both interstellar gas and self-gravitating disk components. In these simulations, the galaxy model to be perturbed (target galaxy) consists of a halo and a disk. The halo was treated as a rigid spherical gravitational field which is assumed to remain fixed during the interaction. The disk is composed of stars and gas. The stellar disk was constructed by 20000 collisionless particles of the same mass. Those particles move in the halo gravitational field, interacting with each other and with the perturber. Therefore, the self-graviy of the disk is properly taken into account. Stellar particles were initially given circular velocities with small random motions required to stabilize the disk against local axisymmetric disturbances. The gravitational field of the stellar disk was calculated by the particle-mesh scheme (e.g. Hockney and Eastwood 1981). The gaseous component was modelled by the cloud-particle scheme (e.g. Roberts and Hausman 1984). Here, the authors represent the gas as an ensemble of small spheres (i.e. clouds) and include the creation of an OB star in a cloud-cloud collision and subsequent velocity push on nearby clouds due to a supernova explosion.

Author

N91-16956*# Leningrad Univ. Observatory (USSR).

GAS FLOWS IN S-E BINARY SYSTEMS OF GALAXIES

N. Ya. Sotnikova *In* NASA, Marshall Space Flight Center, Paired and Interacting Galaxies: International Astronomical Union Colloquium No. 124 Nov. 1990 p 717-726 (For primary document see N91-16858 08-90)

Avail: NTIS HC/MF A99 CSCL 03B

Tidal interaction between the galaxies in binary systems leads to important consequences. Some peculiarities in galactic morphology as well as the transfer of matter from one galaxy to another may be due to this factor. In particular, gas flows in intergalactic space may be formed. Such flows enriching one component with gas from the other may play a substantial role in the evolution of mixed (S-E) pairs. One can mention several facts corroborating the possibility of the gas transfer from the spiral to the elliptical galaxy. High HI content (10(exp 7) to 10(exp 9) solar mass) is detected in nearly 40 E galaxies (Bottinelli and Gougenheim, 1979; Knapp et al., 1985). Such galaxies are often members of pairs or of multiple systems including an S galaxy, which may be the source of gas (Smirnov and Komberg, 1980). Moreover, the gas kinematics and its distribution also indicate an external origin for this gas (Knapp et al., 1985). In many cases there is an outer gaseous disk. The directions of the disk and of stellar rotation don't always coincide (van Gorkom et al., 1985; Varnas et al., 1987). The galaxy colors in S-E pairs are correlated (the Holmberg effect): bluer ellipticals have spiral components that are usually bluer (Demin et al., 1984). The fraction of E galaxies with emission lines (N sub em) in S-E pairs showing traces of tidal interaction is twice as large (N sub em approx. equals 0.24) as in pairs without interaction (N sub em approx. equals 0.12) (Sotnikova, 1988b). Since the presence of emission lines in a galaxy spectrum strongly depends on gas content, this fact also leads to the conclusion that ellipticals in interacting S-E pairs are enriched with gas. These facts may be considered as a serious indication of the existence of gas transfer. Hence, investigation of this process is of interest.

Author

N91-16957*# Naval Research Lab., Washington, DC. Space Science Div.
OBSERVATIONS AND MODELS OF STAR FORMATION IN THE TIDAL FEATURES OF INTERACTING GALAXIES
John F. Wallin, James M. Schombert, and Curtis Struck-Marcell (Iowa State Univ. of Science and Technology, Ames.) *In* NASA, Marshall Space Flight Center, Paired and Interacting Galaxies: International Astronomical Union Colloquium No. 124 Nov. 1990 p 727-730 (For primary document see N91-16858 08-90)
Avail: NTIS HC/MF A99 CSCL 03B

Multi-color surface photometry (BVri) is presented for the tidal features in a sample of interacting galaxies. Large color variations are found between the morphological components and within the individual components. The blue colors in the primary and the tidal features are most dramatic in B-V, and not in V-i, indicating that star formation instead of metallicity or age dominates the colors. Color variations between components is larger in systems shortly after interaction begins and diminishes to a very low level in systems which are merged. Photometric models for interacting systems are presented which suggest that a weak burst of star formation in the tidal features could cause the observed color distributions. Dynamical models indicate that compression occurs during the development of tidal features causing an increase in the local density by a factor of between 1.5 and 5. Assuming this density increase can be related to the star formation rate by a Schmidt law, the density increases observed in the dynamical models may be responsible for the variations in color seen in some of the interacting systems. Limitations of the dynamical models are also discussed. Author

N91-16958*# Max-Planck-Inst. fuer Astronomie, Heidelberg (Germany, F.R.).
STARBURSTS IN INTERACTING GALAXIES: OBSERVATIONS AND MODELS
Konrad Bernloehr *In* NASA, Marshall Space Flight Center, Paired and Interacting Galaxies: International Astronomical Union Colloquium No. 124 Nov. 1990 p 731-736 (For primary document see N91-16858 08-90)
Avail: NTIS HC/MF A99 CSCL 03B

Starbursts have been a puzzling field of research for more than a decade. It is evident that they played a significant role in the evolution of many galaxies but still quite little is known about the starburst mechanisms. A way towards a better interpretation of the available data is the comparison with evolution models of starburst. The modelling of starbursts and the fitting of such model starbursts to observed data is discussed. The models were applied to a subset of starburst and post-starburst galaxies in a sample of 30 interacting systems. These galaxies are not ultraluminous far infrared (FIR) galaxies but rather ordinary starburst galaxies with FIR luminosities of a few 10(exp 10) to a few 10(exp 11) solar luminosities. Author

N91-16959*# Illinois Univ., Urbana. Dept. of Physics.
DYNAMICAL EXPERIMENTS ON MODELS OF COLLIDING DISK GALAXIES
Richard A. Gerber, Dinshaw S. Balsara, and Susan A. Lamb *In* NASA, Marshall Space Flight Center, Paired and Interacting Galaxies: International Astronomical Union Colloquium No. 124 Nov. 1990 p 737-742 (For primary document see N91-16858 08-90)
Avail: NTIS HC/MF A99 CSCL 03B

Collisions between galaxies can induce large morphological changes in the participants and, in the case of colliding disk galaxies, bridges and tails are often formed. Observations of such systems indicate a wide variation in color (see Larson and Tinsley, 1978) and that some of the particpants are experiencing enhanced rates of star formation, especially in their central regions (Bushouse 1986, 1987; Kennicutt et al., 1987, Bushouse, Lamb, and Werner, 1988). Here the authors describe progress made in understanding some of the dynamics of interacting galaxies using N-body stellar dynamical computer experiments, with the goal of extending these models to include a hydrodynamical treatment of the gas so that a better understanding of globally enhanced star formation will eventually be forthcoming. It was concluded that close interactions between galaxies can produce large perturbations in both density and velocity fields. The authors measured, via computational experiments that represent a galaxy's stars, average radial velocity flows as large as 100 km/sec and 400 percent density increases. These can occur in rings that move outwards through the disk of a galaxy, in roughly homologous inflows toward the nucleus, and in off center, non-axisymmetric regions. Here the authors illustrate where the gas is likely to flow during the early stages of interaction and in future work they plan to investigate the fate of the gas more realistically by using an N-body/Smoothed Particle Hydrodynamics code to model both the stellar and gaseous components of a disk galaxy during a collision. Specifically, they will determine the locations of enhanced gas density and the strength and location of shock fronts that form during the interaction. Author

N91-16960*# Iowa State Univ. of Science and Technology, Ames. Astronomy Program.
CAUSTIC WAVES IN GALAXY DISKS PRODUCED IN COLLISIONS WITH LOW MASS COMPANIONS
Curtis Struck-Marcell *In* NASA, Marshall Space Flight Center, Paired and Interacting Galaxies: International Astronomical Union Colloquium No. 124 Nov. 1990 p 743-747 (For primary document see N91-16858 08-90)
(Grant NAGw-1009)
Avail: NTIS HC/MF A99 CSCL 03B

The author lists a few reasons for studying collisions with relatively low mass companions, specifically those that are less than about one third of the mass of the target galaxy. The primary effect of such collisions on a target galaxy with a 'cold' disk component is the generation of waves in the disk. The focus here is on the purely stellar waves in such disks. The example of a ring galaxy case is examined. Author

N91-16961*# Onsala Space Observatory (Sweden).
SIMULATIONS OF GAS CLOUDS IN INTERACTING GALAXIES
Magnus Thomasson *In* NASA, Marshall Space Flight Center, Paired and Interacting Galaxies: International Astronomical Union Colloquium No. 124 Nov. 1990 p 749-753 (For primary document see N91-16858 08-90)
Avail: NTIS HC/MF A99 CSCL 03B

A companion can induce a variety of morphological changes in a galaxy. The author uses N-body simulations to study the effects of different kinds of perturbations on the dynamics of a disk galaxy. The model is two-dimensional, with a disk consisting of about 60,000 particles. Most of the particles (80%) represent the old stellar population with a high velocity dispersion, while the rest (20%) represent gas clouds with a low velocity dispersion. Initially, the velocity dispersion corresponds to $Q = 1$ for the star particles, and $Q = 0$ for the gas particles, where Q is Toomre's (1964) stability parameter. The gas clouds can collide inelastically. The disk is stabilized by a rigid halo potential, and by the random motions of the old star particles. To simulate the effect of an encounter on the disk, a companion galaxy, modelled as a point mass, can move in a co-planar orbit around the disk. A complete description of the N-body code is found in Thomasson (1989). The spiral structures caused by a companion in first a direct and then a retrograde (with respect to the rotation of the disk) parabolic orbit are presented. The associated velocity fields suggest a way to observationally distinguish between leading and trailing spiral arms. The stability of the gas component in a disk in which tidally triggered infall of gas to the center occurs is studied. Finally, the author shows how a ring of gas can form in a disk as a result of a co-planar encounter with another galaxy. Author

N91-16962*# Institute of Astronomy, Cambridge (England).
DO ELLIPTICAL GALAXIES HAVE THICK DISKS
R. C. Thomson and A. E. Wright (Angio-Australian Observatory, Epping.) *In* NASA, Marshall Space Flight Center, Paired and Interacting Galaxies: International Astronomical Union Colloquium No. 124 Nov. 1990 p 755-758 (For primary document see

N91-16858 08-90)
Avail: NTIS HC/MF A99 CSCL 03B

The authors discuss new evidence which supports the existence of thick disks in elliptical/SO galaxies. Numerical simulations of weak interactions with thick disk systems produce shell structures very similar in appearance to those observed in many shell galaxies. The authors think this model presents a more plausible explanation for the formation of shell structures in elliptical/SO galaxies than does the merger model and, if correct, supports the existence of thick disks in elliptical/SO galaxies. Author

N91-16963*# Tokyo Univ. (Japan). Inst. of Astronomy.
WING GALAXIES: A FORMATION MECHANISM OF THE CLUMPY IRREGULAR GALAXY MARKARIAN 297
Yoshiaki Taniguchi and Masafumi Noguchi (Wales Univ., Swansea.) *In* NASA, Marshall Space Flight Center, Paired and Interacting Galaxies: International Astronomical Union Colloquium No. 124 Nov. 1990 p 759-763 (For primary document see N91-16858 08-90)
Avail: NTIS HC/MF A99 CSCL 03B

In order to contribute to an understanding of collision-induced starburst activities, the authors present a detailed case study on the starburst galaxy Markarian 297 (= NGC 6052 = Arp 209; hereafter Mrk 297). This galaxy is classified as a clumpy irregular galaxy (CIG) according to its morphological properties (cf. Heidmann, 1987). Two major clumps and many small clumps are observed in the entire region of Mrk 297 (Hecquet, Coupinot, and Maucherat 1987). The overall morphology of Mrk 297 is highly chaotic and thus it seems difficult to determine possible orbits of galaxy-galaxy collision. However, the authors have serendipitously found a possible orbit during a course of numerical simulations for a radial-penetration collision between galaxies. The radial-penetration collision means that an intruder penetrates a target galaxy radially passing by its nucleus. This kind of collision is known to explain a formation mechanism of ripples around disk galaxies (Wallin and Struck-Marcell 1988). Here, the authors show that the radial-penetration collision between galaxies successfully explains both overall morphological and kinematical properties of Mrk 297. The authors made two kinds of numerical simulations for Mrk 297. One is N-body (1x10(exp 4) particles) simulations in which effects of self gravity of the stellar disk are taken into account. These simulations are used to study detailed morphological feature of Mrk 297. The response of gas clouds are also investigated in order to estimate star formation rates in such collisions. The other is test-particle simulations, which are utilized to obtain a rough picture of Mrk 297 and to analyze the velocity field of Mrk 297. The techniques of the numerical simulations are the same as those in Noguchi (1988) and Noguchi and Ishibashi (1986). In the present model, an intruding galaxy with the same mass of a target galaxy moves on a rectilinear orbit which passes the center of the target. Author

N91-16964*# Johns Hopkins Univ., Baltimore, MD. Dept. of Physics and Astronomy.
PAIRED AND INTERACTING GALAXIES: CONFERENCE SUMMARY
Colin A. Norman (Space Telescope Science Inst., Baltimore, MD.) *In* NASA, Marshall Space Flight Center, Paired and Interacting Galaxies: International Astronomical Union Colloquium No. 124 Nov. 1990 p 765-770 (For primary document see N91-16858 08-90)
Avail: NTIS HC/MF A99 CSCL 03B

The author gives a summary of the conference proceedings. The conference began with the presentation of the basic data sets on pairs, groups, and interacting galaxies with the latter being further discussed with respect to both global properties and properties of the galactic nuclei. Then followed the theory, modelling and interpretation using analytic techniques, simulations and general modelling for spirals and ellipticals, starbursts and active galactic nuclei. Before the conference the author wrote down the three questions concerning pairs, groups and interacting galaxies that he hoped would be answered at the meeting: (1) How do they form, including the role of initial conditions, the importance of subclustering, the evolution of groups to compact groups, and the fate of compact groups; (2) How do they evolve, including issues such as relevant timescales, the role of halos and the problem of overmerging, the triggering and enhancement of star formation and activity in the galactic nuclei, and the relative importance of dwarf versus giant encounters; and (3) Are they important, including the frequency of pairs and interactions, whether merging and interactions are very important aspects of the life of a normal galaxy at formation, during its evolution, in forming bars, shells, rings, bulges, etc., and in the formation and evolution of active galaxies? Where possible he focuses on these three central issues in the summary. Author

N91-16965# Rice Univ., Houston, TX.
POSITRON SURVIVAL IN TYPE II SUPERNOVAE M.S. Thesis
Steven J. Sturner May 1989 65 p
(AD-A226778) Avail: NTIS HC/MF A04 CSCL 03/2

Since the discovery of Supernova 1987A (A Type II supernova) in February of 1987, there has been a flurry of activity in the field of supernova modeling. The fact that the supernova occurred in the nearby Large Magellanic Cloud and that the progenitor star has almost universally been identified has allowed great progress to be made. Prior to exploding, SK 69 202 was seen as a B3-I blue supergiant with a surface temperature of approximately 16,000 K and bolometric magnitude of 7.5 to 8.2. A blue supergiant becoming a Type II supernova shocked many people. It has been suggested that SK 69 202 was once a red supergiant but it evolved back to the blue. Author

N91-16966# Fermi National Accelerator Lab., Batavia, IL.
THE BEST-FIT UNIVERSE
Michael S. Turner (Chicago Univ., IL.) Oct. 1990 14 p Presented at the 1990 Nobel Symposium: The Birth and Early Evolution of Our Universe, Ostersund, Sweden, 11-16 Jun. 1990
(Contract DE-AC02-76CH-03000)
(DE91-004583; FNAL/C-90/226-A; CONF-9006282-3) Avail: NTIS HC/MF A03

Inflation provides very strong motivation for a flat Universe, Harrison-Zel'dovich (constant-curvature) perturbations, and cold dark matter. However, there are a number of cosmological observations that conflict with the predictions of the simplest such model: one with zero cosmological constant. They include the age of the Universe, dynamical determinations of Omega, galaxy-number counts, and the apparent abundance of large-scale structure in the Universe. While the discrepancies are not yet serious enough to rule out the simplest and most well motivated model, the current data point to a best-fit model with the following parameters: Omega(sub B) approximately equal to 0.03, Omega(sub CDM) approximately equal to 0.17, Omega(sub Lambda) approximately equal to 0.8, and H(sub 0) approximately equal to 70 km/(sec x Mpc) which improves significantly the concordance with observations. While there is no good reason to expect such a value for the cosmological constant, there is no physical principle that would rule out such. DOE

N91-16967# Ludwig-Maximilians-Univ., Munich (Germany, F.R.). Fakultaet fuer Physik.
FORMATION AND DEVELOPMENT OF ELLIPTICAL AND DWARF GALAXIES Ph.D. Thesis [ENTSTEHUNG UND ENTWICKLUNG VON ELLIPTISCHEN UND ZWERGGALAXIEN]
Andreas Michael Burkert Jun. 1989 180 p In GERMAN
(Grant DFG-Ku-474/13-1)
(ETN-91-98492) Avail: NTIS HC/MF A09

A consistent model for the formation and development of elliptical and dwarf galaxies is presented. The observed global properties of these galaxies were examined. As galaxies in the late phase of their development are mostly composed of stars, the dynamics of stellar systems plays an important part in the galaxy development. The development of stellar systems was examined, and the results are discussed, using a new star dynamics model. It was found that the development of stellar systems strongly depends on the collapse of this system. A detailed Inter Stellar Medium (ISM) model was presented. The interaction process

between the star components and the gas components was determined. Using this ISM model, the chemidynamical development of the elliptical and dwarf galaxies was analytically and numerically examined. ESA

N91-16968# Los Alamos National Lab., NM.
ORIGIN OF REGULARITIES IN THE REDSHIFT DISTRIBUTIONS OF DISTANT GALAXIES AND QUASARS
Leonid M. Ozernoy 1990 9 p Presented at the Astrophysics Workshop: After the First Three Minutes, College Park, MD, 15-17 Oct. 1990 Submitted for publication
(Contract W-7405-eng-36)
(DE91-004848; LA-UR-90-3920; CONF-9010268-1) Avail: NTIS HC/MF A02

A model in which inhomogeneities originated during inflation and transformed eventually into density peaks with maximum wavelength equal to the horizon size at the decoupling epoch (z(sub dec) approximately equal to 10(exp 3)) would presently give a very large scale structure a periodic distribution: ln(1 + z) approximately equal to 0.04n + 0.04, n = 0,1,2,.... This formula in which the true phase is replaced by its characteristic value fits the data on redshift distribution of distant galaxies fairly well. Some relevant implications are discussed in the paper, such as the difference between the constants of periodicity C equivalent to delta ln(1 + z): C(sub G) for distant galaxies and C(sub Q) for quasars, and a recent finding that quasars close on the sky to low redshifted galaxies shot a higher concentration toward peaks in the quasar redshift distribution than do quasars in general. DOE

N91-16969 Texas Univ., Austin.
DENSE CORES AND YOUNG STELLAR OBJECTS Ph.D. Thesis
Harold Martin Butner 1990 198 p
Avail: Univ. Microfilms Order No. DA9031529

Two kinds of studies were conducted to investigate the physical conditions to be found in nearby low mass star formation regions. The first was a multiple transition study of DCO(+) emission in a sample of low mass dense molecular cores which revealed the presence of denser gas (n = 10(exp 5)/cc) than most previous studies had suggested. In addition, the observations revealed that those cores which are associated with young stars have higher densities than those cores which have no associated star. The DCO(+) linewidths for these cores are significantly broader than the previously observed NH3 linewidths. The broadening of the DCO(+) does not appear to be entirely an opacity effect. Instead, the broader linewidth suggests the presence inside the core of a dense gas component which has some supersonic motion. This component is not traced by NH3. Such a supersonic component, if it is involved in the collapse of a star, will force star formation models to include the effects of turbulence on the star formation process. In the second project, the far-infrared emission at 50 and 100 microns of three nearby, young stellar objects was studied through use of a scanning far-infrared photometer. The three objects, L1551 IRS 5, NGC 2071, and IRAS 16293-2422, are surrounded by spherically distributed dust emission on scales of several thousand AU. The dust emission was modeled with a radiative transfer code assuming various density distributions, n(r), where r is the distance from the object. Two sources, L1551 IRS 5 and NGC 2071, were found to have a density distribution which is in good agreement with current star formation models. IRAS 16293-2422, in contrast, had a much shallower density distribution surrounding it. Current models for individual star formation would appear unable to explain how a star could form in a core with such a shallow density distribution. Dissert. Abstr.

N91-16970 California Inst. of Tech., Pasadena.
MOLECULAR GAS AND STAR FORMATION IN THE CENTRAL REGIONS OF VIRGO SPIRAL GALAXIES Ph.D. Thesis
Blaise Joseph Canzian 1990 351 p
Avail: Univ. Microfilms Order No. DA9031439

The central regions of eight normal spiral galaxies in the Virgo Cluster spanning a wide range of morphological types were observed in CO (J = 1-0) emission using the Owens Valley mm-wave interferometer. Broadband optical and H alpha CCD photometry was obtained using the Palomar 60-inch telescope. The H2 masses in the central five kiloparsecs of the spirals are large, typically several 10(exp 8) solar masses, far exceeding the atomic hydrogen masses. H2 densities in the cloud complexes are comparable to those of Galactic center complexes such as Sgr B2. Molecular gas comprises a substantial fraction of the dynamical mass of the central regions. The H2 masses may be overestimated in some spirals because of cloud heating. The main source of heating is probably dissipation of turbulence, which is probably greater at the centers of spirals based on CO line widths. Current central star formation rates are about a few solar masses per year. The star formation rate in the central regions of most of the spirals has been relatively constant over a Hubble time, although some galaxies are currently undergoing star formation bursts. Several mechanisms are suggested that could supply enough gas to maintain current star formation rates. The current rate of star formation is well correlated with the mean square molecular gas surface density computed from interferometer maps. Such a correlation is expected if cloud-cloud collisions or another stimulation mechanism acting between clouds is the principle means to produce high-mass stars where the concentration of clouds is greatest. The B luminosity is better correlated with the total gas mass surface density, which supports a stochastic or independent mode of forming intermediate-mass stars in the general cloud population. Dissert. Abstr.

N91-16971 Tufts Univ., Medford, MA.
GRAVITON EFFECTS IN VACUUM MAXIMALLY SYMMETRIC SPACES Ph.D. Thesis
Michael Turyn 1990 105 p
Avail: Univ. Microfilms Order No. DA9028616

The two-point functions for perturbations to the metric tensor, or gravitons are found for vacuum-state maximally symmetric backgrounds of arbitrary dimension n. Tensor mode functions are used on the n-sphere and a general gauge-fixing term. The gauge invariant part of the resulting graviton propagator is isolated, and is fully evaluated for de Sitter spaces in terms of functions of the geodesic separation. The metric perturbations in turn induce fluctuations in the various curvature tensors away from their background values. Coordinate independent correlation functions for these fluctuations are found as sums of maximally symmetric bitensors, and physical implications of their behaviors discussed. Dissert. Abstr.

N91-16972# Goettingen Univ. (Germany, F.R.). Mathematisch Naturwissenschaftlichen Fakultaet.
SPECTROMETRIC, CHEMICAL, AND COSMOLOGICAL DEVELOPMENT OF GALAXIES Ph.D. Thesis [SPEKTROPHOTOMETRISCHE, CHEMISCHE UND KOSMOLOGISCHE ENTWICKLUNG VON GALAXIEN]
Uta Fritz-vonAlvensleben 1989 135 p In GERMAN
(Contract DFG-325/21-4/28-1-2)
(ETN-91-98555) Avail: NTIS HC/MF A07

A model is presented, which can be coupled with the Friedmann-Lemaitre model for the cosmological development of the universe to predict spectrophotometric and chemical properties of galaxies, even with high red shift. Thirty-one star spectra were obtained in the ultraviolet and optical area. The superposing of these observed spectra in accordance with the calculated electron numbers of the Hertzprung-Russual diagram states showed the synthetic spectrum of the galaxy at each time point. A good agreement between the model and the observations was observed. ESA

N91-16973# Hamburg Univ. (Germany, F.R.). Fachbereich Physik.
GALACTIC STRUCTURE IN DIRECTION OF VELA-PUPPIS BY MEANS OF UBV BETA OBSERVATIONS Ph.D. Thesis
Lutz Wenskat 1990 150 p In GERMAN; ENGLISH summary
(ETN-91-98556) Avail: NTIS HC/MF A07

The structure of the Milky Way in the region of the southern

constellations Vela and Puppis is studied on the basis of photometric data for 838 stars of the spectral types O and B. UHB values and H-Beta indices were used and homogeneously reduced. Absolute magnitudes were determined with the Crawford calibration to obtain reliable distance data. The spatial distribution of the objects and the interstellar extinction show a continuation of the local spiral arm in the direction of a galactic longitude equal to 265 degrees. ESA

N91-16974 Max-Planck-Inst. fuer Physik und Astrophysik, Garching (Germany, F.R.). Inst. fuer Extraterrestrische Physik.
ION DISTRIBUTIONS AND FLOWS NEAR THE NEUTRAL SHEET
M. Nakamura, G. Paschmann, W. Baumjohannn, and N. Sckopke Apr. 1990 46 p Submitted for publication
(MPE-PREPRINT-179; ETN-91-98603) Copyright Avail: Fachinformationszentrum Karlsruhe, 7514
Leopoldshafen-Eggenstein 2, Fed. Republic of Germany

A survey of the three dimensional ion and electron distributions measured on AMPTE/IRM near the neutral sheet in the near Earth magnetotail is presented. The data is classified according to substorm phases. Individual case studies of velocity distributions reveal that the ions in the neutral sheet consist of a single population. Fast and slow flows both occur during the two extremes of the magnetospheric activity, the substorm expansion phase and quiet times. Ion beams are occasionally observed and their shapes in velocity space are similar to those observed in the plasma sheet boundary layer. A ring distribution is seen only twice in fifty events. The occurrence rate of fast flow is positively correlated with the global magnetic field elevation during disturbed times and anticorrelated with that elevation during quiet times. The global magnetic field elevation angle is related to the magnetic field configuration in the magnetotail. These results indicate a dependence of the flow speed within the neutral sheet on the magnetotail configuration at the point of observation. ESA

N91-16975 Max-Planck-Inst. fuer Physik und Astrophysik, Garching (Germany, F.R.). Inst. fuer Extraterrestrische Physik.
STRUCTURE AND ENERGY BALANCE OF MOLECULAR CLOUDS
Reinhard Genzel May 1990 45 p Presented at Conference on Molecular Clouds, Manchester, England, Mar. 1990 Submitted for publication
(MPE-PREPRINT-181; ETN-91-98605) Copyright Avail: Fachinformationszentrum Karlsruhe, 7514
Leopoldshafen-Eggenstein 2, Fed. Republic of Germany

Maps of millimeter molecular line emission clearly show that molecular clouds have a complex clumpy spatial structure. Recent observations of the structure and energetics of these clouds, as well as possible physical models, such as the effects of radiative and mass outflows from embedded stars, are discussed. The mass spectrum and stability of the clumps is discussed, as well as what might be in between the clumps. The emphasis of the discussion is on clouds in the vicinity of regions of active OB star formation. The possibility that the small, high density condensations in cloud cores are protostars discussed and the role of molecular spectroscopy in studying them is considered. The discovery and possible explanations of the warm molecular gas near the surfaces of these molecular clouds is discussed. ESA

N91-16976 Max-Planck-Inst. fuer Physik und Astrophysik, Garching (Germany, F.R.). Inst. fuer Extraterrestrische Physik.
MOLECULAR ABSORPTION LINES TOWARDS THE NUCLEUS OF CENTAURUS A
A. Eckart, M. Cameron, Reinhard Genzel, J. M. Jackson, H. Rothermel, J. Stutzki, G. Rydbeck, and T. Wiklind (Onsala Space Observatory, Sweden) Apr. 1990 26 p Submitted for publication Sponsored in part by the Royal Society
(MPE-PREPRINT-182; ETN-91-98606) Copyright Avail: Fachinformationszentrum Karlsruhe, 7514
Leopoldshafen-Eggenstein 2, Fed. Republic of Germany

The properties of the molecular interstellar medium in Centaurus A are examined through analysis of molecular absorption lines obtained using the Swedish ESO Submillimeter Telescope (SEST). The results indicate that: the absorption takes place against the compact nuclear continuum source in the line emitting clouds all along the line of sight through the molecular disk of Centaurus A; that the bulk of the absorbing gas is cold; that some absorptions at the systematic velocity of Centaurus A are comparable to typical values found for dense galactic clouds; that abundances, excitation temperature, and density of the absorbing and emitting molecular gas in the disk of Centaurus A are similar to the values obtained for the disk material in other galaxies; and that the absorbing molecular clouds are clumped. The fact that the absorbing molecular gas is cold and dense is in agreement with the finding that at the mean distance of the absorbing gas of 1 kpc radiative excitation from the nuclear source is not important. The molecular abundances found in Centaurus A are within the same range of values obtained for other well studied galaxies. ESA

N91-16977*# Max-Planck-Inst. fuer Physik und Astrophysik, Garching (Germany, F.R.). Inst. fuer Extraterrestrische Physik.
THE 158 MICROMETER (CII) LINE: A MEASURE OF GLOBAL STAR FORMATION ACTIVITY IN GALAXIES
G. J. Stacey, N. Geis, Reinhard Genzel, J. B. Lugten, A. Poglitsch, A. Sternberg, and C. H. Townes (California Univ., Berkeley.) Jul. 1990 54 p Submitted for publication
(Grant NAG2-208)
(NASA-CR-187925; NAS 1.26:187925; MPE-PREPRINT-188; ETN-91-98611) Copyright Avail: NTIS HC/MF A04 CSCL 03B

Some 158 micron (CII) fine structure line observations from a sample of fourteen gas rich galaxies are reported. These measurements confirm and generalize previous basic results that the (CII) line is bright amounting to approximately 0.1 to 1 percent of the Far Infra Red (FIR) luminosity of the nuclear regions of galaxies; the (CII) line is formed in the warm (temperature of the gas is greater than 200 K), dense (n sub H greater than 1000/cu cm) photodissociated gas at the interfaces between giant molecular clouds and ionized gas regions and is therefore associated with the molecular gas component in spiral galaxies; the (CII) line tracks the FIR continuum in a manner consistent with the PDR models; the integrated (CII) to isotope (12)CO (transition 1 to 0) line ratio is large (greater than or equal to 1000) in all galaxies studied, and is similarly large for galactic molecular clouds; the (CII) line is therefore energetically very important for the study of giant molecular clouds. Conclusions obtained from these results are given. ESA

N91-16978 Max-Planck-Inst. fuer Physik und Astrophysik, Garching (Germany, F.R.). Inst. fuer Extraterrestrische Physik.
THE GALACTIC CENTER AT SUBMILLIMETER AND FAR-INFRARED WAVELENGTHS Progress Report
Reinhard Genzel Aug. 1990 24 p Presented at 29th Liege Astrophysical Colloquium, Liege, Belgium, 3-5 Jul. 1990 Submitted for publication
(MPE-PREPRINT-190; ETN-91-98614) Copyright Avail: Max-Planck-Institut fuer Physik und Astrophysik, 8046 Garching-bei-Muenchen, Fed. Republic of Germany

Recent progress in 10 microns to 1 mm observations of the central 100 pc of our galaxy and their interpretations are discussed. The emphasis is on the physical conditions and dynamics in the nucleus derived from spectroscopic and broadband observations of interstellar gas and dust. The radio arc and galactic center molecular clouds in the central 100 pc, the cloud and SgrA east in the central 20 pc and the circum nuclear disk and ionized cavity in the central 5 pc are discussed in detail. ESA

91 LUNAR AND PLANETARY EXPLORATION

Includes planetology; and manned and unmanned flights.

For spacecraft design or space stations see *18 Spacecraft Design, Testing and Performance.*

N91-16979# Deutsche Forschungsanstalt fuer Luft- und Raumfahrt, Oberpfaffenhofen (Germany, F.R.). Abt. Planetare Erkundung.

PHOTOMETRIC ANALYSES FOR THE DETERMINATION OF PHYSICAL AND STRUCTURAL PROPERTIES FOR THE MARTIAN SURFACE IN THE OXIA PALUS REGION Ph.D. Thesis - Ludwig-Maximilians-Univ.

Peter Regner Jun. 1990 177 p In GERMAN; ENGLISH summary Report will also be announced as translation (ESA-TT-1248) Original contains color illustrations

(DLR-FB-90-27; ISSN-0171-1342; ETN-91-98594) Avail: NTIS HC/MF A09; DLR, VB-PL-DO, Postfach 90 60 58, 5000 Cologne, Fed. Republic of Germany, HC 72.50 Deutsche marks

The primary goal is to derive information concerning the physical and structural characteristics of the Martian surface, from measurements of the anisotropy of the diffusely reflected sunlight on the basis of digital Viking orbiter images. The contribution of light scattered on atmospheric dust particles can be identified, calculated and separated from the surface information by using a combined surface atmosphere model, which approximates the reflection behavior of rough surfaces over a wide range of phase angles very accurately and whose parameters can be interpreted in a geologically meaningful sense. The application of this model to phase curves measured in two visible spectral bands gives insight into the mean particle albedo, the state of compaction, and the macroscopic roughness of the surface material as well as into the wavelength dependence of these photometrically derived surface parameters. A pixel by pixel classification results in the development of thematic maps. ESA

92 SOLAR PHYSICS

Includes solar activity, solar flares, solar radiation and sunspots.

For related information see *93 Space Radiation.*

N91-16980# Johns Hopkins Univ., Laurel, MD. Applied Physics Lab.

[ACTIVITIES AND ACCOMPLISHMENTS OF THE CENTER FOR APPLIED SOLAR PHYSICS, 1987 - 1990] Final Report, 1 Dec. 1986 - 30 Apr. 1990

David M. Rust 30 Apr. 1990 16 p

(Grant AF-AFOSR-0077-87; AF Proj. 3484)

(AD-A228773; AFOSR-90-1111TR) Avail: NTIS HC/MF A03 CSCL 03/2

New instruments have been installed at observatories in New Mexico and California for measuring solar magnetic fields and surface velocities. The magnetic fields provide the energy for all eruptive and accelerative processes on the Sun, and the surface velocities reveal the dynamics of the solar interior. Early detection of emerging magnetic fields may give several hours' warning of impending solar flares and interplanetary shocks. The new instruments incorporate several technical innovations, including lithium niobate filter for high spectral resolution. With this filter, circular and linear polarization and Doppler shifts are measured in solar spectral lines to yield estimates of the magnetic field vector in active sunspot regions. A program of daily measurements is planned for study of the current peak in the 11-year solar cycle. GRA

93 SPACE RADIATION

Includes cosmic radiation; and inner and outer earth's radiation belts.

For biological effects of radiation see *52 Aerospace Medicine.* For theory see *73 Nuclear and High-Energy Physics.*

N91-16981*# National Aeronautics and Space Administration. Langley Research Center, Hampton, VA.

CELLULAR TRACK MODEL OF BIOLOGICAL DAMAGE TO MAMMALIAN CELL CULTURES FROM GALACTIC COSMIC RAYS

Francis A. Cucinotta, Robert Katz (Nebraska Univ., Lincoln.), John W. Wilson, Lawrence W. Townsend, John E. Nealy, and Judy L. Shinn Washington Feb. 1991 13 p

(NASA-TP-3055; L-16831; NAS 1.60:3055) Avail: NTIS HC/MF A03 CSCL 03B

The assessment of biological damage from the galactic cosmic rays (GCR) is a current interest for exploratory class space missions where the highly ionizing, high-energy, high-charge ions (HZE) particles are the major concern. The relative biological effectiveness (RBE) values determined by ground-based experiments with HZE particles are well described by a parametric track theory of cell inactivation. Using the track model and a deterministic GCR transport code, the biological damage to mammalian cell cultures is considered for 1 year in free space at solar minimum for typical spacecraft shielding. Included are the effects of projectile and target fragmentation. The RBE values for the GCR spectrum which are fluence-dependent in the track model are found to be more severe than the quality factors identified by the International Commission on Radiological Protection publication 26 and seem to obey a simple scaling law with the duration period in free space. Author

N91-16982# Lawrence Livermore National Lab., CA. Physics Dept.

RESONANT COMPTON SCATTERING IN MODELS OF GAMMA-RAY BURST SOURCES. PART 2: NUMERICAL MODELING

Peter Vitello and Charles D. Dermer 1990 10 p Presented at the Los Alamos Workshop on Gamma-Ray Bursts, Taos, NM, 29 Jul. - 3 Aug. 1990

(Contract W-7405-eng-48)

(DE91-005268; UCRL-JC-105323-PT-2; CONF-9007101-4-PT-2) Avail: NTIS HC/MF A02

Photon spectra produced from the resonant Compton scattering of blackbody photons by a beam of relativistic electrons and positrons were numerically calculated. The beam is assumed to be directed radially outward along the magnetic axis of a highly magnetized neutron star. A dipole magnetic field geometry is assumed, and the effects of magnetic Compton-scattering energy losses on the particles in the beam during transport are included. A range of surface blackbody radiation temperatures near 1 keV and magnetic field strengths near 2 x 10(exp 12) Gauss are studied for power law electron and positron source functions. If the beam is injected with a power law distribution with energy distribution index (Gamma) and low energy cutoff (gamma sub asterisk), then the calculated Compton-scattered photon spectra are similar to observed gamma ray burst spectra, with a spectral index (alpha) which breaks from alpha approx. = 1 to alpha approx. = Gamma. DOE

N91-16983# Max-Planck-Inst. fuer Physik und Astrophysik, Garching (Germany, F.R.). Inst. fuer Extraterrestrische Physik.

INTERPRETATION OF THE DIFFUSIVE GALACTIC CONTINUUM GAMMA RADIATION IN MeV AREA Thesis [INTERPRETATION DER DIFFUSEN GALAKTISCHEN KONTINUUMS-GAMMASTRAHLUNG IM MEV-BEREICH]

Gerhard Youssefi Sep. 1990 127 p In GERMAN

(MPE-220; ISSN-0178-0719; ETN-91-98565) Copyright Avail: NTIS HC/MF A07

A model of the interstellar photon field is presented for wave lengths varying in the interval 100 nm to 1 mm. For the electrons

of the cosmic radiation, the results from direct observations, analysis of synchrotron emission and evaluation of gamma data were used. The calculated photon field was used for the estimation of the source function of the inverse Compton effect and the influence of the photon field anisotropy on the source function was examined and was found to be significant only by high galactic breadths, for which it produces an intensity increasing from the Compton effect of around 30 percent. ESA

99 GENERAL

N91-16984# Argonne National Lab., IL.
[HIGHLIGHTS OF THE CHEMICAL TECHNOLOGY (CMT) DIVISION'S ACTIVITIES] Annual Technical Report, 1989
Mar. 1990 227 p
(Contract W-31-109-eng-38)
(DE90-008242; ANL-90/11) Avail: NTIS HC/MF A11

Highlights of the Chemical Technology (CMT) Division's activities during 1989 are presented. In this period, CMT conducted research and development in the following areas: (1) electrochemical technology, including high-performance batteries (mainly lithium/iron sulfide and sodium/metal chloride), aqueous batteries (lead-acid and nickel/iron), and advanced fuel cells with molten carbonate and solid oxide electrolytes; (2) coal utilization, including the heat and seed recovery technology for coal-fired magnetohydrodynamics plants and the technology for fluidized-bed combustion; (3) methods for recovery of energy from municipal waste and techniques for treatment of hazardous organic waste; (4) nuclear technology related to a process for separating and recovering transuranic elements from nuclear waste and for producing Mo-99 from low-enriched uranium targets, the recovery processes for discharged fuel and the uranium blanket in a sodium-cooled fast reactor (the Integral Fast Reactor), and waste management; and (5) physical chemistry of selected materials in environments simulating those of fission and fusion energy systems. The division also has a program in basic chemistry research in the following areas: (1) fluid catalysis for converting small molecules to desired products; (2) materials chemistry for superconducting oxides and associated and ordered solutions at high temperatures; (3) interfacial processes of importance to corrosion science, high-temperature superconductivity, and catalysis; and (4) the geochemical processes responsible for trace-element migration within the earth's crust. The division continued to be administratively responsible for and the major user of the Analytical Chemistry Laboratory at Argonne National Laboratory (ANL). DOE

N91-16985# Lawrence Livermore National Lab., CA.
ENERGY AND TECHNOLOGY REVIEW, MARCH 1990
Alan K. Burnham, ed., Cara M. Corey, ed., Lauren deVore, ed., Kevin Gleason, ed., Nona M. Sanford, ed., and Shirley O. Taft, ed. 1990 38 p
(Contract W-7405-eng-48)
(DE90-008230; UCRL-52000-90-3) Avail: NTIS HC/MF A03

Energy and Technology is published by Lawrence Livermore Laboratories monthly to report on progress for the several programs currently being conducted. Specific articles are: Materials Engineer to Astronaut; Improving Composite Materials through Mechanistic Cure Modeling; A Test of Newton's Inverse-Square Law of Gravity; A Decision Framework for Verifying Compliance with Test-Limitation Treaties; and Discrimination of Nuclear Explosions and Earthquakes. DOE

N91-16986# Department of Energy, Washington, DC.
ACCOMPLISHMENTS IN TECHNOLOGY TRANSFER FROM DOE AND ITS LABORATORIES
Jan. 1990 213 p
(DE90-002686; DOE/ER-0428) Avail: NTIS HC/MF A11

Technology transfer from DOE laboratories to industry is increasing. Technology transfer opportunities have many forms, including new materials, new and enhanced technologies, improved processes, technical know-how, unique experimental facilities, and computer software. The applied research programs - Nuclear Energy, Conservation and Renewable Energy, and Fossil Energy - include technology transfer activities that are referred to as program directed. When the technology is used for secondary applications or an application that differs from the original purpose for which the technology was developed, spin-off transfer occurs. The laboratories are the predominant implementors of spin-off transfer activities. Private-sector companies, universities, and consortia are also integral participants for program implementation. In this document, the technology transfer accomplishments of DOE's research programs and some of the best from its R and D laboratories are described and illustrated. This document is intended to communicate a few of the many opportunities available for U.S. industry and universities to work with DOE and its laboratories. DOE

N91-16987# Deutsche Forschungsanstalt fuer Luft- und Raumfahrt, Cologne (Germany, F.R.). Hauptabt. Planung.
THE 1989 ANNUAL CATALOG OF THE GERMAN AEROSPACE ESTABLISHMENT: RESEARCH REPORTS AND COMMUNICATIONS [JAHRESVERZEICHNIS 1989: FORSCHUNGSBERICHTE UND MITTEILUNGEN]
W. Wilke Jul. 1990 41 p In GERMAN
(ISSN-0172-357X; ETN-91-98400) Avail: NTIS HC/MF A03

Abstracts of the 1989 aerospace related research reports and communications are presented. Lists of related authors and public institutes are included. Relevant addresses are given. ESA

Typical Subject Index Listing

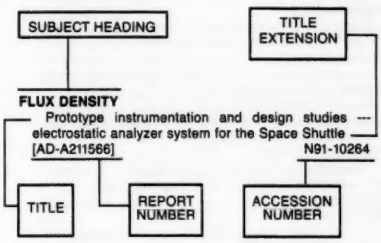

The subject heading is a key to the subject content of the document. Titles, report numbers, and accession numbers of pertinent documents are provided under each subject heading. When the title is insufficiently descriptive of the document content, a title extension has been added, separated from the title by three hyphens. The report number helps to indicate the type of document cited (e.g., NASA report, NASA translation, NASA contractor report). The accession number is the number by which the document abstracts are arranged in this journal and by which the document is sold or requested. The titles, with title extensions if present, are arranged under each subject heading in ascending accession number order. The subject headings have been selected from the latest revision of the *NASA Thesaurus* (NASA SP-7064).

A

ABILITIES
Skill and skilled memory
[AD-A227697] N91-16549

ABLATION
Cluster formation in laser-induced ablation and evaporation of solids observed by laser ionization time-of-flight mass spectrometry and scanning tunneling microscopy
[DE90-010876] N91-16344

ABSORBERS (MATERIALS)
Rotary absorption heat pump sensitivity analysis
[DE90-010006] N91-16256

ABSORPTION
Modeling laser ignition of explosives and pyrotechnics: Effects and characterization of radiative transfer
[DE90-011052] N91-16161
Rotary absorption heat pump sensitivity analysis
[DE90-010006] N91-16256

ABSORPTION SPECTRA
An approximation to true peak absorbance from observed peak absorbance for gas phase Fourier transform spectroscopy
[AD-A228357] N91-16104
Rotational temperature estimation of CO at high temperatures by graphical methods using FTIR spectrometry
[AD-A228370] N91-16105
Photoinduced charge separation by polymer-bound chromophores
[DE90-010997] N91-16140
Molecular absorption lines towards the nucleus of Centaurus A
[MPE-PREPRINT-182] N91-16976

ABSORPTIVITY
Comparison of propagation and absorption of FEL-generated microwaves with theory
[DE90-010369] N91-16181

ABSTRACTS
The 1989 annual catalog of the German Aerospace Establishment: Research reports and communications
[ISSN-0172-357X] N91-16987

ABUNDANCE
A non-LTE analysis of a sample of O stars selected from galactic OB associations N91-16854

ACCELERATED LIFE TESTS
Characterization of the corrosion of a P-130x graphite fiber reinforced 6063 aluminum metal matrix composite
[AD-A228134] N91-16071
Status of Argonne life evaluation of valve regulated lead-acid batteries
[DE90-011098] N91-16229

ACCELERATION STRESSES (PHYSIOLOGY)
Current status of an artificial intelligence-based loss of consciousness monitoring system for advanced fighter aircraft N91-16556
Framework for an efficient two filter GLOC monitor N91-16557

ACCELERATION TOLERANCE
Cerebral oxygen status and G-induced loss of consciousness N91-16554
Detection of loss of consciousness in flight by Doppler method N91-16555
Current status of an artificial intelligence-based loss of consciousness monitoring system for advanced fighter aircraft N91-16556
Framework for an efficient two filter GLOC monitor N91-16557

ACCELERATORS
The new LLNL AMS spectrometer
[DE90-010868] N91-16084
Application of AMS to the biomedical sciences
[DE90-010869] N91-16538

ACCELEROMETERS
A low-cost infrared telemetry system for kilohertz-bandwidth data acquisition
[DE90-010616] N91-16042
Determination of shuttle orbiter center of gravity from flight measurements
[NASA-TM-102627] N91-16058

ACCESS CONTROL
Movable-boundary channel-access schemes for integrated voice/data networks
[AD-A227331] N91-16186

ACCIDENT PREVENTION
Safe venting of hydrogen
[DE90-008964] N91-16174

ACCRETION DISKS
Interacting nuclei in distant galaxies N91-16894

ACCUMULATIONS
Merging galaxies and black hole ejections N91-16929
A statistical study of merging galaxies: Theory and observations N91-16931
On the large-scale structures formed by wakes of open cosmic strings N91-16951

ACETIC ACID
Conversion of acetic acid to methane by thermophiles
[DE90-010993] N91-16086
Formic and acetic acids in the boundary layer over the North Atlantic ocean N91-16530

ACETYLENE
Theoretical study of the C-H bond dissociation energy of acetylene
[NASA-CR-187858] N91-16065

ACID RAIN
Ozone and acid-precipitation on western coniferous forests
[DE90-011014] N91-16462

ACOUSTIC ATTENUATION
Long-range sound propagation: A review of some experimental data N91-16683
Scattering measurements on natural and model trees N91-16691

ACOUSTIC COUPLING
Some comments on the acoustic coupling of elements in an array
[AD-A227762] N91-16239

ACOUSTIC DUCTS
Canonical eigenvalues. Part 2: Application to one-layer, bounded, underwater acoustic ducts
[AD-A227451] N91-16677

ACOUSTIC EMISSION
Some comments on the acoustic coupling of elements in an array
[AD-A227762] N91-16239
Effect of wind and temperature gradients on received acoustic energy N91-16697

ACOUSTIC IMPEDANCE
Some comments on the acoustic coupling of elements in an array
[AD-A227762] N91-16239
Air-ground interface: Surface waves, surface impedance and acoustic-to-seismic coupling coefficient N91-16685
Exponential ground impedance models and their interpretation N91-16686
Preliminary analysis of measured sound propagation over various seasonal snow covers N91-16687
Long-distance sound propagation over discontinuous impedances N91-16688
Using a fast Fourier method to model sound propagation in a stratified atmosphere over a stratified porous-elastic ground N91-16692
Lamina transducer coupler and method of making
[NASA-CASE-LAR-14361-1] N91-16707

ACOUSTIC MEASUREMENT
Acoustical and dynamic mechanical characterization of fiber-matrix interface bonds in ceramic composites
[DE90-010949] N91-16066
Proving experiments on an acoustic transmission suite and its reverberation room
[BBC-RD-1990/13] N91-16681
Fourth International Symposium on Long-Range Sound Propagation
[NASA-CP-3101] N91-16682
Long-range sound propagation: A review of some experimental data N91-16683
ADRPM-VII applied to the long-range acoustic detection problem N91-16689
Infrasonic observations of large-scale HE events N91-16694

ACOUSTIC PROPAGATION
Proving experiments on an acoustic transmission suite and its reverberation room
[BBC-RD-1990/13] N91-16681
Fourth International Symposium on Long-Range Sound Propagation
[NASA-CP-3101] N91-16682
Air-ground interface: Surface waves, surface impedance and acoustic-to-seismic coupling coefficient N91-16685
Vehicular sources in acoustic propagation experiments N91-16690
Using a fast Fourier method to model sound propagation in a stratified atmosphere over a stratified porous-elastic ground N91-16692
Infrasonic observations of large-scale HE events N91-16694
A time-domain finite-element method for the computation of three-dimensional acoustic wave fields in inhomogeneous fluids and solids
[ETN-91-98485] N91-16710

ACOUSTIC PROPERTIES
Vehicular sources in acoustic propagation experiments N91-16690
Comparison of FFP predictions with measurements of a low-frequency signal propagated in the atmosphere N91-16698

ACOUSTIC SCATTERING
Fourth moments of acoustic waves forward scattered by a rough ocean surface
[AD-A227469] N91-16529
Scattering measurements on natural and model trees N91-16691
Scattering of sound by atmospheric turbulence predictions in a refractive shadow zone N91-16703
SCATSPHERE2: A computation for the plane-wave scattering from a submerged, elastic, spherical, evacuated or fluid-filled, thin shell
[AD-A228867] N91-16709

ACOUSTIC SIMULATION
Field measurement of head related transfer functions [AD-A227850] N91-16708
ACOUSTIC VELOCITY
Long-range sound propagation: A review of some experimental data N91-16683
Air-ground interface: Surface waves, surface impedance and acoustic-to-seismic coupling coefficient N91-16685
Meteorological effects on long-range outdoor sound propagation N91-16696
Comparison of FFP predictions with measurements of a low-frequency signal propagated in the atmosphere N91-16698
Effects of large-scale wind driven turbulence on sound propagation N91-16704
ACOUSTICS
Internal solitary waves in compressible fluids [ETN-91-98475] N91-16307
Multiple-frequency surface acoustic wave devices as sensors [DE90-009972] N91-16675
Utilization of polymer viscoelastic properties in acoustic wave sensor applications [DE90-010534] N91-16676
Wind turbine acoustics [NASA-TP-3057] N91-16679
A review of the airborne sound insulation requirements for broadcasting studios and ancillary areas [BBC-RD-1990/10] N91-16680
Air-ground interface: Surface waves, surface impedance and acoustic-to-seismic coupling coefficient N91-16685
Exponential ground impedance models and their interpretation N91-16686
Effect of wind and temperature gradients on received acoustic energy N91-16697
Effects of large-scale wind driven turbulence on sound propagation N91-16704
ACRYLIC RESINS
Model filled polymers versus synthesis of crosslinked monodisperse polymethacrylate beads [AD-A227236] N91-16146
ACTINIDE SERIES
Molecular orbital studies of the bonding in heavy element organometallics [DE90-009732] N91-16711
ACTINIDE SERIES COMPOUNDS
Magnetic structures of actinide materials by pulsed neutron diffraction [DE91-000373] N91-16093
Molecular orbital studies of the bonding in heavy element organometallics [DE90-009732] N91-16711
ACTIVE CONTROL
The NASA controls-structures interaction technology program [NASA-TM-102752] N91-16057
ACTIVE GALACTIC NUCLEI
Paired and Interacting Galaxies: International Astronomical Union Colloquium No. 124 [NASA-CP-3098] N91-16858
New data on the peculiar galaxy MRK 273 N91-16887
Induced starburst and nuclear activity: Faith, facts, and theory N91-16953
Numerical simulations of interacting disk galaxies N91-16955
Paired and interacting galaxies: Conference summary N91-16964
Molecular absorption lines towards the nucleus of Centaurus A [MPE-PREPRINT-182] N91-16976
ACTIVE GALAXIES
Multi-color imaging of selected southern interacting galaxies N91-16867
Dust and ionized gas in active radio elliptical galaxies N91-16919
Paired and interacting galaxies: Conference summary N91-16964
ADA (PROGRAMMING LANGUAGE)
Implementing sporadic servers in Ada [AD-A226723] N91-16584
Understanding the adoption of Ada: Results of an industry survey [AD-A226725] N91-16585
Hartstone benchmark results and analysis [AD-A226817] N91-16587
Scheduler issues for real-time Ada [AD-A227766] N91-16592
Tailoring an Ada runtime environment proof-of-concept [AD-A227767] N91-16593
Distributed issues for Ada real-time systems [AD-A227852] N91-16603
Kernal facilities definition, Kernel version 3.0 [AD-A228027] N91-16610
Ada compiler validation procedures, version 2.1 [AD-A228614] N91-16621
ADAPTATION
An evolutionary approach to designing neural networks [AD-A228874] N91-16643
ADAPTIVE CONTROL
Intra-Pulse Frequency Diversity (IPFD) lab demonstration [AD-A228814] N91-16209
ADAPTIVE FILTERS
Programmable surface acoustic wave detection in silicon: Design of programmable filters [ETN-91-98568] N91-16746
ADHESION
Atomic-scale simulation of adhesion between metallic surfaces [DE91-004722] N91-16127
ADIABATIC CONDITIONS
State of an adiabatic expanding and condensing vapor or slow, medium, and fast explosions into a vacuum [DE90-010815] N91-16263
ADRENERGICS
Computer-assisted determination of minimum energy conformations. Part 4: Alpha1 and alpha2 adrenergiic compounds [AD-A226811] N91-16097
ADSORPTION
Fundamental studies of hydrocarbon conversions over supported bimetallic catalysts [DE90-011744] N91-16089
Synthesis, characterization and catalytic activity of microporous aluminophosphate catalysts N91-16092
Solar refrigeration: Evaluation of technical options and design of a solar-generator-adsorber for a novel adsorption refrigerator, volumes 1 and 2 N91-16440
ADVECTION
Synoptic/planetary-scale interactions and blocking over the North Atlantic Ocean N91-16513
The effect of latent heat release on synoptic-to-planetary scale wave interactions and implications for satellite observations: Observational study N91-16515
AERIAL EXPLOSIONS
Infrasonic observations of large-scale HE events N91-16694
AERIAL PHOTOGRAPHY
The usefulness of MSS pictures for mapping and biomass estimation of macro-algae and seaweed in the Eastern Scheldt [BCRS-90-09] N91-16428
AERIAL RECONNAISSANCE
Army Unmanned Aerial Vehicle (UAV) requirements and the joint UAV program [AD-A228149] N91-16009
AEROACOUSTICS
Long-range vertical propagation N91-16693
AERODYNAMIC CHARACTERISTICS
Large-scale numerical aerodynamic simulations for complete aircraft configurations [NAL-TR-1073-T] N91-15984
Optimal trajectories for an aerospace plane. Part 1: Formulation, results, and analysis [NASA-CR-187868] N91-16013
Developmental tests for shuttle Orbiter N91-16038
AERODYNAMIC COEFFICIENTS
Use of the Magnus force in the modified point mass trajectory model [AD-A228194] N91-15990
Calculation of support interferences on the aerodynamic coefficients for a wind tunnel calibration model [DLR-FB-90-26] N91-15998
AERODYNAMIC CONFIGURATIONS
Aerothermodynamic phenomena and the design of atmospheric hypersonic airplanes [MBB/FE122/S/PUB/0408] N91-16015
Hypersonic model configurations [MBB/FE122/S/PUB/411] N91-16016
AERODYNAMIC DRAG
Aerodynamic drag characterization and deposition studies of irregular particles. Part 3: Analysis of flow and temperature field inside the Combustion Deposition Entrained Reactor (CDER) [DE90-000466] N91-16259
AERODYNAMIC HEATING
Numerical simulations of unsteady shock reflection processes by a ramp N91-16267
Finite element thermo-viscoplastic analysis of aerospace structures [NASA-TM-102761] N91-16407
AERODYNAMIC INTERFERENCE
Finite element thermo-viscoplastic analysis of aerospace structures [NASA-TM-102761] N91-16407
AERODYNAMIC LOADS
Aerodynamic surface pressure measurement in atmosphere and wind tunnel on a vertical axis wind turbine blade using pressure transducers N91-15980
A coupled rotor aeroelastic analysis utilizing advanced aerodynamic modeling N91-16006
Finite element thermo-viscoplastic analysis of aerospace structures [NASA-TM-102761] N91-16407
AERODYNAMIC STALLING
A coupled rotor aeroelastic analysis utilizing advanced aerodynamic modeling N91-16006
Numerical simulation of separated flows around a wing section at steady and unsteady motion by a discrete vortex method N91-16268
AERODYNAMICS
Documents on the history of the Aerodynamic Research Establishment at Goettingen, 1907 - 1925 [DLR-MITT-90-05] N91-15977
Aeronautical engineering: A continuing bibliography with indexes (supplement 260) [NASA-SP-7037(260)] N91-15978
Aeronautical engineering: A continuing bibliography with indexes (supplement 259) [NASA-SP-7037(259)] N91-15979
Analytical and experimental investigation of transverse flow aerodynamic windows for high power lasers [DLR-FB-90-33] N91-16367
AEROELASTICITY
A coupled rotor aeroelastic analysis utilizing advanced aerodynamic modeling N91-16006
The integration of structural optimization in the general design process for aircraft [MBB/FE122/S/PUB/0405] N91-16017
Aeroservoelastic tailoring for lateral control enhancement N91-16025
AERONAUTICAL ENGINEERING
Documents on the history of the Aerodynamic Research Establishment at Goettingen, 1907 - 1925 [DLR-MITT-90-05] N91-15977
Aeronautical engineering: A continuing bibliography with indexes (supplement 260) [NASA-SP-7037(260)] N91-15978
Aeronautical engineering: A continuing bibliography with indexes (supplement 259) [NASA-SP-7037(259)] N91-15979
NASA thesaurus aeronautics vocabulary [NASA-TM-104230] N91-16847
AERONAUTICS
NASA thesaurus aeronautics vocabulary [NASA-TM-104230] N91-16847
AEROSOLS
Aerosol Dynamics Laboratory [DE90-010275] N91-16027
The effect of stratification on gravitational coagulation and settling of aerosols [DE90-010153] N91-16079
Fundamental studies with a monodisperse aerosol-based liquid chromatography/mass spectrometry interface (MAGIC-LC/MS) [DE90-010667] N91-16083
Particle deposition in granular media [DE90-010810] N91-16261
Aerosol cloud generation experiments [DE90-011051] N91-16264
Numerical simulation of aerosol scavenging by ice-bearing convective clouds [DE90-010676] N91-16457
Parameterization of aerosol scavenging in a convective cloud model [DE90-010865] N91-16458
AEROSPACE ENGINEERING
JPRS report: Science and technology. USSR: Space [JPRS-USP-89-006] N91-16036
The Proceedings of the Symposium on Mechanics for Space Flight 1989 [ISAS-SP-12] N91-16266
Software for aerospace education: A bibliography, 2nd edition [NASA-PED-106-ED-2] N91-16601
AEROSPACE ENVIRONMENTS
Determination of shuttle orbiter center of gravity from flight measurements [NASA-TM-102627] N91-16058
AEROSPACE INDUSTRY
Impacts of advanced manufacturing technology on parametric estimating [AD-A228232] N91-16177
Technological management as an element of strategy for an efficient company management [MBB-Z-0307-90-PUB] N91-16834
AEROSPACE MEDICINE
The use of contact lenses in the civil airman population [AD-A227450] N91-16544

Aerospace medicine and biology: A cumulative index to a continuing bibliography (supplement 345)
[NASA-SP-7011(345)] N91-16547

AEROSPACE PLANES
Optimal trajectories for an aerospace plane. Part 2: Data, tables, and graphs
[NASA-CR-187848] N91-16011
Optimal trajectories for an aerospace plane. Part 1: Formulation, results, and analysis
[NASA-CR-187868] N91-16013

AEROSPACE SAFETY
Activities report of the Dutch Civil Aeronautics Board
[ETN-91-98472] N91-16005

AEROSPACE SCIENCES
Activities report of the Space Research Organization Netherlands
[ETN-91-98473] N91-16848

AEROSPACE VEHICLES
Intrepid: A mission to Pluto N91-16047

AEROTHERMODYNAMICS
Aerothermodynamic phenomena and the design of atmospheric hypersonic airplanes
[MBB/FE122/S/PUB/0408] N91-16015
Hypersonic model configurations
[MBB/FE122/S/PUB/411] N91-16016
Finite element thermo-viscoplastic analysis of aerospace structures
[NASA-TM-102761] N91-16407

AFRICA
Magsat investigations over the greater African region N91-16415

AGING (MATERIALS)
Thermal aging of cast stainless steels: Mechanisms and predictions
[DE90-010093] N91-16115
Updated evaluation of polymer films for electrical insulation
[DE91-000544] N91-16148

AGING (METALLURGY)
Thermal aging of cast stainless steels: Mechanisms and predictions
[DE90-010093] N91-16115

AGRICULTURE
Evaluation of crop transpiration with remote sensing and computer simulation models
[REPT-1] N91-16431

AIR
Direct methanol/air fuel cells: Systems considerations
[DE90-011971] N91-16439

AIR DEFENSE
Tactical fighter aircraft: Differences between the Air Force's roadmap and the five year defense plan
[AD-A228882] N91-15976

AIR MASSES
A two-dimensional balanced model of internal frontogenesis in geostrophic and isentropic coordinates
[AD-A227644] N91-16518

AIR NAVIGATION
Terrain matching using image sequence analysis N91-16424

AIR POLLUTION
Analysis of atmospheric diffusion of pollutants based on the limited observation of horizontal wind N91-16274
Biomass and hydrocarb technology for removal of atmospheric CO2
[DE90-010016] N91-16453
Ozone and acid-precipitation on western coniferous forests
[DE90-011014] N91-16462

AIR PURIFICATION
Removal of NO and NO2 from contaminated atmospheres
[AD-A227260] N91-16565

AIR QUALITY
Finalization of the international biospheric model validation study
[DE90-011087] N91-16463

AIR SAMPLING
Determination of airborne organics by direct sampling mass spectrometry
[DE90-009422] N91-16452

AIR TRAFFIC
Activities report of the Dutch Civil Aeronautics Board
[ETN-91-98472] N91-16005

AIR TRAFFIC CONTROL
The European flight safety crisis: Costs and solution
[ETN-91-98490] N91-16000
Activities report of the German Federal Institute for Flight Safety
[ETN-91-98644] N91-16002
Activities report of the Dutch Civil Aeronautics Board
[ETN-91-98472] N91-16005
Results of the Kansas City 1989 Terminal Doppler Weather Radar (TDWR) operational evaluation testing
[AD-A228784] N91-16206

AIR WATER INTERACTIONS
Turbulence and diffusion in the atmospheric boundary layer
[DE90-011582] N91-16471
The vertical structure of the marine atmospheric boundary layer across a sea surface temperature front
[AD-A227931] N91-16525
Variability of latent and sensible heat fluxes over the oceans N91-16531

AIRBORNE EQUIPMENT
A paper-assessment of the performance of a modern airborne multi-mode pulse Doppler radar deployed as a ground-based fire-control radar
[ETN-91-98584] N91-16215
Analysis of wind profile measurements from an instrumented aircraft
[NASA-CR-184084] N91-16523

AIRBORNE/SPACEBORNE COMPUTERS
Framework for an efficient two filter GLOC monitor N91-16557
A comparison of computerized measurement of helicopter pilot performance with atropine sulfate during actual and simulated flight N91-16558

AIRCRAFT CONFIGURATIONS
Large-scale numerical aerodynamic simulations for complete aircraft configurations
[NAL-TR-1073-T] N91-15984

AIRCRAFT CONSTRUCTION MATERIALS
TF89 aircraft centre fuselage
[ETN-91-98579] N91-16018
Metallurgical design of novel metal matrix composites for aerospace applications
[ETN-91-98573] N91-16077

AIRCRAFT CONTROL
Aeroservoelastic tailoring for lateral control enhancement N91-16025

AIRCRAFT DESIGN
Aerothermodynamic phenomena and the design of atmospheric hypersonic airplanes
[MBB/FE122/S/PUB/0408] N91-16015
Hypersonic model configurations
[MBB/FE122/S/PUB/411] N91-16016
The integration of structural optimization in the general design process for aircraft
[MBB/FE122/S/PUB/0405] N91-16017
TF89 aircraft centre fuselage
[ETN-91-98579] N91-16018
TF89 tactical fighter outer wing design
[ETN-91-98580] N91-16019

AIRCRAFT NOISE
Fourth International Symposium on Long-Range Sound Propagation
[NASA-CP-3101] N91-16682
Long-range vertical propagation N91-16693

AIRCRAFT PILOTS
The use of contact lenses in the civil airman population
[AD-A227450] N91-16544
Organization of the mission pattern in the air picture
[IZF-1990-A-12] N91-16568

AIRCRAFT STRUCTURES
Tests for integrating measurements of gas pressures in aircraft mechanisms
[ETN-91-98558] N91-16014
Finite element thermo-viscoplastic analysis of aerospace structures
[NASA-TM-102761] N91-16407

AIRFOILS
Computation of turbulent flow about unconventional airfoil shapes N91-15992
Far-field boundaries and their numerical treatment N91-16281
Smoothing and scaling airfoil coordinates on a personal computer
[DE89-000878] N91-16582

AIRPORTS
Evaluation procedure for reinforced concrete box culverts under airfield pavements
[AD-A227920] N91-16031
Results of the Kansas City 1989 Terminal Doppler Weather Radar (TDWR) operational evaluation testing
[AD-A228784] N91-16206

ALANINE
Molecular crystals and localized vibrational states
[DE90-010602] N91-16786

ALBEDO
Modeling laser ignition of explosives and pyrotechnics: Effects and characterization of radiative transfer
[DE90-011052] N91-16161

ALERTNESS
Study of pilot vigilance during long range flight N91-16561

ALGAE
The usefulness of MSS pictures for mapping and biomass estimation of macro-algae and seaweed in the Eastern Scheldt
[BCRS-90-09] N91-16428
Monitoring challenges and innovative ideas
[DE91-000586] N91-16465

ALGEBRA
Solvable two-dimensional supersymmetric models and the supersymmetric Virasoro algebra
[DE90-012140] N91-16648
Some aspects of quantum groups and supergroups
[DE90-777884] N91-16671

ALGORITHMS
A successive partial-relaxation Gaussian algorithm for area navigation operations with the Microwave Landing System (MLS)
[AD-A228871] N91-16004
Optimal trajectories for an aerospace plane. Part 2: Data, tables, and graphs
[NASA-CR-187848] N91-16011
Numerical modeling tools for transient electromagnetic problems
[DE90-010328] N91-16180
Modeling pulse driven antenna systems with finite differences
[DE90-010682] N91-16182
Shift-invariant image reconstruction of speckle-degraded images using bispectrum estimation
[AD-A227728] N91-16188
Statistically thinned arrays with quantized element weights
[AD-A227965] N91-16196
An algorithm for using a slide-screw tuner as a computer-controlled impedance
[DE90-010657] N91-16226
The use of window functions and Kalman filtering in spectral estimation
[AD-A227482] N91-16236
Incompressible flow simulations using the velocity-pressure formulation N91-16299
Acceleration of iterative algorithms for Euler and Navier-Stokes equations N91-16301
Simulation of the flow past an impulsively started cylinder using a discrete vortex method N91-16303
Research on certain aspects of laser diffraction particle size analysis relevant to autonomous self-diagnosing instrumentation
[AD-A226822] N91-16354
Real-time vergence control for binocular robots
[AD-A228817] N91-16387
A modular stiffness-based approach to rotating systems analysis N91-16400
Terrain matching using image sequence analysis N91-16424
The usefulness of MSS pictures for mapping and biomass estimation of macro-algae and seaweed in the Eastern Scheldt
[BCRS-90-09] N91-16428
Effects of switch leakages upon Nimbus-7 SMMR calibration
[NASA-TM-100705] N91-16536
Framework for an efficient two filter GLOC monitor N91-16557
Development of a test-bed for real-time monitoring of pilot mental status N91-16563
A block QR factorization algorithm for rank-deficient matrices
[DE90-010066] N91-16573
Automatic, high-resolution analysis of low-noise fringes
[DE90-009779] N91-16574
Implementation of the phase gradient algorithm
[DE90-012160] N91-16579
Smoothing and scaling airfoil coordinates on a personal computer
[DE89-000878] N91-16582
Implementing sporadic servers in Ada
[AD-A226723] N91-16584
Real-time filtering and detection of dynamics for compression of HDTV
[NASA-CR-187777] N91-16596
Column reduction of polynomial matrices: An iterative algorithm
[MEMO-COSOR-89-30] N91-16598
Distributed algorithm simulation using input/output automata
[AD-A228113] N91-16611
Implementation and experimentation with motion planning algorithms
[AD-A228278] N91-16612
Alopex optimization algorithm
[AD-A228442] N91-16615
An O(log n) time common CRCW pram algorithm for minimum spanning tree
[AD-A228740] N91-16623

Matrix algorithms in signal processing
[AD-A228851] N91-16625
Linear-time separation algorithms for the three-index assignment polytope
[AD-A228854] N91-16626
Vectorial and parallel algorithms in dynamic programming for optimal control problems
[LAAS-90256] N91-16629
THERMOPT: An optimizer for ESATAN models
[MBB/FW522/S/PUB/427] N91-16630
Artificial intelligence technologies applied to terrain analysis
[DE90-011985] N91-16642
An evolutionary approach to designing neural networks
[AD-A228874] N91-16643
Linear algebra for dense matrices on a hypercube
[DE90-010533] N91-16647
Sparse representation of smooth linear operators
[AD-A228142] N91-16660
Mathematical methods and algorithms for real-time applications
[AD-A228889] N91-16663
Computational physics at the National Energy Research Supercomputer Center
[DE90-010283] N91-16672
New correction procedures for the fast field program which extend its range N91-16699
Field measurement of head related transfer functions
[AD-A227850] N91-16708
A search for good lattice rules based on the reciprocal lattice generator matrix
[DE91-004425] N91-16809
The StarLite project
[AD-A226722] N91-16837
Phased array imaging
[AD-A228774] N91-16855

ALIGNMENT
Self-propelled in-tube shuttle and control system for automated measurements of magnetic field alignment
[DE90-008210] N91-16316
Dynamical theory of dense groups of galaxies N91-16943
Explaining compact groups as change alignments N91-16944
Dynamics and configurations of galaxy triplets N91-16946

ALKANES
Auto-ignition temperatures of binary mixtures of alkanes in a closed vessel: Comparisons between experimental measurements and numerical predictions
[DE90-007856] N91-16082

ALLOYS
Bibliography of the technical literature of the Materials Joining Group, Metals and Ceramics Division, 1951--June 1989
[DE91-000530] N91-16126

ALPHA PARTICLES
Development of liquid xenon imaging gamma-ray spectrophotometers
[AD-A227575] N91-16740

ALPHANUMERIC CHARACTERS
Displaying alphanumeric characters on pixel-planes 5
[AD-A228616] N91-16622

ALUMINIDES
Weldability of nickel aluminides
[DE90-008557] N91-16116
Influence of strain rate on the structure/property of Ti-48Al-1V
[DE91-000172] N91-16122
Elevated temperature crack growth in titanium aluminides
[AD-A227700] N91-16125

ALUMINUM
Synthesis, characterization and catalytic activity of microporous aluminophosphate catalysts N91-16092
Ion beam modification of surface for improved high temperature performance
[AD-A228067] N91-16243
Direct disc impact investigation of dynamic large finite plastic behavior of 1100 aluminum N91-16404

ALUMINUM ALLOYS
Characterization of the corrosion of a P-130x graphite fiber reinforced 6063 aluminum metal matrix composite
[AD-A228134] N91-16071
Mechanical property data on aluminum alloy 7150-T7751 plate
[AD-A227506] N91-16124
The influence of small SO2 contents on the corrosion behavior for NiCrAl alloys in temperature zone from 1000 to 1100 C
[JUEL-2362] N91-16134
Grain-boundary structure in ordered alloys
[ETN-91-98571] N91-16136

ALUMINUM GALLIUM ARSENIDES
Threshold voltage and I-V characteristics of AlGaAs/GaAs MODFETs
[AD-A228844] N91-16248
Two-dimensional simulation of quantum-well lasers including energy transport
[AD-A227487] N91-16356
Integrated semiconductor modulators
[AD-A228615] N91-16820

ALUMINUM OXIDES
Gelcasting of sub-micron alumina, sialon, and silicon nitride powders
[DE91-000618] N91-16145
Domain boundaries formed during epitactical growth of alpha-Al2O3
[DE91-005018] N91-16814

AMMONIUM PERCHLORATES
Space Shuttle Flight Support Motor no. 1 (FSM-1)
[NASA-CR-184078] N91-16064

AMMONIUM SULFATES
Control of industrial crystallizers: The physical aspects
[ETN-91-98488] N91-16179

AMMUNITION
Use of the Magnus force in the modified point mass trajectory model
[AD-A228194] N91-15990

AMORPHOUS MATERIALS
Fatigue of amorphous polymers
[ISBN-90-9003520-6] N91-16157
Correlation between the elastic-shear-instability-mechanism and empirical criteria for irradiation-induced amorphization
[DE91-004481] N91-16810
Domain boundaries formed during epitactical growth of alpha-Al2O3
[DE91-005018] N91-16814

AMPLITUDE MODULATION
Nonlinear optical systems interacting with amplitude-modulated optical fields
[AD-A228221] N91-16742

ANALOG TO DIGITAL CONVERTERS
Time interpolator
[DIGEL-1990-3] N91-16337

ANALOGIES
Extension of transonic flow computational concepts in the analysis of cavitated bearings
[NASA-TM-103214] N91-16304

ANALOGS
Electronic analogue for a biological nose
[ME-78] N91-16541

ANALYZERS
Surface analysis by low-energy ion scattering: Two-dimensional detection and quantification
[ETN-91-98474] N91-16133

ANALYZING
Analytical and experimental investigation of transverse flow aerodynamic windows for high power lasers
[DLR-FB-90-33] N91-16367

ANGLES (GEOMETRY)
Effect of inclination angle on heat transfer characteristics of closed two-phase thermosyphon N91-16278

ANGULAR DISTRIBUTION
A statistical survey of electron pitch angle distributions in the nightside central plasma sheet
[AD-A227763] N91-16486

ANGULAR MOMENTUM
Alignment of cD-galaxies with their surroundings N91-16895
Energy and angular momentum transfer in binary galaxies N91-16940

ANIMALS
Research pathology and special techniques
[NASA-CR-187828] N91-16639

ANIONS
Measurements of scattering processes in negative ion-atom collisions
[DE90-010666] N91-16715

ANISOTROPY
The stationary exterior three dimensional Navier-Stokes problem of viscous flow past a body in anisotropically weighted Sobolev spaces
[REPT-110] N91-16314

ANNEALING
Comparative study of phosphosilicate glass on (100) silicon by furnace and rapid isothermal annealing
[NIAR-90-26] N91-16153
Ion beam modification of surface for improved high temperature performance
[AD-A228067] N91-16243
Thermal emission model for the anneal of radiation-induced trapped holes
[DE90-007285] N91-16718
Characterization of chemically prepared PZT thin films
[DE90-010831] N91-16789

ANNIHILATION REACTIONS
Research in theoretical nuclear physics
[DE90-010792] N91-16828

ANNUAL VARIATIONS
Variability of latent and sensible heat fluxes over the oceans N91-16531
The correction of infrasound signals for upper atmospheric winds N91-16695

ANODES
Electrocatalysis of anodic and cathodic oxygen-transfer reactions
[DE91-000611] N91-16100

ANODIC COATINGS
Studies of the fundamentals of solids state batteries
[AD-A228772] N91-16247

ANOMALIES
Seismic structure of the upper mantle under the Pacific Ocean N91-16492
Computer simulations of medium wavelength irregularities in the equatorial ionosphere resulting from artificially produced density enhancements
[MPE-PREPRINT-186] N91-16496
Variability of latent and sensible heat fluxes over the oceans N91-16531
An experimental study of counter-rotating cores in elliptical galaxies N91-16934

ANTENNA ARRAYS
Statistically thinned arrays with quantized element weights
[AD-A227965] N91-16196
Electronically steerable arrays: Current and future technology and applications
[ETN-91-98581] N91-16254
A Mirnov loop array for field-reversed configurations
[DE90-010607] N91-16750

ANTENNA DESIGN
Modeling pulse driven antenna systems with finite differences
[DE90-010682] N91-16182

ANTENNA RADIATION PATTERNS
Modeling pulse driven antenna systems with finite differences
[DE90-010682] N91-16182
Tactical HF field expedient antenna performance, volume 1
[AD-A228057] N91-16198

ANTIBODIES
Research pathology and special techniques
[NASA-CR-187828] N91-16639

ANTIFERROMAGNETISM
Dynamics of strong-coupling models for cuprate superconductors: Exact results on finite lattices
[DE90-011155] N91-16796
Epitaxial growth and surface morphology of some metal and semiconductor structures N91-16824

ANTIMONY
New surface atomic structures for III-V(110)-p(1 x 1)-Sb(1ML): Chemical bonding and electronic structure
[DE90-011230] N91-16794

ANTIREFLECTION COATINGS
High efficiency silicon concentrator solar cells N91-16441

APERTURES
Statistically thinned arrays with quantized element weights
[AD-A227965] N91-16196
Gabor zone plate apertures for imaging with the mercuric iodide gamma ray camera
[DE90-011193] N91-16321
Low-cost, high-resolution telescopes for imaging low-earth orbit satellites
[DE90-012081] N91-16850

APPLICATIONS PROGRAMS (COMPUTERS)
Evaluation of rotorwash characteristics for tiltrotor and tiltwing aircraft in hovering flight
[SCT-90RR-18] N91-15989
Integrated Refractive Effects Prediction System (IREPS) user's manual, revision PC-2.0
[AD-A228549] N91-16203
X-Ray Detector: An x-ray radiation detector design code
[DE90-008235] N91-16317
Probabilistic fracture mechanics: A validation of predictive capability
[AD-A228877] N91-16409
ANEOS: Analytic equations of state for shock physics codes input manual
[DE90-010198] N91-16575
Using MAPLE for symbolic computations in robotics
[DE90-010405] N91-16576
Distributed issues for Ada real-time systems
[AD-A227852] N91-16603
Massively parallel Fokker-Planck calculations
[DE90-010691] N91-16633

Computational physics at the National Energy Research Supercomputer Center
[DE90-010283] N91-16672
SCATSPHERE2: A computation for the plane-wave scattering from a submerged, elastic, spherical, evacuated or fluid-filled, thin shell
[AD-A228867] N91-16709

APPROXIMATION
Finite element approximations for transonic flows
[ETN-91-98491] N91-15988
Analysis and application of the discrete vortex method N91-16290
Limit behaviors of approximate solutions to conservation laws
[DE90-010069] N91-16646
Mathematical methods and algorithms for real-time applications
[AD-A228889] N91-16663
Wave propagation through random media: A local method of small perturbations based on the Helmholtz equation N91-16701
A dynamical proximity analysis of interacting galaxy pairs N91-16937

ARC SPRAYING
Tensile behavior of tungsten/niobium composites at 1300 to 1600 K
[NASA-TM-103727] N91-16128

ARCHITECTURE (COMPUTERS)
NASA Laboratory telerobotic manipulator control system architecture
[NASA-CR-187751] N91-16385
Living PRAs (Probabilistic Risk Analysis) made easier with IRRAS (Integrated Reliability and Risk Analysis System)
[DE90-010938] N91-16395
Research in optical symbolic tasks
[AD-A228797] N91-16551
Microsupercomputers: Design and implementation
[AD-A228741] N91-16571
Microsupercomputers: Design and implementation
[AD-A228744] N91-16572
POSC: A Partitioning and Optimizing SISAL Compiler
[DE90-010679] N91-16577
A graphical user-interface-driven waveform data acquisition and analysis system
[DE90-011948] N91-16578
Displaying alphanumeric characters on pixel-planes 5
[AD-A228616] N91-16622
Supporting reuse and evolution in software design
[AD-A228782] N91-16624
Vectorial and parallel algorithms in dynamic programming for optimal control problems
[LAAS-90256] N91-16629
Low-level image processing architectures compared for some non-linear recursive neighborhood operations
[ISBN-90-9003713-6] N91-16631
Wakefield calculations on parallel computers
[DE90-009712] N91-16632
Parallel Access Main Memory (PAMM) user's manual, version 1.0
[AD-A227744] N91-16635
Pi: A parallel architecture interface for multi-model execution
[AD-A228345] N91-16640

AREA NAVIGATION
A successive partial-relaxation Gaussian algorithm for area navigation operations with the Microwave Landing System (MLS)
[AD-A228871] N91-16004

ARTHROPODS
Kinematics of arthropod legs: Modeling and measurement N91-16391

ARTIFICIAL INTELLIGENCE
Experimentation and concept formation by an autonomous mobile robot
[DE90-003063] N91-16368
Haptic perception with an articulated, sensate robot hand
[DE90-010195] N91-16371
Safety Network to Detect Performance Degradation and Pilot Incapacitation
[AGARD-CP-490] N91-16553
Current status of an artificial intelligence-based loss of consciousness monitoring system for advanced fighter aircraft N91-16556
Intelligent assistant systems: An artificial intelligence approach to detecting performance degradation and pilot incapacitation N91-16564
Skolem functions and equality in automated deduction
[DE90-009703] N91-16641
Artificial intelligence technologies applied to terrain analysis
[DE90-011985] N91-16642
Implementation and simulation of the manufacturing systems control coordination level: A mixed approach of Petri nets and rule-based systems
[LAAS-90355] N91-16645

ARTIFICIAL SATELLITES
Magnetic-field shielding of satellites from high-energy-electron environments
[DE90-010296] N91-16043
Software for aerospace education: A bibliography, 2nd edition
[NASA-PED-106-ED-2] N91-16601

ARTILLERY
Use of the Magnus force in the modified point mass trajectory model
[AD-A228194] N91-15990

ASTROMETRY
Space research in the Federal Republic of Germany, 1988 and 1989
[ETN-91-98514] N91-16849

ASTRONOMICAL CATALOGS
Quantifying the FIR interaction enhancement in paired galaxies N91-16900

ASTRONOMICAL MODELS
Using tilted-ring models and numerical hydrodynamics to study the structure, kinematics and dynamics of HI disks in galaxies N91-16851
Numerical simulations of interacting disk galaxies N91-16955
Dynamical experiments on models of colliding disk galaxies N91-16959
Do elliptical galaxies have thick disks N91-16962
Positron survival in Type II supernovae
[AD-A226778] N91-16965
The best-fit universe
[DE91-004583] N91-16966
Formation and development of elliptical and dwarf galaxies
[ETN-91-98492] N91-16967
Origin of regularities in the redshift distributions of distant galaxies and quasars
[DE91-004848] N91-16968
Spectrometric, chemical, and cosmological development of galaxies
[ETN-91-98555] N91-16972

ASTRONOMICAL PHOTOGRAPHY
An atlas of mixed-morphology pairs N91-16866

ASTRONOMICAL SPECTROSCOPY
The design and construction of an Automated Multi-Object Spectroscopy system (AMOS)
[DE90-011497] N91-16088

ASTRONOMY
Software for aerospace education: A bibliography, 2nd edition
[NASA-PED-106-ED-2] N91-16601
Fiber optic synthetic aperture interferometer
[AD-A227891] N91-16741
Activities report of the Space Research Organization Netherlands
[ETN-91-98473] N91-16848
Paired and Interacting Galaxies: International Astronomical Union Colloquium No. 124
[NASA-CP-3098] N91-16858

ASTROPHYSICS
Stellar convection and dynamo theory N91-16857

ASYMMETRY
Stellar convection and dynamo theory N91-16857

ASYMPTOTIC METHODS
Asymptotic-induced numerical methods for conservation laws
[NASA-CR-187483] N91-16305
Adaptive bandwidth choice for kernel regression
[AD-A228437] N91-16661
The asymptotic validity of sequential stopping rules for stochastic simulations
[AD-A228896] N91-16668

ASYMPTOTIC SERIES
High frequency scattering by a smooth coated cylinder simulated with generalized impedance boundary conditions
[NASA-CR-187829] N91-16211
Dynamic crack propagation in elastic-plastic solids N91-16402
Experiments with initial transient deletion for parallel, replicated steady-state simulations
[AD-A227879] N91-16636

ATLANTIC OCEAN
Synoptic/planetary-scale interactions and blocking over the North Atlantic Ocean N91-16513
Formic and acetic acids in the boundary layer over the North Atlantic ocean N91-16530
Bio-optical profile data report coastal transition zone program, R/V Thomas Washington, June 24 - July 21, 1988
[NASA-CR-187808] N91-16532
Bio-optical profile data report coastal transition zone program, R/V Point Sur, June 15-28, 1987
[NASA-CR-187807] N91-16533

ATMOSPHERIC ATTENUATION
ADRPM-VII applied to the long-range acoustic detection problem N91-16689

ATMOSPHERIC BOUNDARY LAYER
Turbulence and diffusion in the atmospheric boundary layer
[DE90-011582] N91-16471
Stability criteria for stratocumulus-topped boundary layers evaluated through conditional sampling of turbulence elements
[AD-A228433] N91-16526
Formic and acetic acids in the boundary layer over the North Atlantic ocean N91-16530

ATMOSPHERIC CHEMISTRY
The atmospheric effects of stratospheric aircraft: A current consensus
[NASA-RP-1251] N91-16467

ATMOSPHERIC CIRCULATION
Analysis of atmospheric diffusion of pollutants based on the limited observation of horizontal wind N91-16274
Study of the global distributions of atmospheric radionuclides
[DE90-010749] N91-16455
A comparison of optically measured and radar-derived horizontal neutral winds
[AD-A227690] N91-16483
On the developmental dynamics of sudden stratospheric warmings
[AD-A227731] N91-16485
GCM (General Circulation Model) predictions for surface air temperature and precipitation over the southeastern United States
[DE90-009434] N91-16497
Numerical simulations of the mountain iron tracer data
[DE90-009749] N91-16499
NASA/MSFC FY90 Global Scale Atmospheric Processes Research Program Review
[NASA-CP-3093] N91-16500
South Pacific convergence zone and global-scale circulations N91-16503
Stratiform clouds and their interaction with atmospheric motion N91-16506
A comparison of diagnostic and kinematic vertical motion fields associated with curved and straight jet streak adjustment processes
[AD-A227724] N91-16522
Variability of latent and sensible heat fluxes over the oceans N91-16531
The correction of infrasound signals for upper atmospheric winds N91-16695
Fiber optic synthetic aperture interferometer
[AD-A227891] N91-16741

ATMOSPHERIC COMPOSITION
Analysis of atmospheric diffusion of pollutants based on the limited observation of horizontal wind N91-16274
Solving global environmental problems through technological innovation
[DE90-010018] N91-16446
Biomass and hydrocarb technology for removal of atmospheric CO2
[DE90-010016] N91-16453
Study of the global distributions of atmospheric radionuclides
[DE90-010749] N91-16455
Multi-dimensional aspects of recent climate change in North America
[DE90-010958] N91-16460
The atmospheric effects of stratospheric aircraft: A topical review
[NASA-RP-1250] N91-16466
Use of satellite data and modeling to assess the influence of stratospheric processes on the troposphere N91-16517
Formic and acetic acids in the boundary layer over the North Atlantic ocean N91-16530
Removal of NO and NO2 from contaminated atmospheres
[AD-A227260] N91-16585

ATMOSPHERIC CORRECTION
Ionospheric corrections for SHF satellite radar altimetry N91-16423

ATMOSPHERIC DENSITY
Joint US Navy/US Air Force climatic study of the upper atmosphere. Volume 1: January
[AD-A227122] N91-16476
Joint US Navy/US Air Force climatic study of the upper atmosphere. Volume 2: February
[AD-A227123] N91-16477
Joint US Navy/US Air Force climatic study of the upper atmosphere. Volume 3: March
[AD-A227124] N91-16478

Joint US Navy/US Air Force climatic study of the upper atmosphere. Volume 4: April
[AD-A227125] N91-16479
Joint US Navy/US Air Force climatic study of the upper atmosphere. Volume 7: July
[AD-A227126] N91-16480
Joint US Navy/US Air Force climatic study of the upper atmosphere. Volume 10: October
[AD-A227127] N91-16481
A comparison of optically measured and radar-derived horizontal neutral winds
[AD-A227690] N91-16483

ATMOSPHERIC DIFFUSION

The Proceedings of the Symposium on Mechanics for Space Flight 1989
[ISAS-SP-12] N91-16266
Analysis of atmospheric diffusion of pollutants based on the limited observation of horizontal wind
N91-16274
Numerical simulations of the mountain iron tracer data
[DE90-009749] N91-16499

ATMOSPHERIC EFFECTS

Integrated Refractive Effects Prediction System (IREPS) user's manual, revision PC-2.0
[AD-A228549] N91-16203
The atmospheric effects of stratospheric aircraft: A topical review
[NASA-RP-1250] N91-16466
The atmospheric effects of stratospheric aircraft: A current consensus
[NASA-RP-1251] N91-16467

ATMOSPHERIC GENERAL CIRCULATION MODELS

Climate Caucus report: Opportunities for bridging the gaps from effects to impacts
[DE90-010877] N91-16459
GCM (General Circulation Model) predictions for surface air temperature and precipitation over the southeastern United States
[DE90-009434] N91-16497
Nonlinear dynamics of global atmospheric and Earth-system processes N91-16510

ATMOSPHERIC HEATING

Derivation of exospheric temperature at high latitudes from incoherent-scatter radar data
[AD-A227721] N91-16484
On the developmental dynamics of sudden stratospheric warmings
[AD-A227731] N91-16485
South Pacific convergence zone and global-scale circulations N91-16503
Planetary circulations in the presence of transient and self-induced heating N91-16505
Global-scale, intraseasonal fluctuations of diabatic forcing of the atmosphere N91-16508

ATMOSPHERIC IONIZATION

The role of the equatorial electrojet in the evening ionosphere
[MPE-PREPRINT-184] N91-16494
Theory for modeling the equatorial evening ionosphere and the origin of the shear in the horizontal plasma flow
[MPE-PREPRINT-185] N91-16495

ATMOSPHERIC MODELS

Electron density comparisons between radar observations and 3-D ionospheric model calculations
[AD-A227703] N91-16187
Analysis of atmospheric diffusion of pollutants based on the limited observation of horizontal wind
N91-16274
Carbon dioxide and energy exchanges in a temperate grassland ecosystem N91-16419
Investigation of a remote sensing technique for droplet effective radius N91-16420
Study of the global distributions of atmospheric radionuclides
[DE90-010749] N91-16455
Parameterization of aerosol scavenging in a convective cloud model
[DE90-010865] N91-16458
Multi-dimensional aspects of recent climate change in North America
[DE90-010958] N91-16460
Finalization of the international biospheric model validation study
[DE90-011087] N91-16463
The atmospheric effects of stratospheric aircraft: A current consensus
[NASA-RP-1251] N91-16467
Upper atmosphere IR radiation modeling and analysis
[AD-A227214] N91-16482
On the developmental dynamics of sudden stratospheric warmings
[AD-A227731] N91-16485
A study of the interaction of physical and numerical parameterizations with regard to moisture forecasting in a regional model of the atmosphere
[AD-A227966] N91-16488
Theory for modeling the equatorial evening ionosphere and the origin of the shear in the horizontal plasma flow
[MPE-PREPRINT-185] N91-16495
The value of on-site sodar data in regional modeling
[DE90-009921] N91-16498
Numerical simulations of the mountain iron tracer data
[DE90-009749] N91-16499
NASA/MSFC FY90 Global Scale Atmospheric Processes Research Program Review
[NASA-CP-3093] N91-16500
South Pacific convergence zone and global-scale circulations N91-16503
Planetary circulations in the presence of transient and self-induced heating N91-16505
Stratiform clouds and their interaction with atmospheric motion N91-16506
A two-dimensional balanced model of internal frontogenesis in geostrophic and isentropic coordinates
[AD-A227644] N91-16518
A comparison of diagnostic and kinematic vertical motion fields associated with curved and straight jet streak adjustment processes
[AD-A227724] N91-16522

ATMOSPHERIC MOISTURE

A study of the interaction of physical and numerical parameterizations with regard to moisture forecasting in a regional model of the atmosphere
[AD-A227966] N91-16488
Observation simulation experiments with regional prediction models N91-16502
South Pacific convergence zone and global-scale circulations N91-16503
Global variability of water vapor and condensate from SSM/I N91-16507
Tropical Pacific moisture variability N91-16509
Contents of the NASA ocean data system archive, version 11-90
[NASA-CR-187812] N91-16535

ATMOSPHERIC PHYSICS

NASA/MSFC FY90 Global Scale Atmospheric Processes Research Program Review
[NASA-CP-3093] N91-16500
Comparison of SSM/I measurements to numerically-simulated cloud and precipitation during ERICA N91-16501
Nonlinear dynamics of global atmospheric and Earth-system processes N91-16510

ATMOSPHERIC PRESSURE

Joint US Navy/US Air Force climatic study of the upper atmosphere. Volume 1: January
[AD-A227122] N91-16476
Joint US Navy/US Air Force climatic study of the upper atmosphere. Volume 2: February
[AD-A227123] N91-16477
Joint US Navy/US Air Force climatic study of the upper atmosphere. Volume 3: March
[AD-A227124] N91-16478
Joint US Navy/US Air Force climatic study of the upper atmosphere. Volume 4: April
[AD-A227125] N91-16479
Joint US Navy/US Air Force climatic study of the upper atmosphere. Volume 7: July
[AD-A227126] N91-16480
Joint US Navy/US Air Force climatic study of the upper atmosphere. Volume 10: October
[AD-A227127] N91-16481
An investigation of a gravity wave during GALE: February 6, 1986
[AD-A227655] N91-16519

ATMOSPHERIC REFRACTION

Integrated Refractive Effects Prediction System (IREPS) user's manual, revision PC-2.0
[AD-A228549] N91-16203
ADRPM-VII applied to the long-range acoustic detection problem N91-16689

ATMOSPHERIC SCATTERING

Investigation of a remote sensing technique for droplet effective radius N91-16420
Long-range sound propagation: A review of some experimental data N91-16683
Distorted-wave born approximation calculations for turbulence scattering in an upward-refracting atmosphere N91-16700

ATMOSPHERIC SOUNDING

Definition and preliminary design of the Laser Atmospheric Wind Sounder (LAWS) phase 1. Volume 1: Executive summary
[NASA-CR-184071] N91-16332
Definition and preliminary design of the Laser Atmospheric Wind Sounder (LAWS) phase 1. Volume 2
[NASA-CR-184072] N91-16333
Definition and preliminary design of the Laser Atmospheric Wind Sounder (LAWS) phase 1. Volume 3: Program cost estimates
[NASA-CR-184073] N91-16334
NASA/MSFC FY90 Global Scale Atmospheric Processes Research Program Review
[NASA-CP-3093] N91-16500
Observation simulation experiments with regional prediction models N91-16502

ATMOSPHERIC TEMPERATURE

Joint US Navy/US Air Force climatic study of the upper atmosphere. Volume 1: January
[AD-A227122] N91-16476
Joint US Navy/US Air Force climatic study of the upper atmosphere. Volume 2: February
[AD-A227123] N91-16477
Joint US Navy/US Air Force climatic study of the upper atmosphere. Volume 3: March
[AD-A227124] N91-16478
Joint US Navy/US Air Force climatic study of the upper atmosphere. Volume 4: April
[AD-A227125] N91-16479
Joint US Navy/US Air Force climatic study of the upper atmosphere. Volume 7: July
[AD-A227126] N91-16480
Joint US Navy/US Air Force climatic study of the upper atmosphere. Volume 10: October
[AD-A227127] N91-16481
Derivation of exospheric temperature at high latitudes from incoherent-scatter radar data
[AD-A227721] N91-16484
GCM (General Circulation Model) predictions for surface air temperature and precipitation over the southeastern United States
[DE90-009434] N91-16497
Use of satellite data and modeling to assess the influence of stratospheric processes on the troposphere N91-16517
Meteorological effects on long-range outdoor sound propagation N91-16696
Effect of wind and temperature gradients on received acoustic energy N91-16697

ATMOSPHERIC TURBULENCE

Turbulence and diffusion in the atmospheric boundary layer
[DE90-011582] N91-16471
Comparison of FFP predictions with measurements of a low-frequency signal propagated in the atmosphere N91-16698
Distorted-wave born approximation calculations for turbulence scattering in an upward-refracting atmosphere N91-16700
Wave propagation through random media: A local method of small perturbations based on the Helmholtz equation N91-16701
Scattering of sound by atmospheric turbulence predictions in a refractive shadow zone N91-16703
Effects of large-scale wind driven turbulence on sound propagation N91-16704

ATOMIC BEAMS

Technique for determining the static polarizabilities of refractory metal atoms
[DE90-017088] N91-16724

ATOMIC CLOCKS

Effects of neutron fluence on the operating characteristics of diode lasers used in atomic frequency standards
[AD-A226763] N91-16352
Optimization of hydrogen consumption in hydrogen masers
[AD-A227267] N91-16355

ATOMIC COLLISIONS

Spontaneous force optical traps
[AD-A228539] N91-16363
Upper atmosphere IR radiation modeling and analysis
[AD-A227214] N91-16482
A comparison of optically measured and radar-derived horizontal neutral winds
[AD-A227690] N91-16483
State-to-state inelastic and reactive molecular beam scattering from surfaces
[DE90-010492] N91-16714
Measurements of scattering processes in negative ion-atom collisions
[DE90-010668] N91-16715

ATOMIC ENERGY LEVELS

Comparison of the quadratic configuration interaction and coupled cluster approaches to electron correlation including the effect of triple excitations
[NASA-CR-187855] N91-16727
Triple and quadruple excitation contributions to the binding in Be clusters: Calibration calculations on Be3
[NASA-TM-103391] N91-16728

ATOMIC EXCITATIONS

A tunable x ray microprobe using synchrotron radiation
[DE90-011219] N91-16322

ATOMIC PHYSICS
Technique for determining the static polarizabilities of refractory metal atoms
[DE90-017088] N91-16724
ATOMIC STRUCTURE
In situ studies of potential dependent structural and distributional changes at electrochemical interfaces with x rays
[AD-A226844] N91-16098
High resolution electron microscopy of interfaces in fcc materials
[DE91-004420] N91-16101
High resolution photoelectron spectroscopy of metal clusters and high temperature species
[DE90-011598] N91-16119
Atomic and electronic structure of metals and alloys: Clean surfaces and chemisorbed molecules
[DE91-000267] N91-16123
On the development of in-situ Raman analysis of plasma deposited diamond
[AD-A227453] N91-16147
Optimization of hydrogen consumption in hydrogen masers
[AD-A227267] N91-16355
Linear algebra for dense matrices on a hypercube
[DE90-010533] N91-16647
A new approach for the determination of electronic structure
[DE90-010479] N91-16713
Theoretical studies of atomic transitions
[DE91-000931] N91-16723
Theory of non-equilibrium growth
[DE91-004159] N91-16725
Comparison of the quadratic configuration interaction and coupled cluster approaches to electron correlation including the effect of triple excitations
[NASA-CR-187855] N91-16727
New surface atomic structures for III-V(110)-p(1 x 1)-Sb(1ML): Chemical bonding and electronic structure
[DE90-011230] N91-16794
Photoreflectance studies of electronic transitions in quantum well structures under high pressure
[DE90-011583] N91-16801
Thin film single crystal growth of a nonlinear optical polymer
[AD-A227692] N91-16807
ATOMS
Picosecond multiphoton ionization of atomic and molecular clusters
[DE91-000641] N91-16096
ATROPINE
A comparison of computerized measurement of helicopter pilot performance with atropine sulfate during actual and simulated flight N91-16558
AUDITORY SIGNALS
Field measurement of head related transfer functions
[AD-A227850] N91-16708
AURORAS
A statistical survey of electron pitch angle distributions in the nightside central plasma sheet
[AD-A227763] N91-16486
AUSTENITIC STAINLESS STEELS
HAZ liquation cracking behavior in newly developed lean 316 stainless steels
[DE90-009409] N91-16117
Modeling and identification of cumulative creep fatigue damage in an austenitic stainless steel N91-16131
AUTOCORRELATION
Interferometric second-harmonic-generation autocorrelator for characterizing femtosecond pulses
[DE90-010331] N91-16345
AUTOIONIZATION
The theory of electron-ion collisions: The role of doubly excited states
[DE90-011078] N91-16721
AUTOMATA THEORY
Distributed algorithm simulation using input/output automata
[AD-A228113] N91-16611
Skolem functions and equality in automated deduction
[DE90-009703] N91-16641
AUTOMATIC CONTROL
Developmental tests for shuttle Orbiter N91-16038
Sensor-based automated docking of large payloads
[DE90-011020] N91-16044
Self-propelled in-tube shuttle and control system for automated measurements of magnetic field alignment
[DE90-008210] N91-16316
Ultrasound and visual sensor feedback and fusion
[DE90-005280] N91-16369
Implementation and experimentation with motion planning algorithms
[AD-A228276] N91-16612
AUTOMATIC PILOTS
General designer describes Buran flight control, autopilot systems N91-16039
AUTOMATIC TEST EQUIPMENT
Automatic, high-resolution analysis of low-noise fringes
[DE90-009779] N91-16574
AUTOMOBILE FUELS
Requirements for a fuel cell for transportation application
[DE90-011146] N91-16230
A summary of prospects for methanol vehicles in the United States
[DE90-009719] N91-16370
Greenhouse gas emissions from selected alternative transportation fuels market niches
[DE90-010491] N91-16448
AUTOMOBILES
A summary of prospects for methanol vehicles in the United States
[DE90-009719] N91-16370
AUTONOMY
Experimentation and concept formation by an autonomous mobile robot
[DE90-003063] N91-16368
AVALANCHE DIODES
Design and fabrication of high voltage planar devices
[LAAS-90306] N91-16252
AVIONICS
A successive partial-relaxation Gaussian algorithm for area navigation operations with the Microwave Landing System (MLS)
[AD-A228871] N91-16004
AXIAL LOADS
Plate and butt-weld stresses beyond elastic limit, material and structural modeling
[NASA-TP-3075] N91-16413

B

B STARS
A non-LTE analysis of a sample of O stars selected from galactic OB associations N91-16854
Galactic structure in direction of Vela-Puppis by means of UBV beta observations
[ETN-91-98556] N91-16973
BABOONS
Investigation of effects of 60-Hz electric and magnetic fields on operant and social behavior and on the neuroendocrine system of nonhuman primates
[DE90-010809] N91-16537
BACKGROUND RADIATION
Dragging force on galaxies due to streaming dark matter N91-16947
BACKSCATTERING
Scattering and depolarization by rough terrain and sea: A unified full wave approach
[AD-A228295] N91-16201
Stochastic and chaotic effects in the ring laser N91-16359
BACKWARD FACING STEPS
Autoignition and flameholding in a cylindrical scramjet combustor
[NAL-TR-1067] N91-16102
BACTERIA
Conversion of acetic acid to methane by thermophiles
[DE90-010993] N91-16086
BALANCE
A study of the surface energy balance on slopes in a tallgrass prairie
[NASA-CR-187698] N91-16473
BALL BEARINGS
Wear measurement of ceramic bearings in gas turbines
[AD-A227505] N91-16382
BALLISTICS
Buran and the future of the Soviet space program N91-16037
BALLOON-BORNE INSTRUMENTS
Analysis of wind profile measurements from an instrumented aircraft
[NASA-CR-184084] N91-16523
BANDWIDTH
Stochastic and chaotic effects in the ring laser N91-16359
Adaptive bandwidth choice for kernel regression
[AD-A228437] N91-16661
BARIUM OXIDES
Novel applications of Tl-Ca-Ba-Cu-O thin films to active and passive high frequency devices
[DE91-004507] N91-16240
YBa2Cu3O(7-x) thin film growth on single crystal and polycrystalline yttria-stabilized zirconia
[DE90-010707] N91-16788
Microstructures and dc critical currents in textured Y-Ba-Cu-oxides
[DE91-000895] N91-16803
Observations of vortex structure in YBa2Cu3O7
[DE91-000900] N91-16804
From low to high Tc: An ultrasonic investigation of niobium single crystal and YBaCuO superconducting thin films with surface acoustic waves N91-16822
BAROCLINIC INSTABILITY
Laboratory and theoretical models of planetary-scale instabilities and waves N91-16511
Theoretical and experimental studies of baroclinic processes N91-16512
BAROCLINIC WAVES
Laboratory and theoretical models of planetary-scale instabilities and waves N91-16511
The effect of latent heat release on synoptic-to-planetary wave interactions and its implication for satellite observations: Theoretical modeling N91-16514
BAROCLINITY
South Pacific convergence zone and global-scale circulations N91-16503
Theoretical and experimental studies of baroclinic processes N91-16512
A comparison of diagnostic and kinematic vertical motion fields associated with curved and straight jet streak adjustment processes
[AD-A227724] N91-16522
BAROTROPISM
South Pacific convergence zone and global-scale circulations N91-16503
A comparison of diagnostic and kinematic vertical motion fields associated with curved and straight jet streak adjustment processes
[AD-A227724] N91-16522
BATCH PROCESSING
Estimating the asymptotic variance with batch means
[AD-A228293] N91-16667
BATHING
Whole body cleansing agent
[NASA-CASE-MSC-21589-1] N91-16566
BATHYMETERS
Data base structure to support the production of the digital bathymetric data base
[AD-A227915] N91-16841
BATHYTHERMOGRAPHS
Analysis of satellite and Expendable Bathythermograph (XBT) data for the abrupt topography program
[AD-A228870] N91-16422
BAYES THEOREM
Application of fuzzy-Bayesian analysis to structural reliability
[NAL-TR-1063] N91-16396
Hierarchical Bayesian analysis of change point problems
[AD-A228179] N91-16666
BEADS
Model filled polymers versus synthesis of crosslinked monodisperse polymethacrylate beads
[AD-A227236] N91-16146
BEAM INJECTION
A ring laser gyroscope with optical subtraction N91-16335
Wave-particle power transfer in a steady-state driven system
[DE90-010031] N91-16748
BEAM INTERACTIONS
Some nonlinear problems in the manipulation of beams
[DE91-005211] N91-16358
Advanced methods for the computation of particle beam transport and the computation of electromagnetic fields and beam-cavity interactions
[DE90-011071] N91-16734
BEAMS (SUPPORTS)
Dynamic response of composite beams using shear-deformable finite elements
[AD-A227975] N91-16408
BEARINGS
Extension of transonic flow computational concepts in the analysis of cavitated bearings
[NASA-TM-103214] N91-16304
BEETLES
Kinematics of arthropod legs: Modeling and measurement N91-16391
BEHAVIOR
Investigation of effects of 60-Hz electric and magnetic fields on operant and social behavior and on the neuroendocrine system of nonhuman primates
[DE90-011557] N91-16539
BENDING
Plate and butt-weld stresses beyond elastic limit, material and structural modeling
[NASA-TP-3075] N91-16413
BENZENE
Electronic and ionic transport in processable conducting polymers
[AD-A227857] N91-16154

A comparison of three prospective analytical methods for benzene analysis in jet fuel environments
[AD-A227489] N91-16170

BERYLLIUM
Triple and quadruple excitation contributions to the binding in Be clusters: Calibration calculations on Be3
[NASA-TM-103391] N91-16728

BETATRONS
Diffusion fields in a toroidal conducting shell of circular cross section
[AD-A228021] N91-16197

BIAS
Ionospheric corrections for SHF satellite radar altimetry N91-16423

BIBLIOGRAPHIES
Aeronautical engineering: A continuing bibliography with indexes (supplement 260)
[NASA-SP-7037(260)] N91-15978
Aeronautical engineering: A continuing bibliography with indexes (supplement 259)
[NASA-SP-7037(259)] N91-15979
Bibliography of the technical literature of the Materials Joining Group, Metals and Ceramics Division, 1951--June 1989
[DE91-000530] N91-16126
Aerospace medicine and biology: A cumulative index to a continuing bibliography (supplement 345)
[NASA-SP-7011(345)] N91-16547
Software for aerospace education: A bibliography, 2nd edition
[NASA-PED-106-ED-2] N91-16601
Annotated bibliography of software engineering laboratory literature
[NASA-TM-103415] N91-16602
Subject bibliography of the PMA 205 (Program Manager Air 205) network technical library at Oak Ridge National Laboratory
[DE90-009988] N91-16835
IEEE International Symposium on Information Theory
[AD-A228239] N91-16842

BIMETALS
Fundamental studies of hydrocarbon conversions over supported bimetallic catalysts
[DE90-011744] N91-16089

BINARY MIXTURES
Auto-ignition temperatures of binary mixtures of alkanes in a closed vessel: Comparisons between experimental measurements and numerical predictions
[DE90-007856] N91-16082

BINDERS (MATERIALS)
Method of making contamination-free ceramic bodies
[NASA-CASE-LEW-14984-1] N91-16152

BINOCULAR VISION
Real-time vergence control for binocular robots
[AD-A228817] N91-16387

BIOASTRONAUTICS
Aerospace medicine and biology: A cumulative index to a continuing bibliography (supplement 345)
[NASA-SP-7011(345)] N91-16547

BIOLOGICAL EFFECTS
Ozone and acid-precipitation on western coniferous forests
[DE90-011014] N91-16462
Aerospace medicine and biology: A cumulative index to a continuing bibliography (supplement 345)
[NASA-SP-7011(345)] N91-16547
Radiation physics, biophysics, and radiation biology
[DE90-011544] N91-16722

BIOLOGICAL MODELS (MATHEMATICS)
Carbon dioxide and energy exchanges in a temperate grassland ecosystem N91-16419
Electronic analogue for a biological nose
[ME-78] N91-16541
Cellular track model of biological damage to mammalian cell cultures from galactic cosmic rays
[NASA-TP-3055] N91-16981

BIOMASS
Sahelian vegetation monitoring project
[BCRS-90-04] N91-16426
Biomass and hydrocarb technology for removal of atmospheric CO2
[DE90-010016] N91-16453

BIOPHYSICS
Radiation physics, biophysics, and radiation biology
[DE90-011544] N91-16722

BIOSPHERE
Finalization of the international biospheric model validation study
[DE90-011087] N91-16463

BIOSYNTHESIS
Conversion of acetic acid to methane by thermophiles
[DE90-010993] N91-16086

BIPOLAR TRANSISTORS
Numerical simulation of the comparative electrical performance of the permeable base transistor, opposed gate-source transistor and heterostructure launched ballistic field effect transistor
[AD-A228545] N91-16202

BLACK BODY RADIATION
Analysis of emission data from a Perkin-Elmer 1710 FTIR spectrometer
[AD-A227759] N91-16331

BLACK HOLES (ASTRONOMY)
The x ray emission of SS433
[MPE-PREPRINT-189] N91-16856
Merging galaxies and black hole ejections N91-16929

BLACKOUT (PHYSIOLOGY)
Safety Network to Detect Performance Degradation and Pilot Incapacitation
[AGARD-CP-490] N91-16553
Cerebral oxygen status and G-induced loss of consciousness N91-16554
Detection of loss of consciousness in flight by Doppler method N91-16555
Current status of an artificial intelligence-based loss of consciousness monitoring system for advanced fighter aircraft N91-16556
Framework for an efficient two filter GLOC monitor N91-16557

BLANKETS (FUSION REACTORS)
The measurement of gamma heating in a fusion blanket test assembly
[DE90-011154] N91-16766

BLOCKING
Synoptic/planetary-scale interactions and blocking over the North Atlantic Ocean N91-16513
The effect of latent heat release on synoptic-to-planetary scale wave interactions and implications for satellite observations: Observational study N91-16515
Potential vorticity index N91-16516

BLOOD VOLUME
Electrical resistance volumetry in the circulation N91-16543

BODY KINEMATICS
Kinematics of arthropod legs: Modeling and measurement N91-16391

BODY-WING CONFIGURATIONS
Far-field boundaries and their numerical treatment N91-16281

BOLTS
Failure analysis of a main rotor pitch horn bolt located on the AH-1 Cobra helicopter
[AD-A227679] N91-16007

BOLTZMANN-VLASOV EQUATION
Kinetic stability of field-reversed configurations
[DE90-011530] N91-16767

BONE DEMINERALIZATION
Gallium as a unique anti-resorptive agent in bone: Preclinical studies on its mechanisms of action
[DE90-010650] N91-16542

BONE MINERAL CONTENT
Gallium as a unique anti-resorptive agent in bone: Preclinical studies on its mechanisms of action
[DE90-010650] N91-16542

BOREHOLES
Transient natural convection in heated inclined tubes
[DE90-008217] N91-16255

BORIC ACIDS
A study of the formation and self-lubrication mechanisms of boric acid films on boric oxide coatings
[DE90-010115] N91-16137

BORN APPROXIMATION
Distorted-wave born approximation calculations for turbulence scattering in an upward-refracting atmosphere N91-16700

BORON OXIDES
A study of the formation and self-lubrication mechanisms of boric acid films on boric oxide coatings
[DE90-010115] N91-16137

BOSONS
Chern-Simons and anyonic superconductivity
[DE90-010663] N91-16787
Dynamics of strong-coupling models for cuprate superconductors: Exact results on finite lattices
[DE90-011155] N91-16796

BOUNDARIES
On the propagation of plane waves above an impedance surface N91-16684

BOUNDARY CONDITIONS
Mechanics of interface cracks
[AD-A227579] N91-16067
High frequency scattering by a smooth coated cylinder simulated with generalized impedance boundary conditions
[NASA-CR-187829] N91-16211
Far-field boundaries and their numerical treatment N91-16281
Nonlinear dynamics of global atmospheric and Earth-system processes N91-16510
Synoptic/planetary-scale interactions and blocking over the North Atlantic Ocean N91-16513
Resolution of the 1D regularized Burgers equation using a spatial wavelet approximation
[NASA-CR-187480] N91-16664

BOUNDARY ELEMENT METHOD
Calculations for unsteady aerodynamic characteristics on a 3-D lifting body in subsonic flow using boundary element method
[NAL-TR-1065] N91-15985

BOUNDARY INTEGRAL METHOD
Long-distance sound propagation over discontinuous impedances N91-16688

BOUNDARY LAYER CONTROL
Unsteady separation over maneuvering bodies
[AD-A226829] N91-16285
Experimental parametric study of jet vortex generators for flow separation control
[NASA-CR-187836] N91-16296

BOUNDARY LAYER SEPARATION
Unsteady separation over maneuvering bodies
[AD-A226829] N91-16285
Experimental parametric study of jet vortex generators for flow separation control
[NASA-CR-187836] N91-16296

BOUNDARY LAYER STABILITY
Investigation of the influence of constant adverse pressure gradients on laminar boundary-layer stability at Mach number 8
[AD-A228231] N91-16293
Stability criteria for stratocumulus-topped boundary layers evaluated through conditional sampling of turbulence elements
[AD-A228433] N91-16526

BOUNDARY LAYER TRANSITION
Modelling the transitional boundary layer
[NASA-CR-187487] N91-15995
Streamwise vortices in laminar-turbulent transition N91-16297
Theoretical and experimental examinations of transition behavior of the profile boundary layer at compressor and turbine grids
[ETN-91-98559] N91-16312

BOUNDARY LAYERS
Investigation of transonic flow over segmented slotted wind tunnel wall with mass transfer
[NASA-CR-187760] N91-15981
Natural-convection boundary layers
[ISBN-90-9003467-6] N91-16313
The effect of latent heat release on synoptic-to-planetary wave interactions and its implication for satellite observations: Theoretical modeling N91-16514

BOUNDARY VALUE PROBLEMS
On a class of unsteady three-dimensional Navier Stokes solutions relevant to rotating disc flows: Threshold amplitudes and finite time singularities
[NASA-CR-187482] N91-15991
Time-temperature response of multiphase viscoelastic solids through numerical analysis N91-16401
Adaptive mesh refinement for meshes with singular elements N91-16406
A free boundary problem arising in plasma physics
[DE90-010065] N91-16754

BOXES (CONTAINERS)
Evaluation procedure for reinforced concrete box culverts under airfield pavements
[AD-A227920] N91-16031

BRAIN
A quantum theory of the mind-brain interface
[DE91-004431] N91-16546

BRAYTON CYCLE
Magnetic heat pumps
[DE90-010305] N91-16375

BRAZING
Bibliography of the technical literature of the Materials Joining Group, Metals and Ceramics Division, 1951--June 1989
[DE91-000530] N91-16126

BREEDER REACTORS
Electrical power from inertial confinement fusion: Issues and prospects
[DE90-010332] N91-16759
The measurement of gamma heating in a fusion blanket test assembly
[DE90-011154] N91-16766

BRIGHTNESS
Triple galaxies and a hidden mass problem N91-16875

BROADBAND
Satellite broadcasting: A common-frequency approach to wideband HDTV with a hand-made example plan
[BBC-RD-1990/7] N91-16189

An experimental demonstration of high-resolution Doppler processing
[AD-A228813] N91-16208
Intra-Pulse Frequency Diversity (IPFD) lab demonstration
[AD-A228814] N91-16209

BROADCASTING
Satellite broadcasting: A common-frequency approach to wideband HDTV with a hand-made example plan
[BBC-RD-1990/7] N91-16189
The computer simulation of digital recording systems
[BBC-RD-1990/14] N91-16595
A review of the airborne sound insulation requirements for broadcasting studios and ancillary areas
[BBC-RD-1990/10] N91-16680

BUDGETING
Tactical fighter aircraft: Differences between the Air Force's roadmap and the five year defense plan
[AD-A228882] N91-15976

BUILDINGS
Proving experiments on an acoustic transmission suite and its reverberation room
[BBC-RD-1990/13] N91-16681

BULGING
What determines the bulge to disk ratio of galaxies
N91-16942

BUOYANCY
Laboratory and theoretical models of planetary-scale instabilities and waves N91-16511

BURAN SPACE SHUTTLE
JPRS report: Science and technology. USSR: Space
[JPRS-USP-89-006] N91-16036
Buran and the future of the Soviet space program
N91-16037
Developmental tests for shuttle Orbiter N91-16038
General designer describes Buran flight control, autopilot systems N91-16039
Specialists at flight control center discuss shuttle computer systems N91-16040

BURGER EQUATION
Resolution of the 1D regularized Burgers equation using a spatial wavelet approximation
[NASA-CR-187480] N91-16664

BUTANES
Auto-ignition temperatures of binary mixtures of alkanes in a closed vessel: Comparisons between experimental measurements and numerical predictions
[DE90-007856] N91-16082

C

CABIN ATMOSPHERES
Removal of NO and NO2 from contaminated atmospheres
[AD-A227260] N91-16565

CADMIUM SULFIDES
High-efficiency large-area CdTe panels
[DE91-002117] N91-16443
Low-cost CdZnTe devices for cascade cell application
[DE91-002116] N91-16444

CADMIUM TELLURIDES
Comparison of some x ray sensors for verification
[DE90-011990] N91-16323
High-efficiency large-area CdTe panels
[DE91-002117] N91-16443
Low-cost CdZnTe devices for cascade cell application
[DE91-002116] N91-16444

CALCIUM OXIDES
Novel applications of Tl-Ca-Ba-Cu-O thin films to active and passive high frequency devices
[DE91-004507] N91-16240

CALENDARS
Calendar of selected aeronautical and space meetings: January 1991 onwards
[AGARD-CAL-91/1] N91-16833

CALIBRATING
Aerodynamic surface pressure measurement in atmosphere and wind tunnel on a vertical axis wind turbine blade using pressure transducers N91-15980
Calculation of support interferences on the aerodynamic coefficients for a wind tunnel calibration model
[DLR-FB-90-26] N91-15998
Magnetic measurements with fluxgate magnetometer in rocket flight
[DRI-4-90] N91-16061
An algorithm for using a slide-screw tuner as a computer-controlled impedance
[DE90-010657] N91-16226
Ionospheric corrections for SHF satellite radar altimetry N91-18423
Effects of switch leakages upon Nimbus-7 SMMR calibration
[NASA-TM-100705] N91-16536
Triple and quadruple excitation contributions to the binding in Be clusters: Calibration calculations on Be3
[NASA-TM-103391] N91-16728
A non-LTE analysis of a sample of O stars selected from galactic OB associations N91-16854

CALORIMETERS
Ion beam modification of surface for improved high temperature performance
[AD-A228067] N91-16243
Initial calorimetry experiments in the Physics Divsion, ORNL (Oak Ridge National Laboratory)
[DE90-010301] N91-16756

CAMERAS
Diagnostic of the reaction behaviour of intensive high explosives under jet attack
[MBB-UA-1188-90-PUB] N91-16173
Gabor zone plate apertures for imaging with the mercuric iodide gamma ray camera
[DE90-011193] N91-16321
Camera space manipulation of a mobile robot
N91-16390

CANADA
Potential use of tiltrotor aircraft in Canadian aviation
[NASA-TM-102245] N91-16001
Liquid hydrogen production and commercial demand in the United States N91-16168

CANCELLATION CIRCUITS
Analysis of the performance of a single-auxiliary sidelobe canceller
[RSRE-MEMO-4375] N91-16193

CANS
Experimental study on mercury heat pipes (on effect of screen mesh wick under bottom heat mode)
N91-16280

CAPACITORS
Total-dose degradation of thin film ferroelectric capacitors
[DE90-007152] N91-16218
Properties and characterization of thin film ferroelectric capacitors for nonvolatile memories
[DE91-004037] N91-16242

CAPILLARY FLOW
Experimental study on mercury heat pipes (on effect of screen mesh wick under bottom heat mode)
N91-16280

CAPILLARY TUBES
High speed narrow bore capillary gas chromatography
[ETN-91-98481] N91-16113

CAPILLARY WAVES
Research in nonlinear water waves
[AD-A227948] N91-16292

CAPTURE EFFECT
Measurement of the capture effect of frequency modulation
[AD-A228058] N91-16199

CARBON
Comparison of the thermal stability of the codeposited carbon/hydrogen layer to that of the saturated implant layer in graphite
[DE90-012148] N91-16144

CARBON DIOXIDE
Carbon dioxide and energy exchanges in a temperate grassland ecosystem N91-16419
Biomass and hydrocarb technology for removal of atmospheric CO2
[DE90-010016] N91-16453

CARBON DIOXIDE CONCENTRATION
Biomass and hydrocarb technology for removal of atmospheric CO2
[DE90-010016] N91-16453

CARBON DIOXIDE LASERS
Definition and preliminary design of the Laser Atmospheric Wind Sounder (LAWS) phase 1. Volume 1: Executive summary
[NASA-CR-184071] N91-16332
Definition and preliminary design of the Laser Atmospheric Wind Sounder (LAWS) phase 1. Volume 2
[NASA-CR-184072] N91-16333
Definition and preliminary design of the Laser Atmospheric Wind Sounder (LAWS) phase 1. Volume 3: Program cost estimates
[NASA-CR-184073] N91-16334
Droplet shattering, vaporization, and recondensation in cloud clearing with long pulse infrared chemical lasers
[DE90-010584] N91-16343
Experimental set-up for a pulsed CO2 laser rangefinder with heterodyne detection
[FEL-90-A125] N91-16365
Analytical and experimental investigation of transverse flow aerodynamic windows for high power lasers
[DLR-FB-90-33] N91-16367

CARBON FIBER REINFORCED PLASTICS
Bump examinations of integrally strengthened carbon fiber reinforced plastic panels
[MBB/FE281/CFK/PUB/0013] N91-16076

CARBON MONOXIDE
Rotational temperature estimation of CO at high temperatures by graphical methods using FTIR spectrometry
[AD-A228370] N91-16105
Chemisorption of carbon monoxide on three metal surfaces: Ni(111), Pd(111) and Pt(111): A comparative study
[AD-A228579] N91-16108
Molecular gas and star formation in the central regions of Virgo spiral galaxies N91-16970

CARBON MONOXIDE POISONING
Impurity tolerant electrocatalysts
[DE90-011960] N91-16090

CARBON-CARBON COMPOSITES
The oxidation behavior of carbon-carbon composites and their coatings N91-16074

CARDIOVASCULAR SYSTEM
Electrical resistance volumetry in the circulation
N91-16543

CARGO
Buran and the future of the Soviet space program
N91-16037

CARRIER FREQUENCIES
Nonlinear optical systems interacting with amplitude-modulated optical fields
[AD-A228221] N91-16742

CARRIER TRANSPORT (SOLID STATE)
Photoreflectance studies of electronic transitions in quantum well structures under high pressure
[DE90-011583] N91-16801

CARTESIAN COORDINATES
Simulation of disk-disk encounters with co-moving polar grids N91-16941

CASTING
Gelcasting of sub-micron alumina, sialon, and silicon nitride powders
[DE91-000618] N91-16145
The University of Arizona program in solid propellants
N91-16165

CASTINGS
Gelcasting of sub-micron alumina, sialon, and silicon nitride powders
[DE91-000618] N91-16145

CATACLYSMIC VARIABLES
Interacting nuclei in distant galaxies N91-16894

CATALOGS (PUBLICATIONS)
Dumb-bell galaxies in southern clusters: Catalog and preliminary statistical results N91-16896
The 1989 annual catalog of the German Aerospace Establishment: Research reports and communications
[ISSN-0172-357X] N91-16987

CATALYSIS
Fundamental studies of hydrocarbon conversions over supported bimetallic catalysts
[DE90-011744] N91-16089

CATALYSTS
Fundamental studies of hydrocarbon conversions over supported bimetallic catalysts
[DE90-011744] N91-16089
Synthesis, characterization and catalytic activity of microporous aluminophosphate catalysts N91-16092
High temperature corrosion of alloys in mixed gases
N91-16121
Improved anode catalysts for coal gas-fueled phosphoric acid fuel cells
[DE90-009683] N91-16442

CATALYTIC ACTIVITY
Synthesis, characterization and catalytic activity of microporous aluminophosphate catalysts N91-16092

CATHETERIZATION
Electrical resistance volumetry in the circulation
N91-16543

CAVITATION FLOW
Extension of transonic flow computational concepts in the analysis of cavitated bearings
[NASA-TM-103214] N91-16304

CAVITIES
Void nucleation in nonlinear solid mechanics
[AD-A228890] N91-16410

CELESTIAL MECHANICS
Typical motions in multiple systems N91-16945

CELL ANODES
Improved anode catalysts for coal gas-fueled phosphoric acid fuel cells
[DE90-009683] N91-16442

CELLS (BIOLOGY)
Cellular track model of biological damage to mammalian cell cultures from galactic cosmic rays
[NASA-TP-3055] N91-16981

CENTAURUS CONSTELLATION
Molecular absorption lines towards the nucleus of Centaurus A
[MPE-PREPRINT-182] N91-16976

CENTER OF GRAVITY
Determination of shuttle orbiter center of gravity from flight measurements
[NASA-TM-102627] N91-16058
CENTRAL PROCESSING UNITS
Systematic design of regular VLSI processor arrays
[ETN-91-98482] N91-16250
CENTRIFUGAL FORCE
Fine particle flotation in a centrifugal force field
[ETN-91-98480] N91-16309
CERAMIC MATRIX COMPOSITES
Mechanical behavior of a SiC-fiber/Si3N4 composite
[AD-A228371] N91-16073
Metallurgical design of novel metal matrix composites for aerospace applications
[ETN-91-98573] N91-16077
Fiber-reinforced ceramic composites for Earth-to-orbit rocket engine turbines
[NASA-CR-185264] N91-16150
CERAMICS
Advanced Turbine Technology Applications Project (ATTAP)
[NASA-CR-187039] N91-16021
Acoustical and dynamic mechanical characterization of fiber-matrix interface bonds in ceramic composites
[DE90-010949] N91-16066
Bibliography of the technical literature of the Materials Joining Group, Metals and Ceramics Division, 1951--June 1989
[DE91-000530] N91-16126
Initial studies of electric field effects on ceramic powder formation in flames
[DE90-007571] N91-16138
Development of nondestructive evaluation methods and prediction of effects of flaws on the fracture behavior of structural ceramics
[DE90-011092] N91-16141
Microwave sintering of fuel cell materials
[DE90-011643] N91-16143
Gelcasting of sub-micron alumina, sialon, and silicon nitride powders
[DE91-000618] N91-16145
Sintering stress and microstructure in ceramic powder compacts
[DE91-004415] N91-16149
Method of making contamination-free ceramic bodies
[NASA-CASE-LEW-14984-1] N91-16152
A miniature inexpensive, oxygen sensing element
[DE90-009938] N91-16318
Wear measurement of ceramic bearings in gas turbines
[AD-A227505] N91-16382
Composite ceramic superconducting wires for electric motor applications
[AD-A228359] N91-16818
CEREBRAL CORTEX
Changes in somatosensory responsiveness in behaving monkeys
[AD-A226832] N91-16540
CESIUM IONS
Spatial distributions of the emitting species in a penning surface-plasma source
[DE90-011996] N91-16772
CESIUM VAPOR
Spontaneous force optical traps
[AD-A228539] N91-16363
CHANNEL CAPACITY
IEEE International Symposium on Information Theory
[AD-A228239] N91-16842
CHANNEL FLOW
Heat transfer from water flowing through a chilled-bed open channel
[AD-A226855] N91-16286
Numerical study of a three-dimensional turbulent boundary layer
[AD-A227835] N91-16291
CHANNELS (DATA TRANSMISSION)
A low-cost infrared telemetry system for kilohertz-bandwidth data acquisition
[DE90-010616] N91-16042
Applications of non-linear optics
[AD-A228872] N91-16743
Optical transceiver frontend for high speed bus STANAG 3910 with one fiber only
[MBB-UA-1182-90-PUB] N91-16745
CHAOS
Numerical simulation of a complicated transition-breakdown of vortical flows inside a circular pipe N91-16273
Stochastic and chaotic effects in the ring laser N91-16359
Quasiperiodic transition to chaos in Ge; and magnetic susceptibility of high-T(c) superconductors
[DE90-011304] N91-16797
Triplets of galaxies: Their dynamics, evolution, and the origin of chaos in them N91-16948
CHARACTERIZATION
Synthesis, characterization and catalytic activity of microporous aluminophosphate catalysts N91-16092
Characterization of ultrasonic transducers using pattern recognition techniques
[DE91-000580] N91-16326
Solar refrigeration: Evaluation of technical options and design of a solar-generator-adsorber for a novel adsorption refrigerator, volumes 1 and 2 N91-16440
Characterization of disruptions in the Microwave Tokamak Experiment (MTX)
[DE90-010352] N91-16761
CHARGE COUPLED DEVICES
An atlas of mixed-morphology pairs N91-16866
Multi-color imaging of selected southern interacting galaxies N91-16867
Multi-waveband observations of colliding galaxies N91-16868
The cD galaxy in Abell cluster 1775 N91-16886
The double nucleus galaxies Mkn 423 and Mkn 739 N91-16891
Central activity in 60 micron peakers N91-16913
CHARGED PARTICLES
Radiation physics, biophysics, and radiation biology
[DE90-011544] N91-16722
Advanced methods for the computation of particle beam transport and the computation of electromagnetic fields and beam-cavity interactions
[DE90-011071] N91-16734
CHARON
Aerospace vehicle design, spacecraft section. Volume 1: Project groups 1-4 --- unmanned probe to Pluto
[NASA-CR-186841] N91-16045
PFERD Mission: Pluto flyby exploration/research design N91-16046
Intrepid: A mission to Pluto N91-16047
Project Cerberus: Flyby mission to Pluto N91-16048
OPTIC: Orbiting Plutonian Topographic Image Craft proposal for an unmanned mission to Pluto N91-16049
Aerospace vehicle design, spacecraft section. Volume 2: Project groups 5-7 --- unmanned probe to Pluto
[NASA-CR-186842] N91-16050
Mission management, planning, and cost: PULSE Attitude And Control Systems (AACS) N91-16051
The Copernicus project N91-16052
The Phoenix Pluto Probe N91-16053
CHARPY IMPACT TEST
Thermal aging of cast stainless steels: Mechanisms and predictions
[DE90-010093] N91-16115
Specimen size effects in Charpy impact testing
[DE90-011369] N91-16399
CHEMICAL ANALYSIS
Laboratory testing of chloride 3ET205 6 volt traction battery
[DE90-010926] N91-16225
Contemporary issues in solar pond research
[DE90-010094] N91-16436
Utilization of polymer viscoelastic properties in acoustic wave sensor applications
[DE90-010534] N91-16676
CHEMICAL BONDS
Theoretical study of the C-H bond dissociation energy of acetylene
[NASA-CR-187858] N91-16065
High resolution photoelectron spectroscopy of metal clusters and high temperature species
[DE90-011598] N91-16119
Molecular orbital studies of the bonding in heavy element organometallics
[DE90-009732] N91-16711
Interatomic forces and bonding mechanisms in MgO clusters
[DE90-010148] N91-16719
New surface atomic structures for III-V(110)-p(1 x 1)-Sb(1ML): Chemical bonding and electronic structure
[DE90-011230] N91-16794
CHEMICAL COMPOSITION
Surface analysis by low-energy ion scattering: Two-dimensional detection and quantification
[ETN-91-98474] N91-16133
Aerosol cloud generation experiments
[DE90-011051] N91-16264
CHEMICAL PROPERTIES
Experimental studies of the properties of trihydrogen and tetrahydrogen
[AD-A228869] N91-16110
CHEMICAL REACTIONS
The development of improved capillary supercritical fluid chromatography and mass spectrometry
[AD-A228535] N91-16107
Puzzles of electron transfer
[DE90-010541] N91-16720
CHEMICAL REACTORS
Destruction of propellant components in supercritical water
[DE90-010600] N91-16085
Aerodynamic drag characterization and deposition studies of irregular particles. Part 3: Analysis of flow and temperature field inside the Combustion Deposition Entrained Reactor (CDER)
[DE90-000466] N91-16259
CHEMILUMINESCENCE
New development of laser-based techniques in applications of thin-layer chromatography, microprobe elemental analysis, and gas phase pyrolysis
[DE90-011740] N91-16347
CHEMISORPTION
Chemisorption of carbon monoxide on three metal surfaces: Ni(111), Pd(111) and Pt(111): A comparative study
[AD-A228579] N91-16108
Atomic and electronic structure of metals and alloys: Clean surfaces and chemisorbed molecules
[DE91-000267] N91-16123
A photoemission study of samarium on silicon
[DE90-011509] N91-16799
CHIPS (ELECTRONICS)
Radiation hardening of a high voltage IC technology (BCDMOS)
[DE90-008345] N91-16220
Noise reduction using low weight and constant weight coding techniques
[AD-A228346] N91-16244
ICHARM: Hierarchical CMOS circuit extraction with power bus extraction
[AD-A228613] N91-16245
Timing margin measurement using a laser technique
[AD-A226821] N91-16353
CHLORIDES
Failure analysis of a main rotor pitch horn bolt located on the AH-1 Cobra helicopter
[AD-A227679] N91-16007
CHLOROPHYLLS
Bio-optical profile data report coastal transition zone program, R/V Thomas Washington, June 24 - July 21, 1988
[NASA-CR-187808] N91-16532
Bio-optical profile data report coastal transition zone program, R/V Point Sur, June 15-28, 1987
[NASA-CR-187807] N91-16533
Bio-optical profile data report: Joint Global Ocean Flux Study, Hawaii Ocean Time-Series, HOT-3, R/V Moana Wave, 6-10 January 1989
[NASA-CR-187805] N91-16534
CHROMATOGRAPHY
The development of improved capillary supercritical fluid chromatography and mass spectrometry
[AD-A228535] N91-16107
CHROMIUM
Epitaxial growth and surface morphology of some metal and semiconductor structures N91-16824
CHROMIUM ALLOYS
The influence of small SO2 contents on the corrosion behavior for NiCrAl alloys in temperature zone from 1000 to 1100 C
[JUEL-2362] N91-16134
The use of impedance measurements in corrosion research: The corrosion behaviour of chromium and iron-chromium alloys
[ISBN-90-9003693-8] N91-16135
CHROMIUM OXIDES
Microwave sintering of fuel cell materials
[DE90-011643] N91-16143
CIRCUIT BOARDS
Microwave coupling on printed circuit boards
[DE90-011237] N91-16232
Noise reduction using low weight and constant weight coding techniques
[AD-A228346] N91-16244
CIRCUIT RELIABILITY
ICHARM: Hierarchical CMOS circuit extraction with power bus extraction
[AD-A228613] N91-16245
CIRCULAR CYLINDERS
High frequency scattering by a smooth coated cylinder simulated with generalized impedance boundary conditions
[NASA-CR-187829] N91-16211
Circumfluous motion of a conductive liquid around solid objects in a magnetic field
[DE90-011335] N91-16265
CIRCULAR ORBITS
The spiral-compact galaxy pair AM 2208-251: Computer simulations versus observations N91-16939
CIVIL AVIATION
Potential use of tiltrotor aircraft in Canadian aviation
[NASA-TM-102245] N91-16001

The use of contact lenses in the civil airman population
[AD-A227450] N91-16544

CLASSIFICATIONS
A search for good lattice rules based on the reciprocal lattice generator matrix
[DE91-004425] N91-16809
Hidden interaction in SBO galaxies N91-16880
Correlations between environmental parameters and nuclear activity N91-16920
The role of shocks in NGC 6240 N91-16921
A classification of the galaxy groups N91-16949

CLEANERS
Whole body cleansing agent
[NASA-CASE-MSC-21589-1] N91-16566

CLEARING
Droplet shattering, vaporization, and recondensation in cloud clearing with long pulse infrared chemical lasers
[DE90-010584] N91-16343

CLIMATE
Environmental trends
[DE90-010530] N91-16450
Multi-dimensional aspects of recent climate change in North America
[DE90-010958] N91-16460
Monitoring challenges and innovative ideas
[DE91-000586] N91-16465
Potential vorticity index N91-16516

CLIMATE CHANGE
Solving global environmental problems through technological innovation
[DE90-010018] N91-16446
Potential responses of landscape boundaries to global environmental change
[DE90-008568] N91-16451
International decision making and global climate change: Lessons of prior resource management efforts for consensus building
[DE90-010714] N91-16454
Climate Caucus report: Opportunities for bridging the gaps from effects to impacts
[DE90-010877] N91-16459
Multi-dimensional aspects of recent climate change in North America
[DE90-010958] N91-16460
GCM (General Circulation Model) predictions for surface air temperature and precipitation over the southeastern United States
[DE90-009434] N91-16497

CLIMATOLOGY
Ionospheric corrections for SHF satellite radar altimetry N91-16423
International decision making and global climate change: Lessons of prior resource management efforts for consensus building
[DE90-010714] N91-16454
Climate Caucus report: Opportunities for bridging the gaps from effects to impacts
[DE90-010877] N91-16459
The atmospheric effects of stratospheric aircraft: A topical review
[NASA-RP-1250] N91-16466
Joint US Navy/US Air Force climatic study of the upper atmosphere. Volume 1: January
[AD-A227122] N91-16476
Joint US Navy/US Air Force climatic study of the upper atmosphere. Volume 2: February
[AD-A227123] N91-16477
Joint US Navy/US Air Force climatic study of the upper atmosphere. Volume 3: March
[AD-A227124] N91-16478
Joint US Navy/US Air Force climatic study of the upper atmosphere. Volume 4: April
[AD-A227125] N91-16479
Joint US Navy/US Air Force climatic study of the upper atmosphere. Volume 7: July
[AD-A227126] N91-16480
Joint US Navy/US Air Force climatic study of the upper atmosphere. Volume 10: October
[AD-A227127] N91-16481
Stratiform clouds and their interaction with atmospheric motion N91-16506
Global-scale, intraseasonal fluctuations of diabatic forcing of the atmosphere N91-16508
Tropical Pacific moisture variability N91-16509
The effect of latent heat release on synoptic-to-planetary wave interactions and its implication for satellite observations: Theoretical modeling N91-16514
The effect of latent heat release on synoptic-to-planetary scale wave interactions and implications for satellite observations: Observational study N91-16515
Spatial and temporal climate variations influencing medium-range temperature predictions over south-central European Russia
[AD-A228623] N91-16527

CLOCKS
Time interpolator
[DIGEL-1990-3] N91-16337

CLOSED ECOLOGICAL SYSTEMS
Common approach for planetary habitation systems implementation
[MBB-UO-0115-90-PUB] N91-16570

CLOSURE LAW
Computation of turbulent flow about unconventional airfoil shapes N91-15992
A query model and query and knowledge definition languages for object-oriented databases N91-16580

CLOUD COVER
Comparison of SSM/I measurements to numerically-simulated cloud and precipitation during ERICA N91-16501
Planetary circulations in the presence of transient and self-induced heating N91-16505
Stability criteria for stratocumulus-topped boundary layers evaluated through conditional sampling of turbulence elements
[AD-A228433] N91-16526

CLOUD PHYSICS
Investigation of a remote sensing technique for droplet effective radius N91-16420

CLOUDS
Aerosol cloud generation experiments
[DE90-011051] N91-16264
Droplet shattering, vaporization, and recondensation in cloud clearing with long pulse infrared chemical lasers
[DE90-010584] N91-16343
Geometrical parameters of E+S pairs N91-16865

CLOUDS (METEOROLOGY)
Planetary circulations in the presence of transient and self-induced heating N91-16505

CLUMPS
Cluster formation in laser-induced ablation and evaporation of solids observed by laser ionization time-of-flight mass spectrometry and scanning tunneling microscopy
[DE90-010876] N91-16344
Wing galaxies: A formation mechanism of the clumpy irregular galaxy Markarian 297 N91-16963

CLUTTER
Numeric and symbolic signal processing for very high subclutter visibility
[AD-A228812] N91-16207
An experimental demonstration of high-resolution Doppler processing
[AD-A228813] N91-16208
A paper-assessment of the performance of a modern airborne multi-mode pulse Doppler radar deployed as a ground-based fire-control radar
[ETN-91-98584] N91-16215

CMOS
Properties and characterization of thin film ferroelectric capacitors for nonvolatile memories
[DE91-004037] N91-16242
ICHARM: Hierarchical CMOS circuit extraction with power bus extraction
[AD-A228613] N91-16245
Timing margin measurement using a laser technique
[AD-A226821] N91-16353
Fabrication and electrical characterization of deep-submicron trench-isolated CMOS device structures N91-16802

COAGULATION
The effect of stratification on gravitational coagulation and settling of aerosols
[DE90-010153] N91-16079

COAL
Heat engines program
[DE90-010276] N91-16374

COAL DERIVED GASES
Improved anode catalysts for coal gas-fueled phosphoric acid fuel cells
[DE90-009683] N91-16442

COAL GASIFICATION
Aerodynamic drag characterization and deposition studies of irregular particles. Part 3: Analysis of flow and temperature field inside the Combustion Deposition Entrained Reactor (CDER)
[DE90-000466] N91-16259

COAL UTILIZATION
Aerodynamic drag characterization and deposition studies of irregular particles. Part 3: Analysis of flow and temperature field inside the Combustion Deposition Entrained Reactor (CDER)
[DE90-000466] N91-16259
Highlights of the Chemical Technology (CMT) Division's activities
[DE90-008242] N91-16984

COASTS
Image-based terrain modeling with thematic mapper N91-16418

Comparison of SSM/I measurements to numerically-simulated cloud and precipitation during ERICA N91-16501
Stratiform clouds and their interaction with atmospheric motion N91-16506
Bio-optical profile data report coastal transition zone program, R/V Thomas Washington, June 24 - July 21, 1988
[NASA-CR-187808] N91-16532
Bio-optical profile data report coastal transition zone program, R/V Point Sur, June 15-28, 1987
[NASA-CR-187807] N91-16533

COATING
Assessment of corrosion resistant coatings for a depleted U-0.75 Ti alloy
[AD-A228237] N91-16130

COATINGS
A study of the formation and self-lubrication mechanisms of boric acid films on boric oxide coatings
[DE90-010115] N91-16137
High-frequency techniques for RCS prediction of plate geometries
[NASA-CR-187865] N91-16212
Characterization of chemically prepared PZT thin films
[DE90-010831] N91-16789

COBALT OXIDES
Physico-chemical investigations on Co-Mn-oxide spinels
[ETN-91-98476] N91-16825

CODE DIVISION MULTIPLE ACCESS
Near/far resistant receivers for DS/SSMA communications
[AD-A228147] N91-16200

CODING
Pi: A parallel architecture interface for multi-model execution
[AD-A228345] N91-16640
IEEE International Symposium on Information Theory
[AD-A228239] N91-16842

COEFFICIENTS
Resolution of the 1D regularized Burgers equation using a spatial wavelet approximation
[NASA-CR-187480] N91-16664
Viral coefficient and hidden mass in the galaxy groups N91-16950

COGNITION
Skill and skilled memory
[AD-A227697] N91-16549
Pre-attentive and attentive visual information processing
[AD-A228541] N91-16550
Optimisation of operational workload levels using neurophysiological and cognitive techniques N91-16560

COHERENT RADIATION
Numeric and symbolic signal processing for very high subclutter visibility
[AD-A228812] N91-16207
Mode competition effects in free electron lasers and gyrotrons
[DE90-011084] N91-16346

COLD GAS
Cool infalling gas and its interaction with the hot ISM of elliptical galaxies N91-16915

COLD TOLERANCE
Quantification of lower bounds for endurance times in thermally insulated fingers and toes exposed to cold stress
[AD-A227782] N91-16545

COLLISION PARAMETERS
A multi-frequency study of the peculiar interacting system Arp 206 N91-16870

COLLISIONAL PLASMAS
Massively parallel Fokker-Planck calculations
[DE90-010691] N91-16633

COLLISIONS
Paired and Interacting Galaxies: International Astronomical Union Colloquium No. 124
[NASA-CP-3098] N91-16858
Multi-waveband observations of colliding galaxies N91-16868
A spiral-like disk of ionized gas in IC 1459: Signature of a merging collision N91-16889
Deep Fabry-Perot imaging of NGC 6240: Kinematic evidence for merging galaxies N91-16922
Merging galaxies and black hole ejections N91-16929
A statistical study of merging galaxies: Theory and observations N91-16931
A dynamical proximity analysis of interacting galaxy pairs N91-16937
The spiral-compact galaxy pair AM 2208-251: Computer simulations versus observations N91-16939
Collisional removal of HI from the inner disks of Virgo cluster galaxies N91-16952

Numerical simulations of interacting disk galaxies N91-16955
Dynamical experiments on models of colliding disk galaxies N91-16959
Caustic waves in galaxy disks produced in collisions with low mass companions N91-16960
Wing galaxies: A formation mechanism of the clumpy irregular galaxy Markarian 297 N91-16963

COLOR
Application Principles for Multicolored Displays: A workshop report
[AD-A227961] N91-16567
Chemical beam epitaxy of ZnSe
[AD-A228045] N91-16817
Multi-color imaging of selected southern interacting galaxies N91-16867
Blue ellipticals in compact groups N91-16873
The nature of the emission-line nebulae in powerful far-infrared galaxies N91-16916

COLOR CODING
Organization of the mission pattern in the air picture
[IZF-1990-A-12] N91-16568

COLOR VISION
Application Principles for Multicolored Displays: A workshop report
[AD-A227961] N91-16567

COLORIMETRY
New data on the peculiar galaxy MRK 273 N91-16887

COLUMNS (PROCESS ENGINEERING)
High speed narrow bore capillary gas chromatography
[ETN-91-98481] N91-16113

COMBAT
Organization of the mission pattern in the air picture
[IZF-1990-A-12] N91-16568
Artificial intelligence technologies applied to terrain analysis
[DE90-011985] N91-16642

COMBUSTIBLE FLOW
Development and application of numerical models for reactive flows
[AD-A228884] N91-16295

COMBUSTION
Flammability characteristics of fiber reinforced composite materials
[AD-A228215] N91-16072
Spray combustion modeling and evaluation
[NASA-CR-187887] N91-16078
A numerical study of silane combustion
[DE90-006002] N91-16080
Modelling of flamelet surface-to-volume ratio in turbulent premixed combustion
[DE90-006312] N91-16081
High-loaded combustion chambers stationary constant pressure combustion. Part 2: Research reports
[ETN-91-98511] N91-16112

COMBUSTION CHAMBERS
Autoignition and flameholding in a cylindrical scramjet combustor
[NAL-TR-1067] N91-16102
High-loaded combustion chambers stationary constant pressure combustion. Part 2: Research reports
[ETN-91-98511] N91-16112

COMBUSTION PRODUCTS
Greenhouse gas emissions from selected alternative transportation fuels market niches
[DE90-010491] N91-16448

COMMAND AND CONTROL
ERICC: Construction and application of the Command and Control Research Facility
[IZF-1989-55] N91-16213
Artificial intelligence technologies applied to terrain analysis
[DE90-011985] N91-16642

COMMERCE
Liquid hydrogen production and commercial demand in the United States N91-16168
Report to Congress on the Small Business Program
[DE91-004622] N91-16831

COMMUNICATION NETWORKS
Movable-boundary channel-access schemes for integrated voice/data networks
[AD-A227331] N91-16186
A computer-based instructional support network: Design, development, and evaluation
[AD-A227922] N91-16637
Applications of non-linear optics
[AD-A228872] N91-16743
IEEE International Symposium on Information Theory
[AD-A228239] N91-16842

COMMUNICATION THEORY
Some applications of probability and statistics in communication theory and signal processing
[AD-A226869] N91-16184
IEEE International Symposium on Information Theory
[AD-A228239] N91-16842

COMMUTER AIRCRAFT
Development of a crashworthy seat for commuter aircraft
[AD-A227486] N91-15999

COMPACT GALAXIES
Observational properties of compact groups of galaxies N91-16871
VLA neutral hydrogen imaging of compact groups N91-16872
A study of the compact group of galaxies Shahbazian 4 N91-16877

COMPENSATORS
Longitudinal stability augmentation of a lightweight fighter aircraft model
[ETN-91-98585] N91-16026

COMPILERS
POSC: A Partitioning and Optimizing SISAL Compiler
[DE90-010679] N91-16577
Optimization of a power transient stability program on a vector supercomputer: Theory and applications
[AD-A227884] N91-16607
Ada compiler validation procedures, version 2.1
[AD-A228614] N91-16621

COMPLEMENTS (MATHEMATICS)
Some generalizations of the criss-cross method for quadratic programming
[REPT-90-52] N91-16599

COMPLEX SYSTEMS
Nonlinear dynamics of global atmospheric and Earth-system processes N91-16510

COMPOSITE MATERIALS
TF89 tactical fighter outer wing design
[ETN-91-98580] N91-16019
Acoustical and dynamic mechanical characterization of fiber-matrix interface bonds in ceramic composites
[DE90-010949] N91-16066
Mechanics of interface cracks
[AD-A227579] N91-16067
Composite ceramic superconducting wires for electric motor applications
[AD-A228359] N91-16818
Energy and Technology Review, March 1990
[DE90-008230] N91-16985

COMPOSITE STRUCTURES
Flammability characteristics of fiber-reinforced composite materials for the composite infantry fighting vehicle
[AD-A227783] N91-16068
Dynamic response of composite beams using shear-deformable finite elements
[AD-A227975] N91-16408

COMPRESSED GAS
Effects of high pressure nitrogen on the thermal stability of SiC fibers
[NASA-TM-103245] N91-16075
Time-resolved Coherent Anti-Stokes Raman Spectroscopy (CARS) and the measurement of vibrational spectra in shock-compressed molecular materials
[DE90-012053] N91-16091

COMPRESSIBILITY EFFECTS
An experiment on supersonic turbulent mixing layers: Supersonic-subsonic two-stream layers
[NAL-TR-1066] N91-15983

COMPRESSIBLE FLOW
Calculations for unsteady aerodynamic characteristics on a 3-D lifting body in subsonic flow using boundary element method
[NAL-TR-1065] N91-15985

COMPRESSIBLE FLUIDS
Internal solitary waves in compressible fluids
[ETN-91-98475] N91-16307

COMPTON EFFECT
Multiple-photon Compton scattering in a strong magnetic field: Cross-sections and radiative transport N91-16852
Resonant Compton scattering in models of gamma-ray burst sources. Part 2: Numerical modeling
[DE91-005268] N91-16982
Interpretation of the diffusive galactic continuum gamma radiation in MeV area
[MPE-220] N91-16983

COMPUTATION
Introduction (to a book on applications of local-density-functional methods in chemistry)
[AD-A228769] N91-16109
Decentralized real-time scheduling
[AD-A227856] N91-16604
Expressing user-defined parallelism in EPL (Equational Programming Language)
[AD-A227875] N91-16606
Operating characteristics for weighted energy detector with Gaussian signals
[AD-A226851] N91-16673
Comparison of the quadratic configuration interaction and coupled cluster approaches to electron correlation including the effect of triple excitations
[NASA-CR-187855] N91-16727
Advanced methods for the computation of particle beam transport and the computation of electromagnetic fields and beam-cavity interactions
[DE90-011071] N91-16734

COMPUTATIONAL CHEMISTRY
Introduction (to a book on applications of local-density-functional methods in chemistry)
[AD-A228769] N91-16109
Linear algebra for dense matrices on a hypercube
[DE90-010533] N91-16647

COMPUTATIONAL FLUID DYNAMICS
Large-scale numerical aerodynamic simulations for complete aircraft configurations
[NAL-TR-1073-T] N91-15984
Hypersonic shock/boundary-layer interaction database
[NASA-CR-187769] N91-15986
Rotorcraft application of advanced computational aerodynamics
[NASA-CR-187767] N91-15987
Modelling the transitional boundary layer
[NASA-CR-187487] N91-15995
The Proceedings of the Symposium on Mechanics for Space Flight 1989
[ISAS-SP-12] N91-16266
Numerical simulations of unsteady shock reflection processes by a ramp N91-16267
Some topics of Navier-Stokes solvers N91-16269
Numerical simulation of a complicated transition-breakdown of vortical flows inside a circular pipe N91-16273
Far-field boundaries and their numerical treatment N91-16281
Unsteady separation over maneuvering bodies
[AD-A226829] N91-16285
Evaluation of the HULL and SHARC hydrocodes in simulating the reflection of Mach 2.12 non-decaying shock on wedges of various angles
[AD-A227581] N91-16287
Simulation of the flow past an impulsively started cylinder using a discrete vortex method N91-16303
Extension of transonic flow computational concepts in the analysis of cavitated bearings
[NASA-TM-103214] N91-16304
Modeling the dissipation rate in rotating turbulent flows
[NASA-CR-187485] N91-16306

COMPUTATIONAL GRIDS
Rotorcraft application of advanced computational aerodynamics
[NASA-CR-187767] N91-15987
MmB: A new class of accurate high resolution schemes for conservation laws in two dimensions N91-16275
Study of time accuracy of flow variables across discontinuous boundaries N91-16300
Adaptive mesh refinement for meshes with singular elements N91-16406
Simulation of disk-disk encounters with co-moving polar grids N91-16941

COMPUTER AIDED DESIGN
Applications of fuzzy theories to multi-objective system optimization
[NASA-CR-177573] N91-16012
Developmental tests for shuttle Orbiter N91-16038
X-Ray Detector: An x-ray radiation detector design code
[DE90-008235] N91-16317
Microsupercomputers: Design and implementation
[AD-A228741] N91-16571
Microsupercomputers: Design and implementation
[AD-A228744] N91-16572
Reliability/Maintainability/Logistics support analysis Computer Aided Tailoring Software Program (R/M/L CATSOP)
[AD-A226820] N91-16588

COMPUTER AIDED MANUFACTURING
Geometric modeling applications interface program
[AD-A227651] N91-16591
Geometric modeling application interface program. System components operator's manual
[AD-A227827] N91-16594

COMPUTER ASSISTED INSTRUCTION
A computer-based instructional support network: Design, development, and evaluation
[AD-A227922] N91-16637

COMPUTER GRAPHICS
Living PRAs (Probabilistic Risk Analysis) made easier with IRRAS (Integrated Reliability and Risk Analysis System)
[DE90-010938] N91-16395
A graphical user-interface-driven waveform data acquisition and analysis system
[DE90-011948] N91-16578
Automated design of displays for technical data
[AD-A226729] N91-16586
Introduction to aspects of object oriented graphics
[CWI-CS-R9009] N91-16597

Visualization of surfaces in four-dimensional space
[AD-A227858] N91-16605
PENGUIN: A language for reactive graphical user interfaces
[AD-A228580] N91-16620
Displaying alphanumeric characters on pixel-planes 5
[AD-A228616] N91-16622

COMPUTER NETWORKS
ERICC: Construction and application of the Command and Control Research Facility
[IZF-1989-55] N91-16213
Distributed System Modeling Environment (DSME)
[AD-A226698] N91-16583
XSHELL: A general purpose expert system shell
[AD-A228454] N91-16616
A computer-based instructional support network: Design, development, and evaluation
[AD-A227922] N91-16637
The StarLite project
[AD-A226722] N91-16837

COMPUTER PROGRAMMING
Smoothing and scaling airfoil coordinates on a personal computer
[DE89-000878] N91-16582
Introduction to aspects of object oriented graphics
[CWI-CS-R9009] N91-16597
Annotated bibliography of software engineering laboratory literature
[NASA-TM-103415] N91-16602
A software development specification for nonlinear structural analysis
[AD-A228427] N91-16614
PENGUIN: A language for reactive graphical user interfaces
[AD-A228580] N91-16620
Computational physics at the National Energy Research Supercomputer Center
[DE90-010283] N91-16672
Geographic data transfer N91-16836

COMPUTER PROGRAMS
Evaluation procedure for reinforced concrete box culverts under airfield pavements
[AD-A227920] N91-16031
User's guide to PANCOR: A panel method program for interference assessment in slotted-wall wind tunnels
[NASA-CR-187479] N91-16033
Joint computational/experimental aerodynamics research on a reentry vehicle. Part 2: Computational results
[DE90-012765] N91-16054
Computer-assisted determination of minimum energy conformations. Part 4: Alpha1 and alpha2 adrenergiic compounds
[AD-A226811] N91-16097
Numerical modeling tools for transient electromagnetic problems
[DE90-010328] N91-16180
Diffusion fields in a toroidal conducting shell of circular cross section
[AD-A228021] N91-16197
PCB/transformer techno-economic analysis model: User manual, volume 2
[DE90-010654] N91-16223
Microwave coupling on printed circuit boards
[DE90-011237] N91-16232
Design and fabrication of high voltage planar devices
[LAAS-90306] N91-16252
Integrated Numerical Experiments (INEX) and the Free-Electron Laser Physical Process Code (FELPPC)
[DE90-011957] N91-16348
A modular stiffness-based approach to rotating systems analysis N91-16400
Multimedia Environmental Pollutant Assessment System (MEPAS) sensitivity analysis of computer codes
[DE90-010005] N91-16445
Theoretical and experimental studies of baroclinic processes N91-16512
Framework for an efficient two filter GLOC monitor N91-16557
Understanding the adoption of Ada: Results of an industry survey
[AD-A226725] N91-16585
Reliability/Maintainability/Logistics support analysis Computer Aided Tailoring Software Program (R/M/L CATSOP)
[AD-A226820] N91-16588
BLAST2D computations of the reflection of planar shocks from wedge surfaces with comparison to SHARC and STEALTH results
[AD-A227261] N91-16589
National software capacity: Near-term study executive summary
[AD-A227564] N91-16590
Some generalizations of the criss-cross method for quadratic programming
[REPT-90-52] N91-16599
Annotated bibliography of software engineering laboratory literature
[NASA-TM-103415] N91-16602
The Assistant for Specifying the Quality Software (ASQS). Volume 1: Operational concept document
[AD-A227893] N91-16608
The Assistant for Specifying the Quality Software (ASQS). Volume 2: User's manual. Volume 2
[AD-A227894] N91-16609
A software development specification for nonlinear structural analysis
[AD-A228427] N91-16614
XSHELL: A general purpose expert system shell
[AD-A228454] N91-16616
Practical aspects of repository operations for the Software Technology for Adaptable, Reliable Systems (STARS) program
[AD-A228455] N91-16617
Briefing DTD user's guide for the Software Technology for Adaptable, Reliable Systems (STARS) program
[AD-A228473] N91-16618
DTD creation for the Software Technology for Adaptable, Reliable Systems (STARS) program
[AD-A228475] N91-16619
Supporting reuse and evolution in software design
[AD-A228782] N91-16624
Towards conservative reliability predictions for real-time software
[NASA-CR-187863] N91-16627
THERMOPT: An optimizer for ESATAN models
[MBB/FW522/S/PUB/427] N91-16630
Horizontal fault tolerance in a fully distributed loosely coupled environment
[AD-A227972] N91-16638
ADRPM-VII applied to the long-range acoustic detection problem N91-16689
Electromagnetic computations for fusion devices
[DE90-011097] N91-16765
Investigation and modeling of radiation absorption processes and opacities in dense plasmas
[AD-A228749] N91-16779
Theoretical studies of electron transport in quantum-well structures
[AD-A228429] N91-16819

COMPUTER STORAGE DEVICES
Properties and characterization of thin film ferroelectric capacitors for nonvolatile memories
[DE91-004037] N91-16242
PC-based digital imaging for storing microscopy images for surveillance programs
[DE90-010080] N91-16738

COMPUTER SYSTEMS DESIGN
Microsupercomputers: Design and implementation
[AD-A228741] N91-16571
Microsupercomputers: Design and implementation
[AD-A228744] N91-16572
Tailoring an Ada runtime environment proof-of-concept
[AD-A227767] N91-16593
Research into the design and implementation of knowledge base systems
[AD-A228873] N91-16843

COMPUTER SYSTEMS PERFORMANCE
A block QR factorization algorithm for rank-deficient matrices
[DE90-010066] N91-16573
Distributed System Modeling Environment (DSME)
[AD-A226698] N91-16583
Hartstone benchmark results and analysis
[AD-A226817] N91-16587

COMPUTER SYSTEMS SIMULATION
A trellis-searched APC (Adaptive Predictive Coding) speech coder
[DE91-000866] N91-16581
Analysis of parallel, replicated simulations under a completion time constraint
[AD-A228292] N91-16613

COMPUTER TECHNIQUES
IFDIS: An expert system for diagnosis of failures in jet aircraft engines
[AD-A227757] N91-16020
Computer aided physiological assessment of the functional state of pilots during simulated flight N91-16562
Validity study in multidimensional latent space and efficient computerized adaptive testing
[AD-A227742] N91-16650
Computational physics at the National Energy Research Supercomputer Center
[DE90-010283] N91-16672
Using computer-generated protocols to study writers' planning strategies
[AD-A228875] N91-16844

COMPUTER VISION
Ultrasound and visual sensor feedback and fusion
[DE90-005280] N91-16369
Real-time vergence control for binocular robots
[AD-A228817] N91-16387

COMPUTERIZED SIMULATION
Large-scale numerical aerodynamic simulations for complete aircraft configurations
[NAL-TR-1073-T] N91-15984
Numerical analysis of viscous hypersonic flow past a generic forebody
[MBB/FE122/S/PUB/0407] N91-15997
Spray combustion modeling and evaluation
[NASA-CR-187887] N91-16078
High resolution electron microscopy of interfaces in fcc materials
[DE91-004420] N91-16101
Atomic-scale simulation of adhesion between metallic surfaces
[DE91-004722] N91-16127
Initial parametric results using CYCLEZ: A LMTD-specified, Lorenz-Meutzner cycle refrigerator-freezer model
[DE90-010146] N91-16175
Some topics of Navier-Stokes solvers N91-16269
Simulation of excited shear flows N91-16270
Numerical simulation of buffer flow in a free flow electrophoresis chamber N91-16279
Far-field boundaries and their numerical treatment N91-16281
Evaluation of the HULL and SHARC hydrocodes in simulating the reflection of Mach 2.12 non-decaying shock on wedges of various angles
[AD-A227581] N91-16287
Integrated Numerical Experiments (INEX) and the Free-Electron Laser Physical Process Code (FELPPC)
[DE90-011957] N91-16348
Evaluation of crop transpiration with remote sensing and computer simulation models
[REPT-1] N91-16431
Monte Carlo simulation of atmospheric neutron transport at high altitudes using MCNP
[AD-A226773] N91-16474
Computer simulations of medium wavelength irregularities in the equatorial ionosphere resulting from artificially produced density enhancements
[MPE-PREPRINT-186] N91-16496
Distributed System Modeling Environment (DSME)
[AD-A226698] N91-16583
BLAST2D computations of the reflection of planar shocks from wedge surfaces with comparison to SHARC and STEALTH results
[AD-A227261] N91-16589
The computer simulation of digital recording systems
[BBC-RD-1990/14] N91-16595
Optimization of a power transient stability program on a vector supercomputer: Theory and applications
[AD-A227884] N91-16607
Distributed algorithm simulation using input/output automata
[AD-A228113] N91-16611
Artificial intelligence technologies applied to terrain analysis
[DE90-011985] N91-16642
Computational physics at the National Energy Research Supercomputer Center
[DE90-010283] N91-16672
Investigation and modeling of radiation absorption processes and opacities in dense plasmas
[AD-A228749] N91-16779
Dynamical properties of two-dimensional Josephson junction arrays N91-16823
Data base structure to support the production of the digital bathymetric data base
[AD-A227915] N91-16841
M51's spiral structure N91-16938
The spiral-compact galaxy pair AM 2208-251: Computer simulations versus observations N91-16939
Simulation of disk-disk encounters with co-moving polar grids N91-16941
Typical motions in multiple systems N91-16945
Numerical simulations of interacting disk galaxies N91-16955
Do elliptical galaxies have thick disks N91-16962

COMPUTERS
Specialists at flight control center discuss shuttle computer systems N91-16040
Horizontal fault tolerance in a fully distributed loosely coupled environment
[AD-A227972] N91-16638
Geographic data transfer N91-16836

CONCENTRATING
Shear thickening of concentrated dispersions
[ETN-91-98477] N91-16308

CONCRETES
Evaluation procedure for reinforced concrete box culverts under airfield pavements
[AD-A227920] N91-16031

CONCURRENT PROCESSING
An O(log n) time common CRCW pram algorithm for minimum spanning tree
[AD-A228740] N91-16623
Vectorial and parallel algorithms in dynamic programming for optimal control problems
[LAAS-90256] N91-16629
Real-time system specification and verification
[AD-A227682] N91-16634
CONDENSATES
Comparison of SSM/I measurements to numerically-simulated cloud and precipitation during ERICA N91-16501
Global variability of water vapor and condensate from SSM/I N91-16507
CONDENSED MATTER PHYSICS
Quasiperiodic transition to chaos in Ge; and magnetic susceptibility of high-T(c) superconductors
[DE90-011304] N91-16797
CONDENSING
State of an adiabatic expanding and condensing vapor or slow, medium, and fast explosions into a vacuum
[DE90-010815] N91-16263
CONDUCTING FLUIDS
Circumfluous motion of a conductive liquid around solid objects in a magnetic field
[DE90-011335] N91-16265
CONDUCTING POLYMERS
Electronic and ionic transport in processable conducting polymers
[AD-A227857] N91-16154
CONFERENCES
The Proceedings of the Symposium on Mechanics for Space Flight 1989
[ISAS-SP-12] N91-16266
Preparations for a major international symposium on electricity and the environment
[DE90-010539] N91-16449
Climate Caucus report: Opportunities for bridging the gaps from effects to impacts
[DE90-010877] N91-16459
Fourth International Symposium on Long-Range Sound Propagation
[NASA-CP-3101] N91-16682
Calendar of selected aeronautical and space meetings: January 1991 onwards
[AGARD-CAL-91/1] N91-16833
IEEE International Symposium on Information Theory
[AD-A228239] N91-16842
Paired and Interacting Galaxies: International Astronomical Union Colloquium No. 124
[NASA-CP-3098] N91-16858
Paired and interacting galaxies: Conference summary N91-16964
CONFIGURATION INTERACTION
Comparison of the quadratic configuration interaction and coupled cluster approaches to electron correlation including the effect of triple excitations
[NASA-CR-187855] N91-16727
Triple and quadruple excitation contributions to the binding in Be clusters: Calibration calculations on Be3
[NASA-TM-103391] N91-16728
CONFINEMENT
Materials systems for 2- to 5-micrometers wavelength diode lasers
[AD-A228218] N91-16361
CONGRESSIONAL REPORTS
Moving America; new directions, new opportunities: Assessment of the potential for magnetic levitation transportation systems in the United States
[PB91-104596] N91-16388
CONIFERS
Ozone and acid-precipitation on western coniferous forests
[DE90-011014] N91-16462
CONSCIOUSNESS
Cerebral oxygen status and G-induced loss of consciousness N91-16554
CONSERVATION EQUATIONS
Finite element approximations for transonic flows
[ETN-91-98491] N91-15988
CONSERVATION LAWS
MmB: A new class of accurate high resolution schemes for conservation laws in two dimensions N91-16275
Asymptotic-induced numerical methods for conservation laws
[NASA-CR-187483] N91-16305
Limit behaviors of approximate solutions to conservation laws
[DE90-010069] N91-16646
CONTACT LENSES
The use of contact lenses in the civil airman population
[AD-A227450] N91-16544
CONTACT RESISTANCE
Measurements of 1/f noise in a-Si:H pin diodes and thin-film-transistors
[DE90-011218] N91-16228
CONTAMINANTS
Method of making contamination-free ceramic bodies
[NASA-CASE-LEW-14984-1] N91-16152
The Proceedings of the Symposium on Mechanics for Space Flight 1989
[ISAS-SP-12] N91-16266
Analysis of atmospheric diffusion of pollutants based on the limited observation of horizontal wind N91-16274
Multimedia Environmental Pollutant Assessment System (MEPAS) sensitivity analysis of computer codes
[DE90-010005] N91-16445
Monitoring challenges and innovative ideas
[DE91-000586] N91-16465
CONTAMINATION
Ion contamination of x ray pinhole camera images on PBFA 2
[DE90-012180] N91-16325
Improved anode catalysts for coal gas-fueled phosphoric acid fuel cells
[DE90-009683] N91-16442
Subsurface science program: Program overview and research abstracts
[DE90-010321] N91-16456
CONTINUOUS RADIATION
Materials systems for 2- to 5-micrometers wavelength diode lasers
[AD-A228218] N91-16361
CONTINUUM MECHANICS
Fermions in the hypercharge sector of the standard lattice electroweak theory: Global limit
[DE90-009731] N91-16827
CONTINUUM MODELING
Continuum models of continental deformation N91-16490
CONTROL EQUIPMENT
A paper-assessment of the performance of a modern airborne multi-mode pulse Doppler radar deployed as a ground-based fire-control radar
[ETN-91-98584] N91-16215
CONTROL SIMULATION
ERICC: Construction and application of the Command and Control Research Facility
[IZF-1989-55] N91-16213
CONTROL SURFACES
Aerodynamic surface pressure measurement in atmosphere and wind tunnel on a vertical axis wind turbine blade using pressure transducers N91-15980
Aeroservoelastic tailoring for lateral control enhancement N91-16025
CONTROL SYSTEMS DESIGN
An introduction to modern aero-engine control design
[ETN-91-98583] N91-16024
General designer describes Buran flight control, autopilot systems N91-16039
Sensor-based automated docking of large payloads
[DE90-011020] N91-16044
The NASA controls-structures interaction technology program
[NASA-TM-102752] N91-16057
A decentralized linear quadratic control design method for flexible structures
[NASA-CR-187860] N91-16059
Safety as a design goal for applications of microelectronic control systems
[REPT-23/90] N91-16253
Electronically steerable arrays: Current and future technology and applications
[ETN-91-98581] N91-16254
Design of a telerobotic controller with joint torque sensors using 2-port network theory
[NASA-CR-186543] N91-16379
NASA Laboratory telerobotic manipulator control system architecture
[NASA-CR-187751] N91-16385
The PHD: A Planar, Harmonic Drive robot for joint torque control
[NASA-CR-187924] N91-16386
Real-time vergence control for binocular robots
[AD-A228817] N91-16387
Modeling and control of a two-arm elastic robot in gravity N91-16389
Implementation and simulation of the manufacturing systems control coordination level: A mixed approach of Petri nets and rule-based systems
[LAAS-90355] N91-16645
Analysis of multivariable control systems in the presence of structured uncertainties
[AD-A227976] N91-16665
CONTROL THEORY
Wind tunnel tests on flutter control of a high-aspect-ratio cantilevered wing: Control with leading-edge and trailing-edge control surfaces
[NAL-TR-1070] N91-15982
CONTROLLABILITY
Longitudinal stability augmentation of a lightweight fighter aircraft model
[ETN-91-98585] N91-16026
CONTROLLED FUSION
D3-D research operations
[DE90-008232] N91-16752
Plasma-facing materials
[DE90-008243] N91-16753
CONTROLLERS
Wind tunnel tests on flutter control of a high-aspect-ratio cantilevered wing: Control with leading-edge and trailing-edge control surfaces
[NAL-TR-1070] N91-15982
An introduction to modern aero-engine control design
[ETN-91-98583] N91-16024
CONVECTION
Numerical simulation of buffer flow in a free flow electrophoresis chamber N91-16279
A study of the interaction of physical and numerical parameterizations with regard to moisture forecasting in a regional model of the atmosphere
[AD-A227966] N91-16488
Planetary circulations in the presence of transient and self-induced heating N91-16505
The effect of latent heat release on synoptic-to-planetary wave interactions and its implication for satellite observations: Theoretical modeling N91-16514
An investigation of a gravity wave during GALE: February 6, 1986
[AD-A227655] N91-16519
Prediction of tropical cyclone rapid intensification events
[AD-A227668] N91-16520
The vertical structure of the marine atmospheric boundary layer across a sea surface temperature front
[AD-A227931] N91-16525
An automatic ordering method for incomplete factorization iterative solvers
[DE91-001974] N91-16659
Stellar convection and dynamo theory N91-16857
CONVECTION CELLS
Rotating Rayleigh-Benard convection: The Kueppers-Lortz transition
[DE91-004835] N91-16288
CONVECTION CLOUDS
Numerical simulation of aerosol scavenging by ice-bearing convective clouds
[DE90-010676] N91-16457
Parameterization of aerosol scavenging in a convective cloud model
[DE90-010865] N91-16458
CONVECTIVE FLOW
Computation of turbulent flow about unconventional airfoil shapes N91-15992
Numerical simulation of buffer flow in a free flow electrophoresis chamber N91-16279
Natural-convection boundary layers
[ISBN-90-9003467-6] N91-16313
Laboratory and theoretical models of planetary-scale instabilities and waves N91-16511
Theoretical and experimental studies of baroclinic processes N91-16512
CONVECTIVE HEAT TRANSFER
Transient natural convection in heated inclined tubes
[DE90-008217] N91-16255
Rotating Rayleigh-Benard convection: The Kueppers-Lortz transition
[DE91-004835] N91-16288
CONVERGENCE
Real-time vergence control for binocular robots
[AD-A228817] N91-16387
An automatic ordering method for incomplete factorization iterative solvers
[DE91-001974] N91-16659
Pathwise convexity and its relation to convergence of time-average derivatives
[AD-A228888] N91-16662
CONVEXITY
High frequency scattering by a smooth coated cylinder simulated with generalized impedance boundary conditions
[NASA-CR-187829] N91-16211
A sign-changing global minimizer on a convex domain
[REPT-90-57] N91-16655
Pathwise convexity and its relation to convergence of time-average derivatives
[AD-A228888] N91-16662

COOLERS
Evaporation process and 3 phase flow in a water evaporator assembly
[MBB-UO-0108-90-PUB] N91-16060
COOLING
Spontaneous force optical traps
[AD-A228539] N91-16363
Use of satellite data and modeling to assess the influence of stratospheric processes on the troposphere N91-16517
Modeling the performance of water and liquid gallium cooled x ray optical components: A comparison with experiment
[DE90-010460] N91-16784
COOLING SYSTEMS
Initial parametric results using CYCLEZ: A LMTD-specified, Lorenz-Meutzner cycle refrigerator-freezer model
[DE90-010146] N91-16175
ASTROMAG coil cooling study
[NASA-CR-187768] N91-16813
COORDINATES
On a class of unsteady three-dimensional Navier Stokes solutions relevant to rotating disc flows: Threshold amplitudes and finite time singularities
[NASA-CR-187482] N91-15991
Smoothing and scaling airfoil coordinates on a personal computer
[DE89-000878] N91-16582
COPOLYMERIZATION
Model filled polymers versus synthesis of crosslinked monodisperse polymethacrylate beads
[AD-A227236] N91-16146
COPOLYMERS
Photoinduced charge separation by polymer-bound chromophores
[DE90-010997] N91-16140
COPPER ALLOYS
Grain-boundary structure in ordered alloys
[ETN-91-98571] N91-16136
COPPER OXIDES
Novel applications of Tl-Ca-Ba-Cu-O thin films to active and passive high frequency devices
[DE91-004507] N91-16240
YBa2Cu3O(7-x) thin film growth on single crystal and polycrystalline yttria-stabilized zirconia
[DE90-010707] N91-16788
High Tc oxide solid state reaction kinetics via complex impedance spectroscopy
[DE90-011178] N91-16792
Dynamics of strong-coupling models for cuprate superconductors: Exact results on finite lattices
[DE90-011155] N91-16796
Microstructures and dc critical currents in textured Y-Ba-Cu-oxides
[DE91-000895] N91-16803
Observations of vortex structure in YBa2Cu3O7
[DE91-000900] N91-16804
From low to high Tc: An ultrasonic investigation of niobium single crystal and YBaCuO superconducting thin films with surface acoustic waves N91-16822
CORES
Excursions to the base of the mantle N91-16491
Are extremely luminous far-infrared galaxies the result of merging quasar cores N91-16912
An experimental study of counter-rotating cores in elliptical galaxies N91-16934
CORONAS
Cool infalling gas and its interaction with the hot ISM of elliptical galaxies N91-16915
Triplets of galaxies: Their dynamics, evolution, and the origin of chaos in them N91-16948
CORRELATION
Morphological type correlation between nearest neighbor pairs of galaxies N91-16861
Correlation functions for pairs and groups of galaxies N91-16879
Correlations between environmental parameters and nuclear activity N91-16920
CORROSION
High temperature corrosion of alloys in mixed gases N91-16121
CORROSION PREVENTION
Assessment of corrosion resistant coatings for a depleted U-0.75 Ti alloy
[AD-A228237] N91-16130
CORROSION RESISTANCE
Assessment of corrosion resistant coatings for a depleted U-0.75 Ti alloy
[AD-A228237] N91-16130
CORROSION TESTS
The influence of small SO2 contents on the corrosion behavior for NiCrAl alloys in temperature zone from 1000 to 1100 C
[JUEL-2362] N91-16134
COSMIC DUST
A spiral-like disk of ionized gas in IC 1459: Signature of a merging collision N91-16889
The polar-ring galaxies NGC 2685 and NGC 3808B (VV 300) N91-16892
Infrared images of merging galaxies N91-16904
Central activity in 60 micron peakers N91-16913
The galactic center at submillimeter and far-infrared wavelengths
[MPE-PREPRINT-190] N91-16978
COSMIC GASES
The H I content of non-isolated galaxies N91-16883
Simulations of gas clouds in interacting galaxies N91-16961
COSMIC RAYS
Interpretation of the diffusive galactic continuum gamma radiation in MeV area
[MPE-220] N91-16983
COSMOCHEMISTRY
Spectrometric, chemical, and cosmological development of galaxies
[ETN-91-98555] N91-16972
COSMOLOGY
Observational properties of compact groups of galaxies N91-16871
A tentative explanation of cosmological red shift N91-16928
On the large-scale structures formed by wakes of open cosmic strings N91-16951
The best-fit universe
[DE91-004583] N91-16966
COST EFFECTIVENESS
Aerodynamic surface pressure measurement in atmosphere and wind tunnel on a vertical axis wind turbine blade using pressure transducers N91-15980
COST ESTIMATES
Impacts of advanced manufacturing technology on parametric estimating
[AD-A228232] N91-16177
Definition and preliminary design of the Laser Atmospheric Wind Sounder (LAWS) phase 1. Volume 3: Program cost estimates
[NASA-CR-184073] N91-16334
Technological management as an element of strategy for an efficient company management
[MBB-Z-0307-90-PUB] N91-16834
COST REDUCTION
Low-cost, high-resolution telescopes for imaging low-earth orbit satellites
[DE90-012081] N91-16850
COSTS
The European flight safety crisis: Costs and solution
[ETN-91-98490] N91-16000
COUETTE FLOW
Streamwise vortices in laminar-turbulent transition N91-16297
COUNTER ROTATION
Streamwise vortices in laminar-turbulent transition N91-16297
The double nucleus galaxies Mkn 423 and Mkn 739 N91-16891
An experimental study of counter-rotating cores in elliptical galaxies N91-16934
COUPLERS
Lamina transducer coupler and method of making
[NASA-CASE-LAR-14361-1] N91-16707
COUPLING COEFFICIENTS
Air-ground interface: Surface waves, surface impedance and acoustic-to-seismic coupling coefficient N91-16685
CRACK PROPAGATION
Mechanical property data on aluminum alloy 7150-T7751 plate
[AD-A227506] N91-16124
Elevated temperature crack growth in titanium aluminides
[AD-A227700] N91-16125
Dynamic crack propagation in elastic-plastic solids N91-16402
Attenuation of seismic waves in the near-source region
[AD-A226814] N91-16475
CRACK TIPS
Dynamic crack propagation in elastic-plastic solids N91-16402
CRACKING (FRACTURING)
Weldability of nickel aluminides
[DE90-008557] N91-16116
HAZ liquation cracking behavior in newly developed lean 316 stainless steels
[DE90-009409] N91-16117
Test methods for evaluating hot cracking: Review and perspective
[DE90-009820] N91-16397
CRACKS
Mechanics of interface cracks
[AD-A227579] N91-16067
CRASHWORTHINESS
Development of a crashworthy seat for commuter aircraft
[AD-A227486] N91-15999
CREEP ANALYSIS
Inelastic strain analysis of solder joint in NASA fatigue specimen
[NASA-CR-187864] N91-16132
CREEP PROPERTIES
Elevated temperature crack growth in titanium aluminides
[AD-A227700] N91-16125
Modeling and identification of cumulative creep fatigue damage in an austenitic stainless steel N91-16131
Sintering stress and microstructure in ceramic powder compacts
[DE91-004415] N91-16149
CROSS CORRELATION
A case study of the 19 October 1989 polar cap absorption event using the imaging riometer for ionospheric studies
[AD-A227764] N91-16487
CROSS POLARIZATION
The reflection and transmission properties of a triple band dichroic surface
[NASA-CR-187776] N91-16191
CROSSLINKING
Model filled polymers versus synthesis of crosslinked monodisperse polymethacrylate beads
[AD-A227236] N91-16146
CRUCIBLES
High temperature furnace modeling and performance verifications
[NASA-CR-187831] N91-16032
CRYOGENIC EQUIPMENT
ASTROMAG coil cooling study
[NASA-CR-187768] N91-16813
CRYOGENICS
Debris/Ice/TPS assessment and photographic analysis for shuttle mission STS-41
[NASA-TM-103814] N91-16041
CRYPTOGRAPHY
IEEE International Symposium on Information Theory
[AD-A228239] N91-16842
CRYSTAL DISLOCATIONS
Grain-boundary structure in ordered alloys
[ETN-91-98571] N91-16136
Domain boundaries formed during epitactical growth of alpha-Al2O3
[DE91-005018] N91-16814
CRYSTAL GROWTH
Theory of non-equilibrium growth
[DE91-004159] N91-16725
YBa2Cu3O(7-x) thin film growth on single crystal and polycrystalline yttria-stabilized zirconia
[DE90-010707] N91-16788
Thin film single crystal growth of a nonlinear optical polymer
[AD-A227692] N91-16807
Hanging drop crystal growth apparatus
[NASA-CASE-MFS-26061-1] N91-16815
The role of ledges in phase transformations
[AD-A228750] N91-16821
CRYSTAL LATTICES
Molecular crystals and localized vibrational states
[DE90-010602] N91-16786
Dynamics of strong-coupling models for cuprate superconductors: Exact results on finite lattices
[DE90-011155] N91-16796
Correlation between the elastic-shear-instability-mechanism and empirical criteria for irradiation-induced amorphization
[DE91-004481] N91-16810
Characterization of GaAs/Si interface structure by x ray diffraction
[DE91-004769] N91-16811
CRYSTAL STRUCTURE
Atomic and electronic structure of metals and alloys: Clean surfaces and chemisorbed molecules
[DE91-000267] N91-16123
Atomic-scale simulation of adhesion between metallic surfaces
[DE91-004722] N91-16127
Grain-boundary structure in ordered alloys
[ETN-91-98571] N91-16136
Molecular crystals and localized vibrational states
[DE90-010602] N91-16786
A photoemission study of samarium on silicon
[DE90-011509] N91-16799
Far-infared laser spectroscopy of two dimensional holes in strained-layer heterostructure and superlattices
[DE91-000027] N91-16805
Characterization of GaAs/Si interface structure by x ray diffraction
[DE91-004769] N91-16811

CRYSTAL SURFACES
Chemisorption of carbon monoxide on three metal surfaces: Ni(111), Pd(111) and Pt(111): A comparative study
[AD-A228579] N91-16108
CRYSTALLIZATION
Control of industrial crystallizers: The physical aspects
[ETN-91-98488] N91-16179
The role of ledges in phase transformations
[AD-A228750] N91-16821
CRYSTALLOGRAPHY
Atomic-scale simulation of adhesion between metallic surfaces
[DE91-004722] N91-16127
CRYSTALS
In situ studies of potential dependent structural and distributional changes at electrochemical interfaces with x rays
[AD-A226844] N91-16098
Control of industrial crystallizers: The physical aspects
[ETN-91-98488] N91-16179
Quasiperiodic transition to chaos in Ge; and magnetic susceptibility of high-T(c) superconductors
[DE90-011304] N91-16797
A photoemission study of samarium on silicon
[DE90-011509] N91-16799
Hanging drop crystal growth apparatus
[NASA-CASE-MFS-26061-1] N91-16815
The role of ledges in phase transformations
[AD-A228750] N91-16821
CUES
Changes in somatosensory responsiveness in behaving monkeys
[AD-A226832] N91-16540
CUMULATIVE DAMAGE
Modeling and identification of cumulative creep fatigue damage in an austenitic stainless steel N91-16131
CURING
The University of Arizona program in solid propellants N91-16165
CURRENT DENSITY
Study on ECW transmission lines for NET/ITER
[EUR-FU/80/90-99] N91-16781
CURVE FITTING
Visualization of surfaces in four-dimensional space
[AD-A227858] N91-16605
CUTTERS
Deburring and surface finishing: The past ten years and projections for the next ten years
[DE91-000579] N91-16176
CYANIDES
Electrocatalysis of anodic and cathodic oxygen-transfer reactions
[DE91-000611] N91-16100
CYCLIC LOADS
Modeling and identification of cumulative creep fatigue damage in an austenitic stainless steel N91-16131
CYCLOGENESIS
The effect of latent heat release on synoptic-to-planetary scale wave interactions and implications for satellite observations: Observational study N91-16515
Prediction of tropical cyclone rapid intensification events
[AD-A227668] N91-16520
CYCLONES
Comparison of SSM/I measurements to numerically-simulated cloud and precipitation during ERICA N91-16501
Synoptic/planetary-scale interactions and blocking over the North Atlantic Ocean N91-16513
The effect of latent heat release on synoptic-to-planetary scale wave interactions and implications for satellite observations: Observational study N91-16515
Prediction of tropical cyclone rapid intensification events
[AD-A227668] N91-16520
CYCLOTRON RADIATION
Multiple-photon Compton scattering in a strong magnetic field: Cross-sections and radiative transport N91-16852
CYCLOTRON RESONANCE DEVICES
Mode competition effects in free electron lasers and gyrotrons
[DE90-011084] N91-16346
Microwave generation for magnetic fusion energy applications, task B
[DE90-011079] N91-16763
Microwave generation for magnetic fusion energy applications, task C
[DE90-011080] N91-16764
CYCLOTRONS
Properties of superdeformed bands in the A = 194 region
[DE90-011482] N91-16798
CYGNUS CONSTELLATION
A non-LTE analysis of a sample of O stars selected from galactic OB associations N91-16854
CYLINDERS
High frequency scattering by a smooth coated cylinder simulated with generalized impedance boundary conditions
[NASA-CR-187829] N91-16211
Simulation of the flow past an impulsively started cylinder using a discrete vortex method N91-16303
CYLINDRICAL COORDINATES
On a class of unsteady three-dimensional Navier Stokes solutions relevant to rotating disc flows: Threshold amplitudes and finite time singularities
[NASA-CR-187482] N91-15991
CYLINDRICAL SHELLS
Passive damping concepts for tubular beams with partial rotational and translational end restraints
[NASA-CR-187833] N91-16411

D

DAMAGE ASSESSMENT
Cellular track model of biological damage to mammalian cell cultures from galactic cosmic rays
[NASA-TP-3055] N91-16981
DAMPING
Dynamic aspects of scanning surface instruments and microscopes
[ME-84] N91-16339
DARK MATTER
Pairs of galaxies in low density regions of a combined redshift catalog N91-16860
Dynamics of groups around interacting double ellipticals: Measuring dark matter haloes N91-16863
Dragging force on galaxies due to streaming dark matter N91-16947
Triplets of galaxies: Their dynamics, evolution, and the origin of chaos in them N91-16948
On the large-scale structures formed by wakes of open cosmic strings N91-16951
The best-fit universe
[DE91-004583] N91-16966
DATA ACQUISITION
A low-cost infrared telemetry system for kilohertz-bandwidth data acquisition
[DE90-010616] N91-16042
A graphical user-interface-driven waveform data acquisition and analysis system
[DE90-011948] N91-16578
Annotated bibliography of software engineering laboratory literature
[NASA-TM-103415] N91-16602
DATA BASE MANAGEMENT SYSTEMS
A query model and query and knowledge definition languages for object-oriented databases N91-16580
Parallel Access Main Memory (PAMM) user's manual, version 1.0
[AD-A227744] N91-16635
The USAF STINFO program overview
[AD-A226969] N91-16838
Data base structure to support the production of the digital bathymetric data base
[AD-A227915] N91-16841
DATA BASES
Hypersonic shock/boundary-layer interaction database
[NASA-CR-187769] N91-15986
Jet engine performance estimation from minimal input data
[ETN-91-98582] N91-16023
Cartographic issues in the development of a digital GRASS database
[AD-A227582] N91-16416
Procedure for the correction of errors in the DUTSCAT data 1987/1988
[BCRS-90-14] N91-16430
A query model and query and knowledge definition languages for object-oriented databases N91-16580
Subject bibliography of the PMA 205 (Program Manager Air 205) network technical library at Oak Ridge National Laboratory
[DE90-009988] N91-16835
The StarLite project
[AD-A226722] N91-16837
Data base structure to support the production of the digital bathymetric data base
[AD-A227915] N91-16841
A normative database for, and analysis of, the dual task of the TASKOMAT
[IZF-1990-A-11] N91-16846
DATA COMPRESSION
Real-time filtering and detection of dynamics for compression of HDTV
[NASA-CR-187777] N91-16596
Data base structure to support the production of the digital bathymetric data base
[AD-A227915] N91-16841
IEEE International Symposium on Information Theory
[AD-A228239] N91-16842
DATA CONVERTERS
The design of a meteorological facsimile converter
[ETN-91-98578] N91-16528
DATA MANAGEMENT
Extraction of marketable information from ERS-1 data
[BCRS-90-03] N91-16425
Contents of the NASA ocean data system archive, version 11-90
[NASA-CR-187812] N91-16535
Management information: A key to better acquisition at NIH
[AD-A226867] N91-16830
DATA PROCESSING
Magsat investigations over the greater African region N91-16415
Extraction of marketable information from ERS-1 data
[BCRS-90-03] N91-16425
Seismic signal processing optimized for a specific source and receiver
[DE90-010189] N91-16468
Observation simulation experiments with regional prediction models N91-16502
Synoptic/planetary-scale interactions and blocking over the North Atlantic Ocean N91-16513
Potential vorticity index N91-16516
A sectorial analysis of the information sector in the information economy: Its comparative measurement and new classification model N91-16845
DATA RECORDING
The computer simulation of digital recording systems
[BBC-RD-1990/14] N91-16595
DATA SIMULATION
Dynamics and configurations of galaxy triplets N91-16946
DATA STORAGE
Practical aspects of repository operations for the Software Technology for Adaptable, Reliable Systems (STARS) program
[AD-A228455] N91-16617
Briefing DTD user's guide for the Software Technology for Adaptable, Reliable Systems (STARS) program
[AD-A228473] N91-16618
The USAF STINFO program overview
[AD-A226969] N91-16838
Data base structure to support the production of the digital bathymetric data base
[AD-A227915] N91-16841
DATA STRUCTURES
Distributed issues for Ada real-time systems
[AD-A227852] N91-16603
Geographic data transfer N91-16836
Data base structure to support the production of the digital bathymetric data base
[AD-A227915] N91-16841
DATA TRANSFER (COMPUTERS)
Geographic data transfer N91-16836
DATA TRANSMISSION
The high speed buffer board: A SAIL EIA-485 communications accelerator card for the vector measuring current meter
[AD-A227181] N91-16185
Movable-boundary channel-access schemes for integrated voice/data networks
[AD-A227331] N91-16186
DEBRIS
Debris/Ice/TPS assessment and photographic analysis for shuttle mission STS-41
[NASA-TM-103814] N91-16041
DECAY RATES
Theoretical topics in B-physics
[DE91-004911] N91-16726
DECELERATION
Stellar kinematics of elliptical galaxies in pairs N91-16862
DECISION MAKING
Specialists at flight control center discuss shuttle computer systems N91-16040
Modeling and verification of distributed systems with labeled predicate transition nets
[LAAS-90215] N91-16214
International decision making and global climate change: Lessons of prior resource management efforts for consensus building
[DE90-010714] N91-16454
Intelligent assistant systems: An artificial intelligence approach to detecting performance degradation and pilot incapacitation N91-16564
DECONTAMINATION
Removal of NO and NO2 from contaminated atmospheres
[AD-A227260] N91-16565
DEDUCTION
Skolem functions and equality in automated deduction
[DE90-009703] N91-16641

DEFECTS
High resolution electron microscopy of interfaces in fcc materials
[DE91-004420] N91-16101
Development of nondestructive evaluation methods and prediction of effects of flaws on the fracture behavior of structural ceramics
[DE90-011092] N91-16141
Deburring and surface finishing: The past ten years and projections for the next ten years
[DE91-000579] N91-16176

DEFENSE PROGRAM
Tactical fighter aircraft: Differences between the Air Force's roadmap and the five year defense plan
[AD-A228882] N91-15976

DEFORMATION
Study of the influence of imperfections on the dynamic stability of tanks
[DE90-011094] N91-16398
Finite element solution of steady state axisymmetric penetration problems N91-16403
New methods for producing, recording, and processing interferometric moire patterns N91-16405
Continuum models of continental deformation N91-16490

DEGRADATION
Ultrasensitive molecular fluorescence spectroscopy in levitated microdroplets
[DE91-000621] N91-16095
Tensile behavior of tungsten/niobium composites at 1300 to 1600 K
[NASA-TM-103727] N91-16128

DEGREES OF FREEDOM
Resolution of the 1D regularized Burgers equation using a spatial wavelet approximation
[NASA-CR-187480] N91-16664

DELTA WINGS
The Proceedings of the Symposium on Mechanics for Space Flight 1989
[ISAS-SP-12] N91-16266
Unsteady vortex lattice calculation of the flow around a slender delta wing N91-16272

DEMODULATION
Near/far resistant receivers for DS/SSMA communications
[AD-A228147] N91-16200

DEMODULATORS
Near/far resistant receivers for DS/SSMA communications
[AD-A228147] N91-16200

DENSE PLASMAS
Scaling laws for femtosecond laser-plasma interactions
[DE90-011496] N91-16769
Investigation and modeling of radiation absorption processes and opacities in dense plasmas
[AD-A228749] N91-16779

DENSITY (MASS/VOLUME)
H I studies of the sculptor group galaxies N91-16876

DENSITY (NUMBER/VOLUME)
Pairs of galaxies in low density regions of a combined redshift catalog N91-16860

DENSITY MEASUREMENT
From visco-elasticity towards thermal relaxation: A neutron scattering study of density fluctuations in fluid helium
[ETN-91-98486] N91-16111

DEPOLARIZATION
Scattering and depolarization by rough terrain and sea: A unified full wave approach
[AD-A228295] N91-16201

DEPOSITION
Hydrogen storage in metal hydrides
[AD-A228150] N91-16103
Ion beam modification of surface for improved high temperature performance
[AD-A228067] N91-16243
Research and development on advanced silicon carbide thin film growth techniques and fabrication of high power and microwave frequency silicon carbide-based device
[AD-A228758] N91-16246
Particle deposition in granular media
[DE90-010810] N91-16261

DESERTS
Image-based terrain modeling with thematic mapper N91-16418

DESIGN ANALYSIS
Applications of fuzzy theories to multi-objective system optimization
[NASA-CR-177573] N91-16012
Human factors design guidance during the conceptual design phase of system development: A methodological approach
[AD-A224667] N91-16552

DESORPTION
Desorption of H2O and H2 from steel and LiAO2 by temperature programmed desorption
[DE90-011170] N91-16118
Thermal desorption studies of isotopically-labeled oxygen-induced superconductivity in La2CuO(4+delta)
[DE91-004898] N91-16812

DESTRUCTION
Destruction of propellant components in supercritical water
[DE90-010600] N91-16085

DETECTION
Laser microplasma-gas chromatography detector. 2: Detection of species-specific fragment emission
[AD-A228373] N91-16106
Surface analysis by low-energy ion scattering: Two-dimensional detection and quantification
[ETN-91-98474] N91-16133
Detection of solid lubricant film failure during sliding by vibration monitoring
[NAL-TR-1060] N91-16384
ADRPM-VII applied to the long-range acoustic detection problem N91-16689
Effect of wind and temperature gradients on received acoustic energy N91-16697

DETONATION
Graphical analysis of barrel-tamped explosively accelerated flyer plates
[DE90-010299] N91-16026

DEUTERIUM
Deep inelastic structure functions from electron scattering on hydrogen, deuterium, and iron at 0.6 GeV2 less than or equal to Q2 less than or equal to 30.0 GeV2
[DE90-010169] N91-16785

DIAGNOSIS
Lamina transducer coupler and method of making
[NASA-CASE-LAR-14361-1] N91-16707

DIAMETERS
High speed narrow bore capillary gas chromatography
[ETN-91-98481] N91-16113

DIAMONDS
On the development of in-situ Raman analysis of plasma deposited diamond
[AD-A227453] N91-16147

DICHROISM
The reflection and transmission properties of a triple band dichroic surface
[NASA-CR-187776] N91-16191

DIELECTRIC PROPERTIES
Natural waves of microstrip transmission lines in wave guides
[BER-68] N91-16251
The dielectric properties of wet soils
[BCRS-90-13] N91-16429

DIELECTRICS
The reflection and transmission properties of a triple band dichroic surface
[NASA-CR-187776] N91-16191
Nonradiative dielectric waveguide millimetre-wave integrated circuits: A review
[AD-A227760] N91-16238
Angular dependence of thin-film dielectric coating damage thresholds
[DE91-000237] N91-16351

DIESEL ENGINES
Technical and economic evaluation of diesel engine with oxygen enrichment and water injection
[DE90-009723] N91-16373
Heat engines program
[DE90-010276] N91-16374
Vehicular sources in acoustic propagation experiments N91-16690

DIFFERENTIAL EQUATIONS
Periodic solutions of neutral differential equations
[RR-390] N91-16658
An automatic ordering method for incomplete factorization iterative solvers
[DE91-001974] N91-16659
Sparse representation of smooth linear operators
[AD-A228142] N91-16660
A free boundary problem arising in plasma physics
[DE90-010065] N91-16754

DIFFRACTION
High-frequency techniques for RCS prediction of plate geometries
[NASA-CR-187865] N91-16212
A convenient system for diffraction moire measurements
[DE90-010980] N91-16739

DIFFRACTION PATTERNS
A convenient system for the manufacture of holographic diffraction gratings
[DE90-009481] N91-16319
Research on certain aspects of laser diffraction particle size analysis relevant to autonomous self-diagnosing instrumentation
[AD-A226822] N91-16354
New methods for producing, recording, and processing interferometric moire patterns N91-16405
Automatic, high-resolution analysis of low-noise fringes
[DE90-009779] N91-16574

DIFFUSE RADIATION
Interpretation of the diffusive galactic continuum gamma radiation in MeV area
[MPE-220] N91-16983

DIFFUSION
Understanding the interdiffusion behavior and determining the long term stability of tungsten fiber reinforced niobium-base matrix composite systems
[NASA-CR-187396] N91-16120
High temperature corrosion of alloys in mixed gases N91-16121
Turbulence and diffusion in the atmospheric boundary layer
[DE90-011582] N91-16471
An automatic ordering method for incomplete factorization iterative solvers
[DE91-001974] N91-16659
Comparison of hydrogen diffusion in Ti2PdH(x) to the behavior for Ti2CuH(x) and Zr2PdH(x)
[DE91-002711] N91-16808

DIGITAL DATA
Cartographic issues in the development of a digital GRASS database
[AD-A227582] N91-16416
Geographic data transfer N91-16836
Data base structure to support the production of the digital bathymetric data base
[AD-A227915] N91-16841

DIGITAL ELECTRONICS
Digital time interpolator
[DIGEL-1990-4] N91-16249

DIGITAL SYSTEMS
Research in optical symbolic tasks
[AD-A228797] N91-16551
The computer simulation of digital recording systems
[BBC-RD-1990/14] N91-16595
PC-based digital imaging for storing microscopy images for surveillance programs
[DE90-010080] N91-16738
Managing emerging technology: Case studies in document imaging systems
[AD-A227688] N91-16839
Data base structure to support the production of the digital bathymetric data base
[AD-A227915] N91-16841

DIGITAL TECHNIQUES
Time interpolator
[DIGEL-1990-3] N91-16337

DIMENSIONAL STABILITY
Studies of the fundamentals of solids state batteries
[AD-A228772] N91-16247
Analysis of multivariable control systems in the presence of structured uncertainties
[AD-A227976] N91-16665

DIMENSIONS
Limits of human visual discrimination: Toward a general model of visual geometry
[AD-A226826] N91-16548
Visualization of surfaces in four-dimensional space
[AD-A227858] N91-16605

DIODES
The 1/f frequency noise effects on self-heterodyne linewidth measurements for coherent communications
[AD-A227942] N91-16195

DIPOLE ANTENNAS
The reflection and transmission properties of a triple band dichroic surface
[NASA-CR-187776] N91-16191
Tactical HF field expedient antenna performance, volume 1
[AD-A228057] N91-16198

DIRECT CURRENT
Dynamical properties of two-dimensional Josephson junction arrays N91-16823

DIRECTION
On leading spiral arms in close pairs of galaxies N91-16935

DISCONTINUITY
Study of time accuracy of flow variables across discontinuous boundaries N91-16300
Stochastic and chaotic effects in the ring laser N91-16359

DISILICIDES
A photoemission study of samarium on silicon
[DE90-011509] N91-16799

DISK GALAXIES
Using tilted-ring models and numerical hydrodynamics to study the structure, kinematics and dynamics of HI disks in galaxies N91-16851
The H I content of non-isolated galaxies N91-16883
A spiral-like disk of ionized gas in IC 1459: Signature of a merging collision N91-16889
A multiwavelength survey of interacting galaxies N91-16898
Infrared images of merging galaxies N91-16904
Simulation of disk-disk encounters with co-moving polar grids N91-16941
What determines the bulge to disk ratio of galaxies N91-16942
Collisional removal of HI from the inner disks of Virgo cluster galaxies N91-16952
Stationary orbits of satellites of disk galaxies N91-16954
Numerical simulations of interacting disk galaxies N91-16955
Dynamical experiments on models of colliding disk galaxies N91-16959
Simulations of gas clouds in interacting galaxies N91-16961
Do elliptical galaxies have thick disks N91-16962

DISPERSING
Aerosol cloud generation experiments [DE90-011051] N91-16264

DISPERSIONS
Shear thickening of concentrated dispersions [ETN-91-98477] N91-16308

DISPLACEMENT
A hydraulically driven microdisplacement unit [ME-56] N91-16392
Potential responses of landscape boundaries to global environmental change [DE90-008568] N91-16451

DISPLACEMENT MEASUREMENT
New methods for producing, recording, and processing interferometric moire patterns N91-16405

DISPLAY DEVICES
Application Principles for Multicolored Displays: A workshop report [AD-A227961] N91-16567
Automated design of displays for technical data [AD-A226729] N91-16586
Displaying alphanumeric characters on pixel-planes 5 [AD-A228616] N91-16622
Field measurement of head related transfer functions [AD-A227850] N91-16708

DISSIPATION
Modeling the dissipation rate in rotating turbulent flows [NASA-CR-187485] N91-16306

DISTANCE
ADRPM-VII applied to the long-range acoustic detection problem N91-16689
Correlation functions for pairs and groups of galaxies N91-16879
FIR statistics of paired galaxies N91-16899
A tentative explanation of cosmological red shift N91-16928

DISTORTION
NICAM 728: Factors affecting the assessment of UHF transmitter linearity [BBC-RD-1990/9] N91-16190
Tidal distortions in pairs of early-type galaxies N91-16869

DISTRIBUTED PARAMETER SYSTEMS
Modeling and verification of distributed systems with labeled predicate transition nets [LAAS-90215] N91-16214

DISTRIBUTED PROCESSING
Distributed System Modeling Environment (DSME) [AD-A226698] N91-16583
Distributed issues for Ada real-time systems [AD-A227852] N91-16603
Decentralized real-time scheduling [AD-A227856] N91-16604
Kernal facilities definition, Kernel version 3.0 [AD-A228027] N91-16610
Parallel Access Main Memory (PAMM) user's manual, version 1.0 [AD-A227744] N91-16635

DISTRIBUTION FUNCTIONS
Two-dimensional convolutions, correlations, and Fourier transforms of combinations of Wigner distribution functions and complex ambiguity functions [AD-A226852] N91-16649
Calculation of free energy from the internal-energy distribution function [DE90-011111] N91-16791

DIURNAL VARIATIONS
Spatial and temporal climate variations influencing medium-range temperature predictions over south-central European Russia [AD-A228623] N91-16527

DOCUMENT STORAGE
Managing emerging technology: Case studies in document imaging systems [AD-A227688] N91-16839

DOCUMENTATION
Annotated bibliography of software engineering laboratory literature [NASA-TM-103415] N91-16602

DOMAINS
A sign-changing global minimizer on a convex domain [REPT-90-57] N91-16655

DOPED CRYSTALS
Threshold voltage and I-V characteristics of AlGaAs/GaAs MODFETs [AD-A228844] N91-16248

DOPPLER EFFECT
Properties of the redshift N91-16926

DOPPLER NAVIGATION
Activities report of the German Federal Institute for Flight Safety [ETN-91-98644] N91-16002

DOPPLER RADAR
Results of the Kansas City 1989 Terminal Doppler Weather Radar (TDWR) operational evaluation testing [AD-A228784] N91-16206
An experimental demonstration of high-resolution Doppler processing [AD-A228813] N91-16208
Definition and preliminary design of the Laser Atmospheric Wind Sounder (LAWS) phase 1. Volume 1: Executive summary [NASA-CR-184071] N91-16332
Definition and preliminary design of the Laser Atmospheric Wind Sounder (LAWS) phase 1. Volume 2 [NASA-CR-184072] N91-16333
Definition and preliminary design of the Laser Atmospheric Wind Sounder (LAWS) phase 1. Volume 3: Program cost estimates [NASA-CR-184073] N91-16334
Detection of loss of consciousness in flight by Doppler method N91-16555

DOSIMETERS
Scoping estimates of the LDEF satellite induced radioactivity [NASA-CR-184074] N91-16056

DOWNWASH
Evaluation of rotorwash characteristics for tiltrotor and tiltwing aircraft in hovering flight [SCT-90RR-18] N91-15989

DRAG
Dragging force on galaxies due to streaming dark matter N91-16947

DRAINAGE
Evaluation procedure for reinforced concrete box culverts under airfield pavements [AD-A227920] N91-16031

DROP SIZE
Investigation of a remote sensing technique for droplet effective radius N91-16420

DROPS (LIQUIDS)
State of an adiabatic expanding and condensing vapor or slow, medium, and fast explosions into a vacuum [DE90-010815] N91-16263

DUST
Dust and ionized gas in active radio elliptical galaxies N91-16919
IC5063: A merger with a hidden luminous active nucleus N91-16923

DWARF GALAXIES
H I and mass distribution of GR8 N91-16884
Formation and development of elliptical and dwarf galaxies [ETN-91-98492] N91-16967

DYE LASERS
Interferometric second-harmonic-generation autocorrelator for characterizing femtosecond pulses [DE90-010331] N91-16345
Stochastic and chaotic effects in the ring laser N91-16359

DYNAMIC CHARACTERISTICS
Aerosol Dynamics Laboratory [DE90-010275] N91-16027
AFDM: An Advanced Fluid-Dynamics Model. Volume 2: Topologies, flow regimes and interfacial areas [DE91-000581] N91-16283
Direct disc impact investigation of dynamic large finite plastic behavior of 1100 aluminum N91-16404

DYNAMIC LOADS
Dynamic crack propagation in elastic-plastic solids N91-16402

DYNAMIC MODELS
Control of industrial crystallizers: The physical aspects [ETN-91-98488] N91-16179

DYNAMIC PRESSURE
The magnetospheric response to 8-minute period strong-amplitude upstream pressure variations [AD-A228038] N91-16489

DYNAMIC PROGRAMMING
Vectorial and parallel algorithms in dynamic programming for optimal control problems [LAAS-90256] N91-16629

DYNAMIC RESPONSE
Pilot study of the dynamic impact response of a composite plate [FFA-TN-1990-27] N91-16070
Dynamic response of composite beams using shear-deformable finite elements [AD-A227975] N91-16408

DYNAMIC STABILITY
Study of the influence of imperfections on the dynamic stability of tanks [DE90-011094] N91-16398

DYNAMIC STRUCTURAL ANALYSIS
A decentralized linear quadratic control design method for flexible structures [NASA-CR-187860] N91-16059
Kinematics of arthropod legs: Modeling and measurement N91-16391
A finite element procedure for calculating fluid-structure interaction using MSC/NASTRAN [NASA-TM-102857] N91-16414
Wind turbine acoustics [NASA-TP-3057] N91-16679

DYNAMICAL SYSTEMS
Stratiform clouds and their interaction with atmospheric motion N91-16506
VLA neutral hydrogen imaging of compact groups N91-16872
Properties of the redshift N91-16926

DYNAMO THEORY
Stellar convection and dynamo theory N91-16857

E

EARLY STARS
Observational effects of interaction in the Seyfert galaxy NGC 7469 N91-16906

EARTH (PLANET)
The magnetospheric response to 8-minute period strong-amplitude upstream pressure variations [AD-A228038] N91-16489

EARTH ATMOSPHERE
NASA/MSFC FY90 Global Scale Atmospheric Processes Research Program Review [NASA-CP-3093] N91-16500
Nonlinear dynamics of global atmospheric and Earth-system processes N91-16510
Using a fast Fourier method to model sound propagation in a stratified atmosphere over a stratified porous-elastic ground N91-16692

EARTH CRUST
Seismic imaging for velocity and attenuation structure in geothermal fields [DE90-010742] N91-16469
Continuum models of continental deformation N91-16490

EARTH IONOSPHERE
Ionospheric corrections for SHF satellite radar altimetry N91-16423
The role of the equatorial electrojet in the evening ionosphere [MPE-PREPRINT-184] N91-16494
Theory for modeling the equatorial evening ionosphere and the origin of the shear in the horizontal plasma flow [MPE-PREPRINT-185] N91-16495
Computer simulations of medium wavelength irregularities in the equatorial ionosphere resulting from artificially produced density enhancements [MPE-PREPRINT-186] N91-16496

EARTH MAGNETOSPHERE
Ion distributions and flows near the neutral sheet [MPE-PREPRINT-179] N91-16974

EARTH MANTLE
Continuum models of continental deformation N91-16490
Excursions to the base of the mantle N91-16491
Seismic structure of the upper mantle under the Pacific Ocean N91-16492

EARTH MOVEMENTS
Study of the influence of imperfections on the dynamic stability of tanks [DE90-011094] N91-16398

EARTH OBSERVATIONS (FROM SPACE)
Space research in the Federal Republic of Germany, 1988 and 1989
[ETN-91-98514] N91-16849
EARTH OBSERVING SYSTEM (EOS)
Definition and preliminary design of the Laser Atmospheric Wind Sounder (LAWS) phase 1. Volume 1: Executive summary
[NASA-CR-184071] N91-16332
Definition and preliminary design of the Laser Atmospheric Wind Sounder (LAWS) phase 1. Volume 2
[NASA-CR-184072] N91-16333
Definition and preliminary design of the Laser Atmospheric Wind Sounder (LAWS) phase 1. Volume 3: Program cost estimates
[NASA-CR-184073] N91-16334
Contents of the NASA ocean data system archive, version 11-90
[NASA-CR-187812] N91-16535
EARTH RESOURCES
Extraction of marketable information from ERS-1 data
[BCRS-90-03] N91-16425
EARTH ROTATION
Planetary circulations in the presence of transient and self-induced heating N91-16505
EARTH SURFACE
An inter-comparison of surface energy flux measurement systems used during FIFE, 1987
[NASA-CR-187699] N91-16472
Long-distance sound propagation over discontinuous impedances N91-16688
Using a fast Fourier method to model sound propagation in a stratified atmosphere over a stratified porous-elastic ground N91-16692
EARTH TIDES
The effects of the solid inner core and nonhydrostatic structure on the Earth's forced nutations and Earth tides N91-16417
ECONOMIC ANALYSIS
Technical and economic evaluation of diesel engine with oxygen enrichment and water injection
[DE90-009723] N91-16373
Preparations for a major international symposium on electricity and the environment
[DE90-010539] N91-16449
ECONOMICS
Moving America; new directions, new opportunities: Assessment of the potential for magnetic levitation transportation systems in the United States
[PB91-104596] N91-16388
Electrical power from inertial confinement fusion: Issues and prospects
[DE90-010200] N91-16437
A sectorial analysis of the information sector in the information economy: Its comparative measurement and new classification model N91-16845
ECOSYSTEMS
Potential responses of landscape boundaries to global environmental change
[DE90-008568] N91-16451
The role of quality assurance in the monitoring of terrestrial ecosystems
[DE90-010986] N91-16461
Monitoring challenges and innovative ideas
[DE91-000586] N91-16465
EDDY CURRENTS
Electromagnetic computations for fusion devices
[DE90-011097] N91-16765
EDDY VISCOSITY
Computation of turbulent flow about unconventional airfoil shapes N91-15992
Modelling the transitional boundary layer
[NASA-CR-187487] N91-15995
EDITING ROUTINES (COMPUTERS)
Real-time system specification and verification
[AD-A227682] N91-16634
EDUCATION
Software for aerospace education: A bibliography, 2nd edition
[NASA-PED-106-ED-2] N91-16601
A computer-based instructional support network: Design, development, and evaluation
[AD-A227922] N91-16637
Calendar of selected aeronautical and space meetings: January 1991 onwards
[AGARD-CAL-91/1] N91-16833
EFFERENT NERVOUS SYSTEMS
Changes in somatosensory responsiveness in behaving monkeys
[AD-A226832] N91-16540
EFFICIENCY
Assessment of battery technologies for electric vehicles. Volume 2, part 1: Appendices
[DE90-010907] N91-16227
EIGENVALUES
Matrix algorithms in signal processing
[AD-A228851] N91-16625
Canonical eigenvalues. Part 2: Application to one-layer, bounded, underwater acoustic ducts
[AD-A227451] N91-16677
ELASTIC BENDING
Large space manipulators study
[AD-A227276] N91-16381
ELASTIC PLATES
Scattering of Lamb waves in an elastic plate for ultrasonic nondestructive evaluation of weldments and cracks N91-16412
ELASTIC PROPERTIES
Evaluation procedure for reinforced concrete box culverts under airfield pavements
[AD-A227920] N91-16031
Inelastic strain analysis of solder joint in NASA fatigue specimen
[NASA-CR-187864] N91-16132
Correlation between the elastic-shear-instability-mechanism and empirical criteria for irradiation-induced amorphization
[DE91-004481] N91-16810
ELASTIC SCATTERING
Measurements of scattering processes in negative ion-atom collisions
[DE90-010666] N91-16715
ELASTIC WAVES
Small scale shock tube experiments using a computer controlled active rarefaction wave eliminator
[AD-A227507] N91-16029
ELASTODYNAMICS
A time-domain finite-element method for the computation of three-dimensional acoustic wave fields in inhomogeneous fluids and solids
[ETN-91-98485] N91-16710
ELASTOMERS
Manufacturing guide for elastomeric seals
[AD-A227511] N91-16383
ELECTRIC BATTERIES
Assessment of battery technologies for electric vehicles. Volume 2, part 1: Appendices
[DE90-010907] N91-16227
Development of a moderate rate lithium/thionyl-chloride D cell
[DE90-011909] N91-16233
Electrolyte optimization and electrode material evaluation for the vanadium redox battery N91-16234
Molten salt electrolytes in high temperature batteries
[RAE-TM-MAT/STR-1155] N91-16241
Studies of the fundamentals of solids state batteries
[AD-A228772] N91-16247
ELECTRIC BRIDGES
A transformer coupled semiconductor bridge igniter for low voltage ignition from a high voltage source
[DE90-009974] N91-16221
ELECTRIC CONTACTS
Research and development on advanced silicon carbide thin film growth techniques and fabrication of high power and microwave frequency silicon carbide-based device
[AD-A228758] N91-16246
ELECTRIC FIELDS
Initial studies of electric field effects on ceramic powder formation in flames
[DE90-007571] N91-16138
Applications research studies on microtubules
[AD-A228756] N91-16205
The role of the equatorial electrojet in the evening ionosphere
[MPE-PREPRINT-184] N91-16494
Investigation of effects of 60-Hz electric and magnetic fields on operant and social behavior and on the neuroendocrine system of nonhuman primates
[DE90-010809] N91-16537
Investigation of effects of 60-Hz electric and magnetic fields on operant and social behavior and on the neuroendocrine system of nonhuman primates
[DE90-011557] N91-16539
Programmable surface acoustic wave detection in silicon: Design of programmable filters
[ETN-91-98568] N91-16746
Kinetic stability of field-reversed configurations
[DE90-011530] N91-16767
Stark-effect measurement of high FEL electric fields in MTX by laser-aided particle-probe spectroscopy
[DE90-011911] N91-16771
Applications of strained layer superlattices
[DE90-011204] N91-16793
ELECTRIC MOTOR VEHICLES
Laboratory testing of chloride 3ET205 6 volt traction battery
[DE90-010926] N91-16225
Assessment of battery technologies for electric vehicles. Volume 2, part 1: Appendices
[DE90-010907] N91-16227
ELECTRIC MOTORS
Composite ceramic superconducting wires for electric motor applications
[AD-A228359] N91-16818
ELECTRIC POWER PLANTS
Electrical power from inertial confinement fusion: Issues and prospects
[DE90-010200] N91-16437
Optimization of a power transient stability program on a vector supercomputer: Theory and applications
[AD-A227884] N91-16607
ELECTRIC POWER TRANSMISSION
Optimization of a power transient stability program on a vector supercomputer: Theory and applications
[AD-A227884] N91-16607
ELECTRIC SWITCHES
Effects of switch leakages upon Nimbus-7 SMMR calibration
[NASA-TM-100705] N91-16536
ELECTRICAL FAULTS
Updated evaluation of polymer films for electrical insulation
[DE91-000544] N91-16148
Design and fabrication of high voltage planar devices
[LAAS-90306] N91-16252
ELECTRICAL IMPEDANCE
High frequency scattering by a smooth coated cylinder simulated with generalized impedance boundary conditions
[NASA-CR-187829] N91-16211
ELECTRICAL INSULATION
Updated evaluation of polymer films for electrical insulation
[DE91-000544] N91-16148
ELECTRICAL PROPERTIES
Electrical properties of gas sensor materials
[ETN-91-98572] N91-16114
Numerical simulation of the comparative electrical performance of the permeable base transistor, opposed gate-source transistor and heterostructure launched ballistic field effect transistor
[AD-A228545] N91-16202
Characterization and development report for the SA2859: A silicon controlled rectifier
[DE90-010196] N91-16217
Fabrication and electrical characterization of deep-submicron trench-isolated CMOS device structures N91-16802
ELECTRICAL RESISTANCE
Circumfluous motion of a conductive liquid around solid objects in a magnetic field
[DE90-011335] N91-16265
Electrical resistance volumetry in the circulation N91-16543
ELECTRICAL RESISTIVITY
Investigation of a new concept in semiconductor microwave oscillators
[AD-A226785] N91-16235
High efficiency silicon concentrator solar cells N91-16441
ELECTRICITY
Preparations for a major international symposium on electricity and the environment
[DE90-010539] N91-16449
Electrical power from inertial confinement fusion: Issues and prospects
[DE90-010332] N91-16759
ELECTRO-OPTICS
Applications research studies on microtubules
[AD-A228756] N91-16205
Solid state research
[NASA-CR-187871] N91-16816
Chemical beam epitaxy of ZnSe
[AD-A228045] N91-16817
ELECTROCARDIOGRAPHY
Computer aided physiological assessment of the functional state of pilots during simulated flight N91-16562
ELECTROCATALYSTS
Impurity tolerant electrocatalysts
[DE90-011960] N91-16090
Electrocatalysis of anodic and cathodic oxygen-transfer reactions
[DE91-000611] N91-16100
Improved anode catalysts for coal gas-fueled phosphoric acid fuel cells
[DE90-009683] N91-16442
ELECTROCHEMICAL CELLS
The use of impedance measurements in corrosion research: The corrosion behaviour of chromium and iron-chromium alloys
[ISBN-90-9003693-8] N91-16135
Neutron measurements in search of cold fusion
[DE91-004855] N91-16778

ELECTROCHEMICAL CORROSION
Characterization of the corrosion of a P-130x graphite fiber reinforced 6063 aluminum metal matrix composite
[AD-A228134] N91-16071
The use of impedance measurements in corrosion research: The corrosion behaviour of chromium and iron-chromium alloys
[ISBN-90-9003693-8] N91-16135
ELECTROCHEMICAL OXIDATION
Impurity tolerant electrocatalysts
[DE90-011960] N91-16090
Electrocatalysis of anodic and cathodic oxygen-transfer reactions
[DE91-000611] N91-16100
ELECTROCHEMISTRY
In situ studies of potential dependent structural and distributional changes at electrochemical interfaces with x rays
[AD-A226844] N91-16098
Electrocatalysis of anodic and cathodic oxygen-transfer reactions
[DE91-000611] N91-16100
The use of impedance measurements in corrosion research: The corrosion behaviour of chromium and iron-chromium alloys
[ISBN-90-9003693-8] N91-16135
Electron microscopy and electrochemistry of nickel oxide films for electrochromic devices produced by different techniques
[DE90-011596] N91-16142
Self-discharge study of Li-alloy/FeS2 thermal cells
[DE90-010659] N91-16438
Highlights of the Chemical Technology (CMT) Division's activities
[DE90-008242] N91-16984
ELECTROCHROMISM
Electrochromic sun control coverings for windows
[DE90-000335] N91-16139
ELECTRODE MATERIALS
Evaluation of novel solid electrolyte materials
[DE90-011164] N91-16231
Electrolyte optimization and electrode material evaluation for the vanadium redox battery N91-16234
ELECTRODEPOSITION
Low-cost CdZnTe devices for cascade cell application
[DE91-002116] N91-16444
ELECTRODES
Electrical properties of gas sensor materials
[ETN-91-98572] N91-16114
Electron microscopy and electrochemistry of nickel oxide films for electrochromic devices produced by different techniques
[DE90-011596] N91-16142
Direct methanol/air fuel cells: Systems considerations
[DE90-011971] N91-16439
Initial calorimetry experiments in the Physics Divsion, ORNL (Oak Ridge National Laboratory)
[DE90-010301] N91-16756
ELECTROENCEPHALOGRAPHY
EEG indicators of mental workload: Conceptual and practical issues in the development of a measurement tool N91-16559
Computer aided physiological assessment of the functional state of pilots during simulated flight N91-16562
ELECTROLYSIS
Initial calorimetry experiments in the Physics Divsion, ORNL (Oak Ridge National Laboratory)
[DE90-010301] N91-16756
ELECTROLYTES
Electrical properties of gas sensor materials
[ETN-91-98572] N91-16114
Evaluation of novel solid electrolyte materials
[DE90-011164] N91-16231
Electrolyte optimization and electrode material evaluation for the vanadium redox battery N91-16234
Self-discharge study of Li-alloy/FeS2 thermal cells
[DE90-010659] N91-16438
Direct methanol/air fuel cells: Systems considerations
[DE90-011971] N91-16439
ELECTROLYTIC CELLS
Initial calorimetry experiments in the Physics Divsion, ORNL (Oak Ridge National Laboratory)
[DE90-010301] N91-16756
ELECTROMAGNETIC ABSORPTION
Comparison of propagation and absorption of FEL-generated microwaves with theory
[DE90-010369] N91-16181
ELECTROMAGNETIC FIELDS
Modeling pulse driven antenna systems with finite differences
[DE90-010682] N91-16182
Wakefield calculations on parallel computers
[DE90-009712] N91-16632
Advanced methods for the computation of particle beam transport and the computation of electromagnetic fields and beam-cavity interactions
[DE90-011071] N91-16734
Electromagnetic computations for fusion devices
[DE90-011097] N91-16765
ELECTROMAGNETIC INTERACTIONS
Parity violation and electron scattering
[DE90-010429] N91-16712
ELECTROMAGNETIC INTERFERENCE
Intra-Pulse Frequency Diversity (IPFD) lab demonstration
[AD-A228814] N91-16209
Effects of switch leakages upon Nimbus-7 SMMR calibration
[NASA-TM-100705] N91-16536
ELECTROMAGNETIC NOISE
Shift-invariant image reconstruction of speckle-degraded images using bispectrum estimation
[AD-A227728] N91-16188
ELECTROMAGNETIC PULSES
Numerical modeling tools for transient electromagnetic problems
[DE90-010328] N91-16180
ELECTROMAGNETIC RADIATION
Models for surface scattering from solids and liquids
[RSRE-MEMO-3699] N91-16192
Investigation of effects of 60-Hz electric and magnetic fields on operant and social behavior and on the neuroendocrine system of nonhuman primates
[DE90-011557] N91-16539
ELECTROMAGNETIC SCATTERING
Scattering and depolarization by rough terrain and sea: A unified full wave approach
[AD-A226295] N91-16201
High frequency scattering by a smooth coated cylinder simulated with generalized impedance boundary conditions
[NASA-CR-187829] N91-16211
ELECTROMAGNETIC WAVE TRANSMISSION
Integrated Refractive Effects Prediction System (IREPS) user's manual, revision PC-2.0
[AD-A228549] N91-16203
ELECTRON ACCELERATORS
Testing of lead glass detectors for electron proof in the ELAN experiment
[BONN-IR-90-38] N91-16730
A Moller polarimeter for the extracted ELSA-ray
[BONN-IR-90-42] N91-16731
ELECTRON AVALANCHE
Design and fabrication of high voltage planar devices
[LAAS-90306] N91-16252
ELECTRON BEAMS
Electron microscopy and electrochemistry of nickel oxide films for electrochromic devices produced by different techniques
[DE90-011596] N91-16142
Integrated Numerical Experiments (INEX) and the Free-Electron Laser Physical Process Code (FELPPC)
[DE90-011957] N91-16348
Generation of XUV light by resonant frequency tripling in a two-wiggler FEL amplifier
[DE90-012120] N91-16349
Design requirements and calculated performance of an XUV FEL oscillator operating on a higher harmonic
[DE91-004833] N91-16357
A Moller polarimeter for the extracted ELSA-ray
[BONN-IR-90-42] N91-16731
Microwave generation for magnetic fusion energy applications, task B
[DE90-011079] N91-16763
Resonant Compton scattering in models of gamma-ray burst sources. Part 2: Numerical modeling
[DE91-005268] N91-16982
ELECTRON BOMBARDMENT
Experimental studies of the properties of trihydrogen and tetrahydrogen
[AD-A228869] N91-16110
ELECTRON COUNTERS
Testing of lead glass detectors for electron proof in the ELAN experiment
[BONN-IR-90-38] N91-16730
ELECTRON CYCLOTRON HEATING
A statistical survey of electron pitch angle distributions in the nightside central plasma sheet
[AD-A227763] N91-16486
Texas experimental tokamak
[DE90-011070] N91-16762
Study on ECW transmission lines for NET/ITER
[EUR-FU/80/90-99] N91-16781
ELECTRON DENSITY (CONCENTRATION)
Ionospheric corrections for SHF satellite radar altimetry N91-16423
ELECTRON DIFFRACTION
Atomic and electronic structure of metals and alloys: Clean surfaces and chemisorbed molecules
[DE91-000267] N91-16123
ELECTRON DIFFUSION
A statistical survey of electron pitch angle distributions in the nightside central plasma sheet
[AD-A227763] N91-16486
ELECTRON DISTRIBUTION
A statistical survey of electron pitch angle distributions in the nightside central plasma sheet
[AD-A227763] N91-16486
Ion distributions and flows near the neutral sheet
[MPE-PREPRINT-179] N91-16974
ELECTRON GUNS
Concepts for future developments in electron microscopy
[DE90-010630] N91-16320
ELECTRON MICROSCOPES
Concepts for future developments in electron microscopy
[DE90-010630] N91-16320
ELECTRON MICROSCOPY
High resolution electron microscopy of interfaces in fcc materials
[DE91-004420] N91-16101
Electron microscopy and electrochemistry of nickel oxide films for electrochromic devices produced by different techniques
[DE90-011596] N91-16142
Concepts for future developments in electron microscopy
[DE90-010630] N91-16320
Image interpretation for transmission electron microscopy of thin semiconductor layers and interfaces
[ETN-91-98487] N91-16826
ELECTRON PHONON INTERACTIONS
From low to high Tc: An ultrasonic investigation of niobium single crystal and YBaCuO superconducting thin films with surface acoustic waves N91-16822
ELECTRON PLASMA
Investigation and modeling of radiation absorption processes and opacities in dense plasmas
[AD-A228749] N91-16779
ELECTRON PRECIPITATION
The magnetospheric response to 8-minute period strong-amplitude upstream pressure variations
[AD-A228038] N91-16489
ELECTRON RADIATION
Electron stopping powers of some elements and compounds from 0 to 10,000 eV: A compilation
[DE90-010675] N91-16716
ELECTRON SCATTERING
Parity violation and electron scattering
[DE90-010429] N91-16712
A new approach for the determination of electronic structure
[DE90-010479] N91-16713
The theory of electron-ion collisions: The role of doubly excited states
[DE90-011078] N91-16721
Deep inelastic structure functions from electron scattering on hydrogen, deuterium, and iron at 0.6 GeV2 less than or equal to Q2 less than or equal to 30.0 GeV2
[DE90-010169] N91-16785
Multiple-photon Compton scattering in a strong magnetic field: Cross-sections and radiative transport N91-16852
Resonant Compton scattering in models of gamma-ray burst sources. Part 2: Numerical modeling
[DE91-005268] N91-16982
ELECTRON SOURCES
Development of liquid xenon imaging gamma-ray spectrophotometers
[AD-A227575] N91-16740
ELECTRON STATES
Photoreflectance studies of electronic transitions in quantum well structures under high pressure
[DE90-011583] N91-16801
ELECTRON TRANSFER
Puzzles of electron transfer
[DE90-010541] N91-16720
Theoretical studies of electron transport in quantum-well structures
[AD-A228429] N91-16819
ELECTRON TRANSITIONS
Theoretical studies of atomic transitions
[DE91-000931] N91-16723
Physico-chemical investigations on Co-Mn-oxide spinels
[ETN-91-98476] N91-16825
ELECTRON TUNNELING
Theoretical studies of electron transport in quantum-well structures
[AD-A228429] N91-16819

ELECTRONIC EQUIPMENT
Magnetic-field shielding of satellites from high-energy-electron environments
[DE90-010296] N91-16043
Joint services electronics program
[AD-A227576] N91-16237
Electronic analogue for a biological nose
[ME-78] N91-16541
ELECTRONIC MAIL
A computer-based instructional support network: Design, development, and evaluation
[AD-A227922] N91-16637
ELECTRONS
Design requirements and calculated performance of an XUV FEL oscillator operating on a higher harmonic
[DE91-004833] N91-16357
Comparison of the quadratic configuration interaction and coupled cluster approaches to electron correlation including the effect of triple excitations
[NASA-CR-187855] N91-16727
ELECTROPHORESIS
Numerical simulation of buffer flow in a free flow electrophoresis chamber N91-16279
ELECTROPHYSICS
Magnetic measurements with fluxgate magnetometer in rocket flight
[DRI-4-90] N91-16061
ELECTROSTATIC CHARGE
Parametric study of electrostatically charged sprays
[DE90-010580] N91-16262
ELECTROSTATICS
Development of an external beam ion milliprobe
[AD-A227247] N91-16329
ELEMENTARY PARTICLE INTERACTIONS
Research in theoretical nuclear physics
[DE90-010792] N91-16828
ELEMENTARY PARTICLES
Research in theoretical nuclear physics
[DE90-010792] N91-16828
ELEMENTS
Electron stopping powers of some elements and compounds from 0 to 10,000 eV: A compilation
[DE90-010675] N91-16716
ELLIPSES
Analysis and application of the discrete vortex method N91-16290
ELLIPTIC DIFFERENTIAL EQUATIONS
Finite element approximations for transonic flows
[ETN-91-98491] N91-15988
ELLIPTIC FUNCTIONS
A sign-changing global minimizer on a convex domain
[REPT-90-57] N91-16655
ELLIPTICAL GALAXIES
Stellar kinematics of elliptical galaxies in pairs N91-16862
Dynamics of groups around interacting double ellipticals: Measuring dark matter haloes N91-16863
An atlas of mixed-morphology pairs N91-16866
Tidal distortions in pairs of early-type galaxies N91-16869
Blue ellipticals in compact groups N91-16873
What is the number of spiral galaxies in compact groups N91-16874
The cD galaxy in Abell cluster 1775 N91-16886
A spiral-like disk of ionized gas in IC 1459: Signature of a merging collision N91-16889
Alignment of cD-galaxies with their surroundings N91-16895
Central activity in 60 micron peakers N91-16913
Cool infalling gas and its interaction with the hot ISM of elliptical galaxies N91-16915
Dust and ionized gas in active radio elliptical galaxies N91-16919
Dynamical interactions of galaxy pairs N91-16930
Probing the tides in interacting galaxy pairs N91-16932
Dynamical friction in pairs of elliptical galaxies N91-16933
An experimental study of counter-rotating cores in elliptical galaxies N91-16934
Gas flows in S-E binary systems of galaxies N91-16956
Do elliptical galaxies have thick disks N91-16962
Formation and development of elliptical and dwarf galaxies
[ETN-91-98492] N91-16967
ELLIPTICITY
The effects of the solid inner core and nonhydrostatic structure on the Earth's forced nutations and Earth tides N91-16417
EMBRITTLEMENT
Thermal aging of cast stainless steels: Mechanisms and predictions
[DE90-010093] N91-16115
EMISSION
H I observations of the peculiar galaxy NGC 660 N91-16888
Galaxy interactions and star formation: Results of a survey of global H-alpha emission in spiral galaxies in 8 clusters N91-16905
Nuclear and extended infrared emission in paired and isolated galaxies N91-16917
Signs of interaction of the NGC 1275 nucleus with the high-velocity system according to 0.7 sec seeing observations N91-16918
EMISSION SPECTRA
High resolution photoelectron spectroscopy of metal clusters and high temperature species
[DE90-011598] N91-16119
Analysis of emission data from a Perkin-Elmer 1710 FTIR spectrometer
[AD-A227759] N91-16331
Spatial distributions of the emitting species in a penning surface-plasma source
[DE90-011996] N91-16772
IR plasma emissions
[AD-A227713] N91-16776
X ray emission from low-mass binary systems N91-16853
Interacting nuclei in distant galaxies N91-16894
Cool infalling gas and its interaction with the hot ISM of elliptical galaxies N91-16915
The role of shocks in NGC 6240 N91-16921
IC5063: A merger with a hidden luminous active nucleus N91-16923
The spiral-compact galaxy pair AM 2208-251: Computer simulations versus observations N91-16939
Gas flows in S-E binary systems of galaxies N91-16956
Molecular gas and star formation in the central regions of Virgo spiral galaxies N91-16970
EMITTANCE
Ultrasensitive molecular fluorescence spectroscopy in levitated microdroplets
[DE91-000621] N91-16095
Image-based terrain modeling with thematic mapper N91-16418
EMITTERS
High efficiency silicon concentrator solar cells N91-16441
ENCOUNTERS
Nuclear and extended infrared emission in paired and isolated galaxies N91-16917
A simulation survey of galaxy interactions N91-16936
Numerical simulations of interacting disk galaxies N91-16955
END EFFECTORS
Modeling and control of a two-arm elastic robot in gravity N91-16389
Camera space manipulation of a mobile robot N91-16390
ENDOCRINE SYSTEMS
Investigation of effects of 60-Hz electric and magnetic fields on operant and social behavior and on the neuroendocrine system of nonhuman primates
[DE90-010809] N91-16537
ENDOTHERMIC REACTIONS
State-to-state inelastic and reactive molecular beam scattering from surfaces
[DE90-010492] N91-16714
ENERGY ABSORPTION
Development of a crashworthy seat for commuter aircraft
[AD-A227486] N91-15999
ENERGY BUDGETS
A study of the surface energy balance on slopes in a tallgrass prairie
[NASA-CR-187698] N91-16473
ENERGY CONSUMPTION
Electrochromic sun control coverings for windows
[DE90-000335] N91-16139
ENERGY CONVERSION
Requirements for a fuel cell for transportation application
[DE90-011146] N91-16230
ENERGY CONVERSION EFFICIENCY
Meetings to share advancements in heat pump technologies
[DE90-010008] N91-16257
High efficiency silicon concentrator solar cells N91-16441
ENERGY DISSIPATION
Dynamical friction in pairs of elliptical galaxies N91-16933
ENERGY DISTRIBUTION
Calculation of free energy from the internal-energy distribution function
[DE90-011111] N91-16791
The nature of the emission-line nebulae in powerful far-infrared galaxies N91-16916
ENERGY GAPS (SOLID STATE)
Electronic and ionic transport in processable conducting polymers
[AD-A227857] N91-16154
Applications of strained layer superlattices
[DE90-011204] N91-16793
Integrated semiconductor modulators
[AD-A228615] N91-16820
ENERGY LEVELS
Properties of superdeformed bands in the A = 194 region
[DE90-011482] N91-16798
ENERGY POLICY
A summary of prospects for methanol vehicles in the United States
[DE90-009719] N91-16370
Technological and policy options for mitigating greenhouse gas emissions from mobile sources
[DE90-010151] N91-16447
Greenhouse gas emissions from selected alternative transportation fuels market niches
[DE90-010491] N91-16448
Preparations for a major international symposium on electricity and the environment
[DE90-010539] N91-16449
Report to Congress on the Small Business Program
[DE91-004622] N91-16831
ENERGY TECHNOLOGY
Meetings to share advancements in heat pump technologies
[DE90-010008] N91-16257
Technological and policy options for mitigating greenhouse gas emissions from mobile sources
[DE90-010151] N91-16447
Computational physics at the National Energy Research Supercomputer Center
[DE90-010283] N91-16672
Report to Congress on the Small Business Program
[DE91-004622] N91-16831
Highlights of the Chemical Technology (CMT) Division's activities
[DE90-008242] N91-16984
Energy and Technology Review, March 1990
[DE90-008230] N91-16985
Accomplishments in technology transfer from DOE and its laboratories
[DE90-002686] N91-16986
ENERGY TRANSFER
Two-dimensional simulation of quantum-well lasers including energy transport
[AD-A227487] N91-16356
Carbon dioxide and energy exchanges in a temperate grassland ecosystem N91-16419
Wave-particle power transfer in a steady-state driven system
[DE90-010031] N91-16748
Energy and angular momentum transfer in binary galaxies N91-16940
ENGINE CONTROL
An introduction to modern aero-engine control design
[ETN-91-98583] N91-16024
ENGINE DESIGN
Optimal trajectories for an aerospace plane. Part 2: Data, tables, and graphs
[NASA-CR-187848] N91-16011
Advanced Turbine Technology Applications Project (ATTAP)
[NASA-CR-187039] N91-16021
Jet engine performance estimation from minimal input data
[ETN-91-98582] N91-16023
ENGINE NOISE
Long-distance sound propagation over discontinuous impedances N91-16688
ENGINE TESTS
Advanced Turbine Technology Applications Project (ATTAP)
[NASA-CR-187039] N91-16021
High temperature oxidation-resistant thruster research
[NASA-CR-185233] N91-16063
ENRICHMENT
Technical and economic evaluation of diesel engine with oxygen enrichment and water injection
[DE90-009723] N91-16373
ENTHALPY
Gas solubility in glassy polymers: A correlation with excess enthalpy
[AD-A228202] N91-16155
Ion beam modification of surface for improved high temperature performance
[AD-A228067] N91-16243
ENVIRONMENT EFFECTS
Preparations for a major international symposium on electricity and the environment
[DE90-010539] N91-16449

Potential responses of landscape boundaries to global environmental change
[DE90-008568] N91-16451
International decision making and global climate change: Lessons of prior resource management efforts for consensus building
[DE90-010714] N91-16454
The atmospheric effects of stratospheric aircraft: A topical review
[NASA-RP-1250] N91-16466
Environmental noise from the Naesudden (Sweden) and Maglarp (Sweden) prototype wind turbines: A study of machinery noise
[FFA-TN-1990-34] N91-16706

ENVIRONMENT MANAGEMENT
Environmental uncertainty, planning and organizational performance N91-16464

ENVIRONMENT POLLUTION
Multimedia Environmental Pollutant Assessment System (MEPAS) sensitivity analysis of computer codes
[DE90-010005] N91-16445
Solving global environmental problems through technological innovation
[DE90-010018] N91-16446
International decision making and global climate change: Lessons of prior resource management efforts for consensus building
[DE90-010714] N91-16454

ENVIRONMENT PROTECTION
Is there hope for fusion
[DE90-012095] N91-16736

ENVIRONMENTAL QUALITY
Environmental trends
[DE90-010530] N91-16450

ENVIRONMENTAL SURVEYS
Environmental trends
[DE90-010530] N91-16450
The atmospheric effects of stratospheric aircraft: A topical review
[NASA-RP-1250] N91-16466

EPITAXY
Characterization of GaAs/Si interface structure by x ray diffraction
[DE91-004769] N91-16811
Domain boundaries formed during epitactical growth of alpha-Al2O3
[DE91-005018] N91-16814
Chemical beam epitaxy of ZnSe
[AD-A228045] N91-16817
Epitaxial growth and surface morphology of some metal and semiconductor structures N91-16824

EQUATIONS OF STATE
ANEOS: Analytic equations of state for shock physics codes input manual
[DE90-010198] N91-16575

EQUATORIAL ATMOSPHERE
The role of the equatorial electrojet in the evening ionosphere
[MPE-PREPRINT-184] N91-16494
Theory for modeling the equatorial evening ionosphere and the origin of the shear in the horizontal plasma flow
[MPE-PREPRINT-185] N91-16495
Computer simulations of medium wavelength irregularities in the equatorial ionosphere resulting from artificially produced density enhancements
[MPE-PREPRINT-186] N91-16496

EQUATORIAL ELECTROJET
The role of the equatorial electrojet in the evening ionosphere
[MPE-PREPRINT-184] N91-16494

EQUILIBRIUM FLOW
On a class of unsteady three-dimensional Navier Stokes solutions relevant to rotating disc flows: Threshold amplitudes and finite time singularities
[NASA-CR-187482] N91-15991

ERROR ANALYSIS
IFDIS: An expert system for diagnosis of failures in jet aircraft engines
[AD-A227757] N91-16020
Validity study in multidimensional latent space and efficient computerized adaptive testing
[AD-A227742] N91-16650

ERROR CORRECTING CODES
Procedure for the correction of errors in the DUTSCAT data 1987/1988
[BCRS-90-14] N91-16430

ERROR SIGNALS
Near/far resistant receivers for DS/SSMA communications
[AD-A228147] N91-16200
A ring laser gyroscope with optical subtraction N91-16335

ERS-1 (ESA SATELLITE)
Extraction of marketable information from ERS-1 data
[BCRS-90-03] N91-16425

ESTIMATES
Identification of non-linear mechanical systems for control application
[ISBN-90-9003596-6] N91-16644
Selection effects and binary galaxy velocity differences N91-16927
Viral coefficient and hidden mass in the galaxy groups N91-16950

ESTIMATING
Impacts of advanced manufacturing technology on parametric estimating
[AD-A228232] N91-16177

ETHANE
Auto-ignition temperatures of binary mixtures of alkanes in a closed vessel: Comparisons between experimental measurements and numerical predictions
[DE90-007856] N91-16082
Fundamental studies of hydrocarbon conversions over supported bimetallic catalysts
[DE90-011744] N91-16089

ETHYLENE
Fundamental studies of hydrocarbon conversions over supported bimetallic catalysts
[DE90-011744] N91-16089

EULER EQUATIONS OF MOTION
Study of time accuracy of flow variables across discontinuous boundaries N91-16300
Acceleration of iterative algorithms for Euler and Navier-Stokes equations N91-16301

EUROPE
The European flight safety crisis: Costs and solution
[ETN-91-98490] N91-16000

EVAPORATION
Evaporation process and 3 phase flow in a water evaporator assembly
[MBB-UO-0108-90-PUB] N91-16060
Spray combustion modeling and evaluation
[NASA-CR-187887] N91-16078
Droplet shattering, vaporization, and recondensation in cloud clearing with long pulse infrared chemical lasers
[DE90-010584] N91-16343

EVAPORATORS
Evaporation process and 3 phase flow in a water evaporator assembly
[MBB-UO-0108-90-PUB] N91-16060
Initial parametric results using CYCLEZ: A LMTD-specified, Lorenz-Meutzner cycle refrigerator-freezer model
[DE90-010146] N91-16175
Development of a two-phase cold plate N91-16277

EVAPOTRANSPIRATION
Sahelian vegetation monitoring project
[BCRS-90-04] N91-16426

EVOLUTION (DEVELOPMENT)
An evolutionary approach to designing neural networks
[AD-A228874] N91-16643

EXCITATION
Simulation of excited shear flows N91-16270
Comparison of the quadratic configuration interaction and coupled cluster approaches to electron correlation including the effect of triple excitations
[NASA-CR-187855] N91-16727
Triple and quadruple excitation contributions to the binding in Be clusters: Calibration calculations on Be3
[NASA-TM-103391] N91-16728
IC5063: A merger with a hidden luminous active nucleus N91-16923

EXHAUST EMISSION
Technological and policy options for mitigating greenhouse gas emissions from mobile sources
[DE90-010151] N91-16447
Greenhouse gas emissions from selected alternative transportation fuels market niches
[DE90-010491] N91-16448
The atmospheric effects of stratospheric aircraft: A current consensus
[NASA-RP-1251] N91-16467

EXHAUST GASES
Requirements for a fuel cell for transportation application
[DE90-011146] N91-16230

EXHAUST SYSTEMS
Technological and policy options for mitigating greenhouse gas emissions from mobile sources
[DE90-010151] N91-16447

EXOBIOLOGY
The space flights: Second German Spacelab mission D-2 and Mir 1992
[REPT-25/90] N91-16034
Aerospace medicine and biology: A cumulative index to a continuing bibliography (supplement 345)
[NASA-SP-7011(345)] N91-16547

EXOSPHERE
Derivation of exospheric temperature at high latitudes from incoherent-scatter radar data
[AD-A227721] N91-16484

EXOTHERMIC REACTIONS
State-to-state inelastic and reactive molecular beam scattering from surfaces
[DE90-010492] N91-16714

EXPERIMENT DESIGN
Symmetry and design in mixture experiments
[AD-A226760] N91-16169
ERICC: Construction and application of the Command and Control Research Facility
[IZF-1989-55] N91-16213
The Cabannes-lidar for the examination of the stratosphere: Selected design elements for the experimental construction
[BONN-IR-90-39] N91-16493

EXPERIMENTATION
Analytical and experimental investigation of transverse flow aerodynamic windows for high power lasers
[DLR-FB-90-33] N91-16367

EXPERT SYSTEMS
IFDIS: An expert system for diagnosis of failures in jet aircraft engines
[AD-A227757] N91-16020
Experimentation and concept formation by an autonomous mobile robot
[DE90-003063] N91-16368
A query model and query and knowledge definition languages for object-oriented databases N91-16580
Reliability/Maintainability/Logistics support analysis Computer Aided Tailoring Software Program (R/M/L CATSOP)
[AD-A226820] N91-16588
XSHELL: A general purpose expert system shell
[AD-A228454] N91-16616
Research into the design and implementation of knowledge base systems
[AD-A228873] N91-16843

EXPLOSIONS
State of an adiabatic expanding and condensing vapor or slow, medium, and fast explosions into a vacuum
[DE90-010615] N91-16263

EXPLOSIVES
Graphical analysis of barrel-tamped explosively accelerated flyer plates
[DE90-010299] N91-16028
The search for high energy low vulnerability explosives
[DE90-009436] N91-16158
Paste extrudable explosives: Their history and their current status
[DE90-009438] N91-16159
Modeling laser ignition of explosives and pyrotechnics: Effects and characterization of radiative transfer
[DE90-011052] N91-16161
Diagnostic of the reaction behaviour of intensive high explosives under jet attack
[MBB-UA-1188-90-PUB] N91-16173
Aerosol cloud generation experiments
[DE90-011051] N91-16264

EXPONENTIAL FUNCTIONS
Shift-invariant image reconstruction of speckle-degraded images using bispectrum estimation
[AD-A227728] N91-16188

EXTERNAL TANKS
Debris/Ice/TPS assessment and photographic analysis for shuttle mission STS-41
[NASA-TM-103814] N91-16041

EXTRATERRESTRIAL RADIATION
Scoping estimates of the LDEF satellite induced radioactivity
[NASA-CR-184074] N91-16056

EXTREME ULTRAVIOLET RADIATION
Development of free-electron lasers for XUV projection lithography
[DE90-010566] N91-16342
Generation of XUV light by resonant frequency tripling in a two-wiggler FEL amplifier
[DE90-012120] N91-16349
Design requirements and calculated performance of an XUV FEL oscillator operating on a higher harmonic
[DE91-004833] N91-16357

EXTREMELY HIGH FREQUENCIES
The reflection and transmission properties of a triple band dichroic surface
[NASA-CR-187776] N91-16191

EXTRUDING
Paste extrudable explosives: Their history and their current status
[DE90-009438] N91-16159

EYE MOVEMENTS
Study of pilot vigilance during long range flight N91-16561

F

F-16 AIRCRAFT
Longitudinal stability augmentation of a lightweight fighter aircraft model
[ETN-91-98585] N91-16026
F-18 AIRCRAFT
IFDIS: An expert system for diagnosis of failures in jet aircraft engines
[AD-A227757] N91-16020
FABRICATION
Design and fabrication of the NASA HL-20 full scale research model
[NASA-CR-187801] N91-16008
High-purity silicon soft x ray sensor arrays
[ETN-91-98484] N91-16338
Manufacturing guide for elastomeric seals
[AD-A227511] N91-16383
High efficiency silicon concentrator solar cells N91-16441
Measurements of scattering processes in negative ion-atom collisions
[DE90-010666] N91-16715
Fabrication and electrical characterization of deep-submicron trench-isolated CMOS device structures N91-16802
FABRY-PEROT INTERFEROMETERS
Deep Fabry-Perot imaging of NGC 6240: Kinematic evidence for merging galaxies N91-16922
FACSIMILE COMMUNICATION
The design of a meteorological facsimile converter
[ETN-91-98578] N91-16528
FACTORIZATION
A block QR factorization algorithm for rank-deficient matrices
[DE90-010066] N91-16573
An automatic ordering method for incomplete factorization iterative solvers
[DE91-001974] N91-16659
FAILURE ANALYSIS
Failure analysis of a main rotor pitch horn bolt located on the AH-1 Cobra helicopter
[AD-A227679] N91-16007
Advanced Turbine Technology Applications Project (ATTAP)
[NASA-CR-187039] N91-16021
The oxidation behavior of carbon-carbon composites and their coatings N91-16074
Fatigue of amorphous polymers
[ISBN-90-9003520-6] N91-16157
Detection of solid lubricant film failure during sliding by vibration monitoring
[NAL-TR-1060] N91-16384
Horizontal fault tolerance in a fully distributed loosely coupled environment
[AD-A227972] N91-16638
Theoretical studies of tokamaks
[DE90-011332] N91-16768
FAILURE MODES
Status of Argonne life evaluation of valve regulated lead-acid batteries
[DE90-011098] N91-16229
FALSE ALARMS
Operating characteristics for weighted energy detector with Gaussian signals
[AD-A226851] N91-16673
FAR FIELDS
Far-field boundaries and their numerical treatment N91-16281
FAR INFRARED RADIATION
Far-infared laser spectroscopy of two dimensional holes in strained-layer heterostructure and superlattices
[DE91-000027] N91-16805
Observations of multiple nucleus galaxies N91-16890
FIR statistics of paired galaxies N91-16899
Quantifying the FIR interaction enhancement in paired galaxies N91-16900
Are extremely luminous far-infrared galaxies the result of merging quasar cores N91-16912
The nature of the emission-line nebulae in powerful far-infrared galaxies N91-16916
FAST FOURIER TRANSFORMATIONS
Using a fast Fourier method to model sound propagation in a stratified atmosphere over a stratified porous-elastic ground N91-16692
New correction procedures for the fast field program which extend its range N91-16699
FATIGUE (MATERIALS)
Inelastic strain analysis of solder joint in NASA fatigue specimen
[NASA-CR-187864] N91-16132
Fatigue of amorphous polymers
[ISBN-90-9003520-6] N91-16157
FATIGUE LIFE
Modeling and identification of cumulative creep fatigue damage in an austenitic stainless steel N91-16131
Inelastic strain analysis of solder joint in NASA fatigue specimen
[NASA-CR-187864] N91-16132
FATIGUE TESTS
Test methods for evaluating hot cracking: Review and perspective
[DE90-009820] N91-16397
FAULT TOLERANCE
Safety as a design goal for applications of microelectronic control systems
[REPT-23/90] N91-16253
Horizontal fault tolerance in a fully distributed loosely coupled environment
[AD-A227972] N91-16638
FAULT TREES
Living PRAs (Probabilistic Risk Analysis) made easier with IRRAS (Integrated Reliability and Risk Analysis System)
[DE90-010938] N91-16395
FEASIBILITY ANALYSIS
Potential use of tiltrotor aircraft in Canadian aviation
[NASA-TM-102245] N91-16001
A summary of prospects for methanol vehicles in the United States
[DE90-009719] N91-16370
Technical and economic evaluation of diesel engine with oxygen enrichment and water injection
[DE90-009723] N91-16373
Electrical power from inertial confinement fusion: Issues and prospects
[DE90-010200] N91-16437
Is there hope for fusion
[DE90-012095] N91-16736
FEEDBACK
Experimentation and concept formation by an autonomous mobile robot
[DE90-003063] N91-16368
FEEDBACK CONTROL
Ultrasound and visual sensor feedback and fusion
[DE90-005280] N91-16369
The discrete time H infinity control problem with measurement feedback
[MEMO-COSOR-89-31] N91-16651
The finite horizon singular time-varying H infinity control problem with dynamic measurement feedback
[MEMO-COSOR-89-33] N91-16652
FERMIONS
Chern-Simons and anyonic superconductivity
[DE90-010663] N91-16787
Fermions in the hypercharge sector of the standard lattice electroweak theory: Global limit
[DE90-009731] N91-16827
FERROELECTRICITY
Total-dose degradation of thin film ferroelectric capacitors
[DE90-007152] N91-16218
Properties and characterization of thin film ferroelectric capacitors for nonvolatile memories
[DE91-004037] N91-16242
FERROMAGNETIC MATERIALS
Epitaxial growth and surface morphology of some metal and semiconductor structures N91-16824
FERROMAGNETISM
Magnetic structures of actinide materials by pulsed neutron diffraction
[DE91-000373] N91-16093
FIBER COMPOSITES
Flammability characteristics of fiber-reinforced composite materials for the composite infantry fighting vehicle
[AD-A227783] N91-16068
Characterization of the corrosion of a P-130x graphite fiber reinforced 6063 aluminum metal matrix composite
[AD-A228134] N91-16071
Flammability characteristics of fiber reinforced composite materials
[AD-A228215] N91-16072
Understanding the interdiffusion behavior and determining the long term stability of tungsten fiber reinforced niobium-base matrix composite systems
[NASA-CR-187396] N91-16120
Tensile behavior of tungsten/niobium composites at 1300 to 1600 K
[NASA-TM-103727] N91-16128
Fiber-reinforced ceramic composites for Earth-to-orbit rocket engine turbines
[NASA-CR-185264] N91-16150
FIBER OPTICS
The design and construction of an Automated Multi-Object Spectroscopy system (AMOS)
[DE90-011497] N91-16088
Development of a versatile laser light scattering instrument
[NASA-CR-182474] N91-16350
New methods for producing, recording, and processing interferometric moire patterns N91-16405
Fiber optic synthetic aperture interferometer
[AD-A227891] N91-16741
Applications of non-linear optics
[AD-A228872] N91-16743
FIBER STRENGTH
Effects of high pressure nitrogen on the thermal stability of SiC fibers
[NASA-TM-103245] N91-16075
FIBERS
Mechanics of interface cracks
[AD-A227579] N91-16067
FIBRILLATION
Electrical resistance volumetry in the circulation N91-16543
FIELD EFFECT TRANSISTORS
Numerical simulation of the comparative electrical performance of the permeable base transistor, opposed gate-source transistor and heterostructure launched ballistic field effect transistor
[AD-A228545] N91-16202
Fabrication and electrical characterization of deep-submicron trench-isolated CMOS device structures N91-16802
FIELD EMISSION
Concepts for future developments in electron microscopy
[DE90-010630] N91-16320
FIELD THEORY (PHYSICS)
Analytic Multi-Regge Theory and the Pomeron in QCD
[DE90-012153] N91-16737
Chern-Simons and anyonic superconductivity
[DE90-010663] N91-16787
Dynamics of strong-coupling models for cuprate superconductors: Exact results on finite lattices
[DE90-011155] N91-16796
FIGHTER AIRCRAFT
Tactical fighter aircraft: Differences between the Air Force's roadmap and the five year defense plan
[AD-A228882] N91-15976
TF89 aircraft centre fuselage
[ETN-91-98579] N91-16018
TF89 tactical fighter outer wing design
[ETN-91-98580] N91-16019
Organization of the mission pattern in the air picture
[IZF-1990-A-12] N91-16568
Optical transceiver frontend for high speed bus STANAG 3910 with one fiber only
[MBB-UA-1182-90-PUB] N91-16745
FILE MAINTENANCE (COMPUTERS)
Reliability/Maintainability/Logistics support analysis Computer Aided Tailoring Software Program (R/M/L CATSOP)
[AD-A226820] N91-16588
Ada compiler validation procedures, version 2.1
[AD-A228614] N91-16621
FILLERS
Model filled polymers versus synthesis of crosslinked monodisperse polymethacrylate beads
[AD-A227236] N91-16146
FILM COOLING
Experimental and theoretical examinations of film cooling of gas turbine blades
[ETN-91-98554] N91-16022
FILMS
Updated evaluation of polymer films for electrical insulation
[DE91-000544] N91-16148
FILTERS
Particle deposition in granular media
[DE90-010810] N91-16261
FILTRATION
Particle deposition in granular media
[DE90-010810] N91-16261
FINE STRUCTURE
Fine particle flotation in a centrifugal force field
[ETN-91-98480] N91-16309
The 158 micrometer (CII) line: A measure of global star formation activity in galaxies
[NASA-CR-187925] N91-16977
FINGERS
Quantification of lower bounds for endurance times in thermally insulated fingers and toes exposed to cold stress
[AD-A227782] N91-16545
FINITE DIFFERENCE THEORY
Numerical modeling tools for transient electromagnetic problems
[DE90-010328] N91-16180
Modeling pulse driven antenna systems with finite differences
[DE90-010682] N91-16182

Direct disc impact investigation of dynamic large finite plastic behavior of 1100 aluminum N91-16404
Use of satellite data and modeling to assess the influence of stratospheric processes on the troposphere N91-16517
Wakefield calculations on parallel computers [DE90-009712] N91-16632

FINITE ELEMENT METHOD
Finite element approximations for transonic flows [ETN-91-98491] N91-15988
A coupled rotor aeroelastic analysis utilizing advanced aerodynamic modeling N91-16006
A decentralized linear quadratic control design method for flexible structures [NASA-CR-187860] N91-16059
Inelastic strain analysis of solder joint in NASA fatigue specimen [NASA-CR-187864] N91-16132
Development and application of numerical models for reactive flows [AD-A228884] N91-16295
Finite element solution techniques for the vorticity-stream function formulation of two-dimensional incompressible flows N91-16302
A segregated finite element solution to the incompressible Navier-Stokes equations [ME-69] N91-16315
A modular stiffness-based approach to rotating systems analysis N91-16400
Time-temperature response of multiphase viscoelastic solids through numerical analysis N91-16401
Dynamic crack propagation in elastic-plastic solids N91-16402
Finite element solution of steady state axisymmetric penetration problems N91-16403
Adaptive mesh refinement for meshes with singular elements N91-16406
Finite element thermo-viscoplastic analysis of aerospace structures [NASA-TM-102761] N91-16407
Dynamic response of composite beams using shear-deformable finite elements [AD-A227975] N91-16408
Scattering of Lamb waves in an elastic plate for ultrasonic nondestructive evaluation of weldments and cracks N91-16412
A finite element procedure for calculating fluid-structure interaction using MSC/NASTRAN [NASA-TM-102857] N91-16414
A time-domain finite-element method for the computation of three-dimensional acoustic wave fields in inhomogeneous fluids and solids [ETN-91-98485] N91-16710

FIRE CONTROL
A paper-assessment of the performance of a modern airborne multi-mode pulse Doppler radar deployed as a ground-based fire-control radar [ETN-91-98584] N91-16215

FIRES
Flammability characteristics of fiber reinforced composite materials [AD-A228215] N91-16072
Parameterization of aerosol scavenging in a convective cloud model [DE90-010865] N91-16458

FISSION PRODUCTS
Is there hope for fusion [DE90-012095] N91-16736

FLAME IONIZATION
A comparison of three prospective analytical methods for benzene analysis in jet fuel environments [AD-A227489] N91-16170

FLAME PROPAGATION
Modelling of flamelet surface-to-volume ratio in turbulent premixed combustion [DE90-006312] N91-16081
Development and application of numerical models for reactive flows [AD-A228884] N91-16295

FLAME TEMPERATURE
Initial studies of electric field effects on ceramic powder formation in flames [DE90-007571] N91-16138

FLAMES
Autoignition and flameholding in a cylindrical scramjet combustor [NAL-TR-1067] N91-16102
Initial studies of electric field effects on ceramic powder formation in flames [DE90-007571] N91-16138

FLAMMABILITY
Flammability characteristics of fiber-reinforced composite materials for the composite infantry fighting vehicle [AD-A227783] N91-16068
Flammability characteristics of fiber reinforced composite materials [AD-A228215] N91-16072

FLAT SURFACES
Materials systems for 2- to 5-micrometers wavelength diode lasers [AD-A228218] N91-16361
Linear-time separation algorithms for the three-index assignment polytope [AD-A228854] N91-16626

FLEXIBLE SPACECRAFT
The NASA controls-structures interaction technology program [NASA-TM-102752] N91-16057
A decentralized linear quadratic control design method for flexible structures [NASA-CR-187860] N91-16059

FLIGHT CHARACTERISTICS
Evaluation of rotorwash characteristics for tiltrotor and tiltwing aircraft in hovering flight [SCT-90RR-18] N91-15989

FLIGHT CONTROL
General designer describes Buran flight control, autopilot systems N91-16039
Specialists at flight control center discuss shuttle computer systems N91-16040

FLIGHT MANAGEMENT SYSTEMS
The European flight safety crisis: Costs and solution [ETN-91-98490] N91-16000

FLIGHT SAFETY
The European flight safety crisis: Costs and solution [ETN-91-98490] N91-16000
Activities report of the German Federal Institute for Flight Safety [ETN-91-98644] N91-16002
Safety Network to Detect Performance Degradation and Pilot Incapacitation [AGARD-CP-490] N91-16553

FLIGHT SIMULATION
Use of the Magnus force in the modified point mass trajectory model [AD-A228194] N91-15990
Computer aided physiological assessment of the functional state of pilots during simulated flight N91-16562

FLOQUET THEOREM
A coupled rotor aeroelastic analysis utilizing advanced aerodynamic modeling N91-16006

FLOTATION
Fine particle flotation in a centrifugal force field [ETN-91-98480] N91-16309

FLOW CHAMBERS
Numerical simulation of buffer flow in a free flow electrophoresis chamber N91-16279

FLOW CHARACTERISTICS
Use of satellite data and modeling to assess the influence of stratospheric processes on the troposphere N91-16517

FLOW DISTORTION
On the receptivity and non-parallel stability of travelling disturbances in rotating disk flow [NASA-CR-187486] N91-15996

FLOW DISTRIBUTION
Investigation of transonic flow over segmented slotted wind tunnel wall with mass transfer [NASA-CR-187760] N91-15981
On the receptivity and non-parallel stability of travelling disturbances in rotating disk flow [NASA-CR-187486] N91-15996
Numerical analysis of viscous hypersonic flow past a generic forebody [MBB/FE122/S/PUB/0407] N91-15997
Small scale shock tube experiments using a computer controlled active rarefaction wave eliminator [AD-A227507] N91-16029
Joint computational/experimental aerodynamics research on a reentry vehicle. Part 2: Computational results [DE90-012765] N91-16054
Transient natural convection in heated inclined tubes [DE90-008217] N91-16255
Analytical and numerical studies in flow development [DE90-010424] N91-16258
Aerodynamic drag characterization and deposition studies of irregular particles. Part 3: Analysis of flow and temperature field inside the Combustion Deposition Entrained Reactor (CDER) [DE90-000466] N91-16259
Unsteady vortex lattice calculation of the flow around a slender delta wing N91-16272
Numerical simulation of a complicated transition-breakdown of vortical flows inside a circular pipe N91-16273
MmB: A new class of accurate high resolution schemes for conservation laws in two dimensions N91-16275
Numerical simulation of buffer flow in a free flow electrophoresis chamber N91-16279
Numerical study of a three-dimensional turbulent boundary layer [AD-A227835] N91-16291
Natural-convection boundary layers [ISBN-90-9003467-6] N91-16313
Potential vorticity index N91-16516

FLOW EQUATIONS
Analytical and numerical studies in flow development [DE90-010424] N91-16258
Acceleration of iterative algorithms for Euler and Navier-Stokes equations N91-16301
Natural-convection boundary layers [ISBN-90-9003467-6] N91-16313

FLOW MEASUREMENT
A process for unstationary velocity and turbulence measurements with a pneumatic measuring wedge probe [MITT-33] N91-16310

FLOW STABILITY
On the receptivity and non-parallel stability of travelling disturbances in rotating disk flow [NASA-CR-187486] N91-15996
Analytical and numerical studies in flow development [DE90-010424] N91-16258
Research in nonlinear water waves [AD-A227948] N91-16292
Streamwise vortices in laminar-turbulent transition N91-16297
Local and global instability of heated 2-D jets and wakes N91-16298

FLOW VELOCITY
Investigation of transonic flow over segmented slotted wind tunnel wall with mass transfer [NASA-CR-187760] N91-15981
Safe venting of hydrogen [DE90-008964] N91-16174
The high speed buffer board: A SAIL EIA-485 communications accelerator card for the vector measuring current meter [AD-A227181] N91-16185
Development of a two-phase cold plate N91-16277
Heat transfer from water flowing through a chilled-bed open channel [AD-A226855] N91-16286
The development of laser speckle velocimetry for the study of vortical flows [NASA-CR-187756] N91-16289
Incompressible flow simulations using the velocity-pressure formulation N91-16299
A segregated finite element solution to the incompressible Navier-Stokes equations [ME-69] N91-16315

FLOW VISUALIZATION
Pressure gradient effects on the development of hairpin vortices in an initially laminar boundary layer N91-16282
Rotating Rayleigh-Benard convection: The Kueppers-Lortz transition [DE91-004835] N91-16288
The development of laser speckle velocimetry for the study of vortical flows [NASA-CR-187756] N91-16289
Visualization of unsteady transonic flow by holographic interferometry using photorefractive media [AD-A228802] N91-16336
Full field visualization of surface and bulk acoustic waves [AD-A227676] N91-16678

FLOWMETERS
The high speed buffer board: A SAIL EIA-485 communications accelerator card for the vector measuring current meter [AD-A227181] N91-16185

FLUE GASES
Parametric study of electrostatically charged sprays [DE90-010580] N91-16262

FLUENCE
Effects of neutron fluence on the operating characteristics of diode lasers used in atomic frequency standards [AD-A226763] N91-16352

FLUID BOUNDARIES
Study of time accuracy of flow variables across discontinuous boundaries N91-16300

FLUID DYNAMICS
An experiment on supersonic turbulent mixing layers: Supersonic-subsonic two-stream layers [NAL-TR-1066] N91-15983
MmB: A new class of accurate high resolution schemes for conservation laws in two dimensions N91-16275
Analysis and application of the discrete vortex method N91-16290
Nonlinear waves and inverse scattering [AD-A228757] N91-16294

FLUID FILMS
Extension of transonic flow computational concepts in the analysis of cavitated bearings
[NASA-TM-103214] N91-16304
FLUID FLOW
Far-field boundaries and their numerical treatment N91-16281
The impact of separated flow on heat and mass transfer
[DE91-000592] N91-16284
Theoretical and experimental studies of baroclinic processes N91-16512
FLUID INJECTION
Pressure gradient effects on the development of hairpin vortices in an initially laminar boundary layer N91-16282
FLUID MECHANICS
AFDM: An Advanced Fluid-Dynamics Model. Volume 2: Topologies, flow regimes and interfacial areas
[DE91-000581] N91-16283
FLUID-SOLID INTERACTIONS
A finite element procedure for calculating fluid-structure interaction using MSC/NASTRAN
[NASA-TM-102857] N91-16414
FLUIDS
A new perturbation theory of solids and fluids and its applications to high-pressure melting problems
[DE90-011502] N91-16829
FLUORESCENCE
Ultrasensitive molecular fluorescence spectroscopy in levitated microdroplets
[DE91-000621] N91-16095
Photoinduced charge separation by polymer-bound chromophores
[DE90-010997] N91-16140
FLUOROPOLYMERS
The search for high energy low vulnerability explosives
[DE90-009436] N91-16158
FLUTTER
Wind tunnel tests on flutter control of a high-aspect-ratio cantilevered wing: Control with leading-edge and trailing-edge control surfaces
[NAL-TR-1070] N91-15982
FLUTTER ANALYSIS
Propfan supersonic panel method analysis and flutter predictions N91-15993
FLYBY MISSIONS
Aerospace vehicle design, spacecraft section. Volume 1: Project groups 1-4 --- unmanned probe to Pluto
[NASA-CR-186841] N91-16045
PFERD Mission: Pluto flyby exploration/research design N91-16046
Intrepid: A mission to Pluto N91-16047
Project Cerberus: Flyby mission to Pluto N91-16048
OPTIC: Orbiting Plutonian Topographic Image Craft proposal for an unmanned mission to Pluto N91-16049
Aerospace vehicle design, spacecraft section. Volume 2: Project groups 5-7 --- unmanned probe to Pluto
[NASA-CR-186842] N91-16050
Mission management, planning, and cost: PULSE Attitude And Control Systems (AACS) N91-16051
The Copernicus project N91-16052
The Phoenix Pluto Probe N91-16053
FOKKER-PLANCK EQUATION
Massively parallel Fokker-Planck calculations
[DE90-010691] N91-16633
FORECASTING
Liquid hydrogen production and commercial demand in the United States N91-16168
FORESTS
Ozone and acid-precipitation on western coniferous forests
[DE90-011014] N91-16462
Scattering measurements on natural and model trees N91-16691
FORMALISM
Modeling and verification of distributed systems with labeled predicate transition nets
[LAAS-90215] N91-16214
FORMAT
Automated design of displays for technical data
[AD-A226729] N91-16586
Using computer-generated protocols to study writers' planning strategies
[AD-A228875] N91-16844
FORMIC ACID
Formic and acetic acids in the boundary layer over the North Atlantic ocean N91-16530
FORMING TECHNIQUES
Gelcasting of sub-micron alumina, sialon, and silicon nitride powders
[DE91-000618] N91-16145
FORMULAS (MATHEMATICS)
Geometrical aspects of the production of toothed disks
[MEMO-COSOR-90-02] N91-16178
FORMULATIONS
Symmetry and design in mixture experiments
[AD-A226760] N91-16169
FORWARD SCATTERING
Fourth moments of acoustic waves forward scattered by a rough ocean surface
[AD-A227469] N91-16529
FOSSIL FUELS
Solving global environmental problems through technological innovation
[DE90-010018] N91-16446
Biomass and hydrocarb technology for removal of atmospheric CO2
[DE90-010016] N91-16453
FOURIER ANALYSIS
Nonlinear waves and inverse scattering
[AD-A228757] N91-16294
Effects of large-scale wind driven turbulence on sound propagation N91-16704
FOURIER SERIES
Periodic solutions of neutral differential equations
[RR-390] N91-16658
FOURIER TRANSFORMATION
An approximation to true peak absorbance from observed peak absorbance for gas phase Fourier transform spectroscopy
[AD-A228357] N91-16104
The use of window functions and Kalman filtering in spectral estimation
[AD-A227482] N91-16236
Two-dimensional convolutions, correlations, and Fourier transforms of combinations of Wigner distribution functions and complex ambiguity functions
[AD-A226852] N91-16649
FRACTURE MECHANICS
Effects of high pressure nitrogen on the thermal stability of SiC fibers
[NASA-TM-103245] N91-16075
Weldability of nickel aluminides
[DE90-008557] N91-16116
Elevated temperature crack growth in titanium aluminides
[AD-A227700] N91-16125
Development of nondestructive evaluation methods and prediction of effects of flaws on the fracture behavior of structural ceramics
[DE90-011092] N91-16141
Probabilistic fracture mechanics: A validation of predictive capability
[AD-A228877] N91-16409
FRACTURE STRENGTH
Thermal aging of cast stainless steels: Mechanisms and predictions
[DE90-010093] N91-16115
Mechanical property data on aluminum alloy 7150-T7751 plate
[AD-A227506] N91-16124
FRACTURES (MATERIALS)
Mechanics of interface cracks
[AD-A227579] N91-16067
FRAGMENTS
Fragment mass distribution of debris
[MBB-UA-1187-90-PUB] N91-16669
FREE BOUNDARIES
A free boundary problem arising in plasma physics
[DE90-010065] N91-16754
FREE CONVECTION
Transient natural convection in heated inclined tubes
[DE90-008217] N91-16255
FREE ELECTRON LASERS
Comparison of propagation and absorption of FEL-generated microwaves with theory
[DE90-010369] N91-16181
Nonlinear resonance
[DE90-010428] N91-16341
Development of free-electron lasers for XUV projection lithography
[DE90-010566] N91-16342
Mode competition effects in free electron lasers and gyrotrons
[DE90-011084] N91-16346
Integrated Numerical Experiments (INEX) and the Free-Electron Laser Physical Process Code (FELPPC)
[DE90-011957] N91-16348
Generation of XUV light by resonant frequency tripling in a two-wiggler FEL amplifier
[DE90-012120] N91-16349
Design requirements and calculated performance of an XUV FEL oscillator operating on a higher harmonic
[DE91-004833] N91-16357
Microwave Tokamak Experiment (OMTX): Overview and status
[DE90-010287] N91-16758
Stark-effect measurement of high FEL electric fields in MTX by laser-aided particle-probe spectroscopy
[DE90-011911] N91-16771
FREE ENERGY
Calculation of free energy from the internal-energy distribution function
[DE90-011111] N91-16791
FREE FLOW
An experiment on supersonic turbulent mixing layers: Supersonic-subsonic two-stream layers
[NAL-TR-1066] N91-15983
Numerical simulation of buffer flow in a free flow electrophoresis chamber N91-16279
FREE VIBRATION
Passive damping concepts for tubular beams with partial rotational and translational end restraints
[NASA-CR-187833] N91-16411
FREON
Heat transfer characteristics of a radical heat pipe N91-16276
FREQUENCIES
The 1/f frequency noise effects on self-heterodyne linewidth measurements for coherent communications
[AD-A227942] N91-16195
Measurement of the capture effect of frequency modulation
[AD-A228058] N91-16199
FREQUENCY MEASUREMENT
Measurement of the capture effect of frequency modulation
[AD-A228058] N91-16199
FREQUENCY MODULATION
Measurement of the capture effect of frequency modulation
[AD-A228058] N91-16199
FREQUENCY SHIFT
Intra-Pulse Frequency Diversity (IPFD) lab demonstration
[AD-A228814] N91-16209
FREQUENCY STANDARDS
Effects of neutron fluence on the operating characteristics of diode lasers used in atomic frequency standards
[AD-A226763] N91-16352
FRESH WATER
Heat transfer from water flowing through a chilled-bed open channel
[AD-A226855] N91-16286
FRICTION
Detection of solid lubricant film failure during sliding by vibration monitoring
[NAL-TR-1060] N91-16384
Dynamical friction in pairs of elliptical galaxies N91-16933
FRONTS (METEOROLOGY)
A two-dimensional balanced model of internal frontogenesis in geostrophic and isentropic coordinates
[AD-A227644] N91-16518
Examples of isallobaric forcing in surface frontal motion and surface frontogenesis over the Central United States
[AD-A227687] N91-16521
FUEL CELLS
Impurity tolerant electrocatalysts
[DE90-011960] N91-16090
Microwave sintering of fuel cell materials
[DE90-011643] N91-16143
Requirements for a fuel cell for transportation application
[DE90-011146] N91-16230
Evaluation of novel solid electrolyte materials
[DE90-011164] N91-16231
Direct methanol/air fuel cells: Systems considerations
[DE90-011971] N91-16439
FUEL CONSUMPTION
Technological and policy options for mitigating greenhouse gas emissions from mobile sources
[DE90-010151] N91-16447
FUEL INJECTION
Autoignition and flameholding in a cylindrical scramjet combustor
[NAL-TR-1067] N91-16102
FUEL PRODUCTION
Ionic solid hydrogen fuel: Production and properties of hydrogen ion and energetic neutral clusters
[AD-A227683] N91-16172
FUEL SPRAYS
Spray combustion modeling and evaluation
[NASA-CR-187887] N91-16078
FUEL SYSTEMS
CRC volatility program on the effect of oxygenated fuels and altitude on cold-start drivability at low ambient temperatures
[AD-A227571] N91-16171
FUEL-AIR RATIO
Auto-ignition temperatures of binary mixtures of alkanes in a closed vessel: Comparisons between experimental measurements and numerical predictions
[DE90-007856] N91-16082

FUELS
CRC volatility program on the effect of oxygenated fuels and altitude on cold-start drivability at low ambient temperatures
[AD-A227571] N91-16171
Improved anode catalysts for coal gas-fueled phosphoric acid fuel cells
[DE90-009683] N91-16442
FULL SCALE TESTS
Space Shuttle Flight Support Motor no. 1 (FSM-1)
[NASA-CR-184078] N91-16064
FUNCTIONS (MATHEMATICS)
Introduction (to a book on applications of local-density-functional methods in chemistry)
[AD-A228769] N91-16109
Skolem functions and equality in automated deduction
[DE90-009703] N91-16641
Exponential ground impedance models and their interpretation N91-16686
FURNACES
High temperature furnace modeling and performance verifications
[NASA-CR-187831] N91-16032
Microwave sintering of fuel cell materials
[DE90-011643] N91-16143
FUSELAGES
TF89 aircraft centre fuselage
[ETN-91-98579] N91-16018
FUSION REACTORS
Comparison of the thermal stability of the codeposited carbon/hydrogen layer to that of the saturated implant layer in graphite
[DE90-012148] N91-16144
Is there hope for fusion
[DE90-012095] N91-16736
D3-D research operations
[DE90-008232] N91-16752
Plasma-facing materials
[DE90-008243] N91-16753
Theoretical studies of tokamaks
[DE90-011332] N91-16768
FUZZY SYSTEMS
Applications of fuzzy theories to multi-objective system optimization
[NASA-CR-177573] N91-16012
Application of fuzzy-Bayesian analysis to structural reliability
[NAL-TR-1063] N91-16396
About Petri nets with fuzzy markings
[LAAS-90354] N91-16670

G

GALACTIC BULGE
The spiral-compact galaxy pair AM 2208-251: Computer simulations versus observations N91-16939
GALACTIC CLUSTERS
Paired and Interacting Galaxies: International Astronomical Union Colloquium No. 124
[NASA-CP-3098] N91-16858
Morphological type correlation between nearest neighbor pairs of galaxies N91-16861
Observational properties of compact groups of galaxies N91-16871
VLA neutral hydrogen imaging of compact groups N91-16872
Blue ellipticals in compact groups N91-16873
What is the number of spiral galaxies in compact groups N91-16874
Triple galaxies and a hidden mass problem N91-16875
A study of the compact group of galaxies Shahbazian 4 N91-16877
Isolated galaxies, pairs, and groups of galaxies N91-16878
Correlation functions for pairs and groups of galaxies N91-16879
The cD galaxy in Abell cluster 1775 N91-16886
Alignment of cD-galaxies with their surroundings N91-16895
Dumb-bell galaxies in southern clusters: Catalog and preliminary statistical results N91-16896
Galaxy interactions and star formation: Results of a survey of global H-alpha emission in spiral galaxies in 8 clusters N91-16905
Dynamical theory of dense groups of galaxies N91-16943
Explaining compact groups as change alignments N91-16944
Dynamics and configurations of galaxy triplets N91-16946
Dragging force on galaxies due to streaming dark matter N91-16947
Triplets of galaxies: Their dynamics, evolution, and the origin of chaos in them N91-16948
A classification of the galaxy groups N91-16949
Viral coefficient and hidden mass in the galaxy groups N91-16950
Paired and interacting galaxies: Conference summary N91-16964
GALACTIC COSMIC RAYS
Cellular track model of biological damage to mammalian cell cultures from galactic cosmic rays
[NASA-TP-3055] N91-16981
GALACTIC EVOLUTION
A homogeneous sample of binary galaxies: Basic observational properties N91-16859
Morphological type correlation between nearest neighbor pairs of galaxies N91-16861
Geometrical parameters of E+S pairs N91-16865
An atlas of mixed-morphology pairs N91-16866
Multi-waveband observations of colliding galaxies N91-16868
Blue ellipticals in compact groups N91-16873
The H I content of non-isolated galaxies N91-16883
Alignment of cD-galaxies with their surroundings N91-16895
Global effects of interactions on galaxy evolution N91-16897
A multiwavelength survey of interacting galaxies N91-16898
Star formation in infrared bright and infrared faint starburst interacting galaxies N91-16901
Radio loud far-infrared galaxies N91-16902
Central activity in 60 micron peakers N91-16913
Probing the tides in interacting galaxy pairs N91-16932
Dynamical friction in pairs of elliptical galaxies N91-16933
What determines the bulge to disk ratio of galaxies N91-16942
On the large-scale structures formed by wakes of open cosmic strings N91-16951
Starbursts in interacting galaxies: Observations and models N91-16958
Dynamical experiments on models of colliding disk galaxies N91-16959
Paired and interacting galaxies: Conference summary N91-16964
The best-fit universe
[DE91-004583] N91-16966
Origin of regularities in the redshift distributions of distant galaxies and quasars
[DE91-004848] N91-16968
Spectrometric, chemical, and cosmological development of galaxies
[ETN-91-98555] N91-16972
GALACTIC NUCLEI
The complex nature of the Seyfert galaxy NGC 7592 N91-16882
The cD galaxy in Abell cluster 1775 N91-16886
Observations of multiple nucleus galaxies N91-16890
The double nucleus galaxies Mkn 423 and Mkn 739 N91-16891
Infrared images of merging galaxies N91-16904
Galaxy interactions and the stimulation of nuclear activity N91-16910
Galaxy interactions and strength of nuclear activity N91-16914
The nature of the emission-line nebulae in powerful far-infrared galaxies N91-16916
Signs of interaction of the NGC 1275 nucleus with the high-velocity system according to 0.7 sec seeing observations N91-16918
IC5063: A merger with a hidden luminous active nucleus N91-16923
Paired and interacting galaxies: Conference summary N91-16964
The 158 micrometer (CII) line: A measure of global star formation activity in galaxies
[NASA-CR-187925] N91-16977
The galactic center at submillimeter and far-infrared wavelengths
[MPE-PREPRINT-190] N91-16978
GALACTIC RADIATION
FIR statistics of paired galaxies N91-16899
Interpretation of the diffusive galactic continuum gamma radiation in MeV area
[MPE-220] N91-16983
GALACTIC ROTATION
H I and mass distribution of GR8 N91-16884
An experimental study of counter-rotating cores in elliptical galaxies N91-16934
On leading spiral arms in close pairs of galaxies N91-16935
GALACTIC STRUCTURE
Using tilted-ring models and numerical hydrodynamics to study the structure, kinematics and dynamics of HI disks in galaxies N91-16851
Paired and Interacting Galaxies: International Astronomical Union Colloquium No. 124
[NASA-CP-3098] N91-16858
Geometrical parameters of E+S pairs N91-16865
The complex nature of the Seyfert galaxy NGC 7592 N91-16882
The ringed X-galaxy NGC 7020 N91-16885
Alignment of cD-galaxies with their surroundings N91-16895
Infrared images of merging galaxies N91-16904
The role of shocks in NGC 6240 N91-16921
M51's spiral structure N91-16938
What determines the bulge to disk ratio of galaxies N91-16942
Caustic waves in galaxy disks produced in collisions with low mass companions N91-16960
Do elliptical galaxies have thick disks N91-16962
Origin of regularities in the redshift distributions of distant galaxies and quasars
[DE91-004848] N91-16968
Galactic structure in direction of Vela-Puppis by means of UBV beta observations
[ETN-91-98556] N91-16973
GALAXIES
A homogeneous sample of binary galaxies: Basic observational properties N91-16859
Pairs of galaxies in low density regions of a combined redshift catalog N91-16860
Morphological type correlation between nearest neighbor pairs of galaxies N91-16861
Geometrical parameters of E+S pairs N91-16865
Triple galaxies and a hidden mass problem N91-16875
H I studies of the sculptor group galaxies N91-16876
Correlation functions for pairs and groups of galaxies N91-16879
Hidden interaction in SBO galaxies N91-16880
The double nucleus galaxies Mkn 423 and Mkn 739 N91-16891
The morphology of Sersic-Pastoriza galaxies N91-16893
Dumb-bell galaxies in southern clusters: Catalog and preliminary statistical results N91-16896
Quantifying the FIR interaction enhancement in paired galaxies N91-16900
On a connection between supernova occurrence and tidal interaction in early type galaxies N91-16903
Statistics of associations among IR galaxies N91-16909
Are extremely luminous far-infrared galaxies the result of merging quasar cores N91-16912
The nature of the emission-line nebulae in powerful far-infrared galaxies N91-16916
Nuclear and extended infrared emission in paired and isolated galaxies N91-16917
The role of shocks in NGC 6240 N91-16921
Deep Fabry-Perot imaging of NGC 6240: Kinematic evidence for merging galaxies N91-16922
Radio structures in QSO-galaxy pairs N91-16924
Radio line and continuum observations of quasar-galaxy pairs and the origin of low reshift quasar absorption line systems N91-16925
Properties of the redshift N91-16926
Selection effects and binary galaxy velocity differences N91-16927
Merging galaxies and black hole ejections N91-16929
A statistical study of merging galaxies: Theory and observations N91-16931
Energy and angular momentum transfer in binary galaxies N91-16940
Typical motions in multiple systems N91-16945
Dynamics and configurations of galaxy triplets N91-16946
Dragging force on galaxies due to streaming dark matter N91-16947
Induced starburst and nuclear activity: Faith, facts, and theory N91-16953
Origin of regularities in the redshift distributions of distant galaxies and quasars
[DE91-004848] N91-16968
The 158 micrometer (CII) line: A measure of global star formation activity in galaxies
[NASA-CR-187925] N91-16977
The galactic center at submillimeter and far-infrared wavelengths
[MPE-PREPRINT-190] N91-16978
GALLIUM
Gallium as a unique anti-resorptive agent in bone: Preclinical studies on its mechanisms of action
[DE90-010650] N91-16542
Modeling the performance of water and liquid gallium cooled x ray optical components: A comparison with experiment
[DE90-010460] N91-16784

GALLIUM ARSENIDE LASERS
Two-dimensional simulation of quantum-well lasers including energy transport
[AD-A227487] N91-16356
Integrated semiconductor modulators
[AD-A228615] N91-16820
GALLIUM ARSENIDES
Investigation of a new concept in semiconductor microwave oscillators
[AD-A226785] N91-16235
Threshold voltage and I-V characteristics of AlGaAs/GaAs MODFETs
[AD-A228844] N91-16248
New surface atomic structures for III-V(110)-p(1 x 1)-Sb(1ML): Chemical bonding and electronic structure
[DE90-011230] N91-16794
Dose rate effects on damage formation in ion-implanted gallium arsenide
[DE91-000394] N91-16806
Characterization of GaAs/Si interface structure by x ray diffraction
[DE91-004769] N91-16811
GAMMA RAY ASTRONOMY
Interpretation of the diffusive galactic continuum gamma radiation in MeV area
[MPE-220] N91-16983
GAMMA RAY BURSTS
Multiple-photon Compton scattering in a strong magnetic field: Cross-sections and radiative transport N91-16852
Resonant Compton scattering in models of gamma-ray burst sources. Part 2: Numerical modeling
[DE91-005268] N91-16982
GAMMA RAYS
Gabor zone plate apertures for imaging with the mercuric iodide gamma ray camera
[DE90-011193] N91-16321
Development of liquid xenon imaging gamma-ray spectrophotometers
[AD-A227575] N91-16740
The measurement of gamma heating in a fusion blanket test assembly
[DE90-011154] N91-16766
Properties of superdeformed bands in the A = 194 region
[DE90-011482] N91-16798
GAS ANALYSIS
Rotational temperature estimation of CO at high temperatures by graphical methods using FTIR spectrometry
[AD-A228370] N91-16105
GAS CHROMATOGRAPHY
Synthesis, characterization and catalytic activity of microporous aluminophosphate catalysts N91-16092
Inverse gas chromatography
[AD-A227677] N91-16099
Laser microplasma-gas chromatography detector. 2: Detection of species-specific fragment emission
[AD-A228373] N91-16106
High speed narrow bore capillary gas chromatography
[ETN-91-98481] N91-16113
A comparison of three prospective analytical methods for benzene analysis in jet fuel environments
[AD-A227489] N91-16170
New development of laser-based techniques in applications of thin-layer chromatography, microprobe elemental analysis, and gas phase pyrolysis
[DE90-011740] N91-16347
GAS DETECTORS
Electrical properties of gas sensor materials
[ETN-91-98572] N91-16114
A miniature inexpensive, oxygen sensing element
[DE90-009938] N91-16318
Electronic analogue for a biological nose
[ME-78] N91-16541
GAS DISSOCIATION
On the Goertler instability in hypersonic flows: Sutherland law fluids and real gas effects
[NASA-CR-187481] N91-15994
GAS DYNAMICS
Using tilted-ring models and numerical hydrodynamics to study the structure, kinematics and dynamics of HI disks in galaxies N91-16851
Induced starburst and nuclear activity: Faith, facts, and theory N91-16953
Numerical simulations of interacting disk galaxies N91-16955
GAS EXPANSION
State of an adiabatic expanding and condensing vapor or slow, medium, and fast explosions into a vacuum
[DE90-010815] N91-16263
GAS FLOW
Finite element approximations for transonic flows
[ETN-91-98491] N91-15988
Gas flows in S-E binary systems of galaxies N91-16956
GAS IONIZATION
The role of shocks in NGC 6240 N91-16921
GAS MIXTURES
Laser microplasma-gas chromatography detector. 2: Detection of species-specific fragment emission
[AD-A228373] N91-16106
High temperature corrosion of alloys in mixed gases N91-16121
GAS PRESSURE
Tests for integrating measurements of gas pressures in aircraft mechanisms
[ETN-91-98558] N91-16014
Effects of high pressure nitrogen on the thermal stability of SiC fibers
[NASA-TM-103245] N91-16075
Gas solubility in glassy polymers: A correlation with excess enthalpy
[AD-A228202] N91-16155
GAS STREAMS
Particle deposition in granular media
[DE90-010810] N91-16261
GAS TEMPERATURE
Rotational temperature estimation of CO at high temperatures by graphical methods using FTIR spectrometry
[AD-A228370] N91-16105
GAS TUNGSTEN ARC WELDING
Sensing of metal-transfer mode for process control of GMAW (Gas Metal Arc Welding)
[DE90-010946] N91-16377
GAS TURBINE ENGINES
Advanced structural instrumentation, volume 2
[AD-A227473] N91-16330
Wear measurement of ceramic bearings in gas turbines
[AD-A227505] N91-16382
GAS TURBINES
Advanced Turbine Technology Applications Project (ATTAP)
[NASA-CR-187039] N91-16021
Experimental and theoretical examinations of film cooling of gas turbine blades
[ETN-91-98554] N91-16022
Aerodynamic drag characterization and deposition studies of irregular particles. Part 3: Analysis of flow and temperature field inside the Combustion Deposition Entrained Reactor (CDER)
[DE90-000466] N91-16259
Advanced structural instrumentation, volume 1
[AD-A227226] N91-16328
Heat engines program
[DE90-010276] N91-16374
GATES (CIRCUITS)
Investigation of a new concept in semiconductor microwave oscillators
[AD-A226785] N91-16235
GAUGE INVARIANCE
Graviton effects in vacuum maximally symmetric spaces N91-16971
GAUGE THEORY
Analytic Multi-Regge Theory and the Pomeron in QCD
[DE90-012153] N91-16737
Chern-Simons and anyonic superconductivity
[DE90-010663] N91-16787
GEAR TEETH
Geometrical aspects of the production of toothed disks
[MEMO-COSOR-90-02] N91-16178
GEARS
Geometrical aspects of the production of toothed disks
[MEMO-COSOR-90-02] N91-16178
Environmental noise from the Naesudden (Sweden) and Maglarp (Sweden) prototype wind turbines: A study of machinery noise
[FFA-TN-1990-34] N91-16706
GELS
Gelcasting of sub-micron alumina, sialon, and silicon nitride powders
[DE91-000618] N91-16145
GEOCHEMISTRY
Subsurface science program: Program overview and research abstracts
[DE90-010321] N91-16456
Climate Caucus report: Opportunities for bridging the gaps from effects to impacts
[DE90-010877] N91-16459
Monitoring challenges and innovative ideas
[DE91-000586] N91-16465
Highlights of the Chemical Technology (CMT) Division's activities
[DE90-008242] N91-16984
GEOGRAPHIC INFORMATION SYSTEMS
Cartographic issues in the development of a digital GRASS database
[AD-A227582] N91-16416
Evaluation of crop transpiration with remote sensing and computer simulation models
[REPT-1] N91-16431
GEOLOGICAL SURVEYS
Seismic imaging for velocity and attenuation structure in geothermal fields
[DE90-010742] N91-16469
Principal facts for about 16,000 gravity stations in the Nevada test site and vicinity
[DE90-011521] N91-16470
GEOMETRIC ACCURACY
Geometrical aspects of the production of toothed disks
[MEMO-COSOR-90-02] N91-16178
GEOMETRICAL THEORY OF DIFFRACTION
High frequency scattering by a smooth coated cylinder simulated with generalized impedance boundary conditions
[NASA-CR-187829] N91-16211
Scattering center analysis of simple metallic objects
[DLR-FB-90-32] N91-16216
GEOMETRY
Symmetry and design in mixture experiments
[AD-A226760] N91-16169
Study of the influence of imperfections on the dynamic stability of tanks
[DE90-011094] N91-16398
GEOMORPHOLOGY
Image-based terrain modeling with thematic mapper N91-16418
GEOPHYSICAL FLUID FLOW CELLS
Laboratory and theoretical models of planetary-scale instabilities and waves N91-16511
GEOPHYSICS
Theoretical and experimental studies of baroclinic processes N91-16512
GEOPOTENTIAL HEIGHT
Geopotential harmonics of order 15 and 30 from analysis of 50 orbit determinations of 1967-102B
[RAE-TR-90029] N91-16035
Potential vorticity index N91-16516
GEOSAT SATELLITES
Analysis of satellite and Expendable Bathythermograph (XBT) data for the abrupt topography program
[AD-A228870] N91-16422
GEOSTROPHIC WIND
A two-dimensional balanced model of internal frontogenesis in geostrophic and isentropic coordinates
[AD-A227644] N91-16518
Examples of isallobaric forcing in surface frontal motion and surface frontogenesis over the Central United States
[AD-A227687] N91-16521
GEOTHERMAL RESOURCES
Seismic imaging for velocity and attenuation structure in geothermal fields
[DE90-010742] N91-16469
GERMAN SPACE PROGRAM
Space research in the Federal Republic of Germany, 1988 and 1989
[ETN-91-98514] N91-16849
GERMANIUM
Quasiperiodic transition to chaos in Ge; and magnetic susceptibility of high-T(c) superconductors
[DE90-011304] N91-16797
GERMANY
The space flights: Second German Spacelab mission D-2 and Mir 1992
[REPT-25/90] N91-16034
The 1989 annual catalog of the German Aerospace Establishment: Research reports and communications
[ISSN-0172-357X] N91-16987
GLASS
Comparative study of phosphosilicate glass on (100) silicon by furnace and rapid isothermal annealing
[NIAR-90-26] N91-16153
Gas solubility in glassy polymers: A correlation with excess enthalpy
[AD-A228202] N91-16155
GLASS FIBERS
Fiber optic synthetic aperture interferometer
[AD-A227891] N91-16741
Optical transceiver frontend for high speed bus STANAG 3910 with one fiber only
[MBB-UA-1182-90-PUB] N91-16745
GLASS TRANSITION TEMPERATURE
Gas solubility in glassy polymers: A correlation with excess enthalpy
[AD-A228202] N91-16155
GLOBAL ATMOSPHERIC RESEARCH PROGRAM
NASA/MSFC FY90 Global Scale Atmospheric Processes Research Program Review
[NASA-CP-3093] N91-16500

GLOBAL POSITIONING SYSTEM
Optimal Kalman filter integration of a global positioning system receiver and an LN-94 inertial navigation system
[AD-A227222] N91-16003
GLOBAL WARMING
Solving global environmental problems through technological innovation
[DE90-010018] N91-16446
Potential responses of landscape boundaries to global environmental change
[DE90-008568] N91-16451
GOERTLER INSTABILITY
On the Goertler instability in hypersonic flows: Sutherland law fluids and real gas effects
[NASA-CR-187481] N91-15994
GOES SATELLITES
Evaluation of the GOES 1-M normalization technique with the visible images of GOES-7
[AD-A227462] N91-16055
GOES 7
Evaluation of the GOES 1-M normalization technique with the visible images of GOES-7
[AD-A227462] N91-16055
GOLD ALLOYS
Grain-boundary structure in ordered alloys
[ETN-91-98571] N91-16136
GOVERNMENTS
Potential use of tiltrotor aircraft in Canadian aviation
[NASA-TM-102245] N91-16001
GRADIENTS
Implementation of the phase gradient algorithm
[DE90-012160] N91-16579
GRAIN BOUNDARIES
High resolution electron microscopy of interfaces in fcc materials
[DE91-004420] N91-16101
Weldability of nickel aluminides
[DE90-008557] N91-16116
Grain-boundary structure in ordered alloys
[ETN-91-98571] N91-16136
Domain boundaries formed during epitactical growth of alpha-Al2O3
[DE91-005018] N91-16814
GRAIN SIZE
Development of nondestructive evaluation methods and prediction of effects of flaws on the fracture behavior of structural ceramics
[DE90-011092] N91-16141
GRAMMARS
PENGUIN: A language for reactive graphical user interfaces
[AD-A228580] N91-16620
GRANULAR MATERIALS
Particle deposition in granular media
[DE90-010810] N91-16261
GRAPH THEORY
Stability properties of a flow process in graphs
[REPT-90-58] N91-16656
GRAPHIC ARTS
Distributed algorithm simulation using input/output automata
[AD-A228113] N91-16611
GRAPHITE
Characterization of the corrosion of a P-130x graphite fiber reinforced 6063 aluminum metal matrix composite
[AD-A228134] N91-16071
Comparison of the thermal stability of the codeposited carbon/hydrogen layer to that of the saturated implant layer in graphite
[DE90-012148] N91-16144
GRAPHS (CHARTS)
Automated design of displays for technical data
[AD-A226729] N91-16586
Stability properties of a flow process in graphs
[REPT-90-58] N91-16656
GRASHOF NUMBER
Numerical simulation of buffer flow in a free flow electrophoresis chamber N91-16279
GRASSES
Carbon dioxide and energy exchanges in a temperate grassland ecosystem N91-16419
GRASSLANDS
Carbon dioxide and energy exchanges in a temperate grassland ecosystem N91-16419
GRATINGS (SPECTRA)
A convenient system for the manufacture of holographic diffraction gratings
[DE90-009481] N91-16319
GRAVIMETRY
Principal facts for about 16,000 gravity stations in the Nevada test site and vicinity
[DE90-011521] N91-16470
GRAVITATION
Laboratory and theoretical models of planetary-scale instabilities and waves N91-16511
Galaxy interactions and strength of nuclear activity N91-16914
Dynamical friction in pairs of elliptical galaxies N91-16933
GRAVITATION THEORY
Energy and Technology Review, March 1990
[DE90-008230] N91-16985
GRAVITATIONAL EFFECTS
Determination of shuttle orbiter center of gravity from flight measurements
[NASA-TM-102627] N91-16058
Modeling and control of a two-arm elastic robot in gravity N91-16389
The effects of the solid inner core and nonhydrostatic structure on the Earth's forced nutations and Earth tides N91-16417
Cerebral oxygen status and G-induced loss of consciousness N91-16554
Observational properties of compact groups of galaxies N91-16871
Nuclear and extended infrared emission in paired and isolated galaxies N91-16917
Dynamical theory of dense groups of galaxies N91-16943
GRAVITATIONAL FIELDS
Natural-convection boundary layers
[ISBN-90-9003467-6] N91-16313
Simulation of disk-disk encounters with co-moving polar grids N91-16941
Numerical simulations of interacting disk galaxies N91-16955
GRAVITONS
Graviton effects in vacuum maximally symmetric spaces N91-16971
GRAVITY ANOMALIES
Principal facts for about 16,000 gravity stations in the Nevada test site and vicinity
[DE90-011521] N91-16470
GRAVITY WAVES
Research in nonlinear water waves
[AD-A227948] N91-16292
Internal solitary waves in compressible fluids
[ETN-91-98475] N91-16307
An investigation of a gravity wave during GALE: February 6, 1986
[AD-A227655] N91-16519
A global climatology of middle atmosphere inertio-gravity waves N91-16524
GREAT SALT LAKE (UT)
Image-based terrain modeling with thematic mapper N91-16418
GREEN'S FUNCTIONS
Calculations for unsteady aerodynamic characteristics on a 3-D lifting body in subsonic flow using boundary element method
[NAL-TR-1065] N91-15985
GREENHOUSE EFFECT
Solving global environmental problems through technological innovation
[DE90-010018] N91-16446
Technological and policy options for mitigating greenhouse gas emissions from mobile sources
[DE90-010151] N91-16447
Greenhouse gas emissions from selected alternative transportation fuels market niches
[DE90-010491] N91-16448
Climate Caucus report: Opportunities for bridging the gaps from effects to impacts
[DE90-010877] N91-16459
Multi-dimensional aspects of recent climate change in North America
[DE90-010958] N91-16460
GRID GENERATION (MATHEMATICS)
Rotorcraft application of advanced computational aerodynamics
[NASA-CR-187767] N91-15987
Study of time accuracy of flow variables across discontinuous boundaries N91-16300
Adaptive mesh refinement for meshes with singular elements N91-16406
GROUND BASED CONTROL
Results of the Kansas City 1989 Terminal Doppler Weather Radar (TDWR) operational evaluation testing
[AD-A226784] N91-16206
GROUND TRUTH
Comparison of SSM/I measurements to numerically-simulated cloud and precipitation during ERICA N91-16501
Vehicular sources in acoustic propagation experiments N91-16690
GROUND WATER
Subsurface science program: Program overview and research abstracts
[DE90-010321] N91-16456
GROUND WAVE PROPAGATION
Tactical HF field expedient antenna performance, volume 1
[AD-A228057] N91-16198
GROUND WIND
Global variability of water vapor and condensate from SSM/I N91-16507
Contents of the NASA ocean data system archive, version 11-90
[NASA-CR-187812] N91-16535
GROUP THEORY
Some aspects of quantum groups and supergroups
[DE90-777884] N91-16671
GUANIDINES
Method of making contamination-free ceramic bodies
[NASA-CASE-LEW-14984-1] N91-16152
GUN TURRETS
Flammability characteristics of fiber-reinforced composite materials for the composite infantry fighting vehicle
[AD-A227783] N91-16068

H

H I REGIONS
VLA neutral hydrogen imaging of compact groups N91-16872
H I studies of the sculptor group galaxies N91-16876
The H I content of non-isolated galaxies N91-16883
H I and mass distribution of GR8 N91-16884
H I observations of the peculiar galaxy NGC 660 N91-16888
Collisional removal of HI from the inner disks of Virgo cluster galaxies N91-16952
H II REGIONS
Observational effects of interaction in the Seyfert galaxy NGC 7469 N91-16906
The nature of the emission-line nebulae in powerful far-infrared galaxies N91-16916
Collisional removal of HI from the inner disks of Virgo cluster galaxies N91-16952
HALOS
Dynamics of groups around interacting double ellipticals: Measuring dark matter haloes N91-16863
HAMILTONIAN FUNCTIONS
Solvable two-dimensional supersymmetric models and the supersymmetric Virasoro algebra
[DE90-012140] N91-16648
HARMONIC GENERATIONS
Interferometric second-harmonic-generation autocorrelator for characterizing femtosecond pulses
[DE90-010331] N91-16345
HARMONIC MOTION
On the propagation of plane waves above an impedance surface N91-16684
HARMONIC OSCILLATORS
Design, ultrastructure, and dynamics of nonlinear optical interactions in polymeric thin films
[AD-A228876] N91-16156
HARMONICS
Wind turbine acoustics
[NASA-TP-3057] N91-16679
On the propagation of plane waves above an impedance surface N91-16684
HEARING
Field measurement of head related transfer functions
[AD-A227850] N91-16708
HEART
Electrical resistance volumetry in the circulation N91-16543
HEAT AFFECTED ZONE
HAZ liquation cracking behavior in newly developed lean 316 stainless steels
[DE90-009409] N91-16117
HEAT EXCHANGERS
Initial parametric results using CYCLEZ: A LMTD-specified, Lorenz-Meutzner cycle refrigerator-freezer model
[DE90-010146] N91-16175
Rotary absorption heat pump sensitivity analysis
[DE90-010006] N91-16256
Contemporary issues in solar pond research
[DE90-010094] N91-16436
HEAT FLUX
Heat transfer characteristics of a radical heat pipe N91-16276
An inter-comparison of surface energy flux measurement systems used during FIFE, 1987
[NASA-CR-187699] N91-16472
A study of the surface energy balance on slopes in a tallgrass prairie
[NASA-CR-187698] N91-16473
The vertical structure of the marine atmospheric boundary layer across a sea surface temperature front
[AD-A227931] N91-16525

Variability of latent and sensible heat fluxes over the oceans N91-16531

HEAT MEASUREMENT

An inter-comparison of surface energy flux measurement systems used during FIFE, 1987
[NASA-CR-187699] N91-16472

Initial calorimetry experiments in the Physics Divsion, ORNL (Oak Ridge National Laboratory)
[DE90-010301] N91-16756

HEAT OF DISSOCIATION

Theoretical study of the C-H bond dissociation energy of acetylene
[NASA-CR-187858] N91-16065

HEAT OF FUSION

Initial calorimetry experiments in the Physics Divsion, ORNL (Oak Ridge National Laboratory)
[DE90-010301] N91-16756

HEAT PIPES

The Proceedings of the Symposium on Mechanics for Space Flight 1989
[ISAS-SP-12] N91-16266

Heat transfer characteristics of a radical heat pipe N91-16276

Experimental study on mercury heat pipes (on effect of screen mesh wick under bottom heat mode) N91-16280

HEAT PUMPS

Rotary absorption heat pump sensitivity analysis
[DE90-010006] N91-16256

Meetings to share advancements in heat pump technologies
[DE90-010008] N91-16257

Magnetic heat pumps
[DE90-010305] N91-16375

HEAT RESISTANT ALLOYS

HAZ liquation cracking behavior in newly developed lean 316 stainless steels
[DE90-009409] N91-16117

High temperature corrosion of alloys in mixed gases N91-16121

Phase selection and processing of high temperature intermetallic alloys
[AD-A227910] N91-16129

HEAT TRANSFER

Experimental and theoretical examinations of film cooling of gas turbine blades
[ETN-91-98554] N91-16022

The effect of charge mixture ratio and particle size on igniter plume heat transfer characteristics
[DE90-010833] N91-16160

Initial parametric results using CYCLEZ: A LMTD-specified, Lorenz-Meutzner cycle refrigerator-freezer model
[DE90-010146] N91-16175

The Proceedings of the Symposium on Mechanics for Space Flight 1989
[ISAS-SP-12] N91-16266

Heat transfer characteristics of a radical heat pipe N91-16276

Development of a two-phase cold plate N91-16277

Effect of inclination angle on heat transfer characteristics of closed two-phase thermosyphon N91-16278

AFDM: An Advanced Fluid-Dynamics Model. Volume 2: Topologies, flow regimes and interfacial areas
[DE91-000581] N91-16283

The impact of separated flow on heat and mass transfer
[DE91-000592] N91-16284

Experimental verification of physical model of pulsed laser welding
[DE91-000025] N91-16380

Colorado State University program for developing, testing, evaluating and optimizing solar heating and cooling systems
[DE90-010107] N91-16435

Contemporary issues in solar pond research
[DE90-010094] N91-16436

Direct methanol/air fuel cells: Systems considerations
[DE90-011971] N91-16439

Research on diabatic initialization N91-16504

Stratiform clouds and their interaction with atmospheric motion N91-16506

Global variability of water vapor and condensate from SSM/I N91-16507

Global-scale, intraseasonal fluctuations of diabatic forcing of the atmosphere N91-16508

Synoptic/planetary-scale interactions and blocking over the North Atlantic Ocean N91-16513

The effect of latent heat release on synoptic-to-planetary wave interactions and its implication for satellite observations: Theoretical modeling N91-16514

The effect of latent heat release on synoptic-to-planetary scale wave interactions and implications for satellite observations: Observational study N91-16515

A model for the prediction of Nb3Sn critical current as a function of field, temperature, strain, and radiation damage
[DE91-000656] N91-16775

HEAT TRANSMISSION

Heat transfer characteristics of a radical heat pipe N91-16276

HEAT TREATMENT

Characterization of the corrosion of a P-130x graphite fiber reinforced 6063 aluminum metal matrix composite
[AD-A228134] N91-16071

HEATING

High temperature furnace modeling and performance verifications
[NASA-CR-187831] N91-16032

Experimental study on mercury heat pipes (on effect of screen mesh wick under bottom heat mode) N91-16280

Local and global instability of heated 2-D jets and wakes N91-16298

Observation simulation experiments with regional prediction models N91-16502

Theoretical and experimental studies of baroclinic processes N91-16512

Use of satellite data and modeling to assess the influence of stratospheric processes on the troposphere N91-16517

HEAVY IONS

Cellular track model of biological damage to mammalian cell cultures from galactic cosmic rays
[NASA-TP-3055] N91-16981

HELICOPTER PERFORMANCE

A comparison of computerized measurement of helicopter pilot performance with atropine sulfate during actual and simulated flight N91-16558

HELICOPTERS

Applications of fuzzy theories to multi-objective system optimization
[NASA-CR-177573] N91-16012

Vehicular sources in acoustic propagation experiments N91-16690

Effect of wind and temperature gradients on received acoustic energy N91-16697

HELIUM

From visco-elasticity towards thermal relaxation: A neutron scattering study of density fluctuations in fluid helium
[ETN-91-98486] N91-16111

HELMHOLTZ EQUATIONS

SCATSPHERE2: A computation for the plane-wave scattering from a submerged, elastic, spherical, evacuated or fluid-filled, thin shell
[AD-A228867] N91-16709

HERMES MANNED SPACEPLANE

Evaporation process and 3 phase flow in a water evaporator assembly
[MBB-UO-0108-90-PUB] N91-16060

HETERODYNING

Experimental set-up for a pulsed CO2 laser rangefinder with heterodyne detection
[FEL-90-A125] N91-16365

HETEROJUNCTION DEVICES

Numerical simulation of the comparative electrical performance of the permeable base transistor, opposed gate-source transistor and heterostructure launched ballistic field effect transistor
[AD-A228545] N91-16202

Integrated semiconductor modulators
[AD-A228615] N91-16820

HIERARCHIES

Expressing user-defined parallelism in EPL (Equational Programming Language)
[AD-A227875] N91-16606

Hierarchical Bayesian analysis of change point problems
[AD-A228179] N91-16666

Dynamics and configurations of galaxy triplets N91-16946

HIGH DEFINITION TELEVISION

Satellite broadcasting: A common-frequency approach to wideband HDTV with a hand-made example plan
[BBC-RD-1990/7] N91-16189

Real-time filtering and detection of dynamics for compression of HDTV
[NASA-CR-187777] N91-16596

HIGH ENERGY ELECTRONS

Magnetic-field shielding of satellites from high-energy-electron environments
[DE90-010296] N91-16043

HIGH FREQUENCIES

Tactical HF field expedient antenna performance, volume 1
[AD-A228057] N91-16198

High-frequency techniques for RCS prediction of plate geometries
[NASA-CR-187865] N91-16212

HIGH LEVEL LANGUAGES

Expressing user-defined parallelism in EPL (Equational Programming Language)
[AD-A227875] N91-16606

HIGH POWER LASERS

Picosecond multiphoton ionization of atomic and molecular clusters
[DE91-000641] N91-16096

Stability and accuracy of the sweep rate measurements for LLNL optical streak cameras
[DE90-012080] N91-16324

Generation of high power 1.54 micrometer radiation by stimulated Raman scattering in methane
[FEL-90-B098] N91-16366

Analytical and experimental investigation of transverse flow aerodynamic windows for high power lasers
[DLR-FB-90-33] N91-16367

Scaling laws for femtosecond laser-plasma interactions
[DE90-011496] N91-16769

HIGH PRESSURE

Effects of high pressure nitrogen on the thermal stability of SiC fibers
[NASA-TM-103245] N91-16075

Photoreflectance studies of electronic transitions in quantum well structures under high pressure
[DE90-011583] N91-16801

A new perturbation theory of solids and fluids and its applications to high-pressure melting problems
[DE90-011502] N91-16829

HIGH RESOLUTION

High resolution electron microscopy of interfaces in fcc materials
[DE91-004420] N91-16101

An experimental demonstration of high-resolution Doppler processing
[AD-A228813] N91-16208

MmB: A new class of accurate high resolution schemes for conservation laws in two dimensions N91-16275

Low-cost, high-resolution telescopes for imaging low-earth orbit satellites
[DE90-012081] N91-16850

HIGH REYNOLDS NUMBER

Simulation of the flow past an impulsively started cylinder using a discrete vortex method N91-16303

HIGH SPEED PHOTOGRAPHY

Debris/Ice/TPS assessment and photographic analysis for shuttle mission STS-41
[NASA-TM-103814] N91-16041

HIGH STRENGTH

Method of making contamination-free ceramic bodies
[NASA-CASE-LEW-14984-1] N91-16152

HIGH TEMPERATURE

High temperature furnace modeling and performance verifications
[NASA-CR-187831] N91-16032

Molten salt electrolytes in high temperature batteries
[RAE-TM-MAT/STR-1155] N91-16241

Ion beam modification of surface for improved high temperature performance
[AD-A228067] N91-16243

HIGH TEMPERATURE ENVIRONMENTS

Phase selection and processing of high temperature intermetallic alloys
[AD-A227910] N91-16129

Advanced structural instrumentation, volume 2
[AD-A227473] N91-16330

HIGH TEMPERATURE PLASMAS

US-Japan Workshop on Field-Reversed Configurations with Steady-State High-Temperature Fusion Plasmas and the 11th US-Japan Workshop on Compact Toroids
[DE90-010253] N91-16755

Scaling laws for femtosecond laser-plasma interactions
[DE90-011496] N91-16769

Cool infalling gas and its interaction with the hot ISM of elliptical galaxies N91-16915

HIGH TEMPERATURE RESEARCH

High temperature oxidation-resistant thruster research
[NASA-CR-185233] N91-16063

HIGH TEMPERATURE SUPERCONDUCTORS

Joint services electronics program
[AD-A227576] N91-16237

Novel applications of Tl-Ca-Ba-Cu-O thin films to active and passive high frequency devices
[DE91-004507] N91-16240

Magnetic heat pumps
[DE90-010305] N91-16375

YBa2Cu3O(7-x) thin film growth on single crystal and polycrystalline yttria-stabilized zirconia
[DE90-010707] N91-16788

High Tc oxide solid state reaction kinetics via complex impedance spectroscopy
[DE90-011178] N91-16792

Dynamics of strong-coupling models for cuprate superconductors: Exact results on finite lattices
[DE90-011155] N91-16796
Quasiperiodic transition to chaos in Ge; and magnetic susceptibility of high-T(c) superconductors
[DE90-011304] N91-16797
Microstructures and dc critical currents in textured Y-Ba-Cu-oxides
[DE91-000895] N91-16803
Observations of vortex structure in YBa2Cu3O7
[DE91-000900] N91-16804
Thermal desorption studies of isotopically-labeled oxygen-induced superconductivity in La2CuO(4+delta)
[DE91-004898] N91-16812
Composite ceramic superconducting wires for electric motor applications
[AD-A228359] N91-16818
From low to high Tc: An ultrasonic investigation of niobium single crystal and YBaCuO superconducting thin films with surface acoustic waves N91-16822

HIGH TEMPERATURE TESTS
Mechanical behavior of a SiC-fiber/Si3N4 composite
[AD-A228371] N91-16073
HAZ liquation cracking behavior in newly developed lean 316 stainless steels
[DE90-009409] N91-16117

HIGH VOLTAGES
Design and fabrication of high voltage planar devices
[LAAS-90306] N91-16252

HIGHWAYS
Evaluation procedure for reinforced concrete box culverts under airfield pavements
[AD-A227920] N91-16031

HMX
The search for high energy low vulnerability explosives
[DE90-009436] N91-16158

HOLES (ELECTRON DEFICIENCIES)
Applications of strained layer superlattices
[DE90-011204] N91-16793

HOLES (MECHANICS)
Thermal emission model for the anneal of radiation-induced trapped holes
[DE90-007285] N91-16718

HOLOGRAPHIC INTERFEROMETRY
Visualization of unsteady transonic flow by holographic interferometry using photorefractive media
[AD-A228802] N91-16336

HOLOGRAPHY
A convenient system for the manufacture of holographic diffraction gratings
[DE90-009481] N91-16319
Visualization of unsteady transonic flow by holographic interferometry using photorefractive media
[AD-A228802] N91-16336

HOMOGENEITY
Homogeneously broadened bidirectional ring laser: Theoretical analysis, numerical simulation, and experiment in helium-xenon N91-16360

HORSESHOE VORTICES
Pressure gradient effects on the development of hairpin vortices in an initially laminar boundary layer N91-16282

HOT CORROSION
Weldability of nickel aluminides
[DE90-008557] N91-16116

HOVERING
Evaluation of rotorwash characteristics for tiltrotor and tiltwing aircraft in hovering flight
[SCT-90RR-18] N91-15989

HULLS (STRUCTURES)
Flammability characteristics of fiber-reinforced composite materials for the composite infantry fighting vehicle
[AD-A227783] N91-16068

HUMAN BEHAVIOR
Investigation of effects of 60-Hz electric and magnetic fields on operant and social behavior and on the neuroendocrine system of nonhuman primates
[DE90-010809] N91-16537

HUMAN BEINGS
Limits of human visual discrimination: Toward a general model of visual geometry
[AD-A226826] N91-16548

HUMAN FACTORS ENGINEERING
Human factors design guidance during the conceptual design phase of system development: A methodological approach
[AD-A224667] N91-16552
A graphical user-interface-driven waveform data acquisition and analysis system
[DE90-011948] N91-16578

HUMAN PERFORMANCE
Human factors design guidance during the conceptual design phase of system development: A methodological approach
[AD-A224667] N91-16552
A normative database for, and analysis of, the dual task of the TASKOMAT
[IZF-1990-A-11] N91-16846

HUYGENS PRINCIPLE
A new approach for the determination of electronic structure
[DE90-010479] N91-16713

HYDRAULIC EQUIPMENT
A hydraulically driven microdisplacement unit
[ME-56] N91-16392

HYDRIDES
Comparison of hydrogen diffusion in Ti2PdH(x) to the behavior for Ti2CuH(x) and Zr2PdH(x)
[DE91-002711] N91-16808

HYDRODYNAMICS
Development of a two-phase cold plate N91-16277
Evaluation of the HULL and SHARC hydrocodes in simulating the reflection of Mach 2.12 non-decaying shock on wedges of various angles
[AD-A227581] N91-16287
Fine particle flotation in a centrifugal force field
[ETN-91-98480] N91-16309
Using tilted-ring models and numerical hydrodynamics to study the structure, kinematics and dynamics of HI disks in galaxies N91-16851
Dynamical experiments on models of colliding disk galaxies N91-16959

HYDROGEN
Experimental studies of the properties of trihydrogen and tetrahydrogen
[AD-A228869] N91-16110
Desorption of H2O and H2 from steel and LiAO2 by temperature programmed desorption
[DE90-011170] N91-16118
Safe venting of hydrogen
[DE90-008964] N91-16174
Comparison of hydrogen diffusion in Ti2PdH(x) to the behavior for Ti2CuH(x) and Zr2PdH(x)
[DE91-002711] N91-16808
Using tilted-ring models and numerical hydrodynamics to study the structure, kinematics and dynamics of HI disks in galaxies N91-16851
VLA neutral hydrogen imaging of compact groups N91-16872
Interacting nuclei in distant galaxies N91-16894

HYDROGEN ATOMS
On the development of in-situ Raman analysis of plasma deposited diamond
[AD-A227453] N91-16147
Optimization of hydrogen consumption in hydrogen masers
[AD-A227267] N91-16355

HYDROGEN FUELS
Ionic solid hydrogen fuel: Production and properties of hydrogen ion and energetic neutral clusters
[AD-A227683] N91-16172

HYDROGEN IONS
Comparison of the thermal stability of the codeposited carbon/hydrogen layer to that of the saturated implant layer in graphite
[DE90-012148] N91-16144
Ionic solid hydrogen fuel: Production and properties of hydrogen ion and energetic neutral clusters
[AD-A227683] N91-16172

HYDROGEN ISOTOPES
Comparison of the thermal stability of the codeposited carbon/hydrogen layer to that of the saturated implant layer in graphite
[DE90-012148] N91-16144

HYDROGEN MASERS
Optimization of hydrogen consumption in hydrogen masers
[AD-A227267] N91-16355

HYDROGEN OXYGEN ENGINES
Fiber-reinforced ceramic composites for Earth-to-orbit rocket engine turbines
[NASA-CR-185264] N91-16150

HYDROGEN PLASMA
On the development of in-situ Raman analysis of plasma deposited diamond
[AD-A227453] N91-16147

HYDROGEN PRODUCTION
An assessment of the government liquid hydrogen requirements for the 1995-2005 time frame including addendum, liquid hydrogen production and commercial demand in the United States
[NASA-TM-103812] N91-16166
An assessment of the government liquid hydrogen requirements for the 1995-2005 time frame N91-16167
Liquid hydrogen production and commercial demand in the United States N91-16168
Ionic solid hydrogen fuel: Production and properties of hydrogen ion and energetic neutral clusters
[AD-A227683] N91-16172

HYDROGENOLYSIS
Fundamental studies of hydrocarbon conversions over supported bimetallic catalysts
[DE90-011744] N91-16089

HYDROLOGY
Subsurface science program: Program overview and research abstracts
[DE90-010321] N91-16456

HYDROSTATIC PRESSURE
A hydraulically driven microdisplacement unit
[ME-56] N91-16392

HYPERCUBE MULTIPROCESSORS
Vectorial and parallel algorithms in dynamic programming for optimal control problems
[LAAS-90256] N91-16629
Linear algebra for dense matrices on a hypercube
[DE90-010533] N91-16647

HYPERFINE STRUCTURE
Application of diode lasers to resonance ionization mass spectrometry
[DE91-000614] N91-16094
Hyperfine interactions associated with iron substituted superconducting oxides
[DE90-010411] N91-16783

HYPERGEOMETRIC FUNCTIONS
Relative extrema, zeros, and inequalities for Jacobi functions of the first and second kind
[REPT-90-55] N91-16654

HYPERSONIC AIRCRAFT
Aerothermodynamic phenomena and the design of atmospheric hypersonic airplanes
[MBB/FE122/S/PUB/0408] N91-16015

HYPERSONIC FLIGHT
Optimization and guidance of flight trajectories for the national aerospace plane
[NASA-CR-187837] N91-16010
Optimal trajectories for an aerospace plane. Part 2: Data, tables, and graphs
[NASA-CR-187848] N91-16011
Hypersonic model configurations
[MBB/FE122/S/PUB/411] N91-16016

HYPERSONIC FLOW
Hypersonic shock/boundary-layer interaction database
[NASA-CR-187769] N91-15986
On the Goertler instability in hypersonic flows: Sutherland law fluids and real gas effects
[NASA-CR-187481] N91-15994
Numerical analysis of viscous hypersonic flow past a generic forebody
[MBB/FE122/S/PUB/0407] N91-15997
MmB: A new class of accurate high resolution schemes for conservation laws in two dimensions N91-16275

HYPERSONIC SPEED
Optimal trajectories for an aerospace plane. Part 1: Formulation, results, and analysis
[NASA-CR-187868] N91-16013
Investigation of the influence of constant adverse pressure gradients on laminar boundary-layer stability at Mach number 8
[AD-A228231] N91-16293

HYPERSONIC VEHICLES
Joint computational/experimental aerodynamics research on a reentry vehicle. Part 2: Computational results
[DE90-012765] N91-16054
Finite element thermo-viscoplastic analysis of aerospace structures
[NASA-TM-102761] N91-16407

HYPERSONICS
Optimal trajectories for an aerospace plane. Part 1: Formulation, results, and analysis
[NASA-CR-187868] N91-16013

HYPOXIA
Cerebral oxygen status and G-induced loss of consciousness N91-16554

HYSTERESIS
Numerical simulation of separated flows around a wing section at steady and unsteady motion by a discrete vortex method N91-16268

I

ICE
Debris/ice/TPS assessment and photographic analysis for shuttle mission STS-41
[NASA-TM-103814] N91-16041
Comparison of SSM/I measurements to numerically-simulated cloud and precipitation during ERICA N91-16501
Global variability of water vapor and condensate from SSM/I N91-16507

ICE CLOUDS
Numerical simulation of aerosol scavenging by ice-bearing convective clouds
[DE90-010676] N91-16457

ICE FORMATION
Numerical simulation of aerosol scavenging by ice-bearing convective clouds
[DE90-010676] N91-16457
IDEAL GAS
On the Goertler instability in hypersonic flows: Sutherland law fluids and real gas effects
[NASA-CR-187481] N91-15994
IDENTITIES
An elementary proof of the Ambartzumian-Pleijel identity
[REPT-90-59] N91-16657
IGNITERS
The effect of charge mixture ratio and particle size on igniter plume heat transfer characteristics
[DE90-010833] N91-16160
A transformer coupled semiconductor bridge igniter for low voltage ignition from a high voltage source
[DE90-009974] N91-16221
IGNITION
Flammability characteristics of fiber reinforced composite materials
[AD-A228215] N91-16072
Autoignition and flameholding in a cylindrical scramjet combustor
[NAL-TR-1067] N91-16102
The effect of charge mixture ratio and particle size on igniter plume heat transfer characteristics
[DE90-010833] N91-16160
Modeling laser ignition of explosives and pyrotechnics: Effects and characterization of radiative transfer
[DE90-011052] N91-16161
Safe venting of hydrogen
[DE90-008964] N91-16174
Scaling dimensionally similar tokamak discharges to ignition
[DE90-010079] N91-16749
IGNITION SYSTEMS
A transformer coupled semiconductor bridge igniter for low voltage ignition from a high voltage source
[DE90-009974] N91-16221
IGNITION TEMPERATURE
Auto-ignition temperatures of binary mixtures of alkanes in a closed vessel: Comparisons between experimental measurements and numerical predictions
[DE90-007856] N91-16082
IMAGE ANALYSIS
The development of laser speckle velocimetry for the study of vortical flows
[NASA-CR-187756] N91-16289
New methods for producing, recording, and processing interferometric moire patterns N91-16405
Image-based terrain modeling with thematic mapper N91-16418
Merging panchromatic and multispectral images for enhanced image analysis
[AD-A227902] N91-16421
Terrain matching using image sequence analysis N91-16424
Sahelian vegetation monitoring project
[BCRS-90-04] N91-16426
IMAGE CORRELATORS
The design of a two-dimensional optical image correlator and its application in image tracking N91-16744
IMAGE ENHANCEMENT
Evaluation of the GOES 1-M normalization technique with the visible images of GOES-7
[AD-A227462] N91-16055
IMAGE FILTERS
Real-time filtering and detection of dynamics for compression of HDTV
[NASA-CR-187777] N91-16596
IMAGE INTENSIFIERS
Multiframe x ray images from a single meander stripline coated on a microchannel plate
[DE90-010741] N91-16224
IMAGE MOTION COMPENSATION
Shift-invariant image reconstruction of speckle-degraded images using bispectrum estimation
[AD-A227728] N91-16188
IMAGE PROCESSING
Evaluation of the GOES 1-M normalization technique with the visible images of GOES-7
[AD-A227462] N91-16055
The development of laser speckle velocimetry for the study of vortical flows
[NASA-CR-187756] N91-16289
Gabor zone plate apertures for imaging with the mercuric iodide gamma ray camera
[DE90-011193] N91-16321
Stability and accuracy of the sweep rate measurements for LLNL optical streak cameras
[DE90-012080] N91-16324
Development of free-electron lasers for XUV projection lithography
[DE90-010566] N91-16342
Merging panchromatic and multispectral images for enhanced image analysis
[AD-A227902] N91-16421
The multisensor image map 1:50,000 Rheinhessen N91-16434
Real-time filtering and detection of dynamics for compression of HDTV
[NASA-CR-187777] N91-16596
Low-level image processing architectures compared for some non-linear recursive neighborhood operations
[ISBN-90-9003713-6] N91-16631
PC-based digital imaging for storing microscopy images for surveillance programs
[DE90-010080] N91-16738
The design of a two-dimensional optical image correlator and its application in image tracking N91-16744
Image interpretation for transmission electron microscopy of thin semiconductor layers and interfaces
[ETN-91-98487] N91-16826
Phased array imaging
[AD-A228774] N91-16855
IMAGE RECONSTRUCTION
Shift-invariant image reconstruction of speckle-degraded images using bispectrum estimation
[AD-A227728] N91-16188
IMAGE RESOLUTION
Merging panchromatic and multispectral images for enhanced image analysis
[AD-A227902] N91-16421
Development of liquid xenon imaging gamma-ray spectrophotometers
[AD-A227575] N91-16740
IMAGING TECHNIQUES
Evaluation of the GOES 1-M normalization technique with the visible images of GOES-7
[AD-A227462] N91-16055
Gabor zone plate apertures for imaging with the mercuric iodide gamma ray camera
[DE90-011193] N91-16321
Reports on cartography and topography. Series 1, report 104
[ISSN-0469-4236] N91-16432
Seismic imaging for velocity and attenuation structure in geothermal fields
[DE90-010742] N91-16469
A case study of the 19 October 1989 polar cap absorption event using the imaging riometer for ionospheric studies
[AD-A227764] N91-16487
Research in optical symbolic tasks
[AD-A228797] N91-16551
PC-based digital imaging for storing microscopy images for surveillance programs
[DE90-010080] N91-16738
Development of liquid xenon imaging gamma-ray spectrophotometers
[AD-A227575] N91-16740
Managing emerging technology: Case studies in document imaging systems
[AD-A227688] N91-16839
Low-cost, high-resolution telescopes for imaging low-earth orbit satellites
[DE90-012081] N91-16850
Phased array imaging
[AD-A228774] N91-16855
Multi-color imaging of selected southern interacting galaxies N91-16867
Tidal distortions in pairs of early-type galaxies N91-16869
VLA neutral hydrogen imaging of compact groups N91-16872
The double nucleus galaxies Mkn 423 and Mkn 739 N91-16891
Radio loud far-infrared galaxies N91-16902
Infrared images of merging galaxies N91-16904
Central activity in 60 micron peakers N91-16913
The nature of the emission-line nebulae in powerful far-infrared galaxies N91-16916
Deep Fabry-Perot imaging of NGC 6240: Kinematic evidence for merging galaxies N91-16922
Probing the tides in interacting galaxy pairs N91-16932
IMMUNITY
Research pathology and special techniques
[NASA-CR-187828] N91-16639
IMPACT LOADS
Graphical analysis of barrel-tamped explosively accelerated flyer plates
[DE90-010299] N91-16028
IMPACT STRENGTH
Pilot study of the dynamic impact response of a composite plate
[FFA-TN-1990-27] N91-16070
IMPACT TESTING MACHINES
Diagnostic of the reaction behaviour of intensive high explosives under jet attack
[MBB-UA-1188-90-PUB] N91-16173
IMPACT TESTS
Development of a crashworthy seat for commuter aircraft
[AD-A227486] N91-15999
IMPEDANCE
An algorithm for using a slide-screw tuner as a computer-controlled impedance
[DE90-010657] N91-16226
On the propagation of plane waves above an impedance surface N91-16684
High Tc oxide solid state reaction kinetics via complex impedance spectroscopy
[DE90-011178] N91-16792
IMPEDANCE MEASUREMENT
The use of impedance measurements in corrosion research: The corrosion behaviour of chromium and iron-chromium alloys
[ISBN-90-9003693-8] N91-16135
IMPINGEMENT
Autoignition and flameholding in a cylindrical scramjet combustor
[NAL-TR-1067] N91-16102
Numerical simulations of unsteady shock reflection processes by a ramp N91-16267
IMPURITIES
Impurity tolerant electrocatalysts
[DE90-011960] N91-16090
Transport simulation of the effect of impurity radiation on the high beta, ohmic start-up of the HBT-EP tokamak
[DE90-010333] N91-16760
Texas experimental tokamak
[DE90-011070] N91-16762
Hyperfine interactions associated with iron substituted superconducting oxides
[DE90-010411] N91-16783
IN-FLIGHT MONITORING
Determination of shuttle orbiter center of gravity from flight measurements
[NASA-TM-102627] N91-16058
Detection of loss of consciousness in flight by Doppler method N91-16555
Current status of an artificial intelligence-based loss of consciousness monitoring system for advanced fighter aircraft N91-16556
Framework for an efficient two filter GLOC monitor N91-16557
A comparison of computerized measurement of helicopter pilot performance with atropine sulfate during actual and simulated flight N91-16558
EEG indicators of mental workload: Conceptual and practical issues in the development of a measurement tool N91-16559
Development of a test-bed for real-time monitoring of pilot mental status N91-16563
INCLINATION
Effect of inclination angle on heat transfer characteristics of closed two-phase thermosyphon N91-16278
INCOHERENT SCATTER RADAR
Derivation of exospheric temperature at high latitudes from incoherent-scatter radar data
[AD-A227721] N91-16484
INCOMPRESSIBLE BOUNDARY LAYER
On the Goertler instability in hypersonic flows: Sutherland law fluids and real gas effects
[NASA-CR-187481] N91-15994
INCOMPRESSIBLE FLOW
Incompressible flow simulations using the velocity-pressure formulation N91-16299
Finite element solution techniques for the vorticity-stream function formulation of two-dimensional incompressible flows N91-16302
Simulation of the flow past an impulsively started cylinder using a discrete vortex method N91-16303
A segregated finite element solution to the incompressible Navier-Stokes equations
[ME-69] N91-16315
INDEXES (DOCUMENTATION)
Aeronautical engineering: A continuing bibliography with indexes (supplement 260)
[NASA-SP-7037(260)] N91-15978
Aeronautical engineering: A continuing bibliography with indexes (supplement 259)
[NASA-SP-7037(259)] N91-15979
Aerospace medicine and biology: A cumulative index to a continuing bibliography (supplement 345)
[NASA-SP-7011(345)] N91-16547
Calendar of selected aeronautical and space meetings: January 1991 onwards
[AGARD-CAL-91/1] N91-16833

INDOOR AIR POLLUTION
Determination of airborne organics by direct sampling mass spectrometry
[DE90-009422] N91-16452
INDUSTRIES
An assessment of the government liquid hydrogen requirements for the 1995-2005 time frame N91-16167
Accomplishments in technology transfer from DOE and its laboratories
[DE90-002686] N91-16986
INELASTIC COLLISIONS
Spontaneous force optical traps
[AD-A228539] N91-16363
INELASTIC SCATTERING
State-to-state inelastic and reactive molecular beam scattering from surfaces
[DE90-010492] N91-16714
Measurements of scattering processes in negative ion-atom collisions
[DE90-010666] N91-16715
Deep inelastic structure functions from electron scattering on hydrogen, deuterium, and iron at 0.6 GeV2 less than or equal to Q2 less than or equal to 30.0 GeV2
[DE90-010169] N91-16785
INEQUALITIES
Linear-time separation algorithms for the three-index assignment polytope
[AD-A228854] N91-16626
The discrete time H infinity control problem with measurement feedback
[MEMO-COSOR-89-31] N91-16651
The finite horizon singular time-varying H infinity control problem with dynamic measurement feedback
[MEMO-COSOR-89-33] N91-16652
Relative extrema, zeros, and inequalities for Gegenbauer functions of the first and second kind
[REPT-90-54] N91-16653
Relative extrema, zeros, and inequalities for Jacobi functions of the first and second kind
[REPT-90-55] N91-16654
INERTIA
A global climatology of middle atmosphere inertio-gravity waves N91-16524
INERTIAL CONFINEMENT FUSION
Electrical power from inertial confinement fusion: Issues and prospects
[DE90-010200] N91-16437
Status of target physics for inertial confinement fusion
[DE90-008221] N91-16751
Electrical power from inertial confinement fusion: Issues and prospects
[DE90-010332] N91-16759
INERTIAL NAVIGATION
Optimal Kalman filter integration of a global positioning system receiver and an LN-94 inertial navigation system
[AD-A227222] N91-16003
INFECTIOUS DISEASES
Research pathology and special techniques
[NASA-CR-187828] N91-16639
INFERENCE
Linguistic and pragmatic constraints on utterance interpretation
[AD-A228815] N91-16210
Skolem functions and equality in automated deduction
[DE90-009703] N91-16641
INFILTRATION
Hydrogen storage in metal hydrides
[AD-A228150] N91-16103
INFORMATION DISSEMINATION
Calendar of selected aeronautical and space meetings: January 1991 onwards
[AGARD-CAL-91/1] N91-16833
Subject bibliography of the PMA 205 (Program Manager Air 205) network technical library at Oak Ridge National Laboratory
[DE90-009988] N91-16835
A sectorial analysis of the information sector in the information economy: Its comparative measurement and new classification model N91-16845
INFORMATION MANAGEMENT
Management information: A key to better acquisition at NIH
[AD-A226867] N91-16830
INFORMATION PROCESSING (BIOLOGY)
Skill and skilled memory
[AD-A227697] N91-16549
Pre-attentive and attentive visual information processing
[AD-A228541] N91-16550
Optimisation of operational workload levels using neurophysiological and cognitive techniques N91-16560
INFORMATION RETRIEVAL
Subject bibliography of the PMA 205 (Program Manager Air 205) network technical library at Oak Ridge National Laboratory
[DE90-009988] N91-16835
The USAF STINFO program overview
[AD-A226969] N91-16838
Managing emerging technology: Case studies in document imaging systems
[AD-A227688] N91-16839
Data base structure to support the production of the digital bathymetric data base
[AD-A227915] N91-16841
INFORMATION SYSTEMS
Subject bibliography of the PMA 205 (Program Manager Air 205) network technical library at Oak Ridge National Laboratory
[DE90-009988] N91-16835
Geographic data transfer N91-16836
Information technology policies: A four country comparative study N91-16840
A sectorial analysis of the information sector in the information economy: Its comparative measurement and new classification model N91-16845
INFORMATION THEORY
Modeling and verification of distributed systems with labeled predicate transition nets
[LAAS-90215] N91-16214
A trellis-searched APC (Adaptive Predictive Coding) speech coder
[DE91-000866] N91-16581
IEEE International Symposium on Information Theory
[AD-A228239] N91-16842
INFORMATION TRANSFER
Concepts for future developments in electron microscopy
[DE90-010630] N91-16320
DTD creation for the Software Technology for Adaptable, Reliable Systems (STARS) program
[AD-A228475] N91-16619
INFRARED ASTRONOMY
Quantifying the FIR interaction enhancement in paired galaxies N91-16900
Dense cores and young stellar objects N91-16969
INFRARED ASTRONOMY SATELLITE
A spiral-like disk of ionized gas in IC 1459: Signature of a merging collision N91-16889
Infrared images of merging galaxies N91-16904
Central activity in 60 micron peakers N91-16913
INFRARED DETECTORS
Global-scale, intraseasonal fluctuations of diabatic forcing of the atmosphere N91-16508
INFRARED IMAGERY
Sahelian vegetation monitoring project
[BCRS-90-04] N91-16426
Infrared images of merging galaxies N91-16904
The kinematics and morphology of NGC 520: One, two, or three galaxies N91-16908
INFRARED INSTRUMENTS
A low-cost infrared telemetry system for kilohertz-bandwidth data acquisition
[DE90-010616] N91-16042
INFRARED LASERS
Droplet shattering, vaporization, and recondensation in cloud clearing with long pulse infrared chemical lasers
[DE90-010584] N91-16343
INFRARED RADIATION
Upper atmosphere IR radiation modeling and analysis
[AD-A227214] N91-16482
Infrared response of YBa2Cu3O(7-delta) films to pulsed, broadband synchrotron radiation
[DE90-011519] N91-16800
A multiwavelength survey of interacting galaxies N91-16898
Star formation in infrared bright and infrared faint starburst interacting galaxies N91-16901
Statistics of associations among IR galaxies N91-16909
Nuclear and extended infrared emission in paired and isolated galaxies N91-16917
Deep Fabry-Perot imaging of NGC 6240: Kinematic evidence for merging galaxies N91-16922
INFRARED SIGNATURES
On the development of in-situ Raman analysis of plasma deposited diamond
[AD-A227453] N91-16147
Analysis of emission data from a Perkin-Elmer 1710 FTIR spectrometer
[AD-A227759] N91-16331
INFRARED SOURCES (ASTRONOMY)
Dense cores and young stellar objects N91-16969
INFRARED SPECTRA
An approximation to true peak absorbance from observed peak absorbance for gas phase Fourier transform spectroscopy
[AD-A228357] N91-16104
Rotational temperature estimation of CO at high temperatures by graphical methods using FTIR spectrometry
[AD-A228370] N91-16105
IR plasma emissions
[AD-A227713] N91-16776
INFRARED SPECTROSCOPY
Inverse gas chromatography
[AD-A227677] N91-16099
Analysis of emission data from a Perkin-Elmer 1710 FTIR spectrometer
[AD-A227759] N91-16331
INFRASONIC FREQUENCIES
Infrasonic observations of large-scale HE events N91-16694
The correction of infrasound signals for upper atmospheric winds N91-16695
INORGANIC COMPOUNDS
Electron stopping powers of some elements and compounds from 0 to 10,000 eV: A compilation
[DE90-010675] N91-16716
INPUT/OUTPUT ROUTINES
Distributed algorithm simulation using input/output automata
[AD-A228113] N91-16611
INSPECTION
Debris/Ice/TPS assessment and photographic analysis for shuttle mission STS-41
[NASA-TM-103814] N91-16041
Application of fuzzy-Bayesian analysis to structural reliability
[NAL-TR-1063] N91-16396
INSULATION
A review of the airborne sound insulation requirements for broadcasting studios and ancillary areas
[BBC-RD-1990/10] N91-16680
Proving experiments on an acoustic transmission suite and its reverberation room
[BBC-RD-1990/13] N91-16681
INTEGRAL EQUATIONS
Sparse representation of smooth linear operators
[AD-A228142] N91-16660
INTEGRATED CIRCUITS
Radiation hardening of a high voltage IC technology (BCDMOS)
[DE90-008345] N91-16220
Nonradiative dielectric waveguide millimetre-wave integrated circuits: A review
[AD-A227760] N91-16238
Properties and characterization of thin film ferroelectric capacitors for nonvolatile memories
[DE91-004037] N91-16242
Safety as a design goal for applications of microelectronic control systems
[REPT-23/90] N91-16253
Programmable surface acoustic wave detection in silicon: Design of programmable filters
[ETN-91-98568] N91-16746
INTEGRATED MISSION CONTROL CENTER
Results of the Kansas City 1989 Terminal Doppler Weather Radar (TDWR) operational evaluation testing
[AD-A228784] N91-16206
INTEGRATED OPTICS
Integrated semiconductor modulators
[AD-A228615] N91-16820
INTELLIGENCE
Army Unmanned Aerial Vehicle (UAV) requirements and the joint UAV program
[AD-A228149] N91-16009
INTERACTING GALAXIES
Paired and Interacting Galaxies: International Astronomical Union Colloquium No. 124
[NASA-CP-3098] N91-16858
Dynamics of groups around interacting double ellipticals: Measuring dark matter haloes N91-16863
The interacting pair Mkn 305/306 N91-16864
Multi-color imaging of selected southern interacting galaxies N91-16867
Multi-waveband observations of colliding galaxies N91-16868
A multi-frequency study of the peculiar interacting system Arp 206 N91-16870
Observational properties of compact groups of galaxies N91-16871
Hidden interaction in SBO galaxies N91-16880
The complex nature of the Seyfert galaxy NGC 7592 N91-16882
The H I content of non-isolated galaxies N91-16883
Observations of multiple nucleus galaxies N91-16890
Interacting nuclei in distant galaxies N91-16894
Global effects of interactions on galaxy evolution N91-16897
A multiwavelength survey of interacting galaxies N91-16898
FIR statistics of paired galaxies N91-16899

Quantifying the FIR interaction enhancement in paired galaxies N91-16900
Star formation in infrared bright and infrared faint starburst interacting galaxies N91-16901
Radio loud far-infrared galaxies N91-16902
Infrared images of merging galaxies N91-16904
Galaxy interactions and star formation: Results of a survey of global H-alpha emission in spiral galaxies in 8 clusters N91-16905
The kinematics and morphology of NGC 520: One, two, or three galaxies N91-16908
Galaxy interactions and the stimulation of nuclear activity N91-16910
Central activity in 60 micron peakers N91-16913
Galaxy interactions and strength of nuclear activity N91-16914
The nature of the emission-line nebulae in powerful far-infrared galaxies N91-16916
Probing the tides in interacting galaxy pairs N91-16932
A simulation survey of galaxy interactions N91-16936
A dynamical proximity analysis of interacting galaxy pairs N91-16937
M51's spiral structure N91-16938
Simulation of disk-disk encounters with co-moving polar grids N91-16941
What determines the bulge to disk ratio of galaxies N91-16942
Dynamical theory of dense groups of galaxies N91-16943
Explaining compact groups as change alignments N91-16944
Collisional removal of HI from the inner disks of Virgo cluster galaxies N91-16952
Numerical simulations of interacting disk galaxies N91-16955
Observations and models of star formation in the tidal features of interacting galaxies N91-16957
Starbursts in interacting galaxies: Observations and models N91-16958
Dynamical experiments on models of colliding disk galaxies N91-16959
Simulations of gas clouds in interacting galaxies N91-16961
Paired and interacting galaxies: Conference summary N91-16964

INTERACTIONAL AERODYNAMICS
Hypersonic shock/boundary-layer interaction database [NASA-CR-187769] N91-15986
Rotorcraft application of advanced computational aerodynamics [NASA-CR-187767] N91-15987

INTERATOMIC FORCES
Interatomic forces and bonding mechanisms in MgO clusters [DE90-010148] N91-16719

INTERDIGITAL TRANSDUCERS
Multiple-frequency surface acoustic wave devices as sensors [DE90-009972] N91-16675

INTERFACES
Acoustical and dynamic mechanical characterization of fiber-matrix interface bonds in ceramic composites [DE90-010949] N91-16066
Mechanics of interface cracks [AD-A227579] N91-16067
Fundamental studies with a monodisperse aerosol-based liquid chromatography/mass spectrometry interface (MAGIC-LC/MS) [DE90-010667] N91-16083
AFDM: An Advanced Fluid-Dynamics Model. Volume 2: Topologies, flow regimes and interfacial areas [DE91-000581] N91-16283
Decentralized real-time scheduling [AD-A227856] N91-16604
Horizontal fault tolerance in a fully distributed loosely coupled environment [AD-A227972] N91-16638
Pi: A parallel architecture interface for multi-model execution [AD-A228345] N91-16640

INTERFEROMETERS
A convenient system for diffraction moire measurements [DE90-010980] N91-16739
Fiber optic synthetic aperture interferometer [AD-A227891] N91-16741

INTERGALACTIC MEDIA
The interacting pair Mkn 305/306 N91-16864
The H I content of non-isolated galaxies N91-16883
The polar-ring galaxies NGC 2685 and NGC 3808B (VV 300) N91-16892

INTERMETALLICS
Mechanics of interface cracks [AD-A227579] N91-16067
Phase selection and processing of high temperature intermetallic alloys [AD-A227910] N91-16129
Comparison of hydrogen diffusion in Ti2PdH(x) to the behavior for Ti2CuH(x) and Zr2PdH(x) [DE91-002711] N91-16808

INTERNAL COMBUSTION ENGINES
Requirements for a fuel cell for transportation application [DE90-011146] N91-16230

INTERNATIONAL COOPERATION
Preparations for a major international symposium on electricity and the environment [DE90-010539] N91-16449
International decision making and global climate change: Lessons of prior resource management efforts for consensus building [DE90-010714] N91-16454
Energy and Technology Review, March 1990 [DE90-008230] N91-16985

INTERPLANETARY MAGNETIC FIELDS
The magnetospheric response to 8-minute period strong-amplitude upstream pressure variations [AD-A228038] N91-16489

INTERPLANETARY SPACECRAFT
Aerospace vehicle design, spacecraft section. Volume 1: Project groups 1-4 --- unmanned probe to Pluto [NASA-CR-186841] N91-16045
PFERD Mission: Pluto flyby exploration/research design N91-16046
Project Cerberus: Flyby mission to Pluto N91-16048
OPTIC: Orbiting Plutonian Topographic Image Craft proposal for an unmanned mission to Pluto N91-16049
Aerospace vehicle design, spacecraft section. Volume 2: Project groups 5-7 --- unmanned probe to Pluto [NASA-CR-186842] N91-16050
Mission management, planning, and cost: PULSE Attitude And Control Systems (AACS) N91-16051
The Copernicus project N91-16052
The Phoenix Pluto Probe N91-16053

INTERPOLATION
Mathematical methods and algorithms for real-time applications [AD-A228889] N91-16663

INTERPRETATION
Linguistic and pragmatic constraints on utterance interpretation [AD-A228815] N91-16210

INTERSTELLAR CHEMISTRY
Structure and energy balance of molecular clouds [MPE-PREPRINT-181] N91-16975

INTERSTELLAR EXTINCTION
The complex nature of the Seyfert galaxy NGC 7592 N91-16882

INTERSTELLAR GAS
Numerical simulations of interacting disk galaxies N91-16955
The galactic center at submillimeter and far-infrared wavelengths [MPE-PREPRINT-190] N91-16978

INTERSTELLAR MATTER
Galaxy interactions and the stimulation of nuclear activity N91-16910
Cool infalling gas and its interaction with the hot ISM of elliptical galaxies N91-16915
Collisional removal of HI from the inner disks of Virgo cluster galaxies N91-16952
Molecular absorption lines towards the nucleus of Centaurus A [MPE-PREPRINT-182] N91-16976

INTRAVASCULAR SYSTEM
Electrical resistance volumetry in the circulation N91-16543

INVENTIONS
Whole body cleansing agent [NASA-CASE-MSC-21589-1] N91-16566
Lamina transducer coupler and method of making [NASA-CASE-LAR-14361-1] N91-16707
Hanging drop crystal growth apparatus [NASA-CASE-MFS-26061-1] N91-16815

INVERSE SCATTERING
Nonlinear waves and inverse scattering [AD-A228757] N91-16294
Research on certain aspects of laser diffraction particle size analysis relevant to autonomous self-diagnosing instrumentation [AD-A226822] N91-16354
Some aspects of quantum groups and supergroups [DE90-777884] N91-16671

INVERSIONS
The correction of infrasound signals for upper atmospheric winds N91-16695

INVISCID FLOW
Analysis and application of the discrete vortex method N91-16290
Research in nonlinear water waves [AD-A227948] N91-16292

IODATES
Electrocatalysis of anodic and cathodic oxygen-transfer reactions [DE91-000611] N91-16100

ION ATOM INTERACTIONS
Measurements of scattering processes in negative ion-atom collisions [DE90-010666] N91-16715

ION BEAMS
The new LLNL AMS spectrometer [DE90-010868] N91-16084
Ion beam modification of surface for improved high temperature performance [AD-A228067] N91-16243
Ion contamination of x ray pinhole camera images on PBFA 2 [DE90-012180] N91-16325
Development of an external beam ion milliprobe [AD-A227247] N91-16329
AGS silicon gold collisions measured in the E-810 TPC (Time Projection Chamber) [DE90-010015] N91-16733
Production of high intensity radioactive beams [DE90-011340] N91-16735
V(sup 0) production with 14.5 GeV/c silicon beams [DE90-010014] N91-16747
Wave-particle power transfer in a steady-state driven system [DE90-010031] N91-16748

ION DISTRIBUTION
Ion distributions and flows near the neutral sheet [MPE-PREPRINT-179] N91-16974

ION IMPLANTATION
Dose rate effects on damage formation in ion-implanted gallium arsenide [DE91-000394] N91-16806
Domain boundaries formed during epitactical growth of alpha-Al2O3 [DE91-005018] N91-16814

ION SCATTERING
Surface analysis by low-energy ion scattering: Two-dimensional detection and quantification [ETN-91-98474] N91-16133

ION SOURCES
Fundamental characteristics and applications of an inductively coupled plasma as an ion source for mass spectrometry [DE90-011746] N91-16770

ION TRAPS (INSTRUMENTATION)
Determination of airborne organics by direct sampling mass spectrometry [DE90-009422] N91-16452

IONIC COLLISIONS
Measurements of scattering processes in negative ion-atom collisions [DE90-010666] N91-16715

IONIZATION CROSS SECTIONS
The theory of electron-ion collisions: The role of doubly excited states [DE90-011078] N91-16721

IONIZED GASES
A spiral-like disk of ionized gas in IC 1459: Signature of a merging collision N91-16889
Dust and ionized gas in active radio elliptical galaxies N91-16919
The 158 micrometer (CII) line: A measure of global star formation activity in galaxies [NASA-CR-187925] N91-16977

IONIZING RADIATION
Scoping estimates of the LDEF satellite induced radioactivity [NASA-CR-184074] N91-16056
The 1/f noise in irradiated MOS devices [DE90-007288] N91-16219
Radiation physics, biophysics, and radiation biology [DE90-011544] N91-16722

IONOSPHERIC ELECTRON DENSITY
Electron density comparisons between radar observations and 3-D ionospheric model calculations [AD-A227703] N91-16187

IONOSPHERIC PROPAGATION
Electron density comparisons between radar observations and 3-D ionospheric model calculations [AD-A227703] N91-16187
Tactical HF field expedient antenna performance, volume 1 [AD-A228057] N91-16198

IRIDIUM
High temperature oxidation-resistant thruster research [NASA-CR-185233] N91-16063

IRON
Hyperfine interactions associated with iron substituted superconducting oxides [DE90-010411] N91-16783

Deep inelastic structure functions from electron scattering on hydrogen, deuterium, and iron at 0.6 GeV2 less than or equal to Q2 less than or equal to 30.0 GeV2
[DE90-010169] N91-16785

IRON ALLOYS
The use of impedance measurements in corrosion research: The corrosion behaviour of chromium and iron-chromium alloys
[ISBN-90-9003693-8] N91-16135
Grain-boundary structure in ordered alloys
[ETN-91-98571] N91-16136

IRON COMPOUNDS
Self-discharge study of Li-alloy/FeS2 thermal cells
[DE90-010659] N91-16438

IRRADIANCE
Bio-optical profile data report: Joint Global Ocean Flux Study, Hawaii Ocean Time-Series, HOT-3, R/V Moana Wave, 6-10 January 1989
[NASA-CR-187805] N91-16534

IRRADIATION
Total-dose degradation of thin film ferroelectric capacitors
[DE90-007152] N91-16218
The 1/f noise in irradiated MOS devices
[DE90-007288] N91-16219
Statistical process control for QML (Qualified Manufacturer's List) radiation hardness assurance
[DE90-007413] N91-16394

ISOBARS (PRESSURE)
Examples of isallobaric forcing in surface frontal motion and surface frontogenesis over the Central United States
[AD-A227687] N91-16521

ISOLATION
Proving experiments on an acoustic transmission suite and its reverberation room
[BBC-RD-1990/13] N91-16681
A homogeneous sample of binary galaxies: Basic observational properties N91-16859

ISOTHERMAL PROCESSES
Colorado State University program for developing, testing, evaluating and optimizing solar heating and cooling systems
[DE90-010107] N91-16435

ISOTHERMS
Natural-convection boundary layers
[ISBN-90-9003467-6] N91-16313

ISOTOPE SEPARATION
Surface analysis by low-energy ion scattering: Two-dimensional detection and quantification
[ETN-91-98474] N91-16133
Technique for determining the static polarizabilities of refractory metal atoms
[DE90-017088] N91-16724
Production of high intensity radioactive beams
[DE90-011340] N91-16735

ISOTOPIC ENRICHMENT
Thermal desorption studies of isotopically-labeled oxygen-induced superconductivity in La2CuO(4+delta)
[DE91-004898] N91-16812

ISOTROPIC TURBULENCE
Modeling the dissipation rate in rotating turbulent flows
[NASA-CR-187485] N91-16306

ITERATION
Column reduction of polynomial matrices: An iterative algorithm
[MEMO-COSOR-89-30] N91-16598
A long step barrier method for convex quadratic programming
[REPT-90-53] N91-16600
THERMOPT: An optimizer for ESATAN models
[MBB/FW522/S/PUB/427] N91-16630
An automatic ordering method for incomplete factorization iterative solvers
[DE91-001974] N91-16659
Hierarchical Bayesian analysis of change point problems
[AD-A226179] N91-16666

ITERATIVE SOLUTION
Acceleration of iterative algorithms for Euler and Navier-Stokes equations N91-16301

J

JET AIRCRAFT
Effect of wind and temperature gradients on received acoustic energy N91-16697

JET ENGINE FUELS
A comparison of three prospective analytical methods for benzene analysis in jet fuel environments
[AD-A227489] N91-16170

JET ENGINES
IFDIS: An expert system for diagnosis of failures in jet aircraft engines
[AD-A227757] N91-16020
Jet engine performance estimation from minimal input data
[ETN-91-98582] N91-16023
An introduction to modern aero-engine control design
[ETN-91-98583] N91-16024
Long-distance sound propagation over discontinuous impedances N91-16688

JET FLOW
Experimental parametric study of jet vortex generators for flow separation control
[NASA-CR-187836] N91-16296
Local and global instability of heated 2-D jets and wakes N91-16298

JET MIXING FLOW
Aerodynamic drag characterization and deposition studies of irregular particles. Part 3: Analysis of flow and temperature field inside the Combustion Deposition Entrained Reactor (CDER)
[DE90-000466] N91-16259

JET STREAMS (METEOROLOGY)
A comparison of diagnostic and kinematic vertical motion fields associated with curved and straight jet streak adjustment processes
[AD-A227724] N91-16522

JIMSPHERE BALLOONS
Analysis of wind profile measurements from an instrumented aircraft
[NASA-CR-184084] N91-16523

JOINT EUROPEAN TORUS
Microwave interferometer and reflectometer techniques for thermonuclear plasmas
[ETN-91-98478] N91-16780

JOINTS (JUNCTIONS)
Design of a telerobotic controller with joint torque sensors using 2-port network theory
[NASA-CR-186543] N91-16379
The PHD: A Planar, Harmonic Drive robot for joint torque control
[NASA-CR-187924] N91-16386

JOSEPHSON JUNCTIONS
Dynamical properties of two-dimensional Josephson junction arrays N91-16823

JUNCTION TRANSISTORS
Numerical simulation of the comparative electrical performance of the permeable base transistor, opposed gate-source transistor and heterostructure launched ballistic field effect transistor
[AD-A228545] N91-16202

K

KALMAN FILTERS
Optimal Kalman filter integration of a global positioning system receiver and an LN-94 inertial navigation system
[AD-A227222] N91-16003
The use of window functions and Kalman filtering in spectral estimation
[AD-A227482] N91-16236
Mathematical methods and algorithms for real-time applications
[AD-A228889] N91-16663

KELVIN-HELMHOLTZ INSTABILITY
Numerical examinations of Kelvin-Helmholtz instability in resistive compressible magnetohydrodynamics
[MPE-221] N91-16782

KERNEL FUNCTIONS
Analysis and application of the discrete vortex method N91-16290
Adaptive bandwidth choice for kernel regression
[AD-A228437] N91-16661

KINEMATICS
Applications of fuzzy theories to multi-objective system optimization
[NASA-CR-177573] N91-16012
Global variability of water vapor and condensate from SSM/I N91-16507
Using MAPLE for symbolic computations in robotics
[DE90-010405] N91-16576
Using tilted-ring models and numerical hydrodynamics to study the structure, kinematics and dynamics of HI disks in galaxies N91-16851
Stellar kinematics of elliptical galaxies in pairs N91-16862
H I studies of the sculptor group galaxies N91-16876
The kinematics and morphology of NGC 520: One, two, or three galaxies N91-16908
Galaxy interactions and strength of nuclear activity N91-16914
Deep Fabry-Perot imaging of NGC 6240: Kinematic evidence for merging galaxies N91-16922
Selection effects and binary galaxy velocity differences N91-16927
Gas flows in S-E binary systems of galaxies N91-16956

KINETIC EQUATIONS
Some topics of Navier-Stokes solvers N91-16269

KINETICS
Theoretical study of the C-H bond dissociation energy of acetylene
[NASA-CR-187858] N91-16065
Phase selection and processing of high temperature intermetallic alloys
[AD-A227910] N91-16129
Fine particle flotation in a centrifugal force field
[ETN-91-98480] N91-16309
The role of ledges in phase transformations
[AD-A228750] N91-16821

KNOWLEDGE BASES (ARTIFICIAL INTELLIGENCE)
The Assistant for Specifying the Quality Software (ASQS). Volume 1: Operational concept document
[AD-A227893] N91-16608
The Assistant for Specifying the Quality Software (ASQS). Volume 2: User's manual. Volume 2
[AD-A227894] N91-16609
Research into the design and implementation of knowledge base systems
[AD-A228873] N91-16843

KURTOSIS
Detection of solid lubricant film failure during sliding by vibration monitoring
[NAL-TR-1060] N91-16384

L

LABORATORIES
Status of target physics for inertial confinement fusion
[DE90-008221] N91-16751
Energy and Technology Review, March 1990
[DE90-008230] N91-16985

LABORATORY EQUIPMENT
Aerosol Dynamics Laboratory
[DE90-010275] N91-16027
The new LLNL AMS spectrometer
[DE90-010868] N91-16084

LAMB WAVES
Scattering of Lamb waves in an elastic plate for ultrasonic nondestructive evaluation of weldments and cracks N91-16412

LAMINAR BOUNDARY LAYER
Modelling the transitional boundary layer
[NASA-CR-187487] N91-15995
Pressure gradient effects on the development of hairpin vortices in an initially laminar boundary layer N91-16282
Investigation of the influence of constant adverse pressure gradients on laminar boundary-layer stability at Mach number 8
[AD-A228231] N91-16293

LAMINAR FLOW
Modelling the transitional boundary layer
[NASA-CR-187487] N91-15995
Modelling of flamelet surface-to-volume ratio in turbulent premixed combustion
[DE90-006312] N91-16081
Development and application of numerical models for reactive flows
[AD-A228884] N91-16295
Streamwise vortices in laminar-turbulent transition N91-16297

LAMINATES
Fundamental verification of tailoring technology for control of a coefficient of thermal expansion by composite testing facilities
[NAL-TR-1058] N91-16069
Pilot study of the dynamic impact response of a composite plate
[FFA-TN-1990-27] N91-16070
Updated evaluation of polymer films for electrical insulation
[DE91-000544] N91-16148

LAND USE
Environmental trends
[DE90-010530] N91-16450

LANTHANUM COMPOUNDS
Microwave sintering of fuel cell materials
[DE90-011643] N91-16143

LARGE SPACE STRUCTURES
A decentralized linear quadratic control design method for flexible structures
[NASA-CR-187860] N91-16059
Large space manipulators study
[AD-A227276] N91-16381

LASER ANEMOMETERS
A process for unstationary velocity and turbulence measurements with a pneumatic measuring wedge probe
[MITT-33] N91-16310
Optimization of a laser diode anemometry system
[LSTM-239/T/88] N91-16364
LASER APPLICATIONS
Application of diode lasers to resonance ionization mass spectrometry
[DE91-000614] N91-16094
Laser microplasma-gas chromatography detector. 2: Detection of species-specific fragment emission
[AD-A228373] N91-16106
Droplet shattering, vaporization, and recondensation in cloud clearing with long pulse infrared chemical lasers
[DE90-010584] N91-16343
New development of laser-based techniques in applications of thin-layer chromatography, microprobe elemental analysis, and gas phase pyrolysis
[DE90-011740] N91-16347
Development of a versatile laser light scattering instrument
[NASA-CR-182474] N91-16350
Spontaneous force optical traps
[AD-A228539] N91-16363
LASER BEAMS
Timing margin measurement using a laser technique
[AD-A226821] N91-16353
Research on certain aspects of laser diffraction particle size analysis relevant to autonomous self-diagnosing instrumentation
[AD-A226822] N91-16354
A convenient system for diffraction moire measurements
[DE90-010980] N91-16739
Hanging drop crystal growth apparatus
[NASA-CASE-MFS-26061-1] N91-16815
LASER DAMAGE
Angular dependence of thin-film dielectric coating damage thresholds
[DE91-000237] N91-16351
LASER DOPPLER VELOCIMETERS
The development of laser speckle velocimetry for the study of vortical flows
[NASA-CR-187756] N91-16289
Optimization of a laser diode anemometry system
[LSTM-239/T/88] N91-16364
LASER FUSION
Stability and accuracy of the sweep rate measurements for LLNL optical streak cameras
[DE90-012080] N91-16324
Status of target physics for inertial confinement fusion
[DE90-008221] N91-16751
LASER GYROSCOPES
A ring laser gyroscope with optical subtraction
N91-16335
LASER INDUCED FLUORESCENCE
Direct observation of NF(X) using laser-induced fluorescence: Kinetics of the NF 3 Sigma - ground state
[AD-A228294] N91-16362
LASER MODES
Mode competition effects in free electron lasers and gyrotrons
[DE90-011084] N91-16346
LASER OUTPUTS
Technique for determining the static polarizabilities of refractory metal atoms
[DE90-017088] N91-16724
Hanging drop crystal growth apparatus
[NASA-CASE-MFS-26061-1] N91-16815
LASER PLASMA INTERACTIONS
Scaling laws for femtosecond laser-plasma interactions
[DE90-011496] N91-16769
LASER PLASMAS
Laser microplasma-gas chromatography detector. 2: Detection of species-specific fragment emission
[AD-A228373] N91-16106
IR plasma emissions
[AD-A227713] N91-16776
LASER PROPULSION
Research on certain aspects of laser diffraction particle size analysis relevant to autonomous self-diagnosing instrumentation
[AD-A226822] N91-16354
LASER PUMPING
Nonlinear optical systems interacting with amplitude-modulated optical fields
[AD-A228221] N91-16742
LASER RANGE FINDERS
Experimental set-up for a pulsed CO2 laser rangefinder with heterodyne detection
[FEL-90-A125] N91-16365
LASER SPECTROSCOPY
Stark-effect measurement of high FEL electric fields in MTX by laser-aided particle-probe spectroscopy
[DE90-011911] N91-16771
Far-infared laser spectroscopy of two dimensional holes in strained-layer heterostructure and superlattices
[DE91-000027] N91-16805
LASER TARGETS
Cluster formation in laser-induced ablation and evaporation of solids observed by laser ionization time-of-flight mass spectrometry and scanning tunneling microscopy
[DE90-010876] N91-16344
Status of target physics for inertial confinement fusion
[DE90-008221] N91-16751
Scaling laws for femtosecond laser-plasma interactions
[DE90-011496] N91-16769
LASER WELDING
Experimental verification of physical model of pulsed laser welding
[DE91-000025] N91-16380
LASERS
The 1/f frequency noise effects on self-heterodyne linewidth measurements for coherent communications
[AD-A227942] N91-16195
Cluster formation in laser-induced ablation and evaporation of solids observed by laser ionization time-of-flight mass spectrometry and scanning tunneling microscopy
[DE90-010876] N91-16344
Fiber optic synthetic aperture interferometer
[AD-A227891] N91-16741
Chemical beam epitaxy of ZnSe
[AD-A228045] N91-16817
LATENT HEAT
The effect of latent heat release on synoptic-to-planetary wave interactions and its implication for satellite observations: Theoretical modeling N91-16514
The effect of latent heat release on synoptic-to-planetary scale wave interactions and implications for satellite observations: Observational study N91-16515
Variability of latent and sensible heat fluxes over the oceans N91-16531
LATERAL CONTROL
Aeroservoelastic tailoring for lateral control enhancement N91-16025
LATTICE PARAMETERS
Dynamics of strong-coupling models for cuprate superconductors: Exact results on finite lattices
[DE90-011155] N91-16796
LATTICES (MATHEMATICS)
Unsteady vortex lattice calculation of the flow around a slender delta wing N91-16272
A search for good lattice rules based on the reciprocal lattice generator matrix
[DE91-004425] N91-16809
Fermions in the hypercharge sector of the standard lattice electroweak theory: Global limit
[DE90-009731] N91-16827
LAUNCH VEHICLES
Design and fabrication of the NASA HL-20 full scale research model
[NASA-CR-187801] N91-16008
LAY-UP
Fundamental verification of tailoring technology for control of a coefficient of thermal expansion by composite testing facilities
[NAL-TR-1058] N91-16069
LEAD (METAL)
Chemisorption of carbon monoxide on three metal surfaces: Ni(111), Pd(111) and Pt(111): A comparative study
[AD-A228579] N91-16108
LEAD ACID BATTERIES
Laboratory testing of chloride 3ET205 6 volt traction battery
[DE90-010926] N91-16225
Status of Argonne life evaluation of valve regulated lead-acid batteries
[DE90-011098] N91-16229
LEAD ISOTOPES
Study of the global distributions of atmospheric radionuclides
[DE90-010749] N91-16455
LEAD OXIDES
Characterization of chemically prepared PZT thin films
[DE90-010831] N91-16789
LEADING EDGES
Finite element thermo-viscoplastic analysis of aerospace structures
[NASA-TM-102761] N91-16407
LEARNING
Skill and skilled memory
[AD-A227697] N91-16549
LEDGES
The role of ledges in phase transformations
[AD-A228750] N91-16821
LEG (ANATOMY)
Kinematics of arthropod legs: Modeling and measurement N91-16391
LEGENDRE FUNCTIONS
Relative extrema, zeros, and inequalities for Gegenbauer functions of the first and second kind
[REPT-90-54] N91-16653
Relative extrema, zeros, and inequalities for Jacobi functions of the first and second kind
[REPT-90-55] N91-16654
LENGTH
Fiber optic synthetic aperture interferometer
[AD-A227891] N91-16741
LEPTONS
Theoretical topics in B-physics
[DE91-004911] N91-16726
Measurement of the e+e- annihilation in mu+mu- pairs at the Z sup o resonance
[MPI-PAE/EXP.EL-231] N91-16732
LIBRARIES
Subject bibliography of the PMA 205 (Program Manager Air 205) network technical library at Oak Ridge National Laboratory
[DE90-009988] N91-16835
The StarLite project
[AD-A226722] N91-16837
LIE GROUPS
Advanced methods for the computation of particle beam transport and the computation of electromagnetic fields and beam-cavity interactions
[DE90-011071] N91-16734
LIFE (DURABILITY)
Fatigue of amorphous polymers
[ISBN-90-9003520-6] N91-16157
LIFE SCIENCES
Space research in the Federal Republic of Germany, 1988 and 1989
[ETN-91-98514] N91-16849
LIFTING BODIES
Calculations for unsteady aerodynamic characteristics on a 3-D lifting body in subsonic flow using boundary element method
[NAL-TR-1065] N91-15985
LIGHT AMPLIFIERS
Generation of XUV light by resonant frequency tripling in a two-wiggler FEL amplifier
[DE90-012120] N91-16349
LIGHT BEAMS
Development of a versatile laser light scattering instrument
[NASA-CR-182474] N91-16350
LIGHT EMISSION
Dust and ionized gas in active radio elliptical galaxies
N91-16919
LIGHT EMITTING DIODES
Application of diode lasers to resonance ionization mass spectrometry
[DE91-000614] N91-16094
LIGHT SCATTERING
Development of a versatile laser light scattering instrument
[NASA-CR-182474] N91-16350
Research on certain aspects of laser diffraction particle size analysis relevant to autonomous self-diagnosing instrumentation
[AD-A226822] N91-16354
LIMITERS (FUSION REACTORS)
Plasma-facing materials
[DE90-008243] N91-16753
LINE OF SIGHT COMMUNICATION
Meteor burst communications study
[AD-A228641] N91-16204
LINE SPECTRA
Time-resolved Coherent Anti-Stokes Raman Spectroscopy (CARS) and the measurement of vibrational spectra in shock-compressed molecular materials
[DE90-012053] N91-16091
A tunable x ray microprobe using synchrotron radiation
[DE90-011219] N91-16322
H I and mass distribution of GR8 N91-16884
The nature of the emission-line nebulae in powerful far-infrared galaxies N91-16916
Radio line and continuum observations of quasar-galaxy pairs and the origin of low reshift quasar absorption line systems N91-16925
LINEAR ACCELERATORS
SLED II: A new method of RF pulse compression
[DE91-000058] N91-16183
Development of free-electron lasers for XUV projection lithography
[DE90-010566] N91-16342

Design requirements and calculated performance of an XUV FEL oscillator operating on a higher harmonic
[DE91-004833] N91-16357
LINEAR ARRAYS
Some comments on the acoustic coupling of elements in an array
[AD-A227762] N91-16239
LINEAR OPERATORS
Sparse representation of smooth linear operators
[AD-A228142] N91-16660
Resolution of the 1D regularized Burgers equation using a spatial wavelet approximation
[NASA-CR-187480] N91-16664
LINEAR PREDICTION
An experimental demonstration of high-resolution Doppler processing
[AD-A228813] N91-16208
LINEAR QUADRATIC GAUSSIAN CONTROL
Wind tunnel tests on flutter control of a high-aspect-ratio cantilevered wing: Control with leading-edge and trailing-edge control surfaces
[NAL-TR-1070] N91-15982
Large space manipulators study
[AD-A227276] N91-16381
LINEARITY
NICAM 728: Factors affecting the assessment of UHF transmitter linearity
[BBC-RD-1990/9] N91-16190
Some generalizations of the criss-cross method for quadratic programming
[REPT-90-52] N91-16599
Sparse representation of smooth linear operators
[AD-A228142] N91-16660
LINGUISTICS
Linguistic and pragmatic constraints on utterance interpretation
[AD-A228815] N91-16210
LIPIDS
Applications research studies on microtubules
[AD-A228756] N91-16205
LIQUEFIED GASES
Time-resolved Coherent Anti-Stokes Raman Spectroscopy (CARS) and the measurement of vibrational spectra in shock-compressed molecular materials
[DE90-012053] N91-16091
Development of liquid xenon imaging gamma-ray spectrophotometers
[AD-A227575] N91-16740
LIQUID CHROMATOGRAPHY
Fundamental studies with a monodisperse aerosol-based liquid chromatography/mass spectrometry interface (MAGIC-LC/MS)
[DE90-010667] N91-16083
Inverse gas chromatography
[AD-A227677] N91-16099
A comparison of three prospective analytical methods for benzene analysis in jet fuel environments
[AD-A227489] N91-16170
LIQUID CRYSTALS
Applications research studies on microtubules
[AD-A228756] N91-16205
LIQUID FLOW
Development of a two-phase cold plate N91-16277
LIQUID FUELS
Spray combustion modeling and evaluation
[NASA-CR-187887] N91-16078
LIQUID HELIUM 2
ASTROMAG coil cooling study
[NASA-CR-187768] N91-16813
LIQUID HYDROGEN
An assessment of the government liquid hydrogen requirements for the 1995-2005 time frame including addendum, liquid hydrogen production and commercial demand in the United States
[NASA-TM-103812] N91-16166
An assessment of the government liquid hydrogen requirements for the 1995-2005 time frame N91-16167
Liquid hydrogen production and commercial demand in the United States N91-16168
Safe venting of hydrogen
[DE90-008964] N91-16174
LIQUID PROPELLANT ROCKET ENGINES
High temperature oxidation-resistant thruster research
[NASA-CR-185233] N91-16063
LIQUID ROCKET PROPELLANTS
High temperature oxidation-resistant thruster research
[NASA-CR-185233] N91-16063
LIQUID SURFACES
Models for surface scattering from solids and liquids
[RSRE-MEMO-3699] N91-16192
LIQUID-GAS MIXTURES
Pressure gradient effects on the development of hairpin vortices in an initially laminar boundary layer N91-16282
LIQUID-LIQUID INTERFACES
Polymers at liquid-liquid interfaces: Photophysics and photoredox chemistry
[DE91-005032] N91-16151
A time-domain finite-element method for the computation of three-dimensional acoustic wave fields in inhomogeneous fluids and solids
[ETN-91-98485] N91-16710
LIQUID-SOLID INTERFACES
Test methods for evaluating hot cracking: Review and perspective
[DE90-009820] N91-16397
A time-domain finite-element method for the computation of three-dimensional acoustic wave fields in inhomogeneous fluids and solids
[ETN-91-98485] N91-16710
LIQUIDS
A method for pressure-pulse suppression in fluid-filled piping
[DE90-010408] N91-16260
Utilization of polymer viscoelastic properties in acoustic wave sensor applications
[DE90-010534] N91-16676
LITHIUM CHLORIDES
Development of a moderate rate lithium/thionyl-chloride D cell
[DE90-011909] N91-16233
LITHIUM COMPOUNDS
Studies of the fundamentals of solids state batteries
[AD-A228772] N91-16247
LITHIUM OXIDES
Desorption of H2O and H2 from steel and LiAO2 by temperature programmed desorption
[DE90-011170] N91-16118
LITHIUM SULFUR BATTERIES
Development of a moderate rate lithium/thionyl-chloride D cell
[DE90-011909] N91-16233
Self-discharge study of Li-alloy/FeS2 thermal cells
[DE90-010659] N91-16438
LITHOGRAPHY
New methods for producing, recording, and processing interferometric moire patterns N91-16405
LITHOSPHERE
Magsat investigations over the greater African region N91-16415
Continuum models of continental deformation N91-16490
Seismic structure of the upper mantle under the Pacific Ocean N91-16492
LOAD DISTRIBUTION (FORCES)
TF89 aircraft centre fuselage
[ETN-91-98579] N91-16018
LOADING RATE
Pilot study of the dynamic impact response of a composite plate
[FFA-TN-1990-27] N91-16070
High-loaded combustion chambers stationary constant pressure combustion. Part 2: Research reports
[ETN-91-98511] N91-16112
LOCAL AREA NETWORKS
A software development specification for nonlinear structural analysis
[AD-A228427] N91-16614
Horizontal fault tolerance in a fully distributed loosely coupled environment
[AD-A227972] N91-16638
LOGARITHMS
A long step barrier method for convex quadratic programming
[REPT-90-53] N91-16600
LOGIC PROGRAMMING
Research into the design and implementation of knowledge base systems
[AD-A228873] N91-16843
LOGISTICS
Reliability/Maintainability/Logistics support analysis Computer Aided Tailoring Software Program (R/M/L CATSOP)
[AD-A226820] N91-16588
LONG DURATION EXPOSURE FACILITY
Scoping estimates of the LDEF satellite induced radioactivity
[NASA-CR-184074] N91-16056
LONG WAVE RADIATION
Global-scale, intraseasonal fluctuations of diabatic forcing of the atmosphere N91-16508
LONGERONS
TF89 aircraft centre fuselage
[ETN-91-98579] N91-16018
LONGITUDINAL STABILITY
Longitudinal stability augmentation of a lightweight fighter aircraft model
[ETN-91-98585] N91-16026
LOOP ANTENNAS
A Mirnov loop array for field-reversed configurations
[DE90-010607] N91-16750
LORENTZ FORCE
Investigation of wire motion in superconducting magnets
[DE91-004952] N91-16674
LOSSES
Monitoring challenges and innovative ideas
[DE91-000586] N91-16465
LOW COST
Manufacturing guide for elastomeric seals
[AD-A227511] N91-16383
LOW FREQUENCIES
Long-range sound propagation: A review of some experimental data N91-16683
Long-range vertical propagation N91-16693
Comparison of FFP predictions with measurements of a low-frequency signal propagated in the atmosphere N91-16698
New correction procedures for the fast field program which extend its range N91-16699
LOW PASS FILTERS
Measurement of the capture effect of frequency modulation
[AD-A228058] N91-16199
LOW WEIGHT
Noise reduction using low weight and constant weight coding techniques
[AD-A228346] N91-16244
LOWER ATMOSPHERE
Integrated Refractive Effects Prediction System (IREPS) user's manual, revision PC-2.0
[AD-A228549] N91-16203
LUMINOSITY
A homogeneous sample of binary galaxies: Basic observational properties N91-16859
Blue ellipticals in compact groups N91-16873
H I studies of the sculptor group galaxies N91-16876
Observations of multiple nucleus galaxies N91-16890
Are extremely luminous far-infrared galaxies the result of merging quasar cores N91-16912
The nature of the emission-line nebulae in powerful far-infrared galaxies N91-16916
Deep Fabry-Perot imaging of NGC 6240: Kinematic evidence for merging galaxies N91-16922
IC5063: A merger with a hidden luminous active nucleus N91-16923
Radio structures in QSO-galaxy pairs N91-16924
Probing the tides in interacting galaxy pairs N91-16932
What determines the bulge to disk ratio of galaxies N91-16942
LUMINOUS INTENSITY
The design of a two-dimensional optical image correlator and its application in image tracking N91-16744
LUNAR BASES
Common approach for planetary habitation systems implementation
[MBB-UO-0115-90-PUB] N91-16570

M

MACH NUMBER
Unstationary shock and boundary layer phenomena at profiles and in a plane grid by transonic flow
[ETN-91-98557] N91-16311
MACH REFLECTION
Numerical simulations of unsteady shock reflection processes by a ramp N91-16267
Some topics of Navier-Stokes solvers N91-16269
BLAST2D computations of the reflection of planar shocks from wedge surfaces with comparison to SHARC and STEALTH results
[AD-A227261] N91-16589
MACHINE LEARNING
Experimentation and concept formation by an autonomous mobile robot
[DE90-003063] N91-16368
An evolutionary approach to designing neural networks
[AD-A228874] N91-16643
MACHINE TOOLS
A hydraulically driven microdisplacement unit
[ME-56] N91-16392
MACHINING
Gelcasting of sub-micron alumina, sialon, and silicon nitride powders
[DE91-000618] N91-16145
Deburring and surface finishing: The past ten years and projections for the next ten years
[DE91-000579] N91-16176
A hydraulically driven microdisplacement unit
[ME-56] N91-16392

MACROMOLECULES
Selective excitation, relaxation, and energy channeling in molecular systems
[DE90-010793] N91-16717
MAGNESIUM OXIDES
Interatomic forces and bonding mechanisms in MgO clusters
[DE90-010148] N91-16719
MAGNETIC ANOMALIES
Magsat investigations over the greater African region N91-16415
MAGNETIC COILS
ASTROMAG coil cooling study
[NASA-CR-187768] N91-16813
MAGNETIC DIFFUSION
Diffusion fields in a toroidal conducting shell of circular cross section
[AD-A228021] N91-16197
MAGNETIC DIPOLES
A Moller polarimeter for the extracted ELSA-ray
[BONN-IR-90-42] N91-16731
MAGNETIC DOMAINS
Magnetic domain strain sensor program
[AD-A227225] N91-16327
MAGNETIC FIELD CONFIGURATIONS
Magnetic structures of actinide materials by pulsed neutron diffraction
[DE91-000373] N91-16093
A Mirnov loop array for field-reversed configurations
[DE90-010607] N91-16750
US-Japan Workshop on Field-Reversed Configurations with Steady-State High-Temperature Fusion Plasmas and the 11th US-Japan Workshop on Compact Toroids
[DE90-010253] N91-16755
Kinetic stability of field-reversed configurations
[DE90-011530] N91-16767
MAGNETIC FIELDS
Magnetic measurements with fluxgate magnetometer in rocket flight
[DRI-4-90] N91-16061
Diffusion fields in a toroidal conducting shell of circular cross section
[AD-A228021] N91-16197
Applications research studies on microtubules
[AD-A228756] N91-16205
Circumfluous motion of a conductive liquid around solid objects in a magnetic field
[DE90-011335] N91-16265
Self-propelled in-tube shuttle and control system for automated measurements of magnetic field alignment
[DE90-008210] N91-16316
Magnetic heat pumps
[DE90-010305] N91-16375
Magsat investigations over the greater African region N91-16415
Investigation of effects of 60-Hz electric and magnetic fields on operant and social behavior and on the neuroendocrine system of nonhuman primates
[DE90-010809] N91-16537
Investigation of effects of 60-Hz electric and magnetic fields on operant and social behavior and on the neuroendocrine system of nonhuman primates
[DE90-011557] N91-16539
Transport simulation of the effect of impurity radiation on the high beta, ohmic start-up of the HBT-EP tokamak
[DE90-010333] N91-16760
Microwave generation for magnetic fusion energy applications, task C
[DE90-011080] N91-16764
Kinetic stability of field-reversed configurations
[DE90-011530] N91-16767
Motional Stark effect polarimetry for the current profile diagnostic in D3-D
[DE90-012071] N91-16773
Multiple-photon Compton scattering in a strong magnetic field: Cross-sections and radiative transport N91-16852
MAGNETIC FLUX
Diffusion fields in a toroidal conducting shell of circular cross section
[AD-A228021] N91-16197
The magnetospheric response to 8-minute period strong-amplitude upstream pressure variations
[AD-A228038] N91-16489
MAGNETIC LEVITATION VEHICLES
Moving America; new directions, new opportunities: Assessment of the potential for magnetic levitation transportation systems in the United States
[PB91-104596] N91-16388
MAGNETIC MATERIALS
Magnetic domain strain sensor program
[AD-A227225] N91-16327
MAGNETIC MEASUREMENT
Magnetic measurements with fluxgate magnetometer in rocket flight
[DRI-4-90] N91-16061
MAGNETIC MOMENTS
Epitaxial growth and surface morphology of some metal and semiconductor structures N91-16824
MAGNETIC PERMEABILITY
Quasiperiodic transition to chaos in Ge; and magnetic susceptibility of high-T(c) superconductors
[DE90-011304] N91-16797
MAGNETIC PROPERTIES
Magnetic structures of actinide materials by pulsed neutron diffraction
[DE91-000373] N91-16093
Observations of vortex structure in YBa2Cu3O7
[DE91-000900] N91-16804
MAGNETIC SHIELDING
Magnetic-field shielding of satellites from high-energy-electron environments
[DE90-010296] N91-16043
MAGNETIC SIGNATURES
The magnetospheric response to 8-minute period strong-amplitude upstream pressure variations
[AD-A228038] N91-16489
MAGNETOHYDRODYNAMIC FLOW
Circumfluous motion of a conductive liquid around solid objects in a magnetic field
[DE90-011335] N91-16265
MAGNETOHYDRODYNAMIC GENERATORS
Microwave generation for magnetic fusion energy applications, task C
[DE90-011080] N91-16764
MAGNETOHYDRODYNAMIC STABILITY
A Mirnov loop array for field-reversed configurations
[DE90-010607] N91-16750
D3-D research operations
[DE90-008232] N91-16752
US-Japan Workshop on Field-Reversed Configurations with Steady-State High-Temperature Fusion Plasmas and the 11th US-Japan Workshop on Compact Toroids
[DE90-010253] N91-16755
The Madison symmetric torus
[DE90-010306] N91-16757
Kinetic stability of field-reversed configurations
[DE90-011530] N91-16767
Numerical examinations of Kelvin-Helmholtz instability in resistive compressible magnetohydrodynamics
[MPE-221] N91-16782
MAGNETOHYDRODYNAMIC WAVES
Neoclassical effects on RF current drive
[DE90-010302] N91-16222
The magnetospheric response to 8-minute period strong-amplitude upstream pressure variations
[AD-A228038] N91-16489
MAGNETOHYDRODYNAMICS
IR plasma emissions
[AD-A227713] N91-16776
MAGNETOMETERS
Magnetic measurements with fluxgate magnetometer in rocket flight
[DRI-4-90] N91-16061
MAGNETOSPHERIC ION DENSITY
The magnetospheric response to 8-minute period strong-amplitude upstream pressure variations
[AD-A228038] N91-16489
MAGNETOSTRICTION
Magnetic domain strain sensor program
[AD-A227225] N91-16327
MAGNUS EFFECT
Use of the Magnus force in the modified point mass trajectory model
[AD-A228194] N91-15990
MAGSAT SATELLITES
Magsat investigations over the greater African region N91-16415
MAN MACHINE SYSTEMS
Human factors design guidance during the conceptual design phase of system development: A methodological approach
[AD-A224667] N91-16552
Safety Network to Detect Performance Degradation and Pilot Incapacitation
[AGARD-CP-490] N91-16553
Intelligent assistant systems: An artificial intelligence approach to detecting performance degradation and pilot incapacitation N91-16564
MAN-COMPUTER INTERFACE
A graphical user-interface-driven waveform data acquisition and analysis system
[DE90-011948] N91-16578
PENGUIN: A language for reactive graphical user interfaces
[AD-A228580] N91-16620
MANAGEMENT
Technological management as an element of strategy for an efficient company management
[MBB-Z-0307-90-PUB] N91-16834
MANAGEMENT INFORMATION SYSTEMS
DTD creation for the Software Technology for Adaptable, Reliable Systems (STARS) program
[AD-A228475] N91-16619
Ada compiler validation procedures, version 2.1
[AD-A228614] N91-16621
Management information: A key to better acquisition at NIH
[AD-A226867] N91-16830
The USAF STINFO program overview
[AD-A226969] N91-16838
MANAGEMENT PLANNING
Preparations for a major international symposium on electricity and the environment
[DE90-010539] N91-16449
Managing emerging technology: Case studies in document imaging systems
[AD-A227688] N91-16839
MANEUVERS
Unsteady separation over maneuvering bodies
[AD-A226829] N91-16285
MANGANESE COMPOUNDS
Physico-chemical investigations on Co-Mn-oxide spinels
[ETN-91-98476] N91-16825
MANIPULATORS
Multi-criteria position and configuration optimization for redundant platform/manipulator systems
[DE90-010705] N91-16372
Optimal positioning of redundant manipulator-platform systems for maximum task efficiency
[DE90-011061] N91-16378
Large space manipulators study
[AD-A227276] N91-16381
NASA Laboratory telerobotic manipulator control system architecture
[NASA-CR-187751] N91-16385
Camera space manipulation of a mobile robot N91-16390
Using MAPLE for symbolic computations in robotics
[DE90-010405] N91-16576
MANNED MARS MISSIONS
Common approach for planetary habitation systems implementation
[MBB-UO-0115-90-PUB] N91-16570
MANNED SPACE FLIGHT
Software for aerospace education: A bibliography, 2nd edition
[NASA-PED-106-ED-2] N91-16601
MANUFACTURING
Impacts of advanced manufacturing technology on parametric estimating
[AD-A228232] N91-16177
A convenient system for the manufacture of holographic diffraction gratings
[DE90-009481] N91-16319
Manufacturing guide for elastomeric seals
[AD-A227511] N91-16383
Statistical process control for QML (Qualified Manufacturer's List) radiation hardness assurance
[DE90-007413] N91-16394
Implementation and simulation of the manufacturing systems control coordination level: A mixed approach of Petri nets and rule-based systems
[LAAS-90355] N91-16645
MANY BODY PROBLEM
Dynamical experiments on models of colliding disk galaxies N91-16959
MAP MATCHING GUIDANCE
Terrain matching using image sequence analysis N91-16424
MAPPING
Image-based terrain modeling with thematic mapper N91-16418
The usefulness of MSS pictures for mapping and biomass estimation of macro-algae and seaweed in the Eastern Scheldt
[BCRS-90-09] N91-16428
Reports on cartography and topography. Series 1, report 104
[ISSN-0469-4236] N91-16432
Geographic data transfer N91-16836
MAPS
Cartographic issues in the development of a digital GRASS database
[AD-A227582] N91-16416
MARINE ENVIRONMENTS
The vertical structure of the marine atmospheric boundary layer across a sea surface temperature front
[AD-A227931] N91-16525
MARINE METEOROLOGY
The effect of latent heat release on synoptic-to-planetary wave interactions and its implication for satellite observations: Theoretical modeling N91-16514
MARKARIAN GALAXIES
The environments of Markarian galaxies N91-16881

New data on the peculiar galaxy MRK 273 N91-16887
Wing galaxies: A formation mechanism of the clumpy irregular galaxy Markarian 297 N91-16963

MARKET RESEARCH
Greenhouse gas emissions from selected alternative transportation fuels market niches
[DE90-010491] N91-16448

MARKOV PROCESSES
Hierarchical Bayesian analysis of change point problems
[AD-A228179] N91-16666

MARS SURFACE
Photometric analyses for the determination of physical and structural properties for the Martian surface in the Oxia Palus region
[DLR-FB-90-27] N91-16979

MASS
Selection effects and binary galaxy velocity differences N91-16927
Triplets of galaxies: Their dynamics, evolution, and the origin of chaos in them N91-16948
Viral coefficient and hidden mass in the galaxy groups N91-16950

MASS DISTRIBUTION
Fragment mass distribution of debris
[MBB-UA-1187-90-PUB] N91-16669
H I and mass distribution of GR8 N91-16884

MASS FLOW
Interacting nuclei in distant galaxies N91-16894

MASS SPECTRA
V(sup 0) production with 14.5 GeV/c silicon beams
[DE90-010014] N91-16747

MASS SPECTROMETERS
Fundamental studies with a monodisperse aerosol-based liquid chromatography/mass spectrometry interface (MAGIC-LC/MS)
[DE90-010667] N91-16083
The new LLNL AMS spectrometer
[DE90-010868] N91-16084
Determination of airborne organics by direct sampling mass spectrometry
[DE90-009422] N91-16452
Fundamental characteristics and applications of an inductively coupled plasma as an ion source for mass spectrometry
[DE90-011746] N91-16770

MASS SPECTROSCOPY
Fundamental studies with a monodisperse aerosol-based liquid chromatography/mass spectrometry interface (MAGIC-LC/MS)
[DE90-010667] N91-16083
The new LLNL AMS spectrometer
[DE90-010868] N91-16084
The development of improved capillary supercritical fluid chromatography and mass spectrometry
[AD-A228535] N91-16107
Determination of airborne organics by direct sampling mass spectrometry
[DE90-009422] N91-16452
Application of AMS to the biomedical sciences
[DE90-010869] N91-16538
Fundamental characteristics and applications of an inductively coupled plasma as an ion source for mass spectrometry
[DE90-011746] N91-16770
Thermal desorption studies of isotopically-labeled oxygen-induced superconductivity in La2CuO(4+delta)
[DE91-004898] N91-16812

MASS TO LIGHT RATIOS
H I studies of the sculptor group galaxies N91-16876
A study of the compact group of galaxies Shahbazian 4 N91-16877

MASS TRANSFER
Investigation of transonic flow over segmented slotted wind tunnel wall with mass transfer
[NASA-CR-187760] N91-15981
AFDM: An Advanced Fluid-Dynamics Model. Volume 2: Topologies, flow regimes and interfacial areas
[DE91-000581] N91-16283
The impact of separated flow on heat and mass transfer
[DE91-000592] N91-16284
Experimental verification of physical model of pulsed laser welding
[DE91-000025] N91-16380
Direct methanol/air fuel cells: Systems considerations
[DE90-011971] N91-16439

MASSIVELY PARALLEL PROCESSORS
Wakefield calculations on parallel computers
[DE90-009712] N91-16632
Massively parallel Fokker-Planck calculations
[DE90-010691] N91-16633

MATERIALS HANDLING
Optimal positioning of redundant manipulator-platform systems for maximum task efficiency
[DE90-011061] N91-16378

MATHEMATICAL LOGIC
Skolem functions and equality in automated deduction
[DE90-009703] N91-16641

MATHEMATICAL MODELS
Modelling the transitional boundary layer
[NASA-CR-187487] N91-15995
A coupled rotor aeroelastic analysis utilizing advanced aerodynamic modeling N91-16006
Optimal trajectories for an aerospace plane. Part 2: Data, tables, and graphs
[NASA-CR-187848] N91-16011
Experimental and theoretical examinations of film cooling of gas turbine blades
[ETN-91-98554] N91-16022
High temperature furnace modeling and performance verifications
[NASA-CR-187831] N91-16032
Spray combustion modeling and evaluation
[NASA-CR-187887] N91-16078
The effect of stratification on gravitational coagulation and settling of aerosols
[DE90-010153] N91-16079
A numerical study of silane combustion
[DE90-006002] N91-16080
Modelling of flamelet surface-to-volume ratio in turbulent premixed combustion
[DE90-006312] N91-16081
Modeling and identification of cumulative creep fatigue damage in an austenitic stainless steel N91-16131
The use of impedance measurements in corrosion research: The corrosion behaviour of chromium and iron-chromium alloys
[ISBN-90-9003693-8] N91-16135
Numerical modeling tools for transient electromagnetic problems
[DE90-010328] N91-16180
Shift-invariant image reconstruction of speckle-degraded images using bispectrum estimation
[AD-A227728] N91-16188
Models for surface scattering from solids and liquids
[RSRE-MEMO-3699] N91-16192
Neoclassical effects on RF current drive
[DE90-010302] N91-16222
Threshold voltage and I-V characteristics of AlGaAs/GaAs MODFETs
[AD-A228844] N91-16248
Natural waves of microstrip transmission lines in wave guides
[BER-68] N91-16251
Design and fabrication of high voltage planar devices
[LAAS-90306] N91-16252
Some topics of Navier-Stokes solvers N91-16269
AFDM: An Advanced Fluid-Dynamics Model. Volume 2: Topologies, flow regimes and interfacial areas
[DE91-000581] N91-16283
Numerical study of a three-dimensional turbulent boundary layer
[AD-A227835] N91-16291
Development and application of numerical models for reactive flows
[AD-A228884] N91-16295
Incompressible flow simulations using the velocity-pressure formulation N91-16299
Modeling the dissipation rate in rotating turbulent flows
[NASA-CR-187485] N91-16306
Integrated Numerical Experiments (INEX) and the Free-Electron Laser Physical Process Code (FELPPC)
[DE90-011957] N91-16348
Some nonlinear problems in the manipulation of beams
[DE91-005211] N91-16358
Large space manipulators study
[AD-A227276] N91-16381
Modeling and control of a two-arm elastic robot in gravity N91-16389
Kinematics of arthropod legs: Modeling and measurement N91-16391
Study of the influence of imperfections on the dynamic stability of tanks
[DE90-011094] N91-16398
Time-temperature response of multiphase viscoelastic solids through numerical analysis N91-16401
Direct disc impact investigation of dynamic large finite plastic behavior of 1100 aluminum N91-16404
Dynamic response of composite beams using shear-deformable finite elements
[AD-A227975] N91-16408
Potential responses of landscape boundaries to global environmental change
[DE90-008568] N91-16451
Finalization of the international biospheric model validation study
[DE90-011087] N91-16463
Turbulence and diffusion in the atmospheric boundary layer
[DE90-011582] N91-16471
Continuum models of continental deformation N91-16490
Excursions to the base of the mantle N91-16491
Observation simulation experiments with regional prediction models N91-16502
Laboratory and theoretical models of planetary-scale instabilities and waves N91-16511
Effects of switch leakages upon Nimbus-7 SMMR calibration
[NASA-TM-100705] N91-16536
Quantification of lower bounds for endurance times in thermally insulated fingers and toes exposed to cold stress
[AD-A227782] N91-16545
Heat transfer in clothing during heat radiation
[IZF-1990-B-2] N91-16569
A trellis-searched APC (Adaptive Predictive Coding) speech coder
[DE91-000866] N91-16581
Smoothing and scaling airfoil coordinates on a personal computer
[DE89-000878] N91-16582
Geometric modeling applications interface program
[AD-A227651] N91-16591
Limit behaviors of approximate solutions to conservation laws
[DE90-010069] N91-16646
Solvable two-dimensional supersymmetric models and the supersymmetric Virasoro algebra
[DE90-012140] N91-16648
Validity study in multidimensional latent space and efficient computerized adaptive testing
[AD-A227742] N91-16650
Fragment mass distribution of debris
[MBB-UA-1187-90-PUB] N91-16669
Computational physics at the National Energy Research Supercomputer Center
[DE90-010283] N91-16672
Thermal emission model for the anneal of radiation-induced trapped holes
[DE90-007285] N91-16718
A free boundary problem arising in plasma physics
[DE90-010065] N91-16754
Theoretical studies of tokamaks
[DE90-011332] N91-16768
A model for the prediction of Nb3Sn critical current as a function of field, temperature, strain, and radiation damage
[DE91-000656] N91-16775
IR plasma emissions
[AD-A227713] N91-16776
Hyperfine interactions associated with iron substituted superconducting oxides
[DE90-010411] N91-16783
Molecular crystals and localized vibrational states
[DE90-010602] N91-16786
A search for good lattice rules based on the reciprocal lattice generator matrix
[DE91-004425] N91-16809
Epitaxial growth and surface morphology of some metal and semiconductor structures N91-16824
Image interpretation for transmission electron microscopy of thin semiconductor layers and interfaces
[ETN-91-98487] N91-16826
Dynamics and configurations of galaxy triplets N91-16946
Spectrometric, chemical, and cosmological development of galaxies
[ETN-91-98555] N91-16972
Energy and Technology Review, March 1990
[DE90-008230] N91-16985

MATRICES (MATHEMATICS)
A block QR factorization algorithm for rank-deficient matrices
[DE90-010066] N91-16573
Column reduction of polynomial matrices: An iterative algorithm
[MEMO-COSOR-89-30] N91-16598
Matrix algorithms in signal processing
[AD-A228851] N91-16625
Linear algebra for dense matrices on a hypercube
[DE90-010533] N91-16647
Sparse representation of smooth linear operators
[AD-A228142] N91-16660
A search for good lattice rules based on the reciprocal lattice generator matrix
[DE91-004425] N91-16809

MATRIX MATERIALS
Acoustical and dynamic mechanical characterization of fiber-matrix interface bonds in ceramic composites
[DE90-010949] N91-16066
Mechanics of interface cracks
[AD-A227579] N91-16067
MATRIX METHODS
Using a fast Fourier method to model sound propagation in a stratified atmosphere over a stratified porous-elastic ground N91-16692
MATTER (PHYSICS)
H I studies of the sculptor group galaxies N91-16876
MEASUREMENT
Photometric analyses for the determination of physical and structural properties for the Martian surface in the Oxia Palus region
[DLR-FB-90-27] N91-16979
MEASURING INSTRUMENTS
Self-propelled in-tube shuttle and control system for automated measurements of magnetic field alignment
[DE90-008210] N91-16316
A tunable x ray microprobe using synchrotron radiation
[DE90-011219] N91-16322
Definition and preliminary design of the Laser Atmospheric Wind Sounder (LAWS) phase 1. Volume 1: Executive summary
[NASA-CR-184071] N91-16332
Definition and preliminary design of the Laser Atmospheric Wind Sounder (LAWS) phase 1. Volume 2
[NASA-CR-184072] N91-16333
Definition and preliminary design of the Laser Atmospheric Wind Sounder (LAWS) phase 1. Volume 3: Program cost estimates
[NASA-CR-184073] N91-16334
High-purity silicon soft x ray sensor arrays
[ETN-91-98484] N91-16338
An inter-comparison of surface energy flux measurement systems used during FIFE, 1987
[NASA-CR-187699] N91-16472
MECHANICAL DEVICES
A convenient system for the manufacture of holographic diffraction gratings
[DE90-009481] N91-16319
MECHANICAL DRIVES
The PHD: A Planar, Harmonic Drive robot for joint torque control
[NASA-CR-187924] N91-16386
A hydraulically driven microdisplacement unit
[ME-56] N91-16392
MECHANICAL ENGINEERING
Advanced Turbine Technology Applications Project (ATTAP)
[NASA-CR-187039] N91-16021
MECHANICAL PROPERTIES
Mechanical behavior of a SiC-fiber/Si3N4 composite
[AD-A228371] N91-16073
Development of nondestructive evaluation methods and prediction of effects of flaws on the fracture behavior of structural ceramics
[DE90-011092] N91-16141
Direct disc impact investigation of dynamic large finite plastic behavior of 1100 aluminum N91-16404
Dynamic response of composite beams using shear-deformable finite elements
[AD-A227975] N91-16408
Utilization of polymer viscoelastic properties in acoustic wave sensor applications
[DE90-010534] N91-16676
Development of liquid xenon imaging gamma-ray spectrophotometers
[AD-A227575] N91-16740
MELTING
A new perturbation theory of solids and fluids and its applications to high-pressure melting problems
[DE90-011502] N91-16829
MEMORY
Skill and skilled memory
[AD-A227697] N91-16549
MEMORY (COMPUTERS)
Properties and characterization of thin film ferroelectric capacitors for nonvolatile memories
[DE91-004037] N91-16242
Displaying alphanumeric characters on pixel-planes 5
[AD-A228616] N91-16622
Parallel Access Main Memory (PAMM) user's manual, version 1.0
[AD-A227744] N91-16635
MENTAL PERFORMANCE
A quantum theory of the mind-brain interface
[DE91-004431] N91-16546
Pre-attentive and attentive visual information processing
[AD-A228541] N91-16550
EEG indicators of mental workload: Conceptual and practical issues in the development of a measurement tool N91-16559
Optimisation of operational workload levels using neurophysiological and cognitive techniques N91-16560
Development of a test-bed for real-time monitoring of pilot mental status N91-16563
Organization of the mission pattern in the air picture
[IZF-1990-A-12] N91-16568
MERCURY (METAL)
Circumfluous motion of a conductive liquid around solid objects in a magnetic field
[DE90-011335] N91-16265
Experimental study on mercury heat pipes (on effect of screen mesh wick under bottom heat mode) N91-16280
MESH
Experimental study on mercury heat pipes (on effect of screen mesh wick under bottom heat mode) N91-16280
MESON RESONANCE
Measurement of the e+e- annihilation in mu+mu- pairs at the Z sup o resonance
[MPI-PAE/EXP.EL-231] N91-16732
MESOSCALE PHENOMENA
An investigation of a gravity wave during GALE: February 6, 1986
[AD-A227655] N91-16519
MESOSPHERE
A global climatology of middle atmosphere inertio-gravity waves N91-16524
MESSAGE PROCESSING
Measurement of the capture effect of frequency modulation
[AD-A228058] N91-16199
METAL COATINGS
Assessment of corrosion resistant coatings for a depleted U-0.75 Ti alloy
[AD-A228237] N91-16130
METAL CRYSTALS
Chemisorption of carbon monoxide on three metal surfaces: Ni(111), Pd(111) and Pt(111): A comparative study
[AD-A228579] N91-16108
METAL FATIGUE
Modeling and identification of cumulative creep fatigue damage in an austenitic stainless steel N91-16131
METAL FIBERS
Understanding the interdiffusion behavior and determining the long term stability of tungsten fiber reinforced niobium-base matrix composite systems
[NASA-CR-187396] N91-16120
METAL FINISHING
Deburring and surface finishing: The past ten years and projections for the next ten years
[DE91-000579] N91-16176
METAL FOAMS
Hydrogen storage in metal hydrides
[AD-A228150] N91-16103
METAL FOILS
Scoping estimates of the LDEF satellite induced radioactivity
[NASA-CR-184074] N91-16056
METAL HYDRIDES
Hydrogen storage in metal hydrides
[AD-A228150] N91-16103
METAL MATRIX COMPOSITES
Characterization of the corrosion of a P-130x graphite fiber reinforced 6063 aluminum metal matrix composite
[AD-A228134] N91-16071
Metallurgical design of novel metal matrix composites for aerospace applications
[ETN-91-98573] N91-16077
Understanding the interdiffusion behavior and determining the long term stability of tungsten fiber reinforced niobium-base matrix composite systems
[NASA-CR-187396] N91-16120
METAL OXIDE SEMICONDUCTORS
The 1/f noise in irradiated MOS devices
[DE90-007288] N91-16219
Radiation hardening of a high voltage IC technology (BCDMOS)
[DE90-008345] N91-16220
METAL PLATES
Mechanical property data on aluminum alloy 7150-T7751 plate
[AD-A227506] N91-16124
METAL SURFACES
Hydrogen storage in metal hydrides
[AD-A228150] N91-16103
Chemisorption of carbon monoxide on three metal surfaces: Ni(111), Pd(111) and Pt(111): A comparative study
[AD-A228579] N91-16108
Atomic-scale simulation of adhesion between metallic surfaces
[DE91-004722] N91-16127
METAL-GAS SYSTEMS
Hydrogen storage in metal hydrides
[AD-A228150] N91-16103
METAL-METAL BONDING
Bibliography of the technical literature of the Materials Joining Group, Metals and Ceramics Division, 1951--June 1989
[DE91-000530] N91-16126
METALLIC GLASSES
Magnetic domain strain sensor program
[AD-A227225] N91-16327
METALLIZING
Applications research studies on microtubules
[AD-A228756] N91-16205
METALLOGRAPHY
PC-based digital imaging for storing microscopy images for surveillance programs
[DE90-010080] N91-16738
METALS
Atomic and electronic structure of metals and alloys: Clean surfaces and chemisorbed molecules
[DE91-000267] N91-16123
Scattering center analysis of simple metallic objects
[DLR-FB-90-32] N91-16216
METASTABLE STATE
Experimental studies of the properties of trihydrogen and tetrahydrogen
[AD-A228869] N91-16110
METEOR TRAILS
Meteor burst communications study
[AD-A228641] N91-16204
METEOROLOGICAL CHARTS
The design of a meteorological facsimile converter
[ETN-91-98578] N91-16528
METEOROLOGICAL INSTRUMENTS
Turbulence and diffusion in the atmospheric boundary layer
[DE90-011582] N91-16471
METEOROLOGICAL PARAMETERS
Meteorological effects on long-range outdoor sound propagation N91-16696
Effect of wind and temperature gradients on received acoustic energy N91-16697
Comparison of FFP predictions with measurements of a low-frequency signal propagated in the atmosphere N91-16698
A noise assessment and prediction system N91-16702
METEOROLOGICAL RADAR
Results of the Kansas City 1989 Terminal Doppler Weather Radar (TDWR) operational evaluation testing
[AD-A228784] N91-16206
METEOROLOGICAL SATELLITES
On the developmental dynamics of sudden stratospheric warmings
[AD-A227731] N91-16485
Observation simulation experiments with regional prediction models N91-16502
Synoptic/planetary-scale interactions and blocking over the North Atlantic Ocean N91-16513
METEOROLOGY
NASA/MSFC FY90 Global Scale Atmospheric Processes Research Program Review
[NASA-CP-3093] N91-16500
Comparison of SSM/I measurements to numerically-simulated cloud and precipitation during ERICA N91-16501
Tropical Pacific moisture variability N91-16509
Laboratory and theoretical models of planetary-scale instabilities and waves N91-16511
A noise assessment and prediction system N91-16702
METEOSAT SATELLITE
Sahelian vegetation monitoring project
[BCRS-90-04] N91-16426
METHANE
Auto-ignition temperatures of binary mixtures of alkanes in a closed vessel: Comparisons between experimental measurements and numerical predictions
[DE90-007856] N91-16082
Generation of high power 1.54 micrometer radiation by stimulated Raman scattering in methane
[FEL-90-B098] N91-16366
METHYL ALCOHOL
A summary of prospects for methanol vehicles in the United States
[DE90-009719] N91-16370
Direct methanol/air fuel cells: Systems considerations
[DE90-011971] N91-16439
Greenhouse gas emissions from selected alternative transportation fuels market niches
[DE90-010491] N91-16448

MICHELSON INTERFEROMETERS
Interferometric second-harmonic-generation autocorrelator for characterizing femtosecond pulses
[DE90-010331] N91-16345
MICROANALYSIS
A tunable x ray microprobe using synchrotron radiation
[DE90-011219] N91-16322
New development of laser-based techniques in applications of thin-layer chromatography, microprobe elemental analysis, and gas phase pyrolysis
[DE90-011740] N91-16347
MICROCHANNEL PLATES
Multiframe x ray images from a single meander stripline coated on a microchannel plate
[DE90-010741] N91-16224
MICROCOMPUTERS
Microsupercomputers: Design and implementation
[AD-A228741] N91-16571
Microsupercomputers: Design and implementation
[AD-A228744] N91-16572
MICROELECTRONICS
Safety as a design goal for applications of microelectronic control systems
[REPT-23/90] N91-16253
Solid state research
[NASA-CR-187871] N91-16816
MICROGRAVITY APPLICATIONS
The space flights: Second German Spacelab mission D-2 and Mir 1992
[REPT-25/90] N91-16034
MICROMETEOROLOGY
Carbon dioxide and energy exchanges in a temperate grassland ecosystem N91-16419
A study of the surface energy balance on slopes in a taligrass prairie
[NASA-CR-187698] N91-16473
Comparison of FFP predictions with measurements of a low-frequency signal propagated in the atmosphere N91-16698
MICROPLASMAS
Laser microplasma-gas chromatography detector. 2: Detection of species-specific fragment emission
[AD-A228373] N91-16106
MICROPOROSITY
Synthesis, characterization and catalytic activity of microporous aluminophosphate catalysts N91-16092
MICROPROCESSORS
Timing margin measurement using a laser technique
[AD-A226821] N91-16353
MICROSCOPES
Dynamic aspects of scanning surface instruments and microscopes
[ME-84] N91-16339
PC-based digital imaging for storing microscopy images for surveillance programs
[DE90-010080] N91-16738
MICROSCOPY
Joint services electronics program
[AD-A227576] N91-16237
Kinematics of arthropod legs: Modeling and measurement N91-16391
PC-based digital imaging for storing microscopy images for surveillance programs
[DE90-010080] N91-16738
MICROSTRIP TRANSMISSION LINES
Multiframe x ray images from a single meander stripline coated on a microchannel plate
[DE90-010741] N91-16224
Natural waves of microstrip transmission lines in wave guides
[BER-68] N91-16251
MICROSTRUCTURE
Metallurgical design of novel metal matrix composites for aerospace applications
[ETN-91-98573] N91-16077
Influence of strain rate on the structure/property of Ti-48Al-1V
[DE91-000172] N91-16122
Phase selection and processing of high temperature intermetallic alloys
[AD-A227910] N91-16129
Development of nondestructive evaluation methods and prediction of effects of flaws on the fracture behavior of structural ceramics
[DE90-011092] N91-16141
Electron microscopy and electrochemistry of nickel oxide films for electrochromic devices produced by different techniques
[DE90-011596] N91-16142
Sintering stress and microstructure in ceramic powder compacts
[DE91-004415] N91-16149
Applications research studies on microtubules
[AD-A228756] N91-16205
Test methods for evaluating hot cracking: Review and perspective
[DE90-009820] N91-16397
Microstructures and dc critical currents in textured Y-Ba-Cu-oxides
[DE91-000895] N91-16803
Observations of vortex structure in YBa2Cu3O7
[DE91-000900] N91-16804
Characterization of GaAs/Si interface structure by x ray diffraction
[DE91-004769] N91-16811
Image interpretation for transmission electron microscopy of thin semiconductor layers and interfaces
[ETN-91-98487] N91-16826
MICROWAVE ATTENUATION
Comparison of propagation and absorption of FEL-generated microwaves with theory
[DE90-010369] N91-16181
MICROWAVE CIRCUITS
Novel applications of Tl-Ca-Ba-Cu-O thin films to active and passive high frequency devices
[DE91-004507] N91-16240
MICROWAVE COUPLING
Microwave coupling on printed circuit boards
[DE90-011237] N91-16232
MICROWAVE EQUIPMENT
Microwave sintering of fuel cell materials
[DE90-011643] N91-16143
Research and development on advanced silicon carbide thin film growth techniques and fabrication of high power and microwave frequency silicon carbide-based device
[AD-A228758] N91-16246
Solid state research
[NASA-CR-187871] N91-16816
MICROWAVE FREQUENCIES
Research and development on advanced silicon carbide thin film growth techniques and fabrication of high power and microwave frequency silicon carbide-based device
[AD-A228758] N91-16246
MICROWAVE IMAGERY
Scattering center analysis of simple metallic objects
[DLR-FB-90-32] N91-16216
The dielectric properties of wet soils
[BCRS-90-13] N91-16429
Comparison of SSM/I measurements to numerically-simulated cloud and precipitation during ERICA N91-16501
Observation simulation experiments with regional prediction models N91-16502
Global variability of water vapor and condensate from SSM/I N91-16507
MICROWAVE INTERFEROMETERS
Microwave interferometer and reflectometer techniques for thermonuclear plasmas
[ETN-91-98478] N91-16780
MICROWAVE LANDING SYSTEMS
Activities report of the German Federal Institute for Flight Safety
[ETN-91-98644] N91-16002
A successive partial-relaxation Gaussian algorithm for area navigation operations with the Microwave Landing System (MLS)
[AD-A228871] N91-16004
MICROWAVE OSCILLATORS
Microwave measurements of water vapor partial pressure at temperatures up to 350 C
[DE90-011484] N91-16087
Investigation of a new concept in semiconductor microwave oscillators
[AD-A226785] N91-16235
MICROWAVE RADIOMETERS
Effects of switch leakages upon Nimbus-7 SMMR calibration
[NASA-TM-100705] N91-16536
MICROWAVE TRANSMISSION
Electronically steerable arrays: Current and future technology and applications
[ETN-91-98581] N91-16254
MICROWAVES
Microwave measurements of water vapor partial pressure at temperatures up to 350 C
[DE90-011484] N91-16087
Microwave sintering of fuel cell materials
[DE90-011643] N91-16143
Microwave Tokamak Experiment (OMTX): Overview and status
[DE90-010287] N91-16758
Characterization of disruptions in the Microwave Tokamak Experiment (MTX)
[DE90-010352] N91-16761
Microwave generation for magnetic fusion energy applications, task B
[DE90-011079] N91-16763
Microwave generation for magnetic fusion energy applications, task C
[DE90-011080] N91-16764
Stark-effect measurement of high FEL electric fields in MTX by laser-aided particle-probe spectroscopy
[DE90-011911] N91-16771
Microwave-detected photoconductance decay
[DE90-011505] N91-16795
MILITARY OPERATIONS
Army Unmanned Aerial Vehicle (UAV) requirements and the joint UAV program
[AD-A228149] N91-16009
Artificial intelligence technologies applied to terrain analysis
[DE90-011985] N91-16642
MILITARY TECHNOLOGY
National software capacity: Near-term study executive summary
[AD-A227564] N91-16590
Subject bibliography of the PMA 205 (Program Manager Air 205) network technical library at Oak Ridge National Laboratory
[DE90-009988] N91-16835
MILKY WAY GALAXY
Galactic structure in direction of Vela-Puppis by means of UBV beta observations
[ETN-91-98556] N91-16973
MILLIMETER WAVES
Nonradiative dielectric waveguide millimetre-wave integrated circuits: A review
[AD-A227760] N91-16238
MIMD (COMPUTERS)
Wakefield calculations on parallel computers
[DE90-009712] N91-16632
MINERAL METABOLISM
Gallium as a unique anti-resorptive agent in bone: Preclinical studies on its mechanisms of action
[DE90-010650] N91-16542
MINIATURIZATION
A miniature inexpensive, oxygen sensing element
[DE90-009938] N91-16318
MIR SPACE STATION
The space flights: Second German Spacelab mission D-2 and Mir 1992
[REPT-25/90] N91-16034
MIRRORS
Generation of XUV light by resonant frequency tripling in a two-wiggler FEL amplifier
[DE90-012120] N91-16349
MISSILE CONTROL
Optimal rocket motor design and control for tactical missiles N91-16062
MISSILE DESIGN
Optimal rocket motor design and control for tactical missiles N91-16062
MISSILE SYSTEMS
A transformer coupled semiconductor bridge igniter for low voltage ignition from a high voltage source
[DE90-009974] N91-16221
MISSION PLANNING
Space Station Freedom resource allocation accommodation of technology payload requirements
[NASA-TM-102766] N91-16832
MIXED OXIDES
Hyperfine interactions associated with iron substituted superconducting oxides
[DE90-010411] N91-16783
MIXING
The University of Arizona program in solid propellants N91-16165
Multi-waveband observations of colliding galaxies N91-16868
MIXTURES
The University of Arizona program in solid propellants N91-16165
Symmetry and design in mixture experiments
[AD-A226760] N91-16169
MOBILITY
Optimal positioning of redundant manipulator-platform systems for maximum task efficiency
[DE90-011061] N91-16378
Camera space manipulation of a mobile robot N91-16390
Technique for determining the static polarizabilities of refractory metal atoms
[DE90-017088] N91-16724
MODELS
Use of the Magnus force in the modified point mass trajectory model
[AD-A228194] N91-15990
Calculation of support interferences on the aerodynamic coefficients for a wind tunnel calibration model
[DLR-FB-90-26] N91-15998
Longitudinal stability augmentation of a lightweight fighter aircraft model
[ETN-91-98585] N91-16026
Linguistic and pragmatic constraints on utterance interpretation
[AD-A228815] N91-16210

Experimental verification of physical model of pulsed laser welding
[DE91-000025] N91-16380
Limits of human visual discrimination: Toward a general model of visual geometry
[AD-A226826] N91-16548
Exponential ground impedance models and their interpretation N91-16686

MODFETS
Threshold voltage and I-V characteristics of AlGaAs/GaAs MODFETs
[AD-A228844] N91-16248

MODULATION
Satellite broadcasting: A common-frequency approach to wideband HDTV with a hand-made example plan
[BBC-RD-1990/7] N91-16189

MODULATORS
Integrated semiconductor modulators
[AD-A228615] N91-16820

MODULES
Development of a versatile laser light scattering instrument
[NASA-CR-182474] N91-16350

MOIRE FRINGES
Automatic, high-resolution analysis of low-noise fringes
[DE90-009779] N91-16574

MOIRE INTERFEROMETRY
New methods for producing, recording, and processing interferometric moire patterns N91-16405
Automatic, high-resolution analysis of low-noise fringes
[DE90-009779] N91-16574
A convenient system for diffraction moire measurements
[DE90-010980] N91-16739

MOISTURE
Multi-dimensional aspects of recent climate change in North America
[DE90-010958] N91-16460
Tropical Pacific moisture variability N91-16509

MOLECULAR BEAMS
High resolution photoelectron spectroscopy of metal clusters and high temperature species
[DE90-011598] N91-16119
State-to-state inelastic and reactive molecular beam scattering from surfaces
[DE90-010492] N91-16714

MOLECULAR CLOUDS
Molecular gas and star formation in the central regions of Virgo spiral galaxies N91-16970
Structure and energy balance of molecular clouds
[MPE-PREPRINT-181] N91-16975
The 158 micrometer (CII) line: A measure of global star formation activity in galaxies
[NASA-CR-187925] N91-16977

MOLECULAR COLLISIONS
State-to-state inelastic and reactive molecular beam scattering from surfaces
[DE90-010492] N91-16714

MOLECULAR EXCITATION
Selective excitation, relaxation, and energy channeling in molecular systems
[DE90-010793] N91-16717

MOLECULAR GASES
Galaxy interactions and the stimulation of nuclear activity N91-16910

MOLECULAR ORBITALS
Molecular orbital studies of the bonding in heavy element organometallics
[DE90-009732] N91-16711

MOLECULAR OSCILLATIONS
Direct observation of NF(X) using laser-induced fluorescence: Kinetics of the NF 3 Sigma - ground state
[AD-A228294] N91-16362
Selective excitation, relaxation, and energy channeling in molecular systems
[DE90-010793] N91-16717

MOLECULAR RELAXATION
Direct observation of NF(X) using laser-induced fluorescence: Kinetics of the NF 3 Sigma - ground state
[AD-A228294] N91-16362
Selective excitation, relaxation, and energy channeling in molecular systems
[DE90-010793] N91-16717

MOLECULAR SPECTROSCOPY
Ultrasensitive molecular fluorescence spectroscopy in levitated microdroplets
[DE91-000621] N91-16095

MOLECULAR STRUCTURE
Computer-assisted determination of minimum energy conformations. Part 4: Alpha1 and alpha2 adrenergiic compounds
[AD-A226811] N91-16097
The development of improved capillary supercritical fluid chromatography and mass spectrometry
[AD-A228535] N91-16107
Molecular crystals and localized vibrational states
[DE90-010602] N91-16786

MOLECULAR THEORY
Selective excitation, relaxation, and energy channeling in molecular systems
[DE90-010793] N91-16717

MOLECULAR WEIGHT
Inverse gas chromatography
[AD-A227677] N91-16099

MOLECULES
Ultrasensitive molecular fluorescence spectroscopy in levitated microdroplets
[DE91-000621] N91-16095
Picosecond multiphoton ionization of atomic and molecular clusters
[DE91-000641] N91-16096

MOLTEN SALT ELECTROLYTES
Molten salt electrolytes in high temperature batteries
[RAE-TM-MAT/STR-1155] N91-16241

MOLYBDENUM
Spatial distributions of the emitting species in a penning surface-plasma source
[DE90-011996] N91-16772

MOMENTUM TRANSFER
A global climatology of middle atmosphere inertio-gravity waves N91-16524
Energy and angular momentum transfer in binary galaxies N91-16940

MONITORS
Sensing of metal-transfer mode for process control of GMAW (Gas Metal Arc Welding)
[DE90-010946] N91-16377

MONKEYS
Changes in somatosensory responsiveness in behaving monkeys
[AD-A226832] N91-16540

MONOCHROMATORS
Modeling the performance of water and liquid gallium cooled x ray optical components: A comparison with experiment
[DE90-010460] N91-16784

MONOMERS
Model filled polymers versus synthesis of crosslinked monodisperse polymethacrylate beads
[AD-A227236] N91-16146

MONOTONY
Study of pilot vigilance during long range flight N91-16561

MONTE CARLO METHOD
Monte Carlo simulation of atmospheric neutron transport at high altitudes using MCNP
[AD-A226773] N91-16474
Adaptive bandwidth choice for kernel regression
[AD-A228437] N91-16661
Hierarchical Bayesian analysis of change point problems
[AD-A228179] N91-16666
Theoretical studies of atomic transitions
[DE91-000931] N91-16723
Calculation of free energy from the internal-energy distribution function
[DE90-011111] N91-16791
Epitaxial growth and surface morphology of some metal and semiconductor structures N91-16824
Research in theoretical nuclear physics
[DE90-010792] N91-16828

MOODS
Linguistic and pragmatic constraints on utterance interpretation
[AD-A228815] N91-16210

MORPHOLOGY
Symmetry and design in mixture experiments
[AD-A226760] N91-16169
Epitaxial growth and surface morphology of some metal and semiconductor structures N91-16824
A homogeneous sample of binary galaxies: Basic observational properties N91-16859
Morphological type correlation between nearest neighbor pairs of galaxies N91-16861
The interacting pair Mkn 305/306 N91-16864
Geometrical parameters of E+S pairs N91-16865
An atlas of mixed-morphology pairs N91-16866
Multi-waveband observations of colliding galaxies N91-16868
Tidal distortions in pairs of early-type galaxies N91-16869
The ringed X-galaxy NGC 7020 N91-16885
The morphology of Sersic-Pastoriza galaxies N91-16893
The kinematics and morphology of NGC 520: One, two, or three galaxies N91-16908
Correlations between environmental parameters and nuclear activity N91-16920
The role of shocks in NGC 6240 N91-16921
Radio structures in QSO-galaxy pairs N91-16924
Explaining compact groups as change alignments N91-16944
Wing galaxies: A formation mechanism of the clumpy irregular galaxy Markarian 297 N91-16963

MORSE POTENTIAL
Correlation between the elastic-shear-instability-mechanism and empirical criteria for irradiation-induced amorphization
[DE91-004481] N91-16810

MOTOR VEHICLES
Requirements for a fuel cell for transportation application
[DE90-011146] N91-16230
Technological and policy options for mitigating greenhouse gas emissions from mobile sources
[DE90-010151] N91-16447
Vehicular sources in acoustic propagation experiments N91-16690

MOUNTAINS
Numerical simulations of the mountain iron tracer data
[DE90-009749] N91-16499

MULTIPLE ACCESS
Movable-boundary channel-access schemes for integrated voice/data networks
[AD-A227331] N91-16186

MULTIPLEXING
Applications of non-linear optics
[AD-A228872] N91-16743

MULTIPROCESSING (COMPUTERS)
Microsupercomputers: Design and implementation
[AD-A228744] N91-16572
POSC: A Partitioning and Optimizing SISAL Compiler
[DE90-010679] N91-16577
Analysis of parallel, replicated simulations under a completion time constraint
[AD-A228292] N91-16613
Experiments with initial transient deletion for parallel, replicated steady-state simulations
[AD-A227879] N91-16636

MULTISENSOR APPLICATIONS
Reports on cartography and topography. Series 1, report 104
[ISSN-0469-4236] N91-16432
The multisensor image map 1:50,000 Rheinhessen N91-16434

MULTISPECTRAL BAND SCANNERS
The usefulness of MSS pictures for mapping and biomass estimation of macro-algae and seaweed in the Eastern Scheldt
[BCRS-90-09] N91-16428

MULTISTATIC RADAR
A planar near-field scanning technique for bistatic radar cross section measurements
[NASA-CR-187794] N91-16194

MUONS
Measurement of the e+e- annihilation in mu+mu- pairs at the Z sup o resonance
[MPI-PAE/EXP.EL-231] N91-16732

N

NASA PROGRAMS
The NASA controls-structures interaction technology program
[NASA-TM-102752] N91-16057
Contents of the NASA ocean data system archive, version 11-90
[NASA-CR-187812] N91-16535

NASTRAN
A finite element procedure for calculating fluid-structure interaction using MSC/NASTRAN
[NASA-TM-102857] N91-16414

NATIONAL AEROSPACE PLANE PROGRAM
Optimization and guidance of flight trajectories for the national aerospace plane
[NASA-CR-187837] N91-16010

NATURAL GAS
Greenhouse gas emissions from selected alternative transportation fuels market niches
[DE90-010491] N91-16448

NATURAL SATELLITES
Dynamical interactions of galaxy pairs N91-16930
Stationary orbits of satellites of disk galaxies N91-16954

NAVIER-STOKES EQUATION
Large-scale numerical aerodynamic simulations for complete aircraft configurations
[NAL-TR-1073-T] N91-15984
Some topics of Navier-Stokes solvers N91-16269
Unsteady separation over maneuvering bodies
[AD-A226829] N91-16285
Incompressible flow simulations using the velocity-pressure formulation N91-16299

Acceleration of iterative algorithms for Euler and Navier-Stokes equations N91-16301
The stationary exterior three dimensional Navier-Stokes problem of viscous flow past a body in anisotropically weighted Sobolev spaces
[REPT-110] N91-16314
A segregated finite element solution to the incompressible Navier-Stokes equations
[ME-69] N91-16315

NAVIGATION AIDS
Terrain matching using image sequence analysis N91-16424

NAVIGATION TECHNOLOGY SATELLITES
Principal facts for about 16,000 gravity stations in the Nevada test site and vicinity
[DE90-011521] N91-16470

NEAR FIELDS
A planar near-field scanning technique for bistatic radar cross section measurements
[NASA-CR-187794] N91-16194

NEAR INFRARED RADIATION
Infrared images of merging galaxies N91-16904

NEBULAE
The nature of the emission-line nebulae in powerful far-infrared galaxies N91-16916

NEODYMIUM LASERS
Generation of high power 1.54 micrometer radiation by stimulated Raman scattering in methane
[FEL-90-B098] N91-16366
Experimental verification of physical model of pulsed laser welding
[DE91-000025] N91-16380
The Cabannes-lidar for the examination of the stratosphere: Selected design elements for the experimental construction
[BONN-IR-90-39] N91-16493

NETWORK ANALYSIS
An evolutionary approach to designing neural networks
[AD-A228874] N91-16643

NEURAL NETS
Limits of human visual discrimination: Toward a general model of visual geometry
[AD-A226826] N91-16548
An evolutionary approach to designing neural networks
[AD-A228874] N91-16643
IEEE International Symposium on Information Theory
[AD-A228239] N91-16842

NEUROLOGY
Investigation of effects of 60-Hz electric and magnetic fields on operant and social behavior and on the neuroendocrine system of nonhuman primates
[DE90-010809] N91-16537

NEUROPHYSIOLOGY
Changes in somatosensory responsiveness in behaving monkeys
[AD-A226832] N91-16540
Optimisation of operational workload levels using neurophysiological and cognitive techniques N91-16560
Computer aided physiological assessment of the functional state of pilots during simulated flight N91-16562

NEUTRAL ATMOSPHERES
A comparison of optically measured and radar-derived horizontal neutral winds
[AD-A227690] N91-16483

NEUTRAL GASES
VLA neutral hydrogen imaging of compact groups N91-16872
The morphology of Sersic-Pastoriza galaxies N91-16893

NEUTRAL SHEETS
Ion distributions and flows near the neutral sheet
[MPE-PREPRINT-179] N91-16974

NEUTRON COUNTERS
Neutron measurements in search of cold fusion
[DE91-004855] N91-16778

NEUTRON DIFFRACTION
Magnetic structures of actinide materials by pulsed neutron diffraction
[DE91-000373] N91-16093

NEUTRON EMISSION
The Los Alamos megamp fiber z-pinch experiment
[DE91-004842] N91-16777
Neutron measurements in search of cold fusion
[DE91-004855] N91-16778

NEUTRON IRRADIATION
The radiation hardness test facility
[RAL-90-065] N91-16030

NEUTRON SCATTERING
From visco-elasticity towards thermal relaxation: A neutron scattering study of density fluctuations in fluid helium
[ETN-91-98486] N91-16111

NEUTRON STARS
The x ray emission of SS433
[MPE-PREPRINT-189] N91-16856
Interacting nuclei in distant galaxies N91-16894

NEUTRONS
Effects of neutron fluence on the operating characteristics of diode lasers used in atomic frequency standards
[AD-A226763] N91-16352
Monte Carlo simulation of atmospheric neutron transport at high altitudes using MCNP
[AD-A226773] N91-16474
Radiation physics, biophysics, and radiation biology
[DE90-011544] N91-16722
The measurement of gamma heating in a fusion blanket test assembly
[DE90-011154] N91-16766

NEWTON METHODS
A coupled rotor aeroelastic analysis utilizing advanced aerodynamic modeling N91-16006
Acceleration of iterative algorithms for Euler and Navier-Stokes equations N91-16301
A long step barrier method for convex quadratic programming
[REPT-90-53] N91-16600

NICKEL
Chemisorption of carbon monoxide on three metal surfaces: Ni(111), Pd(111) and Pt(111): A comparative study
[AD-A228579] N91-16108

NICKEL ALLOYS
Weldability of nickel aluminides
[DE90-008557] N91-16116
The influence of small SO2 contents on the corrosion behavior for NiCrAl alloys in temperature zone from 1000 to 1100 C
[JUEL-2362] N91-16134

NICKEL OXIDES
Electron microscopy and electrochemistry of nickel oxide films for electrochromic devices produced by different techniques
[DE90-011596] N91-16142

NIOBIUM
Tensile behavior of tungsten/niobium composites at 1300 to 1600 K
[NASA-TM-103727] N91-16128
From low to high Tc: An ultrasonic investigation of niobium single crystal and YBaCuO superconducting thin films with surface acoustic waves N91-16822

NIOBIUM ALLOYS
Understanding the interdiffusion behavior and determining the long term stability of tungsten fiber reinforced niobium-base matrix composite systems
[NASA-CR-187396] N91-16120

NIOBIUM COMPOUNDS
A model for the prediction of Nb3Sn critical current as a function of field, temperature, strain, and radiation damage
[DE91-000656] N91-16775

NIOBIUM ISOTOPES
Fundamental characteristics and applications of an inductively coupled plasma as an ion source for mass spectrometry
[DE90-011746] N91-16770

NITRIC OXIDE
Removal of NO and NO2 from contaminated atmospheres
[AD-A227260] N91-16565

NITROGEN
Effects of high pressure nitrogen on the thermal stability of SiC fibers
[NASA-TM-103245] N91-16075

NITROGEN DIOXIDE
Removal of NO and NO2 from contaminated atmospheres
[AD-A227260] N91-16565

NITROGEN FLUORIDES
Direct observation of NF(X) using laser-induced fluorescence: Kinetics of the NF 3 Sigma - ground state
[AD-A228294] N91-16362

NITROGEN OXIDES
Parametric study of electrostatically charged sprays
[DE90-010580] N91-16262
The atmospheric effects of stratospheric aircraft: A current consensus
[NASA-RP-1251] N91-16467

NOAA SATELLITES
Evaluation of the GOES 1-M normalization technique with the visible images of GOES-7
[AD-A227462] N91-16055

NOISE (SOUND)
Environmental noise from the Naesudden (Sweden) and Maglarp (Sweden) prototype wind turbines: A study of machinery noise
[FFA-TN-1990-34] N91-16706

NOISE GENERATORS
Long-distance sound propagation over discontinuous impedances N91-16688
Long-range vertical propagation N91-16693

NOISE INTENSITY
A review of the airborne sound insulation requirements for broadcasting studios and ancillary areas
[BBC-RD-1990/10] N91-16680
Fourth International Symposium on Long-Range Sound Propagation
[NASA-CP-3101] N91-16682
Long-range vertical propagation N91-16693
A noise assessment and prediction system N91-16702

NOISE MEASUREMENT
The 1/f frequency noise effects on self-heterodyne linewidth measurements for coherent communications
[AD-A227942] N91-16195
Wind turbine acoustics
[NASA-TP-3057] N91-16679
Long-range vertical propagation N91-16693
Environmental noise from the Naesudden (Sweden) and Maglarp (Sweden) prototype wind turbines: A study of machinery noise
[FFA-TN-1990-34] N91-16706

NOISE POLLUTION
Environmental noise from the Naesudden (Sweden) and Maglarp (Sweden) prototype wind turbines: A study of machinery noise
[FFA-TN-1990-34] N91-16706

NOISE PREDICTION
The 1/f frequency noise effects on self-heterodyne linewidth measurements for coherent communications
[AD-A227942] N91-16195
A noise assessment and prediction system N91-16702

NOISE PROPAGATION
Long-range vertical propagation N91-16693

NOISE REDUCTION
Noise reduction using low weight and constant weight coding techniques
[AD-A228346] N91-16244

NOISE SPECTRA
Fundamental characteristics and applications of an inductively coupled plasma as an ion source for mass spectrometry
[DE90-011746] N91-16770

NONDESTRUCTIVE TESTS
Developmental tests for shuttle Orbiter N91-16038
Acoustical and dynamic mechanical characterization of fiber-matrix interface bonds in ceramic composites
[DE90-010949] N91-16066
Development of nondestructive evaluation methods and prediction of effects of flaws on the fracture behavior of structural ceramics
[DE90-011092] N91-16141
Scattering of Lamb waves in an elastic plate for ultrasonic nondestructive evaluation of weldments and cracks N91-16412

NONLINEAR EQUATIONS
Finite element approximations for transonic flows
[ETN-91-98491] N91-15988
Nonlinear waves and inverse scattering
[AD-A228757] N91-16294

NONLINEAR OPTICS
Design, ultrastructure, and dynamics of nonlinear optical interactions in polymeric thin films
[AD-A228876] N91-16156
Applications of non-linear optics
[AD-A228872] N91-16743
Solid state research
[NASA-CR-187871] N91-16816

NONLINEAR SYSTEMS
Joint services electronics program
[AD-A227576] N91-16237
Research in nonlinear water waves
[AD-A227948] N91-16292
Integrated Numerical Experiments (INEX) and the Free-Electron Laser Physical Process Code (FELPPC)
[DE90-011957] N91-16348
Void nucleation in nonlinear solid mechanics
[AD-A228890] N91-16410
Nonlinear optical systems interacting with amplitude-modulated optical fields
[AD-A228221] N91-16742

NONLINEARITY
Nonlinear waves and inverse scattering
[AD-A228757] N91-16294
Nonlinear resonance
[DE90-010428] N91-16341
Some nonlinear problems in the manipulation of beams
[DE91-005211] N91-16358
Nonlinear dynamics of global atmospheric and Earth-system processes N91-16510
Stellar convection and dynamo theory N91-16857

NONPARAMETRIC STATISTICS
Adaptive bandwidth choice for kernel regression
[AD-A228437] N91-16661
NORTH AMERICA
Multi-dimensional aspects of recent climate change in North America
[DE90-010958] N91-16460
NORTHERN HEMISPHERE
Isolated galaxies, pairs, and groups of galaxies N91-16878
NOSE (ANATOMY)
Electronic analogue for a biological nose
[ME-78] N91-16541
NOTCH TESTS
Specimen size effects in Charpy impact testing
[DE90-011369] N91-16399
NOVA LASER SYSTEM
Stability and accuracy of the sweep rate measurements for LLNL optical streak cameras
[DE90-012080] N91-16324
NUCLEAR BINDING ENERGY
Comparison of the quadratic configuration interaction and coupled cluster approaches to electron correlation including the effect of triple excitations
[NASA-CR-187855] N91-16727
Research in theoretical nuclear physics
[DE90-010792] N91-16828
NUCLEAR CHEMISTRY
Highlights of the Chemical Technology (CMT) Division's activities
[DE90-008242] N91-16984
NUCLEAR EXPLOSIONS
Small scale shock tube experiments using a computer controlled active rarefaction wave eliminator
[AD-A227507] N91-16029
Energy and Technology Review, March 1990
[DE90-008230] N91-16985
NUCLEAR FUSION
Microwave generation for magnetic fusion energy applications, task B
[DE90-011079] N91-16763
Microwave generation for magnetic fusion energy applications, task C
[DE90-011080] N91-16764
Electromagnetic computations for fusion devices
[DE90-011097] N91-16765
Neutron measurements in search of cold fusion
[DE91-004855] N91-16778
NUCLEAR INTERACTIONS
Hyperfine interactions associated with iron substituted superconducting oxides
[DE90-010411] N91-16783
NUCLEAR MAGNETIC RESONANCE
Development of nondestructive evaluation methods and prediction of effects of flaws on the fracture behavior of structural ceramics
[DE90-011092] N91-16141
Comparison of hydrogen diffusion in Ti2PdH(x) to the behavior for Ti2CuH(x) and Zr2PdH(x)
[DE91-002711] N91-16808
NUCLEAR MEDICINE
Application of AMS to the biomedical sciences
[DE90-010869] N91-16538
NUCLEAR PHYSICS
Research in theoretical nuclear physics
[DE90-010792] N91-16828
NUCLEAR REACTIONS
Galaxy interactions and the stimulation of nuclear activity N91-16910
Tidal events and galactic activity N91-16911
Central activity in 60 micron peakers N91-16913
Galaxy interactions and strength of nuclear activity N91-16914
Nuclear and extended infrared emission in paired and isolated galaxies N91-16917
Induced starburst and nuclear activity: Faith, facts, and theory N91-16953
NUCLEAR RESEARCH
Production of high intensity radioactive beams
[DE90-011340] N91-16735
NUCLEAR STRUCTURE
Properties of superdeformed bands in the A = 194 region
[DE90-011482] N91-16798
NUCLEATION
Void nucleation in nonlinear solid mechanics
[AD-A228890] N91-16410
NUMERICAL ANALYSIS
Asymptotic-induced numerical methods for conservation laws
[NASA-CR-187483] N91-16305
Sparse representation of smooth linear operators
[AD-A228142] N91-16660
NUMERICAL CONTROL
An algorithm for using a slide-screw tuner as a computer-controlled impedance
[DE90-010657] N91-16226
Sensing of metal-transfer mode for process control of GMAW (Gas Metal Arc Welding)
[DE90-010946] N91-16377
NUMERICAL INTEGRATION
Homogeneously broadened bidirectional ring laser: Theoretical analysis, numerical simulation, and experiment in helium-xenon N91-16360
NUMERICAL STABILITY
Matrix algorithms in signal processing
[AD-A228851] N91-16625
NUMERICAL WEATHER FORECASTING
GCM (General Circulation Model) predictions for surface air temperature and precipitation over the southeastern United States
[DE90-009434] N91-16497
NASA/MSFC FY90 Global Scale Atmospheric Processes Research Program Review
[NASA-CP-3093] N91-16500
Observation simulation experiments with regional prediction models N91-16502
Research on diabatic initialization N91-16504
NUTATION
The effects of the solid inner core and nonhydrostatic structure on the Earth's forced nutations and Earth tides N91-16417

O

O STARS
A non-LTE analysis of a sample of O stars selected from galactic OB associations N91-16854
Galactic structure in direction of Vela-Puppis by means of UBV beta observations
[ETN-91-98556] N91-16973
OBJECT PROGRAMS
Introduction to aspects of object oriented graphics
[CWI-CS-R9009] N91-16597
OBSERVATORIES
The design and construction of an Automated Multi-Object Spectroscopy system (AMOS)
[DE90-011497] N91-16088
OCEAN BOTTOM
Analysis of satellite and Expendable Bathythermograph (XBT) data for the abrupt topography program
[AD-A228870] N91-16422
Seismic structure of the upper mantle under the Pacific Ocean N91-16492
OCEAN CURRENTS
The high speed buffer board: A SAIL EIA-485 communications accelerator card for the vector measuring current meter
[AD-A227181] N91-16185
OCEAN DATA ACQUISITIONS SYSTEMS
Contents of the NASA ocean data system archive, version 11-90
[NASA-CR-187812] N91-16535
Data base structure to support the production of the digital bathymetric data base
[AD-A227915] N91-16841
OCEAN DYNAMICS
The high speed buffer board: A SAIL EIA-485 communications accelerator card for the vector measuring current meter
[AD-A227181] N91-16185
Analysis and application of the discrete vortex method N91-16290
OCEAN SURFACE
Analysis of satellite and Expendable Bathythermograph (XBT) data for the abrupt topography program
[AD-A228870] N91-16422
Global variability of water vapor and condensate from SSM/I N91-16507
Tropical Pacific moisture variability N91-16509
Synoptic/planetary-scale interactions and blocking over the North Atlantic Ocean N91-16513
The vertical structure of the marine atmospheric boundary layer across a sea surface temperature front
[AD-A227931] N91-16525
Fourth moments of acoustic waves forward scattered by a rough ocean surface
[AD-A227469] N91-16529
Formic and acetic acids in the boundary layer over the North Atlantic ocean N91-16530
Contents of the NASA ocean data system archive, version 11-90
[NASA-CR-187812] N91-16535
OCEAN TEMPERATURE
The high speed buffer board: A SAIL EIA-485 communications accelerator card for the vector measuring current meter
[AD-A227181] N91-16185
OCEANOGRAPHY
Bio-optical profile data report coastal transition zone program, R/V Thomas Washington, June 24 - July 21, 1988
[NASA-CR-187806] N91-16532
Bio-optical profile data report coastal transition zone program, R/V Point Sur, June 15-28, 1987
[NASA-CR-187807] N91-16533
Bio-optical profile data report: Joint Global Ocean Flux Study, Hawaii Ocean Time-Series, HOT-3, R/V Moana Wave, 6-10 January 1989
[NASA-CR-187805] N91-16534
Contents of the NASA ocean data system archive, version 11-90
[NASA-CR-187812] N91-16535
OCEANS
Tropical Pacific moisture variability N91-16509
The effect of latent heat release on synoptic-to-planetary wave interactions and its implication for satellite observations: Theoretical modeling N91-16514
Bio-optical profile data report: Joint Global Ocean Flux Study, Hawaii Ocean Time-Series, HOT-3, R/V Moana Wave, 6-10 January 1989
[NASA-CR-187805] N91-16534
Contents of the NASA ocean data system archive, version 11-90
[NASA-CR-187812] N91-16535
OLFACTORY PERCEPTION
Electronic analogue for a biological nose
[ME-78] N91-16541
OPACITY
Investigation and modeling of radiation absorption processes and opacities in dense plasmas
[AD-A228749] N91-16779
OPERATING SYSTEMS (COMPUTERS)
National software capacity: Near-term study executive summary
[AD-A227564] N91-16590
Scheduler issues for real-time Ada
[AD-A227766] N91-16592
Decentralized real-time scheduling
[AD-A227856] N91-16604
The StarLite project
[AD-A226722] N91-16837
OPERATING TEMPERATURE
Status of Argonne life evaluation of valve regulated lead-acid batteries
[DE90-011098] N91-16229
OPERATORS (MATHEMATICS)
Massively parallel Fokker-Planck calculations
[DE90-010691] N91-16633
OPTICAL COMMUNICATION
A low-cost infrared telemetry system for kilohertz-bandwidth data acquisition
[DE90-010616] N91-16042
The 1/f frequency noise effects on self-heterodyne linewidth measurements for coherent communications
[AD-A227942] N91-16195
Fiber optic synthetic aperture interferometer
[AD-A227891] N91-16741
Applications of non-linear optics
[AD-A228872] N91-16743
Optical transceiver frontend for high speed bus STANAG 3910 with one fiber only
[MBB-UA-1182-90-PUB] N91-16745
IEEE International Symposium on Information Theory
[AD-A228239] N91-16842
OPTICAL COMPUTERS
Research in optical symbolic tasks
[AD-A228797] N91-16551
OPTICAL CORRELATORS
The design of a two-dimensional optical image correlator and its application in image tracking N91-16744
OPTICAL DATA PROCESSING
Research in optical symbolic tasks
[AD-A228797] N91-16551
OPTICAL DISKS
Radio line and continuum observations of quasar-galaxy pairs and the origin of low reshift quasar absorption line systems N91-16925
OPTICAL EQUIPMENT
A convenient system for the manufacture of holographic diffraction gratings
[DE90-009481] N91-16319
Chemical beam epitaxy of ZnSe
[AD-A228045] N91-16817
OPTICAL FIBERS
Tests for integrating measurements of gas pressures in aircraft mechanisms
[ETN-91-98558] N91-16014
Advanced structural instrumentation, volume 2
[AD-A227473] N91-16330
Optical transceiver frontend for high speed bus STANAG 3910 with one fiber only
[MBB-UA-1182-90-PUB] N91-16745

OPTICAL HETERODYNING
A ring laser gyroscope with optical subtraction N91-16335
OPTICAL MEASUREMENT
Stability and accuracy of the sweep rate measurements for LLNL optical streak cameras [DE90-012080] N91-16324
OPTICAL PROPERTIES
Joint services electronics program [AD-A227576] N91-16237
High-efficiency large-area CdTe panels [DE91-002117] N91-16443
Bio-optical profile data report coastal transition zone program, R/V Thomas Washington, June 24 - July 21, 1988 [NASA-CR-187808] N91-16532
Bio-optical profile data report coastal transition zone program, R/V Point Sur, June 15-28, 1987 [NASA-CR-187807] N91-16533
A homogeneous sample of binary galaxies: Basic observational properties N91-16659
OPTICAL RADAR
Definition and preliminary design of the Laser Atmospheric Wind Sounder (LAWS) phase 1. Volume 1: Executive summary [NASA-CR-184071] N91-16332
Definition and preliminary design of the Laser Atmospheric Wind Sounder (LAWS) phase 1. Volume 2 [NASA-CR-184072] N91-16333
Definition and preliminary design of the Laser Atmospheric Wind Sounder (LAWS) phase 1. Volume 3: Program cost estimates [NASA-CR-184073] N91-16334
The Cabannes-lidar for the examination of the stratosphere: Selected design elements for the experimental construction [BONN-IR-90-39] N91-16493
OPTICAL TRACKING
The design of a two-dimensional optical image correlator and its application in image tracking N91-16744
OPTICAL WAVEGUIDES
Integrated semiconductor modulators [AD-A228615] N91-16820
OPTIMAL CONTROL
Optimization and guidance of flight trajectories for the national aerospace plane [NASA-CR-187837] N91-16010
Optimal trajectories for an aerospace plane. Part 2: Data, tables, and graphs [NASA-CR-187848] N91-16011
Aeroservoelastic tailoring for lateral control enhancement N91-16025
A decentralized linear quadratic control design method for flexible structures [NASA-CR-187860] N91-16059
Optimal rocket motor design and control for tactical missiles N91-16062
Modeling and control of a two-arm elastic robot in gravity N91-16389
Identification of non-linear mechanical systems for control application [ISBN-90-9003596-6] N91-16644
OPTIMIZATION
Optimal trajectories for an aerospace plane. Part 1: Formulation, results, and analysis [NASA-CR-187868] N91-16013
The integration of structural optimization in the general design process for aircraft [MBB/FE122/S/PUB/0405] N91-16017
Electrolyte optimization and electrode material evaluation for the vanadium redox battery N91-16234
Optimization of a laser diode anemometry system [LSTM-239/T/88] N91-16364
Multi-criteria position and configuration optimization for redundant platform/manipulator systems [DE90-010705] N91-16372
Optimal positioning of redundant manipulator-platform systems for maximum task efficiency [DE90-011061] N91-16378
Adaptive mesh refinement for meshes with singular elements N91-16406
High efficiency silicon concentrator solar cells N91-16441
Optimization of a power transient stability program on a vector supercomputer: Theory and applications [AD-A227884] N91-16607
Alopex optimization algorithm [AD-A228442] N91-16615
THERMOPT: An optimizer for ESATAN models [MBB/FW522/S/PUB/427] N91-16630
Identification of non-linear mechanical systems for control application [ISBN-90-9003596-6] N91-16644
A sign-changing global minimizer on a convex domain [REPT-90-57] N91-16655
Analysis of multivariable control systems in the presence of structured uncertainties [AD-A227976] N91-16665
A non-LTE analysis of a sample of O stars selected from galactic OB associations N91-16854
ORBIT CALCULATION
Geopotential harmonics of order 15 and 30 from analysis of 50 orbit determinations of 1967-102B [RAE-TR-90029] N91-16035
ORBIT DECAY
Dynamical friction in pairs of elliptical galaxies N91-16933
ORBITAL MANEUVERS
Determination of shuttle orbiter center of gravity from flight measurements [NASA-TM-102627] N91-16058
ORBITAL MECHANICS
Geopotential harmonics of order 15 and 30 from analysis of 50 orbit determinations of 1967-102B [RAE-TR-90029] N91-16035
ORBITS
Stellar kinematics of elliptical galaxies in pairs N91-16862
On leading spiral arms in close pairs of galaxies N91-16935
M51's spiral structure N91-16938
ORGANIC COMPOUNDS
Determination of airborne organics by direct sampling mass spectrometry [DE90-009422] N91-16452
Electron stopping powers of some elements and compounds from 0 to 10,000 eV: A compilation [DE90-010675] N91-16716
ORGANIZATIONS
Environmental uncertainty, planning and organizational performance N91-16464
Calendar of selected aeronautical and space meetings: January 1991 onwards [AGARD-CAL-91/1] N91-16833
Activities report of the Space Research Organization Netherlands [ETN-91-98473] N91-16848
ORGANIZING
Organization of the mission pattern in the air picture [IZF-1990-A-12] N91-16568
ORGANOMETALLIC COMPOUNDS
Molecular orbital studies of the bonding in heavy element organometallics [DE90-009732] N91-16711
ORTHOGONAL FUNCTIONS
Matrix algorithms in signal processing [AD-A228851] N91-16625
OSCILLATING FLOW
On the receptivity and non-parallel stability of travelling disturbances in rotating disk flow [NASA-CR-187486] N91-15996
OSCILLATIONS
The magnetospheric response to 8-minute period strong-amplitude upstream pressure variations [AD-A228038] N91-16489
South Pacific convergence zone and global-scale circulations N91-16503
Viral coefficient and hidden mass in the galaxy groups N91-16950
OXIDATION
The oxidation behavior of carbon-carbon composites and their coatings N91-16074
Destruction of propellant components in supercritical water [DE90-010600] N91-16085
Conversion of acetic acid to methane by thermophiles [DE90-010993] N91-16086
The influence of small SO2 contents on the corrosion behavior for NiCrAl alloys in temperature zone from 1000 to 1100 C [JUEL-2362] N91-16134
Initial studies of electric field effects on ceramic powder formation in flames [DE90-007571] N91-16138
OXIDATION RESISTANCE
High temperature oxidation-resistant thruster research [NASA-CR-185233] N91-16063
The oxidation behavior of carbon-carbon composites and their coatings N91-16074
OXIDATION-REDUCTION REACTIONS
Electrocatalysis of anodic and cathodic oxygen-transfer reactions [DE91-000611] N91-16100
Polymers at liquid-liquid interfaces: Photophysics and photoredox chemistry [DE91-005032] N91-16151
Electronic and ionic transport in processable conducting polymers [AD-A227857] N91-16154
OXIDE FILMS
Electron microscopy and electrochemistry of nickel oxide films for electrochromic devices produced by different techniques [DE90-011596] N91-16142
OXYGEN
A miniature inexpensive, oxygen sensing element [DE90-009938] N91-16318
Technical and economic evaluation of diesel engine with oxygen enrichment and water injection [DE90-009723] N91-16373
Thermal desorption studies of isotopically-labeled oxygen-induced superconductivity in La2CuO(4+delta) [DE91-004898] N91-16812
OXYGEN ANALYZERS
A miniature inexpensive, oxygen sensing element [DE90-009938] N91-16318
OXYGEN ATOMS
A comparison of optically measured and radar-derived horizontal neutral winds [AD-A227690] N91-16483
OXYGEN CONSUMPTION
Cerebral oxygen status and G-induced loss of consciousness N91-16554
OXYGENATION
CRC volatility program on the effect of oxygenated fuels and altitude on cold-start drivability at low ambient temperatures [AD-A227571] N91-16171
OZONE
Ozone and acid-precipitation on western coniferous forests [DE90-011014] N91-16462
The atmospheric effects of stratospheric aircraft: A topical review [NASA-RP-1250] N91-16466
The atmospheric effects of stratospheric aircraft: A current consensus [NASA-RP-1251] N91-16467
Use of satellite data and modeling to assess the influence of stratospheric processes on the troposphere N91-16517

P

P WAVES
Excursions to the base of the mantle N91-16491
P-I-N JUNCTIONS
Measurements of 1/f noise in a-Si:H pin diodes and thin-film-transistors [DE90-011218] N91-16228
Performance measurements of hybrid PIN diode arrays [DE90-010308] N91-16790
PACIFIC OCEAN
Seismic structure of the upper mantle under the Pacific Ocean N91-16492
Tropical Pacific moisture variability N91-16509
PACKET SWITCHING
Meteor burst communications study [AD-A228641] N91-16204
PANEL METHOD (FLUID DYNAMICS)
Propfan supersonic panel method analysis and flutter predictions N91-15993
User's guide to PANCOR: A panel method program for interference assessment in slotted-wall wind tunnels [NASA-CR-187479] N91-16033
Numerical simulation of separated flows around a wing section at steady and unsteady motion by a discrete vortex method N91-16268
PANELS
Bump examinations of integrally strengthened carbon fiber reinforced plastic panels [MBB/FE281/CFK/PUB/0013] N91-16076
High-efficiency large-area CdTe panels [DE91-002117] N91-16443
PARABOLIC DIFFERENTIAL EQUATIONS
Wave propagation through random media: A local method of small perturbations based on the Helmholtz equation N91-16701
PARABOLIC REFLECTORS
A planar near-field scanning technique for bistatic radar cross section measurements [NASA-CR-187794] N91-16194
PARALLEL COMPUTERS
Analysis of parallel, replicated simulations under a completion time constraint [AD-A228292] N91-16613
Wakefield calculations on parallel computers [DE90-009712] N91-16632
PARALLEL PROCESSING (COMPUTERS)
Microsupercomputers: Design and implementation [AD-A228741] N91-16571
POSC: A Partitioning and Optimizing SISAL Compiler [DE90-010679] N91-16577

Expressing user-defined parallelism in EPL (Equational Programming Language)
[AD-A227875] N91-16606
Analysis of parallel, replicated simulations under a completion time constraint
[AD-A228292] N91-16613
An O(log n) time common CRCW pram algorithm for minimum spanning tree
[AD-A228740] N91-16623
Vectorial and parallel algorithms in dynamic programming for optimal control problems
[LAAS-90256] N91-16629
Parallel Access Main Memory (PAMM) user's manual, version 1.0
[AD-A227744] N91-16635
Experiments with initial transient deletion for parallel, replicated steady-state simulations
[AD-A227879] N91-16636
Linear algebra for dense matrices on a hypercube
[DE90-010533] N91-16647

PARALLEL PROGRAMMING
Simulation of the flow past an impulsively started cylinder using a discrete vortex method N91-16303
Microsupercomputers: Design and implementation
[AD-A228744] N91-16572
Massively parallel Fokker-Planck calculations
[DE90-010691] N91-16633
Pi: A parallel architecture interface for multi-model execution
[AD-A228345] N91-16640

PARAMETER IDENTIFICATION
Identification of non-linear mechanical systems for control application
[ISBN-90-9003596-6] N91-16644

PARAMETERIZATION
Impacts of advanced manufacturing technology on parametric estimating
[AD-A228232] N91-16177
Parameterization of aerosol scavenging in a convective cloud model
[DE90-010865] N91-16458
A study of the interaction of physical and numerical parameterizations with regard to moisture forecasting in a regional model of the atmosphere
[AD-A227966] N91-16488
Planetary circulations in the presence of transient and self-induced heating N91-16505

PARITY
Parity violation and electron scattering
[DE90-010429] N91-16712

PARSING ALGORITHMS
PENGUIN: A language for reactive graphical user interfaces
[AD-A228580] N91-16620

PARTIAL DIFFERENTIAL EQUATIONS
Acceleration of iterative algorithms for Euler and Navier-Stokes equations N91-16301
Stellar convection and dynamo theory N91-16857

PARTIAL PRESSURE
Microwave measurements of water vapor partial pressure at temperatures up to 350 C
[DE90-011484] N91-16087

PARTICLE ACCELERATOR TARGETS
Production of high intensity radioactive beams
[DE90-011340] N91-16735

PARTICLE ACCELERATORS
Ion contamination of x ray pinhole camera images on PBFA 2
[DE90-012180] N91-16325
Development of an external beam ion milliprobe
[AD-A227247] N91-16329
Production of high intensity radioactive beams
[DE90-011340] N91-16735

PARTICLE BEAMS
Some nonlinear problems in the manipulation of beams
[DE91-005211] N91-16358
Advanced methods for the computation of particle beam transport and the computation of electromagnetic fields and beam-cavity interactions
[DE90-011071] N91-16734

PARTICLE COLLISIONS
Some nonlinear problems in the manipulation of beams
[DE91-005211] N91-16358

PARTICLE EMISSION
Development of an external beam ion milliprobe
[AD-A227247] N91-16329
Upper atmosphere IR radiation modeling and analysis
[AD-A227214] N91-16482

PARTICLE INTERACTIONS
Upper atmosphere IR radiation modeling and analysis
[AD-A227214] N91-16482
Production of high intensity radioactive beams
[DE90-011340] N91-16735

PARTICLE PRODUCTION
V(sup 0) production with 14.5 GeV/c silicon beams
[DE90-010014] N91-16747

PARTICLE SIZE DISTRIBUTION
The effect of stratification on gravitational coagulation and settling of aerosols
[DE90-010153] N91-16079
The effect of charge mixture ratio and particle size on igniter plume heat transfer characteristics
[DE90-010833] N91-16160
Research on certain aspects of laser diffraction particle size analysis relevant to autonomous self-diagnosing instrumentation
[AD-A226822] N91-16354

PARTICLE THEORY
Theoretical topics in B-physics
[DE91-004911] N91-16726

PARTICLE TRACKS
AGS silicon gold collisions measured in the E-810 TPC (Time Projection Chamber)
[DE90-010015] N91-16733

PARTICLES
Shear thickening of concentrated dispersions
[ETN-91-98477] N91-16308

PASTES
Paste extrudable explosives: Their history and their current status
[DE90-009438] N91-16159
Whole body cleansing agent
[NASA-CASE-MSC-21589-1] N91-16566

PATHOLOGY
Research pathology and special techniques
[NASA-CR-187828] N91-16639

PATTERN RECOGNITION
Characterization of ultrasonic transducers using pattern recognition techniques
[DE91-000580] N91-16326
Organization of the mission pattern in the air picture
[IZF-1990-A-12] N91-16568
Alopex optimization algorithm
[AD-A228442] N91-16615
IEEE International Symposium on Information Theory
[AD-A228239] N91-16842

PAVEMENTS
Evaluation procedure for reinforced concrete box culverts under airfield pavements
[AD-A227920] N91-16031

PAYLOAD INTEGRATION PLAN
Space Station Freedom resource allocation accommodation of technology payload requirements
[NASA-TM-102766] N91-16832

PAYLOADS
Sensor-based automated docking of large payloads
[DE90-011020] N91-16044

PECULIAR GALAXIES
Multi-color imaging of selected southern interacting galaxies N91-16867
The environments of Markarian galaxies N91-16881
New data on the peculiar galaxy MRK 273 N91-16887
H I observations of the peculiar galaxy NGC 660 N91-16888
The polar-ring galaxies NGC 2685 and NGC 3808B (VV 300) N91-16892
Radio emission in peculiar galaxies N91-16907
The kinematics and morphology of NGC 520: One, two, or three galaxies N91-16908

PEEK
TF89 tactical fighter outer wing design
[ETN-91-98580] N91-16019

PENETRATION
Finite element solution of steady state axisymmetric penetration problems N91-16403

PENNING DISCHARGE
Spatial distributions of the emitting species in a penning surface-plasma source
[DE90-011996] N91-16772

PERCOLATION
From low to high Tc: An ultrasonic investigation of niobium single crystal and YBaCuO superconducting thin films with surface acoustic waves N91-16822

PERFORMANCE PREDICTION
Jet engine performance estimation from minimal input data
[ETN-91-98582] N91-16023
Towards conservative reliability predictions for real-time software
[NASA-CR-187863] N91-16627

PERFORMANCE TESTS
Advanced Turbine Technology Applications Project (ATTAP)
[NASA-CR-187039] N91-16021
The effect of charge mixture ratio and particle size on igniter plume heat transfer characteristics
[DE90-010833] N91-16160
CRC volatility program on the effect of oxygenated fuels and altitude on cold-start drivability at low ambient temperatures
[AD-A227571] N91-16171
Numerical simulation of the comparative electrical performance of the permeable base transistor, opposed gate-source transistor and heterostructure launched ballistic field effect transistor
[AD-A228545] N91-16202
Laboratory testing of chloride 3ET205 6 volt traction battery
[DE90-010926] N91-16225
Aerosol cloud generation experiments
[DE90-011051] N91-16264
Development of a versatile laser light scattering instrument
[NASA-CR-182474] N91-16350
The role of quality assurance in the monitoring of terrestrial ecosystems
[DE90-010986] N91-16461
Validity study in multidimensional latent space and efficient computerized adaptive testing
[AD-A227742] N91-16650
Design and testing of a proton detector
[BONN-IR-90-34] N91-16729
Testing of lead glass detectors for electron proof in the ELAN experiment
[BONN-IR-90-38] N91-16730

PERIODIC FUNCTIONS
The use of window functions and Kalman filtering in spectral estimation
[AD-A227482] N91-16236
Periodic solutions of neutral differential equations
[RR-390] N91-16658

PERIODIC VARIATIONS
Electron density comparisons between radar observations and 3-D ionospheric model calculations
[AD-A227703] N91-16187
Origin of regularities in the redshift distributions of distant galaxies and quasars
[DE91-004848] N91-16968

PERSONAL COMPUTERS
Smoothing and scaling airfoil coordinates on a personal computer
[DE89-000878] N91-16582
PC-based digital imaging for storing microscopy images for surveillance programs
[DE90-010080] N91-16738

PERSONNEL SELECTION
A normative database for, and analysis of, the dual task of the TASKOMAT
[IZF-1990-A-11] N91-16846

PERTURBATION
Asymptotic-induced numerical methods for conservation laws
[NASA-CR-187483] N91-16305
The effects of the solid inner core and nonhydrostatic structure on the Earth's forced nutations and Earth tides N91-16417
Wave propagation through random media: A local method of small perturbations based on the Helmholtz equation N91-16701
Characterization of disruptions in the Microwave Tokamak Experiment (MTX)
[DE90-010352] N91-16761
Simulations of gas clouds in interacting galaxies N91-16961
Graviton effects in vacuum maximally symmetric spaces N91-16971

PERTURBATION THEORY
Pathwise convexity and its relation to convergence of time-average derivatives
[AD-A228888] N91-16662
A new perturbation theory of solids and fluids and its applications to high-pressure melting problems
[DE90-011502] N91-16829
The best-fit universe
[DE91-004583] N91-16966

PETRI NETS
Modeling and verification of distributed systems with labeled predicate transition nets
[LAAS-90215] N91-16214
Towards conservative reliability predictions for real-time software
[NASA-CR-187863] N91-16627
Implementation and simulation of the manufacturing systems control coordination level: A mixed approach of Petri nets and rule-based systems
[LAAS-90355] N91-16645
About Petri nets with fuzzy markings
[LAAS-90354] N91-16670

PHASE ERROR
Implementation of the phase gradient algorithm
[DE90-012160] N91-16579

PHASE LOCK DEMODULATORS
Measurement of the capture effect of frequency modulation
[AD-A228058] N91-16199
PHASE TRANSFORMATIONS
Phase selection and processing of high temperature intermetallic alloys
[AD-A227910] N91-16129
Heat transfer from water flowing through a chilled-bed open channel
[AD-A226855] N91-16286
The role of ledges in phase transformations
[AD-A228750] N91-16821
PHASE VELOCITY
Canonical eigenvalues. Part 2: Application to one-layer, bounded, underwater acoustic ducts
[AD-A227451] N91-16677
PHASED ARRAYS
Seismic signal processing optimized for a specific source and receiver
[DE90-010189] N91-16468
A case study of the 19 October 1989 polar cap absorption event using the imaging riometer for ionospheric studies
[AD-A227764] N91-16487
Phased array imaging
[AD-A228774] N91-16855
PHENOMENOLOGY
Dynamical properties of two-dimensional Josephson junction arrays N91-16823
FIR statistics of paired galaxies N91-16899
PHOSPHATES
Synthesis, characterization and catalytic activity of microporous aluminophosphate catalysts N91-16092
PHOSPHORIC ACID FUEL CELLS
Improved anode catalysts for coal gas-fueled phosphoric acid fuel cells
[DE90-009683] N91-16442
PHOSPHORUS COMPOUNDS
Comparative study of phosphosilicate glass on (100) silicon by furnace and rapid isothermal annealing
[NIAR-90-26] N91-16153
PHOTOCHEMICAL REACTIONS
Ultrasensitive molecular fluorescence spectroscopy in levitated microdroplets
[DE91-000621] N91-16095
Photoinduced charge separation by polymer-bound chromophores
[DE90-010997] N91-16140
Polymers at liquid-liquid interfaces: Photophysics and photoredox chemistry
[DE91-005032] N91-16151
Formic and acetic acids in the boundary layer over the North Atlantic ocean N91-16530
PHOTOCONDUCTIVITY
Multiframe x ray images from a single meander stripline coated on a microchannel plate
[DE90-010741] N91-16224
Microwave-detected photoconductance decay
[DE90-011505] N91-16795
PHOTOELECTRIC EMISSION
A photoemission study of samarium on silicon
[DE90-011509] N91-16799
PHOTOELECTRICITY
Timing margin measurement using a laser technique
[AD-A226821] N91-16353
PHOTOGRAMMETRY
Reports on cartography and topography. Series 1, report 104
[ISSN-0469-4236] N91-16432
The photogrammetric evaluation by video technique: A supporting study N91-16433
PHOTOGRAPHIC PLATES
Gabor zone plate apertures for imaging with the mercuric iodide gamma ray camera
[DE90-011193] N91-16321
PHOTOGRAPHS
Jet engine performance estimation from minimal input data
[ETN-91-98582] N91-16023
PHOTOGRAPHY
PC-based digital imaging for storing microscopy images for surveillance programs
[DE90-010080] N91-16738
PHOTOINTERPRETATION
Debris/Ice/TPS assessment and photographic analysis for shuttle mission STS-41
[NASA-TM-103814] N91-16041
PHOTOIONIZATION
Application of diode lasers to resonance ionization mass spectrometry
[DE91-000614] N91-16094
Picosecond multiphoton ionization of atomic and molecular clusters
[DE91-000641] N91-16096
Cluster formation in laser-induced ablation and evaporation of solids observed by laser ionization time-of-flight mass spectrometry and scanning tunneling microscopy
[DE90-010876] N91-16344
PHOTOLITHOGRAPHY
Development of free-electron lasers for XUV projection lithography
[DE90-010566] N91-16342
Dynamical properties of two-dimensional Josephson junction arrays N91-16823
PHOTOLYSIS
Direct observation of NF(X) using laser-induced fluorescence: Kinetics of the NF 3 Sigma - ground state
[AD-A228294] N91-16362
PHOTOMETRY
An atlas of mixed-morphology pairs N91-16866
Multi-color imaging of selected southern interacting galaxies N91-16867
A multiwavelength survey of interacting galaxies N91-16898
Observations and models of star formation in the tidal features of interacting galaxies N91-16957
Photometric analyses for the determination of physical and structural properties for the Martian surface in the Oxia Palus region
[DLR-FB-90-27] N91-16979
PHOTON-ELECTRON INTERACTION
Resonant Compton scattering in models of gamma-ray burst sources. Part 2: Numerical modeling
[DE91-005268] N91-16982
PHOTONS
Comparison of some x ray sensors for verification
[DE90-011990] N91-16323
Multiple-photon Compton scattering in a strong magnetic field: Cross-sections and radiative transport N91-16852
A tentative explanation of cosmological red shift N91-16928
PHOTOSYNTHESIS
Carbon dioxide and energy exchanges in a temperate grassland ecosystem N91-16419
Biomass and hydrocarb technology for removal of atmospheric CO2
[DE90-010016] N91-16453
PHOTOVOLTAIC CELLS
High-efficiency large-area CdTe panels
[DE91-002117] N91-16443
PHYSICAL CHEMISTRY
Linear algebra for dense matrices on a hypercube
[DE90-010533] N91-16647
Highlights of the Chemical Technology (CMT) Division's activities
[DE90-008242] N91-16984
PHYSIOLOGICAL EFFECTS
Gallium as a unique anti-resorptive agent in bone: Preclinical studies on its mechanisms of action
[DE90-010650] N91-16542
PHYSIOLOGICAL FACTORS
Detection of loss of consciousness in flight by Doppler method N91-16555
PHYSIOLOGICAL RESPONSES
Changes in somatosensory responsiveness in behaving monkeys
[AD-A226832] N91-16540
PHYSIOLOGY
Conversion of acetic acid to methane by thermophiles
[DE90-010993] N91-16086
PICOSECOND PULSES
Picosecond multiphoton ionization of atomic and molecular clusters
[DE91-000641] N91-16096
PILOT PERFORMANCE
Safety Network to Detect Performance Degradation and Pilot Incapacitation
[AGARD-CP-490] N91-16553
A comparison of computerized measurement of helicopter pilot performance with atropine sulfate during actual and simulated flight N91-16558
EEG indicators of mental workload: Conceptual and practical issues in the development of a measurement tool N91-16559
Study of pilot vigilance during long range flight N91-16561
Computer aided physiological assessment of the functional state of pilots during simulated flight N91-16562
Development of a test-bed for real-time monitoring of pilot mental status N91-16563
Intelligent assistant systems: An artificial intelligence approach to detecting performance degradation and pilot incapacitation N91-16564
PILOT TRAINING
Current status of an artificial intelligence-based loss of consciousness monitoring system for advanced fighter aircraft N91-16556
PINHOLE CAMERAS
Ion contamination of x ray pinhole camera images on PBFA 2
[DE90-012180] N91-16325
PIPE FLOW
Transient natural convection in heated inclined tubes
[DE90-008217] N91-16255
Numerical simulation of pulsatile flows passing through a pipe with sudden expansion N91-16271
Numerical simulation of a complicated transition-breakdown of vortical flows inside a circular pipe N91-16273
PIPES (TUBES)
A method for pressure-pulse suppression in fluid-filled piping
[DE90-010408] N91-16260
The Proceedings of the Symposium on Mechanics for Space Flight 1989
[ISAS-SP-12] N91-16266
Numerical simulation of pulsatile flows passing through a pipe with sudden expansion N91-16271
Development of a two-phase cold plate N91-16277
Experimental study on mercury heat pipes (on effect of screen mesh wick under bottom heat mode) N91-16280
PITCH (INCLINATION)
A statistical survey of electron pitch angle distributions in the nightside central plasma sheet
[AD-A227763] N91-16486
PITCHING MOMENTS
Numerical simulation of separated flows around a wing section at steady and unsteady motion by a discrete vortex method N91-16268
PITTING
Failure analysis of a main rotor pitch horn bolt located on the AH-1 Cobra helicopter
[AD-A227679] N91-16007
Characterization of the corrosion of a P-130x graphite fiber reinforced 6063 aluminum metal matrix composite
[AD-A228134] N91-16071
PIXELS
Automatic, high-resolution analysis of low-noise fringes
[DE90-009779] N91-16574
Displaying alphanumeric characters on pixel-planes 5
[AD-A228616] N91-16622
PLANE STRESS
Dynamic crack propagation in elastic-plastic solids N91-16402
PLANE WAVES
On the propagation of plane waves above an impedance surface N91-16684
SCATSPHERE2: A computation for the plane-wave scattering from a submerged, elastic, spherical, evacuated or fluid-filled, thin shell
[AD-A228867] N91-16709
PLANETARY COMPOSITION
Photometric analyses for the determination of physical and structural properties for the Martian surface in the Oxia Palus region
[DLR-FB-90-27] N91-16979
PLANETARY WAVES
On the developmental dynamics of sudden stratospheric warmings
[AD-A227731] N91-16485
Nonlinear dynamics of global atmospheric and Earth-system processes N91-16510
The effect of latent heat release on synoptic-to-planetary wave interactions and its implication for satellite observations: Theoretical modeling N91-16514
The effect of latent heat release on synoptic-to-planetary scale wave interactions and implications for satellite observations: Observational study N91-16515
Use of satellite data and modeling to assess the influence of stratospheric processes on the troposphere N91-16517
A global climatology of middle atmosphere inertio-gravity waves N91-16524
PLANNING
Environmental uncertainty, planning and organizational performance N91-16464
Implementation and experimentation with motion planning algorithms
[AD-A228278] N91-16612
Report to Congress on the Small Business Program
[DE91-004622] N91-16831
Using computer-generated protocols to study writers' planning strategies
[AD-A228875] N91-16844
PLANT DESIGN
Production of high intensity radioactive beams
[DE90-011340] N91-16735
PLASMA CLOUDS
Radio line and continuum observations of quasar-galaxy pairs and the origin of low reshift quasar absorption line systems N91-16925

PLASMA CONTROL
Scaling dimensionally similar tokamak discharges to ignition
[DE90-010079] N91-16749
D3-D research operations
[DE90-008232] N91-16752
Plasma-facing materials
[DE90-008243] N91-16753
US-Japan Workshop on Field-Reversed Configurations with Steady-State High-Temperature Fusion Plasmas and the 11th US-Japan Workshop on Compact Toroids
[DE90-010253] N91-16755
The Madison symmetric torus
[DE90-010306] N91-16757
Microwave Tokamak Experiment (OMTX): Overview and status
[DE90-010287] N91-16758
Electromagnetic computations for fusion devices
[DE90-011097] N91-16765
The CIT physics program
[DE90-012134] N91-16774

PLASMA CURRENTS
Electromagnetic computations for fusion devices
[DE90-011097] N91-16765
The Los Alamos megamp fiber z-pinch experiment
[DE91-004842] N91-16777

PLASMA DENSITY
Computer simulations of medium wavelength irregularities in the equatorial ionosphere resulting from artificially produced density enhancements
[MPE-PREPRINT-186] N91-16496
The Los Alamos megamp fiber z-pinch experiment
[DE91-004842] N91-16777

PLASMA DIAGNOSTICS
A Mirnov loop array for field-reversed configurations
[DE90-010607] N91-16750
D3-D research operations
[DE90-008232] N91-16752
The Madison symmetric torus
[DE90-010306] N91-16757
Characterization of disruptions in the Microwave Tokamak Experiment (MTX)
[DE90-010352] N91-16761
Texas experimental tokamak
[DE90-011070] N91-16762
Stark-effect measurement of high FEL electric fields in MTX by laser-aided particle-probe spectroscopy
[DE90-011911] N91-16771
Motional Stark effect polarimetry for the current profile diagnostic in D3-D
[DE90-012071] N91-16773
The CIT physics program
[DE90-012134] N91-16774

PLASMA DIFFUSION
A statistical survey of electron pitch angle distributions in the nightside central plasma sheet
[AD-A227763] N91-16486
Scaling dimensionally similar tokamak discharges to ignition
[DE90-010079] N91-16749

PLASMA DRIFT
Theory for modeling the equatorial evening ionosphere and the origin of the shear in the horizontal plasma flow
[MPE-PREPRINT-185] N91-16495

PLASMA DYNAMICS
The CIT physics program
[DE90-012134] N91-16774

PLASMA HEATING
Scaling dimensionally similar tokamak discharges to ignition
[DE90-010079] N91-16749
Microwave Tokamak Experiment (OMTX): Overview and status
[DE90-010287] N91-16758
Transport simulation of the effect of impurity radiation on the high beta, ohmic start-up of the HBT-EP tokamak
[DE90-010333] N91-16760
The CIT physics program
[DE90-012134] N91-16774
The Los Alamos megamp fiber z-pinch experiment
[DE91-004842] N91-16777

PLASMA INTERACTIONS
Plasma-facing materials
[DE90-008243] N91-16753

PLASMA LAYERS
A statistical survey of electron pitch angle distributions in the nightside central plasma sheet
[AD-A227763] N91-16486

PLASMA OSCILLATIONS
Nonlinear optical systems interacting with amplitude-modulated optical fields
[AD-A228221] N91-16742

PLASMA PHYSICS
A free boundary problem arising in plasma physics
[DE90-010065] N91-16754
Research in theoretical nuclear physics
[DE90-010792] N91-16828

PLASMA PROBES
New development of laser-based techniques in applications of thin-layer chromatography, microprobe elemental analysis, and gas phase pyrolysis
[DE90-011740] N91-16347

PLASMA RADIATION
Investigation and modeling of radiation absorption processes and opacities in dense plasmas
[AD-A228749] N91-16779

PLASMA SPECTRA
Fundamental characteristics and applications of an inductively coupled plasma as an ion source for mass spectrometry
[DE90-011746] N91-16770
IR plasma emissions
[AD-A227713] N91-16776

PLASMA TEMPERATURE
The Los Alamos megamp fiber z-pinch experiment
[DE91-004842] N91-16777

PLASMA WAVES
Wave-particle power transfer in a steady-state driven system
[DE90-010031] N91-16748

PLASMAS (PHYSICS)
Assessment of corrosion resistant coatings for a depleted U-0.75 Ti alloy
[AD-A228237] N91-16130
Computational physics at the National Energy Research Supercomputer Center
[DE90-010283] N91-16672
Microwave interferometer and reflectometer techniques for thermonuclear plasmas
[ETN-91-98478] N91-16780
Study on ECW transmission lines for NET/ITER
[EUR-FU/80/90-99] N91-16781

PLASTIC DEFORMATION
Finite element thermo-viscoplastic analysis of aerospace structures
[NASA-TM-102761] N91-16407

PLASTIC FLOW
Dynamic crack propagation in elastic-plastic solids N91-16402

PLASTIC PROPERTIES
Inelastic strain analysis of solder joint in NASA fatigue specimen
[NASA-CR-187864] N91-16132

PLASTICIZERS
The search for high energy low vulnerability explosives
[DE90-009436] N91-16158
Paste extrudable explosives: Their history and their current status
[DE90-009438] N91-16159

PLASTICS
Finite element solution of steady state axisymmetric penetration problems N91-16403

PLATES (STRUCTURAL MEMBERS)
Pilot study of the dynamic impact response of a composite plate
[FFA-TN-1990-27] N91-16070

PLATINUM
Impurity tolerant electrocatalysts
[DE90-011960] N91-16090
Chemisorption of carbon monoxide on three metal surfaces: Ni(111), Pd(111) and Pt(111): A comparative study
[AD-A228579] N91-16108

PLUMES
The effect of charge mixture ratio and particle size on igniter plume heat transfer characteristics
[DE90-010833] N91-16160

PLUTO (PLANET)
Aerospace vehicle design, spacecraft section. Volume 1: Project groups 1-4 --- unmanned probe to Pluto
[NASA-CR-186841] N91-16045
PFERD Mission: Pluto flyby exploration/research design N91-16046
Intrepid: A mission to Pluto N91-16047
Project Cerberus: Flyby mission to Pluto N91-16048
OPTIC: Orbiting Plutonian Topographic Image Craft proposal for an unmanned mission to Pluto N91-16049
Aerospace vehicle design, spacecraft section. Volume 2: Project groups 5-7 --- unmanned probe to Pluto
[NASA-CR-186842] N91-16050
Mission management, planning, and cost: PULSE Attitude And Control Systems (AACS) N91-16051
The Copernicus project N91-16052
The Phoenix Pluto Probe N91-16053

PNEUMATIC PROBES
A process for unstationary velocity and turbulence measurements with a pneumatic measuring wedge probe
[MITT-33] N91-16310

PNEUMATICS
Self-propelled in-tube shuttle and control system for automated measurements of magnetic field alignment
[DE90-008210] N91-16316

POINT SOURCES
Monte Carlo simulation of atmospheric neutron transport at high altitudes using MCNP
[AD-A226773] N91-16474

POISSON DENSITY FUNCTIONS
Hierarchical Bayesian analysis of change point problems
[AD-A228179] N91-16666

POLAR CAP ABSORPTION
A case study of the 19 October 1989 polar cap absorption event using the imaging riometer for ionospheric studies
[AD-A227764] N91-16487

POLAR COORDINATES
Simulation of disk-disk encounters with co-moving polar grids N91-16941

POLAR REGIONS
On the developmental dynamics of sudden stratospheric warmings
[AD-A227731] N91-16485

POLARIMETERS
A Moller polarimeter for the extracted ELSA-ray
[BONN-IR-90-42] N91-16731

POLARIMETRY
Motional Stark effect polarimetry for the current profile diagnostic in D3-D
[DE90-012071] N91-16773

POLARIZATION (CHARGE SEPARATION)
Photoinduced charge separation by polymer-bound chromophores
[DE90-010997] N91-16140

POLARIZATION (WAVES)
Technique for determining the static polarizabilities of refractory metal atoms
[DE90-017088] N91-16724

POLICIES
JPRS report: Science and technology. USSR: Space
[JPRS-USP-89-006] N91-16036
Information technology policies: A four country comparative study N91-16840

POLLUTION CONTROL
Parametric study of electrostatically charged sprays
[DE90-010580] N91-16262
Technological and policy options for mitigating greenhouse gas emissions from mobile sources
[DE90-010151] N91-16447

POLLUTION TRANSPORT
Subsurface science program: Program overview and research abstracts
[DE90-010321] N91-16456
Numerical simulations of the mountain iron tracer data
[DE90-009749] N91-16499

POLYACETYLENE
Thin film single crystal growth of a nonlinear optical polymer
[AD-A227692] N91-16807

POLYATOMIC MOLECULES
Experimental studies of the properties of trihydrogen and tetrahydrogen
[AD-A228869] N91-16110

POLYBUTADIENE
Time-temperature response of multiphase viscoelastic solids through numerical analysis N91-16401

POLYCHLORINATED BIPHENYLS
PCB/transformer techno-economic analysis model: User manual, volume 2
[DE90-010654] N91-16223

POLYCRYSTALS
Characterization of chemically prepared PZT thin films
[DE90-010831] N91-16789

POLYGONS
An elementary proof of the Ambartzumian-Pleijel identity
[REPT-90-59] N91-16657

POLYMERIC FILMS
Design, ultrastructure, and dynamics of nonlinear optical interactions in polymeric thin films
[AD-A228876] N91-16156

POLYMERIZATION
Gelcasting of sub-micron alumina, sialon, and silicon nitride powders
[DE91-000618] N91-16145
Thin film single crystal growth of a nonlinear optical polymer
[AD-A227692] N91-16807

POLYMERS
Updated evaluation of polymer films for electrical insulation
[DE91-000544] N91-16148
Polymers at liquid-liquid interfaces: Photophysics and photoredox chemistry
[DE91-005032] N91-16151

Fatigue of amorphous polymers
[ISBN-90-9003520-6] N91-16157
Studies of the fundamentals of solids state batteries
[AD-A228772] N91-16247

POLYMETHYL METHACRYLATE
Model filled polymers versus synthesis of crosslinked monodisperse polymethacrylate beads
[AD-A227236] N91-16146

POLYNOMIALS
Column reduction of polynomial matrices: An iterative algorithm
[MEMO-COSOR-89-30] N91-16598
Matrix algorithms in signal processing
[AD-A228851] N91-16625

POLYSTYRENE
Gas solubility in glassy polymers: A correlation with excess enthalpy
[AD-A228202] N91-16155
Time-temperature response of multiphase viscoelastic solids through numerical analysis N91-16401

POLYTOPES
Linear-time separation algorithms for the three-index assignment polytope
[AD-A228854] N91-16626

POMERANCHUK THEOREM
Analytic Multi-Regge Theory and the Pomeron in QCD
[DE90-012153] N91-16737

POMERONS
Analytic Multi-Regge Theory and the Pomeron in QCD
[DE90-012153] N91-16737

POPULATION INVERSION
Homogeneously broadened bidirectional ring laser: Theoretical analysis, numerical simulation, and experiment in helium-xenon N91-16360

POPULATION THEORY
An evolutionary approach to designing neural networks
[AD-A228874] N91-16643

POPULATIONS
Selection effects and binary galaxy velocity differences N91-16927

POSITION (LOCATION)
Vehicular sources in acoustic propagation experiments N91-16690

POSITION ERRORS
Implementation and experimentation with motion planning algorithms
[AD-A228278] N91-16612

POSITRON ANNIHILATION
Measurement of the e+e- annihilation in mu+mu- pairs at the Z sup o resonance
[MPI-PAE/EXP.EL-231] N91-16732

POSITRONS
Positron survival in Type II supernovae
[AD-A226778] N91-16965

POTENTIAL ENERGY
Interatomic forces and bonding mechanisms in MgO clusters
[DE90-010148] N91-16719

POTENTIAL FLOW
Numerical simulation of separated flows around a wing section at steady and unsteady motion by a discrete vortex method N91-16268
Extension of transonic flow computational concepts in the analysis of cavitated bearings
[NASA-TM-103214] N91-16304

POWDER (PARTICLES)
Phase selection and processing of high temperature intermetallic alloys
[AD-A227910] N91-16129
Initial studies of electric field effects on ceramic powder formation in flames
[DE90-007571] N91-16138
Gelcasting of sub-micron alumina, sialon, and silicon nitride powders
[DE91-000618] N91-16145
Method of making contamination-free ceramic bodies
[NASA-CASE-LEW-14984-1] N91-16152

POWDER METALLURGY
Sintering stress and microstructure in ceramic powder compacts
[DE91-004415] N91-16149

POWER SPECTRA
The 1/f frequency noise effects on self-heterodyne linewidth measurements for coherent communications
[AD-A227942] N91-16195

PRANDTL NUMBER
Rotating Rayleigh-Benard convection: The Kueppers-Lortz transition
[DE91-004835] N91-16288

PRECIPITATION (METEOROLOGY)
GCM (General Circulation Model) predictions for surface air temperature and precipitation over the southeastern United States
[DE90-009434] N91-16497
Comparison of SSM/I measurements to numerically-simulated cloud and precipitation during ERICA N91-16501
Global-scale, intraseasonal fluctuations of diabatic forcing of the atmosphere N91-16508

PREDICTION ANALYSIS TECHNIQUES
Propfan supersonic panel method analysis and flutter predictions N91-15993
Fatigue of amorphous polymers
[ISBN-90-9003520-6] N91-16157
Integrated Refractive Effects Prediction System (IREPS) user's manual, revision PC-2.0
[AD-A228549] N91-16203
Probabilistic fracture mechanics: A validation of predictive capability
[AD-A228877] N91-16409
Finalization of the international biospheric model validation study
[DE90-011087] N91-16463
Wind turbine acoustics
[NASA-TP-3057] N91-16679
A noise assessment and prediction system N91-16702

PREDICTIONS
Analysis of atmospheric diffusion of pollutants based on the limited observation of horizontal wind N91-16274

PREDICTOR-CORRECTOR METHODS
Study of time accuracy of flow variables across discontinuous boundaries N91-16300

PREMIXED FLAMES
Modelling of flamelet surface-to-volume ratio in turbulent premixed combustion
[DE90-006312] N91-16081

PREPOLYMERS
Inverse gas chromatography
[AD-A227677] N91-16099

PRESSURE DISTRIBUTION
Large-scale numerical aerodynamic simulations for complete aircraft configurations
[NAL-TR-1073-T] N91-15984
High-loaded combustion chambers stationary constant pressure combustion. Part 2: Research reports
[ETN-91-98511] N91-16112
Incompressible flow simulations using the velocity-pressure formulation N91-16299
A segregated finite element solution to the incompressible Navier-Stokes equations
[ME-69] N91-16315

PRESSURE DROP
Particle deposition in granular media
[DE90-010810] N91-16261

PRESSURE EFFECTS
Effects of high pressure nitrogen on the thermal stability of SiC fibers
[NASA-TM-103245] N91-16075
Particle deposition in granular media
[DE90-010810] N91-16261
Investigation of the influence of constant adverse pressure gradients on laminar boundary-layer stability at Mach number 8
[AD-A228231] N91-16293

PRESSURE GRADIENTS
High-loaded combustion chambers stationary constant pressure combustion. Part 2: Research reports
[ETN-91-98511] N91-16112
Pressure gradient effects on the development of hairpin vortices in an initially laminar boundary layer N91-16282
Numerical study of a three-dimensional turbulent boundary layer
[AD-A227835] N91-16291
Investigation of the influence of constant adverse pressure gradients on laminar boundary-layer stability at Mach number 8
[AD-A228231] N91-16293

PRESSURE MEASUREMENT
Aerodynamic surface pressure measurement in atmosphere and wind tunnel on a vertical axis wind turbine blade using pressure transducers N91-15980
Tests for integrating measurements of gas pressures in aircraft mechanisms
[ETN-91-98558] N91-16014

PRESSURE SENSORS
A process for unstationary velocity and turbulence measurements with a pneumatic measuring wedge probe
[MITT-33] N91-16310
Multiple-frequency surface acoustic wave devices as sensors
[DE90-009972] N91-16675

PRESSURE VESSELS
Study of the influence of imperfections on the dynamic stability of tanks
[DE90-011094] N91-16398

PRIMATES
Investigation of effects of 60-Hz electric and magnetic fields on operant and social behavior and on the neuroendocrine system of nonhuman primates
[DE90-011557] N91-16539

PRIMITIVE EQUATIONS
Planetary circulations in the presence of transient and self-induced heating N91-16505

PRINTED CIRCUITS
Microwave coupling on printed circuit boards
[DE90-011237] N91-16232

PROBABILITY THEORY
Some applications of probability and statistics in communication theory and signal processing
[AD-A226869] N91-16184
Shift-invariant image reconstruction of speckle-degraded images using bispectrum estimation
[AD-A227726] N91-16188
Application of fuzzy-Bayesian analysis to structural reliability
[NAL-TR-1063] N91-16396
About Petri nets with fuzzy markings
[LAAS-90354] N91-16670
Operating characteristics for weighted energy detector with Gaussian signals
[AD-A226851] N91-16673
Dynamics and configurations of galaxy triplets N91-16946

PROBLEM SOLVING
A modular stiffness-based approach to rotating systems analysis N91-16400

PROCESS CONTROL (INDUSTRY)
Phase selection and processing of high temperature intermetallic alloys
[AD-A227910] N91-16129
Development of a high-tensile-strain plastic-bonded TATB explosive
[DE90-011463] N91-16162
Control of industrial crystallizers: The physical aspects
[ETN-91-98488] N91-16179
Sensing of metal-transfer mode for process control of GMAW (Gas Metal Arc Welding)
[DE90-010946] N91-16377
Procedures for Quality Assurance Program
[DE90-010001] N91-16393
Statistical process control for QML (Qualified Manufacturer's List) radiation hardness assurance
[DE90-007413] N91-16394

PROCUREMENT
An assessment of the government liquid hydrogen requirements for the 1995-2005 time frame N91-16167

PRODUCT DEVELOPMENT
Concepts for future developments in electron microscopy
[DE90-010630] N91-16320

PROGRAM VERIFICATION (COMPUTERS)
Hypersonic shock/boundary-layer interaction database
[NASA-CR-187769] N91-15986
Probabilistic fracture mechanics: A validation of predictive capability
[AD-A228877] N91-16409
Ada compiler validation procedures, version 2.1
[AD-A228614] N91-16621

PROGRAMMED INSTRUCTION
Programmable pseudorandom detector pulse pattern generator
[ETN-91-98321] N91-16628

PROGRAMMING (SCHEDULING)
Decentralized real-time scheduling
[AD-A227856] N91-16604

PROGRAMMING LANGUAGES
Distributed algorithm simulation using input/output automata
[AD-A228113] N91-16611
DTD creation for the Software Technology for Adaptable, Reliable Systems (STARS) program
[AD-A228475] N91-16619
PENGUIN: A language for reactive graphical user interfaces
[AD-A228580] N91-16620

PROJECT MANAGEMENT
Space Station Freedom resource allocation accommodation of technology payload requirements
[NASA-TM-102766] N91-16832

PROJECT PLANNING
Tactical fighter aircraft: Differences between the Air Force's roadmap and the five year defense plan
[AD-A228882] N91-15976
Potential use of tiltrotor aircraft in Canadian aviation
[NASA-TM-102245] N91-16001
Preparations for a major international symposium on electricity and the environment
[DE90-010539] N91-16449
Status of target physics for inertial confinement fusion
[DE90-008221] N91-16751

Space Station Freedom resource allocation accommodation of technology payload requirements
[NASA-TM-102766] N91-16832
PROJECTILES
Use of the Magnus force in the modified point mass trajectory model
[AD-A228194] N91-15990
Fragment mass distribution of debris
[MBB-UA-1187-90-PUB] N91-16669
PROJECTION
Development of free-electron lasers for XUV projection lithography
[DE90-010566] N91-16342
PROJECTIVE GEOMETRY
Visualization of surfaces in four-dimensional space
[AD-A227858] N91-16605
PROP-FAN TECHNOLOGY
Propfan supersonic panel method analysis and flutter predictions N91-15993
Long-range vertical propagation N91-16693
PROPAGATION MODES
Mode competition effects in free electron lasers and gyrotrons
[DE90-011084] N91-16346
PROPELLANT BINDERS
Development of a high-tensile-strain plastic-bonded TATB explosive
[DE90-011463] N91-16162
PROPELLANTS
Destruction of propellant components in supercritical water
[DE90-010600] N91-16085
PROPELLER FANS
Propfan supersonic panel method analysis and flutter predictions N91-15993
Long-range vertical propagation N91-16693
PROPORTIONAL COUNTERS
The measurement of gamma heating in a fusion blanket test assembly
[DE90-011154] N91-16766
PROPULSION
High temperature oxidation-resistant thruster research
[NASA-CR-185233] N91-16063
PROPULSION SYSTEM CONFIGURATIONS
Research on certain aspects of laser diffraction particle size analysis relevant to autonomous self-diagnosing instrumentation
[AD-A226822] N91-16354
PROTECTIVE CLOTHING
Heat transfer in clothing during heat radiation
[IZF-1990-B-2] N91-16569
PROTECTIVE COATINGS
High temperature oxidation-resistant thruster research
[NASA-CR-185233] N91-16063
The oxidation behavior of carbon-carbon composites and their coatings N91-16074
Assessment of corrosion resistant coatings for a depleted U-0.75 Ti alloy
[AD-A228237] N91-16130
Angular dependence of thin-film dielectric coating damage thresholds
[DE91-000237] N91-16351
PROTOCOL (COMPUTERS)
Movable-boundary channel-access schemes for integrated voice/data networks
[AD-A227331] N91-16186
Geographic data transfer N91-16836
Using computer-generated protocols to study writers' planning strategies
[AD-A228875] N91-16844
PROTON BEAMS
Ion contamination of x ray pinhole camera images on PBFA 2
[DE90-012180] N91-16325
PROTON SCATTERING
Design and testing of a proton detector
[BONN-IR-90-34] N91-16729
PROTONS
Design and testing of a proton detector
[BONN-IR-90-34] N91-16729
Comparison of hydrogen diffusion in Ti2PdH(x) to the behavior for Ti2CuH(x) and Zr2PdH(x)
[DE91-002711] N91-16808
PROTOSTARS
Positron survival in Type II supernovae
[AD-A226778] N91-16965
Dense cores and young stellar objects N91-16969
PROTUBERANCES
Bump examinations of integrally strengthened carbon fiber reinforced plastic panels
[MBB/FE281/CFK/PUB/0013] N91-16076
PSEUDONOISE
Near/far resistant receivers for DS/SSMA communications
[AD-A228147] N91-16200
PSEUDORANDOM SEQUENCES
Programmable pseudorandom detector pulse pattern generator
[ETN-91-98321] N91-16628
PSYCHOACOUSTICS
Field measurement of head related transfer functions
[AD-A227850] N91-16708
PSYCHOPHYSICS
Changes in somatosensory responsiveness in behaving monkeys
[AD-A226832] N91-16540
Limits of human visual discrimination: Toward a general model of visual geometry
[AD-A226826] N91-16548
Field measurement of head related transfer functions
[AD-A227850] N91-16708
PUBLIC HEALTH
Multimedia Environmental Pollutant Assessment System (MEPAS) sensitivity analysis of computer codes
[DE90-010005] N91-16445
PULSARS
Multiple-photon Compton scattering in a strong magnetic field: Cross-sections and radiative transport N91-16852
PULSE AMPLITUDE
Preliminary analysis of measured sound propagation over various seasonal snow covers N91-16687
PULSE COMPRESSION
SLED II: A new method of RF pulse compression
[DE91-000058] N91-16183
PULSE DOPPLER RADAR
Intra-Pulse Frequency Diversity (IPFD) lab demonstration
[AD-A228814] N91-16209
A paper-assessment of the performance of a modern airborne multi-mode pulse Doppler radar deployed as a ground-based fire-control radar
[ETN-91-98584] N91-16215
PULSE GENERATORS
SLED II: A new method of RF pulse compression
[DE91-000058] N91-16183
Programmable pseudorandom detector pulse pattern generator
[ETN-91-98321] N91-16628
PULSED LASERS
Stability and accuracy of the sweep rate measurements for LLNL optical streak cameras
[DE90-012080] N91-16324
Short pulse driven recombination x ray lasers
[DE90-009945] N91-16340
Experimental verification of physical model of pulsed laser welding
[DE91-000025] N91-16380
PULSED RADIATION
Infrared response of YBa2Cu3O(7-delta) films to pulsed, broadband synchrotron radiation
[DE90-011519] N91-16800
PULSES
A method for pressure-pulse suppression in fluid-filled piping
[DE90-010408] N91-16260
Interferometric second-harmonic-generation autocorrelator for characterizing femtosecond pulses
[DE90-010331] N91-16345
PURITY
High-purity silicon soft x ray sensor arrays
[ETN-91-98484] N91-16338
PYROLYSIS
New development of laser-based techniques in applications of thin-layer chromatography, microprobe elemental analysis, and gas phase pyrolysis
[DE90-011740] N91-16347
PYROLYTIC GRAPHITE
Cluster formation in laser-induced ablation and evaporation of solids observed by laser ionization time-of-flight mass spectrometry and scanning tunneling microscopy
[DE90-010876] N91-16344
PYROMETERS
Advanced structural instrumentation, volume 2
[AD-A227473] N91-16330
PYROTECHNICS
The effect of charge mixture ratio and particle size on igniter plume heat transfer characteristics
[DE90-010833] N91-16160
Modeling laser ignition of explosives and pyrotechnics: Effects and characterization of radiative transfer
[DE90-011052] N91-16161

Q

Q FACTORS
The Assistant for Specifying the Quality Software (ASQS). Volume 1: Operational concept document
[AD-A227893] N91-16608
The Assistant for Specifying the Quality Software (ASQS). Volume 2: User's manual. Volume 2
[AD-A227894] N91-16609
Q SWITCHED LASERS
Experimental set-up for a pulsed CO2 laser rangefinder with heterodyne detection
[FEL-90-A125] N91-16365
QUADRATIC EQUATIONS
Matrix algorithms in signal processing
[AD-A228851] N91-16625
The discrete time H infinity control problem with measurement feedback
[MEMO-COSOR-89-31] N91-16651
The finite horizon singular time-varying H infinity control problem with dynamic measurement feedback
[MEMO-COSOR-89-33] N91-16652
QUADRATIC PROGRAMMING
Some generalizations of the criss-cross method for quadratic programming
[REPT-90-52] N91-16599
A long step barrier method for convex quadratic programming
[REPT-90-53] N91-16600
QUALITATIVE ANALYSIS
Determination of airborne organics by direct sampling mass spectrometry
[DE90-009422] N91-16452
QUALITY
Using computer-generated protocols to study writers' planning strategies
[AD-A228875] N91-16844
QUALITY CONTROL
Developmental tests for shuttle Orbiter N91-16038
Characterization and development report for the SA2859: A silicon controlled rectifier
[DE90-010196] N91-16217
Procedures for Quality Assurance Program
[DE90-010001] N91-16393
Statistical process control for QML (Qualified Manufacturer's List) radiation hardness assurance
[DE90-007413] N91-16394
The role of quality assurance in the monitoring of terrestrial ecosystems
[DE90-010986] N91-16461
QUANTUM CHROMODYNAMICS
Analytic Multi-Regge Theory and the Pomeron in QCD
[DE90-012153] N91-16737
QUANTUM ELECTRONICS
Solid state research
[NASA-CR-187871] N91-16816
Chemical beam epitaxy of ZnSe
[AD-A228045] N91-16817
QUANTUM MECHANICS
A quantum theory of the mind-brain interface
[DE91-004431] N91-16546
Two-dimensional convolutions, correlations, and Fourier transforms of combinations of Wigner distribution functions and complex ambiguity functions
[AD-A226852] N91-16649
Selective excitation, relaxation, and energy channeling in molecular systems
[DE90-010793] N91-16717
Interatomic forces and bonding mechanisms in MgO clusters
[DE90-010148] N91-16719
QUANTUM THEORY
A quantum theory of the mind-brain interface
[DE91-004431] N91-16546
QUANTUM WELLS
Two-dimensional simulation of quantum-well lasers including energy transport
[AD-A227487] N91-16356
Photoreflectance studies of electronic transitions in quantum well structures under high pressure
[DE90-011583] N91-16801
Theoretical studies of electron transport in quantum-well structures
[AD-A228429] N91-16819
QUARK MODELS
Theoretical topics in B-physics
[DE91-004911] N91-16726
QUARKS
Theoretical topics in B-physics
[DE91-004911] N91-16726
QUASARS
Tidal events and galactic activity N91-16911
Are extremely luminous far-infrared galaxies the result of merging quasar cores N91-16912
Radio structures in QSO-galaxy pairs N91-16924
Radio line and continuum observations of quasar-galaxy pairs and the origin of low reshift quasar absorption line systems N91-16925
Merging galaxies and black hole ejections N91-16929

Origin of regularities in the redshift distributions of distant galaxies and quasars
[DE91-004848] N91-16968

QUATERNARY ALLOYS
Materials systems for 2- to 5-micrometers wavelength diode lasers
[AD-A228218] N91-16361

QUENCHING (ATOMIC PHYSICS)
Photoinduced charge separation by polymer-bound chromophores
[DE90-010997] N91-16140

QUERY LANGUAGES
A query model and query and knowledge definition languages for object-oriented databases N91-16580
Research into the design and implementation of knowledge base systems
[AD-A228873] N91-16843

QUEUEING THEORY
Pathwise convexity and its relation to convergence of time-average derivatives
[AD-A228888] N91-16662

R

RADAR
Activities report of the German Federal Institute for Flight Safety
[ETN-91-98644] N91-16002
Electronically steerable arrays: Current and future technology and applications
[ETN-91-98581] N91-16254

RADAR ANTENNAS
Analysis of the performance of a single-auxiliary sidelobe canceller
[RSRE-MEMO-4375] N91-16193

RADAR BEAMS
Intra-Pulse Frequency Diversity (IPFD) lab demonstration
[AD-A228814] N91-16209

RADAR CROSS SECTIONS
A planar near-field scanning technique for bistatic radar cross section measurements
[NASA-CR-187794] N91-16194
High-frequency techniques for RCS prediction of plate geometries
[NASA-CR-187865] N91-16212
A comparison of optically measured and radar-derived horizontal neutral winds
[AD-A227690] N91-16483

RADAR DATA
Derivation of exospheric temperature at high latitudes from incoherent-scatter radar data
[AD-A227721] N91-16484

RADAR DETECTION
Numeric and symbolic signal processing for very high subclutter visibility
[AD-A228812] N91-16207

RADAR EQUIPMENT
Numeric and symbolic signal processing for very high subclutter visibility
[AD-A228812] N91-16207

RADAR IMAGERY
Detection of soil moisture using X-band SLAR records in a sandy area
[BCRS-90-08] N91-16427
Implementation of the phase gradient algorithm
[DE90-012160] N91-16579

RADAR MEASUREMENT
A planar near-field scanning technique for bistatic radar cross section measurements
[NASA-CR-187794] N91-16194

RADAR SCANNING
A planar near-field scanning technique for bistatic radar cross section measurements
[NASA-CR-187794] N91-16194

RADAR SCATTERING
Procedure for the correction of errors in the DUTSCAT data 1987/1988
[BCRS-90-14] N91-16430

RADAR TRACKING
Electron density comparisons between radar observations and 3-D ionospheric model calculations
[AD-A227703] N91-16187

RADIAL VELOCITY
A study of the compact group of galaxies Shahbazian 4 N91-16877
Caustic waves in galaxy disks produced in collisions with low mass companions N91-16960

RADIANCE
Observation simulation experiments with regional prediction models N91-16502

RADIANT FLUX DENSITY
Analysis of emission data from a Perkin-Elmer 1710 FTIR spectrometer
[AD-A227759] N91-16331

RADIANT HEATING
The measurement of gamma heating in a fusion blanket test assembly
[DE90-011154] N91-16766

RADIATION ABSORPTION
Solar refrigeration: Evaluation of technical options and design of a solar-generator-adsorber for a novel adsorption refrigerator, volumes 1 and 2 N91-16440
Investigation and modeling of radiation absorption processes and opacities in dense plasmas
[AD-A228749] N91-16779

RADIATION COUNTERS
Design and testing of a proton detector
[BONN-IR-90-34] N91-16729
AGS silicon gold collisions measured in the E-810 TPC (Time Projection Chamber)
[DE90-010015] N91-16733

RADIATION DAMAGE
Effects of neutron fluence on the operating characteristics of diode lasers used in atomic frequency standards
[AD-A226763] N91-16352
A model for the prediction of Nb3Sn critical current as a function of field, temperature, strain, and radiation damage
[DE91-000656] N91-16775
Dose rate effects on damage formation in ion-implanted gallium arsenide
[DE91-000394] N91-16806
Cellular track model of biological damage to mammalian cell cultures from galactic cosmic rays
[NASA-TP-3055] N91-16981

RADIATION DETECTORS
The radiation hardness test facility
[RAL-90-065] N91-16030
Measurements of 1/f noise in a-Si:H pin diodes and thin-film-transistors
[DE90-011218] N91-16228
X-Ray Detector: An x-ray radiation detector design code
[DE90-008235] N91-16317
Programmable pseudorandom detector pulse pattern generator
[ETN-91-98321] N91-16628
Performance measurements of hybrid PIN diode arrays
[DE90-010308] N91-16790

RADIATION DOSAGE
Total-dose degradation of thin film ferroelectric capacitors
[DE90-007152] N91-16218
Radiation physics, biophysics, and radiation biology
[DE90-011544] N91-16722
Dose rate effects on damage formation in ion-implanted gallium arsenide
[DE91-000394] N91-16806

RADIATION EFFECTS
Scoping estimates of the LDEF satellite induced radioactivity
[NASA-CR-184074] N91-16056
The 1/f noise in irradiated MOS devices
[DE90-007288] N91-16219
Angular dependence of thin-film dielectric coating damage thresholds
[DE91-000237] N91-16351
Application of AMS to the biomedical sciences
[DE90-010869] N91-16538
Thermal emission model for the anneal of radiation-induced trapped holes
[DE90-007285] N91-16718
Radiation physics, biophysics, and radiation biology
[DE90-011544] N91-16722
Transport simulation of the effect of impurity radiation on the high beta, ohmic start-up of the HBT-EP tokamak
[DE90-010333] N91-16760
A model for the prediction of Nb3Sn critical current as a function of field, temperature, strain, and radiation damage
[DE91-000656] N91-16775
Dose rate effects on damage formation in ion-implanted gallium arsenide
[DE91-000394] N91-16806
Correlation between the elastic-shear-instability-mechanism and empirical criteria for irradiation-induced amorphization
[DE91-004481] N91-16810

RADIATION HARDENING
The radiation hardness test facility
[RAL-90-065] N91-16030
Characterization and development report for the SA2859: A silicon controlled rectifier
[DE90-010196] N91-16217
Total-dose degradation of thin film ferroelectric capacitors
[DE90-007152] N91-16218
The 1/f noise in irradiated MOS devices
[DE90-007288] N91-16219
Radiation hardening of a high voltage IC technology (BCDMOS)
[DE90-008345] N91-16220
Properties and characterization of thin film ferroelectric capacitors for nonvolatile memories
[DE91-004037] N91-16242
Statistical process control for QML (Qualified Manufacturer's List) radiation hardness assurance
[DE90-007413] N91-16394
Thermal emission model for the anneal of radiation-induced trapped holes
[DE90-007285] N91-16718

RADIATION HAZARDS
Investigation of effects of 60-Hz electric and magnetic fields on operant and social behavior and on the neuroendocrine system of nonhuman primates
[DE90-011557] N91-16539

RADIATION MEASUREMENT
Scoping estimates of the LDEF satellite induced radioactivity
[NASA-CR-184074] N91-16056

RADIATION PRESSURE
The magnetospheric response to 8-minute period strong-amplitude upstream pressure variations
[AD-A228038] N91-16489

RADIATION PROTECTION
Cellular track model of biological damage to mammalian cell cultures from galactic cosmic rays
[NASA-TP-3055] N91-16981

RADIATION SHIELDING
Electron stopping powers of some elements and compounds from 0 to 10,000 eV: A compilation
[DE90-010675] N91-16716

RADIATION SOURCES
Scoping estimates of the LDEF satellite induced radioactivity
[NASA-CR-184074] N91-16056
Numeric and symbolic signal processing for very high subclutter visibility
[AD-A228812] N91-16207

RADIATIVE HEAT TRANSFER
Heat transfer in clothing during heat radiation
[IZF-1990-B-2] N91-16569

RADIATIVE LIFETIME
Microwave-detected photoconductance decay
[DE90-011505] N91-16795

RADIATIVE TRANSFER
Modeling laser ignition of explosives and pyrotechnics: Effects and characterization of radiative transfer
[DE90-011052] N91-16161
Investigation of a remote sensing technique for droplet effective radius N91-16420

RADIO ALTIMETERS
Ionospheric corrections for SHF satellite radar altimetry N91-16423

RADIO ASTRONOMY
Natural waves of microstrip transmission lines in wave guides
[BER-68] N91-16251
Phased array imaging
[AD-A228774] N91-16855
Paired and Interacting Galaxies: International Astronomical Union Colloquium No. 124
[NASA-CP-3098] N91-16858

RADIO COMMUNICATION
Movable-boundary channel-access schemes for integrated voice/data networks
[AD-A227331] N91-16186

RADIO EMISSION
A multi-frequency study of the peculiar interacting system Arp 206 N91-16870
Dumb-bell galaxies in southern clusters: Catalog and preliminary statistical results N91-16896
Radio loud far-infrared galaxies N91-16902
Radio emission in peculiar galaxies N91-16907
The role of shocks in NGC 6240 N91-16921

RADIO FREQUENCIES
Neoclassical effects on RF current drive
[DE90-010302] N91-16222
Development of free-electron lasers for XUV projection lithography
[DE90-010566] N91-16342
Radio structures in QSO-galaxy pairs N91-16924

RADIO GALAXIES
Multi-color imaging of selected southern interacting galaxies N91-16867
Interacting nuclei in distant galaxies N91-16894
Radio loud far-infrared galaxies N91-16902
Dust and ionized gas in active radio elliptical galaxies N91-16919

RADIO OBSERVATION
Radio loud far-infrared galaxies N91-16902

Radio line and continuum observations of quasar-galaxy pairs and the origin of low reshift quasar absorption line systems N91-16925

RADIO SIGNALS
The design of a meteorological facsimile converter [ETN-91-98578] N91-16528

RADIO STARS
A multiwavelength survey of interacting galaxies N91-16898

RADIO TRANSMISSION
Meteor burst communications study [AD-A228641] N91-16204
The design of a meteorological facsimile converter [ETN-91-98578] N91-16528
Distorted-wave born approximation calculations for turbulence scattering in an upward-refracting atmosphere N91-16700

RADIOACTIVE DECAY
Study of the global distributions of atmospheric radionuclides [DE90-010749] N91-16455
Theoretical topics in B-physics [DE91-004911] N91-16726
Properties of superdeformed bands in the A = 194 region [DE90-011482] N91-16798

RADIOACTIVE ISOTOPES
Finalization of the international biospheric model validation study [DE90-011087] N91-16463
Application of AMS to the biomedical sciences [DE90-010869] N91-16538

RADIOACTIVE MATERIALS
Multimedia Environmental Pollutant Assessment System (MEPAS) sensitivity analysis of computer codes [DE90-010005] N91-16445

RADIOACTIVE WASTES
Principal facts for about 16,000 gravity stations in the Nevada test site and vicinity [DE90-011521] N91-16470
Is there hope for fusion [DE90-012095] N91-16736

RADIOBIOLOGY
Radiation physics, biophysics, and radiation biology [DE90-011544] N91-16722

RADIOMETERS
An inter-comparison of surface energy flux measurement systems used during FIFE, 1987 [NASA-CR-187699] N91-16472

RADIOMETRIC RESOLUTION
Merging panchromatic and multispectral images for enhanced image analysis [AD-A227902] N91-16421

RADIUM 226
Study of the global distributions of atmospheric radionuclides [DE90-010749] N91-16455

RADON ISOTOPES
Study of the global distributions of atmospheric radionuclides [DE90-010749] N91-16455

RAIL TRANSPORTATION
Moving America; new directions, new opportunities: Assessment of the potential for magnetic levitation transportation systems in the United States [PB91-104596] N91-16388

RAMAN SPECTRA
On the development of in-situ Raman analysis of plasma deposited diamond [AD-A227453] N91-16147
Generation of high power 1.54 micrometer radiation by stimulated Raman scattering in methane [FEL-90-B098] N91-16366

RAMAN SPECTROSCOPY
Time-resolved Coherent Anti-Stokes Raman Spectroscopy (CARS) and the measurement of vibrational spectra in shock-compressed molecular materials [DE90-012053] N91-16091

RAMPS (STRUCTURES)
Experimental parametric study of jet vortex generators for flow separation control [NASA-CR-187836] N91-16296

RANDOM ACCESS
An O(log n) time common CRCW pram algorithm for minimum spanning tree [AD-A228740] N91-16623

RANDOM NOISE
Near/far resistant receivers for DS/SSMA communications [AD-A228147] N91-16200
Operating characteristics for weighted energy detector with Gaussian signals [AD-A226851] N91-16673

RANGE (EXTREMES)
Relative extrema, zeros, and inequalities for Gegenbauer functions of the first and second kind [REPT-90-54] N91-16653
Relative extrema, zeros, and inequalities for Jacobi functions of the first and second kind [REPT-90-55] N91-16654

RAY TRACING
Meteorological effects on long-range outdoor sound propagation N91-16696

RAYLEIGH NUMBER
Rotating Rayleigh-Benard convection: The Kueppers-Lortz transition [DE91-004835] N91-16288

RAYLEIGH WAVES
Seismic structure of the upper mantle under the Pacific Ocean N91-16492

RAYLEIGH-BENARD CONVECTION
Rotating Rayleigh-Benard convection: The Kueppers-Lortz transition [DE91-004835] N91-16288

REACTION KINETICS
Effects of high pressure nitrogen on the thermal stability of SiC fibers [NASA-TM-103245] N91-16075
Spray combustion modeling and evaluation [NASA-CR-187887] N91-16078
A numerical study of silane combustion [DE90-006002] N91-16080
Fundamental studies of hydrocarbon conversions over supported bimetallic catalysts [DE90-011744] N91-16089
Electrocatalysis of anodic and cathodic oxygen-transfer reactions [DE91-000611] N91-16100
High temperature corrosion of alloys in mixed gases N91-16121
Diagnostic of the reaction behaviour of intensive high explosives under jet attack [MBB-UA-1188-90-PUB] N91-16173
Puzzles of electron transfer [DE90-010541] N91-16720
High Tc oxide solid state reaction kinetics via complex impedance spectroscopy [DE90-011178] N91-16792
Thermal desorption studies of isotopically-labeled oxygen-induced superconductivity in La2CuO(4+delta) [DE91-004898] N91-16812

REACTOR DESIGN
Electrical power from inertial confinement fusion: Issues and prospects [DE90-010332] N91-16759
Theoretical studies of tokamaks [DE90-011332] N91-16768

REACTOR MATERIALS
Plasma-facing materials [DE90-008243] N91-16753

REACTOR SAFETY
Living PRAs (Probabilistic Risk Analysis) made easier with IRRAS (Integrated Reliability and Risk Analysis System) [DE90-010938] N91-16395
Electrical power from inertial confinement fusion: Issues and prospects [DE90-010332] N91-16759
Theoretical studies of tokamaks [DE90-011332] N91-16768

REACTOR TECHNOLOGY
Study of the influence of imperfections on the dynamic stability of tanks [DE90-011094] N91-16398

REAL GASES
On the Goertler instability in hypersonic flows: Sutherland law fluids and real gas effects [NASA-CR-187481] N91-15994
Numerical analysis of viscous hypersonic flow past a generic forebody [MBB/FE122/S/PUB/0407] N91-15997

REAL TIME OPERATION
Aerosol Dynamics Laboratory [DE90-010275] N91-16027
Real-time vergence control for binocular robots [AD-A228817] N91-16387
New methods for producing, recording, and processing interferometric moire patterns N91-16405
The value of on-site sodar data in regional modeling [DE90-009921] N91-16498
Development of a test-bed for real-time monitoring of pilot mental status N91-16563
Implementation of the phase gradient algorithm [DE90-012160] N91-16579
Implementing sporadic servers in Ada [AD-A226723] N91-16584
Hartstone benchmark results and analysis [AD-A226817] N91-16587
Scheduler issues for real-time Ada [AD-A227766] N91-16592
Tailoring an Ada runtime environment proof-of-concept [AD-A227767] N91-16593
Real-time filtering and detection of dynamics for compression of HDTV [NASA-CR-187777] N91-16596
Distributed issues for Ada real-time systems [AD-A227852] N91-16603
Decentralized real-time scheduling [AD-A227856] N91-16604
Towards conservative reliability predictions for real-time software [NASA-CR-187863] N91-16627
Real-time system specification and verification [AD-A227682] N91-16634
Mathematical methods and algorithms for real-time applications [AD-A228889] N91-16663
The design of a two-dimensional optical image correlator and its application in image tracking N91-16744
The StarLite project [AD-A226722] N91-16837

RECEIVERS
Optimal Kalman filter integration of a global positioning system receiver and an LN-94 inertial navigation system [AD-A227222] N91-16003
Measurement of the capture effect of frequency modulation [AD-A228058] N91-16199
Near/far resistant receivers for DS/SSMA communications [AD-A228147] N91-16200
Seismic signal processing optimized for a specific source and receiver [DE90-010189] N91-16468
Preliminary analysis of measured sound propagation over various seasonal snow covers N91-16687

RECHARGING
Molten salt electrolytes in high temperature batteries [RAE-TM-MAT/STR-1155] N91-16241

RECOMBINATION REACTIONS
Short pulse driven recombination x ray lasers [DE90-009945] N91-16340
The theory of electron-ion collisions: The role of doubly excited states [DE90-011078] N91-16721
Microwave-detected photoconductance decay [DE90-011505] N91-16795

RECTANGULAR PLATES
High-frequency techniques for RCS prediction of plate geometries [NASA-CR-187865] N91-16212

RECURSIVE FUNCTIONS
Low-level image processing architectures compared for some non-linear recursive neighborhood operations [ISBN-90-9003713-6] N91-16631

RED GIANT STARS
Infrared images of merging galaxies N91-16904

RED SHIFT
Pairs of galaxies in low density regions of a combined redshift catalog N91-16860
Observational properties of compact groups of galaxies N91-16871
Correlation functions for pairs and groups of galaxies N91-16879
Radio line and continuum observations of quasar-galaxy pairs and the origin of low reshift quasar absorption line systems N91-16925
Properties of the redshift N91-16926
A tentative explanation of cosmological red shift N91-16928
Origin of regularities in the redshift distributions of distant galaxies and quasars [DE91-004848] N91-16968
Spectrometric, chemical, and cosmological development of galaxies [ETN-91-98555] N91-16972

REDOX CELLS
Electrolyte optimization and electrode material evaluation for the vanadium redox battery N91-16234

REDUCED GRAVITY
The space flights: Second German Spacelab mission D-2 and Mir 1992 [REPT-25/90] N91-16034
Development of a versatile laser light scattering instrument [NASA-CR-182474] N91-16350

REDUNDANCY
Multi-criteria position and configuration optimization for redundant platform/manipulator systems [DE90-010705] N91-16372

REDUNDANT COMPONENTS
TF89 tactical fighter outer wing design [ETN-91-98580] N91-16019

REENTRY VEHICLES
Joint computational/experimental aerodynamics research on a reentry vehicle. Part 2: Computational results
[DE90-012765] N91-16054
REFLECTANCE
Evaluation of the HULL and SHARC hydrocodes in simulating the reflection of Mach 2.12 non-decaying shock on wedges of various angles
[AD-A227581] N91-16287
Photoreflectance studies of electronic transitions in quantum well structures under high pressure
[DE90-011583] N91-16801
REFLECTOMETERS
Microwave interferometer and reflectometer techniques for thermonuclear plasmas
[ETN-91-98478] N91-16780
REFRACTION
Long-range sound propagation: A review of some experimental data N91-16683
The correction of infrasound signals for upper atmospheric winds N91-16695
Effect of wind and temperature gradients on received acoustic energy N91-16697
Distorted-wave born approximation calculations for turbulence scattering in an upward-refracting atmosphere N91-16700
Scattering of sound by atmospheric turbulence predictions in a refractive shadow zone N91-16703
REFRACTIVITY
Visualization of unsteady transonic flow by holographic interferometry using photorefractive media
[AD-A228802] N91-16336
Wave propagation through random media: A local method of small perturbations based on the Helmholtz equation N91-16701
REFRACTORY MATERIALS
Phase selection and processing of high temperature intermetallic alloys
[AD-A227910] N91-16129
Ion beam modification of surface for improved high temperature performance
[AD-A228067] N91-16243
REFRACTORY METALS
Technique for determining the static polarizabilities of refractory metal atoms
[DE90-017088] N91-16724
REFRIGERANTS
Initial parametric results using CYCLEZ: A LMTD-specified, Lorenz-Meutzner cycle refrigerator-freezer model
[DE90-010146] N91-16175
Solar refrigeration: Evaluation of technical options and design of a solar-generator-adsorber for a novel adsorption refrigerator, volumes 1 and 2 N91-16440
REFRIGERATING
Initial parametric results using CYCLEZ: A LMTD-specified, Lorenz-Meutzner cycle refrigerator-freezer model
[DE90-010146] N91-16175
REFRIGERATORS
Magnetic heat pumps
[DE90-010305] N91-16375
Solar refrigeration: Evaluation of technical options and design of a solar-generator-adsorber for a novel adsorption refrigerator, volumes 1 and 2 N91-16440
REGGE POLES
Analytic Multi-Regge Theory and the Pomeron in QCD
[DE90-012153] N91-16737
REGRESSION ANALYSIS
Spatial and temporal climate variations influencing medium-range temperature predictions over south-central European Russia
[AD-A228623] N91-16527
Adaptive bandwidth choice for kernel regression
[AD-A228437] N91-16661
REGULATIONS
Procedures for Quality Assurance Program
[DE90-010001] N91-16393
REINFORCEMENT (STRUCTURES)
Evaluation procedure for reinforced concrete box culverts under airfield pavements
[AD-A227920] N91-16031
REINFORCING FIBERS
Acoustical and dynamic mechanical characterization of fiber-matrix interface bonds in ceramic composites
[DE90-010949] N91-16066
Flammability characteristics of fiber reinforced composite materials
[AD-A228215] N91-16072
RELATIVE BIOLOGICAL EFFECTIVENESS (RBE)
Cellular track model of biological damage to mammalian cell cultures from galactic cosmic rays
[NASA-TP-3055] N91-16981
RELATIVISTIC EFFECTS
Theoretical studies of atomic transitions
[DE91-000931] N91-16723
RELAXATION METHOD (MATHEMATICS)
A successive partial-relaxation Gaussian algorithm for area navigation operations with the Microwave Landing System (MLS)
[AD-A228871] N91-16004
RELIABILITY
Environmental uncertainty, planning and organizational performance N91-16464
RELIABILITY ANALYSIS
Analysis of the performance of a single-auxiliary sidelobe canceller
[RSRE-MEMO-4375] N91-16193
Living PRAs (Probabilistic Risk Analysis) made easier with IRRAS (Integrated Reliability and Risk Analysis System)
[DE90-010938] N91-16395
Towards conservative reliability predictions for real-time software
[NASA-CR-187863] N91-16627
Validity study in multidimensional latent space and efficient computerized adaptive testing
[AD-A227742] N91-16650
Theoretical studies of tokamaks
[DE90-011332] N91-16768
RELIABILITY ENGINEERING
Reliability/Maintainability/Logistics support analysis Computer Aided Tailoring Software Program (R/M/L CATSOP)
[AD-A226820] N91-16588
Practical aspects of repository operations for the Software Technology for Adaptable, Reliable Systems (STARS) program
[AD-A228455] N91-16617
Towards conservative reliability predictions for real-time software
[NASA-CR-187863] N91-16627
REMOTE SENSING
Investigation of a remote sensing technique for droplet effective radius N91-16420
Extraction of marketable information from ERS-1 data
[BCRS-90-03] N91-16425
The dielectric properties of wet soils
[BCRS-90-13] N91-16429
Evaluation of crop transpiration with remote sensing and computer simulation models
[REPT-1] N91-16431
An inter-comparison of surface energy flux measurement systems used during FIFE, 1987
[NASA-CR-187699] N91-16472
NASA/MSFC FY90 Global Scale Atmospheric Processes Research Program Review
[NASA-CP-3093] N91-16500
Observation simulation experiments with regional prediction models N91-16502
REPEATERS
Digital time interpolator
[DIGEL-1990-4] N91-16249
Time interpolator
[DIGEL-1990-3] N91-16337
REPLACING
PCB/transformer techno-economic analysis model: User manual, volume 2
[DE90-010654] N91-16223
REQUIREMENTS
Development of liquid xenon imaging gamma-ray spectrophotometers
[AD-A227575] N91-16740
RESEARCH AND DEVELOPMENT
JPRS report: Science and technology. USSR: Space
[JPRS-USP-89-006] N91-16036
Composite Solid Propellant Predictability and Quality Assurance
[NASA-CR-186404] N91-16163
Introduction to the problem N91-16164
The University of Arizona program in solid propellants N91-16165
The impact of separated flow on heat and mass transfer
[DE91-000592] N91-16284
A summary of prospects for methanol vehicles in the United States
[DE90-009719] N91-16370
Heat engines program
[DE90-010276] N91-16374
Solid state research
[NASA-CR-187871] N91-16816
Space research in the Federal Republic of Germany, 1988 and 1989
[ETN-91-98514] N91-16849
Accomplishments in technology transfer from DOE and its laboratories
[DE90-002686] N91-16986
The 1989 annual catalog of the German Aerospace Establishment: Research reports and communications
[ISSN-0172-357X] N91-16987
RESEARCH FACILITIES
Documents on the history of the Aerodynamic Research Establishment at Goettingen, 1907 - 1925
[DLR-MITT-90-05] N91-15977
Production of high intensity radioactive beams
[DE90-011340] N91-16735
Status of target physics for inertial confinement fusion
[DE90-008221] N91-16751
Activities report of the Space Research Organization Netherlands
[ETN-91-98473] N91-16848
RESIDENTIAL ENERGY
Electrochromic sun control coverings for windows
[DE90-000335] N91-16139
Meetings to share advancements in heat pump technologies
[DE90-010008] N91-16257
RESIDUAL STRENGTH
Bump examinations of integrally strengthened carbon fiber reinforced plastic panels
[MBB/FE281/CFK/PUB/0013] N91-16076
RESIDUAL STRESS
Evaluation procedure for reinforced concrete box culverts under airfield pavements
[AD-A227920] N91-16031
Tensile behavior of tungsten/niobium composites at 1300 to 1600 K
[NASA-TM-103727] N91-16128
RESISTANCE HEATING
Derivation of exospheric temperature at high latitudes from incoherent-scatter radar data
[AD-A227721] N91-16484
RESONANCE
Nonlinear resonance
[DE90-010428] N91-16341
RESONANCE FLUORESCENCE
Nonlinear optical systems interacting with amplitude-modulated optical fields
[AD-A228221] N91-16742
RESONANT FREQUENCIES
Generation of XUV light by resonant frequency tripling in a two-wiggler FEL amplifier
[DE90-012120] N91-16349
Dynamic response of composite beams using shear-deformable finite elements
[AD-A227975] N91-16408
RESOURCE ALLOCATION
Alopex optimization algorithm
[AD-A228442] N91-16615
Space Station Freedom resource allocation accommodation of technology payload requirements
[NASA-TM-102766] N91-16832
RESOURCES MANAGEMENT
International decision making and global climate change: Lessons of prior resource management efforts for consensus building
[DE90-010714] N91-16454
RESPONSE TIME (COMPUTERS)
Implementing sporadic servers in Ada
[AD-A226723] N91-16584
REUSABLE SPACECRAFT
Buran and the future of the Soviet space program N91-16037
REVERBERATION
Proving experiments on an acoustic transmission suite and its reverberation room
[BBC-RD-1990/13] N91-16681
REVERBERATION CHAMBERS
A low cost end-fire acoustic radiator
[ISVR-TR-188] N91-16705
REVERSE FIELD PINCH
A Mirnov loop array for field-reversed configurations
[DE90-010607] N91-16750
The Madison symmetric torus
[DE90-010306] N91-16757
REYNOLDS NUMBER
Numerical simulation of buffer flow in a free flow electrophoresis chamber N91-16279
Theoretical and experimental examinations of transition behavior of the profile boundary layer at compressor and turbine grids
[ETN-91-98559] N91-16312
REYNOLDS STRESS
Numerical study of a three-dimensional turbulent boundary layer
[AD-A227835] N91-16291
RHEOLOGY
Paste extrudable explosives: Their history and their current status
[DE90-009438] N91-16159
Shear thickening of concentrated dispersions
[ETN-91-98477] N91-16308

RICCATI EQUATION
The discrete time H infinity control problem with measurement feedback
[MEMO-COSOR-89-31] N91-16651
The finite horizon singular time-varying H infinity control problem with dynamic measurement feedback
[MEMO-COSOR-89-33] N91-16652
RING GALAXIES
Multi-waveband observations of colliding galaxies N91-16868
The ringed X-galaxy NGC 7020 N91-16885
The polar-ring galaxies NGC 2685 and NGC 3808B (VV 300) N91-16892
Caustic waves in galaxy disks produced in collisions with low mass companions N91-16960
RING LASERS
A ring laser gyroscope with optical subtraction N91-16335
Stochastic and chaotic effects in the ring laser N91-16359
Homogeneously broadened bidirectional ring laser: Theoretical analysis, numerical simulation, and experiment in helium-xenon N91-16360
RISK
Living PRAs (Probabilistic Risk Analysis) made easier with IRRAS (Integrated Reliability and Risk Analysis System)
[DE90-010938] N91-16395
ROBOT ARMS
Sensor-based automated docking of large payloads
[DE90-011020] N91-16044
Ultrasound and visual sensor feedback and fusion
[DE90-005280] N91-16369
Haptic perception with an articulated, sensate robot hand
[DE90-010195] N91-16371
Multi-criteria position and configuration optimization for redundant platform/manipulator systems
[DE90-010705] N91-16372
The PHD: A Planar, Harmonic Drive robot for joint torque control
[NASA-CR-187924] N91-16386
Modeling and control of a two-arm elastic robot in gravity N91-16389
Using MAPLE for symbolic computations in robotics
[DE90-010405] N91-16576
ROBOT CONTROL
Sensor-based automated docking of large payloads
[DE90-011020] N91-16044
The PHD: A Planar, Harmonic Drive robot for joint torque control
[NASA-CR-187924] N91-16386
Real-time vergence control for binocular robots
[AD-A228817] N91-16387
Modeling and control of a two-arm elastic robot in gravity N91-16389
ROBOT DYNAMICS
Ultrasound and visual sensor feedback and fusion
[DE90-005280] N91-16369
Haptic perception with an articulated, sensate robot hand
[DE90-010195] N91-16371
Multi-criteria position and configuration optimization for redundant platform/manipulator systems
[DE90-010705] N91-16372
Optimal positioning of redundant manipulator-platform systems for maximum task efficiency
[DE90-011061] N91-16378
The PHD: A Planar, Harmonic Drive robot for joint torque control
[NASA-CR-187924] N91-16386
Modeling and control of a two-arm elastic robot in gravity N91-16389
Camera space manipulation of a mobile robot N91-16390
ROBOT SENSORS
Sensor-based automated docking of large payloads
[DE90-011020] N91-16044
Ultrasound and visual sensor feedback and fusion
[DE90-005280] N91-16369
Haptic perception with an articulated, sensate robot hand
[DE90-010195] N91-16371
Design of a telerobotic controller with joint torque sensors using 2-port network theory
[NASA-CR-186543] N91-16379
ROBOTICS
Optimal positioning of redundant manipulator-platform systems for maximum task efficiency
[DE90-011061] N91-16378
NASA Laboratory telerobotic manipulator control system architecture
[NASA-CR-187751] N91-16385
Using MAPLE for symbolic computations in robotics
[DE90-010405] N91-16576
Implementation and experimentation with motion planning algorithms
[AD-A228278] N91-16612
ROBOTS
Experimentation and concept formation by an autonomous mobile robot
[DE90-003063] N91-16368
Time optimal trajectories for a two wheeled robot
[DE90-010335] N91-16376
NASA Laboratory telerobotic manipulator control system architecture
[NASA-CR-187751] N91-16385
Camera space manipulation of a mobile robot N91-16390
Implementation and experimentation with motion planning algorithms
[AD-A228278] N91-16612
ROCKET ENGINE CONTROL
Optimal rocket motor design and control for tactical missiles N91-16062
ROCKET ENGINE DESIGN
Optimal rocket motor design and control for tactical missiles N91-16062
ROCKET ENGINES
A transformer coupled semiconductor bridge igniter for low voltage ignition from a high voltage source
[DE90-009974] N91-16221
Long-range sound propagation: A review of some experimental data N91-16683
ROCKET FIRING
The University of Arizona program in solid propellants N91-16165
ROCKET FLIGHT
Magnetic measurements with fluxgate magnetometer in rocket flight
[DRI-4-90] N91-16061
ROCKET PROPELLANTS
Experimental studies of the properties of trihydrogen and tetrahydrogen
[AD-A228869] N91-16110
ROLL
Aeroservoelastic tailoring for lateral control enhancement N91-16025
Determination of shuttle orbiter center of gravity from flight measurements
[NASA-TM-102627] N91-16058
ROOM TEMPERATURE
Mechanical behavior of a SiC-fiber/Si3N4 composite
[AD-A228371] N91-16073
ROOMS
A review of the airborne sound insulation requirements for broadcasting studios and ancillary areas
[BBC-RD-1990/10] N91-16680
Proving experiments on an acoustic transmission suite and its reverberation room
[BBC-RD-1990/13] N91-16681
ROSSBY REGIMES
Stratiform clouds and their interaction with atmospheric motion N91-16506
A comparison of diagnostic and kinematic vertical motion fields associated with curved and straight jet streak adjustment processes
[AD-A227724] N91-16522
ROTARY WING AIRCRAFT
Rotorcraft application of advanced computational aerodynamics
[NASA-CR-187767] N91-15987
ROTATING DISKS
On the receptivity and non-parallel stability of travelling disturbances in rotating disk flow
[NASA-CR-187486] N91-15996
ROTATING FLUIDS
Circumfluous motion of a conductive liquid around solid objects in a magnetic field
[DE90-011335] N91-16265
Rotating Rayleigh-Benard convection: The Kueppers-Lortz transition
[DE91-004835] N91-16288
ROTATING LIQUIDS
Laboratory and theoretical models of planetary-scale instabilities and waves N91-16511
ROTATING MIRRORS
Diagnostic of the reaction behaviour of intensive high explosives under jet attack
[MBB-UA-1188-90-PUB] N91-16173
ROTATION
On a class of unsteady three-dimensional Navier Stokes solutions relevant to rotating disc flows: Threshold amplitudes and finite time singularities
[NASA-CR-187482] N91-15991
Modeling the dissipation rate in rotating turbulent flows
[NASA-CR-187485] N91-16306
A modular stiffness-based approach to rotating systems analysis N91-16400
The effects of the solid inner core and nonhydrostatic structure on the Earth's forced nutations and Earth tides N91-16417
Stratiform clouds and their interaction with atmospheric motion N91-16506
Laboratory and theoretical models of planetary-scale instabilities and waves N91-16511
Dynamical interactions of galaxy pairs N91-16930
The spiral-compact galaxy pair AM 2208-251: Computer simulations versus observations N91-16939
Stationary orbits of satellites of disk galaxies N91-16954
ROTORCRAFT AIRCRAFT
Evaluation of rotorwash characteristics for tiltrotor and tiltwing aircraft in hovering flight
[SCT-90RR-18] N91-15989
ROTORS
Aerodynamic surface pressure measurement in atmosphere and wind tunnel on a vertical axis wind turbine blade using pressure transducers N91-15980
A coupled rotor aeroelastic analysis utilizing advanced aerodynamic modeling N91-16006
Failure analysis of a main rotor pitch horn bolt located on the AH-1 Cobra helicopter
[AD-A227679] N91-16007
Applications of fuzzy theories to multi-objective system optimization
[NASA-CR-177573] N91-16012
Fiber-reinforced ceramic composites for Earth-to-orbit rocket engine turbines
[NASA-CR-185264] N91-16150
RUBBER
Manufacturing guide for elastomeric seals
[AD-A227511] N91-16383
RUBIDIUM ISOTOPES
Fundamental characteristics and applications of an inductively coupled plasma as an ion source for mass spectrometry
[DE90-011746] N91-16770
RULES
The asymptotic validity of sequential stopping rules for stochastic simulations
[AD-A228896] N91-16668
RUN TIME (COMPUTERS)
POSC: A Partitioning and Optimizing SISAL Compiler
[DE90-010679] N91-16577
Implementing sporadic servers in Ada
[AD-A226723] N91-16584
Hartstone benchmark results and analysis
[AD-A226817] N91-16587
Scheduler issues for real-time Ada
[AD-A227766] N91-16592
Tailoring an Ada runtime environment proof-of-concept
[AD-A227767] N91-16593
RUNWAYS
Evaluation procedure for reinforced concrete box culverts under airfield pavements
[AD-A227920] N91-16031

S

S MATRIX THEORY
Analytic Multi-Regge Theory and the Pomeron in QCD
[DE90-012153] N91-16737
S WAVES
Research in nonlinear water waves
[AD-A227948] N91-16292
Interacting nuclei in distant galaxies N91-16894
SAFETY
Assessment of battery technologies for electric vehicles. Volume 2, part 1: Appendices
[DE90-010907] N91-16227
Procedures for Quality Assurance Program
[DE90-010001] N91-16393
The use of contact lenses in the civil airman population
[AD-A227450] N91-16544
SAFETY DEVICES
Safety as a design goal for applications of microelectronic control systems
[REPT-23/90] N91-16253
SAFETY FACTORS
Paste extrudable explosives: Their history and their current status
[DE90-009438] N91-16159
Safe venting of hydrogen
[DE90-008964] N91-16174
Plate and butt-weld stresses beyond elastic limit, material and structural modeling
[NASA-TP-3075] N91-16413
SALINITY
Contemporary issues in solar pond research
[DE90-010094] N91-16436

Bio-optical profile data report coastal transition zone program, R/V Point Sur, June 15-28, 1987
[NASA-CR-187807] N91-16533
SAMARIUM
A photoemission study of samarium on silicon
[DE90-011509] N91-16799
SAMPLING
The role of quality assurance in the monitoring of terrestrial ecosystems
[DE90-010986] N91-16461
Bio-optical profile data report coastal transition zone program, R/V Thomas Washington, June 24 - July 21, 1988
[NASA-CR-187808] N91-16532
Bio-optical profile data report coastal transition zone program, R/V Point Sur, June 15-28, 1987
[NASA-CR-187807] N91-16533
SANDWICH STRUCTURES
Epitaxial growth and surface morphology of some metal and semiconductor structures N91-16824
SATELLITE ALTIMETRY
Analysis of satellite and Expendable Bathythermograph (XBT) data for the abrupt topography program
[AD-A228870] N91-16422
SATELLITE IMAGERY
Evaluation of the GOES 1-M normalization technique with the visible images of GOES-7
[AD-A227462] N91-16055
The multisensor image map 1:50,000 Rheinhessen N91-16434
SATELLITE INSTRUMENTS
Magnetic-field shielding of satellites from high-energy-electron environments
[DE90-010296] N91-16043
SATELLITE OBSERVATION
Investigation of a remote sensing technique for droplet effective radius N91-16420
Sahelian vegetation monitoring project
[BCRS-90-04] N91-16426
An inter-comparison of surface energy flux measurement systems used during FIFE, 1987
[NASA-CR-187699] N91-16472
Planetary circulations in the presence of transient and self-induced heating N91-16505
Tropical Pacific moisture variability N91-16509
The effect of latent heat release on synoptic-to-planetary wave interactions and its implication for satellite observations: Theoretical modeling N91-16514
The effect of latent heat release on synoptic-to-planetary scale wave interactions and implications for satellite observations: Observational study N91-16515
SATELLITE ORBITS
Geopotential harmonics of order 15 and 30 from analysis of 50 orbit determinations of 1967-102B
[RAE-TR-90029] N91-16035
SATELLITE SOUNDING
Tropical Pacific moisture variability N91-16509
SCALE MODELS
Design and fabrication of the NASA HL-20 full scale research model
[NASA-CR-187801] N91-16008
Scattering measurements on natural and model trees N91-16691
SCALING LAWS
Scaling laws for femtosecond laser-plasma interactions
[DE90-011496] N91-16769
SCANNING
Dynamic aspects of scanning surface instruments and microscopes
[ME-84] N91-16339
SCATTERING
Scattering center analysis of simple metallic objects
[DLR-FB-90-32] N91-16216
SCATTERING CROSS SECTIONS
Scattering and depolarization by rough terrain and sea: A unified full wave approach
[AD-A228295] N91-16201
Upper atmosphere IR radiation modeling and analysis
[AD-A227214] N91-16482
Parity violation and electron scattering
[DE90-010429] N91-16712
Testing of lead glass detectors for electron proof in the ELAN experiment
[BONN-IR-90-38] N91-16730
A Moller polarimeter for the extracted ELSA-ray
[BONN-IR-90-42] N91-16731
Measurement of the e+e- annihilation in mu+mu- pairs at the Z sup o resonance
[MPI-PAE/EXP.EL-231] N91-16732
Deep inelastic structure functions from electron scattering on hydrogen, deuterium, and iron at 0.6 GeV2 less than or equal to Q2 less than or equal to 30.0 GeV2
[DE90-010169] N91-16785
Resonant Compton scattering in models of gamma-ray burst sources. Part 2: Numerical modeling
[DE91-005268] N91-16982
SCATTERING FUNCTIONS
Scattering measurements on natural and model trees N91-16691
SCAVENGING
Numerical simulation of aerosol scavenging by ice-bearing convective clouds
[DE90-010676] N91-16457
Parameterization of aerosol scavenging in a convective cloud model
[DE90-010865] N91-16458
SCHEDULES
Application of fuzzy-Bayesian analysis to structural reliability
[NAL-TR-1063] N91-16396
SCHEDULING
Implementing sporadic servers in Ada
[AD-A226723] N91-16584
Scheduler issues for real-time Ada
[AD-A227766] N91-16592
Decentralized real-time scheduling
[AD-A227856] N91-16604
Calendar of selected aeronautical and space meetings: January 1991 onwards
[AGARD-CAL-91/1] N91-16833
SCHROEDINGER EQUATION
Nonlinear waves and inverse scattering
[AD-A228757] N91-16294
A new approach for the determination of electronic structure
[DE90-010479] N91-16713
Molecular crystals and localized vibrational states
[DE90-010602] N91-16786
Theoretical studies of electron transport in quantum-well structures
[AD-A228429] N91-16819
SCINTILLATION COUNTERS
Comparison of some x ray sensors for verification
[DE90-011990] N91-16323
Neutron measurements in search of cold fusion
[DE91-004855] N91-16778
SEA ROUGHNESS
Scattering and depolarization by rough terrain and sea: A unified full wave approach
[AD-A228295] N91-16201
SEA SURFACE TEMPERATURE
The vertical structure of the marine atmospheric boundary layer across a sea surface temperature front
[AD-A227931] N91-16525
Contents of the NASA ocean data system archive, version 11-90
[NASA-CR-187812] N91-16535
SEA WATER
Bio-optical profile data report coastal transition zone program, R/V Thomas Washington, June 24 - July 21, 1988
[NASA-CR-187808] N91-16532
Bio-optical profile data report coastal transition zone program, R/V Point Sur, June 15-28, 1987
[NASA-CR-187807] N91-16533
Bio-optical profile data report: Joint Global Ocean Flux Study, Hawaii Ocean Time-Series, HOT-3, R/V Moana Wave, 6-10 January 1989
[NASA-CR-187805] N91-16534
SEALS (STOPPERS)
Manufacturing guide for elastomeric seals
[AD-A227511] N91-16383
SEATS
Development of a crashworthy seat for commuter aircraft
[AD-A227486] N91-15999
SEAWEEDS
The usefulness of MSS pictures for mapping and biomass estimation of macro-algae and seaweed in the Eastern Scheldt
[BCRS-90-09] N91-16428
SEISMIC WAVES
Seismic signal processing optimized for a specific source and receiver
[DE90-010189] N91-16468
Seismic imaging for velocity and attenuation structure in geothermal fields
[DE90-010742] N91-16469
Attenuation of seismic waves in the near-source region
[AD-A226814] N91-16475
SEISMOGRAPHS
Seismic signal processing optimized for a specific source and receiver
[DE90-010189] N91-16468
SEISMOLOGY
Excursions to the base of the mantle N91-16491
Seismic structure of the upper mantle under the Pacific Ocean N91-16492
Air-ground interface: Surface waves, surface impedance and acoustic-to-seismic coupling coefficient N91-16685
Preliminary analysis of measured sound propagation over various seasonal snow covers N91-16687
SELF CONSISTENT FIELDS
Hyperfine interactions associated with iron substituted superconducting oxides
[DE90-010411] N91-16783
SELF LUBRICATION
A study of the formation and self-lubrication mechanisms of boric acid films on boric oxide coatings
[DE90-010115] N91-16137
SEMICONDUCTING FILMS
Comparative study of phosphosilicate glass on (100) silicon by furnace and rapid isothermal annealing
[NIAR-90-26] N91-16153
Image interpretation for transmission electron microscopy of thin semiconductor layers and interfaces
[ETN-91-98487] N91-16826
SEMICONDUCTOR DEVICES
Electrical properties of gas sensor materials
[ETN-91-98572] N91-16114
A transformer coupled semiconductor bridge igniter for low voltage ignition from a high voltage source
[DE90-009974] N91-16221
Comparison of some x ray sensors for verification
[DE90-011990] N91-16323
Low-cost CdZnTe devices for cascade cell application
[DE91-002116] N91-16444
Programmable surface acoustic wave detection in silicon: Design of programmable filters
[ETN-91-98568] N91-16746
Epitaxial growth and surface morphology of some metal and semiconductor structures N91-16824
SEMICONDUCTOR DIODES
Measurements of 1/f noise in a-Si:H pin diodes and thin-film-transistors
[DE90-011218] N91-16228
Effects of neutron fluence on the operating characteristics of diode lasers used in atomic frequency standards
[AD-A226763] N91-16352
Performance measurements of hybrid PIN diode arrays
[DE90-010308] N91-16790
SEMICONDUCTOR LASERS
Application of diode lasers to resonance ionization mass spectrometry
[DE91-000614] N91-16094
Modeling laser ignition of explosives and pyrotechnics: Effects and characterization of radiative transfer
[DE90-011052] N91-16161
Effects of neutron fluence on the operating characteristics of diode lasers used in atomic frequency standards
[AD-A226763] N91-16352
Two-dimensional simulation of quantum-well lasers including energy transport
[AD-A227487] N91-16356
Materials systems for 2- to 5-micrometers wavelength diode lasers
[AD-A228218] N91-16361
Optimization of a laser diode anemometry system
[LSTM-239/T/88] N91-16364
SEMICONDUCTORS (MATERIALS)
Investigation of a new concept in semiconductor microwave oscillators
[AD-A226785] N91-16235
Materials systems for 2- to 5-micrometers wavelength diode lasers
[AD-A228218] N91-16361
Programmable surface acoustic wave detection in silicon: Design of programmable filters
[ETN-91-98568] N91-16746
Applications of strained layer superlattices
[DE90-011204] N91-16793
Microwave-detected photoconductance decay
[DE90-011505] N91-16795
Photoreflectance studies of electronic transitions in quantum well structures under high pressure
[DE90-011583] N91-16801
Far-infared laser spectroscopy of two dimensional holes in strained-layer heterostructure and superlattices
[DE91-000027] N91-16805
Chemical beam epitaxy of ZnSe
[AD-A228045] N91-16817
SENSITIVITY
Characterization and development report for the SA2859: A silicon controlled rectifier
[DE90-010196] N91-16217
Multimedia Environmental Pollutant Assessment System (MEPAS) sensitivity analysis of computer codes
[DE90-010005] N91-16445
SENSORS
Electronic analogue for a biological nose
[ME-78] N91-16541

SENSORY PERCEPTION
Changes in somatosensory responsiveness in behaving monkeys
[AD-A226832] N91-16540
SEPARATED FLOW
Numerical simulation of separated flows around a wing section at steady and unsteady motion by a discrete vortex method N91-16268
Unsteady separation over maneuvering bodies
[AD-A226829] N91-16285
Experimental parametric study of jet vortex generators for flow separation control
[NASA-CR-187836] N91-16296
SEQUENCING
Pi: A parallel architecture interface for multi-model execution
[AD-A228345] N91-16640
SEQUENTIAL ANALYSIS
The asymptotic validity of sequential stopping rules for stochastic simulations
[AD-A228896] N91-16668
SERVOCONTROL
Design of a telerobotic controller with joint torque sensors using 2-port network theory
[NASA-CR-186543] N91-16379
SERVOMECHANISMS
Design of a telerobotic controller with joint torque sensors using 2-port network theory
[NASA-CR-186543] N91-16379
SETTLING
The effect of stratification on gravitational coagulation and settling of aerosols
[DE90-010153] N91-16079
SEYFERT GALAXIES
Multi-waveband observations of colliding galaxies N91-16868
Observational properties of compact groups of galaxies N91-16871
The environments of Markarian galaxies N91-16881
The complex nature of the Seyfert galaxy NGC 7592 N91-16882
New data on the peculiar galaxy MRK 273 N91-16887
Observations of multiple nucleus galaxies N91-16890
The double nucleus galaxies Mkn 423 and Mkn 739 N91-16891
Observational effects of interaction in the Seyfert galaxy NGC 7469 N91-16906
Galaxy interactions and strength of nuclear activity N91-16914
Signs of interaction of the NGC 1275 nucleus with the high-velocity system according to 0.7 sec seeing observations N91-16918
Correlations between environmental parameters and nuclear activity N91-16920
IC5063: A merger with a hidden luminous active nucleus N91-16923
A simulation survey of galaxy interactions N91-16936
A classification of the galaxy groups N91-16949
SHAPES
Evaluation of the HULL and SHARC hydrocodes in simulating the reflection of Mach 2.12 non-decaying shock on wedges of various angles
[AD-A227581] N91-16287
SHEAR FLOW
Analytical and numerical studies in flow development
[DE90-010424] N91-16258
Simulation of excited shear flows N91-16270
Modeling the dissipation rate in rotating turbulent flows
[NASA-CR-187485] N91-16306
Shear thickening of concentrated dispersions
[ETN-91-98477] N91-16308
Theory for modeling the equatorial evening ionosphere and the origin of the shear in the horizontal plasma flow
[MPE-PREPRINT-185] N91-16495
SHEAR LAYERS
Numerical simulation of separated flows around a wing section at steady and unsteady motion by a discrete vortex method N91-16268
SHEAR PROPERTIES
Correlation between the elastic-shear-instability-mechanism and empirical criteria for irradiation-induced amorphization
[DE91-004481] N91-16810
SHEAR STRESS
Numerical study of a three-dimensional turbulent boundary layer
[AD-A227835] N91-16291
SHOCK HEATING
Numerical simulations of unsteady shock reflection processes by a ramp N91-16267
SHOCK SIMULATORS
Small scale shock tube experiments using a computer controlled active rarefaction wave eliminator
[AD-A227507] N91-16029
SHOCK TUBES
Small scale shock tube experiments using a computer controlled active rarefaction wave eliminator
[AD-A227507] N91-16029
SHOCK WAVE INTERACTION
Hypersonic shock/boundary-layer interaction database
[NASA-CR-187769] N91-15986
SHOCK WAVE PROPAGATION
ANEOS: Analytic equations of state for shock physics codes input manual
[DE90-010196] N91-16575
SHOCK WAVES
Autcignition and flameholding in a cylindrical scramjet combustor
[NAL-TR-1067] N91-16102
Evaluation of the HULL and SHARC hydrocodes in simulating the reflection of Mach 2.12 non-decaying shock on wedges of various angles
[AD-A227581] N91-16287
Unstationary shock and boundary layer phenomena at profiles and in a plane grid by transonic flow
[ETN-91-98557] N91-16311
BLAST2D computations of the reflection of planar shocks from wedge surfaces with comparison to SHARC and STEALTH results
[AD-A227261] N91-16589
The role of shocks in NGC 6240 N91-16921
SHORT WAVE RADIATION
Tactical HF field expedient antenna performance, volume 1
[AD-A228057] N91-16198
SIALON
Gelcasting of sub-micron alumina, sialon, and silicon nitride powders
[DE91-000618] N91-16145
SIDE-LOOKING RADAR
Detection of soil moisture using X-band SLAR records in a sandy area
[BCRS-90-08] N91-16427
SIDELOBE REDUCTION
Analysis of the performance of a single-auxiliary sidelobe canceller
[RSRE-MEMO-4375] N91-16193
SIDELOBES
Analysis of the performance of a single-auxiliary sidelobe canceller
[RSRE-MEMO-4375] N91-16193
Statistically thinned arrays with quantized element weights
[AD-A227965] N91-16196
SIGNAL DETECTION
A ring laser gyroscope with optical subtraction N91-16335
SIGNAL DETECTORS
Operating characteristics for weighted energy detector with Gaussian signals
[AD-A226851] N91-16673
Utilization of polymer viscoelastic properties in acoustic wave sensor applications
[DE90-010534] N91-16676
SIGNAL ENCODING
Noise reduction using low weight and constant weight coding techniques
[AD-A228346] N91-16244
SIGNAL MEASUREMENT
Scattering center analysis of simple metallic objects
[DLR-FB-90-32] N91-16216
SIGNAL PROCESSING
Some applications of probability and statistics in communication theory and signal processing
[AD-A226869] N91-16184
Numeric and symbolic signal processing for very high subclutter visibility
[AD-A228812] N91-16207
An experimental demonstration of high-resolution Doppler processing
[AD-A228813] N91-16208
Intra-Pulse Frequency Diversity (IPFD) lab demonstration
[AD-A228814] N91-16209
Seismic signal processing optimized for a specific source and receiver
[DE90-010189] N91-16468
Implementation of the phase gradient algorithm
[DE90-012160] N91-16579
Matrix algorithms in signal processing
[AD-A228851] N91-16625
IEEE International Symposium on Information Theory
[AD-A228239] N91-16842
SIGNAL TO NOISE RATIOS
Operating characteristics for weighted energy detector with Gaussian signals
[AD-A226851] N91-16673
Motional Stark effect polarimetry for the current profile diagnostic in D3-D
[DE90-012071] N91-16773
SIGNAL TRANSMISSION
A low-cost infrared telemetry system for kilohertz-bandwidth data acquisition
[DE90-010616] N91-16042
Effects of large-scale wind driven turbulence on sound propagation N91-16704
SIGNATURES
Interacting nuclei in distant galaxies N91-16894
Probing the tides in interacting galaxy pairs N91-16932
SILANES
A numerical study of silane combustion
[DE90-006002] N91-16080
SILICATES
Comparative study of phosphosilicate glass on (100) silicon by furnace and rapid isothermal annealing
[NIAR-90-26] N91-16153
SILICON
Comparative study of phosphosilicate glass on (100) silicon by furnace and rapid isothermal annealing
[NIAR-90-26] N91-16153
High-purity silicon soft x ray sensor arrays
[ETN-91-98484] N91-16338
AGS silicon gold collisions measured in the E-810 TPC (Time Projection Chamber)
[DE90-010015] N91-16733
V(sup 0) production with 14.5 GeV/c silicon beams
[DE90-010014] N91-16747
Modeling the performance of water and liquid gallium cooled x ray optical components: A comparison with experiment
[DE90-010460] N91-16784
A photoemission study of samarium on silicon
[DE90-011509] N91-16799
SILICON CARBIDES
Mechanical behavior of a SiC-fiber/Si3N4 composite
[AD-A228371] N91-16073
Effects of high pressure nitrogen on the thermal stability of SiC fibers
[NASA-TM-103245] N91-16075
Fiber-reinforced ceramic composites for Earth-to-orbit rocket engine turbines
[NASA-CR-185264] N91-16150
Research and development on advanced silicon carbide thin film growth techniques and fabrication of high power and microwave frequency silicon carbide-based device
[AD-A228758] N91-16246
SILICON CONTROLLED RECTIFIERS
Characterization and development report for the SA2859: A silicon controlled rectifier
[DE90-010196] N91-16217
SILICON FILMS
Characterization of GaAs/Si interface structure by x ray diffraction
[DE91-004769] N91-16811
SILICON NITRIDES
Mechanical behavior of a SiC-fiber/Si3N4 composite
[AD-A228371] N91-16073
Gelcasting of sub-micron alumina, sialon, and silicon nitride powders
[DE91-000618] N91-16145
SIMD (COMPUTERS)
Wakefield calculations on parallel computers
[DE90-009712] N91-16632
SIMILARITY THEOREM
Analysis of multivariable control systems in the presence of structured uncertainties
[AD-A227976] N91-16665
SIMULATION
Observation simulation experiments with regional prediction models N91-16502
Global-scale, intraseasonal fluctuations of diabatic forcing of the atmosphere N91-16508
Distributed algorithm simulation using input/output automata
[AD-A228113] N91-16611
Experiments with initial transient deletion for parallel, replicated steady-state simulations
[AD-A227879] N91-16636
A simulation survey of galaxy interactions N91-16936
Simulations of gas clouds in interacting galaxies N91-16961
Wing galaxies: A formation mechanism of the clumpy irregular galaxy Markarian 297 N91-16963
SIMULATORS
Two-dimensional simulation of quantum-well lasers including energy transport
[AD-A227487] N91-16356
SINGLE CRYSTALS
Thin film single crystal growth of a nonlinear optical polymer
[AD-A227692] N91-16807
Domain boundaries formed during epitactical growth of alpha-Al2O3
[DE91-005018] N91-16814

From low to high Tc: An ultrasonic investigation of niobium single crystal and YBaCuO superconducting thin films with surface acoustic waves N91-16822

SINGULARITY (MATHEMATICS)
Adaptive mesh refinement for meshes with singular elements N91-16406

SINTERING
Microwave sintering of fuel cell materials [DE90-011643] N91-16143
Sintering stress and microstructure in ceramic powder compacts [DE91-004415] N91-16149
Method of making contamination-free ceramic bodies [NASA-CASE-LEW-14984-1] N91-16152
Microstructures and dc critical currents in textured Y-Ba-Cu-oxides [DE91-000895] N91-16803

SIZE (DIMENSIONS)
Specimen size effects in Charpy impact testing [DE90-011369] N91-16399

SKEWNESS
The reflection and transmission properties of a triple band dichroic surface [NASA-CR-187776] N91-16191

SKIN (ANATOMY)
Heat transfer in clothing during heat radiation [IZF-1990-B-2] N91-16569

SKY SURVEYS (ASTRONOMY)
Pairs of galaxies in low density regions of a combined redshift catalog N91-16860
Geometrical parameters of E+S pairs N91-16865
An atlas of mixed-morphology pairs N91-16866
Isolated galaxies, pairs, and groups of galaxies N91-16878
Dumb-bell galaxies in southern clusters: Catalog and preliminary statistical results N91-16896
A multiwavelength survey of interacting galaxies N91-16898
Radio emission in peculiar galaxies N91-16907

SLEEP DEPRIVATION
Study of pilot vigilance during long range flight N91-16561

SLENDER WINGS
Wind tunnel tests on flutter control of a high-aspect-ratio cantilevered wing: Control with leading-edge and trailing-edge control surfaces [NAL-TR-1070] N91-15982
The Proceedings of the Symposium on Mechanics for Space Flight 1989 [ISAS-SP-12] N91-16266
Unsteady vortex lattice calculation of the flow around a slender delta wing N91-16272

SLIDING
Detection of solid lubricant film failure during sliding by vibration monitoring [NAL-TR-1060] N91-16384

SLOPES
A study of the surface energy balance on slopes in a tallgrass prairie [NASA-CR-187698] N91-16473

SLOTTED WIND TUNNELS
Investigation of transonic flow over segmented slotted wind tunnel wall with mass transfer [NASA-CR-187760] N91-15981
User's guide to PANCOR: A panel method program for interference assessment in slotted-wall wind tunnels [NASA-CR-187479] N91-16033

SLURRIES
The University of Arizona program in solid propellants N91-16165

SMALL PERTURBATION FLOW
On the receptivity and non-parallel stability of travelling disturbances in rotating disk flow [NASA-CR-187486] N91-15996
Scattering and depolarization by rough terrain and sea: A unified full wave approach [AD-A228295] N91-16201

SMOKE
Parameterization of aerosol scavenging in a convective cloud model [DE90-010865] N91-16458

SMOOTHING
Smoothing and scaling airfoil coordinates on a personal computer [DE89-000878] N91-16582

SNOW
Preliminary analysis of measured sound propagation over various seasonal snow covers N91-16687
Using a fast Fourier method to model sound propagation in a stratified atmosphere over a stratified porous-elastic ground N91-16692

SNOW COVER
Preliminary analysis of measured sound propagation over various seasonal snow covers N91-16687

SOBOLEV SPACE
The stationary exterior three dimensional Navier-Stokes problem of viscous flow past a body in anisotropically weighted Sobolev spaces [REPT-110] N91-16314

SOCIAL FACTORS
Information technology policies: A four country comparative study N91-16840

SODAR
The value of on-site sodar data in regional modeling [DE90-009921] N91-16498
Comparison of FFP predictions with measurements of a low-frequency signal propagated in the atmosphere N91-16698

SODIUM NITRATES
Parametric study of electrostatically charged sprays [DE90-010580] N91-16262

SOFTWARE ENGINEERING
Understanding the adoption of Ada: Results of an industry survey [AD-A226725] N91-16585
Annotated bibliography of software engineering laboratory literature [NASA-TM-103415] N91-16602
Practical aspects of repository operations for the Software Technology for Adaptable, Reliable Systems (STARS) program [AD-A228455] N91-16617
Briefing DTD user's guide for the Software Technology for Adaptable, Reliable Systems (STARS) program [AD-A228473] N91-16618
DTD creation for the Software Technology for Adaptable, Reliable Systems (STARS) program [AD-A228475] N91-16619
Supporting reuse and evolution in software design [AD-A228782] N91-16624
Real-time system specification and verification [AD-A227682] N91-16634

SOFTWARE TOOLS
Annotated bibliography of software engineering laboratory literature [NASA-TM-103415] N91-16602
The Assistant for Specifying the Quality Software (ASQS). Volume 1: Operational concept document [AD-A227893] N91-16608
The Assistant for Specifying the Quality Software (ASQS). Volume 2: User's manual. Volume 2 [AD-A227894] N91-16609
Distributed algorithm simulation using input/output automata [AD-A228113] N91-16611
XSHELL: A general purpose expert system shell [AD-A228454] N91-16616

SOIL MAPPING
The dielectric properties of wet soils [BCRS-90-13] N91-16429

SOIL MOISTURE
Detection of soil moisture using X-band SLAR records in a sandy area [BCRS-90-08] N91-16427
The dielectric properties of wet soils [BCRS-90-13] N91-16429

SOILS
The dielectric properties of wet soils [BCRS-90-13] N91-16429
Subsurface science program: Program overview and research abstracts [DE90-010321] N91-16456

SOLAR CELLS
High efficiency silicon concentrator solar cells N91-16441
Low-cost CdZnTe devices for cascade cell application [DE91-002116] N91-16444

SOLAR COOLING
Colorado State University program for developing, testing, evaluating and optimizing solar heating and cooling systems [DE90-010107] N91-16435
Solar refrigeration: Evaluation of technical options and design of a solar-generator-adsorber for a novel adsorption refrigerator, volumes 1 and 2 N91-16440

SOLAR CYCLES
Activities and accomplishments of the Center for Applied Solar Physics, 1987 - 1990 [AD-A228773] N91-16980

SOLAR ENERGY
Image-based terrain modeling with thematic mapper N91-16418

SOLAR FLARES
Activities and accomplishments of the Center for Applied Solar Physics, 1987 - 1990 [AD-A228773] N91-16980

SOLAR FLUX
Variability of latent and sensible heat fluxes over the oceans N91-16531

SOLAR HEATING
Colorado State University program for developing, testing, evaluating and optimizing solar heating and cooling systems [DE90-010107] N91-16435

SOLAR INTERIOR
Activities and accomplishments of the Center for Applied Solar Physics, 1987 - 1990 [AD-A228773] N91-16980

SOLAR MAGNETIC FIELD
Activities and accomplishments of the Center for Applied Solar Physics, 1987 - 1990 [AD-A228773] N91-16980

SOLAR PHYSICS
Space research in the Federal Republic of Germany, 1988 and 1989 [ETN-91-98514] N91-16849
Activities and accomplishments of the Center for Applied Solar Physics, 1987 - 1990 [AD-A228773] N91-16980

SOLAR PONDS (HEAT STORAGE)
Contemporary issues in solar pond research [DE90-010094] N91-16436

SOLAR RADIATION
Solar refrigeration: Evaluation of technical options and design of a solar-generator-adsorber for a novel adsorption refrigerator, volumes 1 and 2 N91-16440

SOLAR SPECTRA
Activities and accomplishments of the Center for Applied Solar Physics, 1987 - 1990 [AD-A228773] N91-16980

SOLAR SYSTEM
Software for aerospace education: A bibliography, 2nd edition [NASA-PED-106-ED-2] N91-16601

SOLAR WIND
The magnetospheric response to 8-minute period strong-amplitude upstream pressure variations [AD-A228038] N91-16489

SOLDERS
Inelastic strain analysis of solder joint in NASA fatigue specimen [NASA-CR-187864] N91-16132

SOLID CRYOGENS
Ionic solid hydrogen fuel: Production and properties of hydrogen ion and energetic neutral clusters [AD-A227683] N91-16172

SOLID ELECTROLYTES
Evaluation of novel solid electrolyte materials [DE90-011164] N91-16231
Studies of the fundamentals of solids state batteries [AD-A228772] N91-16247

SOLID LUBRICANTS
A study of the formation and self-lubrication mechanisms of boric acid films on boric oxide coatings [DE90-010115] N91-16137
Detection of solid lubricant film failure during sliding by vibration monitoring [NAL-TR-1060] N91-16384

SOLID MECHANICS
Void nucleation in nonlinear solid mechanics [AD-A228890] N91-16410

SOLID PHASES
Cluster formation in laser-induced ablation and evaporation of solids observed by laser ionization time-of-flight mass spectrometry and scanning tunneling microscopy [DE90-010876] N91-16344

SOLID PROPELLANT COMBUSTION
Introouction to the problem N91-16164

SOLID PROPELLANT ROCKET ENGINES
Optimal rocket motor design and control for tactical missiles N91-16062
Space Shuttle Flight Support Motor no. 1 (FSM-1) [NASA-CR-184078] N91-16064
Composite Solid Propellant Predictability and Quality Assurance [NASA-CR-186404] N91-16163

SOLID PROPELLANTS
Introduction to the problem N91-16164
The University of Arizona program in solid propellants N91-16165

SOLID ROCKET PROPELLANTS
Inverse gas chromatography [AD-A227677] N91-16099
Composite Solid Propellant Predictability and Quality Assurance [NASA-CR-186404] N91-16163

SOLID STATE
Evaluation of novel solid electrolyte materials [DE90-011164] N91-16231
Studies of the fundamentals of solids state batteries [AD-A228772] N91-16247
High Tc oxide solid state reaction kinetics via complex impedance spectroscopy [DE90-011178] N91-16792

SOLID STATE DEVICES
Electrical properties of gas sensor materials
[ETN-91-98572] N91-16114
SOLID STATE PHYSICS
Solid state research
[NASA-CR-187871] N91-16816
SOLID SURFACES
Models for surface scattering from solids and liquids
[RSRE-MEMO-3699] N91-16192
SOLID-SOLID INTERFACES
A time-domain finite-element method for the computation of three-dimensional acoustic wave fields in inhomogeneous fluids and solids
[ETN-91-98485] N91-16710
Image interpretation for transmission electron microscopy of thin semiconductor layers and interfaces
[ETN-91-98487] N91-16826
SOLIDIFICATION
Phase selection and processing of high temperature intermetallic alloys
[AD-A227910] N91-16129
Test methods for evaluating hot cracking: Review and perspective
[DE90-009820] N91-16397
Theory of non-equilibrium growth
[DE91-004159] N91-16725
SOLIDS
Circumfluous motion of a conductive liquid around solid objects in a magnetic field
[DE90-011335] N91-16265
Time-temperature response of multiphase viscoelastic solids through numerical analysis N91-16401
Dynamic crack propagation in elastic-plastic solids N91-16402
A new perturbation theory of solids and fluids and its applications to high-pressure melting problems
[DE90-011502] N91-16829
SOLITARY WAVES
Selective excitation, relaxation, and energy channeling in molecular systems
[DE90-010793] N91-16717
SOLUBILITY
Gas solubility in glassy polymers: A correlation with excess enthalpy
[AD-A228202] N91-16155
SOLVATION
The development of improved capillary supercritical fluid chromatography and mass spectrometry
[AD-A228535] N91-16107
SOLVENTS
Hanging drop crystal growth apparatus
[NASA-CASE-MFS-26061-1] N91-16815
SORPTION
Gas solubility in glassy polymers: A correlation with excess enthalpy
[AD-A228202] N91-16155
SOUND DETECTING AND RANGING
Turbulence and diffusion in the atmospheric boundary layer
[DE90-011582] N91-16471
SOUND FIELDS
Full field visualization of surface and bulk acoustic waves
[AD-A227676] N91-16678
Effects of large-scale wind driven turbulence on sound propagation N91-16704
A time-domain finite-element method for the computation of three-dimensional acoustic wave fields in inhomogeneous fluids and solids
[ETN-91-98485] N91-16710
SOUND PRESSURE
Meteorological effects on long-range outdoor sound propagation N91-16696
New correction procedures for the fast field program which extend its range N91-16699
Scattering of sound by atmospheric turbulence predictions in a refractive shadow zone N91-16703
SOUND PROPAGATION
Proving experiments on an acoustic transmission suite and its reverberation room
[BBC-RD-1990/13] N91-16681
Fourth International Symposium on Long-Range Sound Propagation
[NASA-CP-3101] N91-16682
Long-range sound propagation: A review of some experimental data N91-16683
Preliminary analysis of measured sound propagation over various seasonal snow covers N91-16687
Long-distance sound propagation over discontinuous impedances N91-16688
Using a fast Fourier method to model sound propagation in a stratified atmosphere over a stratified porous-elastic ground N91-16692
The correction of infrasound signals for upper atmospheric winds N91-16695
Meteorological effects on long-range outdoor sound propagation N91-16696
Comparison of FFP predictions with measurements of a low-frequency signal propagated in the atmosphere N91-16698
New correction procedures for the fast field program which extend its range N91-16699
Scattering of sound by atmospheric turbulence predictions in a refractive shadow zone N91-16703
Effects of large-scale wind driven turbulence on sound propagation N91-16704
SOUND TRANSDUCERS
A low cost end-fire acoustic radiator
[ISVR-TR-188] N91-16705
SOUND TRANSMISSION
A review of the airborne sound insulation requirements for broadcasting studios and ancillary areas
[BBC-RD-1990/10] N91-16680
Proving experiments on an acoustic transmission suite and its reverberation room
[BBC-RD-1990/13] N91-16681
Exponential ground impedance models and their interpretation N91-16686
SOUND WAVES
Acoustical and dynamic mechanical characterization of fiber-matrix interface bonds in ceramic composites
[DE90-010949] N91-16066
Fourth moments of acoustic waves forward scattered by a rough ocean surface
[AD-A227469] N91-16529
Full field visualization of surface and bulk acoustic waves
[AD-A227676] N91-16678
Wind turbine acoustics
[NASA-TP-3057] N91-16679
Long-range sound propagation: A review of some experimental data N91-16683
Air-ground interface: Surface waves, surface impedance and acoustic-to-seismic coupling coefficient N91-16685
Preliminary analysis of measured sound propagation over various seasonal snow covers N91-16687
Effect of wind and temperature gradients on received acoustic energy N91-16697
A noise assessment and prediction system N91-16702
Effects of large-scale wind driven turbulence on sound propagation N91-16704
A low cost end-fire acoustic radiator
[ISVR-TR-188] N91-16705
SCATSPHERE2: A computation for the plane-wave scattering from a submerged, elastic, spherical, evacuated or fluid-filled, thin shell
[AD-A228867] N91-16709
A time-domain finite-element method for the computation of three-dimensional acoustic wave fields in inhomogeneous fluids and solids
[ETN-91-98485] N91-16710
SOUTHERN HEMISPHERE
Multi-color imaging of selected southern interacting galaxies N91-16867
SOUTHERN SKY
Pairs of galaxies in low density regions of a combined redshift catalog N91-16860
SPACE DENSITY
Observational properties of compact groups of galaxies N91-16871
SPACE FLIGHT
Whole body cleansing agent
[NASA-CASE-MSC-21589-1] N91-16566
SPACE HABITATS
Common approach for planetary habitation systems implementation
[MBB-UO-0115-90-PUB] N91-16570
SPACE LABORATORIES
NASA Laboratory telerobotic manipulator control system architecture
[NASA-CR-187751] N91-16385
SPACE LAW
JPRS report: Science and technology. USSR: Space
[JPRS-USP-89-006] N91-16036
SPACE MISSIONS
Introduction to the problem N91-16164
Activities report of the Space Research Organization Netherlands
[ETN-91-98473] N91-16848
SPACE PERCEPTION
Limits of human visual discrimination: Toward a general model of visual geometry
[AD-A226826] N91-16548
SPACE PLASMAS
Numerical examinations of Kelvin-Helmholtz instability in resistive compressible magnetohydrodynamics
[MPE-221] N91-16782
Multiple-photon Compton scattering in a strong magnetic field: Cross-sections and radiative transport N91-16852
Cool infalling gas and its interaction with the hot ISM of elliptical galaxies N91-16915
SPACE PROBES
Aerospace vehicle design, spacecraft section. Volume 1: Project groups 1-4 --- unmanned probe to Pluto
[NASA-CR-186841] N91-16045
PFERD Mission: Pluto flyby exploration/research design N91-16046
Intrepid: A mission to Pluto N91-16047
Project Cerberus: Flyby mission to Pluto N91-16048
OPTIC: Orbiting Plutonian Topographic Image Craft proposal for an unmanned mission to Pluto N91-16049
Aerospace vehicle design, spacecraft section. Volume 2: Project groups 5-7 --- unmanned probe to Pluto
[NASA-CR-186842] N91-16050
Mission management, planning, and cost: PULSE Attitude And Control Systems (AACS) N91-16051
The Copernicus project N91-16052
The Phoenix Pluto Probe N91-16053
SPACE SHUTTLE ORBITERS
Determination of shuttle orbiter center of gravity from flight measurements
[NASA-TM-102627] N91-16058
SPACE SHUTTLE PAYLOADS
ASTROMAG coil cooling study
[NASA-CR-187768] N91-16813
SPACE SHUTTLES
Debris/Ice/TPS assessment and photographic analysis for shuttle mission STS-41
[NASA-TM-103814] N91-16041
Space Shuttle Flight Support Motor no. 1 (FSM-1)
[NASA-CR-184078] N91-16064
SPACE STATION PAYLOADS
Space Station Freedom resource allocation accommodation of technology payload requirements
[NASA-TM-102766] N91-16832
SPACE STATIONS
Common approach for planetary habitation systems implementation
[MBB-UO-0115-90-PUB] N91-16570
ASTROMAG coil cooling study
[NASA-CR-187768] N91-16813
Space Station Freedom resource allocation accommodation of technology payload requirements
[NASA-TM-102766] N91-16832
SPACE TRANSPORTATION
Fiber-reinforced ceramic composites for Earth-to-orbit rocket engine turbines
[NASA-CR-185264] N91-16150
SPACE TRANSPORTATION SYSTEM
Design and fabrication of the NASA HL-20 full scale research model
[NASA-CR-187801] N91-16006
Determination of shuttle orbiter center of gravity from flight measurements
[NASA-TM-102627] N91-16058
SPACE TRANSPORTATION SYSTEM FLIGHTS
Debris/Ice/TPS assessment and photographic analysis for shuttle mission STS-41
[NASA-TM-103814] N91-16041
Determination of shuttle orbiter center of gravity from flight measurements
[NASA-TM-102627] N91-16058
Space Shuttle Flight Support Motor no. 1 (FSM-1)
[NASA-CR-184078] N91-16064
SPACEBORNE ASTRONOMY
Space research in the Federal Republic of Germany, 1988 and 1989
[ETN-91-98514] N91-16849
SPACEBORNE EXPERIMENTS
The space flights: Second German Spacelab mission D-2 and Mir 1992
[REPT-25/90] N91-16034
Laboratory and theoretical models of planetary-scale instabilities and waves N91-16511
Theoretical and experimental studies of baroclinic processes N91-16512
SPACEBORNE LASERS
Definition and preliminary design of the Laser Atmospheric Wind Sounder (LAWS) phase 1. Volume 1: Executive summary
[NASA-CR-184071] N91-16332
Definition and preliminary design of the Laser Atmospheric Wind Sounder (LAWS) phase 1. Volume 2
[NASA-CR-184072] N91-16333
SPACECRAFT CONSTRUCTION MATERIALS
Metallurgical design of novel metal matrix composites for aerospace applications
[ETN-91-98573] N91-16077
SPACECRAFT CONTROL
The NASA controls-structures interaction technology program
[NASA-TM-102752] N91-16057
A decentralized linear quadratic control design method for flexible structures
[NASA-CR-187860] N91-16059

SPACECRAFT DESIGN
Design and fabrication of the NASA HL-20 full scale research model
[NASA-CR-187801] N91-16008
General designer describes Buran flight control, autopilot systems N91-16039
Aerospace vehicle design, spacecraft section. Volume 1: Project groups 1-4 — unmanned probe to Pluto
[NASA-CR-186841] N91-16045
PFERD Mission: Pluto flyby exploration/research design N91-16046
Intrepid: A mission to Pluto N91-16047
Project Cerberus: Flyby mission to Pluto N91-16048
OPTIC: Orbiting Plutonian Topographic Image Craft proposal for an unmanned mission to Pluto N91-16049
Aerospace vehicle design, spacecraft section. Volume 2: Project groups 5-7 — unmanned probe to Pluto
[NASA-CR-186842] N91-16050
Mission management, planning, and cost: PULSE Attitude And Control Systems (AACS) N91-16051
The Copernicus project N91-16052
The Phoenix Pluto Probe N91-16053
The NASA controls-structures interaction technology program
[NASA-TM-102752] N91-16057

SPACECRAFT DOCKING
Sensor-based automated docking of large payloads
[DE90-011020] N91-16044

SPACECRAFT EQUIPMENT
The Proceedings of the Symposium on Mechanics for Space Flight 1989
[ISAS-SP-12] N91-16266
Development of a two-phase cold plate N91-16277

SPACECRAFT GUIDANCE
Optimization and guidance of flight trajectories for the national aerospace plane
[NASA-CR-187837] N91-16010

SPACECRAFT STRUCTURES
The NASA controls-structures interaction technology program
[NASA-TM-102752] N91-16057

SPACECRAFT TRAJECTORIES
Optimization and guidance of flight trajectories for the national aerospace plane
[NASA-CR-187837] N91-16010

SPACECREWS
Design and fabrication of the NASA HL-20 full scale research model
[NASA-CR-187801] N91-16008

SPACELAB
The space flights: Second German Spacelab mission D-2 and Mir 1992
[REPT-25/90] N91-16034
Laboratory and theoretical models of planetary-scale instabilities and waves N91-16511
Theoretical and experimental studies of baroclinic processes N91-16512

SPALLATION
The radiation hardness test facility
[RAL-90-065] N91-16030

SPATIAL DISTRIBUTION
Spatial and temporal climate variations influencing medium-range temperature predictions over south-central European Russia
[AD-A228623] N91-16527
Spatial distributions of the emitting species in a penning surface-plasma source
[DE90-011996] N91-16772
What is the number of spiral galaxies in compact groups N91-16874
Statistics of associations among IR galaxies N91-16909
Origin of regularities in the redshift distributions of distant galaxies and quasars
[DE91-004848] N91-16968

SPATIAL RESOLUTION
Merging panchromatic and multispectral images for enhanced image analysis
[AD-A227902] N91-16421

SPECIFICATIONS
Smoothing and scaling airfoil coordinates on a personal computer
[DE89-000878] N91-16582
Kernal facilities definition, Kernel version 3.0
[AD-A228027] N91-16610

SPECIMEN GEOMETRY
Specimen size effects in Charpy impact testing
[DE90-011369] N91-16399

SPECKLE PATTERNS
The development of laser speckle velocimetry for the study of vortical flows
[NASA-CR-187756] N91-16289

SPECTRA
Wind turbine acoustics
[NASA-TP-3057] N91-16679
The interacting pair Mkn 305/306 N91-16864
The double nucleus galaxies Mkn 423 and Mkn 739 N91-16891
A multiwavelength survey of interacting galaxies N91-16898

SPECTRAL EMISSION
Analysis of emission data from a Perkin-Elmer 1710 FTIR spectrometer
[AD-A227759] N91-16331

SPECTRAL REFLECTANCE
Image-based terrain modeling with thematic mapper N91-16418
Investigation of a remote sensing technique for droplet effective radius N91-16420

SPECTROMETERS
Rotational temperature estimation of CO at high temperatures by graphical methods using FTIR spectrometry
[AD-A228370] N91-16105
Measurements of scattering processes in negative ion-atom collisions
[DE90-010666] N91-16715
Properties of superdeformed bands in the A = 194 region
[DE90-011482] N91-16798
ASTROMAG coil cooling study
[NASA-CR-187768] N91-16813

SPECTROPHOTOMETERS
Development of liquid xenon imaging gamma-ray spectrophotometers
[AD-A227575] N91-16740

SPECTROSCOPY
An approximation to true peak absorbance from observed peak absorbance for gas phase Fourier transform spectroscopy
[AD-A228357] N91-16104
High Tc oxide solid state reaction kinetics via complex impedance spectroscopy
[DE90-011178] N91-16792
Multi-color imaging of selected southern interacting galaxies N91-16867
The double nucleus galaxies Mkn 423 and Mkn 739 N91-16891
Radio loud far-infrared galaxies N91-16902
The kinematics and morphology of NGC 520: One, two, or three galaxies N91-16908
Probing the tides in interacting galaxy pairs N91-16932
The spiral-compact galaxy pair AM 2208-251: Computer simulations versus observations N91-16939

SPECTRUM ANALYSIS
The use of window functions and Kalman filtering in spectral estimation
[AD-A227482] N91-16236
Analysis of emission data from a Perkin-Elmer 1710 FTIR spectrometer
[AD-A227759] N91-16331
Two-dimensional simulation of quantum-well lasers including energy transport
[AD-A227487] N91-16356
New data on the peculiar galaxy MRK 273 N91-16887

SPEECH
A trellis-searched APC (Adaptive Predictive Coding) speech coder
[DE91-000866] N91-16581

SPHERES
MmB: A new class of accurate high resolution schemes for conservation laws in two dimensions N91-16275
Void nucleation in nonlinear solid mechanics
[AD-A228890] N91-16410

SPHERICAL SHELLS
Laboratory and theoretical models of planetary-scale instabilities and waves N91-16511

SPHERICAL WAVES
Air-ground interface: Surface waves, surface impedance and acoustic-to-seismic coupling coefficient N91-16685

SPIN
Properties of superdeformed bands in the A = 194 region
[DE90-011482] N91-16798

SPIN-LATTICE RELAXATION
Comparison of hydrogen diffusion in Ti2PdH(x) to the behavior for Ti2CuH(x) and Zr2PdH(x)
[DE91-002711] N91-16808

SPINEL
Physico-chemical investigations on Co-Mn-oxide spinels
[ETN-91-98476] N91-16825

SPIRAL GALAXIES
Using tilted-ring models and numerical hydrodynamics to study the structure, kinematics and dynamics of HI disks in galaxies N91-16851
An atlas of mixed-morphology pairs N91-16866
Blue ellipticals in compact groups N91-16873
What is the number of spiral galaxies in compact groups N91-16874
Galaxy interactions and star formation: Results of a survey of global H-alpha emission in spiral galaxies in 8 clusters N91-16905
On leading spiral arms in close pairs of galaxies N91-16935
A simulation survey of galaxy interactions N91-16936
M51's spiral structure N91-16938
Gas flows in S-E binary systems of galaxies N91-16956
Molecular gas and star formation in the central regions of Virgo spiral galaxies N91-16970

SPLINE FUNCTIONS
Mathematical methods and algorithms for real-time applications
[AD-A228889] N91-16663

SPRAYERS
Parametric study of electrostatically charged sprays
[DE90-010580] N91-16262

SPREAD SPECTRUM TRANSMISSION
Near/far resistant receivers for DS/SSMA communications
[AD-A228147] N91-16200
IEEE International Symposium on Information Theory
[AD-A228239] N91-16842

STABILITY
Understanding the interdiffusion behavior and determining the long term stability of tungsten fiber reinforced niobium-base matrix composite systems
[NASA-CR-187396] N91-16120
Use of satellite data and modeling to assess the influence of stratospheric processes on the troposphere N91-16517
Stability properties of a flow process in graphs
[REPT-90-58] N91-16656
Stationary orbits of satellites of disk galaxies N91-16954

STABILITY AUGMENTATION
Longitudinal stability augmentation of a lightweight fighter aircraft model
[ETN-91-98585] N91-16026

STABILITY TESTS
A coupled rotor aeroelastic analysis utilizing advanced aerodynamic modeling N91-16006
The search for high energy low vulnerability explosives
[DE90-009436] N91-16158
Homogeneously broadened bidirectional ring laser: Theoretical analysis, numerical simulation, and experiment in helium-xenon N91-16360
High-efficiency large-area CdTe panels
[DE91-002117] N91-16443

STABILIZATION
Monitoring challenges and innovative ideas
[DE91-000586] N91-16465

STAGNATION POINT
On a class of unsteady three-dimensional Navier Stokes solutions relevant to rotating disc flows: Threshold amplitudes and finite time singularities
[NASA-CR-187482] N91-15991

STAINLESS STEELS
Thermal aging of cast stainless steels: Mechanisms and predictions
[DE90-010093] N91-16115
Desorption of H2O and H2 from steel and LiAO2 by temperature programmed desorption
[DE90-011170] N91-16118
Experimental study on mercury heat pipes (on effect of screen mesh wick under bottom heat mode) N91-16280

STANDARDIZATION
The European flight safety crisis: Costs and solution
[ETN-91-98490] N91-16000

STANDARDS
Characterization of ultrasonic transducers using pattern recognition techniques
[DE91-000580] N91-16326
Procedures for Quality Assurance Program
[DE90-010001] N91-16393
Management information: A key to better acquisition at NIH
[AD-A226867] N91-16830
A normative database for, and analysis of, the dual task of the TASKOMAT
[IZF-1990-A-11] N91-16846

STANDING WAVES
In situ studies of potential dependent structural and distributional changes at electrochemical interfaces with x rays
[AD-A226844] N91-16098

STAR CLUSTERS
A non-LTE analysis of a sample of O stars selected from galactic OB associations N91-16854
Observational effects of interaction in the Seyfert galaxy NGC 7469 N91-16906

STAR FORMATION
Paired and Interacting Galaxies: International Astronomical Union Colloquium No. 124 [NASA-CP-3098] N91-16858
Multi-waveband observations of colliding galaxies N91-16868
The H I content of non-isolated galaxies N91-16883
Global effects of interactions on galaxy evolution N91-16897
A multiwavelength survey of interacting galaxies N91-16898
Star formation in infrared bright and infrared faint starburst interacting galaxies N91-16901
Radio loud far-infrared galaxies N91-16902
On a connection between supernova occurrence and tidal interaction in early type galaxies N91-16903
Infrared images of merging galaxies N91-16904
Galaxy interactions and star formation: Results of a survey of global H-alpha emission in spiral galaxies in 8 clusters N91-16905
Galaxy interactions and the stimulation of nuclear activity N91-16910
The spiral-compact galaxy pair AM 2208-251: Computer simulations versus observations N91-16939
Observations and models of star formation in the tidal features of interacting galaxies N91-16957
Dynamical experiments on models of colliding disk galaxies N91-16959
Paired and interacting galaxies: Conference summary N91-16964
Positron survival in Type II supernovae [AD-A226778] N91-16965
Dense cores and young stellar objects N91-16969
Molecular gas and star formation in the central regions of Virgo spiral galaxies N91-16970
The 158 micrometer (CII) line: A measure of global star formation activity in galaxies [NASA-CR-187925] N91-16977

STAR FORMATION RATE
The H I content of non-isolated galaxies N91-16883
Global effects of interactions on galaxy evolution N91-16897
A simulation survey of galaxy interactions N91-16936
Observations and models of star formation in the tidal features of interacting galaxies N91-16957
Molecular gas and star formation in the central regions of Virgo spiral galaxies N91-16970
Spectrometric, chemical, and cosmological development of galaxies [ETN-91-98555] N91-16972

STARBURST GALAXIES
Paired and Interacting Galaxies: International Astronomical Union Colloquium No. 124 [NASA-CP-3098] N91-16858
Observations of multiple nucleus galaxies N91-16890
Galaxy interactions and the stimulation of nuclear activity N91-16910
Starbursts in interacting galaxies: Observations and models N91-16958
Wing galaxies: A formation mechanism of the clumpy irregular galaxy Markarian 297 N91-16963

STARK EFFECT
Stark-effect measurement of high FEL electric fields in MTX by laser-aided particle-probe spectroscopy [DE90-011911] N91-16771
Motional Stark effect polarimetry for the current profile diagnostic in D3-D [DE90-012071] N91-16773
IR plasma emissions [AD-A227713] N91-16776

STARS
Stellar kinematics of elliptical galaxies in pairs N91-16862
The interacting pair Mkn 305/306 N91-16864
Multi-waveband observations of colliding galaxies N91-16868
Star formation in infrared bright and infrared faint starburst interacting galaxies N91-16901
A dynamical proximity analysis of interacting galaxy pairs N91-16937
Simulation of disk-disk encounters with co-moving polar grids N91-16941
Triplets of galaxies: Their dynamics, evolution, and the origin of chaos in them N91-16948
Induced starburst and nuclear activity: Faith, facts, and theory N91-16953
Caustic waves in galaxy disks produced in collisions with low mass companions N91-16960
Simulations of gas clouds in interacting galaxies N91-16961

STATIC TESTS
Space Shuttle Flight Support Motor no. 1 (FSM-1) [NASA-CR-184078] N91-16064

STATIONARY ORBITS
Stationary orbits of satellites of disk galaxies N91-16954

STATISTICAL ANALYSIS
The use of window functions and Kalman filtering in spectral estimation [AD-A227482] N91-16236
Statistical process control for QML (Qualified Manufacturer's List) radiation hardness assurance [DE90-007413] N91-16394
Derivation of exospheric temperature at high latitudes from incoherent-scatter radar data [AD-A227721] N91-16484
Analysis of parallel, replicated simulations under a completion time constraint [AD-A228292] N91-16613
Wave propagation through random media: A local method of small perturbations based on the Helmholtz equation N91-16701
Dumb-bell galaxies in southern clusters: Catalog and preliminary statistical results N91-16896
A statistical study of merging galaxies: Theory and observations N91-16931
Explaining compact groups as change alignments N91-16944
Viral coefficient and hidden mass in the galaxy groups N91-16950

STATISTICAL CORRELATION
Fourth moments of acoustic waves forward scattered by a rough ocean surface [AD-A227469] N91-16529
Statistics of associations among IR galaxies N91-16909

STATISTICAL DISTRIBUTIONS
Statistically thinned arrays with quantized element weights [AD-A227965] N91-16196

STATISTICAL MECHANICS
A new perturbation theory of solids and fluids and its applications to high-pressure melting problems [DE90-011502] N91-16829

STEADY FLOW
Study of time accuracy of flow variables across discontinuous boundaries N91-16300

STEADY STATE
A segregated finite element solution to the incompressible Navier-Stokes equations [ME-69] N91-16315
Homogeneously broadened bidirectional ring laser: Theoretical analysis, numerical simulation, and experiment in helium-xenon N91-16360
Dynamic crack propagation in elastic-plastic solids N91-16402
Finite element solution of steady state axisymmetric penetration problems N91-16403
Experiments with initial transient deletion for parallel, replicated steady-state simulations [AD-A227879] N91-16636
Pathwise convexity and its relation to convergence of time-average derivatives [AD-A228888] N91-16662
Wave-particle power transfer in a steady-state driven system [DE90-010031] N91-16748

STEAM
Magnetic heat pumps [DE90-010305] N91-16375

STEELS
Specimen size effects in Charpy impact testing [DE90-011369] N91-16399

STEERABLE ANTENNAS
Electronically steerable arrays: Current and future technology and applications [ETN-91-98581] N91-16254

STELLAR CORES
Dense cores and young stellar objects N91-16969

STELLAR EVOLUTION
Formation and development of elliptical and dwarf galaxies [ETN-91-98492] N91-16967

STELLAR LUMINOSITY
X ray emission from low-mass binary systems N91-16853
Quantifying the FIR interaction enhancement in paired galaxies N91-16900

STELLAR MAGNITUDE
A non-LTE analysis of a sample of O stars selected from galactic OB associations N91-16854
Triple galaxies and a hidden mass problem N91-16875

STELLAR MASS
A spiral-like disk of ionized gas in IC 1459: Signature of a merging collision N91-16889

STELLAR MODELS
Multiple-photon Compton scattering in a strong magnetic field: Cross-sections and radiative transport N91-16852
Stellar convection and dynamo theory N91-16857
Observations and models of star formation in the tidal features of interacting galaxies N91-16957
Dense cores and young stellar objects N91-16969

STELLAR ROTATION
Gas flows in S-E binary systems of galaxies N91-16956

STELLAR SPECTROPHOTOMETRY
Blue ellipticals in compact groups N91-16873
Spectrometric, chemical, and cosmological development of galaxies [ETN-91-98555] N91-16972
Galactic structure in direction of Vela-Puppis by means of UBV beta observations [ETN-91-98556] N91-16973

STELLAR SYSTEMS
Caustic waves in galaxy disks produced in collisions with low mass companions N91-16960
Formation and development of elliptical and dwarf galaxies [ETN-91-98492] N91-16967

STEP FUNCTIONS
Distorted-wave born approximation calculations for turbulence scattering in an upward-refracting atmosphere N91-16700

STIFFNESS
A hydraulically driven microdisplacement unit [ME-56] N91-16392

STIMULATED EMISSION
Generation of high power 1.54 micrometer radiation by stimulated Raman scattering in methane [FEL-90-B098] N91-16366

STIRLING CYCLE
Magnetic heat pumps [DE90-010305] N91-16375

STOCHASTIC PROCESSES
Stochastic and chaotic effects in the ring laser N91-16359
Alopex optimization algorithm [AD-A228442] N91-16615
Towards conservative reliability predictions for real-time software [NASA-CR-187863] N91-16627
Pathwise convexity and its relation to convergence of time-average derivatives [AD-A228888] N91-16662
Estimating the asymptotic variance with batch means [AD-A228293] N91-16667
The asymptotic validity of sequential stopping rules for stochastic simulations [AD-A228896] N91-16668

STOKES THEOREM (VECTOR CALCULUS)
An elementary proof of the Ambartzumian-Pleijel identity [REPT-90-59] N91-16657

STOPPING
The asymptotic validity of sequential stopping rules for stochastic simulations [AD-A228896] N91-16668

STOPPING POWER
Electron stopping powers of some elements and compounds from 0 to 10,000 eV: A compilation [DE90-010675] N91-16716

STORAGE
Pathwise convexity and its relation to convergence of time-average derivatives [AD-A228888] N91-16662

STORM SURGES
Prediction of tropical cyclone rapid intensification events [AD-A227668] N91-16520

STORMS (METEOROLOGY)
The effect of latent heat release on synoptic-to-planetary wave interactions and its implication for satellite observations: Theoretical modeling N91-16514

STRAIN DISTRIBUTION
Calculation of free energy from the internal-energy distribution function [DE90-011111] N91-16791

STRAIN GAGES
Magnetic domain strain sensor program [AD-A227225] N91-16327
Advanced structural instrumentation, volume 1 [AD-A227226] N91-16328

STRAIN HARDENING
Influence of strain rate on the structure/property of Ti-48Al-1V [DE91-000172] N91-16122

STRAIN RATE
Influence of strain rate on the structure/property of Ti-48Al-1V [DE91-000172] N91-16122

STRANGENESS
V(sup 0) production with 14.5 GeV/c silicon beams [DE90-010014] N91-16747

STRATIFICATION
The effect of stratification on gravitational coagulation and settling of aerosols [DE90-010153] N91-16079

Excursions to the base of the mantle N91-16491
Laboratory and theoretical models of planetary-scale instabilities and waves N91-16511

STRATIFIED FLOW
Using a fast Fourier method to model sound propagation in a stratified atmosphere over a stratified porous-elastic ground N91-16692

STRATOCUMULUS CLOUDS
Stratiform clouds and their interaction with atmospheric motion N91-16506
Stability criteria for stratocumulus-topped boundary layers evaluated through conditional sampling of turbulence elements
[AD-A228433] N91-16526

STRATOSPHERE
The atmospheric effects of stratospheric aircraft: A topical review
[NASA-RP-1250] N91-16466
The atmospheric effects of stratospheric aircraft: A current consensus
[NASA-RP-1251] N91-16467
On the developmental dynamics of sudden stratospheric warmings
[AD-A227731] N91-16485
The Cabannes-lidar for the examination of the stratosphere: Selected design elements for the experimental construction
[BONN-IR-90-39] N91-16493
Use of satellite data and modeling to assess the influence of stratospheric processes on the troposphere N91-16517
A global climatology of middle atmosphere inertio-gravity waves N91-16524

STRATUS CLOUDS
Stratiform clouds and their interaction with atmospheric motion N91-16506

STREAK CAMERAS
Stability and accuracy of the sweep rate measurements for LLNL optical streak cameras
[DE90-012080] N91-16324

STREAM FUNCTIONS (FLUIDS)
Finite element solution techniques for the vorticity-stream function formulation of two-dimensional incompressible flows N91-16302

STRESS (PHYSIOLOGY)
Quantification of lower bounds for endurance times in thermally insulated fingers and toes exposed to cold stress
[AD-A227782] N91-16545

STRESS ANALYSIS
Evaluation procedure for reinforced concrete box culverts under airfield pavements
[AD-A227920] N91-16031
Sintering stress and microstructure in ceramic powder compacts
[DE91-004415] N91-16149
Study of the influence of imperfections on the dynamic stability of tanks
[DE90-011094] N91-16398
Plate and butt-weld stresses beyond elastic limit, material and structural modeling
[NASA-TP-3075] N91-16413

STRESS CORROSION CRACKING
Failure analysis of a main rotor pitch horn bolt located on the AH-1 Cobra helicopter
[AD-A227679] N91-16007
Mechanical property data on aluminum alloy 7150-T7751 plate
[AD-A227506] N91-16124
Attenuation of seismic waves in the near-source region
[AD-A226814] N91-16475

STRESS-STRAIN RELATIONSHIPS
Influence of strain rate on the structure/property of Ti-48Al-1V
[DE91-000172] N91-16122
Plate and butt-weld stresses beyond elastic limit, material and structural modeling
[NASA-TP-3075] N91-16413

STRING THEORY
On the large-scale structures formed by wakes of open cosmic strings N91-16951

STRONGLY COUPLED PLASMAS
Fundamental characteristics and applications of an inductively coupled plasma as an ion source for mass spectrometry
[DE90-011746] N91-16770

STRUCTURAL ANALYSIS
The integration of structural optimization in the general design process for aircraft
[MBB/FE122/S/PUB/0405] N91-16017
Aeroservoelastic tailoring for lateral control enhancement N91-16025
Evaluation procedure for reinforced concrete box culverts under airfield pavements
[AD-A227920] N91-16031
The NASA controls-structures interaction technology program
[NASA-TM-102752] N91-16057
In situ studies of potential dependent structural and distributional changes at electrochemical interfaces with x rays
[AD-A226844] N91-16098
Some applications of probability and statistics in communication theory and signal processing
[AD-A226869] N91-16184
A modular stiffness-based approach to rotating systems analysis N91-16400
Finite element thermo-viscoplastic analysis of aerospace structures
[NASA-TM-102761] N91-16407
Plate and butt-weld stresses beyond elastic limit, material and structural modeling
[NASA-TP-3075] N91-16413
Seismic structure of the upper mantle under the Pacific Ocean N91-16492
A software development specification for nonlinear structural analysis
[AD-A228427] N91-16614
THERMOPT: An optimizer for ESATAN models
[MBB/FW522/S/PUB/427] N91-16630
Structure and energy balance of molecular clouds
[MPE-PREPRINT-181] N91-16975

STRUCTURAL DESIGN
Laboratory testing of chloride 3ET205 6 volt traction battery
[DE90-010926] N91-16225
Design and testing of a proton detector
[BONN-IR-90-34] N91-16729

STRUCTURAL FAILURE
Application of fuzzy-Bayesian analysis to structural reliability
[NAL-TR-1063] N91-16396

STRUCTURAL MEMBERS
Passive damping concepts for tubular beams with partial rotational and translational end restraints
[NASA-CR-187833] N91-16411

STRUCTURAL PROPERTIES (GEOLOGY)
Excursions to the base of the mantle N91-16491

STRUCTURAL RELIABILITY
Application of fuzzy-Bayesian analysis to structural reliability
[NAL-TR-1063] N91-16396

STRUCTURAL VIBRATION
Determination of shuttle orbiter center of gravity from flight measurements
[NASA-TM-102627] N91-16058
Dynamic response of composite beams using shear-deformable finite elements
[AD-A227975] N91-16408
Passive damping concepts for tubular beams with partial rotational and translational end restraints
[NASA-CR-187833] N91-16411

SUBDUCTION (GEOLOGY)
Continuum models of continental deformation N91-16490

SUBJECTS
Calendar of selected aeronautical and space meetings: January 1991 onwards
[AGARD-CAL-91/1] N91-16833

SUBSONIC FLOW
Calculations for unsteady aerodynamic characteristics on a 3-D lifting body in subsonic flow using boundary element method
[NAL-TR-1065] N91-15985

SUBSTRATES
Hydrogen storage in metal hydrides
[AD-A228150] N91-16103

SUCTION
Investigation of transonic flow over segmented slotted wind tunnel wall with mass transfer
[NASA-CR-187760] N91-15981

SULFATES
A comparison of computerized measurement of helicopter pilot performance with atropine sulfate during actual and simulated flight N91-16558

SULFITES
Characterization of the corrosion of a P-130x graphite fiber reinforced 6063 aluminum metal matrix composite
[AD-A228134] N91-16071

SULFUR CHLORIDES
Development of a moderate rate lithium/thionyl-chloride D cell
[DE90-011909] N91-16233

SULFUR DIOXIDES
The influence of small SO2 contents on the corrosion behavior for NiCrAl alloys in temperature zone from 1000 to 1100 C
[JUEL-2362] N91-16134
Parametric study of electrostatically charged sprays
[DE90-010580] N91-16262

SUN
Electrochromic sun control coverings for windows
[DE90-000335] N91-16139
Activities and accomplishments of the Center for Applied Solar Physics, 1987 - 1990
[AD-A228773] N91-16980

SUNSPOTS
Activities and accomplishments of the Center for Applied Solar Physics, 1987 - 1990
[AD-A228773] N91-16980

SUPERCOMPUTERS
Introduction (to a book on applications of local-density-functional methods in chemistry)
[AD-A228769] N91-16109
Microsupercomputers: Design and implementation
[AD-A228741] N91-16571
Microsupercomputers: Design and implementation
[AD-A228744] N91-16572
Optimization of a power transient stability program on a vector supercomputer: Theory and applications
[AD-A227884] N91-16607

SUPERCONDUCTING FILMS
Novel applications of Tl-Ca-Ba-Cu-O thin films to active and passive high frequency devices
[DE91-004507] N91-16240
YBa2Cu3O(7-x) thin film growth on single crystal and polycrystalline yttria-stabilized zirconia
[DE90-010707] N91-16788
Infrared response of YBa2Cu3O(7-delta) films to pulsed, broadband synchrotron radiation
[DE90-011519] N91-16800
From low to high Tc: An ultrasonic investigation of niobium single crystal and YBaCuO superconducting thin films with surface acoustic waves N91-16822

SUPERCONDUCTING MAGNETS
Investigation of wire motion in superconducting magnets
[DE91-004952] N91-16674
ASTROMAG coil cooling study
[NASA-CR-187768] N91-16813

SUPERCONDUCTING SUPER COLLIDER
Self-propelled in-tube shuttle and control system for automated measurements of magnetic field alignment
[DE90-008210] N91-16316
Investigation of wire motion in superconducting magnets
[DE91-004952] N91-16674
Performance measurements of hybrid PIN diode arrays
[DE90-010308] N91-16790

SUPERCONDUCTIVITY
Chern-Simons and anyonic superconductivity
[DE90-010663] N91-16787
Thermal desorption studies of isotopically-labeled oxygen-induced superconductivity in La2CuO(4+delta)
[DE91-004898] N91-16812
Dynamical properties of two-dimensional Josephson junction arrays N91-16823

SUPERCONDUCTORS
Hyperfine interactions associated with iron substituted superconducting oxides
[DE90-010411] N91-16783

SUPERCOOLING
State of an adiabatic expanding and condensing vapor or slow, medium, and fast explosions into a vacuum
[DE90-010815] N91-16263

SUPERCRITICAL FLUIDS
Destruction of propellant components in supercritical water
[DE90-010600] N91-16085
The development of improved capillary supercritical fluid chromatography and mass spectrometry
[AD-A228535] N91-16107

SUPERHIGH FREQUENCIES
The reflection and transmission properties of a triple band dichroic surface
[NASA-CR-187776] N91-16191
Detection of soil moisture using X-band SLAR records in a sandy area
[BCRS-90-08] N91-16427

SUPERLATTICES
Applications of strained layer superlattices
[DE90-011204] N91-16793
Photoreflectance studies of electronic transitions in quantum well structures under high pressure
[DE90-011583] N91-16801
Far-infared laser spectroscopy of two dimensional holes in strained-layer heterostructure and superlattices
[DE91-000027] N91-16805
Dynamical properties of two-dimensional Josephson junction arrays N91-16823

SUPERNOVA REMNANTS
The x ray emission of SS433
[MPE-PREPRINT-189] N91-16856
The morphology of Sersic-Pastoriza galaxies N91-16893

SUPERNOVA 1987A
Positron survival in Type II supernovae
[AD-A226778] N91-16965
SUPERNOVAE
On a connection between supernova occurrence and tidal interaction in early type galaxies N91-16903
Numerical simulations of interacting disk galaxies N91-16955
SUPERSONIC AIRCRAFT
The atmospheric effects of stratospheric aircraft: A current consensus
[NASA-RP-1251] N91-16467
SUPERSONIC COMBUSTION RAMJET ENGINES
Autoignition and flameholding in a cylindrical scramjet combustor
[NAL-TR-1067] N91-16102
SUPERSONIC FLIGHT
Joint computational/experimental aerodynamics research on a reentry vehicle. Part 2: Computational results
[DE90-012765] N91-16054
SUPERSONIC FLOW
Autoignition and flameholding in a cylindrical scramjet combustor
[NAL-TR-1067] N91-16102
SUPERSONIC SPEED
An experiment on supersonic turbulent mixing layers: Supersonic-subsonic two-stream layers
[NAL-TR-1066] N91-15983
Propfan supersonic panel method analysis and flutter predictions N91-15993
Optimal trajectories for an aerospace plane. Part 2: Data, tables, and graphs
[NASA-CR-187848] N91-16011
Optimal trajectories for an aerospace plane. Part 1: Formulation, results, and analysis
[NASA-CR-187868] N91-16013
SUPERSONIC TRANSPORTS
The atmospheric effects of stratospheric aircraft: A topical review
[NASA-RP-1250] N91-16466
SUPERSYMMETRY
Solvable two-dimensional supersymmetric models and the supersymmetric Virasoro algebra
[DE90-012140] N91-16648
SUPPORT INTERFERENCE
Calculation of support interferences on the aerodynamic coefficients for a wind tunnel calibration model
[DLR-FB-90-26] N91-15998
SURFACE ACOUSTIC WAVE DEVICES
Multiple-frequency surface acoustic wave devices as sensors
[DE90-009972] N91-16675
Programmable surface acoustic wave detection in silicon: Design of programmable filters
[ETN-91-98568] N91-16746
From low to high Tc: An ultrasonic investigation of niobium single crystal and YBaCuO superconducting thin films with surface acoustic waves N91-16822
SURFACE CRACKS
Scattering of Lamb waves in an elastic plate for ultrasonic nondestructive evaluation of weldments and cracks N91-16412
SURFACE DEFECTS
On the receptivity and non-parallel stability of travelling disturbances in rotating disk flow
[NASA-CR-187486] N91-15996
SURFACE ENERGY
An inter-comparison of surface energy flux measurement systems used during FIFE, 1987
[NASA-CR-187699] N91-16472
A study of the surface energy balance on slopes in a tallgrass prairie
[NASA-CR-187698] N91-16473
SURFACE FINISHING
Deburring and surface finishing: The past ten years and projections for the next ten years
[DE91-000579] N91-16176
SURFACE LAYERS
Atomic-scale simulation of adhesion between metallic surfaces
[DE91-004722] N91-16127
SURFACE PROPERTIES
Surface analysis by low-energy ion scattering: Two-dimensional detection and quantification
[ETN-91-98474] N91-16133
The reflection and transmission properties of a triple band dichroic surface
[NASA-CR-187776] N91-16191
The impact of separated flow on heat and mass transfer
[DE91-000592] N91-16284
Dynamic aspects of scanning surface instruments and microscopes
[ME-84] N91-16339
Air-ground interface: Surface waves, surface impedance and acoustic-to-seismic coupling coefficient N91-16685
New surface atomic structures for III-V(110)-p(1 x 1)-Sb(1ML): Chemical bonding and electronic structure
[DE90-011230] N91-16794
Photometric analyses for the determination of physical and structural properties for the Martian surface in the Oxia Palus region
[DLR-FB-90-27] N91-16979
SURFACE REACTIONS
Atomic and electronic structure of metals and alloys: Clean surfaces and chemisorbed molecules
[DE91-000267] N91-16123
State-to-state inelastic and reactive molecular beam scattering from surfaces
[DE90-010492] N91-16714
SURFACE ROUGHNESS
On the receptivity and non-parallel stability of travelling disturbances in rotating disk flow
[NASA-CR-187486] N91-15996
Scattering and depolarization by rough terrain and sea: A unified full wave approach
[AD-A228295] N91-16201
Fourth moments of acoustic waves forward scattered by a rough ocean surface
[AD-A227469] N91-16529
SURFACE TEMPERATURE
Analysis of satellite and Expendable Bathythermograph (XBT) data for the abrupt topography program
[AD-A228870] N91-16422
GCM (General Circulation Model) predictions for surface air temperature and precipitation over the southeastern United States
[DE90-009434] N91-16497
SURFACE WAVES
The high speed buffer board: A SAIL EIA-485 communications accelerator card for the vector measuring current meter
[AD-A227181] N91-16185
Fourth moments of acoustic waves forward scattered by a rough ocean surface
[AD-A227469] N91-16529
Full field visualization of surface and bulk acoustic waves
[AD-A227676] N91-16678
Air-ground interface: Surface waves, surface impedance and acoustic-to-seismic coupling coefficient N91-16685
SURFACES
On the propagation of plane waves above an impedance surface N91-16684
SURVEILLANCE
PC-based digital imaging for storing microscopy images for surveillance programs
[DE90-010080] N91-16738
SURVEYS
A homogeneous sample of binary galaxies: Basic observational properties N91-16859
A simulation survey of galaxy interactions N91-16936
SWEPT WINGS
TF69 tactical fighter outer wing design
[ETN-91-98580] N91-16019
SWITCHING
Pi: A parallel architecture interface for multi-model execution
[AD-A228345] N91-16640
SWITCHING CIRCUITS
Timing margin measurement using a laser technique
[AD-A226821] N91-16353
SYMMETRY
Symmetry and design in mixture experiments
[AD-A226760] N91-16169
Stellar convection and dynamo theory N91-16857
SYMPATHETIC NERVOUS SYSTEM
Computer-assisted determination of minimum energy conformations. Part 4: Alpha1 and alpha2 adrenergiic compounds
[AD-A226811] N91-16097
SYNCHRONISM
Pi: A parallel architecture interface for multi-model execution
[AD-A228345] N91-16640
SYNCHROTRON RADIATION
A tunable x ray microprobe using synchrotron radiation
[DE90-011219] N91-16322
Modeling the performance of water and liquid gallium cooled x ray optical components: A comparison with experiment
[DE90-010460] N91-16784
Infrared response of YBa2Cu3O(7-delta) films to pulsed, broadband synchrotron radiation
[DE90-011519] N91-16800
SYNCHROTRONS
AGS silicon gold collisions measured in the E-810 TPC (Time Projection Chamber)
[DE90-010015] N91-16733
SYNOPTIC METEOROLOGY
Research on diabatic initialization N91-16504
SYNTHESIS (CHEMISTRY)
Synthesis, characterization and catalytic activity of microporous aluminophosphate catalysts N91-16092
SYNTHETIC APERTURE RADAR
Implementation of the phase gradient algorithm
[DE90-012160] N91-16579
SYNTHETIC APERTURES
Fiber optic synthetic aperture interferometer
[AD-A227891] N91-16741
SYSTEMS ANALYSIS
A modular stiffness-based approach to rotating systems analysis N91-16400
Distributed issues for Ada real-time systems
[AD-A227852] N91-16603
Analysis of multivariable control systems in the presence of structured uncertainties
[AD-A227976] N91-16665
SYSTEMS ENGINEERING
Cartographic issues in the development of a digital GRASS database
[AD-A227582] N91-16416
Human factors design guidance during the conceptual design phase of system development: A methodological approach
[AD-A224667] N91-16552
Analysis of multivariable control systems in the presence of structured uncertainties
[AD-A227976] N91-16665
SYSTEMS INTEGRATION
Optimal Kalman filter integration of a global positioning system receiver and an LN-94 inertial navigation system
[AD-A227222] N91-16003
Geometric modeling application interface program. System components operator's manual
[AD-A227827] N91-16594
SYSTOLIC ARRAYS
Systematic design of regular VLSI processor arrays
[ETN-91-98482] N91-16250

T

TABLES (DATA)
Automated design of displays for technical data
[AD-A226729] N91-16586
TACTILE SENSORS (ROBOTICS)
Haptic perception with an articulated, sensate robot hand
[DE90-010195] N91-16371
TALKING
Linguistic and pragmatic constraints on utterance interpretation
[AD-A228815] N91-16210
TARGETS
Ion contamination of x ray pinhole camera images on PBFA 2
[DE90-012180] N91-16325
Finite element solution of steady state axisymmetric penetration problems N91-16403
Fragment mass distribution of debris
[MBB-UA-1187-90-PUB] N91-16669
ADRPM-VII applied to the long-range acoustic detection problem N91-16689
TATB
The search for high energy low vulnerability explosives
[DE90-009436] N91-16158
Development of a high-tensile-strain plastic-bonded TATB explosive
[DE90-011463] N91-16162
TEARING MODES (PLASMAS)
Numerical examinations of Kelvin-Helmholtz instability in resistive compressible magnetohydrodynamics
[MPE-221] N91-16782
TECHNICAL WRITING
Using computer-generated protocols to study writers' planning strategies
[AD-A228875] N91-16844
TECHNOLOGIES
JPRS report: Science and technology. USSR: Space
[JPRS-USP-89-006] N91-16036
TECHNOLOGY ASSESSMENT
An assessment of the government liquid hydrogen requirements for the 1995-2005 time frame N91-16167
Assessment of battery technologies for electric vehicles. Volume 2, part 1: Appendices
[DE90-010907] N91-16227
Nonradiative dielectric waveguide millimetre-wave integrated circuits: A review
[AD-A227760] N91-16238
Meetings to share advancements in heat pump technologies
[DE90-010008] N91-16257

Technical and economic evaluation of diesel engine with oxygen enrichment and water injection
[DE90-009723] N91-16373
National software capacity: Near-term study executive summary
[AD-A227564] N91-16590
Status of target physics for inertial confinement fusion
[DE90-008221] N91-16751

TECHNOLOGY TRANSFER
Accomplishments in technology transfer from DOE and its laboratories
[DE90-002686] N91-16986

TECHNOLOGY UTILIZATION
Potential use of tiltrotor aircraft in Canadian aviation
[NASA-TM-102245] N91-16001
Advanced Turbine Technology Applications Project (ATTAP)
[NASA-CR-187039] N91-16021
Electronically steerable arrays: Current and future technology and applications
[ETN-91-98581] N91-16254

TECTONICS
Magsat investigations over the greater African region N91-16415
Continuum models of continental deformation N91-16490

TELECOMMUNICATION
Tactical HF field expedient antenna performance, volume 1
[AD-A228057] N91-16198

TELECONNECTIONS (METEOROLOGY)
Potential vorticity index N91-16516

TELEMETRY
A low-cost infrared telemetry system for kilohertz-bandwidth data acquisition
[DE90-010616] N91-16042

TELEOPERATORS
NASA Laboratory telerobotic manipulator control system architecture
[NASA-CR-187751] N91-16385
The PHD: A Planar, Harmonic Drive robot for joint torque control
[NASA-CR-187924] N91-16386

TELEROBOTICS
Design of a telerobotic controller with joint torque sensors using 2-port network theory
[NASA-CR-186543] N91-16379

TELESCOPES
The design and construction of an Automated Multi-Object Spectroscopy system (AMOS)
[DE90-011497] N91-16088
Fiber optic synthetic aperture interferometer
[AD-A227891] N91-16741
Low-cost, high-resolution telescopes for imaging low-earth orbit satellites
[DE90-012081] N91-16850

TELEVISION EQUIPMENT
NICAM 728: Factors affecting the assessment of UHF transmitter linearity
[BBC-RD-1990/9] N91-16190

TELEVISION SYSTEMS
The computer simulation of digital recording systems
[BBC-RD-1990/14] N91-16595

TELEVISION TRANSMISSION
NICAM 728: Factors affecting the assessment of UHF transmitter linearity
[BBC-RD-1990/9] N91-16190

TEMPERATURE CONTROL
High temperature oxidation-resistant thruster research
[NASA-CR-185233] N91-16063
Development of a two-phase cold plate N91-16277

TEMPERATURE DISTRIBUTION
Aerodynamic drag characterization and deposition studies of irregular particles. Part 3: Analysis of flow and temperature field inside the Combustion Deposition Entrained Reactor (CDER)
[DE90-000466] N91-16259
Development of a two-phase cold plate N91-16277
Variability of latent and sensible heat fluxes over the oceans N91-16531

TEMPERATURE EFFECTS
The oxidation behavior of carbon-carbon composites and their coatings N91-16074
Time-resolved Coherent Anti-Stokes Raman Spectroscopy (CARS) and the measurement of vibrational spectra in shock-compressed molecular materials
[DE90-012053] N91-16091
Desorption of H2O and H2 from steel and LiAO2 by temperature programmed desorption
[DE90-011170] N91-16118
On the development of in-situ Raman analysis of plasma deposited diamond
[AD-A227453] N91-16147
Updated evaluation of polymer films for electrical insulation
[DE91-000544] N91-16148
Multi-dimensional aspects of recent climate change in North America
[DE90-010958] N91-16460
The effect of latent heat release on synoptic-to-planetary wave interactions and its implication for satellite observations: Theoretical modeling N91-16514
The effect of latent heat release on synoptic-to-planetary scale wave interactions and implications for satellite observations: Observational study N91-16515
Meteorological effects on long-range outdoor sound propagation N91-16696
Effect of wind and temperature gradients on received acoustic energy N91-16697
A model for the prediction of Nb3Sn critical current as a function of field, temperature, strain, and radiation damage
[DE91-000656] N91-16775

TEMPERATURE GRADIENTS
High-loaded combustion chambers stationary constant pressure combustion. Part 2: Research reports
[ETN-91-98511] N91-16112
Weldability of nickel aluminides
[DE90-008557] N91-16116
Contemporary issues in solar pond research
[DE90-010094] N91-16436
Theoretical and experimental studies of baroclinic processes N91-16512
Effect of wind and temperature gradients on received acoustic energy N91-16697

TEMPERATURE MEASUREMENT
Rotational temperature estimation of CO at high temperatures by graphical methods using FTIR spectrometry
[AD-A228370] N91-16105
Gas solubility in glassy polymers: A correlation with excess enthalpy
[AD-A228202] N91-16155
The effect of charge mixture ratio and particle size on igniter plume heat transfer characteristics
[DE90-010833] N91-16160

TEMPERATURE PROFILES
High temperature furnace modeling and performance verifications
[NASA-CR-187831] N91-16032
Heat transfer from water flowing through a chilled-bed open channel
[AD-A226855] N91-16286
A global climatology of middle atmosphere inertio-gravity waves N91-16524

TEMPERATURE SENSORS
Advanced structural instrumentation, volume 1
[AD-A227226] N91-16328
Advanced structural instrumentation, volume 2
[AD-A227473] N91-16330
Multiple-frequency surface acoustic wave devices as sensors
[DE90-009972] N91-16675

TEMPORAL DISTRIBUTION
Spatial and temporal climate variations influencing medium-range temperature predictions over south-central European Russia
[AD-A228623] N91-16527
Properties of the redshift N91-16926

TEMPORAL RESOLUTION
Spatial distributions of the emitting species in a penning surface-plasma source
[DE90-011996] N91-16772

TENSILE PROPERTIES
Tensile behavior of tungsten/niobium composites at 1300 to 1600 K
[NASA-TM-103727] N91-16128
Development of a high-tensile-strain plastic-bonded TATB explosive
[DE90-011463] N91-16162

TENSILE STRENGTH
Effects of high pressure nitrogen on the thermal stability of SiC fibers
[NASA-TM-103245] N91-16075
Mechanical property data on aluminum alloy 7150-T7751 plate
[AD-A227506] N91-16124

TENSILE TESTS
Mechanical behavior of a SiC-fiber/Si3N4 composite
[AD-A228371] N91-16073
Thermal aging of cast stainless steels: Mechanisms and predictions
[DE90-010093] N91-16115
Updated evaluation of polymer films for electrical insulation
[DE91-000544] N91-16148

TENSORS
Finite element solution of steady state axisymmetric penetration problems N91-16403
Graviton effects in vacuum maximally symmetric spaces N91-16971

TERMINOLOGY
NASA thesaurus aeronautics vocabulary
[NASA-TM-104230] N91-16847

TERRAIN
Image-based terrain modeling with thematic mapper N91-16418
Terrain matching using image sequence analysis N91-16424
Potential responses of landscape boundaries to global environmental change
[DE90-008568] N91-16451

TERRAIN ANALYSIS
Artificial intelligence technologies applied to terrain analysis
[DE90-011985] N91-16642

TEST CHAMBERS
Proving experiments on an acoustic transmission suite and its reverberation room
[BBC-RD-1990/13] N91-16681

TEST FACILITIES
Small scale shock tube experiments using a computer controlled active rarefaction wave eliminator
[AD-A227507] N91-16029
The radiation hardness test facility
[RAL-90-065] N91-16030

TEST FIRING
Space Shuttle Flight Support Motor no. 1 (FSM-1)
[NASA-CR-184078] N91-16064

THALLIUM COMPOUNDS
Novel applications of Tl-Ca-Ba-Cu-O thin films to active and passive high frequency devices
[DE91-004507] N91-16240

THEMATIC MAPPERS (LANDSAT)
Image-based terrain modeling with thematic mapper N91-16418

THEMATIC MAPPING
The multisensor image map 1:50,000 Rheinhessen N91-16434

THEOREM PROVING
An elementary proof of the Ambartzumian-Pleijel identity
[REPT-90-59] N91-16657
Estimating the asymptotic variance with batch means
[AD-A228293] N91-16667

THEOREMS
Periodic solutions of neutral differential equations
[RR-390] N91-16658

THEORETICAL PHYSICS
Technique for determining the static polarizabilities of refractory metal atoms
[DE90-017088] N91-16724
Research in theoretical nuclear physics
[DE90-010792] N91-16828

THERAPY
Gallium as a unique anti-resorptive agent in bone: Preclinical studies on its mechanisms of action
[DE90-010650] N91-16542

THERMAL ANALYSIS
From visco-elasticity towards thermal relaxation: A neutron scattering study of density fluctuations in fluid helium
[ETN-91-98486] N91-16111
Finite element thermo-viscoplastic analysis of aerospace structures
[NASA-TM-102761] N91-16407

THERMAL BATTERIES
Molten salt electrolytes in high temperature batteries
[RAE-TM-MAT/STR-1155] N91-16241
Self-discharge study of Li-alloy/FeS2 thermal cells
[DE90-010659] N91-16438

THERMAL CYCLING TESTS
The oxidation behavior of carbon-carbon composites and their coatings N91-16074
Inelastic strain analysis of solder joint in NASA fatigue specimen
[NASA-CR-187864] N91-16132

THERMAL EMISSION
Thermal emission model for the anneal of radiation-induced trapped holes
[DE90-007285] N91-16718

THERMAL ENERGY
Heat transfer characteristics of a radical heat pipe N91-16276

THERMAL EXPANSION
Fundamental verification of tailoring technology for control of a coefficient of thermal expansion by composite testing facilities
[NAL-TR-1058] N91-16069
Physico-chemical investigations on Co-Mn-oxide spinels
[ETN-91-98476] N91-16825

THERMAL INSULATION
Advanced Turbine Technology Applications Project (ATTAP)
[NASA-CR-187039] N91-16021

THERMAL PROTECTION
Debris/Ice/TPS assessment and photographic analysis for shuttle mission STS-41
[NASA-TM-103814] N91-16041
THERMAL STABILITY
Effects of high pressure nitrogen on the thermal stability of SiC fibers
[NASA-TM-103245] N91-16075
Phase selection and processing of high temperature intermetallic alloys
[AD-A227910] N91-16129
Comparison of the thermal stability of the codeposited carbon/hydrogen layer to that of the saturated implant layer in graphite
[DE90-012148] N91-16144
The search for high energy low vulnerability explosives
[DE90-009436] N91-16158
THERMAL STRESSES
Updated evaluation of polymer films for electrical insulation
[DE91-000544] N91-16148
Finite element thermo-viscoplastic analysis of aerospace structures
[NASA-TM-102761] N91-16407
THERMOCLINES
The vertical structure of the marine atmospheric boundary layer across a sea surface temperature front
[AD-A227931] N91-16525
THERMOCOUPLES
Advanced structural instrumentation, volume 1
[AD-A227226] N91-16328
Advanced structural instrumentation, volume 2
[AD-A227473] N91-16330
THERMODYNAMIC CYCLES
Rotary absorption heat pump sensitivity analysis
[DE90-010006] N91-16256
THERMODYNAMIC PROPERTIES
Mechanics of interface cracks
[AD-A227579] N91-16067
THERMODYNAMICS
Global-scale, intraseasonal fluctuations of diabatic forcing of the atmosphere N91-16508
ANEOS: Analytic equations of state for shock physics codes input manual
[DE90-010198] N91-16575
Selective excitation, relaxation, and energy channeling in molecular systems
[DE90-010793] N91-16717
THERMOELASTICITY
Fundamental verification of tailoring technology for control of a coefficient of thermal expansion by composite testing facilities
[NAL-TR-1058] N91-16069
Finite element thermo-viscoplastic analysis of aerospace structures
[NASA-TM-102761] N91-16407
THERMOGRAPHY
Advanced structural instrumentation, volume 1
[AD-A227226] N91-16328
THERMOGRAVIMETRY
Hydrogen storage in metal hydrides
[AD-A228150] N91-16103
THERMONUCLEAR REACTIONS
Is there hope for fusion
[DE90-012095] N91-16736
D3-D research operations
[DE90-008232] N91-16752
Initial calorimetry experiments in the Physics Divsion, ORNL (Oak Ridge National Laboratory)
[DE90-010301] N91-16756
Microwave interferometer and reflectometer techniques for thermonuclear plasmas
[ETN-91-98478] N91-16780
THERMOPHILES
Conversion of acetic acid to methane by thermophiles
[DE90-010993] N91-16086
THERMOPLASTIC RESINS
Fatigue of amorphous polymers
[ISBN-90-9003520-6] N91-16157
THERMOSIPHONS
The Proceedings of the Symposium on Mechanics for Space Flight 1989
[ISAS-SP-12] N91-16266
Effect of inclination angle on heat transfer characteristics of closed two-phase thermosyphon N91-16278
THERMOSPHERE
A comparison of optically measured and radar-derived horizontal neutral winds
[AD-A227690] N91-16483
THESAURI
NASA thesaurus aeronautics vocabulary
[NASA-TM-104230] N91-16847
THETA PINCH
A Mirnov loop array for field-reversed configurations
[DE90-010607] N91-16750
THICKNESS
High temperature furnace modeling and performance verifications
[NASA-CR-187831] N91-16032
THIN FILMS
Atomic and electronic structure of metals and alloys: Clean surfaces and chemisorbed molecules
[DE91-000267] N91-16123
A study of the formation and self-lubrication mechanisms of boric acid films on boric oxide coatings
[DE90-010115] N91-16137
Design, ultrastructure, and dynamics of nonlinear optical interactions in polymeric thin films
[AD-A228876] N91-16156
Total-dose degradation of thin film ferroelectric capacitors
[DE90-007152] N91-16218
Measurements of 1/f noise in a-Si:H pin diodes and thin-film-transistors
[DE90-011218] N91-16228
Novel applications of Tl-Ca-Ba-Cu-O thin films to active and passive high frequency devices
[DE91-004507] N91-16240
Properties and characterization of thin film ferroelectric capacitors for nonvolatile memories
[DE91-004037] N91-16242
Ion beam modification of surface for improved high temperature performance
[AD-A228067] N91-16243
Research and development on advanced silicon carbide thin film growth techniques and fabrication of high power and microwave frequency silicon carbide-based device
[AD-A228758] N91-16246
Rotary absorption heat pump sensitivity analysis
[DE90-010006] N91-16256
Magnetic domain strain sensor program
[AD-A227225] N91-16327
Angular dependence of thin-film dielectric coating damage thresholds
[DE91-000237] N91-16351
High-efficiency large-area CdTe panels
[DE91-002117] N91-16443
Low-cost CdZnTe devices for cascade cell application
[DE91-002116] N91-16444
Characterization of chemically prepared PZT thin films
[DE90-010831] N91-16789
Infrared response of YBa2Cu3O(7-delta) films to pulsed, broadband synchrotron radiation
[DE90-011519] N91-16800
Thin film single crystal growth of a nonlinear optical polymer
[AD-A227692] N91-16807
From low to high Tc: An ultrasonic investigation of niobium single crystal and YBaCuO superconducting thin films with surface acoustic waves N91-16822
Image interpretation for transmission electron microscopy of thin semiconductor layers and interfaces
[ETN-91-98487] N91-16826
THIN LAYER CHROMATOGRAPHY
New development of laser-based techniques in applications of thin-layer chromatography, microprobe elemental analysis, and gas phase pyrolysis
[DE90-011740] N91-16347
THIN WALLED SHELLS
SCATSPHERE2: A computation for the plane-wave scattering from a submerged, elastic, spherical, evacuated or fluid-filled, thin shell
[AD-A228867] N91-16709
THREE BODY PROBLEM
Typical motions in multiple systems N91-16945
THREE DIMENSIONAL BOUNDARY LAYER
Unsteady separation over maneuvering bodies
[AD-A226829] N91-16285
Numerical study of a three-dimensional turbulent boundary layer
[AD-A227835] N91-16291
THREE DIMENSIONAL FLOW
On a class of unsteady three-dimensional Navier Stokes solutions relevant to rotating disc flows: Threshold amplitudes and finite time singularities
[NASA-CR-187482] N91-15991
Numerical simulation of buffer flow in a free flow electrophoresis chamber N91-16279
The stationary exterior three dimensional Navier-Stokes problem of viscous flow past a body in anisotropically weighted Sobolev spaces
[REPT-110] N91-16314
THREE DIMENSIONAL MODELS
Electron density comparisons between radar observations and 3-D ionospheric model calculations
[AD-A227703] N91-16187
Numerical simulation of buffer flow in a free flow electrophoresis chamber N91-16279
Magsat investigations over the greater African region N91-16415
THRESHOLD VOLTAGE
Threshold voltage and I-V characteristics of AlGaAs/GaAs MODFETs
[AD-A228844] N91-16248
THRUST CHAMBERS
High temperature oxidation-resistant thruster research
[NASA-CR-185233] N91-16063
THRUST CONTROL
Optimal rocket motor design and control for tactical missiles N91-16062
TIDES
Tidal distortions in pairs of early-type galaxies N91-16869
Tidal events and galactic activity N91-16911
Probing the tides in interacting galaxy pairs N91-16932
Energy and angular momentum transfer in binary galaxies N91-16940
Gas flows in S-E binary systems of galaxies N91-16956
Observations and models of star formation in the tidal features of interacting galaxies N91-16957
TILT ROTOR AIRCRAFT
Evaluation of rotorwash characteristics for tiltrotor and tiltwing aircraft in hovering flight
[SCT 90RR-18] N91-15989
Potential use of tiltrotor aircraft in Canadian aviation
[NASA-TM-102245] N91-16001
TILT WING AIRCRAFT
Evaluation of rotorwash characteristics for tiltrotor and tiltwing aircraft in hovering flight
[SCT-90RR-18] N91-15989
TIME DEPENDENCE
Time optimal trajectories for a two wheeled robot
[DE90-010335] N91-16376
Theoretical studies of electron transport in quantum-well structures
[AD-A228429] N91-16819
TIME MARCHING
Resolution of the 1D regularized Burgers equation using a spatial wavelet approximation
[NASA-CR-187480] N91-16664
TIME MEASUREMENT
Digital time interpolator
[DIGEL-1990-4] N91-16249
Time interpolator
[DIGEL-1990-3] N91-16337
TIME RESPONSE
Meteorological effects on long-range outdoor sound propagation N91-16696
TIME SERIES ANALYSIS
Bio-optical profile data report: Joint Global Ocean Flux Study, Hawaii Ocean Time-Series, HOT-3, R/V Moana Wave, 6-10 January 1989
[NASA-CR-187805] N91-16534
Periodic solutions of neutral differential equations
[RR-390] N91-16658
TIME TEMPERATURE PARAMETER
Time-temperature response of multiphase viscoelastic solids through numerical analysis N91-16401
TIN COMPOUNDS
A model for the prediction of Nb3Sn critical current as a function of field, temperature, strain, and radiation damage
[DE91-000656] N91-16775
TISSUES (BIOLOGY)
Research pathology and special techniques
[NASA-CR-187828] N91-16639
TITANIUM ALLOYS
Influence of strain rate on the structure/property of Ti-48Al-1V
[DE91-000172] N91-16122
Elevated temperature crack growth in titanium aluminides
[AD-A227700] N91-16125
Assessment of corrosion resistant coatings for a depleted U-0.75 Ti alloy
[AD-A228237] N91-16130
TITANIUM OXIDES
Characterization of chemically prepared PZT thin films
[DE90-010831] N91-16789
TOKAMAK DEVICES
Neoclassical effects on RF current drive
[DE90-010302] N91-16222
Scaling dimensionally similar tokamak discharges to ignition
[DE90-010079] N91-16749
D3-D research operations
[DE90-008232] N91-16752
Plasma-facing materials
[DE90-008243] N91-16753
US-Japan Workshop on Field-Reversed Configurations with Steady-State High-Temperature Fusion Plasmas and the 11th US-Japan Workshop on Compact Toroids
[DE90-010253] N91-16755

Microwave Tokamak Experiment (OMTX): Overview and status
[DE90-010287] N91-16758
Transport simulation of the effect of impurity radiation on the high beta, ohmic start-up of the HBT-EP tokamak
[DE90-010333] N91-16760
Characterization of disruptions in the Microwave Tokamak Experiment (MTX)
[DE90-010352] N91-16761
Texas experimental tokamak
[DE90-011070] N91-16762
Theoretical studies of tokamaks
[DE90-011332] N91-16768
Stark-effect measurement of high FEL electric fields in MTX by laser-aided particle-probe spectroscopy
[DE90-011911] N91-16771
The CIT physics program
[DE90-012134] N91-16774

TOMOGRAPHY
Development of nondestructive evaluation methods and prediction of effects of flaws on the fracture behavior of structural ceramics
[DE90-011092] N91-16141

TOPOGRAPHY
The effects of the solid inner core and nonhydrostatic structure on the Earth's forced nutations and Earth tides N91-16417
Analysis of satellite and Expendable Bathythermograph (XBT) data for the abrupt topography program
[AD-A228870] N91-16422
Terrain matching using image sequence analysis N91-16424
Reports on cartography and topography. Series 1, report 104
[ISSN-0469-4236] N91-16432
Potential responses of landscape boundaries to global environmental change
[DE90-008568] N91-16451
A study of the surface energy balance on slopes in a tallgrass prairie
[NASA-CR-187698] N91-16473
Continuum models of continental deformation N91-16490

TOPOLOGY
AFDM: An Advanced Fluid-Dynamics Model. Volume 2: Topologies, flow regimes and interfacial areas
[DE91-000581] N91-16283

TOROIDAL PLASMAS
US-Japan Workshop on Field-Reversed Configurations with Steady-State High-Temperature Fusion Plasmas and the 11th US-Japan Workshop on Compact Toroids
[DE90-010253] N91-16755
The Madison symmetric torus
[DE90-010306] N91-16757

TOROIDAL SHELLS
Diffusion fields in a toroidal conducting shell of circular cross section
[AD-A228021] N91-16197

TOROIDS
Neoclassical effects on RF current drive
[DE90-010302] N91-16222

TORQUE
Multi-criteria position and configuration optimization for redundant platform/manipulator systems
[DE90-010705] N91-16372
Design of a telerobotic controller with joint torque sensors using 2-port network theory
[NASA-CR-186543] N91-16379

TORQUE SENSORS (ROBOTICS)
Haptic perception with an articulated, sensate robot hand
[DE90-010195] N91-16371
The PHD: A Planar, Harmonic Drive robot for joint torque control
[NASA-CR-187924] N91-16386

TOXICITY
Multimedia Environmental Pollutant Assessment System (MEPAS) sensitivity analysis of computer codes
[DE90-010005] N91-16445

TRACKING (POSITION)
Vehicular sources in acoustic propagation experiments N91-16690
Effect of wind and temperature gradients on received acoustic energy N91-16697

TRACKING PROBLEM
A normative database for, and analysis of, the dual task of the TASKOMAT
[IZF-1990-A-11] N91-16846

TRADEOFFS
High efficiency silicon concentrator solar cells N91-16441

TRAINING EVALUATION
Current status of an artificial intelligence-based loss of consciousness monitoring system for advanced fighter aircraft N91-16556

TRAJECTORIES
Use of the Magnus force in the modified point mass trajectory model
[AD-A228194] N91-15990
Optimal trajectories for an aerospace plane. Part 1: Formulation, results, and analysis
[NASA-CR-187868] N91-16013
Typical motions in multiple systems N91-16945

TRAJECTORY CONTROL
Optimization and guidance of flight trajectories for the national aerospace plane
[NASA-CR-187837] N91-16010
Implementation and experimentation with motion planning algorithms
[AD-A228278] N91-16612

TRAJECTORY OPTIMIZATION
Optimization and guidance of flight trajectories for the national aerospace plane
[NASA-CR-187837] N91-16010
Optimal trajectories for an aerospace plane. Part 2: Data, tables, and graphs
[NASA-CR-187848] N91-16011
Applications of fuzzy theories to multi-objective system optimization
[NASA-CR-177573] N91-16012
Time optimal trajectories for a two wheeled robot
[DE90-010335] N91-16376

TRAJECTORY PLANNING
Time optimal trajectories for a two wheeled robot
[DE90-010335] N91-16376
Camera space manipulation of a mobile robot N91-16390

TRANSDUCERS
Lamina transducer coupler and method of making
[NASA-CASE-LAR-14361-1] N91-16707

TRANSFER FUNCTIONS
Field measurement of head related transfer functions
[AD-A227850] N91-16708

TRANSFORMERS
A transformer coupled semiconductor bridge igniter for low voltage ignition from a high voltage source
[DE90-009974] N91-16221
PCB/transformer techno-economic analysis model: User manual, volume 2
[DE90-010654] N91-16223

TRANSIENT HEATING
Planetary circulations in the presence of transient and self-induced heating N91-16505

TRANSISTORS
The 1/f noise in irradiated MOS devices
[DE90-007288] N91-16219
Radiation hardening of a high voltage IC technology (BCDMOS)
[DE90-008345] N91-16220
Measurements of 1/f noise in a-Si:H pin diodes and thin-film-transistors
[DE90-011218] N91-16228

TRANSITION FLOW
Development and application of numerical models for reactive flows
[AD-A228884] N91-16295
Stratiform clouds and their interaction with atmospheric motion N91-16506

TRANSITION POINTS
Theoretical and experimental examinations of transition behavior of the profile boundary layer at compressor and turbine grids
[ETN-91-98559] N91-16312

TRANSITION PRESSURE
Gas solubility in glassy polymers: A correlation with excess enthalpy
[AD-A228202] N91-16155

TRANSMISSION LINES
Nonradiative dielectric waveguide millimetre-wave integrated circuits: A review
[AD-A227760] N91-16238
Study on ECW transmission lines for NET/ITER
[EUR-FU/80/90-99] N91-16781

TRANSMISSION LOSS
Vehicular sources in acoustic propagation experiments N91-16690

TRANSMISSIONS (MACHINE ELEMENTS)
Geometrical aspects of the production of toothed disks
[MEMO-COSOR-90-02] N91-16178
Environmental noise from the Naesudden (Sweden) and Maglarp (Sweden) prototype wind turbines: A study of machinery noise
[FFA-TN-1990-34] N91-16706

TRANSMITTER RECEIVERS
Optical transceiver frontend for high speed bus STANAG 3910 with one fiber only
[MBB-UA-1182-90-PUB] N91-16745

TRANSMITTERS
NICAM 728: Factors affecting the assessment of UHF transmitter linearity
[BBC-RD-1990/9] N91-16190

TRANSONIC FLOW
Investigation of transonic flow over segmented slotted wind tunnel wall with mass transfer
[NASA-CR-187760] N91-15981
Large-scale numerical aerodynamic simulations for complete aircraft configurations
[NAL-TR-1073-T] N91-15984
Finite element approximations for transonic flows
[ETN-91-96491] N91-15988
Extension of transonic flow computational concepts in the analysis of cavitated bearings
[NASA-TM-103214] N91-16304
Unstationary shock and boundary layer phenomena at profiles and in a plane grid by transonic flow
[ETN-91-98557] N91-16311
Visualization of unsteady transonic flow by holographic interferometry using photorefractive media
[AD-A228802] N91-16336

TRANSONIC SPEED
Investigation of transonic flow over segmented slotted wind tunnel wall with mass transfer
[NASA-CR-187760] N91-15981

TRANSPIRATION
Evaluation of crop transpiration with remote sensing and computer simulation models
[REPT-1] N91-16431

TRANSPORT PROPERTIES
Electronic and ionic transport in processable conducting polymers
[AD-A227857] N91-16154
Gas solubility in glassy polymers: A correlation with excess enthalpy
[AD-A228202] N91-16155
Turbulence and diffusion in the atmospheric boundary layer
[DE90-011582] N91-16471

TRANSPORT THEORY
Monte Carlo simulation of atmospheric neutron transport at high altitudes using MCNP
[AD-A226773] N91-16474
Transport simulation of the effect of impurity radiation on the high beta, ohmic start-up of the HBT-EP tokamak
[DE90-010333] N91-16760

TRANSPORTATION
Requirements for a fuel cell for transportation application
[DE90-011146] N91-16230

TRANSVERSE WAVES
Analytical and experimental investigation of transverse flow aerodynamic windows for high power lasers
[DLR-FB-90-33] N91-16367

TRAPPED PARTICLES
Spontaneous force optical traps
[AD-A228539] N91-16363

TREES (MATHEMATICS)
An O(log n) time common CRCW pram algorithm for minimum spanning tree
[AD-A228740] N91-16623
Resolution of the 1D regularized Burgers equation using a spatial wavelet approximation
[NASA-CR-187480] N91-16664

TRENDS
Buran and the future of the Soviet space program N91-16037

TRIATOMIC MOLECULES
Experimental studies of the properties of trihydrogen and tetrahydrogen
[AD-A228869] N91-16110

TRIBOLOGY
A study of the formation and self-lubrication mechanisms of boric acid films on boric oxide coatings
[DE90-010115] N91-16137

TROPICAL REGIONS
South Pacific convergence zone and global-scale circulations N91-16503
Research on diabatic initialization N91-16504
Planetary circulations in the presence of transient and self-induced heating N91-16505
Tropical Pacific moisture variability N91-16509

TROPOSPHERE
Planetary circulations in the presence of transient and self-induced heating N91-16505
Synoptic/planetary-scale interactions and blocking over the North Atlantic Ocean N91-16513
Use of satellite data and modeling to assess the influence of stratospheric processes on the troposphere N91-16517
Prediction of tropical cyclone rapid intensification events
[AD-A227668] N91-16520

TUNERS
An algorithm for using a slide-screw tuner as a computer-controlled impedance
[DE90-010657] N91-16226
TUNGSTEN
Understanding the interdiffusion behavior and determining the long term stability of tungsten fiber reinforced niobium-base matrix composite systems
[NASA-CR-187396] N91-16120
TUNGSTEN ALLOYS
Tensile behavior of tungsten/niobium composites at 1300 to 1600 K
[NASA-TM-103727] N91-16128
TUNING
An algorithm for using a slide-screw tuner as a computer-controlled impedance
[DE90-010657] N91-16226
TURBINE BLADES
Aerodynamic surface pressure measurement in atmosphere and wind tunnel on a vertical axis wind turbine blade using pressure transducers N91-15980
Experimental and theoretical examinations of film cooling of gas turbine blades
[ETN-91-98554] N91-16022
Fiber-reinforced ceramic composites for Earth-to-orbit rocket engine turbines
[NASA-CR-185264] N91-16150
TURBINE ENGINES
Heat engines program
[DE90-010276] N91-16374
TURBINE PUMPS
Fiber-reinforced ceramic composites for Earth-to-orbit rocket engine turbines
[NASA-CR-185264] N91-16150
TURBINES
Advanced Turbine Technology Applications Project (ATTAP)
[NASA-CR-187039] N91-16021
TURBOPROP AIRCRAFT
Long-range vertical propagation N91-16693
TURBULENCE
Numerical analysis of viscous hypersonic flow past a generic forebody
[MBB/FE122/S/PUB/0407] N91-15997
Analytical and numerical studies in flow development
[DE90-010424] N91-16258
Numerical simulation of a complicated transition-breakdown of vortical flows inside a circular pipe N91-16273
Texas experimental tokamak
[DE90-011070] N91-16762
TURBULENCE EFFECTS
Stability criteria for stratocumulus-topped boundary layers evaluated through conditional sampling of turbulence elements
[AD-A228433] N91-16526
Distorted-wave born approximation calculations for turbulence scattering in an upward-refracting atmosphere N91-16700
Scattering of sound by atmospheric turbulence predictions in a refractive shadow zone N91-16703
TURBULENCE MODELS
Hypersonic shock/boundary-layer interaction database
[NASA-CR-187769] N91-15986
Computation of turbulent flow about unconventional airfoil shapes N91-15992
Numerical simulations of the mountain iron tracer data
[DE90-009749] N91-16499
Effects of large-scale wind driven turbulence on sound propagation N91-16704
TURBULENT BOUNDARY LAYER
Hypersonic shock/boundary-layer interaction database
[NASA-CR-187769] N91-15986
Numerical study of a three-dimensional turbulent boundary layer
[AD-A227835] N91-16291
Streamwise vortices in laminar-turbulent transition N91-16297
The vertical structure of the marine atmospheric boundary layer across a sea surface temperature front
[AD-A227931] N91-16525
TURBULENT DIFFUSION
Computation of turbulent flow about unconventional airfoil shapes N91-15992
TURBULENT FLOW
Computation of turbulent flow about unconventional airfoil shapes N91-15992
Modelling the transitional boundary layer
[NASA-CR-187487] N91-15995
High speed narrow bore capillary gas chromatography
[ETN-91-98481] N91-16113
Simulation of excited shear flows N91-16270
Heat transfer from water flowing through a chilled-bed open channel
[AD-A226855] N91-16286
Development and application of numerical models for reactive flows
[AD-A228884] N91-16295
Experimental parametric study of jet vortex generators for flow separation control
[NASA-CR-187836] N91-16296
Modeling the dissipation rate in rotating turbulent flows
[NASA-CR-187485] N91-16306
A process for unstationary velocity and turbulence measurements with a pneumatic measuring wedge probe
[MITT-33] N91-16310
Stochastic and chaotic effects in the ring laser N91-16359
TURBULENT HEAT TRANSFER
Heat transfer from water flowing through a chilled-bed open channel
[AD-A226855] N91-16286
TURBULENT MIXING
An experiment on supersonic turbulent mixing layers: Supersonic-subsonic two-stream layers
[NAL-TR-1066] N91-15983
Modelling of flamelet surface-to-volume ratio in turbulent premixed combustion
[DE90-006312] N91-16081
Simulation of excited shear flows N91-16270
TVD SCHEMES
Large-scale numerical aerodynamic simulations for complete aircraft configurations
[NAL-TR-1073-T] N91-15984
Numerical simulations of unsteady shock reflection processes by a ramp N91-16267
MmB: A new class of accurate high resolution schemes for conservation laws in two dimensions N91-16275
TWISTING
Geometrical parameters of E+S pairs N91-16865
TWO DIMENSIONAL BOUNDARY LAYER
Unstationary shock and boundary layer phenomena at profiles and in a plane grid by transonic flow
[ETN-91-98557] N91-16311
TWO DIMENSIONAL FLOW
Finite element solution techniques for the vorticity-stream function formulation of two-dimensional incompressible flows N91-16302
TWO DIMENSIONAL JETS
Local and global instability of heated 2-D jets and wakes N91-16298
TWO DIMENSIONAL MODELS
A two-dimensional balanced model of internal frontogenesis in geostrophic and isentropic coordinates
[AD-A227644] N91-16518
Solvable two-dimensional supersymmetric models and the supersymmetric Virasoro algebra
[DE90-012140] N91-16648
TWO PHASE FLOW
Pressure gradient effects on the development of hairpin vortices in an initially laminar boundary layer N91-16282

U

U.S.S.R. SPACE PROGRAM
Buran and the future of the Soviet space program N91-16037
UBV SPECTRA
Blue ellipticals in compact groups N91-16873
New data on the peculiar galaxy MRK 273 N91-16887
Galactic structure in direction of Vela-Puppis by means of UBV beta observations
[ETN-91-98556] N91-16973
ULTRAHIGH FREQUENCIES
NICAM 728: Factors affecting the assessment of UHF transmitter linearity
[BBC-RD-1990/9] N91-16190
The reflection and transmission properties of a triple band dichroic surface
[NASA-CR-187776] N91-16191
ULTRASONIC TESTS
Scattering of Lamb waves in an elastic plate for ultrasonic nondestructive evaluation of weldments and cracks N91-16412
ULTRASONIC WAVE TRANSDUCERS
Characterization of ultrasonic transducers using pattern recognition techniques
[DE91-000580] N91-16326
ULTRASONICS
Ultrasound and visual sensor feedback and fusion
[DE90-005280] N91-16369
ULTRAVIOLET RADIATION
Direct observation of NF(X) using laser-induced fluorescence: Kinetics of the NF 3 Sigma - ground state
[AD-A228294] N91-16362
ULTRAVIOLET SPECTRA
Observations of multiple nucleus galaxies N91-16890
Star formation in infrared bright and infrared faint starburst interacting galaxies N91-16901
UNDERGROUND EXPLOSIONS
Seismic signal processing optimized for a specific source and receiver
[DE90-010189] N91-16468
UNDERGROUND STRUCTURES
Evaluation procedure for reinforced concrete box culverts under airfield pavements
[AD-A227920] N91-16031
UNDERWATER ACOUSTICS
Canonical eigenvalues. Part 2: Application to one-layer, bounded, underwater acoustic ducts
[AD-A227451] N91-16577
SCATSPHERE2: A computation for the plane-wave scattering from a submerged, elastic, spherical, evacuated or fluid-filled, thin shell
[AD-A228867] N91-16709
UNDERWATER COMMUNICATION
Chemical beam epitaxy of ZnSe
[AD-A228045] N91-16817
UNITED STATES
An assessment of the government liquid hydrogen requirements for the 1995-2005 time frame including addendum, liquid hydrogen production and commercial demand in the United States
[NASA-TM-103812] N91-16166
Liquid hydrogen production and commercial demand in the United States N91-16168
UNIVERSE
A tentative explanation of cosmological red shift N91-16928
On the large-scale structures formed by wakes of open cosmic strings N91-16951
The best-fit universe
[DE91-004583] N91-16966
UNSTEADY AERODYNAMICS
Calculations for unsteady aerodynamic characteristics on a 3-D lifting body in subsonic flow using boundary element method
[NAL-TR-1065] N91-15985
Propfan supersonic panel method analysis and flutter predictions N91-15993
A coupled rotor aeroelastic analysis utilizing advanced aerodynamic modeling N91-16006
Numerical simulations of unsteady shock reflection processes by a ramp N91-16267
Study of time accuracy of flow variables across discontinuous boundaries N91-16300
UNSTEADY FLOW
Calculations for unsteady aerodynamic characteristics on a 3-D lifting body in subsonic flow using boundary element method
[NAL-TR-1065] N91-15985
Rotorcraft application of advanced computational aerodynamics
[NASA-CR-187767] N91-15987
On a class of unsteady three-dimensional Navier Stokes solutions relevant to rotating disc flows: Threshold amplitudes and finite time singularities
[NASA-CR-187482] N91-15991
The Proceedings of the Symposium on Mechanics for Space Flight 1989
[ISAS-SP-12] N91-16266
Numerical simulation of pulsatile flows passing through a pipe with sudden expansion N91-16271
Unsteady vortex lattice calculation of the flow around a slender delta wing N91-16272
Unsteady separation over maneuvering bodies
[AD-A226829] N91-16285
Visualization of unsteady transonic flow by holographic interferometry using photorefractive media
[AD-A228802] N91-16336
UPPER ATMOSPHERE
Joint US Navy/US Air Force climatic study of the upper atmosphere. Volume 1: January
[AD-A227122] N91-16476
Joint US Navy/US Air Force climatic study of the upper atmosphere. Volume 2: February
[AD-A227123] N91-16477
Joint US Navy/US Air Force climatic study of the upper atmosphere. Volume 3: March
[AD-A227124] N91-16478
Joint US Navy/US Air Force climatic study of the upper atmosphere. Volume 4: April
[AD-A227125] N91-16479
Joint US Navy/US Air Force climatic study of the upper atmosphere. Volume 7: July
[AD-A227126] N91-16480
Joint US Navy/US Air Force climatic study of the upper atmosphere. Volume 10: October
[AD-A227127] N91-16481
Upper atmosphere IR radiation modeling and analysis
[AD-A227214] N91-16482

The correction of infrasound signals for upper atmospheric winds N91-16695

URANIUM ALLOYS

Assessment of corrosion resistant coatings for a depleted U-0.75 Ti alloy
[AD-A228237] N91-16130

USER MANUALS (COMPUTER PROGRAMS)

Integrated Refractive Effects Prediction System (IREPS) user's manual, revision PC-2.0
[AD-A228549] N91-16203

PCB/transformer techno-economic analysis model: User manual, volume 2
[DE90-010654] N91-16223

ANEOS: Analytic equations of state for shock physics codes input manual
[DE90-010198] N91-16575

Geometric modeling applications interface program
[AD-A227651] N91-16591

Geometric modeling application interface program. System components operator's manual
[AD-A227827] N91-16594

The Assistant for Specifying the Quality Software (ASQS). Volume 2: User's manual. Volume 2
[AD-A227894] N91-16609

Briefing DTD user's guide for the Software Technology for Adaptable, Reliable Systems (STARS) program
[AD-A228473] N91-16618

Parallel Access Main Memory (PAMM) user's manual, version 1.0
[AD-A227744] N91-16635

USER REQUIREMENTS

Hartstone benchmark results and analysis
[AD-A226817] N91-16587

V

V/STOL AIRCRAFT

Evaluation of rotorwash characteristics for tiltrotor and tiltwing aircraft in hovering flight
[SCT-90RR-18] N91-15989

VACANCIES (CRYSTAL DEFECTS)

Integrated semiconductor modulators
[AD-A228615] N91-16820

VACILLATION

Theoretical and experimental studies of baroclinic processes N91-16512

VACUUM

State of an adiabatic expanding and condensing vapor or slow, medium, and fast explosions into a vacuum
[DE90-010815] N91-16263

Graviton effects in vacuum maximally symmetric spaces N91-16971

VACUUM APPARATUS

The Madison symmetric torus
[DE90-010306] N91-16757

VANADIUM

Electrolyte optimization and electrode material evaluation for the vanadium redox battery N91-16234

VANADIUM ALLOYS

Influence of strain rate on the structure/property of Ti-48Al-1V
[DE91-000172] N91-16122

VAPOR DEPOSITION

High temperature oxidation-resistant thruster research
[NASA-CR-185233] N91-16063

Hydrogen storage in metal hydrides
[AD-A228150] N91-16103

Electrochromic sun control coverings for windows
[DE90-000335] N91-16139

Comparative study of phosphosilicate glass on (100) silicon by furnace and rapid isothermal annealing
[NIAR-90-26] N91-16153

VAPOR PHASES

An approximation to true peak absorbance from observed peak absorbance for gas phase Fourier transform spectroscopy
[AD-A228357] N91-16104

High temperature corrosion of alloys in mixed gases N91-16121

State of an adiabatic expanding and condensing vapor or slow, medium, and fast explosions into a vacuum
[DE90-010815] N91-16263

VAPOR PRESSURE

Microwave measurements of water vapor partial pressure at temperatures up to 350 C
[DE90-011484] N91-16087

VAPORIZING

Safe venting of hydrogen
[DE90-008964] N91-16174

Cluster formation in laser-induced ablation and evaporation of solids observed by laser ionization time-of-flight mass spectrometry and scanning tunneling microscopy
[DE90-010876] N91-16344

VARIABILITY

Tropical Pacific moisture variability N91-16509

VARIABLE MASS SYSTEMS

Large space manipulators study
[AD-A227276] N91-16381

VARIATIONS

Global-scale, intraseasonal fluctuations of diabatic forcing of the atmosphere N91-16508

Neutron measurements in search of cold fusion
[DE91-004855] N91-16778

VECTOR ANALYSIS

Optimization of a power transient stability program on a vector supercomputer: Theory and applications
[AD-A227884] N91-16607

VECTOR PROCESSING (COMPUTERS)

User's guide to PANCOR: A panel method program for interference assessment in slotted-wall wind tunnels
[NASA-CR-187479] N91-16033

VELOCITY DISTRIBUTION

An experiment on supersonic turbulent mixing layers: Supersonic-subsonic two-stream layers
[NAL-TR-1066] N91-15983

Numerical simulation of pulsatile flows passing through a pipe with sudden expansion N91-16271

Optimization of hydrogen consumption in hydrogen masers
[AD-A227267] N91-16355

Excursions to the base of the mantle N91-16491

Canonical eigenvalues. Part 2: Application to one-layer, bounded, underwater acoustic ducts
[AD-A227451] N91-16677

The interacting pair Mkn 305/306 N91-16864

Observations of multiple nucleus galaxies N91-16890

Triplets of galaxies: Their dynamics, evolution, and the origin of chaos in them N91-16948

Simulations of gas clouds in interacting galaxies N91-16961

VELOCITY MEASUREMENT

A process for unstationary velocity and turbulence measurements with a pneumatic measuring wedge probe
[MITT-33] N91-16310

Optimization of a laser diode anemometry system
[LSTM-239/T/88] N91-16364

Selection effects and binary galaxy velocity differences N91-16927

VENTILATION

Investigation of transonic flow over segmented slotted wind tunnel wall with mass transfer
[NASA-CR-187760] N91-15981

VENTING

Safe venting of hydrogen
[DE90-008964] N91-16174

VERBAL COMMUNICATION

Linguistic and pragmatic constraints on utterance interpretation
[AD-A228815] N91-16210

VERTICAL DISTRIBUTION

The value of on-site sodar data in regional modeling
[DE90-009921] N91-16498

The vertical structure of the marine atmospheric boundary layer across a sea surface temperature front
[AD-A227931] N91-16525

Comparison of FFP predictions with measurements of a low-frequency signal propagated in the atmosphere N91-16698

VERTICAL MOTION

A comparison of diagnostic and kinematic vertical motion fields associated with curved and straight jet streak adjustment processes
[AD-A227724] N91-16522

VERTICAL ORIENTATION

Transient natural convection in heated inclined tubes
[DE90-008217] N91-16255

VERY LARGE ARRAY (VLA)

Systematic design of regular VLSI processor arrays
[ETN-91-98482] N91-16250

VLA neutral hydrogen imaging of compact groups N91-16872

VERY LARGE SCALE INTEGRATION

ICHARM: Hierarchical CMOS circuit extraction with power bus extraction
[AD-A228613] N91-16245

Systematic design of regular VLSI processor arrays
[ETN-91-98482] N91-16250

Timing margin measurement using a laser technique
[AD-A226821] N91-16353

Statistical process control for QML (Qualified Manufacturer's List) radiation hardness assurance
[DE90-007413] N91-16394

Microsupercomputers: Design and implementation
[AD-A228741] N91-16571

Microsupercomputers: Design and implementation
[AD-A228744] N91-16572

VIBRATION

Detection of solid lubricant film failure during sliding by vibration monitoring
[NAL-TR-1060] N91-16384

VIBRATION DAMPING

Passive damping concepts for tubular beams with partial rotational and translational end restraints
[NASA-CR-187833] N91-16411

VIBRATION ISOLATORS

Proving experiments on an acoustic transmission suite and its reverberation room
[BBC-RD-1990/13] N91-16681

VIBRATION TESTS

Detection of solid lubricant film failure during sliding by vibration monitoring
[NAL-TR-1060] N91-16384

VIBRATIONAL SPECTRA

Time-resolved Coherent Anti-Stokes Raman Spectroscopy (CARS) and the measurement of vibrational spectra in shock-compressed molecular materials
[DE90-012053] N91-16091

Molecular crystals and localized vibrational states
[DE90-010602] N91-16786

VIDEO COMMUNICATION

Reports on cartography and topography. Series 1, report 104
[ISSN-0469-4236] N91-16432

The photogrammetric evaluation by video technique: A supporting study N91-16433

VIDEO DATA

The photogrammetric evaluation by video technique: A supporting study N91-16433

Real-time filtering and detection of dynamics for compression of HDTV
[NASA-CR-187777] N91-16596

VIDEO SIGNALS

Real-time filtering and detection of dynamics for compression of HDTV
[NASA-CR-187777] N91-16596

The design of a two-dimensional optical image correlator and its application in image tracking N91-16744

VIRGO GALACTIC CLUSTER

Collisional removal of HI from the inner disks of Virgo cluster galaxies N91-16952

Molecular gas and star formation in the central regions of Virgo spiral galaxies N91-16970

VIRUSES

Research pathology and special techniques
[NASA-CR-187828] N91-16639

VISCOELASTICITY

From visco-elasticity towards thermal relaxation: A neutron scattering study of density fluctuations in fluid helium
[ETN-91-98486] N91-16111

Time-temperature response of multiphase viscoelastic solids through numerical analysis N91-16401

Utilization of polymer viscoelastic properties in acoustic wave sensor applications
[DE90-010534] N91-16676

VISCOPLASTICITY

Inelastic strain analysis of solder joint in NASA fatigue specimen
[NASA-CR-187864] N91-16132

Finite element solution of steady state axisymmetric penetration problems N91-16403

Finite element thermo-viscoplastic analysis of aerospace structures
[NASA-TM-102761] N91-16407

VISCOSITY

Streamwise vortices in laminar-turbulent transition N91-16297

Asymptotic-induced numerical methods for conservation laws
[NASA-CR-187483] N91-16305

Utilization of polymer viscoelastic properties in acoustic wave sensor applications
[DE90-010534] N91-16676

VISCOUS FLOW

Rotorcraft application of advanced computational aerodynamics
[NASA-CR-187767] N91-15987

Numerical analysis of viscous hypersonic flow past a generic forebody
[MBB/FE122/S/PUB/0407] N91-15997

Numerical simulations of unsteady shock reflection processes by a ramp N91-16267

Some topics of Navier-Stokes solvers N91-16269

Simulation of the flow past an impulsively started cylinder using a discrete vortex method N91-16303

The stationary exterior three dimensional Navier-Stokes problem of viscous flow past a body in anisotropically weighted Sobolev spaces
[REPT-110] N91-16314

Continuum models of continental deformation N91-16490

VISIBLE SPECTRUM
Chemical beam epitaxy of ZnSe
[AD-A228045] N91-16817
VISION
The use of contact lenses in the civil airman population
[AD-A227450] N91-16544
VISUAL DISCRIMINATION
Limits of human visual discrimination: Toward a general model of visual geometry
[AD-A226826] N91-16548
VISUAL PERCEPTION
Limits of human visual discrimination: Toward a general model of visual geometry
[AD-A226826] N91-16548
Pre-attentive and attentive visual information processing
[AD-A228541] N91-16550
VOICE COMMUNICATION
Movable-boundary channel-access schemes for integrated voice/data networks
[AD-A227331] N91-16186
VOICE DATA PROCESSING
A trellis-searched APC (Adaptive Predictive Coding) speech coder
[DE91-000866] N91-16581
IEEE International Symposium on Information Theory
[AD-A228239] N91-16842
VOIDS
Void nucleation in nonlinear solid mechanics
[AD-A228890] N91-16410
On the large-scale structures formed by wakes of open cosmic strings N91-16951
VOLT-AMPERE CHARACTERISTICS
Threshold voltage and I-V characteristics of AlGaAs/GaAs MODFETs
[AD-A228844] N91-16248
VOLTAGE REGULATORS
Status of Argonne life evaluation of valve regulated lead-acid batteries
[DE90-011098] N91-16229
VORTEX BREAKDOWN
Numerical simulation of a complicated transition-breakdown of vortical flows inside a circular pipe N91-16273
VORTEX GENERATORS
Experimental parametric study of jet vortex generators for flow separation control
[NASA-CR-187836] N91-16296
VORTEX SHEDDING
Unsteady vortex lattice calculation of the flow around a slender delta wing N91-16272
VORTEX SHEETS
Numerical simulation of separated flows around a wing section at steady and unsteady motion by a discrete vortex method N91-16268
VORTICES
On the Goertler instability in hypersonic flows: Sutherland law fluids and real gas effects
[NASA-CR-187481] N91-15994
The Proceedings of the Symposium on Mechanics for Space Flight 1989
[ISAS-SP-12] N91-16266
Simulation of excited shear flows N91-16270
Unsteady vortex lattice calculation of the flow around a slender delta wing N91-16272
Numerical simulation of a complicated transition-breakdown of vortical flows inside a circular pipe N91-16273
Analysis and application of the discrete vortex method N91-16290
Streamwise vortices in laminar-turbulent transition N91-16297
Simulation of the flow past an impulsively started cylinder using a discrete vortex method N91-16303
Potential vorticity index N91-16516
Observations of vortex structure in YBa2Cu3O7
[DE91-000900] N91-16804
Dynamical properties of two-dimensional Josephson junction arrays N91-16823
VORTICITY
Numerical simulation of pulsatile flows passing through a pipe with sudden expansion N91-16271
The development of laser speckle velocimetry for the study of vortical flows
[NASA-CR-187756] N91-16289
Analysis and application of the discrete vortex method N91-16290
Finite element solution techniques for the vorticity-stream function formulation of two-dimensional incompressible flows N91-16302
Synoptic/planetary-scale interactions and blocking over the North Atlantic Ocean N91-16513
Potential vorticity index N91-16516

W

WAKES
Local and global instability of heated 2-D jets and wakes N91-16298
On the large-scale structures formed by wakes of open cosmic strings N91-16951
WALKING MACHINES
Kinematics of arthropod legs: Modeling and measurement N91-16391
WALL TEMPERATURE
The effect of charge mixture ratio and particle size on igniter plume heat transfer characteristics
[DE90-010833] N91-16160
WALLS
High temperature furnace modeling and performance verifications
[NASA-CR-187831] N91-16032
Proving experiments on an acoustic transmission suite and its reverberation room
[BBC-RD-1990/13] N91-16681
Plasma-facing materials
[DE90-008243] N91-16753
WARFARE
Army Unmanned Aerial Vehicle (UAV) requirements and the joint UAV program
[AD-A228149] N91-16009
WASTE HEAT
Evaporation process and 3 phase flow in a water evaporator assembly
[MBB-UO-0108-90-PUB] N91-16060
WASTE UTILIZATION
Highlights of the Chemical Technology (CMT) Division's activities
[DE90-008242] N91-16984
WATER
Destruction of propellant components in supercritical water
[DE90-010600] N91-16085
Desorption of H2O and H2 from steel and LiAO2 by temperature programmed desorption
[DE90-011170] N91-16118
Global variability of water vapor and condensate from SSM/I N91-16507
WATER FLOW
Heat transfer from water flowing through a chilled-bed open channel
[AD-A226855] N91-16286
WATER HEATING
Colorado State University program for developing, testing, evaluating and optimizing solar heating and cooling systems
[DE90-010107] N91-16435
WATER INJECTION
Technical and economic evaluation of diesel engine with oxygen enrichment and water injection
[DE90-009723] N91-16373
WATER MANAGEMENT
Detection of soil moisture using X-band SLAR records in a sandy area
[BCRS-90-08] N91-16427
WATER QUALITY
Environmental trends
[DE90-010530] N91-16450
Monitoring challenges and innovative ideas
[DE91-000586] N91-16465
WATER RECLAMATION
Whole body cleansing agent
[NASA-CASE-MSC-21589-1] N91-16566
WATER VAPOR
Microwave measurements of water vapor partial pressure at temperatures up to 350 C
[DE90-011484] N91-16087
Droplet shattering, vaporization, and recondensation in cloud clearing with long pulse infrared chemical lasers
[DE90-010584] N91-16343
Global variability of water vapor and condensate from SSM/I N91-16507
Tropical Pacific moisture variability N91-16509
WATER WAVES
Research in nonlinear water waves
[AD-A227948] N91-16292
WAVE AMPLIFICATION
Wave-particle power transfer in a steady-state driven system
[DE90-010031] N91-16748
WAVE ATTENUATION
Seismic imaging for velocity and attenuation structure in geothermal fields
[DE90-010742] N91-16469
Attenuation of seismic waves in the near-source region
[AD-A226814] N91-16475
WAVE EQUATIONS
Natural waves of microstrip transmission lines in wave guides
[BER-68] N91-16251
Wave propagation through random media: A local method of small perturbations based on the Helmholtz equation N91-16701
A tentative explanation of cosmological red shift N91-16928
WAVE INTERACTION
The effect of latent heat release on synoptic-to-planetary wave interactions and its implication for satellite observations: Theoretical modeling N91-16514
The effect of latent heat release on synoptic-to-planetary scale wave interactions and implications for satellite observations: Observational study N91-16515
WAVE PROPAGATION
Comparison of propagation and absorption of FEL-generated microwaves with theory
[DE90-010369] N91-16181
A method for pressure-pulse suppression in fluid-filled piping
[DE90-010408] N91-16260
Attenuation of seismic waves in the near-source region
[AD-A226814] N91-16475
Use of satellite data and modeling to assess the influence of stratospheric processes on the troposphere N91-16517
An investigation of a gravity wave during GALE: February 6, 1986
[AD-A227655] N91-16519
Utilization of polymer viscoelastic properties in acoustic wave sensor applications
[DE90-010534] N91-16676
Full field visualization of surface and bulk acoustic waves
[AD-A227676] N91-16678
On the propagation of plane waves above an impedance surface N91-16684
Wave propagation through random media: A local method of small perturbations based on the Helmholtz equation N91-16701
Caustic waves in galaxy disks produced in collisions with low mass companions N91-16960
WAVE REFLECTION
On the propagation of plane waves above an impedance surface N91-16684
WAVE SCATTERING
Models for surface scattering from solids and liquids
[RSRE-MEMO-3699] N91-16192
Scattering of Lamb waves in an elastic plate for ultrasonic nondestructive evaluation of weldments and cracks N91-16412
WAVEFORMS
A graphical user-interface-driven waveform data acquisition and analysis system
[DE90-011948] N91-16578
Preliminary analysis of measured sound propagation over various seasonal snow covers N91-16687
WAVEGUIDES
Nonradiative dielectric waveguide millimetre-wave integrated circuits: A review
[AD-A227760] N91-16238
Natural waves of microstrip transmission lines in wave guides
[BER-68] N91-16251
WEAK ENERGY INTERACTIONS
Parity violation and electron scattering
[DE90-010429] N91-16712
WEAK INTERACTIONS (FIELD THEORY)
Fermions in the hypercharge sector of the standard lattice electroweak theory: Global limit
[DE90-009731] N91-16827
WEAPON SYSTEMS
Impacts of advanced manufacturing technology on parametric estimating
[AD-A228232] N91-16177
WEAR
Weldability of nickel aluminides
[DE90-008557] N91-16116
Detection of solid lubricant film failure during sliding by vibration monitoring
[NAL-TR-1060] N91-16384
WEAR TESTS
Wear measurement of ceramic bearings in gas turbines
[AD-A227505] N91-16382
WEATHER
NASA/MSFC FY90 Global Scale Atmospheric Processes Research Program Review
[NASA-CP-3093] N91-16500
Effects of large-scale wind driven turbulence on sound propagation N91-16704

WEATHER FORECASTING
Results of the Kansas City 1989 Terminal Doppler Weather Radar (TDWR) operational evaluation testing
[AD-A228784] N91-16205
Research on diabatic initialization N91-16504
Global-scale, intraseasonal fluctuations of diabatic forcing of the atmosphere N91-16508
Tropical Pacific moisture variability N91-16509
Nonlinear dynamics of global atmospheric and Earth-system processes N91-16510
The effect of latent heat release on synoptic-to-planetary wave interactions and its implication for satellite observations: Theoretical modeling N91-16514
Prediction of tropical cyclone rapid intensification events
[AD-A227668] N91-16520
Examples of isallobaric forcing in surface frontal motion and surface frontogenesis over the Central United States
[AD-A227687] N91-16521
Spatial and temporal climate variations influencing medium-range temperature predictions over south-central European Russia
[AD-A228623] N91-16527
A noise assessment and prediction system N91-16702

WEDGES
High-frequency techniques for RCS prediction of plate geometries
[NASA-CR-187865] N91-16212
Some topics of Navier-Stokes solvers N91-16269
Evaluation of the HULL and SHARC hydrocodes in simulating the reflection of Mach 2.12 non-decaying shock on wedges of various angles
[AD-A227581] N91-16287
A process for unstationary velocity and turbulence measurements with a pneumatic measuring wedge probe
[MITT-33] N91-16310
BLAST2D computations of the reflection of planar shocks from wedge surfaces with comparison to SHARC and STEALTH results
[AD-A227261] N91-16589

WEIGHTING FUNCTIONS
Operating characteristics for weighted energy detector with Gaussian signals
[AD-A226851] N91-16673

WEIGHTLESSNESS
The space flights: Second German Spacelab mission D-2 and Mir 1992
[REPT-25/90] N91-16034
Determination of shuttle orbiter center of gravity from flight measurements
[NASA-TM-102627] N91-16058
Whole body cleansing agent
[NASA-CASE-MSC-21589-1] N91-16566

WELD TESTS
HAZ liquation cracking behavior in newly developed lean 316 stainless steels
[DE90-009409] N91-16117

WELDABILITY
Weldability of nickel aluminides
[DE90-008557] N91-16116
HAZ liquation cracking behavior in newly developed lean 316 stainless steels
[DE90-009409] N91-16117

WELDED JOINTS
Test methods for evaluating hot cracking: Review and perspective
[DE90-009820] N91-16397
Plate and butt-weld stresses beyond elastic limit, material and structural modeling
[NASA-TP-3075] N91-16413

WELDED STRUCTURES
Scattering of Lamb waves in an elastic plate for ultrasonic nondestructive evaluation of weldments and cracks N91-16412

WELDING
Test methods for evaluating hot cracking: Review and perspective
[DE90-009820] N91-16397

WEST GERMANY
Documents on the history of the Aerodynamic Research Establishment at Goettingen, 1907 - 1925
[DLR-MITT-90-05] N91-15977
Activities report of the German Federal Institute for Flight Safety
[ETN-91-98644] N91-16002
Space research in the Federal Republic of Germany, 1988 and 1989
[ETN-91-98514] N91-16849

WETTING
Whole body cleansing agent
[NASA-CASE-MSC-21589-1] N91-16566

WHITE NOISE
Near/far resistant receivers for DS/SSMA communications
[AD-A228147] N91-16200

WICKS
Heat transfer characteristics of a radical heat pipe N91-16276
Experimental study on mercury heat pipes (on effect of screen mesh wick under bottom heat mode) N91-16280

WIGGLER MAGNETS
Nonlinear resonance
[DE90-010428] N91-16341

WIND (METEOROLOGY)
Analysis of atmospheric diffusion of pollutants based on the limited observation of horizontal wind N91-16274
Research in nonlinear water waves
[AD-A227948] N91-16292
South Pacific convergence zone and global-scale circulations N91-16503
Research on diabatic initialization N91-16504
Potential vorticity index N91-16516
The correction of infrasound signals for upper atmospheric winds N91-16695
Meteorological effects on long-range outdoor sound propagation N91-16696

WIND DIRECTION
The correction of infrasound signals for upper atmospheric winds N91-16695

WIND EFFECTS
Effect of wind and temperature gradients on received acoustic energy N91-16697
Effects of large-scale wind driven turbulence on sound propagation N91-16704

WIND MEASUREMENT
Definition and preliminary design of the Laser Atmospheric Wind Sounder (LAWS) phase 1. Volume 1: Executive summary
[NASA-CR-184071] N91-16332
Definition and preliminary design of the Laser Atmospheric Wind Sounder (LAWS) phase 1. Volume 2
[NASA-CR-184072] N91-16333
Definition and preliminary design of the Laser Atmospheric Wind Sounder (LAWS) phase 1. Volume 3: Program cost estimates
[NASA-CR-184073] N91-16334
The value of on-site sodar data in regional modeling
[DE90-009921] N91-16498
Prediction of tropical cyclone rapid intensification events
[AD-A227668] N91-16520

WIND PROFILES
The value of on-site sodar data in regional modeling
[DE90-009921] N91-16498
Analysis of wind profile measurements from an instrumented aircraft
[NASA-CR-184084] N91-16523
The correction of infrasound signals for upper atmospheric winds N91-16695
Comparison of FFP predictions with measurements of a low-frequency signal propagated in the atmosphere N91-16698

WIND SHEAR
Global variability of water vapor and condensate from SSM/I N91-16507
Wind turbine acoustics
[NASA-TP-3057] N91-16679

WIND TUNNEL TESTS
Wind tunnel tests on flutter control of a high-aspect-ratio cantilevered wing: Control with leading-edge and trailing-edge control surfaces
[NAL-TR-1070] N91-15982
Joint computational/experimental aerodynamics research on a reentry vehicle. Part 2: Computational results
[DE90-012765] N91-16054
Investigation of the influence of constant adverse pressure gradients on laminar boundary-layer stability at Mach number 8
[AD-A228231] N91-16293
Experimental parametric study of jet vortex generators for flow separation control
[NASA-CR-187836] N91-16296

WIND TUNNEL WALLS
Investigation of transonic flow over segmented slotted wind tunnel wall with mass transfer
[NASA-CR-187760] N91-15981
User's guide to PANCOR: A panel method program for interference assessment in slotted-wall wind tunnels
[NASA-CR-187479] N91-16033

WIND TUNNELS
Calculation of support interferences on the aerodynamic coefficients for a wind tunnel calibration model
[DLR-FB-90-26] N91-15998

WIND TURBINES
Aerodynamic surface pressure measurement in atmosphere and wind tunnel on a vertical axis wind turbine blade using pressure transducers N91-15980
Wind turbine acoustics
[NASA-TP-3057] N91-16679
Environmental noise from the Naesudden (Sweden) and Maglarp (Sweden) prototype wind turbines: A study of machinery noise
[FFA-TN-1990-34] N91-16706

WIND VELOCITY
Analysis of atmospheric diffusion of pollutants based on the limited observation of horizontal wind N91-16274
A comparison of optically measured and radar-derived horizontal neutral winds
[AD-A227690] N91-16483
Research on diabatic initialization N91-16504
Meteorological effects on long-range outdoor sound propagation N91-16696

WIND VELOCITY MEASUREMENT
Analysis of wind profile measurements from an instrumented aircraft
[NASA-CR-184084] N91-16523

WINDOWS (APERTURES)
Electrochromic sun control coverings for windows
[DE90-000335] N91-16139
Analytical and experimental investigation of transverse flow aerodynamic windows for high power lasers
[DLR-FB-90-33] N91-16367

WINDOWS (INTERVALS)
The use of window functions and Kalman filtering in spectral estimation
[AD-A227482] N91-16236

WING LOADING
TF89 tactical fighter outer wing design
[ETN-91-98580] N91-16019

WING OSCILLATIONS
Wind tunnel tests on flutter control of a high-aspect-ratio cantilevered wing: Control with leading-edge and trailing-edge control surfaces
[NAL-TR-1070] N91-15982

WINGS
Wind tunnel tests on flutter control of a high-aspect-ratio cantilevered wing: Control with leading-edge and trailing-edge control surfaces
[NAL-TR-1070] N91-15982
The Proceedings of the Symposium on Mechanics for Space Flight 1989
[ISAS-SP-12] N91-16266
Numerical simulation of separated flows around a wing section at steady and unsteady motion by a discrete vortex method N91-16268

WIRE
Investigation of wire motion in superconducting magnets
[DE91-004952] N91-16674
Composite ceramic superconducting wires for electric motor applications
[AD-A228359] N91-16818

WORK-REST CYCLE
Computer aided physiological assessment of the functional state of pilots during simulated flight N91-16562

WORKING FLUIDS
Heat transfer characteristics of a radical heat pipe N91-16276

WORKLOADS (PSYCHOPHYSIOLOGY)
Safety Network to Detect Performance Degradation and Pilot Incapacitation
[AGARD-CP-490] N91-16553
EEG indicators of mental workload: Conceptual and practical issues in the development of a measurement tool N91-16559
Optimisation of operational workload levels using neurophysiological and cognitive techniques N91-16560
Study of pilot vigilance during long range flight N91-16561
Development of a test-bed for real-time monitoring of pilot mental status N91-16563

X

X RAY ANALYSIS
A tunable x ray microprobe using synchrotron radiation
[DE90-011219] N91-16322

X RAY BINARIES
X ray emission from low-mass binary systems N91-16853
The x ray emission of SS433
[MPE-PREPRINT-189] N91-16856

X RAY DIFFRACTION
Characterization of GaAs/Si interface structure by x ray diffraction
[DE91-004769] N91-16811
X RAY FLUORESCENCE
A tunable x ray microprobe using synchrotron radiation
[DE90-011219] N91-16322
X RAY IMAGERY
Multiframe x ray images from a single meander stripline coated on a microchannel plate
[DE90-010741] N91-16224
Ion contamination of x ray pinhole camera images on PBFA 2
[DE90-012180] N91-16325
X RAY LASERS
Short pulse driven recombination x ray lasers
[DE90-009945] N91-16340
X RAY SOURCES
X ray emission from low-mass binary systems
N91-16853
X RAY SPECTRA
Comparison of some x ray sensors for verification
[DE90-011990] N91-16323
The x ray emission of SS433
[MPE-PREPRINT-189] N91-16856
X RAYS
In situ studies of potential dependent structural and distributional changes at electrochemical interfaces with x rays
[AD-A226844] N91-16098
X-Ray Detector: An x-ray radiation detector design code
[DE90-008235] N91-16317
Comparison of some x ray sensors for verification
[DE90-011990] N91-16323
Development of an external beam ion milliprobe
[AD-A227247] N91-16329
High-purity silicon soft x ray sensor arrays
[ETN-91-98484] N91-16338
Modeling the performance of water and liquid gallium cooled x ray optical components: A comparison with experiment
[DE90-010460] N91-16784
Multiple-photon Compton scattering in a strong magnetic field: Cross-sections and radiative transport N91-16852
X ray emission from low-mass binary systems
N91-16853
XENON
Development of liquid xenon imaging gamma-ray spectrophotometers
[AD-A227575] N91-16740

Y

YAG LASERS
Generation of high power 1.54 micrometer radiation by stimulated Raman scattering in methane
[FEL-90-B098] N91-16366
The Cabannes-lidar for the examination of the stratosphere: Selected design elements for the experimental construction
[BONN-IR-90-39] N91-16493
YAW
Determination of shuttle orbiter center of gravity from flight measurements
[NASA-TM-102627] N91-16058
YTTRIUM OXIDES
YBa2Cu3O(7-x) thin film growth on single crystal and polycrystalline yttria-stabilized zirconia
[DE90-010707] N91-16788
Microstructures and dc critical currents in textured Y-Ba-Cu-oxides
[DE91-000895] N91-16803
Observations of vortex structure in YBa2Cu3O7
[DE91-000900] N91-16804
From low to high Tc: An ultrasonic investigation of niobium single crystal and YBaCuO superconducting thin films with surface acoustic waves N91-16822

Z

ZETA PINCH
The Los Alamos megamp fiber z-pinch experiment
[DE91-004842] N91-16777
ZINC TELLURIDES
Low-cost CdZnTe devices for cascade cell application
[DE91-002116] N91-16444
ZIRCONIUM OXIDES
High temperature furnace modeling and performance verifications
[NASA-CR-187831] N91-16032
YBa2Cu3O(7-x) thin film growth on single crystal and polycrystalline yttria-stabilized zirconia
[DE90-010707] N91-16788
Characterization of chemically prepared PZT thin films
[DE90-010831] N91-16789

Typical Personal Author Index Listing

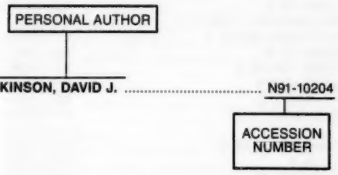

Listings in this index are arranged alphabetically by personal author. The accession number denotes the number by which the citation is identified.

A

AARONSON, H. I. N91-16821
ABELL, G. C. N91-16808
ABEYARATNE, ROHAN N91-16410
ABLOWITZ, MARK J. N91-16294
ABRAHAM, K. M. N91-16247
ABRAHAM, ZULEMA N91-16907
ABRUNA, HECTOR D. N91-16098
ACEVEDO, DAVID N91-16098
ACKERMANS, PAUL ANTON JOSEF N91-16133
ADAMS, L. M. N91-16258
ADELMAN, ROBERT N91-16542
AHMED, SALAHUDDIN N91-15992
AKLONIS, J. J. N91-16146
AKUJOR, CHIDI E. N91-16924
AL-NASSAR, YAAGOUB NASSAR N91-16412
ALAMGIR, M. N91-16247
ALASHQUR, ABDALLAH MOHAMMED N91-16580
ALBERT, DONALD G. N91-16687
ALBERTA, TIMOTHY L. N91-16515
ALBERY, WILLIAM B. N91-16556
ALBRIGHT, SCOT P. N91-16443
ALBRIGHT, STEPHEN LAWRENCE N91-16391
ALEXANDER, DAVID J. N91-16399
ALEXANDER, STEPHEN GEORGE N91-16852
ALLARD, L. F. N91-16320
ALLEN, MIKE J. N91-16344
ALLISON, PAUL N91-16772
ALPERT, BRADLEY KEVIN N91-16660
ALSRUHE, TIMOTHY F. N91-16486
ALTON, LARRY N91-16001
AMEZAWA, HIROO N91-16276
AMIRKHANIAN, A. S. N91-16877
ANDERSON, DANA Z. N91-16743
ANDERSON, R. E. N91-16778
ANDREWS, ANTHONY W. N91-16528
ANOSOVA, JOANNA P. N91-16945
N91-16946
N91-16949
N91-16950
ANSARI, RAFAT R. N91-16350
ANSTREICHER, K. M. N91-16600
ANTONSEN, T. M., JR. N91-16346
N91-16763
N91-16764
AOKI, SINYA N91-16827
APEL, UWE N91-16570
APPLETON, P. N. N91-16868
APRILE, ELENA N91-16740
ARENS, JOHN F. N91-16790
ARENZ, R. W. N91-16318
ARMINI, A. J. N91-16382
ARMSTRONG, RUSSELL A. N91-16776
ARMSTRONG, TONY W. N91-16056
ARMUS, LEE N91-16916
ARNOLD, S. N91-16095
ARRUDA, ANTHONY N91-16690
ASATRIAN, A. S. N91-16887
ASHMAN, WILLIAM P. N91-16097
ASO, SHIGERU N91-16267
N91-16268
ATENCIO, JERRY H. N91-16085
ATHANASSOULA, E. N91-16930
ATTALLA, A. N91-16808
ATTENBOROUGH, K. N91-16692
AUDET, SARAH ANNE STEIGERWALD N91-16338
AVERY, DON E. N91-16832
AXON, D. J. N91-16893
AYERS, MARILYN V. N91-16835
AZEVEDO, J. SOUZA N91-16783
AZUMA, HISAO N91-16279

B

BACK, LLOYD H. N91-16078
BACON, LARRY D. N91-16180
N91-16232
BADDOUR, R. F. N91-16155
BAE, YOUNG K. N91-16172
BAHAR, EZEKIEL N91-16201
BAIN, ADDISON N91-16166
N91-16167
BAKER, D. A. N91-16778
BAKKER, H. C. N91-16428
BAKO, BABOU N91-16645
BALACHANDRAN, U. N91-16792
BALAKUMAR, P. N91-15991
N91-15996
BALANIS, CONSTANTINE A. N91-16212
BALAS, EGON N91-16626
BALCELLS, M. N91-16908
BALOOCH, M. N91-16344
BALSARA, DINSHAW S. N91-16959
BAMBERGER, J. A. N91-16256
BAMBERGER, JUDY N91-16610
BANGERTER, ROGER O. N91-16437
N91-16759
BANKS, S. P. N91-16658
BARCILON, ALBERT N91-16516
BARDSLEY, J. N. N91-16340
BARNARD, STEPHEN N91-16643
BARNES, C. E. N91-16352
BARNES, D. C. N91-16755
BARNETT, D. L. N91-16369
BARNHART, JOHN S. N91-16262
BARNSTABLE, BOB N91-16052
BARTH, MARVIN N91-16182
BARTLETT, RODNEY J. N91-16728
BARTRAM, M. E. N91-16812
BASKETT, RONALD L. N91-16471
N91-16498
BASOL, BULENT M. N91-16444
BASORE, PAUL A. N91-16795
BASS, HENRY E. N91-16703
N91-16704
BATEMAN, G. N91-16774
BATES, BEVAN D. N91-16238
BAUER, PETER N91-16596
BAUM, HUGUES-PIERRE N91-16822
BAUMJOHANNN, W. N91-16974
BAUSCHLICHER, CHARLES W., JR. N91-16065
N91-16728
BEAULIEU, SYLVIE N91-16884
BEAUSANG, C. W. N91-16798
BECKER, J. A. N91-16798
BECKERMAN, M. N91-16369
BEEKE, K. L. N91-16190
BEEKMAN, W. N91-16431
BEHLING, MICHAEL N91-16047
BELL, M. N91-16774
BELL, P. M. N91-16224
BELLAN, JOSETTE N91-16078
BENDER, RALF N91-16862
BENNETT, C. A. N91-16756
BENNETT, E. F. N91-16766
BENSON, D. K. N91-16139
BENTLEY, J. N91-16814
BENZ, SAMUEL PAUL N91-16823
BERGER, HARALD N91-15988
BERGMAN, AVIV N91-16643
BERK, H. L. N91-16748
BERNARDEZ, L. N91-16344
BERNLOEHR, KONRAD N91-16958
BERZINS, G. J. N91-16323
BETTONI, D. N91-16880
BEVINGTON, DENNIS G. N91-16199
BHAT, M. K. N91-15981
BHATTACHARYA, B. N91-16886
BICKES, R. W., JR. N91-16221
BIELICK, E. F. N91-16260
BISCHOF, CHRISTIAN H. N91-16573
BIXLER, JAY V. N91-16088
BJORKEN, JAMES D. N91-16726
BLACKABY, NICHOLAS D. N91-15994
BLADOS, WALTER R. N91-16838
BLAKE, E. H. N91-16597
BLANCHARD, R. C. N91-16058
BLECK, RAINER N91-16514
BLEHA, S. A. N91-16326
BLOEM, J. N91-16365
BLOOM, DAVID M. N91-16237
BLOOM, I. N91-16231
BLOSS, WALTER L. N91-16248
BOCKMAN, RICHARD N91-16542
BOE, CHRISTIAN N91-16061
BOER, L. C. N91-16846
BOERNGEN, F. N91-16887
BOERSMA, WILLEM HEIN N91-16308
BOLTON, R. D. N91-16778
BOMMARITO, MARK N91-16098
BONIFACIO, R. N91-16349
BONIN, KEITH D. N91-16724
BONNER, B. E. N91-16733
N91-16747
BONNER, R. N91-16224
BORNE, KIRK D. N91-16932
BOROSKI, W. N. N91-16316
BOSLEY, DAVID L. N91-16341
BOTTCHER, C. N91-16721
BOWMAN, R. C., JR. N91-16808
BOY, GUY A. N91-16564
BOYER, J. D. N91-16351
BRADLEY, D. K. N91-16224
BRADLEY, GRAHAM WILLIAM N91-16464
BRADLEY, MICHAEL M. N91-16457
N91-16458
BRANSCOME, LEE E. N91-16514
BRAUD, JAMES E. N91-16841
BRAY, K. N. C. N91-16081
BRECKENRIDGE, JOHN L. N91-16841
BRECKENRIDGE, R. P. N91-16461
BREEDON, LORRAINE MARIA N91-16853
BREIZMAN, B. N. N91-16748
BREWE, D. E. N91-16304
BREZOWSKI, C. F. N91-16160
BRIENZO, RICHARD K. N91-16697
BRINKMAN, M. J. N91-16798
BRINKMANN, W. N91-16856
BRINSON, LYNDA CATHERINE N91-16401
BRITTEN, J. A. N91-16080
BROCKMEYER, JERRY W. N91-16150
BRODIE, JEAN P. N91-16088
BRODY, LYNN N91-16542
BROEMME, ANNA DOROTHEA DAGMAR N91-16825
BRONK, B. V. N91-16095
BROWN, C. L. N91-16583
BROWN, HAROLD K. N91-16353
BROWN, RICHARD K. N91-16839
BROWN, RUSSELL D. N91-16208
BROWNER, RICHARD F. N91-16083
BRUNNER, K. N91-16076
BU, JICHUN N91-16250
BUCHANAN, J. A. N91-16733
N91-16747
BUCHANAN, MICHELLE V. N91-16452
BUCHMAN, DONALD N91-16047
BUDAI, J. D. N91-16788
BUDGE, KENT GRIMMETT N91-16854
BUELOW, STEVEN J. N91-16085
BUGG, CHARLES E. N91-16815
BULLOCK, J. S., IV N91-16756
BUNKER, S. N. N91-16382
BUNKER, SUSAN S. N91-16499
BURGESS, D. W. N91-16560
BURKERT, ANDREAS MICHAEL N91-16967
BURNHAM, ALAN K. N91-16985

BURRELL, K. H. N91-16773
BURSTEN, BRUCE E. N91-16711
BUSHOUSE, HOWARD A. N91-16898
N91-16901
BUTA, RONALD N91-16885
BUTLER, DOUGLAS M. N91-16185
BUTLER, KAREN N91-16512
BUTLER, P. L. N91-16385
BUTNER, HAROLD MARTIN N91-16969
BUTTERFIELD, K. B. N91-16778
BYER, R. L. N91-16237
BYRD, GENE G. N91-16936
N91-16938
N91-16939

C

CABO, A. J. N91-16657
CABON, PH. N91-16561
CAFFEE, M. W. N91-16084
CAI, A. N91-16321
CAKIR, S. N91-16495
N91-16496
CALDWELL, J. A., JR. N91-16558
CAMERON, M. N91-16976
CAMPARO, J. C. N91-16352
CANN, DAVID C. N91-16577
CANT, R. S. N91-16081
CANTRELL, J. S. N91-16808
CANZIAN, BLAISE JOSEPH N91-16970
CAPPELLI, MARK A. N91-16147
CARAMANA, E. J. N91-16343
CARDOSO, JANETTE N91-16670
CARIGNAN, CLAUDE N91-16876
N91-16884
CARILLI, C. L. N91-16925
CARIM, A. H. N91-16789
CARLEY, JAMES N91-16159
CARLIN, BRADLEY P. N91-16666
CARLSON, MARTHENA N91-16585
CARLSON, NANCY M. N91-16377
CARMIGNIANI, VINCENT N91-16561
CARON-POPOWICH, RSUE N91-16142
CARR, G. L. N91-16800
CARROLL, M. A. N91-16467
CARTER, DANIEL C. N91-16815
CAUSEY, R. A. N91-16144
CAVASIN, DANIEL N91-16243
CAYAN, DANIEL RICHARD N91-16531
CELIK, I. N91-16259
CERNUSAK, IVAN N91-16728
CHAKMAKJIAN, STEPHEN H. N91-16742
CHAMBERLIN, ALAN N91-16578
CHAMBERLIN, RHODES R. N91-16443
CHAMPAGNE, VICTOR K., JR. N91-16007
CHAN, C. S. N91-16733
N91-16747
CHAN, K. C. D. N91-16348
CHAN, YAT C. N91-16355
CHANDLER-WILDE, SIMON N. N91-16688
CHANDRASEKHAR, H. R. N91-16801
CHANDRASEKHAR, MEERA N91-16801
CHANG, F. N91-16130
CHANG, T. N91-16928
CHANGERY, MICHAEL J. N91-16476
N91-16477
N91-16478
N91-16479
N91-16480
N91-16481
CHAPMAN, K. N91-16322
CHARGIN, MLADEN N91-16414
CHARITAT, GEORGES N91-16252
CHARLTON, JANE C. N91-16860
CHATTERJEE, TAPAN K. N91-16931
N91-16937
CHAUDHURI, J. N91-16153
CHEN, C.-X. N91-16796
CHEN, GUI-QUIANG N91-16646
CHEN, H. L. N91-16273
CHEN, KUAN-LUEN N91-16125
CHEN, YI-JUNG N91-16398
CHENG, RAYMOND S. N91-16709
CHEONG, S. W. N91-16812
CHERNIN, ARTHUR D. N91-16946
N91-16948
CHETWYND, D. G. N91-16392
CHI, TIEN N91-16261
CHILLERY, J. A. N91-16560
CHINZEI, NOBUO N91-15983
N91-16102
CHIOU, C. S. N91-16733
CHIOUS, C. N. N91-16747
CHIU, H. K. N91-16766
CHO, GYUSEONG N91-16228
CHOPRA, O. K. N91-16115
CHOU, SHIH-HUNG N91-16512
CHRIEN, R. N91-16777
CHRISTEN, D. K. N91-16788
CHRISTIE, MICHAEL S. N91-16483
CHRISTODOULOU, DIMITRIS MICHAEL N91-16851
CHRISTY, JOHN R. N91-16508
CHRISTY, STEVEN R. N91-16521
CHRZAS, J. N91-16784
CHU, C.-Y. N91-16141
CHU, MAY-YING N91-16149
CHUI, CHARLES K. N91-16663
CHYBA, THOMAS HERMAN N91-16359
CIESLAK, WENDY R. N91-16233
CIZEWSKI, J. A. N91-16798
CLAMMAE, SHANE S. N91-16353
CLARK, JOHN H. E. N91-16506
CLARK, RAYMOND K. N91-16604
CLEMENT, J. M. N91-16733
N91-16747
CLEMENTS, ROCHELLE E. N91-16162
CLERE, J. M. N91-16555
CLIFFSWALLOW, WILLOW N91-16484
CLOGSTON, A. M. N91-16786
COBLENTZ, A. N91-16561
COCKE, W. J. N91-16926
COHEN, CHARLES N91-16501
COHEN, EDWARD N91-16196
COHEN, R. E. N91-16155
COLBORN, B. L. N91-16056
COLE, R. L. N91-16373
COLEMAN, DAVID M. N91-16031
COLESTOCK, P. N91-16774
COLINA, L. N91-16923
COLKET, CURRIE N91-16610
COLLIER, LISA D. N91-16832
COLLINS, DONALD J. N91-16534
COLLINS, TIM N91-16790
COLUCCI, STEPHEN J. N91-16515
COMBES, FRANCOISE N91-16933
COMPANION, JOHN A. N91-16707
CONANT, J. W. N91-16093
CONSTANTINEAU, E. J. N91-16264
COOK, ROBERT P. N91-16837
COOMBS, DAVID J. N91-16387
COOPER, E. A. N91-16792
COOPER, JAMES A., JR. N91-16235
COPLAND, LISA N91-16565
COPPERSTHWAITE, D. N91-16082
CORCORAN, M. D. N91-16733
N91-16747
COREY, CARA M. N91-16985
CORRIGAN, E. N91-16671
CORT, B. N91-16093
COSBY, PHILIP C. N91-16172
COWAN, C. E. N91-16445
COWLES, S. N91-16462
CRAIG, ROY R., JR. N91-16059
CRAIG, WILLIAM W. N91-16088
CRAIN, JEFFREY SCOTT N91-16770
CRESWICK, F. A. N91-16257
CRIMINALE, W. O. N91-16258
CRONJAEGER, STEFAN N91-16782
CROSIER, RONALD B. N91-16169
CUCINOTTA, FRANCIS A. N91-16981
CULIOLI, JEAN-CHRISTOPHE N91-16372
N91-16378
CULP, DONALD R. N91-16474
CURRENT, JAMES E. N91-16841
CUTRI, ROC M. N91-16917

D

DAHLEH, MARIE DILLON N91-16290
DAIGLE, GILLES N91-16685
DANTASDEMELO, JORGE N91-16629
DARWISH, MOHAMED N. N91-16220
DASGUPTA, ABHIJIT N91-16132
DASILVA, L. N91-16340
DAVID, S. A. N91-16116
N91-16126
DAVIDSON, MASHA B. N91-16694
DAVIES, ELIZABETH A. N91-16557
DAVIS, CURTISS O. N91-16532
N91-16533
DAVIS, J. BRADLEY N91-16041
DAVIS, J. C. N91-16084
N91-16538
DAVIS, ROBERT F. N91-16246
DAVIS, TIMOTHY C. N91-16487
DAVOUST, E. N91-16869
DAWES, WILLIAM R., JR. N91-16220
DAWSON, L. R. N91-16805
DAY, I. N91-16193
DAZEVEDO, E. F. D. N91-16659
DEASON, V. A. N91-16319
N91-16739
DEBLOK, M. N91-16337
DEBOO, J. C. N91-16749
DECHAUMPHAI, PRAMOTE N91-16407
DEES, D. W. N91-16231
DEGEN, GREGG FRANCIS N91-16607
DEJONG, ALAN FRANK N91-16826
DEJONG, T. N91-16889
DEKKER, MENNO N91-16114
DELAROSA, MARK J. N91-16103
DELCAMP, S. B. N91-16352
DELEPLANQUE, M. A. N91-16798
DELOOR, G. P. N91-16429
DELUCA, W. H. N91-16229
DELUCHI, M. A. N91-16448
DEMELLORABACA, DULIA F. N91-16907
DEMETRIADES-SHAH, T. N91-16473
DEMORE, W. B. N91-16467
DENBOW, DAVID A. N91-16255
DENG, XIAOMIN N91-16402
DENHERTOG, D. N91-16600
DENNIS, A. J. N91-16328
N91-16330
DERMER, CHARLES D. N91-16982
DEROSA, F. N91-16800
DERUITER, H. R. N91-16896
DESALVOSOUZA, L. N91-16349
DESAUSSURE, G. N91-16368
DESKO, JOHN C., JR. N91-16220
DESTLER, W. W. N91-16763
N91-16764
DETEMPLE, THOMAS A. N91-16820
DEVALK, C. F. N91-16425
DEVANEY, JOSEPH J. N91-16716
DEVAULT, R. C. N91-16257
DEVORE, LAUREN N91-16985
DEVRED, A. N91-16674
DEVRIES, DANIEL NEVILLE N91-16417
DEWART, J. M. N91-16174
DEXTER, R. N. N91-16757
DEY, ARJUN N91-16902
DHINGRA, A. K. N91-16012
DI, XIAO N91-16700
DIAK, GEORGE N91-16502
DIALETIS, D. N91-16197
DIAMOND, R. M. N91-16798
DICKENSON, MICHAEL L. N91-16476
N91-16477
N91-16478
N91-16479
N91-16480
N91-16481
DIECKMAN, S. L. N91-16141
DIETRICH, MATTHIAS N91-16864
DOBBELAAR, JOHANNES AUGUSTINUS LEONARDUS
N91-16135
DOCTOR, P. G. N91-16445
DODSON, LORI J. N91-15986
DOLLY, MARTIN C. N91-16220
DONALDSON, J. C. N91-16293
DONNELLY, R. HANK N91-16088
DONNELLY, ROBERT N91-16542
DONOHUE, PATRICK N91-16587
DOUGHTY, D. H. N91-16789
DOUGLASS, A. R. N91-16467
DOYON, R. N91-16904
DRAGT, ALEX J. N91-16734
DRESSENDORFER, P. V. N91-16218
N91-16242
DREWERY, J. S. N91-16228
DRIVER, K. DEAN N91-16008
DROTNING, W. D. N91-16044
DUDINOV, V. N. N91-16918
DUKE, C. B. N91-16794
DUNLAP, B. D. N91-16783
DUNLAP, BRETT I. N91-16109
DURBIN, THOMAS E. N91-16262
DUTTA, B. N91-16800
DYER, R. BRIAN N91-16085

E

EBISUZAKI, WESLEY N91-16510
ECCLES, J. V. N91-16494
N91-16495
N91-16496
ECKART, A. N91-16976
ECKE, ROBERT N91-16288
EDESKUTY, F. J. N91-16174
EDWARDS, CHARLES N91-16215
EDWARDS, M. N91-16030
EGETH, HOWARD E. N91-16550
EHST, DAVID A. N91-16222
EICHEL, PAUL H. N91-16579

EKIS, J. W. N91-16326
EL-KADI, MONA N91-16635
ELBEL, JEFFREY P. N91-16048
ELDRED, JIM N91-16053
ELLINGSON, W. A. N91-16141
ELLIOTT, C. J. N91-16348
ELLIS, D. C. N91-16018
ELLIS, D. E. N91-16783
EMBLETON, TONY N91-16685
EMERY, BILL N91-16422
EMMERSON, D. N91-16591
N91-16594
ENDRE, MARK JAMES N91-16049
ENYA, SINTARO N91-16279
EPHREMIDES, ANTHONY N91-16186
ERCK, R. A. N91-16137
ERDEMIR, A. N91-16137
ERICKSON, K. L. N91-16161
ERTEL, PATRICK W. N91-16124
ESSENS, P. J. M. D. N91-16213
N91-16568
ETEMAD, S. N91-16800
ETKIN, A. N91-16733
N91-16747
EUBANK, R. L. N91-16661
EVANS, J. E. N91-16206
EVANS, J. R. N91-16469
EVANS, N. A. N91-16160
N91-16161

F

FAHY, F. J. N91-16705
FAIRCHILD, P. D. N91-16257
FAIRHEAD, A. C. N91-16193
FAIRLIE, D. B. N91-16671
FARKAS, Z. D. N91-16183
FARWIG, REINHARD N91-16314
FASANO, G. N91-16880
FEDRO, A. J. N91-16796
FELDMAN, DAVID L. N91-16454
FELTHAUSER, H. E. N91-16323
FELTON, J. S. N91-16538
FENSKE, G. R. N91-16137
FENSTERMACHER, M. E. N91-16181
FERGUSON, SAMUEL W. N91-15989
FERNANDEZ, J. C. N91-16755
FERNIE, W. A. N91-16026
FETZER, ERIC JOSEPH N91-16524
FIELD, R. T. N91-16472
FIFER, ROBERT A. N91-16104
N91-16105
FINDLAY, A. S. N91-16020
FINEGOLD, LAWRENCE S. N91-16552
FINK, H. H. N91-16856
FINNERTY, ANTHONY E. N91-16565
FIRTH, ROBERT N91-16610
FISCHER, ALBERT K. N91-16118
FISCHER, CHARLOTTE FROESE N91-16723
FISCHER, THOMAS R. N91-16581
FISH, GORDON N91-16327
FISK, Z. N91-16812
FITZGERALD, JAMES N91-16690
FLEETWOOD, D. M. N91-16219
N91-16394
FLETCHER, P. N91-16671
FOLEY, K. J. N91-16733
N91-16747
FOLTYN, S. R. N91-16351
FOOTE, J. N91-16771
FORBES, D. A. N91-16919
FORCH, BRAD E. N91-16106
FORSYTH, P. A. N91-16659
FOUILLOT, J. P. N91-16561
FOWLER, T. KENNETH N91-16736
N91-16768
FRANTZ, F. K. N91-16583
FRICKE, K. J. N91-16920
FRIDMAN, A. M. N91-16935
FRITH, D. A. N91-16020
FRITSCHEN, L. J. N91-16472
FRITZ-VONALVENSLEBEN, UTA N91-16972
FROGEL, JAY A. N91-16913
FRUEHOLZ, R. P. N91-16352
FRYE, G. C. N91-16676
FU, YIBIN B. N91-15994
FUCHS, ULRICH N91-16216
FUEHNE, DOUG N91-16046
FUJIEDA, I. N91-16228
FUJIMOTO, ATSUSHI N91-16268
FUKUNAGA, HISAO N91-16069
FULLER, GLENN C. N91-16353
FULTON, GRAHAM B. N91-16328
N91-16330
FURUKAWA, M. N91-16277
FUTATSUDERA, NAOKI N91-16268

G

GALLAGHER, JOSEPH P. N91-16125
GALLETTA, G. N91-16880
GALLIMORE, JACK F. N91-16909
GANJOO, DEEPAK KUMAR N91-16299
GARBER, DONALD P. N91-16693
GARBEY, MARC N91-16305
GARDNER, K. N91-16126
GARDNER, ROBERT H. N91-16451
GARTMEIER, OTTO N91-16414
GARTRELL, CHARLES F. N91-16832
GARZON, F. H. N91-16778
GATSKI, THOMAS B. N91-16306
GAUSTER, W. B. N91-16753
GAVIN, JOYCE E. N91-16460
GAZDAG, DENYSE N91-16001
GEIMER, RAY M. N91-16223
GEIS, N. N91-16977
GEIST, ROBERT N91-16627
GELFAND, ALAN E. N91-16666
GENZEL, REINHARD N91-16975
N91-16976
N91-16977
N91-16978
GEORGE, THOMAS F. N91-16819
GERBER, RICHARD A. N91-16959
GHAFFARI, SHAHRIAR N91-16744
GIAUQUE, R. D. N91-16322
GIBBONS, GOULD, JR. N91-16565
GIBSON, KEITH J. N91-16588
GIESE, R. F. N91-16375
GILBERT, KENNETH E. N91-16700
N91-16703
GILLESPIE, LAROUX K. N91-16176
GINLEY, D. S. N91-16240
GIORGI, A. L. N91-16093
GLAISTER, DAVID H. N91-16554
GLASS, M. W. N91-16161
GLASSELL, R. L. N91-16385
GLEASON, KEVIN N91-16985
GLEDHILL, B. L. N91-16538
GLUCKSTERN, ROBERT L. N91-16734
GLYNN, PETER W. N91-16613
N91-16636
N91-16662
N91-16667
N91-16668
GO, WILLIAM W. N91-16236
GOBINATH, THULASIRAM N91-16403
GOEDEL, H. N91-16017
GOERKE, WINFRIED N91-16253
GOLDEN, J. N91-16197
GOLDMAN, KENNETH J. N91-16611
GOLDSTEIN, JOHN C. N91-16357
GOLDSTEIN, R. J. N91-16284
GOLDSTON, R. N91-16774
GOLDSTONE, J. A. N91-16093
GOLUB, GENE H. N91-16625
GONDHALEKAR, V. N91-16153
GONIS, A. N91-16713
GONZALES, RICHARD R. N91-16545
GOODWIN, CHARLES A. N91-16220
GOODWIN, G. M. N91-16116
N91-16117
N91-16126
N91-16397
GOPALSAMI, N. N91-16141
GORDON, DAVID F. N91-16677
GOTTESFELD, S. N91-16778
GOTTESMAN, STEPHEN T. N91-16888
GOUDFROOIJ, PAUL N91-16889
GOULDING, C. A. N91-16778
GOWDY, VAN N91-15999
GRANATSTEIN, V. L. N91-16763
N91-16764
GRANDI, STEVEN A. N91-16894
GRAY, GEORGE T., III N91-16122
GREEN, CORDELL N91-16586
GREEN, ROBERT E., JR. N91-16578
GREGORINI, L. N91-16896
GREN, PER N91-16070
GRIEST, LAURA N91-16593
GRIEST, THOMAS E. N91-16592
N91-16603
GRIFFIN, D. C. N91-16721
GRIFFITHS, J. F. N91-16082
GRIFFITHS, S. K. N91-16079
GRIGORIU, MIRCEA N91-16409
GROMOV, S. K. N91-16037
GROSSE, RALF N91-16701
GROSSMAN, L. M. N91-16768
GROTCH, STANLEY L. N91-16497
GROVES, PAULA N91-16602
GROVES, S. H. N91-16361
GRUBB, J. P. N91-16293
GRUBIN, H. L. N91-16202
GUAN, R. N91-16146
GUERIN, MICHAEL N91-16452
GUIDOTTI, RONALD A. N91-16438
GUINAN, M. W. N91-16775
GUNNING, GEORGE R. N91-16053
GUPTA, UDAY N91-16779

H

HAARTSEN, JACOBUS CORNELIS N91-16746
HAAS, WOLFGANG N91-16022
HACKENBURG, R. W. N91-16733
N91-16747
HACKETT, BRUCE E. N91-16048
HACKWORTH, JOHN A. N91-16204
HAERENDEL, G. N91-16494
N91-16495
N91-16496
HAGEDOORN, F. P. N91-16427
HAHN, P. A. N91-16775
HAILEY, CHARLES J. N91-16088
HALBERSTAM, ISADORE M. N91-16488
HALL, A. N91-16560
HALL, E. J. N91-16722
HALL, P. N91-15996
HALL, PHILIP N91-15991
N91-15994
HALL, WILLIAM E. N91-16639
HALLMAN, T. J. N91-16733
N91-16747
HAMAGUCHI, S. N91-16748
HAMMEL, J. E. N91-16777
HAN, DAESOO N91-16536
HANSEN, BARRY R. N91-16795
HANSEN, L. N91-16889
HAPPER, W. N91-16724
HARA, TETSUYA N91-16947
N91-16951
HARDIN, JASPER E. N91-16225
HARMAN, T. C. N91-16361
HARRIOTT, JOSEPH N. B. N91-16688
HARRIS, FREDERICK C., JR. N91-16627
HARRIS, R. N. N91-16470
HARRIS, S. E. N91-16237
HARRISON, JAMES A. N91-16031
HARSHMAN, WILLIAM R. N91-16009
HARSTAD, K. N91-16078
HART, JOHN E. N91-16511
HARTH, E. N91-16615
HARTZHEIM, WOLFGANG N91-16630
HASH, M. C. N91-16231
HATZIS, PATRICIA M. N91-16004
HAUXTHAUSEN, E. M. N91-16925
HAWTHORN, J. BLAND N91-16922
HAYASHI, MASANORI N91-16267
N91-16268
HAYASHI, YOICHI N91-16069
HAYDUK, R. J. N91-16057
HAYES, J. J. E. N91-16886
HAYNES, T. E. N91-16806
HEALEY, D. L. N91-16470
HEALEY, R. J. N91-16482
HECKMAN, TIMOTHY M. N91-16910
N91-16916
HEIDELBERGER, PHILIP N91-16613
N91-16636
HEIDNER, RAYMOND F., III N91-16362
HEIN, RANDALL JOHN N91-16049
HEISLER, CHARLENE A. N91-16913
HELD, MANFRED N91-16173
N91-16669
HELLDOERFER, R. N91-16591
HELVAJIAN, HENRY N91-16362
HENDERSON, FRANCIS M. N91-16709
HENKES, RUDOLPHUS ALOYSIUS WIJNANDUS MARIA N91-16313
HENLE, W. N91-16781
HENLEY, ERNEST M. N91-16712
HENNE, JOERG MICHAEL N91-16311
HENNESSY, JOHN L. N91-16571
N91-16572
HENRIKSEN, G. L. N91-16227
HENRY, E. A. N91-16798
HENTEA, T. N91-16141
HERBSTER, CHRISTOPHER G. N91-16525
HERCHEN, H. N91-16147
HERCHER, MICHAEL N91-16741
HERMAN, H. N91-16803
HERNDON, J. N. N91-16379
N91-16385
HERRING, JASON N91-16046

HERRING, JIM N91-16790
HEYDORN, BARBARA N91-16168
HICKS, M. R. N91-16559
HICKSON, PAUL N91-16871
HIETALA, V. M. N91-16240
HIGGINBOTHAM, SCOTT A. N91-16041
HILL, J. R. N91-16786
HIMED, BRAHAM N91-16207
HINKELMAN, ELIZABETH A. N91-16210
HINSON, E. W. N91-16058
HINTZEN, PAUL N91-16867
HIRLEMAN, E. DAN N91-16354
HIRNING, JAMES LAWRENCE N91-16003
HIRSCH, JOY N91-16548
HIRSCHEL, E. H. N91-16015
N91-16016
HIRSCHMUGL, C. J. N91-16800
HISLEY, DIXIE M. N91-16589
HODGE, JAMES D. N91-16818
HOFFER, LOIS MARION N91-16360
HOFFMAN, F. O. N91-16463
HOFFMANN, CHRISTOPH M. N91-16605
HOFFMANN, ROALD N91-16108
HOGAN, WILLIAM J. N91-16437
N91-16759
HOGREFE, R. L. N91-16229
HOLDER, MICHAEL D. N91-16042
N91-16578
HOLDREN, J. P. N91-16768
HOLLAND, K. R. N91-16705
HOLLAND, O. W. N91-16806
HOLLOWAY, JOHN S. N91-16362
HOLTON, J. R. N91-16467
HONMA, H. N91-16269
HOOPER, E. B. N91-16761
HOROWITZ, MARK A. N91-16571
N91-16572
HORST, RICHARD L. N91-16563
HOSMER, FELL N91-16677
HOSSAIN, MOHAMMAD A. N91-16170
HOTHERSALL, DAVID C. N91-16688
HOUGH, PAUL G. N91-16177
HOUPIS, J. L. J. N91-16462
HOWARD, S. N91-16936
N91-16938
HSIAO, MING-YUAN N91-16767
HUANG, SUJIAN N91-16404
HUBBARD, HARVEY H. N91-16679
HUBER, J. G. N91-16093
HUEY, BEVERLY MESSICK N91-16567
HUFF, JAMES R. N91-16439
HUFF, JOHN H. N91-16436
HUGENHOLTZ, COENRAAD ALBERTUS JACOBUS
N91-16780
HUGHES, PHIL D. N91-16064
HUMPHREY, THEODORE W. N91-16048
HUNG, CHENG-HUNG N91-16138
HUNSAKER, C. T. N91-16465
HUTCHINGS, J. B. N91-16911
HUTCHINSON, D. P. N91-16756
HWANG, CHING-CHYWAN N91-15993

I

ICE, G. E. N91-16811
IIMURA, RUSSELL MAKOTO N91-16245
IKEDA, Y. N91-16280
INGRAFFEA, ANTHONY R. N91-16409
INOUE, OSAMU N91-16270
IP, PRECILA C. F. N91-16776
ISAKSEN, I. S. A. N91-16467
ISHII, MASAHIRO N91-16279
ISHII, Y. N91-16271
N91-16277
ISHIKAWA, TAKASHI N91-16069
ITAGAKI, HIROSHI N91-16396
ITO, HARUHIKO N91-16276
ITO, SEIICHI N91-16396
IVANOV, ALEXEI V. N91-16946
N91-16948

J

JABBARI, M. Y. N91-16284
JACKMAN, B. N91-16130
JACKSON, J. M. N91-16976
JACOBS, A. N91-16781
JACOBS, JEFF N91-16052
JADUSZLIWER, B. N91-16355
JAGER, JOHAN N91-16179
JAHN, ALEXANDER N91-16732
JAKOWATZ, CHARLES V., JR. N91-16579
JAMES, P. A. N91-16904
JANNEY, M. A. N91-16143
JANSEN, J. F. N91-16379
JARDIN, S. N91-16774
JASKOWIAK, MARTHA H. N91-16075
JEDLOVEC, GARY N91-16502
JELLISON, J. L. N91-16380
JENKINS, KEITH N91-16551
JENNINGS, RICHARD LEONARD N91-16857
JENSEN, POUL ANKER N91-16061
JENSEN, S. N91-16560
JEONG, DONG YOUL N91-16845
JERNIGAN, J. GARRETT N91-16790
JIANHUA, HU N91-16392
JING, T. N91-16228
JOG, CHANDA J. N91-16952
JOHANSSON, MELKER N91-16706
JOHNSON, ANDREW DAVID N91-16824
JOHNSON, CARL E. N91-16118
JOHNSON, HELEN SUE N91-16405
JOHNSON, JEFFREY EDWARD N91-16527
JOHNSON, JOHN A. N91-16377
JOHNSON, M. W. N91-16778
JOHNSON, MICHAEL W. N91-16187
JOHNSTON, H. S. N91-16467
JOHNSTON, HAROLD S. N91-16466
JONES, E. C. N91-16788
JONES, E. D. N91-16805
JONES, H. D. N91-16558
JONES, K. B. N91-16461
JONES, K. W. N91-16322
JONES, KEITH W. N91-16542
JONES, R. V. N91-16219
JORDAN, D. L. N91-16192
JORDAN, JOHN F. N91-16443
JORDON, KYM N91-16238
JORGENSEN, H. E. N91-16889
JOSEPH, R. D. N91-16904
JOSHI, A. U. N91-16615
JUNGST, R. G. N91-16161

K

KACKLEY, N. D. N91-16442
KAHN, LARRY N91-16608
N91-16609
KALB, MICHAEL N91-16502
KALINKOV, M. N91-16878
N91-16879
KALOGEROPOULOS, T. N91-16615
KALTSOUNI, MARIA N91-16406
KAMINAGA, FUMITO N91-16276
KANEMASU, E. T. N91-16472
N91-16473
KAPER, HANS G. N91-16754
KAPETANAKOS, C. A. N91-16197
KAPITULNIK, A. N91-16237
KAPLAN, S. N. N91-16228
KAPUR, VIJAY K. N91-16444
KARACHENTSEV, I. D. N91-16859
N91-16875
KARACHENTSEVA, V. E. N91-16875
KARL, THOMAS R. N91-16460
KARNEY, CHARLES F. F. N91-16222
KARNI, S. N91-16281
KASAHARA, AKIRA N91-16504
KASPAREK, W. N91-16781
KATRAGADDA, S. N91-16259
KATZ, JOSEPH L. N91-16138
KATZ, ROBERT N91-16981
KAWAI, N. N91-16856
KAY, BRUCE D. N91-16714
KAZACOS, MICHAEL N91-16234
KEANE, C. J. N91-16340
KEEL, WILLIAM C. N91-16858
N91-16909
N91-16921
N91-16936
KEICHER, D. M. N91-16380
KEITH, T. G., JR. N91-16304
KELLER, STEVE N91-16608
N91-16609
KELLY, JONATHAN E. N91-16049
KEMP, WILLIAM B., JR. N91-16033
KENNEDY, ERIC MILES N91-16092
KENNEDY, RALPH G. N91-16048
KENNICUTT, ROBERT C., JR. N91-16897
KEPES, PAUL N91-16052
KERCHER, J. R. N91-16462
KERST, D. W. N91-16757
KETCHAM, THOMAS D. N91-16788
KEVORKIAN, J. N91-16341
KHACHIKIAN, E. YE. N91-16877
KHALSA, SIRI JODHA SINGH N91-16526
KHOBAIB, M. N91-16125
KHOUNSARY, A. M. N91-16784
KILKENNY, J. D. N91-16224
KILLOUGH, S. M. N91-16369
KIM, J. S. N91-16285
KIM, JOON N91-16419
KIM, SEUNG T. N91-16536
KIM, YOUNGTAE N91-16797
KIMBALL, C. W. N91-16783
KIMREY, H. D. N91-16143
KINDEL, J. L. N91-16343
KING, JOEL DAVID N91-16071
KINNEY, JOANN S. N91-16567
KISELEVA, LJUDMILA G. N91-16946
N91-16950
KISTLER, DORIS J. N91-16708
KLAFSZKY, E. N91-16599
KLARIC, MARIO N91-16939
KLEIN, DANIEL N91-16610
KLEM, J. F. N91-16805
KLUEH, RONALD L. N91-16399
KLUG, HELMUT N91-16696
KNABB, RICHARD D. N91-16513
KNOPOFF, LEON N91-16475
KNOWLTON, L. N91-16488
KO, M. K. W. N91-16467
KOCHHAR, R. K. N91-16903
N91-16940
KOENIG, GERALD N91-16689
KOEPKE, A. N91-16048
KOFFEND, JOHN B. N91-16362
KOIKE, J. N91-16810
KOLB, WERNER N91-16433
KOLLATSCHNY, W. N91-16890
N91-16920
KOLODZIEJSKI, LESLIE A. N91-16817
KOMEN, ERWIN RONALD N91-16631
KOMORI, M. N91-16277
KOMURO, TOMOYUKI N91-15983
N91-16102
KONDA, SURESH N91-16590
KOSEK, J. A. N91-16442
KOTULSKI, JOSEPH D. N91-16180
KRAMER, GORDON N91-16790
KRANEFELD, GEORG N91-16729
KRANTZ, RICHARD J. N91-16248
KRESKOVSKY, J. P. N91-16202
KRONBERG, PHILIPP P. N91-16870
KROTHAPALLI, A. N91-16289
KRUMPELT, M. N91-16231
KUAN, JYH-HORNG N91-16300
KUDOU, KENJI N91-15983
N91-16102
KUHNERT, A. N91-16798
KUKLA, GEORGE J. N91-16460
KULLBERG, M. L. N91-16792
KUMAR, ROMESH N91-16230
KUMRIC, H. N91-16781
KUNERTH, D. C. N91-16066
KUNEVA, I. N91-16878
N91-16879
KUO, AN-YU N91-16125
KUPPERMANN, ARON N91-16110
KUSKA, MICHELLE N91-16345
KUSTAS, W. N91-16472
KUTOROFF, S. N91-16617
N91-16618
N91-16619
KVALE, THOMAS J. N91-16715
KWACK, EUG N91-16078
KWONG, MAN KAM N91-16576

L

LABIJ, DENNIS N91-16053
LACKNER, ANNA M. N91-16205
LAFEMINA, J. P. N91-16794
LAMB, SUSAN A. N91-16898
N91-16901
N91-16959
LAMBERTY, GREGORY L. N91-16513
LAMPERT, CARL M. N91-16142
LANDEN, N. N91-16340
LANDERS, JOSEPH A. N91-16614
LANDRUM, JERRY L. N91-16841
LANG, ROLF N91-16498
LANGHOFF, STEPHEN R. N91-16065
LANSAW, P. TINA N91-16063
LANSMAN, MARCY N91-16844
LAO, L. N91-16773
LAPENTA, WILLIAM N91-16501
LAPYGIN, V. N91-16039
LARKEY, PATRICK D. N91-16590
LARKIN, M. D. N91-16020
LARSEN, ROBERT P. N91-16370
LASSAHN, GORDON D. N91-16574
LASSANYI, RUBY A. N91-16535
LATORRE, VICTOR R. N91-16087

LAUB, R. J. N91-16099
LAURICH, B. K. N91-16793
LAWLESS, MICHAEL T. N91-16552
LAWSON, A. C. N91-16093
LAY, K. W. N91-16788
LAYMAN, W. E. N91-16057
LEAHY, A. M. N91-16019
LEBEDEV, V. S. N91-16875
LEE, I-HSIU N91-16827
LEE, J. N91-16807
LEE, SEUNGSOO N91-16301
LEE, SUNG M. N91-16691
LEE, TIMOTHY J. N91-16727
N91-16728
LEE, W. Y. N91-16011
N91-16013
LEGER, A. N91-16555
LEIDINGER, BERNHARD J. G. N91-16060
LEIGH, RICHARD PETER N91-16423
LEJEUNE, D. N91-16555
LEMKE, GARY N91-16046
LEN, L. K. N91-16197
LENTSCH, STEVEN E. N91-16566
LEO, DONALD J. N91-16048
LEONARD, E. M. N91-16778
LEONG, KENG H. N91-16262
LESLIE, FRED W. N91-16500
N91-16512
LEVINE, D. A. N91-16465
LEVUSH, B. N91-16346
N91-16763
N91-16764
LEVY, M. N91-16130
LIANDRAT, J. N91-16664
LIANG, A. Y. N91-16242
LIENESCH, J. H. N91-16055
LIESKE, ROBERT F. N91-15990
LIM, K. C. N91-16205
LIN, S. Y. N91-16805
LIOU, JIANNTYNG JAMES N91-16302
LIU, KEH-FEI N91-16828
LIU, W. N91-16615
LIU, WING KAM N91-16398
LJUNGGREN, STEN N91-16706
LLORET, JEAN-CHRISTOPHE N91-16214
LO, K.-Y. N91-16898
LOCKE, RANDY J. N91-16106
LORD, S. N91-16898
LOS, S. A. N91-16846
LOTENS, W. A. N91-16569
LOTT, L. A. N91-16066
LOTTERO, RICHARD E. N91-16287
LOTZE, A. N91-16017
LOVBERG, R. N91-16777
LOVELL, T. W. N91-16757
LOWNDES, DOUGLAS H. N91-16788
LOZINO-LOZINSKIY, G. N91-16038
LU, H.-I. N91-16512
LUCAS, N. N91-16811
LUGTEN, J. B. N91-16977
LUI, A. T. N91-16489
LUIK, P. C. N91-16430
LUNARDINI, VIRGIL J. N91-16286
LUNDIN, C. D. N91-16117
LUPO, ANTHONY R. N91-16513
LYKKE, KEITH R. N91-16714
LYKKEN, JOSEPH D. N91-16787
LYNDS, C. R. N91-16877
LYNER, A. G. N91-16190
LYNESS, JAMES N. N91-16809

M

MA, S. N91-16146
MAASCH, KIRK A. N91-16510
MACAIONE, DOMENIC P. N91-16068
MACCHETTO, F. D. N91-16915
N91-16919
N91-16923
MACCRACKEN, MICHAEL C. N91-16459
MACK, ALLAN J. N91-16616
MACKENTY, JOHN W. N91-16881
MACLAREN, STEPHAN A. N91-16329
MADEJSKY, RAINER N91-16862
MAELAND, A. J. N91-16808
MAGNUSON, C. N91-16594
MAGNUSSON, ROBERT N91-16336
MAHON, MARY ELAINE N91-16888
MAHONEY, A. R. N91-16161
MAILHIOT, C. N91-16793
N91-16794
MAIORANA, CHARLIE N91-16838
MAKOWSKI, M. A. N91-16761
MALIK, M. R. N91-15996
MALLOUX, ROBERT J. N91-16196
MALONE, KEVIN T. N91-16581
MAMON, GARY A. N91-16943
N91-16944
MAN, KAM KWONG N91-16754
MANDY, NORMAN H. N91-16518
MARCINIAK, T. J. N91-16373
MARCUS, ANDRES N91-16047
MARGERUM, J. DAVID N91-16205
MARTENS, J. S. N91-16240
MARTIN, STEPHEN J. N91-16675
N91-16676
MARYNICK, DENNIS S. N91-16154
MARZIANI, PAOLO N91-16882
N91-16891
MASON, T. O. N91-16792
MASSIE, N. A. N91-16850
MASUYA, GORO N91-15983
N91-16102
MATHEWS, KIRK A. N91-16474
MATSUDA, H. N91-16807
MATSUOKA, M. N91-16856
MATSUSHIMA, MASAMICHI N91-16069
MATTHEWS, D. N91-16340
MAUEL, M. E. N91-16760
MAURO, B. R. N91-16351
MAXTON, P. M. N91-16786
MAYERGOYZ, I. D. N91-16763
N91-16764
MAYNARD, DAVID P. N91-16604
MAYTAL, BEN-ZION N91-16813
MCADAM, GRANT N91-16121
MCAFEE, JOHN M. N91-16578
MCBRIDE, DENNIS K. N91-16557
MCBRIDE, WALTON E. N91-16703
MCCARTY, C. E. N91-16217
MCCATTY, S. A. N91-16442
MCCOY, H. E., JR. N91-16148
MCCUNE, WILLIAM N91-16641
MCDANIEL, S. T. N91-16529
MCDOWELL, H. K. N91-16786
MCELIGOT, DONALD M. N91-16255
MCENTIRE, R. W. N91-16489
MCGAW, MICHAEL AARON N91-16131
MCGUIRE, RAY N91-16158
MCGUIRE, RAYMOND R. N91-16162
MCGUIRK, JAMES P. N91-16509
MCKEE, J. N91-16348
MCLEAN, BRIAN N91-16881
MCLEAN, I. S. N91-16904
MCLEOD, ROBERT N91-16182
MCMAHON, P. M. N91-16872
MCNESBY, KEVIN L. N91-16104
N91-16105
MCVEY, B. D. N91-16348
MCWHORTER, ALAN L. N91-16816
MCWHORTER, P. J. N91-16718
MEDLEY, S. N91-16774
MEESTER, R. W. J. N91-16656
MEHLHORN, T. A. N91-16325
MEIER, WAYNE R. N91-16759
MEISENHEIMER, T. L. N91-16219
MERCER, LINDEN B. N91-16195
MERKLE, KARL L. N91-16101
MEROLA, JOHN A. N91-16418
MESHII, M. N91-16810
MESSERSMITH, JEAN M. N91-16416
METIK, L. N91-16906
MEULSTEE, C. N91-16428
MEYER, DAVID LEE N91-16049
MEYER, WILLIAM V. N91-16350
MEYYAPPAN, A. N91-16321
MEYYAPPAN, M. N91-16202
MICKIEWICZ, ALEXANDER P. N91-16097
MICKLICH, B. J. N91-16766
MIELE, ANGELO N91-16010
N91-16011
N91-16013
MIESEN, ROBERTUS HENRICUS MARGARETHA N91-16307
MIGLIORI, A. N91-16786
MILEY, GEORGE K. N91-16916
MILEY, T. B. N91-16445
MILLER, J. R. N91-16775
MILLER, JOHN C. N91-16096
MILLER, JOHN R. N91-16720
MILLER, LEROY J. N91-16205
MILLER, R. H. N91-16934
MILLER, S. L. N91-16218
N91-16242
N91-16718
MILLER, TIM N91-16512
MILLER, W. M. N91-16718
MILLER, W. S. N91-16077
MILLS, D. M. N91-16784
MILSTEIN, L. B. N91-16842
MILTENBURG, J. W. N91-16431
MIMURA, K. N91-16277
MINA, STEVE N91-16327
MIRIN, ARTHUR A. N91-16633
N91-16672
MIYAZAKI, Y. N91-16277
MIYOSHI, SHIGERU N91-16947
N91-16951
MIZIOLEK, ANDRZEJ W. N91-16106
MIZUNO, K. N91-16771
MOATS, A. R. N91-16325
MOIN, PARVIZ N91-16291
MOIR, RALPH W. N91-16437
N91-16759
MOLENKAMP, CHARLES R. N91-16457
N91-16458
MOLLARD, R. N91-16561
MOLLISON, TIMOTHY JAMES RAMSAY N91-16636
MONDY, L. A. N91-16027
N91-16079
MONTFROOIJ, WOUTER THEODORUS N91-16111
MONTGOMERY, D. S. N91-16324
MONTI, DAVID L. N91-16474
MOODENBAUGH, A. R. N91-16803
MOODY, GORDON N91-16158
MOORE, B. A. N91-16024
MOORE, D. S. N91-16786
MOORE, DAVID S. N91-16091
MOORE, HARRY H. N91-16830
MOORE, T. L. N91-16084
MORET, R. N91-16811
MORIOKA, SHOJI N91-16951
MORITA, TOSHIYUKI N91-15985
MORKOC, H. N91-16811
MORRIS, JEFFREY B. N91-16108
MORRISON, B. J. N91-16202
MORSE, R. L. N91-16343
MOSS, C. N91-16905
MOSS, C. E. N91-16323
MUELLER, G. A. N91-16781
MUELLER, R. N91-16364
MULLER, H. N91-16804
MUNDELL, DAN B. N91-16520
MUNECHIKA, CURTIS K. N91-16421
MUNK, B. A. N91-16191
MURAKAMI, ATSUO N91-15983
N91-16102
MURAKAMI, M. N91-16278
MURPHY, HUGH D. N91-16255
MURPHY, PATRICK J. N91-16523
MUTSCHLECNER, J. PAUL N91-16694
N91-16695
MUYUNDO, DAVID K. N91-16411
MYERS, JOSEPH DWAN N91-16297

N

NAGARAJAN, R. N91-16259
NAKAGAWARA, VAN B. N91-16544
NAKAISHI, H. N91-16807
NAKAMURA, M. N91-16974
NAM, CHANGHO N91-16025
NAMBOODIRI, P. M. S. N91-16940
NAQWI, A. N91-16364
NARASIMHA, R. N91-15995
NARAYANA, K. T. N91-16634
NASBY, R. D. N91-16218
N91-16242
NASSTROM, JOHN S. N91-16498
NATHAN, TERRENCE N91-16517
NAUMANN, ROBERT J. N91-16815
NEALY, JOHN E. N91-16981
NEBEL, JOHN K. N91-16563
NEFF, S. G. N91-16911
NELSON, A. J. N91-16153
NELSON, D. E. N91-16538
NELSON, RANDALL J. N91-16540
NEMOV, ALEKSANDR N91-16040
NEVEN, W. H. L. N91-16598
NEWMAN, W. N91-16809
NEWNAM, BRIAN E. N91-16342
N91-16357
NEWSOM, JERRY R. N91-16057
NICHOLSON, J. Y. N91-16058
NICKEL, H. N91-16134
NICOL, T. H. N91-16316
NIE, D. N91-16472
N91-16473
NILSON, D. G. N91-16771
NISHIKAWA, N. N91-16269
NISHIMURA, MAKOTO N91-16384
NISKA, HARVEY N91-16327
NITSCHKE, J. M. N91-16735
NOBLE, JOHN M. N91-16702
N91-16704
NOEL, SUSAN D. N91-16694

NOGA, JOZEF N91-16728
NOGUCHI, MASAFUMI N91-16955
N91-16963
NOGUCHI, TATSURU N91-16069
NOLAN, T. A. N91-16320
NOREAU, LOUIS N91-16870
NORGAARD-NIELSEN, H. U. N91-16889
NORMAN, COLIN A. N91-16964
NORRIS, R. P. N91-16912
NORRIS, ROBERT JEFFREY N91-16665
NORTHCUTT, J. DUANE N91-16604
NORTON, DAVID P. N91-16788
NOVICK, ROBERT N91-16740
NOVIKOV, S. B. N91-16918
NOWAK, W. B. N91-16130
NUTTALL, ALBERT H. N91-16649
N91-16673

O

OBAIDAR, M. S. N91-16326
OBERKAMPF, WILLIAM L. N91-16054
OBRIEN, ENDA N91-16514
OCKERT, C. E. N91-16260
ODA, T. N91-16771
ODAJIMA, K. N91-16771
OFFENLOCH, KURT N91-16562
OFFUTT, A. JEFFERSON N91-16627
OGITSU, T. N91-16674
OGLESBY, ROBERT N91-16510
OH, CHAEYOUN N91-16389
OHALLORAN, BERNARD N91-16327
OHASA, K. N91-16771
OKADA, S. N91-16807
OKAMOTO, P. R. N91-16810
OKAMOTO, YOSHIZO N91-16276
OLANDER, D. R. N91-16344
OLIVER, G. N91-16368
OLIVER, H. W. N91-16470
OLOUGHLIN, MICHAEL J. N91-16248
OLSEN, ROBERT O. N91-16702
OLSON, G. L. N91-16481
OLSON, THOMAS J. N91-16387
OLSSON, ROBIN N91-16070
OMATETE, O. O. N91-16145
ONEILL, ROBERT V. N91-16451
N91-16465
OOSTERLOO, T. N91-16880
ORAM, C. E. N91-15980
OREHOTSKY, J. N91-16803
ORLOV, VICTOR V. N91-16946
N91-16950
ORR, JOHN L. N91-16537
N91-16539
ORTH, CHARLES D. N91-16437
N91-16759
OSHIMA, K. N91-16266
N91-16273
OSHIMA, S. N91-16277
OSSARD, G. N91-16555
OSTDIEK, ANN R. N91-16485
OSTER, YALE N91-16850
OSTIC, J. N91-16348
OVERDIJK, D. A. N91-16178
OVERMYER, D. L. N91-16812
OYAN, CHEN N91-16132
OZERNOY, LEONID M. N91-16968
OZTURAN, CAN N91-16606

P

PAFFETT, MARK T. N91-16090
PAIGE, TERRY S. N91-16523
PAINTER, GAYLE S. N91-16719
PANDEY, AJAY K. N91-16407
PANDEY, LAKSHMI N. N91-16819
PANDOLF, KENT B. N91-16545
PANDOLFO, LIONEL N91-16510
PARIDES, GEORGE N91-16690
PARK, M. N91-16146
PARMA, P. N91-16896
PARRISH, ADRIAN JAMES N91-16254
PASCHMANN, G. N91-16974
PATT, B. E. N91-16321
PATTERSON, W. L. N91-16203
PEARSON, RICHARD J. N91-16029
PEDERSEN, MELVIN A. N91-16677
PEDLAR, A. N91-16893
PENNOCK, STEVE N91-16182
PEPIN, FRANCOIS MICHEL N91-16303
PEREPEZKO, J. H. N91-16129
PERERA, ASANGA HIRAN N91-16802
PEREZ-MENDEZ, V. N91-16228
PERKEY, DONALD J. N91-16501
N91-16502
PERKINS, R. N91-16774
PERNAROWSKI, MARK N91-16341
PERRY, D. R. N91-16030
PETERS, C. J. N91-16811
PETERS, JAMES E. N91-16262
PETROSIAN, A. R. N91-16887
PFEIFFER, BERTHOLD N91-16434
PFISTER, K. N91-16076
PHELPS, MALCOM V. N91-16601
PHILIPP, WARREN H. N91-16152
PHILLIPS, C. H. N91-16082
PHILLPOT, S. R. N91-16791
PIDCOE, S. V. N91-16316
PIERINI, P. N91-16349
PIETERS, A. M. J. N91-16569
PIN, F. G. N91-16372
PIN, FRANCOIS G. N91-16378
PINDZOLA, M. S. N91-16721
PITT, MARK N91-16023
PITTS, JOHN H. N91-16437
N91-16759
PITZ, W. J. N91-16082
PLUM, MARTIN M. N91-16223
PLUMB, G. D. N91-16681
POE, GREG N91-16850
POGLITSCH, A. N91-16977
POLITZER, P. N91-16752
N91-16773
POLKA, LESLEY A. N91-16212
POLTE, HANS N91-16052
POLYACHENKO, VALERIJ L. N91-16954
POMERANTZ, MARTIN N91-16154
POMPHREY, N. N91-16774
PONCE, D. A. N91-16470
POPE, S. B. N91-16081
POTEMRA, T. A. N91-16489
POWELL, D. R. N91-16642
POWELL, FREDERIC D. N91-16004
POWELL, G. L. N91-16756
POWER, G. N91-16224
PRAAGMAN, C. N91-16598
PRADO, GERVASIO N91-16690
PRAGER, S. C. N91-16757
PRASAD, PARAS N. N91-16156
PRATHER, M. J. N91-16466
PREM, H. N91-16834
PRIMDAHL, FRITZ N91-16061
PROCOPIS, STEPHANIE N91-16047
PROCTOR, I. D. N91-16084
N91-16538
PRONIK, I. I. N91-16906
N91-16918
PRUGNIEL, PHILIPPE N91-16869
N91-16933
PRUNEDA, CESAR O. N91-16162
PUCHE, DANIEL N91-16876
PUGH, H. LAUREN N91-16637

Q

QI, LIQUN N91-16626
QIAO, C. Y. P. N91-16117
QUADAKKERS, W. J. N91-16134
QUANTE, C. F. N91-16237
QUIGLEY, G. P. N91-16343
QUIJADA, M. N91-16800
QUINN, GEORGE D. N91-16073
QUINTANA, H. N91-16863
QURESHI, S. N91-16228

R

RADER, D. J. N91-16027
RAFANELLI, PIERO N91-16882
N91-16891
RAJ, RISHI N91-16306
RAJESHWAR, KRISHNAN N91-16154
RAMEY, MADISON N91-16381
RAMOHALLI, KUMAR N91-16163
N91-16164
N91-16165
RAMPAZZO, ROBERTO N91-16865
RAMSEY, J. M. N91-16095
RAMSEY, W. Y. N91-16055
RANSICK, MARK H. N91-16738
RAO, S. S. N91-16012
RASMUSON, D. M. N91-16395
RASPET, RICHARD N91-16686
N91-16703
N91-16704
RATNER, E. Z. N91-16227
RATZEL, A. C. N91-16264
RAVAT, DHANANJAY NARENDRA N91-16415
RAZZAQ, ZIA N91-16411
REE, FRANCIS H. N91-16829
REGNER, PETER N91-16979
REHN, L. E. N91-16810
REIN, D. H. N91-16155
REINHARDT, FREDERICK W. N91-16438
REISTER, D. B. N91-16376
REJ, D. J. N91-16755
REMMERSWAAL, JOHANNES ANTONIUS MARIA N91-16157
RENDELL, ALISTAIR P. N91-16727
N91-16728
RESHETNIKOV, V. P. N91-16892
REUTER, RENATE N91-16731
REYNOLDS, JOHN R. N91-16154
REYNOLDS, NATHANIEL N91-16512
RHEA, W. JOSEPH N91-16532
N91-16533
N91-16534
RHEE, GEORGE N91-16895
RHODES, WILLIAM C. N91-16717
RICCO, ANTONIO J. N91-16675
N91-16676
RICE, C. KEITH N91-16175
RICHARDS, R. K. N91-16756
RICHMOND, PAUL W. N91-16286
RICKMAN, J. M. N91-16791
RILEY, DOUGLAS J. N91-16180
RILEY, R. N91-16777
RITCHIE, A. G. N91-16241
RIVERS, M. L. N91-16322
RIZO, P. N91-16141
ROBERTSON, FRANKLIN R. N91-16501
N91-16502
N91-16503
N91-16507
ROBIN, MICHAEL T. N91-16437
ROBINSON, DAVID MARK N91-16049
ROBINSON, R. A. N91-16093
ROBSON, E. I. N91-16868
RODGERS, M. S. N91-16218
N91-16242
RODGERS, MICHAEL A. J. N91-16140
RODRIGUEZ, JEFFREY JOEL N91-16424
ROELOFS, G. R. N91-16934
ROEMER, NICOLAUS N91-16312
ROFER, CHERYL K. N91-16085
ROGERS, J. W., JR. N91-16812
ROGERS, JAMES C. N91-16691
RONCIN, A. N91-16555
ROOS, C. N91-16600
ROOS, NICO N91-16942
ROSEMA, A. N91-16426
ROSEN, M. D. N91-16769
ROSENAU, TODD J. N91-16635
ROSENBLUTH, M. N. N91-16749
ROTH, SUSAN KIES N91-16601
ROTHERMEL, H. N91-16976
ROTTA, JULIUS C. N91-15977
ROWE, J. C. N91-16385
RUCK, GERHARD N91-16310
RUIZ, MARILYN S. N91-16416
RUSSELL, K. D. N91-16395
RUST, DAVID M. N91-16980
RUTH, R. D. N91-16183
RYDBECK, G. N91-16976
RYDER, D. E. N91-16393

S

SAADATMAND, KOUROSH N91-16772
SACK, R. A. N91-16699
SAFFMAN, P. G. N91-16292
SAGAWA, HIROSHI N91-16384
SAHLIN, PER N91-16706
SAHU, DEVARAJ N91-16819
SAIKIA, D. J. N91-16893
SAITO, TAKASI N91-16276
SAITOVICH, E. BAGGIO N91-16783
SAKURAI, AKIRA N91-16272
SALBY, MURRY L. N91-16505
SALO, HEIKKI N91-16941
SALOVEY, R. N91-16146
SALPETER, EDWIN E. N91-16860
N91-16927
SALTZMAN, BARRY N91-16510
SALZER, J. N91-16925
SAMEJIMA, FUMIKO N91-16650
SAMPAS, NICHOLAS MICHAEL N91-16335
SAND, JAMES R. N91-16175
SANDER, MARTIN N91-16630
SANDERS, V. E. N91-16351
SANFORD, NONA M. N91-16985
SANTEE, WILLIAM R. N91-16545
SANTINI, D. J. N91-16448
SARICKS, CHRISTOPHER N91-16447

SARKAR, VIVEK N91-16577
SASAKI, R. N91-16671
SATTISON, M. B. N91-16395
SAUER, KEN D. N91-16596
SAXENA, ASHOK N91-16125
SCHAEFER, HEINZ-JUERGEN N91-16493
SCHAEFFER, JON CONRAD N91-16074
SCHARLEMANN, E. T. N91-16349
SCHAUB, R. L. N91-16393
SCHIAVI, PETER N91-16638
SCHIRBER, J. E. N91-16812
SCHLEITWEILER, PATRICK M. N91-16738
SCHLOBOHM, S. L. N91-16221
SCHMATZ, M. A. N91-15997
SCHMIDT, J. N91-16774
SCHMIDT, STEPHEN C. N91-16091
SCHMITT, M. J. N91-16348
SCHMITZ, ERIC N91-16381
SCHMULTZTOKOS, JOSEPH JOHN N91-16530
SCHNEIDER, J. DAVID N91-16772
SCHNEIDER, S. W. N91-16191
SCHNEIDER, STEPHEN E. N91-16927
SCHNITTGRUND, GARY D. N91-16150
SCHOESSOW, PAUL N91-16632
SCHOMBERT, JAMES M. N91-16868
N91-16957
SCHRAML, STEPHEN J. N91-16029
SCHROEDER, MATTHEW N91-16565
SCHUCANY, WILLIAM R. N91-16661
SCHUELLER, P. G. N91-16781
SCHUELLER, REINER N91-16251
SCHUETTLER, H. B. N91-16796
SCHULLER, S. N91-16249
SCHUMACHER, B. N91-16084
SCHUSTER, H. N91-16134
SCHWANK, J. R. N91-16218
N91-16242
N91-16394
SCHWARTZ, R. W. N91-16789
SCHWEIGER, J. N91-16017
SCKOPKE, N. N91-16974
SCORZELLI, R. B. N91-16783
SCOTT, GEORGE N. N91-16582
SCRIBNER, KEN N91-16158
N91-16159
SCROGGS, JEFFREY S. N91-16305
SCUDDER, D. W. N91-16777
SEARS, MARK P. N91-16647
SEKAR, R. R. N91-16373
SELBY, GREGORY N91-16296
SEMENOV, YU. P. N91-16037
SENSBURG, O. N91-16017
SEPPALA, LYNN G. N91-16088
N91-16850
SESSLER, ANDREW M. N91-16358
SETTLES, GARY S. N91-15986
SEVERING, A. N91-16093
SEXTON, F. W. N91-16394
SHA, LUI N91-16584
SHAKKOTTAI, P. N91-16078
SHALIS, EDWARD N91-16689
SHANEYFELT, M. R. N91-16394
SHAO, MIKE N91-16850
SHAPIRO, RUTH N91-16587
SHAPIRO, STEPHEN L. N91-16790
SHARIR, MICHA N91-16612
SHARKEY, MIKE N91-16046
SHARP, N. A. N91-16868
SHAW, C. T. N91-16315
SHAW, R. W. N91-16094
SHCHERBININ, E. V. N91-16265
SHEN, SHAN-FU N91-16285
SHEPHERD, KEVIN P. N91-16679
SHERMAN, ELENA N91-16205
SHIELDS, JOSEPH C. N91-16902
SHIGEHARA, M. N91-16277
SHIHO, M. N91-16771
SHIN, Y. W. N91-16260
SHINN, JUDY L. N91-16981
SHINN, N. D. N91-16812
SHIRAISHI, M. N91-16278
SHIRER, HAMPTON N. N91-16506
SHITZER, AVRAHAM N91-16545
SHLACHTER, J. S. N91-16777
SHLOSMAN, ISAAC N91-16953
SHOCKLEY, CYNTHIA W. N91-16830
SHOEMAKER, JAMES R. N91-16474
SHROCK, ROBERT E. N91-16827
SHTERN, A. G. N91-16265
SHURMER, H. V. N91-16541
SIBECK, D. G. N91-16489
SIEGEL, JANE A. N91-16590
SIEKHAUS, W. J. N91-16344
SILLIMAN, M. N91-16368
SIMKIN, S. M. N91-16914
SIMPSON, CAROLINE N91-16881
SIMPSON, HENRY N91-16637
SINCLAIR, D. W. N91-16293
SINDONI, J. M. N91-16482
SINGER, ROBIN N91-16185
SINGH, A. N91-16763
N91-16764
SINGH, J. P. N91-16141
SINGH, R. N91-16153
SIVIER, K. N91-16048
SKIGEMITSU, JUNKO N91-16827
SKLAD, P. S. N91-16814
SKOCYPEC, R. D. N91-16161
SLOAN, GEORGE N91-16226
SMAGA, JOHN A. N91-16438
SMALE, MARK WILTON N91-16089
SMARTT, HERSCHEL B. N91-16377
SMITH, ADRIAN F. M. N91-16666
SMITH, B. F. N91-16934
SMITH, D. BARTON N91-16096
SMITH, D. H. N91-16094
SMITH, D. L. N91-16793
SMITH, DAN T. N91-16563
SMITH, E. A. N91-16472
SMITH, ELIZABETH A. N91-16535
SMITH, ERIC P. N91-16867
SMITH, GORDON N. N91-16585
SMITH, H. VERNON, JR. N91-16772
SMITH, JAMES E., JR. N91-16032
SMITH, JOHN B. N91-16844
SMITH, KENNETH S. N91-16519
SMITH, PHILLIP J. N91-16513
SMITH, RICHARD D. N91-16107
SMITH, WILLIS H., JR. N91-16205
SNOHA, DANIEL J. N91-16073
SON, SANG H. N91-16837
SONG, GHIE HUGH N91-16356
SONG, WOOCHUN N91-16840
SOTNIKOVA, N. YA. N91-16956
SOUTHON, J. R. N91-16084
N91-16538
SOWA, ERIC C. N91-16713
SPAPPERI, JEFF N91-16053
SPARGO, ROBERT A. N91-16830
SPARKS, C. J. N91-16811
SPARKS, W. B. N91-16915
N91-16919
N91-16923
SPECHT, E. D. N91-16811
SPELT, P. F. N91-16368
SPEZIALE, CHARLES G. N91-16306
SPIELMAN, RICK B. N91-16317
SPRAGUE, MARK N91-16686
SPRING, JOHN WALTER N91-16400
SPRINGER, T. E. N91-16778
SPROTT, J. C. N91-16757
SPRUNT, BRINKLEY N91-16584
ST.JULIEN, DELL N91-16788
STACEY, G. J. N91-16977
STAM, HENDRIK JOHANNES N91-16710
STANAWAY, SHARON N91-15987
STANFORD, S. A. N91-16908
STANSFIELD, S. A. N91-16371
STAPP, HENRY P. N91-16546
STASZEWSKI, JAMES J. N91-16549
STATE, ANDREI N91-16622
STAUDENMEIER, JOSEPH L. N91-16767
STEARNS, SAMUEL D. N91-16468
STEENDIJK, ANNE MARIE N91-16005
STEINBACH, DIETER N91-15998
STEINBERG, MEYER N91-16446
N91-16453
STEINBERG, VICTOR N91-16288
STEINSIEK, FRANK N91-16570
STEPHENS, F. S. N91-16798
STERNBERG, A. N91-16977
STEWART, J. B. N91-16472
STEWART, W. F. N91-16174
STEWMAN, SHELBY N91-16590
STOCKE, J. T. N91-16925
STOCKMAN, MARK I. N91-16819
STODOLSKY, F. N91-16373
STOORVOGEL, A. A. N91-16651
N91-16652
STOTLER, D. N91-16774
STOTT, J. H. N91-16189
STRAUSS, A. J. N91-16361
STREET, HENRY K. N91-16233
STREET, R. A. N91-16228
STREHLOW, R. A. N91-16145
STRINNI, MEREDITH N91-16053
STROBEL, GEORGE L. N91-16263
STROSCHEIN, LEANDER A. N91-16545
STRUCK-MARCELL, CURTIS N91-16957
N91-16960
STURNER, STEVEN J. N91-16985
STUTZKI, J. N91-16976
SU, TZU-JENG N91-16059
SUDDATH, FRED L. N91-16815
SUENAGA, M. N91-16803
N91-16804
SULENTIC, JACK W. N91-16858
N91-16865
N91-16899
N91-16900
SUMMERS, ERIC W. N91-16049
SUMMERS, L. T. N91-16775
SUN, L. N91-16146
SUTHERLAND, LOUIS C. N91-16683
SUTTON, KEVIN N91-16046
SUZUKI, MINEO N91-16384
SVISHCHEV, G. N91-16038
SWAB, JEFFREY J. N91-16073
SWEERS, GUIDO N91-16655
SWEET, M. R. N91-16323
SWIDERSKI, TANYA N91-16565
SWINDEMAN, R. W. N91-16117
SYED, HASNAIN H. N91-16211

T

TABASSUM, SALIM ABID N91-16440
TABOR, JEFFREY F. N91-16244
TAFT, SHIRLEY O. N91-16985
TAKAHASHI, K. N91-16489
TAKANASHI, SUSUMU N91-15984
TAKANO, MASANORI N91-16267
TAKIYAMA, K. N91-16771
TAN, YANG M. N91-16624
TANAKA, K. N91-16648
TANAKA, Y. N91-16280
TANG, W. P. N91-16659
TANIGUCHI, YOSHIAKI N91-16963
TANNER, D. B. N91-16800
TARRANT, A. D. N91-16077
TASHIRO, M. N91-16280
TATSUMI, SHIGEFUMI N91-15985
TAUCHEN, RUTH N91-16730
TAYLOR, BLAINE KEITH N91-16282
TAYLOR, PAUL A. N91-16127
TAYLOR, PETER R. N91-16065
N91-16727
N91-16728
TCHAMITCHIAN, PH. N91-16664
TELESCO, C. M. N91-16858
TENCH, R. J. N91-16344
TERDTOON, P. N91-16278
TERLAKY, T. N91-16599
N91-16600
TERRY, M. D. N91-16394
TESTROET, FRANK B. N91-16383
TEWARSON, A. N91-16072
THAKUR, R. P. S. N91-16153
THODE, L. E. N91-16348
THOMASSON, MAGNUS N91-16961
THOMPSON, A. C. N91-16322
THOMPSON, BRUCE ROBERT N91-16386
THOMPSON, SAMUEL L. N91-16575
THOMSON, DENNIS W. N91-16698
THOMSON, R. C. N91-16962
THORNTON, EARL A. N91-16407
THUMM, M. N91-16781
TI, SOI-SANG N91-16331
TICHELAAR, FRANS DAVID N91-16136
TIEN, JOHN K. N91-16120
TIFFT, WILLIAM G. N91-16926
TIGGES, C. P. N91-16240
TIKHONOV, N. A. N91-16874
TILLY, BODO N91-16745
TILS, HENRICUS MARTINUS GERARDUS CLEMENS
N91-16309
TIMCHENKO, V. A. N91-16037
TITRAN, ROBERT H. N91-16128
TITUS, JEFFREY L. N91-16220
TKACZYK, J. E. N91-16768
TOBIN, MICHAEL T. N91-16759
TONG, J. N91-16080
TOOMRE, JURI N91-16511
TOOMS, S. N91-16692
TOROK, MICHAEL SCOTT N91-16006
TORR, D. G. N91-16928
TOTH, RICHARD P. N91-16232
TOWNES, C. H. N91-16977
TOWNS, JOHN W. N91-16901
TOWNSEND, LAWRENCE W. N91-16981
TRACY, C. E. N91-16139
TRAN, AN VAN N91-16534
TRENTELMAN, H. L. N91-16652
TRIPATHY, SUKANT N91-16807
TRULL, JEFFREY E. N91-16604
TSINOBER, A. B. N91-16265
TSUCHIYA, K. N91-16674

TSUI, D. C. N91-16805
TSVETKOVA, V. S. N91-16918
TU, PETER K. C. N91-16582
TUDINI, ADRIAN N91-16331
TUHELA-REUNING, S. N91-16194
TULLY, R. B. N91-16922
TUMMILLO, A. F. N91-16229
TUNG, S.-L. N91-16488
TURKES, GURKAN N91-16198
TURNER, C. DAVID N91-16180
TURNER, LARRY R. N91-16765
TURNER, MICHAEL S. N91-16966
TURNER, MONICA G. N91-16451
TURTELTAUB, K. W. N91-16538
TURYN, MICHAEL N91-16971
TUSZEWSKI, MICHEL N91-16750
TUTTLE, BRUCE A. N91-16242
N91-16789

U

UCHIDA, HIROYUKI N91-16279
UCHIHORI, HIROSHI N91-16272
UEMATSU, KAZUO N91-16279
UHL, MARY A. N91-16513
ULLAL, H. S. N91-16153
ULLMAN, JEFFREY D. N91-16843
UNDERWOOD, J. H. N91-16322
UNGER, S. W. N91-16893
URAS, RASIM AZIZ N91-16398

V

V.D.BERG, J. N91-16656
VADER, J. P. N91-16913
VAKILI, A. D. N91-15981
VALENCIA, J. E. N91-16323
VALETT, JON N91-16602
VALLURI, MONICA N91-16952
VALTONEN, M. J. N91-16929
VANAST, CAMILLE I. N91-16205
VANBREUGEL, WIL N91-16902
VANDEMOLENGRAFT, MARINUS JACOBUS GERARDUS N91-16644
VANDERPUTTEN, RONALD N91-16628
VANDOORNE, H. N91-16213
VANES, ANDRIES JOHANNES JOZEF N91-16113
VANGORKOM, J. H. N91-16872
N91-16925
VANHAERINGEN, H. N91-16653
N91-16654
VANKAMPEN, EELCO N91-16895
VANKNOWE, GLENN ERNEST N91-16522
VANMOORHEM, W. K. N91-16684
VANPATTEN, ROBERT E. N91-16556
VANPUTTEN, F. J. M. N91-16366
VANSCIVER, STEVEN W. N91-16813
VANSCOY, ROGER N91-16610
VANSWOL, R. W. N91-16425
VANWIE, C. N91-16591
N91-16594
VASILCHENKO, K. N91-16038
VENEMA, J. C. N91-16425
VENKATESAN, T. N91-16800
VENNERI, F. N91-16777
VERDERAIME, V. N91-16413
VERDU, SERGIO N91-16200
VERMA, S. B. N91-16472
VESS, ROBERT J. N91-16008
VETTOLANI, G. N91-16896
VICCARO, P. J. N91-16784
VIGIL, MANUEL G. N91-16028
VIJAYARAGHAVAN, D. N91-16304
VIJAYASANKAR, M. K. N91-16760
VIJLBRIEF, C. N91-16213
VINCENT, DAYTON G. N91-16503
VITELLO, PETER N91-16982
VITERBI, A. J. N91-16842
VITTITOE, CHARLES N. N91-16043
VOGEL, J. S. N91-16084
N91-16538
VOGT, GREGORY L. N91-16601
VOIGT, J. A. N91-16789
VOLAKIS, JOHN L. N91-16211
VONHOLTZ, ERIC N91-16158
N91-16159
VYAS, A. N91-16448

W

WADE, G. N91-16321
WAGNER, JAMES W. N91-16678
WAGNER, W. G. N91-16590
WAHL, DANIEL E. N91-16579
WAITES, H. B. N91-16057
WALKER, DOREEN M. C. N91-16035
WALKER, KEVIN N91-16052
WALKER, MARY MCWHERTER N91-16054
WALKER, R. N91-16680
WALLACE, BRIAN L. N91-16476
N91-16477
N91-16478
N91-16479
N91-16480
N91-16481
WALLE, GERARDO N91-16014
WALLIN, JOHN F. N91-16957
WALLS, C. A. N91-16145
WALPOLE, J. N. N91-16361
WALSH, D. N91-16144
WALSH, M. N91-16448
WALTON, E. K. N91-16194
WALTZ, R. E. N91-16749
WAMPLER, W. R. N91-16144
WANDER, JOSEPH D. N91-16085
WANG, H.-G. N91-16803
WANG, HONG N91-16208
N91-16209
WANG, LAI-SHENG N91-16119
WANG, LIER N91-16274
WANG, LINTAO N91-16700
WANG, RONGDONG N91-16576
WANG, W. N91-16344
WANIE, K. M. N91-15997
N91-16016
WARD, M. B. N91-16319
N91-16739
WARRELL, RAYMOND N91-16542
WARREN, ROGER W. N91-16357
WAS, GARY S. N91-16243
WASSERFUHR, C. H. N91-16134
WASSGREN, CARL N91-16047
WASSOM, STEVEN R. N91-16062
WATSON, K. N91-16239
WATSON, R. T. N91-16466
WATTS, JOHN D. N91-16728
WDOWINSKI, SHIMON N91-16490
WEAR, STEVEN M. N91-16188
WEAVER, H. N91-16472
WEBBER, S. E. N91-16151
WEBER, IRENE N91-16844
WEBSTER, C. E. N91-16229
WEBSTER, R. B. N91-16343
WEBSTER, ROBIN L. N91-16588
WEIDERMAN, NELSON N91-16587
WEINER, DONALD N91-16207
WELS, BRIAN REID N91-16100
WENG, HENGYI N91-16516
WENSINK, G. J. N91-16425
WENSKAT, LUTZ N91-16973
WERNER, M. N91-16898
WESLEY, DAVID N91-16474
WEST, M. N91-16699
WEST, W. P. N91-16773
WESTBROOK, C. K. N91-16080
N91-16082
WESTFOLD, STEPHEN N91-16586
WETZEL, MELANIE ANN N91-16420
WHIPPLE, RICH N91-16159
WHITAKER, RODNEY W. N91-16694
N91-16695
WHITE, ALAN R. N91-16737
WHITEHOUSE, D. J. N91-16339
WHITEHOUSE, STEPHEN ROBERT N91-16408
WHITLOW, L. W. N91-16785
WHITMORE, BRADLEY C. N91-16873
WHITT, WARD N91-16667
N91-16668
WHITTEN, W. B. N91-16095
WIEDERMANN, A. H. N91-16260
WIEMAN, CARL E. N91-16363
WIERSMA, G. B. N91-16461
WIESELTHIER, JEFFREY E. N91-16186
WIESMANN, H. J. N91-16803
N91-16804
WIGHTMAN, FREDERIC N91-16708
WIKLIND, T. N91-16976
WILBANKS, T. J. N91-16449
WILBURN, COLIN D. N91-16790
WILDERMUTH, D. N91-16228
WILDERMUTH, EBERHARD N91-16367
WILHELM, D. N91-16283
WILKE, W. N91-16987
WILKINSON, JEFFREY P. N91-16053
WILLIAMS, B. A. N91-16872
WILLIAMS, C. H. N91-16595
WILLIAMS, CLAUDE N. N91-16476
N91-16477
N91-16478
N91-16479
N91-16480
N91-16481
WILLIAMS, G. P. N91-16800
WILLIAMS, STEPHEN N91-16052
WILLIAMSON, R. C. N91-16361
WILLS, DONALD SCOTT N91-16640
WILLSHIRE, WILLIAM L., JR. N91-16682
N91-16693
WILSON, A. S. N91-16922
WILSON, DONALD R. N91-16336
WILSON, JOHN W. N91-16981
WILSON, K. KEITH N91-16698
WILSON, P. B. N91-16183
WINOKUR, P. S. N91-16394
WISE, GARY L. N91-16184
WISE, MARCUS B. N91-16452
WITHEROW, WILLIAM K. N91-16815
WONG, YAT-TING N91-16108
WOO, PENG-YUNG N91-16576
WOODARD, JOHN CAMPBELL N91-16543
WOODSON, STANLEY C. N91-16031
WOOTEN, JOHN R. N91-16063
WOOTTON, ALAN J. N91-16762
WORTMAN, JOHN D. N91-16287
WRIGHT, A. E. N91-16962
WRIGHT, G. S. N91-16904
WRIGHT, J. C. N91-16642
WRIGHT, NANCY F. N91-16719
WROBLEWSKI, D. N91-16773
WU, G. D. N91-16011
N91-16013
WU, HUAMO N91-16274
N91-16275
WU, J. M. N91-15981
WU, MICHAEL M. N91-16623
WU, TXUYIN N91-16285
WU, Y. N91-16322

X

XI, X. N91-16800
XIAO, Z. N91-16285
XIE, R. N91-16055
XU, CONG N91-16900

Y

YAKOVLEVA, V. A. N91-16892
YALDA-MOOSHABAD, ISSAC N91-16390
YAMADA, TETSUJI N91-16499
YAMAGATA, TOMOHIKO N91-16861
YAMAGUCHI, HIROMI N91-16279
YAMAMOTO, T. N91-16280
YANAGIZAWA, MITSUNORI N91-15985
YANG, AN-BAN N91-16799
YANG, C. C. N91-16529
YANG, SHULI N91-16275
YAP, B. K. N91-16482
YAP, SUE-KEN N91-16620
YATES, G. J. N91-16893
YATES, S. W. N91-16798
YI, ZHANG N91-16658
YONKER, CLEMENT R. N91-16107
YORK, G. W. N91-16343
YOTSUKURA, TERUMITSU N91-16276
YOUNG, CHRISTOPHER JOHN N91-16491
YOUNG, J. P. N91-16094
YOUSSEFI, GERHARD N91-16983
YU, MING-HUEI N91-16298
YUN, HEE MANN N91-16128

Z

ZAHNER, GISELA N91-16562
ZAIDER, M. N91-16722
ZALONDEK, F. R. N91-16256
ZASOV, ANATOLI V. N91-16883
ZAYED, HUSNI N91-16046
ZEPF, STEPHEN E. N91-16873
ZHANG, X.-G. N91-16713
ZHANG, Y. N91-16658
ZHAO, JIANHUA N91-16441
ZHENG, WEI N91-16894
ZHONG, F. H. N91-16684
ZHONG, FANG N91-16288
ZHOU, JIANHUA N91-16605
ZHU, JIANZHONG N91-16347
ZHU, X.-M. N91-16811
ZIEMER, SARAH N91-16047
ZIMMERMAN, DAVID N91-16586
ZIMMERMAN, SHERY A. N91-16048
ZINDER, S. H. N91-16086
ZINK, R. A. N91-16316
ZIOLKOWSKI, RICHARD N91-16182
ZIPPERIAN, T. E. N91-16240

ZOLOTUSKY, G. N91-16488
ZOU, D. N91-16146
ZOU, KE-SHAN N91-16492
ZUCCA, J. J. N91-16469

Typical Corporate Source Index Listing

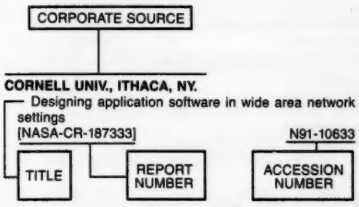

Listings in this index are arranged alphabetically by corporate source. The title of the document provides the user with a brief description of the subject matter. The report number helps to indicate the type of document cited (e.g., NASA report, translation, NASA contractor report). The accession number denotes the number by which the citation is identified. The titles are arranged under each corporate source in ascending accession number order.

A

ACADEMIA SINICA, BEIJING (CHINA).
Analysis of atmospheric diffusion of pollutants based on the limited observation of horizontal wind N91-16274
MmB: A new class of accurate high resolution schemes for conservation laws in two dimensions N91-16275

ACADEMY OF SCIENCES (USSR), MOSCOW.
On leading spiral arms in close pairs of galaxies N91-16935
Stationary orbits of satellites of disk galaxies N91-16954

ADA JOINT PROGRAM OFFICE, ARLINGTON, VA.
Ada compiler validation procedures, version 2.1 [AD-A228614] N91-16621

ADVISORY GROUP FOR AEROSPACE RESEARCH AND DEVELOPMENT, NEUILLY-SUR-SEINE (FRANCE).
Safety Network to Detect Performance Degradation and Pilot Incapacitation [AGARD-CP-490] N91-16553
Calendar of selected aeronautical and space meetings: January 1991 onwards [AGARD-CAL-91/1] N91-16833

AEROJET TECHSYSTEMS CO., SACRAMENTO, CA.
High temperature oxidation-resistant thruster research [NASA-CR-185233] N91-16063

AERONAUTICAL RESEARCH INST. OF SWEDEN, STOCKHOLM.
Pilot study of the dynamic impact response of a composite plate [FFA-TN-1990-27] N91-16070
Environmental noise from the Naesudden (Sweden) and Maglarp (Sweden) prototype wind turbines: A study of machinery noise [FFA-TN-1990-34] N91-16706

AERONAUTICAL RESEARCH LABS., MELBOURNE (AUSTRALIA).
IFDIS: An expert system for diagnosis of failures in jet aircraft engines [AD-A227757] N91-16020

AEROSPACE CORP., EL SEGUNDO, CA.
Threshold voltage and I-V characteristics of AlGaAs/GaAs MODFETs [AD-A228844] N91-16248
Effects of neutron fluence on the operating characteristics of diode lasers used in atomic frequency standards [AD-A226763] N91-16352
Optimization of hydrogen consumption in hydrogen masers [AD-A227267] N91-16355
Direct observation of NF(X) using laser-induced fluorescence: Kinetics of the NF 3 Sigma - ground state [AD-A228294] N91-16362
The magnetospheric response to 8-minute period strong-amplitude upstream pressure variations [AD-A228038] N91-16489

AEROSPACE MEDICAL RESEARCH LABS., WRIGHT-PATTERSON AFB, OH.
Current status of an artificial intelligence-based loss of consciousness monitoring system for advanced fighter aircraft N91-16556

AIR FORCE HUMAN RESOURCES LAB., BROOKS AFB, TX.
Human factors design guidance during the conceptual design phase of system development: A methodological approach [AD-A224667] N91-16552

AIR FORCE INST. OF TECH., WRIGHT-PATTERSON AFB, OH.
Optimal Kalman filter integration of a global positioning system receiver and an LN-94 inertial navigation system [AD-A227222] N91-16003
Electron density comparisons between radar observations and 3-D ionospheric model calculations [AD-A227703] N91-16187
Shift-invariant image reconstruction of speckle-degraded images using bispectrum estimation [AD-A227728] N91-16188
Monte Carlo simulation of atmospheric neutron transport at high altitudes using MCNP [AD-A226773] N91-16474
A comparison of optically measured and radar-derived horizontal neutral winds [AD-A227690] N91-16483
Derivation of exospheric temperature at high latitudes from incoherent-scatter radar data [AD-A227721] N91-16484
On the developmental dynamics of sudden stratospheric warmings [AD-A227731] N91-16485
A two-dimensional balanced model of internal frontogenesis in geostrophic and isentropic coordinates [AD-A227644] N91-16518
An investigation of a gravity wave during GALE: February 6, 1986 [AD-A227655] N91-16519
Prediction of tropical cyclone rapid intensification events [AD-A227668] N91-16520
Examples of isallobaric forcing in surface frontal motion and surface frontogenesis over the Central United States [AD-A227687] N91-16521
A comparison of diagnostic and kinematic vertical motion fields associated with curved and straight jet streak adjustment processes [AD-A227724] N91-16522
Managing emerging technology: Case studies in document imaging systems [AD-A227688] N91-16839

ALABAMA UNIV., HUNTSVILLE.
High temperature furnace modeling and performance verifications [NASA-CR-187831] N91-16032
New methods for producing, recording, and processing interferometric moire patterns N91-16405
Global-scale, intraseasonal fluctuations of diabatic forcing of the atmosphere N91-16508
A tentative explanation of cosmological red shift N91-16928

ALABAMA UNIV., TUSCALOOSA.
The ringed X-galaxy NGC 7020 N91-16885
Interacting nuclei in distant galaxies N91-16894
FIR statistics of paired galaxies N91-16899
Statistics of associations among IR galaxies N91-16909
The role of shocks in NGC 6240 N91-16921
A simulation survey of galaxy interactions N91-16936
The spiral-compact galaxy pair AM 2208-251: Computer simulations versus observations N91-16939

ALLIED-SIGNAL AEROSPACE CO., PHOENIX, AZ.
Magnetic domain strain sensor program [AD-A227225] N91-16327

ALLIED-SIGNAL CORP., KANSAS CITY, MO.
Deburring and surface finishing: The past ten years and projections for the next ten years [DE91-000579] N91-16176
Characterization of ultrasonic transducers using pattern recognition techniques [DE91-000580] N91-16326

AMERICAN SOCIETY OF MECHANICAL ENGINEERS, NAPERVILLE, IL.
Wind turbine acoustics [NASA-TP-3057] N91-16679

AMES LAB., IA.
Fundamental studies of hydrocarbon conversions over supported bimetallic catalysts [DE90-011744] N91-16089
Electrocatalysis of anodic and cathodic oxygen-transfer reactions [DE91-000611] N91-16100
New development of laser-based techniques in applications of thin-layer chromatography, microprobe elemental analysis, and gas phase pyrolysis [DE90-011740] N91-16347
Fundamental characteristics and applications of an inductively coupled plasma as an ion source for mass spectrometry [DE90-011746] N91-16770
A photoemission study of samarium on silicon [DE90-011509] N91-16799

AMSTERDAM UNIV. (NETHERLANDS).
A spiral-like disk of ionized gas in IC 1459: Signature of a merging collision N91-16889

ARGONNE NATIONAL LAB., IL.
High resolution electron microscopy of interfaces in fcc materials [DE91-004420] N91-16101
Thermal aging of cast stainless steels: Mechanisms and predictions [DE90-010093] N91-16115
Desorption of H2O and H2 from steel and LiAO2 by temperature programmed desorption [DE90-011170] N91-16118
A study of the formation and self-lubrication mechanisms of boric acid films on boric oxide coatings [DE90-010115] N91-16137
Development of nondestructive evaluation methods and prediction of effects of flaws on the fracture behavior of structural ceramics [DE90-011092] N91-16141
Neoclassical effects on RF current drive [DE90-010302] N91-16222
Status of Argonne life evaluation of valve regulated lead-acid batteries [DE90-011098] N91-16229
Requirements for a fuel cell for transportation application [DE90-011146] N91-16230
Evaluation of novel solid electrolyte materials [DE90-011164] N91-16231
A method for pressure-pulse suppression in fluid-filled piping [DE90-010408] N91-16260
Parametric study of electrostatically charged sprays [DE90-010580] N91-16262
Circumfluous motion of a conductive liquid around solid objects in a magnetic field [DE90-011335] N91-16265
A summary of prospects for methanol vehicles in the United States [DE90-009719] N91-16370
Technical and economic evaluation of diesel engine with oxygen enrichment and water injection [DE90-009723] N91-16373
Magnetic heat pumps [DE90-010305] N91-16375
Study of the influence of imperfections on the dynamic stability of tanks [DE90-011094] N91-16398
Contemporary issues in solar pond research [DE90-010094] N91-16436
Technological and policy options for mitigating greenhouse gas emissions from mobile sources [DE90-010151] N91-16447

Greenhouse gas emissions from selected alternative transportation fuels market niches
[DE90-010491] N91-16448
A block QR factorization algorithm for rank-deficient matrices
[DE90-010066] N91-16573
Using MAPLE for symbolic computations in robotics
[DE90-010405] N91-16576
Wakefield calculations on parallel computers
[DE90-009712] N91-16632
Skolem functions and equality in automated deduction
[DE90-009703] N91-16641
State-to-state inelastic and reactive molecular beam scattering from surfaces
[DE90-010492] N91-16714
Puzzles of electron transfer
[DE90-010541] N91-16720
Analytic Multi-Regge Theory and the Pomeron in QCD
[DE90-012153] N91-16737
A free boundary problem arising in plasma physics
[DE90-010065] N91-16754
Electromagnetic computations for fusion devices
[DE90-011097] N91-16765
The measurement of gamma heating in a fusion blanket test assembly
[DE90-011154] N91-16766
Hyperfine interactions associated with iron substituted superconducting oxides
[DE90-010411] N91-16783
Modeling the performance of water and liquid gallium cooled x ray optical components: A comparison with experiment
[DE90-010460] N91-16784
Calculation of free energy from the internal-energy distribution function
[DE90-011111] N91-16791
High Tc oxide solid state reaction kinetics via complex impedance spectroscopy
[DE90-011178] N91-16792
A search for good lattice rules based on the reciprocal lattice generator matrix
[DE91-004425] N91-16809
Correlation between the elastic-shear-instability-mechanism and empirical criteria for irradiation-induced amorphization
[DE91-004481] N91-16810
Highlights of the Chemical Technology (CMT) Division's activities
[DE90-008242] N91-16984

ARIZONA STATE UNIV., TEMPE.
High-frequency techniques for RCS prediction of plate geometries
[NASA-CR-187865] N91-16212
Research on certain aspects of laser diffraction particle size analysis relevant to autonomous self-diagnosing instrumentation
[AD-A226822] N91-16354

ARIZONA UNIV., TUCSON.
Composite Solid Propellant Predictability and Quality Assurance
[NASA-CR-186404] N91-16163
Introduction to the problem N91-16164
The University of Arizona program in solid propellants N91-16165
Pairs of galaxies in low density regions of a combined redshift catalog N91-16860
Global effects of interactions on galaxy evolution N91-16897
Nuclear and extended infrared emission in paired and isolated galaxies N91-16917
Properties of the redshift N91-16926

ARMY AEROMEDICAL RESEARCH LAB., FORT RUCKER, AL.
A comparison of computerized measurement of helicopter pilot performance with atropine sulfate during actual and simulated flight N91-16558

ARMY CHEMICAL RESEARCH AND DEVELOPMENT CENTER, ABERDEEN PROVING GROUND, MD.
Computer-assisted determination of minimum energy conformations. Part 4: Alpha1 and alpha2 adrenergiic compounds
[AD-A226811] N91-16097
Symmetry and design in mixture experiments
[AD-A226760] N91-16169

ARMY COLD REGIONS RESEARCH AND ENGINEERING LAB., HANOVER, NH.
Heat transfer from water flowing through a chilled-bed open channel
[AD-A226855] N91-16286
Preliminary analysis of measured sound propagation over various seasonal snow covers N91-16687

ARMY COMMAND AND GENERAL STAFF COLL., FORT LEAVENWORTH, KANSAS.
Army Unmanned Aerial Vehicle (UAV) requirements and the joint UAV program
[AD-A228149] N91-16009

ARMY CONSTRUCTION ENGINEERING RESEARCH LAB., CHAMPAIGN, IL.
Cartographic issues in the development of a digital GRASS database
[AD-A227582] N91-16416

ARMY ENGINEER WATERWAYS EXPERIMENT STATION, VICKSBURG, MS.
Evaluation procedure for reinforced concrete box culverts under airfield pavements
[AD-A227920] N91-16031

ARMY LAB. COMMAND, WATERTOWN, MA.
Failure analysis of a main rotor pitch horn bolt located on the AH-1 Cobra helicopter
[AD-A227679] N91-16007
Mechanical behavior of a SiC-fiber/Si3N4 composite
[AD-A228371] N91-16073
Assessment of corrosion resistant coatings for a depleted U-0.75 Ti alloy
[AD-A228237] N91-16130

ARMY MATERIALS TECHNOLOGY LAB., WATERTOWN, MA.
Flammability characteristics of fiber-reinforced composite materials for the composite infantry fighting vehicle
[AD-A227783] N91-16068

ARMY RESEARCH INST. OF ENVIRONMENTAL MEDICINE, NATICK, MA.
Quantification of lower bounds for endurance times in thermally insulated fingers and toes exposed to cold stress
[AD-A227782] N91-16545

ARMY TANK-AUTOMOTIVE COMMAND, WARREN, MI.
ADRPM-VII applied to the long-range acoustic detection problem N91-16689

ASSISTANT SECRETARY OF THE AIR FORCE, WASHINGTON, DC.
The USAF STINFO program overview
[AD-A226969] N91-16838

ATMOSPHERIC SCIENCES OFFICE, WHITE SANDS MISSILE RANGE, NM.
A noise assessment and prediction system N91-16702
Effects of large-scale wind driven turbulence on sound propagation N91-16704

B

BALLISTIC RESEARCH LABS., ABERDEEN PROVING GROUND, MD.
Use of the Magnus force in the modified point mass trajectory model
[AD-A228194] N91-15990
Small scale shock tube experiments using a computer controlled active rarefaction wave eliminator
[AD-A227507] N91-16029
An approximation to true peak absorbance from observed peak absorbance for gas phase Fourier transform spectroscopy
[AD-A228357] N91-16104
Rotational temperature estimation of CO at high temperatures by graphical methods using FTIR spectrometry
[AD-A228370] N91-16105
Laser microplasma-gas chromatography detector. 2: Detection of species-specific fragment emission
[AD-A228373] N91-16106
Evaluation of the HULL and SHARC hydrocodes in simulating the reflection of Mach 2.12 non-decaying shock on wedges of various angles
[AD-A227581] N91-16287
Removal of NO and NO2 from contaminated atmospheres
[AD-A227260] N91-16565
BLAST2D computations of the reflection of planar shocks from wedge surfaces with comparison to SHARC and STEALTH results
[AD-A227261] N91-16589

BELEIDSCOMMISSIE REMOTE SENSING, DELFT (NETHERLANDS).
Extraction of marketable information from ERS-1 data
[BCRS-90-03] N91-16425
Sahelian vegetation monitoring project
[BCRS-90-04] N91-16426
Detection of soil moisture using X-band SLAR records in a sandy area
[BCRS-90-08] N91-16427
The usefulness of MSS pictures for mapping and biomass estimation of macro-algae and seaweed in the Eastern Scheldt
[BCRS-90-09] N91-16428
The dielectric properties of wet soils
[BCRS-90-13] N91-16429
Procedure for the correction of errors in the DUTSCAT data 1987/1988
[BCRS-90-14] N91-16430

BERKELEY RESEARCH ASSOCIATES, INC., CA.
Development and application of numerical models for reactive flows
[AD-A228884] N91-16295

BONN UNIV. (GERMANY, F.R.).
The stationary exterior three dimensional Navier-Stokes problem of viscous flow past a body in anisotropically weighted Sobolev spaces
[REPT-110] N91-16314
The Cabannes-lidar for the examination of the stratosphere: Selected design elements for the experimental construction
[BONN-IR-90-39] N91-16493
Design and testing of a proton detector
[BONN-IR-90-34] N91-16729
Testing of lead glass detectors for electron proof in the ELAN experiment
[BONN-IR-90-38] N91-16730
A Moller polarimeter for the extracted ELSA-ray
[BONN-IR-90-42] N91-16731

BOWLING GREEN STATE UNIV., OH.
Photoinduced charge separation by polymer-bound chromophores
[DE90-010997] N91-16140

BRADFORD UNIV. (ENGLAND).
Long-distance sound propagation over discontinuous impedances N91-16688

BRITISH AEROSPACE PUBLIC LTD. CO., BRISTOL (ENGLAND).
EEG indicators of mental workload: Conceptual and practical issues in the development of a measurement tool N91-16559

BRITISH BROADCASTING CORP., KINGSWOOD (ENGLAND).
Satellite broadcasting: A common-frequency approach to wideband HDTV with a hand-made example plan
[BBC-RD-1990/7] N91-16189
NICAM 728: Factors affecting the assessment of UHF transmitter linearity
[BBC-RD-1990/9] N91-16190
The computer simulation of digital recording systems
[BBC-RD-1990/14] N91-16595
A review of the airborne sound insulation requirements for broadcasting studios and ancillary areas
[BBC-RD-1990/10] N91-16680
Proving experiments on an acoustic transmission suite and its reverberation room
[BBC-RD-1990/13] N91-16681

BRITISH COLUMBIA UNIV., VANCOUVER.
Observational properties of compact groups of galaxies N91-16871

BRITISH PETROLEUM CO. LTD., SUNBURY-ON-THAMES (ENGLAND).
Metallurgical design of novel metal matrix composites for aerospace applications
[ETN-91-98573] N91-16077

BROOKHAVEN NATIONAL LAB., UPTON, NY.
Solving global environmental problems through technological innovation
[DE90-010018] N91-16446
Biomass and hydrocarb technology for removal of atmospheric CO2
[DE90-010016] N91-16453
Gallium as a unique anti-resorptive agent in bone: Preclinical studies on its mechanisms of action
[DE90-010650] N91-16542
AGS silicon gold collisions measured in the E-810 TPC (Time Projection Chamber)
[DE90-010015] N91-16733
V(sup 0) production with 14.5 GeV/c silicon beams
[DE90-010014] N91-16747
Infrared response of YBa2Cu3O(7-delta) films to pulsed, broadband synchrotron radiation
[DE90-011519] N91-16800
Microstructures and dc critical currents in textured Y-Ba-Cu-oxides
[DE91-000895] N91-16803
Observations of vortex structure in YBa2Cu3O7
[DE91-000900] N91-16804

BRYN MAWR COLL., PA.
Homogeneously broadened bidirectional ring laser: Theoretical analysis, numerical simulation, and experiment in helium-xenon N91-16360

BULGARIAN ACADEMY OF SCIENCES, SOFIA.
Isolated galaxies, pairs, and groups of galaxies N91-16878
Correlation functions for pairs and groups of galaxies N91-16879

BUNDESANSTALT FUER FLUGSICHERUNG, FRANKFURT AM MAIN (GERMANY, F.R.).
Activities report of the German Federal Institute for Flight Safety
[ETN-91-98644] N91-16002

BUNDESMINISTERIUM FUER FORSCHUNG UND TECHNOLOGIE, BONN (GERMANY, F.R.).
The space flights: Second German Spacelab mission D-2 and Mir 1992
[REPT-25/90] N91-16034
BYURAKAN OBSERVATORY, MOUNT ARAGATZ (USSR).
New data on the peculiar galaxy MRK 273
N91-16887

C

CALIFORNIA INST. OF TECH., PASADENA.
Experimental studies of the properties of trihydrogen and tetrahydrogen
[AD-A228869] N91-16110
Research in nonlinear water waves
[AD-A227948] N91-16292
Simulation of the flow past an impulsively started cylinder using a discrete vortex method N91-16303
Time-temperature response of multiphase viscoelastic solids through numerical analysis N91-16401
Dynamic crack propagation in elastic-plastic solids
N91-16402
A non-LTE analysis of a sample of O stars selected from galactic OB associations N91-16854
Induced starburst and nuclear activity: Faith, facts, and theory N91-16953
Molecular gas and star formation in the central regions of Virgo spiral galaxies N91-16970
CALIFORNIA UNIV., BERKELEY.
High resolution photoelectron spectroscopy of metal clusters and high temperature species
[DE90-011598] N91-16119
A software development specification for nonlinear structural analysis
[AD-A228427] N91-16614
Theoretical studies of tokamaks
[DE90-011332] N91-16768
Radio loud far-infrared galaxies N91-16902
CALIFORNIA UNIV., BERKELEY. LAWRENCE BERKELEY LAB.
High resolution photoelectron spectroscopy of metal clusters and high temperature species
[DE90-011598] N91-16119
Electron microscopy and electrochemistry of nickel oxide films for electrochromic devices produced by different techniques
[DE90-011596] N91-16142
Sintering stress and microstructure in ceramic powder compacts
[DE91-004415] N91-16149
Measurements of 1/f noise in a-Si:H pin diodes and thin-film-transistors
[DE90-011218] N91-16228
A tunable x ray microprobe using synchrotron radiation
[DE90-011219] N91-16322
Some nonlinear problems in the manipulation of beams
[DE91-005211] N91-16358
A quantum theory of the mind-brain interface
[DE91-004431] N91-16546
Production of high intensity radioactive beams
[DE90-011340] N91-16735
Quasiperiodic transition to chaos in Ge; and magnetic susceptibility of high-T(c) superconductors
[DE90-011304] N91-16797
CALIFORNIA UNIV., DAVIS.
Use of satellite data and modeling to assess the influence of stratospheric processes on the troposphere
N91-16517
CALIFORNIA UNIV., LOS ANGELES.
Local and global instability of heated 2-D jets and wakes N91-16298
Attenuation of seismic waves in the near-source region
[AD-A226814] N91-16475
A statistical survey of electron pitch angle distributions in the nightside central plasma sheet
[AD-A227763] N91-16486
Seismic structure of the upper mantle under the Pacific Ocean N91-16492
The CIT physics program
[DE90-012134] N91-16774
CALIFORNIA UNIV., SAN DIEGO.
Variability of latent and sensible heat fluxes over the oceans N91-16531
Scaling dimensionally similar tokamak discharges to ignition
[DE90-010079] N91-16749
CALIFORNIA UNIV., SAN DIEGO, LA JOLLA.
Mechanics of interface cracks
[AD-A227579] N91-16067
CALSPAN CORP., ARNOLD AFS, TN.
Investigation of the influence of constant adverse pressure gradients on laminar boundary-layer stability at Mach number 8
[AD-A228231] N91-16293
CARNEGIE-MELLON UNIV., PITTSBURGH, PA.
Implementing sporadic servers in Ada
[AD-A226723] N91-16584
Understanding the adoption of Ada: Results of an industry survey
[AD-A226725] N91-16585
Hartstone benchmark results and analysis
[AD-A226817] N91-16587
National software capacity: Near-term study executive summary
[AD-A227564] N91-16590
Decentralized real-time scheduling
[AD-A227856] N91-16604
Kernal facilities definition, Kernel version 3.0
[AD-A228027] N91-16610
Linear-time separation algorithms for the three-index assignment polytope
[AD-A228854] N91-16626
The role of ledges in phase transformations
[AD-A228750] N91-16821
CASE WESTERN RESERVE UNIV., CLEVELAND, OH.
Modeling and identification of cumulative creep fatigue damage in an austenitic stainless steel N91-16131
Development of a versatile laser light scattering instrument
[NASA-CR-182474] N91-16350
CATHOLIC UNIV., SANTIAGO (CHILE).
Dynamics of groups around interacting double ellipticals: Measuring dark matter haloes N91-16863
CENTER FOR MATHEMATICS AND COMPUTER SCIENCE, AMSTERDAM (NETHERLANDS).
Introduction to aspects of object oriented graphics
[CWI-CS-R9009] N91-16597
CERAMPHYSICS, INC., WESTERVILLE, OH.
A miniature inexpensive, oxygen sensing element
[DE90-009938] N91-16318
CHIBA UNIV. (JAPAN).
Some topics of Navier-Stokes solvers N91-16269
CIVIL AEROMEDICAL INST., OKLAHOMA CITY, OK.
Development of a crashworthy seat for commuter aircraft
[AD-A227486] N91-15999
CLEMSON UNIV., SC.
Towards conservative reliability predictions for real-time software
[NASA-CR-187863] N91-16627
CLEVELAND STATE UNIV., OH.
A modular stiffness-based approach to rotating systems analysis N91-16400
COLORADO STATE UNIV., FORT COLLINS.
Investigation of a remote sensing technique for droplet effective radius N91-16420
Colorado State University program for developing, testing, evaluating and optimizing solar heating and cooling systems
[DE90-010107] N91-16435
COLORADO UNIV., BOULDER.
Nonlinear waves and inverse scattering
[AD-A228757] N91-16294
Study of time accuracy of flow variables across discontinuous boundaries N91-16300
A ring laser gyroscope with optical subtraction
N91-16335
Spontaneous force optical traps
[AD-A228539] N91-16363
Scattering of Lamb waves in an elastic plate for ultrasonic nondestructive evaluation of weldments and cracks N91-16412
The effects of the solid inner core and nonhydrostatic structure on the Earth's forced nutations and Earth tides
N91-16417
Analysis of satellite and Expendable Bathythermograph (XBT) data for the abrupt topography program
[AD-A228870] N91-16422
Planetary circulations in the presence of transient and self-induced heating N91-16505
Laboratory and theoretical models of planetary-scale instabilities and waves N91-16511
A global climatology of middle atmosphere inertio-gravity waves N91-16524
Stability criteria for stratocumulus-topped boundary layers evaluated through conditional sampling of turbulence elements
[AD-A228433] N91-16526
Applications of non-linear optics
[AD-A228872] N91-16743
COLUMBIA UNIV., NEW YORK, NY.
Understanding the interdiffusion behavior and determining the long term stability of tungsten fiber reinforced niobium-base matrix composite systems
[NASA-CR-187396] N91-16120
Radiation physics, biophysics, and radiation biology
[DE90-011544] N91-16722
Development of liquid xenon imaging gamma-ray spectrophotometers
[AD-A227575] N91-16740
Transport simulation of the effect of impurity radiation on the high beta, ohmic start-up of the HBT-EP tokamak
[DE90-010333] N91-16760
COMMONWEALTH SCIENTIFIC AND INDUSTRIAL RESEARCH ORGANIZATION, EPPING (AUSTRALIA).
Are extremely luminous far-infrared galaxies the result of merging quasar cores N91-16912
CONSERVE RESOURCES, INC., PRESCOTT, WA.
Rotary absorption heat pump sensitivity analysis
[DE90-010006] N91-16256
COORDINATING RESEARCH COUNCIL, INC., ATLANTA, GA.
CRC volatility program on the effect of oxygenated fuels and altitude on cold-start drivability at low ambient temperatures
[AD-A227571] N91-16171
CORNELL UNIV., ITHACA, NY.
Conversion of acetic acid to methane by thermophiles
[DE90-010993] N91-16086
In situ studies of potential dependent structural and distributional changes at electrochemical interfaces with x rays
[AD-A226844] N91-16098
Chemisorption of carbon monoxide on three metal surfaces: Ni(111), Pd(111) and Pt(111): A comparative study
[AD-A228579] N91-16108
Unsteady separation over maneuvering bodies
[AD-A226829] N91-16285
Probabilistic fracture mechanics: A validation of predictive capability
[AD-A228877] N91-16409
The effect of latent heat release on synoptic-to-planetary scale wave interactions and implications for satellite observations: Observational study N91-16515
Fabrication and electrical characterization of deep-submicron trench-isolated CMOS device structures
N91-16802
COUNCIL FOR NATIONAL ACADEMIC AWARDS (ENGLAND).
Far-field boundaries and their numerical treatment
N91-16281
Solar refrigeration: Evaluation of technical options and design of a solar-generator-adsorber for a novel adsorption refrigerator, volumes 1 and 2 N91-16440
COUNCIL ON ENVIRONMENTAL QUALITY, WASHINGTON, DC.
Environmental trends
[DE90-010530] N91-16450
CPS SUPERCONDUCTORS, INC., MILFORD, MA.
Composite ceramic superconducting wires for electric motor applications
[AD-A228359] N91-16818
CRANFIELD INST. OF TECH., BEDFORD (ENGLAND).
TF89 aircraft centre fuselage
[ETN-91-98579] N91-16018
TF89 tactical fighter outer wing design
[ETN-91-98580] N91-16019
The design of a meteorological facsimile converter
[ETN-91-98578] N91-16528
CRIMEAN ASTROPHYSICAL OBSERVATORY (USSR).
Observational effects of interaction in the Seyfert galaxy NGC 7469 N91-16906

D

DANISH SPACE RESEARCH INST., LYNGBY.
Magnetic measurements with fluxgate magnetometer in rocket flight
[DRI-4-90] N91-16061
DAVID TAYLOR RESEARCH CENTER, BETHESDA, MD.
SCATSPHERE2: A computation for the plane-wave scattering from a submerged, elastic, spherical, evacuated or fluid-filled, thin shell
[AD-A228867] N91-16709
DAYTON UNIV., OH.
Mechanical property data on aluminum alloy 7150-T7751 plate
[AD-A227506] N91-16124
DEFENSE ADVANCED RESEARCH PROJECTS AGENCY, ARLINGTON, VA.
Framework for an efficient two filter GLOC monitor
N91-16557
DELAWARE UNIV., NEWARK.
VLA neutral hydrogen imaging of compact groups
N91-16872
DEPARTMENT OF ENERGY, WASHINGTON, DC.
Heat engines program
[DE90-010276] N91-16374

Subsurface science program: Program overview and research abstracts
[DE90-010321] N91-16456
Report to Congress on the Small Business Program
[DE91-004622] N91-16831
Accomplishments in technology transfer from DOE and its laboratories
[DE90-002686] N91-16986

DEUTSCHE FORSCHUNGSANSTALT FUER LUFT- UND RAUMFAHRT, COLOGNE (GERMANY, F.R.).
The 1989 annual catalog of the German Aerospace Establishment: Research reports and communications
[ISSN-0172-357X] N91-16987

DEUTSCHE FORSCHUNGSANSTALT FUER LUFT- UND RAUMFAHRT, GOETTINGEN (GERMANY, F.R.).
Documents on the history of the Aerodynamic Research Establishment at Goettingen, 1907 - 1925
[DLR-MITT-90-05] N91-15977
Calculation of support interferences on the aerodynamic coefficients for a wind tunnel calibration model
[DLR-FB-90-26] N91-15998

DEUTSCHE FORSCHUNGSANSTALT FUER LUFT- UND RAUMFAHRT, OBERPFAFFENHOFEN (GERMANY, F.R.).
Scattering center analysis of simple metallic objects
[DLR-FB-90-32] N91-16216
Photometric analyses for the determination of physical and structural properties for the Martian surface in the Oxia Palus region
[DLR-FB-90-27] N91-16979

DEUTSCHE FORSCHUNGSANSTALT FUER LUFT- UND RAUMFAHRT, STUTTGART (GERMANY, F.R.).
Analytical and experimental investigation of transverse flow aerodynamic windows for high power lasers
[DLR-FB-90-33] N91-16367

DEUTSCHE FORSCHUNGSGEMEINSCHAFT, BONN (GERMANY, F.R.).
Space research in the Federal Republic of Germany, 1988 and 1989
[ETN-91-98514] N91-16849

DIALOGICS S.A., LABEGE INNOPOLE (FRANCE).
Intelligent assistant systems: An artificial intelligence approach to detecting performance degradation and pilot incapacitation N91-16564

DYNAMICS RESEARCH CORP., ANDOVER, MA.
The Assistant for Specifying the Quality Software (ASQS). Volume 1: Operational concept document
[AD-A227893] N91-16608
The Assistant for Specifying the Quality Software (ASQS). Volume 2: User's manual. Volume 2
[AD-A227894] N91-16609

E

EDGERTON, GERMESHAUSEN AND GRIER, INC., IDAHO FALLS, ID.
Acoustical and dynamic mechanical characterization of fiber-matrix interface bonds in ceramic composites
[DE90-010949] N91-16066
Laboratory testing of chloride 3ET205 6 volt traction battery
[DE90-010926] N91-16225
Assessment of battery technologies for electric vehicles. Volume 2, part 1: Appendices
[DE90-010907] N91-16227
Sensing of metal-transfer mode for process control of GMAW (Gas Metal Arc Welding)
[DE90-010946] N91-16377
Living PRAs (Probabilistic Risk Analysis) made easier with IRRAS (Integrated Reliability and Risk Analysis System)
[DE90-010938] N91-16395
The role of quality assurance in the monitoring of terrestrial ecosystems
[DE90-010986] N91-16461
Automatic, high-resolution analysis of low-noise fringes
[DE90-009779] N91-16574
A convenient system for diffraction moire measurements
[DE90-010980] N91-16739

EG AND G ENERGY MEASUREMENTS, INC., GOLETA, CA.
Gabor zone plate apertures for imaging with the mercuric iodide gamma ray camera
[DE90-011193] N91-16321

EG AND G ENERGY MEASUREMENTS, INC., PLEASANTON, CA.
Turbulence and diffusion in the atmospheric boundary layer
[DE90-011582] N91-16471

EG AND G MOUND APPLIED TECHNOLOGIES, MIAMISBURG, OH.
Comparison of hydrogen diffusion in Ti2PdH(x) to the behavior for Ti2CuH(x) and Zr2PdH(x)
[DE91-002711] N91-16808

EIC, INC., NORWOOD, MA.
Studies of the fundamentals of solids state batteries
[AD-A228772] N91-16247

ELECTRONICS RESEARCH LAB., ADELAIDE (AUSTRALIA).
Meteor burst communications study
[AD-A228641] N91-16204
Nonradiative dielectric waveguide millimetre-wave integrated circuits: A review
[AD-A227760] N91-16238
Analysis of emission data from a Perkin-Elmer 1710 FTIR spectrometer
[AD-A227759] N91-16331
XSHELL: A general purpose expert system shell
[AD-A228454] N91-16616

ELORET CORP., SUNNYVALE, CA.
Theoretical study of the C-H bond dissociation energy of acetylene
[NASA-CR-187858] N91-16065
Comparison of the quadratic configuration interaction and coupled cluster approaches to electron correlation including the effect of triple excitations
[NASA-CR-187855] N91-16727

EMA, MANSFIELD, TX.
Evaluation of rotorwash characteristics for tiltrotor and tiltwing aircraft in hovering flight
[SCT-90RR-18] N91-15989

ENVIRONMENTAL DYNAMICS RESEARCH, MIAMI, FL.
The effect of latent heat release on synoptic-to-planetary wave interactions and its implication for satellite observations: Theoretical modeling N91-16514

ERLANGEN-NUREMBERG UNIV. (GERMANY, F.R.).
Optimization of a laser diode anemometry system
[LSTM-239/T/88] N91-16364

ERNO RAUMFAHRTTECHNIK G.M.B.H. BREMEN (GERMANY, F.R.).
Common approach for planetary habitation systems implementation
[MBB-UO-0115-90-PUB] N91-16570

EUROPEAN SOUTHERN OBSERVATORY, GARCHING (GERMANY, F.R.).
Tidal distortions in pairs of early-type galaxies N91-16869
Dynamical friction in pairs of elliptical galaxies N91-16933

F

FACTORY MUTUAL RESEARCH CORP., NORWOOD, MA.
Flammability characteristics of fiber reinforced composite materials
[AD-A228215] N91-16072

FEDERAL AVIATION ADMINISTRATION, WASHINGTON, DC.
The use of contact lenses in the civil airman population
[AD-A227450] N91-16544

FEDERAL RAILROAD ADMINISTRATION, WASHINGTON, DC.
Moving America; new directions, new opportunities: Assessment of the potential for magnetic levitation transportation systems in the United States
[PB91-104596] N91-16388

FERMI NATIONAL ACCELERATOR LAB., BATAVIA, IL.
Self-propelled in-tube shuttle and control system for automated measurements of magnetic field alignment
[DE90-008210] N91-16316
Chern-Simons and anyonic superconductivity
[DE90-010663] N91-16787
The best-fit universe
[DE91-004583] N91-16966

FLORIDA STATE UNIV., TALLAHASSEE.
The development of laser speckle velocimetry for the study of vortical flows
[NASA-CR-187756] N91-16289
Potential vorticity index N91-16516
The vertical structure of the marine atmospheric boundary layer across a sea surface temperature front
[AD-A227931] N91-16525
Selective excitation, relaxation, and energy channeling in molecular systems
[DE90-010793] N91-16717

FLORIDA UNIV., GAINESVILLE.
A query model and query and knowledge definition languages for object-oriented databases N91-16580
Analysis of multivariable control systems in the presence of structured uncertainties
[AD-A227976] N91-16665
Triple and quadruple excitation contributions to the binding in Be clusters: Calibration calculations on Be3
[NASA-TM-103391] N91-16728
H I observations of the peculiar galaxy NGC 660 N91-16888

FORSCHUNGSZENTRUM JUELICH G.M.B.H. (GERMANY, F.R.).
The influence of small SO2 contents on the corrosion behavior for NiCrAl alloys in temperature zone from 1000 to 1100 C
[JUEL-2362] N91-16134

FWG ASSOCIATES, INC., TULLAHOMA, TN.
Analysis of wind profile measurements from an instrumented aircraft
[NASA-CR-184084] N91-16523

G

GENERAL ACCOUNTING OFFICE, WASHINGTON, DC.
Tactical fighter aircraft: Differences between the Air Force's roadmap and the five year defense plan
[AD-A228882] N91-15976

GENERAL ATOMIC CO., SAN DIEGO, CA.
Scaling dimensionally similar tokamak discharges to ignition
[DE90-010079] N91-16749
D3-D research operations
[DE90-008232] N91-16752
The CIT physics program
[DE90-012134] N91-16774

GENERAL ELECTRIC CO., PHILADELPHIA, PA.
Definition and preliminary design of the Laser Atmospheric Wind Sounder (LAWS) phase 1. Volume 1: Executive summary
[NASA-CR-184071] N91-16332
Definition and preliminary design of the Laser Atmospheric Wind Sounder (LAWS) phase 1. Volume 2
[NASA-CR-184072] N91-16333
Definition and preliminary design of the Laser Atmospheric Wind Sounder (LAWS) phase 1. Volume 3: Program cost estimates
[NASA-CR-184073] N91-16334

GENERAL MOTORS CORP., INDIANAPOLIS, IN.
Advanced Turbine Technology Applications Project (ATTAP)
[NASA-CR-187039] N91-16021

GEOLOGICAL SURVEY, MENLO PARK, CA.
Principal facts for about 16,000 gravity stations in the Nevada test site and vicinity
[DE90-011521] N91-16470

GEORGIA INST. OF TECH., ATLANTA.
Fundamental studies with a monodisperse aerosol-based liquid chromatography/mass spectrometry interface (MAGIC-LC/MS)
[DE90-010667] N91-16083

GEORGIA UNIV., ATHENS.
Dynamics of strong-coupling models for cuprate superconductors: Exact results on finite lattices
[DE90-011155] N91-16796

GINER, INC., WALTHAM, MA.
Improved anode catalysts for coal gas-fueled phosphoric acid fuel cells
[DE90-009683] N91-16442

GOETTINGEN UNIV. (GERMANY, F.R.).
The interacting pair Mkn 305/306 N91-16864
Spectrometric, chemical, and cosmological development of galaxies
[ETN-91-98555] N91-16972

H

HAMBURG UNIV. (GERMANY, F.R.).
Galactic structure in direction of Vela-Puppis by means of UBV beta observations
[ETN-91-98556] N91-16973

HARVARD UNIV., CAMBRIDGE, MA.
Streamwise vortices in laminar-turbulent transition N91-16297
Continuum models of continental deformation N91-16490
Dynamical properties of two-dimensional Josephson junction arrays N91-16823

HELSINKI UNIV. (FINLAND).
Simulation of disk-disk encounters with co-moving polar grids N91-16941

HIROSHIMA UNIV., TAKEHARA (JAPAN).
Some aspects of quantum groups and supergroups
[DE90-777884] N91-16671

HUGHES RESEARCH LABS., MALIBU, CA.
Applications research studies on microtubules
[AD-A228756] N91-16205

HUMAN SYSTEMS DIV., BROOKS AFB, TX.
A comparison of three prospective analytical methods for benzene analysis in jet fuel environments
[AD-A227489] N91-16170

I

IBARAKI UNIV., HITACHI (JAPAN).
Heat transfer characteristics of a radical heat pipe N91-16276
IBM FEDERAL SYSTEMS DIV., GAITHERSBURG, MD.
Practical aspects of repository operations for the Software Technology for Adaptable, Reliable Systems (STARS) program
[AD-A228455] N91-16617
DTD creation for the Software Technology for Adaptable, Reliable Systems (STARS) program
[AD-A228475] N91-16619
IDAHO NATIONAL ENGINEERING LAB., IDAHO FALLS.
PCB/transformer techno-economic analysis model: User manual, volume 2
[DE90-010654] N91-16223
A convenient system for the manufacture of holographic diffraction gratings
[DE90-009481] N91-16319
ILLINOIS INST. OF TECH., CHICAGO.
Adaptive mesh refinement for meshes with singular elements N91-16406
ILLINOIS UNIV., URBANA.
Two-dimensional simulation of quantum-well lasers including energy transport
[AD-A227487] N91-16356
Integrated semiconductor modulators
[AD-A228615] N91-16820
Star formation in infrared bright and infrared faint starburst interacting galaxies N91-16901
Dynamical experiments on models of colliding disk galaxies N91-16959
ILLINOIS UNIV., URBANA-CHAMPAIGN.
Aerospace vehicle design, spacecraft section. Volume 1: Project groups 1-4
[NASA-CR-186841] N91-16045
PFERD Mission: Pluto flyby exploration/research design N91-16046
Intrepid: A mission to Pluto N91-16047
Project Cerberus: Flyby mission to Pluto N91-16048
OPTIC: Orbiting Plutonian Topographic Image Craft proposal for an unmanned mission to Pluto N91-16049
Aerospace vehicle design, spacecraft section. Volume 2: Project groups 5-7
[NASA-CR-186842] N91-16050
Mission management, planning, and cost: PULSE Attitude And Control Systems (AACS) N91-16051
The Copernicus project N91-16052
The Phoenix Pluto Probe N91-16053
ICHARM: Hierarchical CMOS circuit extraction with power bus extraction
[AD-A228613] N91-16245
Dynamic response of composite beams using shear-deformable finite elements
[AD-A227975] N91-16408
An O(log n) time common CRCW pram algorithm for minimum spanning tree
[AD-A228740] N91-16623
IMPLANT SCIENCES CORP., DANVERS, MA.
Wear measurement of ceramic bearings in gas turbines
[AD-A227505] N91-16382
INDIAN INST. OF ASTROPHYSICS, BANGALORE.
On a connection between supernova occurrence and tidal interaction in early type galaxies N91-16903
Energy and angular momentum transfer in binary galaxies N91-16940
Collisional removal of HI from the inner disks of Virgo cluster galaxies N91-16952
INFO/TEK, WASHINGTON, DC.
The USAF STINFO program overview
[AD-A226969] N91-16838
INSTITUT FUER ANGEWANDTE GEODAESIE, FRANKFURT AM MAIN (GERMANY, F.R.).
Reports on cartography and topography. Series 1, report 104
[ISSN-0469-4236] N91-16432
The photogrammetric evaluation by video technique: A supporting study N91-16433
The multisensor image map 1:50,000 Rheinhessen N91-16434
INSTITUTE FOR COMPUTER APPLICATIONS IN SCIENCE AND ENGINEERING, HAMPTON, VA.
On a class of unsteady three-dimensional Navier Stokes solutions relevant to rotating disc flows: Threshold amplitudes and finite time singularities
[NASA-CR-187482] N91-15991
On the Goertler instability in hypersonic flows: Sutherland law fluids and real gas effects
[NASA-CR-187481] N91-15994
Modelling the transitional boundary layer
[NASA-CR-187487] N91-15995
On the receptivity and non-parallel stability of travelling disturbances in rotating disk flow
[NASA-CR-187486] N91-15996
Asymptotic-induced numerical methods for conservation laws
[NASA-CR-187483] N91-16305
Modeling the dissipation rate in rotating turbulent flows
[NASA-CR-187485] N91-16306
Resolution of the 1D regularized Burgers equation using a spatial wavelet approximation
[NASA-CR-187480] N91-16664
INSTITUTE FOR PERCEPTION RVO-TNO, SOESTERBERG (NETHERLANDS).
ERICC: Construction and application of the Command and Control Research Facility
[IZF-1989-55] N91-16213
Organization of the mission pattern in the air picture
[IZF-1990-A-12] N91-16568
Heat transfer in clothing during heat radiation
[IZF-1990-B-2] N91-16569
A normative database for, and analysis of, the dual task of the TASKOMAT
[IZF-1990-A-11] N91-16846
INSTITUTE OF ASTRONOMY, CAMBRIDGE (ENGLAND).
Galaxy interactions and star formation: Results of a survey of global H-alpha emission in spiral galaxies in 8 clusters N91-16905
Do elliptical galaxies have thick disks N91-16962
INSTITUTE OF AVIATION MEDICINE, FARNBOROUGH (ENGLAND).
Cerebral oxygen status and G-induced loss of consciousness N91-16554
INSTITUTE OF ELECTRICAL AND ELECTRONICS ENGINEERS, NEW YORK, NY.
IEEE International Symposium on Information Theory
[AD-A228239] N91-16842
INTERNATIONAL CENTRE FOR THEORETICAL PHYSICS, TRIESTE (ITALY).
Quantifying the FIR interaction enhancement in paired galaxies N91-16900
INTERSCIENCE, INC., TROY, NY.
Status of target physics for inertial confinement fusion
[DE90-008221] N91-16751
IOWA STATE UNIV. OF SCIENCE AND TECHNOLOGY, AMES.
Computation of turbulent flow about unconventional airfoil shapes N91-15992
Modeling and control of a two-arm elastic robot in gravity N91-16389
Camera space manipulation of a mobile robot N91-16390
Multi-waveband observations of colliding galaxies N91-16868
Caustic waves in galaxy disks produced in collisions with low mass companions N91-16960
ISHIKAWAJIMA-HARIMA HEAVY INDUSTRIES CO. LTD., YOKOHAMA (JAPAN).
Numerical simulation of buffer flow in a free flow electrophoresis chamber N91-16279
ISTITUTO DI RADIOASTRONOMIA, BOLOGNA (ITALY).
Dumb-bell galaxies in southern clusters: Catalog and preliminary statistical results N91-16896

J

JET PROPULSION LAB., CALIFORNIA INST. OF TECH., PASADENA.
Spray combustion modeling and evaluation
[NASA-CR-187887] N91-16078
Bio-optical profile data report coastal transition zone program, R/V Thomas Washington, June 24 - July 21, 1988
[NASA-CR-187808] N91-16532
Bio-optical profile data report coastal transition zone program, R/V Point Sur, June 15-28, 1987
[NASA-CR-187807] N91-16533
Bio-optical profile data report: Joint Global Ocean Flux Study, Hawaii Ocean Time-Series, HOT-3, R/V Moana Wave, 6-10 January 1989
[NASA-CR-187805] N91-16534
Contents of the NASA ocean data system archive, version 11-90
[NASA-CR-187812] N91-16535
JOHANN-WOLFGANG-GOETHE-UNIV., FRANKFURT AM MAIN (GERMANY, F.R.).
Computer aided physiological assessment of the functional state of pilots during simulated flight N91-16562
JOHNS HOPKINS UNIV., BALTIMORE, MD.
Initial studies of electric field effects on ceramic powder formation in flames
[DE90-007571] N91-16138
Pre-attentive and attentive visual information processing
[AD-A228541] N91-16550
Full field visualization of surface and bulk acoustic waves
[AD-A227676] N91-16678
Galaxy interactions and the stimulation of nuclear activity N91-16910
The nature of the emission-line nebulae in powerful far-infrared galaxies N91-16916
Paired and interacting galaxies: Conference summary N91-16964
JOHNS HOPKINS UNIV., LAUREL, MD.
Activities and accomplishments of the Center for Applied Solar Physics, 1987 - 1990
[AD-A228773] N91-16980
JOINT ASTRONOMY CENTRE, HILO, HI.
Infrared images of merging galaxies N91-16904
JOINT PUBLICATIONS RESEARCH SERVICE, ARLINGTON, VA.
JPRS report: Science and technology. USSR: Space
[JPRS-USP-89-006] N91-16036
Buran and the future of the Soviet space program N91-16037
Developmental tests for shuttle Orbiter N91-16038
General designer describes Buran flight control, autopilot systems N91-16039
Specialists at flight control center discuss shuttle computer systems N91-16040

K

KANSAS STATE UNIV., MANHATTAN.
An inter-comparison of surface energy flux measurement systems used during FIFE, 1987
[NASA-CR-187699] N91-16472
A study of the surface energy balance on slopes in a tallgrass prairie
[NASA-CR-187698] N91-16473
KARLSRUHE UNIV. (GERMANY, F.R.).
Experimental and theoretical examinations of film cooling of gas turbine blades
[ETN-91-98554] N91-16022
High-loaded combustion chambers stationary constant pressure combustion. Part 2: Research reports
[ETN-91-98511] N91-16112
Safety as a design goal for applications of microelectronic control systems
[REPT-23/90] N91-16253
KENTUCKY UNIV., LEXINGTON.
Research in theoretical nuclear physics
[DE90-010792] N91-16828
KESTREL INST., PALO ALTO, CA.
Automated design of displays for technical data
[AD-A226729] N91-16586
KHARKOV STATE UNIV. (USSR).
Signs of interaction of the NGC 1275 nucleus with the high-velocity system according to 0.7 sec seeing observations N91-16918
KITT PEAK NATIONAL OBSERVATORY, TUCSON, AZ.
A study of the compact group of galaxies Shahbazian 4 N91-16877
KYOTO SANGYO UNIV. (JAPAN).
Dragging force on galaxies due to streaming dark matter N91-16947
On the large-scale structures formed by wakes of open cosmic strings N91-16951
KYUSHU UNIV., FUKUOKA (JAPAN).
Numerical simulations of unsteady shock reflection processes by a ramp N91-16267
Numerical simulation of separated flows around a wing section at steady and unsteady motion by a discrete vortex method N91-16268
Unsteady vortex lattice calculation of the flow around a slender delta wing N91-16272

L

LABORATOIRE D'AUTOMATIQUE ET D'ANALYSE DES SYSTEMES, TOULOUSE (FRANCE).
Modeling and verification of distributed systems with labeled predicate transition nets
[LAAS-90215] N91-16214
Design and fabrication of high voltage planar devices
[LAAS-90306] N91-16252
Vectorial and parallel algorithms in dynamic programming for optimal control problems
[LAAS-90256] N91-16629

Implementation and simulation of the manufacturing systems control coordination level: A mixed approach of Petri nets and rule-based systems
[LAAS-90355] N91-16645
About Petri nets with fuzzy markings
[LAAS-90354] N91-16670

LABORATOIRE DE MEDECINE AEROSPATIALE, BRETIGNY-SUR-ORGE (FRANCE).
Detection of loss of consciousness in flight by Doppler method
N91-16555

LABTEK CORP., WOODBRIDGE, CT.
Scheduler issues for real-time Ada
[AD-A227766] N91-16592
Tailoring an Ada runtime environment proof-of-concept
[AD-A227767] N91-16593
Distributed issues for Ada real-time systems
[AD-A227852] N91-16603

LAMONT-DOHERTY GEOLOGICAL OBSERVATORY, PALISADES, NY.
Multi-dimensional aspects of recent climate change in North America
[DE90-010958] N91-16460

LANDESSTERNWARTE AUF DEM KOENIGSTUHL, HEIDELBERG (GERMANY, F.R.).
Stellar kinematics of elliptical galaxies in pairs
N91-16862

LAWRENCE LIVERMORE NATIONAL LAB., CA.
A numerical study of silane combustion
[DE90-006002] N91-16080
Auto-ignition temperatures of binary mixtures of alkanes in a closed vessel: Comparisons between experimental measurements and numerical predictions
[DE90-007856] N91-16082
The new LLNL AMS spectrometer
[DE90-010868] N91-16084
Microwave measurements of water vapor partial pressure at temperatures up to 350 C
[DE90-011484] N91-16087
The design and construction of an Automated Multi-Object Spectroscopy system (AMOS)
[DE90-011497] N91-16088
The search for high energy low vulnerability explosives
[DE90-009436] N91-16158
Paste extrudable explosives: Their history and their current status
[DE90-009438] N91-16159
Development of a high-tensile-strain plastic-bonded TATB explosive
[DE90-011463] N91-16162
Comparison of propagation and absorption of FEL-generated microwaves with theory
[DE90-010369] N91-16181
Modeling pulse driven antenna systems with finite differences
[DE90-010682] N91-16182
Multiframe x ray images from a single meander stripline coated on a microchannel plate
[DE90-010741] N91-16224
Stability and accuracy of the sweep rate measurements for LLNL optical streak cameras
[DE90-012080] N91-16324
Short pulse driven recombination x ray lasers
[DE90-009945] N91-16340
Cluster formation in laser-induced ablation and evaporation of solids observed by laser ionization time-of-flight mass spectrometry and scanning tunneling microscopy
[DE90-010876] N91-16344
Generation of XUV light by resonant frequency tripling in a two-wiggler FEL amplifier
[DE90-012120] N91-16349
Electrical power from inertial confinement fusion: Issues and prospects
[DE90-010200] N91-16437
Study of the global distributions of atmospheric radionuclides
[DE90-010749] N91-16455
Numerical simulation of aerosol scavenging by ice-bearing convective clouds
[DE90-010676] N91-16457
Parameterization of aerosol scavenging in a convective cloud model
[DE90-010865] N91-16458
Climate Caucus report: Opportunities for bridging the gaps from effects to impacts
[DE90-010877] N91-16459
Ozone and acid-precipitation on western coniferous forests
[DE90-011014] N91-16462
Seismic imaging for velocity and attenuation structure in geothermal fields
[DE90-010742] N91-16469
GCM (General Circulation Model) predictions for surface air temperature and precipitation over the southeastern United States
[DE90-009434] N91-16497
The value of on-site sodar data in regional modeling
[DE90-009921] N91-16498
Application of AMS to the biomedical sciences
[DE90-010869] N91-16538
POSC: A Partitioning and Optimizing SISAL Compiler
[DE90-010679] N91-16577
Massively parallel Fokker-Planck calculations
[DE90-010691] N91-16633
Computational physics at the National Energy Research Supercomputer Center
[DE90-010283] N91-16672
A new approach for the determination of electronic structure
[DE90-010479] N91-16713
Is there hope for fusion
[DE90-012095] N91-16736
Microwave Tokamak Experiment (OMTX): Overview and status
[DE90-010287] N91-16758
Electrical power from inertial confinement fusion: Issues and prospects
[DE90-010332] N91-16759
Characterization of disruptions in the Microwave Tokamak Experiment (MTX)
[DE90-010352] N91-16761
Theoretical studies of tokamaks
[DE90-011332] N91-16768
Scaling laws for femtosecond laser-plasma interactions
[DE90-011496] N91-16769
Stark-effect measurement of high FEL electric fields in MTX by laser-aided particle-probe spectroscopy
[DE90-011911] N91-16771
Motional Stark effect polarimetry for the current profile diagnostic in D3-D
[DE90-012071] N91-16773
The CIT physics program
[DE90-012134] N91-16774
A model for the prediction of Nb3Sn critical current as a function of field, temperature, strain, and radiation damage
[DE91-000656] N91-16775
Applications of strained layer superlattices
[DE90-011204] N91-16793
New surface atomic structures for III-V(110)-p(1 x 1)-Sb(1ML): Chemical bonding and electronic structure
[DE90-011230] N91-16794
Properties of superdeformed bands in the A = 194 region
[DE90-011482] N91-16798
A new perturbation theory of solids and fluids and its applications to high-pressure melting problems
[DE90-011502] N91-16829
Low-cost, high-resolution telescopes for imaging low-earth orbit satellites
[DE90-012081] N91-16850
Resonant Compton scattering in models of gamma-ray burst sources. Part 2: Numerical modeling
[DE91-005268] N91-16982
Energy and Technology Review, March 1990
[DE90-008230] N91-16985

LEHIGH UNIV., BETHLEHEM, PA.
Pressure gradient effects on the development of hairpin vortices in an initially laminar boundary layer
N91-16282

LEICESTER UNIV. (ENGLAND).
Ionospheric corrections for SHF satellite radar altimetry N91-16423
Epitaxial growth and surface morphology of some metal and semiconductor structures N91-16824
X ray emission from low-mass binary systems
N91-16853

LEIDEN UNIV. (NETHERLANDS).
Alignment of cD-galaxies with their surroundings
N91-16895
What determines the bulge to disk ratio of galaxies
N91-16942

LENINGRAD STATE UNIV. (USSR).
The polar-ring galaxies NGC 2685 and NGC 3808B (VV 300) N91-16892
Triplets of galaxies: Their dynamics, evolution, and the origin of chaos in them N91-16948

LENINGRAD UNIV. OBSERVATORY (USSR).
Typical motions in multiple systems N91-16945
Dynamics and configurations of galaxy triplets
N91-16946
A classification of the galaxy groups N91-16949
Viral coefficient and hidden mass in the galaxy groups
N91-16950
Gas flows in S-E binary systems of galaxies
N91-16956

LOGISTICS MANAGEMENT INST., BETHESDA, MD.
Management information: A key to better acquisition at NIH
[AD-A226867] N91-16830

LOS ALAMOS NATIONAL LAB., NM.
A low-cost infrared telemetry system for kilohertz-bandwidth data acquisition
[DE90-010616] N91-16042
Destruction of propellant components in supercritical water
[DE90-010600] N91-16085
Impurity tolerant electrocatalysts
[DE90-011960] N91-16090
Time-resolved Coherent Anti-Stokes Raman Spectroscopy (CARS) and the measurement of vibrational spectra in shock-compressed molecular materials
[DE90-012053] N91-16091
Magnetic structures of actinide materials by pulsed neutron diffraction
[DE91-000373] N91-16093
Influence of strain rate on the structure/property of Ti-48Al-1V
[DE91-000172] N91-16122
Safe venting of hydrogen
[DE90-008964] N91-16174
Transient natural convection in heated inclined tubes
[DE90-008217] N91-16255
State of an adiabatic expanding and condensing vapor or slow, medium, and fast explosions into a vacuum
[DE90-010815] N91-16263
AFDM: An Advanced Fluid-Dynamics Model. Volume 2: Topologies, flow regimes and interfacial areas
[DE91-000581] N91-16283
Rotating Rayleigh-Benard convection: The Kueppers-Lortz transition
[DE91-004835] N91-16288
Comparison of some x ray sensors for verification
[DE90-011990] N91-16323
Development of free-electron lasers for XUV projection lithography
[DE90-010566] N91-16342
Droplet shattering, vaporization, and recondensation in cloud clearing with long pulse infrared chemical lasers
[DE90-010584] N91-16343
Integrated Numerical Experiments (INEX) and the Free-Electron Laser Physical Process Code (FELPPC)
[DE90-011957] N91-16348
Angular dependence of thin-film dielectric coating damage thresholds
[DE91-000237] N91-16351
Design requirements and calculated performance of an XUV FEL oscillator operating on a higher harmonic
[DE91-004833] N91-16357
Direct methanol/air fuel cells: Systems considerations
[DE90-011971] N91-16439
Numerical simulations of the mountain iron tracer data
[DE90-009749] N91-16499
A graphical user-interface-driven waveform data acquisition and analysis system
[DE90-011948] N91-16578
Artificial intelligence technologies applied to terrain analysis
[DE90-011985] N91-16642
Infrasonic observations of large-scale HE events
N91-16694
The correction of infrasound signals for upper atmospheric winds N91-16695
Electron stopping powers of some elements and compounds from 0 to 10,000 eV: A compilation
[DE90-010675] N91-16716
A Mirnov loop array for field-reversed configurations
[DE90-010607] N91-16750
US-Japan Workshop on Field-Reversed Configurations with Steady-State High-Temperature Fusion Plasmas and the 11th US-Japan Workshop on Compact Toroids
[DE90-010253] N91-16755
Spatial distributions of the emitting species in a penning surface-plasma source
[DE90-011996] N91-16772
The Los Alamos megamp fiber z-pinch experiment
[DE91-004842] N91-16777
Neutron measurements in search of cold fusion
[DE91-004855] N91-16778
Molecular crystals and localized vibrational states
[DE90-010602] N91-16786
M51's spiral structure N91-16938
Origin of regularities in the redshift distributions of distant galaxies and quasars
[DE91-004848] N91-16968

LOUGHBOROUGH UNIV. OF TECHNOLOGY (ENGLAND).
Jet engine performance estimation from minimal input data
[ETN-91-98582] N91-16023
An introduction to modern aero-engine control design
[ETN-91-98583] N91-16024

Longitudinal stability augmentation of a lightweight fighter aircraft model
[ETN-91-98585] N91-16026
A paper-assessment of the performance of a modern airborne multi-mode pulse Doppler radar deployed as a ground-based fire-control radar
[ETN-91-98584] N91-16215
Electronically steerable arrays: Current and future technology and applications
[ETN-91-98581] N91-16254

LOUISIANA STATE UNIV., BATON ROUGE.
Using tilted-ring models and numerical hydrodynamics to study the structure, kinematics and dynamics of HI disks in galaxies N91-16851

LOWELL UNIV., MA.
Thin film single crystal growth of a nonlinear optical polymer
[AD-A227692] N91-16807

LUDWIG-MAXIMILIANS-UNIV., MUNICH (GERMANY, F.R.).
Formation and development of elliptical and dwarf galaxies
[ETN-91-98492] N91-16967

M

MAN-MADE SYSTEMS CORP., ELLICOTT CITY, MD.
Development of a test-bed for real-time monitoring of pilot mental status N91-16563

MARTIN MARIETTA SPACE SYSTEMS, INC., DENVER, CO.
Large space manipulators study
[AD-A227276] N91-16381

MARYLAND UNIV., COLLEGE PARK.
A coupled rotor aeroelastic analysis utilizing advanced aerodynamic modeling N91-16006
Inelastic strain analysis of solder joint in NASA fatigue specimen
[NASA-CR-187864] N91-16132
Mode competition effects in free electron lasers and gyrotrons
[DE90-011084] N91-16346
A case study of the 19 October 1989 polar cap absorption event using the imaging riometer for ionospheric studies
[AD-A227764] N91-16487
Advanced methods for the computation of particle beam transport and the computation of electromagnetic fields and beam-cavity interactions
[DE90-011071] N91-16734
Microwave generation for magnetic fusion energy applications, task B
[DE90-011079] N91-16763
Microwave generation for magnetic fusion energy applications, task C
[DE90-011080] N91-16764

MASSACHUSETTS INST. OF TECH., CAMBRIDGE.
Modelling of flamelet surface-to-volume ratio in turbulent premixed combustion
[DE90-006312] N91-16081
Gas solubility in glassy polymers: A correlation with excess enthalpy
[AD-A228202] N91-16155
Noise reduction using low weight and constant weight coding techniques
[AD-A228346] N91-16244
The PHD: A Planar, Harmonic Drive robot for joint torque control
[NASA-CR-187924] N91-16386
Void nucleation in nonlinear solid mechanics
[AD-A228890] N91-16410
Distributed algorithm simulation using input/output automata
[AD-A228113] N91-16611
Supporting reuse and evolution in software design
[AD-A228782] N91-16624
Pi: A parallel architecture interface for multi-model execution
[AD-A228345] N91-16640
The CIT physics program
[DE90-012134] N91-16774
Chemical beam epitaxy of ZnSe
[AD-A228045] N91-16817

MASSACHUSETTS INST. OF TECH., LEXINGTON.
The 1/f frequency noise effects on self-heterodyne linewidth measurements for coherent communications
[AD-A227942] N91-16195
Results of the Kansas City 1989 Terminal Doppler Weather Radar (TDWR) operational evaluation testing
[AD-A228784] N91-16206
Materials systems for 2- to 5-micrometers wavelength diode lasers
[AD-A228218] N91-16361
Effect of wind and temperature gradients on received acoustic energy N91-16697
Solid state research
[NASA-CR-187871] N91-16816

MASSACHUSETTS UNIV., AMHERST.
Selection effects and binary galaxy velocity differences N91-16927

MAX-PLANCK-INST. FUER ASTRONOMIE, HEIDELBERG (GERMANY, F.R.).
Starbursts in interacting galaxies: Observations and models N91-16958

MAX-PLANCK-INST. FUER PHYSIK UND ASTROPHYSIK, GARCHING (GERMANY, F.R.).
The role of the equatorial electrojet in the evening ionosphere
[MPE-PREPRINT-184] N91-16494
Theory for modeling the equatorial evening ionosphere and the origin of the shear in the horizontal plasma flow
[MPE-PREPRINT-185] N91-16495
Computer simulations of medium wavelength irregularities in the equatorial ionosphere resulting from artificially produced density enhancements
[MPE-PREPRINT-186] N91-16496
Measurement of the e+ e- annihilation in mu+ mu- pairs at the Z sup o resonance
[MPI-PAE/EXP.EL-231] N91-16732
Numerical examinations of Kelvin-Helmholtz instability in resistive compressible magnetohydrodynamics
[MPE-221] N91-16782
The x ray emission of SS433
[MPE-PREPRINT-189] N91-16856
Ion distributions and flows near the neutral sheet
[MPE-PREPRINT-179] N91-16974
Structure and energy balance of molecular clouds
[MPE-PREPRINT-181] N91-16975
Molecular absorption lines towards the nucleus of Centaurus A
[MPE-PREPRINT-182] N91-16976
The 158 micrometer (CII) line: A measure of global star formation activity in galaxies
[NASA-CR-187925] N91-16977
The galactic center at submillimeter and far-infrared wavelengths
[MPE-PREPRINT-190] N91-16978
Interpretation of the diffusive galactic continuum gamma radiation in MeV area
[MPE-220] N91-16983

MAX-PLANCK-INST. FUER RADIOASTRONOMIE, BONN (GERMANY, F.R.).
Natural waves of microstrip transmission lines in wave guides
[BER-68] N91-16251

MCAT INST., SAN JOSE, CA.
Rotorcraft application of advanced computational aerodynamics
[NASA-CR-187767] N91-15987

MCDONNELL AIRCRAFT CO., SAINT LOUIS, MO.
Geometric modeling applications interface program
[AD-A227651] N91-16591

MESSERSCHMITT-BOELKOW-BLOHM G.M.B.H., BREMEN (GERMANY, F.R.).
Evaporation process and 3 phase flow in a water evaporator assembly
[MBB-UO-0108-90-PUB] N91-16060
Common approach for planetary habitation systems implementation
[MBB-UO-0115-90-PUB] N91-16570

MESSERSCHMITT-BOELKOW-BLOHM G.M.B.H., MUNICH (GERMANY, F.R.).
Numerical analysis of viscous hypersonic flow past a generic forebody
[MBB/FE122/S/PUB/0407] N91-15997
Aerothermodynamic phenomena and the design of atmospheric hypersonic airplanes
[MBB/FE122/S/PUB/0408] N91-16015
Hypersonic model configurations
[MBB/FE122/S/PUB/411] N91-16016
The integration of structural optimization in the general design process for aircraft
[MBB/FE122/S/PUB/0405] N91-16017
Bump examinations of integrally strengthened carbon fiber reinforced plastic panels
[MBB/FE281/CFK/PUB/0013] N91-16076
THERMOPT: An optimizer for ESATAN models
[MBB/FW522/S/PUB/427] N91-16630
Optical transceiver frontend for high speed bus STANAG 3910 with one fiber only
[MBB-UA-1182-90-PUB] N91-16745

MESSERSCHMITT-BOELKOW-BLOHM G.M.B.H., OTTOBRUNN (GERMANY, F.R.).
Technological management as an element of strategy for an efficient company management
[MBB-Z-0307-90-PUB] N91-16834

MESSERSCHMITT-BOELKOW-BLOHM G.M.B.H., SCHROBENHAUSEN (GERMANY, F.R.).
Diagnostic of the reaction behaviour of intensive high explosives under jet attack
[MBB-UA-1188-90-PUB] N91-16173
Fragment mass distribution of debris
[MBB-UA-1187-90-PUB] N91-16669

MICHIGAN STATE UNIV., EAST LANSING.
Galaxy interactions and strength of nuclear activity N91-16914

MICHIGAN TECHNOLOGICAL UNIV., HOUGHTON.
Scattering measurements on natural and model trees N91-16691

MICHIGAN UNIV., ANN ARBOR.
High frequency scattering by a smooth coated cylinder simulated with generalized impedance boundary conditions
[NASA-CR-187829] N91-16211
Ion beam modification of surface for improved high temperature performance
[AD-A228067] N91-16243
Excursions to the base of the mantle N91-16491
Theory of non-equilibrium growth
[DE91-004159] N91-16725

MIDWEST RESEARCH INST., GOLDEN, CO.
Electrochromic sun control coverings for windows
[DE90-000335] N91-16139
High-efficiency large-area CdTe panels
[DE91-002117] N91-16443
Low-cost CdZnTe devices for cascade cell application
[DE91-002116] N91-16444
Smoothing and scaling airfoil coordinates on a personal computer
[DE89-000878] N91-16582

MINNESOTA UNIV., MINNEAPOLIS.
The impact of separated flow on heat and mass transfer
[DE91-000592] N91-16284
Incompressible flow simulations using the velocity-pressure formulation N91-16299
Finite element solution techniques for the vorticity-stream function formulation of two-dimensional incompressible flows N91-16302

MISSION RESEARCH CORP., NASHUA, NH.
IR plasma emissions
[AD-A227713] N91-16776

MISSISSIPPI UNIV., UNIVERSITY.
Exponential ground impedance models and their interpretation N91-16686

MISSOURI UNIV., COLUMBIA.
Photoreflectance studies of electronic transitions in quantum well structures under high pressure
[DE90-011583] N91-16801

MISSOURI UNIV., ROLLA.
Finite element solution of steady state axisymmetric penetration problems N91-16403

MITRE CORP., BEDFORD, MA.
A successive partial-relaxation Gaussian algorithm for area navigation operations with the Microwave Landing System (MLS)
[AD-A228871] N91-16004

MITRE CORP., MCLEAN, VA.
Some comments on the acoustic coupling of elements in an array
[AD-A227762] N91-16239

MONTREAL UNIV. (QUEBEC).
H I studies of the sculptor group galaxies N91-16876

MOUND LAB., MIAMISBURG, OH.
PC-based digital imaging for storing microscopy images for surveillance programs
[DE90-010080] N91-16738

N

NATIONAAL INST. VOOR KERNFYSICA EN HOGE ENERGIEFYSICA, AMSTERDAM (NETHERLANDS).
Digital time interpolator
[DIGEL-1990-4] N91-16249
Time interpolator
[DIGEL-1990-3] N91-16337
Programmable pseudorandom detector pulse pattern generator
[ETN-91-98321] N91-16628

NATIONAL ACADEMY OF SCIENCES - NATIONAL RESEARCH COUNCIL, WASHINGTON, DC.
Application Principles for Multicolored Displays: A workshop report
[AD-A227961] N91-16567

NATIONAL AERONAUTICS AND SPACE ADMINISTRATION, WASHINGTON, DC.
Aeronautical engineering: A continuing bibliography with indexes (supplement 260)
[NASA-SP-7037(260)] N91-15978
Aeronautical engineering: A continuing bibliography with indexes (supplement 259)
[NASA-SP-7037(259)] N91-15979
The atmospheric effects of stratospheric aircraft: A topical review
[NASA-RP-1250] N91-16466

Aerospace medicine and biology: A cumulative index to a continuing bibliography (supplement 345)
[NASA-SP-7011(345)] N91-16547
Software for aerospace education: A bibliography, 2nd edition
[NASA-PED-106-ED-2] N91-16601
NASA thesaurus aeronautics vocabulary
[NASA-TM-104230] N91-16847

NATIONAL AERONAUTICS AND SPACE ADMINISTRATION. AMES RESEARCH CENTER, MOFFETT FIELD, CA.

Potential use of tiltrotor aircraft in Canadian aviation
[NASA-TM-102245] N91-16001
A finite element procedure for calculating fluid-structure interaction using MSC/NASTRAN
[NASA-TM-102857] N91-16414
Triple and quadruple excitation contributions to the binding in Be clusters: Calibration calculations on Be3
[NASA-TM-103391] N91-16728
A multiwavelength survey of interacting galaxies N91-16898
An experimental study of counter-rotating cores in elliptical galaxies N91-16934

NATIONAL AERONAUTICS AND SPACE ADMINISTRATION. GODDARD SPACE FLIGHT CENTER, GREENBELT, MD.

The atmospheric effects of stratospheric aircraft: A current consensus
[NASA-RP-1251] N91-16467
Effects of switch leakages upon Nimbus-7 SMMR calibration
[NASA-TM-100705] N91-16536
Annotated bibliography of software engineering laboratory literature
[NASA-TM-103415] N91-16602
Multi-color imaging of selected southern interacting galaxies N91-16867
Tidal events and galactic activity N91-16911

NATIONAL AERONAUTICS AND SPACE ADMINISTRATION. JOHN F. KENNEDY SPACE CENTER, COCOA BEACH, FL.

Debris/Ice/TPS assessment and photographic analysis for shuttle mission STS-41
[NASA-TM-103814] N91-16041
An assessment of the government liquid hydrogen requirements for the 1995-2005 time frame including addendum, liquid hydrogen production and commercial demand in the United States
[NASA-TM-103812] N91-16166
An assessment of the government liquid hydrogen requirements for the 1995-2005 time frame N91-16167

NATIONAL AERONAUTICS AND SPACE ADMINISTRATION. LYNDON B. JOHNSON SPACE CENTER, HOUSTON, TX.

Whole body cleansing agent
[NASA-CASE-MSC-21589-1] N91-16566

NATIONAL AERONAUTICS AND SPACE ADMINISTRATION. LANGLEY RESEARCH CENTER, HAMPTON, VA.

The NASA controls-structures interaction technology program
[NASA-TM-102752] N91-16057
Determination of shuttle orbiter center of gravity from flight measurements
[NASA-TM-102627] N91-16058
Finite element thermo-viscoplastic analysis of aerospace structures
[NASA-TM-102761] N91-16407
Wind turbine acoustics
[NASA-TP-3057] N91-16679
Fourth International Symposium on Long-Range Sound Propagation
[NASA-CP-3101] N91-16682
Long-range vertical propagation N91-16693
Lamina transducer coupler and method of making
[NASA-CASE-LAR-14361-1] N91-16707
Space Station Freedom resource allocation accommodation of technology payload requirements
[NASA-TM-102766] N91-16832
Cellular track model of biological damage to mammalian cell cultures from galactic cosmic rays
[NASA-TP-3055] N91-16981

NATIONAL AERONAUTICS AND SPACE ADMINISTRATION. LEWIS RESEARCH CENTER, CLEVELAND, OH.

Effects of high pressure nitrogen on the thermal stability of SiC fibers
[NASA-TM-103245] N91-16075
Tensile behavior of tungsten/niobium composites at 1300 to 1600 K
[NASA-TM-103727] N91-16128
Method of making contamination-free ceramic bodies
[NASA-CASE-LEW-14984-1] N91-16152
Extension of transonic flow computational concepts in the analysis of cavitated bearings
[NASA-TM-103214] N91-16304
Wind turbine acoustics
[NASA-TP-3057] N91-16679

NATIONAL AERONAUTICS AND SPACE ADMINISTRATION. MARSHALL SPACE FLIGHT CENTER, HUNTSVILLE, AL.

Plate and butt-weld stresses beyond elastic limit, material and structural modeling
[NASA-TP-3075] N91-16413
NASA/MSFC FY90 Global Scale Atmospheric Processes Research Program Review
[NASA-CP-3093] N91-16500
Comparison of SSM/I measurements to numerically-simulated cloud and precipitation during ERICA N91-16501
Observation simulation experiments with regional prediction models N91-16502
South Pacific convergence zone and global-scale circulations N91-16503
Global variability of water vapor and condensate from SSM/I N91-16507
Theoretical and experimental studies of baroclinic processes N91-16512
Hanging drop crystal growth apparatus
[NASA-CASE-MFS-26061-1] N91-16815
Paired and Interacting Galaxies: International Astronomical Union Colloquium No. 124
[NASA-CP-3098] N91-16858

NATIONAL AEROSPACE LAB., TOKYO (JAPAN).

Wind tunnel tests on flutter control of a high-aspect-ratio cantilevered wing: Control with leading-edge and trailing-edge control surfaces
[NAL-TR-1070] N91-15982
An experiment on supersonic turbulent mixing layers: Supersonic-subsonic two-stream layers
[NAL-TR-1066] N91-15983
Large-scale numerical aerodynamic simulations for complete aircraft configurations
[NAL-TR-1073-T] N91-15984
Calculations for unsteady aerodynamic characteristics on a 3-D lifting body in subsonic flow using boundary element method
[NAL-TR-1065] N91-15985
Fundamental verification of tailoring technology for control of a coefficient of thermal expansion by composite testing facilities
[NAL-TR-1058] N91-16069
Autoignition and flameholding in a cylindrical scramjet combustor
[NAL-TR-1067] N91-16102
Detection of solid lubricant film failure during sliding by vibration monitoring
[NAL-TR-1060] N91-16384
Application of fuzzy-Bayesian analysis to structural reliability
[NAL-TR-1063] N91-16396

NATIONAL CENTER FOR ATMOSPHERIC RESEARCH, BOULDER, CO.

Research on diabatic initialization N91-16504

NATIONAL CENTER FOR PHYSICAL ACOUSTICS, UNIVERSITY, MS.

Distorted-wave born approximation calculations for turbulence scattering in an upward-refracting atmosphere N91-16700

NATIONAL CLIMATIC DATA CENTER, ASHEVILLE, NC.

Joint US Navy/US Air Force climatic study of the upper atmosphere. Volume 1: January
[AD-A227122] N91-16476
Joint US Navy/US Air Force climatic study of the upper atmosphere. Volume 2: February
[AD-A227123] N91-16477
Joint US Navy/US Air Force climatic study of the upper atmosphere. Volume 3: March
[AD-A227124] N91-16478
Joint US Navy/US Air Force climatic study of the upper atmosphere. Volume 4: April
[AD-A227125] N91-16479
Joint US Navy/US Air Force climatic study of the upper atmosphere. Volume 7: July
[AD-A227126] N91-16480
Joint US Navy/US Air Force climatic study of the upper atmosphere. Volume 10: October
[AD-A227127] N91-16481

NATIONAL ENVIRONMENTAL SATELLITE SERVICE, WASHINGTON, DC.

Evaluation of the GOES 1-M normalization technique with the visible images of GOES-7
[AD-A227462] N91-16055

NATIONAL LAB. FOR HIGH ENERGY PHYSICS, IBARAKI (JAPAN).

Investigation of wire motion in superconducting magnets
[DE91-004952] N91-16674

NATIONAL OPTICAL ASTRONOMY LAB. TUCSON, AZ.

An atlas of mixed-morphology pairs N91-16866

NATIONAL RESEARCH COUNCIL OF CANADA, OTTAWA (ONTARIO).

Air-ground interface: Surface waves, surface impedance and acoustic-to-seismic coupling coefficient N91-16685

NATIONAL RESEARCH INST. FOR POLLUTION AND RESOURCES, TOKYO (JAPAN).

Experimental study on mercury heat pipes (on effect of screen mesh wick under bottom heat mode) N91-16280

NATIONAL SPACE DEVELOPMENT AGENCY, IBARAKI (JAPAN).

Development of a two-phase cold plate N91-16277

NAVAL ACADEMY, ANNAPOLIS, MD.

Development of an external beam ion milliprobe
[AD-A227247] N91-16329

NAVAL OCEAN RESEARCH AND DEVELOPMENT ACTIVITY, BAY SAINT LOUIS, MS.

Data base structure to support the production of the digital bathymetric data base
[AD-A227915] N91-16841

NAVAL OCEAN SYSTEMS CENTER, SAN DIEGO, CA.

Integrated Refractive Effects Prediction System (IREPS) user's manual, revision PC-2.0
[AD-A228549] N91-16203
Canonical eigenvalues. Part 2: Application to one-layer, bounded, underwater acoustic ducts
[AD-A227451] N91-16677

NAVAL POSTGRADUATE SCHOOL, MONTEREY, CA.

Characterization of the corrosion of a P-130x graphite fiber reinforced 6063 aluminum metal matrix composite
[AD-A228134] N91-16071
Tactical HF field expedient antenna performance, volume 1
[AD-A228057] N91-16198
Measurement of the capture effect of frequency modulation
[AD-A228058] N91-16199
The use of window functions and Kalman filtering in spectral estimation
[AD-A227482] N91-16236

NAVAL RESEARCH LAB., WASHINGTON, DC.

Introduction (to a book on applications of local-density-functional methods in chemistry)
[AD-A228769] N91-16109
Movable-boundary channel-access schemes for integrated voice/data networks
[AD-A227331] N91-16186
Diffusion fields in a toroidal conducting shell of circular cross section
[AD-A228021] N91-16197
Bio-optical profile data report coastal transition zone program, R/V Thomas Washington, June 24 - July 21, 1988
[NASA-CR-187808] N91-16532
Bio-optical profile data report coastal transition zone program, R/V Point Sur, June 15-28, 1987
[NASA-CR-187807] N91-16533
Parallel Access Main Memory (PAMM) user's manual, version 1.0
[AD-A227744] N91-16635
Observations and models of star formation in the tidal features of interacting galaxies N91-16957

NAVAL UNDERWATER SYSTEMS CENTER, NEW LONDON, CT.

Two-dimensional convolutions, correlations, and Fourier transforms of combinations of Wigner distribution functions and complex ambiguity functions
[AD-A226852] N91-16649
Operating characteristics for weighted energy detector with Gaussian signals
[AD-A226851] N91-16673

NAVY PERSONNEL RESEARCH AND DEVELOPMENT CENTER, SAN DIEGO, CA.

A computer-based instructional support network: Design, development, and evaluation
[AD-A227922] N91-16637

NEBRASKA UNIV., LINCOLN.

Scattering and depolarization by rough terrain and sea: A unified full wave approach
[AD-A228295] N91-16201
Carbon dioxide and energy exchanges in a temperate grassland ecosystem N91-16419

NEW SOUTH WALES UNIV., CANBERRA (AUSTRALIA).

Synthesis, characterization and catalytic activity of microporous aluminophosphate catalysts N91-16092
High temperature corrosion of alloys in mixed gases N91-16121
Electrolyte optimization and electrode material evaluation for the vanadium redox battery N91-16234
High efficiency silicon concentrator solar cells N91-16441
Environmental uncertainty, planning and organizational performance N91-16464
Electrical resistance volumetry in the circulation N91-16543
Geographic data transfer N91-16836

NEW YORK UNIV., NEW YORK.
Implementation and experimentation with motion planning algorithms
[AD-A228278] N91-16612
Limit behaviors of approximate solutions to conservation laws
[DE90-010069] N91-16646
NEWCASTLE-UPON-TYNE UNIV. (ENGLAND).
Stellar convection and dynamo theory N91-16857
NIGERIA UNIV., NSUKKA.
Radio structures in QSO-galaxy pairs N91-16924
NORTH CAROLINA STATE UNIV., RALEIGH.
Design and fabrication of the NASA HL-20 full scale research model
[NASA-CR-187801] N91-16008
Research and development on advanced silicon carbide thin film growth techniques and fabrication of high power and microwave frequency silicon carbide-based device
[AD-A228758] N91-16246
NORTH CAROLINA UNIV., CHAPEL HILL.
Displaying alphanumeric characters on pixel-planes 5
[AD-A228616] N91-16622
Using computer-generated protocols to study writers' planning strategies
[AD-A228875] N91-16844
NOTRE DAME UNIV., IN.
Real-time filtering and detection of dynamics for compression of HDTV
[NASA-CR-187777] N91-16596
NUFFIELD RADIO ASTRONOMY LABS., JODRELL BANK (ENGLAND).
The morphology of Sersic-Pastoriza galaxies N91-16893

O

OAK RIDGE NATIONAL LAB., TN.
Application of diode lasers to resonance ionization mass spectrometry
[DE91-000614] N91-16094
Ultrasensitive molecular fluorescence spectroscopy in levitated microdroplets
[DE91-000621] N91-16095
Picosecond multiphoton ionization of atomic and molecular clusters
[DE91-000641] N91-16096
Weldability of nickel aluminides
[DE90-008557] N91-16116
HAZ liquation cracking behavior in newly developed lean 316 stainless steels
[DE90-009409] N91-16117
Bibliography of the technical literature of the Materials Joining Group, Metals and Ceramics Division, 1951–June 1989
[DE91-000530] N91-16126
Microwave sintering of fuel cell materials
[DE90-011643] N91-16143
Gelcasting of sub-micron alumina, sialon, and silicon nitride powders
[DE91-000618] N91-16145
Updated evaluation of polymer films for electrical insulation
[DE91-000544] N91-16148
Initial parametric results using CYCLEZ: A LMTD-specified, Lorenz-Meutzner cycle refrigerator-freezer model
[DE90-010146] N91-16175
Meetings to share advancements in heat pump technologies
[DE90-010008] N91-16257
Concepts for future developments in electron microscopy
[DE90-010630] N91-16320
Experimentation and concept formation by an autonomous mobile robot
[DE90-003063] N91-16368
Ultrasound and visual sensor feedback and fusion
[DE90-005280] N91-16369
Multi-criteria position and configuration optimization for redundant platform/manipulator systems
[DE90-010705] N91-16372
Time optimal trajectories for a two wheeled robot
[DE90-010335] N91-16376
Optimal positioning of redundant manipulator-platform systems for maximum task efficiency
[DE90-011061] N91-16378
Design of a telerobotic controller with joint torque sensors using 2-port network theory
[NASA-CR-186543] N91-16379
NASA Laboratory telerobotic manipulator control system architecture
[NASA-CR-187751] N91-16385
Test methods for evaluating hot cracking: Review and perspective
[DE90-009820] N91-16397
Specimen size effects in Charpy impact testing
[DE90-011369] N91-16399
Preparations for a major international symposium on electricity and the environment
[DE90-010539] N91-16449
Potential responses of landscape boundaries to global environmental change
[DE90-008568] N91-16451
Determination of airborne organics by direct sampling mass spectrometry
[DE90-009422] N91-16452
International decision making and global climate change: Lessons of prior resource management efforts for consensus building
[DE90-010714] N91-16454
Finalization of the international biospheric model validation study
[DE90-011087] N91-16463
Monitoring challenges and innovative ideas
[DE91-000586] N91-16465
An automatic ordering method for incomplete factorization iterative solvers
[DE91-001974] N91-16659
Interatomic forces and bonding mechanisms in MgO clusters
[DE90-010148] N91-16719
The theory of electron-ion collisions: The role of doubly excited states
[DE90-011078] N91-16721
Initial calorimetry experiments in the Physics Divsion, ORNL (Oak Ridge National Laboratory)
[DE90-010301] N91-16756
The CIT physics program
[DE90-012134] N91-16774
YBa2Cu3O(7-x) thin film growth on single crystal and polycrystalline yttria-stabilized zirconia
[DE90-010707] N91-16788
Dose rate effects on damage formation in ion-implanted gallium arsenide
[DE91-000394] N91-16806
Characterization of GaAs/Si interface structure by x ray diffraction
[DE91-004769] N91-16811
Domain boundaries formed during epitactical growth of alpha-Al2O3
[DE91-005018] N91-16814
Subject bibliography of the PMA 205 (Program Manager Air 205) network technical library at Oak Ridge National Laboratory
[DE90-009988] N91-16835
OBSERVATOIRE DE MARSEILLE (FRANCE).
Dynamical interactions of galaxy pairs N91-16930
OBSERVATOIRE DE PARIS-MEUDON (FRANCE).
Dynamical theory of dense groups of galaxies N91-16943
Explaining compact groups as change alignments N91-16944
OHIO STATE UNIV., COLUMBUS.
The reflection and transmission properties of a triple band dichroic surface
[NASA-CR-187776] N91-16191
A planar near-field scanning technique for bistatic radar cross section measurements
[NASA-CR-187794] N91-16194
Solvable two-dimensional supersymmetric models and the supersymmetric Virasoro algebra
[DE90-012140] N91-16648
Molecular orbital studies of the bonding in heavy element organometallics
[DE90-009732] N91-16711
Fermions in the hypercharge sector of the standard lattice electroweak theory: Global limit
[DE90-009731] N91-16827
OKLAHOMA UNIV., NORMAN.
Direct disc impact investigation of dynamic large finite plastic behavior of 1100 aluminum N91-16404
OLD DOMINION UNIV., NORFOLK, VA.
Experimental parametric study of jet vortex generators for flow separation control
[NASA-CR-187836] N91-16296
Passive damping concepts for tubular beams with partial rotational and translational end restraints
[NASA-CR-187833] N91-16411
OLDENBURG UNIV. (GERMANY, F.R.).
Meteorological effects on long-range outdoor sound propagation N91-16696
Wave propagation through random media: A local method of small perturbations based on the Helmholtz equation N91-16701
ONSALA SPACE OBSERVATORY (SWEDEN).
Simulations of gas clouds in interacting galaxies N91-16961
OPEN UNIV., MILTON (ENGLAND).
Using a fast Fourier method to model sound propagation in a stratified atmosphere over a stratified porous-elastic ground N91-16692
OPTICAL SCIENCES CO., PLACENTIA, CA.
Phased array imaging
[AD-A228774] N91-16855
OPTRA, INC., BEVERLY, MA.
Fiber optic synthetic aperture interferometer
[AD-A227891] N91-16741
OREGON STATE UNIV., CORVALLIS.
Kinematics of arthropod legs: Modeling and measurement N91-16391
OSSERVATORIO ASTRONOMICO, BRERA, MILAN (ITALY).
Geometrical parameters of E+S pairs N91-16865

P

PACIFIC NORTHWEST LAB., RICHLAND, WA.
The development of improved capillary supercritical fluid chromatography and mass spectrometry
[AD-A228535] N91-16107
Rotary absorption heat pump sensitivity analysis
[DE90-010006] N91-16256
Procedures for Quality Assurance Program
[DE90-010001] N91-16393
Multimedia Environmental Pollutant Assessment System (MEPAS) sensitivity analysis of computer codes
[DE90-010005] N91-16445
PADUA UNIV. (ITALY).
Hidden interaction in SBO galaxies N91-16880
The complex nature of the Seyfert galaxy NGC 7592 N91-16882
The double nucleus galaxies Mkn 423 and Mkn 739 N91-16891
PARIS V UNIV. (FRANCE).
Study of pilot vigilance during long range flight N91-16561
PATHOLOGY ASSOCIATES, INC., FREDERICK, MD.
Research pathology and special techniques
[NASA-CR-187828] N91-16639
PATTERN ANALYSIS AND RECOGNITION CORP., NEW HARTFORD, NY.
Distributed System Modeling Environment (DSME)
[AD-A226698] N91-16583
PENNSYLVANIA STATE UNIV., UNIVERSITY PARK.
Hypersonic shock/boundary-layer interaction database
[NASA-CR-187769] N91-15986
Acceleration of iterative algorithms for Euler and Navier-Stokes equations N91-16301
Stratiform clouds and their interaction with atmospheric motion N91-16506
Fourth moments of acoustic waves forward scattered by a rough ocean surface
[AD-A227469] N91-16529
Real-time system specification and verification
[AD-A227682] N91-16634
Comparison of FFP predictions with measurements of a low-frequency signal propagated in the atmosphere N91-16698
Kinetic stability of field-reversed configurations
[DE90-011530] N91-16767
Multiple-photon Compton scattering in a strong magnetic field: Cross-sections and radiative transport N91-16852
PHOTON ENERGY, INC., EL PASO, TX.
High-efficiency large-area CdTe panels
[DE91-002117] N91-16443
PHYSICS AND ELECTRONICS LAB. TNO, THE HAGUE (NETHERLANDS).
Experimental set-up for a pulsed CO2 laser rangefinder with heterodyne detection
[FEL-90-A125] N91-16365
Generation of high power 1.54 micrometer radiation by stimulated Raman scattering in methane
[FEL-90-B098] N91-16366
PITTSBURGH UNIV., PA.
The oxidation behavior of carbon-carbon composites and their coatings N91-16074
PLANNING SYSTEMS, INC., SLIDELL, LA.
Scattering of sound by atmospheric turbulence predictions in a refractive shadow zone N91-16703
PLANUNGSBUERO LUFTRAUMNUTZER, FRANKFURT (GERMANY, F.R.).
The European flight safety crisis: Costs and solution
[ETN-91-98490] N91-16000
PRATT AND WHITNEY AIRCRAFT, WEST PALM BEACH, FL.
Geometric modeling applications interface program
[AD-A227651] N91-16591
Geometric modeling application interface program. System components operator's manual
[AD-A227827] N91-16594
PRINCETON UNIV., NJ.
Near/far resistant receivers for DS/SSMA communications
[AD-A228147] N91-16200
Analysis and application of the discrete vortex method N91-16290

Technique for determining the static polarizabilities of refractory metal atoms
[DE90-017088] N91-16724
The CIT physics program
[DE90-012134] N91-16774
Far-infared laser spectroscopy of two dimensional holes in strained-layer heterostructure and superlattices
[DE91-000027] N91-16805
PURDUE UNIV., WEST LAFAYETTE, IN.
Propfan supersonic panel method analysis and flutter predictions N91-15993
Applications of fuzzy theories to multi-objective system optimization
[NASA-CR-177573] N91-16012
Aeroservoelastic tailoring for lateral control enhancement N91-16025
Investigation of a new concept in semiconductor microwave oscillators
[AD-A226785] N91-16235
Magsat investigations over the greater African region N91-16415
Synoptic/planetary-scale interactions and blocking over the North Atlantic Ocean N91-16513
Visualization of surfaces in four-dimensional space
[AD-A227858] N91-16605

R

RAND CORP., SANTA MONICA, CA.
Impacts of advanced manufacturing technology on parametric estimating
[AD-A228232] N91-16177
RENSSELAER POLYTECHNIC INST., TROY, NY.
Expressing user-defined parallelism in EPL (Equational Programming Language)
[AD-A227875] N91-16606
RHODE ISLAND UNIV., KINGSTON.
Formic and acetic acids in the boundary layer over the North Atlantic ocean N91-16530
RICE UNIV., HOUSTON, TX.
Optimization and guidance of flight trajectories for the national aerospace plane
[NASA-CR-187837] N91-16010
Optimal trajectories for an aerospace plane. Part 2: Data, tables, and graphs
[NASA-CR-187848] N91-16011
Optimal trajectories for an aerospace plane. Part 1: Formulation, results, and analysis
[NASA-CR-187868] N91-16013
Deep Fabry-Perot imaging of NGC 6240: Kinematic evidence for merging galaxies N91-16922
Positron survival in Type II supernovae
[AD-A226778] N91-16965
RIJKSLUCHTVAARTDIENST SCHIPHOL (NETHERLANDS).
Activities report of the Dutch Civil Aeronautics Board
[ETN-91-98472] N91-16005
ROCHESTER INST. OF TECH., NY.
Merging panchromatic and multispectral images for enhanced image analysis
[AD-A227902] N91-16421
ROCHESTER UNIV., NY.
Linguistic and pragmatic constraints on utterance interpretation
[AD-A226815] N91-16210
Stochastic and chaotic effects in the ring laser N91-16359
Real-time vergence control for binocular robots
[AD-A228817] N91-16387
PENGUIN: A language for reactive graphical user interfaces
[AD-A228580] N91-16620
Nonlinear optical systems interacting with amplitude-modulated optical fields
[AD-A228221] N91-16742
ROCK ISLAND ARSENAL, IL.
Manufacturing guide for elastomeric seals
[AD-A227511] N91-16383
ROCKWELL INTERNATIONAL CORP., ANAHEIM, CA.
Reliability/Maintainability/Logistics support analysis Computer Aided Tailoring Software Program (R/M/L CATSOP)
[AD-A226820] N91-16588
ROCKWELL INTERNATIONAL CORP., CANOGA PARK, CA.
Fiber-reinforced ceramic composites for Earth-to-orbit rocket engine turbines
[NASA-CR-185264] N91-16150
ROME AIR DEVELOPMENT CENTER, GRIFFISS AFB, NY.
Statistically thinned arrays with quantized element weights
[AD-A227965] N91-16196
ROYAL AEROSPACE ESTABLISHMENT, FARNBOROUGH (ENGLAND).
Geopotential harmonics of order 15 and 30 from analysis of 50 orbit determinations of 1967-102B
[RAE-TR-90029] N91-16035
Molten salt electrolytes in high temperature batteries
[RAE-TM-MAT/STR-1155] N91-16241
Optimisation of operational workload levels using neurophysiological and cognitive techniques N91-16560
ROYAL SIGNALS AND RADAR ESTABLISHMENT, MALVERN (ENGLAND).
Models for surface scattering from solids and liquids
[RSRE-MEMO-3699] N91-16192
Analysis of the performance of a single-auxiliary sidelobe canceller
[RSRE-MEMO-4375] N91-16193
RUTGERS - THE STATE UNIV., NEW BRUNSWICK, NJ.
A sectorial analysis of the information sector in the information economy: Its comparative measurement and new classification model N91-16845
RUTHERFORD APPLETON LAB., CHILTON (ENGLAND).
The radiation hardness test facility
[RAL-90-065] N91-16030

S

SALFORD UNIV. (ENGLAND).
New correction procedures for the fast field program which extend its range N91-16699
SAN DIEGO STATE UNIV., CA.
Inverse gas chromatography
[AD-A227677] N91-16099
Optimization of a power transient stability program on a vector supercomputer: Theory and applications
[AD-A227884] N91-16607
SANDIA NATIONAL LABS., ALBUQUERQUE, NM.
Aerosol Dynamics Laboratory
[DE90-010275] N91-16027
Graphical analysis of barrel-tamped explosively accelerated flyer plates
[DE90-010299] N91-16028
Magnetic-field shielding of satellites from high-energy-electron environments
[DE90-010296] N91-16043
Sensor-based automated docking of large payloads
[DE90-011020] N91-16044
Joint computational/experimental aerodynamics research on a reentry vehicle. Part 2: Computational results
[DE90-012765] N91-16054
The effect of stratification on gravitational coagulation and settling of aerosols
[DE90-010153] N91-16079
Atomic-scale simulation of adhesion between metallic surfaces
[DE91-004722] N91-16127
Comparison of the thermal stability of the codeposited carbon/hydrogen layer to that of the saturated implant layer in graphite
[DE90-012148] N91-16144
The effect of charge mixture ratio and particle size on igniter plume heat transfer characteristics
[DE90-010833] N91-16160
Modeling laser ignition of explosives and pyrotechnics: Effects and characterization of radiative transfer
[DE90-011052] N91-16161
Numerical modeling tools for transient electromagnetic problems
[DE90-010328] N91-16180
Characterization and development report for the SA2859: A silicon controlled rectifier
[DE90-010196] N91-16217
Total-dose degradation of thin film ferroelectric capacitors
[DE90-007152] N91-16218
The 1/f noise in irradiated MOS devices
[DE90-007288] N91-16219
Radiation hardening of a high voltage IC technology (BCDMOS)
[DE90-008345] N91-16220
A transformer coupled semiconductor bridge igniter for low voltage ignition from a high voltage source
[DE90-009974] N91-16221
An algorithm for using a slide-screw tuner as a computer-controlled impedance
[DE90-010657] N91-16226
Microwave coupling on printed circuit boards
[DE90-011237] N91-16232
Development of a moderate rate lithium/thionyl-chloride D cell
[DE90-011909] N91-16233
Novel applications of Tl-Ca-Ba-Cu-O thin films to active and passive high frequency devices
[DE91-004507] N91-16240
Properties and characterization of thin film ferroelectric capacitors for nonvolatile memories
[DE91-004037] N91-16242
Aerosol cloud generation experiments
[DE90-011051] N91-16264
X-Ray Detector: An x-ray radiation detector design code
[DE90-008235] N91-16317
Ion contamination of x ray pinhole camera images on PBFA 2
[DE90-012180] N91-16325
Interferometric second-harmonic-generation autocorrelator for characterizing femtosecond pulses
[DE90-010331] N91-16345
Haptic perception with an articulated, sensate robot hand
[DE90-010195] N91-16371
Experimental verification of physical model of pulsed laser welding
[DE91-000025] N91-16380
Statistical process control for QML (Qualified Manufacturer's List) radiation hardness assurance
[DE90-007413] N91-16394
Self-discharge study of Li-alloy/FeS2 thermal cells
[DE90-010659] N91-16438
Seismic signal processing optimized for a specific source and receiver
[DE90-010189] N91-16468
ANEOS: Analytic equations of state for shock physics codes input manual
[DE90-010198] N91-16575
Implementation of the phase gradient algorithm
[DE90-012160] N91-16579
A trellis-searched APC (Adaptive Predictive Coding) speech coder
[DE91-000866] N91-16581
Linear algebra for dense matrices on a hypercube
[DE90-010533] N91-16647
Multiple-frequency surface acoustic wave devices as sensors
[DE90-009972] N91-16675
Utilization of polymer viscoelastic properties in acoustic wave sensor applications
[DE90-010534] N91-16676
Thermal emission model for the anneal of radiation-induced trapped holes
[DE90-007285] N91-16718
Plasma-facing materials
[DE90-008243] N91-16753
Characterization of chemically prepared PZT thin films
[DE90-010831] N91-16789
Microwave-detected photoconductance decay
[DE90-011505] N91-16795
Far-infared laser spectroscopy of two dimensional holes in strained-layer heterostructure and superlattices
[DE91-000027] N91-16805
Thermal desorption studies of isotopically-labeled oxygen-induced superconductivity in La2CuO(4+delta)
[DE91-004898] N91-16812
SAO PAULO UNIV. (BRAZIL).
Radio emission in peculiar galaxies N91-16907
SCIENCE APPLICATIONS INTERNATIONAL CORP., CLEARWATER, FL.
Briefing DTD user's guide for the Software Technology for Adaptable, Reliable Systems (STARS) program
[AD-A228473] N91-16618
SCIENCE APPLICATIONS INTERNATIONAL CORP., PROSPECT, TN.
Scoping estimates of the LDEF satellite induced radioactivity
[NASA-CR-184074] N91-16056
SCIENTIFIC RESEARCH ASSOCIATES, INC., GLASTONBURY, CT.
Numerical simulation of the comparative electrical performance of the permeable base transistor, opposed gate-source transistor and heterostructure launched ballistic field effect transistor
[AD-A228545] N91-16202
SFA, INC., LANDOVER, MD.
Investigation and modeling of radiation absorption processes and opacities in dense plasmas
[AD-A228749] N91-16779
SHEFFIELD UNIV. (ENGLAND).
Periodic solutions of neutral differential equations
[RR-390] N91-16658
SMITHSONIAN ASTROPHYSICAL OBSERVATORY, CAMBRIDGE, MA.
Radio line and continuum observations of quasar-galaxy pairs and the origin of low reshift quasar absorption line systems N91-16925
SOUTH CAROLINA UNIV., COLUMBIA.
Skill and skilled memory
[AD-A227697] N91-16549
SOUTHAMPTON UNIV. (ENGLAND).
A low cost end-fire acoustic radiator
[ISVR-TR-188] N91-16705

SOUTHERN METHODIST UNIV., DALLAS, TX.
Adaptive bandwidth choice for kernel regression
[AD-A228437] N91-16661
SOUTHWEST RESEARCH INST., SAN ANTONIO, TX.
Investigation of effects of 60-Hz electric and magnetic fields on operant and social behavior and on the neuroendocrine system of nonhuman primates
[DE90-010809] N91-16537
Investigation of effects of 60-Hz electric and magnetic fields on operant and social behavior and on the neuroendocrine system of nonhuman primates
[DE90-011557] N91-16539
SPACE RESEARCH ORGANIZATION NETHERLANDS, UTRECHT.
Activities report of the Space Research Organization Netherlands
[ETN-91-98473] N91-16848
SPACE TELESCOPE SCIENCE INST., BALTIMORE, MD.
Blue ellipticals in compact groups N91-16873
The environments of Markarian galaxies N91-16881
H I and mass distribution of GR8 N91-16884
The cD galaxy in Abell cluster 1775 N91-16886
Cool infalling gas and its interaction with the hot ISM of elliptical galaxies N91-16915
Dust and ionized gas in active radio elliptical galaxies N91-16919
IC5063: A merger with a hidden luminous active nucleus N91-16923
Probing the tides in interacting galaxy pairs N91-16932
SPECIAL ASTROPHYSICAL OBSERVATORY, ZELENCHUKSKAYA (USSR).
A homogeneous sample of binary galaxies: Basic observational properties N91-16859
What is the number of spiral galaxies in compact groups N91-16874
Triple galaxies and a hidden mass problem N91-16875
SRI INTERNATIONAL CORP., MENLO PARK, CA.
Liquid hydrogen production and commercial demand in the United States N91-16168
Ionic solid hydrogen fuel: Production and properties of hydrogen ion and energetic neutral clusters
[AD-A227683] N91-16172
An evolutionary approach to designing neural networks
[AD-A228874] N91-16643
ST SYSTEMS CORP., LEXINGTON, MA.
A study of the interaction of physical and numerical parameterizations with regard to moisture forecasting in a regional model of the atmosphere
[AD-A227966] N91-16488
STANFORD LINEAR ACCELERATOR CENTER, CA.
SLED II: A new method of RF pulse compression
[DE91-000058] N91-16183
Theoretical topics in B-physics
[DE91-004911] N91-16726
Deep inelastic structure functions from electron scattering on hydrogen, deuterium, and iron at 0.6 GeV2 less than or equal to Q2 less than or equal to 30.0 GeV2
[DE90-010169] N91-16785
Performance measurements of hybrid PIN diode arrays
[DE90-010308] N91-16790
STANFORD UNIV., CA.
On the development of in-situ Raman analysis of plasma deposited diamond
[AD-A227453] N91-16147
Joint services electronics program
[AD-A227576] N91-16237
Numerical study of a three-dimensional turbulent boundary layer
[AD-A227835] N91-16291
Microsupercomputers: Design and implementation
[AD-A228741] N91-16571
Microsupercomputers: Design and implementation
[AD-A228744] N91-16572
Analysis of parallel, replicated simulations under a completion time constraint
[AD-A228292] N91-16613
Matrix algorithms in signal processing
[AD-A228851] N91-16625
Experiments with initial transient deletion for parallel, replicated steady-state simulations
[AD-A227879] N91-16636
Pathwise convexity and its relation to convergence of time-average derivatives
[AD-A228888] N91-16662
Hierarchical Bayesian analysis of change point problems
[AD-A228179] N91-16666
Estimating the asymptotic variance with batch means
[AD-A228293] N91-16667
The asymptotic validity of sequential stopping rules for stochastic simulations
[AD-A228896] N91-16668
Research into the design and implementation of knowledge base systems
[AD-A228873] N91-16843
STATE UNIV. OF NEW YORK, BUFFALO.
Design, ultrastructure, and dynamics of nonlinear optical interactions in polymeric thin films
[AD-A228876] N91-16156
Theoretical studies of electron transport in quantum-well structures
[AD-A228429] N91-16819
STATE UNIV. OF NEW YORK, STONY BROOK.
Atomic and electronic structure of metals and alloys: Clean surfaces and chemisorbed molecules
[DE91-000267] N91-16123
STERNBERG ASTRONOMICAL INST., MOSCOW (USSR).
The H I content of non-isolated galaxies N91-16883
STRUCTURAL INTEGRITY ASSOCIATES, INC., SAN JOSE, CA.
Elevated temperature crack growth in titanium aluminides
[AD-A227700] N91-16125
STUTTGART UNIV. (GERMANY, F.R.).
Finite element approximations for transonic flows
[ETN-91-98491] N91-15988
A process for unstationary velocity and turbulence measurements with a pneumatic measuring wedge probe
[MITT-33] N91-16310
Study on ECW transmission lines for NET/ITER
[EUR-FU/80/90-99] N91-16781
SUPERCONDUCTING SUPER COLLIDER LAB., DALLAS, TX.
Investigation of wire motion in superconducting magnets
[DE91-004952] N91-16674
SUTHERLAND (LOUIS C.), RANCHO PALOS VERDES, CA.
Long-range sound propagation: A review of some experimental data N91-16683
SYRACUSE UNIV., NY.
Numeric and symbolic signal processing for very high subclutter visibility
[AD-A228812] N91-16207
An experimental demonstration of high-resolution Doppler processing
[AD-A228813] N91-16208
Intra-Pulse Frequency Diversity (IPFD) lab demonstration
[AD-A228814] N91-16209
Particle deposition in granular media
[DE90-010810] N91-16261
Alopex optimization algorithm
[AD-A228442] N91-16615
SYSTEMS CONTROL TECHNOLOGY, INC., ARLINGTON, VA.
Evaluation of rotorwash characteristics for tiltrotor and tiltwing aircraft in hovering flight
[SCT-90RR-18] N91-15989

T

TECHNISCHE HOCHSCHULE, AACHEN (GERMANY, F.R.).
Unstationary shock and boundary layer phenomena at profiles and in a plane grid by transonic flow
[ETN-91-98557] N91-16311
TECHNISCHE UNIV., BRUNSWICK (GERMANY, F.R.).
Tests for integrating measurements of gas pressures in aircraft mechanisms
[ETN-91-98558] N91-16014
TECHNISCHE UNIV., DELFT (NETHERLANDS).
From visco-elasticity towards thermal relaxation: A neutron scattering study of density fluctuations in fluid helium
[ETN-91-98486] N91-16111
Electrical properties of gas sensor materials
[ETN-91-98572] N91-16114
The use of impedance measurements in corrosion research: The corrosion behaviour of chromium and iron-chromium alloys
[ISBN-90-9003693-8] N91-16135
Grain-boundary structure in ordered alloys
[ETN-91-98571] N91-16136
Fatigue of amorphous polymers
[ISBN-90-9003520-6] N91-16157
Control of industrial crystallizers: The physical aspects
[ETN-91-98488] N91-16179
Systematic design of regular VLSI processor arrays
[ETN-91-98482] N91-16250
Natural-convection boundary layers
[ISBN-90-9003467-6] N91-16313
High-purity silicon soft x ray sensor arrays
[ETN-91-98484] N91-16338
Some generalizations of the criss-cross method for quadratic programming
[REPT-90-52] N91-16599
A long step barrier method for convex quadratic programming
[REPT-90-53] N91-16600
Low-level image processing architectures compared for some non-linear recursive neighborhood operations
[ISBN-90-9003713-6] N91-16631
Relative extrema, zeros, and inequalities for Gegenbauer functions of the first and second kind
[REPT-90-54] N91-16653
Relative extrema, zeros, and inequalities for Jacobi functions of the first and second kind
[REPT-90-55] N91-16654
A sign-changing global minimizer on a convex domain
[REPT-90-57] N91-16655
Stability properties of a flow process in graphs
[REPT-90-58] N91-16656
An elementary proof of the Ambartzumian-Pleijel identity
[REPT-90-59] N91-16657
A time-domain finite-element method for the computation of three-dimensional acoustic wave fields in inhomogeneous fluids and solids
[ETN-91-98485] N91-16710
Programmable surface acoustic wave detection in silicon: Design of programmable filters
[ETN-91-98568] N91-16746
Image interpretation for transmission electron microscopy of thin semiconductor layers and interfaces
[ETN-91-98487] N91-16826
TECHNISCHE UNIV., EINDHOVEN (NETHERLANDS).
High speed narrow bore capillary gas chromatography
[ETN-91-98481] N91-16113
Surface analysis by low-energy ion scattering: Two-dimensional detection and quantification
[ETN-91-98474] N91-16133
Geometrical aspects of the production of toothed disks
[MEMO-COSOR-90-02] N91-16178
Internal solitary waves in compressible fluids
[ETN-91-98475] N91-16307
Shear thickening of concentrated dispersions
[ETN-91-98477] N91-16308
Fine particle flotation in a centrifugal force field
[ETN-91-98480] N91-16309
Column reduction of polynomial matrices: An iterative algorithm
[MEMO-COSOR-89-30] N91-16598
Identification of non-linear mechanical systems for control application
[ISBN-90-9003596-6] N91-16644
The discrete time H infinity control problem with measurement feedback
[MEMO-COSOR-89-31] N91-16651
The finite horizon singular time-varying H infinity control problem with dynamic measurement feedback
[MEMO-COSOR-89-33] N91-16652
Microwave interferometer and reflectometer techniques for thermonuclear plasmas
[ETN-91-98478] N91-16780
Physico-chemical investigations on Co-Mn-oxide spinels
[ETN-91-98476] N91-16825
TECHNISCHE UNIV., GOETTINGEN (GERMANY, F.R.).
Observations of multiple nucleus galaxies N91-16890
Correlations between environmental parameters and nuclear activity N91-16920
TENNESSEE STATE UNIV., NASHVILLE.
Validity study in multidimensional latent space and efficient computerized adaptive testing
[AD-A227742] N91-16650
TENNESSEE UNIV., MEMPHIS.
Changes in somatosensory responsiveness in behaving monkeys
[AD-A226832] N91-16540
TENNESSEE UNIV. SPACE INST., TULLAHOMA.
Investigation of transonic flow over segmented slotted wind tunnel wall with mass transfer
[NASA-CR-187760] N91-15981
TEXAS A&M UNIV., COLLEGE STATION.
Tropical Pacific moisture variability N91-16509
Spatial and temporal climate variations influencing medium-range temperature predictions over south-central European Russia
[AD-A228623] N91-16527
Horizontal fault tolerance in a fully distributed loosely coupled environment
[AD-A227972] N91-16638
Mathematical methods and algorithms for real-time applications
[AD-A228889] N91-16663

TEXAS UNIV., ARLINGTON.
Electronic and ionic transport in processable conducting polymers
[AD-A227857] N91-16154
Visualization of unsteady transonic flow by holographic interferometry using photorefractive media
[AD-A228802] N91-16336

TEXAS UNIV., AUSTIN.
A decentralized linear quadratic control design method for flexible structures
[NASA-CR-187860] N91-16059
Polymers at liquid-liquid interfaces: Photophysics and photoredox chemistry
[DE91-005032] N91-16151
Some applications of probability and statistics in communication theory and signal processing
[AD-A226869] N91-16184
Terrain matching using image sequence analysis N91-16424
The design of a two-dimensional optical image correlator and its application in image tracking N91-16744
Wave-particle power transfer in a steady-state driven system
[DE90-010031] N91-16748
Texas experimental tokamak
[DE90-011070] N91-16762
The CIT physics program
[DE90-012134] N91-16774
Information technology policies: A four country comparative study N91-16840
Dense cores and young stellar objects N91-16969

TEXTRON DEFENSE SYSTEMS, WILMINGTON, MA.
Vehicular sources in acoustic propagation experiments N91-16690

THIOKOL CORP., BRIGHAM CITY, UT.
Space Shuttle Flight Support Motor no. 1 (FSM-1)
[NASA-CR-184078] N91-16064

TOHOKU UNIV., SENDAI (JAPAN).
Simulation of excited shear flows N91-16270

TOKYO ASTRONOMICAL OBSERVATORY, MITAKA (JAPAN).
Morphological type correlation between nearest neighbor pairs of galaxies N91-16861

TOKYO UNIV. (JAPAN).
The Proceedings of the Symposium on Mechanics for Space Flight 1989
[ISAS-SP-12] N91-16266
Numerical simulation of pulsatile flows passing through a pipe with sudden expansion N91-16271
Numerical simulation of a complicated transition-breakdown of vortical flows inside a circular pipe N91-16273
Wing galaxies: A formation mechanism of the clumpy irregular galaxy Markarian 297 N91-16963

TOLEDO UNIV., OH.
Measurements of scattering processes in negative ion-atom collisions
[DE90-010666] N91-16715

TORONTO UNIV. (ONTARIO).
A multi-frequency study of the peculiar interacting system Arp 206 N91-16870

TSUKUBA UNIV., IBARAKI (JAPAN).
Effect of inclination angle on heat transfer characteristics of closed two-phase thermosyphon N91-16278

TUFTS UNIV., MEDFORD, MA.
Graviton effects in vacuum maximally symmetric spaces N91-16971

TURKU UNIV. (FINLAND).
Merging galaxies and black hole ejections N91-16929

U

ULTRAMET, PACOIMA, CA.
Hydrogen storage in metal hydrides
[AD-A228150] N91-16103

UNITED TECHNOLOGIES RESEARCH CENTER, EAST HARTFORD, CT.
Advanced structural instrumentation, volume 1
[AD-A227226] N91-16328
Advanced structural instrumentation, volume 2
[AD-A227473] N91-16330

UNIVERSIDAD AUTONOMA DE PUEBLA (MEXICO).
A statistical study of merging galaxies: Theory and observations N91-16931
A dynamical proximity analysis of interacting galaxy pairs N91-16937

UNIVERSITAET DER BUNDESWEHR MUENCHEN, NEUBIBERG (GERMANY, F.R.).
Theoretical and experimental examinations of transition behavior of the profile boundary layer at compressor and turbine grids
[ETN-91-98559] N91-16312

UNIVERSITY COLL., CARDIFF (WALES).
Aerodynamic surface pressure measurement in atmosphere and wind tunnel on a vertical axis wind turbine blade using pressure transducers N91-15980
Numerical simulations of interacting disk galaxies N91-16955

UNIVERSITY OF CENTRAL FLORIDA, ORLANDO.
Timing margin measurement using a laser technique
[AD-A226821] N91-16353

UNIVERSITY OF SOUTHERN CALIFORNIA, LOS ANGELES.
Model filled polymers versus synthesis of crosslinked monodisperse polymethacrylate beads
[AD-A227236] N91-16146
Research in optical symbolic tasks
[AD-A228797] N91-16551

UTAH STATE UNIV., LOGAN.
Optimal rocket motor design and control for tactical missiles N91-16062

UTAH UNIV., SALT LAKE CITY.
Image-based terrain modeling with thematic mapper N91-16418
On the propagation of plane waves above an impedance surface N91-16684

V

VANDERBILT UNIV., NASHVILLE, TN.
Theoretical studies of atomic transitions
[DE91-000931] N91-16723

VIGYAN RESEARCH ASSOCIATES, INC., HAMPTON, VA.
User's guide to PANCOR: A panel method program for interference assessment in slotted-wall wind tunnels
[NASA-CR-187479] N91-16033

VIRGINIA UNIV., CHARLOTTESVILLE.
The StarLite project
[AD-A226722] N91-16837

W

WARWICK UNIV., COVENTRY (ENGLAND).
A segregated finite element solution to the incompressible Navier-Stokes equations
[ME-69] N91-16315
Dynamic aspects of scanning surface instruments and microscopes
[ME-84] N91-16339
A hydraulically driven microdisplacement unit
[ME-56] N91-16392
Electronic analogue for a biological nose
[ME-78] N91-16541

WASHINGTON UNIV., SEATTLE.
Analytical and numerical studies in flow development
[DE90-010424] N91-16258
Nonlinear resonance
[DE90-010428] N91-16341
Parity violation and electron scattering
[DE90-010429] N91-16712

WEST VIRGINIA UNIV., MORGANTOWN.
Aerodynamic drag characterization and deposition studies of irregular particles. Part 3: Analysis of flow and temperature field inside the Combustion Deposition Entrained Reactor (CDER)
[DE90-000466] N91-16259

WICHITA STATE UNIV., KS.
Comparative study of phosphosilicate glass on (100) silicon by furnace and rapid isothermal annealing
[NIAR-90-26] N91-16153

WINAND STARING CENTRE, WAGENINGEN (NETHERLANDS).
Evaluation of crop transpiration with remote sensing and computer simulation models
[REPT-1] N91-16431

WISCONSIN UNIV., MADISON.
Phase selection and processing of high temperature intermetallic alloys
[AD-A227910] N91-16129
Field measurement of head related transfer functions
[AD-A227850] N91-16708
The Madison symmetric torus
[DE90-010306] N91-16757
ASTROMAG coil cooling study
[NASA-CR-187768] N91-16813
The kinematics and morphology of NGC 520: One, two, or three galaxies N91-16908

WISCONSIN UNIV., MILWAUKEE.
From low to high Tc: An ultrasonic investigation of niobium single crystal and YBaCuO superconducting thin films with surface acoustic waves N91-16822

WOODS HOLE OCEANOGRAPHIC INST., MA.
The high speed buffer board: A SAIL EIA-485 communications accelerator card for the vector measuring current meter
[AD-A227181] N91-16185

Y

YALE UNIV., NEW HAVEN, CT.
Nonlinear dynamics of global atmospheric and Earth-system processes N91-16510
Limits of human visual discrimination: Toward a general model of visual geometry
[AD-A226826] N91-16548
Sparse representation of smooth linear operators
[AD-A228142] N91-16660
Central activity in 60 micron peakers N91-16913

YAP ANALYTICS, INC., LEXINGTON, MA.
Upper atmosphere IR radiation modeling and analysis
[AD-A227214] N91-16482

Typical Contract Number Index Listing

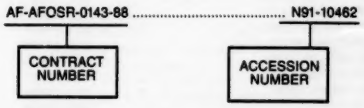

Listings in this index are arranged alphanumerically by contract number. Under each contract number the accession numbers denoting documents that have been produced as a result of research done under that contract are arranged in ascending order. The accession number denotes the number by which the citation is identified.

AF PROJ. MTFI N91-16591
AF PROJ. 7A10 ..... N91-16475
AF PROJ. 2301 ..... N91-16743
AF PROJ. 2302 ..... N91-16409
AF PROJ. 2303 ..... N91-16156
AF PROJ. 2304 ..... N91-16184
N91-16843
AF PROJ. 2305 ..... N91-16235
N91-16551
AF PROJ. 2306 ..... N91-16821
AF PROJ. 2307 ..... N91-16285
N91-16291
AF PROJ. 2308 ..... N91-16354
AF PROJ. 2310 ..... N91-16488
N91-16776
AF PROJ. 2312 ..... N91-16540
AF PROJ. 2313 ..... N91-16548
N91-16550
AF PROJ. 2338 ..... N91-16353
AF PROJ. 2418 ..... N91-16124
AF PROJ. 2527 ..... N91-16608
N91-16609
AF PROJ. 2950 ..... N91-16586
AF PROJ. 3005 ..... N91-16382
AF PROJ. 3017 ..... N91-16552
AF PROJ. 3036 ..... N91-16327
AF PROJ. 3066 ..... N91-16328
N91-16330
AF PROJ. 3484 ..... N91-16980
AF PROJ. 4600 ..... N91-16196
AF PROJ. 5420 ..... N91-16004
AF PROJ. 5581 ..... N91-16604
AF PROJ. 5730 ..... N91-16103
N91-16110
AF PROJ. 7184 ..... N91-16708
AF-AFOSR-0025-90 ..... N91-16106
AF-AFOSR-0026-86 ..... N91-16184
AF-AFOSR-0042-89 ..... N91-15994
AF-AFOSR-0077-86 ..... N91-16548
AF-AFOSR-0077-87 ..... N91-16980
AF-AFOSR-0093-90 ..... N91-16664
AF-AFOSR-0163-87 ..... N91-16743
AF-AFOSR-0179-88 ..... N91-16540
AF-AFOSR-0180-87 ..... N91-16550
AF-AFOSR-0187-84 ..... N91-16354
AF-AFOSR-0193-85 ..... N91-16235
AF-AFOSR-0196-86 ..... N91-16551
AF-AFOSR-0229-88 ..... N91-16285
AF-AFOSR-0248-88 ..... N91-16805
AF-AFOSR-0266-88 ..... N91-16843
AF-AFOSR-0285-87 ..... N91-16291
AF-AFOSR-0334-89 ..... N91-16821
A84/KL/121 ..... N91-16365
A87/KLU/131 ..... N91-16213
N91-16568
A88/M/319 ..... N91-16846
BCRS PROJ. CO-2.20 ..... N91-16425
DA PROJ. 1L1-61102-AH-43 ..... N91-16104
N91-16105
N91-16106
DA PROJ. 1L1-61102-AH-45 ..... N91-16304
DA PROJ. 1L1-62120-AH-25 ..... N91-16029
N91-16589
DA PROJ. 1L1-62618-AH-80 ..... N91-15990
DA PROJ. 3E1-62787-A-878 ..... N91-16545
DA PROJ. 3M2-63763-D-807 ..... N91-16639
DA PROJ. 4A7-62730-A4-AL N91-16286
DA PROJ. 162-63102-D-071 ..... N91-16068
DA PROJ. 162-63102-DO-71 ..... N91-16072
DAAL03-86-G-0052 ..... N91-16243
DAAL03-86-K-0083 ..... N91-16801
DAAL03-86-K-0089 ..... N91-16820
DAAL03-86-K-0149 ..... N91-16336
DAAL03-86-K-0164 ..... N91-16129
DAAL03-86-K-0173 ..... N91-16742
DAAL03-87-K-0016 ..... N91-16410
DAAL03-87-K-0025 ..... N91-16663
DAAL03-87-K-0042 ..... N91-16107
DAAL03-87-K-0062 ..... N91-16200
DAAL03-87-K-0085 ..... N91-16201
DAAL03-87-K-0095 ..... N91-16625
DAAL03-88-K-0063 ..... N91-16613
N91-16636
N91-16662
N91-16667
N91-16668
DAAL03-89-G-0122 ..... N91-16842
DAAL03-90-G-0096 ..... N91-16606
DAAL04-87-C-0078 ..... N91-16072
DACA76-85-C-0001 ..... N91-16210
N91-16387
DARPA ORDER 1133 ..... N91-16571
N91-16572
DARPA ORDER 6090 ..... N91-16622
DARPA ORDER 9525 ..... N91-16818
DE-AC02-76CH-00016 ..... N91-16446
N91-16453
N91-16542
N91-16733
N91-16747
N91-16800
N91-16803
N91-16804
N91-16811
DE-AC02-76CH-03000 ..... N91-16316
N91-16787
N91-16966
DE-AC02-76ER-01198 ..... N91-16811
DE-AC02-76ER-01545 ..... N91-16648
N91-16827
DE-AC02-76ER-03274 ..... N91-16733
N91-16747
DE-AC02-80RA-50219 ..... N91-16537
N91-16539
DE-AC02-83CH-10093 ..... N91-16139
N91-16443
N91-16444
N91-16582
DE-AC02-83ER-40107 ..... N91-16733
N91-16747
DE-AC02-87ER-40325 ..... N91-16827
DE-AC02-89ER-40486 ..... N91-16674
DE-AC03-76SF-00098 ..... N91-16119
N91-16142
N91-16149
N91-16228
N91-16322
N91-16344
N91-16358
N91-16546
N91-16735
N91-16797
N91-16798
DE-AC03-76SF-00515 ..... N91-16183
N91-16726
N91-16785
N91-16790
DE-AC03-89ER-51114 ..... N91-16749
N91-16752
N91-15773
DE-AC04-76DP-00613 ..... N91-16176
N91-16326
DE-AC04-76DP-00789 ..... N91-16027
N91-16028
N91-16043
N91-16044
N91-16054
N91-16079
N91-16127
N91-16144
N91-16160
N91-16161
N91-16180
N91-16217
N91-16218
N91-16219
N91-16220
N91-16221
N91-16226
N91-16232
N91-16233
N91-16240
N91-16242
N91-16264
N91-16317
N91-16325
N91-16345
N91-16371
N91-16380
N91-16394
N91-16438
N91-16468
N91-16575
N91-16579
N91-16581
N91-16647
N91-16675
N91-16676
N91-16718
N91-16753
N91-16789
N91-16795
N91-16805
N91-16812
DE-AC04-88DP-43495 ..... N91-16738
N91-16808
DE-AC05-84OR-21400 ..... N91-16094
N91-16095
N91-16096
N91-16116
N91-16117
N91-16126
N91-16143
N91-16145
N91-16148
N91-16175
N91-16257
N91-16320
N91-16368
N91-16369
N91-16372
N91-16376
N91-16378
N91-16379
N91-16385
N91-16397
N91-16399
N91-16449
N91-16451
N91-16452
N91-16454
N91-16463
N91-16465
N91-16659
N91-16719
N91-16721
N91-16756
N91-16774
N91-16788
N91-16806
N91-16811
N91-16814
N91-16835
DE-AC06-76RL-01830 ..... N91-16393
N91-16445
DE-AC07-76ID-01570 ..... N91-16066
N91-16223

N91-16225
N91-16227
N91-16319
N91-16377
N91-16395
N91-16461
N91-16574
N91-16739
DE-AC08-88NV-10617 ..... N91-16321
N91-16471
N91-16498
DE-AC21-88MC-25170 ..... N91-16442
DE-AI01-76ET-20320 ..... N91-16679
DE-AI01-85CE-50111 ..... N91-16021
DE-AI01-86CE-90237 ..... N91-16078
DE-AI03-86SF-16310 ..... N91-16128
DE-AI05-84OR-21411 ..... N91-16073
DE-AI08-78ET-44802 ..... N91-16470
DE-AS05-80ER-10666 ..... N91-16734
DE-AS05-81ER-40032 ..... N91-16733
N91-16747
DE-FG01-86CE-15256 ..... N91-16256
DE-FG01-88CE-15401 ..... N91-16318
DE-FG02-85ER-13370 ..... N91-16086
DE-FG02-85ER-45189 ..... N91-16725
DE-FG02-85ER-53198 ..... N91-16757
DE-FG02-85ER-60372 ..... N91-16460
DE-FG02-86ER-13529 ..... N91-16711
DE-FG02-86ER-13553 ..... N91-16081
DE-FG02-86ER-45239 ..... N91-16123
DE-FG02-86ER-53222 ..... N91-16760
DE-FG02-87ER-13800 ..... N91-16284
DE-FG02-88ER-13930 ..... N91-16261
DE-FG02-88ER-13942 ..... N91-16140
DE-FG02-88ER-45356 ..... N91-16138
DE-FG02-88ER-60631 ..... N91-16722
DE-FG02-89ER-45402 ..... N91-16801
DE-FG02-90ER-53302 ..... N91-16767
DE-FG03-86SF-16306 ..... N91-16435
DE-FG05-80ET-53088 ..... N91-16748
DE-FG05-84ER-40154 ..... N91-16828
DE-FG05-85ER-13435 ..... N91-16083
DE-FG05-86ER-13629 ..... N91-16151
DE-FG05-86ER-53217 ..... N91-16721
DE-FG05-86ER-60473 ..... N91-16717
DE-FG05-87ER-52147 ..... N91-16346
N91-16763
N91-16764
DE-FG05-88ER-13867 ..... N91-16723
DE-FG05-88ER-13971 ..... N91-16715
DE-FG05-88ER-53267 ..... N91-16762
DE-FG06-86ER-25019 ..... N91-16341
DE-FG06-88ER-25061 ..... N91-16258
DE-FG06-88ER-40427 ..... N91-16712
DE-FG21-86MC-23161 ..... N91-16259
DEN3-336 ..... N91-16021
DFG-KU-474/13-1 ..... N91-16967
DFG-NA-189/1-1 ..... N91-16364
DFG-325/21-4/28-1-2 ..... N91-16972
DTFA01-83-4-10579 ..... N91-16206
DTFA01-87-C-00014 ..... N91-15989
EES-333/88-11/FU-D N91-16781
EY-75-C-02-141500 ..... N91-16648
F04611-86-K-0076 ..... N91-16110
F04611-87-C-0025 ..... N91-16172
F04611-87-K-0006 ..... N91-16099
F04611-89-C-0047 ..... N91-16103
F04701-88-C-0089 ..... N91-16248
N91-16352
N91-16355
N91-16362
N91-16489
F19628-85-C-0003 ..... N91-16584
N91-16585
N91-16587
N91-16590
N91-16610
F19628-86-C-0100 ..... N91-16776
F19628-87-C-0204 ..... N91-16741
F19628-87-K-0020 ..... N91-16475
F19628-88-C-0072 ..... N91-16488
F19628-88-D-0032 ..... N91-16617
N91-16618
N91-16619
F19628-88-K-0042 ..... N91-16661
F19628-89-C-0001 ..... N91-16004
F19628-89-C-0033 ..... N91-16482
F19628-90-C-0002 ..... N91-16195
N91-16361
N91-16816
F30602-86-C-0195 ..... N91-16583
F30602-87-C-0100 ..... N91-16353
F30602-87-C-0133 ..... N91-16588
F30602-87-D-0086 ..... N91-16608
N91-16609
F30602-88-D-0026 ..... N91-16604
F30602-88-D-0027 ..... N91-16207
N91-16208
N91-16209
N91-16615
F30602-88-D-0028 ..... N91-16245
F33615-82-C-5036 ..... N91-16591
F33615-83-C-2330 ..... N91-16328
N91-16330
F33615-85-C-5122 ..... N91-16591
N91-16594
F33615-86-C-2646 ..... N91-16327
F33615-87-C-0534 ..... N91-16708
F33615-88-C-0004 ..... N91-16586
F33615-88-C-5437 ..... N91-16124
F33615-89-C-1848 ..... N91-16622
F33615-89-C-2942 ..... N91-16382
F33615-89-C-3213 ..... N91-16125
F49620-87-C-0042 ..... N91-16156
F49620-87-C-0054 ..... N91-16409
F49620-88-C-0037 ..... N91-16381
F49620-88-C-0055 ..... N91-16779
F49620-89-K-0005 ..... N91-16643
MDA903-85-C-0139 ..... N91-16830
MDA903-86-C-0345 ..... N91-16844
MDA903-87-C-0056 ..... N91-16592
N91-16593
N91-16603
MDA903-88-C-0031 ..... N91-16567
MDA903-89-K-0074 ..... N91-16567
MDA972-88-C-0024 ..... N91-16639
MDA972-88-J-1006 ..... N91-16800
NAGW-1009 ..... N91-16960
NAGW-1331 ..... N91-16008
NAG1-336 ..... N91-16411
NAG1-562 ..... N91-16212
NAG1-1024 ..... N91-16627
NAG1-1029 ..... N91-16010
N91-16011
N91-16013
NAG1-1071 ..... N91-16296
NAG2-193 ..... N91-15981
NAG2-208 ..... N91-16977
NAG2-314 ..... N91-16289
NAG2-541 ..... N91-16211
NAG2-565 ..... N91-15986
NAG2-593 ..... N91-16639
NAG3-720 ..... N91-16120
NAG3-1125 ..... N91-16194
NAG3-1186 ..... N91-16596
NAG5-389 ..... N91-16472
N91-16473
NAG5-1331 ..... N91-16132
NAG5-1417 ..... N91-16813
NAG8-708 ..... N91-16032
NAG8-757 ..... N91-16163
NAG9-357 ..... N91-16059
NAS1-18585 ..... N91-16033
NAS1-18605 ..... N91-15991
N91-15994
N91-15995
N91-15996
N91-16305
N91-16306
N91-16664
NAS3-24643 ..... N91-16063
NAS3-25468 ..... N91-16150
NAS5-25451 ..... N91-16908
NAS5-29386 ..... N91-16536
NAS7-918 ..... N91-16532
N91-16533
N91-16534
N91-16535
N91-16908
NAS8-30490 ..... N91-16064
NAS8-37127 ..... N91-16503
NAS8-37377 ..... N91-16523
NAS8-37589 ..... N91-16332
N91-16333
N91-16334
NAS8-38427 ..... N91-16056
NCA2-223 ..... N91-16012
NCC2-371 ..... N91-16065
N91-16727
N91-16728
NCC2-579 ..... N91-15987
NCC3-74 ..... N91-16350
NCC3-158 ..... N91-16191
NET-88-1-82 ..... N91-16781
NGT-21-002-800 ..... N91-16045
N91-16050
NIH-RR-01838 ..... N91-16542
NR PROJ. 042-267 ..... N91-16666
NR PROJ. 667549 ..... N91-16549
NSF ASC-87-15728 ..... N91-16573
NSF AST-84-51725 ..... N91-16953
NSF AST-88-18900 ..... N91-16922
NSF AST-89-96123 ..... N91-16897
NSF CCR-83-20136 ..... N91-16620
NSF CCR-86-11442 ..... N91-16611
NSF CCR-86-13353 ..... N91-16606
NSF CCR-86-19817 ..... N91-16605
NSF CCR-89-20694 ..... N91-16606
NSF CES-86-14957 ..... N91-16398
NSF DCI-86-01152 ..... N91-16622
NSF DDM-89-01495 ..... N91-16626
NSF DMC-88-07550 ..... N91-16605
NSF DMR-88-02487 ..... N91-16810
NSF DMR-88-09854 ..... N91-16792
NSF DMR-89-13878 ..... N91-16796
NSF DMS-85-0403 ..... N91-16646
NSF DMS-89-02576 ..... N91-16661
NSF DMS-90-12751 ..... N91-16660
NSF DPP-88-18229 ..... N91-16487
NSF IRI-85-19517 ..... N91-16844
NSF NCR-88-21764 ..... N91-16581
NSF PHY-80-08495 ..... N91-16827
NSF RII-86-10669 ..... N91-16936
N91-16938
NSF UPP-84-19272 ..... N91-16487
N00014-82-K-0193 ..... N91-16210
N91-16387
N91-16620
N00014-82-K-0741 ..... N91-16678
N00014-83-K-0125 ..... N91-16611
N00014-83-K-0494 ..... N91-16740
N00014-84-C-0134 ..... N91-16185
N00014-84-K-0405 ..... N91-16526
N00014-84-K-0656 ..... N91-16098
N00014-85-G-0093 ..... N91-16567
N00014-85-K-0124 ..... N91-16244
N91-16624
N91-16640
N00014-85-K-0168 ..... N91-16611
N00014-85-K-0198 ..... N91-16626
N00014-85-K-0524 ..... N91-16549
N00014-85-K-0570 ..... N91-16623
N00014-86-C-0086 ..... N91-16740
N00014-86-C-0567 ..... N91-16202
N00014-86-C-2021 ..... N91-16295
N00014-86-K-0310 ..... N91-16660
N00014-86-K-0442 ..... N91-16606
N00014-86-K-0512 ..... N91-16356
N00014-86-K-0680 ..... N91-16622
N91-16844
N00014-86-K-0685 ..... N91-16386
N00014-87-C-0857 ..... N91-16247
N00014-87-C-2354 ..... N91-16205
N00014-87-K-0320 ..... N91-16650
N00014-87-K-0327 ..... N91-16237
N00014-87-K-0396 ..... N91-16363
N00014-87-K-0517 ..... N91-16155
N00014-87-K-0825 ..... N91-16640
N00014-87-K-0828 ..... N91-16571
N91-16572
N00014-88-C-0512 ..... N91-16818
N00014-88-C-0692 ..... N91-16855
N00014-88-F-0019 ..... N91-16791
N00014-88-K-0302 ..... N91-16146
N00014-88-K-0341 ..... N91-16246
N00014-88-K-0564 ..... N91-16817
N00014-88-K-0738 ..... N91-16640
N00014-88-K-0825 ..... N91-16244
N00014-89-J-1052 ..... N91-16108
N00014-89-J-1164 ..... N91-16292
N00014-89-J-1171 ..... N91-16634
N00014-89-J-1189 ..... N91-16422
N00014-89-J-1197 ..... N91-16147
N00014-89-J-1627 ..... N91-16666
N00014-89-J-1660 ..... N91-16525
N00014-89-J-1690 ..... N91-16529
N00014-89-J-1988 ..... N91-16611
N00014-90-J-1148 ..... N91-16807
N00014-90-J-1193 ..... N91-16819
N00014-90-J-1218 ..... N91-16294
N00014-90-J-1270 ..... N91-16245
N00014-90-J-1284 ..... N91-16612
N00014-90-J-1320 ..... N91-16154
N00014-90-J-1398 ..... N91-16067
N00014-90-J-1495 ..... N91-16185
N00014-90-J-1599 ..... N91-16605
N00014-90-WX-24264 ..... N91-16109
N00173-90-WR-00172 ..... N91-16240
N000143-86-K-0245 ..... N91-16837
SRI PROJ. ECU-7929 ..... N91-16643
SRI PROJ. 8562 ..... N91-16168
STEV-506-266-4 ..... N91-16706
SWRI PROJ. 14-6253 ..... N91-16539
TATP-003604020 ..... N91-16013
W-31-109-ENG-38 ..... N91-16101
N91-16115
N91-16118
N91-16137

N91-16141
N91-16222
N91-16229
N91-16230
N91-16231
N91-16260
N91-16262
N91-16265
N91-16305
N91-16370
N91-16373
N91-16375
N91-16398
N91-16436
N91-16447
N91-16448
N91-16573
N91-16576
N91-16632
N91-16641
N91-16646
N91-16714
N91-16720
N91-16737
N91-16754
N91-16765
N91-16766
N91-16783
N91-16784
N91-16791
N91-16792
N91-16796
N91-16809
N91-16810
N91-16984
W-7405-ENG-36 ..... N91-16042
N91-16085
N91-16090
N91-16091
N91-16093
N91-16122
N91-16174
N91-16255
N91-16263
N91-16283
N91-16288
N91-16323
N91-16342
N91-16343
N91-16348
N91-16351
N91-16357
N91-16439
N91-16499
N91-16578
N91-16642
N91-16716
N91-16750
N91-16755
N91-16772
N91-16777
N91-16778
N91-16786
N91-16968
W-7405-ENG-48 ..... N91-16080
N91-16082
N91-16084
N91-16087
N91-16088
N91-16158
N91-16159
N91-16162
N91-16181
N91-16182
N91-16224
N91-16324
N91-16340
N91-16344
N91-16349
N91-16437
N91-16455
N91-16457
N91-16458
N91-16459
N91-16462
N91-16469
N91-16497
N91-16498
N91-16538
N91-16577
N91-16633
N91-16672
N91-16713
N91-16724
N91-16736
N91-16758

W-7405-ENG-82 ..... N91-16089
N91-16100
N91-16347
N91-16770
N91-16799
199-04-16-11 ..... N91-16981
505-59-54-01 ..... N91-16033
505-61-11-02 ..... N91-16682
505-63-1A N91-16304
505-63-01 ..... N91-16414
505-69-51 ..... N91-16001
505-90-21-01 ..... N91-15991
N91-15994
N91-15995
N91-15996
N91-16306
N91-16664
506-40-21 ..... N91-16407
506-40-91-01 ..... N91-16058
506-42-31 ..... N91-16063
506-49-31-03 ..... N91-16832
510-01-01 ..... N91-16075
590-13-11 ..... N91-16128
590-14-41-02 ..... N91-16057
656-61-12-01 ..... N91-16535
665-10-70 ..... N91-16536
776-33-41 ..... N91-16679

N91-16759
N91-16761
N91-16768
N91-16769
N91-16771
N91-16773
N91-16775
N91-16793
N91-16794
N91-16798
N91-16829
N91-16850
N91-16982
N91-16985

Typical Report Number Index Listing

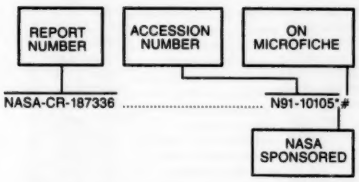

Listings in this index are arranged alphanumerically by report number. The accession number denotes the number by which the citation is identified. An asterisk (*) indicates that the item is a NASA report. A pound sign (#) indicates that the item is available on microfiche.

A-89269 ..... N91-16001* #
A-90262 ..... N91-16414* #
A-91029 ..... N91-16012* #

AAE-241-VOL-1 ..... N91-16045* #
AAE-241-VOL-2 ..... N91-16050* #

AAMRL-TR-90-019 ..... N91-16708 #

AAR-247 ..... N91-16013* #
AAR-248-PT-2 ..... N91-16011* #
AAR-252 ..... N91-16010* #

ACT-114 ..... N91-16623 #

AD-A224667 ..... N91-16552 #
AD-A226698 ..... N91-16583 #
AD-A226722 ..... N91-16837 #
AD-A226723 ..... N91-16584 #
AD-A226725 ..... N91-16585 #
AD-A226729 ..... N91-16586 #
AD-A226760 ..... N91-16169 #
AD-A226763 ..... N91-16352 #
AD-A226773 ..... N91-16474 #
AD-A226778 ..... N91-16965 #
AD-A226785 ..... N91-16235 #
AD-A226811 ..... N91-16097 #
AD-A226814 ..... N91-16475 #
AD-A226817 ..... N91-16587 #
AD-A226820 ..... N91-16588 #
AD-A226821 ..... N91-16353 #
AD-A226822 ..... N91-16354 #
AD-A226826 ..... N91-16548 #
AD-A226829 ..... N91-16285 #
AD-A226832 ..... N91-16540 #
AD-A226844 ..... N91-16098 #
AD-A226851 ..... N91-16673 #
AD-A226852 ..... N91-16649 #
AD-A226855 ..... N91-16286 #
AD-A226867 ..... N91-16830 #
AD-A226869 ..... N91-16184 #
AD-A226969 ..... N91-16838 #
AD-A227122 ..... N91-16476 #
AD-A227123 ..... N91-16477 #
AD-A227124 ..... N91-16478 #
AD-A227125 ..... N91-16479 #
AD-A227126 ..... N91-16480 #
AD-A227127 ..... N91-16481 #
AD-A227181 ..... N91-16185 #
AD-A227214 ..... N91-16482 #
AD-A227222 ..... N91-16003 #
AD-A227225 ..... N91-16327 #
AD-A227226 ..... N91-16328 #
AD-A227236 ..... N91-16146 #
AD-A227247 ..... N91-16329 #
AD-A227260 ..... N91-16565 #
AD-A227261 ..... N91-16589 #
AD-A227267 ..... N91-16355 #
AD-A227276 ..... N91-16381 #
AD-A227331 ..... N91-16186 #
AD-A227450 ..... N91-16544 #
AD-A227451 ..... N91-16677 #
AD-A227453 ..... N91-16147 #
AD-A227462 ..... N91-16055 #
AD-A227469 ..... N91-16529 #
AD-A227473 ..... N91-16330 #
AD-A227482 ..... N91-16236 #
AD-A227486 ..... N91-15999 #
AD-A227487 ..... N91-16356 #
AD-A227489 ..... N91-16170 #
AD-A227505 ..... N91-16382 #
AD-A227506 ..... N91-16124 #
AD-A227507 ..... N91-16029 #
AD-A227511 ..... N91-16383 #
AD-A227564 ..... N91-16590 #
AD-A227571 ..... N91-16171 #
AD-A227575 ..... N91-16740 #
AD-A227576 ..... N91-16237 #
AD-A227579 ..... N91-16067 #
AD-A227581 ..... N91-16287 #
AD-A227582 ..... N91-16416 #
AD-A227644 ..... N91-16518 #
AD-A227651 ..... N91-16591 #
AD-A227655 ..... N91-16519 #
AD-A227668 ..... N91-16520 #
AD-A227676 ..... N91-16678 #
AD-A227677 ..... N91-16099 #
AD-A227679 ..... N91-16007 #
AD-A227682 ..... N91-16634 #
AD-A227683 ..... N91-16172 #
AD-A227687 ..... N91-16521 #
AD-A227688 ..... N91-16839 #
AD-A227690 ..... N91-16483 #
AD-A227692 ..... N91-16807 #
AD-A227697 ..... N91-16549 #
AD-A227700 ..... N91-16125 #
AD-A227703 ..... N91-16187 #
AD-A227713 ..... N91-16776 #
AD-A227721 ..... N91-16484 #
AD-A227724 ..... N91-16522 #
AD-A227728 ..... N91-16188 #
AD-A227731 ..... N91-16485 #
AD-A227742 ..... N91-16650 #
AD-A227744 ..... N91-16635 #
AD-A227757 ..... N91-16020 #
AD-A227759 ..... N91-16331 #
AD-A227760 ..... N91-16238 #
AD-A227762 ..... N91-16239 #
AD-A227763 ..... N91-16486 #
AD-A227764 ..... N91-16487 #
AD-A227766 ..... N91-16592 #
AD-A227767 ..... N91-16593 #
AD-A227782 ..... N91-16545 #
AD-A227783 ..... N91-16068 #
AD-A227827 ..... N91-16594 #
AD-A227835 ..... N91-16291 #
AD-A227850 ..... N91-16708 #
AD-A227852 ..... N91-16603 #
AD-A227856 ..... N91-16604 #
AD-A227857 ..... N91-16154 #
AD-A227858 ..... N91-16605 #
AD-A227875 ..... N91-16606 #
AD-A227879 ..... N91-16636 #
AD-A227884 ..... N91-16607 #
AD-A227891 ..... N91-15741 #
AD-A227893 ..... N91-16608 #
AD-A227894 ..... N91-16609 #
AD-A227902 ..... N91-16421 #
AD-A227910 ..... N91-16129 #
AD-A227915 ..... N91-16841 #
AD-A227920 ..... N91-16031 #
AD-A227922 ..... N91-16637 #
AD-A227931 ..... N91-16525 #
AD-A227941 ..... N91-16816* #
AD-A227942 ..... N91-16195 #
AD-A227948 ..... N91-16292 #
AD-A227961 ..... N91-16567 #
AD-A227965 ..... N91-16196 #
AD-A227966 ..... N91-16488 #
AD-A227972 ..... N91-16638 #
AD-A227975 ..... N91-16408 #
AD-A227976 ..... N91-16665 #
AD-A228021 ..... N91-16197 #
AD-A228027 ..... N91-16610 #
AD-A228038 ..... N91-16489 #
AD-A228045 ..... N91-16817 #
AD-A228057 ..... N91-16198 #
AD-A228058 ..... N91-16199 #
AD-A228067 ..... N91-16243 #
AD-A228113 ..... N91-16611 #
AD-A228134 ..... N91-16071 #
AD-A228142 ..... N91-16660 #
AD-A228147 ..... N91-16200 #
AD-A228149 ..... N91-16009 #
AD-A228150 ..... N91-16103 #
AD-A228179 ..... N91-16666 #
AD-A228194 ..... N91-15990 #
AD-A228202 ..... N91-16155 #
AD-A228215 ..... N91-16072 #
AD-A228218 ..... N91-16361 #
AD-A228221 ..... N91-16742 #
AD-A228231 ..... N91-16293 #
AD-A228232 ..... N91-16177 #
AD-A228237 ..... N91-16130 #
AD-A228239 ..... N91-16842 #
AD-A228256 ..... N91-16639* #
AD-A228278 ..... N91-16612 #
AD-A228292 ..... N91-16613 #
AD-A228293 ..... N91-16667 #
AD-A228294 ..... N91-16362 #
AD-A228295 ..... N91-16201 #
AD-A228345 ..... N91-16640 #
AD-A228346 ..... N91-16244 #
AD-A228357 ..... N91-16104 #
AD-A228359 ..... N91-16818 #
AD-A228370 ..... N91-16105 #
AD-A228371 ..... N91-16073 #
AD-A228373 ..... N91-16106 #
AD-A228427 ..... N91-16614 #
AD-A228429 ..... N91-16819 #
AD-A228433 ..... N91-16526 #
AD-A228437 ..... N91-16661 #
AD-A228442 ..... N91-16615 #
AD-A228454 ..... N91-16616 #
AD-A228455 ..... N91-16617 #
AD-A228473 ..... N91-16618 #
AD-A228475 ..... N91-16619 #
AD-A228535 ..... N91-16107 #
AD-A228539 ..... N91-16363 #
AD-A228541 ..... N91-16550 #
AD-A228545 ..... N91-16202 #
AD-A228549 ..... N91-16203 #
AD-A228579 ..... N91-16108 #
AD-A228580 ..... N91-16620 #
AD-A228613 ..... N91-16245 #
AD-A228614 ..... N91-16621 #
AD-A228615 ..... N91-16820 #
AD-A228616 ..... N91-16622 #
AD-A228623 ..... N91-16527 #
AD-A228641 ..... N91-16204 #
AD-A228691 ..... N91-16386* #
AD-A228740 ..... N91-16623 #
AD-A228741 ..... N91-16571 #
AD-A228744 ..... N91-16572 #
AD-A228749 ..... N91-16779 #
AD-A228750 ..... N91-16821 #
AD-A228756 ..... N91-16205 #
AD-A228757 ..... N91-16294 #
AD-A228758 ..... N91-16246 #
AD-A228769 ..... N91-16109 #
AD-A228772 ..... N91-16247 #
AD-A228773 ..... N91-16980 #
AD-A228774 ..... N91-16855 #
AD-A228782 ..... N91-16624 #
AD-A228784 ..... N91-16206 #
AD-A228797 ..... N91-16551 #
AD-A228802 ..... N91-16336 #
AD-A228812 ..... N91-16207 #
AD-A228813 ..... N91-16208 #
AD-A228814 ..... N91-16209 #
AD-A228815 ..... N91-16210 #
AD-A228817 ..... N91-16387 #
AD-A228844 ..... N91-16248 #
AD-A228851 ..... N91-16625 #
AD-A228854 ..... N91-16626 #
AD-A228867 ..... N91-16709 #
AD-A228869 ..... N91-16110 #

AD-A228870 ..... N91-16422 #
AD-A228871 ..... N91-16004 #
AD-A228872 ..... N91-16743 #
AD-A228873 ..... N91-16843 #
AD-A228874 ..... N91-16643 #
AD-A228875 ..... N91-16844 #
AD-A228876 ..... N91-16156 #
AD-A228877 ..... N91-16409 #
AD-A228882 ..... N91-15976 #
AD-A228884 ..... N91-16295 #
AD-A228888 ..... N91-16662 #
AD-A228889 ..... N91-16663 #
AD-A228890 ..... N91-16410 #
AD-A228896 ..... N91-16668 #

AEDC-TSR-90-V13 ..... N91-16293 #

AFHRL-TP-90-66 ..... N91-16586 #

AFHRL-TR-89-66 ..... N91-16552 #

AFIT/CI/CIA-90-026D ..... N91-16665 #
AFIT/CI/CIA-90-028D ..... N91-16408 #
AFIT/CI/CIA-90-030D ..... N91-16638 #
AFIT/CI/CIA-90-068 ..... N91-16839 #
AFIT/CI/CIA-90-076 ..... N91-16487 #
AFIT/CI/CIA-90-077 ..... N91-16486 #
AFIT/CI/CIA-90-078 ..... N91-16519 #
AFIT/CI/CIA-90-079 ..... N91-16485 #
AFIT/CI/CIA-90-081 ..... N91-16518 #
AFIT/CI/CIA-90-094 ..... N91-16188 #
AFIT/CI/CIA-90-098 ..... N91-16521 #
AFIT/CI/CIA-90-099 ..... N91-16522 #
AFIT/CI/CIA-90-103 ..... N91-16527 #
AFIT/CI/CIA-90-104 ..... N91-16520 #
AFIT/CI/CIA-90-108 ..... N91-16483 #
AFIT/CI/CIA-90-109 ..... N91-16187 #
AFIT/CI/CIA-90-110 ..... N91-16484 #
AFIT/CI/CIA-90-114 ..... N91-16421 #

AFIT/EN-TR-90-5 ..... N91-16474 #

AFIT/GE/ENG/90S-02 ..... N91-16003 #

AFOSR-90-0948TR ..... N91-16285 #
AFOSR-90-0956TR ..... N91-16540 #
AFOSR-90-0965TR ..... N91-16548 #
AFOSR-90-0971TR ..... N91-16235 #
AFOSR-90-0972TR ..... N91-16354 #
AFOSR-90-1027TR ..... N91-16291 #
AFOSR-90-1031TR ..... N91-16381 #
AFOSR-90-1034TR ..... N91-16184 #
AFOSR-90-1066TR ..... N91-16156 #
AFOSR-90-1073TR ..... N91-16779 #
AFOSR-90-1074TR ..... N91-16409 #
AFOSR-90-1103TR ..... N91-16743 #
AFOSR-90-1105TR ..... N91-16821 #
AFOSR-90-1106TR ..... N91-16843 #
AFOSR-90-1111TR ..... N91-16980 #
AFOSR-90-1118TR ..... N91-16550 #
AFOSR-90-1130TR ..... N91-16551 #

AGARD-CAL-91/1 ..... N91-16833 #

AGARD-CP-490 ..... N91-16553 #

AI-TR-1232 ..... N91-16244 #
AI-TR-1245 ..... N91-16640 #
AI-TR-1247 ..... N91-16386* #

AL-TR-90-031 ..... N91-16103 #
AL-TR-90-038 ..... N91-16110 #
AL-TR-90-047 ..... N91-16099 #
AL-TR-90-049 ..... N91-16172 #

ANL-HEP-CP-90-05 ..... N91-16632 #

ANL-HEP-PR-90-28 ..... N91-16737 #

ANL-TRANS-89-52 ..... N91-16265 #

ANL-90/11 ..... N91-16984 #

ANL/ESD-3 ..... N91-16375 #

ANL/FPP/TM-247 ..... N91-16222 #

ARL-PROP-TM-439 ..... N91-16020 #

ARL/PSU/TM-90-227 ..... N91-16529 #

ARO-23802.1-MS-F ..... N91-16243 #
ARO-23915.6-EG ..... N91-16336 #
ARO-23921.5-CH ..... N91-16107 #
ARO-24377.9-EG ..... N91-16410 #
ARO-24543.13-EL ..... N91-16200 #
ARO-24548.3-MS-A ..... N91-16129 #
ARO-24626.155-PH-UIR ..... N91-16742 #
ARO-24862.11-MA-SDI ..... N91-16663 #
ARO-25130.21-GS ..... N91-16201 #
ARO-25323.6-MA-SDI ..... N91-16625 #
ARO-25839.31-MA ..... N91-16668 #
ARO-25839.32-MA ..... N91-16613 #
ARO-25839.33-MA ..... N91-16667 #
ARO-25839.34-MA ..... N91-16636 #
ARO-25839.35-MA ..... N91-16662 #
ARO-27283.1-EL-CF ..... N91-16842 #

ATC-171 ..... N91-16206 #

AVSCOM-TR-91-C-002 ..... N91-16304* #

AWS-TR-89/001-VOL-1 ..... N91-16476 #
AWS-TR-89/002-VOL-2 ..... N91-16477 #
AWS-TR-89/003-VOL-3 ..... N91-16478 #
AWS-TR-89/004-VOL-4 ..... N91-16479 #
AWS-TR-89/007-VOL-7 ..... N91-16480 #
AWS-TR-89/010-VOL-10 ..... N91-16481 #

BBC-RD-1990/7 ..... N91-16189
BBC-RD-1990/9 ..... N91-16190
BBC-RD-1990/10 ..... N91-16680
BBC-RD-1990/13 ..... N91-16681
BBC-RD-1990/14 ..... N91-16595

BCRS-90-03 ..... N91-16425 #
BCRS-90-04 ..... N91-16426 #
BCRS-90-08 ..... N91-16427 #
BCRS-90-09 ..... N91-16428 #
BCRS-90-13 ..... N91-16429 #
BCRS-90-14 ..... N91-16430 #

BER-68 ..... N91-16251 #

BNL-44410 ..... N91-16453 #
BNL-44417 ..... N91-16446 #
BNL-44429 ..... N91-16747 #
BNL-44431 ..... N91-16733 #
BNL-44536 ..... N91-16542 #
BNL-44573 ..... N91-16800 #
BNL-45207 ..... N91-16803 #
BNL-45227 ..... N91-16804 #

BONN-IR-90-34 ..... N91-16729 #
BONN-IR-90-38 ..... N91-16730 #
BONN-IR-90-39 ..... N91-16493 #
BONN-IR-90-42 ..... N91-16731 #

BRA-91-W001R ..... N91-16295 #

BRL-MR-3860 ..... N91-16565 #
BRL-MR-3870 ..... N91-15990 #

BRL-TR-3147 ..... N91-16589 #
BRL-TR-3149 ..... N91-16029 #
BRL-TR-3153 ..... N91-16287 #
BRL-TR-3159 ..... N91-16104 #
BRL-TR-3163 ..... N91-16106 #
BRL-TR-3165 ..... N91-16105 #

BR114980 ..... N91-16192 #
BR115041 ..... N91-16241 #
BR115187 ..... N91-16193 #
BR115205 ..... N91-16035 #

C-937 ..... N91-16247 #

CAL-1811R ..... N91-16740 #

CAR-90-1 ..... N91-16059* #

CDRL-1810 ..... N91-16619 #
CDRL-1820 ..... N91-16618 #

CEQ-90010530 ..... N91-16450 #

CER-90-12 ..... N91-16605 #

CERL-SR-N-90/16 ..... N91-16416 #

CESAR-90/12 ..... N91-16376 #

CMU/SEI-88-TR-16 ..... N91-16610 #
CMU/SEI-90-SR-10 ..... N91-16585 #
CMU/SEI-90-TR-6 ..... N91-16584 #
CMU/SEI-90-TR-7 ..... N91-16587 #

CONF-890770-9 ..... N91-16377 #
CONF-890770-10 ..... N91-16066 #
CONF-890802-27 ..... N91-16784 #
CONF-890802-28 ..... N91-16322 #
CONF-890814-10 ..... N91-16448 #
CONF-890836-24 ..... N91-16224 #
CONF-890836-25 ..... N91-16142 #
CONF-890855-60 ..... N91-16395 #
CONF-890928-24 ..... N91-16087 #
CONF-891007-120 ..... N91-16766 #
CONF-891031-11 ..... N91-16469 #
CONF-891119-132 ..... N91-16792 #
CONF-891163-4 ..... N91-16351 #
CONF-891204-33 ..... N91-16118 #
CONF-891206-12 ..... N91-16720 #
CONF-891208-31 ..... N91-16260 #
CONF-891273-4 ..... N91-16573 #
CONF-900102-5 ..... N91-16373 #
CONF-900121-6 ..... N91-16447 #
CONF-900140-21 ..... N91-16340 #
CONF-900140-22 ..... N91-16714 #
CONF-900140-23 ..... N91-16342 #
CONF-900140-27 ..... N91-16769 #
CONF-900163-8 ..... N91-16632 #
CONF-900163-9 ..... N91-16348 #
CONF-900189-1 ..... N91-16343 #
CONF-900255-2 ..... N91-16497 #
CONF-900264-6 ..... N91-16346 #
CONF-900285-4 ..... N91-16088 #
CONF-900285-5 ..... N91-16850 #
CONF-900302-2 ..... N91-16801 #
CONF-900315-3 ..... N91-16436 #
CONF-900331-2 ..... N91-16733 #
CONF-900331-3 ..... N91-16747 #
CONF-900348-2 ..... N91-16316 #
CONF-900348-5 ..... N91-16790 #
CONF-900419-4 ..... N91-16137 #
CONF-900424-1 ..... N91-16788 #
CONF-900435-1 ..... N91-16499 #
CONF-900450-3 ..... N91-16798 #
CONF-900451-3 ..... N91-16800 #
CONF-900455-1 ..... N91-16713 #
CONF-900466-15 ..... N91-16719 #
CONF-900466-31 ..... N91-16344 #
CONF-900466-38 ..... N91-16791 #
CONF-900466-40 ..... N91-16794 #
CONF-900466-41 ..... N91-16228 #
CONF-900466-42 ..... N91-16793 #
CONF-900486-1 ..... N91-16139 #
CONF-900491-4 ..... N91-16084 #
CONF-900491-5 ..... N91-16538 #
CONF-900505-4 ..... N91-16144 #
CONF-900542-4 ..... N91-16795 #
CONF-900546-2 ..... N91-16141 #
CONF-900546-5 ..... N91-16143 #
CONF-900557-2 ..... N91-16750 #
CONF-900557-5 ..... N91-16771 #
CONF-900557-8 ..... N91-16773 #
CONF-900557-9 ..... N91-16325 #
CONF-900559-14 ..... N91-16576 #
CONF-900563-6 ..... N91-16321 #
CONF-900591-2 ..... N91-16090 #
CONF-900602-7 ..... N91-16749 #
CONF-900602-13 ..... N91-16774 #
CONF-900603-1 ..... N91-16772 #
CONF-900608-17 ..... N91-16044 #
CONF-900617-11 ..... N91-16115 #
CONF-900617-15 ..... N91-16398 #
CONF-900656-1 ..... N91-16091 #
CONF-900704-4 ..... N91-16080 #
CONF-900704-6 ..... N91-16138 #
CONF-900704-7 ..... N91-16081 #
CONF-900704-8 ..... N91-16082 #
CONF-900705-2 ..... N91-16174 #
CONF-900705-3 ..... N91-16453 #
CONF-900712-1 ..... N91-16159 #
CONF-900712-2 ..... N91-16158 #
CONF-900712-3 ..... N91-16162 #
CONF-900723-3 ..... N91-16218 #
CONF-900723-5 ..... N91-16394 #
CONF-900723-6 ..... N91-16219 #
CONF-900723-7 ..... N91-16718 #
CONF-900723-11 ..... N91-16220 #
CONF-900724-6 ..... N91-16452 #
CONF-900729-1 ..... N91-16368 #
CONF-900729-2 ..... N91-16369 #
CONF-900742-1 ..... N91-16175 #
CONF-900756-1 ..... N91-16574 #
CONF-900756-4 ..... N91-16579 #
CONF-900774-1 ..... N91-16116 #
CONF-900775-1 ..... N91-16451 #
CONF-900780-3 ..... N91-16378 #
CONF-900780-5 ..... N91-16379* #
CONF-900789-1 ..... N91-16117 #
CONF-900792-1 ..... N91-16221 #
CONF-900792-3 ..... N91-16160 #
CONF-900792-4 ..... N91-16264 #
CONF-900792-5 ..... N91-16161 #
CONF-900793-1 ..... N91-16641 #
CONF-900795-1 ..... N91-16372 #
CONF-900796-1 ..... N91-16457 #

CONF-900796-2 ..... N91-16458 #
CONF-900799-1 ..... N91-16726 #
CONF-900926-3 ..... N91-16096 #
CONF-900936-9 ..... N91-16806 #
CONF-900936-20 ..... N91-16810 #
CONF-900944-7 ..... N91-16775 #
CONF-900944-10 ..... N91-16803 #
CONF-900944-11 ..... N91-16804 #
CONF-900944-26 ..... N91-16674 #
CONF-901004-5 ..... N91-16093 #
CONF-901008-4 ..... N91-16122 #
CONF-901053-1 ..... N91-16326 #
CONF-901105-15 ..... N91-16805 #
CONF-901105-29 ..... N91-16127 #
CONF-901105-30 ..... N91-16811 #
CONF-901105-36 ..... N91-16812 #
CONF-901105-38 ..... N91-16814 #
CONF-901169-2 ..... N91-16240 #
CONF-910117-3-PT-2 ..... N91-16054 #
CONF-910223-2 ..... N91-16385* #
CONF-910238-2 ..... N91-16659 #
CONF-910251-1 ..... N91-16242 #
CONF-8810423-1 ..... N91-16783 #
CONF-8904308-2 ..... N91-16646 #
CONF-8906270-5 ..... N91-16721 #
CONF-8907189-1 ..... N91-16786 #
CONF-8907191-1 ..... N91-16459 #
CONF-8908106-6 ..... N91-16796 #
CONF-8908128-2 ..... N91-16739 #
CONF-8908134-32 ..... N91-16349 #
CONF-8908178-2 ..... N91-16754 #
CONF-8908185-2 ..... N91-16324 #
CONF-8908222-2 ..... N91-16319 #
CONF-8909192-2 ..... N91-16736 #
CONF-8909331-1 ..... N91-16765 #
CONF-8910401-2 ..... N91-16809 #
CONF-8911130 ..... N91-16755 #
CONF-8911193-1 ..... N91-16399 #
CONF-9002113-1 ..... N91-16446 #
CONF-9002117-1 ..... N91-16712 #
CONF-9002120-1 ..... N91-16370 #
CONF-9002159-1 ..... N91-16546 #
CONF-9003128-3 ..... N91-16182 #
CONF-9003149-2 ..... N91-16042 #
CONF-9003149-3 ..... N91-16578 #
CONF-9003152-1 ..... N91-16787 #
CONF-9003153-1 ..... N91-16085 #
CONF-9004146-8 ..... N91-16738 #
CONF-9004159-5 ..... N91-16633 #
CONF-9004159-6 ..... N91-16647 #
CONF-9004180-1 ..... N91-16498 #
CONF-9004193-1 ..... N91-16789 #
CONF-9004196-2 ..... N91-16229 #
CONF-9004200-1 ..... N91-16461 #
CONF-9004209-1 ..... N91-16735 #
CONF-9005145-3 ..... N91-16101 #
CONF-9005168-1 ..... N91-16262 #
CONF-9005170-1 ..... N91-16542 #
CONF-9005171-1 ..... N91-16454 #
CONF-9005175-1 ..... N91-16226 #
CONF-9005195-1 ..... N91-16231 #
CONF-9005196-1 ..... N91-16230 #
CONF-9005196-2 ..... N91-16439 #
CONF-9005203-1 ..... N91-16829 #
CONF-9005212-1 ..... N91-16323 #
CONF-9005237-8 ..... N91-16288 #
CONF-9006114-1-REV-1 ..... N91-16577 #
CONF-9006146-4 ..... N91-16438 #
CONF-9006146-8 ..... N91-16233 #
CONF-9006149-2 ..... N91-16397 #
CONF-9006162-2 ..... N91-16397 #
CONF-9006171-1 ..... N91-16676 #
CONF-9006172-1 ..... N91-16675 #
CONF-9006179-2 ..... N91-16232 #
CONF-9006189-1 ..... N91-16642 #
CONF-9006282-3 ..... N91-16966 #
CONF-9007101-4-PT-2 ..... N91-16982 #
CONF-9009141-6 ..... N91-16808 #
CONF-9009166-12 ..... N91-16357 #
CONF-9009200-12 ..... N91-16183 #
CONF-9009258-1 ..... N91-16380 #
CONF-9010198-1 ..... N91-16485 #
CONF-9010201-1 ..... N91-16145 #
CONF-9010203-1 ..... N91-16176 #
CONF-9010209-6 ..... N91-16777 #
CONF-9010266-1 ..... N91-16778 #
CONF-9010268-1 ..... N91-16968 #
CONF-9010270-1 ..... N91-16358 #
CONF-9011110-1 ..... N91-16094 #
CONF-9011110-3 ..... N91-16095 #
CONF-9011114-1 ..... N91-16581 #

CPSS-0990-1 ..... N91-16818 #

CRC-569 ..... N91-16171 #

CRDEC-TR-168 ..... N91-16097 #
CRDEC-TR-218 ..... N91-16169 #

CRREL-90-3 ..... N91-16286 #

CSD-TR-960 ..... N91-16605 #

CU-153-1200 ..... N91-16363 #
CU-1531940 ..... N91-16526 #

CWI-CS-R9009 ..... N91-16597 #

DAC-25 ..... N91-16245 #

DE89-000878 ..... N91-16582 #
DE90-000335 ..... N91-16139 #
DE90-000466 ..... N91-16259 #
DE90-002686 ..... N91-16986 #
DE90-003063 ..... N91-16368 #
DE90-005280 ..... N91-16369 #
DE90-006002 ..... N91-16080 #
DE90-006312 ..... N91-16081 #
DE90-007152 ..... N91-16218 #
DE90-007285 ..... N91-16718 #
DE90-007286 ..... N91-16219 #
DE90-007413 ..... N91-16394 #
DE90-007571 ..... N91-16138 #
DE90-007856 ..... N91-16082 #
DE90-008210 ..... N91-16316 #
DE90-008217 ..... N91-16255 #
DE90-008221 ..... N91-16751 #
DE90-008230 ..... N91-16985 #
DE90-008232 ..... N91-16752 #
DE90-008235 ..... N91-16317 #
DE90-008242 ..... N91-16984 #
DE90-008243 ..... N91-16753 #
DE90-008345 ..... N91-16220 #
DE90-008557 ..... N91-16116 #
DE90-008568 ..... N91-16451 #
DE90-008964 ..... N91-16174 #
DE90-009409 ..... N91-16117 #
DE90-009422 ..... N91-16452 #
DE90-009434 ..... N91-16497 #
DE90-009436 ..... N91-16158 #
DE90-009438 ..... N91-16159 #
DE90-009481 ..... N91-16319 #
DE90-009683 ..... N91-16442 #
DE90-009703 ..... N91-16641 #
DE90-009712 ..... N91-16632 #
DE90-009719 ..... N91-16370 #
DE90-009723 ..... N91-16373 #
DE90-009731 ..... N91-16827 #
DE90-009732 ..... N91-16711 #
DE90-009749 ..... N91-16499 #
DE90-009779 ..... N91-16574 #
DE90-009820 ..... N91-16397 #
DE90-009921 ..... N91-16498 #
DE90-009938 ..... N91-16318 #
DE90-009945 ..... N91-16340 #
DE90-009972 ..... N91-16675 #
DE90-009974 ..... N91-16221 #
DE90-009988 ..... N91-16835 #
DE90-010001 ..... N91-16393 #
DE90-010005 ..... N91-16445 #
DE90-010006 ..... N91-16256 #
DE90-010008 ..... N91-16257 #
DE90-010014 ..... N91-16747 #
DE90-010015 ..... N91-16733 #
DE90-010016 ..... N91-16453 #
DE90-010018 ..... N91-16446 #
DE90-010031 ..... N91-16748 #
DE90-010058 ..... N91-16078* #
DE90-010065 ..... N91-16754 #
DE90-010066 ..... N91-16573 #
DE90-010069 ..... N91-16646 #
DE90-010079 ..... N91-16749 #
DE90-010080 ..... N91-16738 #
DE90-010093 ..... N91-16115 #
DE90-010094 ..... N91-16436 #
DE90-010107 ..... N91-16435 #
DE90-010115 ..... N91-16137 #
DE90-010146 ..... N91-16175 #
DE90-010148 ..... N91-16719 #
DE90-010151 ..... N91-16447 #
DE90-010153 ..... N91-16079 #
DE90-010169 ..... N91-16785 #
DE90-010189 ..... N91-16468 #
DE90-010195 ..... N91-16371 #
DE90-010196 ..... N91-16217 #
DE90-010198 ..... N91-16575 #
DE90-010200 ..... N91-16437 #
DE90-010253 ..... N91-16755 #
DE90-010275 ..... N91-16027 #
DE90-010276 ..... N91-16374 #
DE90-010283 ..... N91-16672 #
DE90-010287 ..... N91-16758 #
DE90-010296 ..... N91-16043 #
DE90-010299 ..... N91-16026 #
DE90-010301 ..... N91-16756 #
DE90-010302 ..... N91-16222 #
DE90-010305 ..... N91-16375 #
DE90-010306 ..... N91-16757 #
DE90-010308 ..... N91-16790 #
DE90-010321 ..... N91-16456 #
DE90-010328 ..... N91-16180 #
DE90-010331 ..... N91-16345 #
DE90-010332 ..... N91-16759 #
DE90-010333 ..... N91-16760 #
DE90-010335 ..... N91-16376 #
DE90-010352 ..... N91-16761 #
DE90-010369 ..... N91-16181 #
DE90-010405 ..... N91-16576 #
DE90-010408 ..... N91-16260 #
DE90-010411 ..... N91-16783 #
DE90-010424 ..... N91-16258 #
DE90-010428 ..... N91-16341 #
DE90-010429 ..... N91-16712 #
DE90-010460 ..... N91-16784 #
DE90-010479 ..... N91-16713 #
DE90-010491 ..... N91-16448 #
DE90-010492 ..... N91-16714 #
DE90-010530 ..... N91-16450 #
DE90-010533 ..... N91-16647 #
DE90-010534 ..... N91-16676 #
DE90-010539 ..... N91-16449 #
DE90-010541 ..... N91-16720 #
DE90-010566 ..... N91-16342 #
DE90-010580 ..... N91-16262 #
DE90-010584 ..... N91-16343 #
DE90-010600 ..... N91-16085 #
DE90-010602 ..... N91-16786 #
DE90-010607 ..... N91-16750 #
DE90-010616 ..... N91-16042 #
DE90-010630 ..... N91-16320 #
DE90-010650 ..... N91-16542 #
DE90-010654 ..... N91-16223 #
DE90-010657 ..... N91-16226 #
DE90-010659 ..... N91-16438 #
DE90-010663 ..... N91-16787 #
DE90-010666 ..... N91-16715 #
DE90-010667 ..... N91-16083 #
DE90-010675 ..... N91-16716 #
DE90-010676 ..... N91-16457 #
DE90-010679 ..... N91-16577 #
DE90-010682 ..... N91-16182 #
DE90-010691 ..... N91-16633 #
DE90-010705 ..... N91-16372 #
DE90-010707 ..... N91-16788 #
DE90-010714 ..... N91-16454 #
DE90-010741 ..... N91-16224 #
DE90-010742 ..... N91-16469 #
DE90-010749 ..... N91-16455 #
DE90-010792 ..... N91-16826 #
DE90-010793 ..... N91-16717 #
DE90-010809 ..... N91-16537 #
DE90-010810 ..... N91-16261 #
DE90-010815 ..... N91-16263 #
DE90-010831 ..... N91-16789 #
DE90-010833 ..... N91-16160 #
DE90-010865 ..... N91-16458 #
DE90-010868 ..... N91-16084 #
DE90-010869 ..... N91-16538 #
DE90-010876 ..... N91-16344 #
DE90-010877 ..... N91-16459 #
DE90-010907 ..... N91-16227 #
DE90-010926 ..... N91-16225 #
DE90-010938 ..... N91-16395 #
DE90-010946 ..... N91-16377 #
DE90-010949 ..... N91-16066 #
DE90-010958 ..... N91-16460 #
DE90-010980 ..... N91-16739 #
DE90-010986 ..... N91-16461 #
DE90-010993 ..... N91-16086 #
DE90-010997 ..... N91-16140 #
DE90-011014 ..... N91-16462 #
DE90-011020 ..... N91-16044 #
DE90-011051 ..... N91-16264 #
DE90-011052 ..... N91-16161 #
DE90-011061 ..... N91-16378 #
DE90-011070 ..... N91-16762 #
DE90-011071 ..... N91-16734 #
DE90-011078 ..... N91-16721 #
DE90-011079 ..... N91-16763 #
DE90-011080 ..... N91-16764 #
DE90-011084 ..... N91-16346 #
DE90-011087 ..... N91-16463 #
DE90-011092 ..... N91-16141 #
DE90-011094 ..... N91-16398 #
DE90-011097 ..... N91-16765 #
DE90-011098 ..... N91-16229 #
DE90-011111 ..... N91-16791 #
DE90-011146 ..... N91-16230 #

DE90-011154 ..... N91-16766 #
DE90-011155 ..... N91-16796 #
DE90-011164 ..... N91-16231 #
DE90-011170 ..... N91-16118 #
DE90-011178 ..... N91-16792 #
DE90-011193 ..... N91-16321 #
DE90-011204 ..... N91-16793 #
DE90-011218 ..... N91-16228 #
DE90-011219 ..... N91-16322 #
DE90-011230 ..... N91-16794 #
DE90-011237 ..... N91-16232 #
DE90-011304 ..... N91-16797 #
DE90-011332 ..... N91-16768 #
DE90-011335 ..... N91-16265 #
DE90-011340 ..... N91-16735 #
DE90-011369 ..... N91-16399 #
DE90-011389 ..... N91-16379* #
DE90-011463 ..... N91-16162 #
DE90-011482 ..... N91-16798 #
DE90-011484 ..... N91-16087 #
DE90-011496 ..... N91-16769 #
DE90-011497 ..... N91-16088 #
DE90-011502 ..... N91-16829 #
DE90-011505 ..... N91-16795 #
DE90-011509 ..... N91-16799 #
DE90-011519 ..... N91-16800 #
DE90-011521 ..... N91-16470 #
DE90-011530 ..... N91-16767 #
DE90-011544 ..... N91-16722 #
DE90-011557 ..... N91-16539 #
DE90-011582 ..... N91-16471 #
DE90-011583 ..... N91-16801 #
DE90-011596 ..... N91-16142 #
DE90-011598 ..... N91-16119 #
DE90-011643 ..... N91-16143 #
DE90-011740 ..... N91-16347 #
DE90-011744 ..... N91-16089 #
DE90-011746 ..... N91-16770 #
DE90-011909 ..... N91-16233 #
DE90-011911 ..... N91-16771 #
DE90-011948 ..... N91-16578 #
DE90-011957 ..... N91-16348 #
DE90-011960 ..... N91-16090 #
DE90-011971 ..... N91-16439 #
DE90-011985 ..... N91-16642 #
DE90-011990 ..... N91-16323 #
DE90-011996 ..... N91-16772 #
DE90-012053 ..... N91-16091 #
DE90-012071 ..... N91-16773 #
DE90-012080 ..... N91-16324 #
DE90-012081 ..... N91-16850 #
DE90-012095 ..... N91-16736 #
DE90-012120 ..... N91-16349 #
DE90-012134 ..... N91-16774 #
DE90-012140 ..... N91-16648 #
DE90-012148 ..... N91-16144 #
DE90-012153 ..... N91-16737 #
DE90-012160 ..... N91-16579 #
DE90-012180 ..... N91-16325 #
DE90-012765 ..... N91-16054 #
DE90-017088 ..... N91-16724 #
DE90-777884 ..... N91-16671 #
DE91-000025 ..... N91-16380 #
DE91-000027 ..... N91-16805 #
DE91-000058 ..... N91-16183 #
DE91-000172 ..... N91-16122 #
DE91-000237 ..... N91-16351 #
DE91-000267 ..... N91-16123 #
DE91-000373 ..... N91-16093 #
DE91-000394 ..... N91-16806 #
DE91-000530 ..... N91-16126 #
DE91-000544 ..... N91-16148 #
DE91-000579 ..... N91-16176 #
DE91-000580 ..... N91-16326 #
DE91-000581 ..... N91-16283 #
DE91-000586 ..... N91-16465 #
DE91-000592 ..... N91-16284 #
DE91-000611 ..... N91-16100 #
DE91-000614 ..... N91-16094 #
DE91-000618 ..... N91-16145 #
DE91-000621 ..... N91-16095 #
DE91-000641 ..... N91-16096 #
DE91-000656 ..... N91-16775 #
DE91-000866 ..... N91-16581 #
DE91-000895 ..... N91-16803 #
DE91-000900 ..... N91-16804 #
DE91-000931 ..... N91-16723 #
DE91-001974 ..... N91-16659 #
DE91-002116 ..... N91-16444 #
DE91-002117 ..... N91-16443 #
DE91-002711 ..... N91-16808 #
DE91-002880 ..... N91-16385* #
DE91-004037 ..... N91-16242 #
DE91-004159 ..... N91-16725 #
DE91-004415 ..... N91-16149 #
DE91-004420 ..... N91-16101 #
DE91-004425 ..... N91-16809 #
DE91-004431 ..... N91-16546 #
DE91-004481 ..... N91-16810 #
DE91-004507 ..... N91-16240 #
DE91-004583 ..... N91-16966 #
DE91-004622 ..... N91-16831 #
DE91-004722 ..... N91-16127 #
DE91-004769 ..... N91-16811 #
DE91-004833 ..... N91-16357 #
DE91-004835 ..... N91-16288 #
DE91-004842 ..... N91-16777 #
DE91-004848 ..... N91-16968 #
DE91-004855 ..... N91-16778 #
DE91-004898 ..... N91-16812 #
DE91-004911 ..... N91-16726 #
DE91-004952 ..... N91-16674 #
DE91-005018 ..... N91-16814 #
DE91-005032 ..... N91-16151 #
DE91-005211 ..... N91-16358 #
DE91-005266 ..... N91-16982 #

DIGEL-1990-3 ..... N91-16337 #
DIGEL-1990-4 ..... N91-16249 #

DLR-FB-90-26 ..... N91-15998 #
DLR-FB-90-27 ..... N91-16979 #
DLR-FB-90-32 ..... N91-16216 #
DLR-FB-90-33 ..... N91-16367 #

DLR-MITT-90-05 ..... N91-15977 #

DODA-AR-004-515 ..... N91-16020 #
DODA-AR-005-997 ..... N91-16616 #
DODA-AR-006-413 ..... N91-16331 #
DODA-AR-006-418 ..... N91-16204 #
DODA-AR-006-421 ..... N91-16238 #

DOE/CE-15256/1 ..... N91-16256 #
DOE/CE-15401/T7 ..... N91-16318 #

DOE/DP-0078T ..... N91-16751 #

DOE/ER-0428 ..... N91-16986 #
DOE/ER-0432 ..... N91-16456 #
DOE/ER-01545/439 ..... N91-16648 #
DOE/ER-01545/440 ..... N91-16827 #
DOE/ER-10666/8 ..... N91-16734 #
DOE/ER-13370/1 ..... N91-16086 #
DOE/ER-13435/4 ..... N91-16083 #
DOE/ER-13529/2 ..... N91-16711 #
DOE/ER-13629/4 ..... N91-16151 #
DOE/ER-13800/T2 ..... N91-16284 #
DOE/ER-13867/8 ..... N91-16723 #
DOE/ER-13930/T1 ..... N91-16261 #
DOE/ER-13942/2 ..... N91-16140 #
DOE/ER-13971/6 ..... N91-16715 #
DOE/ER-25019/17 ..... N91-16341 #
DOE/ER-25061/6 ..... N91-16258 #
DOE/ER-40154/T2 ..... N91-16828 #
DOE/ER-40427/04-N90 ..... N91-16712 #
DOE/ER-45189/4 ..... N91-16725 #
DOE/ER-45239/T2 ..... N91-16123 #
DOE/ER-52147/T1 ..... N91-16763 #
DOE/ER-52147/T2 ..... N91-16764 #
DOE/ER-53198/154 ..... N91-16757 #
DOE/ER-53222/102 ..... N91-16760 #
DOE/ER-53267/3 ..... N91-16762 #
DOE/ER-53302/2 ..... N91-16767 #
DOE/ER-60372/5 ..... N91-16460 #
DOE/ER-60473/T1 ..... N91-16717 #
DOE/ER-60631/5 ..... N91-16722 #

DOE/ET-53088/424 ..... N91-16748 #

DOE/FE-0183P ..... N91-16374 #

DOE/ID-10243/2-VOL-2-APP-PT-1 ..... N91-16227 #

DOE/MA-0422 ..... N91-16831 #

DOE/MC-23161/2806 ..... N91-16259 #
DOE/MC-25170/2861 ..... N91-16442 #

DOE/NASA/0336-2 ..... N91-16021* #
DOE/NASA/16310-15 ..... N91-16128* #
DOE/NASA/20320-77 ..... N91-16679* #

DOE/RA-50219/T10 ..... N91-16537 #
DOE/RA-50219/T13 ..... N91-16539 #

DOE/SF-16306/21 ..... N91-16435 #

DOT/FAA/AM-90/10 ..... N91-16544 #
DOT/FAA/AM-90/11 ..... N91-15999 #

DOT/FAA/NR-90/1 ..... N91-16206 #

DOT/FAA/RD-90/16 ..... N91-15989 #

DRI-4-90 ..... N91-16061 #

DTP-89/29 ..... N91-16671 #

DTRC-90/029 ..... N91-16709 #

E-5625 ..... N91-16304* #
E-5663 ..... N91-16679* #
E-5671 ..... N91-16075* #
E-5961 ..... N91-16128* #

EDR-14585 ..... N91-16021* #

EGG-EA-8245-VOL-2 ..... N91-16223 #

EGG-EP-8919 ..... N91-16225 #

EGG-M-89048 ..... N91-16319 #
EGG-M-89148 ..... N91-16377 #
EGG-M-89151 ..... N91-16066 #
EGG-M-89329 ..... N91-16395 #
EGG-M-89360 ..... N91-16739 #
EGG-M-90027 ..... N91-16574 #
EGG-M-90102 ..... N91-16461 #

EGG-10617-2066 ..... N91-16321 #
EGG-10617-7008 ..... N91-16471 #

ERL-0509-RE ..... N91-16616 #
ERL-0517-RR ..... N91-16331 #
ERL-0519-RE ..... N91-16204 #
ERL-0521-RN ..... N91-16238 #

ESD-TR-90-011 ..... N91-16195 #
ESD-TR-90-027 ..... N91-16816* #
ESD-TR-90-066 ..... N91-16361 #
ESD-TR-90-326 ..... N91-16004 #

ESD-88-TR-17 ..... N91-16610 #
ESD-90-TR-207 ..... N91-16584 #
ESD-90-TR-208 ..... N91-16587 #

ESL-FTR-723108-1 ..... N91-16191* #

ESL-TR-723105-1 ..... N91-16194* #

ETN-91-97874 ..... N91-16364 #
ETN-91-98261 ..... N91-15977 #
ETN-91-98305 ..... N91-16213
ETN-91-98310 ..... N91-16846
ETN-91-98311 ..... N91-16568
ETN-91-98321 ..... N91-16628 #
ETN-91-98322 ..... N91-16337 #
ETN-91-98323 ..... N91-16249 #
ETN-91-98390 ..... N91-16569
ETN-91-98392 ..... N91-16365
ETN-91-98395 ..... N91-16366
ETN-91-98400 ..... N91-16987 #
ETN-91-98402 ..... N91-16070 #
ETN-91-98403 ..... N91-16705 #
ETN-91-98408 ..... N91-16030 #
ETN-91-98409 ..... N91-16035 #
ETN-91-98411 ..... N91-16241 #
ETN-91-98412 ..... N91-16192 #
ETN-91-98413 ..... N91-16193 #
ETN-91-98422 ..... N91-16597 #
ETN-91-98428 ..... N91-16598 #
ETN-91-98429 ..... N91-16651 #
ETN-91-98430 ..... N91-16652 #
ETN-91-98433 ..... N91-16178 #
ETN-91-98455 ..... N91-16599 #
ETN-91-98456 ..... N91-16600 #
ETN-91-98457 ..... N91-16653 #
ETN-91-98458 ..... N91-16654 #
ETN-91-98460 ..... N91-16655 #
ETN-91-98461 ..... N91-16656 #
ETN-91-98462 ..... N91-16657 #
ETN-91-98463 ..... N91-16425 #
ETN-91-98464 ..... N91-16426 #
ETN-91-98465 ..... N91-16427 #
ETN-91-98466 ..... N91-16428 #
ETN-91-98468 ..... N91-16429 #
ETN-91-98469 ..... N91-16430 #
ETN-91-98470 ..... N91-16431 #
ETN-91-98472 ..... N91-16005 #
ETN-91-98473 ..... N91-16848 #
ETN-91-98474 ..... N91-16133 #
ETN-91-98475 ..... N91-16307 #
ETN-91-98476 ..... N91-16825 #
ETN-91-98477 ..... N91-16308 #
ETN-91-98478 ..... N91-16780 #
ETN-91-98479 ..... N91-16644 #
ETN-91-98480 ..... N91-16309 #
ETN-91-98481 ..... N91-16113 #

ETN-91-98482 N91-16250 #
ETN-91-98483 N91-16157 #
ETN-91-98484 N91-16338 #
ETN-91-98485 N91-16710 #
ETN-91-98486 N91-16111 #
ETN-91-98487 N91-16826 #
ETN-91-98488 N91-16179 #
ETN-91-98489 N91-16313 #
ETN-91-98490 N91-16000 #
ETN-91-98491 N91-15988 #
ETN-91-98492 N91-16967 #
ETN-91-98503 N91-16781 #
ETN-91-98504 N91-16834 #
ETN-91-98506 N91-16745 #
ETN-91-98507 N91-16669 #
ETN-91-98508 N91-16173 #
ETN-91-98509 N91-16060 #
ETN-91-98511 N91-16112 #
ETN-91-98512 N91-16251 #
ETN-91-98513 N91-16134 #
ETN-91-98514 N91-16849 #
ETN-91-98520 N91-16658 #
ETN-91-98530 N91-16706 #
ETN-91-98541 N91-16214 #
ETN-91-98542 N91-16629 #
ETN-91-98543 N91-16252 #
ETN-91-98544 N91-15997 #
ETN-91-98545 N91-16015 #
ETN-91-98546 N91-16016 #
ETN-91-98547 N91-16017 #
ETN-91-98548 N91-16076 #
ETN-91-98549 N91-16570 #
ETN-91-98550 N91-16630 #
ETN-91-98551 N91-16034 #
ETN-91-98552 N91-16253 #
ETN-91-98553 N91-16310 #
ETN-91-98554 N91-16022 #
ETN-91-98555 N91-16972 #
ETN-91-98556 N91-16973 #
ETN-91-98557 N91-16311 #
ETN-91-98558 N91-16014 #
ETN-91-98559 N91-16312 #
ETN-91-98560 N91-16314 #
ETN-91-98561 N91-16729 #
ETN-91-98562 N91-16730 #
ETN-91-98563 N91-16493 #
ETN-91-98564 N91-16731 #
ETN-91-98565 N91-16983 #
ETN-91-98566 N91-16782 #
ETN-91-98567 N91-16732 #
ETN-91-98568 N91-16746 #
ETN-91-98569 N91-16631 #
ETN-91-98570 N91-16135 #
ETN-91-98571 N91-16136 #
ETN-91-98572 N91-16114 #
ETN-91-98573 N91-16077 #
ETN-91-98574 N91-16392 #
ETN-91-98575 N91-16315 #
ETN-91-98576 N91-16541 #
ETN-91-98577 N91-16339 #
ETN-91-98578 N91-16528 #
ETN-91-98579 N91-16018 #
ETN-91-98580 N91-16019 #
ETN-91-98581 N91-16254 #
ETN-91-98582 N91-16023 #
ETN-91-98583 N91-16024 #
ETN-91-98584 N91-16215 #
ETN-91-98585 N91-16026 #
ETN-91-98591 N91-16670 #
ETN-91-98592 N91-16645 #
ETN-91-98593 N91-15998 #
ETN-91-98594 N91-16979 #
ETN-91-98596 N91-16216 #
ETN-91-98597 N91-16367 #
ETN-91-98603 N91-16974
ETN-91-98605 N91-16975
ETN-91-98606 N91-16976
ETN-91-98608 N91-16494
ETN-91-98609 N91-16495
ETN-91-98610 N91-16496
ETN-91-98611 N91-16977* #
ETN-91-98613 N91-16856
ETN-91-98614 N91-16978
ETN-91-98643 N91-16432 #
ETN-91-98644 N91-16002

EUR-FU/80/90-99 N91-16781 #

FEL-90-A125 N91-16365
FEL-90-B098 N91-16366
FEL-90-C082 N91-16430 #

FERMILAB-CONF-90/72-T N91-16787 #

FFA-TN-1990-27 N91-16070 #
FFA-TN-1990-34 N91-16706 #

FNAL-TM-1654 N91-16316 #

FNAL/C-90/226-A N91-16966 #

FR-20674 N91-16591 #

GA-A-19922 N91-16752 #
GA-A-20077 N91-16749 #

GAO/NSIAD-90-262 N91-15976 #

GL-TR-89-0338 N91-16475 #
GL-TR-90-0129 N91-16482 #
GL-TR-90-0131 N91-16776 #
GL-TR-90-0173 N91-16488 #
GL-TR-90-0277 N91-16661 #

HAC-REF-G3338-1 N91-16205 #

IAF-90-290 N91-16057* #

ICAS-90-6.7.2 N91-15997 #

ICASE-90-83 N91-16664* #
ICASE-90-85 N91-15994* #
ICASE-90-86 N91-15991* #
ICASE-90-87 N91-16305* #
ICASE-90-88 N91-16306* #
ICASE-90-89 N91-15996* #
ICASE-90-90 N91-15995* #

ICW-1942 N91-16427 #

IFSR-424 N91-16748 #

IS-T-1399 N91-16799 #
IS-T-1405 N91-16089 #
IS-T-1413 N91-16770 #
IS-T-1429 N91-16347 #
IS-T-1450 N91-16100 #

ISAS-SP-12 N91-16266 #

ISBN-90-9003467-6 N91-16313 #
ISBN-90-9003520-6 N91-16157 #
ISBN-90-9003596-6 N91-16644 #
ISBN-90-9003693-8 N91-16135 #
ISBN-90-9003713-6 N91-16631 #
ISBN-92-835-0580-8 N91-16553 #
ISBN-92-835-0599-9 N91-16833 #

ISSN-0109-6605 N91-16061 #
ISSN-0171-1342 N91-15998 #
ISSN-0171-1342 N91-16216 #
ISSN-0171-1342 N91-16367 #
ISSN-0171-1342 N91-16979 #
ISSN-0172-357X N91-16987 #
ISSN-0172-8741 N91-16493 #
ISSN-0172-8741 N91-16729 #
ISSN-0172-8741 N91-16730 #
ISSN-0172-8741 N91-16731 #
ISSN-0176-7739 N91-15977 #
ISSN-0178-0719 N91-16782 #
ISSN-0178-0719 N91-16983 #
ISSN-0288-433X N91-16266 #
ISSN-0366-0885 N91-16134 #
ISSN-0389-4010 N91-15982 #
ISSN-0389-4010 N91-15983 #
ISSN-0389-4010 N91-15984 #
ISSN-0389-4010 N91-15985 #
ISSN-0389-4010 N91-16069 #
ISSN-0389-4010 N91-16102 #
ISSN-0389-4010 N91-16384 #
ISSN-0389-4010 N91-16396 #
ISSN-0469-4236 N91-16432 #
ISSN-0922-5641 N91-16599 #
ISSN-0922-5641 N91-16600 #
ISSN-0922-5641 N91-16653 #
ISSN-0922-5641 N91-16654 #
ISSN-0922-5641 N91-16655 #
ISSN-0922-5641 N91-16656 #
ISSN-0922-5641 N91-16657 #

ISVR-TR-188 N91-16705 #

ITP-SB-89-40 N91-16827 #

IZF-1989-55 N91-16213
IZF-1990-A-11 N91-16848
IZF-1990-A-12 N91-16568
IZF-1990-B-2 N91-16569

JPL-D-6847 N91-16078* #

JPL-PUBL-90-36 N91-16534* #
JPL-PUBL-90-39 N91-16533* #
JPL-PUBL-90-40 N91-16532* #
JPL-PUBL-90-49 N91-16535* #

JPRS-USP-89-006 N91-16036

JSR-89-290 N91-16239 #

JUEL-2362 N91-16134 #

KCP-613-4426 N91-16326 #
KCP-613-4437 N91-16176 #

L-16831 N91-16981* #
L-16875 N91-16682* #

LA-UR-90-753 N91-16174 #
LA-UR-90-1125 N91-16342 #
LA-UR-90-1275 N91-16343 #
LA-UR-90-1332 N91-16499 #
LA-UR-90-1338 N91-16085 #
LA-UR-90-1354 N91-16786 #
LA-UR-90-1366 N91-16750 #
LA-UR-90-1434 N91-16042 #
LA-UR-90-1483 N91-16348 #
LA-UR-90-1546 N91-16578 #
LA-UR-90-1603 N91-16090 #
LA-UR-90-1688 N91-16439 #
LA-UR-90-1747 N91-16642 #
LA-UR-90-1809 N91-16091 #
LA-UR-90-1878 N91-16772 #
LA-UR-90-1921 N91-16323 #
LA-UR-90-3129 N91-16351 #
LA-UR-90-3166 N91-16093 #
LA-UR-90-3347 N91-16122 #
LA-UR-90-3788 N91-16357 #
LA-UR-90-3819 N91-16288 #
LA-UR-90-3877 N91-16777 #
LA-UR-90-3920 N91-16968 #
LA-UR-90-3964 N91-16778 #

LA-11625-MS N91-16716 #
LA-11641-MS N91-16263 #
LA-11692-MS-VOL-2 N91-16283 #
LA-11808-C N91-16755 #
LA-11813-MS N91-16255 #

LAAS-90215 N91-16214 #
LAAS-90256 N91-16629 #
LAAS-90306 N91-16252 #
LAAS-90354 N91-16670 #
LAAS-90355 N91-16645 #

LBL-27596 N91-16142 #
LBL-28574 N91-16546 #
LBL-28606 N91-16119 #
LBL-28836 N91-16228 #
LBL-28904 N91-16322 #
LBL-28924 N91-16735 #
LBL-28950 N91-16797 #
LBL-29643 N91-16149 #
LBL-29716 N91-16358 #

LMI-NI801R1 N91-16830 #

LSTM-239/T/88 N91-16364 #

M-651 N91-16500* #
M-652 N91-16858* #
M-654 N91-16413* #

MBB-UA-1182-90-PUB N91-16745 #
MBB-UA-1187-90-PUB N91-16669 #
MBB-UA-1188-90-PUB N91-16173 #

MBB-UO-0108-90-PUB N91-16060 #
MBB-UO-0115-90-PUB N91-16570 #

MBB-Z-0307-90-PUB N91-16834 #

MBB/FE122/S/PUB/411 N91-16016 #
MBB/FE122/S/PUB/0405 N91-16017 #
MBB/FE122/S/PUB/0407 N91-15997 #
MBB/FE122/S/PUB/0408 N91-16015 #
MBB/FE281/CFK/PUB/0013 N91-16076 #

MBB/FW522/S/PUB/427 N91-16630 #

MCAT-91-001 N91-15987* #

MCR-90-513 N91-16381 #

ME-56 N91-16392 #
ME-69 N91-16315 #
ME-78 N91-16541 #
ME-84 N91-16339 #

MEMO-COSOR-89-30 ..... N91-16598 #
MEMO-COSOR-89-31 ..... N91-16651 #
MEMO-COSOR-89-33 ..... N91-16652 #
MEMO-COSOR-90-02 ..... N91-16178 #

MISC-90024-VOL-2-APP-PT-1 ..... N91-16227 #

MIT-AI-M-1256 ..... N91-16624 #

MIT/LCS/TR-490 ..... N91-16611 #

MITT-33 ..... N91-16310 #

MLM-3633(OP) ..... N91-16738 #
MLM-3659(OP) ..... N91-16808 #

MP-90-080 ..... N91-16172 #

MPE-PREPRINT-179 ..... N91-16974
MPE-PREPRINT-181 ..... N91-16975
MPE-PREPRINT-182 ..... N91-16976
MPE-PREPRINT-184 ..... N91-16494
MPE-PREPRINT-185 ..... N91-16495
MPE-PREPRINT-186 ..... N91-16496
MPE-PREPRINT-188 ..... N91-16977* #
MPE-PREPRINT-189 ..... N91-16856
MPE-PREPRINT-190 ..... N91-16978

MPE-220 ..... N91-16983 #
MPE-221 ..... N91-16782 #

MPI-PAE/EXP.EL-231 ..... N91-16732 #

MRC-MSH-R-90-003 ..... N91-16776 #

MSRR-562 ..... N91-16626 #

MTL-TN-90-2 ..... N91-16073 #

MTL-TR-90-41 ..... N91-16072 #
MTL-TR-90-43 ..... N91-16130 #
MTL-TR-90-44 ..... N91-16007 #
MTL-TR-90-45 ..... N91-16068 #

MTR-10910 ..... N91-16004 #

NAL-TR-1058 ..... N91-16069 #
NAL-TR-1060 ..... N91-16384 #
NAL-TR-1063 ..... N91-16396 #
NAL-TR-1065 ..... N91-15985 #
NAL-TR-1066 ..... N91-15983 #
NAL-TR-1067 ..... N91-16102 #
NAL-TR-1070 ..... N91-15982 #
NAL-TR-1073-T ..... N91-15984 #

NAS 1.15:100705 ..... N91-16536* #
NAS 1.15:102245 ..... N91-16001* #
NAS 1.15:102627 ..... N91-16058* #
NAS 1.15:102752 ..... N91-16057* #
NAS 1.15:102761 ..... N91-16407* #
NAS 1.15:102766 ..... N91-16832* #
NAS 1.15:102857 ..... N91-16414* #
NAS 1.15:103214 ..... N91-16304* #
NAS 1.15:103245 ..... N91-16075* #
NAS 1.15:103391 ..... N91-16728* #
NAS 1.15:103415 ..... N91-16602* #
NAS 1.15:103727 ..... N91-16128* #
NAS 1.15:103812 ..... N91-16166* #
NAS 1.15:103814 ..... N91-16041* #
NAS 1.15:104230 ..... N91-16847* #
NAS 1.21:7011(345) N91-16547*
NAS 1.21:7037(259) N91-15979*
NAS 1.21:7037(260) N91-15978*
NAS 1.26:177573 ..... N91-16012* #
NAS 1.26:182474 ..... N91-16350* #
NAS 1.26:184071 ..... N91-16332* #
NAS 1.26:184072 ..... N91-16333* #
NAS 1.26:184073 ..... N91-16334* #
NAS 1.26:184074 ..... N91-16056* #
NAS 1.26:184078 ..... N91-16064* #
NAS 1.26:184084 ..... N91-16523* #
NAS 1.26:185233 ..... N91-16063* #
NAS 1.26:185264 ..... N91-16150* #
NAS 1.26:186404 ..... N91-16163* #
NAS 1.26:186543 ..... N91-16379* #
NAS 1.26:186841 ..... N91-16045* #
NAS 1.26:186842 ..... N91-16050* #
NAS 1.26:187039 ..... N91-16021* #
NAS 1.26:187396 ..... N91-16120* #
NAS 1.26:187479 ..... N91-16033* #
NAS 1.26:187480 ..... N91-16664* #
NAS 1.26:187481 ..... N91-15994* #
NAS 1.26:187482 ..... N91-15991* #
NAS 1.26:187483 ..... N91-16305* #
NAS 1.26:187485 ..... N91-16306* #
NAS 1.26:187486 ..... N91-15996* #
NAS 1.26:187487 ..... N91-15995* #
NAS 1.26:187698 ..... N91-16473* #
NAS 1.26:187699 ..... N91-16472* #
NAS 1.26:187751 ..... N91-16385* #
NAS 1.26:187756 ..... N91-16289* #
NAS 1.26:187760 ..... N91-15981* #
NAS 1.26:187767 ..... N91-15987* #
NAS 1.26:187768 ..... N91-16813* #
NAS 1.26:187769 ..... N91-15986* #
NAS 1.26:187776 ..... N91-16191* #
NAS 1.26:187777 ..... N91-16596* #
NAS 1.26:187794 ..... N91-16194* #
NAS 1.26:187801 ..... N91-16008* #
NAS 1.26:187805 ..... N91-16534* #
NAS 1.26:187807 ..... N91-16533* #
NAS 1.26:187808 ..... N91-16532* #
NAS 1.26:187812 ..... N91-16535* #
NAS 1.26:187828 ..... N91-16639* #
NAS 1.26:187829 ..... N91-16211* #
NAS 1.26:187831 ..... N91-16032* #
NAS 1.26:187833 ..... N91-16411* #
NAS 1.26:187836 ..... N91-16296* #
NAS 1.26:187837 ..... N91-16010* #
NAS 1.26:187848 ..... N91-16011* #
NAS 1.26:187855 ..... N91-16727* #
NAS 1.26:187858 ..... N91-16065* #
NAS 1.26:187860 ..... N91-16059* #
NAS 1.26:187863 ..... N91-16627* #
NAS 1.26:187864 ..... N91-16132* #
NAS 1.26:187865 ..... N91-16212* #
NAS 1.26:187868 ..... N91-16013* #
NAS 1.26:187871 ..... N91-16816* #
NAS 1.26:187887 ..... N91-16078* #
NAS 1.26:187924 ..... N91-16386* #
NAS 1.26:187925 ..... N91-16977* #
NAS 1.55:3093 ..... N91-16500* #
NAS 1.55:3098 ..... N91-16858* #
NAS 1.55:3101 ..... N91-16682* #
NAS 1.60:3055 ..... N91-16981* #
NAS 1.60:3057 ..... N91-16679* #
NAS 1.60:3075 ..... N91-16413* #
NAS 1.61:1250 ..... N91-16466* #
NAS 1.61:1251 ..... N91-16467* #
NAS 1.71:LAR-14361-1 ..... N91-16707* #
NAS 1.71:LEW-14984-1 ..... N91-16152* #
NAS 1.71:MFS-26061-1 ..... N91-16815* #
NAS 1.71:MSC-21589-1 ..... N91-16566* #
NAS 1.84:106-ED-2 ..... N91-16601* #

NASA-CASE-LAR-14361-1 ..... N91-16707* #

NASA-CASE-LEW-14984-1 ..... N91-16152* #

NASA-CASE-MFS-26061-1 ..... N91-16815* #

NASA-CASE-MSC-21589-1 ..... N91-16566* #

NASA-CP-3093 ..... N91-16500* #
NASA-CP-3098 ..... N91-16858* #
NASA-CP-3101 ..... N91-16682* #

NASA-CR-177573 ..... N91-16012* #
NASA-CR-182474 ..... N91-16350* #
NASA-CR-184071 ..... N91-16332* #
NASA-CR-184072 ..... N91-16333* #
NASA-CR-184073 ..... N91-16334* #
NASA-CR-184074 ..... N91-16056* #
NASA-CR-184078 ..... N91-16064* #
NASA-CR-184084 ..... N91-16523* #
NASA-CR-185233 ..... N91-16063* #
NASA-CR-185264 ..... N91-16150* #
NASA-CR-186404 ..... N91-16163* #
NASA-CR-186543 ..... N91-16379* #
NASA-CR-186841 ..... N91-16045* #
NASA-CR-186842 ..... N91-16050* #
NASA-CR-187039 ..... N91-16021* #
NASA-CR-187396 ..... N91-16120* #
NASA-CR-187479 ..... N91-16033* #
NASA-CR-187480 ..... N91-16664* #
NASA-CR-187481 ..... N91-15994* #
NASA-CR-187482 ..... N91-15991* #
NASA-CR-187483 ..... N91-16305* #
NASA-CR-187485 ..... N91-16306* #
NASA-CR-187486 ..... N91-15996* #
NASA-CR-187487 ..... N91-15995* #
NASA-CR-187698 ..... N91-16473* #
NASA-CR-187699 ..... N91-16472* #
NASA-CR-187751 ..... N91-16385* #
NASA-CR-187756 ..... N91-16289* #
NASA-CR-187760 ..... N91-15981* #
NASA-CR-187767 ..... N91-15987* #
NASA-CR-187768 ..... N91-16813* #
NASA-CR-187769 ..... N91-15986* #
NASA-CR-187776 ..... N91-16191* #
NASA-CR-187777 ..... N91-16596* #
NASA-CR-187794 ..... N91-16194* #
NASA-CR-187801 ..... N91-16008* #
NASA-CR-187805 ..... N91-16534* #
NASA-CR-187807 ..... N91-16533* #
NASA-CR-187808 ..... N91-16532* #
NASA-CR-187812 ..... N91-16535* #
NASA-CR-187828 ..... N91-16639* #
NASA-CR-187829 ..... N91-16211* #
NASA-CR-187831 ..... N91-16032* #
NASA-CR-187833 ..... N91-16411* #
NASA-CR-187836 ..... N91-16296* #
NASA-CR-187837 ..... N91-16010* #
NASA-CR-187848 ..... N91-16011* #
NASA-CR-187855 ..... N91-16727* #
NASA-CR-187858 ..... N91-16065* #
NASA-CR-187860 ..... N91-16059* #
NASA-CR-187863 ..... N91-16627* #
NASA-CR-187864 ..... N91-16132* #
NASA-CR-187865 ..... N91-16212* #
NASA-CR-187868 ..... N91-16013* #
NASA-CR-187871 ..... N91-16816* #
NASA-CR-187887 ..... N91-16078* #
NASA-CR-187924 ..... N91-16386* #
NASA-CR-187925 ..... N91-16977* #

NASA-PED-106-ED-2 ..... N91-16601* #

NASA-RP-1250 ..... N91-16466* #
NASA-RP-1251 ..... N91-16467* #

NASA-SP-7011(345) N91-16547*
NASA-SP-7037(259) N91-15979*
NASA-SP-7037(260) N91-15978*

NASA-TM-100705 ..... N91-16536* #
NASA-TM-102245 ..... N91-16001* #
NASA-TM-102627 ..... N91-16058* #
NASA-TM-102752 ..... N91-16057* #
NASA-TM-102761 ..... N91-16407* #
NASA-TM-102766 ..... N91-16832* #
NASA-TM-102857 ..... N91-16414* #
NASA-TM-103214 ..... N91-16304* #
NASA-TM-103245 ..... N91-16075* #
NASA-TM-103391 ..... N91-16728* #
NASA-TM-103415 ..... N91-16602* #
NASA-TM-103727 ..... N91-16128* #
NASA-TM-103812 ..... N91-16166* #
NASA-TM-103814 ..... N91-16041* #
NASA-TM-104230 ..... N91-16847* #

NASA-TP-3055 ..... N91-16981* #
NASA-TP-3057 ..... N91-16679* #
NASA-TP-3075 ..... N91-16413* #

NAVAIR-50-1C-VOL-1 ..... N91-16476 #
NAVAIR-50-1C-VOL-2 ..... N91-16477 #
NAVAIR-50-1C-VOL-3 ..... N91-16478 #
NAVAIR-50-1C-VOL-4 ..... N91-16479 #
NAVAIR-50-1C-VOL-7 ..... N91-16480 #
NAVAIR-50-1C-VOL-10 ..... N91-16481 #

NCEL-CR-90-016 ..... N91-16614 #

NESIDS-31 ..... N91-16055 #

NIAR-90-26 ..... N91-16153 #

NORDA-236 ..... N91-16841 #

NOSC/TD-1874 ..... N91-16203 #

NOSC/TR-1333-PT-2 ..... N91-16677 #

NPRDC-TR-90-6 ..... N91-16637 #

NRL-MR-6706 ..... N91-16186 #
NRL-MR-6719 ..... N91-16197 #

NRL-9267 ..... N91-16635 #

NUSC-TR-8753 ..... N91-16673 #
NUSC-TR-8759 ..... N91-16649 #

ORNL-6603 ..... N91-16148 #

ORNL/FTR-3561 ..... N91-16257 #
ORNL/FTR-3589 ..... N91-16320 #
ORNL/FTR-3602 ..... N91-16449 #
ORNL/FTR-3603 ..... N91-16463 #

ORNL/M-983 ..... N91-16126 #

ORNL/TM-11356 ..... N91-16756 #
ORNL/TM-11510 ..... N91-16376 #
ORNL/TM-11534 ..... N91-16835 #

PB91-104596 ..... N91-16388 #

PNL-MA-70-VOL-1 ..... N91-16393 #

PNL-7296 ..... N91-16445 #

PSU-ME-90/91-003 ..... N91-15986* #

PUBL-910801 ..... N91-16064* #

PWA-FR-20435 ..... N91-16594 #

R-89-2330-VOL-1 ..... N91-16328 #

RA-253 ..... N91-16190

RADC-TR-89-391 ..... N91-16196 #
RADC-TR-90-120 ..... N91-16588 #
RADC-TR-90-140 ..... N91-16583 #
RADC-TR-90-147 ..... N91-16353 #
RADC-TR-90-177 ..... N91-16741 #
RADC-TR-90-182 ..... N91-16604 #
RADC-TR-90-195-VOL-1 ..... N91-16608 #
RADC-TR-90-195-VOL-2 ..... N91-16609 #
RADC-TR-90-205 ..... N91-16615 #
RADC-TR-90-245 ..... N91-16208 #
RADC-TR-90-246 ..... N91-16209 #
RADC-TR-90-251 ..... N91-16207 #

RAE-SS-12 ..... N91-16035 #

RAE-TM-MAT/STR-1155 ..... N91-16241 #

RAE-TR-90029 ..... N91-16035 #

RAL-90-065 ..... N91-16030 #

RAND/P-7543 ..... N91-16177 #

REPT-1 ..... N91-16431 #
REPT-5 ..... N91-16147 #
REPT-21-7574 ..... N91-16327 #
REPT-23/90 ..... N91-16253 #
REPT-25/90 ..... N91-16034 #
REPT-88B0238 ..... N91-16536* #
REPT-90-8 ..... N91-16409 #
REPT-90-52 ..... N91-16599 #
REPT-90-53 ..... N91-16600 #
REPT-90-54 ..... N91-16653 #
REPT-90-55 ..... N91-16654 #
REPT-90-57 ..... N91-16655 #
REPT-90-58 ..... N91-16656 #
REPT-90-59 ..... N91-16657 #
REPT-110 ..... N91-16314 #
REPT-1286-17 ..... N91-16601 #
REPT-1990:1 ..... N91-16816* #
REPT-58922-00-105 ..... N91-16791 #
REPT-025921-17-T ..... N91-16211* #

RI/RD-90-163 ..... N91-16150* #

RPI-TR-90-29 ..... N91-16606 #

RR-CS-90-32 ..... N91-16659 #

RR-390 ..... N91-16658 #

RRK-89-23 ..... N91-16671 #

RSRE-MEMO-3699 ..... N91-16192 #
RSRE-MEMO-4375 ..... N91-16193 #

RU-89/B1/55 ..... N91-16827 #

SAF/AQT-SR-90-001 ..... N91-16838 #

SAIC-90/1462 ..... N91-16056* #

SAND-85-0699 ..... N91-16317 #
SAND-87-0645 ..... N91-16079 #
SAND-88-2174 ..... N91-16217 #
SAND-89-0126C ..... N91-16676 #
SAND-89-2229C ..... N91-16438 #
SAND-89-2245C ..... N91-16233 #
SAND-89-2464C ..... N91-16795 #
SAND-89-2658 ..... N91-16027 #
SAND-89-2769C ..... N91-16232 #
SAND-89-2930C ..... N91-16647 #
SAND-89-2951 ..... N91-16575 #
SAND-89-2956 ..... N91-16043 #
SAND-89-2985C ..... N91-16579 #
SAND-89-8253 ..... N91-16345 #
SAND-90-0001C ..... N91-16221 #
SAND-90-0085 ..... N91-16371 #
SAND-90-0125C ..... N91-16264 #
SAND-90-0139C ..... N91-16675 #
SAND-90-0230C ..... N91-16160 #
SAND-90-0300C ..... N91-16325 #
SAND-90-0344C ..... N91-16718 #
SAND-90-0348C ..... N91-16044 #
SAND-90-0367C ..... N91-16218 #
SAND-90-0368C ..... N91-16394 #
SAND-90-0388 ..... N91-16028 #
SAND-90-0396 ..... N91-16753 #
SAND-90-0410C ..... N91-16219 #
SAND-90-0449C ..... N91-16380 #
SAND-90-0462 ..... N91-16468 #
SAND-90-0501C ..... N91-16220 #
SAND-90-0519 ..... N91-16180 #
SAND-90-0577C ..... N91-16161 #
SAND-90-1077C ..... N91-16789 #
SAND-90-1209C ..... N91-16226 #
SAND-90-1384C-PT-2 ..... N91-16054 #
SAND-90-1394C ..... N91-16144 #
SAND-90-1772C ..... N91-16805 #
SAND-90-1875C ..... N91-16812 #
SAND-90-2192C ..... N91-16240 #
SAND-90-2589C ..... N91-16581 #
SAND-90-2933C ..... N91-16242 #
SAND-90-3057C ..... N91-16127 #

SCT-90RR-18 ..... N91-15989 #

SE-90-04 ..... N91-16383 #

SEI-90-SR-12 ..... N91-16590 #

SEL-82-906 ..... N91-16602* #

SERI/TP-211-4033 ..... N91-16444 #
SERI/TP-211-4034 ..... N91-16443 #
SERI/TP-212-3786 ..... N91-16139 #

SERI/TR-257-3372 ..... N91-16582 #

SFA-0184Z ..... N91-16779 #

SIR-90-017 ..... N91-16125 #

SMU/DS/TR/241 ..... N91-16661 #

SR-1 ..... N91-16482 #

SRA-R90-910032-F ..... N91-16202 #

SSCL-330 ..... N91-16674 #

SSD-TR-89-30 ..... N91-16489 #
SSD-TR-90-21 ..... N91-16352 #
SSD-TR-90-22 ..... N91-16355 #
SSD-TR-90-31 ..... N91-16362 #
SSD-TR-90-44 ..... N91-16248 #

SU-GL-4738 ..... N91-16237 #

SU-SLAC-PUB-5211 ..... N91-16790 #
SU-SLAC-PUB-5330 ..... N91-16183 #
SU-SLAC-PUB-5389 ..... N91-16726 #

SU-SLAC-357 ..... N91-16785 #

SU-TR-56 ..... N91-16613 #
SU-TR-57 ..... N91-16667 #
SU-TR-59 ..... N91-16636 #
SU-TR-437 ..... N91-16666 #

TD-89-4464 ..... N91-16365
TD-89-4553 ..... N91-16213
TD-89-4561 ..... N91-16569
TD-90-0025 ..... N91-16846
TD-90-0026 ..... N91-16568
TD-90-2788 ..... N91-16366

TOSC-DR-514 ..... N91-16855 #

TR-5 ..... N91-16146 #
TR-11 ..... N91-16155 #
TR-14 ..... N91-16807 #
TR-20 ..... N91-16098 #
TR-23 ..... N91-16154 #
TR-52 ..... N91-16108 #
TR-55 ..... N91-16668 #
TR-61 ..... N91-16682 #
TR-288 ..... N91-16210 #
TR-348 ..... N91-16387 #
TR-881 ..... N91-16195 #
TR-898 ..... N91-16361 #
TR-0089(4940-05)-1 ..... N91-16489 #
TR-0090(5925-01)-3 ..... N91-16248 #
TR-0090(5930-04)-3 ..... N91-16382 #
TR-0090(5945-05)-3 ..... N91-16352 #
TR-0090(5945-05)-02 ..... N91-16355 #

TR89-049 ..... N91-16622 #

TR90-033 ..... N91-16844 #

TWR-50068 ..... N91-16064* #

UBUFFALO/DC/90/TR-27 ..... N91-16815 #

UC-700 ..... N91-16345 #
UC-742 ..... N91-16160 #

UCID-21849 ..... N91-16437 #
UCID-21849-REV-1 ..... N91-16759 #

UCRL-CR-103753 ..... N91-16455 #
UCRL-CR-103859 ..... N91-16766 #
UCRL-CR-104249 ..... N91-16724 #

UCRL-ID-103429 ..... N91-16672 #
UCRL-ID-103473 ..... N91-16761 #
UCRL-ID-103486 ..... N91-16758 #
UCRL-ID-103808 ..... N91-16181 #

UCRL-JC-10397 ..... N91-16088 #
UCRL-JC-103166 ..... N91-16497 #
UCRL-JC-103244 ..... N91-16159 #
UCRL-JC-103279 ..... N91-16498 #
UCRL-JC-103302 ..... N91-16182 #
UCRL-JC-103338 ..... N91-16340 #
UCRL-JC-103464 ..... N91-16773 #
UCRL-JC-103520 ..... N91-16713 #
UCRL-JC-103526 ..... N91-16736 #
UCRL-JC-103608 ..... N91-16798 #
UCRL-JC-103629 ..... N91-16344 #
UCRL-JC-103872 ..... N91-16794 #
UCRL-JC-103943 ..... N91-16829 #
UCRL-JC-105323-PT-2 ..... N91-16982 #

UCRL-21221 ..... N91-16462 #
UCRL-52000-90-3 ..... N91-16985 #
UCRL-100531 ..... N91-16775 #
UCRL-100841 ..... N91-16469 #
UCRL-101659 ..... N91-16224 #
UCRL-101660 ..... N91-16324 #
UCRL-101665 ..... N91-16850 #
UCRL-101735 ..... N91-16459 #
UCRL-101866 ..... N91-16087 #
UCRL-101997 ..... N91-16457 #
UCRL-101998 ..... N91-16458 #
UCRL-102393 ..... N91-16158 #
UCRL-102395 ..... N91-16162 #
UCRL-102438 ..... N91-16633 #
UCRL-102484 ..... N91-16769 #
UCRL-102584 ..... N91-16080 #
UCRL-102737-REV-1 ..... N91-16577 #
UCRL-102746 ..... N91-16349 #
UCRL-102758 ..... N91-16793 #
UCRL-102778 ..... N91-16082 #
UCRL-102939 ..... N91-16771 #
UCRL-102963 ..... N91-16084 #
UCRL-102985 ..... N91-16538 #

UDR-TR-90-02 ..... N91-16124 #

UILU-ENG-90-2241 ..... N91-16356 #
UILU-ENG-90-2242 ..... N91-16245 #
UILU-ENG-90-2250 ..... N91-16623 #

ULT/TR-90-7197 ..... N91-16103 #

US-PATENT-APPL-SN-529427 ..... N91-16566* #
US-PATENT-APPL-SN-575708 ..... N91-16815* #
US-PATENT-APPL-SN-587920 ..... N91-16707* #
US-PATENT-APPL-SN-610683 ..... N91-16152* #

USAF-STINFO-MANAGEMENT-90/1 ..... N91-16838 #

USAFOEHL-90-126SA00687HAE ..... N91-16170 #

USARIEM-T18-90 ..... N91-16545 #

USGS-OFR-89-682-A ..... N91-16470 #

USNA-TSPR-170 ..... N91-16329 #

UTRC-R-89-2330-VOL-2 ..... N91-16330 #

UTSI-90 ..... N91-15981* #

UVA/525410/CS91/104 ..... N91-16837 #

WES/TR/GL-90-25 ..... N91-16031 #

WHOI-90-33 ..... N91-16185 #

WRDC-TR-90-2020-VOL-1 ..... N91-16328 #
WRDC-TR-90-2020-V2-VOL-2 ..... N91-16330 #
WRDC-TR-90-2050 ..... N91-16327 #

WRDC-TR-90-2078 ..... N91-16382 #
WRDC-TR-90-3050 ..... N91-16125 #
WRDC-TR-90-4068 ..... N91-16124 #
WRDC-TR-90-8022 ..... N91-16591 #
WRDC-TR-90-8025 ..... N91-16594 #

XA-23383.3-PH ..... N91-16820 #

YAI-TR-101 ..... N91-16482 #

YALEU/DCS/RR-814 ..... N91-16660 #

Appendix

NASA SCIENTIFIC AND TECHNICAL INFORMATION PROGRAM PRODUCTS AND SERVICES

The NASA Scientific and Technical Information (STI) Program provides for the collection and announcement of aerospace-related reports and literature obtained worldwide through agreements and exchanges. The result of the collection is the comprehensive NASA STI Database that covers aeronautics, space, and supporting disciplines.

The STI Database, documents generated or obtained by NASA, and products and services derived from or supporting the database are made available to the NASA research community and to the public. Descriptions and sources of these items are presented in the following pages.

Scientific and Technical Aerospace Reports (*STAR*) is an abstract journal, listing citations with abstracts for aerospace-related reports obtained from worldwide sources. *STAR* is issued on the 8th and 23rd of each month and announces current documents that have been entered into the NASA STI Database during the previous two weeks. The reports are of the following types:

- NASA, NASA contractor, and NASA grantee reports;
- Reports issued by other U.S. Government agencies, domestic and foreign institutions, universities, and private firms;
- Translations in report form;
- NASA-owned patents and patent applications;
- Other U.S. Government agency and foreign patents and patent applications;
- Domestic and foreign dissertations and theses.

Journal, book, and conference literature, journal translations, and certain foreign dissertations having the same subject scope as *STAR* are announced in a companion journal, *International Aerospace Abstracts* (*IAA*). *IAA* is issued on the 1st and 15th of each month and is available from the American Institute of Aeronautics and Astronautics, Technical Information Service, 555 West 57th Street, 12th Floor, New York, NY 10019.

ELIGIBILITY AND REGISTRATION FOR NASA STI PRODUCTS AND SERVICES

Organizations of the type listed below that have registered with NASA can receive products and services.

- NASA offices and installations, contractors, subcontractors, grantees, and consultants;
- Other U.S. Government agencies and their contractors;
- Libraries in the United States that have arrangements with NASA to maintain collections of NASA documents for public reference;
- Other organizations in the United States having a need for NASA documents in work related to aeronautics and space research;
- Organizations abroad that have established reciprocal documents exchange arrangements with NASA.

Only the central service points or central points of document acquisition and control within qualified organizations are eligible to register for NASA STI products and services. Domestic organizations that may be eligible to receive various classes of NASA publications and services should address their requests for registration or further information to:

NASA Center for AeroSpace Information
ATTN: Registration Services
P.O. Box 8757
BWI Airport, MD 21240
301-621-0153

Organizations abroad should direct requests to:

National Aeronautics and Space Administration
Director, Scientific and Technical Information Program
Code NTT
Washington, DC 20546
USA
703-271-5640

SUBJECT SCOPE

The subject scope of *STAR* and *IAA* includes all aspects of aeronautics and space research and development, supporting basic and applied research, and applications. Aerospace aspects of Earth resources, energy development, conservation, oceanography, environmental protection, urban transportation, and other topics of high national priority are also covered.

HOW TO USE *STAR* SUBJECT CATEGORIES

Abstracts in *STAR* are categorized by 10 major subject divisions that are divided further into 76 specific subject categories. The subject divisions and categories are listed in the Table of Contents together with a note for each that defines its scope and provides any cross-references. For example:

16 SPACE TRANSPORTATION
Includes passenger and cargo space transportation, e.g., shuttle operations; and space rescue techniques. For related information see also *03 Air Transportation and Safety* and *18 Spacecraft Design, Testing and Performance.* For space suits see *54 Man/System Technology and Life Support.*

CROSS-REFERENCES

Individual *STAR* abstracts are not ordinarily cross-referenced, except for certain conference reports or book translations that have had separate abstracts written for their component papers or chapters. Citations and abstracts of the components follow immediately after those of the parent document. When the subject content of a component differs sufficiently from the general content of the parent, a cross-reference citation also is printed at the end of the category to which it normally would have been assigned if it were independent.

DOCUMENTS ON MICROFICHE

Documents available on microfiche are designated by a pound sign (#) following the accession number.

LIMITED REPRODUCIBILITY

A note of limited reproducibility appears in the citation, if there are factors affecting the reproducibility of more than 20% of the document. These factors include faint or broken type, color photographs, black and white photographs, foldouts, dot matrix print, or some other factor that limits the reproducibility of the document. This notation also appears on the microfiche header with the specific factor checked off on a list visible in the second frame.

COLOR COPIES

An increasing number of NASA scientific and technical reports are being produced with color graphs, charts, illustrations, and photographs. An indication that a document has color pages follows the source and pricing (SAP) information in the *STAR* citation.

Registered users of the NASA Scientific and Technical Information Program will receive ordered documents with color at no additional cost, as long as stock copies of the document are available. Otherwise, an additional fee of $2.00 per color page will be charged. The NASA Center for AeroSpace Information staff will contact registered users to determine individual user's needs.

NASA PATENTS AND PATENT APPLICATIONS

Patents and patent applications owned by NASA are announced in *STAR* under appropriate subject categories and are referenced in the *STAR* indexes. In the Report/Accession Number Index, patents are indexed by the NASA Case Number, and the U.S. Patent Class. Patent applications are indexed by the NASA Case Number and the U.S. Patent Application Serial Number.

Printed copies of patents (which are not microfiched) are available for purchase from the U.S. Patent and Trademark Office.

NASA patent application specifications are sold in both paper copy and microfiche by the National Technical Information Service (NTIS). The US-Patent-Appl-SN-number should be used in ordering either paper copy or microfiche from NTIS.

When ordering patents, the U.S. Patent Number should be used, and payment must be remitted in advance, by money order or check payable to the Commissioner of Patents and Trademarks. Prepaid purchase coupons for ordering are also available from the U.S. Patent and Trademark Office.

The patents and patent applications announced in *STAR* are owned by NASA and are available for royalty-free licensing. Requests for licensing terms and further information should be addressed to:

National Aeronautics and Space Administration
Associate General Counsel for Intellectual Property
Code GP
Washington, DC 20546

SOURCES FOR DOCUMENTS

One or more sources from which a document announced in *STAR* is available to the public is given in each citation. The most commonly indicated sources and their acronyms or abbreviations are listed on page A-6. If the publication is available from a source other than those listed, the publisher and address will be displayed on the availability line or in combination with the corporate source line.

Avail: NTIS. Sold by the National Technical Information Service. Prices for hard copy (HC) and microfiche (MF) are indicated by a price code following the letters HC or MF in the *STAR* citation. Current values for the price codes are given in the tables on page A-7.

Initially distributed microfiche under the NTIS SRIM (Selected Research in Microfiche) is available at greatly reduced unit prices. For this service and for information concerning subscription to NASA printed reports, consult the NTIS Subscription Section, Springfield, VA 22161.

NOTE ON ORDERING DOCUMENTS: When ordering NASA publications (those followed by the * symbol), use the N accession number. NASA patent applications (only the specifications are offered) should be ordered by the US-Patent-Appl-SN number. Non-NASA publications (no asterisk) should be ordered by the AD, PB, or other *report number* shown on the last line of the citation, not by the N accession number. It is also advisable to cite the title and other bibliographic identification.

Avail: SOD (or GPO). Sold by the Superintendent of Documents, U.S. Government Printing Office, in hard copy. The current price and order number are given following the availability line. (NTIS will fill microfiche requests, as indicated above, for those documents identified by a # symbol.)

Avail: BLL (formerly NLL): British Library Lending Division, Boston Spa, Wetherby, Yorkshire, England. Photocopies available from this organization at the price shown. (If none is given, address inquiry to the BLL.)

Avail: DOE Depository Libraries. Organizations in U.S. cities and abroad that maintain collections of Department of Energy reports, usually in microfiche form, are listed in *Energy Research Abstracts*. Services available from the DOE and its depositories are described in a booklet, *DOE Technical Information Center - Its Functions and Services* (TID-4660), which may be obtained without charge from the DOE Technical Information Center.

Avail: ESDU. Pricing information on specific data, computer programs, and details on Engineering Sciences Data Unit (ESDU) topic categories can be obtained from ESDU International Ltd. Requesters in North America should use the Virginia address while all other requesters should use the London address, both of which are on page A-6.

Avail: Fachinformationszentrum, Karlsruhe. Sold by the Fachinformationszentrum Energie, Physik, Mathematik GMBH, Eggenstein Leopoldshafen, Federal Republic of Germany, at the price shown in deutschmarks (DM).

Avail: HMSO. Publications of Her Majesty's Stationery Office are sold in the U.S. by Pendragon House, Inc. (PHI), Redwood City, CA. The U.S. price (including a service and mailing charge) is given, or a conversion table may be obtained from PHI.

Avail: NASA Public Document Rooms. Documents so indicated may be examined at or purchased from the National Aeronautics and Space Administration, Public Documents Room (Room 126), 600 Independence Ave., S.W., Washington, DC 20546, or public document rooms located at NASA installations, and the NASA Pasadena Office at the Jet Propulsion Laboratory.

Avail: Univ. Microfilms. Documents so indicated are dissertations selected from *Dissertation Abstracts* and are sold by University Microfilms as xerographic copy (HC) and microfilm. All requests should cite the author and the Order Number as they appear in the citation.

Avail: US Patent and Trademark Office. Sold by Commissioner of Patents and Trademarks, U.S. Patent and Trademark Office, at the standard price of $1.50 each, postage free. (See discussion of NASA patents and patent applications below.)

Avail: (US Sales Only). These foreign documents are available to users within the United States from the National Technical Information Service (NTIS). They are available to users outside the United States through the International Nuclear Information Service (INIS) representative in their country, or by applying directly to the issuing organization.

Avail: USGS. Originals of many reports from the U.S. Geological Survey, which may contain color illustrations, or otherwise may not have the quality of illustrations preserved in the microfiche or facsimile reproduction, may be examined by the public at the libraries of the USGS field offices whose addresses are listed on page A-6. The libraries may be queried concerning the availability of specific documents and the possible utilization of local copying services, such as color reproduction.

Avail: Issuing Activity, or Corporate Author, or no indication of availability. Inquiries as to the availability of these documents should be addressed to the organization shown in the citation as the corporate author of the document.

FEDERAL DEPOSITORY LIBRARIES: To provide the general public with greater access to U.S. Government publications, Congress established the Federal Depository Library Program under the Government Printing Office (GPO), with 51 regional depositories responsible for permanent retention of material, inter-library loan, and reference services. (These libraries are not sales outlets.) At least one copy of nearly every NASA and NASA-sponsored publication, either in printed or microfiche format, is received and retained by the 51 regional depositories. A list of the regional GPO libraries, appears on page A-8. A local library can contact a regional depository library to help locate specific reports, or direct contact may be made by an individual.

PUBLIC COLLECTION OF NASA DOCUMENTS

An extensive collection of NASA and NASA-sponsored publications is maintianed by the British Library Lending Divison, Boston Spa, Wetherby, Yorkshire, England, for public access. The British Library Lending Division also has available many of the non-NASA publications cited in *STAR*.

European requesters may purchase facsimile copy or microfiche of NASA and NASA-sponsored documents, those identified by both the symbols # and * from ESA—Information Retrieval Service, European Space Agency, 8-10 rue Mario-Nikis, 75738 Paris CEDEX 15, France.

SUBMITTING DOCUMENTS

All users of this abstract service are urged to forward reports to be considered for announcement in *STAR*. This will aid NASA in its efforts to provide the fullest possible coverage of all scientific and technical publications that might support aeronautics and space research and development. If you have prepared relevant reports (other than those you will transmit to NASA, DOD, or DOE through the usual contract- or grant-reporting channels), please send them for consideration to the NASA Center for AeroSpace Information, P.O. Box 8757, BWI Airport, MD 21240.

Reprints of journal articles, book chapters, and conference papers are also welcome. These will be considered for announcement in *STAR*'s companion journal, *IAA*.

You may specify a particular source to be included in a report announcement if you wish; otherwise the report will be placed on a public sale at the National Technical Information Service. Copyrighted publications will be announced but not distributed or sold.

PURCHASE OF *STAR*

STAR is publicly available on annual subscription from the Superintendent of Documents, U.S. Government Printing Office, Washington, DC 20402.

STAR is available to registered users on annual subscription from the NASA Center for AeroSpace Information, ATTN: Registration Services, P.O. Box 8757, BWI Airport, MD 21240.

Microfiche of the abstract sections of *STAR* are available, on annual subscription only, from NTIS as PB91-911300, Attn: Subscriptions, 5285 Port Royal Road, Springfield, VA 22161. Annual subscription rates are $85.00 North America; $170.00 foreign. Abstract sections for previous years retroactive to 1964 are available at the current rates.

ADDRESSES OF ORGANIZATIONS

American Institute of Aeronautics and Astronautics
Technical Information Service
555 West 57th Street, 12th Floor
New York, New York 10019

British Library Lending Division,
Boston Spa, Wetherby, Yorkshire,
England

Commissioner of Patents and Trademarks
U.S. Patent and Trademark Office
Washington, DC 20231

Department of Energy
Technical Information Center
P.O. Box 62
Oak Ridge, Tennessee 37830

European Space Agency-Information Retrieval Service
ESRIN
Via Galileo Galilei
00044 Frascati (Rome) Italy

Engineering Sciences Data Unit International
P.O. Box 1633
Manassas, Virginia 22110

Engineering Sciences Data Unit International, Ltd.
251-259 Regent Street
London, W1R 7AD, England

Fachinformationszentrum Energie, Physik, Mathematik
GMBH
7514 Eggenstein Leopoldshafen
Federal Republic of Germany

Her Majesty's Stationery Office
P.O. Box 569, S.E. 1
London, England

NASA Center for AeroSpace Information
P.O. Box 8757
BWI Airport, Maryland 21240

National Aeronautics and Space Administration
Scientific and Technical Information Program (NTT)
Washington, DC 20546

National Technical Information Service
5285 Port Royal Road
Springfield, Virginia 22161

Pendragon House, Inc.
899 Broadway Avenue
Redwood City, California 94063

Superintendent of Documents
U.S. Government Printing Office
Washington, DC 20402

University Microfilms
A Xerox Company
300 North Zeeb Road
Ann Arbor, Michigan 48106

University Microfilms, Ltd.
Tylers Green
London, England

U.S. Geological Survey Library National Center
MS 950
12201 Sunrise Valley Drive
Reston, Virginia 22092

U.S. Geological Survey Library
2255 North Gemini Drive
Flagstaff, Arizona 86001

U.S. Geological Survey
345 Middlefield Road
Menlo Park, California 94025

U.S. Geological Survey Library
Box 25046
Denver Federal Center, MS914
Denver, Colorado 80225

NTIS PRICE SCHEDULES

(Effective January 1, 1991)

Schedule A
STANDARD PRICE DOCUMENTS AND MICROFICHE**

PRICE CODE	NORTH AMERICAN PRICE	FOREIGN PRICE
A01	$ 8.00	$ 16.00
A02	11.00	22.00
A03	15.00	30.00
A04-A05	17.00	34.00
A06-A09	23.00	46.00
A10-A13	31.00	62.00
A14-A17	39.00	78.00
A18-A21	45.00	90.00
A22-A25	53.00	106.00
A99	*	*
N01	60.00	120.00
N02	59.00	118.00
N03	20.00	40.00

Schedule E
EXCEPTION PRICE DOCUMENTS AND MICROFICHE**

PRICE CODE	NORTH AMERICAN PRICE	FOREIGN PRICE
E01	$10.00	$ 20.00
E02	12.00	24.00
E03	14.00	28.00
E04	16.50	33.00
E05	18.50	37.00
E06	21.50	43.00
E07	24.00	48.00
E08	27.00	54.00
E09	29.50	59.00
E10	32.50	65.00
E11	35.00	70.00
E12	38.50	77.00
E13	41.00	82.00
E14	45.00	90.00
E15	48.50	97.00
E16	53.00	106.00
E17	57.50	115.00
E18	62.00	124.00
E19	69.00	138.00
E20	80.00	160.00
E99	*	*

* Contact NTIS for price quote.

** Effective January 1, 1991, the microfiche copy of any new document entering the NTIS collection will be priced the same as the paper copy of the document.

IMPORTANT NOTICE

NTIS Shipping and Handling Charges

U.S., Canada, Mexico — ADD $3.00 per TOTAL ORDER

All Other Countries — ADD $4.00 per TOTAL ORDER

Exceptions — Does NOT apply to:

ORDERS REQUESTING NTIS RUSH HANDLING
ORDERS FOR SUBSCRIPTION OR STANDING ORDER PRODUCTS *ONLY*

NOTE: Each additional delivery address on an order requires a separate shipping and handling charge.

FEDERAL REGIONAL DEPOSITORY LIBRARIES

ALABAMA

AUBURN UNIV. AT MONTGOMERY LIBRARY
Documents Department
Montgomery, AL 36193
(205) 279-9110 ext.253

UNIV. OF ALABAMA LIBRARY
Reference Department/Documents
Box S
Tuscaloosa, AL 35486
(205) 348-6046

ARIZONA

DEPT. OF LIBRARY, ARCHIVES, AND PUBLIC RECORDS
Third Floor State Capitol
1700 West Washington
Phoenix, AZ 85007
(602) 255-4121

ARKANSAS

ARKANSAS STATE LIBRARY
Documents Service Section
One Capitol Mall
Little Rock, AR 72201
(501) 371-2090

CALIFORNIA

CALIFORNIA STATE LIBRARY
Govt. Publications Section
914 Capitol Mall
Sacramento, CA 95814
(916) 322-4572

COLORADO

UNIV. OF COLORADO
Norlin Library
Government Publications Division
Campus Box 184
Boulder, CO 80309
(303) 492-8834

DENVER PUBLIC LIBRARY
Govt. Pub. Department
1357 Broadway
Denver, CO 80203
(303) 571-2346

CONNECTICUT

CONNECTICUT STATE LIBRARY
231 Capitol Avenue
Hartford, CT 06106
(203) 566-4971

FLORIDA

UNIV. OF FLORIDA LIBRARIES
Documents Department
Library West
Gainesville, FL 32611
(904) 392-0367

GEORGIA

UNIV. OF GEORGIA LIBRARIES
Government Documents Dept.
Athens, GA 30602
(404) 542-8949

HAWAII

UNIV. OF HAWAII
Hamilton Library
Government Documents Collection
2550 The Mall
Honolulu, HI 96822
(808) 948-8230

IDAHO

UNIV. OF IDAHO LIBRARY
Documents Section
Moscow, ID 83843
(208) 885-6344

ILLINOIS

ILLINOIS STATE LIBRARY
Federal Documents
Centennial Building
Springfield, IL 62756
(217) 782-5012

INDIANA

INDIANA STATE LIBRARY
Serials Section
140 North Senate Avenue
Indianapolis, IN 46204
(317) 232-3686

IOWA

UNIV. OF IOWA LIBRARIES
Government Publications Dept.
Iowa City, IA 52242
(319) 335-5926

KANSAS

UNIVERSITY OF KANSAS
Spencer Research Library
Government Documents
Lawrence, KS 66045
(913) 864-4662

KENTUCKY

UNIV. OF KENTUCKY LIBRARIES
Government Publications/Maps Dept.
Lexington, KY 40506
(606) 257-8400

LOUISIANA

LOUISIANA STATE UNIVERSITY
Middleton Library
Government Documents Dept.
Baton Rouge, LA 70803
(504) 388-2570

LOUISIANA TECHNICAL UNIV.
Prescott Memorial Library
Government Documents Dept.
Ruston, LA 71272
(318) 257-4962

MAINE

UNIVERSITY OF MAINE
Raymond H. Fogler Library
Govt. Documents & Microforms Dept.
Orono, ME 04469
(207) 581-1680

MARYLAND

UNIVERSITY OF MARYLAND
McKeldin Library
Documents/Maps Room
College Park, MD 20742
(301) 454-3034

MASSACHUSETTS

BOSTON PUBLIC LIBRARY
Government Documents Dept.
666 Boylston Street
Boston, MA 02117
(617) 536-5400 ext.226

MICHIGAN

DETROIT PUBLIC LIBRARY
5201 Woodward Avenue
Detroit, MI 48202
(313) 833-1409

LIBRARY OF MICHIGAN
Government Documents
P.O. Box 30007
735 E. Michigan Avenue
Lansing, MI 48909
(517) 373-1593

MINNESOTA

UNIVERSITY OF MINNESOTA
Wilson Library
Government Publications
309 Nineteenth Avenue South
Minneapolis, MN 55455
(612) 373-7813

MISSISSIPPI

UNIV. OF MISSISSIPPI LIB.
Government Documents Dept.
106 Old Gym Bldg.
University, MS 38677
(601) 232-5857

MISSOURI

University of Missouri at Columbia Library
Government Documents
Columbia, MO 65201
(314) 882-6733

MONTANA

UNIV. OF MONTANA
Mansfield Library
Documents Division
Missoula, MT 59812
(406) 243-6700

NEBRASKA

UNIVERSITY OF NEBRASKA - LINCOLN
Love Memorial Library
Documents Department
Lincoln, NE 68588
(402) 472-2562

NEVADA

UNIV. OF NEVADA-RENO LIB.
Govt. Pub. Department
Reno, NV 89557
(702) 784-6579

NEW JERSEY

NEWARK PUBLIC LIBRARY
U.S. Documents Division
5 Washington Street
P.O. Box 630
Newark, NJ 07101
(201) 733-7812

NEW MEXICO

UNIVERSITY OF NEW MEXICO
General Library
Government Publications/Maps Dept.
Albuquerque, NM 87131
(505) 277-5441

NEW MEXICO STATE LIBRARY
325 Don Gaspar Avenue
Santa Fe, NM 87501
(505) 827-3826

NEW YORK

NEW YORK STATE LIBRARY
Documents Sect. Cultural Educ. Ctr.
Empire State Plaza
Albany, NY 12230
(518) 474-5563

NORTH CAROLINA

UNIVERSITY OF NORTH CAROLINA AT CHAPEL HILL
Davis Library 080A
BA/SS Department Documents
Chapel Hill, NC 27514
(919) 962-1151

NORTH DAKOTA

NORTH DAKOTA STATE UNIVERSITY LIBRARY
Government Documents Dept.
Fargo, ND 58105
(701) 237-8352
In cooperation with Univ. of North Dakota, Chester Fritz Library
Grand Forks

OHIO

STATE LIBRARY OF OHIO
Documents Section
65 South Front Street
Columbus, OH 43266
(614) 644-7051

OKLAHOMA

OKLAHOMA DEPT. OF LIBRARIES
Government Documents
200 NE 18th Street
Oklahoma City, OK 73105
(405) 521-2502, ext. 252

OKLAHOMA STATE UNIV. LIB.
Documents Department
Stillwater, OK 74078
(405) 624-0489

OREGON

PORTLAND STATE UNIV.
Millar Library
934 SW Harrison - P.O. Box 1151
Portland, OR 97207
(503) 229-3673

PENNSYLVANIA

STATE LIBRARY OF PENN.
Government Publications Section
Box 1601
Walnut St. & Commonwealth Ave.
Harrisburg, PA 17105
(717) 787-3752

SOUTH CAROLINA

CLEMSON UNIV. COOPER LIB.
Documents Department
Clemson, SC 29634
(803) 656-5174
In cooperation with Univ. of South Carolina, Thomas Cooper Library, Columbia

TEXAS

TEXAS STATE LIBRARY
Public Services Department
P.O. Box 12927 - 1201 Brazos
Austin, TX 78711
(512) 463-5455

TEXAS TECH. UNIV. LIBRARY
Documents Department
Lubbock, TX 79409
(806) 742-2268

UTAH

UTAH STATE UNIVERSITY
Merrill Library & Learning Resources Center, UMC-30
Documents Department
Logan, UT 84322
(801) 750-2682

VIRGINIA

UNIVERSITY OF VIRGINIA
Alderman Library
Government Documents
Charlottesville, VA 22903
(804) 924-3133

WASHINGTON

WASHINGTON STATE LIBRARY
Document Section
Olympia, WA 98504
(206) 753-4027

WEST VIRGINIA

WEST VIRGINIA UNIV. LIB.
Government Documents Section
P.O. Box 6069
Morgantown, WV 26506
(304) 293-3640

WISCONSIN

ST. HIST SOC. OF WISCONSIN LIB.
Government Pub. Section
816 State Street
Madison, WI 53706
(608) 262-2781
In cooperation with Univ. of Wisconsin-Madison, Memorial Library

MILWAUKEE PUBLIC LIBRARY
Documents Division
814 West Wisconsin Avenue
Milwaukee, WI 53233
(414) 278-3065

WYOMING

WYOMING STATE LIBRARY
Supreme Court & Library Bldg.
Cheyenne, WY 82002
(307) 777-5919

National Aeronautics and
Space Administration
Code NTT
Washington, D.C.
20546
Official Business
Penalty for Private Use, $300

SPECIAL FOURTH-CLASS RATE
POSTAGE & FEES PAID
NASA
PERMIT No. G27

POSTMASTER: If Undeliverable (Section 158
Postal Manual) Do Not Return